PETROLOGY, WHOLE ROCK AND MINERAL CHEMISTRY, THERMOBAROMETRY AND INTERPRETATION OF HIGH PRESSURE METAMORPHIC ROCKS

by

Dennis Anthony Carswell
B.Sc., Ph.D. (Edinb.), F.G.S.

Thesis presented for the Degree of Doctor of Science
of the University of Edinburgh in the
Faculty of Science

April, 1988

CONTENTS

1. Abstract 1

2. List of Submitted Publications 2

A. Papers concerned with high pressure metamorphic rocks from the Basal Gneiss Complex of Western Norway 2

B. Papers concerned with xenolith samples brought up in mantle derived magmas 3

C. General papers or papers on high pressure metamorphic rocks from other geological settings 5

3. Statement, as required by Regulation 1.1.4, on the extent of the contribution made to papers with joint authorship 6

4. Review of the research findings contained in the submitted publications 10

A. Papers concerned with high pressure metamorphic rocks from the Basal Gneiss Complex of western Norway 10

B. Papers concerned with xenolith samples brought up in mantle derived magmas 16

C. General papers or papers on high pressure metamorphic rocks from other geological settings 25

5. Copies of Submitted Publications 30

1. ABSTRACT

High pressure metamorphic rocks in two contrasting geological settings have been studied and interpreted.

Occurrences in exposed high grade gneiss complexes (especially in west Norway) have been documented. Petrogenetic interpretations of these rocks have involved the integration of field, mineralogical and microstructural observations with whole rock and mineral composition data, isotopic age data and calculated equilibration temperature and pressure values. Deduced pressure-temperature-time paths for both the prograde (subduction related) and retrograde (uplift related) metamorphic stages have been used to establish tectonothermal models for the formation and survival of such high pressure rocks in orogenic belts involving collision between continental lithospheric plates. Particular emphasis has been placed on interpretation of the chemical, mineralogical and tectonic evolution of alpine-type Mg-Cr rich peridotites of deduced sub-continental mantle origin. However, it has been shown that high pressure mineral asemblages have also developed in original, low pressure, crustal protoliths due to the imposition of high lithostatic pressures during transient A-type subduction.

Complementary studies of high pressure assemblages in xenoliths, brought up in volatile charged magmas of deep mantle origin, have provided important data on the chemical and mineralogical composition of the lower crust and uppermost mantle beneath continental cratonic areas. Particular attention has been paid to evaluation of the reliability of the application of mineral exchange reaction thermometers and barometers to assessment of the pressure-temperature conditions for formation, and depths of origin, of the various xenolith types. It has been demonstrated that, for the garnet lherzolite xenolith suite in the kimberlites of northern Lesotho, earlier pressure-temperature estimates purported to indicate a marked thermal perturbation in the upper mantle palaeogeotherm are invalid. Instead revised pressure-temperature estimates are interpreted to be indicative of only a slightly elevated craton margin geotherm, compatible with derivation of the higher temperature deformed xenoliths in a thermally convecting asthenosphere beneath a ca. 150 kms. thick, thermally conductive, lithosphere.

A revised, three fold, temperature based classification scheme for the formation of high pressure, eclogite facies, mineral assemblages in proposed. Low temperature (<550^{o}C) eclogites have formed in subordinate, fluid deficient, rocks associated with blueschists in B-type subduction zones. Medium temperature (550-900^{o}C) eclogites have been stabilised in tectonically thickened continental crust sequences in A-type subduction zones. High temperature (>900^{o}C) eclogites and associated garnet lherzolites, as witnessed as xenoliths in kimberlites, have equilibrated in the upper mantle.

2. LIST OF PUBLICATIONS SUBMITTED

These publications have been subdivided into three groups according to their content and the location of the rock samples involved in the research work undertaken.

A. Papers concerned with high pressure metamorphic rocks from the Basal Gneiss Region of Western Norway

1. D.A. CARSWELL (1968)
"Picritic magma-residual dunite relationships in garnet peridotite at Kalskaret near Tafjord, south Norway"
Contrib. Mineral. Petrol. 19, 97-124.

2. D.A. CARSWELL (1968)
"Possible primary upper mantle peridotite in Norwegian Basal Gneiss"
Lithos, 1, 322-355.

3. D.A. CARSWELL (1973)
"The age and status of the Basal Gneiss Complex of north-west Southern Norway"
Norsk Geol. Tidsskr. 53, 65-78.

4. D.A. CARSWELL (1973)
"Garnet pyroxenite lens within Ugelvik layered garnet peridotite"
Earth Planet. Sci. Letters 20, 347-352.

5. D.A. CARSWELL (1974)
"Comparative equilibration temperatures and pressures of garnet lherzolites in Norwegian gneisses and in kimberlites"
Lithos 3, 113-121.

6. D.A. CARSWELL, C.D. CURTIS and R. KANARIS-SOTIRIOU (1974)
"Vein metasomatism in peridotite at Kalskaret near Tafjord, South Norway"
J. Petrology 15, 3893-402.

7. R. KANARIS-SOTIRIOU, F.G.F. GIBB, D.A. CARSWELL and C.D. CURTIS (1978)
"Trace-element distribution and ore formation in vein-metasomatised peridotites at Kalskaret, near Tafjord, South Norway.
Contrib. Mineral. Petrol. 67, 289-295.

8. D.A. CARSWELL and F.G.F. GIBB (1980)
"The equilibration conditions and petrogenesis of European crustal garnet lherzolites."
Lithos 13, 19-29.

9. D.A. CARSWELL (1981)
"Clarification of the petrology and occurrence of garnet lherzolites, garnet websterites and eclogite in the vicinity of Rodhaugen, Almklovdalen, West Norway"
Norsk Geol. Tidsskr. 61, 249-260.

10. S.J. CUTHBERT, M.A. HARVEY and D.A. CARSWELL (1983)
"A tectonic model for the metamorphic evolution of the Basal Gneiss Complex, Western South Norway"
J. Metam. Geol. 1, 63-90.

11. D.A. CARSWELL, M.A. HARVEY and A. AL-SAMMAN (1983)
"The petrogenesis of contrasting Fe-Ti amd Mg-Cr garnet peridotite types in the high grade Gneiss Complex of Western Norway"
Bull. Mineral. 106, 727-750.

12. W.L. GRIFFIN and D.A. CARSWELL (1985)
"In-situ metamorphism of Norwegian Eclogites: An example"
In: The Caledonide Orogen - Scandinavia and Related Areas. D.G. Gee and B.A. Sturt (eds), John Wiley & Sons.

13. D.A. CARSWELL, E.J. KROGH and W.L. GRIFFIN (1985)
"Norwegian orthopyroxene eclogites: calcualted equilibration conditions and petrogenetic implications"
In: the Caledonide Orogen - Scandinavia and Related AReas. D.G. Gee and B.A. Sturt (eds), John Wiley and Sons.

14. D.A. CARSWELL and M.A. HARVEY (1985)
"The intrusive history and tectonometamorphic evolution of the Basal Gneiss Complex in the Moldefjord area, West Norway"
In: The Caledonide Orogen - Scandinavia and Related Areas. D.G. Gee and B.A. Sturt (eds), John Wiley & Sons.

15. D.A. CARSWELL (1986)
"The metamorphic evolution of Mg-Cr type Norwegian garnet peridotites"
Lithos 19, 279-297.

B. **Papers concerned with xenolith samples brought up in mantle derived magmas**

16. D.A. CARSWELL and J.B. DAWSON (1970)
"Garnet peridotite xenoliths in South African kimberlite pipes and their petrogenesis"
Contrib. Mineral. Petrol. 25, 163-184.

17. R.H. MITCHELL, D.A. CARSWELL and A.O. BRUNFELT (1973)
"Mineralogy and rare earth geochemistry of an ilmenite-clinopyroxene xenolith from Monastery Mine"
In: Lesotho Kimberlites, P.H. Nixon (ed), Lesotho National Development Corporation.

18. D.A. CARSWELL (1975)
"Primary and secondary phlogopites and clinopyroxenes in garnet lherzolite xenoliths"
Physics Chem. Earth. 9, 145-157.

19. R.H. MITCHELL and D.A. CARSWELL (1976)
"Lanthanum, samarium and ytterbium abundances in some southern African garnet lherzolites"
Earth Planet. Sci. Letters 31, 175-178.

20. D.B. CLARKE and D.A. CARSWELL (1977)
"Green garnets from the Newlands Kimberlite, Cape Province, South Africa"
Earth Planet. Sci. Letters 34, 30-38.

21. D.A. CARSWELL
"Palaeogeotherms: Implications of disequilibrium in garnet lherzolite xenoliths"
Nature 276, 737.

22. W.L. GRIFFIN, D.A. CARSWELL and P.H. NIXON (1978)
"Lower-crustal granulites and eclogites from Lesotho, Southern Africa"
Proc. 2nd Int. Kimberlite Conf. Vol.2, 59-86. Amer. Geophys. Union.

23. D.A. CARSWELL, D.B. CLARKE and R.H. MITCHELL (1978)
"The petrology and geochemistry of ultramafic xenoliths from Pipe 200, Northern Lesotho"
Proc. 2nd Int. Kimberlite Conf. Vol.2, 127-144. Amer. Geophys. Union.

24. D.A. CARSWELL (1980)
"Mantle derived lherzolite nodules associated with kimberlite, carbonatite and basalt magmatism: A review"
Lithos 13, 121-138.

25. D.A. CARSWELL and C.M. RICE (1980)
"The uranium content of garnet lherzolite xenoliths in kimberlites"
Mineral. Mag. 43, 689-693.

26. J.S. DELANEY, J.V. SMITH, D.A. CARSWELL and J.B. DAWSON (1980)
"Chemistry of micas from kimberlites and xenoliths - II. Primary and secondary textured micas from peridotite xenoliths"
Geo. et Cosmochim. Acta 44, 857-872.

27. R.H. MITCHELL, D.A. CARSWELL and D.B. CLARKE (1980)
"Geological implications and validity of calculated equilibration conditions for ultramafic xenoliths from the Pipe 200 kimberlite, northern Lesotho"
Contrib. Mineral. Petrol. 72, 205-217.

28. D.A. CARSWELL and F.G.F. GIBB (1980)
"Geothermometry of garnet lherzolite nodules with special reference to those from the kimberlites of northern Lesotho"
Contrib. Mineral. Petrol. 74, 403-416.

29. D.A. CARSWELL and W.L. GRIFFIN (1981)
"Calculation of equilibration conditions for garnet granulite and garnet websterite nodules in African kimberlite pipes"
Tschermaks Min. Petr. Mitt. 28, 229-244.

30. D.A. CARSWELL, J.B. DAWSON and F.G.F. GIBB (1981)
"Equilibration conditions of upper mantle eclogites: implications for kyanite bearing and diamondiferous varieties"
Mineral. Mag. 44, 79-89.

31. D.A. CARSWELL, W.L. GRIFFIN and P. KRESTEN (1984)
"Peridotite nodules from the Ngopetsoeu and Lipelaneng kimberlites, Lesotho: A crustal or mantle origin"
In: Kimberlites II: The Mantle and Crust-Mantle Relationships. J. Kornprobst (ed), Elsevier, 229-243.

32. D.A. CARSWELL, W.L. GRIFFIN and P. KRESTEN (1984)
"Peridotite nodules from the Ngopetsoeu and Lipelaneng kimberlites, Lesotho: A crustal or mantle origin - Appendix"
Am. Sci. Univ. Clermont-Fd. II. 74, 167-178.

33. D.A. CARSWELL and F.G.F. GIBB (1987)
"Evaluation of mineral thermometers and barometers applicable to garnet lherzolite assemblages"
Contrib. Mineral. Petrol. 95, 499-511.

34. D.A. CARSWELL and F.G.F. GIBB (1987)
"Garnet lherzolite xenoliths in the kimberlites of northern Lesotho: revised P-T equilibration conditions and upper mantle palaeogeotherm"
Contrib. Mineral. Petrol. 97, 473-487.

C. General papers or papers based on high pressure metamorphic rocks from other geological settings

35. D.E. de S. JAYAWARDENA and D.A. CARSWELL (1976)
"The geochemistry of charnockites and their constituent ferro-magnesian minerals from the Precambrian of South East Sri Lanka (Ceylon)"
Mineral. Mag. 40, 541-554.

36. H.G. SCHARBERT and D.A. CARSWELL (1983)
"Petrology of garnet-clinopyroxene rocks in a granulite facies environment, Bohemian Massif of Lower Austria.
Bull. Mineral. 106, 761-774.

37. D.A. CARSWELL and S.J. CUTHBERT (1986)
"Eclogite facies metamorohism in the Lower Continental Crust"
In: the Nature of the Lower Continental Crust. J.B. Dawson, D.A. Carswell, J. Hall and K.H. Wedepohl (eds). Geol. Soc. Special Publ. 24, 193-209.

3. STATEMENT AS REQUIRED BY REGULATION 1.1.4, ON THE EXTENT OF THE CONTRIBUTION MADE TO PAPERS WITH JOINT AUTHORSHIP

For papers in which authorship was shared with others, the extent of involvement and contribution was as follows:

Paper (6) Largely responsible as first author, but analytical data by R. Kanaris-Sotiriou and some interpretative input also by C.D. Curtis

(7) A truely joint effort, with R. Kanaris-Sotiriou largely responsible for final assembly of the paper.

(8) Almost entirely responsible for the content of this paper. F.G.F. Gibb contributed through assistance with the development of the pressure-temperature calculation program employed.

(10) This paper was put together on a collaborative basis with two of my research students. I was pleased to put their names in front in recognition of their efforts.

(11) Totally responsible for writing this paper. Only a minor data input from two of my research students.

(12) A joint effort in terms of analytical data input but the paper mostly written by W.L. Griffin.

(13) A joint effort in terms of input of mineral analyses but wholly responsible for the calculation of the P-T estimates and wrote most of the paper as first author.

(14) Wrote this paper but some input of whole rock analytical data and isotopic age data from one of my research students.

(16) Xenolith samples supplied by J.B. Dawson but wholly responsible for the analytical data and for the content of the paper.

(17) Contribution limited to electron microprobe mineral analyses of the ilmenite-clinopyroxene xenolith.

(19) Contribution limited to supply of samples and background information.

(20) Analyses of the green garnets by D.B. Clarke but the responsibility for writing the paper and for the interpretation was jointly shared.

(22) This paper was a truly joint effort with W.L. Griffin. The role of P.H. Nixon was restricted to the provision of many of the samples studied. Responsible for the whole rock analytical data and for acquiring the modal composition data and the density measurements. The paper was in fact written jointly with W.L. Griffin on an island retreat in the Stockholm archipelago.

(23) Responsible as first author for the co-ordination of this research work with two North American collaborators and for writing the final paper. R.H. Mitchell played only a minor role, but D.B. Clarke was responsible for most of the mineral composition data.

(25) Responsible for writing this paper, incorporating analytical data by C.M. Rice.

(26) Contribution limited to the supply of some of the analysed samples and to certain aspects of the interpretation.

(27) Contribution largely restricted to the calculation and interpretation of the P-T estimates for these xenoliths.

(28) Largely responsible for the paper content as first author. F.G.F. Gibb assisted with the development of the Nodmins 2 calculation program and with data presentation in the paper.

(29) More or less entirely responsible for the content of this paper.

(30) More or less totally responsible as first author for the content of the paper, the analytical data and the calculation of the equilibration conditions.

(31), (32) Responsible for co-ordinating this research work with two collaborators in Scandinavia. Responsible as first author for most of the content of the paper, for the whole rock chemistry and for the P-T estimates and interpretation thereof. Mineral composition data by the two co-authors.

(33), (34) Acted as principal author and largely responsible for the content of both of these papers. F.G.F. Gibb contributed through assisting with the development of the Nodmins 3 calculation program used for calculation of the P-T values, and also advised on presentation of both papers.

(35) Played a major part in writing this paper based on analytical data by a research student.

(36) Analytical data entirely by H.G. Scharbert but played a major role in the calculation of the P-T estimates and in the interpretation.

(37) Largely responsible for the content of this paper as first author, but a significant contribution made by my research student towards the geotectonic model diagram.

I hereby certify that the above is an accurate record of the extent of my involvement in those papers submitted which have co-authorship. This indicates that I have made a substantial contribution to their scientific content in almost all cases.

I also certify that none of the papers submitted here have been submitted previously for any other degree; although the scientific data and interpretations contained in the first two papers listed reflect, to a substantial extent, the content of my earlier Ph.D. thesis.

D. A. Carswell.

D. A. CARSWELL

4. REVIEW OF THE RESEARCH FINDINGS CONTAINED IN THE SUBMITTED PUBLICATIONS

A. Papers concerned with high pressure metamorphic rocks from the Basal Gneiss Complex of western Norway

Papers (1) and (2) are concerned with the geochemical characteristics and upper mantle petrogenesis of garnetiferous peridotite assemblages preserved within the west Norway alpine-type peridotite bodies. These early papers arose largely from my Ph.D. research work.

Paper (4) reported the discovery of a coarse-grained orthopyroxenite lens within the garnetiferous peridotites at the Ugelvik locality on Otrøy. This provides important evidence for the exsolution of garnet from an earlier highly aluminous orthopyroxene phase. Chemical analyses of both the bulk rock and bulk mineral separates from this rock were reported in this early paper, with more detailed electron microprobe analyses of the host and exsolved mineral phases added in a later paper (15). Corroborative evidence for the interpretation, outlined in the synoptic paper (15), that the high pressure garnetiferous peridotite assemblages in these peridotite bodies were predated by an earlier high temperature (lower pressure) assemblage with olivine + aluminous pyroxenes ± spinel ± amphibole, was provided by data for a rock sample from the Sandvika locality on Gurskøy, as documented in paper (11). This further sample demonstrates development of garnet as coronas around earlier pleonaste spinel as well as garnet exsolution from early aluminous orthopyroxene.

Papers (6) and (7) detailed the major and trace element profiles across a mineralogically zoned metasomatic vein in one of the west Norway peridotite bodies. The zoned sequence was interpreted to represent the result of incomplete reaction of the peridotite with a fluid phase introduced along a fracture from the surrounding country rocks under amphibolite facies metamorphic

conditions. It was demonstrated that local equilibrium was maintained at mineral zone interfaces between the introduced fluid and the various silicate, oxide and sulphide mineral phases stabilised by the metasomatic reaction. The mineralogical control on the distribution of both the introduced chemical species and the redistributed elements within the peridotite was outlined and discussed.

Paper (5) presented pressure-temperature estimates for the west Norway garnetiferous peridotites - as well as a comparison with the pressure-temperature extimates calculated for garnetiferus peridotite assembages encountered as xenoliths in kimberlite pipes in southern Africa. The pressure-temperature estimates for the Norwegian garnet peridotites have been up-dated and refined in several subsequent papers (notably in 8, 9, 11, 13 and 15) as better calibrated mineral exchange reactions thermometers and barometers have become available and also as electron microprobe mineral analyses have superceded earlier analyses of bulk mineral separates and thus enabled discrimination between porphyroclast core and rim compositions and also recrystallised neoblast compositions.

My latest assessment is that the porphyroclast core assemblages (Stage II in paper 15) in Norwegian garnet peridotites equilibrated under subcontinental upper mantle conditions at around 850^{o}C and 34-36 Kbars, whilst the porphyroclast rims show evidence of diffusion constrained partial re-equilibration under somewhat lower pressure-temperature conditions. Recrystallised neoblast garnet + spinel peridotite assemblages (Stage III in paper 15) equilibrated at around 725^{o}C and 20-24 Kbars - these values reflecting the pressure-temperature conditions towards the base of a tectonically thickened crustal thrust-nappe stack during tectonic intercalation of thrust slices of uppermost mantle peridotite into the crust during Caledonian plate collision.

Paper (8) also drew a comparison between the calculated equilibration pressures and temperatures for Norwegian garnet peridotites and those in the central Alps and in the Bohemian Massif. Although in all instances an ultimate upper mantle origin was advocated for these peridotite bodies, it was emphasised that the final equilibration of the garnetiferous peridotite assemblages took place during or immediately after emplacement of these peridotite bodies into tectonically thickened crust at the site of major plate collisions.

Paper (13) discussed at length the problems involved in the determination of equilibration pressures using the garnet-orthopyroxene Al barometer in rocks with complex disequilibrium mineral assemblages - especially where orthopyroxenes are appreciably zoned in their alumina content. Nevertheless, it was shown that by careful pairing of garnet and orthopyroxene grain rim compositions comparable pressure-temperature conditions (at around 700-750^{o}C and 20 Kbars) were indicated both for 'internal' orthopyroxene eclogites from within the peridotite bodies and for 'external' orthopyroxene eclogites directly enclosed in quartzo-feldspathic gneisses. As similar pressure-temperature conditions were also deduced for relict high pressure assemblages in the gneisses and also for other varieties of 'external' eclogite, it was argued that a large segment of the crust in western Norway had suffered early Caledonian depression to depths of around 60-70 kms.

Paper (3) provided an early overview of controversies concerning the age and status of the Basal Gneiss Complex in west Norway and to what extent Precambrian and Lower Palaeozoic lithological elements and tectono-metamorphic events were involved. An updated interpretation based on subsequent field, petrographic, chemical and isotopic age data for rocks in the Moldefjord region was presented in paper (14). This later paper stressed the importance of the involvement of large volumes of orthogneisses interpreted to have been origi-

nally emplaced into the crust during major mid-Proterozoic magmatism associated with crustal rifting in an extensional tectonic regime. The original depositional age of the associated metasedimentary paragneiss units is less certain, although at least some Lower Palaeozoic as well as Precambrian lithological units were considered likely to have been involved. Also important in paper (14) was the demonstration that both heterogeneous paragneiss and homogenous orthogneiss units witnessed the early Caledonian high pressure metamorphism. It was further indicated that relicts of the high pressure metamorphic event were best preserved in massive eclogite lenses (earlier basic dykes/sills) within the acid-intermediate augen textured orthogneisses. The more pervasive later deformation of the paragneiss lithologies during subsequent late Caledonian uplift, under conditions of high pore fluid activity, has resulted in more extensive retrogression to amphibolite facies assemblages.

Paper (12) demonstrated partial preservation of original intrusive relationships between the igneous precursors for basic eclogites and the enclosing orthogneisses thereby refuting earlier claims by some workers that all the eclogites represented tectonic inclusions of deep level (mostly mantle derived) rocks within the enclosing quartzo-feldspathic gneisses. Instead it was argued that both these basic igneous rocks and their enclosing rocks (both earlier sediments and igneous rocks) were subjected to high pressure metamorphism as a consequence of subduction of the leading edge of the Baltic lithospheric plate to depths of 60-70 kms early during the Caledonian orogeny.

A more detailed evolutionary tectonic model for the high pressure early Caledonian metamorphism of the Basal Gneiss Complex of western Norway and its subsequent uplift history was provided in paper (10). Tectonic intercalation between continental crust and uppermost sub-continental mantle leading to the emplacement of the garnetiferous peridotite bodies into the gneiss complex was incorporated into this dynamic model. This model has subsequently been widely

accepted and referred to as the 'Sheffield' model. For example thermal modelling of the pressure-temperature-time history of the peridotite bodies by Medaris and co-workers was shown to be compatible with the 'Sheffield' geotectonic model for the Caledonian orogeny in western Norway.

Paper (11) drew attention for the first time to the existence of two chemically contrasted types of garnetiferous peridotites in western Norway. The Mg and Cr-rich type peridotites with minor associated 'internal' garnet pyroxenite (orthopyroxene eclogites) were interpreted to be of upper mantle origin. By contrast, the more Fe and Ti-rich type peridotites, which occur as a subordinate component of layered eclogite-garnet pyroxenite complexes, were interpreted to have originated by metamorphism of relatively low pressure (< 10 Kbar) crustal intrusive complexes originally comprising olivine norite-peridotite cumulates. The latter intrusives were considered to be possibly genetically related to the voluminous rapakivi granite-mangerite-anorthosite suite of mid-Proterozoic anorogenic intrusives - interpreted as the precursors of encompassing orthogneisses.

Another important feature of paper (11) was the demonstration of the existence of two generations of garnet in certain Mg-Cr type peridotite samples. The secondary, Cr-depleted, garnet neoblasts were shown to coexist with Cr spinel as part of a relatively lower pressure 5-phase garnet + spinel lherzolite assemblage. Contrary to suggestions by others these second generation garnets formed before, rather than after, the development of the retrograde granulite-amphibolite facies kelyphite coronas around garnet porphyroclasts.

A more complete documentation of the complex, 7-stage metamorphic evolution of the Mg-Cr type, mantle derived, peridotite bodies in the Basal Gneiss Complex of west Norway was outlined in paper (15) and tabulated in Table 1 of that paper. With the presence of up to 6 generations of certain mineral

phases in these peridotite bodies and the overall prevalence of disequilibrium assemblages, it was emphasised that considerable care has to be exercised when combining mineral composition data to calculate numerical values for the pressure-temperature path followed by these rocks during their long and complex history.

This paper refuted claims by other research workers that these particular peridotites represented pre-Caledonian (Iapetus) ophiolitic material - instead advocating a much older sub-continental mantle origin. It was speculated that the coarse grained Stage II garnet peridotite assemblages equilibrated in the mantle during the Proterozoic (long before the Caledonian high pressure metamophic event) whereas the recrystallised stage III neoblast garnet + spinel peridotite assemblages may well have equilibrated during the Caledonian emplacement of these bodies into the crust. Recent, as yet unpublished, Sm-Nd dating of the high pressure assemblages in these rocks (undertaken in collaboration with B. Jamtveit in the Mineralogisk-Geologisk Museum of the University of Oslo) has indeed confirmed a Caledonian age for the recrystallised Stage III high pressure garnetiferous assemblages (samples U539 and F12 in the Figure overleaf) in contrast to partly reset older Proterozoic ages for the coarse grained Stage III garnetiferous assemblages(samples T96 and T153 in the Figure overleaf). These age dates have been combined with best pressure-temperature estimates for each of the observed sequence of mineral assemblages deduced to have been stable in these peridotite bodies, to derive the synoptic pressure-temperature-time path for the metamorphic evolution of these rocks shown on the further accompanying diagram.

The foregoing resume demonstrates that the integrated field, petrographic, rock chemistry, mineral chemistry, thermometric, barometric and isotopic age data on these west Norway high pressure metamorphic rocks (as documented in the 15 submitted published papers on these rocks) constitute a

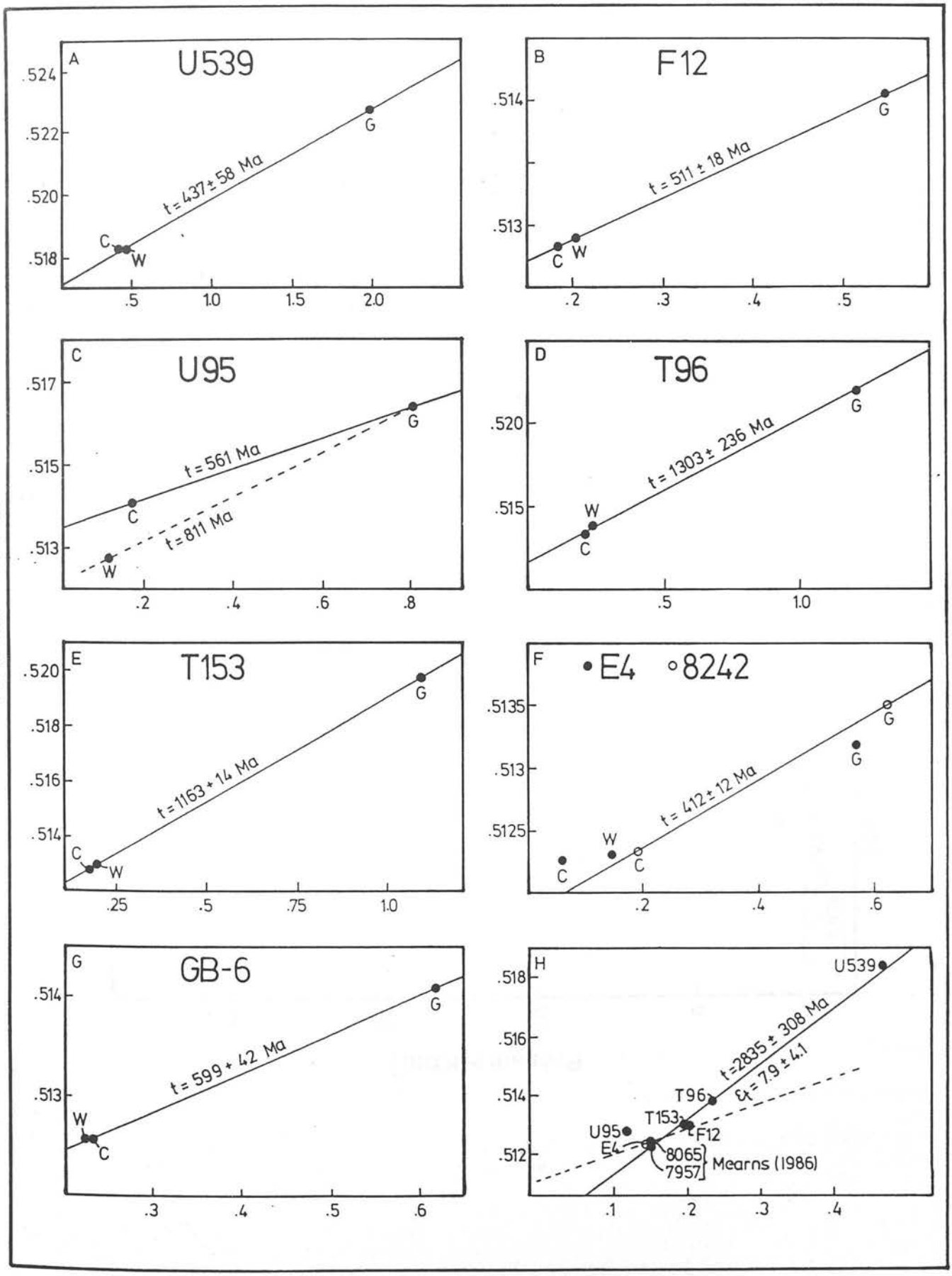
A
U539
t = 437 ± 58 Ma
C
W
G
B
F12
t = 511 ± 18 Ma
C
W
G
C
U95
t = 561 Ma
t = 811 Ma
C
W
G
D
T96
t = 1303 ± 236 Ma
W
C
G
E
T153
t = 1163 ± 14 Ma
C
W
G
F
E4
8242
t = 412 ± 12 Ma
C
W
C
G
G
G
GB-6
t = 599 ± 42 Ma
W
C
G
H
U539
t = 2835 ± 308 Ma
εt = 7.9 ± 4.1
T96
T153
U95
F12
E4
8065
7957
Mearns (1986)
144 Nd / 143 Nd
147 Sm / 143 Nd

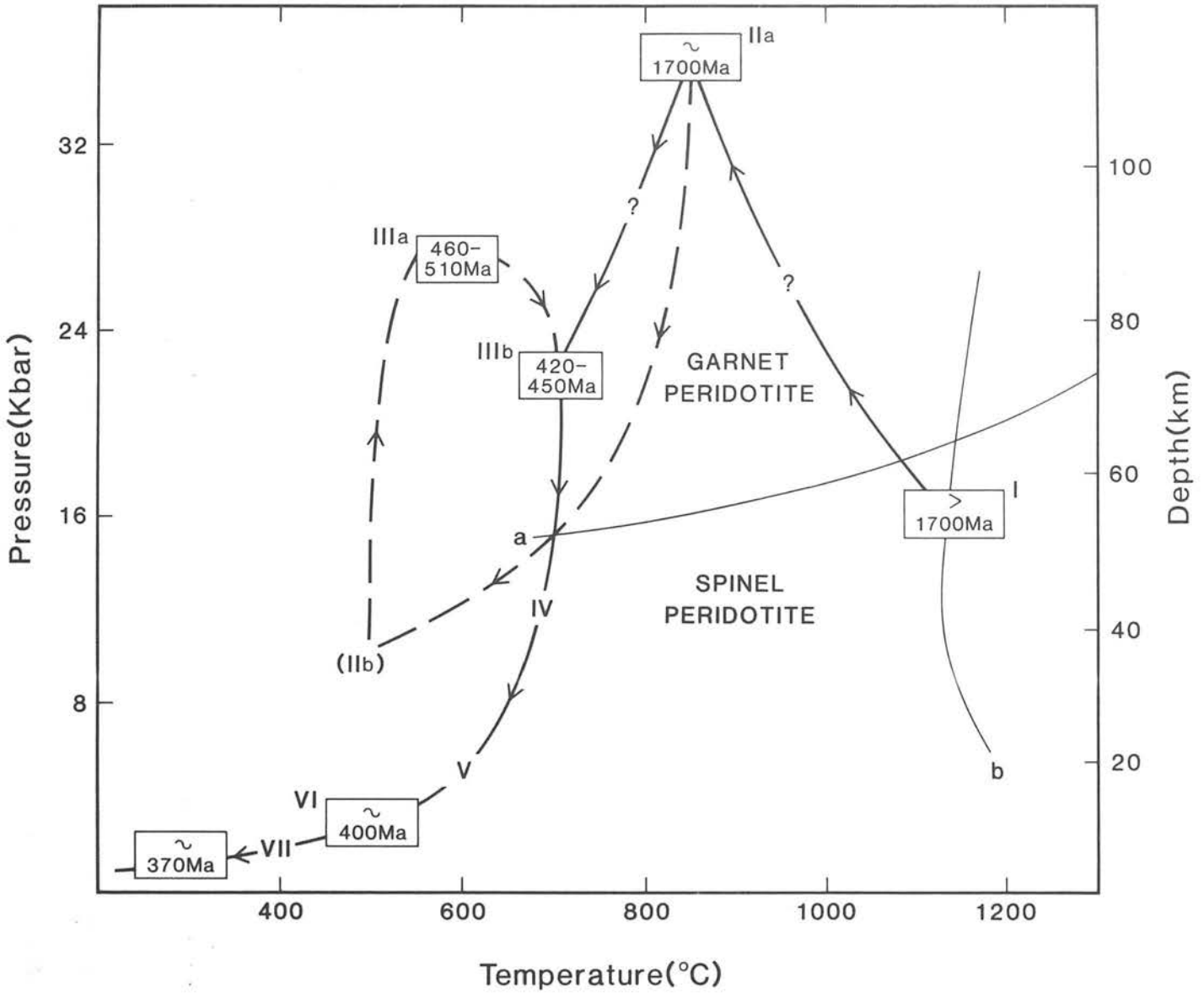
Pressure(Kbar)
32
24
16
8
400
600
800
1000
1200
Temperature(°C)
Depth(km)
100
80
60
40
20
IIa
~ 1700Ma
?
?
IIIa
460-510Ma
IIIb
420-450Ma
GARNET PERIDOTITE
SPINEL PERIDOTITE
I
> 1700Ma
a
b
(IIb)
IV
V
VI
~ 400Ma
VII
~ 370Ma

major contribution to the understanding and interpretation of the geotectonic significance of the occurrences of these rocks within the Scandinavian Caledonides.

B. Papers concerned with xenolith samples brought up in mantle derived magmas

Research work on the high pressure mineral assemblages in xenolithic samples of deep crustal or upper mantle derivation commenced shortly after completion of initial Ph.D. research work on Norwegian rocks. It has since continued in parallel with my research studies of high pressure assemblages in basic and ultrabasic rocks in exhumed high pressure, deep crustal gneiss terranes. These xenolith studies were initially prompted by the International Upper Mantle Project in the late 1960's and were furthered by participation in the International Kimberlite Conferences and related field excursions in South Africa (1973), U.S.A. (1977) and France (1982). These field excursions provided the opportunity for the collection of xenolith samples from kimberlite diatremes, which have been the basis of much of the research work documented in my publications in this research area.

Paper (16), my earlist publication in this research area, detailed the whole rock and mineral chemistry of a suite of garnet lherzolite xenolith samples from South African kimberlites provided by J.B. Dawson. The then existing controversies over the petrogenesis of these xenoliths were reviewed and an upper mantle derivation emphasised.

Papers (17) and (18) documented my first electron microprobe studies of mineral compositions in xenolith samples, undertaken during a visit to the Mineralogisk-Geologisk Museum at the University of Oslo in 1972, as a Royal Society supported Research Fellow. Paper (18) drew attention to the important

chemical distinctions between the two generations of phlogopite mica grains observed in certain xenolith samples, a matter documented in greater detail in a later paper (26).

Paper (20) provided mineral composition data on unusual green coloured, uvarovite-rich, garnet xenocrysts in the Newlands kimberlite and discussed their likely mineral paragenesis from recrystallised spinel wehrlite cumulates of deep mantle origin. Comparisons were drawn with occurrence of rather similar garnets in the kimberlites of Yakutia, U.S.S.R.

Paper (24) constitutes an important review of the whole rock chemistry, mineral assemblages, pressure-temperature equilibration estimates and depths of origin of both spinel- and garnet-bearing lherzolite xenolith types associated with kimberlite, carbonatite or alkali basalt type magmatism. Particular emphasis was placed on the interpretation of the chemical and physical controls on spinel-garnet stability relationships in such xenoliths. Three different classes of spinel lherzolite xenoliths were proposed based on the 100 Cr/(Cr+Al) ratios of the spinels, shown to be inversely correlated with the Al_2O_3 content of the coexisting orthopyroxenes. The extent to which the various xenolith samples were likely to constitute primitive (undepleted) or residual (depleted) upper mantle compositions, in terms of their potential for the generation of basaltic partial melts, was also considered at length. Comparative estimates for the pressure-temperature equilibration conditions of the various mineralogical and textural xenolith types were provided and discussed.

Papers (19) and (25) contain data on the uranium, and certain rare earth element, contents in garnet lherzolite xenoliths. They also include discussion as to what extent these elemental abundances reflect 'normal' upper mantle levels or contamination of the xenolithic peridotite material during transport in the erupting kimberlite magmas.

Papers (23), (31) and (32) provided detailed accounts of the petrography, whole rock and mineral chemistry, pressure-temperature equilibration conditions, and depths of origin of suites of peridotite xenoliths from the Pipe 200, Ngopetsoeu and Lipelaneng kimberlites in northern Lesotho. The controls of whole rock chemistry on the stable mineral parageneses and mineral compositions were detailed, again with particular emphasis on the interpretation of the stability relationships between garnet and spinel in these xenoliths. In the Ngopetsoeu and Lipelaneng kimberlites compositional distinctions were drawn between two groups of spinel bearing peridotite xenoliths interpreted to be of lower crustal origin, and two further groups (one Cr-spinel bearing, the other garnet bearing) considered to be of upper mantle origin. These contrasting depths of derivation were further substantiated by comparative mineral thermometry on the respective mineral assemblages.

Paper (22) reported innovative research on a large suite of lower-crustal granulite and eclogite xenoliths from the kimberlites of southern Lesotho. Previously xenoliths of lower-crustal origin had been largely ignored relative to peridotite xenoliths of upper mantle derivation. This study directed attention to the valuable information to be obtained on the petrological make-up of the lower continental crust from the study of such xenoliths and pioneered such studies of comparable xenolith suites in volatile charged alkaline intrusives in many other parts of the globe. Important points to emerge from this study of lower-crustal xenoliths in the kimberlites of northern Lesotho were:

i. the recognition of a large volume of metabasic granulite material in the lower crust - with implications for the importance of magmatic underplating (or rather interleaving) in the vicinity of the crust-mantle boundary.

ii. that garnet granulite, eclogite and websterite xenoliths were all derived from essentially the same depth range with mineral assemblages (notably the presence or absence of modal plagioclase feldspar) controlled by the bulk rock chemistry.

iii. that calculated pressure-temperature values for the equilibration of the mineral assemblages in these xenoliths were compatible with derivation from the lower continental crust. Consequently, studies of xenolith suites in kimberlites provide an important basis for the establishment of a petrological stratigraphy in the lower continental crust as well as in the sub-continental upper mantle.

Paper (28) provided an assessment of the respective accuracies of the various available calibrations of mineral exchange reaction thermometers applicable to the estimation of equilibration temperatures for xenolithic garnet lherzolite assemblages. Several of the previously proposed thermometer calibrations were rejected as unsatisfactory and on the basis of preferred methods a revised late Cretaceous palaeogeotherm for the upper mantle beneath northern Lesotho was proposed.

Paper (29) applied similarly selected mineral thermometers and barometers to the calculation of 'best' estimates of equilibration temperatures and pressures for lower-crustal garnet granulite and garnet websterite xenoliths. This paper also emphasised the necessity to take into account the Fe^{3+} contents of coexisting garnets and clinopyroxenes in order to obtain geologically meaningful equilibration temperature values by application of the thermometer formulation of Ellis and Green (1979) for Fe^{2+}-Mg^{2+} exchange between garnet-clinopyroxene pairs.

Paper (30) presented new mineral composition data for kyanite eclogite xenoliths from the Roberts Victor Mine and Bellsbank kimberlites. Calculated coefficients for Fe^{2+}-Mg^{2+} partitioning between coexisting garnet and clinopyroxene in these and previously analysed kyanite or diamond bearing eclogite

xenoliths from these kimberlites were used to estimate equilibration temperatures for these xenoliths. Corresponding pressures and depths of origin were deduced with reference to an upper mantle geotherm indicated by garnet lherzolite xenolith thermometry and barometry and to experimental data on the graphite-diamond transition.

The validity of using the array of calculated equilibration pressure-temperature conditions for garnet lherzolite xenoliths to define upper mantle palaeogeotherms, at the time of entrainment of these xenoliths in the transporting kimberlites, was discussed in papers (21) and (27). It was concluded that the transport times of xenoliths within erupting kimberlite were likely to have been too short to permit any significant chemical re-equilibration of mineral assemblages in mantle derived xenoliths. Thus such xenolith suites are considered to effectively retain information on the ambient pressure-temperature conditions at their respective sites of derivation in the upper mantle immediately prior to entrainment in the erupting kimberlite magmas. Whilst this may also hold for xenoliths of lower-crustal origin, it is unlikely to be true for xenoliths incorporated from mid- to upper-crustal levels since at these depths metamorphic mineral assemblages are likely to represent older 'frozen-in' mineral equilibria held at ambient temperatures well below those at which element exchange reactions in mineral assemblages are effectively blocked.

Paper (23) presents an updated evaluation of the accuracy of the various mineral thermometer and barometer calibrations applicable to the mineral assemblages in garnet lherzolite xenoliths. Assessment was based on the ability of the various proposed thermometer and barometer formulations to reproduce the experimental pressure-temperature equilibration conditions of 'natural' multi-component garnet lherzolite assemblages using a large data base assembled from papers by Kushiro et al. (1972), Akella (1976), Mori and Green

(1976) and Nickel (1983). This paper has high-lighted the problems which arise over the application of thermometer and barometer formulations based on experimental data for simple chemical systems to the more chemically complex natural mineral assemblages. Unlike previous assessment which involved tests using selected thermometer-barometer pairings (with consequent cross propagations of errors), in this case thermometers and barometers were tested independently using a specially developed, highly flexible, computer program (Nodmins 3).

The tests reported in paper (33) indicated that no single thermometer formulation was entirely satisfactory throughout the temperature-pressure range of interest and hence that equilibration temperatures for garnet lherzolite assemblages were best evaluated by consideration of the temperature estimates provided by application of a selected number of the most satisfactory thermometer formulations for <u>different</u> element exchange reactions between <u>different</u> coexisting mineral pairs. The Nickel and Green (1985) formulation of the garnet-orthopyroxene Al exchange reaction barometer based on experimental data for the $CaO-MgO-Al_2O_3-SiO_2$ and $CaO-MgO-Al_2O_3-Cr_2O_3-SiO_2$ systems, extrapolated part thermodynamically and part empirically for the additional influence of FeO, most closely models the compositions of natural garnet lherzolite assemblages and accordingly was demonstrated to provide the most satisfactory pressure estimates.

Regardless of which actual formulation of the garnet-orthopyroxene Al exchange reaction barometer is employed, it has been demonstrated that pressure estimates for garnet lherzolite assemblages are critically dependent upon the manner in which the amount of Al in orthopyroxene involved Tschermak's molecule substitution ($Al^{[VI]}Al^{[IV]}Mg^{-1}Si^{-1}$) is assessed from orthopyroxene mineral analyses. Accordingly calculation of the composition parameter [$X^{Ml}_{Al(Ts)}$] is of

fundamental importance to evaluation of equilibration pressures for garnet lherzolite xenoliths.

For garnet-orthopyroxene equilibria in the simple $MgO-Al_2O_3-SiO_2$ system the following simple relationship holds for orthopyroxenes:

$$X^{Ml}_{Al(Ts)} = Al^{Total}/2$$

In applying this barometer to natural garnet-orthopyroxene equilibria, Wood (1974) assumed that this relationship still effectively holds. Similarly, Finnerty and Boyd (1984 and 1987), in applying their favoured barometer formulation based on the $MgO-Al_2O_3-SiO_2$ system experimental data of MacGregor (1974) simply considered the total weight fraction of Al present in the orthopyroxene. Such treatments simply assume that all Al in the orthopyroxenes is present as Tschermak's molecule substitution and will obviously yield inaccurate pressure estimates for natural orthopyroxenes in which some of the Al present is involved in different crystal chemical substitutions.

Paper (34) has demonstrated that in orthopyroxenes from the higher temperature deformed garnet lherzolite xenoliths within the Thaba Putsoa and Mothae kimberlites of northern Lesotho there is a strong positive composition correlation between the cation contents of (Na-Cr) and Al. This indicates that in these particular orthopyroxenes a significant number of Al cations are involved in jadeite molecule substitution. Hence for the orthopyroxenes in these particular xenoliths the assumption that $X^{Ml}_{Al(Ts)} = Al^{Total}/2$ is clearly invalid - such values being too large and thus in turn generating calculated pressure estimates which are too low.

It was thus shown in paper (34) that the pressure-temperature estimates for these higher temperature xenoliths determined by the combinations of barometric and thermometric methods favoured by Finnerty and Boyd (1984 and

1987) are invalid. Consequently the apparent thermal perturbation (inflection) of the upper temperature part of their deduced upper mantle palaeogeotherm, over which they and other research workers have set considerable store and based dynamic mantle models, is considered to be totally spurious.

On the assumption that the orthopyroxenes in garnet lherzolite xenoliths are genuinely stoichiometric, an alternative calculation procedure for assessment of $X^{Ml}_{Al(Ts)}$ is to calculate $Al^{[IV]}$ as $2.000-Si^{4+}$ and hence $Al^{[VI]}$ as $Al^{Total} - Al^{[IV]}$. If some of the $Al^{[VI]}$ in orthopyroxenes is demonstrably present as jadeite molecule substitution then $X^{Ml}_{Al(Ts)}$ is best taken to be equivalent to $Al^{[IV]}$. However, this calculation procedure does not allow for the possibility of additional substitution as represented by $NaTiAlSiO_6$, $M^{2+}TiAl_2O_6$, $M^{2+}CrAlSiO_6$ and $M^{2+}Fe^{3+}AlSiO_6$ molecules. This fact, together with the extreme sensitivity of the calculated $Al^{[IV]}$ value to any errors in the analytical determination of Si, effectively means that $X^{Ml}_{Al(Ts)}$ in natural orthopyroxenes cannot be reliably determined in this manner.

Nickel and Green (1985) proposed that for chemically complex natural orthopyroxenes:

$$X^{Ml}_{Al(Ts)} = [Al^{Total} - Cr - 2Ti + Na]/2$$

The rationale behind this formulation is that it corrects for the amount of Al involved in $M^{2+}CrAlSiO_6$ and $M^{2+}TiAl_2O_6$ substitutions, after first taking into account $NaCrSi_2O_6$ substitution. Allowing for the possible presence of Fe^{3+} in the form of $NaFe^{3+}Si_2O_6$ or $M^{2+}Fe^{3+}AlSiO_6$ substitutions in natural orthopyroxenes this formulation can be expanded to:

$$X^{Ml}_{Al(Ts)} = [Al^{Total} - Cr - Fe^{3+} - 2Ti + Na]/2$$

However, as pointed out in papers (23) and (24) this formulation breaks down for the higher temperature-pressure orthopyroxenes in Thaba Putsoa and Mothae garnet lherzolite xenoliths, as significant jadeite substitution is present in these orthopyroxenes - resulting in their overall chemical composition being such that $Na > Cr + Fe^{3+} + Ti$. Detailed consideration of the crystal chemistry of these Na enriched orthopyroxenes has now led to the conclusion that in these cases $X^{Ml}_{Al(Ts)}$ should instead be calculated as $[Al^{Total} - Na + Cr + Fe^{3+}]/2$.

The result of employment of these recommended procedures for the calculation of the critical $X^{Ml}_{Al(Ts)}$ composition parameter in orthopyroxenes is the generation of pressure-temperature estimates for the garnet lherzolite xenolith suites in these northern Lesotho kimberlites which define pressure-temperature arrays, as shown in paper (34), which lack any significant thermal perturbation. Indeed, the gradient of the deduced upper mantle palaeogeotherm has been shown to decrease rather than increase at the deeper mantle levels, compatible with a conductive heat flux in the lithosphere (the source of the lower temperature coarse grained xenoliths) passing down into a thermally convecting asthenosphere (the source of the higher temperature deformed xenoliths).

Additional important points to emerge in paper (34) from these refined thermometer and barometer applications to the garnet lherzolite xenolith suites in the kimberlites of northern Lesotho included evidence indicative of significant regional variations both in the thickness of the lithosphere and in the mantle heat flux.

In summary, the outlined analytical data and interpretations on the high pressure assemblages in xenolith samples (as contained in the nineteen submitted published papers in this research area) are considered to amount to a significant contribution to knowledge of the chemistry, mineralogical make-up,

petrological evolution and pressure-temperature distribution within the lower crust and uppermost mantle beneath relatively stable continental cratonic areas. It has been shown that assignment of particular xenolith types in kimberlites to particular depths of origin on the basis of calculated equilibration pressure-temperature estimates enables construction of a detailed petrological stratigraphy for both the lower continental crust and the underlying mantle down to depths of about 200 kilometres.

C. General papers or papers on high pressure metamorphic rocks from other geological settings

Included in this section are the research results contained in the published papers which do not fit readily into either of the two previous sections. Nevertheless, the emphasis in these papers was again on the mineral chemistry, equilibration conditions and geotectonic significance of high grade (granulite or eclogite facies) metamorphic rocks.

The work on charnockites from Sri Lanka described in paper (35) arose from the supervision of a British Council supported M.Sc. research student from that country. The petrogenesis of these rocks was interpreted from major and trace element analyses of some fourteen samples, and wet chemical analyses of mineral separates were used as the basis for calculation of equilibration pressure-temperature estimates for the various mineral assemblages.

Studies of the petrography, whole rock and mineral chemistry, equilibration conditions, geochronology and interpretation of the occurrences of high pressure rocks in the Moldanubian Zone of the Bohemian Massif in Lower Austria are being actively persued at present. Paper (36) constitutes an initial interpretative assessment of certain Lower Austrian samples, based largely on analytical data obtained previously by my Austrian collaborator in this research work. Important evidence is provided of high initial temperatures

both in tectonically intercalated, mantle derived, peridotite bodies and in enclosing quartzo-feldspathic granulites of mostly calc-alkaline magmatic origin. These high temperatures and the observed lithological associations are considered to be indicative of evolution in a high heat flux, extensional, geotectonic environment, prior to the major compressional Hercynian plate collision responsible for the stabilisation of the high pressure (eclogite or high pressure granulite facies) assemblages in these lithologies.

Paper (37) comprises a substantial review of the occurrence of medium-temperature, eclogite facies assemblages in the Norwegian Caledonides, Western Alps and Central European Hercynides. The formation and exhumation of these high pressure assemblages were interpreted with reference to a generalised tectono-thermal model involving transient A-type subduction of continental crust in continental plate collision zones. This paper also emphasised how mineralogical features, such as chemical zoning in garnets and the occurrence of armoured mineral inclusions in garnets, may be used to deduce the tectonic location of different crustal segments in an evolving compressional thrust-nappe stack and the contrasting pressure-temperature-time paths which rocks may be expected to have followed depending upon their location prior to the major plate collision.

The survival and ultimate surface exposure of high pressure assemblages necessitates that the uplift rate following maximum tectonic thickening of the continental crust is high relative to the rate of relaxation of the perturbation of the normal temperature-depth profile. Simple isostatic rebound with associated surface erosion was considered to be too slow to permit preservation of high pressure assemblages. Instead a dynamic uplift model involving further tectonic under-thrusting during continued crustal shortening is considered necessary. This paper thus emphasises that exposures of eclogite facies

assemblages in metamorphic terranes are important to the recognition of palaeo-plate suture zones and provide important constraints on evolutionary tectonic and thermal models for plate collision zones.

Paper (37) also proposed a revised three fold, temperature based, subdivision for eclogites which correlates with eclogite formation in what are considered to be three fundamentally different geological environments. The appropriate equilibration temperature estimates for these three groups of eclogites are readily obtained from experimentally based calibrations of the Fe^{2+}-Mg^{2+} exchange reactions between coexisting garnets and clinopyroxenes. The temperatures indicated (< 550°C) for the stability of low temperature eclogites are in line with the likely maximum stability conditions for natural glaucophane in the widely associated blueschists developed in B type (Benioff) subduction zones. The 900°C temperature boundary indicated between the medium and high temperature eclogites is less well constrained but in the majority of cases discriminates between the medium temperature eclogites stabilised in tectonically thickened continental crust in A-type (Amferer) subduction zones and the high temperature eclogites stabilised under ambient conditions in the upper mantle.

Correspondence and comparison of this new classification scheme with previously proposed schemes are shown on the accompanying Table. This new classification scheme for eclogites is considered to be more satisfactory than the currently widely adopted subdivision scheme of Coleman et al. (1965) into Groups A,B and C - based on observed differences in the compositions of the constituent garnets and clinopyroxenes. This previous scheme can be shown to break down in some instances because of the influence of variable rock compositions. In particular the most pyropic garnets and least jadeitic clinopyroxenes are encountered in magnesian eclogite facies meta-peridotites regard-

TABLE 1.1: ECLOGITE CLASSIFICATION SCHEMES

Reference	Eskola (1921)	Coleman et al. (1965)	Smulikowski (1960, 1964, 1968)	Proposed Scheme	
Subdivision Criteria	Geological Occurrences	Largely Mineral Compositions	Geological Settings and Rock and Mineral Compositions	Equilibration Temperature	Likely Origin
Subdivision schemes and inter-correlation	TYPE 1 Xenoliths in kimberlites etc.	GROUP A Garnet › 55 mol. % pyrope	GROUP I (G) Griquaites and garnet websterites associated with peridotites	High T.	Upper Mantle
				900°C - - - - - - - - - - - - - - - - -	
	TYPE 2 Layers and lenses in alpine-type peridotite bodies	Least jadeitic clinopyroxene		Medium T.	Tectonically thickened continental crust
	TYPE 3 Lenses in migmatitic gneiss complexes	GROUP B Garnet 30-55 mol. % pyrope	GROUP III (C) Common eclogites		
				550°C - - - - - - - - - - - - - - - - -	
	TYPE 4 Blocks in blueschist facies terrains	GROUP C Garnet ‹ 30 mol. % pyrope Most jadeitic clinopyroxene	GROUP II (O) Ophiolitic eclogites	Low T.	Subducted oceanic crust and arc-trench sediments

less of whether they occur as xenoliths in kimberlites with mantle derived Group A eclogites or within alpine-type peridotite bodies associated with Group B eclogites in exposed high grade gneiss terranes.

The stability conditions for low, medium and high temperature eclogites are illustrated on the following pressure-temperature petrogenetic grid diagram. It should be noted that this diagram is complicated by the fact that it includes, and attempts to marry, experimentally determined reaction equilibria relevant to eclogite stability for both 'wet' and 'dry' rock systems. The boundary between the eclogite facies and the adjacent amphibole bearing facies (blueschist and amphibolite) should strictly be viewed as a surface in P_{load}-P_{H_2O} - T space. Hence in the presented P_{load} - T section two extreme projected positions - curves (c) and (d) - are indicated for the low pressure boundary of the eclogite facies under conditions ($T < 1000^{o}C$) where amphiboles are potentially stable. Boundary (c) corresponds to the location for water saturated rock systems with $P_{fluid} = P_{H_2O} = P_{load}$, whilst the alternative boundary (d) is for essentially 'dry' rock systems with $P_{H_2O} << P_{load}$. It is clear that under the latter conditions eclogite stability can be expected at substantially and increasingly lower P_{load} conditions at progressively lower temperatures than indicated by boundary (c). Above about $1000^{o}C$ the boundary between the eclogite and granulite facies is fairly well constrained by experimental data on plagioclase elimination in quartz tholeiite (A and B) compositions (Green and Ringwood 1967) and on the stability of garnet lherzolite relative to spinel lherzolite in natural magnesian peridotite (O'Hara et al. 1971). However, the extrapolations of these reaction curves to lower temperatures are less certain. Boundary (d) is considered to be the most realistic indication of the minimum pressures required for stability of

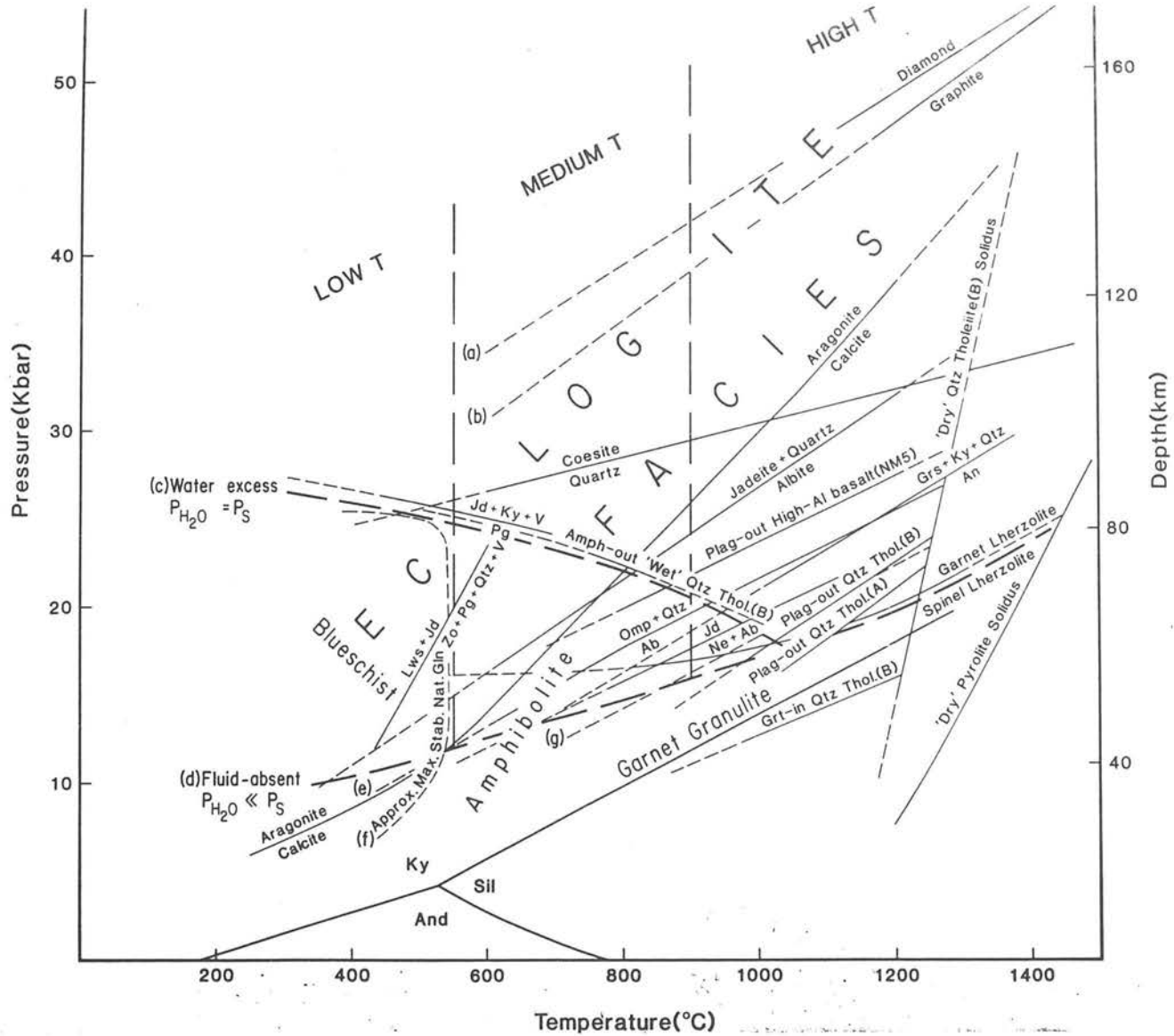
HIGH T
MEDIUM T
LOW T
ECLOGITE FACIES
Diamond
Graphite
(a)
(b)
Aragonite
Calcite
Coesite
Quartz
Jadeite + Quartz
Albite
'Dry' Qtz Tholeiite(B) Solidus
(c)Water excess
$P_{H_2O} = P_S$
Jd + Ky + V
Pg
Amph-out 'Wet' Qtz Thol.(B)
Plag-out High-Al basalt(NM5)
Grs + Ky + Qtz
An
Lws + Jd
Zo + Pg + Qtz + V
Omp + Qtz
Ab
Jd
Ne + Ab
Plag-out Qtz Thol.(B)
Plag-out Qtz Thol.(A)
Garnet Lherzolite
Spinel Lherzolite
Blueschist
Amphibolite
Garnet Granulite
Grt-in Qtz Thol.(B)
'Dry' Pyrolite Solidus
(d)Fluid-absent
$P_{H_2O} \ll P_S$
(e)
(f)Approx.Max.Stab.Nat.Gln
(g)
Aragonite
Calcite
Ky
Sil
And
Pressure(Kbar)
Depth(km)
Temperature(°C)
50
40
30
20
10
160
120
80
40
200
400
600
800
1000
1200
1400

diagnostic eclogite facies assemblages in essentially 'dry', fluid-absent, rock systems. Even if eclogite is in theory thermodynamically stable at somewhat lower pressures in cool 'dry' basaltic rocks, kinetic factors are considered likely to prohibit formation under such conditions.

5. COPIES OF SUBMITTED PUBLICATIONS

A. Papers concerned with high pressure metamorphic rocks from the Basal-Gneiss Complex of Western Norway

Contr. Mineral. and Petrol. 19, 97—124 (1968)

Picritic Magma — Residual Dunite Relationships in Garnet Peridotite at Kalskaret near Tafjord, South Norway

D. A. Carswell*
Grant Institute of Geology, University of Edinburgh, Scotland

Received May 13, 1968

Abstract. Field and textural relationships have indicated the tectonic emplacement of the Norwegian garnet peridotites as relatively cold intrusions into their present environment. Mineralogical data demonstrate considerable heterogeneity. Olivines and orthopyroxenes in garnet rich peridotites are significantly more ferriferous than those in garnet free peridotites. Mineralogical features indicate that the mineral assemblages have been equilibrated at subsolidus temperatures. However, the hypothesis that these garnet peridotites have resulted from the eclogite facies metamorphism in deep levels of the crust of other peridotite mineral facies assemblages is considered and rejected.

Statistical analysis of the bulk rock composition data has substantiated the existence of a very strong linear composition trend, two end members being sufficient to account for almost the whole range of composition variation.

The hypothesis favoured is that these peridotites have been involved in partial melting processes in the upper mantle. The Kalskaret garnet peridotite occurrence is considered to represent a case where the 'picritic' partial melt fraction has not been completely liberated but has remained trapped and mixed with the 'dunitic' residual fraction.

I. Introduction

A. Regional Setting

The village of Tafjord lies at the easternmost extremity of Storfjord, the largest fjord in the Sunnmore district of Norway. Ålesund, the major port for this district, is situated on the coast, just to the north of the mouth of Storfjord, about 150 miles north of Bergen.

The Sunnmore district as a whole is part of the basal gneiss region of southern Norway (Holtedahl, 1944). This gneiss complex was considered by early field workers to be Pre-Cambrian but is now generally recognized as being Caledonian in age (Holtedahl, 1960; Newmann, 1960; Strand, 1961; MacDougall and Green, 1964). Hernes (1957) considered this region as marking a prominent culmination in the Norwegian Caledonide basement, which is consistent with the opinion of Muret (1960) that the rocks of this region represent the structurally lowest levels of the Caledonian orogeny now exposed.

Within the layered gneisses of this district there are numerous occurrences of peridotite in a broad zone from Almklovdalen (62° N. 5°30′ E.) near Åheim on the coast south of Ålesund, north-eastwards to Tafjord (62°13′ N. 7°26′ E.). Eclogites and anorthosites commonly occur in close association with the peridotites throughout this region.

The principal occurrences of peridotite in this district have been indicated by Gjelsvik and Gleditsh (Gjelsvik, 1951), but documented occurrences of garnetiferous peridotite are at present restricted to the Tafjord and Almklovdalen areas (Eskola, 1921).

* Present address: Dept. of Geology, University of Sheffield, England.

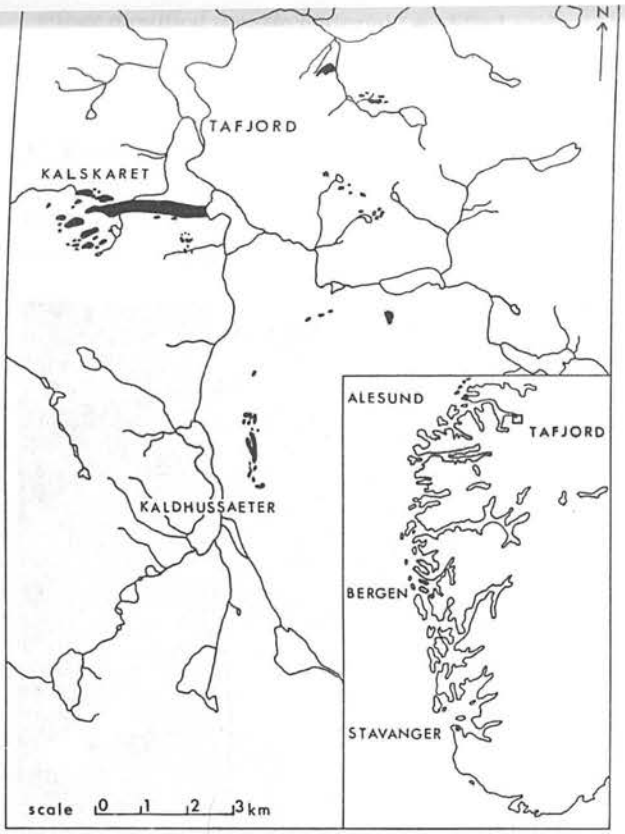

Fig. 1. Map showing the main peridotite outcrops in the Tafjord district. Inset map shows the location of the Tafjord district with respect to the south-western seaboard of Norway

B. Outline of the Problem under Investigation

The mineral assemblage of the garnet peridotites (olivine + garnet + clinopyroxene + orthopyroxene) is distinctive of the eclogite mineral facies, the join olivine-garnet in magnesian compositions being confined to this mineral facies (Eskola, 1920; O'Hara, 1960).

The following four different origins might explain any random body of garnet peridotite exposed at the earth's surface;

(1) Crystallization *in situ* to an eclogite facies assemblage.

(2) Crystallization *in situ* of another mineral facies but subsequently metamorphosed to an eclogite facies assemblage.

(3) Crystallization at depth within the crust or mantle to another mineral facies, then subsequently both metamorphosed to an eclogite facies assemblage and tectonically emplaced into its present position.

(4) Crystallization at depth within the crust or mantle to an eclogite facies assemblage, with subsequent tectonic emplacement into its present position.

This paper considers, in the light of the recent experimental work, whether any of these four hypotheses of origin is most appropriate for the garnet peridotite occurrence at Kalskaret near Tafjord.

C. Previous Work

Early field workers (Reusch, 1877; Brogger, 1880; Vogt, 1883) concluded from the generally conformable contacts and lack of evidence of contact metamorphism that the peridotites were contemporaneous and of the same origin as the gneiss, whatever that origin might have been.

Eskola (1921) recognised the exotic nature of the peridotites and considered that the peridotites, eclogites and anorthosites of this province were all igneous in origin, having been derived through the differentiation of a single magma which also produced the enclosing gneisses.

Lappin (1962, 1966), O'Hara and Mercy (1963) and Bryhni (1966) have all subsequently concluded that the peridotites have been tectonically emplaced at their present level in the gneiss complex, a conclusion substantiated by the author's own field observations (Carswell, 1966).

O'Hara and Mercy (1963) contrasted the eclogite mineral facies of the garnet peridotite assemblages with the almandine-amphibolite facies of the enclosing regional gneisses, indicating that the peridotites are in disequilibrium with their present environment. O'Hara (1963d) considered that these garnet peridotites are themselves equilibrium assemblages, relatively low temperatures of equilibration (about 600° C) being suggested by O'Hara and Mercy (1963).

In comparison with garnet peridotite nodules from kimberlite pipes, O'Hara and Mercy (1963) stressed that the Norwegian garnet peridotites were unlikely to

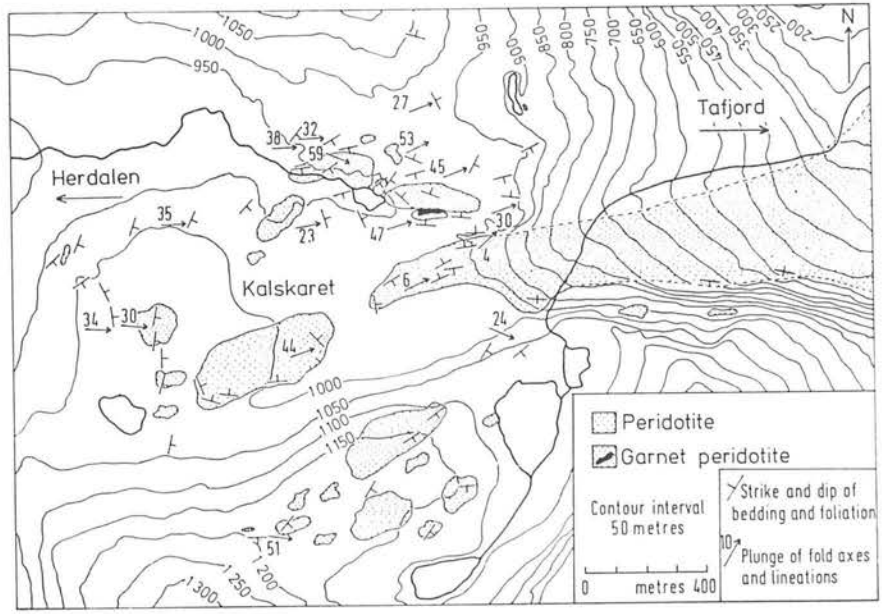

Fig. 2. Map of peridotite outcrops in the Kalskaret area near Tafjord

modified mantle material (modified perhaps by the subtraction of a basaltic fraction) or completely recrystallized peridotites formed by igneous processes near the top of the mantle.

II. Field Relationships of the Kalskaret Garnet Peridotites

The principal peridotite outcrops in the Tafjord district are shown on Fig. 1. Within this district fresh garnetiferous peridotites occur only in the Kalskaret area, the col at about 3,000 feet above sea level, between Tafjord and Herdalen.

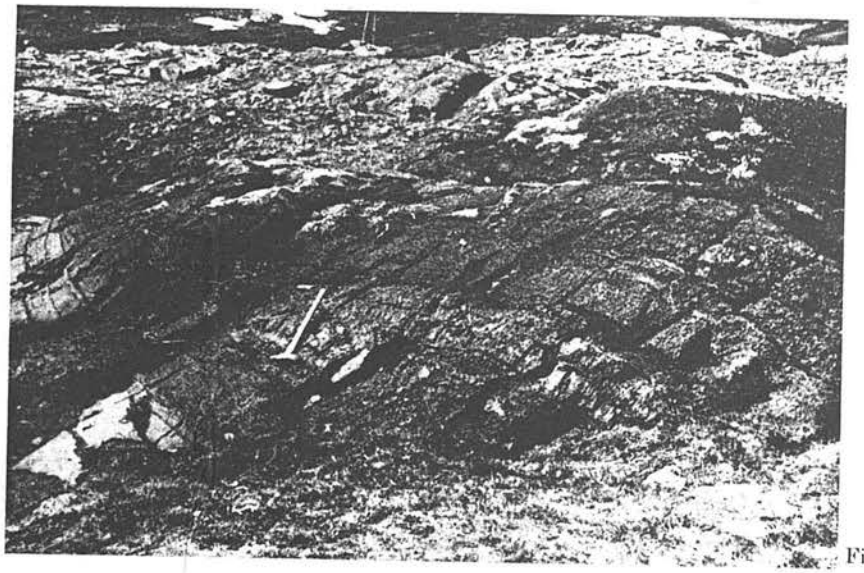

Fig. 3a

Fig. 3b

Garnet peridotite may be seen to occupy only a very small area almost on the eastern lip of the col overlooking Tafjord. These figures are based on more detailed mapping than the preliminary Figs. 3 and 5 of O'Hara and Mercy (1963).

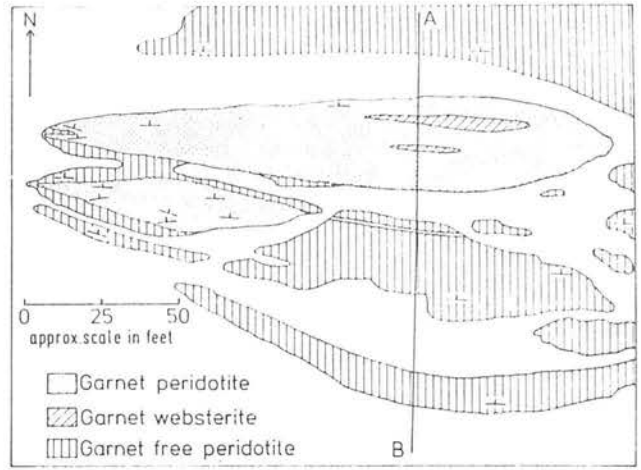

Fig. 4. Map of the rock type relationships at the Kalskaret garnet peridotite locality

Tectonic emplacement of these peridotite masses (cf. O'Hara and Mercy, 1963: Lappin, 1966) is indicated by the sheared nature of their contacts, the lack of any recognisable high temperature thermal aureoles, and the remarkable cataclastic textures often developed, especially in the pyroxene-rich garnet peridotites as at Kalskaret (see Fig. 3b). In other zones, where late stage brittle fracturing has been restricted, there is often a striking dimensional and lattice preferred orientation of the olivine fabric which seems best interpreted as the result of laminar flow through internal recrystallization during movement of these rock masses through the gneisses in an essentially crystalline state.

For the most part the peridotites of the Kalskaret area are exceedingly fresh dunites with only minor amounts of enstatite and chromite as accessories. Tremolitic amphibole and chlorite occur as generally sparse secondary minerals in these peridotites. Neither garnet nor clinopyroxene occurs in the prevalent peridotitse of this area, or for that matter of the Tafjord district as a whole.

The garnet peridotite at Kalskaret occurs predominantly as two lensoid horizons conformable within the prevalent enstatite poor dunite (Fig. 3a and Fig. 4). Taken together these garnetiferous horizons extend for only about 160 feet along the strike and 40 feet at a maximum across the strike. However, a few thin horizons of peridotite with amphibole pseudomorphs after garnet do, in fact, occur in the peridotite immediately below the main garnetiferous layers indicated on Fig. 4.

Fig. 3. a The western extremity of the garnet peridotite lens (the darker rock with the pitted surface) within dunite at Kalskaret near Tafjord. b Photomicrograph of strained and fractured orthopyroxene porphyroclast in Kalskaret garnet peridotite. Cross-polarised light. Magnification $\times 25$

throughout all the garnetiferous materials suggests that the garnet and clinopyroxene bearing rock types are in fact indigenous to the peridotites despite their restricted occurrence.

The margins show some amphibolization, but generally the garnet peridotites are remarkably fresh.

Thirteen rock samples were collected across the garnet peridotite layers along section A—B Fig. 4 and analysed to show the extent of the chemical variation which has resulted in the development of these garnetiferous rock types. The details of the exact horizon of collection, the mineral assemblage and the mode of each specimen are given in Table 2 and Appendix B.

III. The Mineralogy of the Peridotites

A. General

Mineralogical data for the Kalskaret garnet peridotites (O'HARA and MERCY, 1963; MERCY and O'HARA, 1965b) have been supplemented by further data on two other mineral assemblages (T153 and T96). These data, together with the calculated structural formulae, are tabulated in Table 1. The details of location of the analysed mineral assemblages are given in Appendix B; the modes of the assemblages in Table 2. The modal proportions are estimated to be accurate in most cases only to within ±10—15% of the value given, particularly in the case of the garnet lherzolites which have pronounced cataclastic textures, highly variable grain size distribution and a generally inhomogenous distribution of the minerals.

Chemical and X-ray determinations (O'HARA and MERCY, 1963; MERCY and O'HARA, 1965b) of minerals from the Tafjord garnet free peridotites (olivines

Table 1a. *Mineral composition data*

Mineral:	Olivine	Orthopyroxene	Clinopyroxenes		Garnets	
Sample No.:	T96	T96	T96	T153	T96	T153
SiO_2	39.18	55.91[a]	53.75[a]	54.26	41.30	40.61
TiO_2	0.06	0.08	0.15	0.13	0.10	0.11
Al_2O_3	0.44	0.90	3.08	2.94	21.67	21.84
Cr_2O_3	0.01	0.08	0.47	0.16	0.84	0.25
Fe_2O_3	—	—	1.39	2.22	3.26	3.99
FeO	17.12[b]	10.60[b]	2.46	2.58	11.84	13.83
MnO	0.17	0.16	0.06	0.06	0.43	0.42
NiO	0.36	0.08	0.05	0.05	<0.01	<0.01
MgO	42.52	31.74	15.91	15.23	15.58	14.11
CaO	0.16	0.45	20.82	20.40	4.79	4.49
Na_2O	n.d.	n.d.	1.84	2.15	n.d.	n.d.
K_2O	n.d.	n.d.	0.02	<0.01	n.d.	n.d.
total	100.02	100.00	100.00	100.18	99.81	99.65

[a] SiO_2 by difference from 100.00%;
[b] FeO total iron as FeO

Mineral:	Olivine	Orthopyroxene	Clinopyroxenes		Garnets	
Sample No.:	T96	T96	T96	T153	T96	T153
Si^{4+}	0.995	1.968	1.951	1.967	3.015	2.998
Ti^{4+}	0.001	0.002	0.004	0.003	0.006	0.006
Al^{3+}	0.013	0.037	0.132	0.126	1.865	1.900
Cr^{3+}	—	0.002	0.014	0.005	0.049	0.014
Fe^{3+}	—	—	0.038	0.061	0.179	0.222
Fe^{2+}	0.364	0.312	0.075	0.078	0.723	0.854
Mn^{2+}	0.004	0.005	0.002	0.002	0.027	0.026
Ni^{2+}	0.007	0.002	0.002	0.002	—	—
Mg^{2+}	1.609	1.665	0.861	0.823	1.695	1.552
Ca^{2+}	0.004	0.017	0.810	0.793	0.375	0.355
Na^{+}	—	—	0.130	0.151	—	—
K^{+}	—	—	0.001	—	—	—
O^{2-}	4	6	6	6	12	12
Fe × 100 / Fe + Mg	18.43	15.78	Ca 46.41 Mg 49.32	46.80 48.59	Ca 13.29 Mg 60.12	12.74 55.69
		Ca 0.85 Mg 83.50 Fe^{2+} 15.65	Fe^{2+} 4.27	4.61	Fe^{2+} 25.64	30.63
			Jadeite % 7.8	8.5	Mn 0.95	0.94

% jadeite in clinopyroxenes calculated after formation of $NaFe^{3+}$ and $NaCr^{3+}$.

Table 2. *Estimated volume proportions of minerals in analysed specimens collected across the Kalskaret garnet peridotite lens*

Sample No.	OL	GNT	CPX	OPX	Amphibole	Chlorite	Opaques
T200	84	—	—	—	5	11	trace
T268	90	—	—	10	trace	trace	trace
T150	56	—	trace	trace	31	9	4
T151	20	24	41	5	10	—	trace
T152	40	19	26	trace	13	—	2
T153	trace	30	53	5	10	—	2
T154	32	15	45	trace	8	—	trace
T97	17	32	40	—	9	—	2
T96	15	22	27	12	24	—	trace
T155	8	—	trace	4	54	30	4
T156	90	—	—	—	trace	7	3
T162	70	—	—	—	28	—	2
T100	40	—	—	—	40	18	2

OL = olivine, GNT = garnet, CPX = clinopyroxene, OPX = orthopyroxene.

6.6—8.1% Fa, orthopyroxenes 6.6—7.8% Fs) and from the Almklovdalen garnet free peridotites (olivines 7—8.1% Fa, orthopyroxene 7.5% Fs) show the restricted range in composition of these minerals, a feature substantiated in this study by optical 2V determinations on these minerals from garnet free peridotites throughout the Tafjord district.

In the presence of garnet, however, the olivines and orthopyroxenes are significantly more ferriferous in composition and increasingly so with the increasing garnet and clinopyroxene content of the rock type (see Table 3).

mineralogical heterogeneity, the rock types showing considerable variations in the modal contents and composition of olivine, garnet, clinopyroxene and orthopyroxene over very small thicknesses (see Table 2; also Mercy and O'Hara, 1965a, Table 1A).

In Table 3 data demonstrating the extent of the mineral composition variations within the principal solid solution series and in Cr_2O_3 and TiO_2 content for certain Kalskaret and Almklovdalen mineral assemblages are tabulated. Specimens N69, N70 and N71 from Lien, Almklovdalen were collected within a few feet of each other in the field (data from O'Hara and Mercy, 1963). Similarly N21, N23, N26, T96 and T153 are closely associated assemblages from the Kalskaret garnet peridotite lens (data for N21, N23 and N26 from O'Hara and Mercy, 1963).

When contrasted with the limited extent of the mineral composition variations observed as cryptic layering over such small thicknesses in the ultrabasic cumulates of large layered complexes, it appears that the large variations observed in these garnet peridotites cannot be attributed to such layering effects. Hence the hypothesis that the Kalskaret and Almklovdalen garnet peridotites simply represent local segregations of garnet and pyroxenes within unrecrystallized peridotites precipitated by normal igneous crystallization processes, whether *in situ* or at depth, seems untenable.

B. Equilibration of the Assemblages

In all the analysed Norwegian garnet peridotite assemblages the order of decreasing Fe/Fe+Mg ratio is garnet > olivine > orthopyroxene > clinopyroxene. In the light of investigations into the partition of Fe and Mg amongst coexisting olivines and pyroxenes (see in particular Bowen and Schairer, 1935; Hess, 1941; Ramberg and de Vore, 1951) the above order represents the expected equilibrium distribution (cf. O'Hara, 1963d).

C. Physical Conditions of Formation of the Garnet Peridotite Assemblages

Davis and Boyd (1966) have shown that below 1400° C the solubility of enstatite in diopside in the synthetic system is essentially the same at 30 kilobars pressure as at atmospheric pressure (Boyd and Schairer, 1964). Therefore in principal it should be possible to use this solvus curve as a geothermometer that is vitually independent of pressure.

However, to relate this curve to natural coexisting pyroxene pairs the effects of other components, in particular FeO, Fe_2O_3, Cr_2O_3 and Al_2O_3, must be considered. Fortunately contents of these other components in the pyroxenes under consideration are comparatively low, hence the extrapolations involved for comparison with the synthetic system are quite small.

Melting experiments at 30 kilobars pressure (O'Hara, 1963a) on a coexisting pair from a garnet lherzolite nodule in kimberlite (the pyroxenes of which are for the present purposes essentially analogous in composition with the Norwegian pyroxenes under consideration) has indicated considerable mutual solubility between the pyroxenes at high temperatures near the beginning of melting of such garnet peridotite assemblages.

Table 3. *Mineral composition variations*

		Lien, Almklovdalen specimens			Kalskaret, Tafjord specimens				
		N69	N70	N71	N23	N26	T96	T153	N21
	OL	$Fa_{11.2}$	$Fa_{10.2}$	—	—	$Fa_{15.4}$	$Fa_{18.4}$	—	Fa_{12} (X-ray (det.)
	OPX	$Fs_{10.8}$	$Fs_{9.7}$	$Fs_{11.5}$	$Fs_{16.6}$	—	$Fs_{15.8}$	—	
	GNT	$Ca_{30}Mg_{47.7}$	$Ca_{46}Mg_{51.3}$	$Ca_{49}Mg_{48.5}$	$Ca_{17.4}Mg_{48.0}$	$Ca_{45.7}Mg_{49.2}$	$Ca_{46.4}Mg_{49.3}$	$Ca_{46.8}Mg_{45.6}$	
Cr_2O_3 (wt.-%)	Rock	0.43	0.49	0.32	0.21	0.34	0.29	0.12	0.40
	GNT	$Ca_{12}Mg_{66}$	$Ca_{12}Mg_{65}$	$Ca_{12}Mg_{61}$	$Ca_{12}Mg_{60}$	$Ca_{11}Mg_{61}$	$Ca_{12}Mg_{60}$	$Ca_{12}Mg_{56}$	
	CPX	0.80	0.95	0.32	0.39	0.91	0.84	0.25	
	OPX	0.69	0.47	0.20	0.20	0.63	0.47	0.16	
TiO_2 (wt.-%)	Rock	0.08	0.06	0.04	0.03	—	0.08	—	
	GNT	0.19	0.11	0.17	0.45	0.34	0.22	0.64	0.04
	CPX	0.19	0.19	0.15	0.17	0.19	0.10	0.11	
	OPX	0.18	0.16	0.11	0.16	0.22	0.15	0.13	
	OL	0.09	0.07	0.08	0.11	—	0.08	—	
		0.08	0.06	—	—	0.14	0.06	—	

OL = olivine, GNT = garnet, OPX = orthopyroxene, CPX = clinopyroxene.

from the Norwegian garnet peridotites, therefore, suggests equilibration certainly at sub-solidus temperatures, perhaps at temperatures as low as 600—700° C.

Experimental studies (Boyd and England, 1963, 1964; O'Hara, 1963a, b and c; MacGregor and Ringwood, 1964) have demonstrated both for synthetic and natural systems that the Al_2O_3 content of both clinopyroxene and orthopyroxene in equilibrium with pyrope decreases with increasing pressure with constant temperature, and with decreasing temperature at constant pressure.

Attempts have been made to subdivide the garnet peridotite stability field by isopleths giving the expected solubility of Al_2O_3 in orthopyroxene in equilibrium with pyrope under differing temperature and pressure conditions (cf. Boyd and MacGregor, 1964, Fig. 51; Green and Ringwood, 1967a, Fig. 2). The application of such data to the low temperature part of the garnet peridotite stability field, which we appear to be concerned with in the case of these Norwegian assemblages, is complicated by several factors.

1. Early estimates were based primarily on relationships in the synthetic Enstatite-Pyrope system (Boyd and England, 1964). It is now clear that in natural peridotite assemblages the Al_2O_3 content of the orthopyroxene is substantially reduced due to the effects of additional components such as FeO, Fe_2O_3, Cr_2O_3 and CaO, and by the presence of a clinopyroxene phase.

2. The estimates based on the more chemically complex pyrolite composition (Green and Ringwood, 1967a) are not entirely applicable because of compositional differences between the pyrolite model and these Norwegian garnet peridotites. Furthermore, the small amount of data available is restricted to the high temperature range (1300—1500° C).

3. There are doubts about the corrections necessary and hence the accuracy of the pressure measurements in experiments done using apparatus of the solid media type.

Taking these factors into consideration, it does seem likely, however, that the low Al_2O_3 contents (0.90—1.60 wt-%) of the orthopyroxenes from these Norwegian garnet peridotites also reflect equilibration at temperatures well below the temperatures of beginning of melting of such assemblages (about 1425—1450° C at 30 kilobars: O'Hara, 1963a).

The experimental investigations described by Ringwood *et al.* (1964), MacGregor (1965), Green and Ringwood (1967a) and Ito and Kennedy (1967) have thrown some light on but by no means entirely clarified, the stability field of garnet peridotite with respect to the spinel peridotite and aluminous pyroxene peridotite assemblages (cf. Figs. 50, 38, 2 and 3, respectively, in the above papers).

These studies have only in certain cases been extended down to temperatures as low as 1000° C. Hence ideas of the pressure-temperature conditions along the spinel peridotite⇌garnet peridotite reaction boundary at lower temperatures are entirely based on crude linear extrapolations. Furthermore, the transition cannot be expected to be sharp but to extend over a significant pressure interval (cf. Ito and Kennedy, 1967, Fig. 1). However, even at the sub-solidus temperatures envisaged for the formation of these Norwegian garnet peridotite assemblages it seems likely that pressures >10 kilobars are necessary.

within the limitations of the present data it would therefore seem conceivable to interpret these peridotites as either having formed under metamorphic conditions near the base of the crust or alternatively they may represent solid intrusions from the mantle.

Although the solvus limits between coexisting pyroxene pairs and the alumina contents of these pyroxenes suggest low temperatures of equilibration of the present primary mineral assemblages of these garnet peridotites, there is some textural evidence of an original higher temperature history of these rocks.

The principal evidence is the occurrence of rare orientated lamellae of garnet in clinopyroxene similar to textures described in certain eclogite nodules from kimberlite (Williams, 1932, Plates 82 and 83). The best example of this feature occurs in a rather amphibolized but only mildly cataclased garnet lherzolite from the Grubse peridotite mass at Almklovdalen, which contains large clinopyroxene grains with in certain cases regular garnet lamellae (010). Elsewhere, however, more irregular blebs of garnet have been occasionally noted in clinopyroxenes of garnet peridotites from Almklovdalen and also from Kalskaret.

Such exsolution textures suggest that the previous clinopyroxenes had higher R_2O_3 contents than the analysed samples. These rocks may, therefore, have originally crystallized at temperatures above those of the present mineral equilibration, the clinopyroxenes with such exsolution textures being relics which have escaped the subsequent recrystallization.

Abundant textural evidence of recrystallization of the eclogite mineral facies assemblages of these garnet peridotites is apparent, probably being consequent upon the deformation of these rocks during tectonic emplacement. However, as the percentage of unrecrystallized strained porphyroclasts is commonly quite high it seems unlikely that this recrystallization in evidence was the one responsible for the generally complete equilibration of the eclogite mineral facies assemblages at comparatively low temperatures.

This equilibration may well have occurred at regionally attained temperatures near the top of the mantle, or perhaps reflects recrystallization at an early stage during the tectonic emplacement of these rock masses.

IV. The Bulk Rock Chemistry of the Peridotites

A. General

The chemical compositions of the 13 rock samples collected across the Kalskaret garnet peridotite lens are given in Table 4, and the C.I.P.W. norms of these samples in Table 5. As a few of the samples show a moderate degree of serpentinization or amphibolization and hence have significant H_2O^+ contents, the norms of these particular samples have been based on recalculated water free analyses. Recalculation of the relevant analyses assuming that the serpentinization was a constant composition reaction with addition of water and without leaching of other components yielded quite acceptable original compositions when compared with bulk rock compositions calculated using the modal proportions of the minerals and likely mineral compositions (Carswell, 1966).

Field sample No.	T200	T268	T150	T151	T152	T153	T154	T97	T96	T155	T156	T162	T100
SiO_2	41.56	40.66	42.83	44.93	44.44	46.53	44.26	46.45	45.95	44.99	42.57	42.79	43.26
TiO_2	0.04	0.01	0.46	0.44	0.48	0.64	0.38	0.53	0.22	0.22	0.01	0.04	0.04
Al_2O_3	1.66	0.48	6.88	6.40	6.28	11.58	5.76	7.95	6.44	8.17	0.28	0.70	3.60
Cr_2O_3	0.37	0.28	0.18	0.30	0.24	0.12	0.35	0.18	0.29	0.30	0.36	0.40	0.56
Fe_2O_3	2.28	3.40	3.79	3.10	2.78	3.30	2.52	2.43	2.20	2.62	2.44	2.61	2.48
FeO	5.27	3.00	8.03	10.25	11.22	8.65	10.02	8.66	10.07	5.77	4.44	7.58	4.11
MnO	0.12	0.09	0.19	0.16	0.18	0.22	0.18	0.18	0.18	0.12	0.10	0.16	0.10
NiO	0.34	0.36	0.18	0.19	0.18	0.06	0.21	0.13	0.17	0.14	0.38	0.33	0.30
MgO	44.86	46.48	26.34	25.57	24.86	16.08	27.75	22.89	29.10	23.75	47.85	41.74	37.80
CaO	1.36	0.09	5.96	7.36	7.92	11.00	6.90	9.06	4.48	7.94	0.10	2.04	4.12
Na_2O	0.10	0.04	0.53	0.75	0.82	1.01	0.79	0.88	0.59	0.86	0.03	0.26	0.47
K_2O	0.03	0.03	0.07	0.03	0.02	0.02	0.01	0.02	0.03	0.12	0.01	0.04	0.07
H_2O^+	2.41	5.51	4.30	0.48	0.38	0.36	0.48	0.29	0.52	4.73	1.72	1.23	3.48
Σ	100.40	100.43	99.74	99.96	99.80	99.57	99.61	99.65	100.24	99.73	100.29	99.92	100.39

Fig. 5 is a Ca^{2+}:Mg^{2+}:$Fe^{2+}+Fe^{3+}$ plot of the bulk rock compositions of analysed Kalskaret and Almklovdalen peridotites (Table 4; also LAPPIN, 1962; MERCY and O'HARA, 1965a).

The composition points on this diagram define apparent linear correlations between samples from the different localities, a feature first noted by MERCY and O'HARA (1965a). The linear trends of the compositions from the Lien and

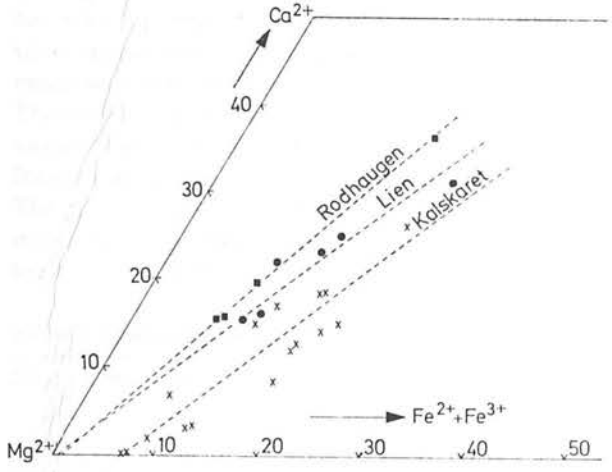

Fig. 5. CMF plot of the bulk rock compositions of analysed Kalskaret and Almklovdalen peridotites. The crosses represent compositions from the Kalskaret locality, solid circles and squares compositions from the Lien and Rodhaugen localities at Almklovdalen, respectively

Rødhaugen localities at Almklovdalen are moderately well defined, that for the Kalskaret locality where appreciably more samples have been analysed less well so. Nevertheless, it is apparent that the samples from Kalskaret have a systematically higher $Fe^{2+}+Fe^{3+}/Mg^{2+}$ ratio for any given Ca^{2+} content than the samples from Lien, and those in turn than the samples from Rodhaugen.

Table 5. *C.I.P.W. norms of analysed Kalskaret peridotites*

	T200 H_2O free	T268 H_2O free	T150 H_2O free	T151	T152	T153	T154	T97	T96	T155 H_2O free	T156 H_2O free	T162	T100 H_2O free
Or	0.18	0.18	0.41	0.18	0.12	0.12	0.06	0.12	0.18	0.71	0.06	0.23	0.41
Ab	0.84	0.34	4.74	6.35	6.94	8.55	6.69	7.45	4.99	7.70	0.25	2.20	4.15
An	4.10	0.45	17.03	14.01	13.39	27.00	12.14	17.68	14.83	19.08	0.50	0.63	7.74
Cor	—	0.25	—	—	—	—	—	—	—	—	0.05	—	—
Di	1.96	—	8.56	14.34	16.04	16.81	14.26	17.56	4.78	14.33	—	6.69	9.38
Hd	0.24	—	2.71	3.58	4.65	5.25	3.32	4.14	1.10	3.58	—	0.79	1.18
En	5.23	9.38	10.79	12.46	7.68	13.91	8.18	13.24	23.08	11.17	11.32	11.95	6.18
Of	0.69	0.95	3.42	3.11	2.23	4.35	1.91	3.12	5.32	2.79	1.21	1.41	0.78
Fo	75.77	79.18	37.91	31.11	32.63	12.68	37.94	24.82	33.02	31.14	76.99	62.27	60.83
Fa	10.36	8.81	13.23	8.57	10.43	4.36	9.74	6.44	8.38	8.58	9.06	8.07	8.40
Mgt				4.49	4.03	4.78	3.65	3.52	3.19			3.78	—
Ilm.	0.07	0.02	0.91	0.84	0.91	1.22	0.72	1.01	0.42	0.44	0.02	0.08	0.08
Cr	0.56	0.44	0.28	0.44	0.35	0.18	0.52	0.26	0.43	0.47	0.54	0.59	0.86
Rest.	—	—	—	0.48	0.38	0.36	0.48	0.29	0.52	—	—	1.23	—
Total	100.00	100.00	99.99	99.96	99.78	99.57	99.61	99.65	100.24	99.99	100.00	99.92	99.99
Fe + Mn + Ni / Fe + Mn + Ni + Mg	0.09	0.07	0.19	0.16	0.18	0.19	0.15	0.15	0.15	0.16	0.08	0.08	0.09
Ab / Ab + An	0.17	0.43	0.22	0.31	0.34	0.24	0.36	0.30	0.25	0.29	0.33	0.78	0.35

Fe + Mn + Ni / Fe + Mn + Ni + Mg — Molecular ratio in normative ferromagnesian silicates.

creased $Fe^{2+} + Fe^{3+}/Mg^{2+}$ ratios with increasing Ca^{2+} contents (ie. increasing modal proportions of garnet and clinopyroxene). This correlates with the fact that in the norms of the Kalskaret and Almklovdalen peridotites (Table 5; also MERCY and O'HARA, 1965a) the Fe + Mn + Ni/Fe + Mn + Ni + Mg ratio in the normative ferromagnesian silicates increases markedly with increasing modal contents of garnet and clinopyroxene in the rock sample.

B. Statistical Analysis of the Composition Variations

The Kalskaret peridotite composition data (the 13 analyses listed in Table 4 together with the compositions of N21, N23 and N26; MERCY and O'HARA, 1965a) have been treated by a totally computerised multivariate statistical technique, namely Q-mode factor analysis as outlined by MASON and IMBRIE (1964). The data were computed by Imbrie and Darland on an IBM computer at Columbia University, New York.

The object of this mathematical treatment was to determine the minimum number of factors required to describe the total composition variations among all the analysed samples, and further to determine the most compositionally extreme end member samples along these factor axes, hence the significant end members in the spectrum of diversity under study. An excellent account of this treatment is given by IMBRIE and VAN ANDEL (1964). Only a brief account of the various computer operations is attempted here.

Firstly theoretical orthogonal vectors were calculated, these representing the principal axes of the multidimensional swarm of composition points. These are the eigenvectors, the corresponding eigenvalues representing the proportions of the total information explained by each vector. Mathematically the problem is to calculate in order the positive eigenvalues of the cos-matrix, hence noting how many axes are required to describe most of the composition variation.

The positive eigenvalues are given in Table 6 and indicate that the first two eigenvalues alone account for 99.8% of the total variation. This points to only two factors being responsible for virtually all the variation.

The positions of the sample vectors in relation to these two factor axes are determined by projecting the vectors on to the axes, the projections being called factor loadings — the size and number indicating the extent to which each factor axis for a specific sample vector is referred to as its communality and reflects the degree of which that sample vector has been explained by the set of factor axes. According to the technique used here a communality of 1.0 indicates a perfect explanation.

As, however, the eigenvectors located by this procedure are rarely in the most meaningful positions and are hence generally difficult to interpret, owing to the fact that the theoretical end-members derived are only sophisticated average samples representing the average orthogonal directions of the composition variations, they have been rotated according to the varimax technique to positions close to the actual extremes of the compositional variation. The theoretical reference vectors in this new orthogonal scheme were selected to fit the data best in a least-squares sense. The resulting rotated factor matrix is given as Table 7. This table gives the communality (the degree of explanation) of all the 16 samples in terms of the two rotated factor axes, together with the factor loadings for each factor axis and the percentage of each factor required to account for each sample.

Table 6. *Positive eigenvalues*

No.	Eigenvalue	% Communality over all 16 factors (Compositions)	Cumulative % Communality over all 16 factors
1	15.446	96.5	96.5
2	0.520	3.2	99.8
3	0.024	0.2	99.9
4	0.006	0.0	100.0
5	0.003	0.0	100.0
6	0.002	0.0	100.0
7	0.000	0.0	100.0

Table 7. *Rotated factor matrix*

Sample No.	Communality 2 factors	Factors		% Factor	
		1	2	1	2
T200	1.000	0.536	0.844	28.7	71.2
T268	0.997	0.494	0.868	24.4	75.3
T150	0.996	0.766	0.640	58.7	41.0
T151	0.999	0.793	0.608	62.9	37.0
T152	0.997	0.801	0.596	64.2	35.5
T153	0.998	0.901	0.432	81.2	18.7
T154	0.998	0.766	0.642	58.7	41.2
T97	0.999	0.831	0.556	69.1	30.9
T96	0.997	0.753	0.656	56.7	43.0
T155	0.992	0.804	0.588	64.6	34.6
T156	0.999	0.506	0.862	25.6	74.3
T162	0.999	0.578	0.815	33.4	66.4
T100	0.997	0.628	0.777	39.4	60.4
N21	0.998	0.588	0.808	34.6	65.3
N23	0.998	0.846	0.532	71.6	28.3
N26	1.000	0.745	0.667	55.5	44.5
Sum squares down columns		8.293	7.673		

It is apparent that with only two factors considered the communalities of all the samples are very high, never less than 0.992 and for only two samples less than 0.997. This indicates that the composition variations involved in this set of data can be almost entirely explained in terms of two factors (end member compositions). From Table 7 it is apparent that the serpentinized dunite T268 and the most eclogitic rock type T153 are compositionally the most extreme of the 16 samples.

rather than the eclogitic compositions. However, the partial secondary amphibolization of a few of the more eclogitic compositions adds a minor complicating factor obscured by the factor analysis treatment. This probably accounts for the two most amphibolized samples T155 and T150 having lowest communalities (Table 7).

To be certain that only two end members are sufficient to account for the composition variations the complete factor analysis treatment was in fact run through assuming that four factors were involved, but the last two proved entirely negligible.

The results of the factor analysis treatment, therefore, indicate that a very strong linear composition trend, which can be interpreted in terms of the mixing of two end members only, exists among the analysed samples from the Kalskaret garnet peridotite locality. The linear composition correlation suggested on the CMF plot (Fig. 5) is therefore substantiated and it is demonstrated that this linear correlation extends to all the components.

Whether or not the most extreme rock samples picked out by the mathematical treatment represent the actual end members of the trend, or whether such end members have more extreme compositions along the trend, is another matter and one which will be further discussed in the next section.

V. The Petrogenesis of the Garnet Peridotites

The development of such a well defined linear composition trend as demonstrated in the Kalskaret garnet peridotites is in general only to be expected with the random mixing of two homogenous end member phases. These phases may have been minerals, rock types or one of either together with a liquid phase. Certainly the repetition of such a linear trend for three independent localities as is suggested on the CMF plot (Fig. 5) would be an exceptional coincidence with the mixing of any more than two phases.

The eclogite facies metamorphism near the base of the crust of a sorted igneous mineral assemblage containing three or more phases therefore appears to be an unsatisfactory mechanism for the production of the present mineral assemblages and bulk rock composition range of these rocks. Even if the metamorphism was not isochemical but involved chemical diffusion processes between rock types of high variance such a linear composition trend would not be expected, as that would imply the unlikely restriction of equality among the diffusion rates of all the components (cf. Clark and Rhines, 1959).

The statistical treatment has shown in the case of the Kalskaret composition trend that the extreme rock types on the trend are essentially dunites (T268 and T156) at one end and the nearest approach to a bimineralic eclogite (T153) at the other. The question then arises as to whether or not these rock types represent the real end member phases of the trend, or whether it is the result of the mixing of compositionally more extreme phases.

Fig. 6 illustrates graphically the linear variation trends amongst the Kalskaret garnet peridotites of the other oxide contents plotted against MgO content.

Clearly one end member is either a rock extremely rich in forsteritic olivine or

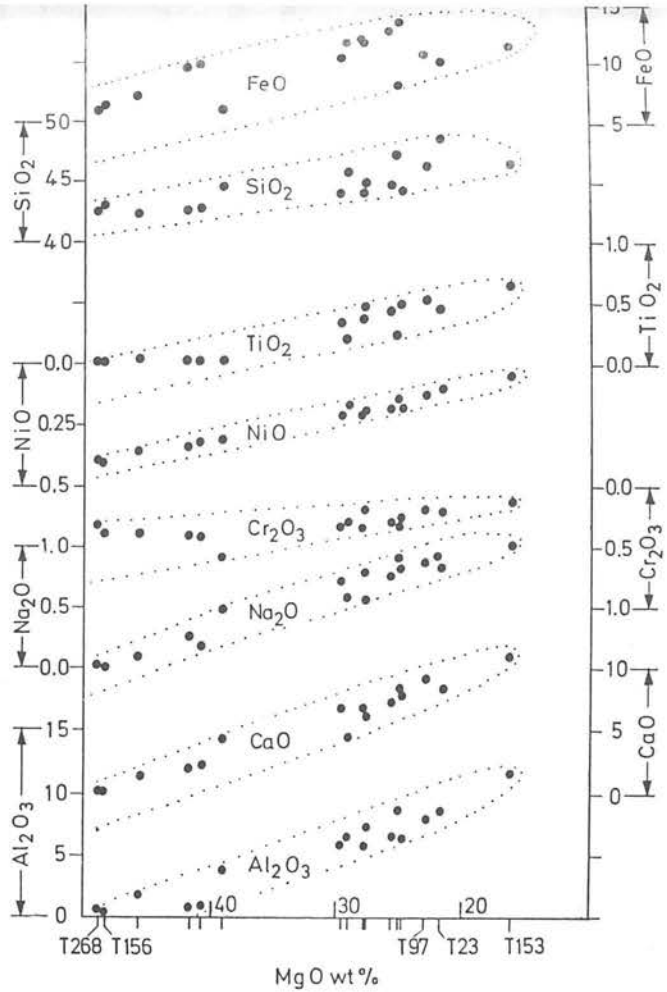

Fig. 6. Variation diagram showing the plot of the contents of the various oxides against MgO content for peridotite compositions from the Kalskaret garnet peridotite locality. The FeO value plotted is total iron calculated as FeO

forsteritic olivine itself. It is notable how the Al_2O_3, CaO, Na_2O and TiO_2 contents all trend to zero in the compositions T268 and T156 suggesting that these compositions closely represent the most extreme end member composition possible in that direction.

The other end member is, however, less well defined. Although the NiO and Cr_2O_3 contents are low in the eclogitic rock type T153 they are not quite zero. The true end member in that direction may therefore have a rather more extreme composition than T153. The chemical characteristics of this phase are clearly high Fe/Mg ratio and high CaO, Al_2O_3, TiO_2 and Na_2O contents with respect to the

bole would seem the only possibilities.

On consideration, however, both these minerals seem unlikely propositions. The Al_2O_3/CaO ratio in the most eclogitic compositions is too high to have been produced only by the sorting of a stable aluminous clinopyroxene of any known composition, even those realized experimentally. A hornblende on the other hand may have a suitable Al_2O_3/CaO ratio, although the conditions for the comagmatic precipitation of such a hydrous mineral with Mg olivine in what is even now an essentially anhydrous environment would appear improbable. It is also unlikely that there would be such a striking increase in Fe/Mg ratio towards the eclogitic compositions solely as a result of an increase in hornblende (or clinopyroxene) content with respect to coexisting olivine. The Fe/Mg ratios of the amphiboles analysed by O'Hara and Mercy (1963, Table 13) are for example too low but then these are secondary, as it would appear are all the amphiboles now present in the peridotites, and not in equilibrium with the olivine. Furthermore, with the mixing of two minerals during or perhaps even after comagmatic precipitation there is no good reason to expect the apparent break in the composition series (Fig. 6).

Extrapolating the linear oxide trends graphically (Carswell, 1966) the NiO content falls to zero at a MgO content of 9.80 wt.-%. Four hypothetical rock compositions slightly more extreme than T153 have therefore been calculated, their compositions and C.I.P.W. norms being given in Table 8.

The features of these increasingly extreme compositions are a notable decrease in the normative olivine contents (the most extreme composition calculated in fact containing normative quartz), an increase in the Fe + Ni + Mn/Fe + Ni + Mn + Mg ratio in the normative ferromagnesian silicates, and slight increases in normative pyroxene and plagioclase contents. This composition trend appears to approach the major element composition of some tholeiitic basalts. However, the low Na_2O contents and negligible K_2O and P_2O_5 contents contrast with all extrusive magma types.

If the end member phases were rock types rather than minerals then the possibility of mechanical mixing of either tholeiitic basalt and dunite, or eclogite and dunite followed by total recrystallization within the eclogite facies has to be considered. Both possibilities raise a major problem regarding the intimate mixing required to produce the present interlayering of the rock types. Mechanical mixing during tectonic transport into their present environment may just supply a feasible explanation of the layering observed in the case of the Kalskaret garnet peridotites which occur in a very restricted lens in which garnet and clinopyroxene rich rock types predominate. It seems altogether unlikely, however, in the case of the Lien locality in Almklovdalen where garnetiferous peridotites occur intimately interlayered with garnet free peridotites over about 200 metres and garnet peridotites with only low modal proportions of garnet and clinopyroxene are much more prevalent.

An even stronger argument against the mechanical mixing hypothesis is that the eclogite facies recrystallization and equilibration of the assemblages in accordance with the 'mixed' bulk rock compositions clearly preceeded the only period of intense mechanical deformation evidenced in these rocks. Hence it seems

Table 8. *Extrapolated "eclogitic" end members of Kalskaret composition trend*

Analyses wt-%	T153	I	II	III	IV
SiO_2	46.53	47.46	47.73	48.04	48.30
TiO_2	0.64	0.66	0.70	0.74	0.77
Al_2O_3	11.58	11.69	12.36	13.12	13.73
Cr_2O_3	0.12	0.11	0.10	0.08	0.07
Fe_2O_3	3.30	3.45	3.52	3.59	3.65
FeO	8.65	9.06	9.31	9.57	9.78
MnO	0.22	0.23	0.24	0.25	0.26
NiO	0.06	0.04	0.02	0.00	0.00
MgO	16.08	14.26	12.22	9.98	8.15
CaO	11.00	11.89	12.58	13.34	13.96
Na_2O	1.01	1.14	1.21	1.28	1.33
K_2O	0.02	(∼0.02)	(∼0.02)	(∼0.02)	(∼0.02)
H_2O+	0.36	—	—	—	—
P_2O_5	0.004	(∼0.004)	(∼0.004)	(∼0.004)	(∼0.004)
Total	99.57	99.99	99.99	99.99	100.00
$\frac{Fe+Ni+Mn}{Fe+Ni+Mn+Mg}$	0.19	0.22	0.25	0.30	0.35
$Ab/Ab+An$	0.24	0.26	0.26	0.26	0.26

C.I.P.W. norms	T153	I	II	III	IV
Qu	—	—	—	—	—
Or	0.12	—	—	—	—
Ab	8.55	9.65	10.24	10.83	11.26
An	27.00	26.78	28.29	30.05	31.49
Di	16.79	18.89	19.10	18.87	18.22
Hd	5.25	6.97	8.43	10.47	12.65
En	13.91	13.71	13.15	12.54	11.38
Of	4.35	5.06	5.80	6.95	7.90
Fo	12.68	8.92	5.65	2.20	—
Fa	4.36	3.63	2.75	1.35	—
Mgt.	4.78	5.00	5.10	5.21	5.29
Ilm	1.22	1.25	1.33	1.41	1.46
Cr.	0.18	0.16	0.15	0.12	0.10
Ap.	0.02	—	—	—	—
Rest	0.36	—	—	—	—
Total	99.57	100.01	99.99	100.00	100.00
$\frac{Fe+Ni+Mn}{Fe+Ni+Mn+Mg}$	0.19	0.22	0.25	0.30	0.35
$Ab/Ab+An$	0.24	0.26	0.26	0.26	0.26

$\frac{Fe+Ni+Mn}{Fe+Ni+Mn+Mg}$ = molecular ratio in normative ferromagnesian silicates.

impossible to relate the mechanical mixing to the tectonic emplacement of these rock masses.

This leads one finally to the possibility of liquid mixing. Two theories involving a liquid end member phase require consideration.

1. Igneous crystallization of olivine ± orthopyroxene cumulates with the residual liquid imperfectly filter pressed out and hence crystallized in pockets within the peridotite

If the crystallization is assumed to have occurred at high crustal levels then the mass must have had an extremely complex tectonic history, namely transport to considerably greater depths in order to produce the eclogite facies mineralogy, followed by transport back up again into its present environment of disequilibrium with the enclosing gneisses.

Furthermore, a low temperature metamorphic origin of the eclogite facies assemblage does not explain the exsolution textures which are considered indicative of an original higher temperature mineral assemblage, unless the original crystallization is assumed to have involved the precipitation of aluminous pyroxenes (granulite or eclogite facies assemblages). In that case original recrystallization must probably be relegated to the upper levels of the mantle and this hypothesis becomes closely akin to the mantle partial melting hypothesis outlined below, except that in this case the composition series would not be expected to include the original upper mantle source composition.

One point against this theory is that the original liquid must have been extremely picritic in order to precipitate such vast thicknesses of olivine cumulates and still remain as relatively picritic in character as the end member composition T 153 is. The existence of such a liquid is very much in doubt.

2. Partial melting of an intermediate peridotite composition resulting in segregation into 'picritic' partial melt and dunitic residual compositional fractions

In this case the garnet free peridotites are considered to represent the residue left after the extraction of a partial melt of 'picritic' composition, and the garnetiferous peridotites the result of imperfect filter pressing out of the partial melt fraction. This hypothesis poses three important questions:

a) Is the most eclogitic rock composition (T 153) or any of the extrapolated rock compositions (Table 8) likely to represent that of either a trapped partial melt or a crystal cumulate from a partial melt?

b) Did the partial melting process take place in the mantle or the crust, and consequently to what mineral facies did the initial and resultant rock types belong?

c) Do any rock types of intermediate composition occur, which are possibly representative of the unmodified source peridotite material?

Recent experimental work (O'Hara, 1963a and b; O'Hara and Yoder, 1963, 1967; Davis and Schairer, 1965; Ito and Kennedy, 1967) indicates that the most extreme Kalskaret eclogitic rock type, T153, has a suitable composition for it to represent a garnet peridotite partial melt extract formed at high pressures (nominally greater than about 20 kilobars; the experimental work cited covering the range 23—40 kilobars). Its composition is, in fact, that of a pyroxenic picrite having a C.I.P.W. norm of Plagioclase 35.7 Clinopyroxene 22.1 Orthopyroxene 18.3 Olivine 17.0, a composition closely similar to that of the primary liquid composition at a nominal 40 kilobars pressure in the synthetic $CaO—MgO—Al_2O_3—SiO_2$ system given by Davis and Schairer (1965). The normative olivine/orthopyroxene ratio in the composition T 153 is somewhat lower than that of the partial melt suggested by some workers (Green and Ringwood, 1967b, say $>30\%$ normative olivine), but has probably been lowered by the effects of partial secondary oxidation increasing the Fe_2O_3/FeO ratio.

Correlation of the composition of T 153 with the partial melting product of garnet peridotite produced at pressures >20 kilobars implies depths of origin >65 kilometres.

Direct evidence of just how far down the crustal disturbance during orogenesis is likely to extend, thus indicating possible depths from which material may have been brought up, is hard to come by although figures of 60—70 kilometres, sometimes as high as 100 kilometres are often mentioned.

Seismic studies (e.g. Gutenberg, 1951; Benioff, 1954, 1962) of earthquakes in the Japanese area have suggested the existence of broad inclined shear zones extending beneath the continental margins. The most frequent earthquakes associated with these movement zones have foci extending down to depths of 60—70 kilometres, but deeper earthquake foci indicate that movement extends down to depths of about 700 kilometres. If such shear zones are commonly directly related to tectogene formation they provide an ideal mechanism for the emplacement of mantle material into the orogenic rock sequence.

It therefore seems possible that during a major orogenic episode the tectogene may extend down to depths of about 70 kilometres, at about which level local partial melting and magma generation may occur. Mantle peridotite material modified by partial melting processes under such conditions may then become involved in the orogenic movements and so be subsequently tectonically emplaced into higher crustal levels.

An alternative suggestion that the composition variation has resulted from the partial melting of granulite facies peridotite at considerably lower pressure (say 10—15 kilobars) at or near the base of the crust is open to the following objections:

a) The lack of evidence of the wholesale production of basalt magmas at such shallow depths. Seismic evidence for the depth of origin of basalt magmas (e.g. Gorshkov, 1958; Eaton and Murata, 1960) suggests depths of the order of 50—70 kilometres, well within the upper mantle. At such depths mantle peridotites are likely to be within the garnet peridotite stability field (cf. MacGregor, 1965, Fig. 38; Green and Ringwood, 1967a, Fig. 2; Ito and Kennedy, 1967 Fig. 3), although at the likely temperatures of melting aluminous pyroxene peridotite may well be the stable assemblage.

b) The partial melt of peridotite under these conditions is likely to be nepheline normative in composition (O'Hara, 1965; Green and Ringwood, 1967b; Kushiro, 1965a and b), which does not fit with the inferred Kalskaret partial melt composition.

It is therefore considered that if the partial melting hypothesis for the explanation of the composition trend among the Kalskaret garnet peridotites is accepted then the partial melting involved rocks of eclogite facies within the upper mantle.

result of partial melting modification of mantle garnet peridotite material, then the mantle peridotite composition must lie within the composition series, obviously being intermediate between the residual and partial melt composition fractions. If the partial melting process has not been carried to completion the possibility exists that some primary mantle peridotite material still persists. It is therefore important to consider whether any peridotites of intermediate composition such that they might represent suitable primary mantle material do occur within the series. Such intermediate mantle peridotite compositions would not be expected with the alternative olivine cumulate — residual liquid hypothesis.

Current theories on the mineralogy and chemistry of the mantle (e.g. O'HARA and MERCY, 1963; MACGREGOR, 1965; RINGWOOD, 1966a, b; GREEN and RINGWOOD, 1967a; ITO and KENNEDY, 1967; MERCY, 1967) mostly favour the idea that the predominant primary upper mantle rock type is a garnet peridotite with low modal contents of garnet and clinopyroxene. Such rock types are scarce among the Kalskaret garnet peridotites most of which are highly garnetiferous but do occur (e.g. N21: O'HARA and MERCY, 1963; MERCY and O'HARA, 1965a). On the evidence at hand at present, however it cannot be proved irrefutably that they represent primary mantle material while the more garnetiferous and also the garnet free peridotites represent modified mantle material. However, it may be possible to test some of the intermediate composition peridotites as possible primary mantle material in terms of their Rb, Sr, K, U and Th contents and Rb/Sr and Sr^{87}/Sr^{86} ratios as suggested by the work of ROE (1964), ALDRICH *et al.* (1964), HART *et al.* (1965), and STUEBER and MURTHY (1966).

Mantle peridotite material must have suitable contents of these trace elements such that the contents of these elements in basalts can be derived from them and their radioactive element contents must be sufficient to produce the observed rates of heat flow from the mantle.

Preliminary determinations of Rb and Sr in the Kalskaret peridotites by X-ray fluorescence techniques indicated Rb values of <10 ppm, probably <5 ppm, in all the samples while Sr values varied from 14—89 ppm.

In view of the likely low contents of Sr, Rb, K and P in the liquid considered to have been involved in the production of the Kalskaret garnet peridotites, together with its picritic nature and major element compositional similarity with the partial melt of garnet peridotite formed experimentally at >20 kilobars pressure, it is considered that this liquid was of a more primitive nature than that of the oceanic tholeiitic basalts (cf. ENGEL *et al.*, 1965) and was hence closer to the composition of a primary partial melt liquid formed at high pressure in the mantle.

The occurrence of other garnet peridotite masses (namely those at Ugelvik) of possible primary mantle composition (unpublished data) close by in the same orogenic belt is also considered to substantiate the proposed mantle partial melting theory for the Kalskaret garnet peridotites.

A problem still remains, however, in trying to explain all the intermediate compositions on the linear composition trend (Fig. 6). According to the partial melt-residual crystals hypothesis, if the most eclogitic composition T153 is taken as representing that of the partial melt liquid itself then compositions occur in the range 0—30% liquid + 70—100% residual crystals and 60—85% liquid + 15 to 40% residual crystals. Thus assuming that MgO content provides a reliable composition index of the composition trend (in effect it appears to represent the best such index) there is a gap in the range 30—60% liquid + 40—70% crystals, which is probably significant but may just be fortuitous due to inadequate sampling. A gap in approximately the same composition range is shown by several of the other elements, namely Al_2O_3, Na_2O, NiO and TiO_2, but is absent with Cr_2O_3, SiO_2 and FeO^T (see Fig. 6).

Compositions in the range 0—30% liquid can be readily explained as representing predominantly residual crystals with tapped interstitial liquid. Alternatively some of these compositions may represent unmodified primary mantle garnet peridotite material. However, compositions which represent 60—85% liquid + 15—40% crystals are more difficult to explain. Such proportions of crystals would be expected to sink out of the liquid phase and a much larger gap in the intermediate crystals + liquid range would be expected.

The intermediate compositions may, however, have been developed according to one or a combination of the following explanations.

1. The liquid composition may not in fact be represented by T153 but may be more intermediate in the composition series. If N23 or T97 represents the liquid composition, rather than T153 which might then represent a crystal cumulate from the liquid, then the composition gap widens somewhat to about the 35—70% liquid range. However, these compositions with high modal orthopyroxene and olivine contents, respectively, are not so satisfactory as T153 as possible partial melt liquids of garnet peridotites at high pressures.
2. It is possible that some of the more eclogitic compositions may represent the product of the mixing of garnet and clinopyroxene crystal cumulates of the partial melt with olivine and orthopyroxene crystals of the residuum. Such a process may explain the deviations from ideal linearity (see Fig. 6) which suggests perhaps a certain amount of segregation of garnet from clinopyroxene or vice versa in several of the more eclogitic compositions. However, any mechanical segregation process cannot have proceeded far, otherwise the compositional linearity would not be expected to be so strong.
3. The liquid is here considered to have developed essentially *in situ* from an intermediate composition in the series. Hence the liquid may have been trapped as minor pockets or stringers within the peridotite with which it was mechanically mixed following crystallization.

Both these last two explanations do, however, bring back the possibility of mechanical mixing and segregation which was previously rejected as a mechanism for the origin of the linear composition sequence through the mixing of basalt or eclogite with crystalline dunite into which it was intruded. It is still considered, however, that an entirely mechanical mixing process is unlikely to have produced the intricate layering and the range of bulk compositions which occur.

The possibility exists, however, that a limited degree of mechanical mixing and segregation superimposed upon the crystal-liquid mixing process has been a

involved in producing the intermediate rock compositions which are difficult to explain by the partial melting process alone.

VI. Conclusion

It is apparent that of the four different origins outlined at the beginning of this paper only case 4 (crystallization at depth to an eclogite facies assemblage followed by tectonic emplacement) appears to fit the available field, mineralogical and chemical evidence for the Kalskaret garnet peridotites. Furthermore, the garnet peridotite stability field outlined by experimental studies, indicates the likelihood that the original eclogite facies crystallization would have occurred within the mantle rather than the lower regions of the crust.

In view of the extensive mineral composition variations involved and the demonstration of a very strong linear composition trend amongst the rock types from the Kalskaret garnet peridotite locality, it is considered that these garnet peridotites do not represent primary mantle material but rather mantle peridotite material which has been modified by involvement in partial melting processes at its site of origin in the upper mantle.

The predominant garnet free peridotites with very low CaO and Al_2O_3 and negligible alkali contents are considered to represent residua after the removal of a partial melt fraction, while the localised garnet and clinopyroxene rich peridotites are considered to represent fossilized attempts at the extraction of such partial melts which have not been carried to completion. The partial melt phase in these instances has not been completely filter pressed out and removed but instead has been trapped and crystallized within the residual peridotite. There are, however some garnet peridotites with only low modal contents of garnet and clinopyroxene, particularly at the Lien locality in Almklovdalen but also at Kalskaret, which may represent original mantle peridotite material which has escaped involvement in such partial melting processes.

It may, however, be necessary to invoke subsequent limited mechanical mixing and segregation during tectonic emplacement to account for certain of the intermediate compositions on the linear composition trend.

It is also recognised that subsequent to their involvement in partial melting processes these garnet peridotites have been modified by recrystallization and equilibration still under eclogite facies conditions at subsolidus temperatures (perhaps as low as 600—700° C) probably prior to, but perhaps during, their emplacement into their present environment and also by partial metamorphic retrogression and serpentinization.

Acknowledgements. This study was carried out at the Grant Institute of Geology, University of Edinburgh during the tenure of a grant from the Natural Environmental Research Council, which is gratefully acknowledged.

The writer is indebted to Dr. M. J. O'Hara for his stimulating comments, his critical reading of this manuscript, and the considerable interest shown by him throughout the course of the study. The writer is also particularly grateful to Dr. E. L. P. Mercy and Dr. N. B. Price for their help and discussions on analytical techniques, and to Dr. R. F. Cheeney and Professor J. Imbrie (Columbia University, New York) for their valuable help and suggestions regarding the statistical treatment of some of the chemical data.

Appendix

A. Definitions

To avoid unnecessary confusion, the following list of definitions of the ultrabasic rock type terms used in this paper is given.

Peridotite	general group name for olivine-rich ultrabasic rocks.
Dunite	peridotite consisting essentially of olivine only (> 90%).
Harzburgite	peridotite consisting of olivine and significant amounts (> 10%) of orthopyroxene.
Wehrlite	peridotite consisting of olivine and significant amounts (> 10%) of clinopyroxene.
Lherzolite	peridotite consisting of olivine and significant amounts of both orthopyroxene and clinopyroxene.
Websterite	pyroxenite consisting essentially of orthopyroxene and clinopyroxene with negligible olivine.
Eclogite	rock type consisting predominantly of a pyrope-rich garnet and an omphacitic clinopyroxene.

B. Locations of Analysed Samples

List of the exact locations of the analysed Kalskaret garnet peridotite rock types collected along section AB Fig. 4. The distances given were measured planimetrically on the ground surface. The estimated modal proportions of minerals in these specimens are given in Table 2.

T200 Peridotite 150′ above top of main garnet peridotite lens.
T268 Dunite 80′ above top of main garnet peridotite lens.
T150 Amphibolized garnet peridotite — 30′ above base of main garnet peridotite lens.
T151 Garnet lherzolite 25′ above base of main garnet peridotite lens.
T152 Garnet wehrlite 21′ above base of main garnet peridotite lens.
T153 Garnet websterite 19′ above base of main garnet peridotite lens.
T154 Garnet wehrlite 14′ above base of main garnet peridotite lens.
T97 Garnet wehrlite 9′ above base of main garnet peridotite lens.
T96 Garnet lherzolite 6′ above base of main garnet peridotite lens.
T155 Amphibolized garnet peridotite — lowest horizon in the main garnet peridotite lens.
T156 Dunite 11′ below base of main garnet peridotite lens.
T162 Amphibolized garnet peridotite — 30′ below base of main garnet peridotite lens.
T100 Altered garnet ? peridotite — 45′ below base of main garnet peridotite lens.

C. Methods of Analysis

11 of the analysed Kalskaret peridotite specimens in Table 4 (all except T97 and T155) were analysed for Si, Al, Ti, Fe (total), Fe^{2+}, Mn, Mg, Ca, Na, K, Cr and H by a combination of recognized gravimetric, spectrophotometric and titration techniques.

Al, Cr, Fe (total), Mn, Ni, Mg and Ca by X-ray fluorescence spectroscopic techniques. In all cases, other than in the determination of small amounts of Cr (<0.4 wt-% Cr_2O_3), a fusion disc preparation with a 1:1:4 ratio of rock powder (100 mesh): La_2O_3:$Li_2B_4O_7$ was used in order to minimize the matrix absorption effects.

Determinative curves were drawn up for each element using a number of recognised standard materials (G_1, W_1, syenite Sy-1 etc.) prepared similarly to the unknown rock and mineral powders. Special standards for the Ni and Cr determinations were prepared by adding appropriate amounts of these elements to one of the unknown rock samples.

In most cases the results obtained by the two methods of analysis were quite comparable. The values listed in Table 4 are therefore averages of those analyses which have been duplicated by the two different analytical methods, except for the low concentrations of CaO in T268 and T156 and the MgO content of T156 for which the X-ray fluorescence values were preferred. Where SiO_2 has been determined for the analysed minerals (Table 1) this was done by a combined gravimetric and spectrophotometric technique, while the MgO values were checked by the recognised E.D.T.A. titration technique.

For a comparison of the results obtained by the two analytical methods and further details on both these methods, in particular the operating conditions of the X-ray fluorescence spectrograph for each element, the reader is referred to Carswell (1966).

References

Aldrich, L. T., S. R. Hart, G. R. Tilton, G. L. Davis, S. N. I. Rama, R. Steiger, J. R. Richards, and J. S. Gerken: Isotope age determination of ultramafic rocks of St. Paul's Islands. Carnegie Inst. Wash. Yearb. **63**, 330—331 (1964).

Benioff, H.: Orogenesis and deep crustal structure. Additional evidence from Seismology. Bull. Geol. Soc. Am. **65**, 465—500 (1954).

— Movements on major transcurrent faults. P. 103—134 in S. K. Runcorn (ed.). Continental Drift. London: Academic Press 1962.

Bowen, N. L., and J. F. Schairer: The system FeO — MgO — SiO_2. Am. J. Sci. **29**, 151—217 (1935).

Boyd, F. R., and J. L. England: Some effects of pressure on phase relations in the system MgO—Al_2O_3—SiO_2. Carnegie Inst. Wash. Yearb. **62**, 121—124 (1963).

— — The system enstatite-pyrope. Carnegie Inst. Wash. Yearb. **63**, 157—161 (1964).

—, and I. D. MacGregor: Ultramafic Rocks. Carnegie Inst. Wash. Yearb. **63**, 152—156 (1964).

—, and J. F. Schairer: The system $MgSiO_3$—$CaMgSi_2O_6$. J. Petrology **5**, 275—309 (1964).

Brøgger, W. C.: Über Olivinfels von Søndmøre. Neues Jb. Miner. Geol. **11**, 187—192 (1880).

Bryhni, I.: Reconnaissance studies of gneisses, ultrabasites, eclogites and anorthosites in Outer Nordfjord, Western Norway. Norg. Geol. Undersökelse **241**, 1—68 (1966).

Carswell, D. A.: Some ultrabasic bodies and related rocks in Sunnmøre, south Norway. Unpublished Ph. D. thesis University of Edinburgh 1966.

Clark, J. B., and F. N. Rhines: Diffusion layer formation in the ternary system Al—Mg—Zn. Trans. Am. Soc. Metals **51**, 199—221 (1959).

Davis, B. T. C., and F. R. Boyd: The join $Mg_2Si_2O_6$ — $CaMgSi_2O_6$ at 30 kilobars pressure and its application to pyroxenes from kimberlites. J. Geophys. Research **71**, 3567—3576 (1966).

at 40 kilobars and at one atmosphere. Carnegie Inst. Wash. Yearb. **64**, 123—126 (1965).

Eaton, J. P., and K. J. Murata: How volcanoes grow. Science **132**, 925—938 (1960).

Engel, A. E. J., C. E. Engel, and R. G. Havens: Chemical characteristics of oceanic basalts and the upper mantle. Bull. Geol. Soc. Am. **76**, 719—734 (1965).

Eskola, P.: The mineral facies of rocks. Norsk. Geol. Tidsskr. **6**, 143—194 (1920).

— On the eclogites of Norway. Kristiania, Videnskapsselskapets-Skrifter, I. Mat.-naturv. Kl. No. 8, 1—118 (1921).

Gjelsvik, T.: Oversikt over bergartene i Sunnmøre og tilgrensende deler av Nordfjord. Norg. Geol. Undersökelse **179**, 1—45 (1951).

Gorshkov, G. S.: On some theoretical problems to volcanology. Bull. volcanol. **19**, 103—114 (1958).

Green, D. H., and A. E. Ringwood: The stability fields of aluminous pyroxene peridotite and garnet peridotite and their revelance in upper mantle structure. Earth Planet. Sci. Letters. **3**, 151—160 (1967a).

— — The genesis of basaltic magmas. Contr. Mineral. and Petrol. **15**, 103—190 (1967b).

Gutenberg, B.: Internal constitution of the earth, 2nd ed. New York: Dover Publications Inc. 1951.

Hart, S. R., L. T. Aldrich, G. R. Tilton, G. L. Davis, T. E. Krogh, and M. Yamaguchi: K/Rb studies of ultrabasic rocks in Japan. Carnegie Inst. Wash. Yearb. **64**, 293—296 (1965).

Hernes, I.: Connections between the Trondheim and Sunnhordland regions, Caledonides of Norway. Norg. Geol. Undersökelse **37**, 247 (1957).

Hess, H. H.: Pyroxenes of common mafic magmas. Parts 1 and 2. Am. Mineralogist **26**, 515—535, 573—594 (1941).

Holtedahl, O.: On the Caledonides of Norway. Vid. Akad. Skr. No. 4 (1944).

— Geology of Norway. Norg. Geol. Undersökelse **208**, 540 p. (1960).

Imbrie, J., and T. H. van Andel: Vector analysis of heavy mineral data. Bull. Geol. Soc. Am. **75**, 1131—1156 (1964).

Ito, K., and G. C. Kennedy: Melting and phase relations in a natural peridotite to 40 kilobars. Am. J. Sci. **265**, 519—538 (1967).

Kushiro, I.: The liquidus relations in the systems forsterite — $CaAl_2SiO_6$ — silica and forsterite-nepheline-silica at high pressures. Carnegie Inst. Wash. Yearb. **64**, 103—109 (1965a).

— Coexistence of nepheline and enstatite at high pressures. Carnegie Inst. Wash. Yearb. **64**, 109—112 (1965b).

Lappin, M. A.: The eclogites, dunites and anorthosites of the Selje and Almklovdalen districts, Nordfjord, S. W. Norway. Unpublished Ph. D. thesis University of Durham 1962.

— The field relationships of basic and ultrabasic masses in the basal gneiss complex of Stadlandet and Almklovdalen, Nordfjord, southwestern Norway. Norsk Geol. Tidsskr. **46**, 439—496 (1966).

MacDougall, I., and D. H. Green: Excess radiogenic argon in pyroxenes and isotopic ages on minerals from Norwegian eclogites. Norsk Geol. Tidsskr. **44**, 183—196 (1964).

MacGregor, I. D.: Stability fields of spinel and garnet peridotites in the synthetic system MgO—CaO—Al_2O_3—SiO_2. Carnegie Inst. Wash. Yearb. **64**, 126—134 (1965).

Mason, V., and J. Imbrie: Fortran Program for factor and vector analysis of geologic data using an IBM 7090 or 7094/1401 computer system. State Geological Survey, The University of Kansas. Special Publication **13**, 46 p. (1964).

Mercy, E. L. P.: Geochemistry of the mantle. In: The earth's mantle (ed. T. F. Gaskell), p. 421—443. London: Academic Press 1967.

—, and M. J. O'Hara: Chemistry of some garnet-bearing rocks from south Norwegian peridotites. Norsk. Geol. Tidsskr. **45**, 323—332 (1965a).

— — Olivines and orthopyroxenes from garnetiferous peridotites and related rocks. Norsk. Geol. Tidsskr. **45**, 457—461 (1965b).

Muret, G.: Partie S. E. de la culmination du Romsdal, Chainne Caledonienne, Norvège. 21st. Int. Geol. Congr. Report, Copenhagen 1960, Sect. 19, 28—32.

Nuemann, H.: Apparent ages of Norwegian minerals and rocks. Norsk. Geol. Tidsskr. **40**, 173—191 (1960).
O'Hara, M. J.: A garnet-hornblende rock from Glenelg Inverness-shire. Geol. Mag. **97**, 145—156 (1960).
— Melting of garnet peridotite at 30 kilobars. Carnegie Inst. Wash. Yearb. **62**, 71—76 (1963a).
— Melting of bimineralic eclogite at 30 kilobars. Carnegie Inst. Wash. Yearb. **62**, 76—77 (1963b).
— The join diopside-pyrope at 30 kilobars. Carnegie Inst. Wash. Yearb. **62**, 116—118 (1963c).
— Distribution of iron between coexisting olivines and Ca-poor pyroxenes in peridotites, gabbros and other magnesian environments. Am. J. Sci. **201**, 32—47 (1963d).
— Primary magmas and the origin of basalts. Scot. J. Geol. **1**, 19—40 (1965).
—, and E. L. P. Mercy: Petrology and petrogenesis of some garnetiferous peridotites. Trans. Roy. Soc. Edinburgh **65**, 251—314 (1963).
—, and H. S. Yoder: Partial melting of the mantle. Carnegie Inst. Wash. Yearb. **62**, 66—71 (1963).
— — Formation and fractionation of basic magmas at high pressures. Scot. J. Geol. **3**, 67—117 (1967).
Ramberg, H., and G. W. de Vore: The distribution of Fe^{2+} and Mg^{2+} in coexisting olivines and pyroxenes. J. Geol. **59**, 193—210 (1951).
Reusch, H. H.: Grundfjeldet i Sondre Sondmore og en del av Nordfjord. Forh. i. Vidensk. i Christ 1877.
Ringwood, A. E.: The chemical composition and origin of the earth. In: Advances in earth Sciences (ed. P. M. Hurley), p. 287—356. Cambridge (Mass.): M. I. T. Press 1966a.
— Mineralogy of the mantle. In: Advances in earth sciences (ed. P. M. Hurley), p. 357—399. Cambridge (Mass.): M. I. T. Press 1966b.
— MacGregor, I. D., and F. R. Boyd: Petrological constitution of th upper mantle. Carnegie Inst. Wash. Yearb. **63**, 147 —152(1964).
Roe, G. D.: Rb/Sr analyses of ultramafic rocks and the origin of peridotites. M. I. T. 12th Annual Progress Report 1964, p. 159—190.
Strand, T.: The Scandinavian Caledonides — a review. Am. J. Sci. **259**, 161—172 (1961).
Stueber, A. M., and V. R. Murthy: Strontium isotope and alkali element abundances in ultramafic rocks. Geochim. et Cosmochim. Acta **30**, 1243—1259 (1966).
Vogt, J. H. L.: Olivinstenen i indre of Sondre Sondmore. Nyt. Mag. for Naturidenskabene. **27**, 125—153 (1883).
Williams, A. F.: The genesis of the diamond, 2 vol.s London: Benn 1932.

Dr. D. A. Carswell
Department of Geology
University of Sheffield, England

POSSIBLE PRIMARY UPPER MANTLE PERIDOTITE IN NORWEGIAN BASAL GNEISS

D.A. CARSWELL

CARSWELL, D.A. 1968: Possible primary upper mantle peridotite in Norwegian basal gneiss. *Lithos 1*, 322–355.

Garnet peridotites at Ugelvik on the island of Oteröy do not show the extensive mineral and bulk rock chemical variations demonstrated by the previously described garnet peridotites at the nearby Kalskaret and Almklovdalen localities. Instead they show striking mineralogical and chemical similarities to the garnet peridotites which occur as nodules in kimberlite pipes and also to those described from the Czech Massif.

In the light of this similarity and their compatibility with likely mantle compositions suggested by the chondrite meteorite and pyrolite models and the likely upper mantle mineralogy indicated by the experimental high pressure and temperature petrology studies, it is postulated that the garnet peridotites from Ugelvik, kimberlite pipes, the Czech Massif and also possibly those from Bellinzona in Switzerland may all be representative of essentially unmodified upper mantle material.

Introduction

In recent years geophysical and geochemical evidence, together with the results of experimental high pressure petrology studies, has swung geological opinion generally in favour of accepting the hypothesis that the earth's mantle is largely of peridotite composition.

Likely mantle compositions (Table 12, columns 3 and 4) derived from the chondrite and pyrolite models respectively (Ringwood 1966), indicate that this mantle peridotite is expected to have low but significant amounts of CaO, Al_2O_3 and alkalies. In the light of experimental studies (Ringwood, MacGregor & Boyd 1964; MacGregor 1965; Green & Ringwood 1967b; Ito & Kennedy 1967) into the pressure-temperature stability fields of the various peridotite mineral assemblages, we can anticipate that the upper mantle will be composed for the most part of eclogite facies peridotite assemblages. It seems likely, therefore, that the principal upper mantle rock type is a garnet peridotite (olivine $\pm$ orthopyroxene + clinopyroxene + garnet assemblage) with low modal contents of garnet and clinopyroxene. At greater depths in the mantle phase transitions may well produce denser higher pressure polymorphs of olivine and pyroxene (see Ringwood & Major 1967; Ringwood 1967).

As a consequence of such speculations, considerable interest has recently been shown in the occurrences of garnet peridotite which are exposed today

at the earth's surface. Such rocks have been observed in only two environments:

1. As nodules in kimberlite pipes,
2. As horizons interlayered with garnet free peridotites in sparse peridotite bodies which occur in the 'basement' rock of certain European orogenic belts, in particular in Norway, Czechoslovakia and Switzerland.

Recently, several attempts have been made to assess whether particular garnet peridotite occurrences from each of these two types of environments are likely to represent primary upper mantle material.

Previous work

The most comprehensive recent analysis of this problem has been that by O'Hara & Mercy (1963). They concluded that... 'both types of garnet peridotite are derived from the mantle, but that only the nodules in kimberlite can be representative of the unmodified composition of the upper mantle'.

Holmes (1936), Nixon et al. (1963), Boyd & MacGregor (1964), and Kryukov (1966) among others have also advocated that the garnet peridotite nodules in kimberlites are derived from the upper mantle. Davidson (1943, 1964), in the latter case following Kopecky & Sattran (1962, 1966), has claimed, however, that such garnet peridotite nodules are xenoliths of crustal origin. O'Hara & Mercy (1963, 1965 & 1966a) have put forward strong arguments against such a hypothesis being the general case, even if a unique specific case as described by Kopecky & Sattran is accepted. In their first paper (1963) they also argue against the hypothesis that these nodules are cognate (i.e. formed by accumulation of crystals from the kimberlite magma) as favoured by Williams (1932) and Dawson (1962).

After considering the earlier petrogenetic hypotheses of Grubenmann (1908) and Dal Vesco (1953) to account for the garnet peridotite and eclogite outcrops in the Alpe Arami peridotite mass near Bellinzona in Switzerland, O'Hara & Mercy (1966b) concluded that these garnet peridotites might well represent a tectonically emplaced slice of the upper mantle; but in view of unexplained chemical peculiarities in enclosed garnet-pyroxene rocks they preferred to retain an alternative hypothesis namely, that they were metamorphosed accumulative igneous peridotites.

As regards the petrogenesis of the garnet peridotites which occur as lenses in granulite facies gneisses of the Bohemian Massif, there are still considerable differences of opinion amongst Czech and Russian geologists. Fiala (1965, 1966) has provided petrochemical information on these rocks, in particular on the coexisting mineral phases. In the latter paper he concluded that these garnet peridotites '...represent deep-seated rocks generated within the range of the Upper Mantle and brought up to the present level by tectonic processes'.

Kryukov (1966) has pointed out the chemical and mineralogical similarities between the garnet peridotites which occur as nodules in kimberlite pipes of

the North-Minusinsk depression in south Siberia, of West Yakutia in Russia and also of South Africa, with those which form lenses in the Bohemian gneiss complex. As he argues the case for garnet peridotites of the first group being derived from the Upper Mantle, he seems to infer a similar origin for those of the second group. Mikhailov & Rovsha (1966) have also stressed the chemical and mineralogical similarities between the garnet peridotites which form xenoliths in the Yakutian kimberlites and those of the Bohemian Massif, and hence assumed analogous ultimate origins. However, they discuss a magmatic emplacement origin of these rocks, envisaging peridotite magma formed in the Upper Mantle bringing up xenocrysts of pyrope.

On the other hand, Kopecky & Sattran (1966) and Rost (1966) have advocated that these garnet peridotites are integral representatives of the crustal metamorphic complex which originally formed at considerable depth.

At present the literature contains references to occurrences of garnet peridotite at only two localities in the basal gneiss region of southern Norway (see Eskola 1921). These are at Almklovdalen in Nordfjord and Tafjord in Sunnmöre.

However, this paper describes a further occurrence of garnet peridotite which has been observed at Ugelvik on the island of Oteröy (62°45′N, 6°40′E) on the north side of Moldefjord in Romsdal district, some 45 miles N.W. of Tafjord.

Lappin (1962, 1966) has advocated the tectonic emplacement of the Almklovdalen peridotites with associated garnetiferous types and thought that they were likely to have been derived from the mantle. Field and petrochemical studies led O'Hara & Mercy (1963) to conclude that the Tafjord and Almklovdalen garnet peridotite masses probably represent somewhat modified mantle peridotite material but they might represent completely recrystallized peridotites formed by igneous processes near the top of the mantle. They stressed several mineralogical and chemical differences between these rocks and the suite of eclogites and garnet peridotites found in South African kimberlite pipes (see also Mercy & O'Hara 1965a).

Following a detailed petrochemical study of the Kalskaret garnet peridotite occurrence at Tafjord, Carswell (1966, 1968) agreed that these garnet peridotites are unlikely to represent primary upper mantle material, but rather, mantle peridotite material which has been modified by involvement in partial melting processes at its site of origin. This particular garnet peridotite occurrence, and also possibly the Almklovdalen one as well, was considered to represent an instance where the 'picritic' partial melt fraction had not been completely liberated but had remained trapped and mixed with the 'dunitic' residual fraction.

General description

As illustrated in Fig. 1, the garnet peridotite occurrence on the island of Oteröy consists of two major closely adjacent masses on the northern side of

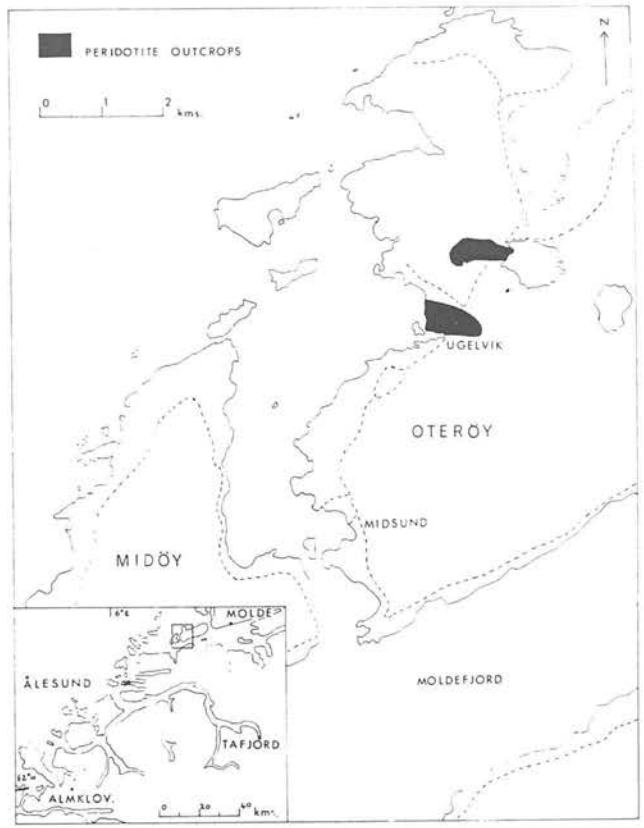

Fig. 1. Map showing the peridotite outcrops on the island of Oteröy. Inset map shows the location of Oteröy with respect to the other garnet peridotite localities in this part of Norway and the principal ports, Ålesund and Molde.

the island – one at the village of Ugelvik and the other about one kilometre north-east of the village. In addition there is a very small outcrop of peridotite independent of the two principal masses.

Nowhere is the actual contact between peridotite and the enclosing gneisses exposed. However, the gneiss appears to be broadly concordant with the peridotite at the contacts, along which both appear to have suffered a greater degree than normal of shearing and deformation. Peridotite and gneiss can

be observed most closely in juxtaposition along the eastern margin of the north-eastern peridotite mass. Specimens of garnet peridotite from here have textures similar to those observed in the Kalskaret garnet peridotites (Carswell 1968), with straining, cataclasis, recrystallization and dimensional orientation of the constituent minerals.

Such cataclastic textures, together with the sheared nature of the adjacent gneisses and the lack of any recognizable high temperature thermal aureole around the peridotite masses, point, therefore, to the tectonic emplacement of these peridotite masses into their present position. O'Hara & Mercy (1963), Lappin (1966), Bryhni (1966) and Carswell (1968) have all argued the case in favour of the tectonic emplacement of the Tafjord and Almklovdalen peridotites.

The gneiss complex adjacent to the Ugelvik peridotites consists predominantly of layered acid gneisses with subordinate mafic horizons. The latter typically occur as restricted lenses or boudins within the acid gneisses.

The typical acid gneiss assemblage consists of large porphyroblasts of antiperthitic oligoclase and microcline, together with quartz ± hornblende ± biotite ± sphene.

It is significant that the large feldspar porphyroblasts so diagnostic of these gneisses are highly deformed adjacent to the peridotite masses. This suggests the emplacement of the peridotites after the main injection, metasomatism and metamorphism of the gneiss complex.

A study of the basic gneiss assemblages indicates that the metamorphic grade was probably initially of granulite facies but later retrogressed to almandine-amphibolite facies.

The critical assemblages observed were:

1. Garnet + Augite + Hornblende + Biotite + Plagioclase + rutile + sphene,
2. Garnet + Augite + Hornblende + Biotite + Plagioclase + Quartz + rutile + sphene,
3. Garnet + Augite + Hypersthene + Hornblende + Biotite + Plagioclase + rutile + sphene.

In these assemblages the pale green augite typically has alteration rims of hornblende and the rutile of sphene. The biotite may well be primary, however.

According to Fyfe et al. (1958), in the granulite facies the garnet-clinopyroxene join is only stable in silica deficient basic assemblages, while in the eclogite facies the assemblage garnet + clinopyroxene + quartz is stable; but then plagioclase is unstable. However, more recently De Waard (1965) and Green & Ringwood (1967a) have advocated the stable appearance of garnet in quartz bearing pyroxene granulites, such assemblages being transitional towards those of the eclogite facies. The latter authors, therefore, have subdivided the granulite facies into low, intermediate and high pressure assemblages, the assemblage garnet + clinopyroxene + plagioclase + quartz being diagnostic of the high pressure granulites.

Microscopic examination of the gneiss assemblages in question indicates that texturally they do not resemble retrogressed eclogite facies assemblages. The garnets do not have kelyphitic reaction rims and the clinopyroxene does not show a symplektite alteration to an intergrowth of hornblende and plagioclase, rather only a broad hornblende rim.

It is, therefore considered likely that these gneiss assemblages correspond to high pressure granulites which have subsequently been partially retrograded to almandine – amphibolite facies assemblages.

Highly retrograded eclogites are, however, occasionally preserved in the gneiss complex. These occur generally as small lenses of boudin form, with extensive outer rims of amphibolite. The primary mineral assemblage of these rocks appears to have been garnet + clinopyroxene ± orthopyroxene ± phlogopitic mica + quartz – rutile. Commonly, however, the clinopyroxene is almost entirely altered to a fine-grained amphibole-plagioclase symplektite, and coarser grained amphibole forms kelyphitic rims round the garnets. These eclogites commonly contain appreciably more quartz than the garnet-pyroxene bearing granulites. Epidote and clinozoisite occur as secondary minerals in some of the altered eclogites.

A discussion of the origin of these eclogites is at present postponed. It is considered, however, that they, like the eclogite facies garnet peridotite assemblages, are extraneous to their present environment.

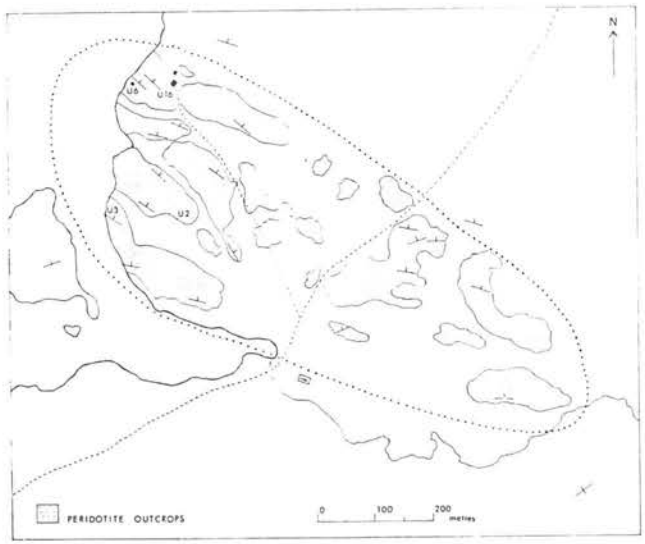

Fig. 2. Map showing the outcrops of the peridotite mass at the village of Ugelvik.

The most distinctive feature of the Ugelvik peridotites when compared with the previously described garnet peridotites in the Tafjord and Almklovdalen districts (O'Hara & Mercy 1963, Carswell 1968) is the widespread occurrence of small amounts of garnet throughout much of the peridotite. The garnet peridotite occurrences at these other localities are remarkably restricted within garnet free peridotites and often contain high modal proportions of garnet and clinopyroxene (15–40% and 25–53%, respectively, amongst analysed specimens). Here, however, peridotite with garnet or pseudomorphs after garnet probably comprises rather more than half the total volume of these peridotite masses, and it is estimated that the modal proportions by volume of garnet average about 10% and of clinopyroxene about < 5% (see Table 11). Slight variations in the proportions of garnet in the peridotite often produce a clear compositional layering.

The general degree of serpentinization of these peridotites is quite high, 50% or more, and quite distinctive from the generally remarkably fresh character of the Tafjord and Almklovdalen peridotites.

The garnets in these rocks often possess very extensive kelyphitic reaction rims (Fig. 3). These reaction rims consist for the most part of pale brown fibrous semi-opaque material which can be observed by detailed optical examination to consist primarily of orthopyroxene with minute inclusions of chrome-spinel. Less prominent fibres of a higher birefringence mineral with oblique extinction and similar relief are probably of clinopyroxene but may be of amphibole.

Occasionally, around the external margins of the reaction rims, the fibrous

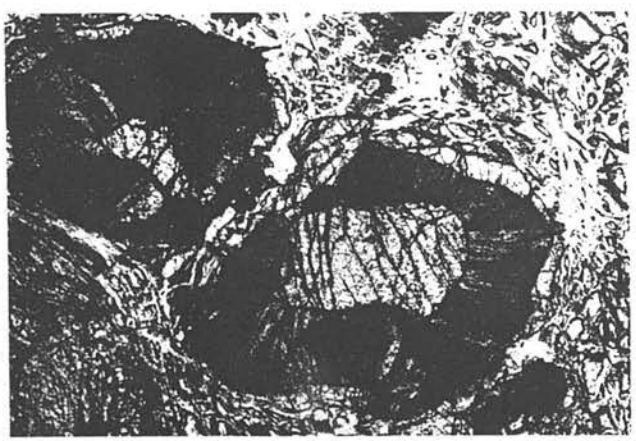

Fig. 3. Photomicrograph of kelyphitic reaction rims around garnets in Ugelvik garnet serpentinite. Plane polarized light. Magnification ×50.

material can be observed to have recrystallized into clear orthopyroxene with separate granules of chrome-spinel. External to this, concentrations of colourless amphibole grains often occur.

The reaction rims may be interpreted in terms of a retrogression of the eclogite facies assemblage (olivine – garnet) to a granulite facies assemblage (pyroxenes + spinel). The reaction involved may be generalized as follows, with an assumed garnet composition:

$$\underset{\text{Olivine}}{(Mg, Fe)_2 SiO_4} + \underset{\text{Garnet}}{(Mg, Fe)_3 Ca (Al, Cr)_2 Si_3 O_{12}}$$

$$= \underset{\text{Orthopyroxene}}{2(Mg, Fe) SiO_3} - \underset{\text{Clinopyroxene}}{Ca(Mg, Fe) Si_2O_6} - \underset{\text{Chrome - Spinel}}{(Mg, Fe), (Al, Cr)_2O_4}$$

The proportion of clinopyroxene formed will depend upon the calcium content of the garnet. The orthopyroxenes from this environment contain only very limited amounts of CaO, hence a restricted amount of clinopyroxene would be expected to form to absorb the excess of CaO released by the breakdown of the calcium poor garnet found in these rocks.

The concentration of amphibole grains often observed as a partial external rim around the garnets probably indicates the later onset of almandine amphibolite facies conditions and introduction of water, perhaps associated with the extensive serpentinization of the peridotites.

In the garnet peridotites, serpentine veins can be observed in several cases to cut across the inner fibrous reaction rims suggesting that the formation of these reaction rims preceded the onset of serpentinization. Furthermore, serpentine veins can be observed passing straight through highly deformed pyroxene and olivine grains, and also pseudomorphing highly distorted grains.

On the other hand, the amphibole grains which are generally clear, unstained and interstitial in habit to the deformed grains, are not shot through with serpentine veins as are all the other minerals; in fact they often appear to be growing over and obscuring serpentine veins. These relationships, therefore, suggest the following conclusions:

1. Serpentinization occurred after the formation of the fibrous reaction rims around the garnets.

2. Serpentinization was subsequent to the deformation of the minerals and hence probably subsequent to the tectonic emplacement of the peridotite masses.

3. Growth of amphibole was a late feature being post deformation and probably also mostly subsequent to or contemporaneous with the serpentinization.

The Ugelvik garnet kelyphitic rims are similar to those described by Nixon et al. (1963) around garnets in peridotite nodules from Basutoland kimberlites. They considered that the kelyphite formed rapidly from chrome pyrope

by the addition of water, the reaction being promoted by a decrease of pressure probably due to kimberlite intrusion.

However, in the case of the Ugelvik garnet peridotites, it seems likely that the addition of water associated with the serpentinization occurred after the formation of the kelyphitic reaction rims. It is considered rather that the inner fibrous reaction rims are possibly just the direct result of decreasing pressure conditions connected with the emplacement of these peridotites initiating from greater depths.

It is interesting to note how the apparent retrogression of the Ugelvik gneisses from the granulite to almandine amphibolite facies appears to be paralleled in the garnet rims with an inner rim of orthopyroxene and spinel, and an outer rim of amphibole.

This does not necessitate, however, these garnet peridotite masses being emplaced in their present position during the apparent partial retrogression of the gneiss complex. Rather, the garnet peridotites probably passed from an environment of granulite facies conditions to one of almandine amphibolite facies conditions during their emplacement. The pressure and temperature conditions of these facies probably, in fact, overlap to a certain extent, the availability of water being the most important distinction between them.

Table 1. Modal proportions by volume of the minerals in the analysed Ugelvik peridotites estimated by point counting

Mineral ↓ Sample No.→	U_2	U_3	U_6	U_8	U_{16}
Olivine	65	10	30	27	40
Serpentine after olivine	21	77		28	47
Orthopyroxene	4	11	8	10	6
Serpentine after orthopyroxene					
Clinopyroxene	2	–	47	10	–
Garnet	7	–	15	23	6
Amphibole	–	–	–	1	–
Opaques	1	2	<1	1	1

Five rock samples from these Ugelvik peridotites were selected for the initial bulk rock and constituent mineral analyses. The modes of these rocks are given in Table 1. Of these rock samples, U_2 and U_{16} are representative of the typical garnet poor peridotites, and U_3 of the garnet free peridotite. U_8 represents a garnet peridotite with approximately the maximum garnet content (about 23%) observed. U_6 is an exceptional rock type being a garnet peridotite with an abnormally high concentration of clinopyroxene (about 47%). This latter rock type is of very limited occurrence, outcropping as a thin band about 1′ 6″ thick at its maximum which can only be followed about 20′ laterally. Within this band there is microlayering with considerable variations in garnet content, but the principal mineral is clinopyroxene.

At a few other localities layers enriched in garnet and clinopyroxene have been observed, but these are generally very thin (2″ or less in thickness) and form a very insignificant fraction of the total volume of these two peridotite masses.

The localities for the collection of analysed samples of U_2, U_3, U_6 and U_{16} are noted in Fig. 2. U_8 was collected from the other principal peridotite mass, to the north-east of Ugelvik village.

Chemistry

The bulk rock analyses of 5 Ugelvik peridotites are given in Table 2. (For methods of analysis see p. 353). The high degree of serpentinization of these rocks, one specimen contains just over 14% H_2O^-, necessitates an attempt to recalculate the original water free composition. Following the discussion given in pages 347–52 it was decided that the constant composition anhydrous recalculations of the whole rock analyses provide the best available approximations to the primary pre-serpentinization compositions of these peridotites. These recalculated water free analyses are also presented in Table 2.

The C.I.P.W. norms based on the recalculated water free analyses of these Ugelvik peridotite samples are given in Table 3.

The most significant feature demonstrated by the normative mineral calculations of these peridotite compositions is the close consistency of the Fe – Mn – Ni/Fe – Mn – Ni + Mg ratios in the normative ferromagnesian silicates of the garnet-free assemblage U_3, the garnet-poor assemblages U_2 and U_{16}, and the garnet-rich assemblage U_8.

Table 2.

	Whole rock analyses of Ugelvik peridotites					Whole rock analyses recalculated on water free basis				
Analysis No.→	846	847	848	849	850	846	847	848	849	850
Field Sample No.→	U_2	U_3	U_6	U_8	U_{16}	U_2	U_3	U_6	U_8	U_{16}
SiO_2	39.67	36.72	49.49	43.39	39.04	44.37	42.86	50.95	46.32	43.26
TiO_2	0.01	<0.005	0.07	0.21	0.01	0.01	<0.005	0.07	0.22	0.01
Al_2O_3	2.00	0.13	3.70	6.27	1.41	2.24	0.15	3.81	6.69	1.56
Cr_2O_3	0.33	0.17	0.71	0.97	0.33	0.37	0.20	0.73	1.04	0.37
Fe_2O_3	4.32	5.22	2.45	3.30	3.93	–	–	–	–	–
FeO	2.21	1.25	4.12	3.25	2.74	6.82	6.95	6.51	6.64	6.96
MnO	0.10	0.10	0.16	0.17	0.11	0.11	0.12	0.16	0.18	0.12
NiO	0.29	0.31	0.12	0.20	0.31	0.32	0.36	0.12	0.21	0.34
MgO	39.65	42.17	25.86	31.68	42.23	44.35	49.22	26.63	33.82	46.81
CaO	1.06	0.05	10.40	4.18	0.38	1.18	0.06	10.71	4.46	0.42
Na_2O	0.14	0.06	0.28	0.37	0.11	0.16	0.07	0.29	0.40	0.12
K_2O	0.06	0.01	0.02	0.02	0.03	0.07	0.01	0.02	0.02	0.03
H_2O^-	10.71	14.02	3.23	6.18	9.38	–	–	–	–	–
Total	100.55	100.21	100.61	100.19	100.01	100.00	100.00	100.00	100.00	100.00

Table 3. C.I.P.W. norms of analyses of Ugelvik peridotites recalculated on a water free basis

Sample No.→	U_2		U_3		U_6		U_8		U_{16}	
Or	0.41		0.06		0.12		0.12		0.18	
Ab	1.35	6.95	0.59	0.71	2.45	11.61	3.38	19.90	1.02	3.28
An	5.19		0.06		9.04		16.40		2.08	
Co	–		–		–		–		0.57	
Di	0.47	0.53	0.17	0.19	29.68	34.92	3.97	4.52	–	
Hd	0.06		0.02		5.24		0.55		–	
En	14.49	16.19	7.94	8.81	25.01	29.43	21.57	24.55	11.21	12.49
Of	1.70		0.87		4.42		2.98		1.28	
Fo	67.09	75.76	80.28	89.99	19.12	22.84	42.60	49.08	73.83	83.09
Fa	8.67		9.71		3.72		6.48		9.26	
Ilm.	0.02		–		0.13		0.42		0.02	
Cr	0.34		0.30		1.08		1.53		0.54	
Total	99.99		100.00		100.01		100.00		99.99	
*Fe – Mn – Ni / Fe – Mn – Ni – Mg	0.08		0.08		0.12		0.10		0.08	
Ab/Ab – An	0.21		0.91		0.21		0.17		0.33	

* $\frac{Fe - Mn - Ni}{Fe - Mn - Ni - Mg}$ = Molecular ratio in normative ferromagnesian silicates.

In the Kalskaret and Almklovdalen peridotites, on the other hand, with increasing garnet and clinopyroxene contents, this ratio in the normative ferromagnesian silicates increases markedly from its value in the garnet free peridotites (see Carswell 1968 Table 5, and Mercy & O'Hara 1965a Table 2).

This feature is also brought out on a $Ca^{2+}:Mg^{2+}:Fe^{2+}+Fe^{3+}$ plot of the bulk rock compositions, (Fig. 4). The composition trend of the Ugelvik peridotites is notable transverse to the linear trends defined by the samples from Kalskaret, Lien and Rödhaugen which were discussed by Carswell (1968). The Ugelvik trend shows only a very slight increase in $Fe^{2+}+Fe^{3+}/Mg^{2+}$ ratio with increasing Ca^{2+} content, a feature which can be attributed solely to the higher $Fe^{2+}-Fe^{3+}/Mg^{2+}$ ratio of the garnet compared with its coexisting minerals. By comparison, the linear composition trends of the Kalskaret, Lien and Rödhaugen peridotite compositions show markedly increased $Fe^{2+}+Fe^{3+}/Mg^{2+}$ ratios with increasing Ca^{2+} content (i.e. increased modal proportions of garnet and clinopyroxene), the whole mineral assemblage becoming more ferriferous.

The mineral compositions for analysed Ugelvik garnet peridotite assemblages, together with the structural formulae, are given in Table 4.

A study of the mineral composition data indicates that the constituent minerals of the Ugelvik garnet peridotites are chemically distinct from those of Kalskaret and Almklovdalen garnet peridotites (O'Hara & Mercy 1963; Carswell 1968) being collectively more magnesium and chromium rich than the latter and also having a far more restricted composition range.

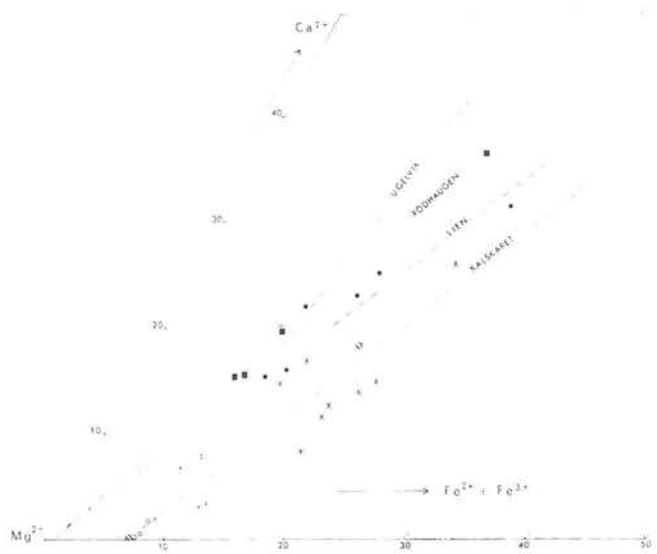

Fig. 4. CMF plot of the bulk rock compositions of analysed Ugelvik, Kalskaret and Almklovdalen peridotites. The *open circles* represent compositions from Ugelvik, *crosses* compositions from Kalskaret, *solid circles* and *squares* compositions from the Lien and Rödhaugen localities at Almklovdalen, respectively.

Optical determinations of the 2V of olivines from 7 different Ugelvik peridotite samples ranging from garnet-rich to garnet-free assemblages gave positive values of 85–87°, thought to be accurate within ± 1.5°. The compositions of these olivines were, therefore, estimated as being within the range 6–9% Fa ± about 2% Fa.

Measurements of the 2V of orthopyroxenes in 3 of the rock samples gave positive values of 74–75°, estimated to be accurate within ± 1°. The compositions of these orthopyroxenes were, therefore, estimated to be in the range 6–7% Fs ± about 1% Fs.

All 2V determinations were made on the universal stage by direct measurement across the acute bisectrix.

The compositions of the chemically analysed olivine U_{16} 7.6% Fa and the orthopyroxene U_8 7.3% Fs are within the composition ranges determined optically.

The compositions of the minerals of rock specimen U_6 are rather exceptional in many respects when compared with the compositions of the minerals from the other analysed Ugelvik assemblages.

The garnet of U_6 is more calcic and ferriferous than all the other analysed

Table 4. Mineral analyses

Mineral→	Olivine	Ortho-pyroxene	Clinopyroxenes			Garnets			
Sample No.→	U_{16}	U_8	U_2	U_8	U_6	U_2	U_8	U_6	U_{16}
SiO_2	41.66	*56.46	*53.28	54.00	*53.49	41.81	*40.89	42.04	41.54
TiO_2	0.04	0.13	0.07	0.08	0.34	0.07	0.10	0.28	0.06
Al_2O_3	0.35	1.29	2.60	0.95	3.26	20.90	20.98	20.71	20.43
Cr_2O_3	0.01	0.15	1.53	0.50	1.30	2.77	2.30	2.32	3.58
Fe_2O_3	–	–	0.34	0.54	0.74	1.71	2.40	1.93	2.02
FeO	7.27	5.10	0.99	1.36	0.93	6.56	9.74	6.95	6.75
MnO	0.09	0.10	0.06	0.05	0.04	0.44	0.50	0.42	0.49
NiO	0.40	0.08	n.d.	0.03	0.04	n.d.	0.02	0.01	<0.01
MgO	49.84	36.34	17.44	18.24	16.60	20.44	17.05	20.30	20.76
CaO	0.12	0.35	21.70	23.44	20.97	4.92	6.02	4.79	4.16
Na_2O	n.d.	n.d.	1.99	0.56	2.28	n.d.	n.d.	n.d.	n.d.
K_2O	n.d.	n.d.	n.d.	0.02	0.01	n.d.	n.d.	n.d.	n.d.
Total	99.78	100.00	100.00	99.77	100.00	99.62	100.00	99.75	99.79

Table 4 contd. Structural formulae.

Si^{4+}	1.011	1.941	1.932	1.963	1.935	2.990	2.976	3.010	2.980
Ti^{4+}	0.001	0.003	0.002	0.002	0.009	0.004	0.006	0.015	0.003
Al^{3+}	0.010	0.052	0.111	0.041	0.139	1.762	1.799	1.748	1.727
Cr^{3+}	–	0.004	0.044	0.014	0.037	0.156	0.132	0.131	0.203
Fe^{3+}	–	–	0.009	0.015	0.020	0.092	0.132	0.104	0.109
Fe^{2+}	0.148	0.147	0.030	0.041	0.028	0.392	0.593	0.416	0.405
Mn^{2+}	0.002	0.003	0.002	0.002	0.001	0.027	0.031	0.025	0.030
Ni^{2+}	0.008	0.002	–	0.001	0.001	–	0.001	<0.001	–
Mg^{2+}	1.802	1.862	0.942	0.988	0.895	2.178	1.849	2.166	2.220
Ca^{2+}	0.003	0.013	0.843	0.913	0.813	0.377	0.469	0.367	0.320
Na^{+}	–	–	0.140	0.040	0.160	–	–	–	–
K^{+}	–	–	–	0.001	–	–	–	–	–
O^{2-}	4.000	6.000	6.000	6.000	6.000	12.000	12.000	12.000	12.000
$\frac{Fe \times 100}{Fe+Mg}$	7.6	7.3	Ca 46.4	47.0	46.8	Ca 12.7	15.9	12.4	10.8
		Ca 0.6	Mg 51.9	50.9	51.6	Mg 73.2	62.9	72.8	74.6
		Mg 92.1	Fe^{2+} 1.7	2.1	1.6	Fe^{2+} 13.2	20.2	14.0	13.6
		Fe^{2+} 7.3	%Jadeite 8.7%	%Jadeite 1.1%	%Jadeite 10.3%	Mn 0.9	1.0	0.8	1.0

% Jadeite in clinopyroxenes calculated after formation of $NaFe^{3+}$ and $NaCr^{3+}$

*SiO_2 By difference from 100.00%

+Total iron as FeO.

Ugelvik garnets. Its high CaO content (6.02 wt%) is unusual as it is appreciably higher than the CaO content of all other garnets from garnet peridotites, analysed in the course of this study or by O'Hara & Mercy 1963.

The clinopyroxene of U_6 has appreciably lower Al_2O_3, Cr_2O_3 and Na_2O contents than the other two analysed Ugelvik clinopyroxenes, and appreciably lower Na_2O and Al_2O_3 contents than all the other clinopyroxenes from Norwegian garnet peridotites (O'Hara & Mercy 1963; Carswell 1968).

The low Al_2O_3 content (0.50 wt%) and Na_2O content (0.56 wt%) of this clinopyroxene indicate the low degree of jadeite substitution (1.1%). However, the degree of substitution of Ca Tschermak's molecule calculated after the formation of $NaR^{3+}Si_2O_6$ is not significantly lower than in certain other Norwegian garnet peridotite clinopyroxenes.

The rock type, U_6, has clearly not resulted solely from the mechanical concentration of the minerals present throughout the Ugelvik peridotite mass in which it occurs, because of the mineral composition anomalies involved.

An obvious explanation of the exceptional mineral chemistry of this assemblage is lacking. The rock sample is the most 'eclogitic' of all the analysed Ugelvik garnet peridotites in the sense that it has by far the lowest modal olivine content (about 30% by volume), yet it contains the clinopyroxene with the lowest jadeite content. This is the converse of the situation in the Kalskaret and Almklovdalen garnet peridotites where the most 'eclogitic' assemblages, T 153 and N 75 respectively, contain the clinopyroxenes with the highest jadeite contents.

Perhaps the most feasible explanation of the development of this rock type which can be put forward at present is that some mechanism of metasomatic concentration (wet or dry diffusion) has somehow produced the high CaO and SiO_2 contents of this thin band resulting in the high modal content of clinopyroxene, the abnormally high CaO content of the garnet, and the apparent general 'disequilibrium' distribution of the elements (Al_2O_3, CaO, Cr_2O_3 etc.) among the mineral phases of this assemblage compared with relatively constant distribution ratios of these elements noted among the mineral phases of the other garnet peridotite assemblages.

However, with the above reservations about the mineral compositions of the assemblage U_6, it is apparent that in general the minerals of the Ugelvik peridotites are relatively uniform in composition, being particularly significantly so in $Fe^{2+} - Fe^{3+}/Mg^{2+}$ ratio. Minor variations do, however, occur with respect to certain minor elements, Cr_2O_3 and TiO_2 in particular. The Cr_2O_3 content of the garnets appears to be closely controlled by the total Al_2O_3 content, which in turn controls the modal proportions of garnet in the assemblage. Hence the Cr_2O_3 content of the garnets decreases with increasing modal garnet content. The whole mineral assemblage of sample U_8 is richer in titanium than all the other analysed Ugelvik assemblages.

For the most part, however, it would appear that the mineral layering observed in the Ugelvik peridotite masses may be adequately explained by the sorting (either igneous or later mechanical sorting) of an eclogite facies assemblage (olivine – garnet + clinopyroxene + orthopyroxene) precipitated by igneous crystallization processes.

Both O'Hara & Mercy (1963) and Carswell (1968) have previously outlined the reasons why a similar explanation cannot explain the garnet peridotite layering at Kalskaret and Almklovdalen.

The distribution of Fe and Mg between the coexisting mineral phases, the limited extent of the mutual solubility between the coexisting pyroxenes of

the assemblage U_4, and the low Al_2O_3 contents of both orthopyroxene and clinopyroxene from the Ugelvik garnet peridotites, are comparable with the situation in the Kalskaret and Almklovdalen garnet peridotites.

High pressure experimental melting studies on both synthetic and naturally occurring garnet-orthopyroxene, garnet-clinopyroxene, and orthopyroxene-clinopyroxene pairs (see Davis & Boyd (1966), Boyd & England (1964), and O'Hara & Yoder (1967)) suggest that all these garnet peridotite assemblages have been equilibrated at temperatures well below those at which such assemblages begin to melt. Both O'Hara & Mercy (1963) and Carswell (1968) have advocated the equilibration of the Kalskaret and Almklovdalen garnet peridotite assemblages at subsolidus temperatures perhaps as low as 600–700° C. It would seem that similar temperatures of equilibration may be inferred for the Ugelvik assemblages. Such temperatures are consistent with being the normal regionally attained ones at the top of the mantle. As it seems likely that all these peridotite masses have at some time been at appreciably higher temperatures (it has been postulated that the Kalskaret and Almklovdalen garnet peridotites have been involved in partial melting processes in the mantle, and probably all the mantle passed through a molten phase during the initial earth differentiation processes) they must subsequently have recrystallized at lower temperatures but still at high pressure prior to or perhaps during their emplacement into their present environment.

Based on the thermodynamic treatment of the $Fe^{2+}:Mg^{2+}$ distribution between co-existing pyroxenes and olivine-calcium poor pyroxene (orthopyroxene) given by Bartholomé (1962), Fiala (1966) derived temperatures of approximately 1300° C and 1200° C for the crystallization of the Czech and Almklovdalen garnet peridotites respectively. However, at such temperatures garnet peridotite assemblages containing enstatites with such low Al_2O_3 contents would, according to the data provided by Boyd & England (1964) and Green & Ringwood (1967b), not be expected to form at pressures and depths less than about 40 kilobars and 130 kilometres, respectively.

Furthermore in deriving these temperatures, Fiala added Fe^{3+} to Fe^{2+} while the equilibrium relationship discussed by Bartholomé considered only the diadochy of Fe^{2+} and Mg^{2+} in the coexisting minerals – the addition of Fe^{3+} to Fe^{2+} being unjustified and confusing (Bartholomé 1961).

Bartholomé derived the following relationships to express the equilibrium distribution of Fe^{2+} and Mg^{2+}:

1. For co-existing Ca – poor pyroxene (Ca-p) and Ca-rich pyroxene (Ca-r):

$$Kp(T) = \frac{(Fe^{2+}/Mg^{2+})_{Ca-p}}{(Fe^{2+}/Mg^{2+})_{Ca-r}}$$

2. For co-existing olivine (Ol) and Ca-poor pyroxene (Ca-p):

$$K_{Ol-Ca-p}(T) = \frac{(Fe^{2+}/Mg^{2+})_{Ol}}{(Fe^{2+}/Mg^{2+})^2_{Ca-p}}$$

Table 5. Estimates of the temperature of formation of various garnet peridotite assemblages

	A		B		C		D		E	
Sample No. ↓	K_p	T°c	K_p	T°c	$K_{Ol-Ca-p}$	T°c	$K_{Ol-Ca-p}$	T°c	K_D	Locality
Sklene	1.27	1250	1.41	1100	9.0	1250 or 400	9.4	1300 or 400	0.71	Czech
Holubov	1.19	1350	1.12	1450	9.3	1300 or 400	10.7	1350 or 400	0.89	
N69	1.40	1100	2.21	150	8.6	1250 or 400	11.2	1350 or 350	0.59	Almklovdalen
N70	1.35	1150	1.65	800	10.0	1300 or 400	11.2	1350 or 350	0.60	
N71	1.86	550	1.98	400	–	–	–	–	0.51	
209	1.49	1000	1.76	650	–	–	–	–	0.57	
N23	1.59	850	1.75	700	–	–	–	–	0.57	
T96	1.57	900	2.16	200	6.3	1150 or 550	6.3	1150 or 550	0.46	Kalskaret
U_4	1.46	1000	2.52	−250	–	–	–	–	0.40	Ugelvik
A_1	0.91	1700	1.76	650	10.5	1350 or 350	14.9	1500 or 200	0.57	Kimberlites
A_4	–	–	–	–	17.7	1600 or 100	21.2	1750 or −50	–	
E_1	–	–	–	–	13.7	1450 or 250	23.7	1850 or −150	–	
E_4	–	–	–	–	14.6	1500 or 200	20.2	1700 or 0	–	
A_7	1.27	1250	1.20	1350	16.2	1550 or 150	12.0	1400 or 300	0.83	Bellinzona

In Table 5, column A gives Bartholomé's equilibrium distribution coefficient Kp calculated by adding Fe^{3+} to Fe^{2+} in deriving the Fe/Mg ratios. Column B gives the Kp values calculated considering only Fe^{2+} except in samples N69, T96 and U8 where only total iron values are available for the orthopyroxene (Ca – poor pyroxene phase) and all this iron was assumed to be in the ferrous state. Consideration of the respective temperatures corresponding to these two sets of Kp values, estimated from Bartholomé's curve (1962) giving the dependence of Kp on temperature, shows that in most cases when taking only the Fe^{2+} into account the derived temperatures are significantly lower than those derived by Fiala's method.

The $K_{Ol-Ca-p}$ values and corresponding temperatures in column C were derived from $Fe^{2+} + Fe^{3+}/Mg^{2+}$ ratios, and in column D from Fe^{2+}/Mg^{2+} ratios with the exception of T96 where only total iron values were available for both the olivine and orthopyroxene and all this iron was assumed to be in the ferrous state.

Taking the values in columns B and D as the correct ones, and the temperature in column D which corresponds most closely to that in column B, the following mean temperatures for the formation of these garnet peridotite assemblages may be derived: Czech 1300° C; Almklovdalen 450° C; Kal-

skaret ~ 500° C; Ugelvik – 250° C; kimberlite ~ 150° C; and Bellinzona ~ 1400° C.

There are obviously several anomalous temperature values amongst these figures. Furthermore, it is exceedingly unlikely that these various garnet peridotite assemblages, similar in many respects, were formed over such a wide range of temperature. It is, therefore, apparent that this theoretical approach does not in general provide reliable temperature data.

Also given in Table 5 in column E are the values of the equilibrium distribution coefficient K_D derived by Kretz (1961) to express the distribution of Fe^{2+} and Mg^{2+} between coexisting pyroxenes. Kretz's approach was essentially analogous to that of Bartholomé; in fact K_D is the inverse of the K_p relationship.

$$K_D = \frac{(Mg\ Mg + Fe^{2+})Ca\text{–}p}{(Fe^{2+}\ Fe^{2+} - Mg)Ca\text{–}p} \times \frac{(Fe^{2+}\ Fe^{2+} + Mg)Ca\text{–}r}{(Mg\ Mg - Fe^{2+})Ca\text{–}r}$$

$$= \frac{Fe^{2+}\ Mg^{2+}\ Ca\text{–}r}{Fe^{2+}\ Mg^{2+}\ Ca\text{–}p} = \frac{1}{Kp}$$

The K_D values similarly show a wide variation (0.40–0.89) corresponding, according to Kretz's interpretation, to crystallization temperatures ranging from above those of gabbros (K_D 0.73) to below those of granulites (K_D 0.54).

O'Hara & Mercy (1963) have pointed out several complicating factors which may invalidate the use of the ideal theoretical Fe^{2+}/Mg^{2+} distribution relationships in natural rock systems for the determination of reliable crystallization temperature data. Although Kretz considered that the differences in K_D values for coexisting pyroxenes were primarily a function of temperature and therefore could be used in determining some estimate of crystallization temperature, he himself demonstrated on theoretical grounds that such distribution coefficients are dependent not only on temperature but also on pressure and compositional differences.

Petrogenesis

In Table Nos. 6–9 the mineral compositions in the Ugelvik garnet peridotites (excepting the mineral assemblage U6) are compared with the available mineral data from other garnet peridotite occurrences.

From Table 6, it is apparent that the Ugelvik garnets are compositionally very similar to those from peridotite nodules in kimberlite pipes both in S. Africa and U.S.S.R. and also to those from peridotite lenses in the Czech Massif. Garnets from the Kalskaret and Almklovdalen garnet peridotites are, on the average, considerably more ferriferous and contain much less chromium. They are also far more variable in $Fe^{2+} + Fe^{3+}/Mg^{2+}$ ratio. The chromium contents of the garnets from the kimberlite, Ugelvik and Czech peridotites are higher but show considerable variations depending on the modal content of garnet in the rock. Fig. 5, which is a $Cr^{3+} : Mg^{2+} : Fe^{2+} + Fe^{3+}$ plot

Table 6. Means and standard deviations of garnet compositions from garnet peridotites

	1	2	3	4	5	6	7	8	9	10
Ca^{2+}	12.0	12.8	11.8	13.0	14.6	13.4	12.4	1.8	12.3	1.2
Mg^{2+}	73.5	73.3	72.1	68.0	76.0	72.0	72.6	2.4	62.5	5.3
Fe^{2+}	13.6	13.2	15.5	18.7	9.0	14.1	14.3	2.6	24.3	4.9
Mn^{2+}	0.9	0.7	0.6	0.3	0.4	0.5	0.7	0.2	0.9	0.2
Cr_2O_3 wt.%	2.89	3.67	1.99	1.40	3.08	–	2.62	1.73	0.59	0.33
$\frac{Fe^{2+} + Fe^{3+}}{Mg^{2+}}$	0.231	0.203	0.229	0.285	0.228	–	0.226	0.028	0.453	0.144

1. Mean of 3 determinations from Ugelvik (U$_6$ garnet excluded)
2. Mean of 8 determinations from South African kimberlite pipes – analyses from O'Hara & Mercy (1963); Nixon et al. (1963) – E_4 garnet excluded owing to the doubts cast about this assemblage by O'Hara & Yoder (1967); and MacGregor & Ringwood (1964)
3. Mean of 12 determinations from the Czech Massif – analyses from Fiala (1965, 1966); and Mikhailov & Rovsha (1966)
4. Mean of 2 determinations from Bellinzona – analyses from Grubenmann (1908); and O'Hara & Mercy (1963)
5. Mean of 2 determinations from Yakutia kimberlite pipes – analyses from Mikhailov & Rovsha (1966)
6. Mean of 15 determinations from Siberian kimberlite pipes – analyses from Sobolev, the mean value being quoted from Fiala (1965)
7. Mean of the 27 determinations listed in columns 1–5
8. Standard deviation of these 27 determinations
9. Mean of 12 determinations from Kalskaret and Almklovdalen – analyses from Eskola (1921); Lappin (1962); O'Hara & Mercy (1963); and Carswell (1968)
10. Standard deviation of these 12 determinations

of the garnet compositions, also demonstrates the restricted range of garnet compositions from the kimberlite, Ugelvik and Czech garnet peridotites while the compositions of the garnets from the Kalskaret and Almklovdalen peridotites trend towards those of garnets in eclogite nodules from kimberlite pipes. This trend is thought to be significant in terms of the postulated origin of the composition variations among the Kalskaret and Almklovdalen garnet peridotites (see Carswell 1968) – namely that they have been involved in partial melting processes in the mantle.

Table 7 similarly demonstrates that the clinopyroxenes from the kimberlite, Ugelvik and Czech garnet peridotites also show limited compositional variation, while those from the Kalskaret and Almklovdalen garnet peridotites have higher mean and more variable $Fe^{2+} - Fe^{3+}/Mg^{2+}$ ratios and contain less chromium. The latter trend in composition towards the clinopyroxenes from eclogite nodules in kimberlites (such as E_4 & E_{16} in Nixon et al. 1963, and 37079 in O'Hara & Yoder 1967).

The olivine compositions in Table 8 again indicate a chemical similarity between the Ugelvik garnet peridotites and those which occur as nodules in kimberlite pipes, while the olivines from the Czech and Bellinzona garnet peridotites are only slightly more ferriferous. Olivines from the Kalskaret and

Almklovdalen garnet peridotites have higher and more variable fayalite contents.

Finally the orthopyroxene composition data in Table 9 demonstrates much the same relationship as the olivine data. The orthopyroxenes from the Ugelvik and kimberlite garnet peridotites are essentially similar compositionally, those from the Czech and Bellinzona garnet peridotites slightly more ferriferous, and those from Kalskaret and Almklovdalen distinctly more so and also more variable compositionally.

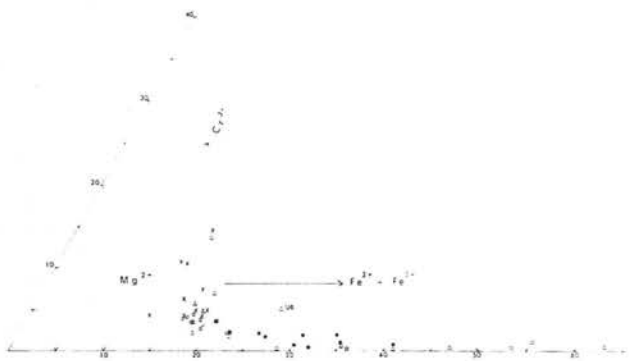

Fig. 5. Cr^{3+}:Mg^{2+}:Fe^{2+} – Fe^{3+} plot of garnet compositions.
Triangles – Ugelvik garnet peridotites
Crosses – Garnet peridotite nodules from kimberlite pipes
Open circles – Czech garnet peridotites
Solid circles – Kalskaret and Almklovdalen garnet peridotites
Solid squares – Bellinzona garnet peridotites
Open squares – Eclogite nodules from kimberlite pipes (Wagner 1914, Williams 1932, Nixon et al. 1963, O'Hara & Yoder 1967)

It is, therefore, apparent that the range of mineral compositions (excepting U_6) from the Ugelvik garnet peridotites is closely analogous to those of the garnet peridotite nodules in kimberlite pipes and also in large measure to those of the garnet peridotites from Bellinzona and the Czech Massif, while the mineral assemblages of these garnet peridotites as a group can be demonstrated to be chemically distinct from those of the Kalskaret and Almklovdalen garnet peridotites as a group.

Furthermore, a consideration of the bulk rock chemical data in Table 10 appears to substantiate the similarities and distinctions just drawn between garnet peridotites from the various occurrences. The garnet peridotites from kimberlite pipes, Ugelvik, Bellinzona and the Czech Massif show only restricted chemical variations, significantly so in Fe/Mg ratio, and as a group are characterised by low Al_2O_3 and CaO contents reflecting the low modal

Table 7. Means and standard deviations of clinopyroxene compositions from garnet peridotites

	1	2	3	4	5	6	7	8	9
Ca^{2+}	46.6	44.7	43.4	43.2	45.6	44.7	2.1	47.9	1.7
Mg^{2+}	51.8	52.4	52.1	53.3	51.7	52.2	1.8	48.7	1.5
Fe^{2+}	1.6	2.9	4.5	3.4	2.7	3.1	1.3	3.4	1.1
Cr_2O_3 wt.%	1.42	1.96	1.06	0.88	1.94	1.52	0.62	0.38	0.21
$\frac{Fe^{2+} - Fe^{3+}}{Mg^{2+}}$	0.048	0.089	0.092	0.078	0.092	0.082	0.019	0.102	0.035

1. Mean of 2 determinations from Ugelvik (U_6 clinopyroxene excluded)
2. Mean of 3 determinations from South African kimberlite pipes – analyses from O'Hara & Mercy (1963); Nixon et al. (1963) – E_1 clinopyroxene excluded; and MacGregor & Ringwood (1964)
3. Mean of 3 determinations from the Czech Massif – analyses from Fiala (1966); and Mikhailov & Rovsha (1966)
4. 1 determination from Bellinzona – analysis from O'Hara & Mercy (1963)
5. Mean of 2 determinations from Yakutia kimberlite pipes – analyses from Mikhailov & Rovsha (1966)
6. Mean of 11 determinations listed in columns 1–5
7. Standard deviation of these 11 determinations
8. Mean of 12 determinations (only 8 of Cr_2O_3 wt.%) from Kalskaret and Almklovdalen – analyses from Eskola (1921); Lappin (1962); O'Hara & Mercy (1963); and Carswell (1968)
9. Standard deviation of these 12 (8) determinations

Table 8. Means and standard deviations of olivine compositions from garnet peridotites

	1	2	3	4	5	6	7	8	9
$Fa\% = \frac{Fe \times 100}{Fe + Mg}$	7.6	7.4	10.1	9.3	8.3	8.4	1.3	13.7	3.6

1. 1 determination from Ugelvik
2. Mean of 5 determinations from South African kimberlite pipes – analyses from Nixon et al. (1963); and Mercy & O'Hara (1965b)
3. Mean of 3 determinations from the Czech Massif – analyses from Fiala (1966); and Mikhailov & Rovsha (1966)
4. 1 determination from Bellinzona – analysis from Mercy & O'Hara (1965b)
5. 1 determination from Yakutia kimberlite pipe – analysis from Mikhailov & Rovsha (1966)
6. Mean of the 11 determinations listed in columns 1–5
7. Standard deviation of these 11 determinations
8. Mean of 4 determinations from Kalskaret and Almklovdalen – analyses from Mercy & O'Hara (1965b); and Carswell (1968)
9. Standard deviation of these 4 determinations

garnet and clinopyroxene contents. The Kalskaret and Almklovdalen garnet peridotites on the other hand contain higher mean and more variable Al_2O_3 and CaO contents and Fe/Mg ratios.

Consideration of the mineralogy and field relations of the garnet peridotites

Table 9. Means and standard deviations of orthopyroxene compositions from garnet peridotites

	1	2	3	4	5	6	7	8
$Fs^{o}_{o} = \frac{Fe \times 100}{Fe + Mg}$	7.3	6.7	10.2	9.0	7.6	1.5	12.9	3.6

1. 1 determination from Ugelvik
2. Mean of 7 determinations from South African kimberlite pipes – analyses from Nixon et al. (1963) – excluding E_3 orthopyroxene; MacGregor & Ringwood (1964); and Mercy & O'Hara (1965b)
3. Mean of 2 determinations from the Czech Massif – analyses from Fiala (1966)
4. 1 determination from Bellinzona – analyses from Mercy & O'Hara (1965b)
5. Mean of the 11 determinations listed in columns 1–4
6. Standard deviation of those 11 determinations
7. Mean of 7 determinations from Kalskaret and Almklovdalen – analyses from Lappin (1962); Mercy & O'Hara (1965b); and Carswell (1968)
8. Standard deviation of these 7 determinations

which occur in the Norwegian gneisses at Kalskaret and Almklovdalen, and those which occur as nodules in kimberlite pipes, led O'Hara & Mercy (1963) to the conclusion that.. 'both types of garnet peridotite are derived from the mantle, but only the nodules in kimberlite can be representative of the unmodified compositions of the upper mantle'.

This author endorsed their conclusion that the Kalskaret and Almklovdalen garnet peridotite from the Norwegian gneisses as a group are unlikely representatives of unmodified upper mantle material, but postulates that the Ugelvik garnet peridotite masses can be correlated both chemically and mineralogically with the garnet peridotites which occur as nodules in kimberlite pipes and that the restricted range of bulk and mineral compositions among the kimberlite and Ugelvik garnet peridotites (and possibly also those from the Czech Massif and from Bellinzona) as a group indicates that they are all possibly representative of primary upper mantle material.

The average modes of the kimberlite, Ugelvik, Czech and Bellinzona garnet peridotites are listed in Table 11, where they can be compared with the mean modal composition of analysed garnet peridotites from the Kalskaret and Almklovdalen localities in Norway. Those from the latter localities clearly have much higher mean garnet and clinopyroxene contents and correspondingly lower olivine and to a lesser extent orthopyroxene contents.

The Ugelvik and Czech peridotites do, however, have lower modal orthopyroxene/olivine ratios than the peridotite nodules in kimberlite pipes described by Wagner (1914), Williams (1932), Holmes (1936), Dawson (1962), Nixon et al. (1963) and O'Hara & Mercy (1963). This may be at least partly attributed to errors in the estimation of the primary modes, resulting from the more extensive fracturing during emplacement and subsequent serpentinization of the Ugelvik and Czech peridotites (see pages 347–52). The serpentinization recalculations suggest mean modal orthopyroxene contents of about 15% by weight in garnet peridotites U_2, U_8 and U_{16}.

Table 10. Means and standard deviations of garnet peridotite bulk rock compositions (recalculated anhydrous and with total iron as FeO)

Wt. %	1	2	3	4	5	6	7	8	9
SiO_2	44.65	45.52	44.07	44.72	44.44	44.66	0.96	46.60	1.71
TiO_2	0.08	0.18	0.17	0.14	0.34	0.19	0.19	0.32	0.18
			(Mean of 3)			(Mean of 17)			
Al_2O_3	3.50	2.42	2.50	3.09	3.06	2.80	1.36	8.11	3.43
Cr_2O_3	0.59	0.33	0.54	0.40	0.33	0.45	0.21	0.34	0.14
		(Mean of 3)				(Mean of 18)			
FeO	6.81	7.32	8.97	8.30	7.76	7.92	1.21	9.99	2.52
MnO	0.14	0.13	0.12	0.13	0.08	0.12	0.04	0.18	0.03
			(Mean of 4)	(1 determ)	(Mean of 2)	(Mean of 15)			
NiO	0.29	0.23	–	0.28	0.46	0.31	0.10	0.17	0.08
		(Mean of 3)		(1 determ)	(Mean of 2)	(Mean of 9)			
MgO	41.66	41.74	41.07	39.88	39.87	40.97	2.84	25.88	5.86
CaO	2.02	2.04	2.60	3.16	3.42	2.59	1.31	7.65	2.21
Na_2O	0.23	0.18	0.43	0.24	0.52	0.30	0.31	0.74	0.20
		(Mean of 4)	(1 determ)	(1 determ)	(Mean of 3)	(Mean of 12)			
K_2O	0.04	0.17	0.04	0.00	0.17	0.12	0.14	0.02	0.01
			(1 determ)	(1 determ)	(Mean of 3)	(Mean of 13)			
Fe/Mg	0.093	0.099	0.123	0.126	0.110	0.109	0.020	0.226	0.080

1. Mean of 3 determinations from Ugelvik (U_2, U_8 and U_{16})
2. Mean of 5 determinations (except where stated otherwise) from South African kimberlite pipes – analyses E_3 and E_{11} from Nixon et al. (1963); No. 370 from Williams (1932); A_3 and A_6 – O'Hara & Mercy personal communication
3. Mean of 6 determinations from the Czech Massif – analyses from Fiala (1965, 1966); and Mikhailov & Rovsha (1966)
4. Mean of 2 determinations from Bellinzona – analyses from Grubenmann (1908); and O'Hara & Mercy (1966b)
5. Mean of 4 determinations from Yakutia kimberlite pipes – analyses from Mikhailov & Rovsha (1966); and Kryukov (1966)
6. Mean of the 20 determinations listed in columns 1–5
7. Standard deviation of these 20 determinations
8. Mean of 14 determinations from Kalskaret and Almklovdalen – analyses from Mercy & O'Hara (1965a); and Carswell (1968)
9. Standard deviation of these 14 determinations

Consideration of the garnet composition data for the Norwegian, Czech and kimberlite garnet peridotite occurrences indicates that the Cr_2O_3 contents are much more variable than the $Ca^{2+}:Mg^{2+}:Mn^{2+}:Fe^{2+}$ ratios, and, therefore, do not provide such a reliable composition index for distinction between different groups of garnet peridotites. The limited analytical data so far available show that the garnets from the Ugelvik and kimberlite peridotites have significantly higher Cr_2O_3 contents than those from the Kalskaret and Almklovdalen peridotites and also higher Cr_2O_3 than most, but not all, garnets from the Czech peridotites (Fiala (1965) recorded one garnet with 6.85 wt. % Cr_2O_3).

Such minor chemical variations as there are amongst the postulated pri-

Table 11. Means of modal analyses of garnet peridotites

	1	2	3	4	5	6
Olivine + serpentine	76	53	71	40	59	24
Orthopyroxene	7	30	14	15	23	7
Clinopyroxene	4	9	6	26	9	32
Garnet	12	8	9	15	9	24
Amphibole	–	–	–	5	–	12
Others	1	–	–	–	–	1

1. Mean of 3 determinations from Ugelvik (U_2, U_8 & U_{16})
2. Mean of 11 determinations from South African kimberlite pipes – data from Nixon et al. (1963); and O'Hara & Mercy (1963)
3. Mean of 2 determinations from the Czech Massif – data from Fiala (1966)
4. 1 determination from Bellinzona – data from O'Hara & Mercy (1963)
5. Mean of the 17 determinations in columns 1–4
6. Mean of 14 determinations from Kalskaret and Almklovdalen – data from Mercy & O'Hara (1965a); and Carswell (1968)

mary upper mantle garnet peridotites (for example the lower mean Cr_2O_3 contents of the Czech garnets and clinopyroxenes, the lower $Fe^{2+}+Fe^{3+}/Mg^{2+}$ ratios in the Ugelvik clinopyroxenes, and the higher $Fe/Fe+Mg$ ratios of the olivines and orthopyroxenes in the Czech specimens) are considered to be within the range of chemical inhomogeneities one might expect in such mantle material. It would certainly be incredible if such mantle material was perfectly homogeneous chemically.

It is, therefore, apparent that the distinction drawn by O'Hara & Mercy (1963, 1966a) between garnet peridotites which occur as xenoliths in kimberlite pipes (and were considered possibly to be representative of primary mantle

Table 12.

	1	2	3	4
SiO_2	44.65	44.66	43.25	45.16
TiO_2	0.08	0.19	–	0.71
Al_2O_3	3.50	2.80	3.90	3.54
Cr_2O_3	0.59	0.45	–	0.43
Fe_2O_3	–	–	–	0.46
FeO	6.81	7.92	9.25	8.04
MnO	0.14	0.12	–	0.14
NiO	0.29	0.31	–	0.20
MgO	41.66	40.97	38.10	37.47
CaO	2.02	2.59	3.72	3.08
Na_2O	0.23	0.30	1.78	0.57
K_2O	0.04	0.12	–	0.13
CoO	–	–	–	0.01
P_2O_5	–	–	–	0.06
Total	100.00	100.00	100.00	100.00
Fe/Mg	0.093	0.109	0.136	0.127

material) and 'crustal' garnet peridotites has become obscured as data has become available on the Ugelvik and Czech garnet peridotites. The present author considers that the true distinction to be made between the various types of garnet peridotites observed at the earth's surface is rather between *primary* upper mantle material and *modified* upper mantle material, irrespective of the environment in which it now occurs.

Both the barren residual garnet-free peridotites and the enriched garnet peridotites with high modal garnet and clinopyroxene contents are considered here to represent modified upper mantle material.

With only sparse chemical data available, the status of the garnet peridotites from Bellinzona is somewhat obscure, although they are tentatively grouped in this paper with the postulated primary upper mantle garnet peridotites.

In Table 12, column 1 gives the mean composition of the analysed Ugelvik garnet peridotites (U_6 excluded), column 2 the mean composition of all the postulated primary upper mantle garnet peridotites (column 6 – Table 10), column 3 the mantle composition derived by Ringwood (1966) from the chondrite meteorite model, and column 4 the hypothetical mantle pyrolite composition derived by Ringwood (1965) on the assumption that the primary mantle peridotite composition must be capable of yielding a basaltic composition partial melt and a dunitic or peridotitic residual.

It is apparent that there is a close but by no means perfect chemical similarity between the garnet peridotite compositions and those derived from the chondrite and pyrolite models. There are quite significant discrepancies in Fe/Mg ratio, TiO_2, CaO, and Na_2O contents between these compositions. However, the compositions derived from the chondrite and pyrolite models are hypothetical and can only be expected to give an indication of the approximate mantle composition. The significance of these hypothetical compositions lies in the fact that combined with the petrological evidence they indicate that the likely primary upper mantle material is expected to be a garnet peridotite with comparatively low modal proportions of garnet and clinopyroxene. The thesis put forward in this paper is that since the garnet peridotites from kimberlite pipes, Ugelvik, the Czech Massif and Bellinzona represent just such rock types and show only very restricted chemical variations as a group, then a good case can be made out for them representing fragments of essentially chemically uniform primary upper mantle material.

Perhaps the most disturbing discrepancy from the chondrite and pyrolite mantle compositions lies in the low alkali contents of the postulated primary upper mantle garnet peridotites, which might appear to raise a major problem concerning the generation of basaltic liquids by the partial fusion of such peridotitic material. Furthermore, the mean alkali content figures quoted in Column 2, Table 12 are probably rather high for those of the fresh garnet peridotite material. Consideration of the range of Na_2O and K_2O contents in the garnet peridotite compositions used for calculating the mean figures indicates that certain of the garnet peridotite nodules from kimberlite pipes

seem to have been contaminated with K_2O from the potassic kimberlite environment, while some of the garnet peridotites which form crustal tectonic slices appear to have picked up K_2O and/or Na_2O from their crustal environment during serpentinization and partial metamorphic retrogression.

Reliable analyses of alkali contents in fresh garnet peridotite nodules from kimberlites are exceedingly scarce. Probably the best available are those quoted by Nixon et al. (1963) for two nodules from Basutoland kimberlites. They note Na_2O contents of 0.24% and 0.18%, and K_2O contents of 0.00 and 0.06%. The low Na_2O and K_2O contents of the constituent minerals from garnet peridotite nodules in kimberlites (O'Hara & Mercy 1963) suggest similarly low bulk rock Na_2O and K_2O contents. Recent bulk rock analyses of two such garnet peridotites (A_3 and A_6) show Na_2O contents of 0.10 and 0.19% (O'Hara & Mercy, personal communication).

It appears likely that the alkali contents of uncontaminated garnet peridotite nodules from kimberlites are of the same order as those found in the Ugelvik peridotites, and that the alkali contents in primary upper mantle garnet peridotite material probably average about 0.20 – 0.25% Na_2O and 0.01–0.05% K_2O.

Tholeiitic basalts, the common basaltic type lowest in alkalies, contain about 2% Na_2O and 0.7% K_2O, while alkali basalts contain considerably greater concentrations. It would, therefore, require some 10 to 20 times concentration at the very least to generate the alkali content of even the low alkali tholeiitic basalt magmas from the partial melting of the postulated primary upper mantle material.

Hamilton & Mountjoy (1965) have discussed the low alkali contents of alpine-type peridotites, which they consider preclude such material as being representative of upper mantle material, from which basalt magma might be derived. However, the alkali contents of these peridotites are appreciably lower than those of the garnet peridotites considered here. They noted median values of 0.004% Na_2O and 0.003% K_2O for 40 analyzed alpine-type peridotite specimens. They suggested that such peridotites have originated either as magmatic crystal precipitates or as mantle residues left after fusion and removal of basalt magmas, a conclusion with which this author would fully concur.

This author knows of no analyses of fresh peridotites of suitable upper mantle mineralogy and composition with higher alkali contents than the garnet peridotites considered here. It is thought that basically two processes may have been involved in producing the remarkable concentration of alkalies observed in basalt magmas compared with the alkali contents of the postulated upper mantle source rocks. First, partial melting in the mantle may involve a 'sweating out' of the low melting fraction of the source rocks, in particular of alkalies. Secondly, the occurrence during transit to the surface of such partial melts of such fractionation processes as outlined by O'Hara (1965) would be expected to result in further appreciable concentration of alkalies in the extruded basalt magmas.

It is, therefore, considered that the relatively low alkali contents of the garnet peridotites under consideration do not preclude such material as possible primary upper mantle material.

Conclusions

Field relationships indicate that the Ugelvik peridotite masses have been tectonically emplaced into a gneiss complex which reached granulite facies grade but was subsequently partially retrograded to almandine-amphibolite facies grade.

Peridotites with low modal proportions of garnet and clinopyroxene probably comprise somewhat more than half the total volume of the peridotite masses exposed here, being interlayered with garnet free peridotites.

These peridotites do not show the extensive mineral and bulk rock chemical variations present among the Kalskaret and Almklovdalen garnet peridotites. The mineral layering within the Ugelvik peridotites (with the exception of the rather anomalous assemblage U_6) may be adequately explained by minor sorting of an eclogite facies assemblage precipitated by igneous crystallization processes. There are, in fact, two possibilities regarding this igneous crystallization. It may have occurred following the mantle melting differentiation process considered by many (e.g. Ringwood 1966) as likely to have followed the terrestrial accretion process, or alternatively it may have occurred through the crystallization of isolated bodies of magma (produced from the mantle) in the upper levels of the mantle. In either case these peridotites are considered to have been derived from the mantle, but in the former case they would represent more primitive mantle material.

The former case is, in fact, preferred here in view of the fact that the Ugelvik garnet peridotites, together with the garnet peridotite nodules in kimberlites and also those from the Czech Massif and from Bellinzona in Switzerland, are mineralogically and chemically suitable as primary upper mantle peridotite representatives in the light of their mineralogical and chemical similarity as a group, and their compatibility with likely mantle compositions suggested by the chondrite meteorite and pyrolite models.

Although it is considered that the Ugelvik garnet peridotites represent fundamentally primary mantle material, it is recognised that they have been modified both by recrystallization and equilibration at subsolidus temperatures (perhaps as low as 600–700° C) which were probably the regionally attained temperatures at the top of the mantle but perhaps temperatures attained during tectonic emplacement into their present environment, and by serpentinization and partial metamorphic retrogression.

On the problem of serpentinization

The serpentinization of peridotites has for long been a controversial subject both as regards the origin of the water producing the reaction and the

nature of the reaction involved (see Turner & Verhoogen 1960, pp. 316–21). In particular, it is uncertain whether the reaction involved is principally a constant volume reaction, involving addition of H_2O and leaching of MgO, FeO, SiO_2 etc., or a constant composition reaction, involving addition of H_2O without leaching and hence a large volume increase.

Thayer (1966) has recently argued the case for serpentinization being essentially a constant volume metasomatic process which requires the removal of about 30% by weight of the original bivalent oxides and SiO_2 in the peridotite.

Green (1964) considering the serpentinization of the Lizard peridotite favoured the hypothesis of 'constant composition serpentinization'.

Hostetler et al. (1966) have drawn attention to the importance of serpentinization reactions producing brucite as a by-product. They considered that volume increases of 35–40% were common during serpentinization and that there was little evidence to substantiate large scale migration of MgO out of the peridotites. Leaching of SiO_2 was considered on thermodynamic grounds even more unplausible as it would call for a chemical potential gradient for SiO_2 away from the markedly SiO_2 undersaturated ultrabasic rocks into more siliceous country rocks.

If the serpentinization is principally a constant composition reaction with addition of water and without significant leaching of other components, then the straightforward anhydrous recalculation of the bulk rock analysis should be in reasonably good agreement with the bulk rock composition calculated using the mineral analyses and the estimated modal proportions of the minerals. This has been tested for the various analysed Ugelvik samples.

In none of the analysed samples have all the constituent minerals been analysed. Mineral analyses and optical determinations on minerals from the suite of Ugelvik rock types indicate, with the exception of U_6, only minor compositional differences, especially in major element content, e.g. Fe/Fe + Mg ratio. Therefore, where necessary, mineral compositions from as closely identical rock types as possible have been used in the calculation of the bulk rock composition. The compositions of the analysed minerals are assumed to represent the original mineral compositions in the unserpentinized peridotites.

Minor amounts of an opaque ore mineral, considered likely to be a chrome spinel, occur in most of the analysed samples. Unfortunately, in none of the samples was it present in large enough amounts to be separated and analysed. However, the composition of a chrome spinel from serpentinite quoted by Deer, Howie & Zussman 1962, Vol. 5, Table 11, No. 8 was considered to give a reasonable approximation and was, therefore, used in the calculations.

A further problem arises regarding the estimation of the proportions by weight of the constituent minerals. The S.G. of the garnet is about 3.7, that of the olivine and both pyroxenes about 3.3. With only small amounts of garnet, differences between the modal proportions by weight and those by volume are within the estimated error of the point-counting technique (± 10–

15% of the value given, in particular for low concentrations). The cataclastic textures, variable grain sizes and partial serpentinization are not conducive to accurate estimations of modes of these rocks by point counting. The volume proportions determined by point counting are given in Table 1, and were used as a first approximation in the calculation of the bulk rock compositions.

In Table 13, column A in each case represents the straightforward water free recalculation of the whole rock analysis with the Fe_2O_3 content recalculated as FeO. Column B in each case represents the whole rock composition calculated using the mineral proportions quoted in Table 1.

It is notable that in all but one case, namely U_3, the analysis in column B has a significantly higher $MgO - FeO/SiO_2$ ratio than that in column A. There seem to be three possible explanations of this discrepancy.

1. Inaccuracies in the estimation of the primary modal proportions of the minerals of these samples,
2. Serpentinization has involved leaching of MgO and FeO with respect to SiO_2,
3. Serpentinization involved the introduction of SiO_2 as well as H_2O without any leaching.

Each of these possibilities may be considered in turn:

1. The primary modal contents of garnet, clinopyroxene and chrome spinel are closely restricted by the present CaO, Al_2O_3, and Cr_2O_3 contents (if no leaching of these elements has occurred). Therefore, considerable underestimation or overestimation of the modal proportions of these minerals can be ruled out.

Considerable underestimation of the orthopyroxene/olivine ratio in the mode is far more of a possibility, however. The extensive cataclastic textures followed by partial or complete serpentinization of both olivine and orthopyroxene in these rocks makes it exceedingly difficult in most cases to estimate accurately the relative proportions of these minerals in the original assemblages. When point counting, the serpentine was considered to be after olivine unless there was clear evidence of relics of orthopyroxene.

In Table 13, column C represents a whole rock analysis calculated from the mineral analyses after adjusting the mineral proportions so as to derive an analysis which corresponds as closely as possible with that of column A in each case. Firstly, minor adjustments were made where necessary in the proportions of garnet, clinopyroxene and chrome spinel so as to fix the Al_2O_3, Cr_2O_3 and CaO contents, then the relative proportions of olivine and orthopyroxene were fixed so as to give a $MgO + FeO/SiO_2$ ratio in the resultant whole rock analysis which closely corresponds to that in column A. The adjusted modal proportions are given in Table 13. Considering the fact that in several cases the mineral analyses used in the calculation where only those of minerals from associated rock samples (in the case of the chrome spinel from a totally unrelated sample), the correlation between columns A and C for most ele-

Table 13. Peridotite pre-serpentinization compositions

Sample No.	846/U_2			847/U_3			848/U_6			849/U_8			850/U_{16}		
	A	B	C	A	B	C	A	B	C	A	B	C	A	B	C
SiO_2	44.37	42.17	44.02	42.86	42.53	42.94	50.95	48.64	50.52	46.32	44.09	46.16	43.26	42.12	43.21
TiO_2	0.01	0.05	0.06	0.005	0.05	0.05	0.07	0.08	0.08	0.22	0.14	0.16	0.01	0.05	0.05
Al_2O_3	2.24	2.30	2.24	0.15	1.29	0.65	3.81	3.81	3.94	6.69	6.06	6.71	1.56	2.04	1.66
Cr_2O_3	0.37	0.47	0.48	0.20	0.48	0.14	0.73	0.60	0.60	1.04	0.94	1.06	0.37	0.46	0.32
FeO	6.82	7.28	6.91	6.95	7.32	7.15	6.51	5.26	5.16	6.64	6.98	6.51	6.96	7.38	7.21
MnO	0.11	0.11	0.11	0.12	0.10	0.09	0.16	0.13	0.14	0.18	0.17	0.17	0.12	0.11	0.11
NiO	0.32	0.35	0.31	0.36	0.36	0.37	0.12	0.14	0.11	0.21	0.24	0.19	0.34	0.35	0.35
MgO	44.35	46.33	44.48	49.22	47.73	48.47	26.63	29.05	28.32	33.82	37.80	34.18	46.81	47.02	46.95
CaO	1.18	0.90	1.31	0.06	0.14	0.14	10.71	12.02	10.89	4.46	3.35	4.52	0.42	0.38	0.34
Na_2O	0.16	0.04	0.08	0.07	–	–	0.29	0.26	0.23	0.40	0.23	0.34	0.12	–	–
K_2O	0.07	–	–	0.01	–	–	0.02	0.01	–	0.02	–	–	0.03	–	–
Total	100.00	100.00	100.00	100.00	100.00	100.00	100.00	100.00	100.00	100.00	100.00	100.00	100.00	100.00	100.00
$\frac{MgO+FeO}{SiO_2}$	1.15	1.27	1.17	1.31	1.29	1.30	0.65	0.71	0.66	0.87	1.02	0.88	1.24	1.29	1.25

ments is quite satisfactory. The worst discrepancies occur with the TiO_2 and alkali contents. The TiO_2 discrepancies are in large measure explicable by the highly variable distribution of TiO_2 amongst these 5 samples. All the minerals of assemblage U_8 are markedly more titaniferous than corresponding minerals in the other samples. The lower Na_2O contents of the whole rock analyses calculated from the mineral analyses are in large measure the result of the alkali contents of the minerals having been determined only for the clinopyroxenes, rather than Na_2O having been introduced in significant amounts during serpentinization. A case for the introduction of minor amounts of K_2O during secondary alteration of the primary assemblages can be made out, however.

Following a further study of the thin sections of these rock samples it was decided that the adjusted modal mineral proportions, in particular with respect to the envisaged changes in orthopyroxene/olivine ratio, were in fact quite feasible for the primary mineral assemblages. Furthermore, the high orthopyroxene content (about 35% by volume) of one relatively uncataclased and unserpentinized Ugelvik garnet lherzolite (U_{10}) suggests that some of the more highly cataclased and serpentinized peridotites may originally have had somewhat higher orthopyroxene contents than is now obvious.

2. At first it was thought that the figures shown in columns A and B, Table 13 provided strong evidence in favour of the leaching of significant amounts of MgO and FeO with respect to SiO_2 durtng the serpentinization of these peridotites. However, as argued in the last section, it is now considered that the $MgO+FeO/SiO_2$ ratio discrepancies may well just be attributable to underestimation of the orthopyroxene/olivine ratio in the original mineral assemblages.

Explanation of Table 13

846/U_2

Mineral compositions used in the calculation of the whole rock analyses (B&C) were: garnet U_2, clinopyroxene U_2, orthopyroxene U_8, olivine U_{16}, chrome spinel (Deer, Howie & Zussman 1962, Vol. 5, Table 11, No. 8).

Estimated modal proportions by weight in the original assemblage used for calculating analysis C were: olivine 74%, orthopyroxene 15%, clinopyroxene 4%, garnet 6%, chrome spinel 1%.

847/U_3

Mineral compositions used in the calculations were: olivine U_{16}, orthopyroxene U_8, chrome spinel (Deer, Howie & Zussman 1962, Vol. 5, Table 11, No. 8).

Estimated modal proportions by weight in the original assemblage used for calculating analysis C were: olivine 90%, orthopyroxene 9.5%, chrome spinel 0.5%.

848/U_6

Mineral compositions used in the calculations were: garnet U_8, clinopyroxene U_6, orthopyroxene U_8, olivine U_{16}.

Estimated modal proportions by weight in the original assemblage used for calculating analysis C were: olivine 18%, orthopyroxene 25%, clinopyroxene 42%, garnet 15%.

849/U_8

Mineral compositions used in the calculations were: garnet U_8, clinopyroxene U_8, orthopyroxene U_8, olivine U_{16}, chrome spinel (Deer, Howie & Zussman 1962, Vol. 5, Table 11, No. 8).

Estimated modal proportions by weight in the original assemblage used for calculating analysis C were: olivine 38%, orthopyroxene 20%, clinopyroxene 15%, garnet 26%, chrome spinel 1%.

850/U_{16}

Mineral compositions used in the calculations were: garnet U_{16}, olivine U_{16}, orthopyroxene U_8, chrome spinel (Deer, Howie & Zussman 1962, Vol. 5, Table 11, No. 8).

Estimated modal proportions by weight in the original assemblage used for calculating analysis C were: olivine 84.5%, orthopyroxene 10%, garnet 5%, chrome spinel 0.5%.

This seems to be borne out when one comes to consider the whole rock analysis recalculated for U_3. This sample had the highest H_2O^+ content (14.02 wt. %), yet comparisons of columns A and B in this case seem contrary to the hypothesis that serpentinization always involves significant leaching of MgO and FeO with respect to SiO_2. In this case the straightforward anhydrous recalculated whole rock analysis in fact has a slightly higher MgO+FeO/SiO_2 ratio than that calculated using the point count mode. It therefore sems that in this case the orthopyroxene/olivine ratio in the original assemblage was slightly overestimated. It is apparent that in this sample the limited degree of cataclasis has resulted in a texture in which it is feasible to determine with a reasonable degree of accuracy the relative proportions of serpentine pseudomorphs after olivine to those after orthopyroxene.

Furthermore, it was found impossible to derive mutually consistent primary whole rock compositions for these peridotite samples from the mineral analyses and the whole rock analyses assuming constant volume serpentinization reactions. A difficult problem arises, however, in making such calculations from uncertainties about the ratio of primary orthopyroxene/olivine involved in the serpentinization.

This author would not entirely rule out the possibility of limited leaching of FeO and MgO with respect to SiO_2 occurring during serpentinization. However, the data for the Ugelvik peridotites, in particular for the sample U_3, provide no evidence that such leaching invariably occurs during serpentinization nor that complete serpentinization consistently involves the removal of as much as 30% by weight of the original bivalent oxides and SiO_2 in the peridotite as envisaged by Thayer (1966).

3. The hypothesis that the serpentinization involved the introduction of SiO_2 as well as H_2O without leaching of MgO and FeO raises problems regarding the origin of the SiO_2 and the even greater volume increase involved. That serpentinization involves only reactions of the type 3 $Mg_2SiO_4 + 4H_2O + SiO_2 \rightarrow 2Mg_3Si_2O_2(OH)_4$ is, therefore, discounted.

This author suspects that taken overall, serpentinization involves a complex series of reactions both of the constant volume and constant composition types although over restricted volumes of peridotite reactions of the one type only may occur or at least predominate.

To summarize, it is considered that in the case of these Ugelvik peridotites, the constant composition anhydrous recalculations of the whole rock analyses provide the best available approximations to the primary pre-serpentinization compositions. It seems quite feasible that the ratio of primary orthopyroxene/olivine was in fact higher in most cases than at first thought. However, as the possibility of leaching during serpentinization of in particular MgO and FeO with respect to SiO_2 cannot be entirely ruled out, the MgO + FeO/SiO_2 ratios of the primary whole rock analyses should be viewed with a certain amount of reservation.

Methods of Analysis

All the rock and mineral samples were analysed for Ti, Al, Cr, Fe (total), Mn, Ni, Mg and Ca by X-ray fluorescence spectroscopic techniques. In all cases, other than in the determination of small amounts of Cr, a fusion disc preparation with a 1:1:4 ratio of rock powder (100 mesh): La_2O_3:$Li_2B_4O_7$ was used in order to minimize the matrix absorption effects. Determinative curves were drawn up for each element using recognized standard materials (G_1, W_1, syenite Sy-1, etc.) for most elements and specially prepared standards for the Ni and Cr determinations. For details of the operating conditions of the X-ray fluorescence spectrograph for each element, the reader is referred to Carswell (1966).

As La interferes with the Cr $K_{\alpha 1}$ peak and Mn with the Cr $K_{\beta 1}$ peak, the determination of Cr raised a problem. This was overcome by determining Cr at low concentrations (<0.40 wt. % Cr_2O_3) on 100 mesh rock powder covering a film of Mylar. For this determination the Cr $K_{\alpha 1}$ peak at a 2θ of 69.31 for LiF was used. It was considered that at such low Cr_2O_3 concentrations the error resulting from differing matrix absorption effects was insignificant. Cr_2O_3 in greater concentrations was determined on fusion discs using the $K_{\beta 1}$ peak at a 2θ of 100.48 for Topaz. It was found possible to determine Cr on this peak down to concentrations of about 0.40 wt. % Cr_2O_3 before interference by Mn, at the low MnO concentrations (<0.60 wt. %) found in these rocks and minerals.

The Cr_2O_3 values of the chrome rich garnets and clinopyroxenes were checked by spectrophometric determination on the yellow chromate colour in strongly alkaline solution following fusion with a 10:1 mixture of Na_2CO_3:KNO_3. The high MgO values were checked by the recognised E.D.T.A. titration technique.

Si and H (as H_2O) were determined gravimetrically, Na and K by flame photometry, and ferrous iron by titration with dichromate.

February 1968

Dept. of Geology, Sheffield University
St. George's Square, Sheffield 1, England

ACKNOWLEDGEMENTS. This study was initiated at the Grant Institute of Geology, University of Edinburgh, during the tenure of a grant from the Natural Environment Research Council, which is gratefully acknowledged. Also acknowledged is a grant from the Sheffield University Research Fund which has enabled the author to continue this study. The author would also like to thank Dr. M.J. O'Hara (University of Edinburgh) and Dr. P.E. Brown (University of Sheffield) for their helpful comments on this manuscript, and the former for valuable suggestions and discussions throughout the course of this study.

REFERENCES

BARTHOLOMÉ, P. 1961: Co-existing pyroxenes in igneous and metamorphic rocks. *Geol. Mag. 98*, 346–48.

BARTHOLOMÉ, P. 1962: Iron-magnesium ratio in associated pyroxenes and olivines. *Petrologic Studies : A volume in honour of A. F. Buddington*, 1–20, Geol. Soc. Amer.

BOYD, F.R. & ENGLAND, J.L. 1964: The system enstatite-pyrope. *Carnegie Inst. Wash. Yearb. 63*, 157–61.

BOYD, F.R. & MACGREGOR, I.D. 1964: Ultramafic rocks. *Carnegie Inst. Wash. Yearb. 63*, 152–56.

BRYHNI, I. 1966: Reconnaissance studies of gneisses, ultrabasites, eclogites and anorthosites in Outer Nordfjord, Western Norway. *Norges Geol. Undersök. 241*, 1–68.

CARSWELL, D.A. 1966: Some ultrabasic bodies and related rocks in Sunnmöre, South Norway. Unpublished Ph.D. thesis. *University of Edinburgh*.

CARSWELL, D.A. 1968: Picritic magma-residual dunite relationships in garnet peridotites at Kalskaret near Tafjord, South Norway. *Contr. Mineral. Petrol.* (in press).

Dal Vesco, E. 1953: Genesi e matamorfosi delle rocce basiche e ultrabasiche nell'ambiente mesozonale dell'orogene Pennidico (Cantone Ticino). *Schweiz. Min. Petrogr. Mitt. 33*, 173–480.

Davidson, C.F. 1943: The Archaean rocks of the Rodil District, South Harris, Outer Hebrides. *Trans. Roy. Soc. Edinb. 61*, 71–112.

Davidson, C.F. 1964: On diamantiferous diatremes. *Econ. Geol. 59*, 1368–80.

Davis, B.T.C. & Boyd, F.R. 1966: The join $Mg_2Si_2O_5$–$CaMgSi_2O_6$ at 30 kilobars pressure and its application to pyroxenes from kimberlites. *J. Geophys. Res. 71*, 3567–76.

Dawson, J.B. 1962: Basutoland kimberlites. *Bull. Geol. Soc. Amer. 73*, 545–60.

Deer, W.A., Howie, R.A. & Zussman, J. 1962: *Rock Forming Minerals. Vol. 5. Non Silicates.* Longmans, London.

De Waard, D. 1965: A proposed subdivision of the granulite facies. *Amer. J. Sci. 263*, 455–61.

Eskola, P. 1921: On the eclogites of Norway. *Skr. Vidensk. Selsk. Christiania, Mat.-Naturv. Kl., I, No. 8*, 1–118.

Fiala, J. 1965: Pyrope in some garnet peridotites of the Czech Massif. *Krystalinikum 3*, 55–74.

Fiala, J. 1966: The distribution of elements in mineral phases of some garnet peridotites from the Bohemian Massif. *Krystalinikum 4*, 31–53.

Fyfe, W.S., Turner, F.J. & Verhoogen, J. 1958: Metamorphic reactions and metamorphic facies. *Geol. Soc. Amer. Mem. 73*, 1–252.

Green, D.H. 1964: The petrogenesis of the high temperature peridotite intrusion in the Lizard area, Cornwall. *J. Petrol. 5*, 134–88.

Green, D.H. & Ringwood, A.E. 1967a: An experimental investigation of the gabbro to eclogite transformation and its petrological implications. *Geochim. et Cosmochim. Acta 31*, 767–833.

Green, D.H. & Ringwood, A.E. 1967b: The stability fields of aluminous pyroxene peridotite and garnet peridotite and their relevance in upper mantle structure. *Earth Planet. Sci. Letters, 3*, 151–60.

Grubenmann, U. 1908: Der Granatolivinfels der Gordunotals, und seine Begleitgesteine. *Virteljahrschr. Naturf. Ges. Zurich. 53*, 129–56.

Hamilton, W. & Mountjoy, W. 1965: Alkali content of alpine ultramafic rocks. *Geochim. et Cosmochim. Acta 29*, 661–71.

Holmes, A. 1936: A contribution to the petrology of kimberlite and its inclusions. *Trans. Geol. Soc. S. Afr. 39*, 379–428.

Hostetler, P.B., Coleman, R.G., Mumpton, F.A. & Evans, B.W. 1966: Brucite in alpine serpentinites. *Amer. Min. 51*, 75–98.

Ito, K. & Kennedy, G.C. 1967: Melting and phase relations in a natural peridotite to 40 kilobars. *Amer. J. Sci. 265*, 519–38.

Kopecký, L. & Sattran, V. 1962: Ke genesi pyropu v Českém Středohoří. *Věstník Ústř. úst. geol. 36, 4*, 269–83.

Kopecký, L. & Sattran, V. 1966: Buried occurrences of pyrope-peridotite and the structure of the crystalline basement in the extreme S.W. of the Ceske Stredohori mountains. *Krystalinikum 4*, 65–86.

Kretz, R. 1961: Some applications of thermodynamics to co-existing minerals of variable composition. Examples: orthopyroxene-clinopyroxene and orthopyroxene-garnet. *J. Geol. 69*, 361–87.

Kryukov, A.V. 1966: Genesis of pyrope peridotite inclusions in the pipes of North Minusinsk Depression and their comparison with peridotites of the České Středohoří Mountains *Krystalinikum 4*, 185–200.

Lappin, M.A. 1962: The eclogites, dunites and anorthosites of the Selje and Almklovdalen districts, Nordfjord, S.W. Norway. Unpublished Ph.D. thesis, *University of Durham.*

Lappin, M.A. 1966: The field relationships of basic and ultrabasic masses in the basal gneiss complex of Stadlandet and Almklovdalen, Nordfjord, south-western Norway. *Norsk Geol. Tidsskr. 46*, 439–96.

MacGregor, I.D. 1965: Stability fields of spinel and garnet peridotites in the synthetic system MgO–CaO–Al_2O_3–SiO_2. *Carnegie Inst. Wash. Yearb. 64*, 126–34.

MacGregor, I.D. & Ringwood, A.E. 1964: The natural system enstatite-pyrope. *Carnegie Inst. Wash. Yearb. 63*, 161–63.

Mercy, E.L.P. & O'Hara, M.J. 1965a: Chemistry of some garnet-bearing rocks from south Norwegian peridotites. *Norsk Geol. Tidsskr. 45*, 323–32.

Mercy, E.L.P. & O'Hara, M.J. 1965b: Olivines and orthopyroxenes from garnetiferous peridotites and related rocks. *Norsk Geol. Tidsskr. 45*, 457–61.

Mikhailov, N.P. & Rovsha, V.S. 1966: Pyrope-bearing peridotites of the Bohemian Massif and their genesis. *Krystalinikum 4*, 87–107.

Nixon, P.H., Knorring, O. Von & Rooke, J.M. 1963: Kimberlites and associated inclusions of Basutoland: A mineralogical and geochemical study. *Amer. Min. 48*, 1090–132.

O'Hara, M.J. 1965: Primary magmas and the origin of basalts. *Scot. J. Geol. 1*, 19–40.

O'Hara, M.J. & Mercy, E.L.P. 1963: Petrology and petrogenesis of some garnetiferous peridotites. *Trans. Roy. Soc. Edin. 65*, 251–314.

O'Hara, M.J. & Mercy, E.L.P. 1965: Diamantiferous diatremes. *Econ. Geol. 60*, 830–1.

O'Hara, M.J. & Mercy, E.L.P. 1966a: Eclogite, peridotite and pyrope from the Navajo Country, Arizona and New Mexico. *Amer. Min. 51*, 336–52.

O'Hara, M.J. & Mercy, E.L.P. 1966b: Garnet-peridotite and eclogite from Bellizona Switzerland. *Earth Planet. Sci. Letters 1*, 295–300.

O'Hara, M.J. & Yoder, H.S. 1967: Formation and fractionation of basic magmas at high pressures. *Scot. J. Geol. 3*, 67–117.

Ringwood, A.E. 1965: The chemical composition and origin of the earth. *Advances in Earth Sciences* (ed. P.M. Hurley), pp. 287–356. M.I.T. Press, Cambridge-Massachusetts.

Ringwood, A.E. 1966: Chemical evolution of the terrestrial planets. *Geochim. et Cosmochim. Acta 30*, 41–104.

Ringwood, A.E. 1967: The pyroxene-garnet transformation in the earth's mantle. *Earth Planet. Sci. Letters 2*, 255–63.

Ringwood, A.E., MacGregor, I.D. & Boyd, F.R. 1964: Petrological constitution of the upper mantle. *Carnegie Inst. Wash. Yearb. 63*, 147–52.

Ringwood, A.E. & Major, A. 1967: Some high pressure transformations of geophysical significance. *Earth Planet. Sci. Letters. 2*, 106–10

Rost, F. 1966: Über ultrabasische einschlüsse in metamorphen gesteinen des südlichen Moldanubikums. *Krystalinikum 4*, 127–62.

Thayer, T.P. 1966: Serpentinization considered as a constant volume metasomatic process. *Amer. Min. 51*, 685–710.

Turner, F.J. & Verhoogen, J. 1960: *Igneous and Metamorphic Petrology*. 2nd Edition. McGraw Hill, New York.

Wagner, P.A. 1914: *The Diamond Fields of Southern Africa*. 347pp. Transvaal Leader, Johannesburg.

Williams, A.F. 1932: *The Genesis of the Diamond*. 2 Vols. Benn, London.

Accepted for publication April 1968 Printed October 1968

THE AGE AND STATUS OF THE BASAL GNEISS COMPLEX OF NORTH-WEST SOUTHERN NORWAY

DENNIS ANTHONY CARSWELL

Carswell, D. A.: The age and status of the Basal Gneiss Complex of north-west southern Norway. *Norsk Geologisk Tidsskrift,* Vol. 53, pp. 65–78. Oslo 1973.

This paper presents a review of the evidence concerning the age and status of the Basal Gneiss Complex of north-west southern Norway. There seems little doubt that both 'Caledonized' Pre-Eocambrian basement rocks and Eocambrian-Lower Palaeozoic cover rocks occur within this complex, although it is extremely difficult to discriminate between them in the field.

It is suggested that occurrences of eclogites, granulites and calcic anorthosites in this region may be restricted to the Pre-Eocambrian basement, and hence may provide the most reliable means of distinguishing between basement and cover rocks in the field.

D. A. Carswell, Department of Geology, University of Sheffield, Sheffield S1 3JD, England.

On the geological map of Norway (Holtedahl & Dons 1960) a large proportion of north-west southern Norway is indicated as consisting mainly of gneissic rocks, of various origin, with a structure wholly or in part Caledonian. Following Holtedahl (1944) this area is usually referred to as the 'Basal Gneiss Region' and the rocks within this area as the 'Basal Gneiss Complex'.

This paper presents an assessment of the often divergent and contradictory results and conclusions of previous workers on the question of the age and status of the Basal Gneiss Complex, in the light of the author's own prejudices, based on field observations in many parts of the region but in particular on recent work in the Romsdalsfjorden region.

Before proceeding it is advisable to discuss some of the geochronological terms which will be used in this paper.

At our present state of knowledge it is perhaps desirable to retain the much used term 'Caledonian' to describe in broad terms the age of the orogenic activity (essentially Lower Palaeozoic) within the Caledonian orogenic belt. Thus within this orogenic belt the deformation, metamorphism and igneous activity may be referred to as being of 'Caledonian' age.

In the past the term 'Caledonian' has also been used very loosely in a time-stratigraphic sense to imply the depositional age of the rocks subjected to deformation and metamorphism during Lower Palaeozoic times in this orogenic belt. It is now apparent, however, that rocks of diverse ages (Early Precambrian basement rocks and both Late Precambrian and Lower Palaeo-

zoic cover rocks) have been subjected to 'Caledonian' deformation and metamorphism in various parts of the orogenic belt.

It is therefore desirable to abandon the use of the term 'Caledonian' in a time-stratigraphic sense, and this procedure will be followed in this paper despite the problems which arise through the present lack of internationally standardized time-stratigraphic terms for the Precambrian.

In this paper emphasis is placed on distinguishing between the sedimentary and igneous rocks formed, metamorphosed and deformed within the Caledonian orogenic belt which are referred to as the *cover rocks*, and the older *basement rocks* upon which the former were deposited. The terms supracrustal and infracrustal rocks (e.g. Bryhni & Grimstad 1970), which are chiefly used with lithological rather than age connotations, will be avoided where possible.

The cover rocks are thought to have been deposited following the extensive Sveconorwegian-Grenville deformation, metamorphism and plutonism of approximately 1200–900 m.y. age (Welin 1966, Kratz et al. 1968) and thus to have depositional ages mostly within the range 900–450 m.y.

The rather unsatisfactory time-stratigraphic term 'Eocambrian' has often been used in the literature with reference to the cover rocks (Sparagmites) of Late Precambrian age ($>$ 600 m.y.) in Norway. However, the use of this term throughout the Caledonides raises problems, and is probably only valuable if it is acceptable to place the base of the Eocambrian at about 900 m.y.

The age of the basal gneisses

Early field geologists (Reusch 1881, Kolderup 1923) regarded the gneisses as forming the Archean (Precambrian) basement to the Cambro-Silurian metasedimentary rocks observed to overlie them, to the east in particular. However, Holtedahl (1936, 1938, 1944) considered these gneisses to have been too strongly influenced by Caledonian metamorphism, migmatization, granitization and deformation to be regarded simply as Precambrian, and described the derivation of some of these gneisses by feldspathization of 'Caledonian' metasediments.

Gjelsvik (1951) and Kolderup (1952, 1960) also thought the gneisses to be primarily of Eocambrian or Cambro-Silurian origin, while more recently Hernes (1965, 1967) has argued that they represent a late Precambrian succession.

Strand (1960) stated that 'work in recent years has in some cases proved and in many cases strongly indicated that the rocks of the Gneiss region are of Caledonian age, in the sense that they were formed from sediments of Sparagmitian or Cambro-Silurian age by metamorphism and metasomatic alterations. It cannot be doubted that rocks of the original Precambrian basement occur in parts of the Gneiss region, but they certainly must be strongly influenced by Caledonian tectonics and be in a "Caledonized" state'.

This statement probably represents the most widely held present view of the basal gneisses.

An imaginative structural interpretation of the north-east part of the region, complying with this view, was advanced by Muret (1960). He postulated the existence of Pennine-style nappe structures with cores of relatively homogeneous Precambrian rocks and envelopes of more heterogeneous Eocambrian and Cambro-Silurian metasediments. Caledonian remobilization of the Precambrian basement rocks was thought to have produced the present general geometrical conformity between the rock series, although it was stated that relics of the original discordance are still in evidence.

The last few years have seen some interesting developments concerning the difficult and challenging problem of differentiating between Eocambrian-Silurian metasediments and transformed Pre-Eocambrian basement in this area. Bryhni (1966, Fig. 2) gave a tentative interpretation of the south-west part of the Basal Gneiss region in which he recognized the existence of a reworked Pre-Eocambrian basement complex (the Jostedal Complex) of relatively homogeneous gneisses (2 feldspar gneisses, migmatite and augen gneiss), overlain by a far more heterogeneous series of rocks (schists, gneisses, quartzite, marble, eclogite, amphibolite, peridotite, anorthosite, etc.) named the Fjordane Complex – thought to contain both rocks of Cambrian-Silurian age and older elements corresponding to the Jotun thrust masses (Fig. 1).

Further to the north-east in the Grotli area, Strand (1969) has mapped a contact on similar lithological grounds between a 'Caledonized' Precambrian basement, and an overlying rock sequence of postulated late Precambrian to Ordovician age.

In the Tafjord area just to the north of Grotli, Brueckner et al. (1968) have obtained a Rb-Sr whole rock isochron age of 1,000 $\pm$ 150 m.y. for comparable homogeneous basement gneisses. They also obtained a K-Ar biotite age of 383 $\pm$ 12 m.y. for these gneisses, implying that although of undoubted Pre-Eocambrian origin these gneisses have, as suspected, recrystallized during the Caledonian orogeny. Brueckner (1969, Fig. 5) followed Bryhni (1966), Strand (1969) and others in supposing that the structurally overlying heterogeneous rocks are of Eocambrian-Silurian age.

The age assumption for the Fjordane Complex, however, is based on rather tenuous lithological grounds, principally the presence of quartzites and peridotites. Gjelsvik (1953), Muret (1960) and Strand (1960) have all correlated quartzites in the Basal Gneiss region with the Eocambrian Sparagmite Complex to the east, and also the peridotites so common in parts of the Basal Gneiss region with occurrences of similar rock types in Cambro-Ordovician metasediments to the east. However, Strand (1949) stated that 'the quartzite of the Grotli area may equally well be Precambrian as Caledonian' and more recently Bryhni & Grimstad (1970) have mentioned that the quartzites and associated metamorphic supracrustal rocks of the Basal Gneiss region may possibly be correlated with similar rocks of the Precam-

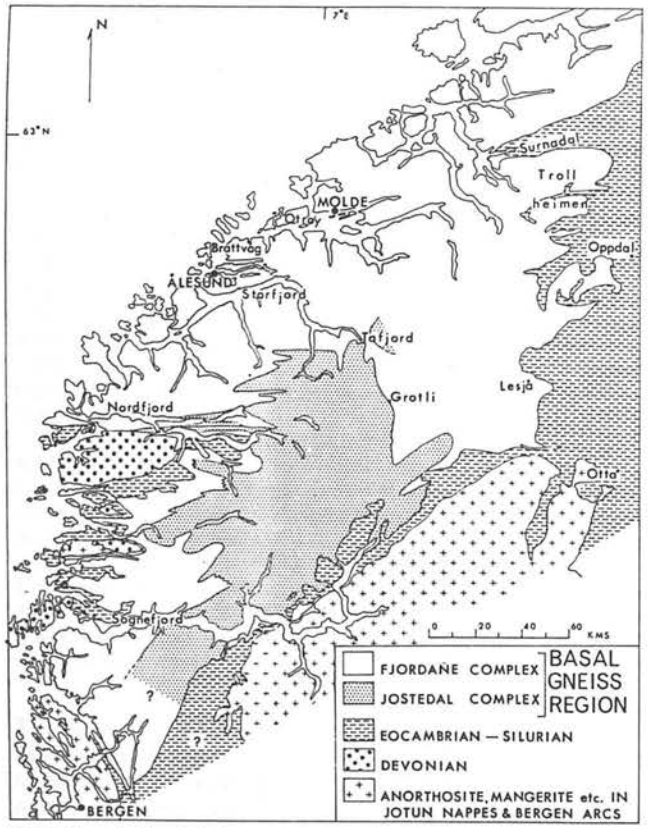

Fig. 1. Generalized geological map of the Basal Gneiss region and adjacent areas of southern Norway – based mainly on Holtedahl & Dons (1960). The outcrops of the Fjordane and Jostedal Complexes within the Basal Gneiss region largely follow the tentative interpretation of Bryhni (1966). The principal localities discussed in the text are indicated on this map.

brian 'Telemark suite' of southern Norway. They state that the age of the Fjordane Complex is not clear, but tentatively regard it as being of Precambrian or Eocambrian age.

An age correlation based on the presence of peridotites appears at least equally dubious. Peridotite intrusions are common in orogenic belts of all

ages (Hess 1955), and as in the Basal Gneiss region (O'Hara & Mercy 1963, Lappin 1966, Carswell 1968a, 1968b), are now generally recognized to have been tectonically emplaced from deeper crustal levels or from the mantle (Wyllie 1967, Moores 1970). Thus during a particular orogeny, peridotite bodies may well be emplaced into both basement and cover rocks. Furthermore, peridotites are considerably more numerous in the Fjordane Complex of the Basal Gneiss region and differ from those in the Cambro-Silurian metasediments to the east in occasionally being garnetiferous and also containing inclusions of 'country rock' eclogites (that is, eclogites of the types commonly found as lenses within the gneisses).

In the Hestbrepiggan area on the south-east margin of the Basal Gneiss region, Banham & Elliott (1965) and Banham (1968) have described gneisses of varied lithology (including quartzite and amphibolite) thought to be of Pre-Eocambrian age, beneath overthrust Eocambrian-Silurian metasedimentary rocks.

Thus that part of the Basal Gneiss Complex consisting of relatively homogeneous granitic gneisses (Bryhni's Jostedal Complex) appears to have recently become justifiably accepted as being of Pre-Eocambrian age, but opinion is still divided regarding the other part consisting of more heterogeneous rocks (Bryhni's Fjordane Complex) although an Eocambrian-Silurian depositional age appears to be most favoured by previous workers.

The contact between the basal gneisses and undisputed Eocambrian–Silurian metasedimentary rocks

A large area of metasedimentary and metavolcanic rocks of undisputed Eocambrian-Silurian age occurs in the Trondheim region to the north-east of the Basal Gneiss region.

In the Oppdal-Trollheimen district the basal gneisses are overlain conformably by feldspathic psammites (Sparagmites) followed by micaschists, amphibolites, etc., often referred to as the Trondheim schists. Holtedahl (1938) and Barth (1938) considered the gneisses beneath the feldspathic psammites to be the products of feldspathization of Eocambrian sediments normally underlying Sparagmitian rocks. However, Rosenqvist (1941) discovered a quartz conglomerate at the base of the Sparagmitian rocks indicating he thought a Precambrian age for the underlying gneisses. Whatever their age, there seems little doubt and indeed general agreement that the underlying gneisses have suffered Caledonian metamorphism, migmatization and deformation.

In the valley areas of Lesja and Otta, Strand (1949) described zones of augen gneisses between homogeneous granitic basal gneisses and Eocambrian-Silurian metasediments to the east. The augen gneiss zones were said to represent a migmatite front, original plagioclase gneisses 'for the most part of Archean age' having been transformed to granitic gneisses by Caledonian granitization and potash feldspar introduction.

In this early paper Strand considered that there were strong arguments for an Archean (Precambrian) origin of the gneisses in great parts of the eastern Basal Gneiss region, although he was inclined to think that tracts of gneisses with quartzites and peridotites were of Eocambrian-Silurian age.

Oftedahl (1964) considered the basal gneisses to be of Pre-Eocambrian age and suggested that the concordant basement contact is possibly a primary effect, the Pre-Eocambrian rocks having been essentially unfolded when the Eocambrian and Cambrian rocks were deposited on them.

Further north, in northern Trøndelag, Birkeland (1958) reported that the younger overlying formations in many places rest with a profound unconformity on the basal gneisses. Oftedahl considered that Birkeland's conclusions were unsubstantiated but Peacey (1964) confirmed Birkeland's conclusion in describing the existence of a primary unconformity in the Tømmerås anticline area.

Roberts et al. (1970) concluded that elsewhere in the northern Trondheim region the Cambro-Silurian rocks rest with tectonic discontinuity upon Precambrian granite gneisses.

The geological map of Norway (Holtedal & Dons 1960) also shows a few isolated outcrops of Cambro-Silurian rocks in the western part of the Basal Gneiss region, between Sognefjorden and Nordfjord. Bryhni & Grimstad (1970) state that to their knowledge these rocks are always bounded by tectonic contacts from basal gneiss supracrustal rocks (Fjordane Complex).

Thus it appears to be becoming increasingly recognized that the contact between the basal gneisses and overlying undisputed Eocambrian-Silurian metasediments is in general a tectonic discontinuity, the structural conformity between the two rock series being a result of the Caledonian deformation they have both suffered.

The relationship between basement and cover rocks in the Surnadalen and Romsdalsfjorden regions

In the Surnadalen area of Nordmøre, Strand (1953) has described the occurrence of Cambro-Ordovician metasediments and metavolcanics (including greenschists, micaschists, micaceous gneisses, limestone and quartzite) which form a narrow synclinal extension of similar rocks in the Trondheim region. These rocks were said to be bounded on both sides by basal gneisses rich in potash feldspar. Both the basal gneisses and overlying rocks were considered to have been subjected to two episodes of Caledonian metasomatism, Na and Ca metasomatism followed by K metasomatism, and it was concluded that 'the upper part at least of the basal gneiss in this region is a Caledonian rock, formed from Caledonian material by metasomatic processes'.

Similar metasedimentary and metavolcanic rocks of postulated Eocambrian-Lower Palaeozoic age (Bugge 1934, Gjelsvik 1953, Hernes 1955) occur in the Romsdalsfjorden region, west south-west along the regional strike from Surnadalen.

Like Strand, Gjelsvik (1953) and Hernes (1955) considered the contact between the basal gneisses and overlying rocks to represent a Caledonian migmatization effect (a migmatite front) – the basal gneisses being extensively migmatized Eocambrian-Lower Palaeozoic rocks.

However, the present author has been studying the contact between basement gneisses and possible Eocambrian-Lower Palaeozoic cover rocks on the islands of Otrøy and Midoy on the northern side of Romsdalsfjorden. Here the abundance of relics of eclogite facies assemblages within the basal gneisses and their apparent absence amongst the overlying rocks where the basic rocks are almost invariably garnet amphibolites, was taken to support the view that the former may be significantly older than the latter and are thus probably part of the 'Caledonized' Pre-Eocambrian basement upon which the Eocambrian-Silurian cover rocks were deposited.

It was also noted that the postulated cover rock sequence includes thick sequences of psammites in addition to the more striking pelites and metavolcanics. Thus not all potash feldspar rich gneisses should be termed basal gneisses, as gneisses of this type occur within both rock complexes. As along the eastern margin of the Basal Gneiss region one is therefore again faced with the extremely difficult task of trying to differentiate between partly migmatized feldspathic psammites of Eocambrian-Lower Palaeozoic age and Pre-Eocambrian granitic injection gneisses.

Other evidence relevant to the question of the age of the Basal Gneiss Complex

Evidence from other parts of the Caledonian orogenic belt which has some bearing on the question of the age of the Basal Gneiss Complex will be considered in this section.

The occurrence of eclogites

Eclogite facies assemblages of two types occur within the Basal Gneiss region (Eskola 1921, Lappin 1966, Bryhni et al. 1969), namely eclogites associated with peridotite bodies, and eclogites directly enclosed in the gneisses (here termed 'country rock' eclogites).

Eclogite facies assemblages of the first type comprise rare indigenous layers of garnet peridotite, garnet websterite and rarely bimineralic eclogite within garnet free peridotite bodies. It has been argued (Carswell 1968a, 1968b) that such assemblages were probably developed in the upper mantle prior to the tectonic emplacement of these peridotite bodies into their present position.

'Country rock' eclogites, on the other hand, occur as tectonic lenses or boudins widely distributed over large areas of the Basal Gneiss region. They frequently contain modal quartz and sometimes kyanite.

Within the Caledonides eclogites associated with peridotites are extremely rare and apparently restricted to the Norwegian Basal Gneiss region. How-

ever, 'country rock' eclogites of comparable types have been reported from north-west Scotland (Alderman 1936), Spitsbergen (Gee 1964) and east Greenland (Kranck 1935, Sahlstein 1935).

Clinopyroxenes from 'country rock' eclogites have yielded K-Ar ages ranging from 780–5050 m.y. (MacDougall & Green 1964, Gayer et al. 1966, Miller et al. 1963). The fact that certain of these ages are undoubtedly erroneous, due to the presence of excess radiogenic argon, prohibits one reaching significant conclusions on the age of the primary eclogite assemblages.

K-Ar ages obtained from secondary amphibole in these eclogites range from 389–1745 m.y., while two secondary phlogopites from Norwegian eclogites gave K-Ar ages of 415 and 950 m.y., and Rb-Sr ages of 401 and 383 m.y. The interpretation of the significance of these ages is again uncertain though MacDougall & Green (1964) have argued that the amphiboles and micas did not contain excess argon, suggesting that secondary amphibole growth, at least in the Norwegian eclogites, was initiated at least 1800 m.y. ago, hence indicating an even older Precambrian age for the eclogite crystallization. The various younger amphibole and mica ages were thought to reflect partial or complete overprinting (argon loss) during subsequent metamorphic events, in particular during the Caledonian orogeny.

The eclogites in the Glenelg and Loch Duich areas of north-west Scotland occur in Lewisian rocks which form the basement for the later cover rocks (the Moines) – see Peach et al. (1910), Ramsay (1957a), Sutton & Watson (1958). These Lewisian rocks are mostly almandine-amphibolite facies schists and gneisses, but occasional partly retrograded pyroxene granulites are preserved. The marked interbanding of the Lewisian basement rocks and Moine cover in this region has been produced either by isoclinal folding (Peach et al. 1910), thrust slicing of the basement into the cover, or most probably (Ramsay 1957a) by a combination of both effects during the Caledonian orogeny.

Thus in the one part of the Caledonian belt where one is reasonably certain of the stratigraphic and structural relationship of the rocks enclosing the eclogites, it is apparent that the eclogites are restricted to the remobilized basement complex.

The geological relationships and radiometric age dates strongly suggest, but do not conclusively prove, that this is also the case for the Norwegian, Spitsbergen and east Greenland eclogite occurrences. In all four areas the eclogites occur as tectonic lenses or boudins of varying sizes but opinion is divided as to whether they are *in situ* crustal metamorphic rocks (Gjelsvik 1952, Hernes 1954, Kolderup 1960, Schmitt 1964, Bryhni et al. 1969, Bryhni et al. 1970) or tectonically emplaced lower crustal or even upper mantle rocks (O'Hara & Mercy 1963, Lappin 1966). However, even if tectonically emplaced their absence from undoubted Eocambrian-Silurian rocks, their observed presence as extensively retrograded and partly injected tectonic inclusions within Norwegian anorthosites (of presumed Precambrian age – see later section) and peridotites (personal observation), and the likelihood that the numerous small lenses of eclogite are deformed fragments of originally much larger masses all suggest that the eclogites were an integral part of the Pre-Eocambrian basement complex rather than Caledonian intrusive rocks.

The age of the granulite facies metamorphism

Relics of granulite facies gneisses occur associated with the eclogites on Otrøy and Midøy in the Norwegian Basal Gneiss region (Carswell 1968b). A similar association has been observed both in Scotland and east Greenland. To the best of my knowledge no regional scale granulite facies gneisses of proven Caledonian age exist within the Caledonides.

Further north in Norway, granulite facies gneisses in the Lofoten-Vesterålen area were originally thought to be of Caledonian age but have recently been reinterpreted by Heier & Compston (1969) as very old Precambrian basement (about 2800 m.y.) broadly comparable in age to the Scourian granulite facies metamorphism (about 2600 m.y.) of the Lewisian of north-west Scotland (Park 1970). In Norway as in Scotland, the granulite facies gneisses show varying degrees of modification by later metamorphism and deformation of Precambrian age – possibly both Laxfordian-Svecofennian (about 1600–1800 m.y.) and Grenville-Sveconorwegian (about 900–1200 m.y.) effects – and Caledonian age (roughly between 370–600 m.y.).

Indeed it would appear that all reliably dated pyroxene granulite facies terrains throughout the world are of Precambrian age (Spooner & Fairbairn 1970).

Basement-cover relationships in the Scottish Caledonides

It is also instructive to compare the Norwegian Basal Gneiss Complex controversy with that concerning the Lewisian 'inliers' within the Moines of central Ross-shire in Scotland. In this latter area the occurrence of Lewisian basement 'inliers' within the Moines was first recognized by the early field geologists (Peach et al. 1913), later discredited by Sutton & Watson (1952, 1954) and Ramsay (1957b) who considered these rocks to be an integral part of the Moine succession, but subsequently substantiated by Sutton & Watson (1962).

It is now generally accepted that the Lewisian rock masses of central Ross-shire represent fragments of the basement which was intensely deformed with, and thrust into, the overlying Moine cover rocks.

Further thrust sheets or nappe cores of Lewisian may also occur in the central part of the fold belt (Ramsay 1963) but it was noted that the original structural and metamorphic distinction between the Lewisian basement and Moine cover has become blurred by the super-position of Caledonian metamorphism, migmatization and probably four fold phases. Hence in the central parts of the fold belt it becomes extremely difficult or even impossible to distinguish certain types of basement and cover rocks, especially Lewisian

quartzo-feldspathic gneisses and feldspathic Moine psammites – a comparable problem to the attempted discrimination between basement gneisses and Sparagmitian rocks in the Basal Gneiss region of Norway.

It would appear that in Norway as in Scotland the collision between the east Greenland and Fennoscandian continental blocks, which ultimately produced the Caledonian fold belt, resulted in the Pre-Ecambrian basement becoming extensively sliced up and thrust upwards and interfolded with the Eocambrian-Lower Palaeozoic cover rocks. On the margins of the fold belt (Moine and Jotun thrust belts), the orogenic compression resulted in thrust slices or nappes of both basement and cover rocks being driven outwards on to the unaffected continental forelands. In the Basal Gneiss region of north-west southern Norway one is apparently looking at a low level in the central part of the fold belt where the basement has been thrust into and interfolded with the cover rocks and has suffered Caledonian metamorphism and migmatization. Consequently the original metamorphic and structural distinctions between the basement and cover rocks have been largely eradicated by Caledonian effects, and one is largely reduced to attempting to discriminate between the two on dubious lithological grounds.

The age of the anorthosites

Anorthosite masses are frequently associated with peridotites and eclogites in the Fjordane Complex of the Basal Gneiss region (Bryhni 1966). The large rather massive and homogeneous sill-like anorthosite masses, as observed by the author in the Tafjord-Grotli area, consist almost entirely of labradorite composition plagioclase $An_{50\text{-}60}$ and thus may be classified as labradorite type massif-type anorthosites – Anderson & Morin (1969). Anderson (1969) and Herz (1969) have pointed out that all reliably dated anorthosite massifs of this type occur in Precambrian terrains – all older than 1000 m.y. They are commonly associated with either fresh or partly retrograded granulite facies rocks. The actual date of primary igneous crystallization of such anorthosites is uncertain, but for the Nain labradorite anorthosite in Canada, Anderson & Morin (1969) have postulated an age $>$ 2000 m.y. The possibility that all such anorthosites are extremely old has led to interesting recent speculation (Anderson & Morin 1969, Yoder 1969, Windley 1970) that calcic anorthosite bodies may represent relics of the primordial continental crust formed during an early phase (perhaps rapid degassing) of the earth's geochemical differentiation.

The anorthosites within the Basal Gneiss Complex, as commonly found elsewhere, have cataclastic fabrics (at least marginally) and tectonic contacts. They may therefore represent tectonically remobilized fragments of the proto-continental crust. However, as with the peridotite and eclogite inclusions in the Basal Gneiss Complex the recognition of tectonic contacts tells one little about how far these rocks may have moved through their enclosing gneisses in a 'cool' crystalline condition. As pointed out by Bryhni et al. (1970) the presence of tectonic margins need not always imply large scale tectonic movements, but may just be a reflection of intense deformation of rocks of widely differing mechanical properties. It is thus not clear whether the anorthosite bodies are indigenous to the gneiss complex or whether they have been tectonically emplaced from lower crustal levels.

However, whichever is the case their absence from undoubted Eocambrian-Silurian rocks in Norway and indeed the apparent world-wide restriction of such anorthosites to Precambrian terrains, strongly suggests a Pre-Eocambrian age for much of the Fjordane Complex of the Basal Gneiss region.

Furthermore, Bryhni et al. (1971) have recently interpreted the ^{40}Ar–^{39}Ar age spectrum of a pyroxene from an augen gneiss in 'Anorthosite Kindred' rocks from the Fjordane Complex of the Nordfjord area as indicating an original age $>$ 1550 m.y.

Concluding remarks

In theory there are several lines of geological evidence one might expect would assist one to differentiate between basement and cover rock complexes in an orogenic belt.

However, where the basement has been reactivated and consequently deformed, metamorphosed and migmatized, together with its cover during a subsequent orogeny, then the geological evidence becomes extremely blurred. In the central regions of an orogenic belt intensive deformation rapidly obliterates the evidence of earlier fold episodes and obscures the contact relationships with the production of a secondary tectonic concordance between the basement and cover. Metamorphic overprinting of the basement eradicates or at least obscures the metamorphic distinctions and also causes partial or complete isotopic re-equilibration, making the interpretation of radiometric dates difficult and often speculative. Migmatization of the cover rocks promotes lithological convergence and obscures primary lithological distinctions.

Unfortunately it is just such a geological situation one is faced with having to decipher in the Basal Gneiss region. A good approach to this problem is to, if possible, first observe the basement-cover relationships and the distinctive features of each where these rocks are in a relatively unmodified state at the margins of the orogenic belt. Working into the orogenic belt from the marginal Moine thrust zone, some success has been achieved in northern Scotland in differentiating between Lewisian basement inliers and Moine cover rocks on lithological grounds. However, the lengthy debate which has occurred concerning these basement inliers shows that even this approach is difficult.

Thus in the opinion of the present author, hopes of producing an accurate geological map of the Pre-Eocambrian basement and Eocambrian-Lower Palaeozoic cover relations in the Norwegian Basal Gneiss region probably depend largely on a confirmation by Rb-Sr isochron or ^{40}Ar-^{39}Ar dating

techniques of the thesis advanced here, that occurrences of 'country rock' eclogites, granulites and calcic anorthosites in this region are restricted to the Pre-Eocambrian basement.

If this thesis is correct then much of Bryhni's Fjordane Complex (Bryhni 1966) as well as his Jostedal Complex must represent reactivated Pre-Eocambrian basement, and is perhaps older rather than younger than the Jostedal Complex.

Acknowledgements. – The author wishes to acknowledge the receipt of financial support from the University of Sheffield Research Fund for field work in Norway, and to thank Dr. P. E. Brown and Dr. N. J. Soper for their most helpful comments and suggestions regarding this paper.

April 1972

REFERENCES

Alderman, A. R. 1936: Eclogites in the neighbourhood of Glenelg, Inverness-shire. *Quart. Jour. Geol. Soc. London 92,* 488–530.

Anderson, A. T. 1969: Massif-type anorthosite: a widespread Pre-Cambrian igneous rock. *In* Isachsen, Y. W. (Ed.): Origin of anorthosite and related rocks. *New York State Mus. Sci. Serv. Mem. 18,* 47–55.

Anderson, A. T. & Morin, M. 1969: Two types of massif anorthosites and their implications regarding the thermal history of the crust. *In* Isachsen, Y. W. (Ed.): Origin of anorthosite and related rocks. *New York State Mus. Sci. Serv. Mem. 18,* 57–69.

Banham, P. H. 1968: The basal gneisses and basement contact of the Hestbrepiggan area, north Jotunheimen, Norway. *Norges geol. undersøkelse 252,* 77 pp.

Banham, P. H. & Elliott, R. B. 1965: Geology of the Hestbrepiggan area, preliminary account. *Norsk geol. tidsskr. 45,* 189–198.

Barth, T. F. W. 1938: Progressive metamorphism of sparagmite rocks of southern Norway. *Norsk geol. tidsskr. 18,* 54–65.

Birkeland, T. 1958: Geological and petrological investigations in northern Trøndelag, western Norway. *Norsk geol. tidsskr. 38,* 327–420.

Brueckner, H. K. 1969: Timing of ultramafic intrusion in the core zone of the Caledonides of southern Norway. *Am. Jour. Sci. 267,* 1195–1212.

Brueckner, H. K., Wheeler, R. L. & Armstrong, R. L. 1968: Rb–Sr isochron of older gneisses of the Tafjord area, basal gneiss region, south-western Norway. *Norsk geol. tidsskr. 48,* 127–131.

Bryhni, I. 1966: Reconnaissance studies of gneisses, ultrabasites, eclogites and anorthosites in outer Nordfjord, western Norway. *Norges geol. undersøkelse 241,* 68 pp.

Bryhni, I., Bollingberg, H. J. & Graff, P. R. 1969: Eclogites in quartz-feldspathic gneisses of Nordfjord, West Norway. *Norsk geol. tidsskr. 49,* 193–225.

Bryhni, I., Green, D. H., Heier, K. S. & Fyfe, W. S. 1970: On the occurrence of eclogite in western Norway. *Contr. Mineral & Petrol. 26,* 12–19.

Bryhni, I. & Grimstad, E. 1970: Supracrustal and infracrustal rocks in the Gneiss Region of the Caledonides west of Breimsvatn. *Norges geol. undersøkelse 266,* 105–140.

Bryhni, I., Fitch, F. J. & Miller, J. A.: $^{40}Ar/^{39}Ar$ dates from recycled Precambrian rocks in the Gneiss region of the Norwegian Caledonides. *Norsk Geol. tidsskr. 51,* 391–406.

Carswell, D. A. 1968a: Picritic magma-residual dunite relationships in garnet peridotite at Kalskaret, near Tafjord, South Norway. *Contr. Mineral. & Petrol. 19,* 97–124.

Carswell, D. A. 1968b: Possible primary upper mantle peridotite in Norwegian basal gneiss. *Lithos 1,* 322–355.

Eskola, P. 1921: On the eclogites of Norway. *Skr. Norske Vidensk.-Akad. i Oslo, Mat.-naturv. Kl., no. 8,* 1–118.

Gayer, R. A., Gee, D. G., Harland, W. B., Miller, J. A., Spall, H. F., Wallis, R. H. & Winsnes, T. S. 1966: Radiometric age determinations on rocks from Spitsbergen. *Norsk. Polarinst. Skr. 137,* 1–39.

Gee, D. G. 1966: A note on the occurrence of eclogites in Spitsbergen. *Norsk. Polarinst. Arb. 1964,* 240–241.

Gjelsvik, T. 1951: Oversikt over bergartene i Sunnmøre og tilgrensende deler av Nordfjord. Med geologisk oversiktskart av Tore Gjelsvik & Chr. Gleditsch. *Norges geol. undersøkelse 279,* 45 pp.

Gjelsvik, T. 1952: Metamorphosed dolerites in the gneiss area of Sunnmøre. *Norsk geol. tidsskr. 30,* 33–134.

Gjelsvik, T. 1953: Det nordvestlige gneis-område i det sydlige Norge, aldersforhold og tektonisk-stratigrafisk stilling. *Norsk. geol. undersøkelse 184,* 71–94.

Heier, K. S. & Compston, W. 1969: Interpretation of Rb–Sr age patterns in high grade metamorphic rocks, North Norway. *Norsk geol. tidsskr. 49,* 257–283.

Hernes, I. 1954: Eclogite-emphibolite on the Molde peninsula, southern Norway. *Norsk geol. tidsskr. 33,* 163–184.

Hernes, I. 1955: Trondhjemsskifrene ved Molde. *Norsk. geol. tidsskr. 34,* 123–137.

Hernes, I. 1965: Die kaledonische Schichtenfolge in Mittelnorwegen. *Neues Jahrb., Geol. Paläont. Mh. 2,* 69–84.

Hernes, I. 1967: The late Pre-Cambrian stratigraphic sequence in the Scandinavian mountain chain. *Geol. Mag. 104,* 557–563.

Herz, N. 1969: Anorthosite belts, continental drift and the anorthosite event. *Science 164,* 944–947.

Hess, H. H. 1965: Serpentines, orogeny and epeirogeny. *Geol. Soc. Amer. Special Paper 62,* 351–407.

Holtedahl, O. 1936: Trekk av det skandinaviske fjellkjedestrøks historie. *Nordiska naturforskarmötet i Helsingfors 1936,* 129–145.

Holtedahl, O. 1938: Geological observations in the Opdal-Sunndal-Trollheimem district. *Norsk geol. tidsskr. 18,* 29–53.

Holtedahl, O. 1944: On the Caledonides of Norway with some scattered local observations. *Skr. Norske Vidensk-Akad. i Oslo, Mat.-naturv. Kl., 1944, no. 4,* 31 pp.

Holtedahl, O. & Dons, J. A. 1960: Geologisk kart over Norge, Bergrunnskart 1:1000000. *Norges geol. undersøkelse 208.*

Kolderup, C. F. 1923: Kvamshestens devonfelt. *Bergens Mus. Årb. 1920–21. Naturvidensk, R. 4,* 96 pp.

Kolderup, N.-H. 1952: The age of gneisses and migmatites in the 'North-West Block' of southern Norway *Trans. Edin. Geol. Soc. 15,* 234–240.

Kolderup, N.-H. 1960: Origin of Norwegian eclogites in gneisses. *Norsk geol. tidsskr. 40,* 73–76.

Kranck, E. H. 1935: On the crystalline complex of Liverpool Land. *Meddelelser om Grönland 95, No. 7,* 122 pp.

Kratz, K. O., Gerling, E. K. & Lobach-Zhuchenko, S. B. 1968: The isotope geology of the Precambrian of the Baltic Shield. *Canadian Jour. Earth Sciences 5,* 657–660.

Lappin, M. A. 1966: The field relationships of basic and ultrabasic masses in the Basal Gneiss Complex of Stadlandet and Almklovdalen, Nordfjord, southwestern Norway. *Norsk geol. tidsskr. 46,* 439–496.

Macdougall, I. & Green, D. H. 1964: Excess radiogenic argon and isotopic ages on minerals from Norwegian eclogites. *Norsk. geol. tidsskr. 44,* 183–196.

Miller, J. A., Barber, A. J. & Kempton, N. H. 1963: A K/Ar age determination from a Lewisian inlier. *Nature 197,* 1095–1096.

Moores, E. 1970: Ultramafics and orogeny, with models of the U.S. Cordillera and the Tethys. *Nature 228,* 837–842.

Muret, C. 1960: Partie S.E. de la culmination du Romsdal, Chainne Caledonienne, Norvège. *Int. Geol. Congr. Norden. 1960, No. 19,* 28–32.

Oftedahl, C. 1964: The nature of the basement contact. *Norges. geol. undersøkelse 227,* 5–12.

O'Hara, M. J. & Mercy, E. L. P. 1963: Petrology and petrogenesis of some garnetiferous peridotites. *Trans. Roy. Soc. Edinburgh. 65,* 251–314.

Park, R. G. 1970: Observations on Lewisian Chronology. *Scottish Jour. Geol. 6,* 379–399.

Peacey, J. S. 1964: Reconnaissance of the Tømmerås anticline. *Norges. geol. undersøkelse 227,* 13–84.

Peach, B. N., Horne, J., Woodward, H. B., Clough, C. T., Harker, A. & Wedd, C. B. 1910: The geology of Glenelg, Lochalsh and south-east part of Skye. *Mem. Geol. Surv. Scotland 71.*

Peach, B. N., Horne, J., Hinxman, L. W., Crampton, C. B., Anderson, E. M., Carruthers, R. G. & Flett, J. S. 1913: The geology of central Ross-shire. *Mem. Geol. Surv. Scotland 82.*

Ramsay, J. G. 1957a.: Moine-Lewisian relations at Glenelg, Inverness-shire. *Quart. Jour. Geol. Soc. London 113,* 487–523.

Ramsay, J. G. 1957b: Superimposed folding at Loch Monar, Inverness-shire, and Ross-shire. *Quart. Jour. Geol. Soc. London 113,* 271–307.

Ramsay, J. G. 1963: Structure and metamorphism of the Moine and Lewisian rocks of the N.W. Caledonides. *In* Johnson, M. R. W. & Stewart, F. W. (Eds.): *The British Caledonides.* Oliver & Boyd, Edinburgh, 143–175.

Reusch, H. H. 1881: Konglomerat-Sandstenfelterne i Nordfjord, Søndfjord og Sogn. *Nyt. Mag. Naturvitensk. 26,* 93–170.

Roberts, D., Springer, J. & Wolff, F. C. 1970: Evolution of the Caledonides in the northern Trondheim region, Central Norway: a review. *Geol. Mag. 107,* 133–145.

Rosenqvist, I. Th. 1941: The Lønset anticline in the Opdal area. *Norsk geol. tidsskr. 21,* 25–48.

Sahlstein, Th. G. 1935: Petrographie der Eklogiteinschlüsse in den Gneisen des südwestlichen Liverpool-Landes in Ost-Grönland. *Meddelelser om Grönland 95, No. 5,* 43 pp.

Schmitt, H. H. 1964: Metamorphic eclogites of the Eiksund area, Sunnmøre, Norway. *Am. Geophys. Union Trans. 43,* 128.

Spooner, C. M. & Fairbairn, H. W. 1970: Sr^{87}/Sr^{86} initial ratios in pyroxene granulite terranes. *M. I. T. 18th Annual Progress Rep. 1970,* 57–64.

Strand, T. 1949: On the gneisses from a part of the north-western Gneiss area of southern Norway. *Norges geol. undersøkelse 173,* 45 pp.

Strand, T. 1953: The relation between the basal gneiss and the overlying metasediments in the Surnadal district (Caledonides of Southern Norway). *Norges geol. undersøkelse 184,* 100–121.

Strand, T. 1960: The region with Basal Gneiss in the N.W. part of S. Norway. *In* Holtedahl, O. (Ed.): Geology of Norway. *Norges geol. undersøkelse 208,* 230–245.

Strand, T. 1969: Geology of the Grotli area. *Norsk. geol. tidsskr. 49,* 341–360.

Sutton, J. & Watson, J. 1952: The supposed Lewisian inlier at Scardroy, central Ross-shire and its relations with the surrounding Moine rocks. *Quart. Jour. Geol. Soc. London 108,* 99–126.

Sutton, J. & Watson, J. 1954: The structure and stratigraphic succession of the Moines of Fannich Forest and Strath Bran, Ross-shire. *Quart. Jour. Geol. Soc. London 110,* 21–53.

Sutton, J. & Watson, J. 1958: Structures in the Caledonides between Loch Duich and Glenelg, north-west Highlands. *Quart. Jour. Geol. Soc. London 114,* 231–257.

Sutton, J. & Watson, J. 1962: An interpretation of the Moine-Lewisian relations in Central Ross-shire. *Geol. Mag. 99,* 525–541.

Welin, E. 1966: The absolute time scale and the classification of Precambrian rocks in Sweden. *Geol. fören. Stockholm Förh. 88,* 29–33.

Wirdley, B. F. 1970: Anorthosites in the early crust of the Earth and on the Moon. *Nature 226,* 333–335.

Wyllie, P. J. 1967: Review: *In* Wyllie, P. J. (Ed.): *Ultramafic and Related Rocks.* John Wiley & Sons. Inc., New York. Pp. 403–416.

Yoder, H. S. Jr. 1969: Experimental studies bearing on the origin of anorthosite. *In* Isachsen, Y. W. (Ed.): Origin of anorthosite and related rocks. *New York State Mus. Sci. Serv. Mem. 18,* 13–22.

EARTH AND PLANETARY SCIENCE LETTERS 20 (1973) 347–352. NORTH-HOLLAND PUBLISHING COMPANY

GARNET PYROXENITE LENS WITHIN UGELVIK LAYERED GARNET PERIDOTITE

D.A. CARSWELL
Department of Geology, University of Sheffield, Mappin Street, Sheffield S1 3JD, England

Received 22 June 1973
Revised version received 12 September 1973

A unique garnet pyroxenite lens is described from within the layered garnet peridotite mass at Ugelvik on the Island of Otrøy, west Norway. Textural evidence, whole rock and mineral analyses suggest the original crystallisation of a high temperature enstatite phase formed at roughly 1500-1600°C and 35-40 kb pressure. This primary enstatite subsequently exsolved chrome diopside and garnet still at upper mantle temperatures and pressures of the order of 950-975°C and 35-37 kb, before the tectonic emplacement of the peridotite mass into its present crustal environment.

1. Introduction

The striking occurrences of layered garnetiferous peridotites close to the village of Ugelvik on the Island of Otrøy on the north side of Romdalsfjord in west Norway, have been previously described [1] and are thought to represent tectonic slices of upper mantle peridotite thrust up into the basal gneisses [2] in this region. This paper describes an interesting new discovery of a coarse garnet pyroxenite lens exposed within the layered garnet peridotites in a new small quarry blasted adjacent to the new harbour at Ugelvik.

2. Petrography

The peridotite exposed around Ugelvik consists largely of interbanded garnetiferous and garnetfree peridotite. Garnetiferous peridotite predominates and contains on the average 10% garnet, 3% chrome diopside, 7% enstatite (7–8% Fs), 78% olivine (8–9% Fa) or serpentinised olivine, 1% spinel and 1% secondary amphibole. The grain size is commonly of the order of 1–2 mm, although single gem quality garnets up to 4–5 mm across can sometimes be found. Also the rocks have partial cataclastic fabrics, most apparent in the garnet- and pyroxene-rich layers, with small granulated grains adjacent to strained 1–2 mm sized porphyroclasts. The extensive late stage serpentinisation tends to mask the cataclastic fabric.

The newly discovered garnet pyroxenite forms an irregularly shaped lens-like mass up to 45 cm across within the usual garnetiferous peridotite. The garnet pyroxenite lens is strikingly coarse grained consisting mainly of large randomly orientated enstatite crystals, commonly 1–2 × 1 cm in size, with the largest single enstatite crystal measured being rougly 3 × 5.5 cm. Forsteritic olivine grains up to 4–6 mm across occur in small interstitial amounts, whilst garnet also occurs interstitially to the enstatite grains and sometimes forms single crystals up to 5 mm across. However, apparently all the chrome diopside and much of the garnet occurs as numerous small grains (of about 0.5 – 1 mm in size) distributed both along crystallographic planes within the enstatites and also, in particular with the garnets, around the margins of the enstatite grains. The chrome diopside forms small discrete grains or in some cases long narrow lamellae orientated // (100) plane of the host enstatite, whilst concentrations of both chrome diopside and garnet grains occur along rather irregular cross-cutting fracture planes (fig. 1).

Thus the overall texture of the garnet pyroxenite lens is undoubtedly that of an exsolution texture in which it appears that probably all of the chrome diopside and much of the garnet present have resulted

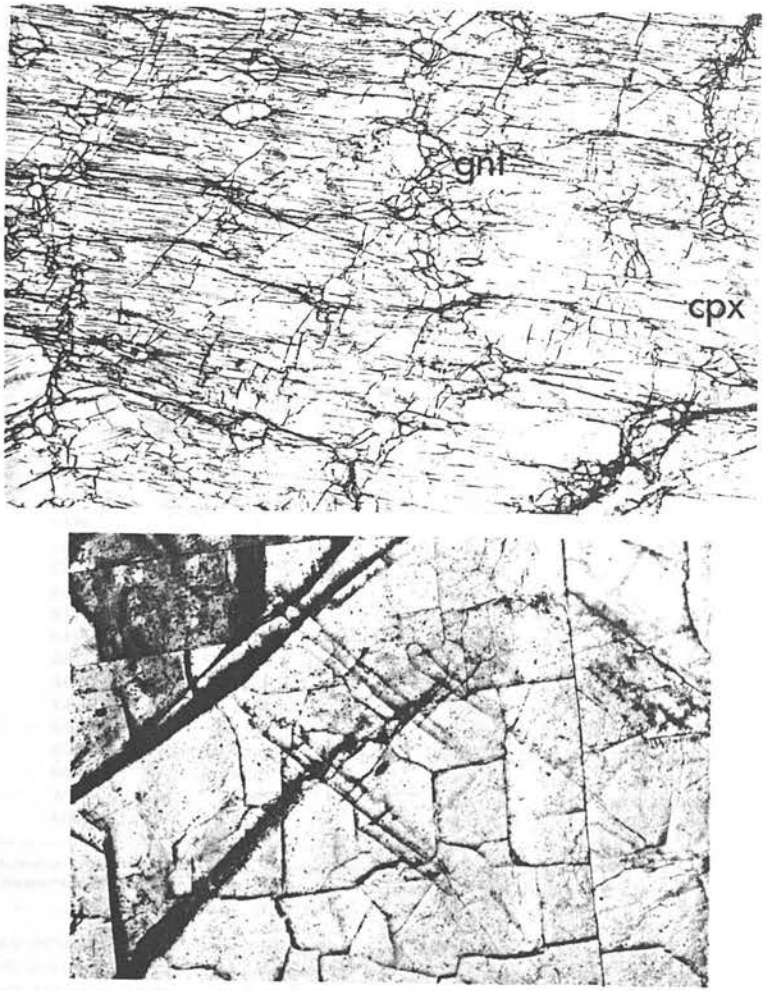

Fig. 1. a. Photomicrograph showing exsolution of chrome diopside (cpx) and garnet (gnt) within enstatite in garnet pyroxenite, U95. Magnification X 10. b. Photomicrograph of narrow exsolution lamellae of chrome diopside within enstatite in garnet pyroxenite, U95. Magnification X 80.

from exsolution from original high temperature enstatite grains.

The garnet pyroxenite lens has a marked sheared marginal zone about 5 mm wide on average, consisting largely of fine grained (up to 0.5 mm) granulated enstatite grains and in which a crude foliation parallel to that in the surrounding garnet peridotites has developed. This strongly suggests that the layering in the surrounding garnet peridotites as a whole is tectonised igneous mineralogical layering.

3. Chemistry

Presented in table 1 are an analysis of a whole rock specimen of the garnet pyroxenite U95, together with analyses of its constituent orthopyroxene, clinopyroxene and garnet. The mineral analyses are very similar to those for equivalent minerals in the associated garnet peridotites [1] and hence appear to have equilibrated as 4-phase garnet lherzolite assemblages under essentially the same temperature and pressure conditions. The equilibration temperatures and pressures of the exsolved pyroxene phases in U95 can be estimated on the basis of the amount of mutal solid solution between the co-existing pyroxenes and the amount of potential garnet molecule in solid solution within the pyroxenes, reflected most simply by the wt.% Al_2O_3 in the pyroxenes.

On the basis of the solid solution limits between the co-existing pyroxenes in the synthetic diopside-enstatite system at 30 kb pressure [3], adjusted slightly to take into account the likely effect of the additional components present in the natural rock systems, and limited experimental data [4] on the wt.% Al_2O_3 in orthopyroxene from 4-phase garnet 'pyrolite' assem-

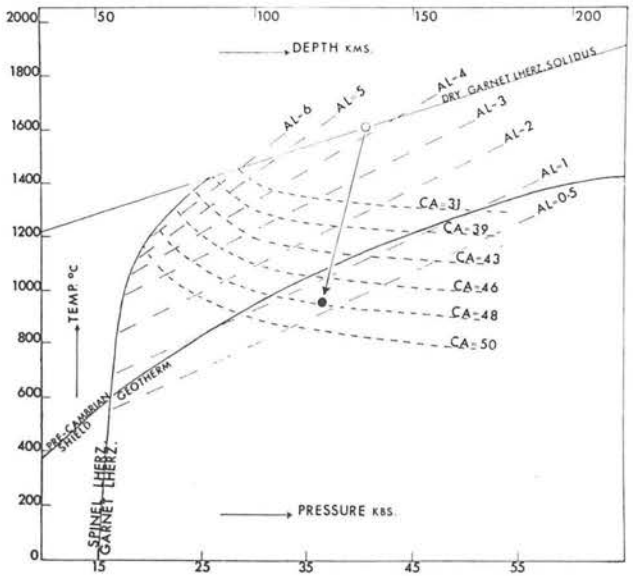

Fig. 2. Estimated equilibration conditions for U95 primary assemblage (open circle) and re-equilibrated assemblage (closed circle) on the basis of the parameters Ca = at.% Ca/Ca + Mg in the clinopyroxene and Al = wt.% Al_2O_3 in the orthopyroxene. The spinel lherzolite ≈ garnet lherzolite boundary is from O'Hara et al. [7], the dry garnet lherzolite solidus extrapolated from Ito and Kennedy [8] and the Pre-Cambrian Shield geotherm from Ringwood et al. [9].

TABLE 1
Whole rock and mineral analyses of garnet websterite, U95 (wt.%)

	Whole rock		Orthopyroxene		Clinopyroxene		Garnet	
SiO_2	55.03		57.66		55.19		42.58	
TiO_2	0.03		0.02		0.14		0.00	
Al_2O_3	4.16		0.66		3.25		21.77	
Cr_2O_3	0.62		0.17		1.92		2.52	
Fe_2O_3	0.55		0.63		0.03		0.77	
FeO	3.91		3.58		1.01		6.90	
MnO	0.10		0.06		0.03		0.32	
NiO	0.10		0.12		0.05		0.00	
MgO	32.66		36.61		15.95		21.02	
CaO	1.98		0.45		20.39		4.34	
Na_2O	0.19		0.03		2.04		0.00	
K_2O	0.00		0.01		0.00		0.00	
Total	99.33		100.00		100.00		100.22	
Structural formulae								
Si	1.906	2.000	1.970	1.997	1.981	2.000	3.014	3.014
Al	0.094		0.027		0.019		0.000	
Al	0.076		0.000		0.119		1.816	1.998
Ti	0.001		0.001		0.004		0.000	
Cr	0.017		0.005		0.054		0.141	
Fe^{3+}	0.014	1.913	0.016	1.993	0.001	1.063	0.041	
Fe^{2+}	0.113		0.102		0.030		0.408	
Mn	0.003		0.002		0.001		0.019	
Ni	0.003		0.003		0.001		0.000	
Mg	1.686		1.864		0.853		2.217	2.973
Ca	0.073	0.086	0.016	0.018	0.784	0.926	0.329	
Na	0.013		0.002		0.142		0.000	
K	0.000		0.000		0.000		0.000	
Total	3.999		4.007		3.990		7.985	
O	6.000		6.000		6.000		12.000	

Mineral analyses by Mr. V.A. Somogyi using 'wet' chemical techniques. Whole rock analysis is an average of 'wet' chemical and X-ray fluorescence determinations performed by Mr. V.A. Somogyi and Dr. R. Sotiriou, respectively.

blages at different temperatures and pressures, it is possible to estimate the equilibration conditions for co-existing pyroxenes by plotting wt.% Al_2O_3 in orthopyroxene against at.% Ca/Ca+Mg in clinopyroxene as shown in fig. 2. However it should be appreciated that fig. 2 involves large extrapolations from the limited experimental data available. It therefore yields only rough estimates of the equilibration temperatures and pressures for particular assemblages, but the relative equilibration conditions deduced for different assemblages should be reliable. Absolute temperatures and pressures determined could perhaps be in error by up to ± 15% in the low temperature part of the diagram.

Fig. 2 suggests an equilibration temperature for the co-existing exsolved pyroxene phases in U95 of about 950–975°C at a pressure of roughly 35–37 kb. Such an equilibration temperature is higher than the 600–700°C previously indicated for the layered garnet peridotites at Ugelvik by Carswell [1] but is now thought to be more realistic for all the Ugelvik 4-phase garnet lherzolite assemblages.

In view of the textural evidence that probably all the clinopyroxene and most, if not all, of the garnet in U95 has been derived as a result of exsolution from the primary high temperature orthopyroxene, it is highly significant that the whole rock analysis of U95 recalculates as a respectable orthopyroxene (table 1). The small amounts of primary olivine present have little significant effect on the whole rock analysis. The postulated primary high temperature orthopyroxene thus has 4.16 wt.% Al_2O_3 and 1.98 wt.% CaO, indicating the presence of significant amounts of potential garnet and clinopyroxene in solid solution. If this primary orthopyroxene crystallised on the peridotite solidus along with garnet and olivine then on the basis of its 4.12 wt.% Al_2O_3 content this suggests from fig. 2 that it crystallised at about 1500–1600°C at 35–40 kb pressure.

4. Discussion

As the textural evidence within U95 in favour of crystallisation of a little primary garnet along with the predominant orthopyroxene and undoubted minor olivine is rather ambiguous, it is important to point out that there is additional evidence suggesting the primary high temperature crystallisation of garnet. This consists of scarce large nodular garnets up to 3 cm across, which are found scattered throughout the layered garnet peridotites. These garnets clearly have small concentrations of clinopyroxenes associated with them suggesting that the clinopyroxene may in fact have exsolved from high temperature garnets or alternatively has formed interstitially to the garnets as the final phase to crystallise. In either case it is felt that the presence of these large garnets, taken in conjunction with the evidence from the garnet pyroxenite lens described in this paper, supports the crystallisation of a primary garnet + orthopyroxene + olivine ± clinopyroxene assemblage. It would appear that the primary assemblage has cooled essentially isobarically down to roughly the Pre-Cambrian Shield geotherm, and there re-equilibrated to a garnet + orthopyroxene + olivine + clinopyroxene assemblage still at upper mantle depths (100–125 km) prior to tectonic emplacement into its present crustal position during a major orogenic event.

The high temperatures and pressures of formation postulated for the primary assemblage clearly necessitate a mantle origin for the garnet pyroxenite lens and its enclosing garnetiferous peridotites, and rule out a crustal metamorphic origin as has been argued by Bryhni et al. [5] and Mysen and Heier [6] for basic eclogite masses in western Norway. However, it is felt that the possibility should be considered that the petrogenesis of the two types of eclogites may be different – the basic eclogites being lower crustal metamorphic rocks as argued by these authors and the ultrabasic eclogites (that is the garnet peridotites) tectonic slices of the underlying upper mantle.

The inferred primary high temperature origin for the Ugelvik garnet pyroxenite lens, combined with previous arguments put forward [10] as indicating that the Kalskaret garnet peridotite lens in the Tafjord district has been involved in a partial melting event at upper mantle pressures, suggests that all the garnet peridotite bodies in the basal gneiss region of western Norway may have had a high temperature upper mantle origin which in general has been masked by secondary recrystallisation at subsolidus temperatures. A further implication is that the sub-continental upper mantle as a whole may have undergone at least partial melting at some stage during its history, but that this high temperature stage has largely been obscured by later recrystallisation. This melting and subsequent crystallisation event may have occurred very early in the earth's history and represent the event largely responsible for the differentiation of the earth into chemically distinct mantle and core units. Alternatively, and perhaps more likely, it may reflect the fact that the uppermost regions of the mantle have undergone extensive partial melting leading to crustal development during geological history.

Acknowledgements

The author wishes to acknowledge the receipt of financial support for field work from the University of Sheffield Research Fund, and to thank Mr. V.A.

Somogyi and Dr. R. Kanaris-Sotiriou for performing the chemical analyses.

References

[1] D.A. Carswell, Possible primary upper mantle peridotite in Norwegian basal gneiss, Lithos 1 (1968) 322.
[2] D.A. Carswell, The age and status of the Basal Gneiss Complex of north-west southern Norway, Norsk Geol. Tidsskr. 53 (1973) 65.
[3] B.T.C. Davis and F.R. Boyd, The join $Mg_2Si_2O_6$-$CaMgSi_2O_6$ at 30 kilobars pressure and its application to pyroxenes from kimberlites, J. Geophys. Res. 71 (1966) 3567.
[4] D.H. Green and A.E. Ringwood, The stability fields of aluminous pyroxene peridotite and garnet-peridotite and their relevance in upper mantle structure, Earth Planet. Sci. Letters 3 (1967) 151.
[5] I. Bryhni, D.H. Green, K.S. Heier and W.S. Fyfe, On the occurrence of eclogite in western Norway, Contr. Mineral. Petrol. 26 (1970) 12.
[6] B.O. Mysen and K.S. Heier, Petrogenesis of eclogites in high grade metamorphic gneisses, exemplified by the Hareidland eclogite, western Norway, Contr. Mineral. Petr. 36 (1972) 73.
[7] M.J. O'Hara, S.W. Richardson and G. Wilson, Garnet-peridotite stability and occurrence in crust and mantle, Contr. Mineral. Petr. 32 (1971) 48.
[8] K. Ito and G.C. Kennedy, Melting and phase relations in a natural peridotite to 40 kilobars, Amer. J. Sci. 165 (1967) 519.
[9] A.E. Ringwood, I.D. Maggregor and F.R. Boyd, Petrological constitution of the upper mantle, Carnegie Inst. Washington Year Book 63 (1964) 147.
[10] D.A. Carswell, Picritic magma-residual dunite relationships in garnet peridotite at Kalskaret near Tafjord, South Norway, Cont. Mineral. Petr. 19 (1968) 97.

Comparative equilibration temperatures and pressures of garnet lherzolites in Norwegian gneisses and in kimberlite

D. A. CARSWELL

LITHOS

Carswell, D. A. 1974: Comparative equilibration temperatures and pressures of garnet lherzolites in Norwegian gneisses and in kimberlite. *Lithos 7*, 113–121.

The chemistry of the pyroxenes suggests that the garnet lherzolites enclosed in the Norwegian basal gneisses have equilibrated at depths greater than 70 kilometres along an expected sub-continental geotherm. Such depths are somewhat shallower than the apparent depths of origin of most garnet lherzolite xenoliths in kimberlite pipes. Distribution coefficients for Fe^{2+}/Mg^{2+} and Mn^{2+}/Mg^{2+} between coexisting clinopyroxenes and garnets support the slightly lower equilibration temperatures deduced for the Norwegian garnet lherzolites compared with the xenolithic garnet lherzolites in kimberlites.

The pressure-temperature equilibration conditions deduced for the Norwegian garnet lherzolites (800–1020°C at 22–37 kbs) contrast with previous estimates ($625 \pm 30°$ at 14 kbs) for basic eclogite masses in the Norwegian gneisses. This suggests a possible dual paragenesis of the Norwegian eclogites, with the garnet lherzolites being tectonic slices of the sub-continental upper mantle and the basic eclogites deep crustal metamorphic rocks.

D. A. Carswell, Dept. of Geology, University of Sheffield, Mappin Street, Sheffield S1 3JD, United Kingdom.

There is now a large body of agreement (Harris et al. 1967, O'Hara 1967, 1970, Carswell & Dawson 1970) that the common granular 4-phase garnet lherzolite xenoliths (garnet + olivine + orthopyroxene + clinopyroxene assemblages) in kimberlite pipes have been derived from the upper mantle – probably in general from depths of the order of 100–150 kilometres. Such xenoliths therefore provide the most direct line of evidence on the mineralogy and composition of the upper mantle at such depths.

However, opinion is still greatly divided (cf. O'Hara & Mercy 1963, Kopecky & Sattran 1966, Rost 1966, Fiala 1966, Carswell 1968a, b, etc.) concerning the petrogenesis of the garnet lherzolites found directly enclosed in gneisses in crustal metamorphic terrains and of which good examples are found in the Basal Gneiss region of the Møre and Romsdal districts of western Norway.

O'Hara & Mercy (1963), Lappin (1966), Carswell (1968a, b, 1973), and O'Hara et al. (1971) have argued that the Norwegian garnet lherzolites and associated eclogites have been tectonically emplaced into their present crustal position as cool bodies during orogenesis, having probably originated from the top of the mantle although possibly (O'Hara 1967) from near the base of the crust in regions of drastically thickened crust. On the other hand Schmitt (1964), Bryhni et al. (1970), and Green & Mysen (1972) have suggested that all the eclogites, both basic and ultrabasic types, one finds in western Norway may be essentially *in situ* crustal metamorphic rocks which developed under the same load pressure and temperature conditions as the enclosing almandine amphibolite facies gneisses but under local conditions of much lower water pressure.

This paper therefore reconsiders the crustal versus mantle origin controversy for the Norwegian garnet lherzolites on the basis of estimates of their likely equilibration temperatures and pressures based on mineralogical considerations and a comparison with the granular garnet lherzolite xenoliths from kimberlite pipes.

Resumé of experimental data

It appears that fairly reasonable values for equilibration temperatures in natural garnet lherzolite assemblages can be obtained by considering the extent of the solid solution

between the coexisting pyroxenes. Experimental studies of the subsolidus relationships concerning the two-pyroxene solvus in the synthetic enstatite-diopside system at atmospheric pressure (Boyd & Schairer 1964) and at 30 kbs pressure (Davis & Boyd 1966) have shown that the extent of enstatite solid solution in diopside increases significantly with temperature, and that the position of the diopside arm of the solvus is virtually independent of pressure. However, one can only use this geothermometer in a semi-quantitative fashion as the effects of the presence of additional chemical components (such as FeO, Al_2O_3, Cr_2O_3, Fe_2O_3 and Na_2O) in natural diopsides on the solvus position are likely to be significant but have not been quantified.

It is clear for example (see Lindsley & Munoz 1969) that enrichment in FeO will progressively shrink the two pyroxene field giving increased solid solution of Mg rich pyroxene in the Ca rich pyroxene phase. There is also some experimental evidence at 30 kbs (O'Hara & Yoder 1967, Boyd 1969) to show that solid solution towards garnet (reflected in increased Al_2O_3 content) has the opposite effect of reducing the solid solution of enstatite in diopside. O'Hara & Yoder (1967) observed appreciable reduction in solid solution at 1500–1600°C for both synthetic $CaSiO_3$–$MgSiO_3$–Al_2O_3 compositions and natural garnet-clinopyroxene-orthopyroxene mixtures, whilst Boyd (1969) observed a much smaller reduction in experiments at 1200°C with similar synthetic compositions.

As the reduction in the solid solution limits due to the presence of Al_2O_3 will most likely be partly offset by the presence of FeO, and since the pyroxenes in most natural garnet lherzolite assemblages have relatively low Al_2O_3 contents (generally <3.5 wt.%) and low $Fe^{2+}/Fe^{2+}+Mg^{2+}$ ratios (generally <0.05) and are in general fairly close in composition to the synthetic enstatite-diopside system, it should be possible to obtain reasonable temperature estimates by application of the experimentally determined diopside solvus at 30 kbs pressure for the synthetic system (Davis & Boyd 1966). The sparse data provided by O'Hara & Yoder (1967: Fig. 8) for the extent of solid solution in natural clinopyroxene-orthopyroxene mixtures suggests that the overall effect of the 'impurities' present in natural clinopyroxenes from garnet lherzolites is to slightly reduce the extent of solid solution of orthopyroxene in clinopyroxene at any particular temperature compared with the synthetic enstatite-diopside system, and hence may lead to an underestimation of the temperature of formation by up to 100 C.

It is also known from experiments with both synthetic and natural systems (Boyd & England 1964, MacGregor & Ringwood 1964, Green & Ringwood 1967, Boyd 1969) that the solubility of potential garnet molecule (which may be expressed most simply as wt.% Al_2O_3 or R_2O_3) in both orthopyroxene and clinopyroxene decreases markedly with pressure at any particular temperature within the garnet lherzolite stability field. Again, however, there are problems involved in interpreting natural garnet lherzolite assemblages in the light of data chiefly obtained on chemically simplified synthetic systems. Experiments with pyrolite model compositions (Green & Ringwood 1967) have shown that under the pressure-temperature conditions of the garnet lherzolite facies, the Al_2O_3 contents of the orthopyroxenes were substantially less at any specific temperature and pressure than in the synthetic and natural enstatite-pyrope systems (Boyd & England 1964, MacGregor & Ringwood 1964), whilst experiments on the synthetic $CaSiO_3$–$MgSiO_3$–Al_2O_3 system by O'Hara & Yoder (1967) and Boyd (1969) similarly showed how solid solution of diopside in enstatite significantly reduced the Al_2O_3 content of the enstatite. The work of MacGregor (1970) has in addition shown that the position of the spinel lherzolite ⇌garnet lherzolite reaction boundary and of the Al_2O_3 isopleths in the garnet lherzolite field may be expected to shift significantly to higher pressures with increasing Cr_2O_3/R_2O_3 ratios, so that inferences drawn from a comparison of natural and experimental garnet lherzolite assemblages should be based on rock systems with broadly comparable Cr_2O_3/R_2O_3 ratios.

However, with the observed reservations in mind it should nevertheless be possible to combine chemical information on the Al_2O_3 or total R_2O_3 content of the pyroxenes with that on the mutual solubility between the coexisting pyroxenes in order to derive a reasonable estimate of the pressure-temperature conditions of crystallization of natural garnet lherzolite assemblages.

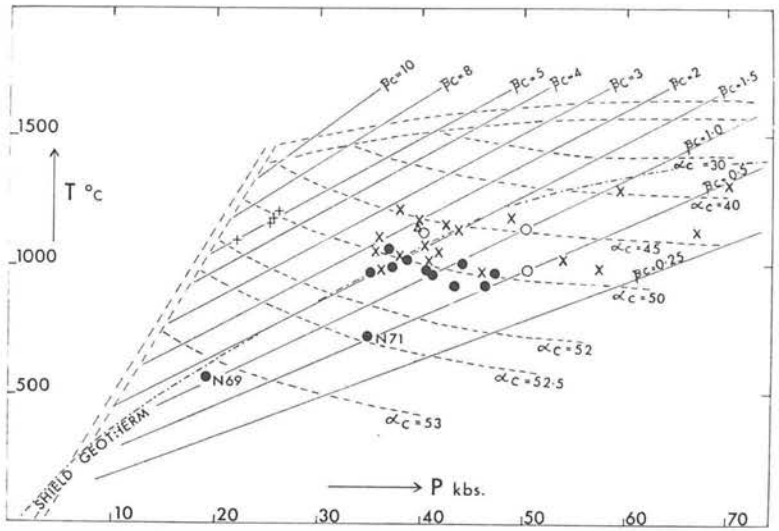

Fig. 1. Estimated pressure-temperature equilibration conditions for natural garnet lherzolite assemblages based on the provisional grid for the variation of the functions α_c and β_c given by O'Hara (1967: Fig. 12.4), extrapolated to somewhat lower β_c values. The data sources and symbol code used are as follows:
Norwegian samples – closed circles (O'Hara & Mercy 1963, Carswell 1968a & b, and unpublished data).
Czech samples – open circles (Fiala 1966, Mikhailov & Rovsha 1966).
Swiss sample – open triangle (O'Hara & Mercy 1963).
Kimberlite samples – crosses (O'Hara & Mercy 1963, Nixon et al. 1963, MacGregor & Ringwood 1964, Mikhailov & Rovsha 1966, Sobolev 1970, Carswell – unpublished data).
Itinome-gata samples – pluses (Kuno & Aoki 1970).

Derived pressure-temperature diagrams

On the basis of the experimental data available up to 1965, O'Hara (1967: Figs. 12.4 and 12.6) derived a pressure-temperature diagram from which the clinopyroxene compositions could be used in order to deduce the equilibration pressures and temperatures for natural 4-phase aluminous lherzolite assemblages. In his diagram the clinopyroxenes were plotted on the basis of two chemical parameters, α_c and β_c, which were calculated after first projecting the clinopyroxene compositions into the $CaSiO_3$–$MgSiO_3$–Al_2O_3 system.

$$\alpha_c = \frac{\text{wt.\% } CaSiO_3 \times 100}{\text{wt.\% } (CaSiO_3 + MgSiO_3)}$$

$$\beta_c = \frac{\text{wt.\% } Al_2O_3 \times 100}{\text{wt.\% } (CaSiO_3 + MgSiO_3 + Al_2O_3)}$$

On O'Hara's diagram (O'Hara 1967: Fig. 12.6) Norwegian and Swiss garnet lherzolites were shown as having equilibrated at about 600–700 C and 15–20 kbs pressure – conditions of equilibration greatly different from those of the xenolithic garnet lherzolites from kimberlite pipes, indicated as having equilibrated at 1000–1200°C and roughly 30–40 kbs.

However, O'Hara's plot of the clinopyroxenes from Norwegian and Swiss garnet lherzol-

ites is a misrepresentation. The new plot (Fig. 1) presented in this paper, of new data together with all previous data, indicates appreciably higher temperatures and pressures of equilibration for most of these garnet lherzolite assemblages. In fact only one Norwegian clinopyroxene (N69) plots in the pressure-temperature field indicated by O'Hara (1967) and the other Norwegian clinopyroxenes plot over the pressure range 35–47 kbs at about 900–1000°C, except N71 which plots at about 750°C and 34 kbs, and anyway should perhaps be omitted as it did not contain olivine although it was interlayered with olivine bearing assemblages. The one Swiss clinopyroxene (A2 – O'Hara & Mercy 1963) plots at about 1200°C and 38 kbs, whilst garnet lherzolites from the Czech Masif (Fiala 1966, Mikhailov & Rovsha 1966) appear to have equilibrated at about 40–51 kbs and 975–1150°C.

Thus contrary to O'Hara's (1967) conclusion, Fig. 1 indicates that there is in fact an overlap in the estimated pressure-temperature equilibration fields and hence inferred depths of origin of the 'crustal' and kimberlite xenolith garnet lherzolites. One Norwegian garnet lherzolite sample, namely N69, does however appear to have equilibrated at significantly lower temperatures and pressures, a possible explanation for this being offered later in this paper.

The fairly wide range of β_c values for both 'crustal' and kimberlite xenolith garnet lherzolite samples with comparable α_c values is probably in large measure due to errors in β_c resulting from incorrect determination of the FeO/Fe_2O_3 ratio and from the high Cr_2O_3/Al_2O_3 ratios in some of the clinopyroxenes.

An alternative plot (Fig. 2) has therefore been constructed in which the equilibration conditions for garnet lherzolite assemblages can be deduced by plotting the wt.% Al_2O_3 content of the orthopyroxene against the $Ca^{2+}/Ca^{2+}+Mg^{2+}$ ratio in the coexisting clinopyroxene. The experimental data used in constructing this diagram have been discussed in the previous section. The wt.% Al_2O_3 in orthopyroxene values are largely based on Green & Ringwood's 1967 Table 2 values for pyrolite compositions and the $Ca^{2+}/Ca^{2+}+Mg^{2+}$ values for the coexisting clinopyroxene on Davis & Boyd's (1966) experimental data with the actual temperature values for particular $Ca^{2+}/Ca^{2+}+Mg^{2+}$ ratios at 30 kbs pressure raised by roughly 100°C in order to take into account the likely effect of the additional chemical components present in the natural rock system.

Projecting natural pyroxene compositions from the $FeSiO_3$ corner of the pyroxene quadrilateral on to the $MgSiO_3$–$CaMgSi_2O_6$ join leads to $Ca^{2+}/Ca^{2+}+Mg^{2+}$ ratios >0.50 for relatively low temperature Ca rich pyroxenes, but on the basis of the modified $Ca^{2+}/Ca^{2+}+Mg^{2+}$ values used in constructing Fig. 2 is thought to give the most realistic temperature estimate.

Fig. 2 is thought to yield somewhat superior pressure-temperature estimates than in Fig. 1 because it avoids inaccuracies resulting from incorrect FeO determinations, also orthopyroxenes have lower contents of Cr_2O_3 and Fe_2O_3 than clinopyroxenes, hence have compositions closer to the experimentally studied synthetic enstatite-pyrope system, and finally because more data are available on wt.% Al_2O_3 in orthopyroxene than R_2O_3 in clinopyroxene for both natural and synthetic systems. However, it must be stressed that Fig. 2, like Fig. 1, involves large extrapolations from the limited experimental data available, especially in the low temperature-pressure part of the garnet lherzolite stability field. Thus the absolute temperatures and pressures estimated may perhaps be in error by up to ±15% in the low temperature part of the diagram, but at least the relative equilibration conditions deduced for different garnet lherzolite assemblages should be reliable.

On the new plot (Fig. 2) the following pressure-temperature equilibration conditions are indicated:

Norwegian garnet lherzolites –
800–1020°C at 22–37 kbs

Swiss garnet lherzolite (A2) –
1100°C at 36 kbs

Czech garnet lherzolites –
1000–1100°C at 33–34 kbs

Kimberlite garnet lherzolites –
960–1240°C at 29–48 kbs

The Norwegian garnet lherzolite N69 which on O'Hara's plot indicated an equilibration temperature of 600°C at 18 kbs now plots at 800°C and 23 kbs somewhat higher temperatures and pressures although still the lowest for all the analysed Norwegian garnet lherzolites.

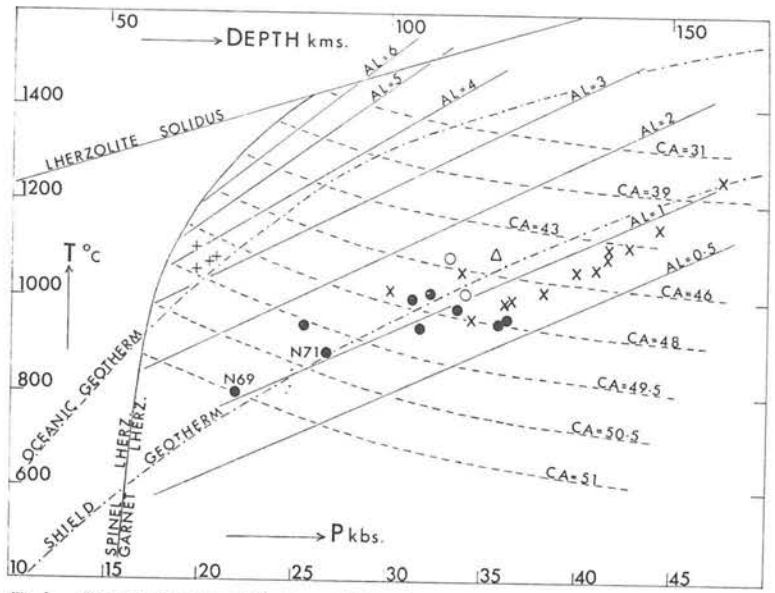

Fig. 2. Pressure-temperature equilibration conditions for natural garnet lherzolite assemblages estimated on the basis of the parameters CA=atomic % Ca/Ca+Mg in the clinopyroxene and AL=wt.% Al_2O_3 in the coexisting orthopyroxene. The spinel lherzolite⇌garnet lherzolite reaction boundary is from O'Hara et al. (1971), the dry garnet lherzolite solidus extrapolated from Ito & Kennedy (1967), and the oceanic and Pre-Cambrian shield geotherms from Ringwood et al. (1964). Data sources and symbols as in Fig. 1.

Thus from Fig. 2 it would appear that the Norwegian, Swiss and Czech garnet lherzolites have equilibrated at depths >70 kilometres along an expected sub-continental geotherm whereas the xenolithic granular garnet lherzolites from kimberlites have in general come from slightly greater sub-continental depths >120 kilometres. As the majority of the 'crustal' garnet lherzolites appear to have formed well within the garnet lherzolite stability field (well away from the spinel lherzolite/garnet lherzolite reaction boundary – O'Hara et al. 1971) it seems unlikely that they represent deep crustal metamorphic rocks and far more likely on chemical and mineralogical grounds that they represent tectonic slices of the uppermost sub-continental upper mantle thrust up into the basal crustal rocks during a major continental collision type orogenic event. The Ugelvik garnet websterite lens, with its postulated high temperature orthopyroxene and exsolved clinopyroxene and garnet phases, Carswell (1973), found within the layered garnet lherzolites at Ugelvik enhances the argument for a mantle origin.

If it is accepted that the Norwegian garnet lherzolites represent tectonic slices of sub-continental mantle then a possible explanation of the fact that they appear to have equilibrated over a fairly wide depth range of about 70–120 km may be that the samples analysed have re-equilibrated to varying degrees during diapiric movement up into the crust. Several of the Norwegian garnet lher-

zolite samples, such as N69, have striking cataclastic textures with large strained porphyroclasts surrounded by smaller granulated grains. These rocks may therefore have partly re-equilibrated at somewhat lower temperatures and pressures during their tectonic emplacement into the crust. It should be borne in mind that the pressure-temperature estimates from Fig. 2 are all based on chemical analysis of bulk mineral separates. Clearly there is a need for comparative microprobe analytical work on both the porphyroclastic and granulated pyroxene grains in certain of these rocks.

Also plotted in Figs. 1 and 2 are the pyroxenes from the Itinome-gata garnet lherzolite nodules from basalts – Kuno & Aoki (1970). It is appropriate to find that they plot close to a postulated oceanic geotherm at 1050–1100°C and 20–22 kbs in Fig. 2.

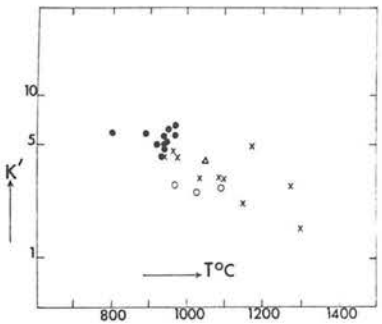

Fig. 3. Plot of K′ against temperature for analysed garnet lherzolite assemblages. Data sources and symbols as in Figs. 1 and 2.

Element partition diagrams

Alternative methods of estimating the temperatures of formation of mineral assemblages have been attempted on the basis of coefficients calculated for the distribution of Fe^{2+} and Mg^{2+} between coexisting pyroxenes (Kretz 1961, Bartholomé 1962) or from coexisting clinopyroxenes and garnets (Banno 1970, Mysen & Heier 1972). Distribution coefficients for coexisting clinopyroxenes and garnets are particularly appropriate to the question of the equilibration conditions of most eclogite facies assemblages, including the garnet lherzolites being considered here. However, it should be noted that O'Hara & Mercy (1963) and O'Hara (1967) pointed out several complicating factors (chiefly composition effects) which may invalidate the distribution coefficient method and hence judged this method to be inferior at present to the calcium-aluminium distribution method discussed in the previous section.

Banno (1970) used the distribution coefficient K′:

$$K' = K_{Ga-Cpx}^{Fe^{2+}-Mg^{2+}} = \left(X_{Fe^{2+}}/X_{Mg^{2+}}\right)^{Ga} / \left(X_{Fe^{2+}}/X_{Mg^{2+}}\right)^{Cpx}$$

in order to obtain temperature estimates for eclogites from a wide range of occurrences. He adjudged the pressure effect on the distribution coefficient to be negligible but argued that significant differences in K′ could arise from composition differences, such as the $Fe^{2+}/Fe^{2+}+Mg^{2+}$ ratio of the minerals, the jadeite and orthopyroxene contents of the clinopyroxene, and the grossular content of the garnet. However, he argued that the dependence of K′ on chemistry was probably small and indeed Mysen & Heier (1972) have recently demonstrated that the effect of variable chemical composition within the large Hareidland eclogite mass on K′ was negligible. Certainly it should be possible to use this method at least to compare the relative equilibration temperatures of the Norwegian and kimberlite garnet lherzolites, as these rocks have identical mineral assemblages and very similar mineral and whole rock chemistry.

Fig. 3 presents a logarithmic plot of K′ against temperature for analysed garnet lherzolite assemblages. The temperature estimates for the clinopyroxene-garnet pairs plotted are based directly on a comparison of the atomic ratio Ca/Ca+Mg in the clinopyroxene with experimental values for the synthetic enstatite-diopside system at 30 kbs pressure (Davis & Boyd 1966). As discussed earlier, temperatures derived in this fashion may be underestimated by up to 100°C in absolute terms.

From Fig. 3 it is apparent that the Norwegian garnet lherzolite assemblages in general have slightly higher K′ values than kimberlite

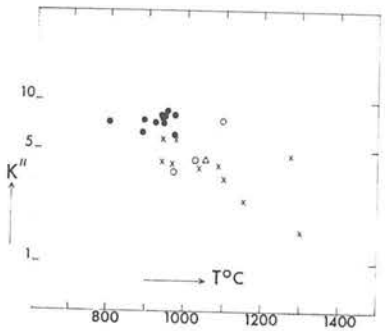

Fig. 4. Plot of K″ against temperature for analysed garnet lherzolite assemblages. Data sources and symbols as in previous figures.

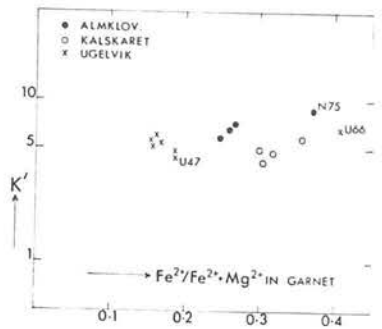

Fig. 5. Plot of K′ against $Fe^{2+}/Fe^{2+}+Mg^{2+}$ ratio in the garnet for various eclogite facies assemblages from the different Norwegian garnet peridotite localities.

garnet lherzolite assemblages, in keeping with the slightly lower equilibration temperatures estimated for them.

As K′ may be expected to be prone to errors resulting from inaccurate Fe^{2+}/Fe^{3+} ratio determination, a notoriously difficult problem with standard geochemical techniques, it is instructive to also consider the distribution of Mn and Mg between coexisting clinopyroxene and garnet.

$$K'' = K_{Ga-Cpx}^{Mn-Mg} = (X_{Mn}/X_{Mg})^{Ga}/(X_{Mn}/_{Mg})^{Cpx}$$

Thus Fig. 4 presents a logarithmic plot of K″ against temperature, again estimated from the $Ca^{2+}/Ca^{2+}+Mg^{2+}$ ratio in the clinopyroxene, for the same garnet lherzolite assemblages. Again it is appropriate to find that the Norwegian garnet lherzolites have in general slightly higher K″ values than kimberlite garnet lherzolites, the scatter of points on this diagram probably being largely due to the use of some rather inaccurate MnO values, especially for clinopyroxenes where MnO figures are commonly low and often not quoted with sufficient precision.

It is clear from Figs. 3 and 4 that both K′ and K″ are strongly temperature dependent and thus can be used to estimate relative equilibrium temperatures, at least when comparing like assemblages of similar overall chemistry as here. However, for determining the actual temperatures and pressures of equilibrium of such assemblages the calcium-aluminium method discussed previously (Figs. 1 and 2) seems superior. Furthermore, from the author's data it would appear that variations in mineral assemblage and mineral chemistry can affect the distribution coefficients and hence may invalidate one comparing the relative equilibration temperatures of say garnet lherzolites and bimineralic eclogites, as attempted by Mysen & Heier (1972).

To check whether the overall mineral assemblage or mineral chemistry has any effect on the distribution coefficients a plot was made (Fig. 5) of the distribution coefficient K′ against the $Fe^{2+}/Fe^{2+}+Mg^{2+}$ ratio in the garnet for various different eclogite facies assemblages from different Norwegian localities. Fig. 5 shows that there is some variation in K′ with mineral chemistry for rocks with identical mineral assemblage from each locality. However, whether this is a genuine composition effect or simply a result of inaccurate determination of the Fe^{2+}/Fe^{3+} ratio in the minerals is uncertain.

However, more significant variations in K′ occur for the different assemblages. For example the two 'internal' eclogites N75 and U66 (that is, bimineralic eclogite lenses enclosed within the garnet lherzolites or associated peridotites) have higher K′ values than the

associated garnet lherzolites, whilst the 'internal' enstatite eclogite U47 has the lowest K′ value of all the Ugelvik samples. Furthermore the two 'external' enstatite eclogites analysed (that is, enstatite eclogites directly enclosed in the gneisses) A44 and U19 have K′ values of only 3.1 and 3.9, respectively, much lower than the K′ values for enstatite free eclogites from the gneisses K′ > 5.6 (e.g. Hareidland eclogite K′ = 7.0 ± 0.4 (Mysen & Heier 1972)).

Thus the admittedly limited data available suggest that the actual mineral assemblage present and possibly also the actual mineral chemistry can have an effect on the distribution coefficients such as K′ calculated for coexisting minerals.

Concluding statements

On the basis of the solid solution between the coexisting pyroxenes and the amount of potential garnet molecule in the orthopyroxene it has been shown that the garnet lherzolites enclosed within the Norwegian gneisses appear in general to have equilibrated at sub-continental upper mantle depths only slightly shallower than the depths of origin of most of the granular garnet lherzolite xenoliths found in kimberlite pipes. The relatively low pressure-temperature equilibration field deduced by O'Hara (1967) for the Norwegian and Swiss garnet lherzolites has not been confirmed. However, a possible explanation of the somewhat lower pressure-temperature equilibration conditions deduced for certain of the Norwegian garnet lherzolites, in particular N69 – O'Hara & Mercy (1963), may be that they have at least in part re-equilibrated at somewhat lower pressures and temperatures during their tectonic emplacement into the crust.

Coefficients calculated for the distribution of Fe^{2+} and Mg^{2+} (K′), and Mn^{2+} and Mg^{2+} (K″) between coexisting clinopyroxenes and garnets also suggest slightly lower equilibration temperatures for the Norwegian garnet lherzolites than the xenolithic garnet lherzolites from kimberlite pipes. The Norwegian garnet lherzolites have generally slightly lower distribution coefficient values than the common eclogites enclosed in the Norwegian gneisses. However, in view of the demonstration that mineral assemblage and chemistry may also affect the distribution coefficients, the author feels that one should beware using the distribution coefficient data to draw any firm conclusions about the relative temperatures and pressures of the garnet lherzolites and eclogites.

Mysen & Heier (1972) estimated that the eclogites in the Norwegian gneisses formed at roughly 625 ± 30 C and 14 kbs pressure, conditions quite different from those deduced in this paper for the Norwegian garnet lherzolites – 800–1020 C at 22–37 kbs pressure. However, it is felt that the possibility should be considered that the two types of eclogites may be of quite different origins, with tectonic slices of upper mantle derived garnet lherzolite having been tectonically emplaced during a major orogenic event into a relatively dry lower crust basement terrain which already contained or was developing indigenous basic eclogite facies assemblages.

Acknowledgements. – This paper was largely written during a study visit to the Mineralogisk-Geologisk Museum in Oslo, where the encouragement of Professor K. S. Heier and Dr. W. L. Griffin was greatly appreciated.

Grants from the University of Sheffield Research Fund for field work on Norwegian garnet peridotites are gratefully acknowledged, and the author also wishes to thank Professor M. J. O'Hara for critically reading the manuscript.

References

Banno, S. 1970: Classification of eclogites in terms of physical conditions of their origin. *Phys. Earth Planet. Inter. 3*, 405–421.

Bartholomé, P. 1962: Iron-magnesium ratio in associated pyroxenes and olivines. *Geol. Soc. Am. (Buddington volume)*, 1–20.

Boyd, F. R. 1969: The system $CaSiO_3$–$MgSiO_3$–Al_2O_3. *Carnegie Inst. Wash. Yearb. 68*, 214–221.

Boyd, F. R. & England, J. L. 1964: The system enstatite-pyrope. *Carnegie Inst. Wash. Yearb. 63*, 157–161.

Boyd, F. R. & Schairer, J. F. 1964: The system $MgSiO_3$–$CaMgSi_2O_6$. *J. Petrol. 5*, 275–309.

Bryhni, I., Green, D. H., Heier, K. S. & Fyfe, W. S. 1970: On the occurrence of eclogite in western Norway. *Contrib. Miner. Petrol. 26*, 12–19.

Carswell, D. A. 1968a: Picritic magma-residual dunite relationships in garnet peridotite at Kalskaret, near Tafjord, South Norway. *Contrib. Miner. Petrol. 19*, 97–124.

Carswell, D. A. 1968b: Possible primary upper mantle peridotite in Norwegian basal gneiss. *Lithos 1*, 322–355.

Carswell, D. A. 1973: Garnet websterite nodule within layered garnet peridotite. *Earth Planet. Sci. Lett. 20*, 347–352.

Carswell, D. A. & Dawson, J. B. 1970: Garnet peridotite xenoliths in South African kimberlite pipes and their petrogenesis. *Contrib. Miner. Petrol. 25*, 163–184.

Davis, B. T. C. & Boyd, F. R. 1966: The join $Mg_2Si_2O_6$–$CaMgSi_2O_6$ at 30 kilobars pressure and its application to pyroxenes from kimberlites. *J. Geophys. Res. 71*, 3567–3576.

Fiala, J. 1966: The distribution of elements in mineral phases of some garnet peridotites from the Bohemian Massif. *Krystalinikum 4*, 31–53.

Green, D. H. & Mysen, B. O. 1972: Genetic relationship between eclogite and hornblende–plagioclase pegmatite in western Norway. *Lithos 5*, 147–161.

Green, D. H. & Ringwood, A. E. 1967: The stability fields of aluminous pyroxene peridotite and garnet peridotite and their relevance in upper mantle structure. *Earth Planet. Sci. Lett. 3*, 151–160.

Harris, P. G., Reay, A. & White, I. G. 1967: Chemical compositions of the upper mantle. *J. Geophys. Res. 72*, 6359–6369.

Ito, K. & Kennedy, G. C. 1967: The melting and phase relations in a natural peridotite to 40 kilobars. *Am. J. Sci. 265*, 519–538.

Kopecky, L. & Sattran, V. 1966: Buried occurrence of pyrope-peridotite and the structure of the crystalline basement in the extreme south-west of the Ceske Stredohori mountains. *Krystalinikum 4*, 65–86.

Kretz, R. 1961: Some applications of thermodynamics to co-existing minerals of variable composition. Examples: orthopyroxene-clinopyroxene and orthopyroxene-garnet. *J. Geol. 69*, 361–387.

Kuno, H. & Aoki, K. 1970: Chemistry of ultramafic nodules and their bearing on the origin of basaltic magmas. *Phys. Earth Planet. Inter. 3*, 273–301.

Lappin, M. A. 1966: The field relationships of basic and ultrabasic masses in the basal gneiss complex of Stadlandet and Almklovdalen, Nordfjord southwestern Norway. *Nor. Geol. Tidsskr. 46*, 439–496.

Lindsley, D. A. & Munoz, J. L. 1969: Subsolidus relations along the join hedenbergite-ferrosilite. *Am. J. Sci. (Schairer volume), 267A*, 295–324.

MacGregor, I. D. 1970: The effect of CaO, Cr_2O_3, Fe_2O_3 and Al_2O_3 on the stability of spinel and garnet peridotites. *Phys. Earth Planet. Inter. 3*, 372–377.

MacGregor, I. D. & Ringwood, A. E. 1964: The natural system enstatite-pyrope. *Carnegie Inst. Wash. Yearb. 63*, 161–163.

Mikhailov, N. P. & Rovsha, V. S. 1966: Pyrope-bearing peridotites of the Bohemian Massif and their genesis. *Krystalinikum 4*, 87–107.

Mysen, B. O. & Heier, K. S. 1972: Petrogenesis of eclogites in high grade metamorphic gneisses, exemplified by the Hareidland eclogite, western Norway. *Contr. Miner. Petrol. 36*, 73–94.

Nixon, P. H., Knorring, O. von & Rooke, J. M. 1963: Kimberlite and associated inclusions of Basutoland: a mineralogical and geochemical study. *Am. Mineral. 48*, 1090–1132.

O'Hara, M. J. 1967: Mineral parageneses in ultrabasic rocks, pp. 393–403 in Wyllie, P. J. (ed.), *Ultramafic and Related Rocks*, J. Wiley, New York.

O'Hara, M. J. 1970: Upper mantle composition inferred from laboratory experiments and observation of volcanic products. *Phys. Earth Planet. Inter. 3*, 236–245.

O'Hara, M. J. & Mercy, E. L. P. 1963: Petrology and petrogenesis of some garnetiferous peridotites. *Trans. Roy. Soc. Edinb. 65*, 251–314.

O'Hara, M. J., Richardson, S. W. & Wilson, G. 1971: Garnet peridotite stability and occurrence in crust and mantle. *Contrib. Miner. Petrol. 32*, 48–68.

O'Hara, M. J. & Yoder, H. S., Jr. 1967: Formation and fractionation of basic magmas at high pressure. *Scott. J. Geol. 4*, 67–117.

Ringwood, A. E., MacGregor, I. D. & Boyd, F. R. 1964: Petrological constitution of the upper mantle. *Carnegie Inst. Wash. Yearb. 63*, 147–152.

Rost, F. 1966: Über ultrabasische einschlusse in metamorphen gesteinen des südlichen Moldanubikums. *Krystalinikum 4*, 127–162.

Schmitt, H. H. 1964: Metamorphic eclogites of the Eiksund area, Sunmøre, Norway. *Am. Geophys. Union Trans. 43*, 128.

Sobolev, N. V. 1970: Eclogites and pyrope peridotites from the Kimberlites of Yakutia. *Phys. Earth Planet. Inter. 3*, 398–404.

Accepted for publication January 1974
Printed April 1974

Vein Metasomatism in Peridotite at Kalskaret near Tafjord, South Norway

by D. A. CARSWELL, C. D. CURTIS, *and* R. KANARIS-SOTIRIOU

Department of Geology, The University, Sheffield, S1 3JD, England

(*Received 26 June 1973; in revised form 20 October 1973*)

ABSTRACT

Enstatite, anthophyllite, tremolite, and chlorite are developed in a zoned sequence as a vein cross cutting a peridotite body located within the basal gneiss region of southern Norway. They are believed to have formed during the main regional metamorphic event at temperatures around 700 C and P_{total} in excess of 6 kb.

It is thought that metasomatic reaction occurred by means of (and to a lesser extent directly involved) a pore fluid phase rich in alkali halides. The zonal sequence now found represents the results of incomplete reaction of the peridotite body with pore fluids derived from the acid gneiss country rocks. Each zone illustrates partial attainment of equilibrium one component at a time. Local equilibrium was maintained between the fluid phase and the various silicates during reaction. Questions of component 'mobility' are considered.

There appears to be no doubt that enstatite developed by metasomatic reaction on this small scale. This raises interesting possibilities of metasomatic development on a larger scale: enstatite occurs as a major constituent of some ultrabasic bodies in this region of southern Norway.

INTRODUCTION

THIS paper describes the mineral sequence developed in a vein which cuts a small peridotite body on the southern flank of the Kalskaret col above Tafjord (see Carswell, 1968, figs. 1 and 2 for location). The silicates present in the vein constitute a particularly well-developed example of zoned metasomatic alteration.

The petrology and field relationships of the peridotite bodies in this part of the Basal Gneiss Region of southern Norway have been described by O'Hara & Mercy (1963), Carswell (1968), and Brueckner (1969). The last paper also gives some mineralogical information on the alteration assemblages observed both in cross-cutting fractures and at peridotite lens margins.

Metasomatic assemblages are not true equilibrium assemblages, but represent partial reaction states 'frozen' by lowering of temperature or removal of the reaction medium. As such they should be particularly useful in providing general information about the reactions that take place in metamorphic environments. In spite of much theoretical discussion, however, relatively few examples of metasomatic alteration have been studied in detail. One such description was given by Curtis & Brown (1969, 1971) for zoned ultrabasic bodies in Unst, Shetland. However, the metasomatic assemblages they described

differed significantly from those observed in the Kalskaret vein, although some common features are of special interest.

FIELD OCCURRENCE AND PETROGRAPHY

Field exposure of the vein is limited to some 4–5 metres. Centrally placed chlorite is bounded on both sides by tremolite, anthophyllite, and enstatite zones in that order. Zonal boundaries are not sharp in particular being crossed by large crystals (up to 2 cm) of anthophyllite and tremolite. In general, however, the zonal form of the vein is clear and the zonal sequence constant.

The original width of the vein is difficult to estimate since later deformation has caused some redistribution of the material, particularly of the innermost chlorite zone, which has been squeezed out in places to form pods up to 40 cm across. The enstatite–tremolite sequence is, however, less variable in thickness (about 8–18 cm over-all). Some lateral variation in vein thickness might well have been present prior to the deformation of the vein.

The 'normal' peridotite of the ultrabasic bodies in the Kalskaret and other parts (Kaldhussaeter, Ranukdalen, etc.) of the Tafjord district is essentially a dunite with about 90 per cent olivine ($Fo_{93\cdot4\text{-}91\cdot9}$), 10 per cent enstatite ($En_{93\cdot4\text{-}92\cdot2}$), and small amounts of chromite. Most of the bodies are relatively unaltered although minor amounts of secondary tremolite, chlorite, enstatite, serpentine, and talc are not uncommon. Chemical and mineralogical data on these assemblages have been published by O'Hara & Mercy (1963), and Mercy & O'Hara (1965).

Some of the smaller bodies in the district, however, have been extensively altered to enstatite, chlorite, tremolite or less commonly serpentine, and marginal metasomatism is common. Late-stage deformation has apparently produced considerable variability in the width of the marginal metasomatic skin, so that whilst in some places a wide zone exists, elsewhere it apparently has been stripped off completely.

It seems probable that both the vein metasomatism and the marginal metasomatism can be attributed to the same episode of metasomatic activity. The vein assemblages differ from the marginal assemblages only in the obvious sense of not being in direct contact with reactant acid country rock material. These relationships are outlined schematically in Fig. 1.

Three hand specimens were taken from the vein: samples T412, T410, and T413. These samples were sliced normal to the vein and then one slice from each cut parallel to the vein to give a sequence of sub-samples starting from little altered dunite and ending with virtually pure chlorite from the centre of the vein. Thin section petrography revealed the following assemblages:

T412A. Mostly olivine with enstatite and minor serpentine, talc, and chlorite.
T412B. As T412A but roughly equal proportions of olivine and enstatite.
T412C. Mostly enstatite with minor anthophyllite, chlorite, and traces of talc and tremolite.

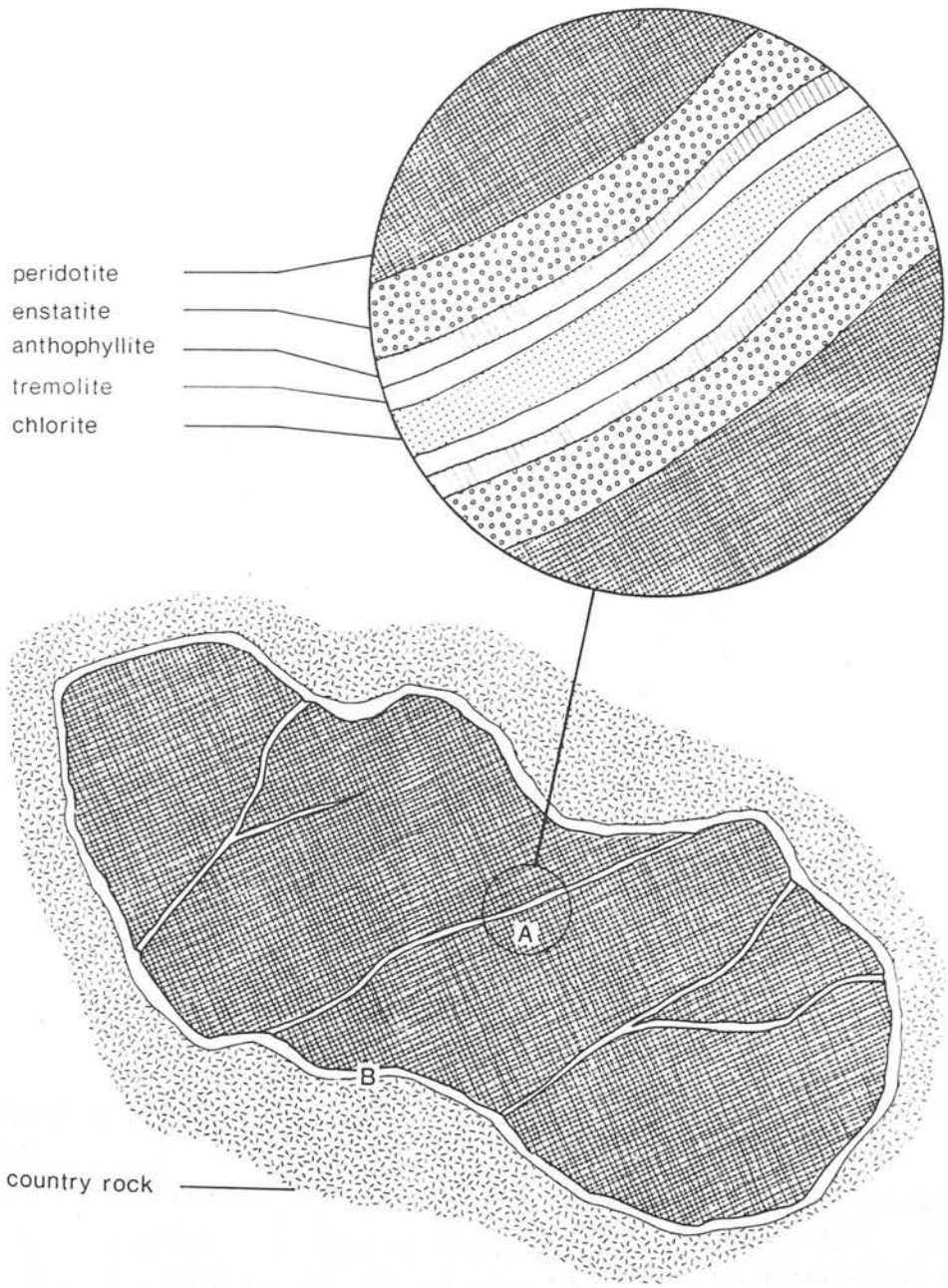

FIG. 1. Schematic representation of the vein mineral assemblage and inferred relationships between vein (A) and contact (B) metasomatic assemblage development.

T410A. Mostly enstatite but overlaps into the anthophyllite zone with a definite concentration of talc between the enstatite and anthophyllite zones. No olivine but minor chlorite and tremolite.

T410B. Anthophyllite zone: largely anthophyllite with minor chlorite and tremolite.

T410C. Anthophyllite and tremolite as major phases with minor chlorite.

T410D. Tremolite zone: abundant tremolite together with appreciable chlorite and trace anthophyllite.

T410E. Chlorite and tremolite with some anthophyllite.

T413A. Mostly chlorite with some anthophyllite and minor tremolite.

T413B. Chlorite zone: almost pure chlorite with trace anthophyllite.

CHEMICAL MINERALOGY

Table 1 lists the chemical analyses of the ten sub-samples. Na_2O and FeO were determined by wet chemical methods, the remaining oxides by X-ray fluorescence analysis. The H_2O^+ figure represents glass fusion loss corrected for iron oxidation and sulphur.

The chemical variation in Table 1 largely reflects the differing proportions of the minerals present. This assertion was justified by a modified 'norm' calculation procedure, and checked by semi-quantitative X-ray diffraction analysis.

Sample T413B proved to be essentially monomineralic chlorite (XRD) and recalculation of this analysis to 36 (O+OH) gave:

$$(Al_{1\cdot9}Fe^{3+}_{0\cdot2}Fe^{2+}_{0\cdot4}Mg_{9\cdot9})[Si_{6\cdot0}Al_{2\cdot0}O_{20\cdot7}](OH)_{15\cdot3}$$

This chemical formula corresponds closely to that of a clinochlore. It was then assumed that chlorite of this composition was responsible for all the Al in the remaining samples. Hence percentage chlorite figures were calculated and appropriate oxide percentages subtracted from these analyses.

Sample T410D was considered next as this proved (XRD) to be essentially tremolite plus chlorite. The residue after subtraction of chlorite recalculated to:

$$Ca_{2\cdot1}(Fe^{3+}_{0\cdot1}Fe^{2+}_{0\cdot3}Mg_{4\cdot4})[Si_{8\cdot1}O_{21\cdot9}](OH)_{2\cdot1}$$

It was then assumed that tremolite of this composition was responsible for all the Ca in the remaining analyses and hence an equivalent amount of material was subtracted and recorded as percentage tremolite.

Samples T410B, T410E, and T413A were considered next as they proved to contain chlorite, tremolite, and anthophyllite. After corrective subtraction of chlorite and tremolite, the residues were recalculated on the basis of 24(O+OH) and gave:

$$\text{T410B } (Fe^{3+}_{0\cdot1}Fe^{2+}_{0\cdot7}Mg_{6\cdot3})[Si_{8\cdot0}O_{22\cdot0}](OH)_{2\cdot0}$$

$$\text{T410E } (Fe_{0\cdot1}Fe_{0\cdot6}Mg_{6\cdot1})[Si_{8\cdot1}O_{22}](OH)_2$$

in the latter case the recalculation assumed 22(O) and 2 (OH).

$$\text{T413A } (Fe^{3+}_{0\cdot1}Fe^{2+}_{0\cdot7}Mg_{6\cdot2})[Si_{7\cdot9}O_{21\cdot8}](OH)_{2\cdot2}$$

All three give remarkably good anthophyllite formulae, especially when in the last two cases the correction for chlorite and tremolite accounts for 83·7 and 63·8 per cent, respectively, of the total analysis.

A similar routine was developed for the olivine–enstatite–antigorite–chlorite assemblages. Chlorite equivalent to the Al content was calculated and subtracted, then any water remaining attributed to antigorite (talc being ignored).

TABLE 1

Chemical analyses

Sample number	*412A*	*412B*	*412C*	*410A*	*410B*	*410C*	*410D*	*410E*	*413A*	*413B*
SiO_2	43·47	48·06	54·56	53·40	54·92	54·80	52·80	44·18	44·60	31·38
Al_2O_3	0·85	1·22	1·54	2·30	2·40	2·50	4·20	9·18	9·25	17·35
TiO_2	0·02	0·02	0·02	0·01	0·01	0·02	0·03	0·04	0·04	0·06
Fe_2O_3	1·48	1·72	1·98	1·87	0·73	0·66	0·70	0·89	1·19	1·20
FeO	6·07	5·74	5·64	4·51	5·38	4·20	2·80	3·04	3·95	2·37
MgO	44·08	39·93	34·01	32·36	31·49	28·16	24·89	30·06	32·06	34·62
CaO	0·02	0·03	0·10	0·16	0·37	4·96	10·33	4·43	1·49	0·004
Na_2O	0·005	0·008	0·010	0·025	0·044	0·187	0·385	0·133	0·064	0·004
K_2O	0·003	0·001	0·004	0·002	0·000	0·018	0·049	0·018	0·006	0·002
MnO	0·13	0·12	0·13	0·08	0·11	0·09	0·09	0·05	0·10	0·08
P_2O_5	0·000	0·001	0·003	0·004	0·031	0·031	0·086	0·040	0·041	0·000
S	0·05	0·10	0·19	0·22	0·13	0·08	0·01	0·00	0·00	0·01
H_2O^+	2·44	2·49	1·43	3·72	3·52	3·23	3·21	7·98	7·28	13·21
Σ	98·62	99·44	98·62	98·66	99·14	98·94	99·58	100·04	100·07	100·29
O≡S	0·02	0·05	0·09	0·11	0·06	0·04	0·00	0·00	0·00	0·00
TOTAL	98·60	99·39	98·53	98·55	99·08	98·90	99·58	100·04	100·07	100·29

See text for details of methods.

The residuum was then partitioned between olivine and enstatite on the basis of assumed ideal cation silica ratios. This procedure almost certainly gives good estimates of olivine and enstatite but very little certainty can be attributed to the antigorite figure based on residual water. A precisely similar routine attributes residual water to anthophyllite in the chlorite–tremolite–anthophyllite–enstatite samples—again with uncertain precision. Also, any talc present has essentially been calculated as anthophyllite.

These procedures allow 'normative' mineral assemblages to be calculated for all the samples and the estimates so obtained are listed in Table 2. This table also lists semi-quantitative estimates of the mineral proportions based on X-ray diffraction peak intensities. The agreement between the two approaches is very reasonable apart from sample T410A where significant enstatite is missed by the normative calculation, anthophyllite being overestimated at the expense of enstatite and talc.

The chemical 'norm' estimates are plotted in Fig. 2 except for sample T410A where the X-ray diffraction estimate, although crude, is obviously better than the 'norm'. This diagram shows clearly that the over-all chemical variation is due to a definite mineral zonation sequence from (pure) chlorite in the vein centre through tremolite, anthophyllite, and enstatite to the peridotite, which has been partially serpentinized. The statistical overlap of zones is partially due to the method of sampling, the samples themselves showing some internal zonation. It is clear, therefore, that the metasomatic reaction which formed the vein involved the growth of four new silicate minerals. All grew at the expense of olivine and all show distinctive zonal culminations.

TABLE 2

Estimated mineralogical composition of samples T412, T410, T413 per cent (a) Based on 'normative' calculations, (b) Based on XRD intensity data

	Chlorite		*Tremolite*		*Anthophyllite*		*Enstatite*		*Olivine*		*Antigorite*		*Talc*	
	a	*b*	*a*	*b*	*a*	*b*	*a*	*b*	*a*	*b*	*a*	*b*	*a*	*b*
T412A	4·9	5	—	—	—	—	17·9	30	61·2	60	14·7	p	—	p
T412B	7·0	5	—	—	—	—	49·8	45	29·6	50	13·0	p	—	p
T412C	8·8	5	0·7	10	16·3	10	72·6	75	—	—	—	—	—	*
T410A	13·1	10	1·2	10	84·1	50	—	30	—	—	—	—	—	*
T410B	13·7	10	2·4	—	82·8	90	—	—	—	—	—	—	—	*
T410C	14·3	10	36·4	50	48·1	40	—	—	—	—	—	—	—	*
T410D	24·0	10	75·4	90	—	—	—	—	—	—	—	—	—	—
T410E	52·4	30	31·3	60	16·3	10	—	—	—	—	—	—	—	*
T413A	52·8	60	11·0	10	36·3	30	—	—	—	—	—	—	—	*
T413B	100·0	100	—	—	—	—	—	—	—	—	—	—	—	—

p = present, quantitative estimate impossible.
* = correspondence of anthophyllite and talc lines prevents positive identification of talc in anthophyllite-rich specimens.

However, the presence and distribution of the minor amount of serpentine and talc in certain of the analysed samples requires further comments. Serpentine occurs as a sparse secondary mineral formed from both primary olivine and enstatite in the peridotite adjacent to the vein and from the secondary enstatite in the outermost parts of the vein. Likewise, talc is only sparsely developed but its distribution is informative. There is a distinct concentration of talc at the contact between the enstatite and anthophyllite zones (within sample T410A), whilst elsewhere within the vein traces of talc occur marginal to anthophyllite or enstatite grains. As argued in the following section, it appears that both serpentine and talc grew subsequently to the formation of the primary metasomatic sequence in the vein.

PHYSICAL CONDITIONS PREVAILING AT THE TIME OF VEIN FORMATION

This section largely concerns an appraisal of the likely physical conditions (T, P_{total}, P_{H_2O}, P_{CO_2}, etc.) under which the vein formed, in the light of the relevant experimental data at present available.

First, it is important to consider the physical conditions pertaining to the metamorphic grade of the enclosing country rocks. These are largely almandine–amphibolite facies psammitic gneisses with the assemblage: Quartz + Perthitic Potash Felspar + Plagioclase + Biotite ± Muscovite ± Hornblende ± Garnet. However, certain horizons of more pelitic gneisses occur which sometimes

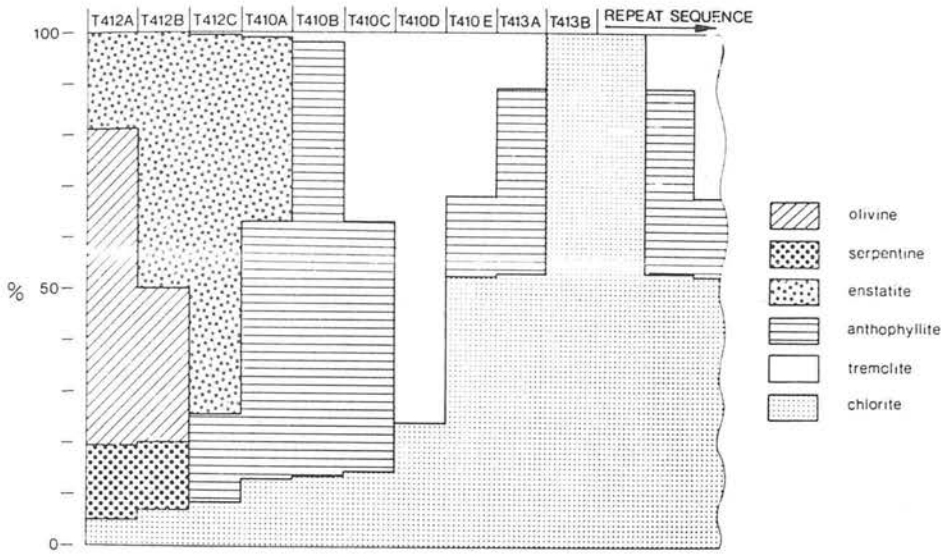

FIG. 2. Relative development of different minerals within the analysed samples as deduced by chemical 'norm' calculations. The presence of four distinct metasomatic zones is seen: chlorite occupies the vein centre and is bounded on both sides by tremolite, anthophyllite, and enstatite in that order (olivine represents unreacted material, serpentine developed later).

contain kyanite, whilst sillimanite development has also occasionally been reported—Brueckner (1969), Schmitt (1964). There is also clear evidence of local anatexis producing 'granitic' fluids during the main metamorphism. Eclogite and/or amphibolite lenses are common in certain horizons within the gneisses.

Temperatures of about 600–700 °C seem appropriate for the main regional metamorphism but estimates of the load pressures involved vary from 6–8 kb (O'Hara *et al.* (1971)) to > 8 kb, more likely about 14 kb (Mysen & Heier (1972) and Green & Mysen (1972)).

Let us now consider the question of whether the vein metasomatism may have occurred under essentially similar physical conditions to those operating during the main regional metamorphism. The answer to this question has important implications concerning the timing of the emplacement of the peridotite bodies. To date Brueckner (1969) has argued largely on structural grounds in favour of early emplacement during or before the main metamorphism and firstfold episode in the country rocks, whilst O'Hara & Mercy (1963) and O'Hara *et al.* (1971) have argued on largely mineralogical grounds in favour

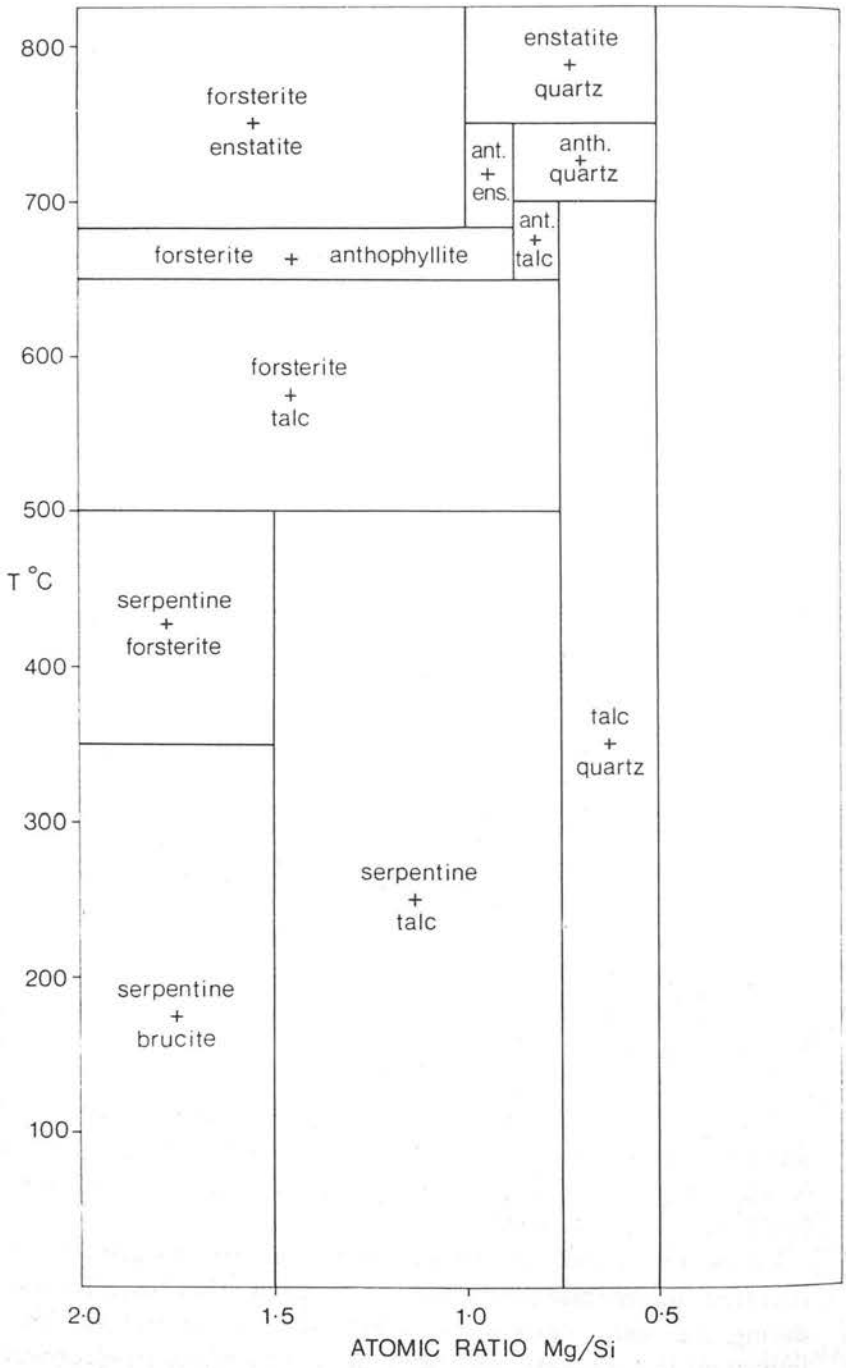

FIG. 3. Mineral assemblages in the system MgO–SiO_2–H_2O expected to be stable at about 2 kb P_{H_2O} (largely after Turner, 1968).

of much later emplacement after the main regional metamorphism and deformation.

Phase relations in the system MgO–SiO_2–H_2O have been extensively studied (see Bowen & Tuttle (1949), Fyfe (1962), Greenwood (1963), and Kitahara *et al.* (1966)) over a wide range of temperatures and pressures.

Fig. 3 which largely follows Turner (1968) table 4–4, summarizes the mineral assemblages expected to be stable in the system MgO–SiO_2–H_2O at various temperatures and a water pressure of about 2 kb. Markedly increased P_{H_2O} only slightly raises the temperature at which the various hydrous minerals breakdown. It is therefore apparent that at P_{H_2O} of 1 kb or greater, the mineral sequence forsterite → enstatite → anthophyllite observed in the vein is only expected at temperatures of roughly 680–750 °C.

Boyd (1954) showed that tremolite is stable with respect to the assemblage diopside+enstatite+quartz at temperatures up to 850 °C at $P_{H_2O} = 1$ kb and also on the basis of the study of phase relations along the join

$$Mg_{3\cdot5}Fe_{3\cdot5}Si_8O_{22}(OH)_2\text{–}Ca_2Mg_{2\cdot5}Fe_{2\cdot5}Si_8O_{22}(OH)_2$$

at $P_{H_2O} = 2$ kb by Cameron (1971), it is reasonable to predict that the assemblage anthophyllite+tremolite would be stable relative to talc+tremolite (lower T assemblage) and enstatite+tremolite (higher T assemblage) over the temperature range of about 650–720 °C at $P_{H_2O} = 2$ kb.

Similarly studies of phase relations in the system MgO–Al_2O_3–SiO_2–H_2O by Yoder (1952) and Fawcett & Yoder (1966) have shown that the magnesian chlorite–clinochlore is expected to remain stable in quartz-free assemblages to temperatures of about 720 °C at $P_{H_2O} = 2$ kb and markedly higher temperatures at higher water-pressures (e.g. 830 °C at $P_{H_2O} = 10$ kb). Thus one can predict that the assemblage chlorite+anthophyllite is probably stable over the temperature range of about 650–720 °C at $P_{H_2O} = 2$ kb. Fig. 4 summarizes the expected mineral assemblages at $P_{H_2O} = 2$ kb and temperatures of 700 °C and 450 °C in both the MgO–CaO–SiO_2–H_2O and MgO–Al_2O_3–SiO_2–H_2O systems.

In conclusion, the available experimental data suggest that the observed mineral sequence forsterite → enstatite → anthophyllite → tremolite → chlorite can have formed at temperatures of roughly 700±20 °C at P_{H_2O} of about 2 kb, or greater. As already discussed, temperatures of that order seem appropriate for the main regional metamorphism of the enclosing gneisses, whilst P_{total} was certainly greater than 6 kb, more likely about 10–14 kb. Either P_{H_2O} was significantly less than P_{total} during the metamorphism, as suggested by the common occurrence of eclogites, or at least there was a sharp drop in the activity of H_2O across the country rock/peridotite and fracture vein/peridotite contacts.

Accepting the structural arguments put forward by Brueckner (1969) for early emplacement, and bearing in mind the widespread development of small amounts of secondary enstatite, tremolite, and chlorite in the peridotites

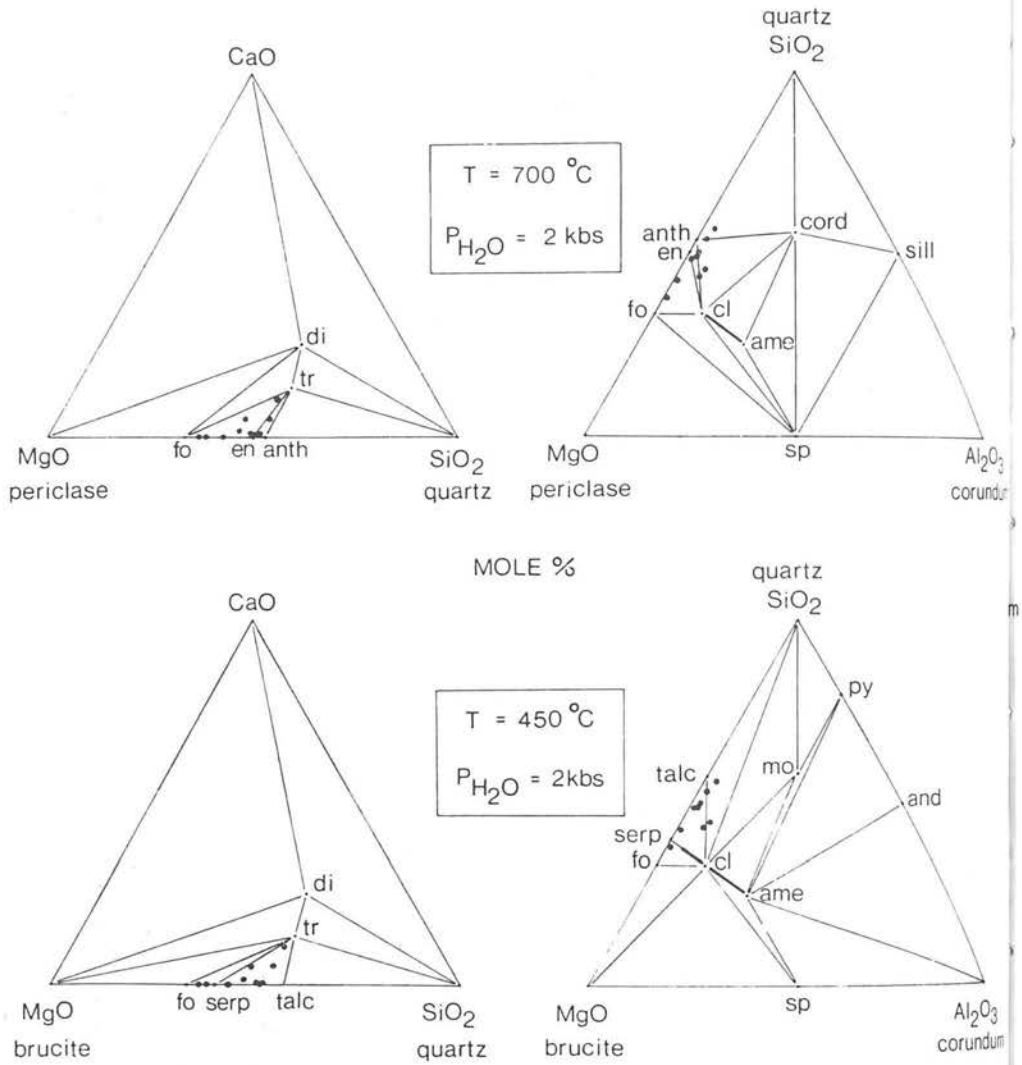

FIG. 4. Mineral assemblages expected at P_{H_2O} = 2 kb and 450 and 700 °C for the systems MgO-CaO-SiO_2-H_2O and MgO-Al_2O_3-SiO_2-H_2O. Abbreviations used: fo—forsterite, en—enstatite, anth—anthophyllite, tr—tremolite, di—diopside, cl—clinochlore, ame—amesite, cord—cordierite, sill—sillimanite, serp—serpentine, mo—montmorillonite, py—pyrophyllite, and—andalusite, sp—spinel.

throughout this region, it seems eminently reasonable to conclude that the growth of these minerals as exemplified by the metasomatic vein in question, occurred during the main metamorphic and migmatitic event affecting the region.

It is also clear (see Fig. 3) that serpentine and talc cannot have formed during the same high-temperature metamorphic event, but rather formed as secondary minerals in the presence of residual water at temperatures of the

order of 400–500 °C during the subsequent cooling history. The petrographic evidence that talc is concentrated between the enstatite and anthophyllite zones enhances this argument.

THE CONCEPT OF LOCAL EQUILIBRIUM IN OPEN SYSTEMS

It has been known amongst metallurgists for many years that high-temperature solid-state reactions proceed via intermediate stages characterized by sharply defined (often monominerallic) zones. These apparently develop as a result of two-way diffusion with simultaneous reaction in response to maintained concentration gradients.

The geological significance of this style of reaction was also noticed long ago (Read, 1934) and was actively investigated by the Russian School, led by Korzhinskii (1959 for review in English) who sought to develop a theory of metasomatism that was generally applicable. More recently Thompson (1959) once again drew the attention of western geologists to 'local equilibrium' theory. There followed an extended and heated discussion of the true value of the whole 'metasomatic phase rule' approach (Weill & Fyfe, 1964, 1967; Korzhinskii, 1964, 1967; and Thompson, 1970).

In the opinion of one of us (C. D. C.) this discussion had the rather unfortunate result of clouding the issue rather than resolving matters. Serious criticisms of the Korzhinskii–Thompson phase-rule approach were made which were not clearly answered. An impression was left that the whole approach was suspect, yet physical chemists for years have been studying systems with simultaneous diffusion and reaction. Their behaviour is very well known as is amply illustrated by such basic texts as Crank (1957) and Jost (1960). There is thus no need to define behavioural patterns in terms of 'perfectly mobile' or 'immobile' components and the resulting 'metasomatic phase rule' is of little predictive or interpretive help in understanding real systems. In fact it is difficult to see exactly how the rule is meant to be applied constructively. Certainly it cannot give information about the relative juxtaposition of different monominerallic zones nor about the relative dimensions of those zones. These are the factors of principle interest to geologists studying metasomatic systems.

The real value of the 'local equilibrium' approach resides in the fundamental postulate. As defined by Thompson (1959) this is: 'Equilibrium tends to be maintained locally within a reacting system even though the system as a whole may be distinctly out of equilibrium.' An alternative definition which draws attention to the essentially kinetic assumptions implicit is 'provided that the rate of material transfer within a reacting system is much less than the rate of reaction between components, reaction will proceed via compositionally distinct zones separated by sharp compositional discontinuities'. That this must be so was illustrated by Thompson (1959) although a slight element of uncertainty might have been introduced by the statement (p. 434) that '. . . a diffusion process can actually produce discontinuities in bulk composition where none

existed before'. A more general conclusion from the same treatment would have been 'in spontaneous metasomatic processes major sharp compositional discontinuities tend to be replaced by a number of lesser, although still sharp, compositional discontinuities'. Periclase and cristobalite in contact would react to give forsterite and enstatite intermediate zones with lesser, although sharp, compositional boundaries between each phase. Such a statement is also less at variance with classical thermodynamic reasoning.

THE MECHANISM OF VEIN FORMATION

Local equilibria in vein metasomatism: reaction style

It has been argued that the mineral zones at Kalskaret developed at high temperatures ($\sim$ 700 °C) and pressures. It seems likely that chemical reactions within silicate assemblages proceed via the intermediary of some fluid phase (obviously supercritical here) in which chemical constituents of the assemblage have finite solubilities. In an elegant series of experiments, Vidale (1969) demonstrated the importance of such fluids by producing typical metasomatic calc–silicate assemblages under hydrothermal conditions in the laboratory. It was found that reaction was favoured by:

(*a*) increasing temperature
(*b*) increasing pore fluid content
(*c*) increasing salt content of the pore fluid

Direct evidence of the presence of such salt-rich fluids is offered by fluid inclusion data. A comprehensive literature survey (including very extensive Soviet investigations) together with an excellent summary of both data and interpretation has been published recently by Roedder (1972). By far the most common type of inclusion material consists of a low-viscosity liquid with a gas bubble. The liquid almost invariably turns out to be a strong salt solution and the gas is dominated by either water or carbon dioxide. Roedder (1972, p. 58) states 'the residual fluids from the crystallisation of most igneous rocks also are strong sodium chloride brines as evidenced by the common presence of halite daughter crystals in their inclusions'.

Following from this survey and from the experimental demonstration of zone development, it is not unreasonable to postulate that the Kalskaret (acid) country rocks were permeated by supercritical fluids containing SiO_2, Al_2O_3, Na^+, K^+, Ca^{2+}, So_4^{2-}, Cl^-, with H_2O and some CO_2 as 'solvent'. It is noteworthy that Mg^{2+} is seldom recorded in fluid inclusions from quartz or quartz containing assemblages even though it is normally a major constituent of saline brines and inclusions in evaporite minerals. The metasomatic assemblages described here presumably developed by reaction of ultrabasic (peridotite) material with these fluids or, more likely, the fluids acted as a medium for peridotite/acid country rock reaction. Another way of looking at this is to think in terms of catalytic activity of the pore fluids with their great capacity

for carrying chemical constituents in solution. Reaction was not purely catalytic, however, since hydrous zonal minerals demonstrate direct reaction between peridotite and pore fluids.

The final 'true equilibrium' configuration

Classical thermodynamic reasoning suggests that a small volume of peridotite allowed to react with a large volume of (say) quartz–muscovite–biotite–potash felspar–oligoclase gneiss would equilibriate with an increase in biotite content (slightly higher Mg Fe ratio) with minor adjustments to the proportions of other phases.

In general terms, reaction of peridotite should lead to total conversion to the ferromagnesian member of the country rock assemblage stable under the prevailing regional conditions. Total conversion of the Kalskaret body to biotite, for example, would be truly stable in the sense that one very large biotite crystal would be. The activities of all species would be the same at all points in the entire system.

The metasomatic zoned bodies of Unst, Shetland, described by Read (1934), and Curtis & Brown (1969), formed by reaction of serpentine with oligoclase–biotite gneiss. The outermost reaction zone, always in sharp contact with country rock, invariably was pure, monominerallic biotite, exactly as suggested by the example given above. In the Kalskaret case, the central part of the vein represents the closest approach to the outermost zone in contact metasomatic assemblages. That this is chlorite might perhaps suggest that the regional conditions prevailing at the time of reaction were chlorite-grade. The composition of the chlorite, however, is far from that expected in an acid environment, being very much more magnesian, and the country rocks are usually free from any sign of chlorite. One obvious explanation is that the innermost (chlorite) zone is not fully in equilibrium with the country rock in the sense that the outermost zone of a contact assemblage is. In the Unst assemblages, for example, chlorite was always present and tended to form the second outermost zone. Again the chlorite was magnesium-rich. If the relationship between vein and contact metasomatism is as depicted in Fig. 1, material involved in the vein reaction must have traversed the contact zone and is likely to have been modified by reaction in that region. The vein sequence, therefore, probably does not represent a complete metasomatic assemblage. Any simple test of this hypothesis is precluded by field exposure or rather the lack of it in this particular instance. Biotite, however, has been observed in the contact metasomatic assemblage of other peridotite bodies in the Tafjord area.

Initiation of reaction

Fig. 5 outlines, in schematic fashion, the probable composition of the hydrous reaction fluid. This would have finite activity levels for all the common rock-forming metals and water. Contrast this with the probable composition

of any fluid in equilibrium (at the same T, P) with an olivine-dominated assemblage.

Now consider the outcome of connecting these two fluids. There would be immediate spontaneous diffusion of material down concentration gradients; Si, Al, H_2O, etc. would migrate into the pore fluid associated with the peridotite mass. Mg would migrate outwards for the same reason. It is important to

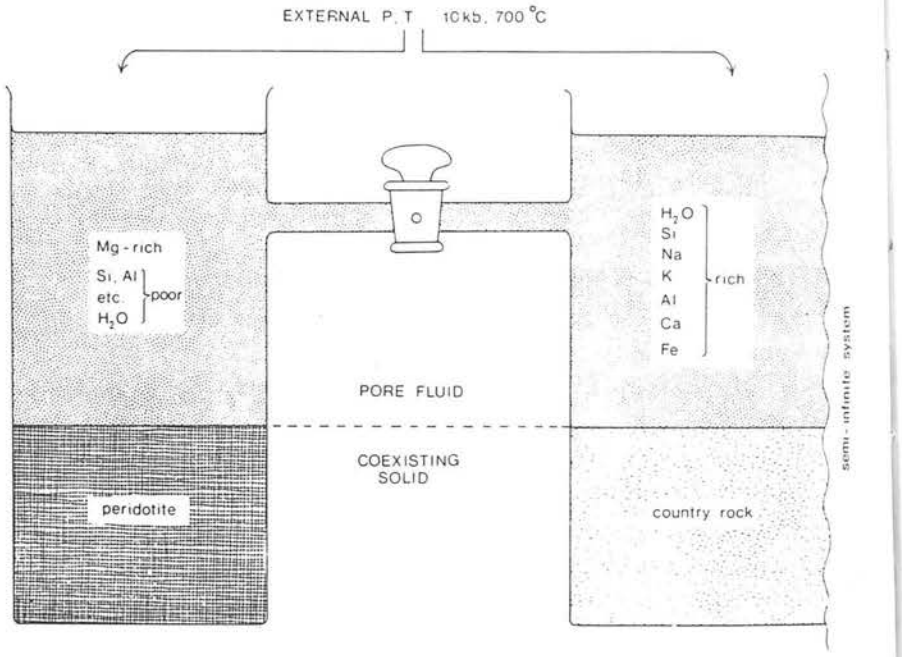

FIG. 5. Involvement of pore-fluids. Country-rock pore fluid would be dominated by alkali halides, H_2O and CO_2 with significant Si, Al, Ca, Fe, etc. Any link between this and fluids in equilibrium with peridotite at the same T, P (Mg, CO_2-rich, H_2O, Si-poor, etc.) would cause spontaneous inward migration of Si, Al, H_2O, and outward migration of Mg. Solid/fluid reactions would precipitate new solids and maintain diffusive migration tendency. The ultimate assemblage would be dictated by the semi-infinite volume of country rock acting as a buffer.

note, however, that all points within a fluid system must be electrostatically neutral. This means that in net movement all cationic species must either be accompanied by anionic species or the charge effect must be negated by the counter movement of a different cationic species. Ionic diffusion is thus seen to be subject to rather complex controls. In the present example is is likely that inward migration of Ca^{2+} and Al^{3+} would be linked with outward migration of Mg^{2+} as well as with individual ion concentration gradients as stipulated by Fick's Law. Further restrictions are imposed by reactions between fluid and solid.

This simple analysis tells us something about the initiation of reaction whereas the thermodynamic analysis of the preceding section tells us what the ultimate

reaction product ought to be. But neither can tell us anything about the incomplete reaction stage that constitutes a metasomatic assemblage. Undoubtedly the assemblage olivine–enstatite–anthophyllite–tremolite–chlorite is unstable just as is the cristobalite–enstatite–forsterite–periclase assemblage cited in Thompson's (1959) illustration. To make sense of these assemblages it is essential to return to the 'Principle of Local Equilibrium'.

Local equilibrium in vein metasomatism

Analysis of 'reaction tendency' from Fig. 5 suggests establishment of concentration gradients. Provided that equilibrium between pore fluid and solid phases is reached rapidly relative to component migration within the pore fluid, local equilibrium conditions should prevail and metasomatic zonation develop. The character of the reaction intermediate state may be inferred directly from the actual zonal sequence of solid phases preserved—this is outlined in Fig. 6.

Consider the pore fluid phase. Reaction at the chlorite/tremolite front removes Al^{3+} from the fluid phase in converting tremolite to chlorite (this is accompanied by migration of the front). In the reaction silica, water and calcium are also involved but the inward migration flux of aluminium is terminated whereas silica, water, and calcium pass on through. In other words the activity level dictated by the assemblage tremolite plus chlorite plus fluid is sufficiently low to prevent aluminium taking part in any further replacement reaction. This low level is maintained at the front and is responsible for preserving the concentration gradient, thereby ensuring continued inward migration of aluminium.

By similar reasoning, Ca^{2+} is seen to be the critical ion at the tremolite/anthophyllite front and its immigration is terminated there with only silica and water passing beyond. Analogous reasoning leads to the four stage (Al, Ca, H_2O, Si) model that is Fig. 6. Equilibrium is maintained at all points within the reacting system although no two points taken in a line perpendicular to the vein have identical composition. This is always true for the fluid phase but may not be so for the solid phase; hence the apparent compositional discontinuities.

The above interpretation takes no account of two alternative reactions that might be responsible for the anthophyllite and enstatite fronts. Silicification and hydration are inferred to be more or less independent processes, yet the $Si(OH)_4^0$ species (which is present in dilute aqueous solutions) would liberate water at the olivine/enstatite front. It is by no means certain that this silica species is present in high-temperature salt solutions. Further discussion of actual reactions seems pointless in the absence of factual information about the composition of such solutions.

The second point also concerns the enstatite and anthophyllite fronts. Mg^{2+} must diffuse outwards from the system into the vein fluid. If the Mg^{2+} activity in the peridotite fluid drops to (or slightly below) the level in

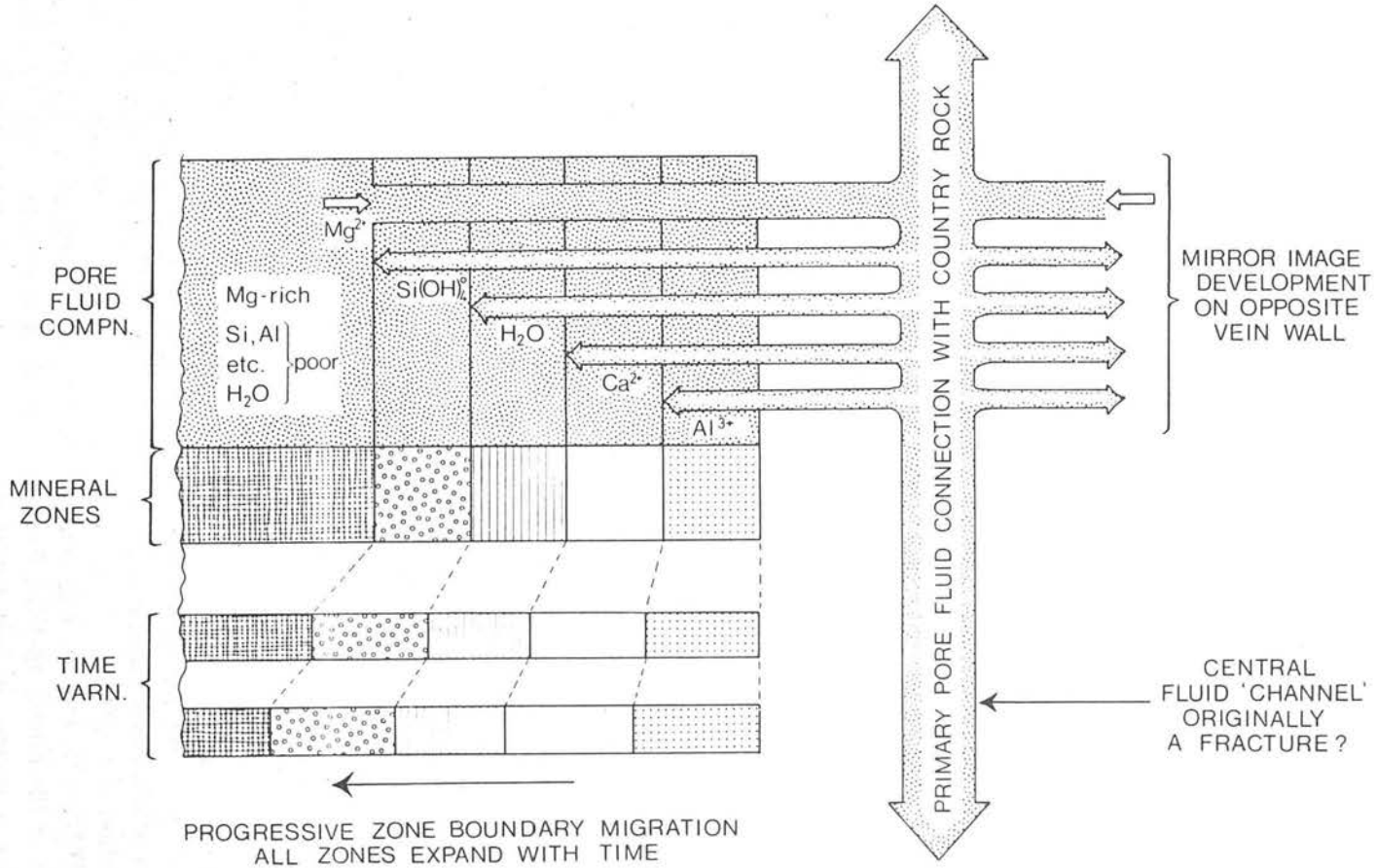

FIG. 6. Local equilibria between pore fluid and successive zonal minerals. Over-all reaction is one of cation (including H^+) exchange between olivine and pore fluids emanating from (and originally in equilibrium with) acid country rock. Each zonal boundary represents the maximum metasomatic penetration of a single species at any time during reaction. The over-all sequence represents equilibration of peridotite with country-rock pore fluids, one component at a time, such that the chlorite zone is most nearly in equilibrium with country rock (very high magnesium activities presumably stabilize chlorite within vein assemblages whereas biotite should occur in contact assemblages).
(Key to mineral composition: as in Fig. 1.)

equilibrium with the solid assemblage olivine plus enstatite, olivine will spontaneously alter to enstatite, liberating Mg^{2+} ions. A good analogy is removal of heat from the system ice plus water: the temperature does not fall until all water is converted to ice. An externally applied temperature low is responsible for the migration of a phase transition front (water/ice). Similarly, an externally applied Mg^{2+} activity low is responsible for the olivine–enstatite transformation.

There is no real discrepancy, however, between this interpretation and the earlier one (Fig. 6) suggesting inward silica flux. Both are partially correct as can be seen from an analysis of the simplest replacement front—tremolite anthophyllite. The replacement reaction is:

$$Mg_7Si_8O_{22}(OH)_2 + 2Ca^{2+} = Mg_5Ca_2Si_8O_{22}(OH)_2 + 2Mg^{2+}$$

(Local) Equilibrium may be described by the expression:

$$K_{\text{Trem/anthoph.}} = \frac{a_{Mg^{2+}}}{a_{Ca^{2+}}} \text{ (Activity of solids} \sim \text{unity)}$$

either an increase in Mg^{2+} activity *or* a decrease in Ca^{2+} activity will drive the reaction in the direction of anthophyllite. Only at this specific activity ratio may both solid phases stably coexist. The tremolite front in Fig. 6 therefore occurs at that point in the system where the values of Ca^{2+} and Mg^{2+} activity satisfy this condition. A similar (although more complex) condition may be written for each of the other fronts.

The meaning of mobility

The zonal sequence in the Kalskaret vein appears to represent a clear-cut example of a metasomatic process in which equilibrium between pore fluid and solid phases was maintained locally. At the outset of reaction migrating pore fluids reacted with vein walls and four very thin zones developed. These migrated inwards as reaction proceeded to constitute four replacement fronts. Had reaction gone to completion, all the peridotite would have been converted to enstatite and the enstatite successively replaced by anthophyllite, tremolite, chlorite, and, presumably, biotite.

Reaction would then have ceased since biotite, being a member of the country-rock assemblage would have no tendency to react with country-rock pore fluids. The fundamental characteristic of this reaction is that the peridotite equilibriated with the migrating fluids one component at a time. This picture is less obvious from the solid-phase sequence than from the probable reacting system configuration. The essential nature of a boundary (front) is that it separates (at any point in time) a region of flux from a region of zero flux for one component. In the case of the peridotite/enstatite boundary it is not clear whether this was the maximum inward extent of the inward Si flux or the outward Mg flux or possibly both. The Al and Ca fronts are unambiguous.

The reacting metasomatic system may therefore be regarded as a series of

reaction fronts which pass all ions except one: this is the critical front-determining ion. It is not difficult to envisage a realistic thermodynamic basis for this: the factor which determines which particular ion will be removed at a given front is the free energy released in that particular replacement reaction as opposed to the free energy released by possible alternative replacement reactions. It will depend upon the free energies of the two solids involved, upon the free energies of the solvated species involved, and upon their concentration levels. Free-energy considerations of this type therefore will determine the nature of a given metasomatic sequence. The relative width of the zones will depend upon kinetic factors such as the concentration differentials present and upon individual species diffusion coefficients.

All this leads to an interesting appraisal of 'mobility'. One thing is clear: simple considerations of ionic size or charge or even of measured solid or solution diffusion rates relate only to mobility within an inert system. The geologist examining metasomatic phenomena is looking at systems that have reacted. Solvated species migrate in response to concentration gradients. These gradients are maintained whenever a replacement reaction involves the particular solvate species or ion in question. The maximum migration of any ion depends on the nearest replacement front of the special type for which the ion is 'critical'. The presence of anions such as Cl^- and SO_4^{2-} increases the capacity of fluids to transport cations but they will not be effective in replacement reactions unless conditions of the type described above are met.

Departure from perfect zonality

The development of the model of Fig. 6 from the real mineral assemblages seen in Fig. 1 neglected compositional overlap. The only truly monomineralic zone is the chlorite zone. All others show varying degrees of complexity, this generally increasing away from the central chlorite zone. There is one simple and fairly obvious explanation for this in terms of the model already proposed. Unless the rate of component migration through the fluid pore space is much faster than the rate of equilibration between pore fluid and solid, the boundaries between zones must be diffuse. In the limiting case of the total reverse situation (i.e. diffusion rate much faster than reaction rate), there will be no tendency for zonal development. All types of intermediate situation have been investigated experimentally and complete mathematical analyses are available in basic texts (Crank, 1957; Jost, 1960).

In the case of metasomatic zonation developed in ultrabasic bodies in Unst (Curtis & Brown, 1969) it was argued that boundaries in multi-component systems should become increasingly diffuse away from the initial compositional discontinuity. Such is also the case in the present work.

Hofmann (1972) has extended Korzhinsky's treatment of infiltration metasomatism to take account of well-developed chromatographic theory. It is thought that the presence of anhydrous phases in the assemblages being interpreted in

CAMERON, K. L., 1971. Amphibole phase relations along the join $Mg_{3\cdot5}Fe_{3\cdot5}Si_8O_{22}(OH)_2$–$Ca_2Mg_{2\cdot5}Fe_{2\cdot5}Si_8O_{22}(OH)_2$. *Yb. Carnegie Instn Wash.* **70,** 145–50.

CARSWELL, D. A., 1968. Picritic magma–residual dunite relationships in garnet peridotite at Kalskaret near Tafjord, South Norway. *Contr. Miner. Petrol.* **19,** 97–124.

CRANK, J., 1957. *The mathematics of diffusion.* Oxford: Clarendon Press.

CURTIS, C. D., & BROWN, P. E., 1969. The metasomatic development of zoned ultrabasic bodies in Unst, Shetland. *Contr. Miner. Petrol.* **24,** 275–92.

—— —— 1971. Trace element behaviour in the zoned ultrabasic bodies of Unst, Shetland. *Contr. Miner. Petrol.* **31,** 87–93.

FAWCETT, J. J., & YODER, H. S., 1966. Phase relationships of chlorites in the system MgO–Al_2O_3–SiO_2–H_2O. *Am. Miner.* **51,** 353–80.

FYFE, W. S., 1962. On the relative stability of talc, anthophyllite and enstatite. *Am. J. Sci.* **260,** 460–6.

GREEN, D. H., & MYSEN, B. E., 1972. On the mineralogy of hornblende and plagioclase pegmatite and gneisses associated with eclogite in western Norway. *Lithos,* **5,** 147–61.

GREENWOOD, H. J., 1963. The synthesis and stability of anthophyllite. *J. Petrology,* **4,** 317–51.

HOFMANN, A., 1972. Chromatographic theory of infiltration metasomatism and its application to feldspars. *Am. J. Sci.* **272,** 60–90.

JOST, W., 1960. *Diffusion in solids, liquids, gases.* New York, Academic Press.

KITAHARA, S., TAKENOUCHI, S., & KENNEDY, G. C., 1966. Phase relations in the system MgO–SiO_2–H_2O at high temperatures and pressures. *Am. J. Sci.* **264,** 223–33.

KORZHINSKII, D. S., 1959. *Physicochemical basis of the analysis of the paragenesis of minerals.* New York, Consultant's Bureau.

—— 1966. On thermodynamics of open systems and the phase rule (a reply to D. F. Weill and W. S. Fyfe). *Geochim. cosmochim. Acta,* **30,** 829–35.

—— 1967. On thermodynamics of open systems and the phase rule (a reply to the second critical paper of D. F. Weill and W. S. Fyfe). *Geochim. cosmochim. Acta,* **31,** 1177–80.

MERCY, E. L. P., & O'HARA, M. J., 1965. Olivines and orthopyroxenes from garnetiferous peridotites and related rocks. *Norsk geol. Tidsskr.* **45,** 457–61.

MYSEN, B. O., & HEIER, K. S., 1972. Petrogenesis of eclogites in high grade metamorphic gneisses, exemplified by the Hareidland eclogite, Western Norway. *Contr. Miner. Petrol.* **36,** 73–94.

O'HARA, M. J., & MERCY, E. L. P., 1963. Petrology and petrogenesis of some garnetiferous peridotites. *Trans. R. Soc. Edinb.* **65,** 251–314.

—— RICHARDSON, S. W., & WILSON, G., 1971. Garnet peridotite stability and occurrence in crust and mantle. *Contr. Miner. Petrol.* **32,** 48–68.

READ, H. H., 1934. On zoned associations of talc, actinolite, chlorite and biotite in Unst, Shetland Islands. *Miner. Mag.* **23,** 519–40.

ROEDDER, E., 1972. Composition of fluid inclusions. *in* Data of geochemistry, ed. M. Fleischer, Chapter JJ. *U.S.G.S. Prof. Paper,* **440-JJ.**

SCHMITT, H. H., 1964. Metamorphic eclogites of the Eiksund area, Sunnmore, Norway. *Am. Geophys. Union Trans.* **43,** 128.

THOMPSON, J. B., 1959. Local equilibrium in metasomatic processes. *in* ABELSON, P. H. (ed.), *Researches in Geochemistry.* New York, John Wiley & Sons.

—— 1970. Geochemical reaction and open systems. *Geochim. cosmochim. Acta.* **34,** 529–51.

TURNER, F. J., 1968. *Metamorphic petrology.* New York, McGraw-Hill.

VIDALE, R., 1969. Metasomatism in a chemical gradient and the formation of calc-silicate bands. *Am. J. Sci.* **267,** 857–74.

WEILL, D. F., & FYFE, W. S., 1964. A discussion of the Korzhinskii and Thompson treatment of thermodynamic equilibrium in open systems. *Geochim. cosmochim. Acta,* **28,** 565–76.

—— —— 1967. On equilibrium thermodynamics of open systems and the phase rule (a reply to D. S. Korshinskii). Ibid. **31,** 1167–76.

YODER, H. S., 1952. The MgO–Al_2O_3–SiO_2–H_2O system and the related metamorphic facies. *Am. J. Sci., Bowen Volume,* 569–627.

the present paper is sufficient evidence to reject the chromatographic model which relies on solvent movement for material transfer.

CONCLUSIONS

The mineralogy and geochemistry of a complex silicate assemblage vein cross-cutting a peridotite body at Kalskaret, Norway has been described in some detail. The principle minerals (enstatite, anthophyllite, tremolite, and chlorite) are concluded to have developed simultaneously in a zoned sequence by reaction between the peridotite body and both supercritical fluids and acid country rock (via the fluids) during the main regional metamorphic event. A second reaction phase (possibly a much later stage of the same regional event) caused certain lower temperature phases (notably talc and serpentine) to grow on a small scale throughout the ultrabasic bodies and the metasomatic vein assemblages.

One interesting and perhaps important finding of the study was the undoubted presence of enstatite as a zonal mineral. Enstatization therefore occurred as a metasomatic process on this very small scale and suggests the possibility of the same or a similar mechanism accounting for the development of the enstatite-rich, ultrabasic masses which occur in some parts of this region of southern Norway.

A considerable part of the discussion was devoted to largely hypothetical considerations of the nature of the controls acting upon this classic example of metasomatic alteration. There were many features in common with an earlier described example of contact metasomatic alteration (Curtis & Brown, 1969, 1971). The same basic explanation for reaction was found to be valid: each reaction front representing equilibration with respect to a single important chemical species. Zoned metasomatic assemblages represent step-by-step adjustment (partial equilibration) one component at a time, to the over-all component activity levels determined by country rock (regional) conditions. In this sense, metasomatic assemblages may be able to provide much more information about regional conditions than true equilibrium assemblages. Further work not only is required but seems eminently worth while.

ACKNOWLEDGEMENTS

We wish to acknowledge financial support for field-work from the University of Sheffield Research Fund, and to thank Dr. H. K. Brueckner for pointing out the occurrence of this metasomatic vein, V. A. Somogyi for his assistance with chemical analysis, and Miss Pat Mellor for typing the manuscript.

REFERENCES

Bowen, N. L., & Tuttle, O. F., 1949. The system MgO–SiO_2–H_2O. *Bull. geol. Soc. Am.* **60**, 430–60.

Boyd, F. R., 1954. Tremolite. *Yb. Carnegie Instn Wash.* **53**, 109–10.

Brueckner, H. K., 1969. Timing of ultramafic intrusion in the core zone of the Caledonides of southern Norway. *Am. J. Sci.* **267**, 1195–1212.

Contrib. Mineral. Petrol. 67, 289–295 (1978)

Contributions to Mineralogy and Petrology

Trace-Element Distribution and Ore Formation in Vein-Metasomatised Peridotite at Kalskaret, Near Tafjord, South Norway

R. Kanaris-Sotiriou, F.G.F. Gibb, D.A. Carswell, and C.D. Curtis

Department of Geology, The University of Sheffield, S1 3JD, Great Britain

Abstract. The concentration profiles of the trace elements, S, Ti, V, Cr, Mn, Co, Ni, Cu, Zn, Sr, and Y have been determined across a metasomatic vein in peridotite. The introduced elements Ti, V, Sr, and Y show specific enrichment in particular silicate phases in accordance with the availability of suitable lattice sites. In contrast, the other introduced trace elements (Cu and S) behave more like the redistributed elements, Cr, Ni, Mn, and Co which do not show concentration 'fronts' that can be simply related to the silicate minerals. Concentration of pentlandite, chalcopyrite, and Cr-magnetite near the boundary between the enstatite and anthophyllite zones gives rise to maxima in the Ni, Cu, S, and Cr distributions, while in the chlorite zone significant concentrations of Cr and Ni occur in the chlorite itself. Control of the distribution of Ni, Cu, and Cr is ascribed to the oxidation/reduction reactions involved in the formation of pentlandite, chalcopyrite and Cr-magnetite, together with the critical role of Al in limiting chlorite formation during metasomatism.

Introduction

The mineralogy and major-element geochemistry of a complex assemblage of silicates in a vein cross-cutting a peridotite body at Kalskaret, Norway, have previously been reported in some detail (Carswell et al., 1974). The symmetrically zoned sequence of vein minerals on either side of a fracture in the peridotite was concluded to have developed by the reaction of the peridotite with supercritical hydrous fluids that originated from the acid gneiss country rocks. Each half of the sequence is around 10 cm thick with a common central zone of chlorite occupying the position of the fracture and zones of tremolite, anthophyllite and enstatite between this and the peridotite on either side (Fig. 1).

The sequence is believed to have formed at temperatures of about 700° C and at a P_{total} of greater than 6 kb. A later reaction episode was thought to account for the presence on a small scale of lower temperature phases (talc and serpentine) which occur to a limited extent throughout the ultrabasic bodies and in the metasomatic vein assemblage. Ultramafic fracture assemblages from Almklovdalen, further west in the Norwegian Basal Gneiss Complex, have been tentatively dated as having formed in the late Caledonian (c. 400 m.y.) by Brueckner (1975), although it was recognised that the metamorphic histories of the ultramafic bodies may extend as far back as the Svecofennian (1600–1800 m.y.).

It was suggested (Carswell et al., 1974) that each mineral zone represented a local attainment of equilibrium, although overall the reaction was incomplete. The outer boundary (towards the peridotite) of each zone was thought to represent the limit of penetration of the particular chemical species from the fluid controlling the growth of the mineral phase forming that zone. In this way, the zone 'front' for chlorite was determined by Al^{3-}, tremolite by Ca^{2-}, anthophyllite by H_2O and enstatite possibly by $Si(OH)^0_4$. With progressive influx of fluids all zones simultaneously expanded towards the peridotite.

The study is here extended to the trace elements of the same sequence, with a view to establishing the ways in which the distribution of these elements may be controlled in metasomatic systems of this type. Detailed elemental distributions for other examples of similar complexity to the Kalskaret vein sequence do not appear to have been recorded although work illustrating the mobility of Ni in altered ultramafic rocks has been reported (e.g., Rucklidge (1972), Eckstrand (1975), and Groves et al. (1974)). Curtis and Brown (1971) discussed trace-element behaviour in the zoned metasomatic bodies of Unst, Shetland but, in case, the complete zonal sequence is rarely seen.

0010-7999/78/0067/0289/$01.40

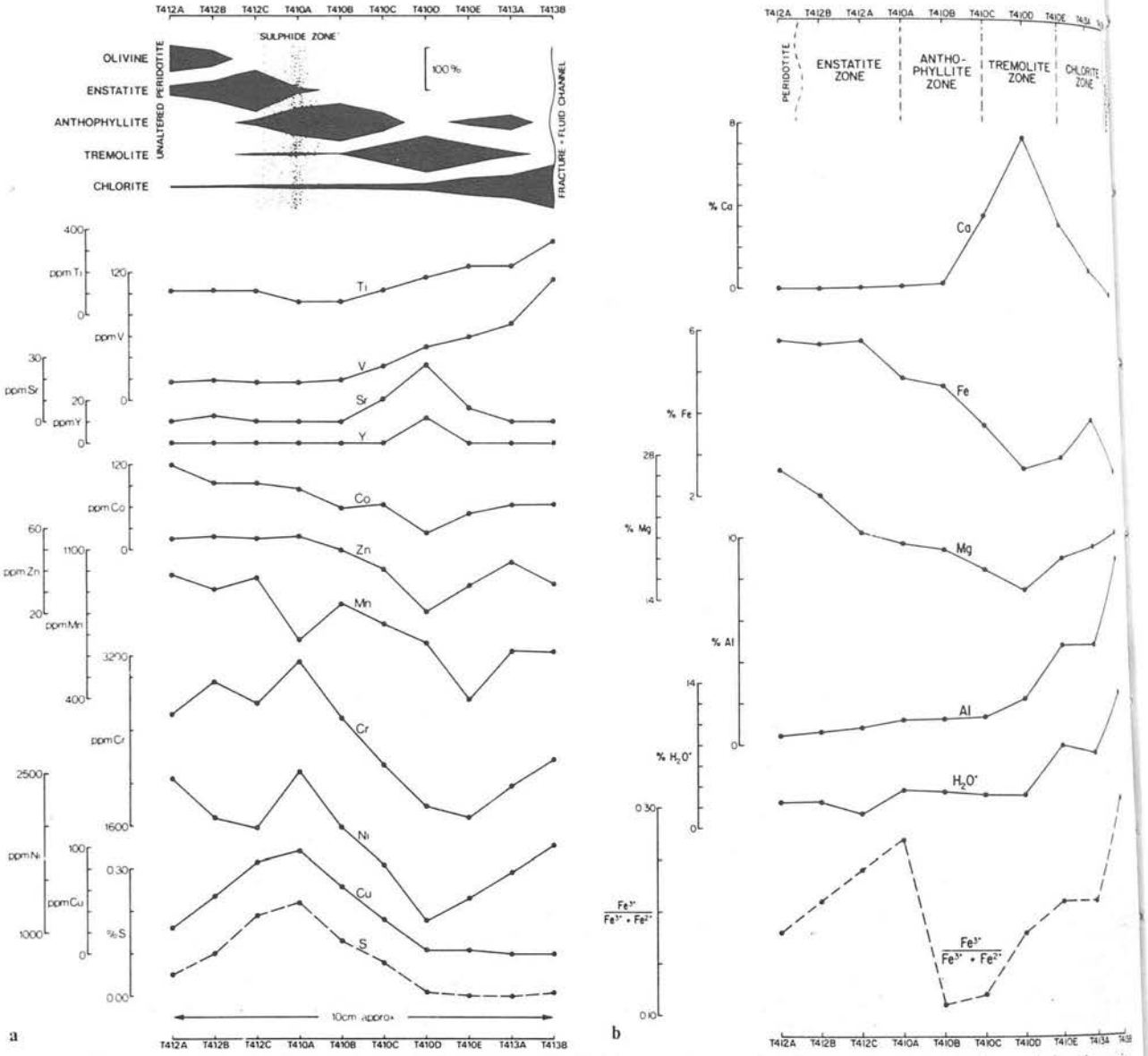

Fig. 1a and b. Chemical and mineralogical variations across the Kalskaret metasomatic vein. **(a)** shows (top) the variation in major silicate mineral contents and the position of the sulphide concentration which accounts for up to 0.5% by volume of the rock. Plotted below are the distributions of the various trace elements. **(b)** shows the corresponding critical variations in major element geochemistry

The same bulk samples from the Kalskaret vein that were previously analysed for major elements were used for the determination of trace elements by X-ray Fluorescence Spectrometry using pressed-powder specimens. The elements determined were Zr, Y, Sr, Rb, Zn, Cu, Mn, V, Ni, Cr, Co, Ba, and Pb, but of these Zr, Rb, Ba, and Pb were close to the limit of detection (about 2 ppm) and showed little variation. The remaining trace-element contents are plotted in Figure 1a together with values for Ti and S determined by XRFS using a fusion sample preparation technique. A schematic representation of the mineralogy of the sequence as determined by a combination of X-ray diffraction modal analysis and normative calculations is given in Figure 1a.

Sources of the Trace-Elements

The following assumptions have been made in attempting to establish the sources of the various elements:

(a) The trace elements contained in the zonal sequence were derived either from the original peridotite *or* were introduced with the incoming fluids.

(b) The original trace elements within the peridotite were uniformly distributed on the scale of a hand specimen.

(c) Any volume changes as a result of the metasomatism were relatively small and/or uniformly distributed over the region of the peridotite affected.

Table 1. Electron microprobe partial analyses of Kalskaret silicate and oxide phases

Zone	Mineral	wt % Cr^a	wt % Ni^a	wt % FeO^a	wt % $Al_2O_3{}^a$
	Oxide	33.29	0.13	45.84	3.91
	Enstatite	0.02	0.11	n.d.	n.d.
	Anthophyllite	0.04	0.12	n.d.	n.d.
Enstatite	Chlorite A	2.16	n.d.	n.d.	n.d.
	Chlorite B	1.96	n.d.	n.d.	n.d.
	Chlorite C	1.64	0.23	3.25	15.35
	Oxide	34.38	0.11	36.85	7.21
	Anthophyllite	0.03	0.11	n.d.	n.d.
Anthophyllite	Chlorite	1.55	0.20	3.37	15.40
	Tremolite	0.03	0.10	n.d.	n.d.
	Talc	0.03	0.18	n.d.	n.d.
	Oxide	29.15	0.32	45.40	7.18
	Anthophyllite	0.03	0.11	n.d.	n.d.
Tremolite	Chlorite A	0.60	0.22	3.25	17.29
	Chlorite B	0.72	0.18	n.d.	n.d.
	Tremolite	0.01	0.13	n.d.	n.d.
Chlorite	Chlorite	0.17	0.25	3.37	16.76

n.d. = not determined

[a] ZAF correction factors derived from mineral compositions calculated from bulk analyses except for oxide for which a spinel composition of similar Fe, Cr, and Al content was used

Table 2. Electron microprobe analyses of Kalskaret sulphide minerals

(a) Pentlandite

Sample/ Analysis No.	T410/0/A	T410/0/B	T412/0/B	T412/1/B	T412/1/C	[a]
wt %						
S	33.1	33.3	32.7	32.7	35.0	32.81
Cu	0.0	0.0	0.14	0.0	0.0	
Ni	32.6	34.5	32.7	33.1	28.6	35.12
Fe	33.6	32.7	34.8	33.0	34.3	29.48
Co	n.d.	n.d.	n.d.	0.57	0.55	2.20
Total	99.30	100.50	100.34	99.37	98.45	99.61

[a] Average of twenty pentlandite analyses from pentlandite-pyrrhotite assemblages after Harris and Nickel (1972)

(b) Chalcopyrite

Sample/ Analysis No.	T412/1/A	T412/2/A	[b]
wt %			
S	34.4	34.8	34.95
Cu	34.5	34.6	34.20
Ni	0.13	0.22	
Fe	29.8	29.8	30.65
Co	0.04	0.05	
Total	98.87	99.47	99.80

[b] Average of three chalcopyrite analyses from Dana's System of Mineralogy, Vol. 1, (Palance, Berman and Frondel, 1958) p. 221, analyses 1, 2, and 6

If these conditions are accepted it seems clear that elements occurring in much greater quantities overall in the zonal sequence than in the relatively unaltered peridotite must have been introduced by the metasomatizing fluids. Components of this type are Ti, V, Sr, Y, Cu, and S, all of which occur in virtually negligible quantities in the peridotite and yet show a significant build-up in various parts of the vein sequence (see Fig. 1). By contrast, Co, Mn, Cr, and Ni all occur in adequate quantities in the peridotite to account for the amounts of these elements present in the zones.

A sample of peridotite, T156 (90% olivine, 7% chlorite and 3% opaque minerals), from an adjacent body unaffected by vein metasomatism has whole-rock contents of 0.30 wt % Ni and 0.25 wt % Cr (Carswell, 1968) which are close to the values found for the least-altered zone of the present example (T412A) which has 0.25 wt % Ni and 0.26 wt % Cr.

Trace-Element Contents of the Minerals

It is evident from Figure 1 that there is only a limited correlation between the distribution of the various trace elements and the silicate phases forming the bulk of the metasomatic sequence. For example, peaks in the Cr, Ni, and Cu distributions are located near the *junction* between the enstatite and anthophyllite zones. These particular trace elements do, however, show a strong correlation with the sulphur content, indicating that they may be in part associated with phases other than the silicates. The mineralogical distribution of these trace elements has been ascertained by electron microprobe analyses of both silicate and opaque phases. Sulphides and oxides are common constituents of the samples and both are relatively concentrated in the region of the boundary between the enstatite and anthophyllite zones. The sulphide phase is mainly pentlandite with minor chalcopyrite intergrowths. The microprobe analyses of these sulphides are similar to previously reported compositions (see Table 2). The oxide phases are identified as Cr-rich magnetite (see Table 1), with lesser amounts of Cr-free magnetite. The Cr-rich magnetite may be classified as a 'ferritchromit' (Spangenberg, 1943) the occurrence of which may be of some genetic significance (see later). Original (i.e., peridotite derived) chromite is not found in the Kalskaret vein sequence, but evidence from nearby peridotite bodies suggests that chromite was almost certainly the source of Cr. Sample T156 (unaltered peridotite from an adjacent body) contains chromite with approximately 40 wt % Cr and olivine with 0.3 wt % Ni.

It is evident from Table 1 that, with the exception of chlorite, the contents of the quantitatively important trace elements, Cr and Ni, in the silicate phases show remarkably little variation both between different grains of the same phase and between different phases. Average values for these silicates are:

enstatite	0.02 wt % Cr	0.11 wt % Ni
anthophyllite	0.03 wt % Cr	0.11 wt % Ni
tremolite	0.02 wt % Cr	0.12 wt % Ni

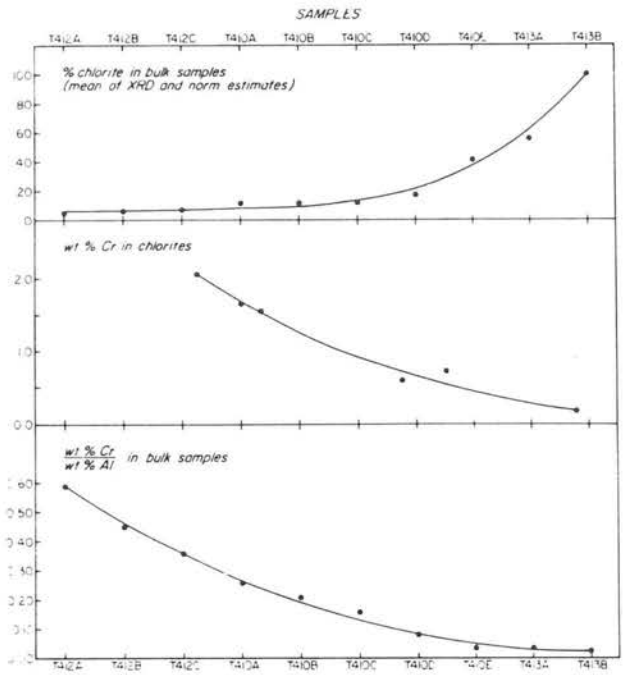

Fig. 2. Variations in modal % chlorite (top), Cr content of chlorite (determined by EMP analysis) (centre) and Cr: Al ratio (bottom) across the vein

In contrast to the Ni content of the chlorite which shows a comparatively small variation (0.18–0.25 wt % Ni) the Cr content exhibits a wide range (0.17–2.16 wt % Cr) and varies systematically across the zonal sequence. The lowest values for Cr content occur in the chlorite zone itself (see Fig. 2), the Cr content decreasing with increasing chlorite concentration in the zonal sequence.

Zonal Trace-Element Distributions

As previously noted, only limited correlation exists between the distribution of the various trace elements and the silicate phases and this is due to the incorporation of significant quantities of some elements into the opaque phases.

The exact coincidence of the distributions of Cu and S throughout the sequence and the identification of chalcopyrite as one of the opaque phases indicates that Cu occurs almost entirely in the chalcopyrite and, like the S, has clearly been introduced during the metasomatism.

The distribution pattern of Ni is irregular, rising to a peak between the enstatite and anthophyllite zones and then decreasing into the tremolite zone before increasing again in the chlorite zone. In the part of the sequence (around sample T410A) where the sulphides are concentrated (about 0.5% by volume) Ni in the pentlandite (about 33 wt % Ni) accounts for a large proportion of the Ni in the bulk sample. Towards the fluid channel it is obvious that chlorite becomes the most important host for Ni, with the whole-rock Ni content of 0.18 wt % being in reasonable agreement with the microprobe value of 0.25 wt % Ni for chlorite in the chlorite zone. Apart from the obvious peak corresponding to the concentration of pentlandite, the Ni distribution pattern closely follows that of Mg (Fig. 1a and b).

This is not unexpected as Mg and Ni vary sympathetically in almost all rocks. It is clear that there has been an overall loss of Mg, Ni and Fe from the metasomatic sequence rather than any influx.

The Co and Mn contents also show a gradual decrease towards the fluid channel with only minor irregularities.

The distribution pattern of Cr, like Ni, is very irregular. Cr rises to a peak in sample T410A in which it is located in chrome-magnetite (about 33 wt % Cr), chlorite (about 2 wt % Cr) and anthophyllite (about 0.04 wt % Cr). The Cr content then drops steadily outwards from the enstatite/anthophyllite boundary to the tremolite zone, but then increases again in samples T413A and T413B. This increase is due to the progressively larger amounts of Cr-bearing chlorite in this part of the vein (see Fig. 2) even though the chlorite itself has a considerably lower Cr content (about 0.17 wt % Cr) in comparison with the chlorite in sample T410A.

Brady (1977), from a theoretical standpoint, offered a completely novel geological explanation for the Kalskaret vein sequence, namely, that it was initially a granitic dyke. The justification for this was that it is difficult to envisage movement of an 'immobile' species such as Al (the critical element in chlorite formation). Because of this, Brady suggested that the initial wall-rock/'fluid' channel boundary in metasomatically zoned systems of the Kalskaret type may be identified by discontinuities in the weight ratios of two components such as Al and Cr. In the present example the Al: Cr ratio decreases steadily from the peridotite to the centre of the chlorite zone (see Fig. 2) without any such discontinuity. There is therefore no evidence, using Brady's own criterion, to support his implication that the chlorite zone does not represent part of the altered peridotite. His alternative model, that the fracture may have been originally occupied by granitic material, is consequently untenable and in any case does not fit the observed field relationships.

Of the undoubtedly introduced elements, V and Ti have distributions that show a direct correlation with chlorite content. Both elements apparently substitute for Al^{3+} in the chlorite. In contrast, the striking restrictions of Sr and Y to the tremolite zone indicate that these elements have predictably substi-

tuted for Ca^{2+} and are preferentially incorporated into the tremolite lattice.

The various introduced trace elements therefore tend to show quite specific concentration in particular mineral species in accordance with the availability of suitable lattice sites for their incorporation. This behaviour contrasts markedly with that of the re-distributed trace elements, notably Ni and Cr, which do not show such simple concentration 'fronts' probably because these elements were originally present throughout the region of the peridotite that has undergone reaction.

Origins of the Trace-Element Distributions

The distributions of Ti, V, Sr, and Y are compatible with the previously proposed mechanism for the origin of the zoning (Carswell et al., 1974), each of these incoming elements being preferentially incorporated where lattice sites are favourable. The behaviour of the Cr and Ni derived from the peridotite and the Cu introduced via the incoming fluids is less easily understood. Several possibilities exist, based on the following observations:

(a) The Cr, Ni, and Cu distributions show coincident maxima at the junctionof the enstatite and anthophyllite zones. This position also marks the transition from anhydrous to OH-bearing phases in the zonal sequence.

(b) A concentration of talc and magnetite occurs at the same position.

(c) At the position of maximum concentrations of Ni and Cu, i.e., in the 'sulphide zone', these elements occur mainly in pentlandite and chalcopyrite respectively.

(d) In the chlorite zone most of the Ni occurs in the chlorite itself, pentlandite being absent.

(e) The Cr is mainly located in chlorite in which the concentration of Cr varies systematically across the sequence, and in chromiferous magnetite which exhibits a maximum concentration in the 'sulphide zone'.

(f) The Cr and Ni contents of the zonal sequence were derived from the original peridotite where the Cr was located in the chromite and the Ni in the olivine. Cu and S were introduced via the incoming fluids.

It was previously suggested (Carswell et al., 1974) that the talc and serpentine were low temperature reaction products formed after the main zonal sequence was established. In view of the correlation between the 'sulphide zone' and the talc-oxide concentration it is appropriate to consider here whether the location of the Cr, Ni and Cu was related to either the high or low temperature reaction episodes or to both.

The occurrence in the zonal sequence of a chromiferous magnetite may reveal something about the way the original chromite has been broken down and the chromium relocated in other phases. Bliss and McLean (1975), cite numerous reported instances where the breakdown of chromite to form ferritchromit ± chlorite has occurred in serpentinites, although this reaction has been variously ascribed to the serpentinisation process itself, to the subsequent metamorphism of the serpentinite or to alteration prior to serpentinisation. Although ferritchromit (Spangenberg, 1943) does not represent a specific composition of chromiferous magnetite, the characteristic features of the reaction seem to have some uniformity, with the ferritchromit being relatively depleted in Mg and Al (and sometimes in Cr) and enriched in Fe relative to the parent chromite. Beeson and Jackson (1969), for example, describe the chemistry of altered primary chromites from the Stillwater complex where one chromite (47.1 wt % Cr_2O_3, 18.6 wt % Al_2O_3, 2.1 wt % Fe_2O_3, 19.7 wt % FeO, 10.0 wt % MgO) shows alteration to ferritchromit (42.0 wt % Cr_2O_3, 3.1 wt % Al_2O_3, 22.4 wt % Fe_2O_3, 30.1 wt % FeO, 2.1 wt % MgO) and chlorite (1.5 wt % Cr_2O_3, 21.0 wt % Al_2O_3, 6.6 wt % FeO, 29.4 wt % MgO). This is obviously similar to the situation in the Kalskaret vein, where, although the original chromite is not seen, the Cr-Fe oxide (approx. 47 wt % Cr_2O_3, 6 wt % Al_2O_3, 43 wt % total iron oxide as FeO) seems to be of the ferritchromit type and occurs in a part of the sequence where the small amounts of the chlorite present contain up to 2 wt % Cr_2O_3.

It is clear that the decomposition of primary chromite in the Kalskaret vein sequence must have taken place during the high-temperature reaction episode since Cr derived from the chromite (the major source of Cr) has been partially incorporated in silicates (notably chlorite) formed as a direct result of this reaction episode. This implies that the re-distribution of Cr may have been a stepwise process partially dependent upon redox potential (chromite ⇆ ferritchromit) and partially on the availability of Al to form chlorite. There is a strong tendency for Cr to be incorporated in chlorite. Where the availability of Al limits the quantity of chlorite formed, this results in chlorite with a high (c. 2 wt %) Cr content (see Fig. 2).

It is suggested that in the Kalskaret vein the distribution of Cr was controlled by two sequential reactions. Firstly, the original primary chromite was completely broken down to form ferritchromit plus small amounts of Cr-rich chlorite, this part of the

process being seen in the inner part of the zonal sequence (in the 'sulphide zone') where little or no introduced Al was present. Secondly, as the development of the zone sequence progressed, more Al became available via diffusion from the fluid channel, thus enabling the formation of more chlorite which incorporated the Cr released by the further breakdown of the ferritchromit, as seen in the outer parts of the sequence where no oxide phase remains and virtually all the Cr is located in chlorite.

It is interesting to note that Trommsdorff and Evans (1974) have observed the exact reverse of these reactions in metamorphosed serpentinised peridotite and associated the progressive reaction chlorite→ferritchromit→chromite with increasing grade of metamorphism.

The occurrence of pentlandite (often with chalcopyrite) as ores associated with serpentinites is well known (Ramdohr, 1967) although the pentlandite may be primary (i.e., magmatic) (Groves et al., 1974) or derived from Ni originally contained in silicates (Eckstrand, 1975). In the Kalskaret sequence the Ni in the pentlandite is clearly derived from the original olivine of the peridotite.

Eckstrand (op. cit.) described a model for the development of the nickel-bearing opaque mineral assemblages of the Dumont serpentinite controlled by redox mechanisms that may be relevant here. He indicated that serpentinisation reactions involving the production of magnetite resulted in strongly reducing environments that ultimately control the formation of nickel sulphides. It therefore seems probable that the pentlandite in the Kalskaret vein resulted from such a reducing reaction with the S being introduced by the fluids as SO_4^{2-}. Complimentary oxidations may be involved in the formation of either the ferritchromit or the magnetite.

The overall reaction may be expressed as:

$$SO_4^{2-} + 8FeO \rightleftharpoons S^{2-} + 4Fe_2O_3$$

However, although the formation of the ferritchromit may be convincingly assigned to the high-temperature reaction episode, the formation of the magnetite could have resulted from the low-temperature reactions in which talc and antigorite were formed. The essential part of the equation for this reaction would be:

$$3\,FeO + H_2O \rightleftharpoons Fe_3O_4 + H_2$$

(In olivine or enstatite) (Magnetite)

Oxidation reactions compensating for the reduction by which pentlandite formed may therefore be ascribed to either the high or low-temperature reaction episodes. Because the original Ni site (in the olivine) must have been destroyed as a result of the high-temperature reaction episode and because the Ni contents of the high-temperature reaction silicates are inadequate to account for the released Ni, it seems most likely that during the high-temperature reaction episode a significant proportion of the Ni was relocated in pentlandite where the conditions were favourable, i.e., in the 'sulphide zone'.

Experimental data from non-silicate systems suggest an upper stability limit for pentlandite of about 600° C (Kullerud, 1963) but evidence from Mg-rich silicate systems (e.g., Rajamani, 1976) indicates that it is possible for pentlandite to exist at much higher temperatures (c. 900° C). Thus experimental data do not preclude the possibility of pentlandite formation in the Kalskaret vein during the high-temperature reaction episode. However, this requires that with the continued expansion of the zonal sequence, pentlandite breaks down to provide Ni for incorporation in the chlorite which is the sole Ni-bearing mineral in the outer part of the sequence. Alternatively, Ni could have been temporarily located in another host (now destroyed) during the high-temperature reaction episode and relocated in pentlandite as a result of the low-temperature reactions.

On the balance of the evidence available, we favour the development of the pentlandite during the high-temperature reaction episode, but in either event it seems clear that the distribution of Cr and Ni has been controlled by a complex interplay of oxidation-reduction mechanisms coupled with the availability of Al as the critical factor in chlorite formation.

References

Beeson, M.H., Jackson, E.D.: Chemical composition of altered chromites from the Stillwater complex, Montana. Am. Mineral. **54**, 1084–1100 (1969)

Bliss, N.W., MacLean, W.H.: The paragenesis of zoned chromite from Central Manitoba. Geochim. Cosmochim. Acta **39**, 973–990 (1975)

Brady, J.B.: Metasomatic zones in metamorphic rocks. Geochim. Cosmochim. Acta **41**, 113–125 (1977)

Brueckner, H.K.: Contact and fracture ultramafic assemblages from Norway: Rb-Sr evidence for crustal contamination. Contrib. Mineral. Petrol. **49**, 39–48 (1975)

Carswell, D.A., Curtis, C.D., Kanaris-Sotiriou, R.: Vein metasomatism in peridotite at Kalskaret, near Tafjord, South Norway. Contrib. Mineral. Petrol. **19**, 97–124 (1968)

Carswell, D.A., Curtis, G.D., Kanaris-Sotirou, R.: Vein metasomatism in peridotite at Kalskaret, near Tefjord, South Norway. J. Petrol. **15**, 383–402 (1974)

Curtis, C.D., Brown, P.E.: Trace element behaviour in the zoned ultrabasic bodies of Unst, Shetland. Contrib. Mineral. Petrol. **31**, 87–93 (1971)

Eckstrand, O.R.: The Dumont Serpentinite: a model for control of nickeliferous opaque mineral assemblages by alteration reactions in ultramafic rocks. Econ. Geol. **70**, 183–201 (1975)

Groves, D.I., Hudson, D.R., Hack, J.B.C.: Modification of iron-nickel sulphides during serpentinisation and talc-carbonate alteration at Black Swan, Western Australia. Econ. Geol. **69**, 1265–1281 (1974)

Harris, D.C., Nickel, E.H.: Pentlandite compositions and associations in some mineral deposits. Can. Mineral. **11**, 861–878 (1972)

Kullerud, G.: Thermal stability of pentlandite. Can. Mineral. **7**, 353–366 (1963)

Palache, C., Berman, H., Frondel, C.: Dana's system of mineralogy, Vol. I, 7th Ed. New York: John Wiley & Sons 1978

Rajamani, V.: Distribution of iron, cobalt and nickel between synthetic sulphide and orthopyroxene at 900° C. Econ. Geol. **71**, 795–802 (1976)

Ramdohr, P.: A widespread mineral association, connected with serpentinisation. N. Jb. Mineral. Abh. **107**, 241–265 (1967)

Rucklidge, J.C.: A study of the redistribution of nickel in the serpentinisation of olivine. Proc. 6th Inter. Conf. X-ray Optics and Microanalysis, Tokyo (1972)

Spangenberg, K.: Die chromitlagenstätte von Tampadel in Zobten. Z. Prakt. Geol. **51**, 13–35 (1943)

Trommsdorf, V., Evans, B.W.: Alpine metamorphism of peridotitic rocks. Schweiz. Mineral Petrol. Mitt. **54**, 333–352 (1974)

Received April 19, 1978 / Accepted June 21, 1978

The equilibration conditions and petrogenesis of European crustal garnet lherzolites

D. A. CARSWELL & F. G. F. GIBB

LITHOS

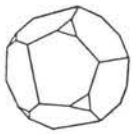

Carswell, D. A. & Gibb, F. G. F. 1980: The equilibration conditions and petrogenesis of European crustal garnet lherzolites. *Lithos 13*, 19–29. Oslo. ISSN 0024-4937.

Consideration of various element partition geothermometers yields new mean temperature estimates of 734–776°C and 836–893°C for garnet lherzolites from West Norway and the Central Alps, respectively. Reservations are expressed over the current 'best' pressure estimates of 20.7–23.1 kbars and 29.4–33.0 kbars. An ultimate mantle origin for the peridotite masses is thought likely but it is emphasized that in all probability these rocks were tectonically interleaved with their enveloping gneisses *before* rather than *after* equilibration of the present garnet lherzolite assemblages. This requires that exceptionally high pressures were attained in the lower continental crust possibly as a consequence of transient subduction during a major plate collision event. The higher pressure/temperature values for the Central Alpine garnet lherzolites are taken to indicate greater depression of the continental plate in that area.

D. A. Carswell & F. G. F. Gibb, Department of Geology, University of Sheffield, Mappin Street, Sheffield S1 3JD, U.K.

There is now general agreement that the common garnet lherzolite xenoliths found in kimberlite pipes are of upper mantle origin but still considerable controversy over the petrogenesis of the rare occurrences of garnet lherzolites directly enclosed within crustal orogenic rock sequences. In Europe such rocks have been described as layers or tectonically bounded lenses within 'alpine-type' peridotite bodies in the Basal Gneiss Region of West Norway (O'Hara & Mercy 1963; Lappin 1966, 1974; Carswell 1968a and b), in the lower Pennine Adula/Cima Lunga Nappe of the Lepontine Belt of the Central Alps (O'Hara & Mercy 1966; Ernst 1978; Evans & Trommsdorff 1978), and in the high grade gneiss basement of the Bohemian Massif in northwest Czechoslovakia (Fiala 1966; Kopecky & Sattran 1966).

Experimental studies of the spinel lherzolite ⇌ garnet lherzolite transition (Green & Ringwood 1967; O'Hara et al. 1971) and previous estimates of the P (pressure)/T (temperature) equilibration conditions of the crustal garnet lherzolites (Table 1) led most authors to interpret these rocks as slices of upper mantle tectonically emplaced into lower crustal gneiss sequences. O'Hara (1967) and Carswell (1974) have demonstrated that these rocks have been derived from shallower depths than most of the garnet lherzolite xenoliths in kimberlites but there remain serious doubts over their exact depth of origin. Further, if an upper mantle origin is to be seriously entertained, viable dynamic processes must be found to explain their solid state movement from previously implied depths of up to about 120 kms into the lower crustal gneisses.

Early P/T estimates (O'Hara 1967; Carswell 1974) for these crustal garnet lherzolites were based on variants of the two pyroxene solvus geothermometer [with reference to the Davis & Boyd (1966) experimental data for the $Mg_2Si_2O_6$ – $CaMgSi_2O_6$ system at 30 Kbars pressure] in combination with the P/T dependent Al_2O_3 isopleths (MacGregor & Ringwood 1964; Green & Ringwood 1967) for garnet–pyroxenes equilibria in the garnet lherzolite stability field. More recently not only have improved experimental calibrations (Nehru & Wyllie 1974; Mori & Green 1976; Lindsley & Dixon 1976; MacGregor 1974) and semi-empirical derivations (Wood & Banno 1973; Wood 1974; Wells 1977) become available for this particular geothermometer/geobarometer combination but additional mineralogical thermometers utilizing other element exchange reactions have been experimentally calibrated (Råheim & Green 1974; Mysen 1976; Mori & Green 1978).

We have developed a Fortran IV computer program (NODMINS) to calculate the P/T equilibration conditions of garnet lherzolites and pyroxenites from analyses of the garnet and coexisting pyroxenes. Temperature calculations based on the various available calibrated element exchange geothermometers are combined

with pressure calculations using equation 12 of Wood (1974) for garnet-orthopyroxene equilibria, with and without his proposed corrections to account for the presence of trivalent cations other than Al. An option to calculate the Fe^{3+} content of these minerals on a charge balance basis is also available as experience has shown that in some eclogite facies assemblages failure to take account of Fe^{3+}, in clinopyroxenes especially, results in clearly anomalous P/T estimates (Carswell & Griffin, in preparation).

Temperature estimates

Previous P/T estimates for Norwegian, Alpine and Czechoslovakian garnet lherzolites are summarized in Table 1 and our new estimates are listed in Table 2.

Early estimates (O'Hara 1967; Carswell 1974) on crustal garnet lherzolites were critically dependent on the two pyroxene solvus data of Davis & Boyd (1966). However, more recent experimental studies of the two pyroxene miscibility gap in the $Mg_2Si_2O_6$ – $CaMgSi_2O_6$ system (Nehru & Wyllie 1974; Mori & Green 1975; Lindsley & Dixon 1976) have indicated that the diopside arm of the solvus is much steeper below about 1200°C than previously indicated and hence the early temperature estimates obtained from this geothermometer are likely to be erroneously high for assemblages which equilibrated below about 1000°C. In addition, pressure dependence of the two pyroxene solvus has now been convincingly demonstrated (Mori & Green 1975; Lindsley & Dixon 1976) but it would appear that below 1000°C any errors introduced through ignoring the pressure effect are likely to be minor compared with the overall level of uncertainty attached to the data.

Of the new temperature values for the crustal garnet lherzolites (Table 2) those obtained by the method of Wood & Banno (1973), which involves a semi-empirical extrapolation of the Davis & Boyd (1966) solvus data, are broadly in line with those previously indicated by Carswell (1974) and are now likewise thought to be too high. Table 2 shows that these values are typically some 100–125°C higher than ones obtained from the preferred calibrations of this geothermometer provided by Wells (1977) and Mori & Green (1978). It is reassuring that the Wells (1977) calibration, based on an updated but similar semi-empirical approach to that pioneered by Wood & Banno (1973) yields temperature values which are closely comparable to those based on the Mori & Green (1978) experimetally determined miscibility gap for coexisting pyroxenes in natural garnet lherzolite assemblages. The Mori & Green (1978) calibration is strictly only valid in the ranges 950–1500°C and 30–40 Kbar and with X_{Fe}^{opx} between 0.04 and 0.13, whilst Wells (1977) applied a straight line best fit to $\ln\left(\frac{a^{Cpx}_{Mg_2Si_2O_6}}{a^{Opx}_{Mg_2Si_2O_6}}\right)$ versus 1/T°K together with a factor to allow for the strong dependence of this partition coefficient on the iron content of the pyroxenes. As variation in $\ln\left(\frac{a^{Cpx}_{Mg_2Si_2O_6}}{a^{Opx}_{Mg_2Si_2O_6}}\right)$ with 1/T°K may in fact be slightly curved (Mori & Green 1978; Evans & Trommsdorff 1978) application of such straight line calibrations could result in systematic errors which could become significant at either end of the experimentally calibrated temperature range.

In view of this and the overall poor sensitivity of the two pyroxene solvus geothermometer below about 1000°C it is clearly important to examine results from other potential mineralogical geothermometers which may be applied to these rocks. For some time now it has been appreciated (e.g. Banno 1970; Carswell 1974) that Fe^{2+}–Mg^{2+} partitioning between coexisting garnets and clinopyroxenes is strongly temperature dependent. The P/T dependence of $K_{D\,Fe-Mg}^{Gnt-Cpx}$ for basaltic rock compositions was calibrated experimentally by Råheim & Green (1974). However, Wood (1976) presented data which strongly indicated that the pressure dependence of $K_{D\,Fe-Mg}^{Gnt-Cpx}$ in ultramafic rock compositions is much smaller than indicated by Råheim & Green (1974) and this has been confirmed by Mori & Green's (1978) experimental calibration of $K_{D\,Fe-Mg}^{Gnt-Cpx}$ in natural garnet lherzolite assemblages in which they were unable to detect any consistent pressure effect over the range 30–40 Kbars.

Application of the Mori & Green (1978) $K_{D\,Fe-Mg}^{Gnt-Cpx}$ calibration to Norwegian and Alpine garnet lherzolites yields equilibration temperatures (Table 2) which are encouragingly close to those obtained by the Wells (1978) and Mori & Green (1978) calibrations of the two pyroxene solvus geothermometer. The correspondence is especially close if only microprobe data are considered. One must beware of the possibility of serious errors in temperatures calculated from

Table 1. Summary of previous pressure/temperature estimates for crustal garnet lherzolites.

West Norway
800–1020°C and 22–37 Kbars – Carswell (1974)
600–700°C and 15–20 Kbars – O'Hara (1967), although Carswell (1974) showed that using the P/T grid of O'Hara (1967) only one Norwegian sample plots in this field, the others yielding
900–1000°C and 35–47 Kbars
Lappin (1974) interpreted eclogites within a peridotite body to be cumulates from melting of the ultramafic rocks which crystallized at 1500–1600°C and 25–28 Kbars and underwent subsequent eclogite facies equilibration at *500–700°C and 17–19 Kbars*. He implied that similar conditions were appropriate for associated garnet lherzolites.

Central Alps (Alpe Arami)
1100°C and 36 Kbars – Carswell (1974)
O'Hara (1967) indicated similar equilibration conditions to the Norwegian garnet lherzolites (*600–700°C and 15–20 Kbars*) but in fact plotting his sample A2 correctly on his P/T grid gives *1200°C and 38 Kbars* for this sample (Carswell 1974).
996 ± 78°C and 40 ± 10 Kbars – Ernst (1978)
800 ± 50°C and >20 Kbars – Evans and Trommsdorff (1978) – samples from Cima di Gagnone and Monte Duria as well as Alpe Arami.

Bohemian Massif
1000–1100°C and 33–34 Kbars – Carswell (1974)

the two pyroxene solvus geothermometer for analyses of bulk mineral separates as our calculations show that contamination of a clinopyroxene separate by only 1% orthopyroxene will result in a positive error of upwards of 50°C in the 700–800°C range.

We should make it clear that the temperatures listed in Table 2 as obtained from the Mori & Green (1978) calibration of $K_{D\,Fe-Mg}^{Gnt-Cpx}$ are based on the assumption that all iron is ferrous in both minerals. This was done in order to be consistent in the treatment of both microprobe and mineral separates analytical data. Unfortunately charge balance calculation of $Fe^{3+}/Fe^{2+}+Fe^{3+}$ for microprobe analyses of garnets and pyroxenes yields unrealistically high ratios for these minerals in most garnet lherzolites. As wet chemical analyses show that the clinopyroxenes in eclogite facies assemblages typically have higher $Fe^{3+}/Fe^{2+}+Fe^{3+}$ ratios than coexisting garnets, these calculated temperatures should be viewed strictly as maximum values for this particular method. Excluding analytically determined Fe^{3+} from the $K_{D\,Fe-Mg}^{Gnt-Cpx}$ calculation for analyses of mineral separates lowers the mean temperature from 730°C to 680 ± 39°C for eleven Norwegian garnet lherzolite samples and gives 824°C as opposed to 887°C for the one Alpine sample for which mineral separates have been analysed.

The experimentally calibrated coefficient for Al^{VI} – Cr partitioning between coexisting pyroxenes (Mysen 1976) is another potentially useful geothermometer which may be applied to garnet lherzolite assemblages. For the Norwegian and Alpine examples it yields mean temperatures (Table 2) which are reasonably close to those obtained by the favoured methods discussed above, although values for individual samples tend to be rather more variable.

From the above considerations of these various geothermometers the 'best' estimates for the equilibration temperatures of the Norwegian and Alpine garnet lherzolites appear to be within the ranges 734–776°C and 836–893°C respectively. The fact that four independent calibrations of various element exchange reactions yield reasonably close temperatures encourages us to think that these values are geologically meaningful. Certainly there seems little doubt about the higher equilibration temperatures of the garnet lherzolites in the Central Alps as compared with those in the West Norway Basal Gneiss Region.

The situation regarding the equilibration temperatures of the garnet lherzolites in the Bohemian Massif is, however, confused. Data are currently available on mineral separates from only two samples and these yield quite inconsistent temperature estimates (Table 2) by the various geothermometers. It is difficult to decide whether analytical, contamination or disequilibrium factors are responsible but it is clear that further analytical data are required on these rocks before any of the temperature estimates on the Czechoslovakian garnet lherzolites can be accepted with any conviction.

Table 2. New pressure/temperature estimates for crustal garnet lherzolites.

			T,°C Wells (1977)	P,Kbars Wood (1974)	T,°C Mori & Green (1978) Two pyroxene Solvus	P,Kbars Wood (1974)	T,°C Wood & Banno (1973)	P,Kbars Wood (1974)	T,°C Mysen (1976)	P,Kbars Wood (1974)	T,°C Mori & Green (1978) $K_{D_{Fe-Mg}}^{Gnt-Cpx}$	P,Kbars Wood (1974)	T,°C Range of preferred Values	P,Kbars Range of preferred Values
West Norway	Probe and mineral separate analyses	$\bar{X}$	759	22.1	776	23.1	880	29.2	738	21.1	734	20.7		
	$n = 15$	σ n	105	7.5	114	7.8	100	8.0	106	8.7	54	4.2		
	Probe analyses only	$\bar{X}$	742	24.8	750	25.3	875	33.0	677	21.0	747	25.3	734–776	20.7–23.1
	$n = 4$	σ n	77	5.0	85	5.5	71	4.7	132	12.1	53	3.6		
	Analyses of mineral separates only	$\bar{X}$	765	21.1	786	22.4	882	27.9	758	21.2	730	19.0		
	$n = 11$	σ n	112	8.0	122	8.3	109	8.4	88	7.2	54	2.8		
Central Alps	Probe analyses only	$\bar{X}$	836	29.4	854	30.4	959	36.9	893	33.0	846	29.9		
	$n = 6$	σ n	27	1.6	29	1.7	25	1.7	121	9.2	50	3.1		
	Analyses of mineral separates $n = 1$		989	30.3	1029	32.4	1088	35.6	696	14.4	887	24.7	836–893	29.4–33.0
Bohemian Massif	Analyses of mineral separates	Sample 1	749	20.6	765	21.5	872	27.7	1048	37.8	1036	37.1	?	?
		Sample 2	998	28.8	1046	31.3	1086	33.4	680	12.1	1071	32.7		

Details of calculation methods employed are given in the text. Sources of data: Lappin (1962); O'Hara & Mercy (1963); Fiala (1966); Carswell (1968a, b, 1973 & unpublished data); Ernst (1978) and Evans & Trommsdorff (1978).

Pressure estimates

At present the only experimentally calibrated geobarometer applicable to garnet lherzolites is that based on the Al_2O_3 contents of orthopyroxenes coexisting with garnets. Hence the equilibration pressures presented in this work were calculated using equation (12) of Wood (1974): a semi-empirical expression derived for this geobarometer primarily from the experimental data of MacGregor (1974) for orthopyroxene-garnet equilibria in the MgO-Al_2O_3-SiO_2 system.

It is important to appreciate that X_{VI}^{VI} in orthopyroxene coexisting with garnet is both pressure and temperature dependent. Thus any errors in the initial temperature estimates will be compounded in the calculated pressures.

The pressures listed in Table 2 were calculated with X_{VI}^{VI} in orthopyroxene fixed as half the number of aluminium atoms present. Taking into account substitution of Cr for Al in the octahedral sites in both orthopyroxenes and garnets, in the manner suggested by Wood (1974), slightly lowers the pressure estimates in the majority of cases. However, the decrease is small (generally < 1 Kbar) compared to the overall uncertainty which we feel should be attached to these pressure estimates. No correction has been applied for substitution of Al^{3+} by Fe^{3+} because of uncertainties over the Fe^{3+} contents in these minerals. If significant amounts of Fe^{3+} do in fact occur in the garnets, then calculated pressures would be lowered slightly further.

Certainly we have much less confidence in these pressure estimates than we have in the temperature values. A major source of concern and possible error stems from the high Cr/Cr + Al ratios in most of the garnet lherzolites. The experimental data of MacGregor (1970) and petrographic observations related to whole rock compositions (e.g. Carswell et al. 1979) clearly indicate that variations in Cr/Cr + Al profoundly affect garnet-pyroxene-spinel equilibria. Indeed it seems likely in reality that between the stability fields of spinel lherzolite and garnet lherzolite (O'Hara et al. 1971) there is a five phase garnet-spinel lherzolite field the width of which may be expected to increase with increasing Cr/Cr + Al ratio (MacGregor 1970). Thus further experimental data on garnet-orthopyroxene equilibria in the system MgO-Al_2O_3-Cr_2O_3-SiO_2 are necessary before more reliable pressure estimates can be obtained for these natural garnet lherzolite assemblages.

Petrogenetic considerations

The higher calculated equilibration pressures for the garnet lherzolites from the Central Alps region compared to those from West Norway mainly reflect the higher temperature estimates entered into the pressure calculation equation. The mean value of 0.017 ± 0.005 for X_{VI}^{VI} in orthopyroxene from the Alpine garnet lherzolites is not appreciably lower than the corresponding mean value of 0.020 ± 0.006 in orthopyroxenes from the Norwegian samples. As isopleths for X_{VI}^{VI} in orthopyroxene in equilibrium with garnet are essentially sub-parallel to expected geotherms (Fraser & Lawless 1978; Carswell 1978) it is therefore possible to interpret the Alpine garnet lherzolites simply as having equilibrated at slightly deeper levels than the Norwegian garnet lherzolites on a similar geotherm – indeed a geotherm (Fig. 1) fairly closely approximated by the shield geotherm of Clark & Ringwood (1964).

In Fig. 1 calculated P/T equilibration conditions for individual crustal garnet lherzolite samples are shown and compared with the values obtained for garnet lherzolite xenoliths in Lesotho kimberlites using the same calculation methods (data from Carswell & Dawson 1970; Cox et al. 1973; Nixon & Boyd 1973; Dawson & Smith 1975; Carswell et al. 1979). For Fig. 1A temperatures were calculated from the $K_{D_{Fe-Mg}}^{Gnt-Cpx}$ calibration of Mori & Green (1978), whilst for Fig. 1B temperatures were calculated from the Wells (1977) 'best fit' calibration of the two pyroxene solvus geothermometer. For both plots pressure values are uncorrected for substitution of Al by Cr in orthopyroxenes and garnets and all iron has been assumed to be divalent in garnet and pyroxenes.

We prefer the P/T values of Fig. 1A to those of Fig. 1B because of the smaller range of values indicated for the Norwegian garnet lherzolites and the contrastingly wider range of values indicated for the kimberlite xenoliths – extending as it does from uppermost mantle depths down into the diamond stability field for certain xenoliths, although admittedly the diamond bearing garnet lherzolite xenolith reported by Dawson & Smith (1975) still plots just outside the diamond stability field of Bundy et al. (1961). However, as discussed earlier, we do have reservations about the accuracy of the pressure estimates, in particular for rocks with high Cr/Cr + Al ratios. It should also be borne in mind that, since the $K_{D_{Fe-Mg}}^{Gnt-Cpx}$ values used to calculate the temperatures for Fig. 1A are based on the assumption of all iron as Fe^{2+}, one could justifiably argue that these temperature values (and hence, in turn, the pressure values) should all be slightly lower, if the higher $Fe^{3+}/Fe^{2+} + Fe^{3+}$ ratios of clinopyroxenes relative to garnets determined on mineral separates from Norwegian samples holds in general.

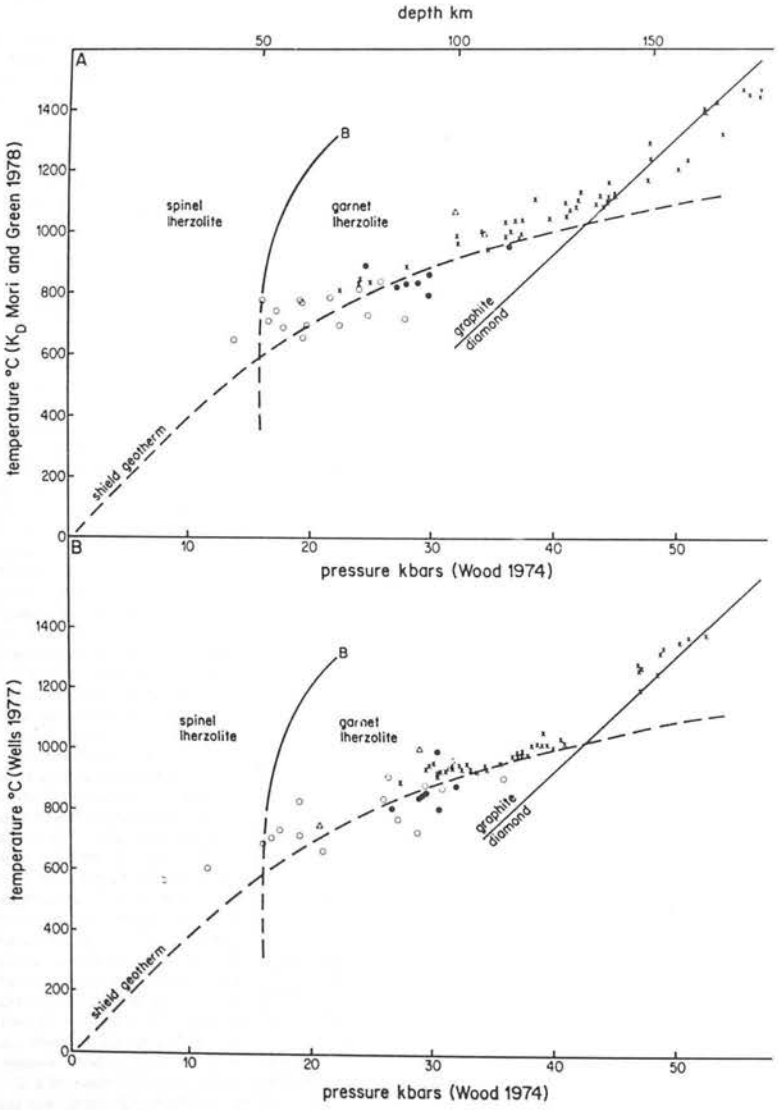

Fig. 1. Pressure/Temperature diagram showing estimates of equilibration conditions for garnet lherzolites from West Norway (open circles), Central Alps (closed circles), Bohemian Massif (triangles) and kimberlites (crosses). References to data sources are given in the text as are descriptions of the calculation methods used to obtain the different temperature values for plots A and B. The diamond/graphite inversion curve is from Bundy et al. (1961) and the Precambrian shield geotherm from Clark & Ringwood (1964). Curve B is the experimentally determined spinel lherzolite/garnet lherzolite boundary for natural materials from O'Hara et al. (1971).

The wide ranges of equilibration conditions indicated in Fig. 1 for both West Norway and Central Alpine garnet lherzolites require comment. For Norwegian samples the range shown in Fig. 1B is particularly wide in comparison with that in Fig. 1A but this is almost certainly due to the extreme sensitivity of the two pyroxene solvus temperatures to analytical errors and cross-contamination of the mineral separates. However, a further explanation has to be sought for the sizable spread of P/T values still indicated on Fig. 1A. There is a close geographic and geotectonic association of sample localities in both regions and considerable variation is apparent even for samples from the same localities. For example, the highest P/T point for an Alpine garnet lherzolite is for a sample from the same locality (Alpe Arami) as samples for four of the other points.

Textural evidence in both the Norwegian and Alpine garnet lherzolites indicates that the rocks have had a complex history of deformation and recrystallization. Variable degrees of recrystallization and re-equilibration during tectonic emplacement up into their present crustal environment could therefore account for much of the apparent variation in P/T estimates for closely associated samples. Certainly porphyroclastic textures are particularly in evidence amongst the Norwegian garnet lherzolite samples and a detailed microprobe study of the relationships between mineral chemistry and the various deformation fabrics in these rocks seems called for.

Microprobe analyses used to obtain the P/T values listed in Table 2 and plotted in Fig. 1 were all made on the central parts of grains. Comparison with microprobe analyses of clinopyroxene grain rims (Evans & Trommsdorff 1978) in three Alpine garnet lherzolite samples suggest the presence of retrograde zoning as evidenced by increased $K_D^{\frac{Gnt-Cpx}{Fe-Mg}}$ values. The mean temperature calculated for these rim analyses from the Mori & Green (1978) calibration of $K_D^{\frac{Gnt-Cpx}{Fe-Mg}}$ is 702 ± 39°C, some 144°C lower than the mean value based on microprobe analyses of grain cores.

In the light of the foregoing analysis of the various P/T estimates it is appropriate to consider just what conclusions can now be drawn concerning the ultimate origin and site of equilibration of these crustal garnet lherzolites.

It must be re-emphasized that these garnet lherzolite assemblages occur as rare layers or tectonically disrupted lenses within larger bodies of garnet free peridotite. Field relationships and geochemical considerations (O'Hara & Mercy 1963; Mercy & O'Hara 1965; Carswell 1968a, b) suggest that the garnet lherzolites are endogenous to these peridotite bodies and hence that the peridotite masses as a whole must have undergone the same tectonic and metamorphic history. The peridotite masses themselves have tectonic contacts against their enclosing gneisses. No thermal metamorphism of the adjacent rocks by the peridotites has ever been noted although tectonically disrupted selvages of zoned metasomatic reaction rinds are sometimes in evidence (Brueckner 1975). The main point of controversy concerns the extent of possible tectonic transport of the peridotite masses through the enclosing gneisses and whether the garnet lherzolite assemblages developed before or after these masses came into contact with the enveloping gneisses.

In the case of the Alpe Arami garnet lherzolite body in the Alps, Ernst (1978) has argued in favour of a sub-continental upper mantle derivation from depths approaching 150 kilometres on the basis of equilibration conditions estimated to be 966 ± 78°C and 40 ± 10 Kbars although, as he admitted, the mechanism and driving force of the process required to account for the proposed solid state rise of this peridotite mass through a considerable thickness of the upper mantle and then its tectonic emplacement into the old Lepontine sialic crust of the European lithospheric plate are obscure. Even if a suitable dynamic model can be conceived we find it difficult to envisage just how such solid state movement could be accomplished without attendant recrystallization and re-equilibration. Our analysis of the various P/T estimates for garnet lherzolites from the three reported localities in the Central Alps (including Alpe Arami) leads us to conclude that the 'best' estimates are within the range 836–893°C and 29.4–33.0 Kbars. These estimates are more in line with the values of 800 ± 50°C and > 20

Kbars deduced by Evans & Trommsdorff (1978) and suggest that the P/T estimates and implied depths of origin given by Ernst (1978) are excessive.

In marked contrast to the petrogenetic model of Ernst (1978), Evans & Trommsdorff (1978) have proposed that the Central Alpine peridotite bodies containing the garnet lherzolites have undergone prograde metamorphism in a subduction zone environment from ophiolitic ultramafic bodies which, at least at the Cima di Gagnone locality, had suffered early serpentinization. Unfortunately their microprobe analyses of the garnet lherzolite minerals show evidence of retrograde rather than prograde zoning. However, this does not in itself rule out their petrogenetic model if it is accepted that complete equilibration at the peak of the progressive metamorphism during subduction was followed by limited re-equilibration of the garnet lherzolite assemblage during subsequent uprise into a lower P/T environment. Evans & Trommsdorff (1978) in fact interpreted the garnet lherzolite assemblages as having predated and hence having survived the metamorphic 'high' in the surrounding gneisses – indicated as having taken place at 600–700°C and very much lower pressures. Thus they still found it necessary to advocate tectonic emplacement of the peridotite masses up into their present envelope of gneisses after the development of the garnet lherzolites, although the distances involved would obviously be much less than those envisaged by Ernst (1978).

The petrogenetic interpretation of the West Norway garnet lherzolites is certainly no less controversial and is best viewed in the light of the long running debate over the formation of the common metabasic eclogites occurring as boudins within the gneisses in this region. Advocates of an 'in situ' crustal metamorphic origin of these eclogites (Bryhni et al. 1970; Mysen & Heier 1972; Krogh 1977; Bryhni et al. 1977) have emphasized the striking prograde zoning observed in certain eclogites, the likely metasedimentary origin of some of the eclogites, corona development of eclogite assemblages from original low pressure assemblages in metaigneous rocks, and that the deduced P/T conditions of formation for these eclogites (which according to Krogh (1977) show a systematic regional variation from ~8 Kbars and 300°C to ~22 Kbars and 800°C) are not inconsistent with appropriate stability conditions for the early high grade assemblages in the enclosing gneisses (Green & Mysen 1972; Mysen & Heier 1972). The pressures necessary for formation of both the eclogites and gneiss assemblages were envisaged by Krogh (1977) as having been attained during partial subduction of a plate of continental crust during a major continent-continent collision event. On the other hand, Lappin (1974, 1977) and Lappin & Smith (1978) have argued strongly in favour of initial eclogite facies equilibration at mantle depths (in some cases exceeding 100 kilometres) of orthopyroxene eclogites enclosed both directly within gneisses and within one of the peridotite bodies. By implication the peridotite masses, including the garnet lherzolite layers or lenses, had the same deep level mantle origin. These rocks were envisaged to have subsequently been tectonically emplaced up into the continental gneiss environment by obduction-type processes during plate collisions.

Contrasting P/T equilibration estimates have, however, led one of us (Carswell 1974) to propose earlier a dual origin for the West Norway eclogite facies rocks, with the peridotite bodies (together with their enclosed garnet lherzolites and eclogites) interpreted as being of mantle derivation whilst the eclogites directly enclosed within the gneisses were believed to have been formed essentially in situ in a deep crustal gneiss environment. Support for this view came from Brueckner (1977), who presented Sr isotopic evidence for separate origins for these two groups of rocks. It should be pointed out, however, that the previous contrasting P/T estimates on these two groups of eclogite facies rocks were based on different methods applied to contrasting rock compositions.

In this paper we have shown that recent refinements to the methods used to obtain P/T estimates for garnet lherzolites result in revised values of 734–776°C and 20.7–23.1 Kbars for the Norwegian samples; values which are significantly different to those indicated by Carswell (1974). Allowing realistic margins for errors, these P/T conditions overlap the upper end of the range of values given by Krogh (1977) for the eclogites directly enclosed in the gneisses. It is particularly significant that application of the same P/T calculation methods to identical eclogite facies assemblages both within and external to peridotite bodies yields closely similar values (Carswell, in preparation). Thus it appears increasingly likely that the final equilibration of the garnet lherzolite assemblages took place in the same P/T environment as that responsible for the formation of the eclogite facies assemblages in the gneisses and that such conditions were attained in a lower crustal gneiss environment, possibly near the base of a continental crustal plate depressed to unusually deep levels during a major plate collision event. Such a petrogenetic model does not exclude the possibility that the peridotite masses were initially derived as tectonic slices of the underlying mantle but it does require that any tectonic transport and interleaving of crustal and mantle rocks was effectively accomplished *before* the equilibration of the present garnet lherzolite assemblages.

Whilst we accept that there is strong evidence that certain of the West Norway eclogites directly enclosed in gneisses have undergone a prograde metamorphic history from original sediments, it is equally clear that the occasional preservation of exsolution textures in pyroxenes (Carswell 1968a, 1973; Lappin 1974; Lappin & Smith 1978), especially in garnet pyroxenites enclosed both within the peridotite masses and directly in the gneisses, indicates an initial high temperature igneous origin in these instances. The pressures, and hence depths, at which this igneous crystallization is considered to have taken place depends on the role ascribed to garnet. If garnet is judged to have been a liquidus phase, high pressure (30–40 Kbars), deep mantle crystallization is indicated (Carswell 1973; Lappin & Smith 1978) but the evidence is somewhat ambiguous. Hence the possibility that these garnet pyroxenites developed through exsolution from cumulates of aluminous pyroxenes which crystallized directly from basaltic magmas which were intruded towards the base of a thickened continental crust prior to the main eclogite facies equilibration cannot be excluded. Further whole rock composition data are necessary before we can be certain whether in particular instances initial igneous crystallization processes taking place at upper or lower crustal or even mantle depths were responsible for observed chemical and mineralogical variations (Carswell 1968a, b; Mysen & Heier 1972). Nevertheless at this stage it seems probable that the various eclogite facies assemblages in the West Norway Basal Gneiss Region have developed in rocks which have had multifarious origins.

Returning to the specific question of the petrogenesis of the garnet lherzolites we feel that the revised P/T equilibration estimates which we have presented for both Norwegian and Alpine occurrences go some way towards clarifying the present confused picture. Certainly, in contrast to most previous estimates, these new lower P/T estimates are more in line with conditions which can reasonably be expected to occur either towards the base of a continental crustal plate depressed during plate collisions or in the uppermost sub-continental mantle. Geochemical considerations (e.g. Carswell 1968a, b) lead us to conclude that in all probability these garnet lherzolite bearing peridotite bodies were initially of upper mantle origin and have been tectonically interleaved with lower crustal gneisses during plate collision processes. However we stress that in West Norway, and possibly also in the Central Alps region, the final equilibration of the garnet lherzolite assemblages most likely occurred after emplacement of the peridotite bodies into the lower continental crust and hence that the surrounding gneisses were also subjected to similar load pressure and temperature conditions to those necessary for garnet lherzolite formation. Such an interpretation avoids the serious dynamic problems inherent in previous petrogenetic models.

Finally we note that the P/T equilibration estimates for garnet lherzolites in both the West Norway and Central Alps regions lie on similar continental type geotherms but that the higher P/T conditions estimated for the Alpine garnet lherzolites indicates equilibration at a deeper level perhaps due to greater depression of the continental plate in that area.

Acknowledgements. – D. A. Carswell wishes to acknowledge financial support for fieldwork in West Norway from the Natural Environmental Research Council and the University of Sheffield. We both wish to thank L. G. Medaris, Jr. for his review and helpful comments on the manuscript.

References

Banno, S. 1970: Classification of eclogites in terms of physical conditions of their origin. *Phys. Earth Planet. Inter. 3*, 405–421.

Brueckner, H. K. 1975: Contact and fracture ultramafic assemblages from Norway: Rb-Sr evidence for crustal contamination. *Contrib. Mineral. Petrol. 49*, 39–48.

Brueckner, H. K. 1977: A crustal origin for eclogites and a mantle origin for garnet peridotites: strontium isotopic evidence from clinopyroxenes. *Contrib. Mineral. Petrol. 60*, 1–15.

Bryhni, I., Green, D. H., Heier, K. S. & Fyfe, W. S. 1970: On the occurrence of ecologite in western Norway. *Contrib. Mineral. Petrol. 26*, 12–19.

Bryhni, I., Krogh, E. & Griffin, W. L. 1977: Crustal derivation

of Norwegian eclogites: a review. *Neues Jahrb. Mineral. Abh. 130*, 49–68.

Bundy, F. R., Bovenkerk, H. P., Strong, H. M. & Wentorf, R. H. Jr. 1961: Diamond graphite equilibrium line from growth and graphitisation of diamond. *J. Chem. Phys. 35*, 383–391.

Carswell, D. A. 1968a: Picritic magma-residual dunite relationships in garnet peridotite at Kalskaret, near Tafjord, south Norway. *Contrib. Mineral. Petrol. 19*, 97–124.

Carswell, D. A. 1968b: Possible primary upper mantle peridotite in Norwegian basal gneiss. *Lithos 1*, 322–355.

Carswell, D. A. 1973: Garnet websterite nodule within layered garnet peridotite. *Earth Planet. Sci. Lett. 20*, 347–352.

Carswell, D. A. 1974: Comparative equilibration temperatures and pressures of garnet lherzolites in Norwegian gneisses and in kimberlite. *Lithos 7*, 113–121.

Carswell, D. A. 1978: Palaeogeotherms: implications of disequilibrium in garnet lherzolite xenoliths. *Nature 276*, 737.

Carswell, D. A. & Dawson, J. B. 1970: Garnet peridotite xenoliths in South African kimberlite pipes and their petrogenesis. *Contrib. Mineral. Petrol. 25*, 163–184.

Carswell, D. A., Clarke, D. B. & Mitchell, R. H. 1979: The petrology and geochemistry of ultramafic nodules from Pipe 200, northern Lesotho. *Proceedings 2nd Inter. Kimberlite Conference*, Vol. 2, 127–144. Am. Geophys. Union.

Clark, S. P., Jr. & Ringwood, A. E. 1964: Density distribution and constitution of the mantle. *Rev. Geophys. 2*, 35–88.

Cox, K. G., Gurney, J. J. & Harte, B. 1973: Xenoliths from the Matsoku Pipe, pp. 76–92 in Nixon, P. H. (ed.), *Lesotho Kimberlites*, Lesotho National Devel. Corp. Maseru, Lesotho.

Davis, B. T. C. & Boyd, F. R. 1966: The join $Mg_2Si_2O_6$ – $CaMgSi_2O_6$ at 30 kilobars pressure and its application to pyroxenes from kimberlites. *J. Geophys. Res. 71*, 3567–3576.

Dawson, J. B. & Smith, J. V. 1975: Occurrence of diamond in mica-garnet lherzolite xenolith from kimberlite. *Nature 254*, 580–581.

Ernst, W. G. 1978: Petrochemical study of lherzolitic rocks from the Western Alps. *J. Petrol. 19*, 341–392.

Evans, B. W. & Trommsdorff, V. 1978: Petrogenesis of garnet lherzolite, Cima di Gagnone, Lepontine Alps. *Earth Planet. Sci. Lett. 40*, 333–348.

Fiala, J. 1966: The distribution of elements in mineral phases of some garnet lherzolites from the Bohemian Massif. *Krystalinikum 4*, 31–53.

Fraser, D. G. & Lawless, P. J. 1978: Palaeogeotherms: implications of disequilibrium in garnet lherzolite xenoliths. *Nature 273*, 220–222.

Green, D. H. & Mysen, B. O. 1972: Genetic relationship between eclogite and hornblende + plagioclase pegmatite in western Norway. *Lithos 5*, 147–161.

Green, D. H. & Ringwood, A. E. 1967: The stability fields of aluminous pyroxene peridotite and garnet peridotite and their relevance in upper mantle structure. *Earth Planet. Sci. Lett. 3*, 151–160.

Kopecky, L. & Sattran, V. 1966: Buried occurrences of pyrope-peridotite and the structure of the crystalline basement in the extreme southwest of the Ceske Stredohori mountains. *Krystalinikum 4*, 65–86.

Krogh, E. J. 1977: Evidence of Precambrian continent-continent collision in Western Norway. *Nature 267*, 17–19.

Lappin, M. A. 1962: The eclogites, dunites and anorthosites of the Selje and Almklovdalen districts, Nordfjord, S.W. Norway. Unpublished Ph.D. thesis University of Durham (Kings College).

Lappin, M. A. 1966: The field relationships of basic and ultrabasic masses in the basal gneiss complex of Stadtlandet and Almklovdalen, Nordfjord, Southwestern Norway. *Nor. Geol. Tidsskr. 46*, 439–496.

Lappin, M. A. 1974: Eclogites from the Sunndal-Grubse ultramafic mass, Almklovdalen, Norway and the T-P history of the Almklovdalen masses. *J. Petrol. 15*, 567–601.

Lappin, M. A. 1977: Crustal and in situ origin of Norwegian eclogites. *Nature 269*, 730.

Lappin, M. A. & Smith, D. C. 1978: Mantle-equilibrated orthopyroxene eclogite pods from the Basal Gneisses in the Selje District, Western Norway. *J. Petrol. 19*, 530–584.

Lindsley, D. H. & Dixon, S. A. 1976: Diopside-enstatite equilibria at 850° to 1400°C, 5 to 35 Kb. *Am. J. Sci. 276*, 1285–1301.

MacGregor, I. D. 1970: The effect of CaO, Cr_2O_3, Fe_2O_3 and Al_2O_3 on the stability of spinel and garnet peridotites. *Phys. Earth Planet. Int. 3*, 372–377.

MacGregor, I. D. 1974: The system MgO-Al_2O_3-SiO_2: solubility of Al_2O_3 in enstatite for spinel and garnet peridotite compositions. *Am. Mineral. 59*, 110–119.

MacGregor, I. D. & Ringwood, A. E. 1964: The natural system enstatite-pyrope. *Carnegie Inst. Wash. Yearb. 63*, 161–163.

Mercy, E. L. P. & O'Hara, M. J. 1965: Chemistry of some garnet-bearing rocks from South Norwegian peridotites. *Nor. Geol. Tidsskr. 45*, 323–332.

Mori, T. & Green, D. H. 1975: Pyroxenes in the system $Mg_2Si_2O_6$ – $CaMgSi_2O_6$ at high pressure. *Earth Planet. Sci. Lett. 26*, 277–286.

Mori, T. & Green, D. H. 1976: Subsolidus equilibria between pyroxenes in the CaO-MgO-SiO_2 system at high pressures and temperatures. *Am. Mineral. 61*, 616–625.

Mori, T. & Green, D. H. 1978: Laboratory duplication of phase equilibria observed in natural garnet lherzolites. *J. Geol. 86*, 83–97.

Mysen, B. O. 1976: Experimental determination of some geochemical parameters relating to conditions of equilibration of peridotite in the upper mantle. *Am. Mineral. 61*, 677–683.

Mysen, B. O. & Heier, K. S. 1972: Petrogenesis of eclogites in high grade metamorphic gneisses, exemplified by the Hareidland eclogite, western Norway. *Contrib. Mineral. Petrol. 36*, 73–94.

Nehru, C. E. & Wyllie, P. J. 1974: Electron-microprobe measurement of pyroxenes coexisting with H_2O undersaturated liquid in the join $CaMgSi_2O_6$ – $Mg_2Si_2O_6$-H_2O, at 30 kilobars with application to geothermometry. *Contrib. Mineral. Petrol. 48*, 221–228.

Nixon, P. H. & Boyd, F. R. 1973: Petrogenesis of the granular and sheared ultrabasic nodule suite in kimberlites, pp. 48–56 in Nixon, P. H. (ed.), *Lesotho Kimberlites*, Lesotho National Devel. Corp. Maseru, Lesotho.

O'Hara, M. J. 1967: Mineral parageneses in ultrabasic rocks, pp. 393–403 in Wyllie, P. J. (ed.), *Ultramafic and Related Rocks*, J. Wiley, New York.

O'Hara, M. J. & Mercy, E. L. P. 1963: Petrology and petrogenesis of some garnetiferous peridotites. *Trans. Roy. Soc. Edinb. 65*, 251–314.

O'Hara, M. J. & Mercy, E. L. P. 1966: Garnet peridotite and eclogite from Bellinzona, Switzerland. *Earth Planet. Sci. Lett. 1*, 295–300.

O'Hara, M. J., Richardson, S. W. & Wilson, G. 1971: Garnet peridotite stability and occurrence in crust and mantle. *Contrib. Mineral. Petrol. 32*, 48–68.

Råheim, A. & Green, D. H. 1974: Experimental determination of the temperature and pressure dependence of the Fe-Mg partition coefficient for coexisting garnet and clinopyroxene. *Contrib. Mineral. Petrol. 48*, 179–203.

Wells, P. R. A. 1977: Pyroxene thermometry in simple and complex systems. *Contrib. Mineral. Petrol. 62*, 129–139.

Wood, B. J. 1974: Solubility of alumina in orthopyroxene coexisting with garnet. *Contrib. Mineral. Petrol. 46*, 1–15.

Wood, B. J. 1976: The partitioning of iron and magnesium between garnet and clinopyroxene. *Carnegie Inst. Wash. Yearb. 75*, 571–574.

Wood, B. J. & Banno, S. 1973: Garnet-orthopyroxene and orthopyroxene-clinopyroxene relationships in simple and complex systems. *Contrib. Mineral. Petrol. 42*, 109–142.

Accepted for publication June 1979
Printed January 1980

Clarification of the petrology and occurrence of garnet lherzolites, garnet websterites and eclogite in the vicinity of Rødhaugen, Almklovdalen, West Norway

DENNIS ANTHONY CARSWELL

Carswell, D. A.: Clarification of the petrology and occurrence of garnet lherzolites, garnet websterites and eclogite in the vicinity of Rødhaugen, Almklovdalen, west Norway. *Norsk Geologisk Tidskrift*, Vol. 61, pp. 249–260. Oslo 1981. ISSN 0029-196X.

Re-examination of the so-called Rødhaugen eclogite specimens analysed by Eskola (1921) and Mercy & O'Hara (1965), together with new field observations, demonstrate that these specimens were not petrographically analogous nor from precisely the same locality. Eskola apparently overlooked the presence of appreciable orthopyroxene in his specimen. New microprobe mineral analyses are presented both for these earlier specimens and for a further suite of eight associated garnet lherzolite, garnet websterite and eclogite samples from the Rødhaugen area. The petrogenesis and tectono-metamorphic evolution of these rocks are discussed with reference to the differing compositions of porphyroclast cores and rims, and recrystallised matrix grains. New pressure/temperature equilibration estimates for these assemblages are taken to indicate that these rocks shared a common eclogite facies metamorphic event with the surrounding eclogite bearing gneiss complex.

D. A. Carswell, Department of Geology, University of Sheffield, Mappin Street, Sheffield S1 3JD, England.

In his classic early paper on the eclogites of Norway, Eskola (1921) described and presented chemical analyses for co-existing garnet and clinopyroxene in an eclogite from within one of the large peridotite masses in Almklovdalen near Åheim in Sunnmøre. He made it clear that his analysed specimen, previously unnumbered but hereon referred to as sample ESK 75, was from the collection in the Mineralogisk-Geologisk Museum at Oslo and was simply labelled 'Almklovdalen'. However, comparison with specimens which he later collected himself convinced him that it was from the hill called Rødhaugen about 500 metres to the north-east of Hellebust (Fig. 1). According to Eskola this eclogite contained rounded 'phenocrysts' of a pyropic garnet and a diopsidic pyroxene set in an evenly granular millimetre-sized groundmass of the same pyroxene. Small amounts of pale green amphibole were noted at the contacts between garnet and clinopyroxene and traces of chlorite and rutile were also observed. From the measured specific gravity of the rock, Eskola calculated a mode which he then used to calculate a bulk rock chemical composition for this eclogite from the garnet and pyroxene analyses (see Table 2). In his Fig. 5, Eskola sketched the Rødhaugen eclogite as occuring as 5–70 cm wide bands within olivine-rock which sometimes contains garnets and calcic pyroxenes as in the eclogite.

In their much later papers on Norwegian garnetiferous peridotites, O'Hara & Mercy (see both O'Hara & Mercy 1963 and Mercy & O'Hara 1965) presented petrographic data and a bulk rock analysis of what was claimed to be a petrographically similar porphyroclastic textured garnet-chrome diopside rock (field no. N75). They likewise indicated the locality for this rock to be at Rødhaugen within the Eikremsæter peridotite mass in Almklovdalen and implied that this was essentially the same eclogite as studied by Eskola. However, they did observe that their analysed eclogite sample was appreciably more ferriferous and must have contained a more sodic clinopyroxene than Eskola's Rødhaugen eclogite.

In order to resolve this confusion over the so-called Rødhaugen eclogite, it seemed desirable to undertake a reinvestigation of the samples analysed by these earlier workers in the light of my own field observations of the garnetiferous rocks within the Eikremsæter peridotite mass on, and in the vicinity of, the hill called Rødhaugen. It is apparent from this study that not only were the Eskola and O'Hara & Mercy

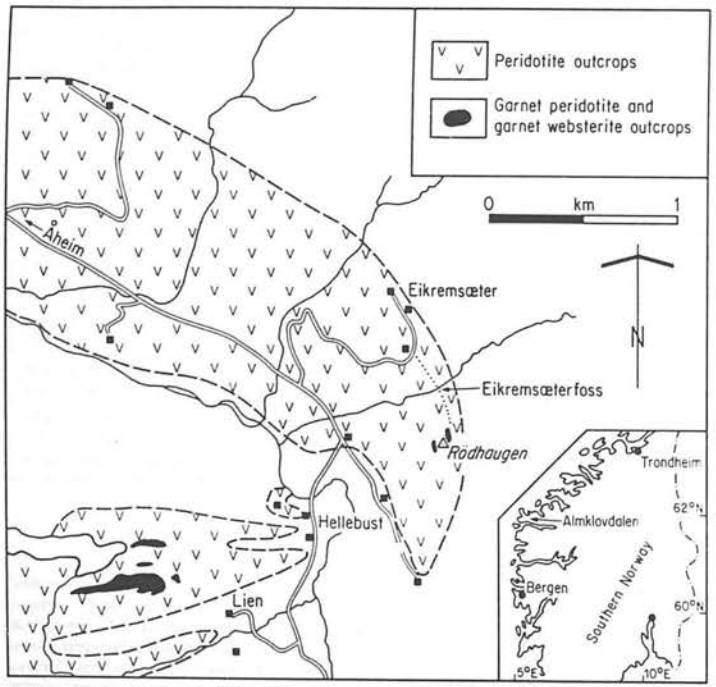

Fig. 1. Geological sketch map showing the locality for the analysed eclogite samples in relation to the garnet peridotite and garnet websterite outcrops in the Rødhaugen and Lien areas of Almklovdalen.

samples not identical petrographically, as well as chemically, but that they cannot have come from the same locality.

Field locations and petrography

It is now clear that the O'Hara & Mercy sample N75, though a true eclogite, did not come from the outcrops on the flanks of Rødhaugen but rather from a locality, perhaps best referred to as Eikremsæterfoss, about 250 metres north of Rødhaugen (see Fig. 1). Here a 130 cm wide lens of eclogite is exposed within chloritic peridotite on the eastern bank of a minor stream just below a small waterfall and above the rough track from Eikremsæter to Rødhaugen.

The eclogite at Eikremsæterfoss is indeed an essentially bimineralic red garnet-green clinopyroxene rock except for traces of both rutile and sulphide and the development of increasing amounts of secondary darker green amphibole towards the contact with the adjacent peridotite. Much of this eclogite is of relatively uniform grain-size with garnets 3–5 mm across and slightly smaller clinopyroxenes. However, it has a strikingly porphyroclastic texture in places, especially in pyroxene rich portions, with large strained clinopyroxene porphyroclasts up to 1 cm in length, set in a mosaic of strain-free recrystallised 0.3–0.5 mm sized clinopyroxenes.

TABLE 1 MODAL ANALYSES (VOL. %) OF ANALYSED SAMPLES

SAMPLE NUMBER	ROCK TYPE	% OLIVINE	% ORTHOPYROXENE	% CLINOPYROXENE	% GARNET	% AMPHIBOLE	% CHLORITE
A41	Eclogite	-	-	32	56	12	-
A84	Eclogite	-	-	67	26	7	-
ESK 75	Garnet Websterite	-	10	56	26	8	-
A33	Garnet Websterite	-	21	25	36	16	-
A49	Garnet Websterite	-	26	22	14	38	-
A6	Garnet Lherzolite	41	11	14	21	13	-
A7A	Garnet Lherzolite	47	9	19	17	8	-
A7B	Garnet Lherzolite	25	18	15	26	16	-
ESK 76	Garnet Lherzolite	17	22	21	32	8	-
ESK 77	Garnet Lherzolite	55	17	8	6	11	3

Mineral analyses are presented in this paper for two new samples of eclogite from this locality. Sample A41 is essentially identical to the original N75 sample of O'Hara & Mercy, whilst sample A84 is of the associated porphyroclastic textured variant.

By contrast, Eskola's analysed sample (ESK 75) was not a bimineralic eclogite as described by him. Re-examination of a residual piece of this sample retained in the Mineralogisk-Geologisk Museum at Oslo confirmed my earlier suspicions that this rock contains a minor, though significant, amount of orthopyroxene (see Table 1). This orthopyroxene takes the form of both rare large strained porphyroclasts and more abundant smaller recrystallised grains. This rock is thus strictly a garnet websterite and as such is indeed more akin to the rocks exposed on Rødhaugen, where garnet and clinopyroxene rich rocks occur interbanded with garnet and clinopyroxene free peridotite in the manner illustrated by Eskola. I myself have observed that at Rødhaugen there are in fact no true bimineralic eclogites and that the most garnet and clinopyroxene rich rocks are garnet websterites – in other words they invariably contain orthopyroxene.

In an attempt to confirm whether or not Eskola's specimen came from Rødhaugen, new petrographic and mineral composition data on the original Museum specimen have been obtained and compared with data on a further suite of garnetiferous samples from this locality. Two of these samples, ESK 76 and ESK 77, were also from Eskola's original collection housed in the Museum at Oslo, but in both cases specifically labelled as being from Rødhaugen. Sample ESK 76, recorded as *Eclogite in dunite*, in fact contains both orthopyroxene and olivine (Table 1). Sample ESK 77, recorded as *Garnet dunite*, likewise has a 4-phase garnet lherzolite assemblage but with much scarcer garnet and clinopyroxene, and the former heavily kelyphitised. In addition, the following five specimens were selected for analysis out of my own field collection from the Rødhaugen locality. Samples A33 and A49 are both olivine free but orthopyroxene bearing, and are therefore garnet websterites. Of these, sample A33 is petrographically the closest in appearance to Eskola's original Rødhaugen

TABLE 2 ANALYSES OF BULK ROCKS AND MINERAL SEPARATES

SAMPLE	BULK ROCK ANALYSES		ANALYSES OF MINERAL SEPARATES				
			GARNET		CLINOPYROXENE		AMPHIBOLE
	N75	ESK 75	A41	ESK 75	A41	ESK 75	A41
SiO_2	44.42	48.7	40.61	41.52	54.14	54.49	45.07
TiO_2	0.14	tr.	0.01	tr.	0.11	tr.	0.35
Al_2O_3	18.59	11.7	22.50	23.01	8.26	2.50	16.19
Cr_2O_3	0.11	0.2	0.10	0.22	0.15	0.20	0.08
Fe_2O_3	2.23	1.4	0.41	1.22	0.76	1.63	0.15
FeO	7.56	6.8	12.30	12.86	1.57	1.98	4.91
MnO	0.18	0.2	0.29	0.33	0.01	0.06	0.04
NiO	0.03	n.d.	0.00	0.00	0.05	0.03	0.11
MgO	12.09	16.7	11.56	16.64	12.72	16.74	16.06
CaO	13.69	13.9	11.92	4.71	19.31	21.40	11.59
Na_2O	1.41	0.4	0.06	0.00	2.68	0.83	3.10
K_2O	<0.01	0.2	0.02	0.00	0.12	0.40	0.08
P_2O_5	0.01	n.d.	0.02	n.d.	0.06	n.d.	0.01
H_2O	0.19	0.1	n.d.	0.16	n.d.	0.12	n.d.
TOTAL	100.15	100.3	99.82	100.67	99.96	100.38	97.74

ESK 75: Analyses of mineral separates and calculated bulk rock analysis from Eskola (1921).

N75: Bulk rock analysis from Mercy & O'Hara (1965).

A41: New analyses of mineral separates from the Eikremsæter eclogite, performed by a combination of gravimetric, colometric and titration techniques in the Geology Department, University of Sheffield, U.K.

'eclogite' sample ESK 75, and is from the widest (approx. 75 cm.) olivine free layer observed at Rødhaugen. By contrast, sample A49 shows more extensive secondary amphibolitisation. As overall there are considerable variations in the proportions of primary garnet, pyroxenes and olivine in the various garnetiferous layers within the peridotite mass at Rødhaugen, the remaining three analysed samples, A6, A7a and A7b, were selected to span the gap between the olivine free garnet websterite samples and the relatively garnet impoverished lherzolite sample ESK 77.

All the analysed garnet websterite and garnet lherzolite samples have strikingly porphyroclastic textures with highly strained clasts of garnet, pyroxenes and olivines (in lherzolites only) up to 1 cm. in maximum dimension, set in a recrystallised matrix, consisting of a mosaic of small (typically 0.2–0.5 mm.) strain-free grains (neoblasts) of garnets, pyroxenes, olivines and amphiboles. Secondary amphibole has clearly formed at the expense of both primary garnets and clinopyroxenes and in certain samples, notably A49 and ESK 77, is intergrown with fine-grained chrome spinel as pronounced kelyphite rims around the garnets.

Mineral chemistry

Eikremsæterfoss eclogite

As might be predicted from comparison of the bulk rock analyses, the new mineral analyses confirm that all the clinopyroxene in the Eikremsæter eclogite is substantially more jadeitic than in Eskola's sample (ESK 75), and that garnets and clinopyroxenes both have higher Fe/Mg ratios (compare Tables 2–4). In addition the garnets in the Eikremsæterfoss eclogite are very much more calcic, reflecting the bimineralic eclogite paragenesis (Fig. 2). On the other hand, comparison with other analysed eclogite, garnet websterite and garnet lherzolite assemblages (O'Hara & Mercy 1963, Lappin 1974, Lappin & Smith 1978, Carswell 1968, 1973 and Medaris 1980) indicates that the limitation of the CaO content in the garnet in Eskola's sample to only 4.71 wt.% reflects equilibration within an orthopyroxene bearing assemblage (as indeed has been confirmed by the petrographic reinvestigation of this sample).

There is no interbanding of this eclogite with olivine bearing rocks, but instead sharp contacts between the eclogite and peridotite, adjacent to

TABLE 3 MICROPROBE ANALYSES OF MINERAL PHASES IN SAMPLES OF THE EIKREMSÆTER ECLOGITE

Sample No.	A41	A41	A41	A41	A84	A84	A84	A84	A41	A41
Description	Grt Core	Grt Rim	Cpx Core	Cpx Rim	Grt Unzoned	Cpx Clast Core	Cpx Clast Rim	Cpx Recryst.	Amph. in Grt	Amph. in Cpx Fol. Grt
SiO_2	41.12	41.36	54.49	54.65	41.02	54.01	53.51	54.55	44.78	45.48
TiO_2	0.04	0.02	0.16	0.11	0.04	0.16	0.14	0.14	0.47	0.44
Al_2O_3	22.83	22.81	7.42	7.40	22.62	8.42	8.04	7.81	14.44	14.18
Cr_2O_3	0.13	0.07	0.11	0.16	0.14	0.14	0.10	0.16	0.07	0.07
T_{FeO}	12.19	11.51	1.97	1.96	14.69	2.12	2.24	2.11	5.07	4.98
MnO	0.26	0.27	0.02	0.02	0.27	0.04	0.02	0.01	0.05	0.05
NiO	0.00	0.00	0.03	0.00	0.00	0.01	0.00	0.00	0.03	0.03
MgO	11.57	11.53	12.47	12.40	10.44	11.71	11.74	12.06	14.13	14.12
CaO	10.25	11.13	19.19	19.05	11.00	19.03	19.07	19.07	11.51	11.51
Na_2O	0.02	0.01	3.37	3.44	0.00	4.03	4.04	4.06	1.53	1.59
TOTAL	100.41	100.11	99.25	99.57	100.01	99.84	98.91	100.01	96.23	96.45
Cation Proportions										
Si	3.016	3.024	1.991	1.993	3.017	1.983	1.981	1.990		
Ti	0.002	0.001	0.004	0.003	0.002	0.004	0.004	0.004		
Al	1.974	1.970	0.320	0.318	1.959	0.364	0.351	0.336		
Cr	0.008	0.004	0.003	0.004	0.008	0.004	0.003	0.004		
Fe	0.748	0.703	0.059	0.059	0.774	0.064	0.069	0.064		
Mn	0.016	0.017	0.001	0.000	0.018	0.001	0.000	0.000		
Ni	0.000	0.000	0.001	0.002	0.000	-	-	0.000		
Mg	1.264	1.259	0.679	0.674	1.167	0.641	0.648	0.656		
Ca	0.963	0.948	0.749	0.745	1.036	0.749	0.757	0.747		
Na	0.003	0.002	0.239	0.240	0.000	0.287	0.290	0.287		
TOTAL	7.993	7.958	3.995	3.994	7.981	4.000	4.003	4.008		
O	12.0	12.0	6.0	6.0	12.0	6.0	6.0	6.0		

T:- All Fe expressed as FeO

Microprobe IR wavelength dispersion analyses performed in Department of Geology, University of Sheffield, U.K.

which the eclogite is heavily amphibolitised. This secondary amphibole develops at the expense of both garnet and clinopyroxene and varies in composition depending on location. The two electron microprobe analyses given in Table 3 represent the extremes of the composition range observed in the amphibole grains, whilst the pargasitic amphibole separate analysis (Table 2) represents an average composition.

Despite the lack of interbanding of this eclogite with the adjacent peridotite, the fact that its bulk rock composition (N75 in Table 2) lies on the continuation of the linear composition trend shown on the Ca:Mg:Fe plot of Mercy & O'Hara (1965) for the interlayered garnet websterites and lherzolites from Rødhaugen suggests that this eclogite may well be genetically related to the associated peridotitic rocks rather than that it represents a tectonic inclusion of eclogite of the type found in the nearby gneisses. Such an interpretation is further supported by the relatively magnesian and chromiferous nature of the garnets and clinopyroxenes in this eclogite,

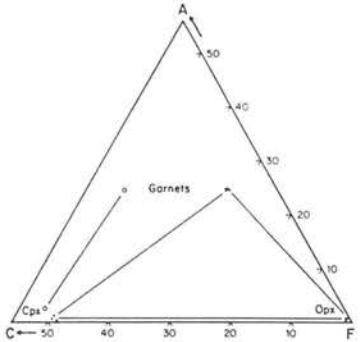

Fig. 2. ACF diagram showing a comparison of mean garnet, clinopyroxene and orthopyroxene porphyroclast core compositions in both the Rødhaugen garnet lherzolite and garnet websterite samples (filled circles) with the corresponding mineral compositions in Eskola's original 'eclogite' specimen (crosses) and in the Eikremsæterfoss eclogite (open circles).

TABLE 4 MICROPROBE ANALYSES OF PRIMARY MINERAL PHASES IN GARNET WEBSTERITE SAMPLES

Mineral Description	Garnet Clast Cores			Garnet Clast Rims & Recryst. Grains		Clinopyroxene Clast Cores			Clinopyroxene Clast Rims & Recryst. Grains			Orthopyroxene Clast Cores			Orthopyroxene Clast Rims & Recryst. Grains		
Sample No.	ESK 75	A33	A49	ESK 75	A33	ESK 75	A33	A49	ESK 75	A33	A49	ESK 75	A33	A49	ESK 75	A33	A49
SiO_2	42.19	41.67	41.92	42.18	41.75	55.14	53.50	53.60	55.48	53.88	53.36	56.39	58.10	57.71	57.74	58.17	57.7
TiO_2	0.04	0.02	0.02	0.02	0.02	0.09	0.15	0.15	0.06	0.11	0.11	0.14	0.01	0.04	0.02	0.02	0.0
Al_2O_3	22.59	24.22	23.08	24.47	22.90	2.65	3.06	3.38	2.26	2.65	4.04	0.77	0.76	1.7	0.31	0.74	0.6
Cr_2O_3	0.16	0.06	0.02	0.18	0.06	0.18	0.41	0.42	0.11	0.29	0.35	0.02	0.04	0.04	0.01	0.01	0.0
FeO*	14.70	9.53	9.06	15.29	9.51	2.53	1.38	1.51	2.52	1.28	1.54	5.67	1.90	1.91	4.27	1.68	1.5
MnO	0.37	0.18	0.45	0.43	0.44	0.03	0.02	0.03	0.03	0.02	0.03	0.09	0.06	0.10	0.06	0.05	0.0
NiO	0.00	0.00	0.00	0.00	0.00	0.02	0.02	0.02	0.04	0.02	0.02	0.14	0.05	0.04	0.11	0.01	0.0
MgO	20.28	20.40	20.00	15.70	19.74	15.28	15.51	15.41	15.59	15.02	16.00	1.64	35.47	35.03	32.64	35.45	35.0
CaO	1.33	4.26	4.29	4.47	4.21	21.92	22.23	22.02	22.14	22.51	22.53	0.30	0.18	0.14	0.11	0.37	0.3
Na_2O	0.00	0.00	n.d.	0.00	0.00	1.96	1.90	1.97	1.52	1.56	1.64	0.02	0.01	0.01	0.01	0.01	0.0
TOTAL	101.96	101.02	99.84	100.74	101.03	99.91	100.08	100.51	100.08	99.44	100.16	99.18	99.37	99.42	100.42	100.46	99.7
Ionic Proportions																	
Si	3.054	3.057	2.993	3.055	3.073	1.995	1.994	1.990	2.004	2.017	1.978	1.986	1.992	1.986	2.004	2.014	1.9
Ti	0.002	0.001	0.001	0.001	0.001	0.002	0.004	0.004	0.002	0.003	0.003	0.005	0.001	0.001	0.001	0.001	0.0
Al	1.928	1.956	1.942	1.919	1.896	0.122	0.130	0.142	0.096	0.113	0.170	0.032	0.031	0.029	0.013	0.030	0.0
Cr	0.009	0.026	0.015	0.010	0.026	0.005	0.012	0.010	0.004	0.003	0.016	0.001	0.002	0.002	0.000	0.001	0.0
Fe	0.890	0.583	0.571	0.926	0.559	0.076	0.042	0.045	0.076	0.078	0.046	0.251	0.137	0.141	0.249	0.133	0.1
Mn	0.023	0.011	0.027	0.026	0.026	0.001	0.001	0.001	0.001	0.001	0.001	0.002	0.002	0.003	0.002	0.001	0.0
Ni	0.000	0.000	0.000	0.000	0.000	0.001	0.001	0.001	0.001	0.001	0.001	0.004	0.001	0.001	0.003	0.001	0.0
Mg	1.735	2.128	2.128	1.695	2.067	0.824	0.830	0.819	0.839	0.808	0.852	0.099	1.813	1.808	1.687	1.810	1.8
Ca	0.336	0.320	0.329	0.347	0.317	0.849	0.856	0.842	0.868	0.871	0.863	0.011	0.007	0.005	0.004	0.002	0.0
Na	0.000	0.000	0.000	0.000	0.000	0.130	0.125	0.129	0.106	0.109	0.114	0.001	0.002	0.001	0.001	0.001	0.0
TOTAL	7.976	7.972	8.018	7.979	7.965	4.005	3.994	3.990	3.998	3.972	4.003	3.993	3.997	3.998	3.967	3.990	4.0
O	12.0	12.0	12.0	12.0	12.0	6.0	6.0	6.0	6.0	6.0	6.0	6.0	6.0	6.0	6.0	6.0	6.0

* Total Fe as FeO

Microprobe IR wavelength dispersion analyses performed in Department of Geology, University of Sheffield, U.K.

compared with those in eclogites directly enclosed in the gneisses at the nearby Lien locality (Medaris 1980).

Both Krogh (1977) and Medaris (1980) have interpreted mineral compositional zoning in eclogite lenses directly enclosed in the gneisses to indicate a prograde metamorphic evolution of such rocks. This contrasts and converges with the retrograde metamorphic P./T. trend defined on mineral zoning evidence by Medaris (1980) for interbanded garnet peridotite and pyroxenites in the Lien mass at Almklovdalen. However, probe analyses of the different samples of the Eikremsæterfoss eclogite (Table 3) indicate only minimal overall compositional zoning. Indeed mineral composition differences between the two samples (A41 and A84) are greater than the within grain variations observed in either sample. What little compositional zoning there is in the garnets and clinopyroxenes in sample A41 indicates a slight increase in the K_D partition co-efficient

$$[=(Fe^{2+}/Mg^{2+})\ \text{garnet}/(Fe^{2+}/Mg^{2+})\ \text{clinopyroxene}].$$

On the other hand, no significant zoning was detected in garnets in sample A84, and even the composition differences between the large strained porphyroclasts and the smaller recrystallised grains of clinopyroxene in that sample are surprisingly small.

Garnet websterite samples

Electron microprobe analyses of the primary mineral phases in the two garnet websterite samples (A33 and A49) from Rødhaugen are given in Table 4, where they can be compared with the new analyses for Eskola's original 'Rødhaugen eclogite' sample (ESK 75). All three samples lack modal olivine. It is noticeable that whilst the mineral compositions in Rødhaugen samples A33 and A49 are fairly similar, those in Eskola's sample are much less magnesian and chromiferous. For example, orthopyroxenes in ESK 75 are En_{86-87}, compared with En_{92-93} in the other two samples. In view of this, and the fact that I have been unable to match closely in appearance Eskola's original sample with any sample which I have collected at Rødhaugen, it is thought that Eskola's sample may not have come from that locality. Instead it is suspected that it may have originated from the nearby Lien locality, where Medaris (1980) has found that the

TABLE 5 GARNET AND CLINOPYROXENE ANALYSES IN GARNET LHERZOLITE SAMPLES

mineral assemblages in comparable rocks extend to similarly more ferriferous compositions (e.g. orthopyroxenes are En_{87-92}).

In all three analysed garnet websterite samples, porphyroclasts of garnet and both pyroxenes are compositionally zoned. The most obvious features are an increase in Fe/Mg ratio from cores to rims in garnets, a decrease in Al and Na from cores to rims in clinopyroxenes, and a decrease in Al, Cr and Ca from cores to rims in orthopyroxenes. It was found that the compositions of the smaller recrystallised matrix grains of these phases are essentially the same as the rims of the large porphyroclasts. It was not possible to obtain a realistic garnet rim analysis in sample A49 because of the extensive kelyphitisation, but in the other two samples the change in Fe-Mg partitioning between garnets and clinopyroxenes is reflected in an increase in the K_D value from grain cores to rims (see Table 7).

The electron microprobe analyses for the garnets in ESK 75 are broadly similar to Eskola's original analysis (cf. Tables 2 and 4) for the garnet mineral separate. However, the new analyses for the clinopyroxenes in this rock are, significantly different from Eskola's original analysis. In particular, they indicate lower Fe and Mg, and higher Ca, Al and Na contents. From this it is concluded that Eskola's analysed clinopyroxene mineral separate may well have been contaminated with about 10% of orthopyroxene, the presence of which he appears to have overlooked in this rock sample. That said, it is still difficult to reconcile Eskola's value for Na_2O in the clinopyroxene with the roughly doubled values determined in the electron microprobe analyses.

Garnet lherzolite samples

The range of mineral compositions determined in the five garnet lherzolite samples from Rødhaugen (Tables 4 and 5) is fairly limited. The olivines are Fo_{90-91} and the orthopyroxenes En_{91-92} in all samples. Overall the garnets and pyroxenes have broadly similar Fe/Mg ratios to those determined in the associated garnet websterite samples from Rødhaugen, but are generally more chromiferous. Indeed, the chrome contents appear in general to increase in sympathy with decreasing modal contents of these minerals, relative to olivine.

There are again some significant composition differences between the cores and rims of por-

phyroclasts, with the smaller recrystallised matrix grains having essentially the same compositions as the porphyroclast rims. Moreover, the nature of these differences is much the same as in the olivine-free garnet websterites. K_D values are again consistently somewhat higher for clast rims than for cores (Table 7). Likewise, clinopyroxene clast rims and recrystallised grains have generally lower Al and Na (i.e. jadeite) contents and equivalent orthopyroxenes lower Al, Cr and Ca contents than corresponding clast cores.

Equilibration conditions and petrogenetic implications

Medaris (1980) has reported that core and rim compositions of minerals in garnet lherzolite and garnet pyroxenite assemblages from the nearby Lien locality (Fig. 1) define a retrograde metamorphic trend from 820° C., 28.1 Kbars. to 645° C., 17.6 Kbars. By contrast, eclogite lenses directly enclosed in the adjacent gneisses were reported to record a prograde metamorphic trend, which converges with the retrograde trend observed in the ultramafic rocks.

For comparison, calculated equilibration temperature-pressure estimates for respective core and rim (+neoblast) assemblages in the various analysed rocks are given in Table 7. All pressures have been calculated through use of the garnet-orthopyroxene geobarometer as formulated by Wood (1974), with substitution of Cr for Al in the octahedral sites taken into account in the manner which he proposed. Only results obtained from those geothermometers judged to give fairly consistent and reliable values have been included in Table 7. For example, results based on Fe^{2+}–Mg^{2+} partitioning between garnet and olivine in garnet lherzolite assemblages as experimentally calibrated by O'Neill & Wood (1979, 1980) vary from 706° C./21.6 Kbars. to 1086° C./48.4 Kbars. for grain cores alone, and have therefore been excluded. More detailed discussion of the likely validity of the various available mineralogical thermometers and barometers, especially those applicable to garnet lherzolite assemblages, have been given elsewhere (Carswell & Gibb 1980 a & b). It should, however, be noted here that in the case of the Wells (1977)/Wood (1974) and Ellis & Green (1979)/ Wood (1974) combinations, the paired temperature/pressure values have been obtained through simultaneous solution of two temperature and pressure dependent equations. Hence in these instances the temperature and pressure values given are interdependent, and each susceptible to errors in the other. For the other paired temperature/ pressure values given in Table 7, temperatures were calculated before pressures. Thus these pressure values are susceptible to any temperature errors but not vice-versa.

Both the Wells (1977) and Mori & Green (1978) calibrations of the two pyroxene solvus geothermometer give closely similar and encouragingly consistent temperature estimates for porphyroclast core assemblages. The mean values are 724° C./23 Kbars. and 732° C./23.5 Kbars. for the respective temperature/pressure pairings. However, it seems necessary to attach uncertainties of at least ± 50° C. to these particular temperature estimates, in view of the relative temperature insensitivity of the two pyroxene solvus at such low temperatures. Co-existing pyroxene clast rims and recrystallised matrix grains yield much less consistent temperature estimates by this method, although the mean values are fortuitously similar to those for co-existing pyroxene clast cores.

Fe^{2+}–Mg^{2+} partitioning between co-existing garnet and clinopyroxene, usually expressed by the distribution co-efficient $K_D = (Fe^{2+}/Mg^{2+})$ garnet/(Fe^{2+}/Mg^{2+}) clinopyroxene, is much more temperature sensitive. It is therefore reasonable to expect that the temperature/pressure values obtained from this geothermometer in combination with the garnet-orthopyroxene geobarometer should be the most reliable. However, results calculated in this manner are critically dependent on whether or not all the iron in the co-existing garnet-clinopyroxene mineral pairs is taken to be divalent. If it is all taken as Fe^{2+}, the mean K_D values for the combined garnet lherzolite and garnet websterite samples are 4.51 and 5.40 for clast core and rim (+neoblast) assemblages, respectively. However, if one assumes equivalent $Fe^{2+}/(Fe^{2+} + Fe^{3+})$ ratios in the garnets and clinopyroxenes to those determined in analysis of bulk mineral separates from comparable assemblages (Table 2 and O'Hara & Mercy 1963), the mean K_D values are raised to 6.22 and 7.46, respectively. Consequently, calculated equilibration temperatures (Table 7) are on average around 100° C. lower.

The fact that the Mori & Green (1978) calibration of the K_D geothermometer involved some experiments on mineral assemblages separated from Norwegian garnet lherzolites of much the same composition as those being considered in this study, encourages one to consider that it should be more directly applicable to the present garnet lherzolite and garnet websterite assemblages than the Ellis & Green (1979) experimental calibration, which was based on garnet-clinopyroxene mineral pairs, in generally more siliceous and ferriferous basaltic compositions. However, it should be appreciated that Mori & Green's formulation of the K_D geothermometer was based on experiments run at either 30 or 40 Kbars. pressure and, unlike the Ellis & Green calibration, does not include a pressure dependence factor. There were also important differences in the experimental procedures employed, which have a bearing on the crucial question as to whether or not all the iron in the garnets and clinopyroxenes should be taken as Fe^{2+} when calculating K_D values. As pointed out by Medaris (1980), the garnets and clinopyroxenes produced in Mori & Green's experiments almost certainly contained small amounts of Fe^{3+}, as do the natural mineral pairs in these Norwegian rocks. However, since Mori & Green formulated their K_D geothermometer from microprobe mineral analyses in which all the iron was taken as Fe^{2+}, it seems desirable to make the same assumption when dealing with the natural assemblages in question. On the other hand, Ellis & Green carefully controlled the oxygen fugacity in their experiments on synthetic rock compositions in order to ensure that all iron remained divalent. Hence application of their K_D calibration to natural garnet-clinopyroxene pairs should take account of the presence of any Fe^{3+}.

With these considerations in mind, the temperature/pressure values based on the Mori & Green K_D calibration (assuming all Fe as Fe^{2+}) in combination with the garnet-orthopyroxene geobarometer of Wood (1974) are judged to be the most reliable as far as the garnet lherzolite and garnet websterite samples are concerned. On this basis, the averaged 'best' temperature/pressure estimates for the porphyroclast core assemblages in these rocks are 770° C. and 25.8 Kbars. Such values are very much in line with those obtained by Medaris (1980, Table 3) for comparable samples from the Lien locality on the same calculation basis, and are compatible with experimental evidence (O'Hara et al. 1971, Jenkins & Newton 1979) on the temperature/pressure conditions necessary for stability of such garnet lherzolite assemblages.

The consistently higher K_D values for co-existing garnet and clinopyroxene porphyroclast rims and recrystallised matrix grains, compared with the values for porphyroclast cores, suggests that cataclasis and attendant recrystallisation occurred as temperatures were falling. If, as seems likely, this took place as these rocks were being thrust towards the surface, subsequent to the metamorphic 'high', one would reasonably expect that pressures would also be lower. However, it is apparent from Table 7 that in many cases the calculated equilibration pressures for porphyroclast rim and neoblast assemblages are actually higher than those for corresponding porphyroclast cores. This is a consequence of the consistently lower Al contents of orthopyroxene porphyroclast rims and neoblasts compared with the porphyroclast cores (Tables 4 and 6). However, it is considered that the low Al contents in such orthopyroxenes at least in part reflect the uptake of Al in associated secondary amphiboles, a feature also noted in partly amphibolitised orthopyroxene eclogite assemblages (Carswell et al. 1981). Hence it is probably invalid to calculate equilibration pressures for such clast rim and neoblast assemblages using the garnet-orthopyroxene geobarometer based on anhydrous assemblages (Wood 1974, MacGregor 1974) and considered unlikely that the temperature/pressure estimates (Table 7) calculated in that manner for the porphyroclast rim and neoblast assemblages are geologically meaningful. Thus, although the K_D variation suggests recrystallisation in a falling temperature (and pressure?) environment, it is not possible to confirm the actual values indicated by Medaris (1980) for the retrograde metamorphic trend in garnetiferous assemblages in the nearby Lien peridotite.

The absence of primary plagioclase and quartz means that it is not possible to estimate the equilibration pressures for the Eikremsæterfoss eclogite sample from the jadeite content of its clinopyroxene (Kushiro 1969). The lack of orthopyroxene similarly rules out use of the garnet-orthopyroxene geobarometer. However, if one assumes a pressure value of 25.8 Kbars. (taken to be the 'best' pressure estimate for the garnet lherzolites and websterites), then from the Ellis & Green (1979) K_D calibration, which encompasses broadly comparable rock compositions, calculated equilibration temperatures for

TABLE 6 ORTHOPYROXENE AND OLIVINE ANALYSES IN GARNET LHERZOLITE SAMPLES

Mineral Description	Orthopyroxene Clast Cores					Orthopyroxene Clast-Rim & Recryst. Grains					Olivines				
Sample No.	A6	A7A	A7b	ESK 76	ESK 77	A6	A7A	A7b	ESK 76	ESK 77	A6	A7A	A7b	ESK 76	ESK 77
SiO_2	57.84	57.57	58.37	57.69	57.23	57.99	57.84	58.54	57.72	58.70	40.93	40.61	41.16	40.62	40.14
TiO_2	0.04	0.03	0.03	0.02	0.02	0.03	0.02	0.03	0.03	0.01	n.d.	n.d.	n.d.	0.00	n.d.
Al_2O_3	0.81	0.84	0.62	0.66	1.06	0.48	0.60	0.53	0.61	0.46	0.06	0.06	0.00	0.00	0.04
Cr_2O_3	0.22	0.17	0.08	0.12	0.15	0.11	0.08	0.05	0.09	0.07	n.d.	n.d.	n.d.	0.00	n.d.
FeO	5.07	5.63	5.86	5.33	6.06	4.36	5.93	5.15	5.69	4.15	9.24	8.59	9.45	8.54	9.11
MnO	0.13	0.11	0.12	0.11	0.14	0.14	0.07	0.06	0.11	0.13	0.11	0.11	0.16	0.15	0.15
NiO	0.04	0.06	0.05	0.03	0.04	0.05	0.06	0.05	0.04	0.07	0.41	0.42	0.21	0.38	0.41
MgO	34.41	34.93	35.10	35.74	34.41	34.64	35.07	35.52	35.21	34.76	49.11	50.01	48.96	49.93	49.45
CaO	0.16	0.10	0.10	0.11	0.13	0.09	0.10	0.09	0.09	0.07	0.06	0.06	0.00	0.06	0.04
Na_2O	0.01	0.00	0.00	0.00	0.01	0.00	0.00	0.00	0.03	0.00	n.d.	n.d.	n.d.	0.00	n.d.
TOTAL	99.78	99.44	100.33	100.01	99.42	99.49	99.41	100.07	99.59	100.47	99.75	99.74	100.02	99.69	99.54
Cation Proportions															
Si	1.995	1.987	1.996	1.983	1.971	1.997	1.987	2.000	1.989	1.999	0.991	0.994	1.007	0.995	0.991
Ti	0.001	0.001	0.001	0.001	0.001	0.001	0.001	0.001	0.001	0.001	-	-	-	0.000	-
Al	0.033	0.034	0.025	0.027	0.043	0.020	0.024	0.021	0.025	0.019	0.002	0.000	0.000	0.000	0.002
Cr	0.006	0.005	0.002	0.003	0.004	0.001	0.002	0.001	0.002	0.002	-	-	-	0.000	-
Fe	0.175	0.162	0.168	0.153	0.174	0.126	0.171	0.147	0.164	0.119	0.191	0.173	0.193	0.175	0.190
Mn	0.004	0.003	0.004	0.003	0.004	0.004	0.002	0.002	0.003	0.004	0.002	0.002	0.004	0.003	0.003
Ni	0.001	0.002	0.001	0.001	0.001	0.001	0.002	0.001	0.001	0.002	0.008	0.008	0.004	0.008	0.008
Mg	1.767	1.796	1.789	1.825	1.774	1.774	1.807	1.809	1.808	1.771	1.066	1.825	1.782	1.824	1.811
Ca	0.007	0.004	0.004	0.004	0.007	0.003	0.004	0.003	0.003	0.003	0.000	0.000	0.000	0.000	0.000
Na	0.002	0.000	0.000	0.000	0.000	0.000	0.000	0.002	0.000	0.000	-	-	-	0.000	-
TOTAL	3.986	3.993	3.989	4.001	3.991	3.991	3.999	3.989	3.997	3.993	3.064	3.004	2.993	3.005	3.005
O	6.0	6.0	6.0	6.0	6.0	6.0	6.0	6.0	6.0	6.0	4.0	4.0	4.0	4.0	4.0

Fe* Total Fe as FeO

Microprobe EX wavelength dispersion analyses performed in Department of Geology, University of Sheffield, U.K.

garnet-clinopyroxene grain cores average out at 879° C (if all Fe is taken as Fe^{2+}) or 778° C. (if analytical $Fe^{2+}/Fe^{2+} + Fe^{3+}$ ratios are taken into consideration). The latter value is clearly to be preferred both in the light of earlier discussions on the iron valency state problem and its similarity with the preferred mean value of 770° C. for porphyroclast core assemblages in the garnet lherzolites and websterites. Whilst the close agreement between these two values is encouraging, concern over the disparity in the various individual temperature estimates listed in Table 7 and doubts over the accuracy of the garnet-orthopyroxene geobarometer, when applied to chromiferous garnet lherzolite assemblages (Carswell & Gibb 1980 a & b), demand that fairly wide error brackets should be attached to the favoured temperature/pressure estimates.

In my opinion the most judicious though still somewhat subjective, interpretation which can be placed on the available temperature/pressure estimates is that the equilibration conditions for the porphyroclast core assemblages in the rocks described are probably encompassed by the values 740 ± 50° C. and 22 ± 5 Kbars. These values are compatible with several other estimates for the metamorphic 'high'-responsible for the development of eclogite facies assemblages enclosed both within other peridotite bodies and directly in the surrounding gneisses throughout much of Møre and Romsdal (Krogh 1977, Medaris 1980, Carswell & Gibb 1980a, Carswell et al. 1981) – but are significantly lower, especially in pressure terms, than the values of 700–850° C. and 30–45 Kbars. given by Lappin & Smith (1978). They are also in line with the temperature/presure estimates derived by Krogh (1980) for relict high grade assemblages occasionally preserved in the quartzofeldspathic gneisses themselves.

The available evidence therefore points to such temperature/pressure conditions having been operative on a regional scale, and indicates that the emplacement of the peridotite bodies into a lower crustal gneiss sequence occurred prior to the regional metamorphic 'high' (Carswell & Gibb 1980a). Since geochemical considerations (e.g. Carswell 1968, Brueckner 1977) suggest an ultimate mantle origin for the peridotite bodies, a possible scenario is that tectonic intercalation of these sub-Moho rocks occurred in the nose of a continental lithospheric plate as it was being temporarily subducted beneath another such plate with which it had collided

TABLE 7 CALCULATED TEMPERATURE-PRESSURE ESTIMATES FOR THE VARIOUS ANALYSED SAMPLES

			Two Pyroxene Solvus				GNT—CPX $^1K_D Fe^{2+}—Mg^{2+}$					GNT—CPX $^2K_D Fe^{2+}—Mg^{2+}$				
	Samples	Methods	T°C Wells (1977)	P. Kbars Wood (1974)	T°C Mori & Green (1978)	P. Kbars Wood (1974)	^1K_D	T°C Ellis & Green (1979)	P. Kbars Wood (1974)	T°C Mori & Green (1978)	P. Kbars Wood (1974)	^2K_D	T°C Ellis & Green (1979)	P. Kbars Wood (1974)	T°C Mori & Green (1978)	P. Kbars Wood (1974)
Garnet Websterites	ESK 75	CLAST CORES	691	19.7	711	20.9	5.52	729	22.0	693	19.8	7.31	642	15.5	608	13.5
		CLAST RIMS	722	28.1	749	29.8	6.02	726	28.3	665	24.2	7.94	642	21.4	585	17.7
	A33	CLAST CORES	693	20.9	693	20.9	4.73	783	26.4	747	24.2	6.31	687	20.5	651	18.3
		CLAST RIMS	699	29.6	699	29.6	5.65	751	33.3	685	28.7	7.48	660	26.1	601	22.1
	A49	CLAST CORES	747	25.2	751	25.4	4.88	773	26.7	736	24.5	6.47	677	20.0	643	18.0
Garnet Lherzolites	A6	CLAST CORES	719	21.7	728	22.2	3.94	856	30.0	820	27.8	5.57	724	21.5	690	19.4
		CLAST RIMS	704	26.0	713	26.6	5.26	763	29.9	710	26.4	7.44	652	22.4	603	19.2
	A7A	CLAST CORES	719	22.4	725	22.8	4.06	840	29.8	808	27.8	5.74	711	21.4	680	19.6
		CLAST RIMS	802	30.7	817	31.6	4.55	805	30.8	762	28.1	6.45	682	22.5	644	20.0
	A7B	CLAST CORES	759	27.6	770	28.3	3.99	869	34.6	815	31.2	5.65	733	25.5	685	22.4
		CLAST RIMS	816	31.9	828	32.6	6.04	715	25.4	664	22.1	8.56	612	18.3	566	15.4
	ESK 76	CLAST CORES	731	25.6	736	25.9	4.14	843	32.7	800	30.0	5.86	712	24.0	674	21.6
		CLAST RIMS	621	18.9	620	18.9	4.91	779	29.0	734	26.1	6.91	664	21.1	623	18.6
	ESK 77	CLAST CORES	735	20.7	745	21.3	4.86	764	22.4	737	20.8	6.85	653	15.4	626	13.9
Mean Values		CLAST CORES (n = 8)	724	23.0	732	23.5	4.51	807	28.1	770	25.8	6.22	692	20.5	657	18.3
		CLAST RIMS (n = 6)	727	27.5	738	28.2	5.40	757	29.4	703	25.9	7.46	652	22.0	604	18.8
Eclogite	A41	CLAST CORES					6.67	861	25.8 Kbars. P. assumed			9.37	770	25.8 Kbars. P. assumed		
		CLAST RIMS					6.92	846				9.74	756			
	A84	CLAST CORES					6.71	878				9.40	787			

^1K_D—all Fe taken as Fe^{2+} in calculation.
^2K_D—calculation takes account of $Fe^{2+}/(Fe^{2+} + Fe^{3+})$ ratios in garnets and clinopyroxenes as follows:
0.924 and 0.656 in garnet lherzolite assemblages
0.879 and 0.660 in garnet websterite assemblages
0.921 and 0.574 in the Eikremsaeterfoss eclogite

(see Cuthbert et al. 1981). It does not seem unreasonable to expect that the sorts of temperature/pressure conditions deduced above for the metamorphic 'high' were established within the overridden plate, prior to its rapid upwards recovery which led to the eventual exposure of such high grade assemblages at the earth's surface.

Acknowledgements.– Access to Eskola's original specimens housed in the Mineralogisk-Geologisk Museum at Oslo was kindly arranged by I. Bryhni. Financial support was provided by a grant from the Natural Environment Research Council. F. G. F. Gibb and V. A. Somogyi are thanked for their assistance with the electron microprobe and 'wet' chemical analyses, respectively.

Manuscript received August 1981

References

Brueckner, H. K. 1977: A crustal origin for eclogites and a mantle origin for garnet peridotites: strontium isotopic evidence from clinopyroxenes. *Contrib. Mineral. Petrol. 60*, 1–15.

Carswell, D. A. 1968: Possible primary upper mantle peridotite in Norwegian basal gneiss. *Lithos 1*, 322–355.

Carswell, D. A. & Gibb, F. G. G. 1980a: The equilibration conditions and petrogenesis of European crustal garnet lherzolites. *Lithos 13*, 19–29.

Carswell, D. A. & Gibb, F. G. F. 1980b: Geothermometry of garnet lherzolite nodules with special reference to those from the kimberlites of northern Lesotho. *Contrib. Mineral. Petrol., 74*, 403–416.

Carswell, D. A., Griffin, W. L. & Krogh, E. J. 1981: Petrogenetic implications of calculated equilibration conditions for Norwegian orthopyroxene eclogites. *Proceedings of the 1981 Uppsala Caledonide Symposium* (in preparation).

Cuthbert, S. J., Harvey, M. A. & Carswell, D. A. 1981: A plate tectonic model for the metamorphic evolution of the basal gneiss complex in western Norway. *Proceedings of the 1981 Uppsala Caledonide Symposium* (in preparation).

Ellis, D. J. & Green, D. H. 1979: An experimental study of the effect of Ca upon garnet-clinopyroxene Fe-Mg exchange equilibrium. *Contrib. Mineral. Petrol. 71*, 13–22.

Eskola, P. 1921: On the eclogites of Norway. *Skr. Norske Vidensk. – Akad. i Oslo. Mat. – naturv. Kl., no. 8*, 1–118.

Jenkins, D. M. & Newton, R. C. 1979: Experimental determination of the spinel peridotite to garnet peridotite inversion at 900°C. and 1000°C. in the system CaO-MgO-Al_2O_3-SiO_2 and at 900°C. with natural garnet and olivine. *Contrib. Mineral. Petrol. 68*, 407–420.

Krogh, E. J. 1977: Evidence of Precambrian continent-continent collision on western Norway. *Nature 267*, 17–19.

Krogh, E. J. 1980: Compatible P-T conditions for eclogites and surrounding gneisses in the Kristiansund area, Western Norway. *Contrib. Mineral. Petrol. 75*, 387–393.

Kushiro, I. 1969: Clinopyroxene solid solutions formed by reactions between diopside and plagioclase at high pressures. *Mineral. Soc. Am. Spec. Pap. 2*, 179–191.

Lappin, M. A. & Smith, D. C. 1978: Mantle-equilibrated orthopyroxene eclogite pods from the Basal Gneisses in the Selje district, western Norway. *J. Petrol 19*, 530–584.

MacGregor, I. D. 1974: The system MgO-Al_2O_3-SiO_2: Solubility of Al_2O_3 in enstatite for spinel and garnet peridotite compositions. *Am. Mineral. 59*, 110–119.

Medaris, L. G. Jr. 1980: Petrogenesis of the Lien peridotite and associated eclogites, Almklovdalen, Western Norway. *Lithos. 13*, 339–353.

Mercy, E. L. P. & O'Hara, M. J. 1965: Chemistry of some garnetbearing rocks from south Norwegian peridotites. *Nord. Geol. Tidsskr. 45*, 323–332.

Mori, R. & Green, D. H. 1978: Laboratory duplication of phase equilibria observed in natural garnet lherzolites. *J. Geol. 86*, 83–97.

O'Hara, M. J. & Mercy, E. L. P. 1963: Petrology and petrogenesis of some garnetiferous peridotites. *Trans. Roy. Soc. Edinb. 65*, 251–314.

O'Hara, M. J., Richardson, S. W. & Wilson, G. 1971: Garnet peridotite stability and occurrence in crust and mantle. *Contrib. Mineral. Petrol. 32*, 48–67.

O'Neill, H. St. C. & Wood, B. J. 1979: An experimental study of Fe-Mg partitioning between garnet and olivine and its calibration as a geothermometer. *Contrib. Mineral. Petrol. 70*, 59–70.

O'Neill, H. St.C. & Wood, B. J. 1980: An experimental study of Fe-Mg partitioning between garnet and olivine and its calibration as a geothermometer: corrections. *Contrib. Mineral. Petrol. 72*, 337.

Wells, P. R. A. 1977: Pyroxene thermometry in simple and complex systems. *Contrib. Mineral. Petrol., 62*, 129–139.

Wood, B. J. 1974: Solubility of alumina in orthopyroxene coexisting with garnet. *Contrib. Mineral. Petrol. 46*, 1–15.

J. metamorphic Geol. 1983, **1**, 63–90

A tectonic model for the metamorphic evolution of the Basal Gneiss Complex, Western South Norway

S. J. CUTHBERT, M. A. HARVEY & D. A. CARSWELL, *Department of Geology, University of Sheffield, Mappin Street, Sheffield S1 3JD, UK*

Abstract. A review of currently available information relevant to the Basal Gneiss Complex (BGC) of Western South Norway, combined with the authors' own observations, leads to the following conclusions.

1. Most of the BGC consists of Proterozoic crystalline rocks and probably subordinate Lower Palaeozoic cover.
2. The last major deformation of these rocks was during the Caledonian orogeny and involved large-scale thrusting, recumbent folding and doming. The structural development of the BGC is closely tied in with that of the Caledonian allochthon.
3. The whole eclogite-bearing part of the BGC has suffered a high pressure metamorphism with conditions of between 550°C, 12.5 kbar (Sunnfjord) and about 750°C, 20 kbar (Møre og Romsdal) at the metamorphic climax.
4. This metamorphism was of Caledonian age, probably rather early in the Caledonian tectonic history of the BGC and is considered to have been a rather transient event.

By setting these conclusions in a framework provided by geophysical evidence for the deep structure of the crust in southern Norway we have constructed a geotectonic model to explain the recorded metamorphic history of the BGC. It is suggested that considerable crustal thickening was caused by imbrication of the Baltic plate margin during continental collision with the Greenland plate. This resulted in high pressure metamorphism in the resulting nappe stack. Progradation of the suture caused underthrusting of the Baltic foreland below the eclogite-bearing terrain causing it to emerge at the Earth's surface, aided by tectonic stripping and erosion.

Application of isostacy equations to the model shows that eclogites can be formed by *in-situ* metamorphism in crustal rocks and reappear at the land surface above a normal thickness of crust in a single orogenic episode of approximately 65–70 Ma duration.

0263–4929/83/0300–0063 $02.00

Key-words: Caledonides; eclogites; geothermobarometry; isostacy; tectonics

INTRODUCTION

The Basal Gneiss Complex (*BGC*) of Western South Norway forms the deepest exposed structural level of the Scandinavian Caledonides (Fig. 1), being the largest of a number of basement windows in the extensive area of Caledonian nappes in Norway and Sweden (Holtedal & Dons, 1960; Roberts, Thon, Gee & Stephens, 1981).

It seems likely that this gneiss region has had a complex structural and metamorphic history, containing as it does elements resulting from Proterozoic (Svecofennian and Sveconorwegian–Grenvillian) and Caledonian orogenic events.

A particular feature of this basement window is the common occurrence of lithologies with relict high-pressure mineral assemblages, the most obvious being eclogites and garnetiferous peridotites. The gneissic hosts to these relics are commonly metamorphosed in the almandine–amphibolite or epidote–amphibolite facies. However, both low-pressure and high-pressure granulitic parageneses have been increasingly recognized in recent years (see, for instance, Griffin & Mørk, 1981).

The origin and age of these high-pressure relics are still highly controversial. Garnet peridotites and eclogites have been interpreted as solid intrusions from deeper crustal levels or from the mantle (O'Hara & Mercy, 1963; Carswell, 1968b; Lappin & Smith, 1978; Gebauer, Lappin, Gruenefelder, Koestler & Wyttenbach, 1982) or to have been metamorphosed *in-situ* in their host gneisses from low pressure protoliths (Bryhni, Krogh & Griffin, 1977; Griffin & Qvale, 1981; Griffin, Austrheim, Grastad, Bryhni, Krill, Mørk, Qvale & Tørudbakken, 1981). Geochronological results have been variously interpreted as showing a Proterozoic age for the 'main metamorphism' of eclogite-bearing gneisses (Råheim, 1977, 1979, 1981), a Caledonian 'eclogite forming event' (Griffin & Brueckner, 1980, 1982) and tectonic

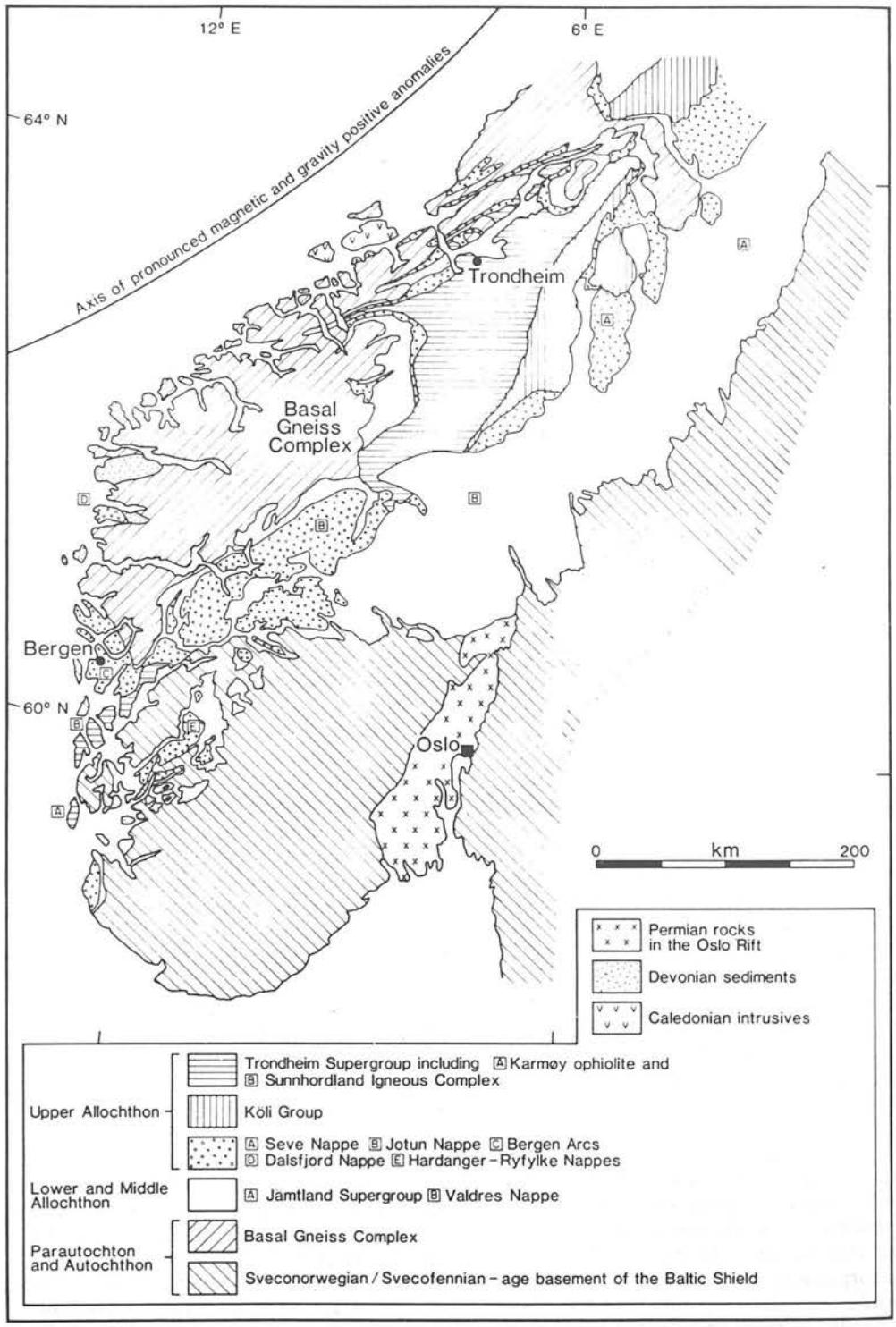

Fig. 1. Map showing the main tectonostratigraphic units of southern Scandinavia (after Roberts *et al.*, 1981).

juxtaposition of units with widely differing provenances (Mearns & Lappin, 1982 a,b,c).

The BGC is surrounded by outcrops of overlying allochtonous nappes which include units of postulated ophiolites, island-arc sequences, continental sediments and deep-seated continental crust. Some of these units also contain eclogites and garnet peridotites (Gee, 1975, 1978; Gee, Guezou, Roberts & Wolff, 1982; Guezou, 1981; Stephens & Gee, 1981; Andresen & Faerseth, 1982; van Roermund, 1981). Locations for place names are given in Fig. 2.

The aim of this paper is to develop a tectonic model which fits the petrological features of the high pressure parageneses in the BGC whilst attempting to be consistent with geochronological, tectonostratigraphic and geophysical data currently available for this part of the Caledonide belt. We hope that presentation of this model as a working hypothesis will stimulate future research, which will doubtless lead to its refinement.

THE GEOLOGICAL SETTING OF THE BASAL GNEISS COMPLEX

The history of the development of interpretation of geological relationships within the BGC and between the BGC and its cover has been characterized by an increasing awareness of the effect of the Caledonian orogeny (for reviews see Bryhni & Grimstad, 1970, pp. 106–109 and Carswell, 1973a).

Recent work by Gee (1980) has shown that the autochthonous Proterozoic crystalline basement at the thrust front of the Central Scandinavian Caledonides in Sweden has a characteristic cover sequence of late Precambrian and Lower Palaeozoic sediments including quartzites, greywackes, locally limestones and green or red shales and a radiogenic black shale. These form the Jämtland Supergroup. The sole thrust of the Caledonian allochthon and parautochthon rides in the black shales which have acted as a plane of

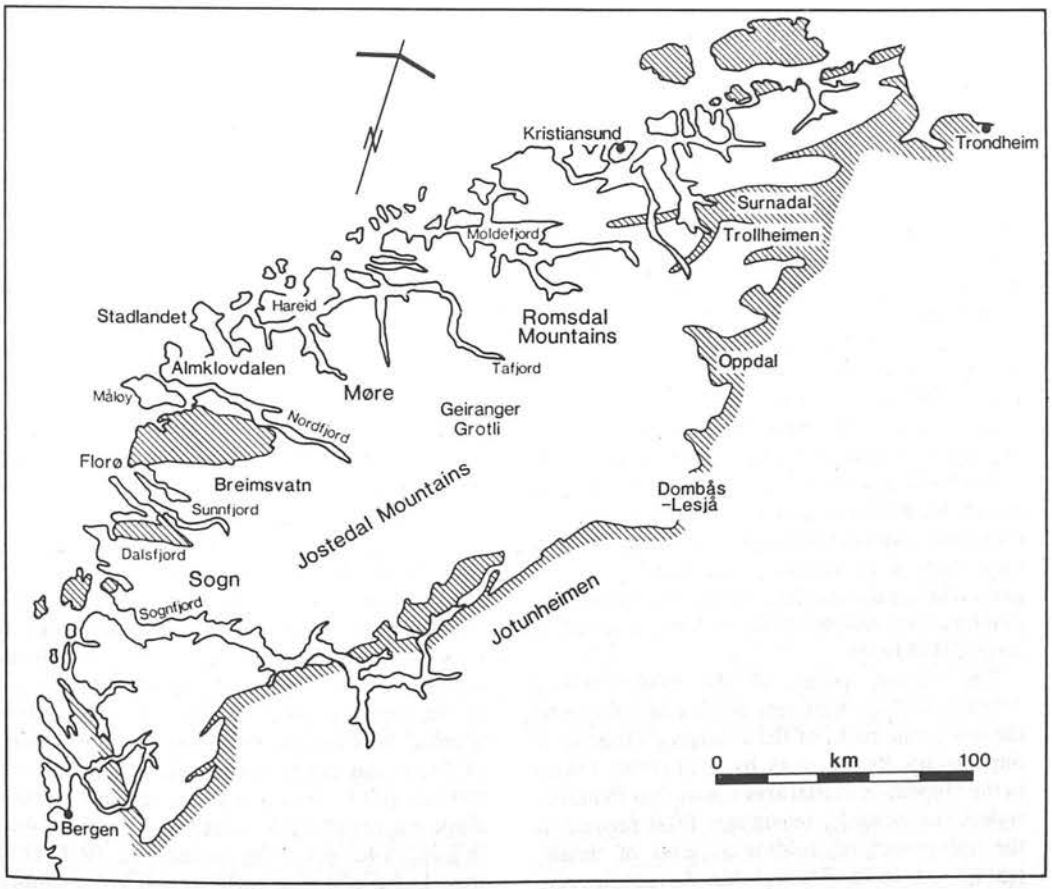

Fig. 2. Map of western south Norway showing the positions of localities mentioned in the text. Basal Gneiss Complex unshaded, higher tectonostratigraphic units shaded.

décollement (Gee, 1978, 1980). This horizon can be traced westwards below the parautochthon and allochthon within the Jämtland basement window, the Grong-Olden culmination, the Tømmerås window and the Trollheimen antiform, the last of which lies on the eastern margin of the BGC (Fig. 1).

Near the Swedish–Norwegian border the detachment surface passes into an imbricated basement, where the basement-cover sequence is repeated parautochthonously. Gee (1980), therefore, suggests that the allochthon has an origin far to the W of its present position, possibly as much as 1000 km. Imbrication of the basement in the windows implies basement shortening of at least 70 km. The metamorphic grade of the black shale increases westwards, as does the pervasive foliation in the basement associated with Caledonian thrusting.

The tectonostratigraphy of the allochthon, parautochthon and autochthon in central Scandinavia is summarized in Fig. 1. The major elements of this sequence have now been recognized in the Trollheimen antiform (Gee, 1980). They can be found further S in Oppdal (Krill, 1980; Gee, 1980) and the Dombås-Lesjå area (Guezou, 1978) and to the N and W in the Surnadal and Kristiansund areas (Krill, 1981a; Hernes, 1955; Råheim, 1972). Further to the W in the BGC strong deformation and metamorphism makes correlation more difficult. However, broadly similar sequences with a heterogeneous 'cover' sequence over a more homogeneous 'basement' are seen at Grotli (Strand, 1969; Bryhni, 1977), Tafjord (Bryhni, 1977; Brueckner, 1977), Breimsvatn (Bryhni, 1977; Bryhni & Grimstad, 1970) and possibly Sunnfjord (Skjerlie, 1969; Skjerlie & Pringle, 1978). In most of these areas it has been demonstrated that units with differing origins have been tectonically juxtaposed prior to recumbent isoclinal folding and doming. Most of these units W of Surnadal contain eclogites and garnetiferous ultrabasites. These and other high pressure metamorphic relics will be discussed in more detail below.

The eastern margin of the BGC exhibits 'Stockwerk'-type tectonics in its relationship to the low-grade rocks of the overlying Trondheim Supergroup. Recent work by Krill (1980, 1981a) in the Oppdal-Surnadal area shows that Pennine-style Caledonian F_1 recumbent folds formed in the 'infrastructure', folding a series of thrust-juxtaposed units. These folds do not involve the 'superstructure' (the Støren unit of the Trondheim Supergroup). Younger, upright folds involve both the infrastructure and the superstructure and become tighter downwards from the base of the Støren unit. Metamorphic grade increases westwards (downwards) in the superstructure, as it does in the infrastructure. Eclogites appear within 20 km of the base of the infrastructure except at Surnadal where they appear within 5 km, apparently by prograde metamorphism via amphibolites. Rb-Sr studies of metabasic dykes in the Saetra nappe and late granitic intrusions (see below) suggest that both the folding and metamorphism is Caledonian (Krill, 1981b).

It would therefore appear that the main Caledonian deformation and metamorphism occured *in-situ* beneath the superstructure apparently formed by the allochthon. Whether the present superstructure is the same as that which originally formed the overburden to the BGC during the early period of metamorphism, or whether it has tectonically replaced an earlier overburden seems equivocal at present (Krill, 1980).

The history of the nappe-pile overlying the BGC and the basement to the E has been summarized by Gee (1975, 1978) and Gee *et al.* (1982). They suggest that the early development of the nappes follows obduction of ophiolites onto the Baltic continental margin in the early Ordovician. Then final closure of the Iapetus ocean resulted in the Greenland continental margin overthrusting that of the Baltic plate during the Middle and Upper Silurian. The resulting compressional regime led to considerable basement shortening and imbrication of basement and cover. Subsequent basement uplift then resulted in translation and stretching of the nappes towards the present Caledonian front in the east.

The Seva nappe of Jämtland, Central Scandinavian Caledonides, also contains eclogite and garnet-peridotite bodies. Roermund (1981) has found that the eclogites are comparable to those in the BGC and restoration of the Seve to its possible pre-translation position reveals that the regional P–T variation seen in eclogites from this nappe complex matches that of western Norway (van Roermund, 1981; Bryhni *et al.*, 1977; Krogh, 1977a; Griffin & Mørk, 1981). As Seve lithostratigraphic units are recognized in the eastern BGC (Table 1) and can be traced into eclogite-bearing terrains (Krill, 1981a) it seems sensible to conclude that the allochthonous Seve nappe now seen in Sweden was originally rooted in the BGC, or at least had a common early metamorphic history with it.

Bordering the BGC to the S and SW is the huge Jotun nappe which consists of Precambrian anor-

Table 1. Summary of the metamorphic evolution of the coronitic metadolerites, after Griffin & Råheim (1973) and Griffin & Bryhni (1977). The development of corona types is shown for reactions between (A) igneous plagioclase and olivine; (B) igneous plagioclase and clinopyroxene; and (C) igneous plagioclase and orthopyroxene. Each column represents the order of corona shells observed at each stage in the metamorphic evolutionary sequence, with short solid lines separating successive shells. Numbers indicate the reactions responsible for each stage of corona formation, as outlined at the bottom of the table. Plag = plagioclase; Ol = Mg-rich olivine; Cpx = clinopyroxene; Opx = orthopyroxene; Sp = spinel; Gnt = garnet; Omph = omphacite; Qtz = quartz; Rt = rutile

Decreasing T, increasing P	→		→		→		→	Decreasing P T constant?
(A)								
Plag Ol	(1)	Plag Cpx *I* + Sp Opx Ol	(2) (3) (4)	Plag Cpx I + Sp Gnt Cpx II Opx Ol	(2) (3) (4) (5) (8) (9)	Plag Gnt Omph ± Opx ± Ol	(10) (11) (12)	Plag Gnt Plag II low Na Cpx high Na ± Opx, Ol
(B)								
Plag Igneous Cpx			(6) (7)	Plag Gnt Omph Cpx II + Rt	(6) (7) (8) (9)	Plag Gnt Omph + Rt	(10) (11) (12)	Plag Gnt Plag II low Na Cpx High Na
(C)								
Plag Igneous Opx			(4) (5)	Plag Gnt low Al Opx	(4) (5) (7) (8) (9)	Plag Gnt ± Qtz Omph Opx	(10) (11) (12)	Plag Gnt ± Qtz Plag II low Na Cpx high Na ± Cpx

Reactions:
(1) Ol + plag → Al-Opx + Al-CpxI + Sp. (2) Al-px's + Sp + plag → Gnt + low Al-Cpx II + low Al-Opx. (3) $6MgSiO_3 + CaAl_2Si_2O_8 + MgAl_2O_4 \rightarrow CaMgSi_2O_6 + 2Mg_3Al_2Si_3O_{12}$. (4) $4MgSiO_3 + CaAl_2Si_2O_8 \rightarrow CaMgSi_2O_6 + Mg_3Al_2Si_3O_{12} + SiO_2$. (5) $MgAl_2SiO_6 + 2MgSiO_3 \rightarrow Mg_3Al_2Si_3O_{12}$. (6) $CaMgSi_2O_6 + MgAl_2SiO_6 \rightarrow CaMg_2Al_2Si_3O_{12}$. (7) $NaAlSi_3O_8 + CaAl_2SiO_6 \rightarrow NaAlSi_2O_6 + CaAl_2Si_2O_8$. (8) $CaAl_2Si_2O_8 + CaMgSi_2O_6 \rightarrow Ca_2MgAl_2Si_3O_{12} + SiO_2$. (9) $NaAlSi_3O_8 \rightarrow NaAlSi_2O_6 + SiO_2$. (10) $CaMg_2Al_2Si_3O_{12} \rightarrow MgAl_2SiO_6 + CaMgSi_2O_6$. (11) $Ca_2MgAl_2Si_3O_{12} + SiO_2 \rightarrow CaMgSi_2O_6 + CaAl_2Si_2O_8$. (12) $NaAlSi_2O_6 + SiO_2 \rightarrow NaAlSi_3O_8$.

thosites, ultramafites, pyroxene granulites, etc., with a peripheral group of amphibolite-facies gabbroic and granitic rocks (Battey & McRitchie, 1973). It lies in a large, synclinal depression known as the 'Faltungsgraben'. Gravity studies of the nappe have shown it to be a wedge-shaped prism with a deep, dense root and a thickness of 10–15 km (Smithson, Ramberg & Grønlie, 1974). It is structurally overlain by the Trondheim nappe and underlain by Eocambrian (Sparagmitic) to

Cambro-Silurian sediments. In the S (Valdres area) the autochthonous Proterozoic basement has an autochthonous veneer of Middle Cambrian shale. This is overlain by two imbricate duplex sheets of sediments, roofed by the Valdres nappe composed of Eocambrian–Ordovician sediments, on an allochthonous gneissic basement. The Valdres nappe is in turn overlain by the Jotun nappe whose southward movement here is well established (Hossack, 1978; Hossack, Nickelson & Garton, 1981), and has caused considerable telescoping of the cover sequence. From this it has often been assumed that the Jotun nappe is a large, far-travelled thrust nappe. The existence of smaller, Jotun-like thrust sheets on the W coast of Norway (e.g. the Dalsfjord nappe) has led to the suggestion that these outcrops represent the trailing edge of the Jotun nappe and that the BGC is a tectonic window within it (Skjerlie, 1969; Hossack, 1982).

However, structural evidence from the northern margin of the Jotun nappe against the BGC may suggest that it has moved to the NW here (Battey & McRitchie, 1973; Banham, Gibbs & Hopper, 1979). This has led to the alternative suggestion that the Jotun nappe has had a local derivation, whereby it has risen directly from the root of the Faltungsgraben as an 'Ivrea-type flake' (Battey & McRitchie, 1973; Smithson *et al.*, 1974; Banham *et al.*, 1979). Underlying the northern margin of the Jotun nappe is a sequence of parautochthonous sediments and metavolcanics, locally with pillow-lavas and serpentinites (Banham *et al.*, 1979; Elliot & Cowan, 1966) and a postulated 'exotic olistostrome melange' (Gibbs, 1982). Two explanations for this are: either the northern Jotun nappe front represents a Caledonian suture zone (Banham *et al.*, 1979) or the opposing senses of motion of the nappe margins and underlying tectonostratigraphy are the result of the compressive telescoping of a rifted marginal basin, the nappe representing the root of the central graben high (Gibbs, 1982).

Along the SW extension of the Faltungsgraben lie the nappes of the Hardangervidda area and those of the Bergen arcs. Andresen & Faerseth (1982) have summarized the relationships here, which show close similarities to the Jotunheim and, to some extent, the Trondheim areas. Lying above the foreland Proterozoic basement and its cover (Vidda Group) is the Hardangervidda-Ryfylke nappe complex, whose lower unit (Hosmasjø/Nupsfonn allochton) correlates with the nappes of the Valdres area and whose upper units, the Dyrskard, Kvitenut and Revsegg units, are correlated with the Jotun nappe and perhaps, in part, the Røros schists at Surnadal. Overlying this is the Sunnhordland nappe complex, consisting of ophiolites and island-arc volcanics, possible continental rift volcanics and intrusives, allochthonous basement and later sediments associated with uplift of this sequence.

In their synthesis of this area, Andresen & Faerseth (1982) suggest that the ophiolites were obducted onto an Andean-type Baltic margin prior to the Ashgillian. Following intrusion by granodiorites this sequence was thrust over the Proterozoic basement (Dyrskard-Kvitenut-Revsegg allochthon) and the whole stack was then translated over the autochthonous basement and the Vidda Group.

Similar rocks to those of the Jotun-Hardanger areas occur in the Bergen arcs (Sturt, Skarpenes, Ohanian & Pringle, 1975; Sturt & Thon, 1976; Andresen & Faerseth, 1982). However, here the eugeoclinal rocks (Major and Minor Arcs) correspond to the Sunnhordland Nappe Complex and presumably the Trondheim nappe, but form the lowest tectonic unit above the basement gneisses and are overlain by allochthonous Proterozoic crystalline rocks (Ulrikkens Gneiss Complex, Anorthosite Complex). The Anorthosite Complex contains eclogites of postulated Caledonian, or possibly Sveconorwegian age (Austrheim & Råheim, 1981; Austrheim, 1981; Austrheim & Griffin, 1982) and may be correlated with the Jotun nappe. However, as it has had a different structural history it may represent a higher structural level than that observed in the Jotun nappe (Andresen & Faerseth, 1982). The Bergen Arcs are also commonly thought to comprise far-travelled nappes with a source off the present W coast of Norway (Sturt *et al.*, 1975; Austrheim, 1981).

A similar sequence to that in the northern Jotunheimen is found in the Dalsfjord area, Sunnfjord, where a sheet of mangerites (the Dalsfjord nappe) has been thrust over metagreywackes (Askvoll Group) and in turn overthrust by a eugeoclinal ophiolite/island arc sequence (Stavfjord anticline) prior to emplacement of the thrust stack onto the Baltic margin (now the BGC) (Skjerlie, 1969, 1974; Furnes, Skjerlie & Tysseland, 1976).

Suggested correlations of the Hardanger, Bergen and Dalsfjord nappe sequences with the Jotun nappe mitigate against its local origin and favour its evolution as a far-travelled sheet. In this case its huge thickness must have greatly contributed to the load over the eclogite-bearing BGC. However, resolution of the problems of interpretation of the structures and lithologies of

northern Jotunheimen will be necessary before a local origin can be discounted. If such an origin should be ultimately proven some very large scale mechanism must be invoked to explain the upward travel of such a large, dense mass and its super-position over less dense crustal material.

In summary, the BGC appears to consist of an intensely imbricated and interfolded mass of crystalline pre-Caledonian basement and autochthonous and allochthonous cover, the major part of which bears common relics of high pressure assemblages. It forms a window within overlying nappes of basement, cover and oceanic rocks of considerable overall thickness. Representatives of most of these allochthonous units can be found within the BGC. Three stages in the development of the orogen appear to have occurred. The first involved obduction of oceanic crust and island-arcs in the early-middle Ordovician, the second involved stacking and recumbent folding of imbricate sheets of basement, cover and obducted rocks during the early-middle Silurian continental collision and the third involved 'basement' uplift, uprooting of the nappes and their translation on a dècollement plane towards the Swedish and S Norwegian foreland. Following this, in the early-middle Devonian, late orogenic intermontane basins formed controlled by either hinged normal faults or strike-slip faults (Bryhni, 1981).

GEOCHRONOLOGY

From the foregoing it is apparent that the Caledonian history of the BGC is bracketed by two ages; the upper age of the rocks formed prior to the development of the allochthon, corresponding to the Llandoverian of the Köli Supergroup (Gee, 1975, 1978) and the early-middle Devonian age of the late-orogenic, unmetamorphosed sediments found in fault-bounded basins on the W coast of Norway. These sediments overlie eclogite-bearing gneisses and must therefore mark the end of a period of very considerable uplift, especially if a Caledonian age and crustal *in-situ* metamorphic origin for the eclogites is accepted (see below).

Viewing the ages obtained from whole-rock Rb-Sr isochron studies of gneisses in the BGC (e.g. Brueckner, 1972, 1979) it is noticeable that they bear a close similarity to those seen in the Svecofennian and Sveconorwegian provinces in the foreland of southern Norway and Sweden, although perhaps the age distribution in the BGC is more complex. However, mineral ages are markedly different. Mineral ages in the Baltic foreland unaffected by the Caledonian orogeny are usually similar to the whole-rock ages (Brueckner, 1972) but in the BGC Rb-Sr mineral ages generally show late Caledonian provenance, clustering tightly between 380 Ma, and 405 Ma. This is perhaps not surprising in view of the position of the BGC in relation to the rest of the Caledonide belt, but considerable controversy revolves around the interpretation of these ages.

One school of thought is that the Proterozoic whole-rock Rb-Sr ages represent a metamorphic event, usually at amphibolite facies, and that the Caledonian Rb-Sr mineral ages are a result of post-orogenic cooling related to uplift or of a relatively unimportant thermal event resetting the isotopic system (Råheim, 1977, 1979; Pigeon & Råheim 1972; Skjerlie & Pringle, 1978; Solheim, 1980; Mearns & Lappin, 1982 a,b,c). That implies that most, if not all the major metamorphism in the BGC occurred in the Sveconorwegian or Svecofennian and the Caledonian effect is minimal. The pervasive nature of the amphibolite-facies metamorphism, allied with independent evidence for a Caledonian eclogite-forming event has led Mearns & Lappin (1982 a,c) and Gebauer *et al.* (1982) to suggest that the eclogites were tectonically introduced into the gneisses from deeper lithospheric levels during the Caledonian orogeny. Mearns & Lappin (1982c) from a study of granulite-facies 'mangerites' in the Selje area, Stadlandet, further suggest the influence of a 700 Ma granulite-facies event which seriously disturbed the Rb-Sr system by Rb loss after intrusion at 1520 Ma. However, Lappin, Pidgeon & van Breemen (1979) have shown that the composition of these rocks has not changed significantly since intrusion except for some K-metasomatism. Furthermore, there are no other records of an important 700 Ma granulite-facies event. This age comes from a plagioclase–garnet whole-rock Sm-Nd isochron for a basic dyke and may either be a mixed age or a relict igneous age.

Research workers who consider whole-rock Rb-Sr isochrons to record a metamorphic event clearly recognize that the low initial ratios of these isochrons puts severe constraints on the time which elapsed between magmatic crystallization of the rock suite and metamorphism. In fact the time period may easily lie within the error envelope of the isochron age. Upper intersection U-Pb ages from discordant zircons are often close to Rb-Sr whole rock ages and are taken to indicate the time of magmatic crystallization (Pigeon & Råheim, 1972; Lappin *et al.*, 1979). Lower inter-

section ages are usually around 400 Ma suggesting a pervasive Caledonian event.

The other school of thought considers that whole rock Rb-Sr isochrons represent magmatic crystallization ages and that subsequent events have only caused minor disturbance to the isotopic system (Brueckner, 1972, 1979; Carswell & Harvey, 1983; Harvey, unpublished data; Krill & Griffin, 1981). The significance of the Caledonian mineral ages is less certain. Brueckner (op. cit.) gives two possibilities; that the metamorphism was Proterozoic but a slight re-heating event reset the mineral ages ('limited Caledonization') or that the most severe recrystallization was Caledonian ('severe Caledonization'). With respect to the latter, Brueckner (1979) points out that the youngest good whole-rock ages for the gneisses are 960 Ma (granodiorite near Geiranger) and 975 Ma (Hestbrepiggan granite). Both of these rock suites have a pervasive tectonic fabric which must have been imposed during either the late Sveconorwegian or the Caledonian. In addition to this we note that the evidence of Gee (1980) and Krill (1980) in favour of a Caledonian age for the main deformation in the BGC strongly supports a 'severe Caledonization'. Also, Krill (1981a) reports a 745 Ma whole rock Rb-Sr date for a pretectonic dyke in the Saetra unit near Oppdal and a 345 Ma Rb-Sr mineral isochron age from a granitic intrusion cutting a regionally mapped thrust surface in the same area, bracketing tte tectonic events within the Caledonian orogeny.

A recent study of coexisting green (Caledonian) and brown (Sveconorwegian) biotites from near the Caledonian front in SW Norway (Verschure, Andressen, Boelrijk, Hebden, Maier, Priem & Verdurmen, 1980) shows that resetting of biotite Rb-Sr and K-Ar ages at temperatures of up to 400°C may require complete recrystallization. This brings into question the validity of models requiring a limited Caledonian heating event. Krill & Griffin (1981) comparing interpretations of whole rock Rb-Sr ages from the BGC with those in the Alps suggest that such ages can record magmatic events despite very strong tectonism and metamorphism. They reject the likelihood of large-scale homogenization of isotope systems during orogenesis.

Whilst it is not intended to review the distribution of whole-rock ages within the BGC, it is significant that all reliable ages for gneisses are either Svecofennian or Sveconorwegian, dominantly the former. Good evidence for Caledonian protolith ages comes from Gee's (1980) correlation of Cambrian sediments into the Trollheimen area. Other evidence comes from the common lithological comparison of metaquartzites and arkoses with the Eocambrian Sparagmites of southern Norway.

We, therefore, prefer the interpretation that whilst the main crust-forming events for lithologies in the BGC were Proterozoic, the tectonic and metamorphic events responsible for the present state of this area were dominantly Caledonian.

Outside the BGC in S Norway granulite-facies assemblages are common in Proterozoic gneisses. Also, relict granulite-facies parageneses are sometimes found within amphibolite-facies gneisses of the BGC (Lappin *et al.* 1979; Krogh, 1980a, Mearns, 1982; Cuthbert, unpublished data). In view of the Proterozoic provenances of the BGC gneisses, it seems reasonable to expect to encounter relics of such older parageneses. Bryhni, Fitch & Miller (1971) carried out $^{39}Ar/^{40}Ar$ age spectrum analysis on a clinopyroxene from an augen-gneiss in the Fjordane complex, Gloppen. The most retentive argon gave an age of 1550 Ma, which may record the age of its crystallization, under granulite-facies conditions.

However, eclogite-facies relics are also found in the gneisses, as eclogites, garnet peridotites and isolated gneissic domains containing omphacitic pyroxene or diopside–plagioclase symplectites. These also show the influence of pervasive later amphibolitization. At Flekke, Sunnfjord, low-pressure granulites are preserved (Opx + Cpx + plag + K-feldspar + quartz) with garnet coronas forming on orthopyroxene aggregates (Cuthbert & Carswell, 1982). This is taken to indicate a superimposed higher pressure (and lower temperature) event, correlated with similar textural development in partially eclogitized metabasites. Identical relationships are seen at Flatraket, Stadlandet (Cuthbert, unpublished data) and in the Bergen Arcs (Austrheim & Griffin, 1982). In all these areas subsequent pervasive amphibolite-facies recrystallization has occurred. Hence there is evidence here that a high pressure event postdates the Proterozoic granulites and predates the amphibolite-facies metamorphism. Resolution of the complex polymetamorphic history of the BGC undoubtedly requires very careful petrographic observations before any *a-priori* assumptions can be made about the relative (or absolute) ages of the mineral parageneses.

Recent evidence has begun to throw light on the age of eclogite formation. Krogh, Myson & Davis (1973) reported a U-Pb zircon age of 401 ± 20 Ma from the Ulsteinvik eclogite, Hareidland. The zircons contained inclusions of eclogite-facies

minerals but no secondary minerals, hence the age was taken as a minimum age for formation of the eclogite. However, this age is not entirely unambiguous in that it only provides an upper limit for this event and there is evidence for some older, inherited zircon in the rock.

Griffin & Brueckner (1980) have presented five two-point Sm-Nd mineral isochrons using garnets and clinopyroxenes from eclogites. Ages in the range 407–477 Ma were obtained, in close agreement with the results of Krogh *et al.* (1973) and slightly older than, but overlapping with, Rb-Sr mineral ages from the gneisses. Sm-Nd and Rb-Sr isotope systematics suggest that at least some of the eclogite protoliths had a long crustal history prior to the Caledonian orogeny. Further work (Griffin & Brueckner, 1982) has demonstrated the difficulty of obtaining meaningful Sm-Nd ages from eclogites with equilibrium temperatures below about 700°C due to disequilibrium distribution of REE between garnet and pyroxene. Samples with zoned garnets tend to give much older ages. A five-point Rb-Sr mineral isochron from the Verpeneset eclogite, Nordfjord, gave an age of 398 ± 1 Ma with an initial ratio of 0.7034, suggesting that the protolith is probably Palaeozoic and thus the metamorphism Caledonian.

Mearns & Lappin (1982b) have reported Sm-Nd garnet–clinopyroxene whole-rock isochron ages for garnet lherzolites and associated garnet pyroxenites as well as for an 'external' or 'country-rock' eclogite and a garnet whole-rock age from a grey gneiss. The eclogite gave an age of 408 ± 8 Ma, the gneiss 414 ± 31 Ma, suggesting recrystallization or 'thermal resetting' of Proterozoic material during the Caledonian orogeny. The ultramafites gave much older ages and a low εNd (1029 ± 34 Ma, $\varepsilon Nd = -1.6$; 1316 ± 138 Ma, $\varepsilon Nd = -1.4$) suggesting crystallization soon after formation of the whole-rock in the mantle and that these rocks have apparently not been disturbed by any Caledonian metamorphic events.

Gebauer *et al.* (1982) have also reported Caledonian ages for eclogites from U-Pb zircon discordia, which suggest protolith formation in the Svecofennian and Sveconorwegian and eclogite metamorphism at about 400 Ma.

Krill (1981) has produced a Rb-Sr whole rock isochron for an intermediate gneiss which is interbanded with eclogite-bearing mica schists of the Blåho unit W of Oppdal, giving an age of 583 ± 69 Ma. This further supports a Caledonian age for the eclogite metamorphism.

Some indication of the severity of the Caledonian thermal event is given by Devonian mineral ages from pegmatites which cut eclogites, indicating temperatures high enough to cause anatexis well into the waning stages of the orogeny (Griffin & Mørk, 1981).

Together these various data strongly indicate that the major crust-forming events for the lithologies in the BGC were Proterozoic, dominantly in the Svecofennian but with significant contributions from the Sveconorwegian and Caledonian events. It is quite possible that much of this crustal (and mantle?) material suffered high-grade amphibolite and/or granulite facies metamorphism prior to the early Palacozoic, but a growing body of evidence supports a major tectonometamorphic event in the BGC during the Caledonian orogeny, commencing at least as early as 420 Ma. The significance of the eclogite mineral ages depends upon prejudicial interpretation of the origins of these controversial rocks (*cf.* Bryhni *et al.*, 1977; Lappin & Smith, 1978; Smith, 1980; Carswell & Gibb, 1980; Griffin *et al.*, 1981), but it is possible that this orogenic event involved depression of very large masses of continental crust to great depths prior to their exhumation and exposure at the land surface by the early to middle Devonian.

METAMORPHIC EVOLUTION OF THE BASAL GNEISS COMPLEX

Much of the research carried out in the BGC has centred around two rather exotic and enigmatic rock-types, the eclogites and the garnetiferous peridotites. This is especially true of work during the last 20 years; a result of the surge of interest in the nature of the upper mantle. The fact that these eclogite-facies assemblages occur in a terrain apparently consisting largely of amphibolite-facies assemblages has caused discussion of an intensity which is out of all proportion to their rather insignificant volume. This metamorphic contrast has led to the eclogites being described as 'foreign inclusions' (e.g. Lappin, 1966) and evolutionary models involving tectonic transport of eclogites and peridotites from sub-crustal depths to high lithospheric levels have been developed to explain their presence (Lappin & Smith, 1978; O'Hara, 1976; Smith, 1980).

There is, however, a growing body of evidence (outlined below) to suggest that in many cases eclogites and even garnet peridotites have been formed by metamorphism *in-situ* within their country rocks. Conclusive proof of this has profound tectonic consequences as it implies that large masses of buoyant continental crust have

been subjected to unusually large confining pressures.

Occurrence of eclogite-facies rocks

Eclogites occur in both the Jostedal and Fjordane complexes of Bryhni (1966), but are more common in the latter unit. They are also reported from the Vikvatn sequence in the Tafjord area, but not in the basal Fetvatn gneisses (Brueckner, 1977). They occur in the Frei group of the Kristiansund area (Råheim, 1972; Griffin & Råheim, 1973; Krogh, 1980b) and in Surnadal (Tørudbakken, 1981). Hence the eclogites occur in most, if not all, of the lithologic units of the BGC, to within 25 km of its border with the overlying allochthon in the E. However, eclogites are apparently absent in the BGC to the S of Sognfjord.

In the more heterogeneous rock sequences (e.g. the Fjordane complex) eclogites are frequently associated with anorthosites (Eskola, 1921; Brueckner, 1977; Bryhni, 1966; Brastad, 1983; Griffin & Mørk, 1981) as well as obvious supracrustal rocks (Bryhni, 1966; Carswell & Harvey, 1983; Harvey, unpublished data). Garnet peridotites appear to be confined to these heterogeneous gneisses (Bryhni, 1966; Carswell, 1973a; Brueckner, 1977) but are generally absent to the S of Nordfjord, where hydrous peridotites are more normally present. The close association of some peridotites to what are apparently layered basic bodies and to anorthosites has often been noted (Schmitt, 1964; Eskola, 1921; Brueckner, 1977; Bryhni, 1966; Brastad, 1982). Some authors have noted the common occurrence of garnet peridotites in steeply inclined shear belts (Bryhni, 1966; Lappin, 1966) but Brueckner (1977) considers this to be due to their 'stratigraphic' position on the limbs of large-scale folds.

Lappin (1966) suggested that eclogites share most of the structural history of the surrounding gneisses at Selje, Stadlandet, and Almklovdalen, but that anorthosites and garnet peridotites were introduced at successively later stages. However, Medaris (1980) has found that all the structural elements in the gneisses at Almklovdalen are shared by the peridotites. Similar relationships occur in peridotites at Rødskaret, Gurksøy (Griffin and Mørk, 1981). At Kalskaret, Tafjord, peridotites, anorthosites, eclogites and gneisses have all undergone the same structural history (Brueckner, 1977). At Bjørkedalen, eclogites show gradational contacts towards anorthosites and close association with peridotites, all of which have at least two fold episodes in common with the gneisses (Brastad, 1982, 1983). In all these examples the earliest obvious pervasive foliation is associated with amphibolite facies assemblages which postdate the eclogite-facies parageneses. Hence the eclogites and garnet peridotites can be described as relics whose mineral facies would appear to have converged with that of the gneisses during deformation associated with amphibolite-facies metamorphism.

Foreign versus in-situ metamorphism

Early arguments in favour of the foreign tectonic origin of eclogites and peridotites stemmed from the apparent difference in metamorphic grade between these rocks and their host gneisses, the commonly sheared margins of the bodies and, in the case of the peridotites, the lack of a thermal metamorphic aureole around them (O'Hara & Mercy, 1963; Lappin, 1966; Carswell, 1968a). Later evidence in favour of this hypothesis came from geothermometric/geobarometric studies. Lappin & Smith (1978) derived temperatures of 700–800 C and pressures of 30–45 kbar for primary assemblages in orthopyroxene-eclogites from Stadlandet, using the

$$K_D^{\text{Gt–Cpx}}{}_{Fe^{2+}/Mg^{2+}}$$

method of Råheim & Green (1975), the two-pyroxene solvus of Wood & Banno (1973) and the solubility of alumina in orthopyroxene and garnet (Wood & Banno, 1973). Reconstruction of the composition of an early high-Al orthopyroxene, now containing exsolution lamellae of garnet, and an early clinopyroxene with lamellae of orthopyroxene allowed estimates of pre-exsolution conditions at 1200–1370°C, and 30–40 kbar. Similar results were obtained by Carswell (1973b) for an exsolved orthopyroxene lens within a garnet-peridotite. In both cases it was postulated that the rocks formed in the upper mantle prior to tectonic intercalation into the crustal rocks.

More recent arguments in favour of the foreign origin of the eclogites and garnet-peridotites have centred around the radiometric age differences between these rocks and their host gneisses, the arguments for and against which are outlined above. The emphasis of interpretation for the eclogites has now shifted from an origin in the upper mantle to one in subducted or deeply obducted oceanic crust (O'Hara, 1976; Gebauer *et al.*, 1982; Mearns & Lappin, 1982a; Smith, 1981). Smith (1980, 1981) has expanded upon this idea, suggesting that the diversity of lithologies and mineral facies found within the BGC is a result of

production of a 'gigantic tectonic mèlange' during Caledonian orogenesis which shuffled rocks from a range of lithospheric levels with little mineralogical or isotopic re-equilibration. While this idea may provide a crude description of the tectonostratigraphy of the BGC, it is considered that the information presented in this synthesis shows that Smith's (1980) model breaks down under detailed scrutiny.

Much of the geological evidence in favour of the foreign origin hypothesis is equivocal. The sheared margins often seen on bodies of eclogite in the gneisses can be more simply explained by differential movement of the eclogite during boudinage of a continuous metabasic sheet within the less competant gneisses. At Flemsøy, Sunnmøre, bodies of corona-bearing metadolerite are frequently boudinaged. Sheared margins are frequently transformed to eclogite and field evidence suggests that bodies of eclogite in the country-rock have been torn from the dolerite margins during deformation. These are indeed 'foreign inclusions', but movements of no more than a few metres are required to explain their present position (Mørk, 1982).

The lack of a thermal metamorphic aureole around the peridotites is perhaps not surprising in view of their complex structural history, during which deformation would surely have obliterated the evidence for any such aureole and has certainly frequently disrupted any observed backwall metasomatic reaction zones. Geochemical evidence (Carswell, Krogh & Griffin, 1983) from some of the more iron-rich garnetiferous peridotites such as in the Eiksunddal eclogite complex (Schmitt, 1964) suggest that these were probably of low pressure igneous origin, originally having been olivine gabbro–peridotite cumulates.

Unequivocal geological evidence in favour of a foreign origin for the eclogite-facies inclusions in the gneisses is difficult to envisage. As the most feasible mechanism for tectonic emplacement might be introduction along large crustal dislocations, one might expect to find eclogites strongly associated with major lithological boundaries. This has not been demonstrated as yet, to our knowledge, although such a situation may be complicated by polyphase folding following emplacement. However the observation that peridotites are sometimes associated with shear zones (Bryhni, 1966; Lappin, 1966) is interesting in the light of continuing assertions that these rocks were indeed foreign to the continental crust prior to the eclogite-forming metamorphism (Carswell & Gibb, 1980; Medaris, 1980).

Geological evidence in favour of crustal eclogite-facies metamorphism can perhaps be divided into two types. The first is the preservation of features demonstrating that the rock was indigenous to its surrounding crustal rocks prior to eclogite-facies metamorphism. The second is the preservation of features within the rock showing that its protolith had a low-pressure origin. If evidence for only the latter exists it is difficult to deny a foreign origin, as deep level obduction (Lappin, 1977; Lappin & Smith, 1978; Smith, 1980, 1981) of eclogitic oceanic crust may explain its present position. If the surrounding crustal rocks have co-facial high-pressure parageneses then *in-situ* metamorphism is likely to have occurred, but this says little about the pre-metamorphic tectonic history of the eclogite. In view of the known tectonostratigraphy of the BGC it is not unlikely that fragments of oceanic crust formed part of the early nappe pile (*c.f.* Krill, 1980, 1981).

Evidence for the crustal derivation of eclogites has been reviewed by Bryhni *et al.* (1977), Krogh (1977a) and Griffin *et al.* (1981) and in several contributions in Griffin & Mørk (1981). Perhaps the most obvious indigenous crustal eclogites are the sills and dykes of metadolerites and metabasalts which preserve relics and eclogitic pseudomorphs of low-pressure igneous phases. These are known from the Surnadal synform (Tørudbakken, 1981; Tørubakken & Råheim, 1981), the Molde peninsula (Harvey, unpublished data; Carswell & Harvey, 1983), Kristiansund (Råheim, 1972; Griffin & Råheim, 1973), Sunnmøre (Mørk, 1982; Gjelsvik, 1952), Flatraket, Stadlandet (Lappin, 1966), Måløy (Bryhni *et al.* 1977) and Dalsfjord, Sunnfjord (Cuthbert & Carswell, 1982; Cuthbert, unpublished data). Original igneous margins are preserved at Midøy, Moldefjord (Griffin & Carswell, 1983), at Flatraket and Måløy, where the dykes intrude granulite facies mangerites (Bryhni *et al.*, 1977) and at Dalsfjord (Cuthbert & Carswell, 1982; Cuthbert, unpublished data). Where the margins of these bodies are sheared but not hydrated, granoblastic aggregates of garnet and omphacite occur which are often indistinguishable from the eclogite pods found elsewhere in the gneisses.

Within these metadolerites the original igneous assemblage appears to have been plagioclase + clinopyroxene ± olivine ± orthopyroxene ± oxides. The common coexistence of plagioclase and olivine indicates crystallization at pressures certainly less than 10 kbar (Mysen & Heier, 1972) and temperatures greater than 1100°C. A sequence of corona-forming reactions has pro-

gressively transformed this assemblage to essentially bimineralic eclogite. These reactions are summarized in Table 1, and discussed further below.

Layering is a common feature of both eclogites and garnet peridotites. At Ulsteinvik and Eiksunddal eclogite mineralogical layering has been demonstrated to mimic original igneous layering, sometimes rhythmic in character (Schmitt, 1964; Mysen & Heier, 1972; Carswell *et al.*, 1983). Other types of layering in eclogites may be a result of eclogitization of sediments, or interbanded sediments and igneous rocks. A number of occurrences of eclogite along western Nordfjord expose interbanded pyroxene-rich or quartz-rich layers (Bryhni, 1966; Bryhni & Griffin, 1971; Bryhni, 1981) and in the Moldefjord area marble lenses occur within a large area of retrograded eclogite. The marbles contain silica-rich layers and grade into eclogites (Hernes, 1954; Carswell & Harvey, 1983; Harvey, unpublished data). Carswell & Harvey (1983) consider these rocks to have been submarine basic volcanics interbedded with limestones.

High-pressure assemblages in the gneisses

It has been recognized for some time that high-pressure parageneses are occasionally preserved in the gneisses.

Pelitic gneisses adjacent to the Ulsteinvik eclogite, Hareidlandet, contain the assemblage garnet + omphacite + biotite + plagioclase + quartz, the omphacite now being represented by a diopside–plagioclase symplectite. Gneissic meta-xenoliths in this eclogite have the assemblages garnet + orthopyroxene + plagioclase + quartz and garnet + kyanite + clinopyroxene + plagioclase + quartz. Garnets in these xenoliths contain inclusions of omphacitic pyroxene (Mysen & Heier, 1972; Griffin & Mørk, 1981). These assemblages suggest metamorphism under the same conditions as the eclogite (800°C, and 18 kbar–Griffin *et al.*, 1981).

Syenitic gneisses from Tafjord also locally contain symplectic clinopyroxenes (Brueckner, 1977), as do some augen gneisses in the Moldefjord area (Carswell, 1981; Carswell & Harvey, 1983). In the latter case the symplectites are rimmed by rather grossular-rich garnet coronas, suggesting equilibration at >9 kbar at 700–800°C (*cf.* Green and Mysen, 1972).

In the intermediate augen-gneisses (mangerites) at Flatraket, Stadlandet, and Måløy, the assemblage garnet $\pm$ clinopyroxene + plagioclase + K-feldspar + quartz $\pm$ kyanite is found, garnet–clinopyroxene pairs giving the same equilibration temperatures as the adjacent eclogites (Krogh, 1977b, using

$$K_D \begin{matrix} \text{Gt–Cpx} \\ Fe^{2+}/Mg^{2+} \end{matrix}$$

as for Ellis & Green, 1979).

Krogh (1980a,b) has demonstrated co-facial eclogites and gneisses from two areas; Førde, Sunnfjord and Kristiansund. At Førde, rather low-temperature eclogites record conditions of 630 ± 35°C, 15.0 ± 2.5 kbar (Naustdal) and 540 ± 35°C, 12.5 ± 2.5 kbar (Kvineset). In the gneisses garnet-omphacite pairs give similar temperatures (Ellis & Green, 1979). The assemblages annite + K-feldspar + magnetite + quartz, ferropargasite + garnet + plagioclase + clinopyroxene + magnetite + quartz, garnet + acmitic clinopyroxene + plagioclase + magnetite and garnet + phengite + annite + quartz which occur in the gneisses are also compatible with the conditions deduced for the eclogites. At Kristiansund, three garnet granulite samples contain garnet + clinopyroxene + quartz + epidote $\pm$ plagioclase $\pm$ amphibole $\pm$ rutile, the garnets containing inclusions of clinopyroxene, quartz and rutile or clinopyroxene, quartz, biotite and white mica. Using garnet–clinopyroxene pairs, jadeite content of omphacite, garnet + clinopyroxene + plagioclase + quartz in the absence of orthopyroxene and $CaAl_2Si_2O_6$-rich clinopyroxene + quartz, conditions for the granulites are estimated at 18.5 $\pm$ 3.0 kbar and 750 ± 50°C (see Fig. 4).

On Midøy, Moldefjord, anatectic backveins of gneiss in eclogites preserve the assemblage Ca-rich garnet + kyanite + plagioclase + quartz $\pm$ K-feldspar $\pm$ omphacite. Geobarometry on this assemblage (method of Ghent, 1976) gives a pressure of 19–21 kbar at 750°C. This pressure is the same as that deduced for many eclogites in this area. Hence, in this case, both geological and mineral-chemical data suggest an *in-situ* metamorphic origin for the eclogite (Griffin & Mørk, 1981; Griffin & Carswell, 1983). The assemblage garnet + plagioclase + kyanite + quartz is being discovered widely in the BGC and gives metamorphic conditions compatible with those for adjacent eclogites (Griffin, pers. comm., 1982).

Similar anatectic backveins are known from the Førde area (Krogh, 1980a) and the Dalsfjord area (Cuthbert, unpublished data) in Sunnfjord, where they contain garnet + (diopside + plagioclase symplectite) or omphacite + phengite + quartz and are gradational into garnet + omphacite + phengite eclogites.

Hence it is becoming apparent that high-

pressure assemblages are not uncommon in the gneisses. Indeed, they may prove to be as common as the more obvious eclogites and garnet peridotites. However, in common with the latter, these assemblages are often retrograded to hydrous amphibolite-facies assemblages.

Orthopyroxene eclogites and garnet peridotites

In a recent review of orthopyroxene-bearing eclogites in the BGC, Carswell *et al.* (1983) have derived metamorphic equilibration pressures considerably lower than those obtained earlier by Lappin & Smith (1978). Eclogites within gneisses ('external eclogites') have values of 700–740°C, and 17–18 kbar, whilst 'eclogites' (garnet websterites) forming layers within garnet peridotite gave 710 C, and 20 kbar. Hence conditions deduced for these rock types appear to be mutually compatible and also match conditions for more aluminous eclogites and high-pressure granulites in the NW coastal areas of the BGC.

Considerable disequilibrium among orthopyroxene, clinopyroxene and garnet exists in these rocks and may have been the cause of previous anomolously high pressure estimates. Furthermore Carswell *et al.* (1983) suggest that the pyroxenes with exsolution features were probably never in equilibrium with garnet, invalidating the high pressure and temperature values derived from the reconstructed mineral analyses (Carswell, 1973a; Lappin & Smith, 1978).

An upper mantle origin for some of the peridotites is still postulated (Carswell, 1968a, b, 1973b; Carswell & Gibb, 1980; Carswell *et al.*, 1983; Medaris, 1980, 1982) on the basis of bulk-rock geochemistry, mineralogical comparisons with nodules from kimberlites and geothermobarometry. Until recently there has been a tacit assumption that they represented primary sub-continental mantle, but recent evidence has complicated the issue. Griffin & Qvale (1981, see also Griffin & Mørk, 1981) have favourably compared the composition of an eclogite body within the Almklovdalen peridotite at Raudkleivane with that of ferroan basaltic amphibolite dykes in Caledonian alpine-type serpentinites from the Bergen area. The Raudkleivane eclogite contains garnets with strong prograde zoning (see below) and amphibolite facies mineral relics and it is inferred that this peridotite has evolved by prograde ('crustal') metamorphism of a serpentinized peridotite.

Carswell *et al.* (1983) have reported the presence of early spinel relics with garnet coronas in geochemically similar peridotites to that at Almklovdalen, providing further evidence of prograde metamorphism. This raises the possibility that some of the garnet peridotites may have been derived from sub-oceanic mantle. Some features of garnetiferous peridotites like those at Kalskaret, Tafjord (Carswell, 1968a) are similar to those described in some ophiolites containing primary high P–T mantle assemblages (Spray, 1982). These are thought to be fragments of lithosphere from incipient rifts or marginal basins where large scale mantle diapirism has taken place. This similarly deserves further investigation, particularly in view of the contention of Gebauer *et al.* (1982) that some eclogites had basaltic protoliths originating in back-arc basins.

The uniformity of P–T estimates for eclogites and garnet peridotites indicates that, whatever their origin, they have been metamorphosed under very high confining pressure. Carswell & Gibb (1980) have suggested that the peridotites gained their present mineralogical constitution *after* emplacement into their present host rocks during high P/T metamorphism operative on a regional scale.

Prograde and retrograde metamorphism and P/T trajectories

Evidence for a low-pressure pre-eclogite facies metamorphism is commonly preserved in eclogites in the BGC, in the form of corona structures and compositional zoning in minerals, usually in garnets.

Table 1 shows the sequence of corona-forming reactions, as described by Griffin & Bryhni (1977), Griffin & Råheim (1973) and Griffin & Heier (1973). Early reactions consume the solidus phases, producing low-pressure granulite assemblages (e.g. aluminous pyroxenes + spinel + plagioclase) then high-pressure granulites (garnet + low Al pyroxenes + plagioclase) before final consumption of plagioclase to produce omphacitic pyroxene and almandine-pyrope-grossular garnet. Griffin & Råheim (1973) considered that these reactions were a continuous sequence occurring during cooling and compression from solidus conditions. However, studies in the anorthosites of the Bergen Arcs show that although this may have been the case for the granulite-facies coronas, the eclogite event was superimposed at a later, separate stage (Austrheim & Griffin, 1982). Also at Dalsfjord, Sunnfjord, low-temperature breakdown of plagioclase predates the eclogite-facies corona assemblage, implying considerable cooling prior to eclogitization (Cuthbert & Carswell, 1982; Cuthbert, unpublished data). Late

stage breakdown of omphacite and garnet produce secondary plagioclase coronas, which Griffin and Råheim (1973) have interpreted as being a result of strong decompression.

Although the coronites provide striking examples of eclogitization of low-pressure protoliths, the likelihood of temporal breaks in their evolution and strong overstepping of the stability fields of the minerals involved (*cf.* Griffin & Råheim, 1973) makes construction of P/T trajectories for their evolution difficult.

Chemical zoning in garnets is common in the eclogites and, locally, the gneisses southwards from Nordfjord. Relict mineral suites (including amphibole, zoisite, white mica, feldspars and pyroxenes) are often preserved within garnets. Thus these rocks provide a useful window for examination of the pre-eclogitic history of the BGC.

Two early studies (Bryhni & Griffin, 1971; Råheim & Green, 1975) discussed the interpretation of compositional zonation in garnets. The factors affecting zoning patterns include rates of intergrain and volume diffusion (controlled by temperature, fluids, deformation and cooling rate), fractionation due to removal of components from the reacting system into earlier grains, distribution coefficients (K_D) for continuous exchange reactions and availability of new components during mineral breakdown resulting from discontinuous reactions. The latter two are P/T dependent. The good correlation between mineral compositional variation and zonal changes in inclusion suites (e.g. Bryhni *et al.*, 1977; Krogh, 1980a, and unpublished data) suggests a strong P/T effect and therefore confirms the usefulness of these features in the deduction of P/T histories.

Figure 3 shows zoning profiles from three eclogite garnets, from Gjørlanger by Dalsfjord, Sunnfjord (Cuthbert, unpublished data), Verpeneset, Nordfjord (Bryhni & Griffin, 1971; Krogh, unpublished data) and Langvatnet, Molde peninsula (Harvey, unpublished data). The examples from Gjørlanger and Verpeneset both contain relict amphibolite-facies assemblages in garnet cores and eclogite-facies assemblages nearer the rims. The amphibolite–eclogite transition is marked by a strong rimward increase in pyrope content and a decrease in spessartine and almandine. In the Verpeneset example amphibole compositions show a systematic variation from the core, with a marked change at the eclogite transition. Similar patterns are found in eclogites from the Naustdal area, Sunnfjord (Krogh, 1980a) but the rim zone assemblages and the eclogite matrices are characterized by the presence of glaucophanitic amphibole. Although these patterns can be partly explained by chemical fractionation, the evidence for prograde metamorphism is particularly convincing here.

Suggested P/T paths for the Sunnfjord eclogites and gneisses (after Krogh, 1980a) and the Verpeneset and Romsdalshorn eclogites are shown in Fig. 4. Maximum conditions for the Sunnfjord area are 510–630°C, and 12–15 kbar (Krogh, 1980a; Cuthbert & Carswell, 1982; Cuthbert, unpublished data) and for the Verpeneset eclogite are 740°C, and 17–19 kbar.

In contrast to the above, the Langvatnet eclogite garnets show rather flat profile (Fig. 3) and narrow, retrogressive rims (decreasing $Mg^{2+}/(Mg^{2+} + Fe^{2+})$; Mn and Ca show similar profiles). The garnets sometimes contain inclusions of rutile, omphacite and quartz, with no obvious zonal arrangement. Similar profiles are reported for an eclogite garnet from Reset, outer Romsdal (Krogh, unpublished data) and appear to be common in eclogites where

$$K_{D\,Fe^{2+}/Mg^{2+}}^{Gt\text{–}Cpx}$$

is less than 6.0, corresponding to temperatures above about 725°C. This may be a result of more effective volume diffusion in garnets at these high temperatures, wiping out any prograde zoning. The narrow, retrograde rims may thus represent late growth or restricted re-equilibration due to limited intergrain diffusion below this threshold temperature. The matrix omphacites have lower jadeite contents than the inclusions, possibly reflecting a significant drop in pressure at a late stage. This is the opposite to the situation found in prograde eclogite garnets at Naustdal (Krogh, 1980a) and Verpeneset (Krogh, unpublished data).

Secondary, retrogressive features of eclogites include breakdown of omphacite to diopside–plagioclase or amphibole–plagioclase symplectites, breakdown of garnet + quartz to produce enstatite + plagioclase, and reaction of garnet + clinopyroxene to produce amphibole + plagioclase ± enstatite symplectites. Phengites in eclogites and gneisses breakdown to biotite + phengite or biotite + K-feldspar + kyanite. Glaucophane and barroisite may be replaced by amphiboles more similar to those in garnet cores. Prograde garnets (e.g. Fig. 3c) show narrow retrograde rims in some cases. Latest stage alteration involves the formation of chlorite and epidote after garnet (Krogh, 1977a, and un-

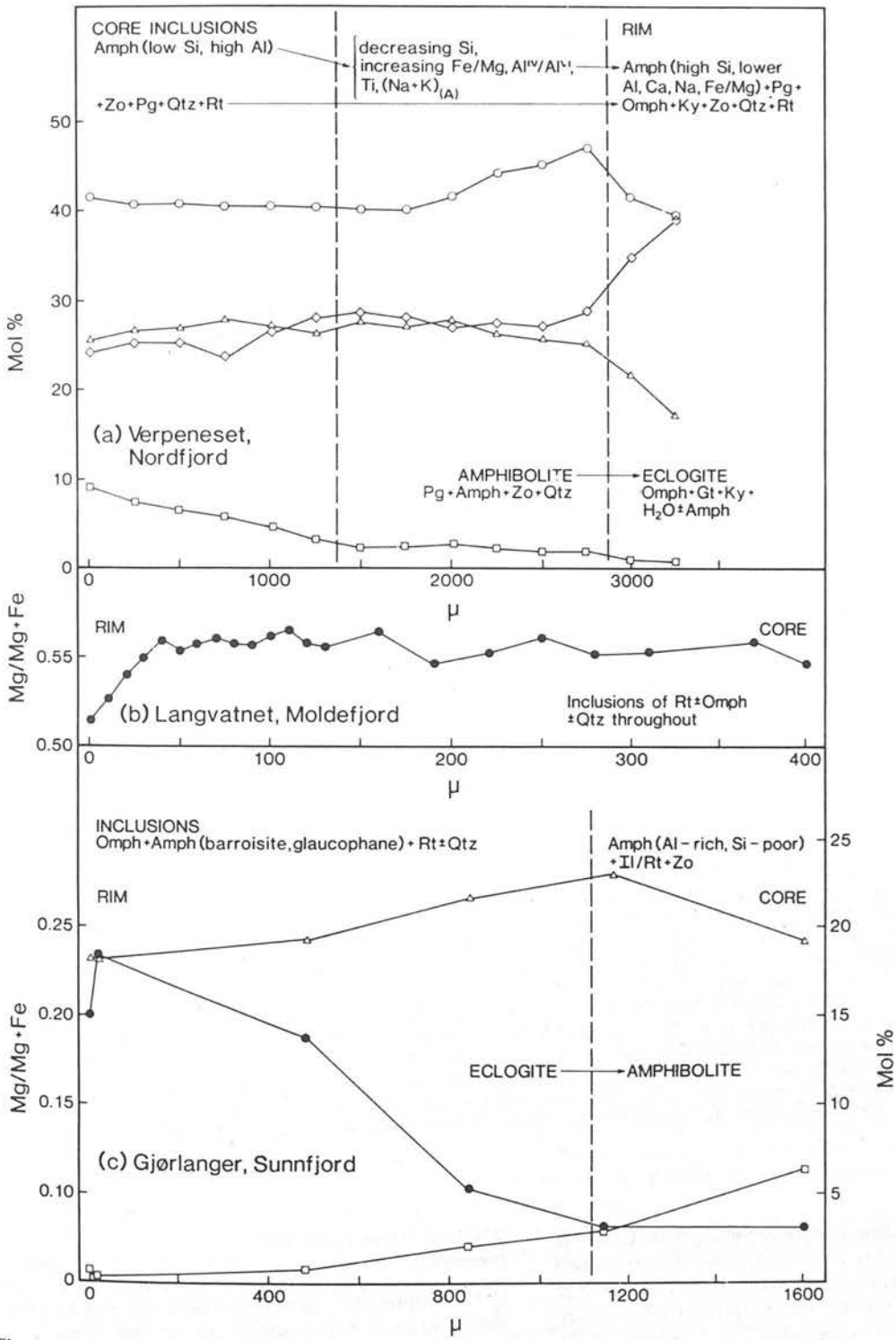

Fig. 3. Compositional zoning profiles and mineral inclusion suites for garnets from Verpeneset, Nordfjord (Krogh, unpublished data), Langvatnet, Moldefjord (Harvey, unpublished data) and Gjørlanger, Sunnfjord (Cuthbert, unpublished data). Open circles—almandine component; triangles—grossular component; diamonds—pyrope component; squares—spessartine component; closed circles—$Mg^{2+}/(Mg^{2+}/Fe^{2+})$. Amph = amphibole; Zo = zoisite; Pg = paragonite; Qtz = quartz; Rt = rutile; Omp = omphacite; Ky = kyanite; and Il = ilmenite.

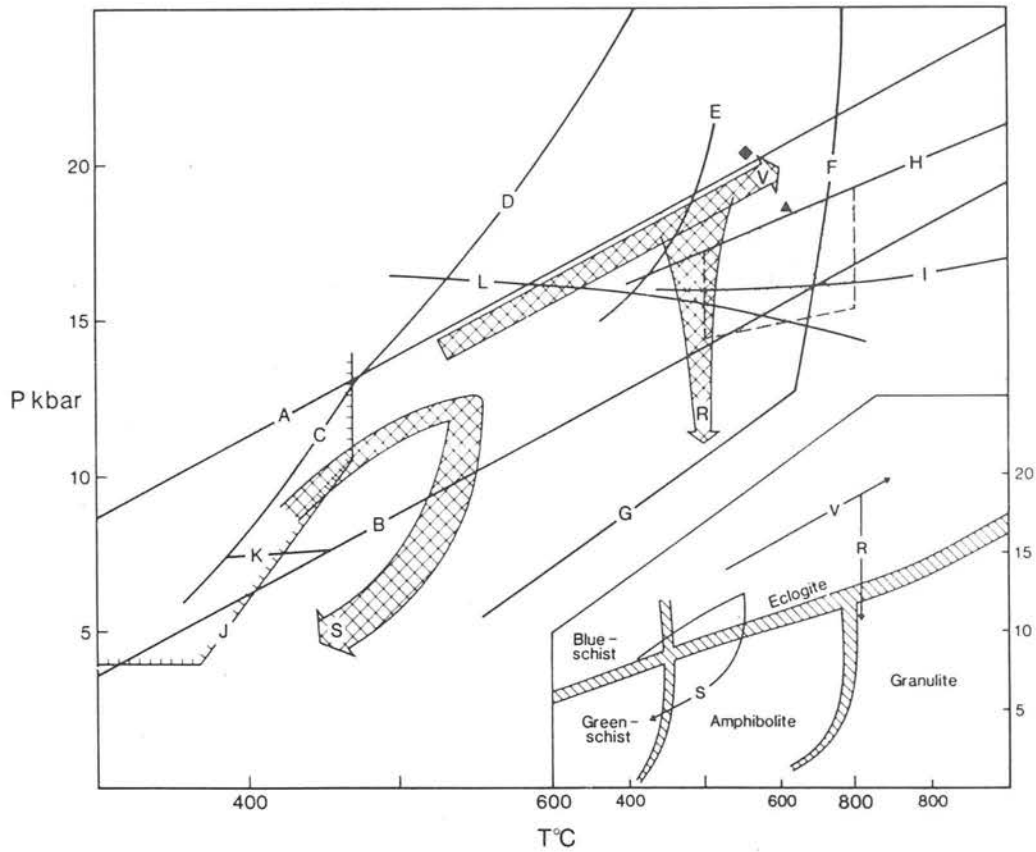

Fig. 4. Petrogenetic grid showing P/T trajectories for eclogites from Sunnfjord (s) (after Krogh, 1980a). Verpeneset (V) and Romsdalshorn (R), Møreog Romsdal (Krogh, unpublished data). A—Ab = Jd + Qtz (Holland, 1979, 1980), B—lower stability of $DiJd_{40}$ + Qtz (Holland, 1979, 1980), C—Lws + Ab = Zo + Pg + Qtz + vapour (Holland, 1979), D—Lws + Jd = Zo + Pg + Qtz + vapour (Holland, 1979), E—wet eclogite solidus (Lambert & Wyllie, 1972), F—Zo + Ky + Qtz = liq. + vapour (Boettcher, 1970), G—Zo + Ky + Qtz = An + vap (Boettcher, 1970), H—plagioclase out in high-Al basalt/andesite (extrapolated from Stern, Hung & Wyllie, 1975), I—special iherzolite–garnet lherzolitetransition (O'Hara, Richardson & Wilson, 1971), J—maximum stability field for glaucophane, ticks point towards stability field (Maresch, 1977), K—Marg + Ab = Pg + Zo + Qtz (Franz & Althaus, 1977), L—Pg = $DiJd_{40}$ + Ky + vapour (Holland, 1979). Stippled area—P/T conditions deduced for granulites near Kristiansund (Krogh, 1980b). Triangle—best estimate of P/T for orthopyroxene eclogites in the BGC (Carswell *et al.*, 1983). Diamond—best estimate of P/T for garnet lherzolites in the BGC (Carswell & Gibb, 1980). Inset—P/T trajectories plotted against generalized metamorphic facies boundaries.

published data; Lappin & Smith, 1978; Griffin & Carswell, 1983). These features are thought to be a result of strong decompression with little change in temperature, imparting a rather hairpin-shaped profile to P/T trajectories (Fig. 4) (Krogh, 1977a, 1980a; Griffin *et al.*, 1981). Similar profiles are reported from other orogenic belts containing eclogites implying, perhaps, a common tectonic process for their metamorphic evolution (e.g. Ernst & dal Piaz, 1978; Ernst, 1977, 1981; Maresch & Abraham, 1981).

Regional temperature and pressure variation

It will be apparent from what has been said above that a range of P/T conditions occurs not only within individual eclogites, but also between them. Bryhni *et al.* (1977); Krogh (1977a); Griffin & Mørk (1981) and Griffin *et al.* (1981) have plotted

$$K_D \overset{Gt\text{–}Cpx}{Fe^{2+}/Mg^{2+}}$$

values for rim compositions and estimated temperature on a map of the BGC and find a systematic increase in K_D and T towards the NW coast. The lowest temperatures are recorded in Sunnford, where 'type C' glaucophane-bearing eclogites outcrop. The highest temperatures are recorded between Stadlandet and Kristiansund. Pressures also increase in the same sense for the eclogites and continuing research suggests a similar pattern is recorded in garnet + plagioclase + kyanite + quartz assemblages in the gneisses (Griffin, pers. comm.).

This regional pattern is thought to be a result of crustal 'subduction' during continental collision (Krogh, 1977a), now thought to be of Caledonian age, as discussed above. The variation is consistent with the findings of Krill (1981b) who reported decreasing

$$K_D \begin{matrix} \text{Gt–Biot} \\ Fe^{2+}/Mg^{2+} \end{matrix}$$

values (*cf.* Ferry & Spear, 1978) westwards from the eastern margin of the BGC and westward change of metabasites from amphibolites to eclogites.

The superimposition of this regional variation of temperature and pressure on the structurally complex BGC puts strong constraints on tectonic models for the origin of the eclogite-facies assemblages. First, it implies superimposition of high-pressure metamorphism on existing major structures. Second, it considerably reduces the credibility of foreign origin hypotheses unless some special mechanism can be explained for the variation which is consistent with regional geological relationships. Further resolution of this matter urgently requires extensive fieldwork to map out the major tectonic units, and detailed petrographic and geothermobarometric studies across large amplitude structures to ascertain the relative age of eclogite metamorphism with respect to deformation episodes.

In order for the regional variaton to have remained intact the BGC must have emerged as a fairly rigid, coherent body. The pressure variation implies that the uplift hinged somewhere in the SE, possibly near to Jotunheimen. Some disturbance of the iso-K_D lines seems to have occurred in Sunnfjord, perhaps due to late movement at the base of the Sunnfjord nappe (Griffin & Mørk, 1981; Cuthbert, unpublished data).

Summary of metamorphic evolution

High-pressure assemblages seem to have formed early in the observed tectonic history of the BGC, probably early in the formation of the present tectonostratigraphy. This metamorphism has affected all the lithologies and any 'foreign' fragments (oceanic crust, and upper oceanic, back-arc or sub-continental mantle) have equlibrated essentially in their present position relative to their host gneisses. A P/T history is recorded in which low-pressure protoliths suffered a rapid compression with some heating, followed by a rapid decompression which may have been nearly adiabatic or isothermal. Disequilibrium on all scales, including preservation of pre-Caledonian parageneses, prograde Caledonian parageneses and mineral zoning and only partial retrogression implies that the high-pressure event was rather short-lived. The regional P/T variation implies superimposition of an increasing overburden towards the W, up to about 65 km in thickness. The preservation of blueschist-type parageneses in Sunnfjord implies short-lived depression of rather cold (upper?) continental crust to considerable depths (up to 45 km).

GEOPHYSICS

The aim of this section is twofold. The first part will discuss evidence for the deep structure of the BGC and adjacent areas. The second part will explore the isostatic constraints on the evolution of the eclogite bearing terrain and attempt to throw some light on the possible thermal evolution of the BGC.

Deep structure

It is now generally accepted that the Caledonian orogenic belt has formed as a result of the collision of the Baltic–European continental plate with the Greenland–American continental plate following closure of the Iapetus ocean (e.g. Dewey, 1969, 1982; Phillips, Stillman & Murphy, 1976). The presence of ophiolite fragments in thrusted nappes in the Scandinavian Caledonides suggests that a geosuture exists close to the present coast of western Norway, marking the line of continental collision (Gale & Roberts, 1974; Gee, 1975, 1978; Furnes *et al.*, 1976; Andresen & Faerseth, 1982).

A comprehensive geophysical survey off the Norwegian coast (Talwani & Eldholm, 1972) has revealed the presence of a marked belt of high gravity and magnetic anomalies parallel to the coast between Trondheim and Stadlandet, trending towards Shetland and the N coast of Scotland. These are attributed to intrabasement density contrasts of pre-Permian age and have been related to dense Lewisian mafic granulites, as seen

in NW Scotland (Talwani & Eldholm, 1972; Watts, 1971). Gee (1975) suggests that these anomalies mark a dramatic change in the nature of the basement crust and may mark the junction between the ancient, Lewisian-type crust of Greenland and Scotland and the granitic, Gothogrenvillian-type crust of the Baltic shield. In this case the line may well represent a geosuture. However, the close proximity of these anomalies to the ophiolites on the W coast of Norway, and in particular to that on Shetland (Mcquillan & Brooks, 1967; Pritchard, 1981) may suggest that they represent an ophiolite-lined suture. Interpretation of the significance of these anomalies is complicated by their proximity to the Great Glen transform fault. Very large strike-slip movements on this fault may put the Lewisian rocks in close proximity to present northern Norway (Kent & Opdyke, 1979) perhaps invalidating these hypotheses. However, smaller movements (< 500 km) constrained by the geometry of the Barrovian metamorphic zones of Scotland, may only slightly affect the continuity of the anomalies as they lie essentially parallel to the fault.

The presence of a geosuture so close to the BGC may mean that the leading edge of the Greenland Plate may have over-ridden the BGC and therefore could provide at least part of the great overburden required to satisfy the geobarometric estimates. Such a hypothesis can only be very simplistic in view of the complex nature of the plate-margin collisions (Dewey, 1982). The presence of eclogites and garnet peridotites on the corresponding east coast of Greenland (Smith & Cheeney, 1981) suggests depression of the Greenland margin to great depths implying also either that this part of the E Greenland Caledonides represents part of the same structural entity as the BGC and the suture lies further west still, or that both margins have been depressed below some intervening structure, perhaps a microcontinent, an Andean-type orogen or just a telescoped continental margin similar to that envisaged here for the BGC but thrust in an opposing direction. Thus, although at present we may be able to pin-point the primary geosuture (if such a structure exists), we still cannot precisely reconstruct the nature of the upper collided plate. Seismic reflection studies akin to the COCORPS or BIRPS experiments may help to resolve this problem in the future.

Seismic refraction and reflection studies in S Norway give some clues to the deep structure of the BGC. A recent COCORP reflection profile has revealed the presence of a crustal low velocity layer (LVL) at approximately 12–14 km below the present land surface in the Møre area (Mykkeltveit, Husebye & Oftedahl, 1980). This LVL has been best defined over a length of about 50 km, and seems to be about 4 km thick with a westward dip of $< 2^{\circ}$ (Fig. 5E). It cannot be explained by heat flow anomalies and Mykkeltveit *et al.* (1980) suggested that the LVL results from incorporation of oceanic crust and sediments during overthrusting of the BGC over the Baltic margin. Such a model has many faults, on the basis of the information outlined in this paper, not the least of which is that it precludes the development of Caledonian eclogites in the BGC.

Seismic refraction studies carried out by workers at the Seismological Observatory at Bergen show similar results to those of Mykkeltveit *et al.* (1980). Sellevoll & Warrick (1971) discussed the results of two traverses across S Norway, from Fedje (Bergen Arcs) to Grimstad (S coast) and Florà (W coast, BGC) to Åsnes (near Swedish border in Proterozoic foreland). They constructed a model in which the crust outside the Caledonides has a 6.00 km/sec P-wave velocity for the upper crustal layer, underlain by a 6.51 km/sec layer below about 18 km, with the Moho reflector at about 33 km. An interesting observation is that within the area corresponding to the BGC and the Bergen Arcs an additional upper high-velocity layer (6.32 km/sec) is present. It was suggested that this is underlain by a low velocity layer with a base at about 14–17 km. The velocity of the LVL was taken as that of the surface layer at Grimstad (6.00 km/sec). Also Kanestrøm (1977) has described a detailed refraction study in the Møre area to the W of that by Mykkeltveit *et al.* (1980) and found evidence for a LVL (5.00 km/sec) 7 km thick with its top at 9 km. The upper layer velocity was 6.20 km/sec, also higher than that in the foreland.

From these studies another interpretation for the velocity reversal may be suggested in which the LVL results from the superposition of a high velocity layer over crust of normal velocity distribution. This does not entirely discount the presence of supracrustal material in the LVL. The anomolously high upper layer velocity is interesting in that it coincides with the outcrop of an eclogite-bearing terrain where dense high-pressure parageneses may still be common, despite retrogression.

In recent years seismic mapping of velocity changes and reversals has made significant contributions to our knowledge of orogenic belts, indicating the superposition of large masses of crystalline continental crust over each other and over supracrustal layers in, for example, the

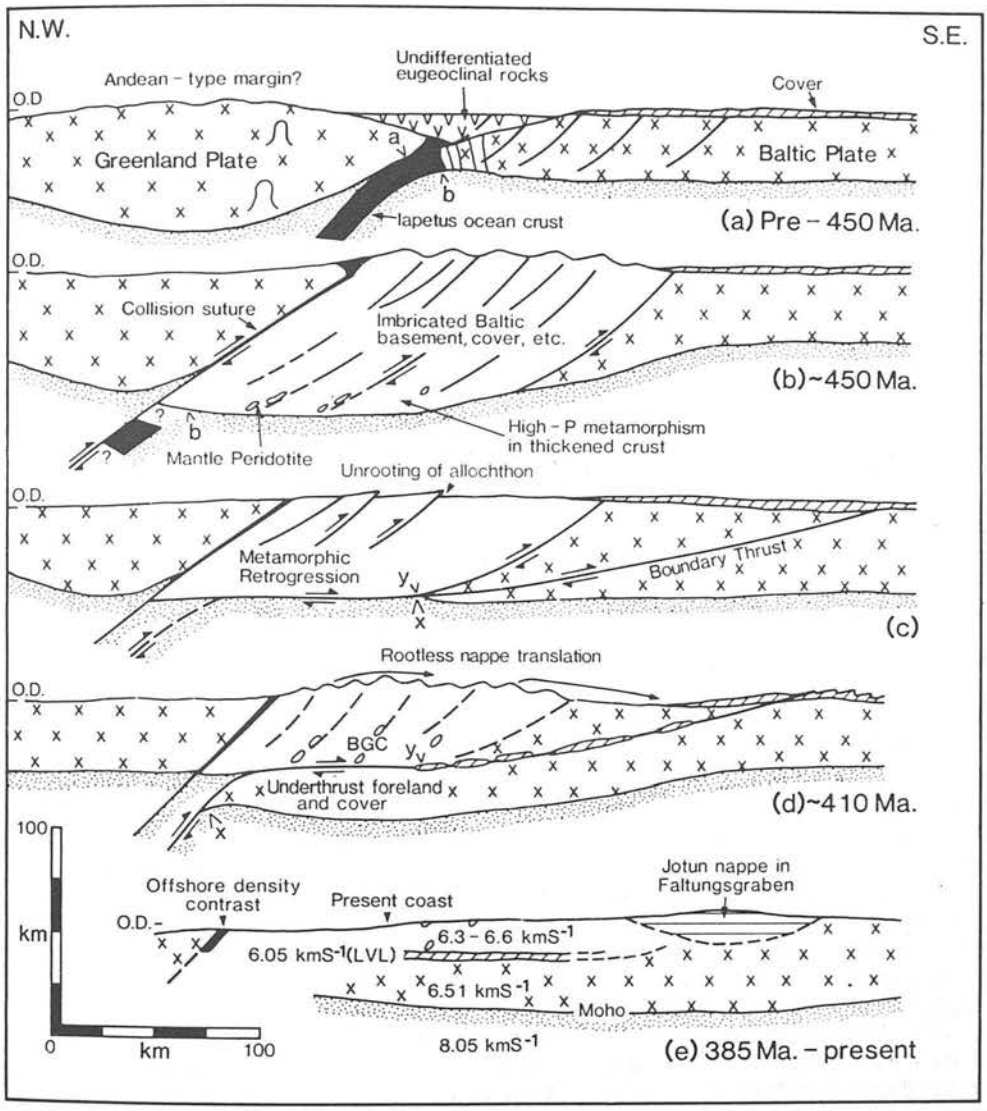

Fig. 5. Evolutionary model for the Basal Gneiss Complex, as described in the text. For details see Table 2.

Appalachians (Cook, Albaugh, Brown, Kaujman, Oliver & Hatcher, 1979), the Alps (Hsü, 1979) and the Scottish Caledonides (Soper & Barber, 1982). The latter two examples suggest crustal-scale imbrication. A major problem in developing a tectonic model for the BGC is to find a viable mechanism by which crust which has been buried to depths of up to 70 km can be restored to the Earth's surface and still have a crust of near-normal thickness beneath it. We suggest that following the early phase of collision, in which the eclogitic parageneses formed in a tectonically thickened and overthrust continental margin, a phase of suture progradation (Roeder, 1979) caused underthrusting of continental crust (and supracrustal cover?) below the eclogite-bearing terrain, hence providing the isostatic impetus for its uplift.

Isostasy and thermal history

Bird, Toksöz & Sleep (1975) have made a theoretical study of the mechanical and thermal effects of continent–continental collision. They found that when subduction of continental crust follows that of the oceanic slab, the greater thickness of the

continental lithosphere tends to resist bending, so that downwarping tends to occur at some distance in front of the original suture zone. Furthermore, the buoyancy of the continental crust introduces large deviatoric stresses on the downgoing slab. A combination of these factors causes a large, low angle thrust to form in the underthrust plate, making it easier for the continental crust to continue underthrusting. This results in suture progradation. Should the contact between the dense oceanic crust and the continental crust be disrupted by this shearing, the oceanic slab will become detached and sink, perhaps removing the driving force for continental underthrusting. In this case crustal doubling will cease and isostatic compensation, aided by surface erosion, will act to restore the crust to a more normal thickness. Bird *et al.* (1975) and Toksöz & Bird (1977) have applied this model to the Zagros mountains and the Himalayas.

Dewey (1982) shows that during continental convergence crustal imbrication will tend to occur by reversal of listric normal faults formed during the early phases of basin development. The form taken by this 'tectonic telescoping' will vary between thin-skinned flaking and whole-crust imbrication, depending on the previous thermal history of the margin. Where the cold, 'elastic lid' is of crustal depth, faulting may take in slivers of upper mantle material during thrusting.

A combination of the latter two mechanisms would tend to produce a prism of imbricated crust, possibly of great thickness, between the primary geosuture and a low angle prograde suture, a situation apparently developing at present in the Zagros mountains and the Himalayas (Bird *et al.*, 1975; Powell & Conaghan, 1973; Barazangi & Ni, 1982; Shackelton, 1981) and one which may be directly analogous to the S Norwegian Caledonides.

The thermal effect of this geotectonic scenario will depend on a number of factors, including the rate of underthrusting (and, therefore, frictional heat production), the rate of surface erosion, the effect of density changes due to metamorphic reactions with high ΔV, the effect of radiogenic self-heating and the previous thermal history of the continental margins (England & Richardson, 1977; Bird *et al.*, 1975; Toksöz & Bird, 1977; Richardson & England, 1979; Draper & Bone, 1981). The existence of blueschist mineralogy in parts of the BGC suggests downward transport of fairly cold crustal material. Its preservation suggests high initial uplift rates and rapid exhumation, which may require tectonic stripping in addition to erosion (Draper & Bone, 1981). However, the P–T conditions for garnet peridotites and eclogites in the Molde-Kristiansund area ($\sim 750°C$, and 20 kbar) lie along the Precambrian shield geotherm (Carswell & Gibb, 1980) and may indicate some thermal relaxation to a more stable geotherm prior to uplift here, in an area which may be closer to the mantle heat flux source.

Most recent thermal models of overthrust orogenic belts (England & Richardson, 1977; Richardson & England, 1979; Thompson, 1981) result in a P–T path where some heating follows the metamorphic pressure peak. Although this may be the case in the north-western part of the BGC, where retrograde garnet zoning is prevalent, it does not appear to be the case further S where very little change in T or even some cooling has occurred during decompression. Rubie (1982) has produced a model for the history of the Alpine Sezia-Lanzo zone in which a temperature rise during uplift is prevented by continuing subduction of cold oceanic crust beneath the emerging crustal slab. Bird *et al.* (1975) show that significant heat transfer and self-heating do not occur in an underthrust continental slab until about 30 Ma after collision. Hence preservation of low-T parageneses in the overlying thickened crust may be a result of the blanketing effect of the under thrust slab.

An alternative to this model might be that the recorded P–T trajectory is a result of interruption of thermal relaxation by very rapid uplift. It is interesting that the known volume of late orogenic Devonian sediments does not balance the removal of up to 65 km of crust by erosion. The known volume includes that found in seismic studies of the Norwegian Sea and Northern North Sea where basin accumulations of up to 6 km occur (Talwani & Eldholm, 1972). This discrepancy may be accounted for by considerable tectonic stripping, which would be the result of the unrooting and eastward translation of the nappe pile, as envisaged by Gee (1975, 1978, 1980). Very rapid unloading would have resulted from this.

Griffin *et al.* (1981) and Griffin & Mørk (1981) have noted the close similarity between the apparent regional P–T variation in the BGC and that occurring at present at the top of the underthrust continental slab in the Zagros mountains (Bird *et al.*, 1975). This may support the ideas outlined above, but far better resolution of this variation will be necessary before this similarity can be seen as anything but fortuitous. Indeed, it seems likely that in a tectonic window such as the BGC any observed P–T variation may be a result

of erosion to different crustal levels, a situation which may prove very useful for resolution of the thermal structure of the crust if its detailed tectonic structure is ever resolved. Moreover, the possibility that the P–T variation is diachronous cannot be ruled out as yet.

In order to test the feasibility of the collision–underthrusting–recovery scenario outlined above we have applied the isostacy equations of Ahnert (1970) as used by England & Richardson (1977) to a geotectonic model embodying the geological, geochronological, petrological and geophysical features outlined above. The equations relate crust and mantle densities, surface height and erosion as follows:

$$H = H_0 - Fe$$

(2b of England & Richardson, 1977)

and

$$E = E_{max}(1 - \exp(-t/\lambda))$$

(4b of England & Richardson, 1977)

where H_0 is the surface height at time $t = 0$, H is the surface height at time t, $F = (1 - \rho c/\rho m)$, ρc and ρm being the densities of eroded material and the mantle respectively. E is the amount eroded after time t, E_{max} the amount eroded after infinite time and λ the erosional time constant. The values for these parameters were set by observing the follwing constraints.

1. Maximum estimated pressures from mineral geobarometry are about 20 kbar, indicating burial depths of about 65 km for rocks now at the present land surface. Hence $E_{max} = 65$ km.
2. Ahnert (1970) suggests that erosion rates seen in large mid-latitude drainage basins indicate erosional time constants as small as 55 km. This may be a maximum value if exhumation is enhanced by tectonic stripping, depending on the rate of nappe translation. A value of $\lambda = 55$ km is taken here.
3. Radiometric ages on eclogite minerals cluster around 420–400 Ma, with some as early as 447 Ma. If these are taken to be fairly early closure ages then maximum crustal depth for the BGC was reached at least as early as 420 Ma. A lower bracket for commencement of final continental collision is set by the lowest Silurian age for part of the Köli supergroup (at least 450 Ma). We have set the maximum crustal depth achieved during collision at about 450 Ma for the purposes of this calculation.
4. The end of orogenesis (i.e. uplift) was achieved by the time of deposition of the Devonian clastics in middle Devonian times, and we use an age of about 385 Ma here.
5. The total custal thickness achieved during collision is equal to E_{max} plus the depth to the present LVL, taken at ~ 14 km. This level is assumed to have been the Moho. Hence the crustal thickness at that time was about 80 km. The distance from the LVL to the present Moho is rather variable due to the coastwards rise in Moho level away from the Jotun nappes (Sellevol & Warrick, 1971; Ramberg & Grønlie, 1969; Kanestrøm, 1973), but is generally about 25 km. For the purposes of the calculation it is assumed that this amount was added to the base of the imbricate prism at some time after primary collision (the 'secondary underthrusting event').
6. The present crustal thickness is about 40 km (maximum) with a surface elevation of about 1.5 km. The crustal thickness at time $t = 0$ is arbitrarily set at 35 km, although it may have been somewhat thinner due to marginal extension during opening of Iapetus.

Manipulation of these figures led, by trial and error, to a three stage scheme in which crustal protoliths could be depressed to 65 km and returned to the surface within 73 Ma (Table 2). This is slightly longer than the period indicated by the time constraints. It was found necessary to divide the secondary underthrusting event into two periods with a small thickening phase after the main one. Division of these main events into a number of smaller increments would probably further reduce the time needed. It is clear that a single stage thickening event would not have returned the eclogites to the surface in the time available, indicating the importance of the secondary underthrusting to provide the buoyancy impetus for their exhumation. Any delayed recovery due to the development of an 'eclogite anchor' (Richardson & England, 1979) would also result in a poor fit with the time constraints. Maximum surface heights were broadly compatible with those of the Himalayan belt at the present time.

AN EVOLUTIONARY MODEL FOR THE BASAL GNEISS COMPLEX

The model present here is intended to relate the main geological and geophysical features of the South Norwegian Caledonides to the metamorphic evolution of the BGC as indicated by studies of relict high pressure assemblages. We make no detailed attempt to explain the pre-collisional history of this part of the orogen. For reviews of this see Gee (1975, 1978), Gee *et al.* (1981), Stevens & Gee (1981) and Andresen & Faerseth (1982).

Table 2. Calculated crustal thickening and erosion scheme for the evolution of the Basal Gneiss Complex during the Caledonian orogeny using equations 2b and 4b of England & Richardson (1977)

Time Interval t (Ma)	Crustal Thickness (km)	Surface Height H (km)	Crust Eroded E (km)	Event	Fig.	Age
	32	0			5A	Pre-450 Ma
			−48	Continental collision, crustal thickening by imbrication		
33	80	8.75		Partial thermal recovery, high P/T metamorphism	5B	~ 450 Ma
			+28.2	Isostatic recovery and erosion, retrogressive metamorphism	5C	
	51.8	3.6				
			−25	Second suture develops with underthrusting of Baltic foreland	5D	
	76.8	8.2				
15			+15.5	Isostatic recovery, tectonic stripping and erosion, continuing retrogressive metamorphism	5D	~ 410 Ma
	61.2	5.3				
			− 2.5	Further crustal thickening, final eastward translation of allochthon		
	63.7	5.8				
25			+23.7	Isostatic recovery and erosion		
	40	1.5				
				Deposition of Devonian molasse	5E	~ 385 Ma

Figure 5 presents a series of sections showing the main features of the evolutionary model, which are also summarized in Table 2.

In developing the model the following assumptions were made.

1. The eclogites and garnet peridotites equilibrated *in-situ* within their present host gneisses. Hence the whole BGC has suffered eclogite facies metamorphism.
2. The major structures in the BGC are of Caledonian age.
3. The eclogite facies metamorphism was of Caledonian age.
4. The LVL represents a structural discontinuity in the crust.

All these assumptions are still matters of intense debate, but we believe that the information outlined in this paper strongly supports them as correct assumptions. The model is described below.

Following closure of the Iapetus ocean and obduction of ophiolites and eunimatic island-arc sequences in the early Ordovician (A in Fig. 5), the Greenland and Baltic margins collided. The Baltic margin underthrust that of Greenland and was tectonically telescoped, possibly along pre-existing faults, leading to the development of a stack of thrust sheets consisting largely of Proterozoic crystalline basement and cover, including some early Palaeozoic cover rocks. Caledonian ophiolites were also incorporated in the thrust stack and in the suture zone. Incorporation of ultrabasic fragments probably occurred at this stage, either due to thrusts transecting the upper sub-continental mantle or due to incorporation of basal oceanic or marginal basin lithosphere. The thrust stack included not only rocks now present in the BGC, but also those in the allochthon.

The considerable horizontal shortening resulting from this collision caused great crustal thickening (up to 80 km) so that pressures large enough to form eclogite facies assemblages prevailed. Initially compression was much more rapid than warming, so that low-temperature amphibolites and low-T glaucophane eclogites formed. Ultimately thermal relaxation due to conduction of mantle heat flux and radiogenic self-heating would have occurred, but this seems to have affected only those rocks which have attained the greatest depths (i.e. those which record the highest pressures) as they record the highest temperatures and show no prograde garnet zoning. However, the widespread disequilibrium shown in the BGC by mineral zoning, carona formation and relict granulite and igneous assemblages, as well as the preservation of low-T eclogites, implies that in large volumes of this early nappe pile, thermal relaxation was every limited and hence this high pressure event was only transient. Our isostatic calculations indicate a period of 33 Ma for this event, which is consistent with the thermal modelling of Bird *et al.*

(1975), and the time available between the deposition of the Köli supergroup and eclogite mineral (closure?) ages. Andréasson & Gorbatschev (1980) describe the metamorphism of the nappes in the Trondheim-Østersund area and suggest that common inverted metamorphic gradients are a result of incomplete thermal equilibration during early nappe thrusting. They also note evidence for early high-P metamorphism in some of the nappes as well as a westward increase in metamorphic grade. These features are consistent with the model. Andréasson & Gorbatschev (1980) suggested that the high-P event may have only lasted 15 Ma.

The overburden for the high-P metamorphism was probably largely provided by the great thickness of the nappe pile. The value of 65 km for the overburden may be an overestimate if there was a large amount of dense oceanic crust in the thrust stack.

At this stage the strong positive buoyancy of the thickened prism of nappes caused strong uplift, aided by surface erosion upon its emergence above sea level. This would have had two effects. Firstly, the decompression would have caused retrogression of the high-pressure mineral assemblages, observed as symplectitization of omphacitic pyroxene and phengitic mica, followed by development of amphibolite-facies assemblages. The completeness of retrogression was probably aided by deformation—relict mineral assemblages are most commonly observed in the least deformed rocks. Geothermometry indicates that very little change in temperature occurred during decompression. This may have been a consequence of the low rate of thermal conduction relative to uplift, as a result of which the uplift was essentially adiabatic. Thus the lack of extra thermal energy to drive reactions across kinetic barriers may have resulted in the common preservation of high pressure relics (Lappin & Smith, 1978). Griffin & Mørk (1981) note that many retrogressive assemblages record pressures equivalent to 8–10 km. This may be a result of either a slowing down of the rate of uplift or a major deformational event.

The second effect of the uplift would have been to cause gravitational instability in the higher parts of the nappe pile. This could have caused the commencement of translation of the allochthon away from its root zone in the nappe pile and towards the foreland. We speculate that the stretching involved in this translation may have been responsible for the pervasive amphibolite-facies foliation in the gneisses and the common boudinage seen in the eclogites. Recumbent isoclinal folding occurred at or slightly before this stage. Some eclogite-bearing units were involved in the nappe translation now seen in the Seve nappe in Sweden (Roermund, 1981).

At some time during this uplift period a major low-angle crustal fracture formed in the Baltic foreland (suture progradation). The foreland was then underthrust along this fracture below the eclogite-bearing base of the BGC. The thrust surface is now seen as the LVL, either as a result of emplacement of normal density upper crust below eclogite-bearning gneisses, or due to the incorporation of some supracrustal sedimentary cover into this fracture system. The former alternative implies that little or no mineralogical equilibration to higher pressure parageneses took place at the top of the underthrust slab.

The surface expression of this thrust may be where the basal décollement to the allochthon in central Sweden passes into the basement in the Grong-Olden culmination. This 'boundary thrust' would be analogous to the Main Boundary Thrust of the southern Himalayas (Powell & Conaghan, 1973; Shackleton, 1981; Baraganzi & Ni, 1982). The geometry of the boundary thrust further SW depends upon interpretation of the Jotun nappe. If it is accepted that the nappe has travelled from a source in the NW then its outcrop may simply cover the boundary thrust. If, however, this Nappe has had a local, deep rooted source, its emplacement may have been a direct consequence of this suture progradation, either as a result of the detachment of an 'Ivrea-type flake' (Battey & McRitchie, 1973; Smithson & Ramberg, 1974; Banham *et al.*, 1979) or telescoping an ensialic marginal basin (Gibbs, 1982). In either case the formation of the duplex thrust system in the Valdres area may be at least partly a result of off-scraping of the supracrustal sediments against the upper end of the boundary thrust as the foreland moved north-westwards below the hanging wall.

This phase of crustal doubling provided further impetus for uplift and nappe translation, with the unrooted allochthon being replaced by higher units from the NW. In Sunnfjord, a break of about 3.5–6.0 kbar is indicated by the different parageneses in the eclogite-bearing basement and the overlying Cambro-Silurian schists (Griffin & Mørk, 1981), but retrogressive assemblages in the gneisses may be broadly consistent with the conditions indicated by the schists, indicating that their final juxtapositioning occurred after uplift of at least 25 km. Hence the final uplift stage was probably only accompained by surface erosion and not tectonic stripping. The effect of adiabatic

upward transport of rather warm crust to these higher levels may well have had a strong thermal effect on the overlying allochthon, but this does not seem to be well documented, although Andréasson & Gorbatschev (1980) mention a 'thermal pulse' succeeding nappe translation.

Final emergence of the BGC in the early middle Devonian produced the present geometry of this part of the orogen, with the development of molasse-filled intermontaine basins controlled by late faulting. Guezou (pers. comm., 1981), associates this with late transverse movement near the primary suture due to oblique collision. The appearance of the BGC as a culmination within the surrounding allochthon may be associated with frequently observed late dome structures (e.g. Løset, 1977). If the regional P–T variation observed by Krogh (1977a) and Griffin *et al.* (1981) survives detailed scrutiny, it would appear that after imbrication and inter-folding of the lithologies forming the BGC it acted as a coherent body during uplift, except for minor movements as may be observed in the Sunnfjord area.

Elucidation of the history of the BGC has great importance in geodynamic modelling of the Caledonides as it is likely that its uplift provided the driving force for final translation of the allochthon into its present position. Studies of high-pressure relics such as eclogites, garnet peridotites and high-pressure granulites play an important part in this modelling.

ACKNOWLEDGEMENTS

This paper has grown considerably since its original conception and has benefited from critical comments by D. G. Gee and anonymous referees, as well as discussions with N. J. Soper, J. -C. Guezou, I. Bryhni and many others. S. J. Cuthbert and M. A. Harvey acknowledge studentships from the Natural Environment Research Council and D. A. Carswell, financial support from the University of Sheffield.

REFERENCES

Ahnert, F., 1970. Functional relationship between denudation, relief and uplift in large mid-latitude drainage basins. *Am. J. Sci.*, **268**, 243–63.

Andréasson, P. G. & Gorbatschev, R., 1980. Metamorphism in extensive nappe terrains: a study of the Central Scandinavian Caledonides. *Geol. För. Stockholm Förh.*, **102**, 335–57.

Andresen, A. & Faerseth, R., 1982. An evolutionary model for the south-west Norwegian Caledonides. *Am. J. Sci.*, **282**, 756–82.

Austrheim, H., 1981. Bergen Arcs. In: *Excursions in the Scandinavian Caledonides. U.C.S. Excursion No. B1: Eclogites and Basal Gneisses in West Norway.* (eds. W. L. Griffin & M. B. E. Mørk), pp. 74–82. Uppsala Caledonide Symposium.

Austrheim, E. & Griffin, W. L., 1982. Shear deformation and eclogite formation within granulite-facies anorthosites of the Bergen Arcs, western Norway. *Abstr. First Int. Eclogite Conf., Clermont Ferrand, Terra Cognita*, **2**, 315.

Austrheim, H. & Råheim, A., 1981. Age relationships within the high grade metamorphic rocks of the Bergen Arcs, western Norway. *Abstr. Uppsala Caledonide Symp. Terra Cognita*, **1**, 33.

Banham, P. H., Gibbs, A. D. & Hopper, F. W. M., 1979. Geological evidence in favour of a Jotunheimen Caledonian suture. *Nature*, **277**, 289–91.

Barazangi, M. & Ni, J., 1982. Velocities and propagation characteristics of Pn and Sn beneath the Himalayan arc and Tibetan plateau: Possible evidence for underthrusting of Indian continental lithosphere beneath Tibet. *Geology*, **10**, 179–85.

Battey, M. H. & McRitchie, W. D., 1973. A geological traverse across the pyroxene-granulites of Jotenheimen in the Norwegian Caledonides. *Nor. Geol. Tidsskr.*, **53**, 237–65.

Bird, P., Toksoz, M. N. & Sleep, N. H., 1975. Thermal and mechanical models of continent-continent convergence zones. *J. Geophys. Res.*, **80**, 4405–16.

Boettcher, A. L., 1970. The system $CaO-Al_2O_3-SiO_2-H_2O$ at high pressures and temperatures. *J. Petrol.*, **11**, 337–79.

Brastad, K., 1982. Eclogites within the Bjørkedalen peridotite, western Norway. *Abstr. First Int. Eclogite Conf., Clermont Ferrand. Terra Cognita*, **2**, 327.

Brastad, K., 1983. Relations between anorthosites, eclogites and ultramafics in Bjørkedalen, west Norway. *Proc. Uppsala Caledonides Symp.* (In press).

Brueckner, H. K., 1972. Interpretation of Rb-Sr ages from the Precambrian and Palaeozoic rocks of southern Norway. *Am. J. Sci.*, **272**, 334–58.

Brueckner, H. K., 1977. A structural, stratigraphic and petrologic study of anorthosites, eclogites and ultramafic rocks and their country rocks, Tafjord area, western south Norway. *Nor. Geol. Unders.*, **332**, 1–53.

Brueckner, H. K., 1979. Precambrian ages from Geiranger-Tafjord-Grotli area of the Basal Gneiss Region, west Norway. *Nor. Geol. Tidsskr.*, **59**, 141–53.

Bryhni, I., 1966. Reconnaissance studies of gneisses, ultrabasites, eclogites and anorthosites in outer Nordfjord, western Norway. *Nor. Geol. Unders.*, **241**, 1–68.

Bryhni, I., 1977. The gneiss region west and northwest of Jotunheimen. In: *The Norwegian Geotraverse Project. A Norwegian Contribution to the International Upper Mantle Project and the International Geodynamics Project.* (ed. K. S. Heier), pp. 227–246.

Bryhni, I., 1981. Nordfjord-Sognfjord Devonian Basins. In: *Excursion in the Scandinavian Caledonides, U.C.S. Excursion No. B1: Eclogites and Basal Gneisses in west Norway.* (eds. W. L. Griffin & M. B. E. Mørk), pp. 58–63. Uppsala Caledonide Symposium.

Bryhni, I., Fitch, F. J. & Miller, J. A., 1971. $^{40}Ar/^{39}Ar$ dates from recycled precambrian rocks in the gneiss

region of the Norwegian Caledonides. *Nor. Geol. Tidsskr.*, **51**, 391–406.

Bryhni, I. & Griffin, W. L., 1971. Zoning in eclogite garnets from Nordfjord, west Norway. *Contrib. Mineral. Petrol.*, **32**, 112–25.

Bryhni, I. & Grimstad, E., 1970. Supracrustal and infracrustal rocks in the gneiss region of the Caledonides west of Breimsvatn. *Nor. Geol. Unders.*, **266**, 105–40.

Bryhni, M., Kroph, E. & Griffin, W. L., 1977. Crustal derivation of Norwegian eclogites: A review. *N. Jb. Mineral. Abh.*, **130**, 49–68.

Carswell, D. A., 1968a. Picritic magma—residual dunite relationships in garnet peridotite at Kalskaret near Tafjord, southern Norway. *Contrib. Mineral. Petrol.*, **19**, 97–124.

Carswell, D. A., 1968b. Possible primary upper mantle peridotite in Norwegian basal gneiss. *Lithos*, **1**, 322–355.

Carswell, D. A., 1973a. The age and status of the basal gneiss complex of north-west southern Norway. *Nor. Geol. Tidsskr.*, **53**, 65–78.

Carswell, D. A., 1973b. Garnet pyroxenite lens within Ugelvik layered garnet peridotite. *Earth Planet. Sci. Lett.*, **20**, 347–52.

Carswell, D. A. & Gibb, F. G. F., 1980. The equilibration conditions and petro-genesis of European crustal garnet lherzolites. *Lithos*, **13**, 19–29.

Carswell, D. A. & Harvey, M. A., 1983. The intrusive history and tectono-metamorphic evolution of the Basal Gneiss Complex in the Moldefjord area, west Norway. *Proc. Uppsala Caledonide Symp.* (In press).

Carswell, D. A., Krogh, E. J. & Griffin, W. L., 1983. Norwegian orthopyroxene eclogites: Calculated equilibration conditions and petrogenetic implications. *Proc. Uppsala Caledonide Symp.* (In press).

Cook, F. A., Albaugh, D. S., Brown, L. D., Kaufman, S., Oliver, J. E. & Hatcher, Jr., R. D., 1979. Thin-skinned tectonics in the crystalline southern Appalachians, COCORP seismic profiling of the Blue-Ridge and Piedmont. *Geology*, **7**, 563–7.

Cuthbert, S. J. & Carswell, D. A., 1982. Petrology and tectonic setting of eclogites and related rocks from the Dalsfjord area, Sunnfjord, west Norway. *Abstr. First Int. Eclogite Conf., Clermont Ferrand. Terra Cognita*, **2**, 315.

Dewey, J. F., 1969. Evolution of the Appalachian/Caledonian orogen. *Nature*, **222**, 124–9.

Dewey, J. F., 1982. Plate tectonics and the evolution of the British Isles. *J. geol. Soc. London*, **139**, 371–412.

Draper, G. & Bone, R., 1981. Denudation rates, thermal evolution and preservation of blueschist terrains. *J. Geol.*, **89**, 601–13.

Elliot, R. B. & Cowan, D. R., 1966. The petrochemistry of the amphibolites of the Holleindalen Greenstone Group, Jotunheimen, Norway. *Nor. Geol. Tidsskr.*, **46**, 309–25.

Ellis, D. J. & Green, D. H., 1979. An experimental study of the effect of Ca upon Garnet-Clinopyroxene Fe-Mg exchange equilibria. *Contrib. Mineral. Petrol.*, **71**, 13–22.

England, P. C. & Richardson, S. W., 1977. The influence of erosion upon the mineral facies of rocks from different metamorphic environments. *J. geol. Soc. Lond.*, **134**, 201–13.

Ernst, W. G., 1977. Tectonics and prograde versus retrograde P-T trajectories of high pressure metamorphic belts; In: High pressure-low temperature metamorphism of the Oceanic and Continental Crust in the Western Alps. *Rendiconti Societa Italiana di Mineralogia e Petrologia*, **33**, 221–252.

Ernst, W. G., 1981. Petrogenesis of eclogites and peridotites from the western and Ligurian Alps. *Am. Mineral.*, **66**, 443–72.

Ernst, W. G. & dal Piaz, G. V., 1978. Mineral parageneses of eclogitic rocks and related mafic schists of the Piedmont ophiolite nappe, Breuil-St. Jacques area, Italian western Alps. *Am. Mineral.*, **63**, 621–40.

Eskola, P., 1921. On the eclogites of Norway. *Skr. Norske Vidensk-Akad. i Oslo, Mat-naturv., kl.*, **8**, 1–118.

Ferry, J. M. & Spear, F. S., 1978. Experimental calibration of partitioning of Fe and Mg between biotite and garnet. *Contrib. Mineral. Petrol.*, **66**, 113–7.

Franz, G. & Althaus, E., 1977. The stability relations of the paragenesis paragonite-zoisite-quartz. *N. Jb. Miner. Abh.*, **130**, 159–67.

Furnes, H., Skjerlie, F. J. & Tysseland, M., 1976. Plate tectonic model based on greenstone geochemistry in the late Precambrian-Lower Palaeozoic sequence in the Solund-Stavfjorden areas, west Norway. *Nor. Geol. Tidsskr.*, **56**, 161–86.

Gale, H. G. & Roberts, D., 1974. Trace-element geochemistry of Norwegian lower Palaeozoic basic volcanics and its tectonic implications. *Earth Planet. Sci. Lett.*, **22**, 380–90.

Gebauer, D., Lappin, M. A., Gruenefelder, M., Koestler, A. & Wyttenbach, A., 1982. Age and origin of some Norwegian eclogites: a U-Pb zircon and REE study. *Abstr. First Int. Eclogite Conf., Clermont Ferrand. Terra Cognita*, **2**, 323.

Gee, D. G., 1975. A geotraverse through the Scandinavian Caledonies—Ostersund to Trondheim. *Sver. Geol. Unders. Ser. C.*, **417**, 1–66.

Gee, D. G., 1978. Nappe displacement in the Scandinavian Caledonides. *Tectonophysics*, **47**, 393–419.

Gee, D. G., 1980. Basement-cover relationships in the central Scandinavian Caledonides. *Geol. För. Stockholm. Förh.*, **102**, 455–74.

Gee, D. G., Guezou, J. C., Roberts, D. & Wolff, J. C., 1982. The central-southern segment of the Scandinavian Caledonides. *Abstr. Uppsala Caledonide Symp. Terra Cognita*, **1**, 45.

Gent, E. D., 1976. Plagioclase–garnet–Al_2SiO_5–quartz, a potential geobarometer–geothermometer. *Am. Mineral.*, **61**, 710–14.

Gibbs, A. D., 1982. Northerly transport and exotic olistostrome in northern Jotunheim: Possible implications. *Abstr. Scandinavian Caledonides Research Seminar, Bedford College, London.* Convenor: P. Banham.

Gjelsvik, T., 1952. Metamorphosed dolerites in the gneiss area of Sunnmøre on the west coast of southern Norway. *Nor. Geol. Tidsskr.*, **30**, 31–134.

Green, D. H. & Mysen, B. A., 1972. Genetic relationship between eclogite and hornblende + plagioclase pegmatite in W. Norway. *Lithos*, **5**, 147–161.

Griffin, W. L., 1972. Formation of eclogites and the

coronas in anorthosites, Bergen Arcs, Norway. *Geol. Soc. Am. Memoir*, **135**, 37–63.

Griffin, W. L., Austrheim, H., Grastad, K., Bryhni, I., Krill, A., Mørk, M. B. E., Qvale, H. & Tørudbakken, B., 1981. High pressure metamorphism in the Scandinavian Caledonides. *Abstr. Uppsala Caledonide Symp. Terra Cognita*, **1**, 48.

Griffin, W. L. & Brueckner, H. K., 1980. Caledonian Sm-Nd ages and a crustal origin for Norwegian eclogites. *Nature*, **285**, 319–21.

Griffin, W. L. & Brueckner, H. K., 1982. Rb-Sr and Sm-Nd studies of Norwegian eclogites *Abstr. First Int. Eclogite Conf., Clermont Ferrand. Terra Cognita*, **2**, 324.

Griffin, W. L. & Bryhni, I., 1977. Corona reactions and the eclogite problem. In: *The Norwegian Geotraverse Project. A Norwegian Contribution to the International Upper Mantle Project and the International Geodynamics Project* (ed. K. S. Heier), pp. 247–264.

Griffin, W. L. & Carswell, D. A., 1983. Geochronological setting of in-situ eclogite metamorphism in western Norway. *Proc. Uppsala Caledonide Symp.* (in press).

Griffin, W. L. & Heier, K. S., 1973. Petrological implications of some corona structures. *Lithos*, **6**, 315–35.

Griffin, W. L. & Mørk, M. B. E., 1981. Introduction. In: *Excursion in the Scandinavian Caledonides Excursion No. B1: Eclogites and Basal Gneisses in West Norway* (eds. W. L. Griffin & M. B. E. Mørk), pp. 2–12, Uppsala Caledonide Symposium.

Griffin, W. L. & Qvale, H., 1981. Superferric eclogites and the crustal origin of garnet peridotite. *Abstr. Uppsala Caledonide Symp. Terra Cognita*, **1**, 48.

Griffin, W. L. & Råheim, A., 1973. Convergent metamorphism of eclogites and dolerites, Kristiansund area, Norway. *Lithos*, **6**, 21–40.

Guezou, J.-C., 1978. Geology and structure of the Dombås-Lesja area, southern Trondheim region, south central Norway. *Nor. Geol. Unders.*, **340**, 1–34.

Guezou, J.-C., 1981. A geodynamic model for the central and southern parts of the Scandinavian Caledonides. *Abstr. Uppsala Caledonide Symp. Terra Cognita*, **1**, 49.

Hernes, I., 1954. Eclogite-amphibolite on the Molde peninsula, southern Norway. *Nor. Geol. Tidsskr.*, **33**, 163–84.

Hernes, I., 1955. Geologisk oversikt over Molde-Kristiansundsområdet. *Det. kyl. Norske Vidensk, Selsk, Skifter*, **5**, 1–17.

Holland, T. J. B., 1979. Experimental determination of the reaction paragonite = jadeite + kayanite + H_2O, and internally consistent thermodynamic data for part of the system Na_2O–Al_2O_3–SiO_2–H_2O, with applications to eclogites and blueschists. *Contrib. Mineral. Petrol.*, **68**, 293–301.

Holland, J. T. B., 1980. The reaction albite = jadeite + quartz determined experimentally in the range 600–1200°C. *Am. Mineral.*, **65**, 129–34.

Holtedahl, O. & Dons, R. F., 1960. Geologiske kart over Norge, Bergrunnskart 1:1000,000. *Nor. Geol. Unders.* **208**.

Hossack, J. R., 1978. The correction of stratigraphic sections for tectonic finite strain the Bygdin area, Norway. *J. geol. Soc. London*, **135**, 229–41.

Hossack, J. R., 1982. A geological section from the foreland across the Valdres and Jotunheim areas to the west coast of Norway. *Abstr. Scandinavian Caledonides Research Seminar, Bedford College, London*, Convenor: P. Banham.

Hossack, J. R., Nickelsen, R. P. & Garton, M., 1981. The geological section from the foreland up to the Jotun sheet in the Veldres area, south Norway. *Abstr. Uppsala Caledonide Symp. Terra Cognita*, **1**, 52.

Hsü, K. F., 1979. Thin skinned plate tectonics during Neo-Alpine orogenesis. *Am. J. Sci.*, **279**, 353–66.

Kanestrøm, R., 1973. A crust-mantle model for the NORSAR area. *Pure Appl. Geophys.*, **105**, 729–40.

Kanestrøm, R., 1977. Seismic investigations of the crust and Moho in southern Norway. In: *The Norwegian Geotraverse Project. A Norwegian Contribution to the International Upper Mantle Project and the International Geodynamics Project.* (ed. K. S. Heier), pp. 143–9.

Kent, D. V. & Opdyke, N. D., 1979. The early Carboniferous palaeomagnetic field of North America and its bearing on the tectonics of the Northern Appalachians. *Earth Planet. Sci. Lett.*, **44**, 365–72.

Krill, A. G., 1980. Tectonics of the Oppdal area, central Norway. *Geol. För. Stockholm Förh.*, **102**, 523–30.

Krill, A. G., 1981a. Rb-Sr study of metamorphosed dolerite dykes and psammite: 'Precambrian' *vs.* 'Caledonian' orogenesis in the western gneiss region of Norway. *Abstr. Uppsala Caledonide Symp., Terra Cognita*, **1**, 56.

Krill, A. G., 1981b. 'Stockwerk' tectonic relationships between the Trondheim synclinorium and the Western Gneiss Region of Norway. *Abstr. Uppsala Caledonide Symp., Terra Cognita*, **1**, 56.

Krill, A. G. & Griffin, W. L., 1981. Interpretation of Rb-Sr dates from the Western Gneiss Region: A cautionary note. *Nor. Geol. Tidsskr.* **61**, 83–6.

Krogh, E. J., 1977a. Evidence of Precambrian continent–continent collision in Western Norway. *Nature*, **267**, 17–9.

Krogh, E. J., 1977b. Crustal and in-situ origin of Norwegian eclogites. Reply. *Nature*, **269**, 730.

Krogh, E. J., 1980a. Geochemistry and petrology of glaucophane-bearing eclogites and associated rocks from Sunnfjord, western Norway. *Lithos*, **13**, 355–80.

Krogh, E. H., 1980b. Compatible P-T conditions for eclogites and surrounding gneisses in the Kristiansund area, western Norway. *Contrib. Mineral. Petrol.*, **75**, 387–93.

Krogh, T. E., Mysen, B. O. & Davis, G. L., 1973. A Palaeozoic age for the primary minerals of a Norwegian eclogite. *Carnegie Inst. Wash. Yearb.*, **73**, 575–6.

Lambert, I. B. & Wyllie, P. J., 1972. Melting of gabbro 'quartz eclogite' with excess water to 35 kilobars, with geological applications. *J. Geol.*, **80**, 693–708.

Lappin, M. A., 1966. The field relationships of basic and ultrabasic masses in the Basal Gneiss Complex of Stadlandet and Almklovdalen, Nordfjord, S. W. Norway. *Nor. Geol. Tidsskr.*, **46**, 439–95.

Lappin, M. A., 1977. Crustal and in-situ origin of Norwegian eclogites. *Nature*, **269**, 730.

Lappin, M. A., Pidgeon, R. T. & van Breemen, O., 1977. Geochronology of basal genisses and mangerite syenites of Stadlandet, west Norway. *Nor. Geol. Tidsskr.*, **59**, 161–81.

Lappin, M. A. & Smith, D. C., 1978. Mantle equilibrated orthopyroxene eclogite pods from the Basal Gneisses in the Selje district, western Norway. *J. Petrol.*, **19**, 530–84.

Løset, F., 1977. Three fold phases in the northern part of Trollheimen in the Norwegian Caledonides. *Nor. Geol. Tidsskr.*, **57**, 121–31.

Lund, G. E., 1979. Crustal structure along the Blue Road Profile in northern Scandinavia. *Geol. För. Stockholm Förh.*, **101**, 191–204.

Maresch, W. V., 1977. Experimental studies on glaucophane: An analysis of present knowledge. *Tectonophysics*, **43**, 109–25.

Maresch, W. V. & Abraham, K., 1981. Petrography, mineralogy and metamorphic evolution of an eclogite from the island of Margarita, Venezuela. *J. Petrol.*, **22**, 337–62.

Mearns, E. W. & Lappin, M. A., 1982a. The origin and age of 'external eclogites' and gneisses from the Selje district of the western gneiss region, Norway. *Abstr. First Int. Eclogite Conf., Clermont Ferrand. Terra Cognita*, **2**, 324.

Mearns, E. W. & Lappin, M. A., 1982b. A Sm-Nd isotopic study of 'internal' and 'external' eclogites, garnet lherzolites and grey gneiss from Almklovdalen, western Norway. *Abstr. First Int. Eclogite Conf., Clermont ferrand. Terra Cognita*, **2**, 324.

Mearns, E. W. & Lappin, M. A., 1982c. Poster Contribution. *First Int. Eclogite Conf., Clermont Ferrand.*

Medaris, Jr. L. G., 1980. Petrogenesis of the Lien peridotite and associated eclogites, Almklovdalen, western Norway. *Lithos*, **13**, 339–53.

Medaris, Jr. L. G., 1982. A review of garnet peridotites within gneiss in western Norway. *Abstr. First Int. Eclogite Conf., Clermont Ferrand. Terra Cognita*, **2**, 303.

Mørk, M. B. E., 1982. A gabbro-eclogite transition of Flemsøy, Sunnmøre, western Norway. *Abstr. First Int. Eclogite Conf., Cleremont Ferrand. Terra Cognita*, **2**, 316.

Mykkeltveit, S., Husebye, E. S., Oftedahl, C., 1980. Subduction of the Iapetus Ocean crust beneath the Møre Gneiss Region, Southern Norway. *Nature*, **288**, 473–5.

Mysen, B. O. & Heier, K. S., 1972. Petrogenesis of eclogites in high grade metamorphic gneisses exemplified by the Hareidland eclogite, western Norway. *Contrib. Mineral. Petrol.*, **36**, 73–94.

McQuillin, R. & Brooks, M., 1967. Geophysical surveys in the Shetland Islands. *Institute of Geological Sciences, Geophysical Paper No. 2.* HMSO, London.

O'Hara, M. J., 1976. Origin of the Norwegian eclogites. *Progr. Expt. N.E.R.C.*, **3**, 252.

O'Hara, M. J. & Mercy, E. L. P. 1963. Petrology and petrogenesis of some garnetiferous peridotites. *Trans. Roy. Soc. Edin.*, **65**, 251–314.

O'Hara, M. J., Richardson, S. W. & Wilson, G., 1971. Garnet-peridotite stability and occurrence in crust and mantle. *Contrib. Mineral. Petrol.*, **32**, 48–68.

Phillips, W. E. A., Stillman, C. J. & Murphy, J., 1976. A Caledonian plate tectonic model. *J. geol. Soc. Lond.*, **132**, 579–609.

Pidgeon, R. T. & Råheim, A., 1972. Geochronological investigation of the gneisses and minor intrusive rocks from Kristiansund, west Norway. *Nor. geol. Tidsskr.*, **52**, 241–56.

Powell, C. Mc.A. & Conaghan, P. J., 1973. Plate tectonics and the Himalyas. *Earth Planet. Sci. Lett.*, **20**, 1–12.

Prichard, H. M., 1981. The Shetland Ophiolite. *Abstr. Uppsala Caledonide Symp. Terra Cognita*, **1**, 65.

Råheim, A., 1972. Petrology of high grade metamorphic rocks of the Kristiansund area. *Nor. Geol. Unders.*, **279**, 1–75.

Råheim, A., 1977. A Rb, Sr study of the rocks of the Surnadal syncline *Nor Geol. Tidsskr.*, **57**, 193–204.

Råheim, A., 1979. Structural and metamorphic break between the Trondheim basin and the surnadal synform. *Nor. Geol. Tidsskr.*, **59**, 195–8.

Råheim, A., 1981. Age relationships in the western gneiss region. *Abstr. Uppsala Caledonide Symp. Terra Cognita*, **1**, 67.

Råheim, A. & Green, D. A., 1975. P,T paths of natural eclogites during metamorphism—a record of subduction. *Lithos*, **8**, 317–28.

Ramberg, I. B. & Grønlie, G., 1969. A crustal section across the Caledonian mountain belt (Norway) based on gravity data. *Bolletino di Geofisica Teorica ed Applicata*, **11**, 219–26.

Richardson, S. W. & England, P. C., 1979. Metamorphic consequences of crustal eclogite production in overthrust orogenic zones. *Earth Planet. Sci. Lett.*, **42**, 183–90.

Roberts, D., Thon, A., Gee, D. G. & Stephens, M. B., 1981. Scandinavian Caledonides–Tectonostratigraphy map, scale 1:1,000,000. *Uppsala Caledonide Symp.*

Roeder, D., 1979. Continental collisions. *Rev. Geophys.*, **17**, 1098–1109.

Roermund, H. L. M. van, 1981. On the eclogites of the Seve Nappe central Scandinavian Caledonides. *Abstr. Uppsala Caledonides. Abstr. Uppsala Caledonide Symp. Terra Cognita*, **1**, 70.

Rubie, D. C., 1982. A kinematic model for metamorphism and deformation in the Sesia-Lanzo zone, western Alps. *Abstr. First Int. Eclogite Conf. Clermont Ferrand. Terra Cognita*, **2**, 308–9.

Schmitt, H. H., 1964. Metamorphic eclogites of the Eiksund area, Sunnmøre Norway. *Abstr. Am. Geophys. Union*, **43**, 128.

Sellevoll, M. A. & Warrick, R. E., 1971. A refraction study of the crustal structure in southern Norway. *Bull. Seismol. Soc. Am.*, **61**, 457–71.

Shackleton, R. M., 1981. Structure of southern Tibet: Report on a traverse from Lhasa to Khatmandu organised by Academia Sinica. *J. Struct. Geol.*, **3**, 97–105.

Skjerlie, F. J., 1969. The pre-Devonian rocks in the Askvoll-Gaular area and the adjacent districts, western Norway. *Nor. Geol. Unders.* **258**, 325–59.

Skjerlie, F. J., 1974. The lower Palaeozoic sequence of the Stavfjord district, Sunnfjord. *Nor. Geol. Unders*, **302**, 1–32.

Skjerlie, F. J. & Pringle, I. R., 1978. A Rb/Sr whole rock isochron date from the lowermost gneiss complex of the Gaular area, west Norway and its regional implications. *Nor. Geol. Tidsskr.*, **58**, 259–65.

Smith, D. C., 1980. A tectonic melange of foreign eclogites and ultramafites in west Norway. *Nature*, **287**, 366–7.

Smith, D. C., 1981. A reappraisal of factual and mythical evidence concerning the metamorphic and tectonic evolution of eclogite-bearing terrain in the Caledonides. *Abstr. Uppsala Caledonide Symp. Terra Cognita*, **1**, 73.

Smith, D. C. & Cheeny, R. F., 1981. A new occurrence of garnet ultrabasite in the Caledonides: A Cr-rich chromite-garnet-lherzolite from Tvaerdalen, Liverpool land, east Greenland. *Abstr. Uppsala Caledonide Symp. Terra Cognita*, **1**, 74.

Smithson, S. B., Ramberg, I. B. & Grønlie, G., 1974. Gravity interpretation of the Jotun Nappe of the Norwegian Caledonides. *Tectonophysics*, **22**, 205–22.

Solheim, S., 1980. Geochronological investigations in the Oppdal area, central Norway. *Nor. Geol. Tidsskr.*, **60**, 175–88.

Soper, N. J. & Barber, A. J., 1982. A model for the deep structure of the Moine thrust zone. *J. geol. Soc. Lond.*, **139**, 127–38.

Spray, J. G., 1982. Mafic segregations in ophiolite mantle sequences. *Nature*, **299**, 524–8.

Stephens, M. B. & Gee, D. G., 1981. A plate-tectonic model for Caledonian orogenesis in the central Scandinavian Caledonides. *Abstr. Uppsala Caledonide Symp. Terra Cognita*, **1**, 76.

Stern, C. R., Huang, W.-L, & Wyllie, P. J., 1975. Basalt-andesite-rhyolite H_2O: Crystallisation intervals with excess H_2O and H_2O-undersaturated liquidus surfaces to 35 kbars with implications for magma genesis. *Earth Planet Sci. Lett.*, **28**, 189–96.

Strand, T., 1969. Geology of the Grotli area. *Nor. Geol Tidsskr.*, **49**, 341–60.

Sturt, B. A., Skarpenes, O., Ohanian, A. T. & Pringle, I. R., 1975. Reconnaissance Rb/Sr isochron study in the Bergen Arc System and regional implications. *Nature*, **253**, 589–99.

Sturt, B. A. & Thon, A., 1974. The age of orogenic deformation in the Swedish Caledonides. *Am. J. Sci.*, **276**, 385–9 .

Talwani, M. & Eldholm, O., 1972. Continental margin off Norway: A geophysical study. *Geol. Soc. Am. Bull.*, **83**, 3575–606.

Thompson, A. B., 1981. The pressure-temperature (P,T) plane viewed by geophysicists and petrologists. *Abstr. Uppsala Caledonide Symp. Terra Cognita*, **1**, 11–20.

Toksöz, M. N. & Bird, P., 1977. Modelling of temperatures in continental convergence zones. *Tectonophysics*, **41**, 181–93.

Tørudbakken, B., 1981. Trondheim-Surnadal. In: *Excursions in the Scandinavian Caledonides U.C.S. Excursion No. B: Eclogites and Basal Gneisses in west Norway* (eds. W. L. Griffin & M. B. E. Mørk), pp. 13–19. Uppsala Caledonide Symposium.

Tørudbakken, B. & Råheim, A., 1982. An in-situ metamorphosed eclogite near the Surnadal syncline and its implications for the metamorphic relationships in the Surnadal area. *Abstr. First Int. Eclogite Conf., Clermont Ferrand. Terra Cognita*, **2**, 79.

Verschure, R. H., Andressen, P. A. M., Boelrijk, N. A. I. M., Hebden, E. H., Maier, C., Priem, H. N. A. & Verdurmen, E. A. Th., 1980. On the thermal stability of Rb-Sr and K-Ar biotite systems: Evidence from coexisting Sveconorwegian (ca. 870 Ma) and Caledonian (ca. 400 Ma) biotites in S. W. Norway. *Contrib. Mineral. Petrol.*, **74**, 245–52.

Watts, A. B., 1971. Geophysical investigations on the continental shelf and slope north of scotland. *Scott. J. Geol.*, **7**, 189–218.

Wood, B. J. & Banno, S., 1973. Garnet-orthopyroxena and orthopyroxene-clinopyroxene relationships in simple and complex systems. *Contrib. Mineral. Petrol.*, **42**, 109–24.

Received 9 July 1982; revision accepted 10 December 1982.

Note added in proof

It has been brought to our attention that the Griffin & Mørk (1981) reference is not widely available. Readers are advised instead to refer to the major new review paper on 'High-pressure metamorphism in the Scandinavian Caledonides' by W. L. Griffin, H. Austrheim, K. Brastad, I. Bryhni, A. G. Knill, E. J. Krogh, M. B. E. Mørk, H. Qvale & T. Tørudbakken to be published shortly in: *The Caledonian Orogen—Scandinavia and Related Areas* (eds. B. A. Sturt & D. G. Gee), John Wiley.

Bull. Minéral.
(1983), **106**, 727-750

The petrogenesis of contrasting Fe-Ti and Mg-Cr garnet peridotite types in the high grade gneiss complex of Western Norway

by DENNIS A. CARSWELL, MARTIN A. HARVEY and AZZAM AL-SAMMAN,
Department of Geology, University of Sheffield, Mappin Street, Sheffield, S1 3JD, England.

Abstract. — Attention is drawn to the existence of two compositionally different types of garnetiferous peridotites within the west Norway gneiss region. The Fe-Ti type comprises relatively ferriferous garnet peridotites (olivines Fo_{67-82}) with conspicuous amounts of Fe and Ti oxide phases. New whole rock and mineral analyses suggest that in the Eiksunddal Complex on Hareidlandet these rocks, together with dominant garnet pyroxenites and eclogites, developed from a layered intrusive complex of original low pressure (< 10 kbar) olivine norite-peridotite cumulates perhaps genetically related to the rapakivi granite (augen gneiss)-mangerite-anorthosite igneous rock suite. The more restricted occurrences of comparable rocks at Raknestangen (Otrøy), Kolmannskog (Molde area) and Lyngenes (Selje area) have probably had similar origins. By contrast the Mg-Cr garnet peridotites (olivines Fo_{82-92}) have significantly lower Ti and higher Cr and Ni contents and, together with associated garnet pyroxenites, are sporadically preserved within large mantle derived olivine dominated (Fo_{93-95}) 'alpine-type' peridotites bodies. New data on an occurrence of these rocks at Sandvik on Gurskøy demonstrate the development of garnetiferous peridotite from an original high temperature spinel-aluminous pyroxenes peridotite assemblage. Possible pressure-temperature trajectories for the metamorphic evolution of both the Fe-Ti garnet peridotites and the Mg-Cr garnetiferous peridotites are outlined and compared. It is emphasised that in both garnet peridotite types the eclogite facies mineralogies developed in a deep crustal environment under similar pressure-temperature conditions.

Key words : garnet peridotite, Norway, P-T conditions, Eiksunddal, protoliths.

Pétrogenèse des péridotites à grenat riches en Fe-Ti et de celles riches en Mg-Cr qui leur font contraste dans le complexe métamorphique de haut grade de l'Ouest de la Norvège.

Résumé. — L'accent est mis sur l'existence de deux types de péridotites à grenat de composition différente dans la région gneissique de l'Ouest de la Norvège. Le type Fe-Ti est formé de péridotites à grenat relativement ferrifères (olivines Fo 67-82) avec une teneur remarquable en oxydes de Fe et de Ti. De nouvelles analyses de roche totale et de minéraux suggèrent que dans le complexe de Eiksunddal en Hareidlandet ces roches, comme les pyroxénites à grenat et les éclogites associées plus abondantes, se sont développées à partir d'un complexe stratifié intrusif formé initialement de cumulats de norite à olivine-péridotite de basse pression (< 10 kbar) peut-être génétiquement liés à la séquence ignée granite rapikiwi (gneiss œillé)-mangérite-anorthosite. Les gisements plus restreints de roches comparables à Raknestangen (Otrøy), Kolmannskog (région de Molde) et Lyngenes (région de Selje) ont probablement des origines semblables. En revanche, les péridotites à grenat riches en Mg-Cr (olivines Fo 82-92) ont des teneurs particulièrement plus faibles en Ti et plus élevées en Cr et Mi et, comme les pyroxénites à grenat associées, sont sporadiquement préservées dans de grands massifs de péridotite de "type alpin" à olivine prépondérante (Fo 93-95) issus du manteau. De nouvelles données sur un gisement de ces roches à Sandvik près de Gurskøy illustrent le développement d'une péridotite à grenat à partir d'une péridotite à pyroxènes et spinelle de haute température. Les trajectoires pression-température probables de l'évolution métamorphique des péridotites à grenat riches en Fe-Ti et des péridotites à grenat riches en Mg-Cr sont présentées et comparées. Il est fortement suggéré pour les deux types de péridotites à grenat que les paragenèses du faciès éclogite se sont formées dans un environnement infra-crustal sous des conditions pression-température similaires.

Mots-clés : péridotite grenat, Norvège, conditions pression-température, Eiksunddal, protolithe.

INTRODUCTION

In their review of occurrences of alpine-type ultramafic rocks in the Norwegian Caledonides and associated Basal Gneiss Complex, Moore and Qvale (1977) drew attention to the existence of three types of such rocks, distinguished on the basis of mineralogical and textural characteristics and field associations. They stressed that their type three ultramafic rocks are particularly in evidence within the high grade Basal Gneiss Complex in the Sunnmøre district of western Norway and have to date received most attention because of the spectacular, although controver-

sial, occurrences of garnetiferous variants, notably garnet peridotites and garnet pyroxenites (garnet websterites). However it does not appear to have been appreciated that two compositionally contrasting types of garnet peridotites in fact occur within the gneisses of the Møre and Romsdal regions of west Norway.

To highlight their chemical distinctions we propose to refer to these as *Fe-Ti garnet peridotites* and *Mg-Cr garnet peridotites*, respectively. Only the latter type, as exemplified by the occurrences at Almklovdalen near Åheim, Kalskaret near Tafjord and Ugelvik on Otrøy, was recognised and discussed by Moore and Qvale (1977).

In this paper, we emphasise the contrasting whole rock and mineral chemistries and lithological associations of these two types of garnet peridotites by particular reference to new data on the occurrences of these different garnet peridotite types at Eiksunddal on Hareidlandet and at Sandvik on Gurskøy. The locations of these and other documented occurrences of the two garnet peridotite types are shown on figure 1. We shall also show that the two types are likely to have had quite separate origins from different protoliths.

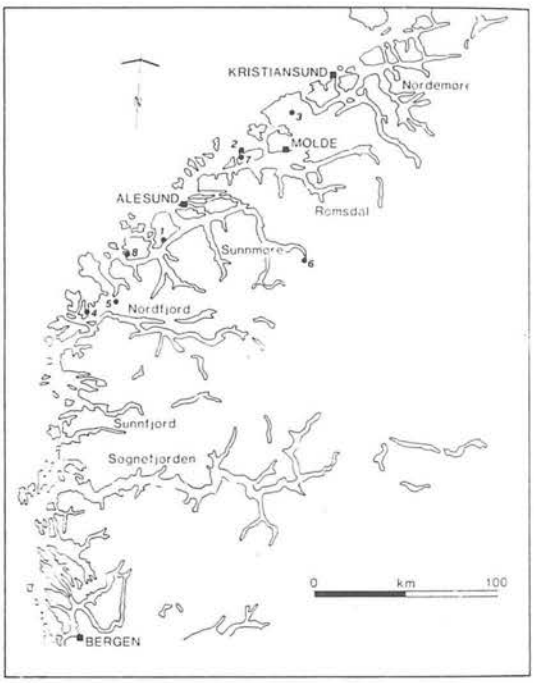

FIG. 1. — *Geographic map of western Norway showing the locations of garnet peridotite samples discussed in this paper*. Fe-Ti Type : 1. Eiksunddal ; 2. Raknestangen ; 3. Kolmannskog ; 4. Lyngenes. Mg-Cr Type : 5. Almklovdalen ; 6. Kalskaret ; 7. Ugelvik ; 8. Sandvik.

Carte géographique de la partie Ouest de la Norvège montrant la localisation des exemples discutés dans cet article. Type Fe-Ti : 1. Eiksunddal ; 2. Raknestangen ; 3. Kolmannskog ; 4. Lyngenes. Type Mg-Cr : 5. Almklovdalen ; 6. Kalskaret ; 7. Ugelvik ; 8. Sandvik.

PETROGRAPHY, MINERAL COMPOSITIONS AND FIELD ASSOCIATIONS

Type One : Fe-Ti garnet peridotites

The occurrence of such rocks at Eiksunddal on Hareidlandet has previously been documented in a short published abstract by Schmitt (1964), although in the absence of data on their whole rock and mineral chemistries no mention was made of their distinctive chemical character. Schmitt described these garnet peridotites and associated garnet pyroxenites as being interlayered with hypersthene-, biotite- and hornblende-bearing varieties of eclogite in a large (0.4-1.0 km^3) layered mafic-ultramafic complex. The hazardous access to critical parts has so far prevented a detailed study of this important rock complex, but we present here data on what we take to be a representative suite of samples from this locality.

Coarse-grained olivine free, hypersthene-biotite eclogite appears to be the dominant rock type in the Eiksunddal Complex with the garnetiferous peridotites restricted to distinct layers (typically from 0.1-2 metres in width) in the more central parts of the complex, where they perhaps comprise about 10 % by volume. The narrower layer widths typically reflect small scale rhythmic interlayering of olivine free and olivine bearing rocks. Modal olivine contents vary widely (2-60 vol.%) in different layers but in the most conspicuous garnet peridotites average about 20 vol.%.

Electron microprobe analyses (Tables I-VI) indicate olivine compositions to be in the range Fo_{67-78}. Garnets ($Pyr_{39-53}Alm_{35-47}Gross_{1-10}$) and

Locality	Eiksunddal								Raknes Tangen		Kolmann skog
Type	Fe-Ti Type										
Sample No.	E4	E4	E29	E29	E30	E31	E31	E32	U125	U125	H185
Details wt.%	Emp. Aver.	Min. Sep.	Emp. Cores	Emp. Rims	Emp. Aver.	Emp. Cores	Emp. Rims	Emp. Aver.	Emp. Cores	Emp. Rims	Emp. Aver.
SiO_2	39.9	39.9	39.4	39.9	39.9	39.1	39.7	38.8	40.5	40.5	40.8
TiO_2	0.04	0.05	-	-	0.06	0.04	0.05	-	0.02	0.02	0.01
Al_2O_3	22.0	21.7	21.9	22.7	21.8	21.6	21.8	21.6	22.0	22.0	22.6
Cr_2O_3	-	0.03	-	-	-	-	-	-	0.00	0.00	-
Fe_2O_3	-	2.73	-	-	-	-	-	-	-	-	-
FeO^T	19.9	18.0	21.6	19.7	21.1	21.1	19.9	23.6	17.0	17.3	15.6
MnO	0.50	0.54	-	-	0.66	0.65	0.65	-	0.72	0.78	0.90
NiO	-	0.00	-	-	-	-	-	-	0.02	-	-
MgO	12.5	12.1	12.1	13.4	12.3	12.2	14.1	10.1	13.7	13.7	15.3
CaO	4.77	4.61	4.25	4.17	4.22	4.53	4.10	5.05	4.92	5.12	4.94
Total	99.6	99.6	99.2	99.8	100.0	99.2	100.3	99.2	99.6	99.4	100.2
Structural Formulae Calculated on Basis of 12 Oxygens											
Si	2.985	2.994	2.977	2.967	2.994	2.956	2.941	2.973	3.011	3.013	2.983
Ti	0.002	0.003	-	-	0.003	0.002	0.003	-	0.001	0.001	0.001
Al	1.942	1.923	1.952	1.990	1.924	1.928	1.904	1.953	1.938	1.932	1.951
Cr	-	0.002	-	-	-	-	-	-	0.000	0.000	-
$*Fe^{3+}$	0.070	0.154	0.093	0.076	0.082	0.156	0.208	0.102	0.037	0.039	0.082
Fe^{2+}	1.180	1.128	1.269	1.152	1.241	1.178	1.023	1.407	1.056	1.038	0.869
Mn	0.032	0.034	-	-	0.042	0.042	0.041	-	0.045	0.049	0.056
Ni	-	0.000	-	-	-	-	-	-	0.001	-	-
Mg	1.397	1.355	1.364	1.482	1.373	1.373	1.554	1.152	1.518	1.518	1.672
Ca	0.383	0.371	0.344	0.332	0.339	0.366	0.326	0.414	0.392	0.409	0.387
% Pyr	46.7	46.9	45.8	50.0	45.8	46.5	52.8	38.8	51.3	51.4	56.0
% Alm	39.5	39.1	42.6	38.8	41.5	39.7	34.8	47.3	34.0	33.1	29.1
% Gross	9.5	4.7	6.9	7.4	7.4	4.3	0.5	8.8	11.4	11.8	8.8
% Spess	1.1	1.2	-	-	1.4	1.4	1.4	-	1.5	1.7	1.9
% And	3.3	8.0	4.7	3.8	3.8	8.0	10.5	5.1	1.8	2.0	4.1
% Uvar	-	0.1	-	-	-	-	-	-	-	-	-

$*Fe^{3+}$ Calculated by charge balance in structural formulae

FeO^T Total Fe as FeO in Emp (Electron Microprobe) analyses

Locality	Sandvik							
Type	Mg-Cr Type							
Sample No.	E35	E35	E38	E38	E39A	E39A	E97	E97
Details wt.%	Emp. Cores	Emp. Cores	Emp. Exsolv Opx	Emp. Corona Spinel	Emp. Cores	Emp. Rims	Emp. Aver. Prim.	Emp. Aver. Sec.
SiO_2	41.9	41.9	40.7	40.8	41.8	42.2	42.4	42.4
TiO_2	0.03	0.03	0.09	0.02	0.17	0.15	0.22	0.02
Al_2O_3	20.7	20.6	21.9	22.7	22.6	22.8	22.7	23.5
Cr_2O_3	4.36	4.57	0.83	0.34	1.77	1.56	1.68	0.65
Fe_2O_3	-	-	-	-	-	-	-	-
FeO^T	7.78	8.56	13.6	14.4	7.97	8.14	8.43	8.65
MnO	0.42	0.53	0.68	0.80	0.43	0.30	0.37	0.24
NiO	0.03	0.04	0.01	0.02	0.00	0.00	0.01	0.01
MgO	19.7	19.3	15.5	15.8	20.5	20.8	20.4	20.9
CaO	5.36	5.08	6.01	4.48	4.16	4.10	4.22	4.02
Total	100.2	100.5	99.3	99.4	99.5	100.0	100.4	100.1
Structural Formulae Calculated on Basis of 12 Oxygens								
Si	2.999	3.002	2.995	2.998	2.987	2.996	3.003	2.982
Ti	0.002	0.002	0.005	0.001	0.009	0.008	0.012	0.001
Al	1.745	1.738	1.902	1.963	1.906	1.903	1.892	1.954
Cr	0.247	0.259	0.048	0.020	0.100	0.087	0.094	0.036
$*Fe^{3+}$	0.006	0.000	0.050	0.019	0.002	0.002	0.000	0.043
Fe^{2+}	0.460	0.513	0.783	0.867	0.474	0.480	0.499	0.468
Mn	0.026	0.032	0.042	0.050	0.026	0.018	0.022	0.014
Ni	0.002	0.002	0.001	0.001	0.000	0.000	0.001	0.001
Mg	2.103	2.062	1.700	1.780	2.178	2.194	2.157	2.196
Ca	0.411	0.390	0.474	0.352	0.318	0.312	0.320	0.304
% Pyr	70.2	68.9	56.7	57.7	72.9	73.4	72.4	73.6
% Alm	15.2	17.0	26.1	28.9	15.6	15.6	16.1	15.7
% Gross	1.1	0.1	10.9	9.8	5.5	5.9	6.0	6.2
% Spess	0.9	1.1	1.4	1.7	0.9	0.6	0.7	0.5
% And	0.2	-	2.3	0.9	-	0.1	-	2.1
% Uvar	12.4	13.0	2.4	1.0	5.0	4.4	4.7	1.8

$*Fe^{3+}$ Calculated by charge balance in structural formulae

FeO^T Total Fe as FeO in Emp (Electron Microprobe) analyses

TABLE I. — *Garnet compositions in analysed garnet peridotite samples. Compositions des grenats des échantillons de péridotite à grenat analysés.*

Locality	Eiksunddal				Raknes.	Kol Manns	Sandvik						
Type	Fe-Ti Type						Mg-Cr Type						
Sample No.	E4	E4	E42	E42	U125	H185	E35	E35	E38	E39A	E39A	E97	E97
Details wt.%	Emp. Aver.	Min. Sep.	Emp. Aver.	Emp. Aver.	Emp. Aver.	Emp. Aver.	Emp. Cores	Emp. Rims	Emp. Aver.	Emp. Cores	Emp. Rims	Emp. Cores	Emp. Rims
SiO_2	53.1	54.0	54.2	54.3	54.1	54.4	54.4	54.8	51.8	55.1	54.8	55.1	55.2
TiO_2	-	0.05	0.01	-	0.03	-	0.01	0.02	0.57	0.24	0.25	0.29	0.28
Al_2O_3	0.73	1.28	1.41	1.10	0.76	0.92	2.58	2.56	4.51	3.66	3.55	3.20	3.16
Cr_2O_3	-	0.01	-	-	0.02	-	2.98	2.72	0.47	1.36	1.41	1.29	1.36
Fe_2O_3	-	0.76	-	-	-	-	-	-	-	-	-	-	-
FeO^T	4.40	4.01	5.77	6.49	3.81	3.50	1.62	1.23	3.71	1.23	1.26	1.51	1.56
MnO	-	0.07	0.02	-	0.09	0.23	0.09	0.06	0.09	0.07	0.06	0.08	0.07
NiO	-	0.00	-	-	0.03	-	0.04	0.06	0.01	0.05	0.03	0.01	0.03
MnO	16.8	16.5	15.3	15.2	16.9	17.0	16.3	15.2	15.7	16.1	15.3	15.3	16.1
CaO	22.2	22.3	22.0	21.9	23.6	23.7	19.4	20.3	21.9	20.2	20.9	20.2	20.0
Na_2O	0.49	0.44	1.60	1.47	0.21	0.27	1.91	2.21	0.84	2.03	2.08	2.43	2.17
Total	98.8	99.6	100.3	100.4	99.6	99.9	99.3	99.2	99.7	99.4	99.6	99.6	100.0
	Structural Formulae on Basis of 6 Oxygens												
Si	1.994	1.980	1.961	1.977	1.986	1.981	1.978	1.996	1.890	1.992	1.981	1.998	1.984
Ti	-	0.001	0.000	-	0.001	-	0.001	0.001	0.016	0.006	0.007	0.008	0.007
Al	0.032	0.055	0.060	0.047	0.033	0.040	0.111	0.110	0.194	0.130	0.151	0.136	0.134
Cr	-	0.000	-	-	0.001	-	0.086	0.078	0.014	0.039	0.040	0.037	0.039
$*Fe^{3+}$	0.015	0.021	0.113	0.102	0.016	0.017	0.000	0.000	0.041	0.000	0.000	0.000	0.000
Fe^{2+}	0.121	0.123	0.062	0.095	0.101	0.090	0.049	0.038	0.072	0.037	0.038	0.046	0.047
Mn	-	0.002	0.001	-	0.003	0.007	0.003	0.002	0.003	0.002	0.002	0.002	0.002
Ni	-	0.000	-	-	0.001	-	0.001	0.002	0.001	0.002	0.001	0.001	0.003
Mg	0.925	0.904	0.827	0.822	0.924	0.922	0.882	0.827	0.853	0.865	0.823	0.821	0.862
CaO	0.878	0.878	0.855	0.853	0.925	0.924	0.756	0.791	0.857	0.784	0.811	0.781	0.771
Na	0.035	0.031	0.113	0.104	0.015	0.019	0.135	0.156	0.059	0.142	0.146	0.170	0.151

$*Fe^{3+}$ Calculated by Charge Balance in Structural Formulae
FeO^T Total Fe as FeO in EMP (Electron Microprobe) Analyses

TABLE II. — *Clinopyroxene compositions in analysed garnet peridotite samples.*
Compositions des clinopyroxènes des échantillons de péridotite à grenat analysés.

orthopyroxenes (En_{74-81}) are usually the dominant mineral phases. Diopsidic clinopyroxene is absent in some garnet peridotites but increases up to about 20 vol.% in others. All garnet peridotite samples contain several percent of oxide phases. Granular intergrowths of magnetite ($Magn_{93-97}Ulvosp_{3-7}$) and ilmenite (Ilm_{95-99} $Haem_{1-5}$) are particularly in evidence but there are often also some discrete grains of green pleonaste spinel ($Sp_{92-97}Magn_{3-8}$). In addition, these rocks variably contain olivines crowded with thin magnetite lamellae, coarse symplectite intergrowths of magnetite and bronzitic orthopyroxene, and fine grained symplectite intergrowths of green pleonaste spinel and pyroxenes developed as coronas between adjacent garnets and olivines (Figure 2). Full discussion of the mineral reactions responsible for symplectite and corona development is deferred until later, but it is clear that the latter coronas reflect the breakdown of the earlier high pressure eclogite facies garnet + olivine assemblage in these rocks. Further retrogression is often witnessed by the growth of late interstitial hornblendic amphibole as a replacement phase of the garnets and pyroxenes (including symplectitic varieties).

We have observed occurrences of comparable Fe-Ti enriched garnet peridotites at two other localities further to the North, namely at Raknestangen on the northernmost coast of Otrøy and at Kolmannskog approximately 18 km North of the town of Molde. At Raknestangen garnet peridotites again occur interlayered with orthopyroxene enriched garnet pyroxenites and with eclogites in an elongate lens roughly 24 × 10 metres enclosed in quartzofeldspathic gneisses. Petrographic features and mineral compositions are in large measure similar to those of the Eiksunddal garnet peridotites. Olivine (Fo_{79-80}) is subordinate to garnet (Pyr_{51} $Alm_{34}Gross_{12}$) and orthopyroxene (En_{82}) whilst the clinopyroxene is again diopsidic and jadeite poor (Tables I-VI). Magnetite, ilmenite and green pleonaste spinel ($Sp_{95}Magn_5$) together again comprise several percent of the mode. An additional feature is the presence of some 2-3

Locality	Eiksunddal									Raknes Tangen		Kolmann Skogs		Sandvik				
Type	Fe-Ti Type													Mg-Cr Type				
Sample No.	E4	E4	E29	E29	E30	E30	E31	E31	E32	U125	U125	H185	H185	E35	E35	E38	E38	E97
Details wt.%	Emp. Aver	Min. Sep.	Emp. Prim.	Emp. Symp. Magn.	Emp. Prim.	Emp. Symp. Magn.	Emp. Inclu. In Ol.	Emp. Symp. Magn.	Emp. Aver.	Emp. Aver.	Emp. Rim Against Gnt	Emp. Max. Al	Emp. Min. Al.	Emp. Cores	Emp. Rims Against	Emp. Aver	Calc. Prim. Recon.	Emp. Aver.
SiO_2	55.5	55.3	55.8	54.9	55.6	55.4	55.1	55.6	54.5	55.8	55.4	55.9	57.0	58.3	57.5	54.8	53.8	58.1
TiO_2	0.04	0.05	-	-	0.01	0.03	0.00	0.03	-	0.02	0.02	0.05	0.02	0.02	0.01	0.10	0.10	0.06
Al_2O_3	0.29	0.48	0.09	0.37	0.12	0.48	0.08	0.48	0.20	0.86	1.27	1.87	0.81	0.64	1.45	3.39	4.79	1.05
Cr_2O_3	-	0.00	-	-	-	-	-	-	-	0.01	0.02	0.00	0.02	0.23	0.24	0.19	0.24	0.09
Fe_2O_3	-	1.46	-	-	-	-	-	-	-	-	-	-	-	-	-	-	-	-
FeO^T	13.1	12.1	13.9	13.6	14.1	13.8	13.4	13.5	17.6	11.8	12.2	12.0	10.8	4.85	5.76	8.80	9.16	4.97
MnO	-	0.15	-	-	0.18	0.20	0.10	0.08	-	0.21	0.24	-	-	0.10	0.14	0.18	0.24	0.10
NiO	-	0.04	-	-	-	-	-	-	-	-	-	-	-	0.05	0.05	0.10	0.09	0.09
MgO	30.6	30.2	30.4	30.2	29.5	29.5	30.4	30.5	27.3	30.0	30.0	30.2	31.4	35.8	34.6	31.6	30.1	35.3
CaO	0.23	0.24	0.18	0.18	0.17	0.18	0.16	0.22	0.22	0.25	0.27	0.26	0.23	0.20	0.14	0.35	0.77	0.17
Na_2O	0.02	0.04	0.02	0.02	0.03	0.02	0.04	0.02	-	-	-	0.05	0.01	0.01	0.00	0.01	0.01	0.01
Total	99.8	100.0	100.4	99.4	99.6	99.6	99.2	100.4	99.7	99.6	99.4	100.3	100.3	99.8	99.9	99.6	99.6	100.0
%En	82	81	80	80	79	79	80	80	74	82	81	80	83	93	91	86	86	93
Structural Formulae on Basis of 6 Oxygens																		
Si	1.976	1.967	1.981	1.971	1.992	1.982	1.978	1.974	1.978	1.981	1.974	1.966	1.993	1.995	1.978	1.922	1.892	1.987
Ti	0.001	0.001	-	-	0.000	0.001	0.000	0.001	-	0.001	0.001	0.001	0.001	0.001	0.000	0.003	0.003	0.002
Al	0.012	0.020	0.004	0.015	0.005	0.020	0.003	0.020	0.009	0.036	0.053	0.078	0.033	0.026	0.059	0.140	0.199	0.042
Cr	-	0.000	-	-	-	-	-	-	-	0.000	0.001	0.000	0.001	0.006	0.006	0.005	0.007	0.002
$^*Fe^{3+}$	-	0.039	-	-	-	-	-	-	-	-	-	-	-	-	-	-	-	-
Fe^{2+}	0.390	0.360	0.413	0.409	0.421	0.414	0.404	0.401	0.532	0.351	0.362	0.353	0.316	0.139	0.166	0.258	0.270	0.142
Mn	-	0.004	-	-	0.005	0.006	0.003	0.002	-	0.006	0.007	-	-	0.003	0.004	0.005	0.003	0.003
Ni	-	0.001	-	-	-	-	-	-	-	-	-	-	-	0.001	0.001	0.003	0.002	0.003
Mg	1.625	1.600	1.612	1.617	1.573	1.575	1.625	1.610	1.490	1.616	1.590	1.583	1.638	1.810	1.770	1.653	1.595	1.801
Ca	0.009	0.009	0.007	0.007	0.006	0.007	0.006	0.008	0.009	0.010	0.010	0.010	0.009	0.007	0.005	0.013	0.029	0.006
Na	0.001	0.003	0.001	0.001	0.002	0.001	0.003	0.001	-	-	-	0.003	0.001	0.001	0.000	0.001	0.001	0.001
Total	4.013	4.004	4.018	4.020	4.006	4.008	4.022	4.017	4.018	4.001	3.998	3.995	3.990	3.989	3.990	4.003	4.004	3.989

FeO^T Total Fe as FeO in Emp (Electron Microprobe) Analyses

TABLE III. — *Orthopyroxene compositions in analysed garnet peridotite samples.*
Compositions des orthopyroxènes des échantillons de péridotite à grenat analysés.

Locality	Eiksunddal					Raknes.	Kol Manns.	Sandvik				
Type	Fe-Ti Type							Mg-Cr Type				
Sample No.	E4	E29	E30	E31	E32	U125	H185	E35	E38	E38A	E97	E97
Details wt.%	Emp. Aver.	Emp. Aver.	Emp. Aver.	Emp. Aver.	Emp. Aver.	Emp. Aver.	Emp. Aver.	Emp. Aver.	Emp. Aver.	Emp. Aver.	Emp. Clasts	Emp Neobl.
SiO_2	38.4	37.4	37.7	37.6	36.1	39.1	39.7	41.3	40.1	41.7	41.4	42.5
TiO_2	0.01	-	0.02	0.01	-	-	0.01	-	-	-	-	-
Al_2O_3	0.01	0.01	0.00	0.01	0.02	-	-	-	-	-	-	-
FeO^T	20.7	22.7	23.1	22.5	29.4	19.2	17.4	7.40	13.2	6.45	7.49	7.26
MnO	-	-	0.02	0.12	-	0.29	0.28	0.08	0.19	0.03	0.06	0.09
NiO	-	-	-	-	-	0.17	-	0.41	0.37	0.41	0.41	0.41
MgO	41.1	39.1	38.2	39.0	33.7	41.6	42.8	50.5	45.6	51.5	50.8	49.9
CaO	0.04	0.03	0.03	0.03	0.04	-	-	-	-	-	-	-
Total	100.3	99.2	99.2	99.1	99.2	100.4	100.2	99.6	99.5	100.1	100.2	100.1
%Fo	78	75	75	76	67	79	81	92	86	93	92	92

TABLE IV. — *Olivine compositions in analysed garnet peridotite samples.*
Compositions des olivines des échantillons de péridotite à grenat analysés.

vol.% of phlogopitic mica occurring as discrete plates in apparent textural equilibrium with the garnet lherzolite assemblage. Similar symplectite intergrowths and secondary reaction coronas occur as in the Eiksunddal garnet peridotites.

The analysed garnet peridotite sample from Kolmannskog (Tables I-VI) is almost identical to that from Raknestangen with predominant olivine (Fo_{81}), orthopyroxene (En_{85}) and garnet ($Pyr_{56}Alm_{29}Gross_9$) and minor diopsidic clino-

Locality	Eiksunddal										Raknes Tangen		Kol Manns.	Sandvik	
Type	Fe-Ti Type													Mg-Cr Type	
Sample No.	E4	E4	E29	E29	E29	E30	E30	E30	E31	E31	U125	U125	H185	E35	E38
Oxide Type	Magn.	Ilm.	Magn.	Ilm.	Spinel	Magn.	Ilm.	Spinel	Magn.	Spinel	Magn.	Spinel	Spinel	Sec. Spinel	Prim Spinel
O^{2-}	4	3	4	3	4	4	3	4	4	4	4	4	4	4	4
% Magn.	93	-	97	-	-	95	-	-	95	-	91.6	-	-	-	-
% Ulvo-Spinel	7	-	3	-	-	5	-	-	5	-	8.4	-	-	-	-
% Ilm.	-	95	-	99	-	-	99	-	-	-	-	-	-	-	-
% Haem.	-	5	-	1	-	-	1	-	-	-	-	-	-	-	-
% Spinel	-	-	-	-	96	-	-	92	-	97	-	95.1	95.4	76.5	87.2
% Magn.	-	-	-	-	4	-	-	8	-	3	-	4.7	4.5	0.0	4.8
% Chrom.	-	-	-	-	-	-	-	-	-	-	-	0.2	0.1	23.5	8.0

End member values above are based on microprobe analyses with stoichiometrically calculated Fe_2O_3 contents.

Magn. = magnetite; Ilm. = ilmenite; Haem. = haematite; Chrom = chromite

TABLE V. — *Oxide compositions in analysed garnet peridotite samples.*
Compositions des oxydes des échantillons de péridotite à grenat analysés.

Location	Eiksunddal				Raknes.	Kolmannskog		Sandvik		
Type	Fe-Ti Type							Mg-Cr Type		
Sample No.	E4	E30	E31	E31	U125	H185	H185	E35	E38	E39A
Details wt.%	Sec. Amph.	Sec. Amph.	Sec. Amph.	Mica	Sec. Amph.	Mica	Sec. Amph.	Sec. Amph.	Prim Amph.	Sec. Amph.
SiO_2	45.1	47.0	46.1	40.5	44.3	38.2	43.8	39.4	42.0	41.4
TiO_2	-	0.27	-	0.48	0.46	0.83	0.43	0.11	1.81	0.57
Al_2O_3	12.6	10.8	9.60	14.3	12.9	16.7	14.7	21.0	13.0	17.6
Cr_2O_3	-	-	-	-	0.02	-	-	3.78	0.57	1.78
FeO^T	7.69	8.49	8.75	5.44	7.60	6.17	7.80	3.28	6.15	2.59
MnO	0.41	0.11	-	0.00	0.11	0.03	-	0.10	0.06	0.06
NiO	-	-	-	-	0.05	-	-	0.08	0.11	0.06
MgO	17.0	18.8	18.5	23.7	15.9	21.6	15.4	17.21	17.2	17.8
CaO	11.6	10.3	10.8	0.02	12.2	-	12.7	10.38	11.4	11.2
Na_2O	2.02	2.85	2.53	0.63	1.05	0.18	0.93	-	2.39	-
K_2O	-	-	-	8.41	1.40	9.78	1.54	-	1.13	-
Total	96.4	98.5	96.3	93.5	95.9	93.4	97.3	95.3	95.8	93.2

TABLE VI. — *Partial analyses of amphiboles and micas.*
Analyses partielles des amphiboles et des micas.

pyroxene, magnetite, ilmenite, pleonaste spinel ($Sp_{95}Magn_5$) and phlogopitic mica. This lithology is associated with a clinopyroxene rich garnet pyroxenite, a partial analysis for which is thought to be that given in Matsui *et al.* (1966), and rather retrograded bimineralic eclogite. However, exposures of this garnet peridotite bearing body are limited to a small, rather weathered, roadside outcrop roughly 6 metres high and 15 metres long. Much of the western end of the outcrop comprises a tremolitic amphibole rich zone which probably represents a reaction selvage developed between the ultramafic body and the surrounding migmatitic semipelitic gneisses. On the other hand, the eastern contact of the body is tectonic and occupied by a late quartz vein.

A further Fe-Ti garnet peridotite sample, comparable to those described above but not referred to as such, is that previously recorded and analysed by Eskola (1921) and Lappin and

Smith (1978). This analysed sample, labelled *Ly* by the latter authors, was from the collection at the Mineralogisk-Geologisk Museum in Oslo, where it is recorded to have been collected by H. Reusch in 1886 from Lyngenes, Sørpollen near Selje on Stadlandet (See figure 1). Lappin and Smith (1978) reported that they were unable to locate the field occurrence of this rock, so nothing is known about its field relations. Eskola (1921) recorded this rock as an olivine bearing, orthopyroxene free, eclogite and obtained the whole rock analysis reproduced in table X. However, the more detailed mineralogical study of Lappin and Smith (1978) has shown it to contain the assemblage garnet ($Pyr_{51}Alm_{37}Gross_{12}$), diopsidic clinopyroxene, orthopyroxene (En_{84}), olivine (Fo_{82}), spinel and opaque oxides. This sample therefore has a chemical and mineralogical similarity to the other Fe-Ti garnet peridotites reported in this paper.

The mineral compositions listed in tables I-VI were mainly obtained by electron microprobe analysis ; those for Eiksunddal samples on the ARL-EMX microprobe at the Central Institute for Industrial Research (Oslo) all others on the Cambridge Microscan IX instrument in the Department of Geology, University of Sheffield. Observed variations in chemical composition both within and between the individual grains of particular mineral phases were small in most samples. Hence reported mineral analyses in most cases represent the average value obtained for several point analyses. Slight chemical zoning was observed in garnets from certain Eiksunddal samples, with a slight decrease in Fe/Mg ratio in rims compared to cores, suggestive of garnet growth along a prograde metamorphic path (cf. Bryhni and Griffin, 1971 ; Råheim, 1975). The 'wet' chemical analyses of mineral separates from the Eiksunddal garnet peridotite sample, E4, are probably only of value to the extent that they indicate the $Fe^{3+}/(Fe^{2+} + Fe^{3+})$ ratios and contents of certain minor elements in these minerals. Oxide analyses in the Eiksunddal samples obtained by the ARL-EMX microprobe and related data reduction procedure have rather poor analytical totals and only provide a generalised indication of the compositions of the various oxide types. On the other hand, the oxide analyses in the other samples, obtained on the Microscan IX, give a more precise indication of mineral compositions.

FIG. 2. — *Photomicrograph of Eiksunddal garnet lherzolite showing :* (a) the development of fine grained coronas of secondary pleonaste spinel and pyroxenes between garnet (left) and olivines (bottom right) ; (b) adjacent coarser symplectite intergrowths of orthopyroxene and magnetite ; (c) the abundance of fine grained magnetite lamellae in the nearby olivines. Photograph width approx. 2 mm.

Photomicrographie de la lherzolite à grenat de Eiksunddal montrant : a) le développement de couronnes à grain fin de pléonaste secondaire et de pyroxènes entre grenat (à gauche) et olivines (en bas à droite) ; b) l'intercroissance symplectitique grossière voisine formée d'orthopyroxène et magnétite ; c) l'abondance de fines lamelles de magnétite dans les olivines voisines. Dimension approx. de la photographie : 2 mm.

As previously noted oxide-pyroxene symplectite intergrowths sometimes in obvious coronitic disposition, are a characteristic petrographic feature of the Fe-Ti garnet peridotites. Two principal types of such symplectite intergrowths have been observed (See figure 2). The first type comprises extremely fine grained intergrowths of green pleonaste spinel and pyroxenes (mostly orthopyroxene but also minor clinopyroxene). Occasionally, fine grained magnetite occurs with, although generally subordinate to, the green spinel. Such symplectite intergrowths occur for the most part as irregularly developed reaction coronas at the contacts between garnet and olivine grains. Garnet grain margins are often highly irregular with embayments of such replacement symplectite. Further from garnet grain margins, these fine grained spinel-pyroxene symplectites characteristically pass into the second type of symplectite. These comprise much coarser grained orthopyroxene-magnetite symplectites within which the distri-

bution of magnetite is highly variable and both the orthopyroxene and the magnetite appear to have primarily nucleated on (hence are in optical continuity with) pre-existing orthopyroxene and magnetite grains. Outside of an irregularly developed zone of such coarse orthopyroxene-magnetite symplectite, pale coloured amphibole is often developed as a late replacement phase in the most hydrated rocks. Adjacent olivine grains typically have 'fronts' of fine grained magnetite inclusions extending in from their margins.

We consider that the various symplectite intergrowth textures reflect the fact that the retrograde (decompression) replacement reaction of the eclogite facies garnet peridotite assemblage to a granulite facies pyroxenes + spinel peridotite assemblage has occurred concommitantly with oxidation reactions buffered by the high content of 'initial'* oxide phases. Excluding the grossular content of the garnet and the resultant secondary clinopyroxene, the integrated reactions may be represented by the following simplified reaction equation :

$$Mg_{1.5}Fe_{1.5}Al_2Si_3O_{12} + 7Mg_1Fe_1SiO_4 + O_2 \quad \uparrow\downarrow \quad Mg_{0.5}Fe_{0.5}Al_2O_4 + 5Mg_{1.6}Fe_{0.4}Si_2O_6 + 2Fe_3O_4 \qquad [1]$$

However, in some samples oxidation of olivine, leading to the development of associated orthopyroxene-magnetite symplectite and olivine with enclosed abundant fine grained magnetite, may have occurred independently of garnet breakdown according to the reaction equation :

$$12Mg_{1.5}Fe_{0.5}SiO_4 + O_2 \quad \uparrow\downarrow \quad 6Mg_2SiO_4 + 6MgSiO_3 + 2Fe_3O_4 \qquad [2]$$

It is significant that orthopyroxenes occurring in coarse symplectite intergrowths with magnetite have somewhat higher Al_2O_3 contents than the 'initial' orthopyroxene grains (Table III) as might be expected from reaction [1]. Unfortunately it was not found to be possible to analyse the fine grained secondary orthopyroxene intergrown with green spinel immediately adjacent to garnet grain margins but it is reasonable to expect it to be even more aluminous.

It is also noteworthy that in these Fe-Ti garnet peridotites the 100 $Mg^{2+}/(Mg^{2+} + Fe^{2+})$ ratios in the olivines and orthopyroxenes tend to be negatively correlated with the 100 $Fe^{2+}/(Fe^{2+} + Fe^{3+})$ value in the rock (compare tables III, IV, VII and X, cols. B-D), whereas there is no correlation whatsoever with the overall 100 Mg/(Mg + Fe) value in the rock, which in fact varies little in the various rock samples. In other words, the more highly oxidised the rock the more magnetite has formed and consequently the higher the 100 $Mg^{2+}/(Mg^{2+} + Fe^{2+})$ ratios in the silicate minerals. Consequently, of the Eiksunddal samples, the least oxidised rock, E32, contains the most ferriferous silicate minerals. As this relationship holds for the garnets and clinopyroxenes, as well as the olivines and orthopyroxenes, it is apparent that the oxygen fugacity has controlled the 100 $Mg^{2+}/(Mg^{2+} + Fe^{2+})$ contents of the 'initial' eclogite facies assemblages as well as in the secondary replacement assemblages. 'Initial' magnetite, ilmenite and spinel all form some discrete grains independent of secondary symplectites and coronas, and also occur as inclusions in the garnets. The compositions of the coexisting 'initial' magnetites and ilmenites are somewhat variable (Table V) but indicate that during the formation of the Fe-Ti garnet peridotite assemblages the oxygen fugacity was almost certainly buffered to values in excess of the fayalite-magnetite-quartz buffer (Buddington and Lindsley, 1964).

Type Two : Mg-Cr garnet peridotites

This second group of garnetiferous peridotites is exemplified by the well documented rocks at the Kalskaret (near Tafjord), Ugelvik (Otrøy) and various Almklovdalen (near Åheim) localities (Eskola, 1921 ; O'Hara and Mercy, 1963 ; Lappin, 1966, 1974 ; Bryhni, 1966 ; Carswell, 1968*a* and *b*, 1973, 1981 ; Medaris, 1980, 1982). Such rocks and associated olivine free garnet pyroxenites are sporadically preserved as layers or tectonically bounded lenses within large forsteritic olivine (Fo_{93-95}) dominated 'alpine-type' peridotite bodies. The gradational character of undeformed contacts and the considerable overall variability in modal mineral contents emphasise that these garnet peridotites

* *'Initial'* is used here and elsewhere in this paper to denote an early metamorphic phase formed at or close to the metamorphic maximum. *'Primary'*, by contrast, is used to describe deduced earlier high temperature igneous ? phases.

Sample No.	E4	E29	E31	E32	E47	E49	E51	E52	E30	*E48
Rock Type (wt.%)	Garnet Lherz.	Garnet Lherz.	Garnet Lherz.	Garnet Lherz.	Garnet Lherz.	Garnet Lherz.	Garnet Lherz.	Garnet Harz.	Garnet Harz.	Garnet Webr.
SiO_2	42.51	38.42	37.54	39.36	42.45	39.50	39.87	45.90	37.40	41.07
TiO_2	0.98	0.65	0.87	0.81	0.77	0.80	0.80	0.76	1.05	0.96
Al_2O_3	8.07	8.71	11.06	4.99	6.02	4.27	3.89	4.91	12.11	14.76
Cr_2O_3	0.04	0.03	0.01	0.03	0.04	0.03	0.02	0.03	0.01	0.03
Fe_2O_3	6.84	7.40	5.57	5.50	6.76	6.84	6.46	6.73	5.67	6.09
FeO	13.19	14.09	18.30	19.84	16.46	19.47	14.80	16.49	18.64	12.61
MnO	0.21	0.43	0.39	0.44	0.27	0.34	0.23	0.22	0.53	0.52
NiO	0.07	0.09	0.08	0.09	0.09	0.09	0.07	0.08	0.08	0.04
MgO	20.57	22.04	22.13	23.99	23.17	25.52	20.20	23.74	21.84	12.91
CaO	6.58	4.10	2.59	3.34	3.46	2.26	6.06	1.08	2.41	10.72
Na_2O	0.18	0.18	0.05	0.14	0.09	0.05	0.33	0.01	0.02	0.63
K_2O	0.03	0.004	0.02	0.00	0.002	0.00	0.03	0.01	0.01	0.01
P_2O_5	0.12	0.02	0.14	0.15	0.16	0.18	0.11	0.01	0.12	0.52
S	0.02	0.02	0.01	0.06	0.01	0.00	0.00	0.01	0.01	0.00
H_2O^+	0.44	4.11	1.12	1.15	0.70	1.29	1.36	0.54	1.09	0.24
Total	99.85	100.29	99.88	99.89	100.46	100.67	100.22	100.11	100.99	101.63
100 $Mg/(Mg+Fe^T)$	65.4	65.4	62.8	63.3	64.5	64.0	63.6	65.2	62.1	56.0
100 $Cr/(Cr+Al)$	0.3	0.2	0.1	0.4	0.4	0.4	0.1	0.4	0.1	0.1
100 $Fe^{2+}/(Fe^{2+}+Fe^{3+})$	68.2	67.9	78.5	80.0	73.0	76.0	71.8	73.1	78.5	69.7
ppm: V	84	38	31	84	86	67	68	82	41	88
Sr	139	108	69	81	144	59	210	-	36	308
Rb	1	0	2	8	0	2	1	3	0	0
CIPW Normative Mineralogy										
Or	0.18	-	0.12	-	-	-	0.18	0.06	0.06	0.06
Ab	1.52	1.52	0.42	1.18	0.76	0.42	2.79	0.08	0.17	5.33
An	21.12	20.21	11.94	12.99	16.02	10.04	25.42	5.29	11.17	37.42
Cor	-	1.01	6.58	-	-	0.51	-	2.94	7.97	-
Di	8.60	-	-	2.11	0.08	-	3.16	-	-	10.02
Hy	33.99	28.37	33.60	26.48	44.47	33.60	21.04	72.05	35.67	13.70
Ol	21.58	32.47	35.55	45.42	26.36	42.47	34.82	7.55	33.72	21.82
Mt	9.92	10.73	8.08	7.97	9.80	9.92	9.37	9.76	8.22	8.83
Il	1.86	1.24	1.65	1.54	1.46	1.52	1.52	1.44	1.99	1.82
Ap	0.28	0.05	0.32	0.35	0.37	0.42	0.26	0.02	0.28	1.21
Oliv.%Fo	73	73	64	64	69	67	69	70	64	64
Plag.%An	93	93	97	92	95	92	90	98	99	88

*E48 contains only minor olivine invariably in reaction relationship with garnet

TABLE VII. — *Analyses of Fe-Ti garnet peridotite samples from the Eiksunddal Complex.*
Analyses des échantillons de péridotite à grenat riche en Fe-Ti du Complexe de Eiksunddal.

and garnet pyroxenites comprise an integral part of these peridotite bodies, they are not 'foreign' tectonic inclusions. Hence any origin and tectono-metamorphic evolutionary history proposed for these garnetiferous rocks must also pertain to the enclosing dominant garnet free peridotites (Moore and Qvale, 1977).

There is good petrographic evidence (e.g. Medaris, 1980) that these garnet peridotites were originally much more widely developed in these peridotite bodies than is currently apparent at all localities other than Ugelvik (Carswell, 1968*b*), but have been extensively retrograded to foliated chlorite and tremolite bearing assemblages. This strongly suggests that all the magnesian peridotite bodies in this part of western Norway witnessed an early eclogite facies metamorphism before the extensive recrystallisation to amphibolite facies assemblages (Medaris, 1982).

Mineral compositions in these Mg-Cr garnet peridotites (O'Hara and Mercy, 1963 ; Mercy and O'Hara, 1965 ; Medaris, 1980 ; Carswell, 1968*a* and *b*, 1981, and unpublished data) are more magnesian and chromiferous than those in the Fe-Ti garnet peridotites. Reported olivine compositions are in the range Fo_{82-92} and orthopyroxenes En_{84-93}. The majority of analysed samples have mineral compositions towards the magnesian end of these ranges but the more ferriferous compositions reported in certain Kalskaret garnet peridotites (O'Hara and Mercy, 1963 ; Carswell, 1968*a*) do just overlap with those reported in certain of the Fe-Ti garnet peridotite samples, specifically with those from Kolmannskog and Lyngenes. However, in common with the other Mg-Cr garnet peridotites, these Kalskaret samples contain significantly more chromiferous garnets and clinopyroxenes than in all of the analysed Fe-Ti garnet peridotite samples. Overall the Cr_2O_3 contents recorded in the pyropic garnets (approx. 60-75 % pyrope) of the Mg-Cr garnet peridotites range from 0.60-4.35 wt.% and in the diopsidic clinopyroxenes from 0.47-2.60 wt.%. By contrast Cr_2O_3

Sample No.	E1	E3	E22	E41	E42	E43	E44	E45	E50A	E50B
Rock Type (wt.%)	Biotite Garnet Pyrox.	Biotite Garnet Pyrox.	Eclogite	Eclogite Trace Opx.	Biotite Garnet Pyrox.	Eclogite	Biotite Eclogite	Discordant Omphacite Vein	Eclogite Cpx Rich Layer+	Eclogite Gnt Rich Layer+
SiO_2	45.51	45.39	45.71	45.00	43.55	45.98	43.64	55.53	47.39	38.57
TiO_2	1.07	1.00	1.14	0.96	1.04	1.11	1.20	0.13	0.86	1.18
Al_2O_3	15.24	15.21	15.35	15.50	14.90	16.52	14.84	10.49	7.09	17.80
Cr_2O_3	0.02	0.02	0.02	0.01	0.01	0.01	0.01	0.005	0.04	0.03
Fe_2O_3	2.74	3.18	2.57	0.92	2.45	2.81	2.93	2.67	3.66	5.25
FeO	12.06	11.67	12.11	13.29	13.91	11.96	13.12	3.55	8.38	16.15
MnO	0.30	0.19	0.19	0.32	0.22	0.17	0.20	0.08	0.14	0.30
NiO	0.05	0.04	0.04	0.02	0.04	0.05	0.04	0.02	0.06	0.05
MgO	13.36	13.05	10.82	11.68	12.85	10.51	12.04	8.90	15.82	13.95
CaO	6.94	7.38	8.17	8.11	6.89	7.81	6.71	12.19	15.84	6.84
Na_2O	2.20	2.17	2.85	2.88	2.16	3.17	2.25	5.25	0.67	0.04
K_2O	0.35	0.70	0.003	0.01	0.27	0.02	1.40	0.02	0.01	0.01
P_2O_5	0.05	0.16	0.30	0.09	0.30	0.18	0.27	0.21	0.09	0.24
S	0.02	0.01	0.03	0.85	0.13	0.02	0.05	0.03	0.00	0.00
H_2O^+	0.23	0.33	0.24	0.16	0.35	0.26	0.50	0.50	0.33	0.34
Total	100.14	100.52	99.52	99.80	99.09	100.56	99.19	99.55	100.37	100.75
100 Mg/(Mg+Fe^T)	62.1	61.5	57.2	59.6	58.7	56.4	57.7	78.5	70.7	54.4
ppm: V	87	83	120	76	78	97	105	132	113	74
Sr	187	249	377	230	341	258	321	301	478	98
Rb	22	33	-	5	2	1	22	1	1	2
CIPW Normative Mineralogy										
Or	2.07	4.14	-	0.06	1.60	0.12	8.27	0.12	0.06	0.06
Ab	18.61	18.36	24.11	21.90	18.27	26.82	16.22	39.34	5.67	0.34
An	30.68	29.70	29.09	29.34	30.16	30.79	26.26	5.00	16.31	32.37
Ne	-	-	-	1.34	-	-	1.52	2.75	-	-
Cor	-	-	-	-	-	-	-	-	-	5.86
Di	2.78	4.76	7.74	8.43	1.68	5.54	4.30	42.9	49.2	-
Hy	10.73	6.31	4.78	-	6.57	0.33	-	-	7.59	31.80
Ol	28.50	29.75	27.66	33.06	33.66	30.84	35.61	4.22	1.63	19.20
Mt	3.97	4.61	3.73	1.33	3.55	4.07	4.25	3.87	5.31	7.61
Il	2.03	1.90	2.16	1.82	1.98	2.11	2.28	0.25	1.63	2.24
Ap	0.12	0.37	0.70	0.21	0.70	0.42	0.63	0.49	0.21	0.56
Oliv. %Fo	63	63	55	57	57	55	57	83	77	57
Plag. %An	62	62	55	57	62	53	62	11	74	99

+Contains traces of olivine

TABLE VIII. — *Analyses of garnet pyroxenites, eclogites, etc., from the Eiksunddal Complex. Analyses des pyroxénites à grenat, éclogites, etc., du Complexe de Eiksunddal.*

contents in both garnets and clinopyroxenes in the Fe-Ti garnet peridotites are consistently < 0.05 wt.%.

Electron microprobe mineral analyses are presented in tables I-VI for Mg-Cr garnet peridotites from a locality at Sandvik on the south-west part of Gurskøy (Figure 1). The small outcrop of these rocks at this locality has previously been mentioned by Green and Mysen (1972) and by Griffin and Mørk (1981), but no analyses were given. Garnet peridotites with up to about 20 vol.% garnet and 10 vol.% clinopyroxene (samples E35, E36, E39A and E97) occur intimately interlayered with, and gradational into, garnet free Cr spinel dunites (sample E37) and olivine free orthopyroxene poor garnet pyroxenites (samples E39B and E99). Olivines, where present, are Fo_{92-93} and the orthopyroxenes En_{92-95}. The large chrome rich garnets (1.56-4.75 wt.% Cr_2O_3) in the peridotites invariably have conspicuous orange-brown kelyphite reaction coronas ; in a few cases the garnets have been completely replaced. These fine grained kelyphites consist largely of an intimate intergrowth of secondary Cr spinel and pyroxenes (and/or amphibole). Sometimes there is a coarser grained outer corona of pale green secondary amphibole and orange Cr spinel developed.

A notable feature is the occurrence in the outermost parts of some of the kelyphites of ragged grains of a secondary less chromiferous garnet alongside the Cr spinel (Figure 3). This feature appears to be similar to that previously mentioned by Griffin and Heier (1973) and by O'Hara (1975) to occur in certain garnet peridotite samples at Lien, Almklovdalen. Griffin and Heier (1973) interpreted this feature to indicate a reversal of the kelyphite forming reaction garnet + olivine → orthopyroxene + clinopyroxene + spinel, due to the effects of cooling subsequent to initial rapid decompression on the retrograde P-T path followed by these rocks during their exhumation. However, the less chromiferous character of the secondary garnet and its close

Sample No.	E35	E36	E37	E38	E39B	E99
Rock Type wt.%	Gnt. Lherz.	Gnt. Lherz.	Chromite Dunite	Gnt-Sp. Lherz.	Gnt Pyrox.	Gnt. Pyrox.
SiO_2	41.67	44.06	41.75	39.44	46.76	46.78
TiO_2	0.01	0.13	0.02	0.48	0.23	0.25
Al_2O_3	1.08	4.34	0.48	6.45	14.98	16.53
Cr_2O_3	0.29	0.48	0.18	0.53	0.67	0.79
Fe_2O_3	1.50	0.89	0.82	4.39	0.94	0.27
FeO	6.23	5.73	6.26	6.53	4.35	4.68
MnO	0.10	0.11	0.10	0.16	0.16	0.16
NiO	0.33	0.27	0.33	0.20	0.09	0.06
MgO	46.82	40.41	49.51	31.32	23.92	21.99
CaO	0.53	3.35	0.25	2.66	7.39	7.74
Na_2O	0.12	0.34	0.10	0.30	0.52	0.53
K_2O	0.02	0.01	0.00	0.11	0.02	0.01
P_2O_5	0.05	0.04	0.07	0.31	0.05	0.05
S	0.02	0.03	0.00	0.07	0.05	0.04
H_2O^+	0.42	0.33	0.61	7.08	0.05	0.24
Total	99.19	100.52	100.48	100.03	100.18	100.12
100 Mg/(Mg+Fe^T)	91.7	91.7	92.7	84.2	89.1	89.3
100 Cr/(Cr+Al)	15.3	6.9	20.1	5.2	2.9	3.1
CIPW Normative Mineralogy						
Or	0.12	0.06	-	0.65	0.12	0.06
Ab	1.02	2.88	0.85	2.54	4.40	4.49
An	2.30	10.29	0.78	11.17	36.34	38.07
Cor	0.02	-	0.03	1.74	0.79	1.70
Di	-	4.76	-	-	-	-
Hy	9.18	11.42	5.02	25.30	29.76	31.11
Ol	83.07	68.22	91.20	42.52	26.09	22.38
Mt	2.18	1.29	1.19	6.37	1.36	0.39
Il	0.02	0.25	0.04	0.91	0.44	0.48
Ap	0.12	0.09	0.16	0.72	0.12	0.12
Oliv.%Fo	91	91	91	91	89	86
Plag.%An	69	78	48	81	89	89

TABLE IX. — *Analyses of Mg-Cr garnet peridotites and associated rocks from Sandvik, Gurskoy.*

Analyses des péridotites à grenat riches en Mg-Cr et des roches associées de Sandvik, Gurskoy.

association with Cr spinel would appear to support O'Hara's (1975) contention that the secondary garnet may simply have developed during the down pressure multivariant reaction Cr rich garnet + olivine → Cr poor garnet + Cr spinel + orthopyroxene + clinopyroxene. Certainly the experimental data of MacGregor (1970) and O'Neill (1981) indicate that for natural Mg-Cr garnet peridotite rock compositions the garnet lherzolite ⇌ spinel lherzolite reaction will constitute a multivariant sliding equilibrium with an intermediate 5-phase garnet spinel lherzolite assemblage stable over an increasingly wide pressure interval in rocks with increased Cr/(Cr + Al) ratios.

Sample E39 shows a characteristically rather poorly defined and somewhat gradational contact between typical Mg-Cr garnet peridotite (sub-sample E39A) and a 4 cm wide layer of garnet pyroxenite (sub-sample E39B). Overall the mineral assemblage in the garnet pyroxenite is slightly less ferriferous than that observed in the associated garnet peridotite, the garnet being $Pyr_{78}Alm_{11}Gross_8$ and the minor orthopyroxene En_{95}. This relationship is the reverse of that previously observed (O'Hara and Mercy, 1963 ; Carswell, 1968*a*, 1981 ; Medaris, 1980) at the Kalskaret (Tafjord) and various Almklovdalen localities. However, as at these other localities, the mineral phases in the garnet pyroxenite layer are less chromiferous than in the associated garnet peridotites — the average Cr_2O_3 contents being : garnet (0.90 wt.%), clinopyroxene (0.78 wt.%) and orthopyroxene (0.12 wt.%).

A further analysed sample, E38, from the Sandvik garnet peridotite locality is petrographically unusual but particularly important from a petrogenetic viewpoint. In hand specimen,it is a

	A	B	C	D	E	F	G	H	I	J
wt.% n	9	2	1	1	2	16	16	7	1	10
SiO_2	40.28	40.12	45.33	44.22	42.86	44.94	42.79	44.97	48.24	47.62
TiO_2	0.83	0.71	1.35	0.42	0.07	0.36	0.11	1.07	0.90	0.36
Al_2O_3	7.78	7.41	13.06	6.50	2.71	6.76	4.84	15.37	8.99	12.26
Cr_2O_3	0.03	0.03	tr.	0.03	0.39	0.29	0.53	0.01	0.11	0.21
Fe_2O_3	6.42	10.74	1.58	6.17	1.20	2.61	2.82	2.51	5.95	1.16
FeO	16.81	13.61	12.73	10.77	5.98	8.84	4.09	12.59	5.30	6.21
MnO	0.34	0.28	0.22	0.29	0.10	0.16	0.14	0.23	0.23	0.20
NiO	0.08	0.06	n.d.	0.06	0.30	0.17	0.21	0.04	0.02	0.06
MgO	22.58	21.20	17.28	26.39	43.62	27.04	33.51	12.04	13.92	17.88
CaO	3.54	4.19	7.57	3.59	1.94	6.52	4.27	7.43	14.73	12.35
Na_2O	0.12	0.09	0.79	0.07	0.23	0.70	0.28	2.53	1.94	0.90
K_2O	0.01	0.26	0.16	0.79	0.02	0.04	0.02	0.39	0.09	0.01
P_2O_5	0.11	0.22	0.19	0.03	0.04	0.02	0.07	0.19	0.03	0.03
S	0.02	0.01	n.d.	0.01	0.02	0.06	0.05	0.16	0.00	0.04
H_2O^+	1.31	0.52	0.22	0.75	0.38	1.12	6.34	0.30	0.39	0.92
Total	100.26	99.45	100.48	100.40	99.86	99.63	100.07	99.83	99.90	100.41
100 Mg/Mg+Fe^T)	64.0	61.9	69.5	74.5	91.7	81.2	90.0	59.1	70.0	81.1
100 Cr/(Cr+Al)	0.3	0.3	-	0.3	8.8	2.8	6.8	<0.1	0.8	1.1
100 $Fe^{2+}/(Fe^{2+}+Fe^{3+})$	74.4	58.5	90.0	66.0	84.7	79.0	61.7	84.8	49.7	83.5

A Fe-Ti garnet peridotites from Eiksunddal Complex.
B Fe-Ti garnet peridotites from Raknestangen, Otrøy.
C Fe-Ti garnet peridotite from Lyngenes, Sørpollen - Analyses from Eskola (1921).
D Fe-Ti garnet peridotite from Kolmannskog, Molde Area.
E Mg-Cr garnet peridotites from Sandvik, Gurskøy.
F Mg-Cr garnet peridotites from Kaskaret, Tafjord - Analyses from Mercy & O'Hara (1965), Carswell (1968a), and Al-Samman, unpublished.
G Mg-Cr garnet peridotites from Uqelvik, Otrøy - Analyses from Carswell (1968b) and unpublished data.
H Associated eclogites and garnet pyroxenites from Eiksunddal Complex.
I Associated eclogite from Kolmannskog, Molde Area.
J Associated eclogites and garnet pyroxenites from Uqelvik, Otrøy.

TABLE X. — *Comparison of averaged whole rock analyses.*
Comparaison des analyses moyennes de roches totales.

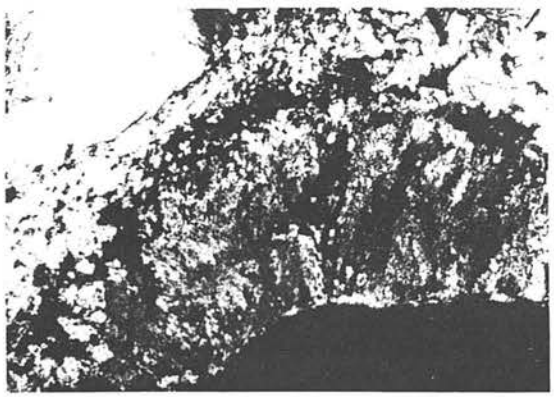

FIG. 3. — *Photomicrograph* (crossed polars) *of Sandvik garnet peridotite showing the development of secondary less chromiferous garnet towards the outside of the broad kelyphite reaction rim on the more chromiferous 'initial' garnet* (bottom right). Photograph width approx. 1 mm.

Photomicrographie (polariseurs croisés) *de la péridotite à grenat de Sandvik montrant le développement d'un grenat secondaire moins chromifère vers l'extérieur de l'auréole réactionnelle kélyphitique autour du grenat ''initial'' le plus chromifère* (en bas à droite). Dimension approximative de la photographie 1 mm.

dark coloured rather heavily serpentinised peridotite lacking any obvious garnet, but containing somewhat strained and disrupted large orthopyroxene porphyroclasts up to about 2.5 cm across. Careful thin section examination, however, shows that garnet is indeed present — the mode (vol.%) of this rock being 48 % olivine (Fo_{86}), 25 % orthopyroxene, 13 % amphibole, 6 % clinopyroxene, 6 % spinel and only 2 % garnet. Ragged shaped grains of dark green pleonaste spinel ($Sp_{87}Magn_5Chrom_8$), typically 0.1-0.4 mm across, are conspicuous throughout this rock and are frequently fringed (Figure 4) by coronas of garnet only a few microns wide or by necklaces of similarly minute garnet grains. More obvious garnets of somewhat larger size (0.05-0.2 mm) occur as crudely orientated clusters (Figure 5) within the large orthopyroxene grains (En_{86}), suggestive of an exsolution origin. It is noteworthy that the garnets forming coronas on the spinels have significantly lower Cr_2O_3 contents (average 0.34 wt.% as against 0.83 wt.%) and CaO contents (average 4.48 wt.% as against 6.01 wt.%) compared to the garnets considered to have been exsolved from the orthopyroxenes. Local environmental control on the garnet grain compositions thus

FIG. 4. — *Photomicrograph showing the growth of garnet as coronas on primary green pleonaste spinels in the Sandvik peridotite sample E38.* Also note the adjacent large primary amphibole grain (top left) with abundant rutile inclusions. Photograph width approx. 2 mm.

Photomicrographie montrant la croissance de couronnes de grenat autour de spinelles pléonaste vert primaires dans l'échantillon E38 de la péridotite de Sandvik. Noter également le grand cristal d'amphibole primaire voisin (en haut à gauche) contenant d'abondantes inclusions de rutile. Dimension approximative de la photographie 2 mm.

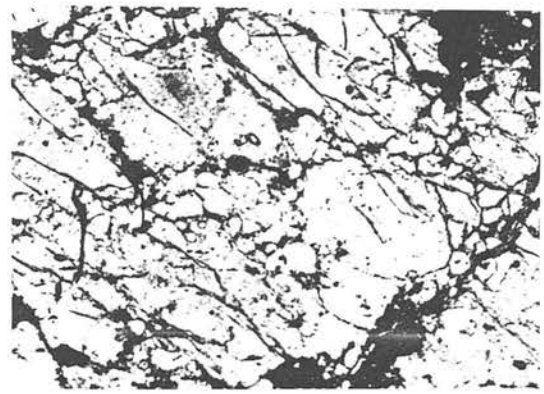

FIG. 5. — *Photomicrograph showing clusters of small garnet grains considered to have exsolved from an originally more aluminous orthopyroxene in the Sandvik peridotite sample E38.* Also note the presence of primary dark coloured pleonaste spinel inclusions in the orthopyroxene megacryst - which typically develop extremely narrow (< 10 microns) garnet coronas. Photograph width approx. 5 mm.

Photomicrographie montrant les amas de petits grains de grenat considérés comme ayant été exsolvés à partir d'un orthopyroxène initial plus alumineux dans l'échantillon E38 de la péridotite de Sandvik. Noter aussi la présence d'inclusions de spinelle pléonaste primaire très colorées dans le cristal d'orthopyroxène, lequel développe de manière typique des couronnes de grenat extrêmement fines (< 10 microns). Dimension approximative de la photographie 5 mm.

confirms the arrested nature of the spinel lherzolite → garnet lherzolite reaction in this rock and the overall lack of chemical equilibrium.

Despite the garnet exsolution the orthopyroxenes in sample E38 are still considerably more aluminous (average 3.39 wt.% of Al_2O_3) than those in the associated garnet peridotites (E35, E39A, and E97). Point counts on three mutually perpendicular sections cut through a large orthopyroxene porphyroclast indicated the presence of 6.4 vol.% of garnet (equivalent to approx. 7.5 wt.%) within the orthopyroxene. The reconstituted primary orthopyroxene calculated on the reasonable assumption that all this garnet was exsolved from a primary high temperature more aluminous orthopyroxene indicates an original Al_2O_3 content of 4.79 wt.% (Table III). As it was not possible to satisfactorily integrate the fine scale clinopyroxene exsolution lamellae present in these orthopyroxenes by direct analysis or by calculation, the CaO content of the derived primary orthopyroxene is almost certainly an underestimate. Amounts of primary clinopyroxene in this rock are fairly limited but analyses show (Table II) that it is also somewhat more aluminous (average 4.51 wt.% Al_2O_3) than that in the analysed throughgoing garnet peridotite samples. However, this clinopyroxene has not been observed to show any evidence of garnet exsolution. A further unusual feature of this peridotite sample is the presence of considerable amounts of pale coloured hornblende full of minute rutile inclusions (Figure 4). This amphibole appears to be in textural equilibrium with the pyroxenes and as it occurs together with olivine, clinopyroxene and spinel as inclusions in the large orthopyroxenes, it would appear to have formed in association with the primary spinel lherzolite assemblage.

In common with most other documented occurrences of Norwegian Mg-Cr garnet peridotites, the rocks at Sandvik characteristically have partly recrystallised mosaic porphyroclastic textures with large strained porphyroclasts (typically 0.2-1.0 cm across) surrounded by much smaller recrystallised neoblasts. As observed el-

sewhere (e.g. Medaris, 1980 ; Carswell, 1981), compositions of pyroxene porphyroclast rims and recrystallised neoblasts are mostly indistinguishable but generally slightly different from porphyroclast core compositions. Where such differences have been observed separate averaged analyses are given (Tables I-VI) for grain cores and rims, the latter incorporating any available neoblast analyses.

The main composition differences recognised are a slight increase in Fe/Mg ratios in garnet rims (+ neoblasts) compared to garnet cores and an increase in the Al_2O_3 content of orthopyroxene grain rims adjacent to garnets. Such features are similar to those observed in the more detailed zoning profiles obtained from large garnet and pyroxene porphyroclasts in Mg-Cr garnet peridotites from the Kalskaret (Tafjord) locality (Figure 6), the most obvious features of which are the existence of uniform grain cores and compositionally distinct rims only 100-200 microns wide. Garnets show the most striking composition changes at grain rims with marked increases in Fe, Mn and Ca contents and corresponding decreases in Mg content. Compositional zoning in the clinopyroxenes is less distinct but tends to be in the opposite direction in terms

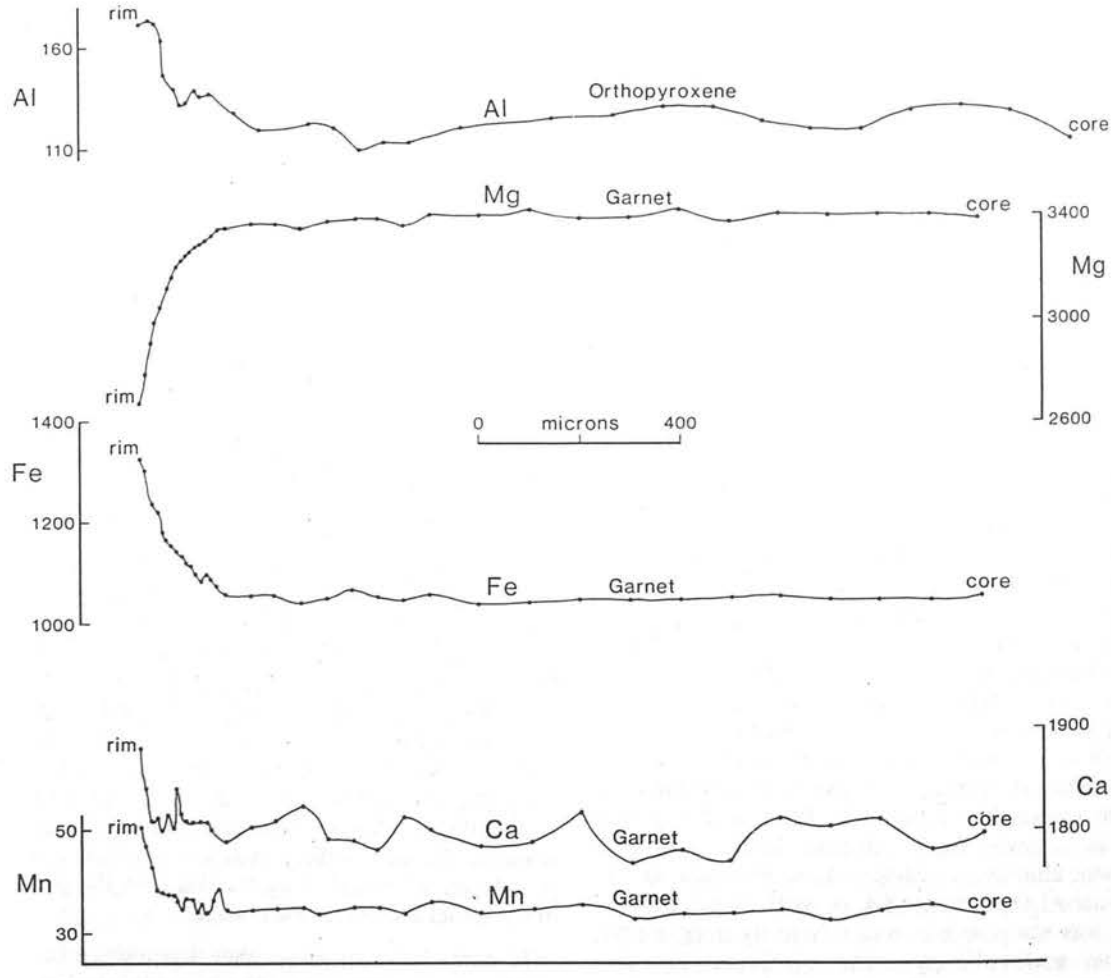

FIG. 6. — *Compositional zoning profiles* (presented as counts/sec) *for Al in orthopyroxene and Mg, Fe and Ca and Mn in garnet from a Kalskaret garnet peridotite sample T337.*

Profils de composition (en coups/sec) *pour Al dans l'orthopyroxène et Mg, Fe, Ca et Mn dans le grenat de l'échantillon T337 de la péridotite à grenat de Kalskaret.*

of Fe and Mg contents. Hence the overall result is a marked increase in the partition coefficient $K_D = \frac{\text{Fe/Mg garnet}}{\text{Fe/Mg clinopyroxene}}$ close to grain edges, a feature which may be conventionally interpreted (Råheim and Green, 1974 ; Ellis and Green, 1979) to indicate that the final stages of growth occurred under declining temperature (and pressure ?) conditions. However, such compositional zoning may simply represent a diffusion controlled arrested attempt by these mineral grains to adjust their element partitioning during the declining P-T conditions which must have followed the metamorphic peak. Neither in the Sandvik nor the Kalskaret samples have we observed instances of more prolonged retrograde Fe/Mg zoning profiles as reported by Medaris (1980) in a sample from Lien, Almklovdalen.

WHOLE ROCK CHEMICAL COMPOSITIONS

In tables VII-IX, new analyses for major and various trace elements and calculated CIPW norms are presented for representative whole rock samples of Fe-Ti garnet peridotites and associated garnet pyroxenites and eclogites from the Eiksunddal Complex and for Mg-Cr garnet peridotites and associated rocks from the Sandvik locality on Gurskøy. These analyses were obtained for the most part by X-ray fluorescence although analyses of FeO and H_2O were performed by classical 'wet' techniques and those of Na_2O by atomic absorption. In table X, averaged analyses for the rocks from these two localities are compared with analyses of Fe-Ti garnet peridotites from Kolmannskog and Raknestangen (new analyses) and from Lyngenes (Eskola, 1921) and with averaged analyses of Mg-Cr garnet peridotites from Kalskaret and Ugelvik and also of related 'internal' garnet pyroxenites and eclogites from the latter locality.

These analyses confirm the much more ferriferous and titaniferous and less chromiferous character of the garnet peridotites from Eiksunddal (mean value for 100 Mg/(Mg + Fe) = 64.0 ; ranges in Cr_2O_3 and TiO_2 contents are 0.01-0.04 wt.% and 0.65-1.05 wt.% respectively), from Raknestangen (mean 100 Mg/(Mg + Fe) = 61.9 ; mean Cr_2O_3 = 0.03 wt.%, mean TiO_2 = 0.71 wt.%), from Kolmannskog (100 Mg/(Mg + Fe) = 74.9 ; Cr_2O_3 = 0.03 wt.%, TiO_2 = 0.42 wt.%) and from Lyngenes (100 Mg/(Mg + Fe) = 68.5 ; TiO_2 = 1.35 wt.%) compared with the garnet peridotites from Sandvik (100 Mg/(Mg + Fe) = 84.2-91.7 ; Cr_2O_3 = 0.29-0.53 wt.%, TiO_2 = 0.01-0.48 wt.%), from Kalskaret (mean 100 Mg/(Mg + Fe) = 81.2 ; mean Cr_2O_3 = 0.29 wt.% ; mean TiO_2 = 0.36 wt.%) and Ugelvik (mean 100 Mg/(Mg + Fe) = 90.0 ; mean Cr_2O_3 = 0.53 wt.% ; mean TiO_2 = 0.11 wt.%). It is clear that these particular chemical distinctions also extend to the associated garnet pyroxenites and eclogites at these various localities. Other significant chemical differences are the higher MnO and P_2O_5 contents and lower NiO contents of the Fe-Ti peridotites compared with the Mg-Cr garnet peridotites.

The contrasting chemistries of the two groups of garnet peridotites (+ associated rocks) are further illustrated on figure 7, in which the composition fields for the two groups are quite separate. Figure 7 also demonstrates that other than at Sandvik, the garnet peridotites and associated rocks at the various localities define fairly well constrained composition arrays with the more

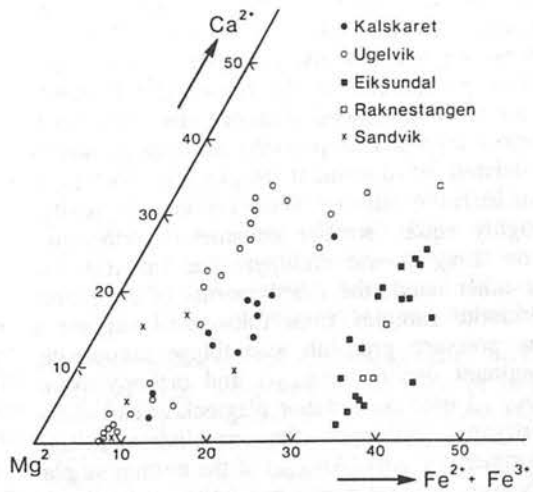

FIG. 7. — *CMF diagram showing the whole rock compositions for garnet peridotites and associated eclogites and garnet pyroxenites from various localities discussed in this paper.*

Diagramme CMF montrant les compositions chimiques, en roche totale, des péridotites à grenat, des éclogites associées et des pyroxénites à grenat des différents gisements présentés dans cet article.

calcic, aluminous and sodic garnet pyroxenites and eclogites characteristically having somewhat lower 100 Mg/(Mg + Fe) ratios than the related garnet peridotites. However, at the Sandvik locality the amphibole bearing garnet spinel lherzolite sample E38 is distinctly more ferriferous both in its overall whole rock composition and in its constituent minerals (Tables I-VI) than the analysed samples of associated peridotites and pyroxenites. The explanation of this and the precise nature of the relationship of this exceptional and important sample to the surrounding rocks at Sandvik currently remains unclear.

The highly oxidised character of some of the metamorphic mineral assemblages in the Eiksunddal Complex and the likelihood of chemical transfer during metamorphic evolution complicate any attempt to interpret the variations in chemical compositions between the various whole rock samples in terms of original igneous layering of low pressure gabbro-peridotite assemblages as represented by the calculated CIPW norms (Tables VII-VIII). The occurrences of cross cutting omphacite veins at Eiksunddal (e.g. sample E45) and Kolmannskog and of discordant metasomatically zoned garnet-omphacite veins at Raknestangen bear witness not only to chemical mobility during the eclogite facies metamorphism, but also to the existence of substantial fluid pressures for the development of these fracture controlled veins. Nevertheless, despite these reservations, the CIPW norms suggest that the dominant eclogites and garnet pyroxenites in the Eiksunddal Complex could have developed from original olivine rich norites with a low pressure mineralogy which consisted of dominant plagioclase (An_{53-62}), considerable olivine (Fo_{55-63}) and typically, roughly equal, smaller amounts of orthopyroxene (En_{66-75}) and clinopyroxene (augite). On the other hand, the CIPW norms of the garnet peridotite samples from Eiksunddal suggest a low pressure protolith assemblage comprising dominant olivine (Fo_{64-73}) and orthopyroxene (En_{66-75}) with only minor plagioclase and clinopyroxene. However, the unrealistically high anorthite contents (An_{90-98}) of the normative plagioclases in these garnet peridotites make it probable that such rocks developed from original plagioclase free olivine and orthopyroxene rich peridotite layers. Furthermore, because of the current highly oxidised character of these particular rocks, the original ferromagnesian silicates can reasonably be expected to have had lower $Mg^{2+}/(Mg^{2+} + Fe^{2+})$ ratios than the values indicated by the CIPW norms.

The previously highlighted geochemical distinctions, indicate that it is extremely unlikely that the Mg-Cr garnet peridotites, such as those from Sandvik, have originated from igneous assemblages which were in any way directly related genetically to the protoliths for the Fe-Ti garnet peridotites. Whole rock compositions and derived CIPW norms for the Sandvik samples by themselves provide little insight into the likely origins of these rocks, other than to indicate their consistently highly magnesian and chromiferous refractory character which is in keeping with other forsteritic olivine dominated 'alpine-type' peridotite bodies of proposed upper mantle or ophiolitic origins (e.g. Carswell, 1968*b* ; Ringwood, 1975 ; Ernst, 1978 ; Spray, 1982 ; Dick, 1982). The subordinate garnet pyroxenite or eclogite layers enclosed within such peridotite bodies appear most likely to represent the modified products of complex partial melting and crystal fractionation processes operative at upper mantle depths (e.g. Carswell, 1968*a* ; Dickey *et al.*, 1977 ; Lappin, 1974 ; Loubet and Allègre, 1982).

PRESSURE-TEMPERATURE ESTIMATES AND IMPLICATIONS

Various calibrated mineralogical thermometers such as those for the two pyroxene solvus (Wells, 1977) and for Fe^{2+}/Mg^{2+} distribution between garnet and clinopyroxene (Mori and Green, 1978 ; Ellis and Green, 1979) and garnet and olivine (O'Neill and Wood, 1979, 1980) are appropriate for evaluation of the likely equilibration temperatures of garnet peridotite assemblages (Carswell and Gibb, 1980*a* and *b*). These values can then be combined with the Wood (1974) geobarometer for Al partitioning in garnet-orthopyroxene equilibra to yield absolute values for both temperature and pressure. Alternatively, for 5-phase garnet + spinel lherzolite assemblages absolute P-T values may be obtained by the method provided by O'Neill (1981).

Fe-Ti garnet peridotites and associated rocks

Problems can be expected with the application

of the above geothermometric/barometric methods to these rocks because of the gross chemical differences between these rock compositions and the experimentally calibrated rock systems. The common occurrence of secondary reaction features in these rocks is a further complication. Hence any P-T values calculated for these rocks must be carefully scrutinised.

The following mean values (and standard deviations) have been obtained for a total of 13 separate P-T determinations based on core and/or rim analyses of largely unzoned grains in the Fe-Ti garnet peridotites and associated garnet pyroxenites :

Wells/Wood
808 °C (70 °C) / 28.6 kbar (8.1 kbar)
Mori and Green/Wood
747 °C (57 °C) / 24.9 kbar (10.4 kbar)
Ellis and Green/Wood
692 °C (59 °C) / 21.3 kbar (6.7 kbar)
O'Neill and Wood/Wood
620 °C (51 °C) / 21.6 kbar (11.1 kbar).

It should be pointed out that the Mori and Green (1978) K_D $^{Gnt\text{-}Cpx}_{Fe^{2+}\text{-}Mg^{2+}}$ calibration has been employed assuming all Fe as Fe^{2+} in both minerals, whereas with the Ellis and Green (1979) calibration analytically determined or stoichiometrically calculated $Fe^{2+}/(Fe^{3+} + Fe^{3+})$ values have been taken into consideration. These contrasting procedures are in line with the different experimental and data treatments employed to obtain these different calibrations (see also Medaris, 1980 ; Carswell, 1981).

It seems likely that the Wells two pyroxene solvus temperatures are too high, a conclusion substantiated by other evidence (Carswell and Griffin, 1981) which suggests that the empirical correction applied by Wells (1977) to take account of the effect of Fe on the solvus is probably inadequate. Furthermore, these high Wells temperatures in turn lead to pressure estimates which also seem excessively high. By contrast the O'Neill and Wood temperatures based on $K^{Gnt\text{-}Ol}_{Fe^{2+}\text{-}Mg^{2+}}$ look to be rather low, perhaps reflecting the influence of the widely prevalent secondary reactions at garnet-olivine grain contacts.

It therefore would appear that the P-T values obtained by the Mori and Green/Wood and Ellis and Green/Wood pairings are likely to be the most realistic, the former being somewhat higher at least partly because the Mori and Green K_D calibration is based on experiments at 30-40 kilobars pressure and unlike that of Ellis and Green does not provide a correction factor for the influence of pressure on K_D. All things considered it is perhaps surprising that these 'best' P-T values at least approach the values of around 750 °C and 20 kbar indicated for the metamorphic maximum in this part of western Norway from several studies of other relict high grade mineral assemblages (Krogh, 1980 ; Medaris, 1980 ; Carswell and Gibb, 1980*b* ; Griffin and Mørk, 1981 ; Carswell *et al.*, 1983). The mean pressure estimates for these rocks from the Wood (1974) garnet-orthopyroxene geobarometer are however, > 20 kbar, but are somewhat lowered if only orthopyroxene-garnet grain rim compositions are considered. For example, for the Mori and Green/Wood pairings the mean P-T values for grain rim compositions are 726 °C/19.7 kbar compared with 757 °C/27.2 kbar for grain core compositions. Unfortunately, the Fe rich nature of the garnet + pleonaste spinel bearing peridotites prohibits calculation of meaningful pressure values by the method of O'Neill (1981) because of uncertainties over the appropriate correction factors required to take account of the likely opposing effects of Fe^{2+} and Fe^{3+} on the garnet peridotite-spinel peridotite equilibrium (MacGregor, 1970 ; O'Neill, 1981). Application of the more recently published garnet-orthopyroxene barometer of Harley and Green (1982), which has been experimentally calibration for FeO bearing systems, raises the pressure estimates by on average about 2 kbar relative to the values obtained from the Wood (1974) calibration. Such differences are well within the large overall uncertainty which must be attached to the pressure estimates because of the low values of X^{Ml}_{Al} in the orthopyroxenes concerned.

The existence of compositionally homogeneous grain cores and the absence of obvious relict mineral inclusions in the garnets restrain interpretation of the prograde metamorphic path followed by these rocks. However, if the original igneous crystallisation of these rocks took place in a reasonably stable continental crust environment and involved coexisting olivines and plagioclases, as seems plausible for the associated garnet pyroxenites and eclogites, then pressures less than about 10 kbar (Figure 8) seems likely (Ito and Kennedy, 1971 ; Ringwood, 1975). Geochemical affinities and field associa-

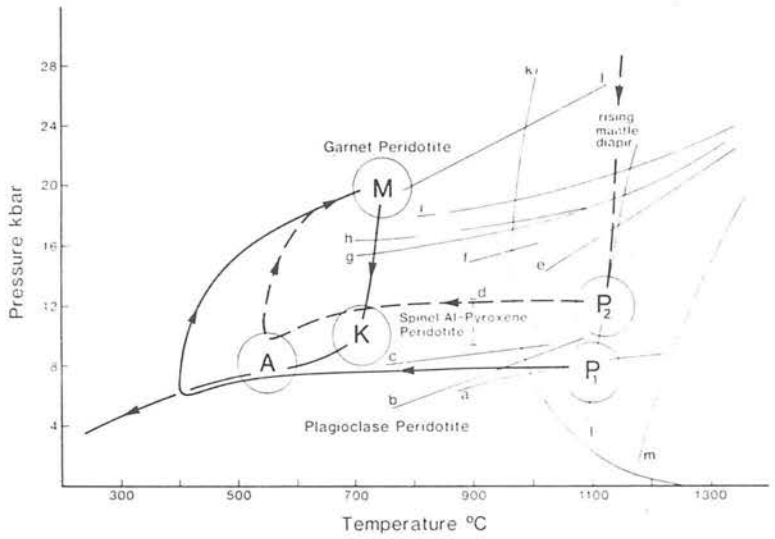

FIG. 8. — *Diagram illustrating possible P-T trajectories* (directions arrowed) *for the metamorphic evolution of protoliths for the Fe-Ti garnet peridotites (P1) and the Mg-Cr garnet peridotites (P2).* Note the separate but essentially parallel early cooling paths, the convergence on tectonic interdigitation just prior to the eclogite facies metamorphic peak (M) and the common retrograde path passing through appropriate conditions for the development of secondary Al pyroxenes + spinel kelyphites (K) and amphibolites (A). The various experimentally determined equilibria shown are as follows : a) Calculated univariant curve for the reaction anorthite + forsterite (low P) = clinopyroxene + orthopyroxene + spinel (high P) in the system CaO-MgO-Al_2O_3-SiO_2 (Obata, 1976). b and j) Up pressure garnet-in and plagioclase-out reaction curves respectively, for basaltic composition NM5 of Ito and Kennedy (1971) which provides a reasonable approximation to the bulk composition of eclogites/garnet pyroxenites in the Eiksunddal Complex. c) Reaction boundary between plagioclase pyrolite (peridotite) and spinel-Al pyroxenes pyrolite from figure 6-4 of Ringwood (1975). d) Pressure brackets for the garnet + olivine $\rightleftharpoons$ pyroxenes + spinel reaction at 900 °C determined by Jenkins and Newton (1979) in hydrothermal reversal runs on a mixture of natural pyropic garnet and forsteritic olivine. e) Garnet + olivine $\rightleftharpoons$ pyroxenes + spinel reaction curve in the CaO-MgO-Al_2O_3-SiO_2 system of MacGregor (1970). f) The same reaction curve determined by Jenkins and Newton (1979) from hydrothermal reversal runs in the CMAS system. g) The univariant curve for the spinel lherzolite $\rightleftharpoons$ garnet lherzolite reaction in Almklovdalen garnet peridotite sample N14A. O'Hara (1975). h) The same reaction curve for slightly more magnesian natural compositions. O'Hara *et al.* (1971). i) Univariant reaction curve for pyrope + forsterite $\rightleftharpoons$ enstatite + spinel in the MgO-Al_2O_3-SiO_2 system determined by Perkins *et al.* (1981). k, l and m) Represent the approximate locations and form of the 'wet' (P_{H_2O} = P total), 0.1 % H_2O and 'dry' mantle peridotite solidus, respectively, from data given by Ringwood (1975) and Wyllie (1977, 1979).

Diagramme illustrant les trajectoires P-T possibles (flèches) pour l'évolution métamorphique des protolithes pour les péridotites à grenat riches en Fe-Ti (P1) et les péridotites à grenat riches en Mg-Cr (P2). Noter les trajectoires initiales de refroidissement séparées mais parallèles, la convergence de l'interdigitation tectonique juste avant le maximum du métamorphisme éclogitique (M) et la trajectoire rétromorphique commune au travers de conditions requises pour le développement de kélyphites (K) de pyroxènes secondaires alumineux + spinelle et d'amphibolites (A). Les différents équilibres expérimentaux représentés sont les suivants : a) Courbe univariante calculée pour la réaction anorthite + forstérite (basse Pression) = clinopyroxène + orthopyroxène + spinelle (haute Pression) dans le système CaO-MgO-Al_2O_3-SiO_2 (Obata, 1976). b et j) Courbes réactionnelles respectives limitant le domaine du grenat de haute pression et celui de l'existence du plagioclase pour la composition basaltique NM5 de Ito et Kennedy (1971) qui représente une approximation raisonnable de la composition moyenne de l'ensemble éclogites/pyroxénites à grenat dans le complexe de Eiksunddal. c) Limite réactionnelle entre pyrolite à plagioclase (péridotite) et pyrolite à pyroxènes et spinelle alumineux d'après les figure 6-4 de Ringwood (1975). d) Domaines de pression pour la réaction grenat + olivine $\rightleftharpoons$ pyroxènes + spinelle à 900 °C déterminés par Jenkins et Newton (1979) lors d'expériences hydrothermales réversibles sur un mélange de grenat riche en pyrope et d'olivine riche en forstérite. e) Courbe réactionnelle grenat + olivine $\rightleftharpoons$ pyroxène + spinelle dans le système CaO-MgO-Al_2O_3-SiO_2 d'après MacGregor (1970). f) La même courbe

réactionnelle déterminée par Jenkins et Newton (1979) à partir d'expériences hydrothermales réversibles dans le système CMAS. g) Courbe univariante pour la réaction lherzolite à spinelle $\rightleftharpoons$ lherzolite à grenat dans l'échantillon N14A de la péridotite à grenat de l'Almklovdalen. O'Hara (1975). h) La même courbe réactionnelle pour des compositions légèrement plus magnésiennes. O'Hara *et al.* (1971). i) Courbe réactionnelle univariante pour la réaction pyrope + forstérite $\rightleftharpoons$ enstatite + spinelle dans le système $MgO\text{-}Al_2O_3\text{-}SiO_2$ déterminée par Perkins *et al.* (1981). k, l et m) Localisation et forme approximatives respectives des solidus de péridotite mantellaire "humide" (P_{H_2O} = P totale), 0,1 % H_2O et "sèche" d'après les données de Ringwood (1973) et Wyllie (1977, 1979).

tions lead us to speculate that the Fe-Ti garnet peridotites and associated rocks in the Basal Gneiss Complex may be genetically related to the typically Fe and Ti enriched rapakivi granite (augen gneiss)-mangerite-anorthosite rock suite (Emslie, 1978) which appears to have been emplaced extensively throughout this part of Scandinavia at around 1 500 Ma (Harvey, 1983). Thus the prolonged initial cooling and subsequent prograde P-T paths shown on figure 8 for these rocks prior to the metamorphic culmination (M) are drawn so as to be compatible with the notion that the protoliths of these Fe-Ti garnet peridotites were old mid-Proterozoic igneous rocks intruded into the lower continental crust. Subsequent to the eclogite facies metamorphic 'high' these rocks appear likely to have followed a retrograde P-T path which initially involved rapid decompression (Cuthbert *et al.*, 1983) with the restricted development of granulite facies assemblages (pyroxenes + spinel kelyphites at garnet-olivine grain contacts) before cooling and partial hydration led to replacive amphibolite facies assemblages.

Mg-Cr garnet peridotites and associated rocks

For the Sandvik Mg-Cr garnet peridotites 'best' P-T estimates are limited to an average for only two sample assemblages, namely those for E97 and E35 grain rims, since estimates based on the exsolved assemblages in E38 and on E35 grain cores give unrealistically low (3-12 kbar) and high (28-38 kbar) pressures respectively. These P-T estimates based on the same four methods as used to evaluate the equilibration conditions for the Fe-Ti garnet peridotites are as follows :

Wells/Wood	836 °C/23.4 kbar
Mori and Green/Wood	754 °C/18.6 kbar
Ellis and Green/Wood	770 °C/21.8 kbar
O'Neill and Wood/Wood	620 °C/11.6 kbar

As before, the values based on the Mori and Green/Wood and Ellis and Green/Wood pairings are considered to be superior not least because they are most in line with previous determinations of P-T equilibration conditions for other Mg-Cr garnet peridotites in the Basal Gneiss Complex (Carswell and Gibb, 1980*b* ; Medaris, 1980 ; Carswell, 1981) and the 'best' P-T estimates derived above for the Fe-Ti garnet peridotites. As with the Fe-Ti garnet peridotites, the Harley and Green (1982) calibration raises the pressure estimates by about 2 kbar compared with the values obtained from the Wood (1974) calibration. However, uncertainties attributable to the low X_{Al}^{MI} values in the orthopyroxenes are exacerbated by the significant Cr_2O_3 contents in these particular mineral assemblages.

The recognition in sample E38 of garnet coronas on earlier pleonaste spinels and of garnet exsolution from originally more highly aluminous orthopyroxenes are clearly important to any interpretation of the metamorphic evolution of these rocks. Evaluation of the likely primary olivine-orthopyroxene (reconstituted composition - table III)-spinel assemblage in this rock indicates a temperature of about 1 110 °C, employing the method of Sachtleben and Seck (1981).

Other evidence for the existence of original high Al pyroxene megacrysts within the Mg-Cr garnet peridotite bearing bodies has been provided by Carswell (1973) and Lappin (1973, 1974). At Ugelvik, Carswell (1973) has described in a garnet pyroxenite sample exsolution of abundant garnet and clinopyroxene from orthopyroxene judged to have had an original Al_2O_3 content of around 4.16 wt.% very similar to the primary orthopyroxene composition deduced for the Sandvik sample. At Raudkleivane, Sunndal-Grubse, Almklovdalen, Lappin (1973, 1974) has described exsolution of garnet and orthopyroxene from large lamellar clinopyroxenes within a garnet poor clinopyroxenite. The pre-exsolution clinopyroxenes at this locality were also deduced to have originally contained around 4 wt.% Al_2O_3 and to have formed at around 1 100 °C.

The assumption of cotectic crystallisation of these early high Al pyroxenes with garnets, led Carswell (1973) and Lappin (1974) to deduce crystallisation from high pressure melts indicative of a deep mantle origin for these rocks. However, at neither of these localities is there unequivocal evidence that these high Al pyroxenes coexisted with garnet or indeed with spinel as at Sandvik. However, the evidence from the Sandvik locality strongly suggests a lower pressure origin for these high Al pyroxene bearing assemblages than previous interpretations. Nevertheless, in the absence of a suitable mineral barometer for spinel peridotite assemblages uncertainty persists over the precise pressures of formation and depths of origin of these rocks. The temperature of around 1 100 °C obtained for the primary olivine-orthopyroxene-spinel assemblage in the Sandvik sample E38 is reasonably in line with the expected solidus temperatures for such a peridotite composition with small amounts of water and/or CO_2 (Ringwood, 1975 ; Wyllie, 1977, 1979). Under hydrous melting conditions amphibole, also observed as an apparent primary phase in this rock, may bé expected to crystallise on the peridotite solidus at temperatures around 1 050 °C, at 10-20 kbar. Hence, allowing for uncertainties in the derived temperature estimate, it is just conceivable that the deduced primary assemblage in E38 may have been a true igneous assemblage (Figure 8). Alternatively, it may represent an early high P-T sub-solidus assemblage equilibrated on the ambient mantle geotherm subsequent to a partial melting event induced by diapirism but before thrust related tectonic emplacement into the crust, as proposed by Obata (1979) for the Ronda peridotite body in southern Spain. Certainly, the presence of garnet pyroxenite and eclogite layers and lenses within these peridotite bodies, some as at Kalskaret of picritic composition (Carswell, 1968*a*), strongly suggests that the development of the deduced early high P-T assemblages was at least a consequence of partial melting in a rising mantle peridotite diapir, as indicated in figure 8.

The recent recognition by Griffin and Qvale (1981) of superferric eclogites containing prograde zoned garnets intimately associated with the exsolved garnet clinopyroxenites within the Mg-Cr garnet peridotite body at Raudkleivane, imposes an important constraint on the subsequent P-T trajectory followed by these peridotite bodies. The preservation of Cl-rich, Al-rich ferropargasite inclusions in the cores of these prograde zoned garnets was taken by these authors as evidence that amphibolitisation (and possibly even serpentinisation of the associated peridotites) preceded the prograde metamorphism of these rocks.

Geochronological constraints on the P-T trajectory for these particular alpine-type peridotite bodies are currently rather inadequate, but there is some evidence that the diapiric melting event which established the isotope systems in these rocks may have occurred as long ago as 1 500 Ma (Gebauer *et al.*, 1982 ; Mearns and Lappin, 1982), whilst the current eclogite facies mineralogies were probably established much later (around 400-450 Ma) during the Caledonian orogeny (Griffin and Brueckner, 1980, 1982 ; Gebauer *et al.*, 1982). Hence a possible scenario might be that the initial diapirism and resultant partial melting which affected these rocks occurred around 1 500 Ma ago during a major episode of continental rifting which ultimately led to the opening of Iapetus Ocean. These mantle peridotites may consequently have been welded on to the edge of the Baltic continental plate in a highly vulnerable position (see models in Spray, 1982 and Gebauer *et al.*, 1982) from which they were subsequently tectonically emplaced into the crustal gneisses of the Baltic plate on its collision with the Greenland plate when Iapetus ocean finally closed during the Caledonian orogeny (see tectonic model of Cuthbert *et al.*, 1983). It is interesting that the timing of the initial mantle diapirism and continental rifting at around 1 500 Ma would indicate that it was essentially contemporaneous with the episode of extensive intrusion into the crust of rapakivi granite-mangerite-anorthosite suite magmas (Harvey, 1983), to which, as previously indicated, the protoliths of the Fe-Ti garnet peridotites and associated rocks may well have been related. It is also significant that the emplacement of the latter suite of crustal intrusives into the North American continental crust at around the same time has also been considered to relate to the onset of major continental rifting (Bridgewater and Windley, 1973 ; Emslie, 1978).

With these various considerations and constraints in mind, we have indicated on figure 8 what we consider to be a plausible overall P-T trajectory leading to the development of the

eclogite facies mineralogies in these Norwegian Mg-Cr garnet peridotite bodies. It is envisaged that in order for the early high P-T spinel-Al pyroxenes assemblages to have been at least sporadically preserved, these rocks must have been fairly rapidly cooled down below the diffusion 'blocking' temperatures of around 800-900 °C (Harte and Freer, 1982) following the diapirically induced partial melting event. On figure 8 this initial cooling episode is shown as ultimately extending down to temperatures appropriate for partial amphibolitisation. Subsequent to early Caledonian thrust related tectonic emplacement of these rocks into the crustal gneiss sequence, both the Mg-Cr peridotites and the Fe-Ti peridotites are shown as having followed a common P-T trajectory, first to the eclogite facies metamorphic peak on superposition of maximum crustal overburden (Cuthbert *et al.*, 1983) and then down the subsequent retrograde metamorphic path on fairly rapid unloading and exhumation. Retrogressive metamorphism in the Mg-Cr garnet peridotites involved first the development of kelyphites around garnets of spinel + Al pyroxenes and subsequently amphibolitisation giving tremolite-chlorite peridotite assemblages. It is important to emphasise that the P-T trajectory shown for the Mg-Cr mantle derived 'alpine type' peridotite bodies indicates that the garnet peridotite assemblages in these rocks have not been inherited from upper mantle depths as proposed in many earlier papers (e.g. Carswell, 1968*a.b*, 1973 ; Lappin, 1974 ; O'Hara and Mercy, 1963 ; Medaris, 1980 ; Smith, 1980) but have developed in association with equivalent assemblages formed in undoubted crustal lithologies, including the protoliths of the Fe-Ti garnet peridotites described in this paper.

CONCLUSIONS

1. Two chemically distinct types of garnet peridotites occur in the Basal Gneiss Complex of western Norway, here designated as the Fe-Ti type and the Mg-Cr type. The former typically has 100 Mg/(Mg + Fe) values of 60-75, Cr_2O_3 and TiO_2 contents of < 0.05 wt.% and around 1 wt.% respectively, with mineral compositions of : olivine (Fo_{67-82}), garnet ($Pyr_{39-56}Alm_{29-47}Gross_{1-12}$), and orthopyroxene ($En_{74-85}$). The latter typically has 100 Mg/(Mg + Fe) values of 80-92, Cr_2O_3 and TiO_2 contents of around 0.5 wt.% and 0.25 wt.% respectively ; with mineral compositions of : olivine (Fo_{82-92}), garnet ($Pyr_{60-75}Alm_{15-30}Gross_{5-10}$) and orthopyroxene ($En_{84-93}$).

2. CIPW norms for whole rock analyses of the Fe-Ti garnet peridotites and associated garnet pyroxenites and eclogites are compatible with derivation from layered intrusions of olivine norite-peridotite cumulates originally crystallised at < 10 kbar pressure. On the other hand, geochemical considerations and new petrographic evidence from the Sandvik locality are taken to indicate that the Mg-Cr garnet peridotites evolved from original high temperature aluminous pyroxenes-spinel peridotite bodies of ultimate mantle origin. Such early high temperature assemblages and the occurrence of indigenous layers or lenses of garnet pyroxenites and eclogites of picritic composition are considered to be indicative of diapirically induced partial melting at mantle depths prior to the tectonic emplacement of these rocks into the lower crustal gneiss complex.

3. The crystallisation of the high temperature protolith assemblages for both types of garnet peridotites may have occurred at around 1 500 Ma. (mid-Proterozoic) and have been related to the initial continental rifting leading to the opening of Iapetus Ocean. The Fe-Ti type is tentatively linked with the rapakivi granite-mangerite-anorthosite suite of magmatic intrusives of that age.

4. The Mg-Cr peridotite bodies are considered most likely to have been tectonically intercalated into the lower crustal gneiss complex early during the Caledonian orogeny. Subsequently, both peridotite types are envisaged to have followed essentially the same P-T trajectory leading to the development of the garnetiferous assemblages.

5. Temperature and pressure estimates for the metamorphic culmination in both garnet peridotite types are broadly similar at around 750 °C and 20 kbar and are also compatible with other P-T estimates from relict high-grade assemblages in this part of western Norway.

6. Prior to their eventual exposure at the surface, both peridotite types are judged to have followed comparable retrograde P-T paths in-

volving firstly development of anhydrous kelyphites around garnets of spinel + pyroxenes, in response to rapid decompression, and subsequently extensive amphibolitisation. Secondary Cr poor garnet is sometimes observed in kelyphites around Cr rich garnets in the Mg-Cr garnet peridotites whilst abundant secondary magnetite forms coarse symplectite intergrowths with pyroxenes on garnet breakdown in the Fe-Ti garnet peridotites.

ACKNOWLEDGEMENTS

D.A. Carswell wishes to acknowledge financial support for field studies in Norway from the University of Sheffield and the Natural Environment Research Council, and M.A. Harvey the receipt of a research studentship from the latter body. Thanks are also due to R. Kanaris-Sotiriou, F.G.F. Gibb and W.L. Griffin for assistance and advice with X-ray fluorescence and electron microprobe analyses.

REFERENCES

BRIDGEWATER, D. and WINDLEY, B.F. (1973). — Anorthosites, post-orogenic granites, acid volcanic rocks, and crustal development in the North Atlantic Shield during the mid-Proterozoic. *In* : Symp. on Granites, Gneisses and Related Rocks. L.A. Lister ed. *Geol. Soc. S. Afr. Sp. Publ., 3,* 307-318.

BRYHNI, I. (1966). — Reconnaissance studies of gneisses, ultrabasites, eclogites and anorthosites in outer Nordfjord, western Norway. *Nor. Geol. Unders., 241,* 1-68.

BRYHNI, I. and GRIFFIN, W.L. (1971). — Zoning in eclogite garnets from Nordfjord, west Norway. *Contrib. Mineral. Petrol., 32,* 112-125.

BUDDINGTON, A.F. and LINDSLEY, D.H. (1964). — Iron-titanium oxide minerals and synthetic equivalents. *J. Petrol., 5,* 310-357.

CARSWELL, D.A. (1968*a*). — Picritic magma - residual dunite relationships in garnet peridotite at Kalskaret near Tafjord, southern Norway. *Contrib. Mineral. Petrol., 19,* 97-124.

CARSWELL, D.A. (1968*b*). — Possible primary upper mantle peridotite in Norwegian basal gneiss. *Lithos, 1,* 322-255.

CARSWELL, D.A. (1973). — Garnet pyroxenite lens within Ugelvik layered garnet peridotite. *Earth Planet. Sci. Lett., 20,* 347-352.

CARSWELL, D.A. (1981). — Clarification of the petrology and occurrence of garnet lherzolites, garnet websterites and eclogite in the vicinity of Rödhaugen, Almklovdalen, West Norway. *Nor. Geol. Tidsskr., 61,* 249-260.

CARSWELL, D.A. and GIBB, F.G.F. (1980*a*). — Geothermometry of garnet lherzolite nodules with special reference to those from the kimberlites of northern Lesotho. *Contrib. Mineral. Petrol., 74,* 403-416.

CARSWELL, D.A. and GIBB, F.G.F. (1980*b*). — The equilibration conditions and petrogenesis of European crustal garnet lherzolites. *Lithos, 13,* 19-29.

CARSWELL, D.A. and GRIFFIN, W.L. (1981). — Calculation of equilibration conditions for garnet granulite and garnet websterite nodules in African kimberlite pipes. *Tschermaks Min. Petr. Mitt., 28,* 229-244.

CARSWELL, D.A., KROGH, E.J. and GRIFFIN, W.L. (1983). — Norwegian orthopyroxene eclogites : calculated equilibration conditions and petrogenetic implications. *In* : The Caledonide Orogen. D.G. Gee and B.A. Sturt ed., John Wiley (in press).

CUTHBERT, S.J., HARVEY, M.A. and CARSWELL, D.A. (1983). — A tectonic model for the metamorphic evolution of the Basal Gneiss Complex, Western South Norway. *J. metamorphic Geol., 1,* 63-90.

DICK, H.J.B. (1982). — Mineralogy and composition of abyssal and alpine-type peridotites. Abstr. Third Int. Kimberlite Conf., Clermont-Ferrand. *Terra Cognita, 2,* 242.

DICKEY, J.S., OBATA, M. and SUEN, C.J. (1977). — Partial fusion versus fractional crystallisation : hypotheses for the differentiation of the Ronda ultramafic massif of southern Spain. *Oregon Dept. Geol. Min. Indust., Bull., 96,* 79-89.

ELLIS, D.J. and GREEN, D.H. (1979). — An experimental study of the effect of Ca upon garnet-clinopyroxene Fe-Mg exchange equilibria. *Contrib. Mineral. Petrol., 71,* 13-22.

EMSLIE, R.F. (1978). — Anorthosite massifs, rapakivi granites and late Proterozoic rifting of North America. *Precambrian Res., 7,* 61-98.

ERNST, W.G. (1978). — Petrochemical study of lherzolitic rocks from the Western Alps. *J. Petrol., 19,* 341-392.

ESKOLA, P. (1921). — On the eclogites of Norway. *Skr. Norske, Vidensk - Akad. i Oslo, Mat. Natur. Kl., 8,* 1-118.

GEBAUER, D., LAPPIN, M., GRUENENFELDER, M., KOESTLER, A. and WYTTENBACH, A. (1982). —

Age and origin of some Norwegian eclogites : A U-Pb zircon and REE study. Abstr. First Int. Eclogite Conf., Clermont-Ferrand. *Terra Cognita, 2*, 323.

GREEN, D.H. and MYSEN, B.O. (1972). — Genetic relationship between eclogite and hornblende plagioclase pegmatite in western Norway. *Lithos, 5*, 147-161.

GRIFFIN, W.L. and BRUECKNER, H.K. (1980). — Caledonian Sm-Nd ages and a crustal origin for the Norwegian eclogites. *Nature, 285*, 319-321.

GRIFFIN, W.L. and BRUECKNER, H.K. (1982). — Rb-Sr and Sm-Nd studies of Norwegian eclogites. Abstr. First Int. Eclogite Conf., Clermont-Ferrand. *Terra Cognita, 2*, 324.

GRIFFIN, W.L. and HEIER, K.S. (1973). — Petrological implications of some corona structures. *Lithos, 6*, 315-335.

GRIFFIN, W.L. and MÖRK, M.B.E. (1981). — Excursions in the Scandinavian Caledonides. UCS Excursion No. B1 : Eclogites and Basal Gneiss in West Norway. Uppsala, Sweden, 88 p.

GRIFFIN, W.L. and QVALE, H. (1981). — Super ferric eclogites and the crustal origin of garnet peridotites, Almklovdalen, Norway. Abstr. Uppsala Caledonide Symp. *Terra Cognita, 1*, 48.

HARLEY, S.L. and GREEN, D.H. (1982). — Garnet-orthopyroxene barometry from granulites and peridotites. *Nature, 300*, 697-701.

HARTE, B. and FREER, R. (1982). — Diffusion data and their bearing on the interpretation of mantle nodules and the evolution of the mantle lithosphere. Abstr. Third Int. Kimberlite Conf. Clermont-Ferrand. *Terra Cognita, 2*, 273-275.

HARVEY, M.A. (1983). — A geochemical and Rb-Sr study of the Proterozoic augen orthogneisses on the Molde peninsula, west Norway. *Lithos* (in press).

ITO, K. and KENNEDY, G.C. (1971). — An experimental study of the basalt-garnet granulite-eclogite transition. *In* : The Structure and Physical Properties of the Earth's Crust. *Amer. Geophys. Union Geophys. Monograph, 14*, 303-314.

JENKINS, D.M. and NEWTON, R.C. (1979). — Experimental determination of the spinel peridotite to garnet peridotite inversion at 900 °C and 1 000 °C in the system CaO-MgO-Al_2O_3-SiO_2 and at 900 °C with natural garnet and olivine. *Contrib. Mineral. Petrol., 68*, 407-420.

KROGH, E.J. (1980). — Compatible P-T conditions for eclogites and surrounding gneisses in the Kristiansund area, Western Norway. *Contrib. Mineral. Petrol., 75*, 387-393.

LAPPIN, M.A. (1966). — The field relationships of basic and ultrabasic masses in the Basal Gneiss Complex of Stadlandet and Almklovdalen, Nordfjord, S.W. Norway. *Nor. Geol. Tidsskr., 46*, 439-495.

LAPPIN, M.A. (1973). — An unusual clinopyroxene with complex lamellar intergrowths from an eclogite in the Sunndal-Grubse ultramafic mass, Almklovdalen, Nordfjord, Norway. *Mineral. Mag., 39*, 313-320.

LAPPIN, M.A. (1974). — Eclogites from the Sunndal-Grubse Ultramafic Mass, Almklovdalen, Norway and the T-P History of the Almklovdalen Masses. *J. Petrol., 15*, 567-601.

LAPPIN, M.A. and SMITH, D.C. (1978). — Mantle equilibrated orthopyroxene eclogite pods from the Basal Gneisses in the Selje district, western Norway. *J. Petrol., 19*, 530-584.

LOUBET, M. and ALLÈGRE, C.J. (1982). — Trace elements in orogenic lherzolites reveal the complex history of the upper mantle. *Nature, 298*, 809-814.

MACGREGOR, I.D. (1970). — The effect of CaO, Cr_2O_3, Fe_2O_3 and Al_2O_3 on the stability of spinel and garnet peridotite. *Phys. Earth. Planet. Int., 3*, 372-377.

MATSUI, Y., BANNO, S. and HERNES, I. (1966). — Distribution of some elements among minerals of Norwegian eclogites. *Nor. Geol. Tidsskr., 46*, 364-368.

MEARNS, E.W. and LAPPIN, M.A. (1982). — A Sm-Nd isotopic study of 'internal' and 'external' eclogites, garnet lherzolite and grey gneiss from Almklovdalen, western Norway. Abstr. First Int. Eclogite Conf., Clermont-Ferrand. *Terra Cognita, 2*, 324.

MEDARIS, L.G. Jr. (1980). — Petrogenesis of the Lien peridotite and associated eclogites, Almklovdalen, Western Norway. *Lithos, 13*, 339-353.

MEDARIS, L.G. Jr. (1982). — A review of garnet peridotites within gneiss in western Norway. Abstr. First Int. Eclogite Conf., Clermont-Ferrand. *Terra Cognita, 2*, 303.

MERCY, E.L.P. and O'HARA, M.J. (1965). — Chemistry of some garnet bearing rocks from south Norwegian peridotites. *Nor. Geol. Tidsskr., 45*, 323-332.

MOORE, A.C. and QVALE, H. (1977). — Three varieties of alpine-type ultramafic rocks in the Norwegian Caledonides and Basal Gneiss Complex. *Lithos, 10*, 149-161.

MORI, T. and GREEN, D.H. (1978). — Laboratory duplication of phase equilibria observed in natural garnet lherzolites. *J. Geol., 86*, 83-97.

OBATA, M. (1976). — The solubility of Al_2O_3 in orthopyroxenes in spinel and plagioclase peridotites and spinel pyroxenite. *Amer. Mineral., 61*, 804-816.

OBATA, M. (1979). — The Ronda peridotite : garnet, spinel- and plagioclase-lherzolite facies and the P-T trajectories of a high-temperature mantle intrusion. *J. Petrol., 21*, 533-572.

O'HARA, M.J. (1975). — Pressure required to stabilise garnet-peridotite and eclogite at low temperatures. Abstr. Int. Conf. Geotherm. Geobarom. Penn. State University, U.S.A.

O'HARA, M.J. and MERCY, E.L.P. (1963). — Petro-

logy and petrogenesis of some garnetiferous peridotites. *Trans. Roy. Soc. Edinb., 65*, 251-314.

O'HARA, M.J., RICHARDSON, S.W. and WILSON, G. (1971). — Garnet peridotite stability and occurrence in crust and mantle. *Contrib. Mineral. Petrol., 32*, 48-67.

O'NEILL, H.St.C. (1981). — The transition between spinel lherzolite and garnet lherzolite, and its use as a geobarometer. *Contrib. Mineral. Petrol., 77*, 185-194.

O'NEILL, H.St.C. and WOOD, B.J. (1979). — An experimental study of Fe-Mg partitioning between garnet and olivine and its calibration as a geothermometer. *Contrib. Mineral. Petrol., 70*, 59-70.

O'NEILL, H.St.C. and WOOD, B.J. (1980). — An experimental study of Fe-Mg partitioning between garnet and olivine and its calibration as a geothermometer : corrections. *Contrib. Mineral. Petrol., 72*, 337.

PERKINS, D. III, HOLLAND, T.J.B. and NEWTON, R.C. (1981). — The Al_2O_3 contents of enstatite in equilibrium with garnet in the system MgO-Al_2O_3-SiO_2 at 15-40 kbar and 900-1 600 °C. *Contrib. Mineral. Petrol., 78*, 99-109.

RÅHEIM, A. (1975). — Mineral zoning as a record of P,T history of Precambrian eclogites and schists in western Tasmania. *Lithos, 8*, 221-236.

RÅHEIM, A. and GREEN, D.H. (1974). — Experimental determination of the temperature and pressure dependence of the Fe-Mg partition coefficient for coexisting garnet and clinopyroxene. *Contrib. Mineral. Petrol., 48*, 179-203.

RINGWOOD, A.E. (1975). — Composition and Petrology of the Earth's Mantle. McGraw Hill ed., New York, 618 p.

SACHTLEBEN, Th. and SECK, H.A. (1981). — Chemical control on the Al-solubility in orthopyroxene and its implications on pyroxene geothermometry. *Contrib. Mineral. Petrol., 78*, 157-165.

SCHMITT, H.H. (1964). — Metamorphic eclogites of the Eiksund area, Sunnmore, Norway. *Abstr. Amer. Geophys. Union, 43*, 128.

SMITH, D.C. (1980). — A tectonic mélange of foreign eclogites and ultramafites in the Basal Gneiss Region, West Norway. *Nature, 287*, 366-368.

SPRAY, J.G. (1982). — Mafic segregations in ophiolite mantle sequences. *Nature, 299*, 524-528.

WELLS, P.R.A. (1977). — Pyroxene thermometry in simple and complex systems. *Contrib. Mineral. Petrol., 46*, 1-15.

WOOD, B.J. (1974). — Solubility of alumina in orthopyroxene coexisting with garnet. *Contrib. Mineral. Petrol., 46*, 1-15.

WYLLIE, P.J. (1977). — Effects of H_2O and CO_2 on magma generation in the crust and mantle. *Jl. geol. Soc. Lond., 134*, 215-324.

WYLLIE, P.J. (1979). — Kimberlite magmas from the system peridotite-CO_2-H_2O. Proc. 2nd Kimberlite Conference, Sante Fe, Vol. 1, 'Kimberlites, Diatremes, and Diamonds : Their Geology, Petrology and Geochemistry'. *Amer. Geophys. Union*, 319-329.

The Caledonide Orogen—Scandinavia and Related Areas
Edited by D. G. Gee and B. A. Sturt

In situ metamorphism of Norwegian eclogites: an example

W. L. Griffin* and **D. A. Carswell†**

**Mineralogisk–Geologisk Museum, Sarsgate 1, Oslo 5. Norway*
†Dept. of Geology, Sheffield Univ., Sheffield S1 3JD, England

ABSTRACT

Field relations and petrographic observations on the west coast of Midøy, W. of Molde, show the following sequence of events: 1. Intrusion of the igneous protoliths of the augen orthogneiss complex; 2. Intrusion of dolerite dykes; melting of wall rocks, back-veining of dolerites by anatectic melt (intrusive relations of gneiss into eclogite are preserved locally); 3. Metamorphism to *ca.* T = 750°C, P = 17–21 Kb; dolerites boudinaged and converted to eclogites, felsic veins to Ca-rich garnet + kyanite + plagioclase + quartz ± K-feldspar ± omphacite; 4. Extreme flattening, ENE–WSW shearing and development of blastomylonite in gneisses; further boudinage of eclogites, formation of granitic pegmatites, amphibolite-facies mineral assemblages in gneiss and along eclogite margins.

This sequence is now recognized over much of the Western Gneiss Region. Radiometric data suggest that (1) occurred *ca.* 1500 Ma ago, while (3) and (4) are Caledonian (450–380 Ma). The high-pressure metamorphism of the eclogites must have occurred *in situ*; the surrounding segment of continental crust was depressed to 60–70 km depths. This 'subduction' was probably related to continent–continent collision during the Caledonian orogeny.

Introduction

The origin of the eclogites that occur as lenses in the Western Gneiss Region of Norway is still a matter of debate, sixty years after the classic descriptions of Eskola (1921). Many investigators see compelling evidence for *in situ* metamorphism of the eclogite lenses enclosed in gneiss ('country-rock' or 'external' eclogites; Bryhni *et al.* 1977; Krogh 1977; Griffin *et al.* 1984). Others, noting the presence of apparently mantle-derived garnet peridotite bodies in the gneisses, also interpret the 'country-rock' eclogites as mantle fragments (Lappin 1966; Lappin and Smith 1978; O'Hara *et al.* 1971). If eclogites can be shown to have formed by *in situ* metamorphism at high P and T, this would imply an overthickening of the continental crust, with important tectonic ramifications.

The main argument generally used against an *in situ* formation of the eclogites is that the surrounding gneisses are usually in amphibolite facies. The eclogites are thus 'out of equilibrium' with their country rocks, as evidenced by the zone of marginal amphibolitization that is typically present. Models have been presented to show that this difference in facies could be due to local variations in f_{H_2O} (Bryhni *et al.* 1977; Green and Mysen 1972) and these models have experimental support (Fry and Fyfe 1969). However, our experience suggests that *in situ* metamorphism of the eclogites and their country rock has been followed by extensive deformation and retrograde metamorphism, involving relative movement (especially along eclogite/gneiss contacts) and introduction of water. The observed eclogites therefore, in this interpretation, represent relics of an earlier high-pressure regional metamorphism. Many eclogites have been completely retrograded to garnet amphibolites, and are recognizable only by the occasional relics of omphacite found as inclusions in garnet grains. Similar relict assemblages are also found in the gneisses. Omphacite relics occur in gneiss near the Ulsteinvik eclogite, and omphacite – pyroxene–garnet–K-feldspar–quartz-kyanite assemblages occur in mangeritic rocks at several localities

(Mysen 1972; Bryhni 1966; Griffin and Mørk 1981). Krogh (1980a, b) has demonstrated in two localities that the metamorphic mineral assemblages of the gneisses are compatible with those of the associated eclogites.

Field work on Otrøy and Midøy, southwest of Molde has recently revealed rare examples of preserved 'primary' eclogite/gneiss contacts, showing relations that not only imply the *in situ* metamorphism of some country-rock eclogites, but which give detailed evidence of the relative age relations in the gneiss complex there.

Field Relations

The islands of Midøy and Otrøy (Fig. 1) expose several zones of eclogite boudins within a massive intermediate gneiss, mapped by Carswell (see Carswell and Harvey 1984) as part of an 'augen orthogneiss complex'. This complex, which includes rocks with original rapakivi-type feldspar megacrysts and relict high-P granulite mineralogy, intrudes an older supracrustal sequence. Eclogites occur in elongate concentrations, resembling basic dyke swarms, within the complex (Carswell and Harvey 1984). We will discuss one locality in detail: Litledigerneset, map sheet 1220 III, series M711, coordinates 521/769. Relations similar to those described here have also been observed at several other localities on Otrøy, Midøy, and other islands to the west (Carswell unpublished; Mørk and Griffin unpublished).

The gneiss at Litledigerneset contains abundant feldspathic lenses 1–5 cm thick and 10–100 cm long, which are isoclinally folded about a marked foliation (S_1). The origin of these lenses is ambiguous. They may be anatectic segregations, formed during high-grade metamorphism of the gneiss, or they may be of essentially tectonic origin. In other localities on Otrøy and Midøy, deformation of coarse-grained rapakivi-type structures (S_1) has flattened feldspar megacrysts into elongate ovoid lenses. More extreme deformation locally results in coalescence and segregation of this feldspathic material into the cores of tight small-scale folds. The less strongly deformed augen gneiss on Litledigerneset point, between two main eclogite zones, does not have this 'migmatitic' appearance.

The eclogites at this locality, as elsewhere on Otrøy and Midøy, occur in elongated zones of lensoid boudins, typically from 1–20 m long and $\frac{1}{2}$–10 m across, enclosed in strongly flattened gneiss. The boudins are often bordered by zones of intense amphibolitization 1–10 cm thick. Both the gneisses and the eclogites are cross-cut by coarse-grained granite pegmatites up to several decimetres thick. In the gneisses, these pegmatites are usually folded, stretched, and finally disrupted into trains of feldspar and quartz augen, easily distinguishable from the feldspathic lenses mentioned above. Where the pegmatites cut the eclogites, they are bordered by decimetre-wide amphibolite zones. Some of the pegmatites within the eclogites show very little deformation, but others have developed a strong foliation parallel to their length.

The Midøy locality is interesting because several of the eclogite boudins *do* preserve the original contact relations. In these cases the blastomylonitic foliation (S_2) swings around the eclogite bodies in such a

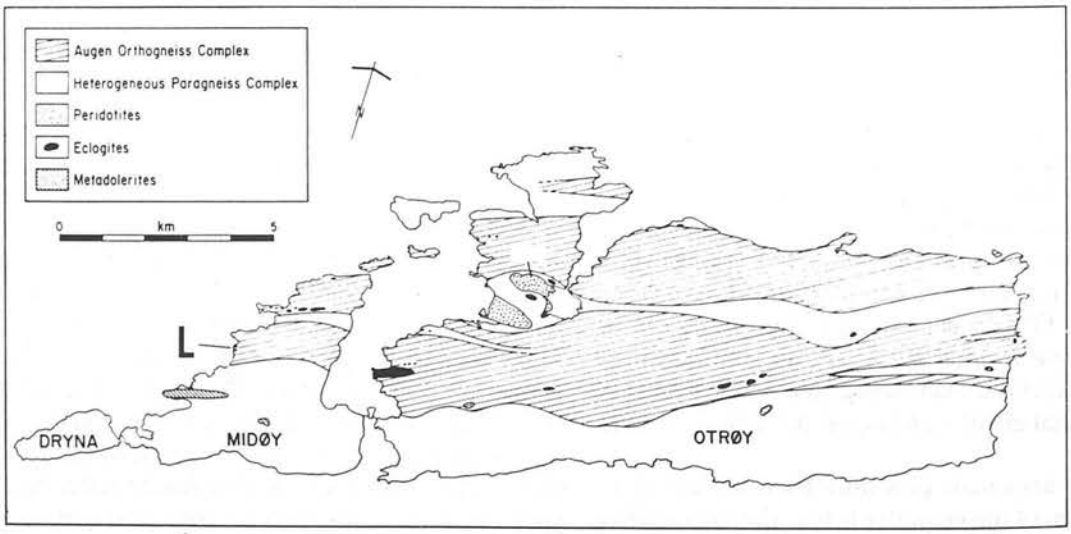

Fig. 1 Geological map of Otrøy and Midøy

way as to leave some of the surrounding gneiss relatively little affected by S_2, in a 'pressure shadow' area adjacent to the eclogite. These eclogites also have the form of irregular pods, but they are bordered by a 20–60 cm zone of massive, fine-grained quartz-dioritic gneiss lacking the feldspathic lenses common in the rest of the gneiss. This zone grades outward into the 'migmatitic' gneiss through the appearance of scattered coarser feldspathic lenses in the fine-grained matrix (Fig. 2).

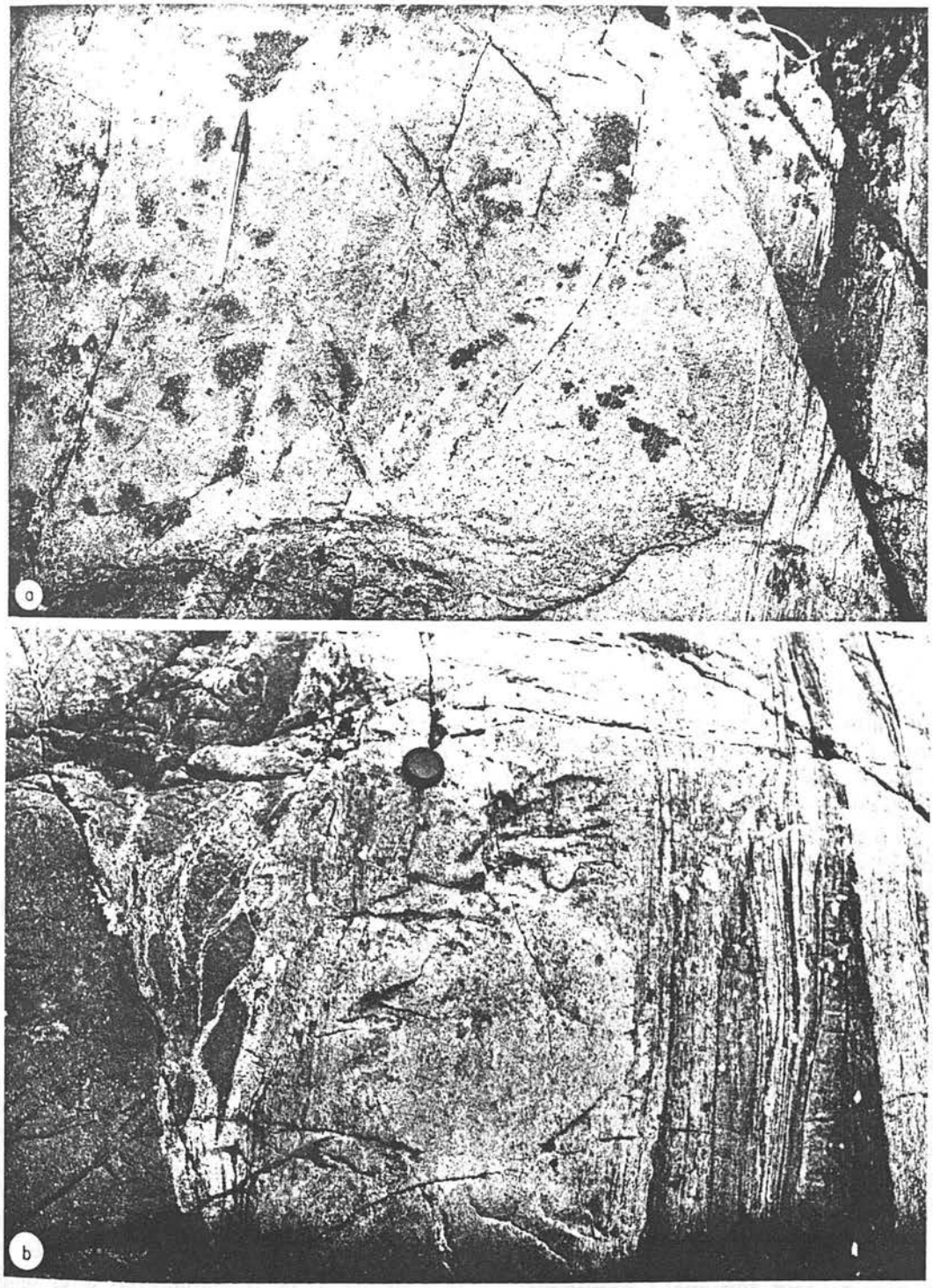

Fig. 2 Eclogite-gneiss contact relations, showing back-veining. (a) 'Migmatitic' augen orthogneiss (right) grades into fine-grained quartz dioritic gneiss toward contact with eclogite (left) and material from the fine-grained zone intrudes eclogite as irregular veins. Contact outlined for visibility. (b) Similar relations to (a), but showing blastomylonite development in migmatitic gneiss outside the fine-grained quartz-dioritic zone

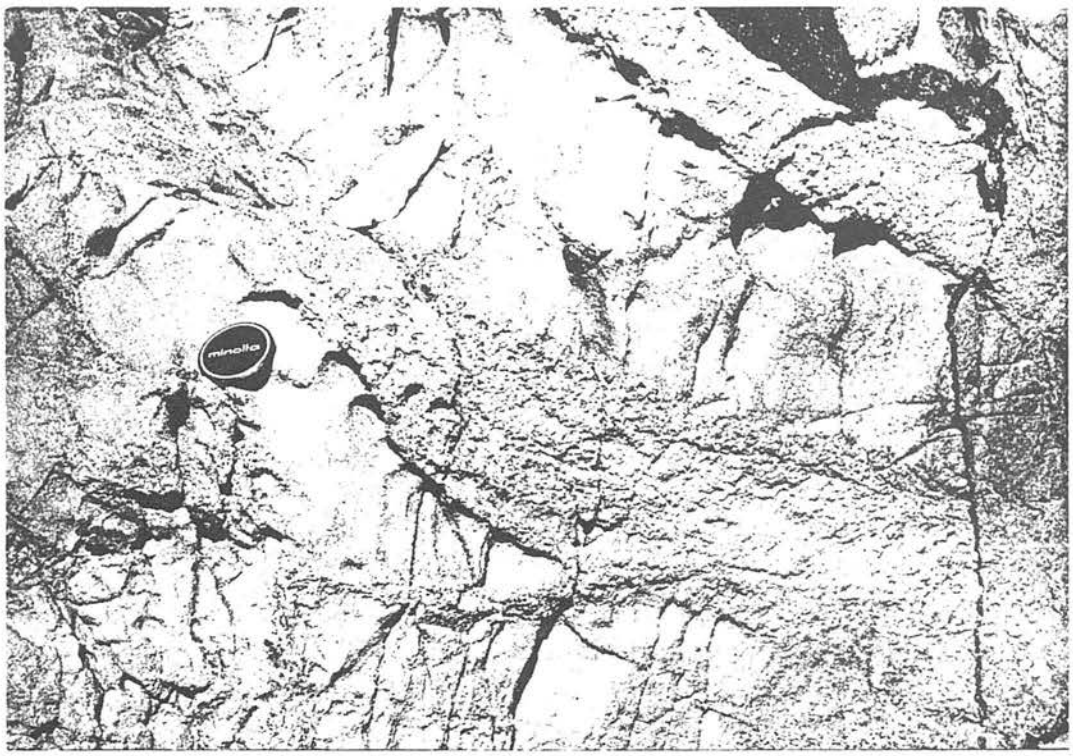

Fig. 3 Irregular, zoned felsic veins in eclogite. Note absence of any amphibolitization along veins

The contact between the fine-grained massive zone and the eclogite is generally sharp, but in several cases the former appears to intrude the eclogite in irregular veins 1–50 cm thick (Fig. 2). These felsic veins, unlike the granite pegmatites, are *not* bordered by amphibolite (Fig. 3), but contain pyroxene, kyanite and garnet (see below). The fine-grained quartz-dioritic zone, the unretrograded eclogite, and the felsic veins in the eclogite are cut by a weak foliation. This foliation appears to be the same (S_1) as that which is parallel to the axial planes of isoclinal folds in the migmatitic gneiss.

The field relations strongly suggest that the fine-grained quartz-dioritic zone and the veins in the eclogites were formed by local anatexis of the gneiss adjacent to the eclogites. We interpret this as an example of the 'Sederholm effect'–melting of the country rock adjacent to the basic intrusion, and back-veining of the chilled basic magma by the anatectic melt. The relatively wide zone of melting suggests that the country rock was at rather high T at the time of intrusion. Comparable relations, in similar rocks, have been described from the Raftsund mangerite in Lofoten (Griffin *et al.* 1974).

Petrography and Mineral Chemistry

The eclogites at Litledigerneset, where least amphibolitized, show a retrograded-eclogite mineral assemblage, consisting of garnet and symplectitic masses of clinopyroxene + plagioclase (An_{23}), with minor secondary hornblende. Quartz and rutile are locally present. The pyroxene–plagioclase symplectites are common in Norwegian eclogites and are widely recognized as the result of exsolution of the jadeite (Jd) component from high-pressure omphacite pyroxene, probably at lower pressure. The chemistry of this breakdown has been described in detail elsewhere (Mysen and Griffin 1973; Mysen 1972). The larger grains in the pyroxene–plagioclase symplectites contain up to 20 per cent Jd (Table 1); the original pyroxene apparently contained *ca.* 50 per cent Jd. The eclogite garnets are zoned to higher Fe/Mg at the rims, suggesting partial reequilibration at lower T (Table 1). Adjacent to the felsic veins, the eclogite may be enriched in garnet and/or biotite; the latter appears to have coexisted with both clinopyroxene and garnet.

The thin (*ca.* 1.5 cm) anatectic veins, where not subjected to later amphibolitization, consist of quartz, K-feldspar ($Or_{85}Ab_{15}$), plagioclase (An_{20-25}), biotite, kyanite, garnet, and clinopyroxene. The clinopyroxene occurs in pyroxene + plagioclase symplectites texturally similar to those in the adjacent eclogites. This symplectite occurs in patches that appear to be pseudomorphs after omphacite grains (Fig. 4). Microprobe analyses show that the cpx is a sodic augite with *ca.* 10% Jd (Table 1). Point-counting of photomicrographs yielded Jd con-

Table 1 Mineral analyses: eclogite and veins

	Eclogite				Vein G1			Vein U502		Vein 521G		Vein 521C		Vein U518×6	
	cpx cores	cpx rims	gnt cores	gnt rims	cpx	gnt cores (4)	gnt rims (4)	biotite (3)	Kspar (3)	gnt cores (4)	gnt rims (4)	gnt cores (2)	gnt rims (4)	gnt cores (3)	gnt rims (3)
SiO_2	51.0	50.9	40.0	39.2	51.6	39.6	39.6	37.66	64.03	39.05	39.24	38.77	38.30	39.12	39.21
TiO_2	0.38	0.46	—	—	0.19	—	—	2.79	0.30	0.0	0.0	0.0	0.0	0.0	0.0
Al_2O_3	10.7	5.1	23.0	22.8	4.6	23.0	23.0	20.24	18.61	21.89	22.07	21.94	21.37	21.64	22.05
Fe_2O_3*	1.9	1.3	—	—	0.0	—	—	—	—	—	—	—	—	—	—
FeO	5.9	7.4	19.6	21.2	9.3	19.2	18.8	8.65	0.0	19.53	21.90	19.13	23.80	19.64	21.37
MnO	0.10	0.15	0.30	0.30	0.25	0.30	0.35	0.0	0.0	0.10	0.21	0.10	0.24	0.20	0.20
MgO	9.3	11.0	7.6	6.6	11.8	7.7	7.6	16.74	0.10	4.98	6.97	5.14	5.94	5.30	6.46
CaO	17.3	20.1	10.9	10.7	20.3	11.4	11.9	0.0	0.15	14.82	10.16	14.64	9.75	14.30	11.15
Na_2O	3.6	1.8	—	—	1.2	—	—	0.36	1.52	—	—	—	—	—	—
K_2O	—	—	—	—	—	—	—	9.91	14.36	—	—	—	—	—	—
	100.18	98.21	101.4	100.8	99.24	101.2	101.25	96.35	98.97	100.37	100.55	99.72	99.40	100.20	100.44
Si	1.861	1.922	2.989	2.971	1.937	2.971	2.967	5.375	2.972	2.994	2.994	2.987	2.989	3.003	2.997
Al^{IV}	0.139	0.078	0.011	0.029	0.063	0.029	0.033	0.625	0.028	0.006	0.006	0.013	0.011	—	0.003
Al^{VI}	0.319	0.148	2.020	2.013	0.139	2.003	0.020	2.779	0.990	1.972	1.979	1.979	1.954	1.958	1.983
Ti_3	0.010	0.013	—	—	0.005	—	—	0.299	0.010	—	—	—	—	—	—
Fe_3	0.051	0.035	—	—	—	—	—	—	—	—	—	—	—	—	—
Fe_2	0.180	0.233	1.225	1.348	0.291	1.201	1.181	1.032	—	1.252	1.398	1.233	1.553	1.261	1.366
Mn	0.003	0.005	0.025	0.025	0.010	0.020	0.021	—	—	0.006	0.014	0.007	0.016	0.013	0.013
Mg	0.508	0.622	0.846	0.745	0.659	0.862	0.848	3.561	0.007	0.569	0.793	0.590	0.691	0.606	0.736
Ca	0.676	0.813	0.874	0.872	0.813	0.917	0.952	—	0.007	1.217	0.831	1.208	0.815	1.176	0.913
Na	0.252	0.131	—	—	0.081	—	—	0.100	0.137	—	—	—	—	—	—
K	—	—	—	—	—	—	—	1.804	0.850	—	—	—	—	—	—
Plag:	An_{23} (symplectite)				An_{25} (symplectite, grains)			An_{15}		An_{30}(28–35)		An_{35}(33–43)		An_{35}(33–40)	

Analyses by energy-dispersive microprobe techniques (LINK system, ZAF–4 reduction program, ARL–EMX probe).
*Fe_2O_3 calculated by charge balance for cpx (4 cations); all Fe as FeO in garnets (12 oxygen) and biotites (22 oxygen).

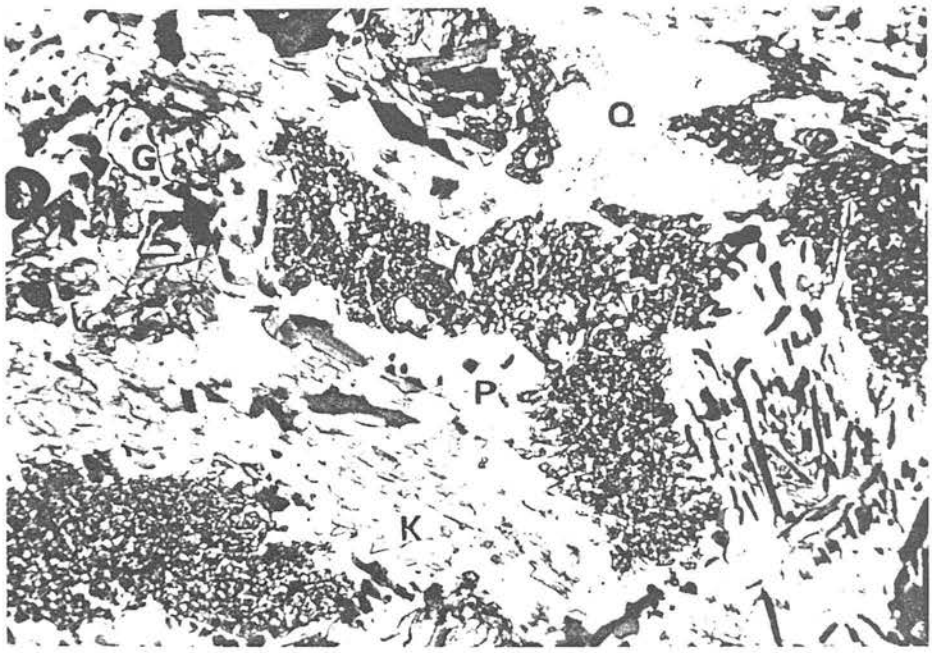

Fig. 4 Photomicrograph of sample G1, showing cpx + plag (P) symplectites, biotite + K-feldspar (K) + kyanite intergrowths and minor garnet (G) and quartz (Q)

tents of 30–40 per cent for the original omphacite. The presence of large homogeneous plagioclase grains, not in contact with symplectite, suggests that this pyroxene may have coexisted with plagioclase, but this is difficult to establish with certainty.

Hornblende + plagioclase + quartz symplectites are common in samples that lack pyroxene, and appear to have formed by amphibolitization of pre-existing cpx + plag symplectites, or of primary omphacite. Biotite occurs mainly in skeletal or radial aggregates, intergrown with K-feldspar + quartz + kyanite. These are interpreted as pseudomorphs after phengite, according to the reaction:

$$\underset{\text{Phengite}}{6K_2Al_{4-x}(Mg,Fe)_xSi_{6-x}Al_{2-x}O_{20}(OH)} \rightarrow \underset{\text{Biotite}}{XK_2(Mg,Fe)_6Si_6Al_2O_{10}(OH)_4} + \underset{\text{Kyanite}}{12-2x\ Al_2SiO_5} + \underset{\text{K-feldspar}}{12-2x\ KAlSi_3O_8} + \underset{\text{Quartz}}{(12x-12)SiO_2} + 12-2x\ H_2O$$

Thicker veins commonly show a marked zoning, with dark outer zones and a felsic central zone. The adjacent eclogite is typically enriched in garnet and/or biotite. The dark outer zones are similar in mineralogy and texture to the thinner veins, but with higher biotite contents. Again, much of the biotite, and all of the K-feldspar appear to be breakdown products of phengite flakes. The felsic cores contain a coarse-grained (1–3 mm) equilibrium assemblage of gnt + kyanite + plag + qtz. Kyanite blades are commonly, but not always, separated from quartz by a collar of plagioclase grains. Biotite + kspar and cpx/hbl + plag intergrowths occur in some samples. The garnets are rich in Ca; they are typically zoned from *ca*. $Gros_{40-45}$ in the cores to $Gros_{30-33}$ or less at the rims. Fe/Mg typically decreases rimward as well (Table 1). Plagioclase varies from *ca*. An_{28} to An_{40}, with more calcic varieties (aver. An_{35}) adjacent to the garnets.

The fine-grained quartz-dioritic zones consist dominantly of antiperthitic plagioclase (An_{18-25}) and minor quartz. The foliation is defined by dark green–brown hornblende and minor very dark brown biotite in ragged flakes. Small grains of garnet are common, and minor cpx was seen in one section. The fine-grained zone is thus depleted in K_2O compared to the surrounding gneisses (Table 2), which contain abundant microcline and biotite, but rarely garnet or hornblende. This depletion is ascribed to removal of the anatectic melt now represented by the veins in the eclogites.

Rock Chemistry

One retrograded eclogite from Litledigerneset (U517) has a Ne normative composition, whereas the others are tholeiitic (Table 2). Similar, better-preserved eclogites elsewhere on Midøy and Otrøy have the composition of olivine tholeiites (Carswell and Harvey 1984).

Analyses of two thin veins (one from Otrøy), and three samples taken across a thicker one, are presented in Table 3. Microprobe analyses have been made on glasses prepared by fusing rock powders on a Mo strip in an Ar atmosphere. Tests on standard rocks have shown that the method produces no loss of alkalies, and that the results are comparable in precision and accuracy with XRF data, for concentrations > 0.5 per cent.

One of the thin veins (U502), and the outer part of a thicker one, are granitic in composition. The other thin vein (G1) is more mafic; this vein has a diffuse margin, and appears to have been contaminated by basic material, now represented by the eclogite. The other analyses show that the central parts of the zoned veins are higher in Al and Ca, and much lower in K, than the marginal zones.

These relations suggest that originally granitic to quartz-monzonitic veins have interacted with the surrounding basic material. Mg has migrated into the veins, while K and Na have moved toward the vein margins. These variations are now seen as enrichment of clinopyroxene, phengite, and/or biotite in the vein margins, and of biotite and/or garnet in the adjacent eclogite. The removal of K and Na from the centres of larger veins resulted in an excess of Al and the presence of abundant kyanite. These contamination and differentiation processes may have occurred either during intrusion of the veins, or during later metamorphism. The relatively small size (20–50 cm) of the zoned veins suggests small-scale, subsolidus diffusion; we therefore prefer the latter interpretation.

Table 2 Whole rock analyses

	Eclogite U514	Average oliv. thol. eclogite (n = 4)	Average augen orthogneiss (n = 12)
SiO_2	46.65	46.42	65.02
TiO_2	2.45	1.30	0.85
Al_2O_3	12.16	15.82	15.11
Fe_2O_3	0.45	2.22	1.48
FeO	9.85	11.14	4.08
MnO	0.18	0.20	0.11
MgO	9.81	10.56	1.80
CaO	12.98	9.10	3.62
Na_2O	2.65	2.39	3.14
K_2O	0.08	0.08	3.64
P_2O_5	0.80	0.18	0.32
S	0.44	0.03	0.05
H_2O^-	0.45	0.31	0.65
Total	99.03	100.08	99.91
ppm			
Ni	184	259	4
V	263	182	53
Cr	814	301	13
Zn	104	112	85
Cu	45	61	18
Rb	5	2	44
Sr	534	231	264
Y	40	23	42
Zr	346	89	345
Pb	9	40	16
Ba	254	69	1151

XRF analyses by D. A. Carswell.

Table 3 Analyses of felsic veins in eclogite

	G1	U502	U518 ×4	U518 ×5	U518 ×6
SiO_2	53.95	70.69	78.94	78.52	79.12
TiO_2	0.91	0.39	0.22	0.37	0.27
Al_2O_3	18.50	15.67	10.82	12.40	12.30
Fe_2O_3	1.01	n.a.	n.a.	n.a.	n.a.
FeO	6.48	2.82	2.17	2.93	2.57
MnO	0.16	0.0	0.0	0.0	0.0
MgO	5.34	2.09	1.56	0.88	0.89
CaO	5.30	1.78	1.48	2.60	2.13
Na_2O	3.83	2.84	1.86	1.26	1.58
K_2O	3.30	3.98	3.09	0.17	0.52
P_2O_5	0.49	n.a.	n.a.	n.a.	n.a.
H_2O^-	0.88	n.a.	n.a.	n.a.	n.a.
	100.15	100.25	100.13	99.14	99.53

G1, wet-chemical analysis by B. Bruun. Other vein analyses by microprobe on fused samples.

G1: 2-cm wide irregular vein, abundant cpx + plag symplectite.
U502: 2.5-cm felsic vein, scattered large garnets, bio + kyan + ksp symplectite.
U518: 20-cm wide zoned felsic vein.
×4: Mica-rich outer zone with rare garnets, bio + kyan + ksp symplectite.
×5: Outer part of central zone, with large gnt and kyanite grains.
×6: Central zone with gnt + kyan + plag + qtz, and minor hbl + plag symplectite.

Metamorphic Conditions

The original presence of the metamorphic omphacite + garnet + feldspar + quartz assemblage in the veins corroborates the field evidence that these veins were metamorphosed together with the surrounding eclogite. The vein assemblage may have included phengite at the metamorphic peak, or this phase have formed at an earlier stage of prograde metamorphism and broken down at high-T conditions. An accurate estimate of the metamorphic T is difficult, since no omphacite is preserved well enough to be considered in equilibrium with garnet. However, studies of eclogites on a regional basis have documented a metamorphic gradient across the Western Gneiss Region (Griffin *et al.* 1984), and

many of the data points are from the area around Midøy. These data suggest that the temperature at the metamorphic peak here lay near 750°C.

The assemblage calcic garnet + plagioclase + kyanite + quartz is indicative of relatively high P, and several attempts have been made to calibrate the reaction:

$$An \leftrightharpoons Gros + kyan + qtz \qquad (2)$$

for P and T. We have used the calibration of Schmid and Wood (1976) and Wood (1977), with the value of ω_{Ca}^{gnt} suggested by Jenkins and Newton (1979) and $\gamma_{An}^{plag} = 1.28$ (Orville 1972). This method gives results that are identical (within the probable error) to those obtained by the method of Ghent (1976). We have assumed that the rims of the analysed garnet ($Gros_{30}$) equilibrated with the adjacent plagioclase (An_{35}). This leads to P = 19–21 Kb at 750°C for the four samples of this assemblage (Table 1). This P estimate lies near the upper end of the P–T array for the eclogites of the Western Gneiss Region (Griffin *et al.* this volume) and is similar to the average P estimate (17–18 Kb at 700–750°C) derived from orthopyroxene-bearing eclogites by Carswell *et al.* (this volume). An error of 50° in T leads to a positively correlated error in P of *ca.* 1.5 Kb. This estimate, therefore, represents an independent confirmation of the high pressures reached during the metamorphism of the Western Gneiss Region.

The zoning of the garnets in the veins suggests growth during increasing T (reflected by a rimward decrease in Fe/Mg). The rimward decline in CaO could be interpreted as reflecting a moderate drop in P as T increased; England and Richardson (1977) predict such a thermal evolution for subducted or overthrust terranes. However, we have no evidence on the composition of the plagioclase that may have coexisted with garnet cores. It is therefore possible that the rimward drop in CaO seen in the garnets mainly reflects depletion of Ca from the coexisting plagioclase.

Discussion

The field relations described here, and the evidence of high-P mineral assemblages in the anatectic back-veins, clearly show that the eclogites and the surrounding gneiss have been metamorphosed together at high P and T (F_1). Both gneiss and eclogite have suffered a later, lower-grade hydrous metamorphism, accompanied by extreme local flattening (F_2), boudinage, and local anatexis. The preservation of the eclogite and high-P granulite has depended heavily on the size of the eclogite bodies and the large difference in competence between the basic bodies and the more ductile gneiss.

The Litledigerneset locality shows a rather detailed sequence of events.

1. Formation of the host rock, probably as an intermediate plutonic intrusive.
2. Intrusion of the basic magma, probably as dykes: marginal anatexis, back-veining of the dykes.
3. Metamorphism at high T, P: development of S_1 foliation, 'migmatization', either anatectic or tectonic, of orthogneiss, boudinage of basic dykes, formation of eclogite/high-P granulite mineral assemblages.
4. Strong *ca.* N–S compression (ENE–WSW shearing): blastomylonite formation, further boudinage of basic bodies, formation of coarse-grained granitic pegmatites around and locally cross-cutting the eclogite boudins.

The oldest foliation that can be recognized is that which forms the axial plane to isoclinal folds in feldspathic lenses in the gneiss (S_1). This foliation is also found in the eclogites and in the fine-grained quartz-dioritic zone around the eclogites.

If the feldspathic lenses in the gneiss represent deformed feldspar megacrysts, their absence from the quartz-dioritic marginal zones can be a result of the local anatexis associated with intrusion of the basic dykes. If these lenses were formed by anatexis during (F_1) regional metamorphism they would not have formed in the quartz-dioritic zones, which were already depleted in granitic components. Thus we cannot be sure that the formation of these lenses post-dates the intrusion of the dykes; the sequence given here is the simplest that fits the observed relations.

Several workers (Bryhni *et al.* 1969; Green and Mysen 1972) have suggested that the formation of pegmatites by anatexis was important in lowering f_{H_2O} locally and thus promoting the formation of eclogites. The field relations at Litledigerneset show that on the contrary the granitic pegmatites there clearly post-date the high-grade metamorphic event. They have been important in introducing water, leading to amphibolitization of the eclogites. This retrograde step occurred either prior to, or during the latest intense deformation phase.

Several of the steps in this sequence can be dated, at least tentatively, on the basis of available radiometric data. The formation of the augen orthogneiss complex has been dated as 1478 ± 42 Ma by Rb–Sr whole-rock studies, along the strike from the present locality (Carswell and Harvey 1984). This agrees with U–Pb and Rb–Sr data from similar rocks in the Nordfjord area (Lappin *et al.* 1979; Malinconico personal communication). These ages are signifi-

cantly younger than those on the surrounding supracrustal rocks (1600–1800 Ma: Tørudbakken and Ilebekk in prepartion).

The intrusion of the basic magma has not been dated directly, but is believed to have occurred soon after the intrusion of the orthogneiss complex, as discussed above. Tørudbakken (1981) has obtained a Rb–Sr whole-rock age of 1517 ± 60 Ma on a partially eclogitized gabbro of similar composition, in the Trollheimen area.

The high-P metamorphism may be dated by Sm–Nd ages of cpx + gnt pairs, which cluster tightly around 425 Ma (Griffin and Brueckner 1980; in preparation). U–Pb data on zircons from several Norwegian eclogites also indicate metamorphism in this time range (Krogh *et al.* 1974; Gebauer personal communication). Rb–Sr dates on micas and other phases from eclogites cluster in the period 380–430 Ma (Griffin and Brueckner in preparation). It is not clear whether these ages are related only to cooling and uplift, or represent a real metamorphic episode—step (4) of the above sequence. Similar Rb–Sr ages are given by mica + whole-rock pairs from various types of gneiss (Brueckner 1972; Krill and Griffin in preparation).

Brueckner (1972) has given a biotite-rock Rb–Sr date of 396 Ma on a granite pegmatite cutting a retrograded (oliv + opx + chlor + amph) garnet peridotite on Gurskøy. Feldspar–mica pairs from similar dykes in eclogites yield ages as low as 355 Ma (Krill and Griffin in preparation), suggesting that intrusion and local deformation continued into Devonian time.

These radiometric data suggest that all of the *metamorphic* events recognized at the Litlediger-neset locality occurred during the Caledonian orogeny, while the igneous protoliths date from the end of the Svecofennian period. This sequence of events is recognizable over larger areas of the Western Gneiss Region, wherever eclogites occur within massive or migmatitic orthogneisses. A metamorphic event older than step (1) may be recognized where metasupracrustal rocks occur; we interpret this as a Svecofennian amphibolite-facies metamorphism. The garnets of eclogites in metamorphosed supracrustal rocks commonly contain inclusions of amphibolite-facies minerals (Bryhni *et al.* 1977; Krogh 1982) that may derive from this metamorphic event.

The relations between gneiss and eclogite described here leave little doubt that the formation of the eclogites has occurred *in situ*. Other evidence, summarized by Bryhni *et al.* (1977) and Griffin *et al.* (this volume) suggests that this conclusion is valid for many, if not all, of the eclogites in the Western Gneiss Region. This requires in turn that this edge of the Baltic Shield was depressed to depths of *ca.* 60–70 km, probably in a continent–continent collision zone, during the Caledonian orogeny (Bryhni *et al.* 1977; Krogh 1977; Griffin *et al.* this volume; Cuthbert *et al.* 1981).

Acknowledgements

This work has been supported by NAVF (grant D 48–22.08) and NERC (grant GR3/3085). Discussions with M. B. E. Mørk have contributed much to our understanding of the field relations.

References

Brueckner, H. K. 1972. Interpretation of Rb–Sr ages from the Precambrian and Paleozoic rocks of southern Norway. *Am. Journal of Science*, **272**, 334–358.

Bryhni, I. 1966. Reconnaissance studies of gneisses, ultrabasites, eclogites and anorthosites in outer Nordfjord western Norway *Norges geol. Unders.*, **241**, 1–68.

Bryhni, I., Fyfe, W. S., Green, D. H. and Heier, K. S. 1970. On the occurrence of eclogite in Western Norway. *Contr. Mineral. Petrol.*, **26**, 12–19.

Bryhni, I., Krogh, E. J. and Griffin, W. L. 1977. Crustal derivation of Norwegian eclogites: a review. *N. Jb. Miner. Abh.*, **130**, 49–68.

Carswell, D. A. and Harvey, M. 1981. Molde–Otrøy–Midøy. In Griffin, W. L. and Mørk M.-B. E. (Eds), *Excursion B1. Excursions in the Scandinavian Caledonides.* Geologisk Museum, Oslo.

Carswell, D. A. and Harvey, M. this volume. The intrusive history and tectonometamorphic evolution of the basal gneiss complex in the Moldefjord region. W. Norway.

Carswell, D. A., Krogh, E. J. and Griffin, W. L. this volume. Norwegian orthopyroxene eclogites: calculated equilibration conditions and petrogenetic implications.

Cuthbert, S., Harvey, M. and Carswell, D. A. 1981. A plate tectonic model for the metamorphic evolution of the Basal Gneiss Complex in Western Norway. *Terra Cognita*, **1**, 41.

England, P. C. and Richardson, S. W. 1977. The influence of erosion upon the mineral facies of rocks from different metamorphic environments. *J. geol. Soc. London*, **134**, 201–219.

Eskola, P. 1921. On the eclogites of Norway. *Skr. Vidensk. Selsk. Christiania, Mat.–Natv. KII*, No 8, 1–118.

Fry, N. and Fyfe, W. S. 1969. Eclogites and water pressure. *Contr. Mineral. Petrol*, **24**, 1–6.

Ghent, E. D. 1976. Plagioclase–garnet–Al_2SiO_5–quartz: a potential geobarometer–geothermometer. *Am. Mineral*, **61**, 710–714.

Green, D. H. and Mysen, B. O. 1972. Genetic relationship between eclogite and hornblende + plagioclase pegmatite in western Norway. *Lithos*, **5**, 147–161.

Green, D. H. and Ringwood, A. E. 1967. An experimental investigation of the gabbro to eclogite transformation and its petrological implications. *Geochim. Cosmochim. Acta.*, **31**, 767–833.

Griffin, W. L., Austrheim, H., Brastad, K., Bryhni, I., Krill, A., Mørk, M.-B. E., Qvale, H. and Tørudbakken,

B.' this volume. High-pressure metamorphism in the Scandinavian Caledonides.

Griffin, W. L., Heier, K. S., Taylor, P. N. and Weigand, P. W. 1974. General geology, age and chemistry of the Raftsund mangerite intrusion, Lofoten–Vesterålen. *Norges geol. Unders.*, **312**, 1–30.

Griffin, W. L. and Brueckner, H. K. 1980. Caledonian Sm–Nd ages and a crustal origin for Norwegian eclogites. *Nature, London*, **285**, 319–321.

Griffin, W. L. and Mørk, M.-B. E. 1981. Eclogites and basal gneisses in western Norway. *Excursion B1. Excursions in the Scandinavian Caledonides.* Geolisk Museum, Oslo.

Jenkins, D. M. and Newton, R. C. 1979. Experimental determination of the spinel peridotite to garnet peridotite inversion at 900°C and 1000°C in the system $CaO–MgO–Al_2O_3–SiO_2$, and at 900°C with natural olivine and garnet. *Contr. Miner. Petrol.*, **68**, 407–419.

Krogh, E. J. 1977. Evidence for a Precambrian continent–continent collision in western Norway. *Nature, London*, **267**, 17–19.

Krogh, E. J. 1980a. Geochemistry and petrology of glaucophane-bearing eclogites and associated rocks from Sunnfjord, western Norway. *Lithos*, **13**, 355–380.

Krogh, E. J. 1980b. Compatible P–T conditions for eclogites and surrounding gneisses in the Kristiansund area, western Norway. *Contrib. Mineral. Petrol.*, **75**, 387–393.

Krogh, E. J. 1982. Metamorphic evolution deduced from mineral inclusions and compositional zoning in garnets from Norwegian country-rock eclogites. *Lithos*, **15**, 305–321.

Krogh, T. E., Mysen, B. O. and Davis, G. L. 1974. A Paleozoic age for the primary minerals of a Norwegian eclogite. *Ann. Rep. Geophys. Lab. Carnegie I not. Washington*, **73**, 575–576.

Lappin, M. A. 1966. The field relationships of basic and ultrabasic masses in the basal gneiss complex of Stadlandet and Almklovdalen, Nordfjord, northwestern Norway. *Norsk geol. Tidsskr.*, **46**, 439–495.

Lappin, M. A. and Smith, D. C. 1978. Mantle-equilibrated orthopyroxene eclogite pods from the basal gneisses in the Selje district, western Norway. *J. Petrol.*, **19**, 530–584.

Lappin, M. A., Pidgeon, R. T. and Breemen, O. Van. 1979. Geochronology of basal gneisses and mangerite syenite of Stadlandet, west Norway. *Norsk geol. Tidsskr.*, **59**, 161–181.

Mysen, B. O. 1972. Five clinopyroxenes in the Hareidlandet eclogite, western Norway. *Cont. Mineral. and Petrol.*, **34**, 315–325.

Mysen, B. O. and Griffin, W. L. 1973. Pyroxene stoichiometry and the breakdown of omphacite. *Am. Miner.*, **58**, 60–63.

O'Hara, M. J., Richardson, S. W. and Wilson, G. 1971. Garnet peridotite stability and occurrence in crust and mantle. *Contr. Mineral. Petrol.*, **32**, 48–68.

Orville, P. M. 1972. Plagioclase cation exchange equilibria with aqueous chloride solution: results at 700°C and 2000 bars in the presence of quartz. *Am. J. Sci.*, **272**, 234–272.

Schmid, R. and Wood, B. J. 1976. Phase relationships in granulitic metapelites from the Ivrea–Verbano Zone (Northern Italy). *Contr. Miner. Petrol.*, **54**, 255–279.

Tørudbakken, B. 1981. Vindøldalen dolerite. In Griffin, W. L. and Mørk, M.-B. E. (Eds), *Excursion B1. Excursions in the Scandinavian Caledonides.* Geologisk Museum, Oslo.

Wood, B. E. 1977. The activities of components in clinopyroxene and garnet solid solutions and their application to rocks. *Phil. Trans. R. Soc. London*, **A286**, 331–342.

Yoder, H. S. and Tilly, C. E. 1964. Origin of basalt magmas: an experimental study of natural and synthetic rock systems. *J. Petrol.*, **3**, 342–532.

The Caledonide Orogen—Scandinavia and Related Areas
Edited by D. G. Gee and B. A. Sturt

Norwegian orthopyroxene eclogites: calculated equilibration conditions and petrogenetic implications

D. A. Carswell* E. J. Krogh† and W. L. Griffin‡

**Department of Geology, University of Sheffield, Mappin Street, Sheffield S1 3JD, England*
†*Institute of Biology & Geology, University of Tromsø, Tromsø, Norway*
‡*Mineralogisk–Geologisk Museum, Sarsgate 1, N–Oslo 5, Norway*

ABSTRACT

Within the Western Gneiss Region of Norway, orthopyroxene-bearing eclogites occur as part of garnetiferous ultramafic rocks ('internal' or 'A' type) and as layers and lenses enclosed in gneisses ('external' or 'B' type). Calculation of metamorphic pressure–temperature conditions is complicated by apparent disequilibrium among orthopyroxene, clinopyroxene, and garnet. Garnets commonly show minor retrograde Fe/Mg zoning, while in some external orthopyroxene eclogites, garnets are prograde zoned and preserve amphibolite facies mineral assemblages as inclusions. Orthopyroxene grains are commonly zoned from low Al in cores to maximum Al in rims in contact with garnet and clinopyroxene. Some orthopyroxene eclogites show phase intergrowths which may reflect exsolution from primary high Al pyroxenes, comparable to those found elsewhere in anorthosites or spinel peridotites. There is no evidence that these high-Al pyroxenes ever have coexisted with garnets; they are high temperature, but not necessarily high pressure, phases. The low Al contents of some orthopyroxene grain cores may reflect disequilibrium during prograde metamorphism. These low-Al compositions cannot be paired with particular garnet compositions as meaningful mineral equilibria. Hence the high pressure values (30–50 Kbars) calculated for many orthopyroxene–garnet composition pairs are probably spurious.

Calculated pressure–temperature conditions using maximum values of Al in orthopyroxenes, average: external orthopyroxene eclogites *ca.* 700–740°C, 17–18 Kbars; internal orthopyroxene eclogites *ca.* 710°C, 20 Kbars; garnet lherzolites, *ca.* 725°C, 20 Kbars. As similar pressure–temperature values have been calculated for associated granulite facies gneisses and orthopyroxene free external eclogites, it is considered that all of these rock types equilibrated together at high pressures. This may have occurred during a transient subduction event, prior to the extensive retrograde metamorphism which occurred during the ensuing uplift of these rocks towards the surface.

Introduction

The Gneiss Region of western Norway, extending from Bergen to Kristiansund, is a classic area for the study of eclogites. Within this area, two general types are commonly distinguished:

1. 'Internal' or Type A eclogites are layers or lenses enclosed within ultramafic rocks, sometimes garnet-bearing. The peridotites are dominated by the amphibolite facies assemblage olivine + orthopyroxene + amphibole + chlorite, which overprints the garnetiferous assemblages (Medaris 1980).
2. 'External' or Type B eclogites are layers, lenses, and pods from centimetres to kilometres in size, enclosed within gneisses of both sedimentary and igneous origin. The gneisses locally contain relict high-pressure granulite assemblages, but are dominated by the amphibolite facies mineral assemblages that also overprint the eclogites.

It appears obvious from field and petrographic data that the eclogite facies assemblages are relics of

Table 1 Summary of field relations and petrography of analysed samples

Sample no.	Locality	Field type	Primary mineral assemblage	Secondary minerals	Special features
KR1	Hornindal	B	Gnt+cpx+opx+amph +magnetite+spinel?	Sec. green amph around cpx	Uncertain if green spinel associated with magnetite is primary or secondary. Sub- to euhedral gnt inclusions in pyroxenes may reflect exsolution from original higher T. Al-rich pyroxenes.
KR6	Hellesylt	B	Gnt+cpx+opx +(colourless)amph +rutile	none	Rounded irregular gnt grains enclosed in larger opx, cpx and amph grains.
KR2A KR2B	Kvalneset	B	Gnt+cpx+opx +amph+rutile	none	Large opx grains contain sub- to euhedral grains of gnt. Primary amph is colourless in thin sections in contrast to inclusions of green amph in some gnt.
KR3	Hjørungavåg	B	Gnt+cpx+opx+amph +qtz+rutile	Secondary reactions as follows: (a) CpxI+gnt → CpxII+plag +opxII	Cpx grains contain thin spindles of quartz // to cleavage planes—perhaps exsolved during oxidation.
KR3	Hjørungavåg	B	Gnt+cpx+opx+amph +qtz+rutile	(b) CpxI+gnt+H_2O → cpxII+amphII+plag (c) OpxI+gnt+H_2O → amphII (d) Gnt+qtz → opxII+plag	
KR4	Kvalvåg	B	Gnt+cpx+opx +qtz+rutile	Considerable sec. cpx after both gnt and cpx. Sec. reaction (d) Gnt+qtz → OpxII+plag	Resembles KR3 but sec. reaction products not so abundant. Green amph inclusions in some gnt.
U206 U243	Solholm Otrøy	B	Gnt+cpx+opx +mica+rutile	Sec. amph after cpx and gnt especially in U206; also extensive alteration of opx	Red–brown mica in apparent textural equil. with primary phases and also as inclusions in gnt.
U19	Skarshaugen Otrøy	B	Gnt+cpx+opx+mica? +qtz+rutile	Minor sec. amph	Numerous gnt inclusions in pyroxenes. Pale brown mica is enigmatic—sometimes in text. equil. with primary phases elsewhere of apparent replacement origin.
KR5 A44A			Gnt+cpx+opx+rutile		Pegmatitic opx bearing variants.
A44B	Grytingvåg	B	Gnt+cpx+opx+rutile	Sec. amph abundant in broad zones towards margin of lens	Contains contact of coarse opx eclogite with finer grained, foliated, opx free eclogite.
A45			Gnt+cpx+mica+rutile		Interlayered opx free eclogite with pale brown mica. Many cpx+mica inclusions in gnt.
V80/19	Høydalsneset	B	Gnt+cpx+opx+amph +qtz+rutile	Some sec. amph	Gnt contain inclusions of pyroxenes and amph., foliation defined by pyroxenes and amph.
U95	Ugelvik (Harbour)	A	Gnt+opx+cpx	none	All cpx and much (all?) gnt exsolved from original high Al–opx. Details and data in Carswell (1973).
U47	Ugelvik (Raudhaugene)	A	Gnt+opx+cpx+rutile	Pyroxenes extensively hydrated	Sharply bounded layer in serp. gnt peridotite body. Porphyroclastic texture with clasts up to 6 mm in recryst. mosaic of 0.2–0.5 mm grains.

an early high-pressure metamorphic event, now largely obliterated by later amphibolite facies metamorphism. The nature, tectonic setting, and timing of the high-P metamorphism have been a matter of heated controversy for at least 50 years. One group (O'Hara and Mercy 1963; O'Hara 1967; O'Hara *et al.* 1971; Lappin 1966, 1974; Lappin and Smith 1978), regard the ultramafic rocks as tectonic slices of the subcontinental mantle, and have extended this interpretation to include the external eclogites. Others (Bryhni 1966; Bryhni *et al.* 1970, 1977; Carswell 1974; Griffin 1972; Griffin and Råheim 1973; Krogh 1977a,b; Mysen and Heier 1972; Råheim 1972) regard the external eclogites as an integral part of the gneiss terrane and implicitly or explicitly consider a dual origin: essentially *in situ* metamorphism of the external eclogites, and tectonic introduction of the ultramafic rocks and their associated internal eclogites. Recent geotectonic models relate both processes to limited transient subduction of the west Norwegian continental crust in a Himalaya-type collision belt, probably in an early stage of the Caledonian orogeny (Bryhni *et al.* 1977; Krogh, 1977a; Cuthbert *et al.* 1983; Griffin *et al.* this volume).

One approach to the resolution of this controversy is the determination of the P–T conditions involved in the metamorphism of both types. Garnet websterites are especially pertinent to this problem, since the assemblage orthopyroxene + clinopyroxene + garnet allows estimation of both P and T by comparison with experimental work, assuming that these phases have equilibrated under metamorphism. Garnet websterites occur in both 'internal' and 'external' situations in the Western Gneiss Region. Although these rocks contain clinopyroxene, they have traditionally been called 'orthopyroxene eclogites', and we will follow this practice. 'Internal' orthopyroxene eclogites may contain olivine and grade into garnet lherzolites. 'External' orthopyroxene eclogites may contain quartz and rutile, as well as hydrous phases.

Mineralogical data and P–T estimates for the internal orthopyroxene eclogites and garnet lherzolites are summarized by Carswell and Gibb (1980a), and Medaris (1980). Data on external orthopyroxene eclogites are less extensive. Lappin (1974) and Lappin and Smith (1978) presented data from several bodies in the Selje area; they concluded that these originated deep in the upper mantle, and have been tectonically emplaced into the crust ($\Delta P \sim 20$ Kbars). This paper presents data on a wider range of orthopyroxene eclogite occurrences, mostly of the external type. Special attention is paid to evidence of chemical disequilibrium and the difficulty of calculating meaningful P–T estimates for these rocks.

The locations of the analysed samples are given in Griffin *et al.* (this volume), and field relations, petrography, etc. are summarized in Table 1.

Mineral Chemistry

Analytical techniques

Mineral separates were analysed by D. A. Carswell at the University of Sheffield using a combination of atomic absorption, flame photometry, spectrophotometric, and titration techniques. All other mineral analyses were by electron microprobe using either the ARL–EMX microprobe at Oslo (analysts: A. J. Krogh and W. L. Griffin) or the Microscan IX microprobe at Sheffield (analyst: D. A. Carswell). The Oslo analyses include both WDS and some EDS (LINK system, ZAF–4 reduction program) analyses; Sheffield analyses are all WDS data. Analyses of low-Al orthopyroxene standards are shown in Table 2.

Microprobe point analyses of the primary mineral

Table 2 Microprobe analyses of 'standard' orthopyroxenes

	R 2537		R 1742		Shallow water	
	Oslo	nominal	Oslo	nominal	Oslo	nominal
SiO_2	51.91	52.2	49.92	50.2	59.13	59.98
Al_2O_3	1.78	1.8 (2.2)	1.40	1.1 (1.8)	0.11	0.13
TiO_2	0.11	0.1	0.12	0.1	—	—
MgO	22.45	22.8	13.25	13.8	40.04	39.96
FeO	21.91	21.3	32.97	33.3	—	—
MnO	0.61	0.6	0.78	0.7	—	—
CaO	0.54	0.6	0.69	0.6	0.09	0.10
	99.31		99.13		99.37	

Nominal values for R 2537, R 1742 are probe analyses by Howie and Smith (1966); wet chemical values in parentheses. Shallow water enstatite, probe analysis by K. Fredriksson (pers. comm. 1977). Oslo analyses done using ARL–EMX manual probe, mixed synthetic and natural mineral standards, Bence–Albee correction methods. Analyst: E. J. Krogh.

Table 3 Analyses of primary orthopyroxenes

	KR 1 No zoning	KR 2A–1 Cores	KR 2A–1 Rims ADJ gnt	KR 2B–1 Rims ADJ gnt	KR 2B–2 Cores	KR 3–1 Min. Al	KR 3–2 Max. Al	KR 3–3 Aver. Al	KR 4–1 Min. Al	KR 4–2 Max. Al	KR 4–3 Aver. Al	KR 6–1 Rims ADJ gnt	KR 6–2 Cores	U 206 No zoning	U 243–1 Large grains	U 243–2 Inc. in gnt	U 19–1 Min. Al	U 19–2 Max. Al
SiO_2	55.3	56.1	55.5	54.4	55.3	56.3	54.7	55.8	55.2	55.2	54.9	55.6	55.9	55.4	55.7	54.6	56.4	55.8
TiO_2	n.d.	n.d.	n.d.	0.03	0.02	n.d.	n.d.	n.d.	n.d.	n.d.	n.d.	0.06	0.09	n.d.	n.d.	n.d.	0.02	0.02
Al_2O_3	0.88	0.28	0.57	0.78	0.33	0.77	2.58	1.16	0.90	2.41	1.53	0.69	0.35	0.86	0.73	1.11	1.24	1.99
Cr_2O_3	n.d.	n.d.	n.d.	0.06	0.02	n.d.	n.d.	n.d.	n.d.	n.d.	n.d.	0.05	0.02	n.d.	n.d.	n.d.	0.04	0.05
FeO*	14.4	15.0	15.8	15.4	15.0	13.5	13.3	13.6	11.4	10.7	11.8	12.1	12.2	13.0	12.7	13.2	8.40	8.04
MnO	0.21	n.d.	n.d.	0.14	0.13	0.34	0.34	0.34	0.16	0.10	0.17	0.10	0.15	0.18	n.d.	n.d.	0.15	0.15
NiO	n.d.	n.d.	n.d.	n.d.	n.d.	n.d.	n.d.	n.d.	n.d.	n.d.	n.d.	n.d.	n.d.	n.d.	n.d.	n.d.	n.d.	n.d.
MgO	29.6	28.2	27.7	28.2	28.8	29.1	28.5	28.9	32.0	30.8	30.8	30.8	31.1	30.5	31.1	30.4	34.0	34.1
CaO	0.14	0.19	0.26	0.25	0.10	0.23	0.14	0.21	0.23	0.17	0.37	0.16	0.15	0.29	0.28	0.27	0.21	0.13
Na_2O	n.d.	n.d.	n.d.	n.d.	n.d.	n.d.	n.d.	n.d.	n.d.	n.d.	n.d.	n.d.	n.d.	0.02	n.d.	n.d.	0.01	0.02
Total	100.5	99.8	99.9	99.3	99.7	100.2	99.6	100.0	99.9	99.4	99.5	99.6	100.0	100.3	100.5	99.6	100.4	100.3
								Structural formulae O = 6										
Si	1.968	2.011	1.996	1.971	1.988	1.998	1.953	1.986	1.953	1.951	1.951	1.976	1.980	1.965	1.966	1.954	1.954	1.934
Al^{IV}	0.032	0.000	0.004	0.029	0.012	0.002	0.047	0.014	0.038	0.049	0.049	0.024	0.015	0.035	0.030	0.046	0.046	0.066
Al^{VI}	0.005	0.012	0.020	0.004	0.002	0.030	0.066	0.035	0.000	0.051	0.015	0.005	0.000	0.001	0.000	0.001	0.005	0.015
Ti	—	—	—	0.001	0.001	—	—	—	—	—	—	0.002	0.002	—	—	—	0.001	0.001
Cr	—	—	—	0.002	0.001	—	—	—	—	—	—	0.001	0.001	—	—	—	0.001	0.001
Fe	0.428	0.451	0.477	0.467	0.451	0.400	0.398	0.404	0.337	0.315	0.351	0.360	0.361	0.387	0.375	0.395	0.243	0.233
Mn	0.006	—	—	0.004	0.004	0.010	0.010	0.010	0.005	0.003	0.005	0.003	0.005	0.005	—	—	0.004	0.004
Ni	—	—	—	—	—	—	—	—	—	—	—	—	—	—	—	—	—	—
Mg	1.568	1.503	1.485	1.523	1.542	1.537	1.516	1.534	1.686	1.622	1.631	1.631	1.642	1.613	1.637	1.617	1.757	1.763
Ca	0.005	0.007	0.010	0.010	0.004	0.009	0.005	0.008	0.009	0.006	0.014	0.006	0.006	0.011	0.011	0.010	0.008	0.005
Na	—	—	—	—	—	—	—	—	—	—	—	—	—	0.001	—	—	0.001	0.001
Total	4.013	3.984	3.992	4.011	4.006	3.986	3.992	3.990	4.028	3.998	4.017	4.008	4.012	4.018	4.019	4.023	4.020	4.024

* All Fe as FeO; analytically determined FeO contents in mineral separates are U19: 8.61 wt%, U47: 4.41 wt%, A44: 8.42 wt%.

Table 3 (*continued*)

	U 19–3 Aver. Al	U 19–4 Min. Sep.	U 95–1 Min. Al	U 95–2 Max. Al	U 95–3 Aver. Al	U 47–1 Aver. clasts	U 47–2 Aver. recrysts.	U 47–3 Min. sep.	KR 5–1 Rims ADJ gnt	KR 5–2 Core	KR 5–3 Rims ADJ cpx	A 44–1 Aver. cores	A 44–2 Rims ADJ gnt	A 44–3 Rims ADJ cpx/amp	A 44–4 Min. sep.	V80/17 1 High-Al	V80/17 2 Min. Al
SiO_2	56.0	53.5	58.4	57.4	58.0	57.7	58.1	58.0	56.4	56.6	56.8	57.2	56.9	57.0	56.7	55.9	55.7
TiO_2	0.02	0.05	n.d.	n.d.	n.d.	n.d.	n.d.	0.08	n.d.	n.d.	n.d.	0.02	0.02	0.02	0.03	n.d.	n.d.
Al_2O_3	1.52	6.66	0.54	2.03	1.22	0.15	0.38	0.75	0.78	0.53	0.38	0.35	0.68	0.48	0.82	1.18	0.59
Cr_2O_3	0.05	0.13	0.15	0.28	0.24	n.d.	n.d.	0.04	0.03	0.03	0.03	0.03	0.02	0.02	0.02	n.d.	n.d.
FeO*	8.17	8.88	4.14	4.18	4.26	4.93	5.11	4.96	10.0	10.4	10.1	9.67	10.0	9.82	8.84	12.1	11.9
MnO	0.15	0.20	0.12	0.14	0.13	n.d.	n.d.	0.08	0.14	0.15	0.15	0.06	0.09	0.10	0.08	0.0	0.14
NiO	n.d.	0.07	n.d.	n.d.	n.d.	n.d.	n.d.	0.11	n.d.	n.d.	n.d.	0.21	0.17	0.19	0.21	n.d.	n.d.
MgO	34.0	27.2	36.0	35.6	35.4	37.3	37.3	35.4	31.7	30.8	30.6	32.3	32.0	32.0	32.8	31.0	31.0
CaO	0.18	2.15	0.20	0.20	0.20	0.17	0.13	0.39	0.17	0.14	0.18	0.13	0.13	0.14	0.63	0.15	0.25
Na_2O	0.02	0.39	n.d.	n.d.	n.d.	0.01	0.02	0.09	n.d.	n.d.	n.d.	n.d.	n.d.	n.d.	0.06	n.d.	n.d.
Total	100.1	99.2	99.6	99.8	99.5	100.3	101.0	99.9	99.2	98.7	98.2	100.0	100.1	99.8	100.1	100.3	99.6
Structural formulae O = 6																	
Si	1.946	1.890	1.999	1.961	1.987	1.972	1.971	1.989	1.982	2.009	2.020	1.999	1.990	1.997	1.976	1.979	1.978
Al^{IV}	0.054	0.110	0.001	0.039	0.013	0.006	0.015	0.011	0.011	0.000	0.000	0.001	0.010	0.003	0.024	0.021	0.022
Al^{VI}	0.008	0.167	0.021	0.043	0.036	0.000	0.000	0.019	0.021	0.022	0.016	0.013	0.018	0.017	0.010	0.003	0.002
Ti	0.001	0.001	—	—	—	—	—	0.002	—	—	—	0.001	0.001	0.001	0.001	—	—
Cr	0.001	0.004	0.004	0.008	0.006	—	—	0.001	0.001	0.001	0.001	0.001	0.001	0.001	0.001	—	—
Fe	0.238	0.262	0.118	0.120	0.122	0.141	0.145	0.142	0.296	0.309	0.302	0.283	0.294	0.288	0.258	0.353	0.353
Mn	0.004	0.006	0.004	0.004	0.004	—	—	0.002	0.004	0.005	0.005	0.002	0.003	0.003	0.002	0.004	0.004
Ni	—	0.002	—	—	—	—	—	0.003	—	—	—	0.006	0.005	0.005	0.006	—	—
Mg	1.763	1.432	1.834	1.813	1.810	1.899	1.886	1.807	1.666	1.628	1.622	1.683	1.670	1.673	1.703	1.639	1.641
Ca	0.007	0.081	0.007	0.007	0.007	0.006	0.005	0.014	0.006	0.005	0.007	0.005	0.005	0.005	0.024	0.010	0.010
Na	0.001	0.027	—	—	—	0.001	0.001	0.006	—	—	—	—	—	—	0.004	—	—
Total	4.023	3.982	3.988	3.994	3.985	4.025	4.023	3.997	3.995	3.980	3.972	3.993	3.995	3.992	4.008	4.009	4.010

*All Fe as FeO; analytically determined FeO contents in mineral separates are U19: 8.61 wt%, U47: 4.41 wt%, A44: 8.42 wt%.

Table 4 Analyses of

	KR 1 Not zoned	KR 2A–1 Cores	KR 2A–2 Rims	KR 2B–1 Cores	2B–2 Rims	KR 3–1 Cores	KR 3–2 Rims	KR 4–1 Cores	KR 4–2 Rims	KR 6 Not zoned	U 206 No zoning	U 243 No zoning	U 19–1 No zoning
SiO_2	54.9	55.3	55.1	53.9	54.0	54.7	53.7	54.3	54.2	54.1	54.4	53.8	54.5
TiO_2	n.d.	n.d.	n.d.	0.03	0.03	n.d.	n.d.	n.d.	n.d.	0.13	0.04	n.d.	0.08
Al_2O_3	1.11	1.91	2.25	1.48	1.49	3.96	4.18	5.41	5.82	2.45	1.83	1.78	2.99
Cr_2O_3	n.d.	n.d.	n.d.	0.15	n.d.	n.d.	0.24	n.d.	0.28	n.d.	n.d.	n.d.	n.d.
FeO*	5.01	4.65	4.06	5.56	4.18	5.63	5.78	4.51	4.59	4.09	4.20	4.16	3.88
MnO	0.11	n.d.	n.d.	0.03	0.08	0.10	0.12	0.07	0.08	0.04	0.05	n.d.	0.08
MgO	16.3	14.9	15.3	14.3	15.4	13.7	13.9	12.6	12.6	15.1	16.01	15.9	15.2
CaO	22.8	22.1	22.3	21.8	22.7	18.6	19.1	19.2	19.1	21.6	23.1	22.6	21.1
Na_2O	1.10	1.54	1.55	1.78	1.30	2.86	2.37	3.37	3.15	1.88	1.10	1.15	2.20
Total	101.3	100.5	100.5	99.1	99.3	99.5	99.2	99.5	99.6	99.7	100.7	99.5	100.4
					Structural formulae O = 6								
Si	1.987	2.007	1.995	1.998	1.988	1.999	1.975	1.979	1.971	1.979	1.974	1.976	1.975
Al^{IV}	0.013	0.000	0.005	0.002	0.012	0.001	0.025	0.021	0.029	0.021	0.026	0.024	0.025
Al^{IV}	0.034	0.082	0.091	0.063	0.053	0.170	0.156	0.211	0.221	0.085	0.052	0.053	0.103
Ti	—	—	—	0.001	0.001	—	—	—	—	0.004	0.001	—	0.002
Cr	—	—	—	0.007	0.004	—	—	—	—	0.008	—	—	0.011
Fe	0.152	0.141	0.123	0.172	0.129	0.172	0.178	0.138	0.140	0.125	0.128	0.128	0.118
Mn	0.003	—	—	0.001	0.002	0.003	0.004	0.002	0.002	0.001	0.002	—	0.002
Mg	0.879	0.807	0.824	0.790	0.845	0.744	0.759	0.683	0.686	0.823	0.867	0.872	0.821
Ca	0.883	0.860	0.864	0.866	0.896	0.726	0.754	0.751	0.746	0.847	0.897	0.891	0.821
Na	0.077	0.108	0.109	0.128	0.093	0.203	0.169	0.238	0.222	0.133	0.077	0.082	0.155
Total	4.028	4.006	4.012	4.028	4.023	4.017	4.019	4.024	4.016	4.026	4.024	4.026	4.032

*All Fe as FeO; analytically determined FeO contents in mineral separates are U19: 2.71 wt%, U47: 1.49 wt%, A44: 2.10 wt%.

phases in many of the analysed samples have shown significant within-grain compositional variations. As the zoning is important to interpretations of the metamorphic evolution of these rocks, averages for both grain core and rim analyses are given in these instances (Tables 3–7).

Orthopyroxene compositional variability

Al_2O_3 contents of orthopyroxenes are crucial to the calculation of equilibration pressures for these rocks but often vary significantly within single grains. Our observations indicate that the Al_2O_3 content of the orthopyroxene is typically highest adjacent (20–50 μm distance) to garnet grains and appreciably lower in the cores of grains and adjacent to clinopyroxenes. Secondary amphibolitization in some of the orthopyroxene eclogites results in a notable decrease in the Al_2O_3 contents of both orthopyroxenes and clinopyroxenes. Inclusions of pyroxenes within garnets, which are shielded from the effects of secondary amphibolitization, typically have higher Al_2O_3 contents than matrix pyroxene grains. In Table 3 several different orthopyroxene analyses are given for most samples. In most instances we have elected to give analyses with both maximum and minimum Al_2O_3 contents in addition to an 'average' analysis, that is probably not very meaningful.

Lappin and Smith (1978) reported very low values for Al_2O_3 (0.24–0.65 wt. per cent) in orthopyroxenes from a number of orthopyroxene eclogite lenses directly enclosed in gneisses. However, our Al_2O_3 determinations have indicated a much wider range (0.28–2.58 wt. per cent) for the orthopyroxenes of such bodies. It is of particular interest to compare our various analyses for orthopyroxenes in samples from the Grytingvåg locality with the microprobe determination of 0.39 wt. per cent Al_2O_3 given by Lappin and Smith (1978). This latter value lies within our microprobe-determined ranges of 0.38–0.78 wt. per cent (sample KR5—analyst: Krogh, Oslo microprobe) and 0.35–0.68 wt. per cent (sample A44—analyst: Carswell, Sheffield microprobe). However, it is clearly more in line with the values that we have measured in orthopyroxene grain cores (or rims adjacent to clinopyroxene or amphibole) than with the higher values of 0.78 wt. per cent (Krogh) and 0.68 wt. per cent (Carswell) for orthopyroxene rims adjacent to garnets. Likewise in other orthopyroxene eclogites the values for Al_2O_3 in orthopyroxenes given by Lappin and Smith (1978) are much more comparable to our determinations for grain cores than for rims adjacent to garnets. Our microprobe studies thus suggest that equilibrium between orthopyroxene, garnet, and clinopyroxene has been attained over very short dis-

primary clinopyroxenes

	U 19–2 Min. sep.	U 95 No zoning	U 47–1 Aver. clasts	U 47–2 Aver. recryst.	U 47–3 Min. sep.	KR 5–1 Cores	KR 5–2 Rims ADJ gnt	A 44–1 Cores	A 44–2 Rims	A 44–3 Min. sep.	A 45–1 Cores	A 45–2 Rims	U80/19 Not zoned
SiO_2	54.2	55.1	54.9	54.8	54.7	55.1	55.1	55.3	55.4	54.7	55.2	55.1	54.0
TiO_2	0.20	n.d.	n.d.	n.d.	0.26	n.d.	n.d.	0.34	0.03	0.12	0.02	0.04	0.17
Al_2O_3	3.22	4.04	3.29	3.10	3.76	3.34	2.94	2.96	2.50	2.72	1.82	2.22	1.43
Cr_2O_3	0.33	1.67	n.d.	n.d.	0.37	0.19	0.20	0.26	0.18	0.18	0.11	0.10	n.d.
FeO*	3.67	1.12	2.06	1.93	2.49	3.39	3.50	3.07	3.32	2.76	2.16	2.24	3.65
MnO	0.08	0.10	n.d.	n.d.	0.05	0.11	0.08	0.03	0.03	0.04	0.01	0.00	0.10
MgO	15.3	15.2	16.2	15.9	16.1	14.8	15.5	14.9	15.2	16.7	16.0	15.7	16.3
CaO	20.0	20.8	21.6	21.4	19.9	21.1	21.4	20.9	21.2	20.2	22.6	22.3	22.7
Na_2O	2.54	2.45	2.30	2.33	2.37	1.97	1.80	2.06	1.86	2.13	1.31	1.36	1.20
Total	99.7	100.5	100.3	99.5	100.0	100.0	100.5	99.8	99.7	99.6	99.4	99.1	99.6
						Structural formulae O = 6							
Si	1.976	1.973	1.975	1.986	1.970	1.993	1.987	2.000	2.008	1.981	2.008	2.006	1.979
Al^{IV}	0.024	0.027	0.025	0.014	0.030	0.007	0.013	0.000	0.000	0.019	0.000	0.000	0.021
Al^{VI}	0.114	0.143	0.115	0.118	0.130	0.136	0.112	0.126	0.107	0.097	0.078	0.095	0.041
Ti	0.005	—	—	—	0.007	—	—	0.009	0.001	0.003	0.001	0.001	0.005
Cr	0.010	0.047	—	—	0.010	0.005	0.006	0.007	0.005	0.005	0.003	0.003	—
Fe	0.112	0.034	0.062	0.058	0.075	0.103	0.106	0.093	0.101	0.084	0.066	0.068	0.112
Mn	0.002	0.003	—	—	0.002	0.003	0.002	0.001	0.001	0.001	0.000	0.000	0.003
Mg	0.830	0.810	0.868	0.857	0.865	0.797	0.834	0.803	0.821	0.904	0.866	0.851	0.890
Ca	0.780	0.796	0.831	0.832	0.766	0.819	0.825	0.810	0.823	0.783	0.882	0.872	0.891
Na	0.180	0.170	0.160	0.164	0.165	0.138	0.126	0.144	0.131	0.150	0.092	0.096	0.085
Total	4.034	4.003	4.035	4.030	4.020	4.002	4.011	3.992	3.998	4.026	3.997	3.992	4.028

*All Fe as FeO; analytically determined FeO contents in mineral separates are U19: 2.71 wt%, U47: 1.49 wt%, A44: 2.10 wt%.

tances at best. This being the case, it is clearly important to calculate P–T values, based on element distribution considerations, on analyses of adjacent grain rims rather than the grain cores.

Al_2O_3 contents determined in orthopyroxene bulk mineral separates are invariably higher (as are the CaO contents) than in microprobe determinations for the same sample. Values determined for example on an orthopyroxene mineral separate from the Grytingvåg eclogite are 0.82 wt. per cent Al_2O_3 and 0.63 wt. per cent CaO, which compare closely with the values of 0.90 wt. per cent Al_2O_3 and 0.55 wt. per cent CaO independently determined by Green (1969). These significantly higher values undoubtedly reflect minor contamination by both garnet and clinopyroxene. Certainly this is the case in the orthopyroxene of sample U19. The contents of 6.66 wt. per cent Al_2O_3 and 2.15 wt. per cent CaO in the orthopyroxene separate reflect the presence of abundant small inclusions of both garnet and clinopyroxene, which prohibit preparation of a pure orthopyroxene separate.

Sample U47 is the only one with a notably porphyroclastic texture. Al_2O_3 contents are low in both the large strained porphyroclasts (0.15 wt. per cent) and the much smaller recrystallized grains (0.38 wt. per cent), but none the less significantly higher in the latter.

Clinopyroxene compositions (Table 4)

Unlike the orthopyroxenes these show little in the way of significant within-grain compositional variation of Al_2O_3 content. There is no consistent variation in the Na_2O content between grain cores and rims, so that Jd contents are fairly uniform. Similarly there is a little significant difference between the analyses of the large clinopyroxene porphyroclasts and smaller recrystallized grains in sample U47.

Garnets and $K_{D_{Fe-Mg}}^{Gnt-Cpx}$ values

The metamorphic evolution of eclogite facies assemblages is often conveniently monitored by changes in Fe^{2+}–Mg^{2+} partitioning between the coexisting garnets and clinopyroxenes—usually expressed by $K_D = (Fe^{2+}/Mg^{2+}$ garnet$)/(Fe^{2+}/Mg^{2+}$ clinopyroxene). K_D values are strongly temperature dependent (Banno 1970) but are also influenced by pressure and compositional factors, notably the Ca content of the garnet (Råheim and Green 1974; Ellis and Green 1979). The appreciable compositional zonation observed in eclogite minerals from the Nordfjord and Sunnfjord regions (Bryhni and Griffin 1971; Bryhni *et al.* 1977 Krogh 1977a, 1980a, 1982) provides a convincing record of the prograde metamorphic history suffered by these

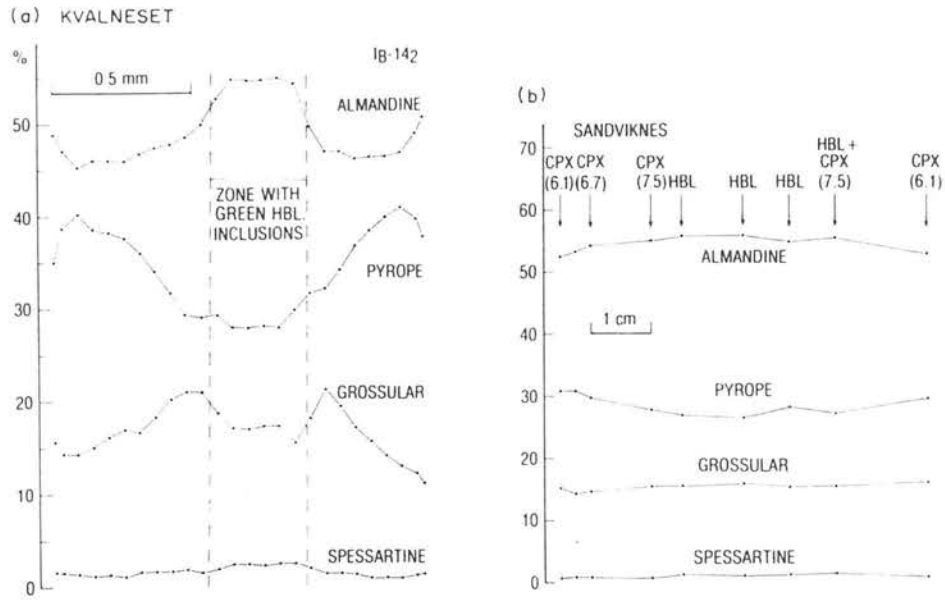

Fig. 1 Zoning profiles across garnet grains in two orthopyroxene bearing eclogite bodies. (a). Kvalneset, orthopyroxene eclogite, sample KR2A (IB–14$_2$). (b) Sandviknes, quartz eclogite, sample V80/33. Note radial variation in inclusions and K_D

rocks. This evolution is further documented by the existence of amphibolite facies inclusion suites in the cores of many eclogite garnets (Bryhni *et al.* 1977; Krogh 1982).

The compositional zonation of the garnets in the orthopyroxene eclogites is not usually so pronounced (Table 5). The most extreme prograde zonation that we have observed occurs in sample KR2A from Kvalneset (Fig. 1) in which the Fe/Mg of the garnet (with all Fe taken as Fe^{2+}) decreases from 1.81 (cores) to 1.08 (rims). Comparison with the coexisting clinopyroxene suggests that the zoning represents a decrease in K_D from 10.3 to 7.3 as the garnets grew. A less extreme example, from the Sandviknes body described by Lappin and Smith (1978), is shown in Fig. 1B. More typically, any sig-

Table 5 Analyses of

	KR 1 Not zoned	KR 2A–1 Cores	KR 2A–2 Rims	KR 2B–1 Cores	KR 2B–2 Rims	KR 3–1 Cores	KR 3–2 Rims	KR 4–1 Cores	KR 4–2 Rims	KR 6 Not zoned	U 206 No zoning	U 243 No zoning	U 19–1 No zoning
SiO_2	39.7	38.8	39.4	38.1	39.6	40.0	39.6	40.2	40.1	40.2	39.9	39.5	40.8
TiO_2	n.d.	n.d.	n.d.	0.17	0.09	n.d.	n.d.	n.d.	n.d.	0.08	0.02	n.d.	0.04
Al_2O_3	23.3	22.4	22.9	22.3	22.4	23.2	23.0	22.8	22.9	23.1	21.8	22.0	22.8
Cr_2O_3	n.d.	n.d.	n.d.	0.30	0.19	n.d.	n.d.	n.d.	n.d.	0.21	n.d.	n.d.	0.46
FeO*	20.5	25.6	22.0	25.5	21.8	18.3	19.9	17.4	19.0	19.0	18.5	18.1	13.3
MnO	0.58	n.d.	n.d.	1.17	0.75	1.39	1.32	0.65	0.84	0.68	0.82	n.d.	0.79
MgO	12.0	7.96	11.4	7.27	10.9	13.3	11.9	14.1	12.5	13.9	13.1	13.2	17.5
CaO	5.22	5.07	4.30	6.17	5.43	3.67	3.90	4.32	4.43	3.98	5.66	5.63	4.22
Total	101.2	99.8	100.0	100.9	101.2	99.8	99.6	99.5	99.8	101.2	99.9	98.5	99.9
					Structural formulae O = 12								
Si	2.947	2.987	2.966	2.930	2.968	2.975	2.981	2.984	2.993	2.959	2.988	2.982	2.970
Al^{IV}	0.053	0.013	0.034	0.070	0.032	0.025	0.019	0.016	0.007	0.04	0.012	0.018	0.030
Al^{VI}	1.983	2.019	2.002	1.952	1.947	2.013	2.016	1.985	2.011	1.962	1.915	1.946	1.925
Ti	—	—	—	0.010	0.005	—	—	—	—	0.004	0.001	—	0.002
Cr	—	—	—	0.018	0.011	—	—	—	—	0.012	—	—	0.026
Fe	1.273	1.648	1.384	1.640	1.366	1.139	1.252	1.081	1.185	1.169	1.160	1.146	0.812
Mn	0.036	—	—	0.076	0.048	0.088	0.084	0.041	0.053	0.042	0.052	—	0.049
Mg	1.325	0.913	1.283	0.833	1.218	1.474	1.335	1.564	1.396	1.52	1.465	1.486	1.894
Ca	0.416	0.418	0.347	0.510	0.436	0.293	0.314	0.344	0.354	0.314	0.454	0.456	0.329
Total	8.035	7.997	8.016	8.039	8.031	8.006	8.002	8.015	7.998	8.02	8.048	8.036	8.038

*All Fe as FeO; analytically determined FeO contents in mineral separates are: U19: 11.99 wt%, U47: 8.17 wt%, A44: 13.15 wt%.

nificant zoning is of a retrograde nature and is confined to narrow zones at the grain rims. Retrograde zoning also appears to be the norm in the orthopyroxene eclogites enclosed within the peridotite bodies (see Medaris 1980).

'Primary' amphiboles and micas

The primary or secondary status of the amphiboles and micas in these eclogites is often enigmatic from textural evidence alone. Some grains of these minerals are in apparent textural equilibrium with the primary anhydrous eclogite facies phases (garnets and pyroxenes) or occur as inclusions within these minerals. Other grains (even in the same rock) show obvious replacement relationships. While the latter are undoubtedly secondary, in the sense that they post-date and replace the primary eclogite facies mineral assemblages the former would appear to be primary. This is especially obvious in the case of hornblende inclusions in the cores of garnets, which apparently are relicts of pre-eclogite amphibolite assemblages (Krogh 1982). However, Lappin and Smith (1978) considered them to have developed later than the primary anhydrous eclogite facies assemblage and referred to such hydrous phases as 'early' rather than primary.

Like Lappin and Smith (1978) we have found it impossible to distinguish on chemical grounds between the 'primary' (or 'early') amphiboles in these rocks and the undoubted secondary replacement amphiboles (Table 6), as both show wide compositional ranges, especially in their Al_2O_3 and Na_2O contents. It seems reasonable to expect that different generations of amphibole may have similar compositions if they formed under similar P–T conditions on either the prograde or retrograde metamorphic paths (Krogh 1982). However, amphiboles replacing garnet clearly have higher Al_2O_3 contents than those replacing pyroxenes.

The pale brown micas in these rocks all appear to be Ti-rich phlogopites, regardless of their textural relationships. Primary phengitic micas were not found in these particular rocks and appear to be restricted to more aluminous eclogites (Krogh and Råheim 1978; Lappin and Smith 1978; Krogh 1980a).

Secondary pyroxenes (Table 7)

Breakdown of the primary garnet–clinopyroxene assemblage in the Hjørungavåg orthopyroxene eclogite, according to reactions (a) and (b) listed in Table I, results in the development of a secondary labradoritic plagioclase (An_{50-63}). The secondary orthopyroxene has a higher Fe/(Fe+Mg) ratio and an Al_2O_3 content similar to the minimum value recorded in the primary orthopyroxene grains. Breakdown of the garnet + quartz assemblage according to reaction (d) in both the Hjørungavåg

primary garnets

	U 19–2 Min. sep.	U 95 No zoning	U 47–1 No zoning	U 47–2 Min. sep.	KR 5–1 Cores	KR 5–2 Rims ADJ opx	A 44–1 Cores	A 44–2 Rims	A 44–3 Min. sep.	A 45–1 Cores	A 45–2 Rims	V80/19 1 Cores	V80/19 2 Rims
SiO_2	41.2	42.2	41.9	41.6	40.3	40.9	40.8	40.4	40.9	41.7	41.5	40.3	40.4
TiO_2	0.10	n.d.	n.d.	0.14	n.d.	n.d.	n.d.	0.02	0.16	0.02	0.02	n.d.	n.d.
Al_2O_3	23.3	22.7	23.3	23.2	22.5	22.5	22.5	22.5	22.4	23.1	23.1	22.9	22.7
Cr_2O_3	0.28	1.85	n.d.	0.37	0.25	0.27	0.23	0.38	0.24	0.09	0.12	n.d.	n.d.
FeO*	12.0	7.73	9.75	10.0	18.3	16.5	16.9	16.3	15.1	13.9	14.3	17.8	18.0
MnO	0.50	0.35	n.d.	0.41	0.61	0.57	0.41	0.38	0.37	0.28	0.30	0.37	0.55
MgO	17.5	21.2	20.4	20.1	14.7	15.6	15.0	15.4	16.0	17.1	16.9	14.4	14.2
CaO	4.02	4.37	3.85	3.79	4.28	4.23	4.19	4.23	4.46	4.15	4.37	4.66	4.73
Total	100.1	100.4	99.5	99.5	100.9	100.5	100.1	99.7	99.6	100.4	100.6	100.4	100.6
					Structural formulae O = 12								
Si	2.985	2.983	2.989	2.978	2.969	2.993	3.002	2.982	3.001	3.012	3.000	2.972	2.980
Al^{IV}	0.015	0.017	0.011	0.022	0.031	0.007	0.000	0.018	0.000	0.000	0.000	0.028	0.020
Al^{VI}	1.972	1.876	1.951	1.935	1.922	1.936	1.955	1.940	1.941	1.964	1.964	1.962	1.953
Ti	0.005	—	—	0.008	—	—	—	0.001	0.009	0.001	0.00	—	—
Cr	0.016	0.103	—	0.021	0.014	0.016	0.013	0.022	0.014	0.005	0.007	—	—
Fe	0.791	0.457	0.582	0.601	1.127	1.010	1.042	1.008	0.925	0.840	0.862	1.098	1.110
Mn	0.031	0.021	—	0.024	0.038	0.035	0.026	0.024	0.023	0.017	0.018	0.023	0.034
Mg	1.882	2.232	2.202	2.146	1.609	1.699	1.646	1.698	1.748	1.842	1.823	1.583	1.561
Ca	0.312	0.331	0.294	0.291	0.338	0.332	0.330	0.334	0.351	0.231	0.338	0.368	0.374
Total	8.008	8.020	8.030	8.026	8.048	8.028	8.014	8.027	8.013	8.002	8.013	8.033	8.033

*All Fe as FeO; analytically determined FeO contents in mineral separates are: U19: 11.99 wt%, U47: 8.17 wt%, A44: 13.15 wt%.

Table 6 Partial analyses of amphiboles and micas

	Amphiboles															Micas		
	KR 1–1 Prim.	KR 1–2 Sec.	KR 2A Inc. in gnt	KR 2B–1 Inc. in gnt	KR 2B–2 Prim.	KR 3 Prim.	KR 4 Inc. in gnt	KR 6 Prim.	U 206 Sec.	U 243 Inc. in gnt	U 19–1 Inc. in gnt	U 19–2 Sec.	U 95–1 Sec. ADJ pyrox.	U 95–2 Sec. ADJ gnt	A 44 Sec.	V80/19 Prim.	U 206 Prim?	U 19 Prim.	A 45 Prim.
SiO_2	48.5	53.7	40.8	49.8	56.5	53.4	51.2	55.5	48.2	47.6	54.0	52.5	47.6	43.4	55.0	51.8	38.4	40.2	41.4
TiO_2	n.d.	n.d.	n.d.	0.24	0.07	n.d.	n.d.	0.03	0.42	n.d.	0.09	0.11	n.d.	n.d.	0.09	0.14	1.24	1.42	1.11
Al_2O_3	9.70	6.41	18.2	8.12	1.51	4.43	8.79	2.97	10.2	10.1	3.53	5.96	12.8	18.6	3.58	5.67	17.1	14.0	14.6
Cr_2O_3	n.d.	n.d.	n.d.	n.d.	n.d.	n.d.	n.d.	0.08	n.d.	n.d.	0.17	0.22	2.02	1.52	0.08	n.d.	n.d.	0.30	0.08
FeO*	8.58	11.4	12.8	7.89	5.70	7.86	5.26	4.88	6.14	5.46	4.11	4.49	1.73	2.07	3.96	5.42	8.16	4.69	3.84
MnO	0.09	0.10	n.d.	0.17	0.09	0.18	0.08	0.12	0.02	n.d.	0.10	0.13	0.09	0.12	0.02	0.05	n.d.	n.d.	0.02
NiO	n.d.	n.d.	n.d.	n.d.	n.d.	n.d.	n.d.	n.d.	n.d.	n.d.	n.d.	n.d.	n.d.	n.d.	0.23	n.d.	n.d.	n.d.	n.d.
MgO	17.7	13.2	12.1	18.0	21.6	19.9	19.5	21.6	18.1	18.2	22.7	21.4	18.6	17.2	21.14	20.7	19.5	24.0	22.4
CaO	11.9	12.2	10.5	11.8	11.4	11.7	9.72	11.4	11.7	11.5	11.0	11.1	11.6	10.8	10.92	11.7	0.03	0.04	n.d.
Na_2O	0.84	0.46	3.13	1.85	0.72	1.14	2.22	1.16	1.52	1.85	1.03	1.44	2.65	3.04	1.19	1.19	1.59	0.32	0.24
K_2O	n.d.	n.d.	n.d.	0.17	0.13	n.d.	n.d.	0.18	n.d.	n.d.	0.58	0.44	n.d.	n.d.	n.d.	0.12	9.28	9.32	9.43
Total	97.4	97.4	97.6	98.0	97.7	98.6	96.8	97.9	96.3	94.7	97.3	97.8	99.2	96.8	96.2	96.8	95.4	94.3	93.1

*All Fe as FeO.

Table 7 Analyses of phases in reaction coronas

Sample	KR	KR	KR	KR	KR	KR	KR	KR	KR
No.	3	3	3	3	3	3	3	3	4
Phase	cpx II	opx II	cpx II	amph IIA	amph IIB	amph IIA	amph IIB	opx II	opx II
Reaction type (see text)	(a)	(a)	(b)	(b)	(b)	(c)	(c)	(d)	(d)
SiO_2	55.1	54.9	52.7	51.0	44.7	53.2	45.5	55.3	55.6
TiO_2	n.d.	n.d.	n.d.	n.d.	n.d.	n.d.	n.d.	n.d.	n.d.
Al_2O_3	2.47	0.79	3.89	7.58	13.2	6.20	14.4	0.69	0.75
FeO	7.37	16.8	7.40	7.75	9.03	6.52	8.30	18.4	14.6
MnO	0.16	0.29	0.14	0.17	0.17	0.14	0.15	0.44	0.20
MgO	14.6	26.5	16.2	18.7	17.0	20.0	16.7	25.3	28.3
CaO	19.2	0.36	18.4	11.0	11.3	10.4	10.6	0.10	0.20
Na_2O	0.94	n.d.	0.85	1.34	2.25	1.27	2.52	n.d.	0.20
Total	99.8	99.7	99.6	97.5	97.6	97.7	98.2	100.2	99.6

and Kvalvåg samples gives secondary orthopyroxenes of similar composition coexisting with oligoclase (An_{23-29}).

Pressure–Temperature Estimates

A number of experimentally calibrated mineralogical geothermometers/barometers based on element partition relationships are now available; together they allow calculation of absolute P–T estimates for the equilibration of garnet + orthopyroxene + clinopyroxene assemblages. Extensive discussions of these methods exist in the literature (Carswell 1980; Carswell and Gibb 1980a, b; Carswell and Griffin 1981) mainly in connection with their application to garnet lherzolite assemblages. From these considerations it appears that either the Wells (1977) 'best fit' calibration of the two-pyroxene solvus geothermometer or the Ellis and Green (1979) calibration of the $K_{D_{Fe-Mg}}^{Gnt-Cpx}$ geothermometer, used in conjunction with the garnet–orthopyroxene geobarometer of Wood (1974), can be expected to yield the most reliable P–T estimates for orthopyroxene eclogite assemblages. There are nevertheless problems with the application of both geothermometers to these particular rocks. The two-pyroxene solvus geothermometer is relatively insensitive below about 1000°C and use of the $K_{D_{Fe-Mg}}^{Gnt-Cpx}$ geothermometer is hampered by lack of knowledge of the $Fe^{2+}/(Fe^{2+} + Fe^{3+})$ ratios in the minerals in the case of microprobe analyses. However, the two independent methods do at least provide a cross check on the temperature estimates.

Our calculated P–T estimates for the various orthopyroxene eclogite samples analysed by us or reported in the literature are given in Table 8. In the case of the Ellis and Green/Wood combination alternative P–T values are given, depending on whether (a) all Fe is taken as Fe^{2+} in both garnets and clinopyroxene, (b) Fe^{3+} calculated on a charge balance basis (Neumann 1976) is excluded from the K_D calculation, or (c) K_D calculation is based on Fe^{2+} values determined in mineral separates.

For the majority of samples there is reasonably good agreement between the P–T values given by the Wells/Wood and Ellis and Green/Wood combinations, especially when all Fe is taken as Fe^{2+} in the latter case (Table 8). However, in certain instances the Ellis and Green/Wood combination yields much higher P–T estimates. For these samples the correspondence with the Wells/Wood values is considerably improved if wet-chemical Fe^{2+} values are used in the K_D calculation. On the other hand the Ellis and Green/Wood values which exclude calculated Fe^{3+} contents from the K_D calculation are rather erratic. Calculation of the $Fe^{2+}/(Fe^{2+}+Fe^{3+})$ ratio in these magnesian garnets and clinopyroxenes is apparently too sensitive to analytical errors (notably in SiO_2) to yield consistently reliable results. The Wells/Wood values for mineral separates tend to be higher than those based on microprobe analyses of the same sample. Even very small amounts of contamination in pyroxene mineral separates (or the existence of exsolution lamellae) will result in erroneously high temperature estimates from the two-pyroxene solvus geothermometer.

The profound influence that intrasample variations in orthopyroxene composition have on the P–T estimates is also illustrated in Table 8. In the case of the Wells/Wood values only the P value is affected as this has been obtained after calculation of the T by the Wells (1977) geothermometer. However, with the Ellis and Green/Wood combination both the T and P values are affected, and decrease as the Al_2O_3 contents of the orthopyroxene increase, since these values were obtained by simultaneous solution of the two P–T dependent equations. In several of

Table 8 P–T estimates for Norwegian orthopyroxene eclogites

Locality	Sample no.	Features	Data ref.	T°C Wells	P Kbars Wood	all Fe as Fe^{2+} T°C Ellis & Green*	all Fe as Fe^{2+} P Kbars Wood	calc. Fe^{3+} excl. T°C Ellis & Green†	calc. Fe^{3+} excl. P Kbars Wood	analyz. Fe^{3+} excl. T°C Ellis & Green‡	analyz. Fe^{3+} excl. P Kbars Wood
					'External' opx eclogites						
Hornindal	KR 1	Unzoned minerals	1	770	21.0	740	19.1	545	8.0		
Hellesylt	KR 6	Max. Al opx against gnt	1	674	19.3	752	24.1	499	8.5		
		Min. Al opx in cores	1	674	26.1	781	33.6	515	15.2		
Kvalneset	KR 2A	Grain cores	1	739	31.5	600	21.8	567	19.3		
		Grain rims		726	23.8	653	19.2	570	14.2		
	KR 2B	Grain rims Max. Al opx	1	600	11.5	659	15.0	501	5.7		
		Grain cores Min. Al opx	1	529	13.7	649	21.8	511	12.4		
Hjørungavåg	KR 3	Min. Al opx Gnt & cpx cores	1	833	27.2	910	31.8	767	23.1		
		Max. Al opx Gnt & cpx rims	1	853	13.9	782	10.6	652	4.5		
		Aver. Al opx Gnt & cpx cores	1	834	22.4	888	25.3	750	17.6		
Kvalvåg	KR 4	Min. Al opx Gnt & cpx cores	1	566	10.2	910	30.2	657	15.8		
		Max. Al opx Gnt & cpx rims	1	711	8.4	786	11.9	652	5.6		
		Aver. Al opx Gnt & cpx cores	1	568	5.5	881	22.0	638	9.4		
Solholm	U 206	Unzoned minerals	1	713	17.7	759	20.3	564	9.1		
	U 243	Large opx	1	730	21.0	779	23.9	548	10.2		
		Opx inc. in gnt		730	16.4	761	18.0	538	5.9		
Skarshaugen	U 19	Min. Al opx	1	694	15.2	955	29.6	954	29.3	755	18.5
		Max. Al opx		696	10.6	928	22.2	482	0.2	736	12.5
		Aver. Al opx		695	13.2	943	26.4	488	2.5	747	15.8
		Min. separates		814	3.9	847	5.1		—	766	2.0
Grytingvåg	KR 5	Opx rims adj. gnt Gnt & cpx rims	1	808	26.4	780	24.7	689	19.1	674	18.1
		Grain cores		776	28.6	743	26.5	777	28.4	688	22.5
	A 44	Grain cores		799	35.3	759	32.6	775	33.6	707	28.6
		Opx rims adj. gnt Gnt & cpx rims	1	803	27.9	777	26.3	810	28.2	684	20.3
		Min. separates		882	30.5	717	20.6		—	678	18.1
	2539	Min. separates	2	735	10.6	737	20.7		—	652	15.6
	8G	Min. sep. analy. except Ca & Al in opx	3	880	39.0	807	34.1	759	30.4	714	27.6
Liseter	D 171	Aver. probe Anal.	3	774	27.2	835	31.0	721	24.0		
Sørpollen	C 411	Aver. probe Anal.	3	722	33.2	820	40.3	713	32.5		
Sandviknes	66/87/ 11	Aver. probe Anal.	3	685	22.2	961	40.2	612	17.4		
Ganges–Kardneset	127 M	Aver. probe Anal.	3	660	24.4	684	26.1	360	3.9		
Høydalsneset	V80/19	High Al opx Gnt rims	1	690	14.5	710	15.5	423	−0.4		
		Low Al opx Gnt cores	1	689	21.5	743	24.9	743	24.9		
					'Internal' opx eclogites						
Ugelvik	U 95	Min. Al opx	1	757	28.8	783	30.5	707	25.4		
		Max. Al opx		761	14.6	729	13.0	661	9.5		
		Aver. Al opx	4	760	20.0	749	19.4	678	15.3		
		Min. separates		904	35.8	735	25.2		—	759	26.6
	U 47	Opx & cpx clasts		605	31.4	966	60.1		—	896	54.5
		Opx & cpx recryst.	1	533	17.8	890	42.6		—	856	40.1
		Min. separates		881	32.8	936	36.2		—	803	28.1

Table 8 (*continued*)

Locality	Sample no.	Features	Data ref.	TC Wells	P Kbars Wood	all Fe as Fe^{2+} T°C Ellis & Green*	all Fe as Fe^{2+} P Kbars Wood	calc. Fe^{3+} excl. T°C Ellis & Green†	calc. Fe^{3+} excl. K Bars Wood	analyz. Fe^{3+} excl. T°C Ellis & Green‡	analyz. Fe^{3+} excl. P Kbars Wood
Sunndal	6912	Aver. probe anal.	5	722	23.9	714	23.4	—		640	18.5
Grubse	6095	Aver. probe anal.		752	21.1	731	19.8	—		657	15.2
Lien	1 J	Grain cores	6	623	20.2	801	31.8	—		797	31.3
		Grain rims		608	19.7	734	28.1	—		730	27.6
	N71	Min. separates	7	686	16.0	675	15.4	—		647	14.7

*All Fe taken as Fe^{2+} in K_D calculation
†Calculated Fe^{3+} excluded from K_D calculation
‡K_D calculation excludes Fe^{3+} indicated by analytical Fe^{2+} determination
Data references: 1—This paper
2—Green (1969)
3—Lappin and Smith (1978)
4—Carswell (1973)
5—Lappin (1974)
6—Medaris 1980
7—O'Hara and Mercy (1963)

our analysed samples orthopyroxenes have highest Al_2O_3 contents adjacent to garnets, and the lower P–T estimates yielded by such analyses (calculated in conjunction with garnet and clinopyroxene rim analyses) are probably the most appropriate to the garnet + orthopyroxene + clinopyroxene assemblages.

We have underlined in Table 8 those P–T values which we judge from the foregoing considerations to give the 'best' indication of the actual equilibration conditions for the primary eclogite facies assemblages in these rocks. For the orthopyroxene eclogites directly enclosed in the gneisses these values range from 674–853°C and 8.4–27.9 Kbars (mean values 743°C and 18.2 Kbars) with the Wells/Wood combination and from 653–786°C and 10.6–26.3 Kbars (mean values 737°C and 18.6 Kbars) with the Ellis and Green/Wood combination, assuming all Fe as Fe^{2+} in the K_D calculation.

Although the ranges for the different samples are considerable the mean values given by these different calculation procedures are remarkably close. This may be fortuitous, as taking all Fe as Fe^{2+} in K_D yields P–T estimates, using the Ellis and Green/Wood pair, which are effectively maxima for this particular method. We consider the somewhat lower values, ranging from 674–736°C and 12.5–20.3 Kbars (mean values 698°C and 17.0 Kbars) and which utilize K_D based on analytically determined Fe^{2+} values, to be more accurate. We suspect that the variation in P–T estimates between the different analysed orthopyroxene eclogite samples essentially reflects analytical errors, Fe^{2+}–Fe^{3+} uncertainties, or disequilibrium effects. These data cannot be used to demonstrate any regional P–T variation over the Sunnmøre–Romsdal–Nordmøre area even though such a gradient is apparent in data from other types of eclogites (Krogh 1977a,b; Griffin *et al.* this volume).

Our 'best' estimates for the equilibration conditions of the 'external' orthopyroxene eclogites (Table 8) are substantially lower than the equivalent estimates of 700–850°C and 30–45 Kbars given by Lappin and Smith (1978) for their 'Regime B'. The differences arise partly from the fact that they used the obsolete Wood and Banno (1973) calibration of the garnet–orthopyroxene geobarometer instead of the improved Wood (1974) calibration, and partly from the lower analytical values for Al_2O_3 in the orthopyroxenes given by Lappin and Smith (values which in our experience do not represent equilibrium with garnet.).

We have also calculated T values for garnet–phlogopite in the three samples containing apparently primary mica, using the data of Ferry and Spear (1978). Assuming P = 17 Kbars, these temperatures are: U206, 855°C; U19, 789°C; A45, 690°C. The value for A45 is within the range of other estimates, while the other two are considerably higher. Errors may well result from failure to take account of the influence of the significant TiO_2 contents in the micas on K_{Fe-Mg}^{Gnt-Bi}.

Olivine-free 'internal' orthopyroxene eclogites, enclosed within the west Norwegian peridotite bodies, are rare and P–T estimates for these, based on currently available data (Table 8), present a somewhat more confused picture (especially as sample U47 yields consistently high values). We have again underlined those P–T values that we judge to be the 'best' indication of the eclogite facies equilibration conditions. These P–T estimates range from 608–761°C and 13.0–28.1 Kbars for the different

methods, with overall mean 'best' values of 707°C and 20.4 Kbars.

When realistic allowances are made for errors in the various P–T estimates, we feel justified in concluding that the eclogite facies assemblages in both the 'internal' and 'external' orthopyroxene eclogites equilibrated in similar P–T regimes. Our preferred mean P–T estimates for the West Norwegian garnet lherzolite assemblages are likewise closely similar at 726°C and 20.3 Kbars, although again this disguises a substantial range of estimates (651–834°C and 11.3–31.8 Kbars) for individual samples. These estimates for the garnet lherzolite assemblages are slightly lower than those given recently by Carswell and Gibb (1980a). This is the result of incorporation of additional data, provided by the new experimental calibrations for $K_{D\text{Fe-Mg}}^{\text{Gnt-Cpx}}$ and for $K_{D\text{Fe-Mg}}^{\text{Gnt-Ol}}$ (Ellis and Green 1979); O'Neill and Wood 1979, 1980), and the use of analytically determined $Fe^{2+}/(Fe^{2+}+Fe^{3+})$ ratios in the calculations.

Discussion

Prograde metamorphism of external eclogites

There is abundant evidence that many of the 'external' or Type B eclogites of the Western Gneiss Region have formed through prograde metamorphism of crustal rocks (see summaries by Bryhni *et al.* 1977; Griffin *et al.* this volume). The evidence includes (1) observation of partial to complete eclogitization in rocks of demonstrably low-P origin (sediments, anorthosites, gabbros, dolerites); (2) preservation of relict amphibolite facies mineral assemblages in the garnet grains of many eclogites; (3) marked prograde zoning in eclogite minerals; and (4) a regional gradient in the maximum T calculated from $K_{D\text{Fe-Mg}}^{\text{Gnt-Cpx}}$, reflecting increasing grade of metamorphism toward the W and NW. Maximum P–T conditions are estimated at 750–800°C, 16–18 Kbars (Krogh 1977; Griffin *et al.* this volume; this paper).

In the high-grade part of this regional gradient, homogenization appears to have occurred in both garnets and clinopyroxenes. Prograde zoning is generally found only in coarse-grained rocks, while many samples show some retrograde zoning near grain contacts. Most of the external orthopyroxene eclogites in this study are from this high-grade area, and show only minor retrograde zoning. However, some evidence of prograde metamorphic evolution is found locally. As noted above (see Fig. 1), prograde zoning is obvious in the minerals of the Kvalneset orthopyroxene eclogite, suggesting an increase in T, and presumably of P, with time.

The 'Sandviksnes' orthopyroxene eclogite at Årheimneset on Stadlandet has been described by Lappin and Smith (1978), who considered it to be a mantle derived fragment. A restudy of this strongly layered body shows layers of coarse-grained (1 cm) clinopyroxene + garnet + quartz eclogite, in which the garnets show a clear prograde zoning (Fig. 1B). The cores contain abundant euhedral hornblende inclusions; the rims contain only omphacite inclusions (aver. $Jd_{25}Acm_7Ts_1$). $K_{D\text{Fe-Mg}}^{\text{Gnt-Cpx}}$ calculated for clinopyroxene inclusions and adjoining garnet declines from 7.5 to 6.1 across the outer rim. The lowest K_D implies a T of *ca.* 675° at an assumed P of 18 Kbar, and is thus compatible with the calculated T for the orthopyroxene eclogite in the same body (Table 7). The zoning, and the preservation of hornblende grains in the garnet cores (none is seen in the matrix) of this layer, strongly suggest that the orthopyroxene-bearing layers of this body also have had a crustal, prograde history.

Disequilibrium model

As noted above, most of the orthopyroxene eclogites, both internal and external, show a minor retrograde zoning (Fe/Mg of garnet increasing toward the rim, Fe/Mg of clinopyroxene decreasing), suggesting a partial adjustment to declining T. Many also show a marked zoning in Al_2O_3 content of the orthopyroxene, from low values in grain cores to high values near garnet. These two trends could be interpreted as reflecting *large* drops in P, together with modest drops in T (as, for example, in the 'internal' garnet pyroxenites studied by Medaris (1980)).

However, it is not necessary to postulate a variety of tectonic/metamorphic histories to reconcile these data with the (apparently conflicting) evidence for prograde metamorphism of other eclogites. There is abundant evidence that *disequilibrium* was common during the eclogite-forming event in western Norway; the existence of zoned minerals and relict inclusion assemblages is in itself such evidence. Partial reaction to eclogite (corona structures) is common in the basic rocks of the region (Griffin and Heier 1973). Several examples are known of gabbros in which apparently unmetamorphosed portions alternate with completely eclogitized zones, and in which the gabbro textures are pseudomorphed by garnet and omphacite (Mørk in prep.; Tørudbakken 1981; Cuthbert 1981).

We can suggest two ways in which disequilibrium during prograde metamorphism could produce the commonly observed zoning of orthopyroxene from low-Al cores to high-Al rims.

1. The orthopyroxene + clinopyroxene + garnet assemblage forms at relatively low T (and P),

where the orthopyroxene in equilibrium with garnet would have low Al. During a relatively rapid T increase, Al_{opx} equilibrates slowly compared to equilibration of Fe/Mg between clinopyroxene and garnet.

2. The orthopyroxene cores are relics from a lower-P, T assemblage, such as orthopyroxene + amphibole ± chlorite. Such rocks are seen in lower-grade parts of the area and as retrograde assemblages in the high-T part. With increasing metamorphic grade this assemblage would react to orthopyroxene + clinopyroxene + garnet, but the original low-Al orthopyroxenes might not equilibrate with the new assemblage, especially in coarse-grained rocks.

In either case, the use of the low-Al orthopyroxene core compositions to calculate P, after T has been calculated from the garnet–clinopyroxene pair, will lead to spurious P–T estimates (Fig. 2). In general, the use of the core compositions from zoned grains to calculate P–T must be regarded with suspicion, unless other evidence can show which of these compositions originally were in mutual equilibrium. In our view, the use of such data has misled Lappin and Smith (1978) to propose (erroneously) a very high-P origin for the orthopyroxene eclogites.

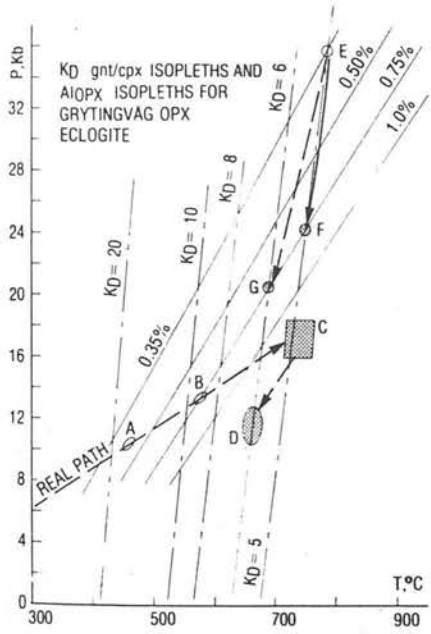

Fig. 2 K_D and Al_{opx} isopleths for Grytingvåg eclogite, calculated from relations of Ellis and Green (1979) and Wood (1974). Path A–B–C is a possible regional P–T development derived for the West Norwegian eclogites by Krogh (1977a). Assume that (1) low-Al cores of orthopyroxenes formed in equilibrium with amphibole + chlorite ± clinopyroxene at T < 600°C, (2) this assemblage reacted to opx + cpx + gnt at higher T, and (3) equilibration of Al between cpx and gnt lagged behind equilibration of Fe/Mg between cpx and gnt. When rock is at C, opx has Al_2O_3 content appropriate to, for example, B. Uplift is accompanied by minor retrograde readjustment of Fe/Mg to D. Calculated P/T conditions will be: E for cores of opx + cpx + gnt; F for rim opx + core cpx + core gnt; G for rims of all phases. E–F and E–G illustrate the types of spurious P–T paths that might be deduced from particular combinations of mineral composition data

Origin of orthopyroxene eclogites

Most orthopyroxene eclogites, unlike the Sandviknes and Kvalneset bodies discussed above, retain no structural or textural clues to the nature of the protolith. Many of the 'external' orthopyroxene eclogites may be high-pressure equivalents of the Mg(–Al–Si) rich rocks found in lower-P gneiss terranes as cordierite + anthophyllite assemblages. It is striking that *all* analysed external orthopyroxene eclogites, but only a few orthopyroxene-free ones, contain very high unsupported $^{87}Sr/^{86}Sr$ ratios (Brueckner 1977; Griffin and Brueckner 1980, in prep.), implying that they have at least undergone chemical exchange with the surrounding gneisses.

However, certain orthopyroxene eclogites contain pyroxenes apparently showing extensive exsolution, notably of garnet. Lappin (1973, 1974) and Lappin and Smith (1978) have 'reconstituted' some of these pyroxenes from modal and microprobe analyses. By assuming that these reconstituted phases coexisted with other pyroxenes, they have calculated very high temperatures (*ca.* 1000°C). By assuming coexistence of the reconstituted orthopyroxene with garnet at these temperatures, they have then calculated very high pressures (30–45 Kbars) which have been used as evidence for a mantle origin. Likewise Carswell (1973) argued for an upper mantle P–T regime for the crystallization of the primary aluminous orthopyroxene of the orthopyroxene eclogite (garnet pyroxenite) lens within the garnet peridotite body at Ugelvik, Otrøy. However, high primary crystallization pressures (35–40 Kbars) are only required on the assumption that some garnet coexisted with the original high temperature orthopyroxene, and the petrographic evidence for that is equivocal.

The exsolution textures described by Lappin and Smith (1978) in the Sandviknes orthopyroxene eclogite are difficult to reconcile with our described zoning and solid-inclusion evidence for a prograde metamorphism history in the associated layers of quartz eclogite. However, the petrographic features attributed by these authors to exsolution are somewhat enigmatic, and in the case of the amphibole lamellae may reflect parallel growth or replacement rather than exsolution. Evidence for garnet and pyroxene exsolution in the pyroxenites at Sunn-

dal–Grubse (Lappin 1973, 1974) and Ugelvik (Carswell 1973) is more convincing.

Accepting that exsolution textures in certain orthopyroxene eclogites imply a high temperature origin for the protoliths of those particular rocks, the following considerations indicate that very high (mantle) pressures may not be necessary.

1. Many anorthosites contain high-Al orthopyroxenes as primary magmatic phases, even though these cannot have formed at mantle depths. Morse (1975) concluded that the high Al content is controlled by kinetic factors rather than being a pressure effect. In the layered anorthosites of the Bergen Arcs, the primary low-pressure mineral assemblages of olivine + plagioclase + clinopyroxene ± orthopyroxene have been metamorphosed to granulite facies, then to eclogite facies conditions (Griffin 1972; Austrheim 1981). Pods of coarsely granular 'primary' orthopyroxene and clinopyroxene show intragrain and interstitial exsolution of garnet. The least-exsolved (not 'reconstituted') orthopyroxene bears a strong compositional resemblance to Lappin and Smith's (1978) 'reconstituted' orthopyroxene from an external eclogite pod (Table 9).

   The Fiskå anorthosite, north of Åheim in Sunnmøre, contains large (10–20 cm) primary orthopyroxene crystals bordered by clinopyroxene + garnet coronas and choked with garnet and clinopyroxene exsolution lamellae (Griffin and Mørk 1981). This pyroxene is again similar to those proposed by Lappin and Smith (1978) as protoliths for the orthopyroxene eclogites. Obviously extreme pressures are not necessary for the production of such pyroxenes, since the primary olivine + plagioclase assemblage of the Bergen anorthosites (Griffin 1972) limits crystallization of the anorthosites to $P < 8$–10 Kbars (Griffin and Heier 1973). Maquil (1978) has experimentally produced such pyroxenes in anorthosite compositions at 1000°C, 10 Kbars.
2. T. H. Green and Ringwood (1968) showed experimentally that subliquidus clinopyroxenes coexisting with garnet in tholeiitic melts contain up to 13.6 per cent Al_2O_3 at 18 Kbars, 1230–1300°C. Subsolidus clinopyroxenes coexisting with plagioclase, orthopyroxene, and amphibole at 920–1040°C and 9–10 Kbars contained 9.9–11.3 per cent Al_2O_3, while coexisting orthopyroxene contains 7.3–8.4 per cent Al_2O_3. Thompson (1974) has produced similar pyroxenes at liquidus to subliquidus T and intermediate P, from a range of basalts. Na and Al contents rise rapidly with falling T or rising P for each

Table 9 Exsolved pyroxenes in anorthosites—comparison with 'reconstituted' pyroxenes from opx eclogites

	Bergen–cpx POD 113 A				Bergen–opx POD 119 A			
	cpx	cpx by gnt	exs. gnt	gran. gnt	opx	exs. cpx	exs. gnt	gran. gnt
SiO_2	49.8	53.4	39.2	39.3	51.4	50.4	38.9	39.5
TiO_2	1.2	0.2	—	—	0.1	0.7	—	—
Al_2O_3	9.2	6.7	22.3	22.9	3.8	5.7	21.9	21.9
FeO^+	7.2	6.0	21.7	17.6	20.6	9.3	24.3	22.5
MnO	—	—	0.8	0.6	—	—	1.1	0.9
MgO	11.1	12.4	9.7	11.3	21.8	11.7	7.5	9.6
CaO	19.3	19.8	5.1	7.3	0.3	20.3	5.5	5.3
Na_2O	2.2	1.9	—	—	—	1.7	—	—
	100.0	100.4	98.8	99.0	98.0	99.8	99.2	99.7

	Fiskå–opx megacryst		'Reconstituted' eclogite pyroxenes		
	opx	exs. gnt	opx 68/88*	cpx 68/87*	6912†
SiO_2	53.1	39.2	51.83	55.20	52.3
TiO_2	0.16	0.0	0.02	0.07	0.0
Al_2O_3	3.00	22.5	3.58	4.50	4.2
FeO	16.3	21.0	17.45	10.17	7.80
MnO	0.18	0.97	0.17	0.06	0.1
MgO	27.0	10.7	25.38	14.93	16.3
CaO	0.18	5.86	0.72	12.04	17.0
Na_2O	0.0	0.0	0.07	3.44	1.18
	99.9	100.2	99.22	100.51	99.30

*Lappin and Smith (1978).
†Lappin (1974).

composition. Extrapolation of Thompson's data also suggests that at T = 1100–1200°C, P = 15–18 Kbars, many basalts will precipitate pyroxenes with high Na/Ca ratios and high Al contents.

3. Rost and Brenneis (1978) have described exsolution of garnet in the pyroxenes of spinel peridotites in the Ultenthal, and suggested that the associated garnet peridotites and garnet pyroxenites have evolved by crustal metamorphism of the Al-rich primary pyroxenes of the spinel lherzolites and pyroxenites.

We conclude that cumulates of various igneous pyroxenes, formed at moderate pressures, may well have been the protoliths for at least some orthopyroxene eclogites, both internal and external. These may stem from magmas intruded into the crust during the eclogite metamorphism. Alternatively, they may represent much older rocks, carried to depth and recrystallized during the eclogite forming event (*cf.* Griffin and Qvale this volume). Isotopic data on some external orthopyroxene eclogites (Griffin and Brueckner 1980) tend to support the latter interpretation. These older rocks may include both pyroxenites, related to the ultramafics and the anorthosites, and metasupracrustal rocks; further analytical data are obviously necessary.

Internal vs. external eclogites

Most discussions of the garnetiferous ultramafic rocks and associated internal 'eclogites' (± orthopyroxene) in the Western Gneiss Region have concluded that these rocks represent tectonic slices of the subcontinental mantle. This conclusion has been based on (a) the assumption (based on early experimental work) that the garnet–peridotite mineral assemblage is only stable at very high P, (b) high calculated P–T values, (c) a decompression history, derived both from observation of pyroxene + spinel symplectites around garnet (O'Hara and Mercy 1963; Carswell 1968), and from compositional zoning in constituent minerals (Medaris 1980).

We have shown here that careful evaluation of both the analytical data and of published barometers and thermometers points to substantially lower pressures of formation for all the orthopyroxene eclogites than previously indicated. We have also shown how the zoning profiles can be reconciled with a prograde, rather than retrograde, metamorphic history (Fig. 2). Recent experimental evidence (Jenkins and Newton 1979) demonstrates that a garnet–peridotite-like assemblage is stable to pressures as low as 13 Kbars at 800°C. Our work shows that, when appropriate error brackets are attached to the various calculated values, there is no resolvable difference in the average P and T of equilibration among the garnet peridotites, internal orthopyroxene eclogites, external orthopyroxene eclogites, and external orthopyroxene-free eclogites in the coastal parts of the Western Gneiss Region. Finally, the widespread high-pressure granulite facies relics within the gneisses of the region (Mysen and Heier 1972; Krogh 1980a,b; Griffin and Carswell this volume; Griffin and Mørk 1981; Griffin *et al.* this volume) suggest that the gneisses have had a metamorphic history similar to that of the eclogites. Krogh (1980a,b) has demonstrated this point in detail for two localities at extremes of the regional P–T gradient.

All the available data are therefore consistent with a unified model for the genesis of all the observed eclogite facies assemblages during a major, regional scale, high pressure metamorphic event. This may have resulted from transient subduction (Bryhni *et al.* 1977; Krogh 1977a; Cuthbert *et al.* 1983) of a large continental lithospheric slab during a major continent–continental collision event. Recent geochronological data suggest that this event was part of the Caledonian orogeny (Griffin and Brueckner 1980, in prep.; Griffin and Carswell this volume).

There are two possible origins for the garnetiferous ultramafic rocks and 'internal' eclogites in this geotectonic scenario: (a) tectonic introduction of mantle slices into the descending slab; (b) progressive metamorphism of older 'alpine-type' peridotites or serpentinites already lodged in the crust during earlier orogenic episodes (Griffin and Qvale this volume). In either case the data and arguments presented here imply final 'equilibration' of all the eclogite facies types under similar conditions. Further evidence of the metamorphic and tectonic history of the ultramafic association will have to come from studies of their field associations and geochemistry, especially isotopic geochemistry.

Acknowledgements

This research has been supported by grants from N.E.R.C. (grant GR3/3085), N.A.V.F. (grant D48–22.08) and Nansenfondet. The manuscript was considerably improved after a perceptive review by Simon Harley.

References

Austrheim, H. 1981. Bergen Arc. In Griffen, W. L. and Mørk, M. B. E. (Eds), *Excursion B1, Excurs. in Scand. Caledonides*, 74–82.

Banno, S. 1970. Classification of eclogites in terms of physical conditions of their origin. *Phys. Earth Planet. Inter.*, **3**, 405–421.

Brueckner, H. K. 1977. A crustal origin for eclogites and a mantle origin for garnet peridotites: Strontium isotopic evidence from clinopyroxenes. *Contr. Miner. Petrol.*, **60**, 1–15.

Bryhni, I. 1966. Reconnaissance studies of gneisses, ultrabasites, eclogites and anorthosites in outer Nordfjord, western Norway. *Norges geol. Unders.*, **241**, 1–68.

Bryhni, I., Fyfe, W. S., Green, D. H. and Heier, K. S. 1970. On the occurrence of eclogite in western Norway. *Contr. Miner. Petrol.*, **26**, 12–19.

Bryhni, I. and Griffin, W. L. 1971. Zoning in eclogite garnets from Nordfjord, West Norway. *Contr. Miner. Petrol.*, **32**, 112–125.

Bryhni, I., Krogh, E. J. and Griffin, W. L. 1977. Crustal derivation of Norwegian eclogites: a review. *N. Jb. Miner. Abh.*, **130**, 46–68.

Carswell, D. A. 1968. Possible primary upper mantle peridotite in Norwegian basal gneiss. *Lithos*, **1**, 322–355.

Carswell, D. A. 1973. Garnet pyroxenite lens within Uglevik layered garnet peridotite. *Earth Planet. Sci. Lett.*, **20**, 347–352.

Carswell, D. A. 1974. Comparative equilibration temperatures and pressures of garnet lherzolites in Norwegian gneisses and in kimberlite. *Lithos*, **7**, 113–121.

Carswell, D. A. 1980. Mantle derived lherzolite nodules associated with kimberlite, carbonatite and basalt magmatism: a review. Lithos, **13**, 121–138.

Carswell, D. A. 1982. Clarification of the petrology and occurrence of garnet lherzolites, garnet websterites and eclogites in the vicinity of Rødhaugen, Almklovdalen, west Norway. *Norsk geol. Tidsskr.*, **62**, 249–260.

Carswell, D. A. and Gibb, F. G. F. 1980a. The equilibration conditions and petrogenesis of European crustal garnet lherzolites. *Lithos*, **13**, 19–29.

Carswell, D. A. and Gibb, F. G. F. 1980b. Geothermometry of garnet lherzolite nodules with special reference to those from the kimberlites of Northern Lesotho. *Contr. Miner. Petrol.*, **74**, 403–416.

Carswell, D. A. and Griffin, W. L. 1981. Calculation of equilibration conditions for garnet granulite and garnet websterite nodules in African kimberlite pipes. *Tscher. Min. Petr. Mitt.*, **28**, 229–244.

Cuthbert, S. J. 1981. Gørlangen–Sørdal area. In Griffin, W. L. and Mørk, M. B. E. (Eds), *Excursion B1, Excurs. in Scand. Caledonides*, 70–73.

Cuthbert, S. J., Harvey, M. A. and Carswell, D. A. 1983. A tectonic model for the metamorphic evolution of the Basal Gneiss Complex, Western South Norway—a working hypothesis. *J. Metamorphic Geol.*, **1**, 63–90.

Ellis, D. J. and Green, D. H. 1979. An experimental study of the effect of Ca upon garnet–clinopyroxene Fe–Mg exchange equilibria. *Contr. Miner. Petrol.*, **71**, 13–22.

Eskola, P. 1921. On the eclogites of Norway. *Skr. Vidensk. Selsk. Christiania, Mat.-Naturv. Kl.*, **I**, 8, 1–118.

Ferry, J. M. and Spear, I. S. 1978. Experimental calibration of the partitioning of Fe and Mg between biotite and garnet. *Contr. Miner. Petrol.*, **66**, 113–117.

Green, D. H. 1969. On the mineralogy of two Norwegian eclogites. *Contr. to Physico-chemical Petrology*, **1**, 37–44.

Green, T. H. and Ringwood, A. E. 1968. Genesis for the calc-alkaline igneous rock suite. *Contr. Miner. Petrol.*, **18**, 105–162.

Griffin, W. L. 1972. Formation of eclogites and the coronas in anorthosite, Bergen Arcs, Norway, *Mem. Geol. Soc. Am.*, **135**, 37–63.

Griffin, W. L., Austrheim, H., Brastad, K., Bryhni, I., Krill, A. G., Krogh, E. J. Mørk, M.|B. E., Qvale, H. and Tørudbakken, B. this volume. High-Pressure metamorphism in the Scandinavian Caledonides.

Griffin, W. L. and Brueckner, H. K. 1980. Caledonian Sm–Nd ages and a crustal origin for Norwegian eclogites. *Nature*, London, **285**, 319–321.

Griffin, W. L. and Carswell, D. A. this volume. *In situ* metamorphism of Norwegian eclogites: an example. this volume.

Griffin, W. L. and Heier, K. S. 1973. Petrological implications of some corona structures. *Lithos*, **6**, 315–335.

Griffin, W. L. and Mørk, M. B. E. 1981. Eclogites and basal gneisses in western Norway. *Excursion B1, Excurs. in Scand. Caledonides*.

Griffin, W. L. and Råheim, A. 1973. Convergent metamorphism of eclogites and dolerites, Kristiansund area, Norway. *Lithos*, **6**, 21–40.

Griffin, W. L. and Qvale, H. this volume. Superferric eclogites and the crustal origin of garnet peridotites.

Howie, R. A. and Smith, J. V. 1966. X-ray emission microanalysis of rock-forming minerals. V. Orthopyroxenes. *J. Geol.*, **74**, 443–462.

Jenkins, D. M. and Newton, R. C. 1979. Experimental determination of the spinel peridotite to garnet peridotite inversion at 900°C and 1000°C in the system $CaO–MgO–Al_2O_3–SiO_2$, and at 900°C with natural olivine and garnet. *Contr. Miner. Petrol.*, **68**, 407–419.

Krogh, E. J. 1977a. Evidence for a Precambrian continent–continent collision in western Norway. *Nature*, London, **267**, 17–19.

Krogh, E. J. 1977b. Crustal and *in situ* origin of Norwegian eclogites. Reply. *Nature*, London, **269**, 730.

Krogh, E. J. 1980a. Geochemistry and petrology of glaucophane-bearing eclogites and associated rocks from Sunnfjord, western Norway. *Lithos*, **13**, 355–380.

Krogh, E. J. 1980b. Compatible P–T conditions for eclogites and surrounding gneisses in the Kristiansund area, western Norway. *Contr. Miner. Petrol.*, **75**, 387–393.

Krogh, E. J. 1982. Metamorphic evolution of Norwegian country rock eclogites, as deduced from mineral inclusions and compositional zoning in garnets. *Lithos*, **15**, 305–321.

Krogh, E. J. and Råheim, A. 1978. Temperature and pressure dependence of Fe–Mg partitioning between garnet and phengite, with particular reference to eclogites. *Contr. Miner. Petrol.*, **66**, 75–80.

Lappin, M. A. 1966. The field relationships of basic and ultrabasic masses in the basal gneiss complex of Stadlandet and Almklovdalen, Nordfjord, southwestern Norway. *Norsk geol. Tidsskr.*, **46**, 439–495.

Lappin, M. A. 1973. An unusual clinopyroxene with complex lamellar intergrowths from an eclogite in the Sunndal–Grubse ultramafic mass, Almklovdalen, Nordfjord, Norway. *Miner. Mag.*, **39**, 313–320.

Lappin, M. A. 1974. Eclogites from the Sunndal–Grubse ultramafic mass, Almklovdalen, Norway, and the T–P history of the Almklovdalen mass. *J. Petrol.*, **15**, 567–601.

Lappin, M. A. and Smith, D. C. 1978. Mantle-equilibrated orthopyroxene eclogite pods from the basal gneisses in the Selje district, western Norway. *J. Petrol.*, **19**, 530–584.

Maquil, R. 1978. Preliminary investigation on giant

orthopyroxenes with plagioclase exsolution lamellae from the Egersund–Ogna anorthositic massif (S. Norway). In *Progress in Experimental Petrology. N.E.R.C. Series D, no. 11*, 144–146.

Medaris, L. G. Jr. 1980. Petrogenesis of the Lien peridotite and associated eclogites, Almklovdalen, western Norway. *Lithos*, **13**, 339–353.

Morse, S. A. 1975. Plagioclase lamellae in hypersthene, Tikkoatokhakh Bay, Labrador. *Earth Planet. Sci. Lett.*, **26**.

Mysen, B. O. and Heier, K. S. 1972. Petrogenesis of eclogites in high grade metamorphic gneisses, exemplified by the Hareidlandet eclogite, western Norway. *Contr. Miner. Petrol.*, **36**, 73–94.

Mørk, M. B. E. 1982. A gabbro–eclogite transition on Flemsøy, Sunnmøre, Western Norway. *Proc. 1st Int. Eclogite Conf.* (Abst.).

Neumann, E.-R. 1976. Two refinements for the calculations of structural formulae for pyroxenes and amphiboles. *Norsk geol. Tidsskr.*, **56**, 1–6.

O'Hara, M. J. 1967. Garnetiferous ultrabasic rocks of orogenic zones. In *Ultramafic and Related Rocks* (Ed. P. J. Wyllie), Wiley, New York, 167–172.

O'Hara, M. J. and Mercy, E. L. P. 1963. Petrology and petrogenesis of some garnetiferous peridotites. *Trans. Roy. Soc. Edinburgh*, **65**, 251–314.

O'Hara, M. J., Richardson, S. W. and Wilson, G. 1971. Garnet peridotite stability and occurrence in crust and mantle. *Contr. Miner. Petrol.*, **32**, 48–68.

O'Neill, H. St. C. and Wood, B. J. 1979. An experimental study of Fe–Mg partitioning between garnet and olivine and its calibration as a geothermometer. *Contr. Miner. Petrol.*, **70**, 59–70.

O'Neill, H. St. C. and Wood, B. J. 1980. Corrections. *Contr. Miner. Petrol.*, **72**, 337.

Råheim, A. 1972. Petrology of high grade metamorphic rocks of the Kristiansund area. *Norges geol. Unders.*, **270**, 1–75.

Råheim, A. and Green, D. H. 1974. Experimental determination of the temperature and pressure dependence of the Fe–Mg partition coefficient for coexisting garnet and clinopyroxene. *Contr. Miner. Petrol.*, **48**, 179–203.

Rost, F. and Brenneis, P. 1978. Die Ultramafite in Bergzug südlich des Ultenthales, Provinz Alto Adige (Oberitalien). *Tscherm. Min. Petr. Mitt.*, **25**, 257–286.

Thompson, R. N. 1974. Some high-pressure pyroxenes. *Mineral Mag.*, **39**, 768–787.

Tørudbakken, B. 1981. Vindøladalen dolerite. In *Excursion B1. Excurs. in Scand. Caledonides*.

Wells, P. R. A. 1977. Pyroxene thermometry in simple and complex systems. *Contr. Miner. Petrol.*, **62**, 129–139.

Wood, B. J. 1974. The solubility of alumina in orthopyroxene coexisting with garnet. *Contr. Miner. Petrol.*, **46**, 1–15.

Wood, B. J. and Banno, S. 1973. Garnet–orthopyroxene and orthopyroxene–clinopyroxene relationships in simple and complex systems. *Contr. Miner. Petrol.*, **42**, 109–124.

The Caledonide Orogen – Scandinavia and Related Areas
Edited by D. G. Gee and B. A. Sturt

The intrusive history and tectonometamorphic evolution of the Basal Gneiss Complex in the Moldefjord area, west Norway

D. A. Carswell and **M. A. Harvey**
Department of Geology, University of Sheffield, Mappin Street, Sheffield S1 3JD, U.K.

ABSTRACT

Field, petrographic and geochemical data are presented which indicate that the voluminous quartz monzonitic augen gneisses in this area, together with subordinate granitic gneisses, are orthogneisses originally emplaced in the mid-Proterozoic (Rb–Sr isochron age of 1506 ± 22 Ma) but extensively deformed and recrystallized during the Caledonian orogeny. Least deformed samples retain porphyritic igneous textures with coronitic development of garnet and scarce relict clinopyroxene, mineralogical features considered to reflect the influence of an early Caledonian high pressure metamorphism more obviously evidenced by the associated metabasic eclogite lenses. These lenses are interpreted as tectonically disrupted intrusive sheets, mostly with olivine tholeiite basaltic chemistry. Original intrusive back-veining relationships have occasionally been preserved between these metabasic intrusives and the enclosing gneisses. A few of the larger metabasic bodies also retain igneous textures with impressive coronitic development of the eclogite facies mineral phases. However, both the eclogites and the augen orthogneisses show extensive deformation which induced retrogression to late Caledonian amphibolite facies mineral assemblages.

A more variable sequence of quartzo-feldspathic gneisses, pelites, calc silicate gneisses, marbles and metabasites (the Paragneiss Complex) has not been dated isotopically but is considered most likely to represent an older Svecofennian rock sequence intruded by the mid-Proterozoic Orthogneiss Complex. Metabasic rocks in the Paragneiss Complex only rarely retain eclogite facies mineralogies and are mostly garnet granulites (as on Tverrfjella) or amphibolites (as on Bolsøy and other islands in Moldefjord). The lower metamorphic grade of the rocks along Moldefjord is associated with the imposition of a near pervasive protomylonitic fabric and is considered to reflect the more intensive late Caledonian deformation and recrystallization of these rocks. However, the occasional preservation of kyanite in pelites and of eclogite facies mineralogies in metabasic rocks indicate that the rocks of the Paragneiss Complex have also witnessed the earlier high pressure metamorphism.

Introduction and Previous Studies

This paper summarizes the results of a study of the rocks in the Moldefjord area of west Norway (62°52′N, 7°W) in the so-called Basal Gneiss Complex (Holtedahl 1944; Carswell 1973).

The rocks of this Complex (Fig. 1) have been the subject of several conflicting interpretations. The earliest workers (e.g. Reusch 1881) regarded the gneisses as Precambrian basement to the overlying Palaeozoic sediments. Later it was considered that part (e.g. Holtedahl 1944; Gjelsvik 1951; Kolderup 1960) or all (e.g. Hernes 1967) of the gneisses were derived by feldspathization of 'Caledonian' or late Precambrian/Cambro-Silurian sediments, respectively. The situation was further complicated by the suggestion that perhaps the basement was composed of two distinct elements. These were first defined by Bryhni (1966) as the homogeneous Jostedal Complex, of reworked Precambrian gneisses and the overlying heterogeneous Fjordane Complex. Strand (1969), Brueckner (1977a), and Skjerlie (1969) discerned similar units at Grotli, Tafjord, and Sunnfjord, respectively.

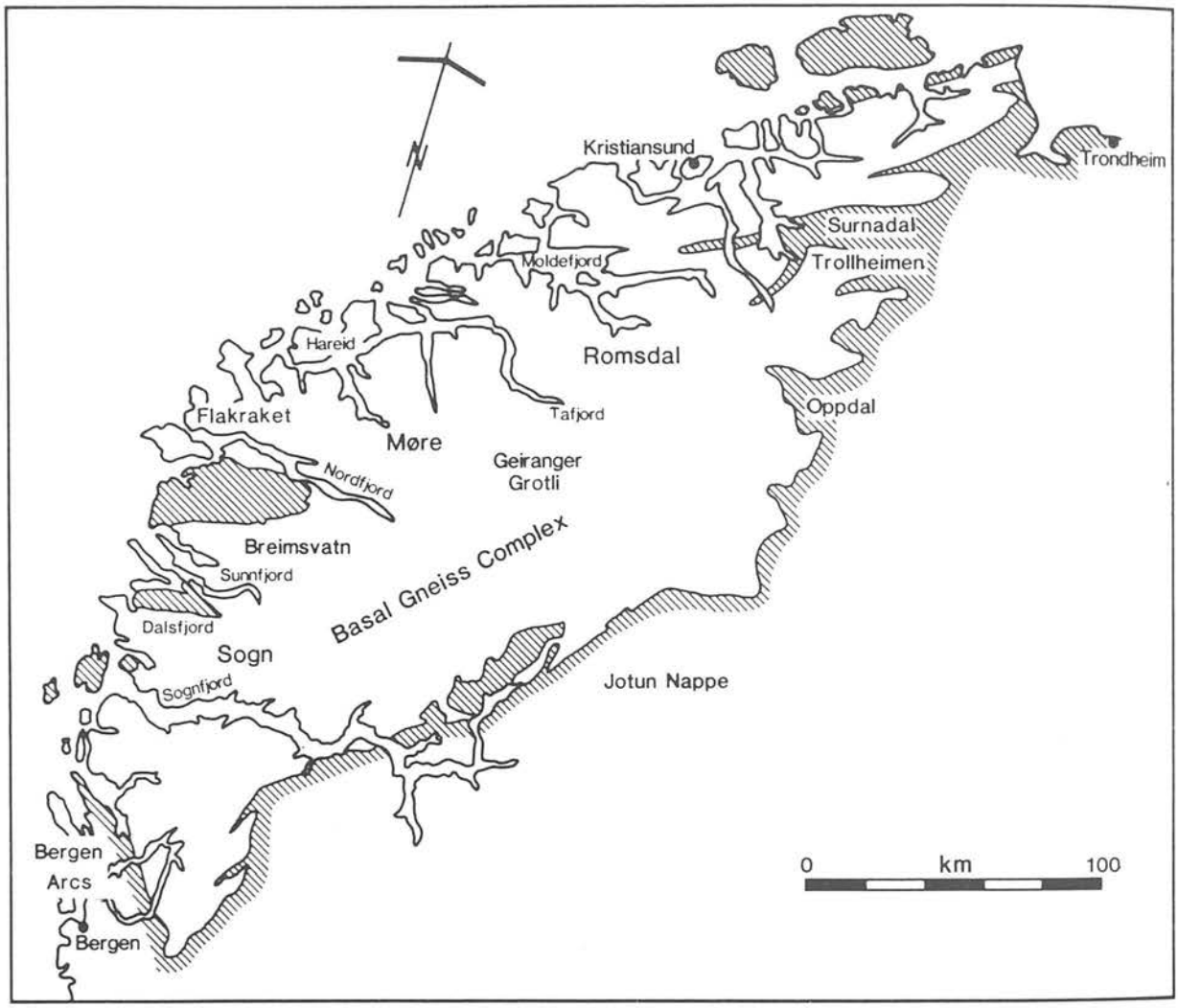

Fig. 1 Location of area of study within the Basal Gneiss Complex, of western Norway. Basal Gneiss Complex unshaded, higher lithological units shaded

In the northern part of the Complex the gneisses are directly overlain by a sequence of heterogeneous rocks of late Precambrian to Ordovician age, with intercalated portions of the basement, shown to be a series of allochthonous nappes with a supposed origin at least 500 km to the west (Gee 1978, 1980). These are separated from the basement Complex by a thin veneer of sediment considered to have acted as a décollement surface for the movement (Gee 1980). The nature of the nappe/basement contact here is crucial to the interpretation of the Moldefjord rocks.

The southern part of the Complex is bordered by further allochthonous material in the Jotun nappe and the Bergen arcs. The origin of the former, consisting of anorthosites and granulites, is equivocal; often thought to be a far-travelled thrust nappe (e.g. Hossack *et al.* 1981). Gravity studies have suggested a deep dense root, and a local derivation from the lower crust as an 'Ivrea-type flake' (Smithson *et al.* 1974; Banham *et al.* 1979). The Bergen Arcs, consisting of a series of arcuate belts of lower Palaeozoic metasediments and metavolcanics, and gneisses with migmatites and anorthosites, have been interpreted as a series of nappes thrust onto a Precambrian gneiss complex of probable autochthonous nature (Sturt *et al.* 1975; Sturt and Thon 1976). The anorthosite portion contains eclogites of postulated Caledonian or possibly Sveconorwegian age and may correlate with the Jotun Nappe (Austrheim and Råheim 1981).

Field studies at Moldefjord have so far been concentrated (Fig. 2) between Moldefjord and Langvatnet–Nåsvatnet, just north of Tverrfjella on the Molde peninsula and on the nearby islands of Otrøy, Midøy, and Dryna to the west and Bolsøy to the south.

Bugge (1934) described the discovery of greenschists, micaschists, quartz schists, and marble on Bolsøy, Saeterøy, and Hjertøy in Moldefjord. Later

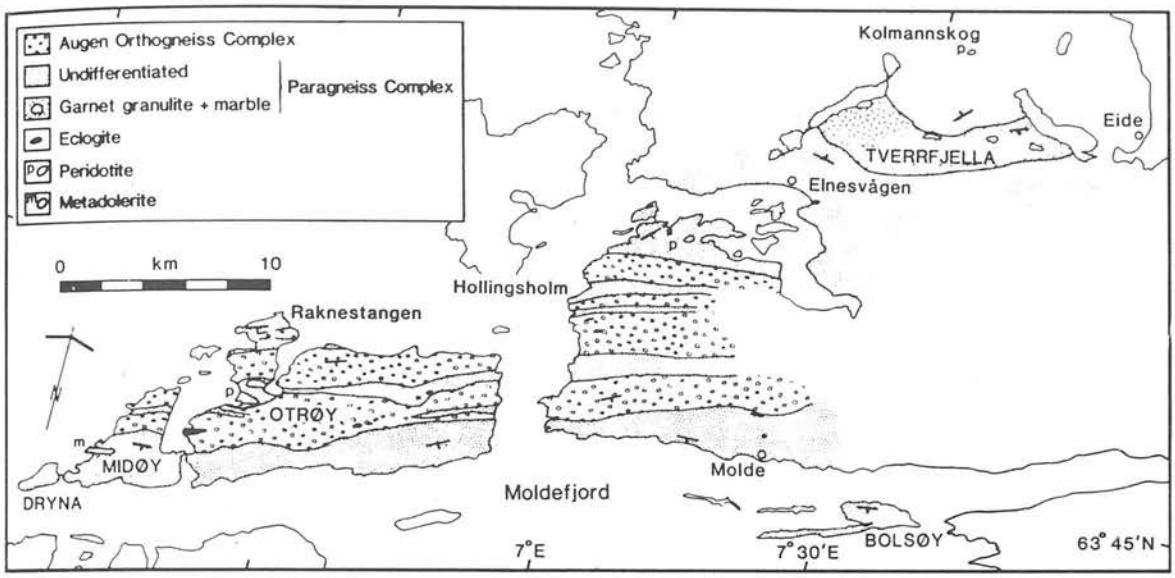

Fig. 2 Generalized geological map of the northern Moldefjord region, only the largest observed lenses of eclogite, peridotite, and metadolerite are indicated

Hernes (1954a, 1956) mapped a narrow synclinal outcrop of similar rocks along the south side of Fannefjord to the east of Molde. These rocks were thought to be contained in a discontinuous westward extension, along the regional strike of the Surnadal syncline which contains comparable rocks (Strand 1952); they were shown as such on the map of Hernes (1955). Furthermore, as Strand considered that the Surnadal rocks could be traced eastwards directly into the Cambro-Silurian rocks of the Trondheim region (as shown on the geological map of Norway—Holtedahl and Dons 1960) it was presumed that the greenschists and associated rocks in the Moldefjord area were of similar age. Gjelsvik (1953) has described rocks near Brattvåg to the southwest of Moldefjord; here micaschists associated with greenschists contain porphyroblasts of feldspar which increase in number over a distance of 50 m across the strike so that the schists pass into an augen gneiss and then into uniform grey gneisses. Thus Gjelsvik, like Hernes (1954a, 1956) apparently considered the contact between the 'basal gneisses' and the supracrustal metasedimentary and metavolcanic rocks to represent a Caledonian migmatite front—the basal gneisses therefore being interpreted as extensively migmatized Eocambrian–Lower Palaeozoic rocks.

Hernes (1955) published a map of the geology between Moldefjord and Kristiansund, including Surnadalen, and constructed a tectonostratigraphy based on a eugeosynclinal sequence of assumed late Precambrian age (Hernes 1967). From his studies near Kristiansund Råheim (1972) expanded upon Hernes's sequence but questioned the Caledonian age for the formation of the gneisses. Subsequently, Pidgeon and Råheim (1972) demonstrated that at least some of the rocks (Tingvoll Group) had a Svecofennian age (1708 ± 60 Ma). The apparent lack of any structural or metamorphic break between these rocks and those of the Surnadal synform suggested that the latter (Røros Group) were of a similar age which Råheim (1977) showed to be so, although the isochron was not well constrained. In addition he demonstrated the existence of a metamorphic and structural break between these Svecofennian-aged rocks in the synform and those higher in the sequence, which he equated with the Støren nappe of Gale and Roberts (1974) and Råheim (1979).

This suggested that the Surnadal synform was not an integral part of the Palaeozoic rocks of the Trondheim Basin. However, Krill (1981) regarded this tectonic break as a zone separating an infrastructure of high-grade metamorphism from a superstructure of low-grade metamorphism as found at Oppdal (Krill 1980). He also correlated an allochthonous Caledonian-aged unit at Oppdal (Blåhø unit) with part of the Surnadal sequence, thereby contradicting the Svecofennian age given for them by Råheim (1977). Furthermore Gee (1980) has correlated the Blåhø unit with the Seve nappe thereby implying that the cover rocks of the Surnadal syncline were allochthonous and Caledonian in age. These contrasting interpretations of the rocks at Surnadal have cast serious doubt over the age and nature of the supracrustal rocks in Moldefjord.

According to the previous mapping and interpretation of Hernes (1956) and Råheim (1972) in the

area between Molde and Kristiansund, the rocks of the actual Basal Gneiss Complex on the northern side of Moldefjord should correspond to Hernes' Frei Group. This lithologically heterogeneous group of rocks was reported to include migmatites, augen gneisses, amphibole and diopside bearing schists and gneisses, marbles and calc-silicate gneisses, garnet amphibolites, eclogites, metaperidotites, metapyroxenites, and metadolerites. On his map, Hernes (1955) indicated that a lithological boundary exists within the Frei Group rocks about 3 km north of Molde which can be followed for tens of kilometres northeast along strike. Our mapping has shown (Fig. 2) that this boundary can also be followed southwestwards across the islands of Otrøy and Midøy and separates contrasting lithological units which we refer to as the Heterogeneous Paragneiss Complex and the more homogeneous Augen Orthogneiss Complex. However, the rocks of the Paragneiss Complex are not restricted to the southern side of this boundary but also occur further north, notably at Raknestangen (the most northerly point at Otrøy) in the area north of Hollingsholm, and on Tverrfjella about 18 km north of Molde (see Fig. 2).

The Augen Orthogneiss Complex

The dominant lithology in this unit is an impressive coarse augen-textured gneiss. The conspicuous pink feldspar augen are usually somewhat flattened and are typically about 1 cm across, although they may be up to 5 cm long. However, dependent upon the degree of deformation, the size, shape, and apparent proportion of feldspar augen may be quite variable, as therefore is the overall appearance of the rock. Nevertheless, where least deformed, the rock has the appearance of a consistently porphyritic igneous rock. An igneous origin is also indicated by the relative uniformity in chemical composition of the augen gneiss (Table 1, column E). On a normative feldspar

Table 1 Averaged whole rock analyses

	A		B		C		D		E		F		G
	$\bar{x}$	σ_n	$\bar{x}$	σ_n	$\bar{x}$	σ_n	$\bar{x}$	σ_n	$\bar{x}$	σ_n	$\bar{x}$	σ_n	$\bar{x}$
SiO_2	46.11	1.98	50.06	1.33	48.59	1.31	46.77	1.20	66.39	2.93	77.54	0.78	66.03
TiO_2	1.76	1.23	0.29	0.04	1.23	0.27	1.78	0.59	0.76	0.23	0.09	0.07	0.71
Al_2O_3	14.87	1.54	8.50	0.78	14.72	0.63	16.43	0.79	14.84	0.74	12.10	0.27	15.88
Fe_2O_3	2.35	0.82	1.75	0.26	3.53	0.76	1.47	0.51	1.75	0.74	0.39	0.32	1.87
FeO	12.23	2.78	7.62	1.14	7.38	1.21	11.41	1.15	3.33	1.55	0.53	0.39	3.24
MnO	0.20	0.05	0.19	0.01	0.17	0.04	0.32	0.33	0.09	0.03	0.02	0.02	0.08
MgO	9.72	2.19	18.52	1.02	8.60	1.98	8.47	2.21	1.55	0.48	0.30	0.13	1.70
CaO	10.11	1.75	10.12	0.18	11.09	1.09	8.81	0.94	3.23	0.72	0.99	0.27	3.00
Na_2O	2.15	0.56	0.76	0.11	3.11	0.84	2.70	0.41	3.13	0.43	2.88	0.54	2.80
K_2O	0.06	0.06	0.42	0.25	0.37	0.28	0.81	0.33	4.12	0.75	4.85	0.90	4.21
P_2O_5	0.18	0.12	0.34	0.37	0.10	0.04	0.33	0.16	0.27	0.10	0.02	0.02	0.15
S	0.02	0.03	0.02	0.01	0.01	0.02	0.03	0.05	0.02	0.04	0.01	0.01	—
H_2O^+	0.35	0.12	0.89	0.60	0.74	0.20	0.65	0.47	0.58	0.19	0.35	0.23	0.90
TOTAL	100.11		99.48		99.64		99.98		100.06		100.07		100.57
100Na/(Na + Ca)	27.8		11.9		33.7		35.7		63.7		84.0		62.8
100Mg/(Mg + Fe)	57.4		78.3		64.8		56.1		42.1		45.6		44.7
ppm													
Ni	217	132	498	41	163	95	155	93	3	2	0	0	
V	341	315	139	3	303	44	220	48	45	17	5	5	
Cr	279	199	1960	55	412	178	101	37	12	3	11	4	
Zn	109	28	86	13	76	16	103	22	85	20	18	10	
Cu	67	39	29	11	67	52	70	14	18	10	7	3	
Rb	2	2	23	4	6	4	21	6	80	20	139	60	
Sr	206	123	102	38	105	40	368	49	231	96	82	74	
Y	23	8	8	6	29	6	30	10	38	12	21	17	
Zr	90	38	30	8	70	21	132	43	339	85	65	44	
Ba	77	27	149	83	84	30	403	185	1123	403	253	106	

A—Average of 11 essentially unmetasomatized olivine normative tholeiitic eclogites
B—Average of 3 somewhat metasomatized 'eucritic' orthopyroxene eclogites
C—Average of 11 garnet granulites from Tverrfjella
D—Average of 5 metadolerites
E—Average of 19 augen orthogneisses
F—Average of 9 granites in orthogneiss complex
G—Average mangerite syenite, Flatraket (Lappin *et al.* 1979)

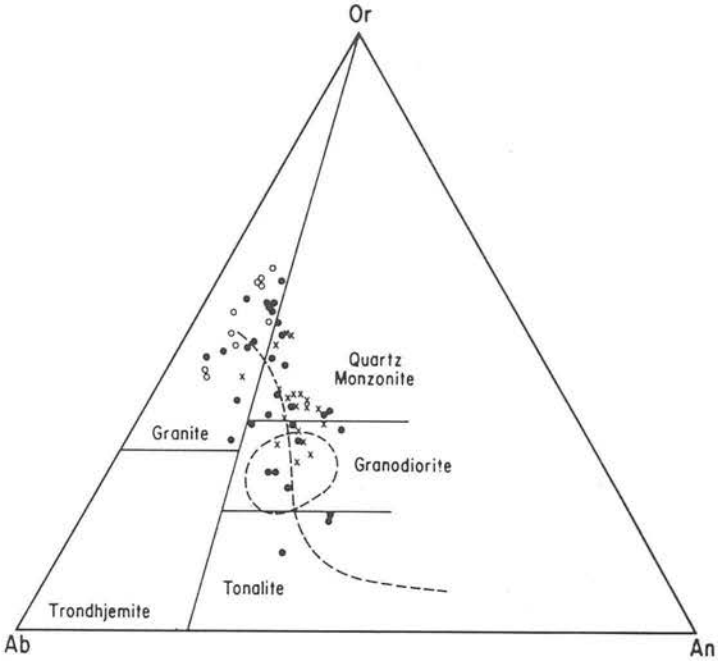

Fig. 3 Normative feldspar plot of whole rock compositions for coarse augen orthogneisses (crosses) and associated granitic sheets (open circles) and miscellaneous augen free gneisses (closed circles). The labelled classification fields outlined by solid lines are those of O'Conner (1965), the field encircled by a broken line the granodiorite field of Streckeisen (1976), and the curved dashed line corresponds to the chemical trend recognized by de Waard (1969) for anorthosite–norite–jotunite–mangerite–farsundite–opdalite–charnockite suite rocks

classification basis (Fig. 3) the augen gneiss compositions straddle the quartz monzonite and granodiorite fields of O'Conner (1965) and lie partly within the granodiorite field of Streckeisen (1976).

Where relatively undeformed it is apparent that the feldspar augen are of rapakivi type with cores of finely perthitic microcline (Or_{90-94} Ab_{5-10}) mantled by oligoclase (An_{20-30}). This plagioclase is commonly antiperthitic enclosing coarse patches of microcline and is often myrmekitic adjacent to the potash feldspar core. A further conspicuous feature of the augen gneiss is the presence of appreciable fine-grained garnet developed in a crude corona fashion between the feldspar augen and the clots of mafic minerals which include rare clinopyroxene relicts, more common dark green hornblende, and significant amounts of both magnetite and sphene. The fabric of these predominantly quartz monzonitic augen gneisses is invariably to some extent porphyroclastic with 'ribbons' of finely granulated quartz. With extreme deformation the feldspar augen clasts are drawn out into long 'pencils' and the content of garnet clearly diminishes whilst that of biotite increases as the rocks are transformed into finely banded, grey, hornblende–biotite gneisses.

Locally the augen-gneisses are sheeted by more nearly equigranular pink granites (Table 1, column F). Despite their low mafic content these granites sometimes contain scarce pyralspite garnet.

Isotopic studies have shown that the augen gneisses and associated granitic rocks give a Rb–Sr isochron age of 1506 ± 22 Ma (Fig. 4). In view of the low initial $^{87}Sr/^{86}Sr$ ratio of 0.7035 and the lack of disturbance of the LIL elements in general (including Rb) we consider this to represent essentially the magmatic crystallization age of these rocks rather than a metamorphic recrystallization age (*cf.* Krill and Griffin 1981). It is of interest that this age is essentially identical to the U–Pb magmatic crystallization age obtained by Lappin *et al* (1979) for the mangerite syenite intrusion within the Basal Gneiss Complex at Flakraket, Nordfjord and to the age for other rapakivi-like orthogneisses in Scandinavia (Point 1975; Röshoff 1978; Krill 1980). The fairly high M.S.W.D. of 14.78 is considered to be the result of subsequent high grade metamorphism during the Caledonian (see below).

We also note the close similarity in chemical composition between the Flakraket mangerite syenite and the Moldefjord quartz monzonitic augen gneisses (compare columns E and G, Table 1), and the fact that together with the associated granitic rocks and miscellaneous augen free gneisses the augen-textured orthogneisses define a chemical trend (Fig. 3) which closely corresponds to that recognized by de Waard (1969) for the anorthosite–norite– jotunite– mangerite– farsundite– opdalite– charnockite suite of rocks. Although anorthosites appear to be

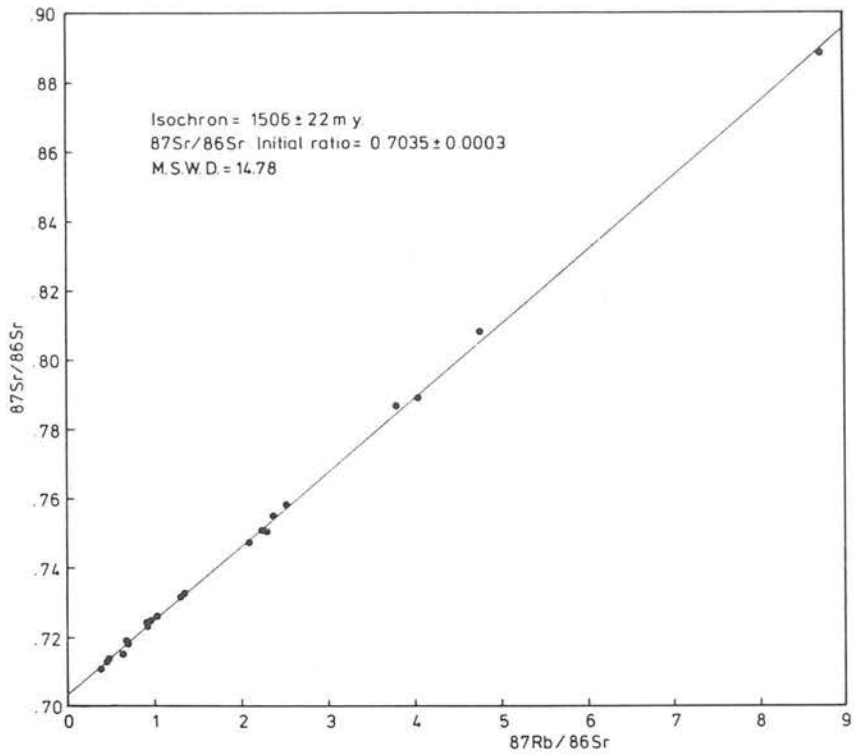

Fig. 4 Rb–Sr isochron diagram for augen textured gneisses and associated granitic rocks from the Augen Orthogneiss Complex on the north side of Moldefjord

absent in the Moldefjord area, they are not uncommon elsewhere in the Basal Gneiss Complex (Bryhni 1966; Brueckner 1977a). We suggest that the anorthosite–augen orthogneiss (mangerite)–granite suite of plutonic intrusives within the Basal Gneiss Complex may be related to the voluminous emplacement of such anorogenic plutonic igneous rocks which appears to have occurred between 1450–1700 Ma, in a broad belt across Scandinavia and North America (Emslie 1978, Bridgewater and Windley 1973).

Lenses of essentially bimineralic eclogite frequently occur throughout the Augen Orthogneiss Complex in this area. Only the outcrops of the largest lenses are shown on Fig. 2. When unaffected by later metasomatism associated with their transformation into biotite amphibolites, the majority of these lenses have broadly similar basaltic rock chemistries (Table 1, columns A and B). In normative terms the dominant eclogites are olivine tholeiites, whilst the scarcer orthopyroxene bearing eclogites (garnet pyroxenites) (Carswell *et al.* this volume) appear to have had a eucritic (i.e. hypersthene–olivine gabbro) parentage. There seems little doubt that these eclogite types represent metamorphosed basic igneous rocks which originally sheeted the intermediate–acid plutonic complex. Typically the eclogite facies metabasites occur as tectonically bounded 'strings' of lenses indicating extensive boudinage of the original intrusive sheets or dykes. This tectonic disruption clearly post-dated the development of the eclogite facies assemblages as witnessed by disorientated internal layering of such assemblages in certain lenses. Particularly large eclogite lenses at Kolmannskog and Raknestangen illustrate internal layering from bimineralic eclogite through garnet websterite to iron-rich garnet–spinel lherzolite, similar to the layering in the Eiksunddal eclogite complex further south on Hareidlandet (Schmitt 1963). Some degree of marginal amphibolitization of all eclogite lenses against the surrounding gneisses is normally apparent.

In rare instances where, as at Litledigerneset on the west coast of Midøy, the contacts between the eclogite bodies and the gneisses have escaped tectonism, original intrusive backveining relationships have been preserved (Griffin and Carswell this volume). Field evidence demonstrates that the higher temperature basic sheets have caused partial remelting of the igneous precursors of the augen gneisses into which they were intruded, leading to the injection of acid backveins into the basic rocks. Quartz and alkali feldspars are the dominant mineral phases in these veins but the preservation of small amounts of symplectitic clinopyroxene, garnet, and kyanite strongly suggests that the emplacement of these veins predated the high pressure eclogite facies metamorphism. These early quartzo-feldspathic

veins contrast with the much more conspicuous post-eclogite facies granitic pegmatites which lack high pressure mineral phases and produce amphibolite haloes where they cross-cut eclogite lenses.

The presence of almandine garnets with significant grossular contents (Table 3, columns H and J) in the intermediate–acid plutonic rocks of the Augen Orthogneiss Complex, is taken to indicate pressures of at least 9 Kbars at the likely 700–800°C metamorphic recrystallization temperatures (Green and Mysen 1972). Likewise the occasional preservation of symplectitic clinopyroxenes in the augen gneisses and the general observation that eclogites have developed in basaltic sheets intruded into the igneous precursors of the augen gneisses, requires that these intermediate–acid plutonic rocks were subjected to the high pressure metamorphic conditions responsible for the development of the eclogite facies assemblages in the metabasic rocks.

Utilizing the garnet–symplectitic clinopyroxene–plagioclase–quartz assemblage equilibria (Newton and Perkins 1981) and the Fe^{2+}/Mg^{2+} partitioning between garnet and symplectitic clinopyroxene (Ellis and Green 1979) pressure and temperature conditions for this assemblage both in augen gneisses and in retrograded eclogites (garnet granulites) were calculated as ~800°C and 9–10 Kbars. The original omphacitic clinopyroxene in these rocks must therefore have been formed at $P > 9$ Kbars.

The Heterogeneous Paragneiss Complex

This rock complex includes migmatitic gneisses (sometimes garnetiferous but invariably with hornblende and/or biotite), diopside ± scapolite-bearing calc-silicate gneisses, marbles, garnet–mica pelites (sometimes with conspicuous kyanite), and garnet and/or epidote bearing amphibolites. The undoubted metasedimentary parentage of many of these rocks and their dominant almandine–amphibolite facies mineralogy led one of us (Carswell 1973) to suggest previously that the rocks of this Complex, which outcrop on the southern sides of Otrøy and Midøy and on the smaller islands nearer Molde, represent a sequence of Caledonian supracrustal rocks deposited on an older Precambrian gneiss basement within which the high grade eclogite facies assemblages were thought to be restricted. However, this interpretation is now recognized to be at least partly incorrect. Firstly, recent Sm–Nd dating of garnet–clinopyroxene mineral pairs from several eclogite lenses within the Basal Gneiss Complex (including samples from the Moldefjord area) has indicated a Caledonian age of around 425 Ma for the eclogite facies metamorphism contrary to the earlier interpretations by Pidgeon and Råheim (1972) and Krogh (1977) of a Svecofennian age (1700–1800 Ma) for this event. Secondly, although the majority of metabasic rocks within the Paragneiss Complex in the near vicinity of Moldefjord are amphibolites, it is now appreciated that eclogite assemblages are in fact occasionally preserved within such amphibolite lenses. Moreover, there are large numbers of eclogite lenses enclosed within migmatitic metasedimentary gneisses around Raknestangen on the extreme north of Otrøy and abundant partly retrograded eclogitic rocks associated with marbles on Tverrfjella (Hernes 1954b). In addition we now recognize that the Paragneiss Complex as mapped (Fig. 2) in places includes conspicuous volumes of possible orthogneisses which may be related to comparable rocks in the more homogeneous Augen Orthogneiss Complex.

So far the Paragneiss Complex around Molde has failed to give a suitably constrained whole-rock Rb–Sr isochron. However, the rocks dated by Pidgeon and Råheim (1972) as 1708 ± 60 Ma near Kristiansund were from the Frei Group, whilst Brueckner (1979) dated eclogite-bearing supracrustal rocks at Tafjord as 1775 ± 57 Ma. These dates for possibly equivalent rocks to those of the Paragneiss Complex suggest that they might be of similar age.

As previously mentioned the Paragneiss Complex on Bolsøy has been related to rocks in the Surnadal syncline (Strand 1952; Hernes 1955; Råheim 1972) but no agreement exists over the interpretation of the latter as either Svecofennian basement (Råheim 1979) or allochthonous Caledonian rocks (Krill 1981; Gee 1980).

However, we question the validity of Råheim's (1977) dating of the Røros Group at Surnadal as Svecofennian on three points. Firstly, no actual isochron was produced for this age. Secondly, the samples described were not of the same lithology and therefore were unlikely to possess the same $^{87}Sr/^{86}Sr$ initial ratio. Thirdly, the 1700 Ma age was suggested because some of the Røros Group rocks fell on the Tingvoll Group isochron, but again the lithologies were different and this superimposition may be purely fortuitous. Furthermore, the concordance of the Røros and underlying Tingvoll groups, taken to indicate a single lithological sequence (Råheim 1977) may well be an artifact of the intense flattening suffered by these rocks during the Caledonian orogeny (*cf.* Carswell 1973). On the other hand the interpretation of Krill and Gee for the Surnadal rocks seems better founded and is preferred on present evidence.

If the lithostratigraphic correlation of the paragneisses on Bolsøy and Tverrfjella eastwards with the rocks at Surnadal is accepted, this would suggest that

the former may also be allochthonous Caledonian rocks. However, as such an interpretation is at odds with the Svecofennian whole rock Rb–Sr isochron age for the Frei Group rocks to the south of Kristiansund (Pidgeon and Råheim 1972), it appears that the key question of the age of the Paragneiss Complex rocks in the Moldefjord area cannot be satisfactorily resolved at present.

Due to this uncertainty over their age, two interpretations are possible for their relationship to the Orthogneiss Complex. The simplest explanation is that the igneous precursors to the augen gneisses intruded and partially migmatized a sequence of pre-existing sediments. Such a model explains the appearance of apparent orthogneisses within the Paragneiss Complex and vice versa, although these relationships have undoubtedly been complicated by later (Caledonian) crustal imbrication. The more complex alternative model requires one, or possibly both, of the complexes to be allochthonous. The augen gneisses could correlate with the Tännäs Augen Gneiss nappe in Sweden which contains Proterozoic rapakivi-like augen orthogneisses with anorthosites and anorthositic gabbros in the Oppdal area (Krill 1980), although the last two rock types are absent at Moldefjord, whilst the Paragneisses could possibly correlate with allochthonous Caledonian rocks of the overlying nappes (e.g. the Seve nappe). To achieve the close intercalation of Orthogneisses and Paragneiss Complexes large scale folding and/or faulting movements would clearly have been required.

It is feasible that the Paragneiss Complex in the Moldefjord area (Fig. 2) may in fact contain both Svecofennian (basement) and Caledonian (cover) lithostratigraphic units. However, the currently available data do not enable us to discriminate between two such rock units, if indeed both do exist in this area.

Metabasic eclogite lenses within the Paragneiss Complex on northern Otrøy have undergone deformation-induced retrogression which has converted the rocks into plagioclase-bearing garnet-granulites. The sporadic preservation of inclusions of omphacitic clinopyroxene within garnets indicates the original presence of eclogite facies assemblages in these granulites. Jadeite-poor clinopyroxenes now occur in equilibrium with oligoclase in the same rocks (Table 2, columns B–D). The conspicuous metabasaltic rocks associated with the marbles on Tverrfjella, described by Hernes (1954b) as eclogite–amphibolites, contain clinopyroxenes with low jadeite contents, intergrown with oligoclase as a symplectite (Table 2, column E) and thus are also garnet-granulites. Further retrogression of such garnet-granulites, ultimately to garnet-free epidote amphibolites would have depended upon the accessibility of water in a declining P/T environment. Metabasic rocks on Bolsøy and adjacent islands in Moldefjord, previously described as greenschists (Bugge 1934; Gjelsvik 1953) are better termed epidote amphibolites. Our recent discovery of relict kyanite in garnetiferous pelites on Bolsøy suggests that these paragneisses may have suffered the same high metamorphic pressures as experienced further north. It would appear that the appearance of fine-grained, well-foliated epidote amphibolites on Bolsøy and adjacent islands and the paucity of eclogite facies assemblages in the Paragneiss Complex along Moldefjord are related to the imposition of a late Caledonian protomylonitic fabric on the rocks in that area.

One of us (MAH) has recently been particularly concerned with the interpretation of the relationships between garnet-granulites (eclogite-amphibolites), marbles, and associated schists and gneisses in the Tverrfjella area. From his earlier study, Hernes (1954b) was uncertain as to whether the conspicuous mafic rocks there (his eclogite-amphibolites) represented metabasaltic rocks or some form of reaction skarn between the marbles and the surrounding gneisses. Since the marbles occur as megaboudins and can be traced along presumed original sedimentary horizons, a further possibility to be considered is that they are of metasedimentary origin and have been derived from impure carbonate rocks.

From geochemical studies the Tverrfjella garnet-granulites display a basaltic chemistry (compare columns A and C in Table 1). These are plotted on a Pearce and Cann (1973) diagram (Fig. 5a), together with various eclogites, amphibolites, and other garnet-granulites from elsewhere in the region. The Tverrfjella garnet-granulites are fairly well separated from the eclogites, the majority of which form a compact group although there are a few with anomalously high or low titanium contents. The majority of the eclogites lie in or near the field defined as ocean island or continental basalts by Pearce and Cann (1973) which is consistent with our hypothesis of them originally being basic dykes intruded into continental crust rocks. By contrast the Tverrfjella garnet-granulite samples lie predominantly in the field of ocean floor basalts as do the majority of the amphibolite and garnet-granulite samples from elsewhere, suggesting that all of these rocks are of an igneous origin. However, another scattered group of amphibolites and garnet-granulites appear towards the Zr apex and are interpreted as having a different, possibly sedimentary, parentage with the high Zr resulting from concentrations of detrital zircon.

Table 2 Representative electron microprobe clinopyroxene analyses

Analysis	A	B	C	D	E	F	G	H	J	K
Sample No.	U484	U160 Inc.	U160 Symp. Max. Al	U160 Symp. Min. Al	1410 Symp.	U263 Prim.	U263 Corona	U262 Inner corona	U262 Outer corona	U332
SiO_2	55.90	55.39	49.64	50.87	49.86	52.09	52.64	53.16	53.28	50.71
TiO_2	0.12	0.31	0.32	0.51	0.42	0.25	0.17	0.07	0.08	0.12
Al_2O_3	8.24	10.08	5.71	1.78	5.07	2.81	3.22	2.15	5.59	2.21
FeO^T	3.97	8.11	10.35	9.38	11.42	8.41	8.78	5.78	5.67	15.08
MnO	0.02	0.09	0.24	0.22	0.11	0.17	0.14	0.14	0.13	0.30
MgO	11.15	8.32	10.79	13.02	10.74	13.52	13.08	14.19	13.51	9.45
CaO	16.26	14.34	20.43	22.00	20.52	21.94	20.35	22.75	18.78	20.89
Na_2O	4.86	6.05	1.68	1.09	1.22	0.99	1.86	1.43	2.63	0.63
TOTAL	100.53	99.69	99.15	99.32	99.36	100.18	100.24	99.67	99.67	99.39
Si	1.989	1.960	1.956	1.931	1.892	1.937	1.952	1.968	1.947	1.950
Ti	0.003	0.008	0.010	0.015	0.012	0.007	0.005	0.002	0.002	0.004
Al	0.346	0.421	0.107	0.080	0.227	0.123	0.141	0.094	0.241	0.101
Fe	0.118	0.240	0.341	0.312	0.362	0.262	0.272	0.179	0.173	0.490
Mn	0.001	0.003	0.008	0.007	0.004	0.005	0.005	0.004	0.004	0.010
Mg	0.591	0.439	0.633	0.736	0.608	0.749	0.723	0.783	0.736	0.547
Ca	0.620	0.544	0.862	0.895	0.834	0.874	0.809	0.902	0.735	0.870
Na	0.335	0.415	0.128	0.080	0.090	0.072	0.134	0.103	0.186	0.048

A —Unaltered grains in large eclogite body at Torveneset, W. Otrøy.
B —Omphacite inclusions in garnets from partly retrograded eclogite lens in roadcut between Rakvåg and Ugelvik, Otrøy.
C, D —Symplectitic grains intergrown with plagioclase An_{16}. Same sample as Analysis B but showing the range of alumina contents observed in different spot analyses.
E —Symplectitic grains in garnet–granulite from Tverrfjella.
F —Primary 'igneous' grains in metadolerite from Drynasund Lighthouse, W. Midøy.
G —Corona grains around clusters of orthopyroxene grains in same sample as F.
H —Inner part of corona adjacent to corona orthopyroxene around primary olivines (Fo_{67}) in metadolerite from Drynasund Lighthouse, W. Midøy.
J —Outer part of corona adjacent to garnet in same sample as H.
K —Relict grains intergrown with plagioclase in augen gneiss from Sundsbø roadcut, N.E. Otrøy.
FeO^T—Total Fe as FeO.

Table 3 Representative electron microprobe garnet analyses

Analysis	A	B	C	D	E	F	G	H	J
Sample No.	U484	U160	1410	U263 Inner corona	U263 Outer corona	U262 Inner corona	U262 Outer corona	U332 High Fe + Mn	U332 Low Fe + Mn
SiO_2	40.89	38.65	38.03	38.68	38.64	39.04	38.66	37.32	37.67
TiO_2	0.02	0.05	0.02	0.05	0.05	0.07	0.06	0.02	0.04
Al_2O_3	23.10	21.31	20.92	21.12	21.18	22.37	22.68	20.58	20.63
FeO^T	18.49	23.88	27.59	25.34	26.04	20.95	14.82	29.64	27.81
MnO	0.29	0.24	0.80	1.14	1.12	0.81	0.70	2.33	0.83
MgO	13.94	7.88	4.57	7.36	6.90	10.32	4.70	2.14	3.26
CaO	4.01	7.34	8.25	6.27	5.88	6.33	17.56	7.95	9.44
Na_2O	0.02	0.02	n.d.	0.02	0.01	0.03	0.02	n.d.	n.d.
TOTAL	100.76	99.87	100.18	99.98	99.82	99.94	99.40	99.98	99.68
Si	6.003	5.973	5.877	5.977	6.015	5.923	5.933	5.989	5.993
Ti	0.004	0.008	0.004	0.008	0.008	0.012	0.010	0.004	0.007
Al	3.998	3.882	3.811	3.848	3.888	4.000	4.104	3.894	3.870
Fe	2.270	3.087	3.566	3.275	3.390	2.658	1.902	3.978	3.701
Mn	0.001	0.097	0.105	0.150	0.148	0.104	0.091	0.316	0.112
Mg	3.050	1.814	1.052	1.695	1.600	2.334	1.075	0.512	0.773
Ca	0.631	1.216	1.366	1.038	0.981	1.029	2.887	1.367	1.609
Na	0.005	0.006	—	0.006	0.004	0.009	0.006	—	—

Sample locations as in Table 2.
FeO^T—total Fe as FeO.

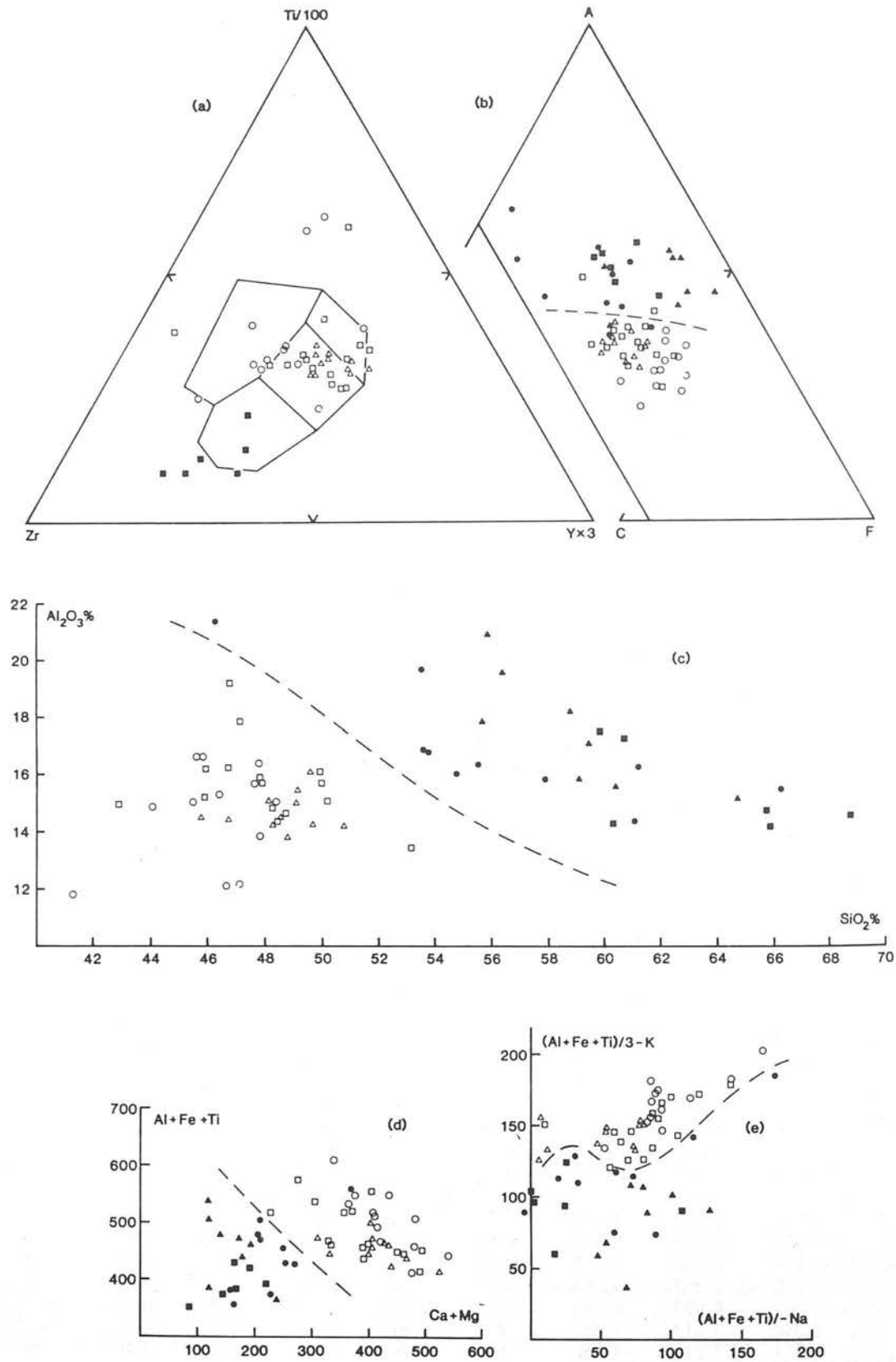

Fig. 5 (a) to (e): various discrimination diagrams showing plots of whole rock analyses of samples from the Moldefjord region as follows: open circles—eclogites; open triangles—garnet granulites from Tverrfjella; open squares—ortho-amphibolites and granulites; solid circles—various calc-silicate bearing and semipelitic gneisses; solid triangles—pelites; solid squares—para-amphibolites and granulites

In an attempt to clarify further the origin of the various garnet-granulites and amphibolites, several discrimination plots were constructed including analyses of pelites and calc-silicate bearing rocks from the Tverrfjella and Molde sequences.

In all these figures (5b–e) the meta-igneous basaltic rocks lie in a cluster (i.e. eclogites, garnet-granulites, and amphibolites) which does not include the apparent metasedimentary amphibolites. Rather, these occur with the undoubted metasedimentary rocks (pelites and calc-silicates). The para-amphibolites are rather more alkali-rich (Fig. 5b) and siliceous, often extremely so (Fig. 5c). The diagrams of Moine and of de la Roche (1968) (Figs. 5d and 5e) were devised specifically to discriminate between meta-igneous and metasedimentary rocks. Although the data do not fall exactly within the fields defined by de la Roche we feel that there is sufficient consistancy of pattern to define two contrasting groups of amphibolites.

From the relative compositional unconformity of the Tverrfjella garnet-granulite and the evidence of the discrimination plots we conclude that this rock may represent submarine basalt flows interbedded with sedimentary material now represented by the associated marbles; calc-silicate gneisses (composed of garnet, diopside, scapolite, feldspar, and sphene) appearing as bands within the marble; amphibolites (often feldspathic and rarely garnetiferous), kyanite-bearing garnet–biotite pelites and quartzo-feldspathic schists. These rocks appear as a definite sequence passing from quartzofeldspathic schists, through the garnet-granulite with marbles, amphibolites, to pelites at the top of the Tverrfjella sequence.

Petrogenetic Significance of Metaperidotites and Metadolerites

Variably sized bodies of both of these rocks types are conspicuous within the area which we have studied. Particularly noteworthy are the garnetiferous peridotites outcropping between Ugelvik and Raknes on the island of Otrøy and the large metadolerite body at Drynasund on western Midøy.

The metadolerites are characterized by the fact that for the most part they retain an igneous fabric but with obvious development of coronas of fine-grained garnet and secondary pyroxenes around primary orthopyroxenes and, if present, olivines. There are considerable variations in composition within these corona phases (Tables 2 and 3) but it is clear that the overall metamorphic trend is towards the development of high pressure eclogite facies assemblages with pyropic garnets and omphacitic clinopyroxenes (*cf.* Griffin and Råheim 1973). Although these dolerites have a basaltic rock chemistry (Table 1, column D) similar to the common bimineralic eclogite lenses, there are certain minor chemical differences, notably in K, Rb, Ba, Zr, P, and Cr contents. Two splits of hand-picked clinopyroxenes from a coarse metadolerite lens exposed at Bolgavatnet within the Frei Group (Råheim 1972), some 45 km northeast of Molde and just south of Kristiansund, have yielded ^{39}Ar–^{40}Ar weighted mean plateau ages on stepwise degassing, of 428 ± 23 Ma and 421 ± 25 Ma (Lynch 1976) with little evidence from the Ar release pattern that these rocks have had an older origin. Hence, we consider that it is more likely that these metadolerites represent a suite of later Caledonian intrusives (probably emplaced close in time to the attainment of the metamorphic 'high') rather than them being older (~ 1500 Ma) rocks of the extensive early basaltic dyke suite (now represented by the thoroughly recrystallized coarse grained eclogites).

For kinetic reasons these metadolerites have partly retained their parent igneous mineralogy through having remained as essentially passive bodies during the subsequent tectonic events. What is certain is that their intrusion and high pressure corona development predates the emplacement of the common Caledonian granite pegmatite suite observed throughout both the Augen Orthogneiss and the Paragneiss Complexes. As in eclogite lenses, amphibolite haloes are developed around such pegmatites where they cut the metadolerite bodies. In addition the metadolerites are converted into foliated amphibole schists where intersected by ENE-striking late Caledonian shear zones.

Geochemical studies of the garnet peridotite bodies in the Basal Gneiss Complex suggest an ultimate mantle origin for these rocks (Carswell 1968; Brueckner 1977b). However, it is now considered (Carswell and Gibb 1980; Medaris 1980) that these peridotite bodies were tectonically intercalated into the gneiss complex prior to the equilibration of the garnet peridotite assemblages. Indeed these eclogite facies assemblages are now thought to have developed contemporaneously with the high pressure assemblages sporadically preserved in metabasic, pelitic, and gneissic rocks of the surrounding Basal Gneiss Complex.

Tectonometamorphic Implications of Deduced P/T Equilibrium Conditions for the High Pressure Metamorphic Assemblages

Judicious interpretation of P/T values obtained from various experimentally calibrated mineral ther-

mometers and barometers applicable to garnet + clinopyroxene ± orthopyroxene ± olivine assemblages indicates values of around 740 ± 50°C and 22 ± 5 Kbars for the P/T equilibration conditions responsible for the high grade metabasic and metaperidotitic assemblages outcropping in this area (Krogh 1977; Carswell and Gibb 1980; Carswell *et al* this volume). In view of the evidence for early high pressure assemblages in a wide range of rock types (including the extensive augen orthogneisses) we envisage that these conditions were operative over a wide area in this part of Møre and Romsdal region. However, observations of regional variations in Fe^{2+}–Mg^{2+} partition coefficients for garnet–clinopyroxene pairs in eclogites indicate that the P/T conditions responsible for the metamorphic culmination in the Basal Gneiss Complex were at a maximum around Moldefjord and adjacent areas along the Norwegian coast and decreased significantly to the southeast (Krogh 1977). Taking into consideration both this and recent isotopic age evidence (Griffin and Brueckner 1980) of a Caledonian age for the metamorphic culmination responsible for the generation of the eclogite facies assemblages, we propose a revised plate tectonic model for the evolution of the Basal Gneiss Complex as outlined more fully in Cuthbert *et al*. (1981, 1983).

We envisage that, following collision of the Greenland and Baltic plates during the Caledonian orogeny, the Baltic plate was underthrust beneath the Greenland plate down a northwesterly dipping Benioff Zone (relative to present geography). Imbrication of mantle peridotite into crustal gneisses situated close to the nose of the downgoing plate is thought to have preceded imposition of the P/T conditions for the metamorphic 'high' which may be expected to have occurred shortly after cessation of subduction and attainment of maximum crustal thickness. Subsequent rapid recovery of these rocks to near surface by mid-Devonian times is considered to have led to varying degrees of retrogression of the high grade assemblages depending upon the extent of strain induced recrystallization.

It is apparent throughout the Moldefjord area that rocks of both the Augen Orthogneiss and Paragneiss Complexes show widespread development of a protomylonitic fabric associated with which the early high grade mineral assemblages are extensively retrograded to lower almandine amphibolite facies assemblages. This deformation attenuates and progressively eliminates early fabrics and structures and is responsible for the dominant steeply dipping ENE striking foliation and prominent rodding lineation in many of the rocks. We consider that this deformation occurred late in the Caledonian orogenic cycle, during the final stages of the recovery of these rocks to the surface. It is our thesis that the virtual elimination of early high grade metamorphic assemblages within the Paragneiss Complex rocks in the southern part of the area can be attributed to the fact that the intensity of this late deformation was at a maximum roughly along the present line of Moldefjord itself.

Summary of the Geological Evolution of the Basal Gneiss Complex

Due to the uncertainty over the age and nature of the Paragneiss Complex two alternatives are given in the following sequence of events for its role in the geological evolution of the Basal Gneiss Complex in the Moldefjord area.

1. Possible deposition and subsequent almandine amphibolite facies metamorphism and migmatization of the sedimentary and volcanic rocks of the Paragneiss Complex at around 1700–1800 Ma.
2. Intrusion into the Paragneiss Complex at around 1500 Ma of the rapakivi-textured quartz monzonites/granodiorites with subsidiary granitic and doleritic sheets now seen as the Orthogneiss Complex. This plutonic igneous activity may have been related to the extensive suite of anorthosite–mangerite–rapakivi granite intrusions emplaced between 1450–1700 Ma in a broad belt across Scandinavia and North America connected with the incipient break-up of the old North American–European continent prior to the Grenville (Sveconorwegian) orogeny.
3. Although we have no definite evidence it seems unlikely that the rocks in this area entirely escaped the tectonometamorphic effects of the Grenville (Sveconorwegian) orogeny at around 900–1200 Ma. Certainly they lie within the Grenville front in Scandinavia as depicted by Shackleton (1979).
4. Our model for the closure and collision of the Baltic and Greenland plates, resulting in the Caledonian orogeny, is presented in Cuthbert *et al*. (1983); only a synopsis relevant to the rocks in Moldefjord is given here but is tenable for both possible suggested relationships between the Paragneiss and Orthogneiss Complexes. During collision the leading edge of the Baltic plate underthrust the Greenland plate and suffered intense telescoping and imbrication of both basement and cover giving a crustal thickness of around 80 km. The possible juxtapositioning of the two Complexes by thrusting could have occurred at that time, with the Orthogneisses thrust over basement or perhaps a parautochthonous unit, and the Paragneisses in turn thrust

over the Orthogneisses. The alternative intrusive relationship of the two Complexes would require that the two behaved as a single unit of crust which escaped much of this imbrication. The metaperidotites are considered to have been incorporated during this imbrication perhaps due to thrusts transecting the subcontinental upper mantle. There also appears to have been an episode of emplacement of mantle derived basaltic magma, resulting in the metadolerite bodies, at around the time of maximum crustal thickness, approximately 450 Ma.

5. Imposition of the P/T conditions (740 ± 50°C, 22 ± 5 Kbars) for the Caledonian metamorphic culmination in the Basal Gneiss Complex occurred shortly afterwards, following thermal 'recovery' in the imbricated pile (Richardson and England 1979). During this high pressure metamorphic event eclogite facies mineral assemblages were developed in 'dry' metabasic rocks and in the metaperidotite bodies and garnet (and rare jadeitic clinopyroxene) formed in the intermediate–acid orthogneisses. By contrast, almandine amphibolite assemblages may have remained stable (Bryhni *et al.* 1977) in certain 'wetter' metasedimentary/metavolcanic rocks of the Paragneiss Complex. Partial melting of the latter rocks under the high P_{H_2O} conditions may have been responsible for the generation of the extensive suite of Caledonian granite pegmatites.
6. During the ensuing rapid, isostatically induced, recovery of these rocks towards the surface, the early high pressure metamorphic assemblages suffered varying degrees of retrogression to low almandine amphibolite and ultimately greenschist facies assemblages, depending upon the extent to which the rocks were affected by associated deformation. Where eclogite facies assemblages remained essentially 'dry', but deformation prompted recrystallization, retrogression proceeded only as far as the development of granulite facies assemblages. The pervasive imposition of a low grade protomylonitic fabric in the paragneisses in the vicinity of Moldefjord suggests that the final transfer of these rocks to close to the surface by mid-Devonian times (~ 385 Ma) involved extensive shearing, thrusting, and isoclinal folding presumably associated with continued compression in the orogen.

Acknowledgements

We wish to thank R. Kanaris-Sotiriou and F. G. F. Gibb for assistance and advice with X-ray fluorescence and electron microprobe analyses performed at the University of Sheffield; W. L. Griffin for his cooperation and encouragement with Rb–Sr isotopic analyses conducted at the Mineralogisk–Geologisk Museum in Oslo; and P. Mellor for cheerfully typing several versions of the manuscript of this paper. In addition, D. A. Carswell acknowledges financial support for field studies in Norway from the University of Sheffield and the Natural Environment Research Council, and M. A. Harvey the receipt of a research studentship from the latter body.

References

Austrheim, H. and Råheim, A. 1981. Age relationships within the high grade metamorphic rocks of the Bergen Arcs, western Norway. *Abstr. Uppsala Caledonide Symp. Terra Cognita*, **1**, 33.

Banham, P. H., Gibbs, A. D. and Hopper, F. W. M. 1979. Geological evidence in favour of Jotunheimen Caledonian suture. *Nature*, London, **277**, 289–291.

Bridgewater, D. and Windley, B. F. 1973. Anorthosites, post-orogenic granites, acid volcanic rocks, and crustal development in the North Atlantic Shield during the mid-Proterozoic. In Lister, L. A. (Ed.), *Symposium on Granites, Gneisses and Related Rocks*, *Geol. Soc. S. Africa Sp. Publ.*, **3**, 307–318.

Brueckner, H. K. 1977a. A structural, stratigraphic and petrologic study of anorthosites, eclogites and ultramafic rocks and their country rocks, Tafjord area, western south Norway. *Norges geol. Unders.*, **332**, 1–53.

Brueckner, H. K. 1977b. A crustal origin for eclogites and a mantle origin for garnet peridotites: strontium isotopic evidence from clinopyroxenes. *Contrib. Mineral. and Petrol.*, **60**, 1–15.

Brueckner, H. K. 1979. Precambrian ages from the Geiranger–Tafjord–Grotli area of the Basal Gneiss region, west Norway. *Norsk geol. Tidsskr.*, **59**, 141–153.

Bryhni, I. 1966. Reconnaissance studies of gneisses, ultrabasites, eclogites and anorthosites in outer Nordfjord, western Norway. *Norges geol. Unders.*, **241**, 1–60.

Bryhni, I., Krogh, E. and Griffin, W. L. 1977. Crustal derivation of Norwegian eclogites: a review. *N. Jb. Miner. Abh.*, **130**, 49–68.

Bugge, C. 1934. Grønne trondhjemsskifre på øyene ved Molde. *Norges geol. Unders.*, **43**, 167–175.

Carswell, D. A. 1968. Possible primary upper mantle peridotite in Norwegian basal gneiss. *Lithos*, **1**, 322–355.

Carswell, D. A. 1973. The age and status of the basal gneiss complex of north-west southern Norway. *Norsk geol. Tidsskr.*, **53**, 65–78.

Carswell, D. A. and Gibb, F. G. F. 1980. The equilibrium conditions and petrogenesis of European crustal garnet lherzolites. *Lithos*, **13**, 19–29.

Carswell, D. A., Krogh, E. J. and Griffin, W. L. this volume. Norwegian orthopyroxene eclogites: calculated equilibration conditions and petrogenetic implications.

Claesson, S. 1981. Caledonian metamorphism of Proterozoic Seve rocks in Mt. Åreskutan, southern Swedish Caledonides. *Geol. För. Stockholm Förh.*, **103**, 291–304.

Cuthbert, S. J., Harvey, M. A. and Carswell, D. A. 1981. A plate tectonic model for the Basal Gneiss Complex of

Western South Norway—a working hypothesis. *Abstr. Uppsala Caledonide Symp. Terra Cognita*, **1**, 41.

Cuthbert, S. J., Harvey, M. A. and Carswell, D. A. 1983. A tectonic model for the metamorphic evolution of the Basal Gneiss Complex, Western South Norway. *J. Metam. geol.*, **1**, 63–90.

de Waard, D. 1969. The anorthosite problem: the problem of the anorthosite–charnockite suite of rocks. In Isachesen, Y. W. (Ed.), *Origin of Anorthosite and Related Rocks*, pp. 466.

Ellis, D. J. and Green, D. H. 1979. An experimental study of the effect of Ca upon garnet–clinopyroxene Fe–Mg exchange equilibria. *Contrib. Mineral. Petrol*, **71**, 13–22.

Emslie, R. F. 1978 Anorthosite massifs, rapakivi granites and late Proterozoic rifting of North America. *Precambrian Res.*, **7**, 61–98.

Gale, H. G. and Roberts, D. 1974. Trace-element geochemistry of Norwegian lower Palaeozoic basic volcanics and its tectonic implications. *Earth Planet. Sci. Lett.*, **22**, 380–390.

Gee, D. G. 1978. Nappe displacement in the Scandinavian Caledonides. *Tectonophysics*, **47**, 393–419.

Gee, D. G. 1980. Basement–cover relationships in the central Scandinavian Caledonides. *Geol. För. Stockholm Förh.*, **102**, 455–474.

Gjelsvik, T. 1951. Oversikt over bergartene i Sunnmøre og tilgrensende deler av Nordfjord. *Norges geol. Unders.*, **179**, 1–45.

Gjelsvik T. 1953. Det nordvestlige gneis-område i det sydlige Norge, aldersforhold og tektonisk–stratigrafisk stilling. *Norges geol. Unders.*, **184**, 71–94.

Green, D. H. and Mysen, B. O. 1972. Genetic relationship between eclogite and hornblende plagioclase pegmatite in western Norway. *Lithos*, **5**, 147–161.

Griffin, W. L. and Råheim, A. 1973. Convergent metamorphism of eclogites and dolerites, Kristiansund area, Norway. *Lithos*, **6**, 21–40.

Griffin, W. L. and Brueckner, H. K. 1980. Caledonian Sm–Nd ages and crustal origin for Norwegian eclogites. *Nature*, London, **285**, 319–321.

Griffin, W. L. and Carswell, D. A. this volume. In-situ metamorphism of Norwegian eclogites: an example.

Hernes, I. 1954a. Trondhjemsskifrene ved Molde. *Norsk geol. Tidsskr.*, **34**, 123–137.

Hernes, I. 1954b. Eclogite amphibolite on the Molde peninsula, southern Norway. *Norsk geol Tidsskr.*, **33**, 163–184.

Hernes, I. 1955. Geologisk oversikt over Molde–Kristiansundsområdet. *Det. Kongl. Norske Vidensk. Selsk. Skrifter.*, **5**, 16.

Hernes, I. 1956. Surnadalssynklinalen. The Surnadal syncline, central Norway. *Norsk geol. Tidsskr.*, **36**, 35–39.

Hernes, I. 1967. The late Pre-Cambrian stratigraphic sequence in the Scandinavian mountain chain. *Geol. Mag.*, **104**, 557–563.

Holtedahl, O. 1944. On the Caledonides of Norway with some scattered local observations. *Skr. Norske Vidensk-Akad. i Oslo, Mat.-Naturv. Kl.*, **4**, 31.

Holtedahl, O. and Dons, J. A. 1960. Geologiske kart over Norge, Bergrunnskart 1: 1,000,000. *Norges geol. Unders.*, **208**.

Hossack, J. R., Nickelsen, R. P. and Garton, M. 1981. The geological section from the foreland up to the Jotun Sheet in the Valdres area, South Norway. *Abstr. Uppsala Caled. Symp. Terra Cognita*, **1**, 52.

Kolderup, N.–H. 1960. Origin of Norwegian eclogites in gneisses. *Norsk geol. Tidsskr.*, **40**, 73–76.

Krill, A. G. 1980. Tectonics of the Oppdal area, central Norway. *Geol. För. Stockholm Förh.*, **102**, 523–530.

Krill, A. G. 1981. 'Stockwerk' tectonic relationships between the Trondheim synclinorium and the Western Gneiss Region of Norway. *Abstr. Uppsala Caledonides Symp. Terra Cognita*, **1**, 56.

Krill, A. G. and Griffin, W. L. 1981. Interpretation of Rb–Sr dates from the western gneiss region: a cautionary note. *Norsk geol. Tidsskr.*, **61**, 83–86.

Krogh, E. J. 1977. Evidence of Precambrian continent–continent collision in western Norway. *Nature*, London, **267**, 17–19.

Lappin, M. A., Pidgeon, R. T. and van Breemen, O. 1979. Geochronology of basal gneisses and mangerite syenites of Stadlandet, west Norway. *Norsk geol. Tidsskr.*, **59**, 161–181.

Lynch, M. C. F. 1976. *Application of the ^{39}Ar–^{40}Ar technique to terrestrial rocks and minerals with special reference to the Lewisian of N.W. Scotland*. Unpublished Ph.D Thesis, University of Sheffield, U.K.

Medaris, L. G. 1980. Petrogenesis of the Lien peridotite and associated eclogites, Almklovdalen, Western Norway. *Lithos*, **13**, 339–353.

Moine, B. and de la Roche, H. 1968. Nouvelle approche de probleme de l'origine des amphibolites a partir de leur composition chimique. *Comptes Rendues Acad. Sci. Paris, seire D*, **267**, 2084–2087.

Newton, R. C. and Perkins, D. III 1981. Thermodynamic calibration of geobarometers based on the assemblages garnet–plagioclase–orthopyroxene (clinopyroxene)–quartz. *Am. Mineral.*, **67**, 203–222.

O'Conner, J. T. 1965. A classification for quartz-rich igneous rocks based on feldspar ratios. *U.S. geol. Surv. Prof. Paper*, **525–B**, 79–84.

Pearce, J. A. and Cann, J. 1973. Tectonic setting of basic volcanic rocks using trace element analysis. *Earth Planet. Sci. Lett.*, **19**, 290–300.

Pidgeon, R. T. and Råheim, A. 1972. Geochronological investigation of the gneisses and minor intrusive rocks from Kristiansund, west Norway. *Norsk geol. Tidsskr.*, **52**, 241–256.

Point, R. 1975. Mylonites et orogenèse tangentielle nature, geochemie, origine et âge des gneiss oeillés dans les nappes calédoniennes externes. *Bulletin de la Societe Geologique de France*, **7**, 17, 664–679.

Råheim, A. 1972. Petrology of high grade metamorphic rocks of the Kristiansund area. *Norges geol. Unders.*, **279**, 1–75.

Råheim, A. 1977. A Rb, Sr study of the rocks of the Surnadal syncline. *Norsk. geol. Tidsskr.*, **57**, 193–204.

Råheim, A. 1979. Structural and metamorphic break between the Trondheim basin and the Surnadal synform. *Norsk geol. Tidsskr.*, **59**, 195–198.

Reusch, H. H. 1881. Konglomerat–Sandstenfelterne i Nordfjord, Søndfjord og Sogn. *Nytt. Mag. Naturvitensk.*, **26**, 93–170.

Richardson, S. W. and England, P. C. 1979. Metamorphic consequences of crustal eclogite production in overthrust orogenic zones. *Earth Planet. Sci. Lett.*, **42**, 183–190.

Roberts, D., Thon, A., Gee, D. G. and Stephens, M. B. 1981. Scandinavian Caledonides-tectonostratigraphy map, scale 1:1,000,000. *Uppsala Caledonide Symp.*

Röshoff, K. 1978. Structure of the Tännäs Augen Gneiss Nappe and its relation to under- and overlying units in

the central Scandinavian Caledonides. *Sver. geol. Unders.*, **C739**, 1–35.

Schmitt, H. H. 1963. *Petrology and Structures of the Eiksundal Eclogite Complex, Hareidland, Sunnmøre, Norway*. Unpublished|Ph.D.|thesis, Harvard University.

Shackleton, R. M. 1979. The British Caledonides: comment and summary. In Harris, A. L. Holland, C. H. and Leake, B. E. (Eds), *The Caledonides of the British Isles, Reviewed*, pp. 768.

Skjerlie, F. J. 1969. The Pre-Devonian rocks in the Askvoll–Gaular area and adjacent districts, Western Norway. *Norges geol. Unders.*, **28**, 325–359.

Smithson, S. B., Ramberg, I. B. and Grønlie, G. 1974. Gravity interpretation of the Jotun Nappe of the Norwegian Caledonides. *Tectonophysics.*, **22**, 205–222.

Strand, T. 1952. The relation between the basal gneiss and the overlying meta-sediments in the Surnadal district (Caledonides of Southern Norway). *Norges geol. Unders.*, **184**, 100–123.

Strand, T. 1969. Geology of the Grotli area. *Norsk geol. Tidsskr.*, **49**, 341–360.

Streckeisen, A. 1976. Classification of the common igneous rocks by means of their chemical composition. A provisional attempt. *N. Jb. Miner. Mh.*, **1**, 1–15.

Sturt, B. A. and Thon, A. 1976. The age of orogenic deformation in the Swedish Caledonides. *Am. J. Sci.*, **276**, 385–390.

Sturt, B. A., Skarpenes, O., Ohanian, A. T. and Pringle, I. R. 1975. Reconnaissance Rb/Sr isochron study in the Bergen Arc system and regional implications. *Nature*, London, **253**, 595–599.

Lithos, 19 (1986) 279–297
Elsevier Science Publishers B.V., Amsterdam – Printed in The Netherlands

The metamorphic evolution of Mg-Cr type Norwegian garnet peridotites

D.A. CARSWELL

Department of Geology, University of Sheffield, Mappin Street, Sheffield S1 3JD (Great Britain)

LITHOS

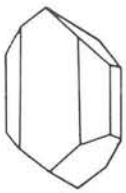

Carswell, D.A., 1986. The metamorphic evolution of Mg-Cr type Norwegian garnet peridotites. In: W.L. Griffin (Editor), Second International Eclogite Conference. Lithos, 19: 279–297.

Mineralogical and microstructural data are presented which demonstrate that the garnet peridotites variably preserved in Alpine-type bodies within the Western Gneiss Region of Norway have had a prolonged, 7-stage, evolutionary history. High-temperature Al-pyroxene ± spinel protolith assemblages (ass. I) are only rarely preserved but predate the coarse-grained P_{max} garnet lherzolite assemblages (ass. II). Porphyroclastic textured samples demonstrate subsequent recrystallisation to a lower-pressure 5-phase garnet + spinel lherzolite assemblage (ass. III). Most samples show development of kelyphites of intimately intergrown replacement pyroxenes + spinel (ass. IV) around garnets. These are in turn frequently overgrown by late coarser-grained coronas of orthopyroxene + pargasitic amphibole + spinel (ass. V). The chrome-depleted secondary garnets are interpreted to have predated kelyphite formation contrary to most previous interpretations. Assemblages VI and VII reflect the late-stage stability at reduced temperatures of firstly aluminous chlorite and finally serpentine + talc assemblages.

As the peridotites may contain up to six generations of certain mineral phases (notably orthopyroxene) and individual grains are frequently compositionally zoned, considerable care has been exercised over the selection of mineral compositions appropriate to the various mineral equilibria used to deduce the overall *P-T* path followed by these rocks. Finally, general aspects of the origin and tectonic setting of these rocks and of the age of the various observed assemblages are discussed. Whilst the early assemblages (I and II) appear to be mid-Proterozoic in age, the later assemblages (III → VII) are probably all Caledonian).

(Received November 20, 1985; accepted for publication February 15, 1986)

1. General considerations and regional setting

Two compositionally contrasted types of garnet peridotite bodies occur within the Western Gneiss Region of Norway (Carswell et al., 1983). The Fe-Ti type occurs, together with volumetrically dominant eclogites and garnet websterites, as a component of metamorphosed layered complexes judged to have originally comprised low-pressure (< 10 kbar), plagioclase + olivine bearing, cumulates (Schmitt, 1964; Jamtveit, 1985). Evidence suggests that the prograde high-pressure (eclogite facies) assemblages in these rocks, in common with those in associated supracrustal lithologies, formed at *P-T* conditions of around 750–800°C and 20 kbar during the underthrusting of this continental crust segment (effectively the leading edge of the Baltic Plate) beneath the Greenland Plate during the Caledonian orogeny (see, e.g., Krogh, 1977; Cuthbert et al., 1983; Griffin et al., 1985).

By contrast the Mg-Cr type garnetiferous peridotite assemblages occur as sporadically preserved layers or boudinaged lenses within typical Mg + Cr rich (forsteritic olivine dominated), Alpine-type peridotite bodies. Occurrences of such garnet peridotites (Fig. 1) have been described by Eskola (1921), Bryhni (1961), O'Hara and Mercy (1963), Lappin (1966, 1974), Carswell (1968a, b, 1973, 1981), Medaris (1980, 1984), Carswell et al. (1983) and Jamtveit (1984), but details of their origin,

0024-4937/86/$03.50

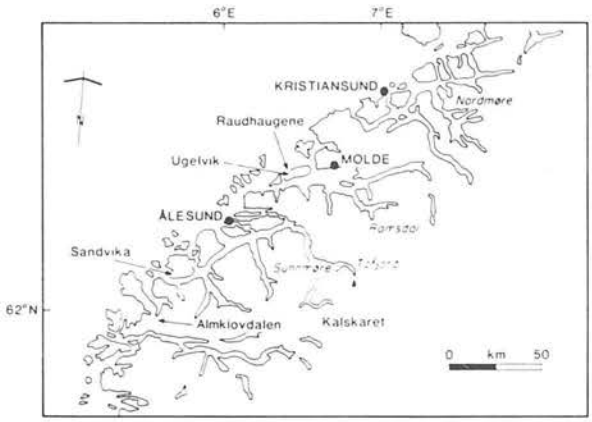

Fig. 1. Locality map for Mg-Cr garnet peridotite occurrences in western Norway discussed in this paper.

age and mode of emplacement into the high-grade crustal gneiss complex remain controversial. The majority of these authors has interpreted such peridotite bodies to comprise tectonically intercalated slices of sub-continental upper-mantle rocks which have had a different, though possibly convergent (Medaris, 1980), metamorphic history to the eclogite-facies assemblages formed from low-pressure crustal protoliths. However, there have been some recent suggestions that the Mg-Cr garnet peridotites may represent prograde metamorphosed ophiolitic rocks (Jamtveit, 1984; Griffin and Qvale, 1985). Either origin seems feasible in the vicinity of a major plate suture but contrasts in the *P-T* paths expected to have been followed, as witnessed by compositional zoning and mineral inclusion evidence in garnets, should enable discrimination between the two alternatives (Carswell and Cuthbert, 1986). This paper examines the question of these two possible origins for the Norwegian Mg-Cr garnet peridotites in the light of a full documentation of their metamorphic evolution as deduced from petrographic evidence and mineral composition data.

2. Stages in the metamorphic evolutionary history

It has long been recognised that these garnet peridotites represent relicts of early high-pressure assemblages which, in common with other eclogite-facies assemblages in the Western Gneiss Region, have been extensively overprinted and partly replaced by later amphibolite-facies assemblages. However, integration of mineralogical and microstructural observations from the various occur-

TABLE 1

Metamorphic evolution of west Norway Mg-Cr 'Alpine'-type peridotites

Stage	Assemblage	Interpretation
I	$Ol + Opx_1 + Cpx_1 \pm Sp_1 \pm Amp_1$	high-temperature protolith
		(near pervasive ductile deformation)
		↓
II	$Ol_2 + Opx_2 + Cpx_2 + Gnt_1$	coarse-grained eclogite-facies assemblage
		(extensive shear deformation)
		↓
III	$Ol_3 + Opx_3 + Cpx_3 + Gnt_2 + Sp_2$	fine-grained neoblast eclogite-facies assemblage
		↓ (strain-free decompression)
IV	$Ol_4 + Opx_4 + Cpx_4 + Sp_3$	kelyphitic granulite-facies assemblage
		(limited deformation)
		↓
V	$Ol_5 + Opx_5 + Amp_2 + Sp_4$	coronitic/foliated high amphibolite-facies assemblage
		(restricted deformation in high-strain zones)
		↓
VI	$Ol_6 + Opx_6 + Amp_3 + Chl_1$	foliated low amphibolite-facies assemblage
		(late-stage brittle fracturing)
		↓
VII	$Serp + Talc + Amp_4 + Chl_2$	localised greenschist-facies assemblage

rences (especially those at Ugelvik and Raudhaugene on the island of Otrøy in Moldefjord) indicate that overall these rocks have in fact had a more complex and prolonged metamorphic history.

The idealised equilibrium mineral assemblages considered to have been stable at each of the seven stages recognised in the metamorphic evolution of these peridotite bodies are outlined in Table 1. However, individual samples from particular localities invariably contain disequilibrium assemblages which reflect the association of mineral phases which grew during two or more, but never all seven, of the metamorphic stages.

2.1. Stage I: olivine$_1$ + orthopyroxene$_1$ + clinopyroxene$_1$ ± spinel$_1$ ± amphibole$_1$

Mineral phases (Table 2) which predate the development of garnetiferous peridotite assemblages in these west Norway bodies are only rarely preserved. However, relict early aluminous orthopyroxene megacrysts (opx_1) which show evidence of extensive garnet and clinopyroxene exsolution have been described from Ugelvik, Otrøy (Carswell, 1973; sample U95) and from Sandvika, Gurskøy (Carswell et al., 1983; sample E38). The sample from the latter locality also contains early aluminous spinel (Sp_1) with reaction coronas of garnet, clinopyroxene with extensive fine-scale orthopyroxene and rutile exsolution, and an early amphibole in apparent textural equilibrium with the aluminous pyroxenes + spinel + olivine assemblage. It is of interest to note that this amphibole (Amp_1) has a relatively TiO_2 + K_2O enriched composition comparable to that occurring as rare early strained porphyroclasts in garnet peridotites at Kalskaret, Tafjord (Al-Samman, 1985; sample T98). On the other hand, petrographic evidence is compatible with the interpretation that this latter amphibole in certain Kalskaret samples was in equilibrium with the Stage II garnet lherzolite assemblage and adjacent small recrystallised amphibole grains with the Stage III garnet + spinel lherzolite neoblast assemblage. Large clinopyroxene clasts in peridotite at the Kalskaret locality occasionally contain elongated garnet blebs (Carswell, 1968a; Al-Samman, 1985; Figs. 4–10), which strongly suggests that they originally had more aluminous compositions. In addition, Lappin (1973, 1974) has described convincing evidence of exsolution of both garnet and orthopyroxene lamellae and blebs from large clinopyroxene clasts within a garnet-poor pyroxenite (samples 6912 and 6095) in the peridotite body at Sunndal-Grubse, Almklovdalen.

Taken together these various pieces of evidence, albeit from geographically scattered localities, indicate that the garnet-bearing assemblages in these peridotite bodies were predated by higher-tempera-

TABLE 2

Compositions of mineral phases in Stage I protolith assemblages

Mineral phase	Opx_1	Opx_1	Cpx_1	Cpx_1	Cpx_1	Sp_1	Amp_1	Amp_1
Sample No.	E38	U95	6912	6095	E38	E38	E38	T98
Locality	Sandvika	Ugelvik	Sunndal-Grubse	Sunndal-Grubse	Sandvika	Sandvika	Sandvika	Kalskaret
SiO_2	53.8	55.0	52.3	52.6	51.8	0.11	42.0	46.5
TiO_2	0.10	0.03	0.01	0.05	0.57	0.04	1.81	0.81
Al_2O_3	4.79	4.16	4.21	3.88	4.51	55.6	13.0	11.2
Cr_2O_3	0.24	0.62	0.17	0.17	0.47	7.60	0.57	0.27
Fe_2O_3	n.d.	0.55	1.52	1.52	n.d.	4.76*	n.d.	n.d.
FeO	9.16	3.91	6.41	5.90	3.71	13.5	6.15	5.24
MnO	0.24	0.10	0.14	0.25	0.09	0.12	0.06	0.02
NiO	0.09	0.10	0.06	0.03	0.04	0.46	0.11	n.d.
MgO	30.4	32.7	16.3	16.4	15.7	17.5	17.2	18.6
CaO	0.77	1.98	17.0	17.5	21.9	n.d.	11.4	11.6
Na_2O	0.01	0.19	1.18	1.26	0.84	n.d.	2.39	3.21
K_2O	n.d.	0.00	n.d.	n.d.	n.d.	n.d.	1.13	0.24
Total	99.6	99.3	99.3	99.6	99.7	99.7	95.8	97.6

The first 4 analyses represent calculated compositions for Stage I pyroxenes assuming integration of exsolved phases. Other analyses are direct electron microprobe determinations. Calculated analyses for the clinopyroxenes from the Sunndal-Grubse body at Almklovdalen are from Lappin (1974). n.d. = not determined.
*Stoichiometrically calculated value.

ture assemblages involving markedly aluminous pyroxenes (around 4–5 wt.% Al_2O_3) with aluminous spinel ($X_{Al}^{Sp} \simeq 0.9$) and pargasitic amphibole as possible additional phases.

2.2. *Stage II: olivine$_2$ + orthopyroxene$_2$ + clinopyroxene$_2$ + garnet$_1$*

The west Norway garnet-bearing peridotites characteristically have markedly inequigranular textures with large strained clasts (up to 2 cm across) of orthopyroxene, clinopyroxene, garnet and more rarely olivine set in a much finer-grained matrix of essentially strain-free grains. Close petrographic observation indicates that the matrix comprises recrystallised neoblasts of all four phases, although in the majority of samples garnet and clinopyroxene have been at least partly replaced by later pargasitic amphibole and spinel. An additional petrographic feature is that garnets are usually mantled by broad, mineralogically complex, kelyphite reaction rims (Figs. 5C and D) developed in response to the instability of the P_{max} garnet + olivine assemblage on the declining *P-T* path which led to the ultimate surface exposure of these rocks.

Garnet peridotite sample U8 from Raudhaugene, Otrøy, is an important, although relatively uncommon, type in that it retains evidence of recrystallisation of a coarse-grained Stage II clast assemblage to a subsequent fine-grained Stage III neoblast assemblage without the superimposed effects of later kelyphite development and growth of replacement amphibole. Accordingly in the following account petrographic features, mineral compositions and zoning profiles in sample U8 are detailed and contrasted with those in sample U92 from the small quarry by the harbour at Ugelvik, Otrøy, which is typical of those garnet peridotites which show extensive development of kelyphites around garnets and of later replacement amphibole. In view of its importance further data are also presented and discussed for sample U95 from Ugelvik (cf. Carswell, 1973). Mineral analyses are given not only for the large (1–5 cm) orthopyroxene megacrysts and the exsolved garnet and clinopyroxene, but also for the immediately adjacent foliated garnet peridotite assemblage observed to have formed through recrystallisation at the margins of the strained orthopyroxene porphyroclasts. Garnets in this adjacent foliated garnet peridotite typically have narrow kelyphite reaction rims mantled by later coarse-grained replacement amphibole.

Electron microprobe analyses of the various mineral phases in these three samples are detailed in Tables 3–5. Most quoted analyses are averages for several point analyses of the particular types of mineral grains indicated. However, since the larger garnet grains are compositionally zoned especially with respect to Fe/Mg ratios, the most extreme compositions determined for grain rims are also quoted in these instances. All compositions were obtained by wavelength dispersion analysis using a Cambridge Instruments Microscan IX at the University of Sheffield.

As in most other garnet peridotite samples, the porphyroclast phases in U8 are compositionally zoned – most notably and importantly the garnets and orthopyroxenes (Fig. 2). Such zoning is considered to have evolved through inter- and intra-crystalline element diffusion in response to element exchange reactions operational during subsequent stages in the metamorphic history of these rocks.

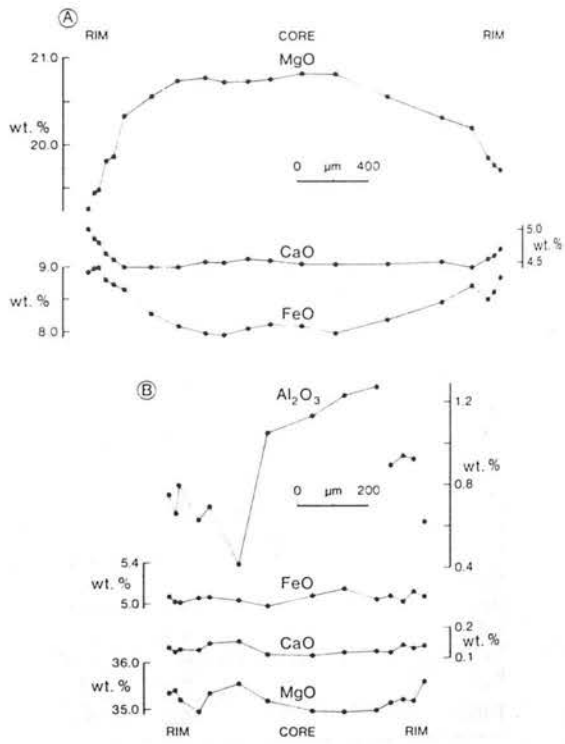

Fig. 2. A. Zoning profile across garnet porphyroclast (Gnt_1) in garnet peridotite sample U8 from Raudhaugene, Otrøy. B. Zoning profile across orthopyroxene porphyroclast (Opx_2) in sample U8.

TABLE 3

Mineral compositions in porphyroclastic garnet peridotite U8 – Raudhaugene, Otrøy

Mineral	Garnet	Garnet	Garnet	Garnet	Opx	Opx	Opx	Cpx	Cpx	Cpx	Spinel	Olivine	Olivine
Textural type	Clast cores	Clast rims	Most extreme clast rim	Small neoblasts	Clast cores	Clast rims	Neoblasts	Clast cores	Clast rims	Neoblasts	With Gnt neoblasts	Clasts	Neoblasts
Growth stage	II	II	II	III	II	II	III	II	II	III	III	II	III
Mineral generation	1	1^m	1^m	2	2	2^m	3	2	2^m	3	2	2	3
SiO_2	41.8	41.8	42.4	42.2	57.9	58.4	58.5	55.0	54.8	55.1	0.00	41.7	41.5
TiO_2	0.24	0.16	0.04	0.01	0.07	0.06	0.04	0.12	0.19	0.15	0.02	n.d.	n.d.
Al_2O_3	22.0	22.1	22.5	23.3	1.05	0.74	0.52	2.57	3.18	3.05	34.8	n.d.	n.d.
Cr_2O_3	2.20	2.05	1.70	0.91	0.17	0.23	0.11	1.38	1.49	1.52	34.2	n.d.	n.d.
FeO^T	8.40	8.84	9.09	9.18	4.98	5.17	4.96	1.49	1.54	1.61	14.2^s	7.73	7.84
MnO	0.42	0.44	0.41	0.41	0.11	0.10	0.08	0.09	0.06	0.05	0.18	0.07	0.11
NiO	0.01	0.00	0.02	0.01	0.08	0.06	0.08	0.05	0.03	0.04	0.02	0.38	0.41
MgO	20.5	19.6	19.4	20.4	35.4	35.5	35.6	15.8	15.2	15.1	15.9	50.4	50.4
CaO	4.54	4.89	5.04	3.87	0.14	0.13	0.11	21.3	21.0	20.8	0.00	n.d.	n.d.
Na_2O	n.d.	n.d.	n.d.	n.d.	0.01	0.00	0.01	2.05	2.25	2.34	n.d.	n.d.	n.d.
K_2O	n.d.	n.d.	n.d.	n.d.	n.d.	n.d.	n.d.	n.d.	n.d.	n.d.	n.d.	n.d.	n.d.
Total	100.1	99.9	100.5	100.3	99.3	100.4	100.1	99.8	99.7	99.8	99.3	100.3	100.3
					$En_{92.7}$	$En_{92.4}$	$En_{92.8}$					$Fo_{92.1}$	$Fo_{92.0}$

FeO^T – total Fe as FeO; m – signifies that mineral composition subsequently modified during later metamorphic stage; s – stoichiometrically calculated Fe_2O_3 = 1.49 with residual FeO = 12.9; n.d. – not determined.

TABLE 4

Mineral compositions in partly amphibolitised garnet peridotite U92 – Ugelvik, Otrøy

Mineral	Garnet	Garnet	Garnet	Opx	Opx	Opx	Opx
Textural type	Grain cores	Grain rims	Most extreme rim	Grain cores	Grain rims	Secondary in coarse kelyphite	Collars around kelyphite
Growth stage	II	II	II	III	III	IV	V
Mineral generation	1	1^m	1^m	3	3^m	4	5
SiO_2	41.4	41.2	40.7	57.7	57.2	56.9	56.5
TiO_2	0.02	0.03	n.d.	0.04	0.05	0.05	0.05
Al_2O_3	21.7	21.5	21.4	0.68	1.21	1.53	2.16
Cr_2O_3	2.35	2.62	2.71	0.11	0.17	0.29	0.11
FeO^T	11.2	11.6	12.4	7.78	8.10	8.70	8.89
MnO	0.82	0.92	0.98	0.21	0.18	0.32	0.26
NiO	n.d.	n.d.	0.05	0.06	0.03	0.11	0.10
MgO	17.7	17.1	17.0	33.7	33.2	32.5	32.2
CaO	5.06	5.38	4.79	0.18	0.20	0.24	0.25
Na_2O	n.d.	n.d.	n.d.	0.01	0.01	0.00	0.01
K_2O	n.d.	n.d.	n.d.	n.d.	n.d.	n.d.	n.d.
Total	100.2	100.2	100.1	100.4	100.3	100.6	100.6
				$En_{88.5}$	$En_{87.9}$	$En_{86.9}$	$En_{86.6}$

FeO^T – total Fe as FeO; m – signifies that mineral composition subsequently modified during later metamorphic stage; s – stoichiometrically calculated values, Sp_2: Fe_2O_3 = 2.35, residual FeO = 21.9, and Sp_{3-4}: Fe_2O_3 = 1.64, residual FeO = 15.6; n.d. – not determined.

The zoning profiles of the large garnet clasts in U8 (Fig. 2A), characterised by notably increasing FeO/MgO ratios from cores to rims, are similar to those recorded in many other west Norway garnet peridotite samples (Carswell et al., 1983; Medaris, 1984; D.A. Carswell and A.H. Al-Samman, unpublished data, 1985). However, the degree to which such zoning is preserved in individual garnet grains in particular samples clearly depends on the extent of subsequent garnet breakdown reactions (e.g., kelyphite development). Fe-Mg zonation is less marked in clinopyroxene clasts but calculated $K_{Fe^{2+}\text{-}Mg}^{Gnt\text{-}Cpx}$ partition coefficients increase from clast cores to rims, indicating that the zonation has probably developed in response to declining temperatures and possibly also pressures (Ellis and Green, 1979).

Zoning profiles for orthopyroxene clasts in U8 (Fig. 2B) show decreasing Al_2O_3 contents from cores (mean value 1.05 wt.%), to rims (mean value 0.74 wt.%). This trend correlates with the observed decreased Al_2O_3 contents of the orthopyroxene neoblasts in U8 (mean value 0.52 wt.%) which have formed through recrystallisation of the strained orthopyroxene clasts. Fig. 3 illustrates the full extent of the variation in Al_2O_3 content in individual spot analyses of the various textural types of orthopyroxene grains in U8, with the highest contents being for clast cores and the lowest for recrystallised neoblasts. By contrast, large matrix orthopyroxenes in sample U92 (Fig. 4B) show a significant increase in Al_2O_3 content from grain cores (mean value 0.68 wt.%) to grain rims (mean value 1.21 wt.%). Similar Al_2O_3 values and zoning profiles have been determined in texturally comparable orthopyroxenes from most other analysed west Norway garnet peridotite samples (cf. Carswell et al., 1983, fig. 6; Medaris, 1984, fig. 8). It is

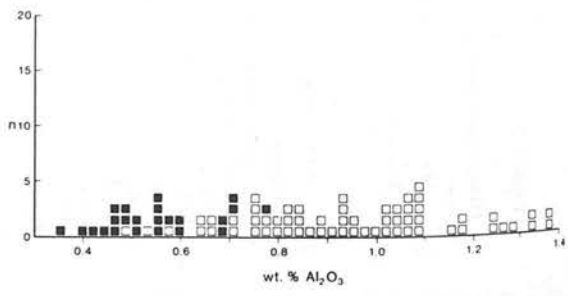

Fig. 3. Al_2O_3 contents for single spot analyses of orthopyroxene porphyroclasts Opx_2 (open squares) and neoblasts Opx_3 (solid squares) in garnet peridotite sample U8 from Raudhaugene, Otrøy.

Cpx	Cpx	Cpx	Spinel	Spinel	Olivine	Olivine	Amph	Amph
Grain cores	Grain rims	Secondary in coarse kelyphite	Grain cores in matrix	Secondary in kelyphite	Clasts	Neoblasts	Outer collars to kelyphite	Discrete in matrix
III	III	IV	III	IV–V	II	III	V	V
3	3[III]	4	2	3–4	2	3	2	2
54.5	54.5	54.4	0.00	0.00	40.6	40.2	47.4	46.7
0.04	0.04	0.12	0.16	0.05	n.d.	n.d.	0.61	0.27
1.07	0.83	1.17	23.5	46.5	n.d.	n.d.	12.0	12.7
0.68	0.34	0.39	43.0	20.0	n.d.	n.d.	1.08	1.71
1.82	1.90	2.37	24.0[S]	17.1[S]	11.6	13.4	4.01	3.40
0.08	0.06	0.11	0.46	0.23	0.19	0.28	0.09	0.08
0.03	0.03	0.03	0.06	0.17	0.41	0.39	0.08	0.09
17.1	17.5	17.1	8.89	15.2	47.6	46.4	18.6	18.6
23.5	24.6	24.0	n.d.	n.d.	n.d.	n.d.	12.8	12.6
0.48	0.33	0.23	n.d.	n.d.	n.d.	n.d.	1.79	2.14
n.d.	n.d.	n.d.	n.d.	n.d.	n.d.	n.d.	0.04	0.08
99.3	100.0	99.9	100.0	99.3	100.4	100.6	98.3	98.5
					$Fo_{88.0}$	$Fo_{86.1}$		

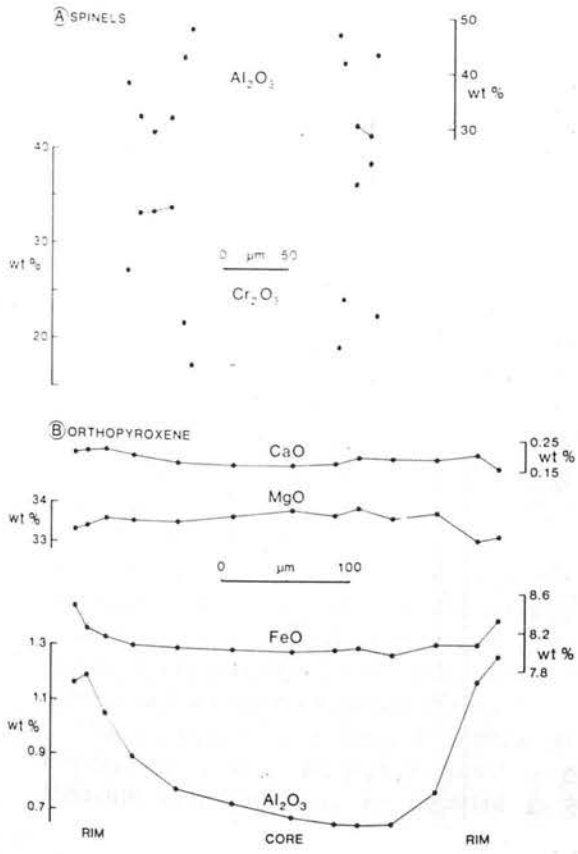

important to appreciate that, unlike in U8, these latter samples are all characterised by kelyphitic reaction rims around garnets and considerable growth of late replacement amphibole. Accordingly it is significant that in respect of their higher Al_2O_3 contents and lower Mg/(Mg + Fe) ratios (cf. Table 4) the rims of the large matrix orthopyroxenes in these samples approach the composition of the later orthopyroxene phases (Opx_4 and Opx_5) which have, on textural evidence, clearly grown as a result of garnet breakdown reactions.

On the basis of the above observations porphyroclast core compositions in sample U8 (Table 3) are judged to be best representative of the 4-phase garnet lherzolite assemblage stabilised during stage II of the metamorphic evolution of these peridotite bodies. On the other hand, orthopyroxene clast rim compositions in U8 are considered to have been modified during the subsequent deformation induced recrystallisation to the stage III 5-phase garnet + spinel lherzolite assemblage.

Fig. 4. A. Zoning profiles across two matrix spinel grains (Sp_{2-3}) in garnet peridotite sample U92 from Ugelvik, Otrøy.
B. Zoning profile across large matrix orthopyroxene (Opx_{3-4}) in sample U92.

TABLE 5

Mineral compositions in sample U95 comprising exsolved orthopyroxene megacrysts + adjacent foliated partly amphibolitised garnet peridotite – Ugelvik, Otrøy

Mineral	Garnet	Garnet	Opx	Opx	Opx	Opx	Cpx	Cpx	Spinel	Olivine	Amph	Amph
Textural type	Exsolved from Opx megacrysts	Adjacent foliated peridotite	Megacryst remote from the exsolution	Megacryst adjacent to Gnt exsolution	Grain cores foliated peridotite zone	Grain rims foliated peridotite zone	Exsolved from Opx megacryst	Adjacent foliated peridotite zone	Discrete foliated peridotite zone	Foliated peridotite zone	Adjacent to Gnt	Discrete foliated peridotite zone
Growth stage	II	II	I	I	III	III	II	III	III	III	V	V
Mineral generation	1	1	2^m	2^m	3	3^m	2	3	2	3–5	2	2
SiO_2	41.6	41.5	58.6	58.3	58.6	58.2	55.0	55.3	0.00	41.6	43.8	45.7
TiO_2	0.03	0.03	0.00	0.00	0.00	0.00	0.00	0.02	0.02	n.d.	0.06	0.13
Al_2O_3	21.3	21.3	0.41	0.82	0.42	0.64	2.69	2.75	14.2	n.d.	15.6	12.1
Cr_2O_3	3.52	3.44	0.16	0.21	0.09	0.17	2.40	2.58	55.8	n.d.	2.33	2.05
FeO^T	8.64	8.82	4.48	4.70	4.86	4.79	1.26	0.99	18.8	7.61	2.35	2.18
MnO	0.48	0.53	0.07	0.10	0.12	0.13	0.07	0.07	0.34	0.08	0.12	0.09
NiO	0.01	0.01	0.09	0.10	0.09	0.11	0.02	0.02	0.01	0.42	0.10	0.11
MgO	20.2	19.9	35.9	35.6	35.7	35.6	15.4	14.8	10.20	50.2	17.6	19.1
CaO	4.61	4.53	0.13	0.13	0.10	0.13	20.6	20.6	0.00	n.d.	10.4	11.0
Na_2O	n.d.	n.d.	0.01	0.01	0.01	0.01	2.22	2.52	n.d.	n.d.	4.23	3.79
Total	100.3	100.1	99.8	100.0	100.0	99.8	99.8	99.6	99.3	99.9	96.6	96.2
			$En_{93.4}$	$En_{93.1}$	$En_{92.9}$	$En_{93.0}$				$Fo_{92.2}$		

FeO^T – total Fe as FeO; m – signifies that mineral composition subsequently modified during later metamorphic stage; n.d. – not determined.

Despite the previously mentioned uncertainty over the interpretation of the scarce early amphibole porphyroclasts in certain Kalskaret samples, it is apparent that at least for the most part the garnetiferous assemblages of both Stages II and III were amphibole free. This implies that in general the activity of H_2O in these peridotites was too low to stabilise amphibole in these particular assemblages under the then prevailing *P-T* conditions.

2.3. Stage III: olivine$_3$ + orthopyroxene$_3$ + clinopyroxene$_3$ + garnet$_2$ + spinel$_2$

In sample U8 the large garnet porphyroclasts (Gnt_1) can be observed to have recrystallised, both at margins and along internal fractures (Figs. 5A and B), to a fine-grained mosaic aggregate of secondary garnet and red chrome spinel (X_{Cr}^{Sp} = 0.39). The garnet neoblasts (Gnt_2) are notably less chromiferous (mean value 0.91 wt.% Cr_2O_3) than the primary garnet clasts (mean value 2.20 wt.% Cr_2O_3 in cores). They also characteristically have lower TiO_2 contents. Similar, lower chrome, secondary garnets have been recorded in other samples from the Otrøy localities (D.A. Carswell, unpublished data, 1984) and from Kalskaret (Al-Samman, 1985), Sandvika (Carswell et al., 1983) and Almklovdalen (Griffin and Heier, 1973). However, in these other samples textural relationships between the two generations of garnet grains have been partly obscured by the subsequent development of kelyphite at garnet grain boundaries (cf. Figs. 5C and D; also Carswell et al., 1983, fig. 3).

Griffin and Heier (1973) concluded that the secondary garnet has grown after kelyphite formation through reversal of the reaction garnet + olivine → orthopyroxene + clinopyroxene + spinel responsible for kelyphite development. However, this is clearly not the case in sample U8, where microstructural evidence and its intimate association with chrome spinel indicates that the secondary garnet developed through direct strain-induced breakdown and recrystallisation of original more chromiferous garnet according to the multivariant reaction of Cr-rich garnet$_1$ + olivine$_2$ + orthopyroxene$_2$ + clinopyroxene$_2$ → Cr poor garnet$_2$ + Cr spinel$_2$ + orthopyroxene$_3$ + clinopyroxene$_3$.

This reaction from a Stage II 4-phase garnet lherzolite to a Stage III 5-phase garnet + spinel lherzolite assemblage may be expected to have occurred in response to deformation at decreased ambient lithostatic pressures during the exhumation history of such deep-level, high-pressure, rocks (MacGregor, 1970; O'Hara, 1975; O'Neill, 1981).

Compositions of neoblasts of all five mineral phases stable at Stage III in the metamorphic evolution of these peridotites are best represented in sample U8 (Table 3). As in other samples, olivine neoblasts are somewhat less forsteritic than porphyroclasts. Precise characterisation of olivine compositions during each of the metamorphic stages I–VI is not possible since it is difficult to assess the extent of olivine re-equilibration during the various stages. An overall trend towards lower forsterite contents in the later-stage olivines (especially on garnet breakdown) is, however, apparent.

As noted above in U8 the lower-Al_2O_3 orthopyroxene clast rim compositions (mean value 0.74 wt.%) reflect re-equilibration with the Stage III 5-phase garnet + spinel lherzolite assemblage. The cores of the matrix orthopyroxenes in other garnet peridotite samples (e.g., U92, Table 4) mostly have similar low Al_2O_3 contents (e.g., range 0.29–0.68 wt.%, mean 0.50 wt.% in fourteen Otrøy samples). The implication of the evidence from orthopyroxenes in sample U8 is that such low-Al_2O_3 orthopyroxene compositions probably also reflect re-equilibration with a Stage III 5-phase garnet + spinel lherzolite assemblage. In this connection, orthopyroxene compositions (Table 5) and zoning profiles (Fig. 6) determined in sample U95, with the large exsolved orthopyroxene megacrysts, are also enlightening.

The orthopyroxene megacrysts in U95 have uniformly low Al_2O_3 contents (mean value 0.41 wt.%) except immediately adjacent to the garnet exsolution lamellae where the Al_2O_3 content dramatically increases to an average of 0.82 wt.%. Such an increase cannot be related to the exsolution stage, rather it must have evolved during subsequent metamorphic stages. Indeed the optically visible presence of minor replacement amphibole along some garnet-orthopyroxene interfaces suggests that it may well reflect later instability of garnet. Such an interpretation seems to be borne out by evidence from the immediately adjacent foliated garnet peridotite which contains discrete orthopyroxenes with low-Al_2O_3 cores and higher-Al_2O_3 rims. This garnet peridotite is heavily retrograded with kelyphite rims around garnets and considerable growth of late amphibole in the rock matrix.

It is also important to note the presence of discrete chrome spinel grains in the matrix of the adjacent foliated garnet peridotite in U95 as well as numerous minute chrome spinel inclusions directly enclosed in the exsolved orthopyroxene megacrysts. Hence, the low Al_2O_3 contents of the orthopyroxene megacrysts (away from garnet exsolution lamellae) and in the cores of the matrix orthopyroxenes are considered to reflect equilibration with a Stage III garnet + spinel lherzolite assemblage during attendant deformation, as likewise with the low-Al_2O_3 core compositions of matrix orthopyroxenes in most other west Norway garnet peridotite samples.

The compositional zoning in the larger matrix spinels, as in sample U92 (Fig. 4A) is also significant. The chrome-rich spinel cores (X_{Cr}^{Sp} = 0.53) are considered to have equilibrated with the low-Al

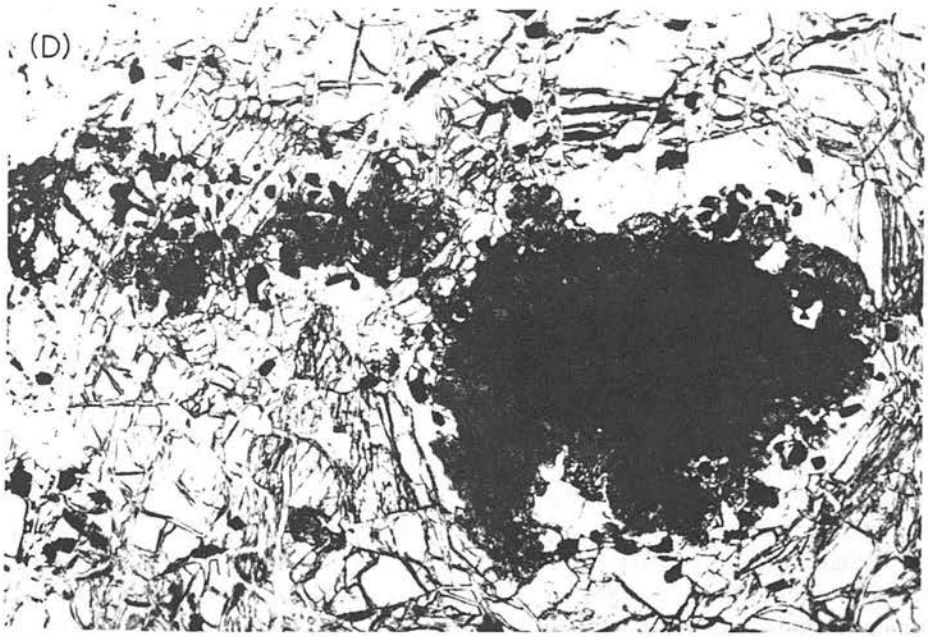

Fig. 5. A and B. Deformation induced recrystallisation at margins of garnet porphyroclasts (Gnt_1) to finer-grained neoblasts of secondary less chromiferous garnet (Gnt_2) together with chrome spinel (Sp_2) which appears opaque. Sample U8 from Raudhaugene, Otrøy. Width of field of view across photographs is approximately 2 mm.

C. Relict garnet porphyroclast core (Gnt_1) preserved within broad kelyphite reaction rim of secondary pyroxenes and spinel (assemblage IV). Note how smaller garnet neoblasts (Gnt_2) adjacent to the large deformed and elongated garnet clast have been entirely replaced by kelyphite. Hence the deformation and garnet neoblast formation predated kelyphite development. Garnet peridotite sample U29 from Ugelvik, Otrøy – field of view approximately 5 mm.

D. Large garnet porphyroclast entirely replaced by semi-opaque kelyphite of secondary pyroxenes + spinel (assemblage IV) in turn mantled by a corona of coarser-grained orthopyroxene + pargasitic amphibole + spinel (assemblage V). Heavily amphibolitised garnet peridotite sample U92 from Ugelvik, Otrøy – field of view approximately 5 mm.

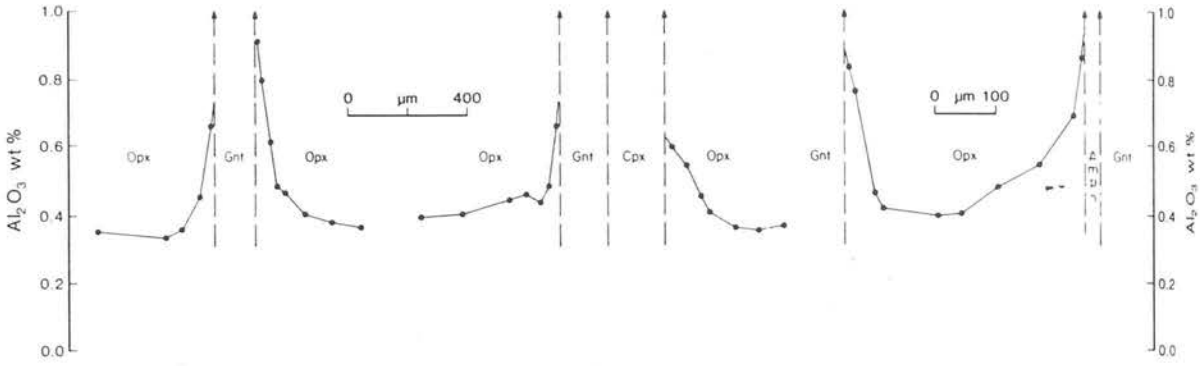

Fig. 6. Al_2O_3 zonation across orthopyroxene megacryst (Opx_1) with exsolution lamellae of garnet and clinopyroxene in sample U95 from Ugelvik, Otrøy. Note the development of visibly apparent amphibole along at least some garnet-orthopyroxene interfaces.

orthopyroxene cores as part of a Stage III garnet + spinel lherzolite assemblage, whereas the more aluminous spinel rims are comparable in composition to later spinels ($X_{Cr}^{Sp} = 0.22$) formed as a result of garnet breakdown (Table 4) which equilibrated with later higher-Al orthopyroxene compositions (viz. matrix grain rims + grains spatially associated with garnet breakdown).

2.4. Stage IV: olivine$_4$ + orthopyroxene$_4$ + clinopyroxene$_4$ + spinel$_3$

The coexisting pyroxenes and spinel of this assemblage take the form of fine-grained filamental intergrowths which comprise the inner, radial growth, parts of the kelyphite reactions rims (Figs. 5C and D) around garnets. This assemblage has developed as a result of the down-pressure reaction garnet + olivine → orthopyroxene + clinopyroxene + spinel. It is reasonable to expect these replacement pyroxenes and spinel all to be significantly more aluminous than those associated with the earlier garnet-bearing assemblages of Stages II and III. Unfortunately, the spinels are too small to analyse and their wide dispersal throughout the associated pyroxenes mostly prevents their analysis as well. However, analysis was possible of occasional spinel-free areas of the pyroxenes, which occur towards the outer edges of some radial kelyphites. Such analyses (Table 4) confirm the more aluminous character of Opx_4 and Cpx_4.

Kelyphite reaction rims are most strikingly developed around the large chromiferous garnet clasts (Gnt_1). However, petrographic evidence in the Otrøy garnet peridotite samples (e.g., Fig. 5C) demonstrates that kelyphites have frequently also formed around the smaller garnet neoblasts (Gnt_2) observed adjacent to the large deformed garnet clasts. Clearly kelyphite formation postdates the deformation responsible for the development of the impressive mosaic porphyroclastic texture associated with recrystallisation to the Stage III assemblage in these rocks. There is in fact little or no post-kelyphite deformation apparent in most Otrøy garnet peridotite samples unlike at many other west Norway localities (notably at Almklovdalen) where kelyphites commonly have been deformed, attenuated and ultimately recrystallised into the later amphibole + chlorite bearing assemblages of Stages V and VI (e.g., Medaris, 1980, fig. 4A).

2.5. Stage V: olivine$_5$ + orthopyroxene$_5$ + amphibole$_1$ + spinel$_4$

The inner radial kelyphite intergrowths of secondary pyroxenes + spinel are frequently mantled by coarser-grained coronas of orthopyroxene + amphibole + spinel (Fig. 5D). This later orthopyroxene (Opx_5) frequently forms nearly continuous collars around the inner fibrous kelyphites. It characteristically has a lower Mg/(Mg + Fe) ratio and is distinctly more aluminous than the orthopyroxenes (Opx_2 and Opx_3) equilibrated with the earlier garnet-bearing assemblages. The spinel is a relatively aluminous variety ($X_{Al}^{Sp} \simeq 0.7$–0.8) and the amphibole a green, chrome-bearing, pargasite.

The lower temperatures and/or increased water activity at this stage in the metamorphic history

have commonly resulted in further growth of comparable amphibole grains in the rock matrix. There is often textural evidence that such amphibole has replaced, at least in part, the earlier matrix clinopyroxenes (Cpx_2 and Cpx_3).

2.6. Stage VI: olivine$_6$ + orthopyroxene$_6$ + amphibole$_3$ + chlorite$_1$

Further reduction in temperature and/or increased water activity has resulted in the stability of a chrome-bearing magnesian chlorite as the dominant Al-bearing phase in these rocks, at the expense of Opx_5, $Amph_2$ and Sp_4. This stage in the overall metamorphic evolution has been reached only in those peridotite bodies which have been subjected to significant late-stage deformation and is consequently absent in the analysed Otrøy samples. The chlorite frequently coexists with a low-Al tremolitic amphibole and an essentially Al-free orthopyroxene (e.g., 0.00–0.02 wt.% Al_2O_3 in nine Tafjord area samples; Al-Samman, 1985).

The foliated chlorite + tremolitic amphibole + enstatitic orthopyroxene bearing peridotites which dominate most of the peridotite bodies within the Western Gneiss Region of Norway have evolved to this metamorphic stage. It is reasonable to conclude that garnet + clinopyroxene bearing assemblages were previously present in such rocks but have been entirely replaced by low amphibolite facies assemblages in response to extensive deformation under retrograde metamorphic conditions. Certain metasomatic fracture veins, notably in peridotite bodies in the Tafjord area (Carswell et al., 1974; Al-Samman, 1985) comprise similar low amphibolite facies mineral phases – chlorite, tremolitic amphibole, enstatitic orthopyroxene and locally anthophyllite. More dispersed metasomatic growth of late (Stage VI) essentially Al-free enstatitic orthopyroxene at the expense of olivine, is also quite common in certain of these peridotite bodies.

2.7. Stage VII: serpentine + talc + amphibole$_4$ + chlorite$_2$

Petrographic evidence for the very late-stage replacement of earlier olivines by serpentine and of orthopyroxenes by talc and serpentine is common place along late fracture veins but more pervasively in the Otrøy peridotite bodies which are now for the most part heavily serpentinised. Essentially Al-free tremolitic amphibole and relatively ferriferous chlorite may also be stable phases at this stage but are difficult to discriminate from possible relict Stage VI phases. Increased CO_2 activity has resulted in localised magnesite formation at this stage and in addition magnetite grains are often conspicuously present as a result of oxidation during serpentinisation. Serpentinisation has invariably resulted in an increased $Fe^{3+}/(Fe^{2+} + Fe^{3+})$ ratio in the rocks concerned.

3. Pressure-temperature path for metamorphic evolution

From the foregoing account it is apparent that these peridotite bodies have had a prolonged and complex metamorphic history. The general form of the *P-T* path followed by these bodies (see Fig. 8) may be deduced through reference to available experimental data on the stability fields of the various peridotite assemblages (O'Hara, 1967; O'Hara et al., 1971; Evans, 1977; Jenkins, 1981, etc.). More precise values for the actual *P-T* conditions of equilibration of particular assemblages may be obtained through application of various experimental or semi-empirical calibrations of thermometers and barometers based on element exchange between coexisting minerals. Particularly useful in this respect are considerations of the extent of solid solution between coexisting pyroxenes (Wells, 1977), of Fe^{2+}-Mg^{2+} partitioning between garnet-clinopyroxene (Mori and Green, 1978; Ellis and Green, 1979), garnet-orthopyroxene (Harley, 1984) and garnet-olivine (O'Neill and Wood, 1979) pairs, and of the content of octahedrally coordinated aluminium (X_{Al}^{M1}) in orthopyroxenes involved in garnet-orthopyroxene (Wood, 1974; Harley and Green, 1982; Nickel and Green, 1985), and spinel-orthopyroxene-olivine (Sachtleben and Seck, 1981) equilibria.

Exsolution of coexisting pyroxene as well as garnet lamellae from the earliest pyroxenes (Opx_1 and Cpx_1) clearly indicates the high-temperature character of the Stage I spinel lherzolite protolith assemblage. The Stage I pyroxene compositions in samples E38 and U95 (Table 1) may well represent igneous phases which crystallised directly on the solidus curve for peridotite with small amounts of H_2O and/or CO_2 at *P-T* conditions of around

1100–1200°C and 10–20 kbar during an upper-mantle melting event. Certainly the subsequent Stage II garnet lherzolite assemblage can be confidently taken to have formed at markedly lower, sub-solidus, temperatures.

Overall six different generations of orthopyroxene have been recognised in these Norwegian peridotites. Moreover, exsolution and chemical zoning in individual grains indicate that the compositions of the earlier orthopyroxenes have been modified, at least in part, during the later stages of the metamorphic history. Considerable care must obviously be exercised over the selection of mineral compositions to be combined when considering the various element-exchange mineral equilibria. In particular the identification of the orthopyroxene compositions which equilibrated with Gnt_1 and Gnt_2 in these rocks is crucial to the deduction of equilibration pressures for the assemblages concerned.

Textural relationships provide important, but not always entirely unequivocal, evidence on equilibrium or disequilibrium between associated mineral phases. In addition a comparison between observed and experimentally determined element partition data can also be used to confirm whether selected assemblages (combined compositions) represent equilibrated systems. Such a test can be performed with reference to Figs. 7A and B, in which analytically determined Fe-Mg partition data in the three samples detailed in this paper (together with data for two other Otrøy garnet peridotite samples U29 and U88 – which show more extreme compositional zonation in garnets) are plotted with reference to experimentally determined element distributions (Mori and Green, 1978). Such diagrams confirm that sample U8 contains the best equilibrated and highest-temperature, porphyroclast core, garnet lherzolite assemblage. By contrast the garnet lherzolite clast core assemblages in samples U29, U88 and U92 (all characterised by lower-Al orthopyroxene core compositions) do not appear to represent suitably equilibrated assemblages.

Following confirmation that the clast core assemblage in U8 seems best representative of an equilibrated 4-phase garnet lherzolite assemblage formed during Stage II in the metamorphic evolution, corresponding *P-T* conditions for this metamorphic stage have been calculated (Table 6) from available calibrations of appropriate *P-T* dependent

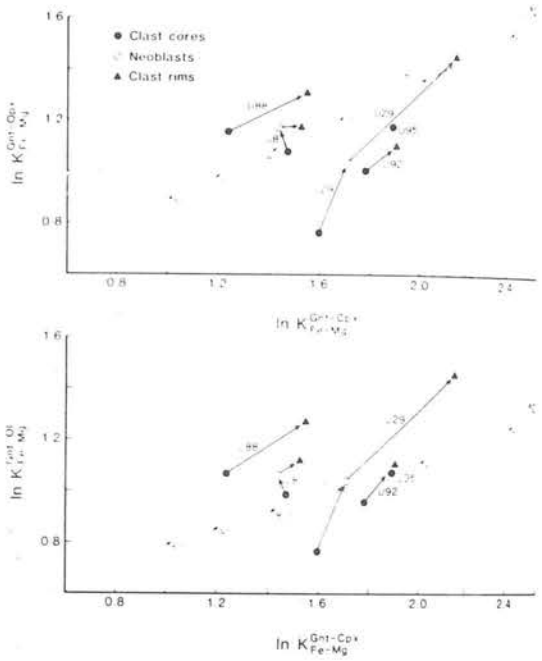

Fig. 7. Correlation diagrams for Fe-Mg partitioning between garnet-clinopyroxene, garnet-orthopyroxene and garnet-olivine pairs in specified garnet peridotite samples from Otrøy. Note that the values indicated for sample U95 are for grain core assemblages in the foliated garnet peridotite adjacent to the exsolved orthopyroxene megacrysts. The temperature-calibrated correlation lines have been calculated from the experimental data of Mori and Green (1978). In keeping with Mori and Green's formulation of the Fe/Mg partition coefficients all Fe present in these minerals was taken as Fe^{2+}.

mineral equilibria. However, even with a limited choice of permutations of available thermometers and barometers there is a considerable range in calculated temperatures (715–847°C) and pressures (18.4–29.3 kbar). Such variations may be attributed to factors such as different closure temperatures for element exchange in different minerals and hence different susceptibilities of minerals to modification during the subsequent cooling history of these rocks. There are further problems connected with the rather low X_{Al}^{M1} content of the orthopyroxene and the corrections necessary to take account of Fe^{2+}, Fe^{3+} and Cr^{3+} contents in the M1 sites.

All calculated paired *P-T* values for the Stage II assemblage in U8 lie within the experimentally determined garnet lherzolite stability field (O'Hara et al., 1971) and there are no additional constraints available which permit unprejudiced rejection or

TABLE 6

Calculated temperature/pressure estimates for equilibration of assemblages II and III in porphyroclastic garnet peridotite sample U8 from Raudhaugene, Otrøy, west Norway

Thermometer/barometer used in calculation	Assemblage II		Assemblage III
	Clast cores	Clast rims	Neoblasts
Wells (1977), Wood (1974)	759°C, 20.8 kbar	738°C, 24.6 kbar	745°C, 29.4 kbar
Ellis and Green (1979), Wood (1974)	805°C, 23.5 kbar	831°C, 30.4 kbar	840°C, 35.7 kbar
Mori and Green (1978) – $K_{Fe\text{-}Mg}^{Gnt\text{-}Cpx}$, Wood (1974)	779°C, 22.0 kbar	772°C, 26.7 kbar	792°C, 32.5 kbar
O'Neill and Wood (1979), Wood (1974)	715°C, 18.4 kbar		685°C, 25.4 kbar
Harley (1984); Harley and Green (1982)	847°C, 29.3 kbar	853°C, 35.5 kbar	836°C, 37.9 kbar
Wells (1977), Nickel and Green (1985)	759°C, 26.1 kbar	738°C, 30.4 kbar	745°C, 33.8 kbar
Wells (1977), O'Neill (1981) 5-phase assemblage			745°C, 21.2 kbar

selection of particular values. Mean values and standard deviations are 777 ± 41°C and 23.4 ± 3.6 kbar, but there is no real justification for averaging the various *P-T* estimates.

It is clear from the Fe^{2+}-Mg partition plots in Fig. 7 that the clast rim compositions in U8, as indeed in other samples, reflect the influence of decreased temperatures during the subsequent metamorphic stages. However, the extent of Fe^{2+}-Mg zonation in porphyroclasts in U8 is small compared that observed in samples such as U29. This probably reflects the fact that clast compositions in U8 have been essentially unaffected and unmodified by reactions associated with metamorphic stages IV and V, unlike in most of the other Otrøy garnet peridotite samples. Calculated mean *P-T* values and standard deviations for the clast rim assemblage in U8, using the same thermo-/barometric methods (Table 6) as for the clast cores, are 786 ± 55°C and 29.5 ± 3.7 kbar. Corresponding values for the neoblast assemblage in U8 are 773 ± 55°C and 32.4 ± 4.1 kbar. Although there is again no real justification for averaging the various values obtained, these mean values for the clast rim and neoblast assemblages do serve to emphasise their anomalous character, since general mineralogical considerations such as the Fe^{2+}-Mg partitioning between the mineral phases (Fig. 7) and the observed breakdown of a 4-phase garnet lherzolite assemblage to a 5-phase garnet + spinel lherzolite assemblage strongly indicate decreasing *P-T* conditions from Stages II to III.

The erroneous higher *P-T* values calculated for the Stage III neoblast assemblage stem from the reduced X_{Al}^{M1} contents of the orthopyroxenes concerned. However, the various *P-T* dependent calibrations of the garnet-orthopyroxene geobarometer utilised (Wood, 1974; Harley and Green, 1982; Nickel and Green, 1985) take no account of the influence of spinel as an additional Al-bearing phase in the peridotite assemblage. The experimental studies of MacGregor (1970) and O'Neill (1981) have demonstrated that the presence of Cr_2O_3 in natural peridotites will result in the stability of a 5-phase garnet + spinel lherzolite assemblage at pressures intermediate between the higher-pressure garnet lherzolite and lower-pressure spinel lherzolite fields. Accordingly, it is necessary to consider mineral equilibria in the 5-phase garnet + spinel + orthopyroxene + clinopyroxene + olivine assemblage rather than just the 4-phase assemblage (without spinel) in order to derive the equilibration conditions for the Stage III assemblage. Appropriate experimental data for this are currently rather limited. However, it seems significant that, at an estimated temperature of 745°C as indicated by the two-pyroxene solvus thermometer of Wells (1977), an appreciably lower pressure of 21.2 kbar is indicated for the Stage III neoblast assemblage in sample U8 using the geobarometric expression derived by O'Neill (1981) for such 5-phase assemblages. It should be noted that this pressure has been calculated after adoption of a −10% correction (H.St.C. O'Neill, pers. commun., 1982) to the provisional pressure calculated for the garnet lherzolite ⇌ spinel lherzolite reaction in the *CMAS* system, compared with the values indicated by O'Neill (1981).

There is some uncertainty over the composition of Opx_4 and Cpx_4 in inner fibrous Stage IV kelyphites due to the disseminated fine-grained spinel but the observed garnet breakdown reaction is clearly indicative of a further pressure drop. The Stage V high amphibolite facies assemblage in U92 (plus other Otrøy samples) indicates an equilibration temperature of around 600°C from consideration of the X^{M1}_{Al} content of Opx_5 coexisting with aluminous spinel (Sachtleben and Seck, 1981). Observations (e.g., Harvey, 1983) that sillimanite rather than kyanite was the stable Al-silicate polymorph in the amphibolite-facies assemblages widely displayed by the gneisses enclosing these west Norway peridotite bodies points to a further substantial decompression by Stage V. Mineralogical evidence thus indicates that the segment of the metamorphic path from Stages II → V is characterised by an overall drop in pressure (around 20 kbar) which is large relative to the decrease in temperature (150–200°C). On the other hand, development of aluminous chlorite (Stage VI) and finally of serpentine (Stage VII) most probably reflect late-stage cooling of these peridotite bodies immediately prior to their eventual exposure.

4. Petrogenetic and geochronological considerations

A synoptic pressure-temperature evolutionary path for these peridotite bodies based on the foregoing evidence is shown in Fig. 8. From general geochemical considerations (Carswell, 1968a, b; Brueckner, 1977; Carswell et al., 1983) an ultimate origin of these Mg + Cr rich peridotite bodies as predominately somewhat depleted upper-mantle material, though with localised enrichment related to trapped partial melts (Carswell, 1968a), does not seem to be in doubt. Much more uncertainty prevails over the age of formation of the protolith (Stage I) and high-pressure (Stages II and III) assemblages, the nature and timing of emplacement of the peridotite bodies into the crustal gneisses, and whether they represent slices of sub-continental mantle or dismembered lower portions of ophiolite complexes (subducted oceanic crust/uppermost mantle). The latter origin has been indicated by Griffin and Qvale (1985) following their recognition within the peridotites at the Almklovdalen locality of superferrian eclogites with prograde zoned garnets interpreted as metamorphosed basic dykes of the type frequently observed to intrude along transform fault zones.

New Sm-Nd data for associated garnet lherzolite and garnet websterite samples from Almklovdalen reported by Mearns (1986 in this special issue) provide some further important constraints on such

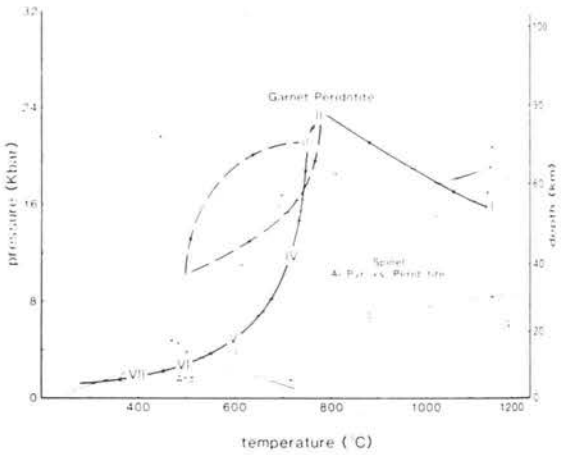

Fig. 8. Pressure-temperature path for the development of the various assemblages associated with evolution stages I → VII in these peridotite bodies. As discussed in the text, a possible alternative path (dashed heavy line) between II and III is also indicated commensurate with a long time interval between these stages. The retrograde segment of such an alternative path would correspond to long slow cooling to ambient sub-continental uppermost mantle conditions and the prograde segment to the influence of Caledonian continental plate collision. The various reaction curves shown (fainter lines) are as follows:

a. Calculated invariant curve for the reaction anorthite + forsterite (low P) = clinopyroxene + orthopyroxene + spinel (high P) in the system $CaO\text{-}MgO\text{-}Al_2O_3\text{-}SiO_2$ (Obata, 1976).

b. Garnet + olivine = pyroxenes + spinel reaction curve for the $CaO\text{-}MgO\text{-}Al_2O_3\text{-}SiO_2$ system from MacGregor (1970).

c. The same reaction curve determined by Jenkins and Newton (1979) from hydrothermal reversal runs in the *CMAS* system.

d. The univariant curve for the spinel lherzolite = garnet lherzolite reaction in Almklovdalen garnet peridotite sample N14A (O'Hara, 1975).

e. The same reaction curve for slightly more magnesian natural peridotite compositions (O'Hara et al., 1971).

f. Univariant reaction curve for pyrope + forsterite = enstatite + spinel in the $MgO\text{-}Al_2O_3\text{-}SiO_2$ system determined by Perkins et al. (1981).

g. Approximate location of the mantle peridotite melting curve in the presence of H_2O and Co_2 vapour ($X^V_{CO_2}$ = 0.75) (Wyllie, 1977).

h. Reaction curves defining the stability fields of the alumino-silicate polymorphs (Holdaway, 1971).

petrogenetic considerations. Importantly, and rather surprisingly in view of other Sm-Nd isotopic evidence of a Caledonian age (407–447 Ma) for the formation of eclogites enclosed directly in the west Norway gneisses (Griffin and Brueckner, 1980, 1985), a mid-Proterozoic age of around 1703 ± 29 Ma is indicated both for the age of formation (upper-mantle melting and depletion) of the peridotite protoliths (Stage I) and the crystallisation of the coarse-grained garnet lherzolite assemblage (Stage II). In view of the apparent short time interval between Stages I and II and the petrographic evidence (exsolution features, absence of prograde garnet zonation) the most straightforward interpretation (as favoured by Mearns) is of recrystallisation of spinel lherzolite (Stage I) to garnet lherzolite (Stage II) soon after the upper-mantle melting event as the rocks following a cooling path as illustrated in Fig. 8. The calculated Stage II *P-T* conditions lie close to the ambient conditions on a 55 mW m^{-2} continental geotherm (Chapman, 1986). Establishment of such a low geotherm so soon (< 60 Ma) after an upper-mantle melting event seems rather surprising, especially in an entirely sub-continental environment. Hence, actual continental splitting and establishment of an oceanic basin, however ephemeral, during this mid-Proterozoic event should not be completely discounted, especially as it might better explain the short cooling interval and the origin of the superferrian eclogites the age of which is currently unknown. A pressure increase during cooling and recrystallisation to the Stage II assemblage is indicated in Fig. 8, on the basis of the calculated *P-T* conditions for this assemblage. Some pressure increase seems feasible if, as seems likely, the cooling occurred during transition from an extensional (melting) regime to a compressional one, with possible overthrusting. However, it should be borne in mind that there are large uncertainties (possibly ± 5 kbar) associated with the pressure estimates for the Stage II assemblage. Furthermore, different experimental data sets indicate different slopes in *P-T* space for the spinel lherzolite → garnet lherzolite transition (see Fig. 8), but overall do not exclude the possibility of the transition occurring in response to effectively isobaric cooling.

Mearns (1986 in this special issue) also presents evidence that the gneisses enclosing the peridotite bodies at Almklovdalen are younger in age than the Stage II garnet peridotite assemblages. Accordingly, the latter must have formed prior to the emplacement of the peridotites bodies against their now enclosing gneisses. Hence, it is conjectured here that these peridotite bodies were emplaced into the lower continental gneisses during the major Caledonian continental plate collision (cf. Cuthbert et al., 1983, fig. 5) and that the deformation responsible for this tectonic intercalation was that which produced the impressive mosaic porphyroclastic fabrics in these rocks, associated with partial recrystallisation of the Stage II garnet lherzolite assemblage to a somewhat lower-pressure Stage III garnet + spinel lherzolite. The *P-T* conditions deduced for the stability of the Stage III 5-phase neoblast assemblage are similar to those indicated (e.g., Griffin et al., 1985) for the development of the Caledonian prograde metabasic eclogites enclosed in this gneiss complex. If this latter correlation is valid then there must have been an extremely long time interval (ca. 1200 Ma) between the development of the Stage II and III assemblages in these peridotites. It is unlikely that these peridotites would have been held at the *P-T* conditions for stabilisation of the Stage III garnet lherzolite assemblages throughout that period of time. If, as seems feasible, these peridotite bodies represent tectonic slices of sub-continental uppermost mantle detached and upthrust from the lower portion of the leading edge of the Baltic Plate during the Caledonian plate collision, they are more likely to have been held at appreciably lower *P-T* conditions (say 400–550°C and 10–15 kbar) prior to then, with their Stage II garnet lherzolite assemblages frozen in. In that case the enigmatic dyke protoliths for enclosed prograde superferrian eclogites as at Almklovdalen may have been intruded during the extensional continental rifting and opening of the Iapetus ocean which preceded the main Caledonian orogeny.

In comparison with the uncertainties concerning the details and timing of the *P-T* path linking the assemblages of Stages I → III in these peridotite bodies, the ensuing retrograde metamorphic path from Stages III → VII is uncontroversial. A late Caledonian age (ca. 385–420 Ma) for the development of the retrograde amphibolite and greenschist facies assemblages seems clear by analogy with the widespread early Palaeozoic K-Ar and Rb-Sr mineral ages determined from amphibolite-facies assemblages throughout the Western Gneiss Region. In addition, Brueckner (1972) has reported a Rb-Sr

whole rock-mineral isochron age of 408 Ma for an olivine + chlorite + amphibole assemblage in a late stage (i.e. Stage VI) vein within the peridotite body at Almklovdalen. Overall the retrograde metamorphic path for these peridotite bodies (Fig. 8) is characterised by an initial large drop in pressure relative to temperature (Stages III → V) followed by more notable cooling during Stages VI and VII, as these rocks approached the surface. Comparable retrograde paths have been deduced for metabasic eclogite bodies directly enclosed in the quartzo-feldspathic gneisses of this region of western Norway – for example, at Romsdalshorn (Krogh, 1982). Such uplift paths reflect the relatively rapid exhumation of such high-pressure rocks from their depths of origin, following significant lithospheric thickening in a major compressional tectonic regime (Cuthbert et al., 1983; Carswell and Cuthbert, 1986).

Acknowledgements

Research on these rocks over several years has been supported by grants from the Natural Environment Research Council and the University of Sheffield. In addition, the assistance of Fergus Gibb over provision of the electron microprobe facility at Sheffield and of Euan Mearns through provision of a preprint of his paper in this special issue were both much appreciated.

References

Al-Samman, A.H., 1985. Mineralogy and geochemistry of ultramafic rocks in the west Norway basement gneiss terrain. Ph.D. Thesis, University of Sheffield, Sheffield (unpublished).

Brueckner, H.K., 1972. Interpretation of Rb-Sr ages from the Precambrian and Palaeozoic rocks of southern Norway. Am. J. Sci., 272: 334–358.

Brueckner, H.K., 1977. A crustal origin for eclogites and a mantle origin for garnet peridotites: Strontium isotope evidence from clinopyroxenes. Contrib. Mineral. Petrol., 60: 1–15.

Bryhni, I., 1966. Reconnaissance studies of gneisses, ultrabasites, eclogites and anorthosites in outer Nordfjord, western Norway. Nor. Geol. Unders., 241: 1–68.

Carswell, D.A., 1968a. Picritic magma-residual dunite relationships in garnet peridotite at Kalskaret near Tafjord, southern Norway. Contrib. Mineral. Petrol., 19: 97–124.

Carswell, D.A., 1968b. Possible primary upper mantle peridotite in Norwegian basal gneiss. Lithos, 1: 322–355.

Carswell, D.A., 1973. Garnet pyroxenite lens within Ugelvik layered garnet peridotite. Earth Planet. Sci. Lett., 20: 347–352.

Carswell, D.A., 1981. Clarification of the petrology and occurrence of garnet lherzolites, garnet websterites and eclogite in the vicinity of Rødhaugen, Almklovdalen, west Norway. Nor. Geol. Tidsskr., 61: 249–260.

Carswell, D.A. and Cuthbert, S.J., 1986. Eclogite facies metamorphism in the Lower Continental Crust. In: J.B. Dawson, D.A. Carswell, J. Hall and K.H. Wedepohl (Editors), The Nature of the Lower Continental Crust. Geol. Soc. London, Spec. Publ. No. 25, pp. 193–209.

Carswell, D.A., Curtis, C.D. and Kanaris-Sotiriou, R., 1974. Vein metasomatism in peridotite at Kalskaret, near Tafjord, south Norway. J. Petrol., 15: 383–402.

Carswell, D.A., Harvey, M.A. and Al-Samman, A.H., 1983. The petrogenesis of contrasting Fe-Ti and Mg-Cr garnet peridotite types in the high grade gneiss complex of western Norway. Bull. Mineral., 106: 727–750.

Chapman, D.S., 1986. Thermal gradients in the continental crust. In: J.B. Dawson, D.A. Carswell, J. Hall and K.H. Wedepohl (Editors), The Nature of the Lower Continental Crust. Geol. Soc. London, Spec. Publ. No. 25, pp. 63–40.

Cuthbert, S.J., Harvey, M.A. and Carswell, D.A., 1983. A tectonic model for the metamorphic evolution of the basal gneiss complex, western south Norway. J. Metamorph. Geol., 1: 63–90.

Ellis, D.J. and Green, D.H., 1979. An experimental study of the effect of Ca upon garnet-clinopyroxene Fe-Mg exchange equilibria. Contrib. Mineral. Petrol., 71: 13–22.

Eskola, P., 1921. On the eclogites of Norway. Skr. Nor. Vidensk.-Akad. Oslo, 1. Mat.-Naturvidensk. Kl., 8: 1–118.

Evans, B.W., 1977. Metamorphism of Alpine peridotite and serpentinite. Annu. Rev. Earth Planet. Sci., 5: 397–447.

Griffin, W.L. and Brueckner, H.K., 1980. Caledonian Sm-Nd ages and a crustal origin for Norwegian eclogites. Nature (London), 285: 319–321.

Griffin, W.L. and Brueckner, H.K., 1985. REE, Rb–Sr and Sm–Nd studies of Norwegian eclogites. In: D.C. Smith and Ph. Vidal (Guest-Editors), Isotope Geochemistry and Geochronology of Eclogites. Chem. Geol. (Isot. Geosci. Sect.), 52: 249–271.

Griffin, W.L. and Heier, K.S., 1973. Petrological implications of some corona structures. Lithos, 6: 315–335.

Griffin, W.L. and Qvale, H., 1985. Superferrian eclogites and the crustal origin of garnet peridotites, Almklovdalen, Norway. In: D.G. Gee and B.A. Sturt (Editors), The Caledonide Orogen – Scandinavia and Related Areas. Wiley, Chichester, pp. 803–812.

Griffin, W.L., Austrheim, H., Brastad, K., Bryhni, I., Krill, A., Mørk, M.B.E., Qvale, H. and Tørudbakken, B., 1986. High pressure metamorphism in the Scandinavian Caledonides. In: D.G. Gee and B.A. Sturt (Editors), The Caledonide Orogen – Scandinavia and Related Areas. Wiley, Chichester, pp. 783–801.

Harley, S.L., 1984. An experimental study of the partition-

ing of Fe and Mg between garnet and orthopyroxene. Contrib. Mineral. Petrol., 86: 359–373.

Harley, S.L. and Green, D.H., 1982. Garnet-orthopyroxene barometry for granulites and peridotites. Nature (London), 300: 697–701.

Harvey, M.A., 1983. A geochemical and structural study of the gneisses and eclogites on the Molde Peninsula, west Norway. Ph.D. Thesis, University of Sheffield, Sheffield (unpublished).

Holdaway, M.J., 1971. Stability of andalusite and the aluminium phase diagram. Am. J. Sci., 271: 97–131.

Jamtveit, B., 1984. High-*P* metamorphism and deformation of the Gurskebotn Garnet Peridotite, western Norway. Nor. Geol. Tidsskr., 64: 97–110.

Jamtveit, B., 1985. Magmatic and chemical controls on chemical variations within the Eiksundal complex. Terra Cognita, 5: 422 (abstract).

Jenkins, D.M., 1981. Experimental phase relations of hydrous peridotites modelled in the system H_2O-CaO-MgO-Al_2O_3-SiO_2. Contrib. Mineral. Petrol., 77: 166–176.

Jenkins, D.M. and Newton, R.C., 1979. Experimental determination of the spinel peridotite to garnet peridotite inversion at 900°C and 1100°C in the system CaO-MgO-Al_2O_3-SiO_2 and at 900°C with natural garnet and olivine. Contrib. Mineral. Petrol., 75: 387–393.

Krogh, E.J., 1977. Evidence of Precambrian continent-continent collision in western Norway. Nature (London), 267: 17–19.

Krogh, E.J., 1982. Metamorphic evolution of Norwegian country-rock eclogites, as deduced from mineral inclusions and compositional zoning in garnets. Lithos, 15: 305–321.

Lappin, M.A., 1966. The field relationships of basic and ultrabasic masses in the basal gneiss complex of Stadlandet and Almkovdalen, Nordfjord, S.W. Norway. Nor. Geol. Tidsskr., 46: 439–495.

Lappin, M.A., 1973. An unusual clinopyroxene with complex lamellar intergrowths from an eclogite in the Sunndal-Grubse ultramafic mass, Almklovdalen, Nordfjord, Norway. Mineral. Mag., 39: 313–320.

Lappin, M.A., 1974. Eclogites from the Sunndal-Grubse ultramafic mass, Almklovdalen, Norway and the *T-P* history of the Almklovdalen masses. J. Petrol., 15: 567–601.

MacGregor, I.D., 1970. The effect of CaO, Cr_2O_3, Fe_2O_3, and Al_2O_3 on the stability of the spinel and garnet peridotite. Phys. Earth Planet. Int., 3: 372–377.

Mearns, E.W., 1986. Sm-Nd ages for Norwegian garnet peridotite. In: W.L. Griffin (Editor), Second International Eclogite Conference. Lithos, 19: 269–278 (this special issue).

Medaris, Jr., L.G., 1980. Petrogenesis of the Lien peridotite and associated eclogites, Almklovdalen, western Norway. Lithos, 13: 339–353.

Medaris, Jr., L.G., 1984. A geothermobarometric investigation of garnet peridotites in the western gneiss region of Norway. Contrib. Mineral. Petrol., 87: 72–86.

Mori, T. and Green, D.H., 1978. Laboratory duplication of phase equilibria observed in natural garnet lherzolites. J. Geol., 86: 83–97.

Nickel, K.G. and Green, D.H., 1985. Empirical geothermobarometry for garnet peridotites and implications for the nature of the lithosphere, kimberlites and diamonds. Earth Planet. Sci. Lett., 73: 158–170.

Obata, M., 1976. The solubility of Al_2O_3 in orthopyroxene in spinel and plagioclase peridotites and spinel pyroxenite. Am. Mineral., 61: 804–816.

O'Hara, M.J., 1967. Mineral paragenesis in ultrabasic rocks. In: P.J. Wyllie (Editor), Ultramafic and Related Rocks. Wiley, New York, N.Y., pp. 393–403.

O'Hara, M.J., 1975. Pressure required to stabilise garnet-peridotite and eclogite at low temperatures. Abstr. Int. Conf. on Geothermometry and Geobarometry, Pennsylvanian State University, University Park, Pa., 4 pp.

O'Hara, M.J. and Mercy, E.L.P., 1963. Petrology and petrogenesis of some garnetiferous peridotites. Trans. R. Soc. Edinburgh, 65: 251–314.

O'Hara, M.J., Richardson, S.W. and Wilson, G., 1971. Garnet peridotite stability and occurrence in crust and mantle. Contrib. Mineral. Petrol., 32: 48–68.

O'Neill, H.St.C., 1981. The transition between spinel lherzolite and garnet lherzolite, and its use as a geobarometer. Contrib. Mineral. Petrol., 77: 185–194.

O'Neill, H.St.C. and Wood, B.J., 1979. An experimental study of Fe-Mg partitioning between garnet and olivine and its calibration as a geothermometer. Contrib. Mineral. Petrol., 70: 59–70.

Perkins, III, D., Holland, T.J.B. and Newton, R.C., 1981. The Al_2O_3 contents of enstatite in equilibrium with garnet in the system MgO-Al_2O_3-SiO_2 at 15–40 kbar and 900°–1600°C. Contrib. Mineral. Petrol., 78: 99–109.

Sachtleben, Th. and Seck, H.A., 1981. Chemical control on the Al-solubility in orthopyroxene and its implications on pyroxene geothermometry. Contrib. Mineral. Petrol., 78: 157–165.

Schmitt, H.H., 1964. Metamorphic eclogites of the Eiksund area, Sunnmøre, Norway. Abstr. Am. Geophys. Union, 43: 128.

Wells, P.R.A., 1977. Pyroxene thermometry in simple and complex systems. Contrib. Mineral. Petrol., 62: 129–139.

Wood, B.J., 1974. Solubility of alumina in orthopyroxene coexisting with garnet. Contrib. Mineral. Petrol., 46: 1–15.

Wyllie, P.J., 1977. Effects of H_2O and CO_2 on magma generation in the crust and mantle. J. Geol. Soc. London, 134: 215–234.

B. Papers concerned with xenolith samples brought up in mantle derived magmas

Contr. Mineral. and Petrol. 25, 163—184 (1970)

Garnet Peridotite Xenoliths in South African Kimberlite Pipes and Their Petrogenesis

D. A. CARSWELL
Department of Geology, University of Sheffield, St. George's Square, Sheffield 1, England
J. B. DAWSON
Department of Geology, University of St. Andrews, Fife, Scotland

Received October 10, 1969

Abstract. Whole rock analyses are presented for nine garnet peridotite, two garnet pyroxenite, one garnet free peridotite and two highly altered garnet peridotite xenoliths from South African kimberlite pipes. Garnets from eight of these samples have also been chemically analysed, while olivine compositions in the twelve fresh samples have been estimated by X-ray diffraction. The chemistry and mineralogy of these specimens are compared with the results of previous studies, and the controversies concerning the petrogenesis of these xenoliths are discussed in detail.

I. Introduction

Garnet peridotite xenoliths in kimberlite pipes have been widely recognised as being extremely important in speculations about the chemistry and mineralogy of the earth's upper mantle. Whole rock analyses of such xenoliths may surprisingly, however, still be counted in single figures and certain of these are of dubious reliability. It is therefore not surprising that Wyllie (1967) in his review section on the petrogenesis of ultramafic and ultrabasic rocks was cautious in his conclusions about the xenoliths, pointing out that ... 'the chemical variation of garnet peridotite nodules is inadequately known.'

The paucity of garnet peridotite analyses is even more remarkable when it is seen that the geological literature contains about six times as many analyses of eclogite xenoliths from kimberlite pipes, yet eclogite xenoliths are widely reported (Wagner, 1928; Williams, 1932; Dawson, 1962; Nixon *et al.*, 1963; Rickwood *et al.*, 1968) to be much scarcer than those of garnet peridotite. The reason for this numerical disparity amongst published analyses probably lies both in the more uniform chemical and mineralogical composition of the garnet peridotite xenoliths and the more spectacular appearance in the field of the eclogites. Much more mineral data on garnet peridotites is available, in particular for garnets, but is still subordinate to the data available on the eclogites.

It is hoped that the analyses presented in this paper will go some way towards redressing the balance, and will therefore place theories on the relevance of garnet peridotite as a possible upper mantle rock type on a firmer footing.

II. Field Occurrence

The fourteen rocks investigated in this study were collected from five kimberlite occurrences in South Africa (Fig. 1). The specimens are listed in Table 1, with the

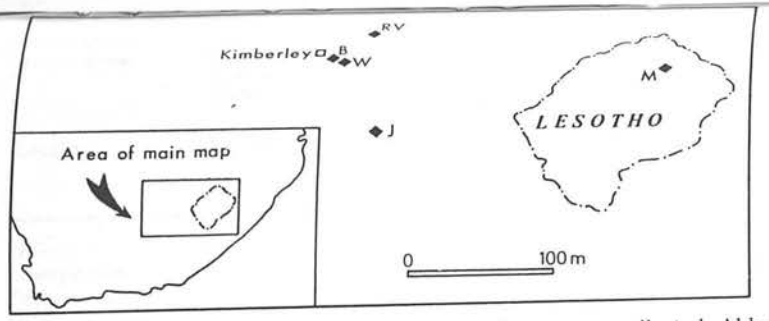

Fig. 1. Map showing the localities where the specimens were collected. Abbreviation: *B* Bultfontein, *J* Jagersfontein, *M* Matsoku, *RV* Roberts Victor, *W* Wesselton

estimated volume proportions of the minerals. Of these samples, nine were of garnet peridotite, two of garnet pyroxenite, one of garnet-free peridotite, and two are extensively silicified and carbonated garnet peridotite. The terms garnet peridotite and garnet pyroxenite are used in the mineralogical sense defined by Rickwood *et al.* (1968), i.e. garnet peridotite consists of $<19\%$ garnet, and olivine $>$ orthopyroxene + clinopyroxene; garnet pyroxenite consists of $<19\%$ garnet, and olivine $<$ orthopyroxene + clinopyroxene.

Nine of the samples are from the Jagersfontein, Bultfontein, Wesselton and Roberts Victor mines, which have been described by Wagner (1914) and Williams (1932), and were collected from the old dumps surrounding the mines. The garnet peridotites at Jagersfontein are part of a xenolith suite comprising eclogite (some with kyanite and corundum), dunite and phlogopite peridotites. The garnet peridotites at Bultfontein are accompanied by a wide variety of peridotite types composed of various combinations of garnet, ortho- and clino-pyroxene and olivine, and also more unusual rock types such as glimmerite, mica pyroxenite, amphibole mica pyroxenite, and magnetite rich dunite. At Wesselton the accompanying rocks are garnet pyroxenite, phlogopite wehrlite, pyroxenite and bronzite peridotite. The garnet peridotites from Roberts Victor mine are subordinate to the eclogite xenoliths for which this locality is justifiably famous. The extremely altered nature of the garnet peridotites studied from here is in keeping with the extensive hydration, carbonation and silicification that is characteristic of most of the xenoliths from this intrusion.

The Lesotho samples were collected from the Matsoku pipe, a small diatreme in eastern Lesotho that has only been briefly described previously (Dawson, 1968). The intrusion is a small elliptically shaped pipe, measuring 50 by 100 yards, which crops out on a Karroo basalt ridge between the valleys of the Matsoku and Lipitsaneng rivers (29°05′ S, 28°44′ E). The pipe is exposed at a height of 9,300 feet and is topographically one of the highest kimberlites in the world. The intrusion is unusual in that it contains an unusually high percentage of 'deep-seated' xenoliths. These comprise 20—30 per cent of the pipe filling (Fig. 2a), and some of the xenoliths are much larger than those recorded in other kimberlite diatremes. One elliptically shaped block of garnet peridotite measured 2′5″ along its longest axis (Fig. 2b). The garnet peridotites, which are only slightly serpentinized when compared with similar rocks from other kimberlites (see water content, Table 2), are accompanied by xenoliths of garnet pyroxenite, mica garnet peridotite, eclogite, mica granulite and scapolite granulite.

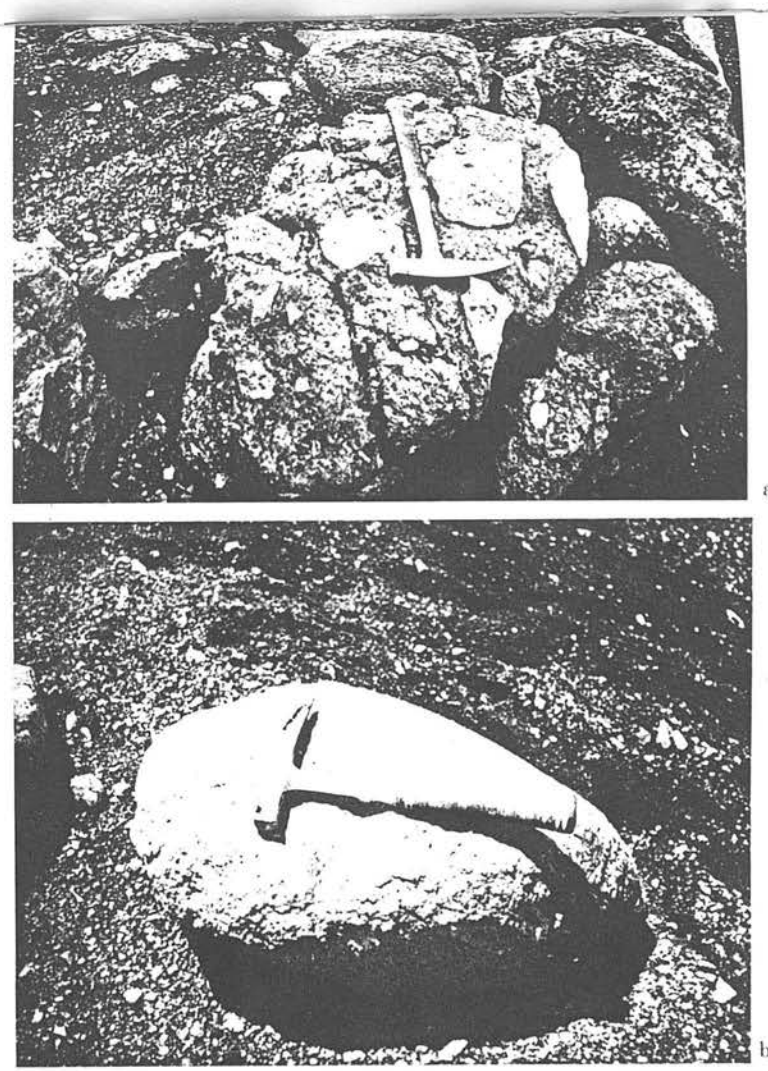
a

b

Fig. 2. a Xenolith-rich kimberlite, Matsoku pipe, Lesotho. b An unusually large xenolith of garnet peridotite, Matsoku pipe, Lesotho

III. Chemical Composition

The whole rock analyses and C.I.P.W. norms of the fourteen samples are listed in Table 2.

Table 1. *Modal proportions by volume in analysed samples*

Sample No. Rock name	BD 1354 Garnet pyroxenite	BD 1355 Garnet peridotite	BD 1356 Garnet peridotite	BD 1360 Garnet peridotite	BD 1364 Garnet pyroxenite	BD 1127 Garnet peridotite
Locality	Matsoku	Matsoku	Matsoku	Matsoku	Matsoku	Jagersfontein
Olivine + serpentine	38	54	56	62	17	75
Orthopyroxene	28	34	30	24	35	16
Clinopyroxene	14	4	5	4	30	3
Garnet	17	7	5	4	18	5
Phlogopite	—	—	3	4	—	—
Amphibole	trace	trace	—	—	trace	1
Chlorite	—	—	—	—	—	—
Spinel	3	1	1	trace	trace	trace
Calcite	trace	trace	trace	trace	trace	trace
Quartz	—	—	—			
Rutile	—	—	—	2		

BD 1133 Garnet peridotite	BD 1140 Garnet peridotite	BD 1143 Garnet peridotite	BD 1150 Garnet peridotite	BD 1200 Peridotite	BD 1201 Garnet peridotite	BD 1195 Altered garnet peridotite	BD 1196 Altered garnet peridotite
Jagersfontein	Bultfontein	Bultfontein	Bultfontein	Wesselton	Wesselton	Roberts Victor Mine	Roberts Victor Mine
58	67	62	52	64	62	—	—
30	12	27	17	32	27	—	—
2	7	2	15	—	5	—	2
4	12	8	9	—	3	7	6
4	2	1	7	1	2	8	2
2		trace		trace	—	—	—
—				—	—	1	1
trace	trace	trace	trace	2	1	trace	1
trace	trace	trace	trace	1	trace	13	51
						71	37
						—	—

Methods of Analysis

Si, Ti, Mn, P and Fe (total) were determined by recognised spectrophotometric methods, Na and K by flame photometry, H_2O and CO_2 gravimetrically, and Fe^{2+} by titration with dichromate. Mg, Ca and Al were determined by atomic absorption as was Cr in the garnets, while the Cr and Ni values for the whole rocks are averages of atomic absorption and X-ray fluorescence determinations.

It is apparent that all nine garnet peridotites have a fairly restricted composition range, significantly so in Al_2O_3 (1.04—2.93 wt.%), CaO (0.83—3.35 wt.%) and $Fe^{2+} + Fe^{3+}/Mg^{2+}$ ratio (0.076—0.121). It will be observed, however, that BD 1360 has an exceptionally high TiO_2 content, more than ten times the concentration in any of the other samples. This can be attributed to thin veins of secondary rutile which cut through this sample.

The two garnet pyroxenites, on the other hand, have significantly higher Al_2O_3 (4.81 and 4.85 wt.%), CaO (4.34 and 7.28 wt.%) and Cr_2O_3 (0.60 and 0.84 wt.%) contents reflecting their higher modal garnet and clinopyroxene contents, and also higher $Fe^{2+} + Fe^{3+}/Mg^{2+}$ ratios (0.153—0.214).

The garnet and clinopyroxene free peridotite (BD 1200) has, as might be expected, the lowest Al_2O_3 and CaO contents of all the analysed samples.

In thin section limited secondary alteration may be seen to have affected most samples. This takes the form of partial serpentinization of olivine, carbonation — the growth of interstitial calcite plates, and phlogopitization — mainly in the form of rims of phlogopite around garnet. The contents of H_2O, CO_2 and also to a considerable extent K_2O reflect this alteration, but it is thought unlikely that the primary concentrations of the other principal chemical components have been appreciably altered.

On the other hand the two samples analysed from Roberts Victor mine (BD 1195 and BD 1196) represent extensively altered garnet peridotite xenoliths. Both have appreciable contents of secondary calcite and quartz while olivine is now totally lacking and contain chrome pyrope rich garnets both compositionally very similar and in the same volume percentage to garnets in the garnet peridotite xenoliths. BD 1196 also contains unaltered crystals of chrome diopside. Williams (1932, p. 392—394) has described in detail a similar silicified garnet peridotite xenolith from Roberts Victor mine. This sample also had an appreciable content of secondary calcite, though not nearly as much in BD 1196.

It has already been pointed out that complete and reliable analyses of garnet peridotite xenoliths are scarce. However, in Table 3 columns A and B the mean of the nine analyses presented in this paper may be compared with that of six previous analyses. There can be seen to be close agreement for most elements except TiO_2, the exceptionally high TiO_2 content of BD 1360 being the reason for this descrepancy. Most of the TiO_2 in this sample is almost definitely of secondary origin associated with the veins of rutile.

The full composition range in these fifteen garnet peridotites is given in column C, and may be seen to be quite restricted. It is therefore apparent that garnet peridotite xenoliths represent a distinctive rock type essentially uniform chemically and mineralogically.

On the other hand eclogite xenoliths from kimberlite pipes have a much wider composition range characterized by much higher Al_2O_3, CaO, FeO^T, Na_2O and K_2O contents and lower MgO, NiO and Cr_2O_3 contents. The wide composition gap between eclogite and garnet peridotite xenoliths is well illustrated on the CMF plot Fig. 3.

It is significant that the two garnet pyroxenite samples analysed, BD 1354 and BD 1364, have compositions intermediate between the eclogites and garnet peridotites on the CMF plot. Furthermore, their Al_2O_3, Na_2O and NiO contents

Table 2

	Sample No.					
	BD 1354	BD 1355	BD 1356	BD 1360	BD 1364	BD 1127
A. Whole Rock Analyses						
SiO_2	47.55	46.84	45.80	44.31	49.91	42.57
TiO_2	0.20	0.04	0.07	2.25	0.08	0.09
Al_2O_3	4.81	1.50	1.16	2.28	4.85	1.04
Cr_2O_3	0.84	0.36	0.38	0.34	0.60	0.29
Fe_2O_3	2.45	2.30	2.89	2.47	2.16	2.67
FeO	8.90	3.69	3.28	5.95	5.35	3.50
MnO	0.18	0.10	0.10	0.12	0.18	0.09
NiO	0.19	0.34	0.31	0.30	0.18	0.31
MgO	29.09	41.80	41.76	37.82	26.80	43.32
CaO	4.34	1.03	1.12	1.51	7.28	0.95
Na_2O	0.44	0.06	0.12	0.19	0.70	0.12
K_2O	0.08	0.04	0.13	0.26	0.04	0.04
P_2O_5	0.02	0.02	0.01	0.03	0.02	0.01
CO_2	0.08	0.10	0.17	0.18	0.18	0.30
H_2O^+	1.23	1.71	2.55	1.61	1.40	4.62
Total	100.40	99.93	99.85	99.62	99.73	99.92
$\frac{Fe^{2+}+Fe^{3+}}{Mg^{2+}}$	0.214	0.077	0.079	0.121	0.153	0.076
B. C.I.P.W. Norms						
Or	0.47	0.24	0.77	1.54	0.24	0.23
Ab	3.72	0.51	1.02	1.61	5.92	1.02
An	10.91	3.71	2.24	4.60	9.97	2.18
Di	6.64	0.48	1.64	1.15	17.50	0.43
Hd	1.28	0.02	0.06	0.07	2.10	0.02
En	34.66	39.19	35.48	32.78	35.26	23.58
Of	6.66	1.99	1.34	1.96	4.25	0.99
Fo	24.28	45.33	47.48	42.65	16.30	58.93
Fa	5.14	2.54	1.97	2.81	2.16	2.73
Mt	3.55	3.33	4.19	3.58	3.13	3.87
Ilm	0.38	0.08	0.13	4.27	0.15	0.17
Cr	1.24	0.53	0.56	0.50	0.88	0.43
Ap	0.05	0.05	0.02	0.07	0.04	0.02
Calc	0.18	0.23	0.39	0.41	0.41	0.68
H_2O	1.23	1.71	2.55	1.61	1.40	4.62
Co	—	—	—	—	—	—
Qz	—	—	—	—	—	—

BD 1133	BD 1140	BD 1143	BD 1150	BD 1200	BD 1201	BD 1195	BD 1196
46.14	42.98	45.32	44.95	45.43	45.82	81.89	43.82
0.15	0.16	0.05	0.11	0.09	0.07	0.10	0.16
1.14	2.46	1.97	2.93	0.90	1.49	1.95	1.52
0.41	0.32	0.39	0.50	0.34	0.33	0.42	0.28
1.61	2.99	2.39	2.23	1.89	1.84	0.50	1.09
4.60	4.26	3.91	4.82	4.35	5.00	1.19	0.80
0.10	0.10	0.10	0.13	0.09	0.11	0.07	0.42
0.32	0.30	0.34	0.26	0.40	0.34	0.24	0.15
41.93	39.94	40.95	36.12	43.97	41.35	6.26	4.70
1.03	1.67	0.83	3.35	0.56	1.30	2.95	24.91
0.11	0.20	0.10	0.38	0.05	0.12	0.15	0.10
0.26	0.08	0.07	0.28	0.07	0.14	0.25	0.05
0.03	0.02	0.02	0.03	0.02	0.03	0.05	0.02
0.17	0.17	0.38	0.20	0.24	0.13	1.73	19.35
2.08	4.50	3.60	3.56	2.08	1.91	1.84	2.30
100.08	100.15	100.42	99.85	100.48	99.98	99.59	99.67
0.081	0.098	0.083	0.106	0.077	0.090	0.147	0.213
1.54	0.47	0.41	1.65	0.41	0.83	1.48	0.30
0.93	1.69	0.85	3.22	0.42	1.02	1.27	0.85
1.85	5.58	1.58	5.46	1.13	3.11	3.37	1.13
1.46	1.11	—	7.06	—	1.69	—	—
0.10	0.06	—	0.56	—	0.13	—	—
32.26	24.35	38.51	24.07	32.08	31.04	15.59	11.70
2.24	1.35	2.10	1.90	2.01	2.43	1.80	1.11
50.09	52.27	44.48	43.85	54.25	49.86	—	—
3.84	3.20	2.68	3.81	3.74	4.30	—	—
2.33	4.34	3.47	3.23	2.74	2.67	0.72	1.58
0.28	0.30	0.09	0.21	0.17	0.13	0.19	0.30
0.60	0.47	0.57	0.74	0.50	0.49	0.62	0.41
0.07	0.05	0.05	0.07	0.05	0.07	0.12	0.05
0.39	0.39	0.86	0.45	0.55	0.30	3.93	44.01
2.08	4.50	3.60	3.56	2.08	1.91	1.84	2.30
—	—	1.15	—	0.33	—	0.20	0.89
—	—	—	—	—	—	68.46	35.05

are also intermediate in character. On the other hand they have higher Cr_2O_3 contents than even the garnet peridotites.

The compositions of analysed garnets from certain of the kimberlite xenoliths are given in Table 4, together with structural formulae and the percentage of the various garnet end-member molecules calculated according to the procedure outlined by Rickwood (1968). All the garnets are characterised by high pyrope and significant uvarovite contents, while two of them also contain the rarer chrome garnet molecule knorringite.

Hanléite (Fermor, 1952) has been discredited (Sastri, 1963) as the name for the chrome garnet molecule, $Mg_3Cr_2(SiO_4)_3$, and superseded by the name knorringite (Nixon and Hornung, 1968).

Table 5 column A gives the mean composition, in terms of garnet end-member molecules, of forty garnets from garnet peridotite xenoliths. This may be contrasted with the mean composition of forty-five garnets from eclogite xenoliths given in column B. The garnets from the eclogites are characterized by considerably higher grossular and almandine, lower pyrope and negligible uvarovite

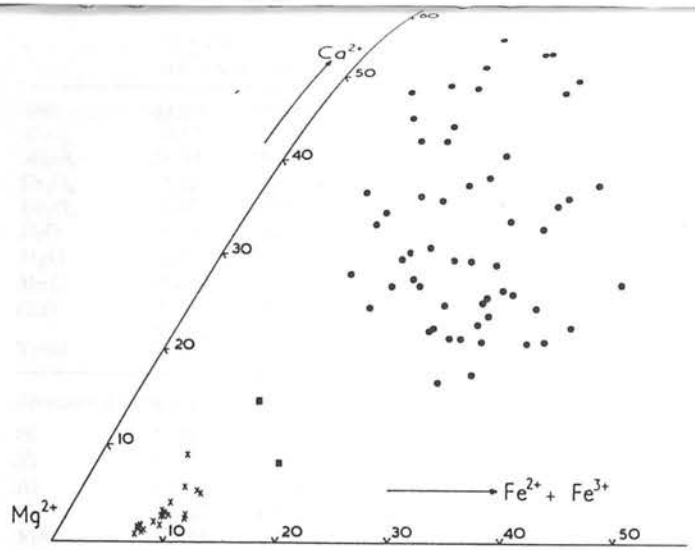

Fig. 3. Ca^{2+}: Mg^{2+}: $Fe^{2+} + Fe^{3+}$ plot of the whole rock compositions of garnet bearing peridotite (crosses), pyroxenite (squares) and eclogite (dots) xenoliths from kimberlite pipes. Data from Holmes (1936), Ito and Kennedy (1967); Kryukov (1966); Kushiro and Aoki (1968); Mikhailov and Rovsha (1966); Nixon *et al.* (1963); Sobolev and Kuznetsova (1965, 1966); Sobolev *et al.* (1968); Wagner (1928), Williams (1932) and this paper

Table 3. *Whole rock analyses of garnet peridotites recalculated to 100.00%. H_2O and CO_2 free and with total iron as FeO*

	A	B	C
SiO_2	46.53	45.46	44.54—47.85
TiO_2	0.33	0.16	0.02— 2.30
Al_2O_3	1.84	2.65	1.09— 3.26
Cr_2O_3	0.38	0.31	0.21— 0.52
FeO^T	6.70	6.99	5.89— 8.38
MnO	0.11	0.12	0.09— 0.15
NiO	0.32	0.30	0.25— 0.43
MgO	41.98	41.90	37.68—45.74
CaO	1.47	1.89	0.86— 3.50
Na_2O	0.16	0.19	0.06— 0.40
K_2O	0.15	0.14	0.00— 0.35
P_2O_5	0.02	0.03	0.00— 0.05
$\frac{Fe^{2+}(T)}{Mg^{2+}}$	0.082	0.094	0.076— 0.121

FeO^T = total iron as FeO.

A = Mean of nine analyses present in this paper. B = Mean of six previous analyses of garnet peridotite xenoliths. Only four and five determinations for NiO and Cr_2O_3, respectively. Analyses used were: A3 (O'Hara and Mercy, 1963) — equivalent to Wesselton No. 3 (Holmes, 1936); A6 (O'Hara and Mercy, 1963) — personal communication; E3 and E11 (Nixon *et al.*, 1963); No. 6 (Kryukov, 1966); and KA64-16 (Ito and Kennedy, 1967). C = Composition range in all fifteen analysed garnet peridotites.

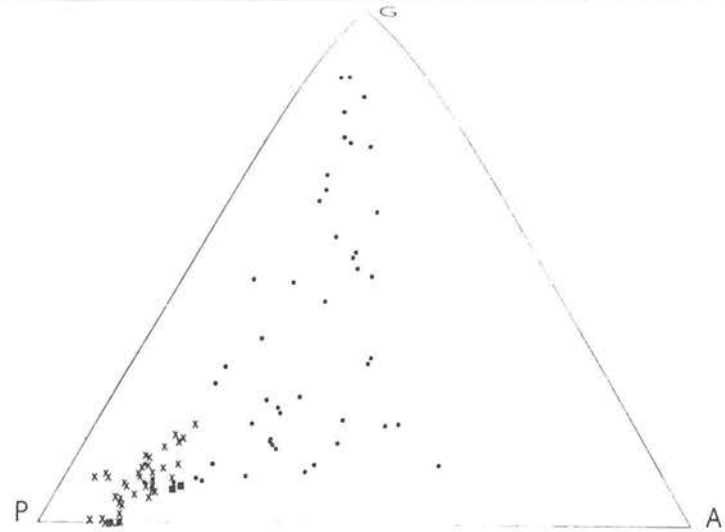

Fig. 4. Composition diagram for garnets from peridotite (crosses), pyroxenite (squares) and eclogite (dots) xenoliths in kimberlite pipes. The garnet compositions were plotted according to the proportions of the various garnet end-member molecules, calculated by the scheme of Rickwood (1968), and grouped as follows: *P*-pyrope ($Mg_3Al_2Si_3O_{12}$) + uvarovite ($Ca_3Cr_2Si_3O_{12}$) + knorringite ($Mg_3Cr_2Si_3O_{12}$). *G*-grossular ($Ca_3Al_2Si_3O_{12}$) + andradite ($Ca_3Fe^{3+}_2Si_3O_{12}$) + schlorlomite ($Ca_3Fe^{3+}_2Ti_3O_{12}$). *A*-almandine ($Fe^{2+}_3Al_2Si_3O_{12}$) + spessartine ($Mn_3Al_2Si_3O_{12}$) + skiagite ($Fe^{2+}_3Fe^{3+}_2Si_3O_{12}$). Data from Kushiro and Aoki (1968); MacGregor and Ringwood (1964); Nixon *et al.* (1963); O'Hara and Mercy (1963, 1966), O'Hara and Yoder (1967); Sobolev (1963, 1964); Sobolev and Kuznetsova (1965, 1966); Sobolev *et al.* (1968) and this paper

contents. In compiling these averages certain analyses in the literature have been deliberately omitted because either they are incomplete or $< 90\%$ of the cations can be allocated to end-member molecules.

The compositional distinctions amongst garnets are further illustrated on the ternary composition diagram presented as Fig. 4. As with the whole rock compositions, the compositions of garnets from garnet peridotite xenoliths are far more uniform than those from eclogite xenoliths.

Some overlap of the garnet compositions from these two different types of xenoliths is indicated on Fig. 4, the analyses of the six garnets from eclogites responsible for the overlap all being from Sobolev (1963, Nos. 70—73, 76 and 78). All these six garnets are described as being from eclogite xenoliths, but detailed petrographic descriptions were not given. The absence of similar garnets from South African eclogite xenoliths suggests that they may in fact be from olivine bearing xenoliths (peridotites and/or pyroxenites). As both garnet peridotite and eclogite (sensu stricto) are eclogite facies assemblages some confusion has arisen in the literature through some authors referring to both rock types as eclogites (e.g. Eskola, 1921). The mean composition of thirty-nine garnets from eclogite xenoliths, excluding the six ambiguous analyses, is given in Table 5, column C.

Table 4. *Garnet Analyses*

	Sample No.							
	BD 1355	BD 1356	BD 1364	BD 1127	BD 1140	BD 1201	BD 1195	BD 1196
SiO_2	41.90	42.03	41.33	42.28	41.75	41.82	42.01	41.55
TiO_2	0.17	0.31	0.28	0.38	0.11	0.18	0.21	0.45
Al_2O_3	21.44	20.73	21.83	21.05	22.39	21.71	21.22	20.29
Cr_2O_3	4.21	4.26	1.73	4.22	1.73	2.66	3.88	4.74
Fe_2O_3	1.35	0.96	1.44	1.34	1.34	1.14	1.15	1.46
FeO	4.79	5.49	9.00	4.41	6.84	6.83	5.10	5.31
MgO	23.91	20.87	19.60	21.53	20.94	20.26	20.71	20.55
MnO	0.30	0.32	0.44	0.25	0.38	0.43	0.29	0.30
CaO	1.58	5.37	4.40	4.95	4.20	4.78	5.46	4.97
Total	99.65	100.34	100.05	100.41	99.68	99.81	100.03	99.62
Structural formulae								
Si	2.957	2.984	2.967	2.982	2.972	2.985	2.983	2.976
Ti	0.009	0.017	0.015	0.020	0.006	0.010	0.011	0.024
Al	1.783	1.735	1.847	1.750	1.879	1.826	1.776	1.713
Cr	0.235	0.239	0.098	0.235	0.097	0.150	0.218	0.268
Fe^{3+}	0.072	0.051	0.078	0.071	0.072	0.061	0.061	0.079
Fe^{2+}	0.283	0.326	0.540	0.260	0.407	0.408	0.303	0.318
Mg	2.514	2.208	2.097	2.263	2.222	2.155	2.192	2.193
Mn	0.018	0.019	0.027	0.015	0.023	0.026	0.017	0.018
Ca	0.119	0.408	0.338	0.374	0.320	0.366	0.415	0.381
O	12.000	12.000	12.000	12.000	12.000	12.000	12.000	12.000
Molecular perecentages								
Uvarovite	4.1	12.1	4.9	12.1	4.9	7.6	11.2	13.1
Andradite	—	1.7	3.4	0.7	3.6	3.1	3.0	—
Pyrope	77.8	74.6	70.3	77.7	74.8	73.0	74.9	74.6
Spessartine	0.6	0.7	0.9	0.5	0.8	0.9	0.6	0.6
Grossular	—	—	2.5	—	2.2	1.6	—	—
Almandine	9.6	11.0	17.4	8.9	13.7	13.8	10.4	10.9
Knorringite	7.9	—	—	—	—	—	—	0.7
Schlorlomite	—	—	0.5	—	—	—	—	—
% Cations allocated	97.9	98.9	99.3	97.4	99.1	98.6	97.9	97.4

The garnet from the garnet pyroxenite xenolith BD 1364 is similar in composition to that from another pyroxenite xenolith G12 (Nixon *et al.*, 1963). Both are rather intermediate in character between undoubted garnet peridotite and eclogite xenoliths, in agreement with the conclusion of Rickwood *et al.* (1968).

Olivine compositions estimated by X-ray diffraction are given in Table 6. Determinations are made of 2θ (LiF_{220} — $Olivine_{062}$) essentially by the method outlined by Jackson (1960), except that a step-scanning counting technique was used rather than direct measurements of the chart. The calibration curve for variation of 2θ with mol.% fayalite was checked with two previously chemically analysed olivines (Carswell, 1968a and b).

Table 5. *Garnet compositions expressed as percentages of end member molecules calculated according to the scheme outlined by Rickwood (1968)*

	A	B	C	D
Uvarovite	6.2	0.6	0.2	5.5
Andradite	5.0	6.0	6.1	6.0
Pyrope	74.3	41.7	37.0	74.2
Spessartine	0.6	0.6	0.6	0.7
Grossular	1.7	28.2	32.1	2.0
Almandine	11.0	22.7	23.9	10.8
Schlorlomite	0.1	—	—	0.2
Knorringite	0.5	—	—	0.2
Skiagite	0.4	0.1	—	0.5

A = Mean of forty garnet analyses from garnet peridotite xenoliths. Source of analyses: A3, A4 and A6, O'Hara and Mercy (1963); E1, E3, E10 and E11, Nixon *et al.* (1963); 1—4, 6—11, 13—18, 20—21, 23—25, 28—30, Sobolev (1963); 5, Sobolev (1964); BLT-1, MacGregor and Ringwood (1964); and seven analyses presented in this paper.

B = Mean of forty-five garnet analyses from eclogite xenoliths. Source of analyses: E4, E7 and E16, Nixon *et al.* (1963); 70—73, 76, 78, 81—82, 126, Sobolev (1963); IX and X, Wagner (1914); 1 and 2, Sobolev and Kuznetsova (1965); 6, 7 and 8, Sobolev and Kuznetsova (1966); 37077, O'Hara and Mercy (1966); 37079, O'Hara and Yoder (1967); 1—6, Kushiro and Aoki (1968); Z3, Z6, Z8, Z15, Z24, Z28, Z33, Z34, Z37, Z38, Z43, Z48, Z49, Z52, Z59, Z63, RV15 and 1, Sobolev *et al.* (1968).

C = Mean of thirty-nine garnet analyses from eclogite xenoliths — namely those listed under B, but excluding 70—73, 76 and 78, Sobolev (1963).

D = Mean of twenty-four garnet analyses from kimberlite matrix ("blue ground"). Source of analyses: 2, Mennell (1910); III and IV, Wagner (1914); II, Williams (1932); 42—52, 56—59, 61, 64—66, Sobolev (1963); 5, Mikhailov and Rovsha (1966).

Table 6. *Olivine compositions determined by X-ray diffraction*

	Sample No.											
	BD 1354	BD 1355	BD 1356	BD 1360	BD 1364	BD 1127	BD 1133	BD 1140	BD 1143	BD 1150	BD 1200	BD 1201
fayalite %	18	8	7	10	14	8	7	8	8	9	7	9

Olivines from the garnet peridotites vary from 7—10 mol.% fayalite, with a mean value of 8 mol.% Fa corresponding closely to published chemically analysed olivines from garnet peridotite xenoliths (E9 — 7.9 mol.% Fa — Nixon *et al.*, 1963; A3 — 8.3 mol.% Fa — O'Hara and Mercy, 1963; No. 3 — 8.3 mol.% Fa — Mikhailov and Rovsha, 1966). All these xenoliths are in fact garnet lherzolites (Ol + OPX + CPX + GNT). Olivines from garnet harzburgite xenoliths (Ol + OPX + GNT) on the scant data so far available may have slightly lower fayalite contents (E8 — 7.5 mol.% Fa — Nixon *et al.*, 1963; A4 — 7.1 mol.% Fa, A6 — 6.4 mol.% Fa, A5 — 7 mol.% Fa, A6 — 5 mol.% Fa — all from O'Hara and Mercy, 1963), as also olivines from garnet free xenoliths of harzburgite (A1 — 6.4 mol.% Fa — O'Hara and Mercy, 1963; BD 1200 — 7 mol.% Fa) and lherzolite (A10 — 7.5 mol.% Fa, A15 — 6.5 mol.% Fa, O'Hara and Mercy, 1963). On

the other hand, olivines from the two analysed garnet pyroxenite xenoliths, BD 1354 and BD 1364, clearly have significantly higher fayalite contents, 18 and 14 mol.% respectively.

IV. Petrogenesis

Basically three different theories have been in vogue in recent years to explain the occurrence of garnet peridotite xenoliths in kimberlites. These are that they are:

a) fragments of high grade metamorphic zones situated deep in the crust.

b) xenoliths derived from the upper mantle.

c) segregations or 'cognate xenoliths' derived from the kimberlite magma.

Dawson (1967) elaborated on the original cognate xenolith theory (Wagner, 1914; Williams, 1932; Dawson, 1962) with a suggestion that they were formed by partial fragmentation of ultrabasic skarns formed at depth in the crust by reaction between carbonatite and crustal rocks. However, Dawson (1968) has since pointed out that the demonstration by Sarsadskikh *et al.* (1966) that xenoliths in Russian kimberlites give older ages than phlogopite in the kimberlite groundmass casts considerable doubt on the 'cognate' xenolith theory, assuming that these K-Ar ages are reliable. Furthermore it is difficult to reconcile the regularity in mineral and whole rock chemistry of the four phase garnet peridotite xenoliths with the cognate xenolith theory. O'Hara and Mercy (1963) have stressed other mineralogical and chemical arguments against such an origin.

One therefore appears to be left with a choice between the theory that they are crustal metamorphic xenoliths (Davidson, 1964, 1965, 1967b) or the currently more popular view that they are upper mantle xenoliths (O'Hara and Mercy, 1963; Nixon *et al.*, 1963; Boyd and Macgregor, 1964; O'Hara and Yoder, 1967; Harris *et al.*, 1967; Rickwood *et al.*, 1968; and others).

Davidson (1967b) has raised an impressive series of points in favour of a crustal origin for these xenoliths. As these points must clearly be answered if one is to unanimously accept the mantle origin theory, they will now be considered in turn.

1) It was claimed that the entire range of petrographic types among kimberlite xenoliths can be paralleled in several high grade metamorphic terrains.

Although O'Hara and Mercy (1963, 1966) and O'Hara, 1967a have argued that mineralogical and chemical distinctions exist between 'crustal' and 'kimberlite xenolith' garnet peridotites which refute this claim, this argument is now far from convincing as further investigations of 'crustal' garnet peridotites in Norway (Carswell, 1968b) and Czechoslovakia (Fiala, 1965, 1966; Mikhailov and Rovsha, 1966; and Kryukov, 1966) have produced descriptions of rocks, which although more serpentinized are basically similar mineralogically and chemically to garnet peridotites which form xenoliths in kimberlite pipes. At the same time, however, none of these particular authors has considered these garnet peridotites as representing 'in situ' crustal metamorphic rocks, rather they are thought to have originated in the mantle.

More serious objections can be raised when one looks into the volume distribution of garnet peridotites and eclogites in different environments. In metamorphic terrains eclogites predominate over garnet peridotites, while the reverse is true in kimberlite pipes. Furthermore Coleman *et al.* (1965) and Smulikowski (1964, 1965, 1968) have stressed mineralogical and chemical differences between eclogites in different environments in their propositions of a three fold subdivision of eclogites. Clearly the *average* eclogites in kimberlite pipes and metamorphic terrains are quite distinct both mineralogically and chemically as illustrated by Smulikowski (1968). This also contradicts Davidson's point 3 discussed below. However, one must take careful note of Smulikowski's statement that ... 'Only analyses of typical rocks (i.e. those which could be assigned to one of the groups without any hesitation) have been used in the calculation of the averages.' In fact, the validity of the proposed three fold subdivision of eclogites may be seriously questioned as intermediate types are far from unusual, a fact appreciated by Smulikowski (1968) himself.

2) The validity was doubted of selecting the garnet peridotite xenoliths as a distinctive type likely to be representative of the upper mantle from the range of ultrabasic and eclogitic xenoliths found in kimberlite pipes.

To settle this question conclusively quantitative data on the types of xenoliths in a large number of kimberlite pipes is required. Unfortunately the difficulties involved in acquiring such data may well prohibit it ever becoming available.

Davidson (1967b) has cited the instance of the Obnazhennaya pipe in Siberia where Milashev *et al.* (1963) have described an unusual suite of banded eclogite and ultrabasic xenoliths of highly variable composition.

Eclogite xenoliths are widely recognized as being both chemically and mineralogically variable (see Fig. 1, also Kushiro and Aoki, 1968; Sobolev *et al.* 1968) — a point strongly against the idea of a primary eclogite layer in the mantle and in favour of theories such as that of O'Hara and Yoder (1967) which explain such rocks as being high pressure crystal cumulates from fractionating 'basaltic' liquids.

Concerning the variability of garnet bearing peridotite xenoliths the most comprehensive survey to date has been that by Rickwood *et al.* (1968). They obtained samples of eclogite and garnet bearing peridotite xenoliths from kimberlite pipes and fissures at seventeen localities in Southern Africa. Every garnet bearing sample available to them at the time is reported to have been examined, a total of one hundred and thirty-seven. Of the seventy-six garnet + olivine bearing xenoliths examined, seventy-two were classified as garnet peridotite and four as garnet pyroxenite. The highest volume percentage of garnet in the garnet peridotites was 18.5% and the average 6.8%, the highest in the garnet pyroxenites 14.0% and the average 10.7%. The mean value for the garnet volume percentage in the eclogites was much higher at 50.5% and the range 28.6—81.6%. Furthermore, estimates of the chemical composition of these garnets based on their unit cell edge length and refractive indices indicated a fairly narrow range of compositions for those from peridotites contrasted with the much wider and chemically different range for those from eclogites, those from pyroxenites tending to be of intermediate chemical character.

The new data presented in this paper substantiates the distinctions and conclusions pointed out by Rickwood *et al.* (1968). Garnet peridotite xenoliths in kimberlite pipes, both from Siberia and southern Africa, are remarkably uniform

in terms of their modal mineral contents, and bulk rock and mineral compositions. Furthermore, they are the most common type of 'deep-seated' xenolith and whereas eclogites are not ubiquitous garnet peridotite is, either as intact nodules or else in a finely fragmented form as xenocrysts in the kimberlite matrix. It is therefore apparent that they must have been derived from a widespread and essentially uniform source at depth, most likely as we shall see in the mantle.

3) It was stated that a distinction between 'true' kimberlite eclogites and 'crustal' eclogites is ill-founded.

This question is not really relevant to the problem of the genesis of garnet peridotites, and has anyway already been dealt with to some extent in the previous discussion in point 1.

4) It was stated that the suggestion that garnet peridotites in metamorphic terrains represent cold intrusions of mantle material emplaced late in the metamorphic history is not in accordance with radiometric dating nor with independent field observations.

The radiometric dates referred to are those for Norwegian garnet peridotite and enclosed eclogite given by MacDougall and Green (1964). Diopsides in these rocks gave K-Ar ages of 8,100 and 7,350 m.y. respectively — these 'impossible' ages being explained by these pyroxenes containing an excess of radiogenic argon, the mobility of radiogenic argon in a deep-seated metamorphic environment clearly being established. Amphibole from the eclogite within peridotite gave a K-Ar age of 1,850 m.y. tentatively accepted by MacDougall and Green as a valid age, dating a clearly Pre-Cambrian retrogressive metamorphic event. This single date is the only one available to support Davidson's contention (1965) ... 'that the eclogites and garnet peridotites are undigested residues of the Pre-Cambrian shield.' On the other hand the published results of field studies by O'Hara and Mercy (1963), Lappin (1966), Bryhni (1966) and Carswell (1968a, b) all support the theory that the Norwegian garnet peridotites and enclosed eclogites are tectonic inclusions in the Caledonian gneisses. Against this only Schmitt (1964) has thought that they are 'in situ' crustal metamorphics and unfortunately the detailed results of his study have not so far been published.

The significance of the single K-Ar amphibole age date must be considered in the light of the accompanying statement by MacDougall and Green ... 'The presence of excess radiogenic argon in the pyroxenes makes it difficult to interpret K-Ar ages from these rocks or their secondary alteration products. Thus the dates on amphiboles ... may be true ages, ages that are too old due to excess argon, or ages that are too low due to partial argon loss.' It is noteworthy that age determinations on different mineral fractions from a composite eclogite lens directly enclosed in Norwegian gneiss gave the following figures — phlogopite (K-Ar 950 m.y., Rb-Sr 401 m.y.) phlogopite (K-Ar 415 m.y., Rb-Sr 382 m.y.), amphibole (K-Ar 980 m.y.) amphibole (K-Ar 1,160 m.y.), amphibole (K-Ar 1,745 m.y.). As MacDougall and Green point out there is no unique interpretation of these results, and despite their arguments to the contrary the K-Ar ages of the phlogopites and amphiboles, as well as the pyroxenes, appear of dubious validity. The only Rb-Sr determinations both give Caledonian ages for secondary phlogopite.

5) The occurrence of scapolite and kelyphitic rims around garnets in kimberlite xenoliths were said to be typical features of high grade basement rocks.

This point is unconvincing as both features may be expected in partially retrograded eclogites in any environment. Scapolite would not be expected as a primary crystal phase from a kimberlite liquid.

6) It was pointed out that the garnet peridotite xenoliths are 'cognate' with kimberlite only in the sense that through the trituration and fluidization of some xenoliths they have provided the pyrope, chrome-spinellids and part of the kimberlite breccia slurry.

This point is probably valid and is supported by the chemical similarity of garnet xenocrysts in the kimberlite matrix with garnets in the garnet peridotite xenoliths. The mean of twenty-four analyses of garnet xenocrysts in the kimberlite matrix, recalculated in terms of garnet end-member molecules, is given in Table 5 column D where it can be directly compared with the mean of garnets from xenoliths.

7) It was stated that the rare occurrence of diamond bearing eclogite xenoliths does not necessitate that they have come from great depth. Instead both eclogite and diamond were claimed to have formed in the deeper levels of the crust.

Davidson (1964) developed a 'two-stage' kimberlite emplacement hypothesis to explain apparent discrepancies between the K-Ar ages of phlogopites from Russian kimberlites and the field evidence on age of emplacement (Mikheyenko and Nenashev, 1962). Kimberlite, eclogite and garnet peridotite were all thought to have formed and consolidated in the lower parts of the crust in Pre-Cambrian times. At a much later geological date the kimberlite was fragmented, diamond formed, and eclogite and garnet peridotite xenoliths incorporated and transported from depth by a fluidization process. However, as Davidson (1964) himself pointed out a crustal origin for diamond is contrary to all current conceptions on its pressure-temperature stability field. Although in recent years diamond has been synthesized at much lower pressure-temperature conditions than previously (e.g. 800—1,600 °K and pressures as low as 15,000 atmospheres, Bezrukov *et al.*, 1966), the minimum pressure-temperature conditions still suggest formation within the mantle (see Dawson, 1968, Fig. 4).

Moreover, a more recent paper on the age of the Yakutian kimberlites (Sarsadskikh *et al.*, 1966) appears to contradict the 'two stage' hypothesis, as it was pointed out that the earlier Pre-Cambrian dates were obtained on xenoliths while new datings on phlogopite from the kimberlite matrix have given much younger ages in accordance with the field relationships. Davidson (1967a) has not differentiated between ages obtained on phlogopite from xenoliths and phlogopite in the kimberlite matrix in his discussion on the age of Yakutian kimberlites. Davidson (1967a) Table 8.2 should be compared with Sarsadskikh *et al.* (1966) Tables 1 and 2.

As only K-Ar ages are available one might suspect their validity, especially in the light of the data presented by MacDougall and Green (1964). Moreover it is not made clear whether the phlogopite in the xenoliths is primary or secondary and thus what event one is in fact dating in this case. However, Sarsadskikh *et al.* (1966) point out that in most, but not all, cases the K-Ar age of kimberlite emplacement obtained from phlogopites in the kimberlite matrix approximates closely to the age based on geological field evidence.

8) It was claimed that diamond has not yet been recorded from any xenolith of garnet peridotite.

Diamond bearing xenoliths in general are certainly rare and most documented occurrences are of diamond in eclogite xenoliths, such as the famous specimens from Newlands mine. However, Wagner (1928) referred to the presence of diamond in some xenoliths of both eclogite and peridotite. Williams (1932) also makes it clear that diamonds have been recorded in peridotite xenoliths in the Kimberley mines. It was not specificially stated that the diamond bearing peridotite xenoliths observed were garnetiferous although it is virtually inferred, especially as most peridotite xenoliths are in fact garnetiferous. Furthermore, the occurrence of inclusions of chrome-pyrope garnet, chrome-diopside and forsteritic olivine (6—9 mole% Fa) in diamonds (Meyer and Boyd, 1968; Williams, 1932) strongly suggests that these diamonds have developed in an environment where garnet peridotite was a prominent rock type.

9) There was said to be irrefutable evidence that the source of garnet peridotite and eclogite xenoliths in the Linorka kimberlite diatreme in Czechoslovakia lies at depths of only a few hundred metres in the crust.

Much of the weight behind Davidson's argument centred on this final point which must now be considered in detail.

Kopecky and Sattran (1962) reported that a borehole sunk 80 metres from the margin of the Linorka diatreme at depths of 209—436 metres passed through a massive body of serpentinized peridotite with pyrope and pyroxene, and with zones of pyroxenite and eclogite. Mineralogical and chemical studies (Kopecky and Sattran, 1962; Fiala, 1965; Mikhaikov and Rovsha, 1966; Kryukov, 1966) of samples of garnet peridotite from the borehole have shown them to be basically similar to the garnet peridotite xenoliths found in this and other kimberlite diatremes, and to samples of other garnet peridotite masses enclosed in the granulites of the Bohemian Massif (Fiala, 1966).

However, although an instance of a diatreme intersecting a garnet peridotite body directly enclosed in crustal metamorphic rocks has been demonstrated, this does not prove Davidson's case unless it can be further demonstrated that the garnet peridotite body intersected or any of the other similar bodies in the Bohemian Massif, are in fact crustal metamorphic rocks.

Kopecky and Sattran (1966) themselves do not regard these garnet peridotites as straightforward 'in situ' crustal metamorphic rocks, although they say that they form bodies ... 'connected both in genesis and time with the origin of granulite and granulitic gneiss.' They appear to favour the idea that the present garnet peridotite bodies represent fragments of plutonic igneous bodies kneaded in tectonically into the rocks of the granulite facies. It is only a short step from this interpretation to Fiala's conclusions (1966) that these garnet peridotites — 'represent deep-seated rocks generated within the range of the Upper Mantle and brought up to their present level by tectonic processes.' Also relevant is the statement by Weiss (1966) that ... 'the pyrope-bearing ultrabasic rocks are arranged into distinct linear zones of NW and NNE trends, indicating deep-reaching fault-zones which served as channels for their ascent'.

There are still clearly differences of opinion amongst Czech, Russian and German geologists who have studied the garnet peridotites of the Bohemian Massif. Nevertheless collectively their support to Davidson's theory that the garnet peridotites are crustal metamorphic rocks is slender. Certainly it is not inconceivable that the garnet peridotite body intersected by the Linorka diatreme may itself represent a fragment of tectonically-emplaced upper mantle material. Furthermore it has been pointed out (Dawson, 1968) that the diatremes of the České Středohoří mountains in Czechoslovakia do not have true kimberlitic affinities and hence are perhaps not strictly relevant to the issue being considered.

The preceding assessment of the points raised by Davidson (1967b) makes it clear that there is little firm evidence in favour of his interpretation, that the garnet peridotite xenoliths in kimberlite pipes are crustal metamorphic rocks. Whilst it is not possible to say what occurs in the Basement terrains beneath the sedimentary Karroo rocks that cover much of South Africa, when the Basement is seen in the deepest parts of the diamond mines in the Kimberley area, the pipes are intruded through granitic gneiss without any apparent garnet peridotite and eclogite bodies. It would indeed be fortuitous if each kimberlite intrusion during its ascent through the crust were to intersect pods of these rock-types known to be rare in crustal metamorphic terrains.

Published experimental data on the pressure-temperature stability field of garnet peridotite (MacGregor, 1965; Green and Ringwood, 1967b; Ito and Kennedy, 1967) suggests that the formation of garnet peridotite under metamorphic conditions in the crust is unlikely though not impossible. O'Hara (1967b) considered in the light of the chemistry of the pyroxenes that the mineral assemblages of the garnet peridotites from kimberlites have been equilibrated at pressures in excess of 30 kilobars and temperatures in the range 1,000—1,250 °C (see O'Hara, 1967b, Fig. 12.6). Such pressure-temperature conditions are consistent with an environment at depths of 100—140 kilometres on the Pre-Cambrian shield geothermal gradient — pointing to a derivation well within the realm of the upper mantle.

The regularity in the mineralogy and chemistry of garnet peridotite xenoliths from kimberlite pipes, as far apart as Russia and South Africa strongly suggests a widespread source of such rocks at depth in the mantle. Moreover a predominately garnet peridotite upper mantle provides a resonable fit to the mantle composition crudely predicted by the chondrite meteorite model (see Ringwood, 1966; Mercy, 1967), and provides a suitable source rock for the generation of basaltic magmas (see O'Hara, 1965, 1968; Green and Ringwood, 1967a). Certainly the model outlined by O'Hara and Yoder (1967) in which they have stressed the genetic association of xenoliths of garnet peridotite (a possible source rock for basaltic magmas, and mantle material) with xenoliths of eclogite (possible high pressure crystal cumulates from the garnet peridotite partial melt liquid) in kimberlite (a possible residual fluid of high pressure fractionation) is extremely elegant and attractive.

It seems likely that the garnet peridotite xenoliths represent essentially original or primitive upper mantle material largely undepleted in the 'readily fusible' constituents (Al_2O_3, CaO, Na_2O and K_2O) which may be selectively extracted by partial melting to form basaltic type liquids, rather than the 'infusible' mantle residue left after such a process (see Harris *et al.*, 1967). Unfortunately due to

contamination, in particular with K_2O as witnessed by the common growth of secondary phlogopite, garnet peridotite xenoliths as they are now found in kimberlite pipes fail to provide a reliable indication of the alkali concentrations in the primitive mantle material.

Garnet peridótite also appears to possess the requisite physical properties of upper mantle material necessitated by geophysical measurements (Birch, 1952; Clark and Ringwood, 1964, 1967).

O'Hara (1968, Figs. 8—11) considered that partial melting of garnet lherzolite (Ol + OPX + CPX + GNT) of the common kimberlite xenolith type at pressures of about 30 kilobars or greater will yield garnet harzburgite residua (Ol + OPX + GNT) with less than about 20% partial melting, and harzburgite and dunite residua with progressively higher degrees of melting. Petrological support for this was derived from estimates of the relative abundances of peridotite xenoliths based on Williams (1932). Garnet lherzolites are reported to be the most common type followed by garnet harzburgites, then harzburgites, with lherzolites and dunites quite scarce. Rickwood *et al.* (1968) unfortunately do not give the relative proportions of garnet lherzolites and garnet harzburgites amongst the seventy-two peridotite xenoliths studied by them. Both types are reported to occur, however, along with only one garnet dunite (GNT + Ol) and one garnet wehrlite (GNT + Ol + CPX).

No garnet harzburgites similar to rock types A4, A5, A6 and A9 listed by O'Hara and Mercy (1963) have been collected or analysed in the course of this study. As no attempt was made to distinguish between garnet lherzolites and garnet harzburgites in the field this may just be fortuitous, however. One harzburgite (BD 1200) was collected and analysed. The fact that it has the lowest contents of Al_2O_3, CaO and Na_2O amongst the analysed xenoliths supports the idea that it represents a residuum after partial melting.

Rare lherzolite xenoliths such as A10 (O'Hara and Mercy, 1963) were thought (O'Hara, 1968) to be either residua produced by partial melting at slightly lower pressures or cognate accumulates. The latter explanation was thought to be the most likely for the garnet poor websterite (A17). The scarcity of dunite xenoliths may be explained if the generation of advanced partial melts (>40% liquid phase) from garnet lherzolite is a rare event.

As indicated in the earlier discussion of the data presented in Table 6, the suggestion that olivine from garnet harzburgite, harzburgite and lherzolite xenoliths may have slightly lower fayalite contents than olivines from garnet lherzolite xenoliths would also support the idea of the three former types of xenoliths being residua after partial melting of garnet lherzolite.

Finally it remains to explain the occurrence of garnet pyroxenite xenoliths such as samples BD 1354 and BD 1364 analysed during this study. Rickwood *et al.* (1968) have listed four further xenoliths of this type, and Nixon *et al.* (1963) yet another (G12).

Two possible explanations are that either such rocks represent unusually high concentrations of garnet and clinopyroxene in the primary unmodified upper mantle material, or they represent mantle material enriched in 'fusible' constituents (notably Al_2O_3, CaO and Na_2O) perhaps during some earlier partial melting event in the mantle.

It is difficult, however to account for the chemical differences between minerals from garnet pyroxenite and garnet peridotite xenoliths with the former explanation. It has already been pointed out that olivines from the two analysed garnet pyroxenite xenoliths have significantly higher fayalite contents than those from garnet peridoties, while garnets have higher almandine/pyrope ratios than those from peridotite xenoliths, being chemically rather intermediate between the garnets from peridotite and eclogite xenoliths. It is apparent that compared with the garnet peridotites the higher $Fe^{2+} + Fe^{3+}/Mg^{2+}$ ratios of the analysed garnet pyroxenite xenoliths cannot be attributed solely to their increased modal garnet content. Rather the whole mineral assemblage is more ferriferous as illustrated by the analysed garnets and olivines.

Garnet pyroxenites with similarly higher $Fe^{2+} + Fe^{3+}/Mg^{2+}$ ratios and higher Al_2O_3, CaO and Na_2O contents than postulated primary upper mantle material have been described from peridotite bodies in Norwegian gneisses (Carswell, 1968a), and interpreted as mantle derived material 'enriched' during involvement in partial melting processes in the mantle. It is thought that the garnet pyroxenite xenoliths in kimberlite pipes may have been derived from lenses of 'enriched' mantle material representing crystallized pockets of tapped partial melt liquid.

The unusual suite of banded eclogite and ultrabasic xenoliths of highly variable composition in the Obnazhennaya pipe in Siberia cited by Davidson (1967b),may indicate that this pipe has sampled an unusually complex series of crystal cumulates from a large pocket of partial melt liquid which was trapped in the mantle. The presence of banded eclogites in the Roberts Victor mine (Wagner, 1914; Dawson, 1968) may be indicative of a similar process.

In conclusion it may be stated that the evidence at present available suggests that in the upper mantle regions where kimberlites originate, garnet peridotite or more specifically garnet lherzolite, as it was before the secondary alteration within the kimberlite pipes where it is now found as xenoliths, is an important and probably the predominant rock type. The theory that such xenoliths represent inclusions of crustal metamorphic rocks seems far less likely.

Residua of garnet harzburgite, harzburgite and dunite may well occur in regions of the upper mantle where extensive partial melting of the primary garnet peridotite has occurred, along with isolated lenses of garnet pyroxenite and eclogite representing the crystallization products of trapped pockets of partial melt liquid.

Acknowledgements. The specimens on which this paper is based were collected by J. B. Dawson during a visit to South Africa in 1966, the visit being made possible by grants from the Carnegie Trust for the Universities of Scotland, the Institute of Mining and Metallurgy (G. Vernon Hobson Bequest Fund) and the Travel Fund of the University of St. Andrews. Field-work in South Africa was carried out with the assistance of geologists of De Beers Consolidated Mines Ltd. of whom Mr. C. D. Hallam is especially acknowledged for his unstinting and generous help.

D. A. Carswell gratefully acknowledges the cooperation of Dr. P. E. Brown and Mr. P. Wilkinson and assistance of Mr. V. Somogyi with analytical procedures. Dr. R. Till kindly assisted with writing a computer program for calculating structural formulae and molecular percentages of garnets.

References

Bezrukov, V. A., Bezrukov, G. N., Butuzov, V. P., Varagin, V. S., Voroscikin, K. F., Kirova, N. F., Litkin, Yu. A.: Morphology of crystals of diamond, synthesized at wide intervals of temperature and pressure. [Russian.] Zap. Vses. Mineralog. Obshchestva **95**, 1—9 (1966).

Birch, F.: Elasticity and constitution of the earth's interior. J. Geophys. Res. **57**, 227—286 (1952).

Boyd, F. R., Macgregor, I. D.: Ultramafic rocks. Carnegie Inst. Wash. Yearb. **63**, 152—156 (1964).

Bryhni, I.: Reconnaissance studies of gneisses, ultrabasites, eclogites and anorthosites in Outer Nordfjord, Western Norway. Norg. Geol. Undersokelse **241**, 1—68 (1966).

Carswell, D. A.: Picritic magma-residual dunite relationships in garnet peridotite at Kalskaret near Tafjord, South Norway. Contr. Mineral. and Petrol. **19**, 97—124 (1968a).

— Possible primary upper mantle peridotite in Norwegian basal gneiss. Lithos **1**, 322—355 (1968b).

Clark, S. P., Jr., Ringwood, A. E.: Density distribution and constitution of the mantle. Rev. Geophys. **2**, 35—88 (1964).

— — Density, strength and constitution of the mantle. In: Gaskell, T. F. (ed.): The earth's mantle, p. 111—124. London: Academic Press 1967.

Coleman, R. G., Lee, D. E., Beatty, L. B., Brannock, W. W.: Eclogites and eclogites; their differences and similarities. Bull. Geol. Soc. Am. **76**, 483—508 (1965).

Davidson, C. F.: On diamantiferous diatremes. Econ. Geol. **59**, 1368—1380 (1964).

— Diamentiferous diatremes: a reply. Econ. Geol. **60**, 1735—1739 (1965).

— The kimberlites of the U.S.S.R. In: Wyllie, P. J. (ed.), Ultramafic and related rocks, p. 251—261. New York: John Wiley & Sons 1967a.

— The so-called "cognate xenoliths" of kimberlite. In: Wyllie, P. J. (ed.), Ultramafic and related rocks, p. 342—346. New York: John Wiley & Sons 1967b.

Dawson, J. B.: Basutoland kimberlites. Bull. Geol. Soc. Am. **73**, 545—560 (1962).

— Geochemistry and origin of kimberlite. In: Wyllie, P. J. (ed.), Ultramafic and related rocks, p. 269—278. New York: John Wiley & Sons 1967.

— Recent researches on kimberlite and diamond geology. Econ. Geol. **63**, 504—511 (1968).

Eskola, P.: On the eclogites of Norway. Skrifter Vidensk. Selsk. Christiania, Mat.-Naturv. Kl., I, No. 8, 1—118 (1921).

Fermor, L. L.: On a new chrome-garnet. Geol. Mag. **89**, 145—147 (1952).

Fiala, J.: Pyrope in some garnet peridotites of the Czech Massif. Krystalinikum **3**, 55—74 (1965).

— The distribution of elements in mineral phases of some garnet peridotites of the Bohemian Massif. Krystalinikum **4**, 31—53 (1966).

Green, D. H., Ringwood, A. E.: The genesis of basaltic magmas. Contr. Mineral. and Petrol. **15**, 103—190 (1967a).

— — The stability fields of aluminous pyroxene peridotite and garnet peridotite and their relevance in upper mantle structure. Earth Planet. Sci. Letters **3**, 151—160 (1967b).

Harris, P. G., Reay, A., White, I. G.: Chemical composition of the upper mantle. J. Geophys. Res. **72**, 6359—6369 (1967).

Holmes, A.: A contribution to the petrology of kimberlite and its inclusions. Trans. Geol. Soc. S. Afr. **39**, 379—428 (1936).

Ito, K., Kennedy, G. C.: Melting and phase relations in a natural peridotite to 40 kilobars. Am. J. Sci. **265**, 519—538 (1967).

Jackson, E. D.: X-ray determinative curve for natural olivine of composition Fo_{80-90}. U.S. Geol. Surv. Profess. Papers **400-B**, 432—434 (1960).

Kopecký, L., Sattran, V.: Zur Genese der Pyrope im tschechischen Mittelgebirge. Vestn. Ustredniho Ustavu Geol. **37**, 269—283 (1962).

— Buried occurrences of pyrope-peridotite and the structure of the crystalline basement in the extreme S.W. of the České Středohoří mountains. Krystalinikum **4**, 65—86 (1966).

Kryukov, A. V.: Genesis of pyrope-peridotite inclusions in the pipes of North Minusinsk Depression and their comparison with peridotites of the České Středohoří Mountains. Krystalinikum **4**, 185—200 (1966).

Kushiro, I., Aoki, Ken-Ichiro: Origin of some eclogite inclusions in kimberlite. Am. Mineralogist **53**, 1347—1367 (1968).

Lappin, M. A.: The field relationship of basic and ultrabasic masses in the basal gneiss complex of Stadlandet and Almklovdalen, Nordfjord, south-western Norway. Norsk Geol. Tidsskr. **46**, 439—494 (1966).

MacDougall, I., Green, D. H.: Excess radiogenic argon in pyroxenes and isotopic ages on minerals from Norwegian eclogites. Norsk Geol. Tidsskr. **44**, 183—196 (1964).

MacGregor, I. D.: Stability fields of spinel and garnet peridotites in the synthetic system MgO–CaO–Al_2O_3–SiO_2. Carnegie Inst. Wash. Yearb. **64**, 126—134 (1965).

— Ringwood, A. E.: The natural system enstatite-pyrope. Carnegie Inst. Wash. Yearb. **63**, 161—163 (1964).

Mennell, L. P.: The geological structure of Southern Rhodesia. Quart. J. Geol. Soc. London **66**, 353—375 (1910).

Mercy, E. L. P.: Geochemistry of the mantle. In: Gaskell, T. F. (ed.), The earth's mantle, p. 421—443. London: Academic Press 1967.

Meyer, H. O. A., Boyd, F. R.: Mineral inclusions in diamonds. Carnegie Inst. Wash. Yearb. **67**, 130—135 (1968).

Mikhailov, N. P., Rovsha, V. S.: Pyrope-bearing peridotites of the Bohemian Massif and their genesis. Krystalinikum **4**, 87—107 (1966).

Mikheyenko, V. I., Nenashev, N. I.: Absolute age of the kimberlites of Yakutia. Intern. Geol. Rev. **4**, 916—924 (1962).

Milashev, V. A., Krutoyarski, M. A., Rabhkin, M. I., Zirlich, Z. N.: Kimberlitic rocks and picritic porphyries of the north-eastern part of the Siberian platform. [Russian.] Tr. Nauchno-Issled. Inst. Geol. Arktiki **126**, 1—215 (1963).

Nixon, P. H., Hornung, G.: A new chromium garnet end member, knorringite, from kimberlite. Am. Mineralogist **53**, 1833—1840 (1968).

— Knorring, O. von, Rooke, J. M.: Kimberlites and associated inclusions of Basutoland: a mineralogical and geochemical study. Am. Mineralogist **48**, 1090—1132 (1963).

O'Hara, M. J.: Primary magmas and the origin of basalts. Scot. J. Geol. **1**, 19—40 (1965).

— Garnetiferous ultrabasic rocks of orogenic regions. In: Wyllie, P. J. (ed.), Ultramafic and related rocks, p. 167—172. New York: John Wiley & Sons 1967a.

— Mineral paragenesis in ultrabasic rocks. In: Wyllie, P. J. (ed.), Ultramafic and related rocks, p. 393—403. New York: John Wiley & Sons 1967b.

— The bearing of phase equilibria studies in synthetic and natural systems on the origin and evolution of basic and ultrabasic rocks. Earth-Sci. Rev. **4**, 69—133 (1968).

— Mercy, E. L. P.: Petrology and petrogenesis of some garnetiferous peridotites. Trans. Roy. Soc. Edinburgh **65**, 251—314 (1963).

— — Eclogite, peridotite and pyrope from the Navajo Country, Arizona and New Mexico. Am. Mineralogist **51**, 336—352 (1966).

— Yoder, H. S.: Formation and fractionation of basic magmas at high pressures. Scot. J. Geol. **3**, 67—117 (1967).

Rickwood, P. C.: On recasting analyses of garnet into end-member molecules. Contr. Mineral. and Petrol. **18**, 175—198 (1968).

— Mathias, M., Siebert, J. C.: A study of garnets from eclogite and peridotite xenoliths found in kimberlite. Contr. Mineral. and Petrol. **19**, 271—301 (1968).

Ringwood, A. E.: Chemical evolution of the terrestrial planets. Geochim. Cosmochim. Acta **30**, 41—104 (1966).

Sarsadskikh, N. N., Blagulkina, V. A., Silin, Yu. I.: Absolute age of Yakutian kimberlites. Dokl. Akad. Nauk SSSR Earth Sci. Sect. **168**, 48—50 (1966).

Sastri, G. G. K.: Note on a chrome and two manganese garnets from India. Mineral. Mag. **33**, 508—511 (1963).

Schmitt, H. H.: Metamorphic eclogites of the Eiksund area, Sunnmore, Norway. (Abstract). Trans. Am. Geophys. Union **45**, 128 (1964).

Smulikowski, K.: An attempt at eclogite classification. Bull. Acad. Polon. Sci., Sér. Géol. Géograph. **12** (I), 27—33 (1964).

— Chemical differentiation of garnet and clinopyroxene in eclogites. Bull. Acad. Polon. Sci., Sér. Géol. Géogr. **13** (I), 11—18 (1965).

Smulikowski, K.: Differentiation of eclogites and its possible causes. Lithos **1**, 89—101 (1968).
Sobolev, N. V.: Paragenetic types of garnet. I. Pyrope-almandine garnets from ultrabasic rocks and eclogites. [Russian.] Tr. Inst. Geol. i Geofiz. Sibirskoe otd. Akad. Nauk SSSR **15**, 42—73 (1963).
— Rhombic pyroxenes from garnet peridotite and eclogite. Dokl. Akad. Nauk SSSR Earth Sci. Sect. **154**, 110—111 (1964).
— Kuznetsova, I. K.: More facts on the mineralogy of eclogite from Yakutian kimberlite pipes. Dokl. Akad. Nauk SSSR Earth Sci. Sect. **163**, 137—140 (1965).
— — Mineralogy of diamond-bearing eclogites. Dokl. Akad. Nauk SSSR Earth Sci. Sect. **167**, 112—115 (1966).
— — Zyuzin, N. I.: The petrology of grospydite xenoliths from the Zagadochnaya kimberlite pipe in Yakutia. J. Petr. **9**, 253—280 (1968).
Wagner, P. A.: The diamond fields of Southern Africa. Transvaal Leader, Johannesburg. 347 p. (1914).
— The evidence of kimberlite pipes on the constitution of the outer part of the earth. S. African J. Sci. **25**, 127—148 (1928).
Weiss, J.: Ultrabasic rocks of the West Moravian crystalline complex. Krystalinikum **4**, 171—183 (1966).
Williams, A. F.: The genesis of the diamond. 2 vols. London: Benn 1932.
Wyllie, P. J.: Review. In: Wyllie, P. J. (ed.), Ultramafic and related rocks, p. 403—416. New York: John Wiley & Sons 1967.

D. A. Carswell
Department of Geology
University of Sheffield
St. George's Square
Sheffield 1, England

J. B. Dawson
Department of Geology
University of St. Andrews
Fife, Scotland

From "Lesotho Kimberlites" (ed. P. H. Nixon) 224-239 (1973)

Ilmenite Association Trace Element Studies

Part I: *Mineralogy and Rare Earth Geochemistry of an Ilmenite-Clino-pyroxene Xenolith from the Monastery Mine*

R. H. MITCHELL, D. A. CARSWELL and A. O. BRUNFELT

ABSTRACT

Homogeneous ilmenite (27,3 mol. % $MgTiO_3$) and subcalcic clinopyroxene are the major phases of the intergrowth. Secondary alteration has resulted in the formation of MnO-rich ilmenite (11,6 mol. % $MnTiO_3$), and a phlogopite rich in TiO_2 (3,33%) and poor in Al_2O_3 (7,84%). Abundant secondary fluid inclusions in the clinopyroxene confined to healed fractures are interpreted as indicating formation of the intergrowth by eutectic crystallization rather than by solid state exsolution. Rare earth element distribution patterns of the clinopyroxene and Monastery kimberlite indicate that the clinopyroxene could have been in equilibrium with kimberlite magma but was unlikely to be formed as a result of breakdown of high pressure garnet.

INTRODUCTION

A summary of the views on the origin of the ilmenite-pyroxene lamellar intergrowths in kimberlite has been given by Gurney *et al.* (this volume, p.239). Data are presented here for a single inclusion, *1860J*, from Monastery Mine, in which the ilmenite shows exsolution features, marked chemical zoning and marginal reaction to secondary phlogopite.

ANALYTICAL METHODS

The major element composition of the phases of the xenolith was determined by microprobe at the University of Oslo. Standards similar in composition to the samples were used for constructing calibration curves for the analyses.

The clinopyroxene was separated from the xenolith, leached with 10% HCl to remove any possible carbonate contamination and then analysed by neutron activation analysis for rare earth elements. The analytical procedure was as described by Ragland *et al.* (1970), except that U.S.G.S. standard BCR-1 was used as a standard using assigned values for the rare earth element abundances given by Brunfelt and Steinnes (1971).

Ilmenite

Ilmenite analyses are given in table 63 (nos. 1, 2, and 3). Calculations assuming a stoichiometric structural formula, ABO_3, shows that the ilmenites are deficient in Ti and hence must contain some Fe^{3+}. Oxygen anion proportions were calculated on the basis of two cations, with total Fe expressed as FeO, and then

considerably in their abundances. Hypothetical pyroxenes in equilibrium with the Monastery kimberlite behave in a similar fashion. However, Schnetzler and Philpotts' (1970) distribution coefficients result in hypothetical pyroxenes which are slightly more fractionated than the actual pyroxene.

The data could be interpreted to imply that the clinopyroxene was in equilibrium with the kimberlite, since discrepancies between hypothetical and actual REE abundances are considered to lie within the variations of determined distribution coefficients (Schnetzler and Philpotts, 1970). Furthermore, Philpotts *et al.*, (1972) have argued that eclogite omphacites which have similar patterns (figure 59B) are in equilibrium with kimberlite.

The variations in abundances of REE in the liquid may not be due to fractionation but to simple dilution or concentration after pyroxene crystallization. Alternatively, the phenocryst-matrix partition coefficients of Onuma *et al.* (1968) and Schnetzler and Philpotts (1970) determined on lavas, may be incorrect for this higher pressure system of different composition. Masuda and Kushiro (1970) and Nagasawa and Schnetzler (1971) have demonstrated changes in the *magnitude* of the partition coefficients with pressure and composition respectively and the clinopyroxene could, therefore, be genetically related to the kimberlite. However, this would not hold if the *relative* values of the REE partition coefficients change with pressure and liquid composition.

CONCLUSIONS

If the pyroxene-ilmenite intergrowth was formed by the breakdown of a high pressure phase, and assuming that no REE were lost during exsolution, the REE distribution of the clinopyroxene should be representative of the parent phase if no REE enter the ilmenite lattice. Ringwood and Lovering (1970) have suggested garnet as a possible parental phase. Garnets in eclogites and garnet lherzolites are known to preferentially incorporate the heavy REE and to show distribution patterns with a strong depletion in light REE (Philpotts *et al.*, 1972; Reid and Frey, 1971). As the "parent phase" distribution pattern, as represented by the pyroxene, is unlike that of garnet, support for Ringwood and Lovering's (1970) conclusions would be obtained only if very high pressure garnets have different REE patterns to those in garnet lherzolites. The distribution patterns are, therefore, more in keeping with Dawson and Reid's (1970) hypothesis of breakdown of an ilmenite-structured pyroxene. However, Mitchell (1973a) has proposed that the compositional range seen in kimberlite ilmenites is the result of *fractional crystallization*, and since the intergrowth ilmenite, is poorer in Mg, Cr, Nb and Ta (Mitchell *et al.*, part II, this volume, p. 231) it might be one of the later fractions of a protokimberlite magma, at a time when silicates were just taking the place of ilmenite in the liquidus phase. Fluid inclusions in healed fractures can be taken as evidence for crystallization of the clinopyroxene from a magma, and the REE geochemical study indicates that it was possibly in equilibrium with a magma of kimberlite composition. Alteration of ilmenite to MnO-rich rims and secondary phlogopite are interpreted as magmatic effects that occurred deep in the mantle.

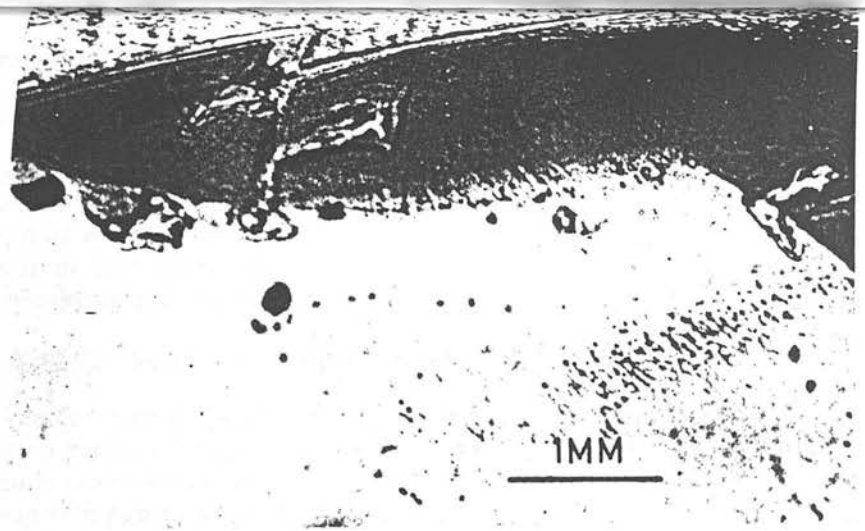

Plate 66A Phlogopite showing iron- and titanium-enriched dark rim, in ultrabasic nodule *1859N*, Monastery Mine. (*Boyd*)

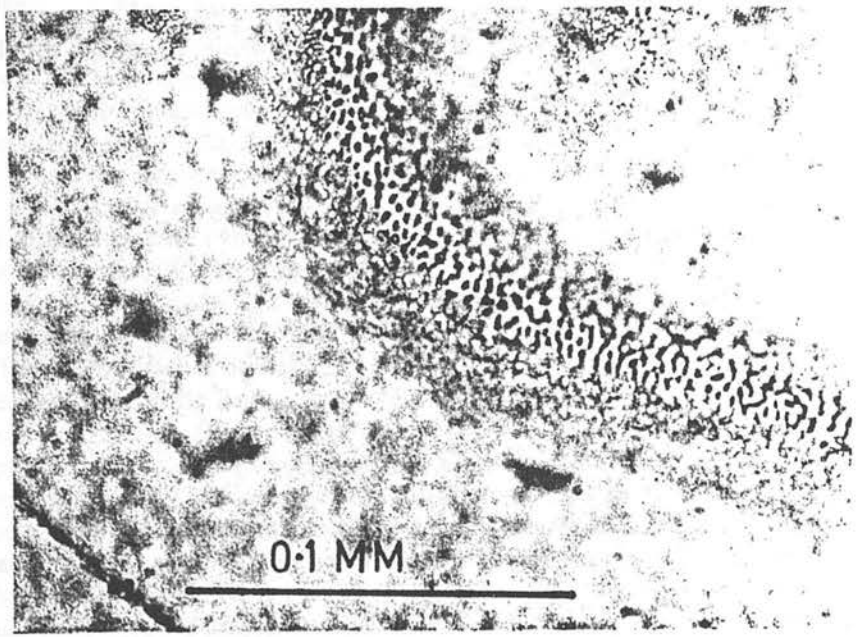

Plate 66B Arcuate zone of secondary fluid inclusions occupying a healed fracture in clinopyroxene, *1860J*, Monastery Mine. (*Mitchell*)

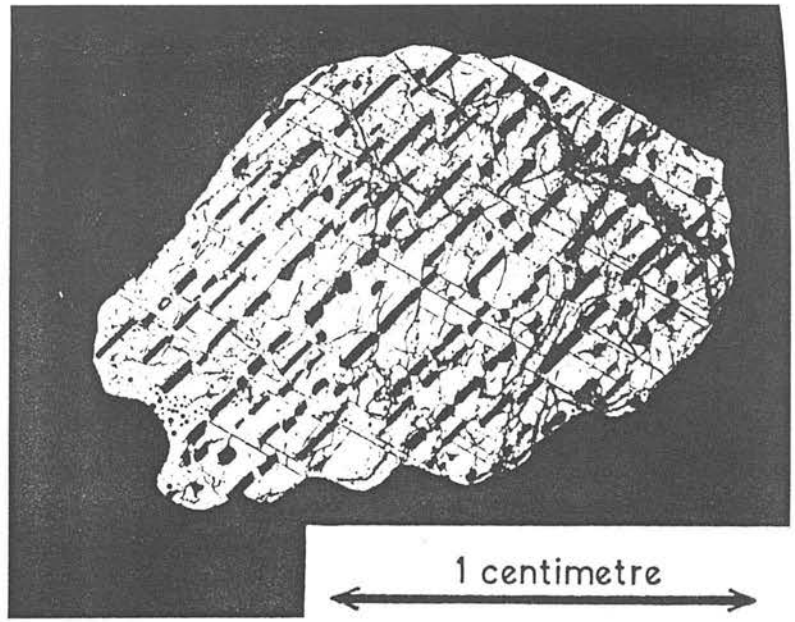

Plate 67A Photomicrograph of clinopyroxene-ilmenite intergrowth from kimberlite in Kentucky, *KEN 1*. Note the fine ilmenite lamellae. Plain light. (*Gurney*)

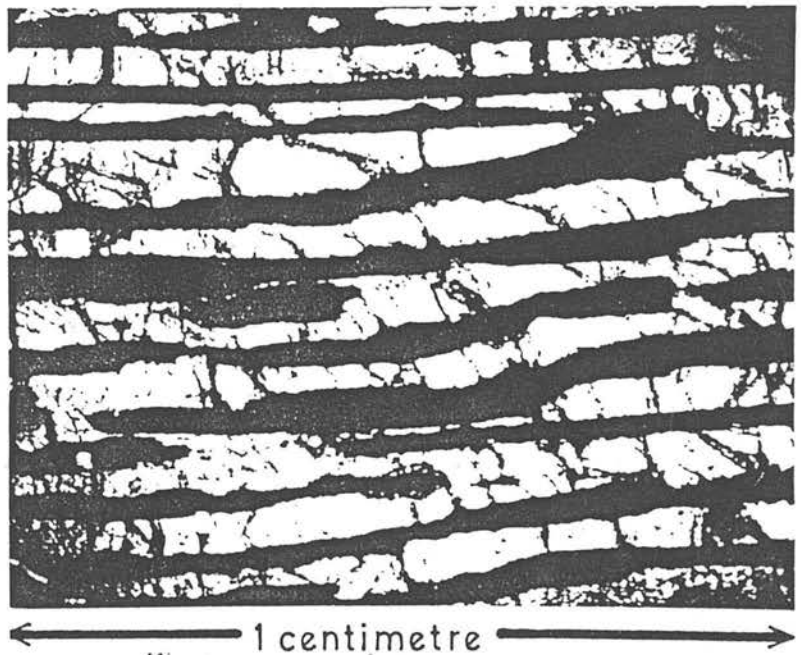

Plate 67B Photomicrograph of lamellar intergrowth of enstatite and ilmenite,

Clinopyroxene

The clinopyroxene analysis (table 63, no. 5) agrees closely with those of other lamellar intergrowths (Boyd, 1971) apart from a threefold increase in MnO.

The pyroxene is colourless but with sinuous and arcuate dark grey discolouration zones cross cut by later fractures. Under high magnification the zones were observed to be composed of large numbers of reddish, rounded to tubular, fluid inclusions (plate 66B), similar to the CO_2 inclusions in ultrabasic nodules from kimberlite, which Roedder (1965) has interpreted as secondary and as occupying healed fractures in the crystal.

RARE EARTH ELEMENT GEOCHEMISTRY OF CLINOPYROXENE

Rare earth element (REE) abundances and chondrite normalized REE distribution patterns for pyroxene and whole rock kimberlite from Monastery are given in table 64 and figure 59A respectively. The pyroxene REE pattern is convex-up with a maxima in the neighbourhood of Nd. The kimberlite pattern is almost linear and shows the strong enrichment in the light REE, typical of

TABLE 64 RARE EARTH ELEMENT ABUNDANCES (IN P.P.M.) IN MONASTERY CLINOPYROXENE AND WHOLE ROCK KIMBERLITE

	La	Ce	Sm	Eu	Tb	Yb	Lu	REE total
Clinopyroxene	3,18	15,24	2,86	1,08	0,54	0,347	0,051	23,3
Kimberlite	97	243	12,58	3,70	1,30	0,985	—	358,6

other South African kimberlites (Philpotts *et al.*, 1972; Mitchell and Brunfelt, in prep.). The pronounced difference in the REE distribution patterns and, in particular, the low abundance of La in the pyroxene, indicates that the pyroxene is not contaminated by the REE-rich kimberlite.

The Monastery clinopyroxene pattern (figure 59B) resembles those patterns found by Philpotts *et al.* (1972) of omphacites from kimberlitic eclogites (although abundances in these pyroxenes are lower), but it contrasts with the pattern for chrome diopside from a garnet lherzolite, which is strongly fractionated and similar to that of whole rock kimberlite.

In assessing the relationship of the Monastery clinopyroxene to kimberlite the following approach is utilized. Equilibrium is assumed between the analysed pyroxene or kimberlite and a coexisting hypothetical kimberlite liquid or pyroxene respectively (Philpotts *et al.*, 1972). Measured phenocryst-matrix REE partition coefficients (Schnetzler and Philpotts, 1970; Onuma *et al.*, 1968) are applied to the REE concentrations for the hypothetical phases, which can then be compared with the distributions actually measured. If good agreement between the actual and hypothetical REE distribution patterns of pyroxenes in equilibrium with kimberlite is obtained, then it is likely that the pyroxene was in equilibrium with the kimberlite and, thus, is in some way genetically related to the kimberlite.

In figure 59A, hypothetical liquids B and D in equilibrium with the pyroxene, have similar REE distribution patterns to that of the kimberlite but differ

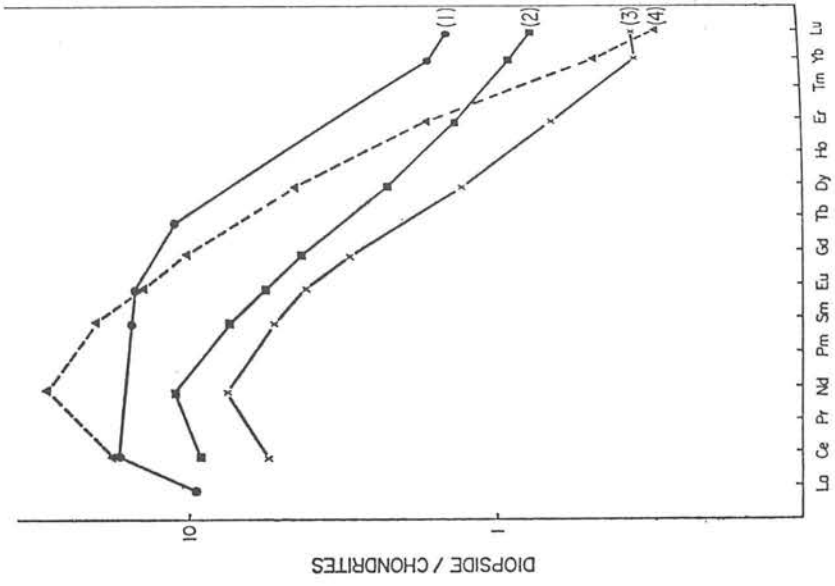

Figure 59B Rare earth element distribution patterns of Monastery diopside *1860J* (1), omphacitic pyroxenes (2 and 3) from Roberts Victor eclogite, and chrome diopside (4) from Roberts Victor garnet lherzolite. Roberts Victor data from Philpotts *et al.* (1972).

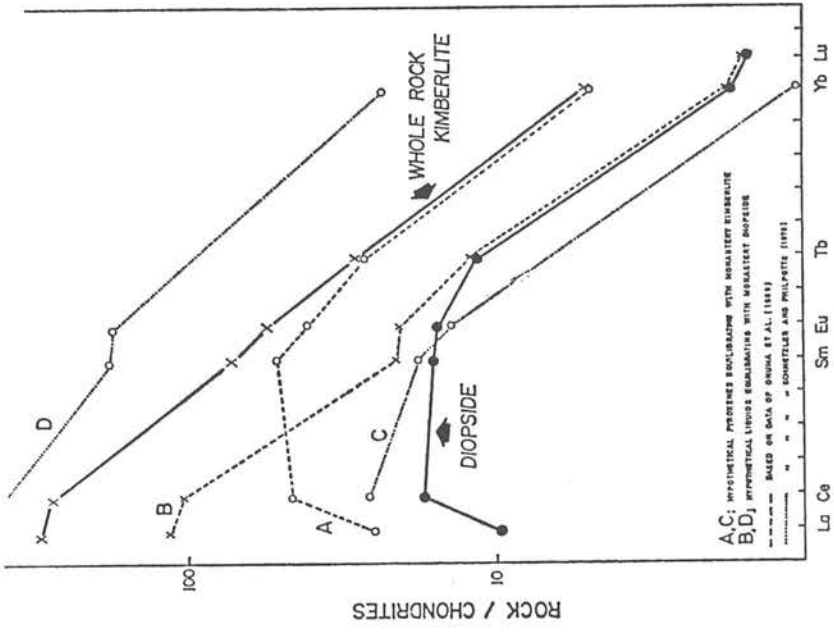

Figure 59A Rare earth element distribution patterns for clinopyroxene and whole rock kimberlite from the Monastery Mine (solid curves). Curves A,B and C,D represent the composition of hypothetical phases in equilibrium with the Monastery material calculated using crystal-liquid partition coefficients determined by Onuma *et al.* (1968) and Schnetzler and Philpotts (1970) respectively. A and C represent the hypothetical pyroxenes in equilibrium with analyzed Monastery kimberlite and B and D the hypothetical liquids in equilibrium with the analyzed pyroxene, *1860J*.

adjusted (in all cases, increased) to three, by converting the necessary proportion of FeO to Fe_2O_3. This gives an Fe_2O_3/FeO ratio (table 63, no. 1) similar to the chemical determination (Ringwood and Lovering, 1970) and calculated ratios (Boyd, 1971a) for ilmenites from comparable xenoliths. Slight variations in total iron and MgO content were found in 10 determinations on large ilmenite plates but otherwise all analyses were very similar. A single analysis from the edge of a large plate (table 63, no. 2) shows a significant increase in TiO_2 and MgO, and decrease in total iron and Fe_2O_3, compared with analysis 1. Previous analyses of ilmenite from ilmenite-clinopyroxene xenoliths (Dawson and Reid, 1970; Ringwood and Lovering, 1970; Boyd, 1971a) are similar to analyses 1 and 2, apart from a somewhat lower MnO content.

TABLE 63 MINERAL ANALYSES OF ILMENITE-CLINOPYROXENE INCLUSION *1860J*

	Ilmenite			Phlogopite	Clinopyroxene
	1	2	3	4	5
SiO_2	—	—	—	41,28	54,58
TiO_2	50,51	54,19	53,32	3,33	0,42
Al_2O_3	0,55	0,60	0,77	7,84	2,42
Cr_2O_3	0,06	0,06	0,07	0,01	0,02
Fe_2O_3	11,64*	5,85*	0,73*	—	—
FeO	30,05*	31,25*	39,35*	9,42†	6,36†
MnO	0,61	0,44	5,35	0,21	0,45
MgO	7,62	9,02	0,81	23,36	17,26
CaO	0,06	0,05	0,06	0,03	17,64
Na_2O	0,05	0,04	0,11	0,22	1,96
K_2O	0,25	0,24	0,37	9,89	0,05
Totals	101,40	101,74	100,94	95,59‡	101,16
	Number of cations for *n* oxygens				
n =	3§	3§	3§	22	6
Si	—	—	—	6,020	1,95
Ti	0,895	0,945	0,990	0,365	0,012
Al	0,015	0,016	0,023	1,348	0,103
Cr	0,001	0,001	0,002	0,001	0,001
Fe^{2+}	0,206	0,102	0,014	—	—
Fe^{3+}	0,592	0,606	0,812	1,149	0,192
Mn	0,012	0,009	0,112	0,026	0,014
Mg	0,267	0,312	0,030	5,077	0,928
Ca	0,002	0,001	0,001	0,004	0,682
Na	0,002	0,002	0,005	0,061	0,137
K	0,008	0,007	0,012	1,840	0,002
$FeTiO_3$	60,8	62,0	84,4		
$MgTiO_3$	27,4	31,9	3,1		
$MnTiO_3$	1,2	0,9	11,6		
Fe_2O_3	10,6	5,2	0,8		

* Fe_2O_3 and FeO calculated for ilmenites from total Fe assuming stoichiometry.
† Total Fe expressed as FeO.
‡ Total does not include F or H_2O.
§ Total cations normalized to 2 in the course of ferric ion calculation.

Analyst: D. A. Carswell.
1 Average of 10 determinations on large plates intergrown with clinopyroxene.
2 Single analysis from edge of a large ilmenite plate.
3 Average of 7 determinations of Mn-rich ilmenite forming very narrow rims around some ilmenite plates.
4 Average of 7 determinations of secondary phlogopite rimming ilmenite plates.
5 Average of 4 determinations of clinopyroxene intergrown with ilmenite.

An average of 7 determinations on Mn-rich ilmenite forming very narrow discontinuous rims around some of the ilmenite plates (table 63, no. 3) is very poor in the *geikielite* molecule, but rich in the *pyrophanite* molecule, compared with analyses 1 and 2. The rims are not noticeable under reflected light.

Trace element analyses of ilmenite from this xenolith have shown that the ilmenite is poor in Cr, Nb and Ta, compared to the monomineralic ilmenite nodules found in kimberlite (Mitchell *et al.*, this volume, p. 231).

Exsolution lamellae are present, but are too fine to be analysed with the microprobe (as noted by Boyd, 1971a), but qualitative scans indicate that the lamellae contain significantly more Fe and A1 than the host ilmenite. (cf. Wittkop, 1971). Optically identical lamellae in a Cr, Nb and Ta deficient ilmenite nodule (not associated with pyroxene) from Monastery have been identified by X-ray diffraction as magnetite (Mitchell, 1973a), and it is considered that the lamellae in the intergrowth ilmenite are also magnetite (with possibly some solid solution towards $FeA1_2O_4$).

Phlogopite

Several of the ilmenite plates have rims of secondary phlogopite. Although F, H_2O and ferric iron were not determined, recalculation of the analysis (table 63, no. 4) anhydrously on a basis of 22 oxygens, shows that the distribution of cations between the various sites agrees well with the general formula of phlogopite. It has a fairly high TiO_2 content, varying from 4,92 wt.%, immediately adjacent to the ilmenite, to as low as 2,25 wt.% further from the ilmenite (7 determinations). Boyd and Nixon (this volume, p. 257) have found 4,1% TiO_2 and enriched iron in the dark rims of phlogopite in ultrabasic nodule, 1859N, from Monastery, compared with 0,9% TiO_2 in the pale cores (plate 66A).

Compared with phlogopites from eclogite xenoliths and kimberlite matrix (Kushiro and Aoki, 1968; Dawson *et al.*, 1970; Rimsaite, 1971; Carswell, unpublished data) the secondary phlogopite is characterized by a rather low Al_2O_3 content.

Seifert and Schreyer (1971) have discussed the occurrence of alumina-free high-silica phlogopite, and postulated that such micas should be found in alumina-poor rocks such as kimberlites. However, the secondary phlogopite here, has 3,01 Si cations per formula unit and an octahedral site occupancy of 2,993 cations per formula unit and, hence, is very close in composition to ideal phlogopite, with very little solid solution towards high Si phlogopite or muscovite. The composition indicates formation in a relatively alumina-rich environment, and if Seifert and Schreyer's (1971) hypothesis is correct, such an environment might have been available at the time garnet was a liquidus phase in the kimberlite magma. Secondary mica would in this case, form deep in the mantle by reaction of the ilmenite-pyroxene intergrowth with potassium and alumina-rich magma. Such an origin is in agreement with kimberlite petrogenetic theories involving limited partial fusion of the mantle to produce alkali-rich liquids (Dawson, 1971; Mitchell, 1973a).

30

PRIMARY AND SECONDARY PHLOGOPITES AND CLINOPYROXENES IN GARNET LHERZOLITE XENOLITHS

By D. A. CARSWELL

Department of Geology, University of Sheffield, Mappin Street, Sheffield, S1 3JD, U.K.

ABSTRACT

Microprobe analyses are presented for primary and secondary phlogopites in six garnet lherzolite xenoliths from South African kimberlite pipes, together with the wet chemical analysis of a bulk mineral separate of phlogopite from a similar xenolith. The primary phlogopites form rare large (2–3 × 1 mm) discrete plates which do not show any textural evidence of disequilibrium towards the other primary phases, whilst the secondary phlogopites form narrow rims around garnets.

The primary phlogopites have lower TiO_2, Cr_2O_3 and Al_2O_3 contents, lower Fe^{2+}/Mg^{2+} and Na^+/K^+ ratios, and higher SiO_2 contents than the secondary phlogopites. They also have much lower TiO_2 contents and Fe^{2+}/Mg^{2+} ratios than the previously postulated TiO_2 rich primary phlogopites from a Lashaine garnet lherzolite xenolith (DAWSON *et al.*, 1970) and from Jan Mayen alkali basalts (FLOWER, 1971). They are thought more likely to represent a primary phase in equilibrium with the four phase garnet lherzolite assemblage in the upper mantle than the Lashaine and Jan Mayen phlogopites.

The presence of on average 1% by volume of primary phlogopite in these xenoliths, thought to have originated from depths of 100–150 km, suggests that the upper mantle material at such depths may contain on average about 0.09 wt.% K_2O and 0.03 wt.% H_2O^+ in phlogopite.

The clinopyroxenes in the xenoliths examined commonly have marginal zones which are significantly depleted in jadeite molecule compared with the primary cores. As no felspar or other Na_2O and Al_2O_3 rich phase could be detected associated with the marginal zones, it appears that the jadeite released has probably been taken up in secondary phlogopite and amphibole.

INTRODUCTION

This paper largely concerns the question of the possible stability of phlogopite in the upper mantle and its bearing on the likely contents of K_2O and H_2O in the upper mantle.

Garnet lherzolite xenoliths are the most common ultramafic xenolith type found in the majority of kimberlite pipes (MATHIAS *et al.*, 1970). They therefore appear to represent the predominant rock type in regions of the upper mantle from which kimberlite originates or through which it passes during its emplacement up into the crust, and hence the possible source rock (O'HARA, 1970) for basalt and other mantle derived magmas. If diamond at least nucleates within its own thermodynamic stability field (MITCHELL and CROCKET, 1971), it is likely that the volatile charged kimberlite magma samples the upper mantle down to depths of at least 150 km. Furthermore, the chemistry of the pyroxenes in the garnet lherzolite xenoliths suggests depths of origin in general in the range 100–200 km (O'HARA, 1967; BOYD and NIXON, 1973).

Whilst whole rock analyses of garnet lherzolite xenoliths can be expected to yield reasonably good data on the major element chemistry of the upper mantle (CARSWELL and DAWSON, 1970; CHEN, 1971) they do not produce reliable figures for K_2O and H_2O because of the possibility of contamination by the relatively K_2O- and H_2O-rich kimberlite magma into which they have been incorporated. It is therefore necessary to deduce the likely K_2O and H_2O values from a consideration of the primary mineralogy and mineral chemistry of the garnet lherzolite xenoliths.

The four principal mineral phases in garnet lherzolites are essentially anhydrous and of these only clinopyroxenes (usually <0.05 wt.% K_2O) contain significant K_2O. That both K_2O and H_2O must be present in the upper mantle is beyond dispute in view of their presence, sometimes in appreciable concentrations, in mantle derived magmas (e.g. alkali olivine basalts, kimberlites, etc.). However, what is in dispute is just how much is present and in which phases it is incorporated. For example, NICHOLLS (1967) estimated the undepleted upper mantle material beneath the mid-oceanic ridges to contain 9.7 wt.% H_2O, whilst WYLLIE's (1971) model for partial melting in the upper mantle assumed a more realistic figure of 0.1 wt.% H_2O. The low K_2O and modal contents of the clinopyroxenes in garnet lherzolites yield whole rock K_2O contents (< 0.005 wt.%) which appear insufficient to account for the K_2O contents of alkali basalts and kimberlites by normal partial melting/fractional crystallization processes, as enrichment factors of 200 or even greater would in general be involved. Thus it would seem likely that both K_2O and H_2O in the upper mantle are contained in an additional phase or phases.

DAWSON and POWELL (1969), FLOWER (1969, 1971) and others have recently argued that most of the K_2O and H_2O in at least the uppermost regions (say first 100 km) of the mantle is contained in small amounts of phlogopite, while OXBURGH (1964) and VARNE (1970) have argued in favour of the presence of amphiboles. Alternatively it has been suggested (WYLLIE, 1971) that these elements may be largely incorporated in small amounts of a water-rich intergranular liquid phase, especially at depths where the temperatures are expected to be above the breakdown temperatures of amphiboles and phlogopites. Further suggestions are that in the upper mantle H_2O may be incorporated in the nominally anhydrous silicates through hydroxyl substitution in limited amounts in certain oxygen point-positions (MARTIN and DONNAY, 1972) or in high pressure so-called hydroxylated pyroxenes and garnets (LAMBERT and WYLLIE, 1970; FYFE, 1970; SCLAR, 1970).

PETROGRAPHY

All six rock specimens, for which microprobe mineral analyses are presented in this paper, are of the common four-phase granular garnet lherzolite xenolith type, such as were the majority of those previously analysed by CARSWELL and DAWSON (1970). Like the previously studied specimens they contain on average about 60 vol.% olivine, 25 vol.% orthopyroxene, 3–8 vol.% clinopyroxene and 5–10 vol.% garnet, together with minor amounts of phlogopite, amphibole and spinel.

Specimens CK1, CK2, CK3 and CK4 were from mines in the Kimberley area; specimens CB4 and CB6 from the Bultfontein dumps.

Although phlogopite is only present as a minor phase, petrographic examination of these xenoliths suggests the common presence of two generations of phlogopite growth. On the one hand, it forms rare, large discrete plates (Fig. 1A)—commonly about 2-3 mm

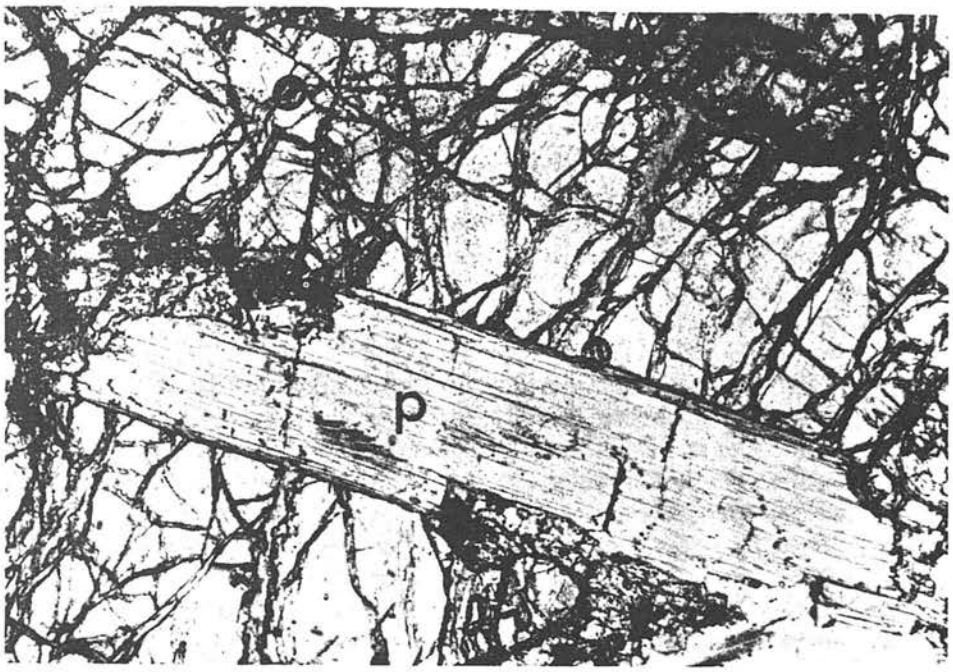

A. Primary phlogopite plate (labelled p) in garnet lherzolite CK1—approximate magnification × 30. Plane-polarized light.

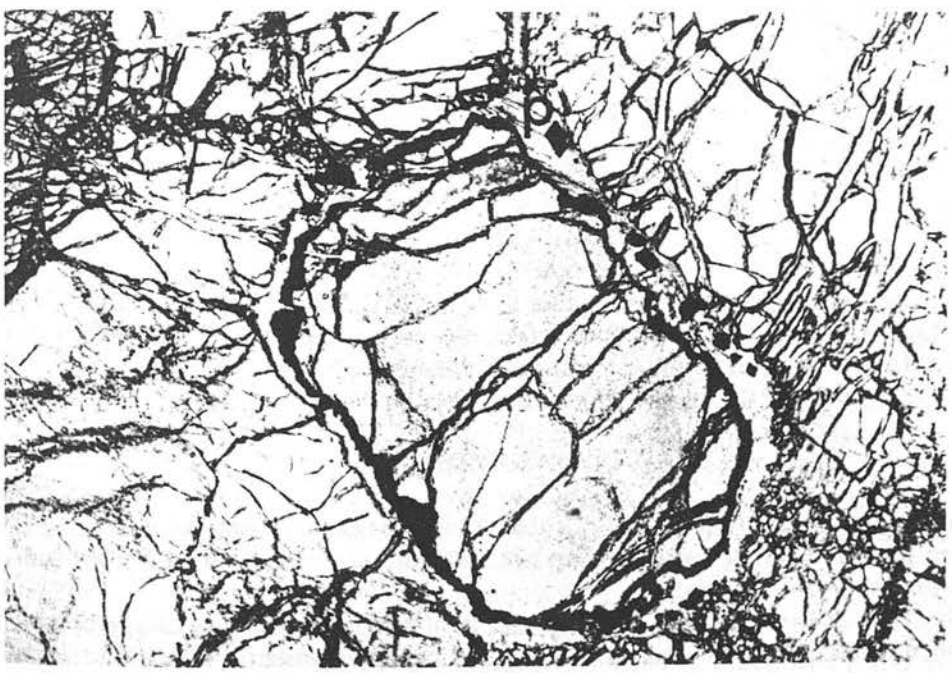

B. Rim of secondary phlogopite (labelled p) around garnet in garnet lherzolite xenolith CB2—approximate magnification × 30. Plane-polarized light.

FIG. 1

in length and 1 mm across and only two or three plates in any particular 2 × 3-cm section—showing no apparent textural evidence of being in disequilibrium with the other primary minerals and hence thought itself to be primary, in the sense that it crystallized in equilibrium with the primary, albeit sub-solidus, four-phase garnet lherzolite assemblage. In addition it forms generally narrow (0.1–0.4 mm) rims around some garnets (Fig. 1B) where it is undoubtedly of secondary growth. Of the six xenoliths studied with the microprobe four contained both primary and secondary phlogopite together in the same polished thin section, whilst of the other two CK2 only contained primary phlogopite and CB4 only secondary phlogopite.

An interesting petrographic feature of the clinopyroxenes in all the xenoliths except CB6, is the existence in most grains of rather cloudy "porous" outer zones around clear pale-green cores. These "porous" rims are variable in width even in the same grain and in places cut right across the grains and almost completely replace the original clear clinopyroxene. The "porous" zone always extinguishes in the same position as the unaltered part of the grain and is clearly an alteration feature within an original homogeneous clinopyroxene grain, the whole grain having the same birefringence colour.

Similar alteration zones have previously been described in clinopyroxenes in spinel lherzolite xenoliths from basalts, for example see ERNST (1936), WILSHIRE and BINNS (1961), WHITE (1966), and KUTOLIN and FROLOVA (1970). ERNST (1936) and WILSHIRE and BINNS (1961) have interpreted the porous alteration zones as being due to the presence of devitrified glass cavities in the pyroxene, whilst with X-ray powder photographs and microprobe examination WHITE (1966) thought that he could detect the presence of felspar together with jadeite depleted diopside and sometimes brown spinel octahedra in the alteration zones.

It is also worthy of note that the overall textural relationship of the clinopyroxene in xenolith CB4 is quite different from that in the other five xenoliths, or indeed in all the other garnet lherzolite xenoliths observed by the author to date. All the other xenoliths have an essentially granoblastic fabric, but in CB4 the texture is strikingly igneous in character with the clinopyroxene growing in a markedly poikilitic habit with respect to garnet in particular, but also towards both the orthopyroxene and olivine. It is also worth noting that this xenolith was the only one of the six studied which did not contain apparent primary phlogopite.

MINERAL CHEMISTRY

The minerals were analysed by the author using an ARL-EMX microprobe by courtesy of the Mineralogisk-Geologisk Museum in Oslo. Selected natural mineral standards were used and the results corrected using the method of BENCE and ALBEE (1968).

PHLOGOPITES

Analyses of five primary phlogopites (Table 1) and five secondary phlogopites (Table 2) are given together with the corresponding structural formulae calculated anhydrous with respect to twenty-two oxygens.

Each of the analyses given is an average of from two to six analyses of appropriate phlogopite grains in the xenolith in question. In the majority of cases the internal variation

TABLE 1. PRIMARY PHLOGOPITES

Wt.%	CK1	CK2	CK3	CK4	CB6
SiO_2	40.7	41.2	41.1	41.5	41.7
TiO_2	0.28	0.22	0.15	0.26	0.68
Al_2O_3	12.8	12.4	13.2	12.5	12.2
Cr_2O_3	0.86	0.70	0.60	0.75	0.61
*FeO	2.63	2.64	2.56	2.52	2.78
MnO	0.01	0.05	0.01	0.03	0.02
MgO	26.5	26.6	27.9	26.5	26.5
CaO	0.02	0.02	0.02	0.01	0.01
Na_2O	0.75	0.76	0.99	0.91	0.31
K_2O	9.31	9.32	8.78	9.16	10.2
Total	93.9	93.9	95.3	94.1	95.0

*FeO — total iron as FeO
CK — samples from Kimberley Mines
CB — samples from Bultfontein Dumps

STRUCTURAL FORMULAE CALCULATED ANHYDROUS WITH RESPECT TO TWENTY-TWO OXYGENS

Si^{4+}	5.82	7.98	5.89	7.97	5.77	7.96	5.90	7.99	5.90	7.94
Al^{3+}	2.16		2.08		2.19		2.09		2.04	
Ti^{4+}	0.030		0.024		0.032		0.028		0.072	
Cr^{3+}	0.098		0.079		0.066		0.084		0.068	
Fe^{2+}	0.314	6.09	0.315	6.07	0.300	6.23	0.300	6.03	0.329	6.06
Mn^{2+}	0.001		0.006		0.001		0.003		0.003	
Mg^{2+}	5.65		5.65		5.83		5.62		5.59	
Ca^{2+}	0.003		0.003		0.003		0.002		0.002	
Na^{+}	0.208	1.91	0.211	1.91	0.270	1.84	0.251	1.91	0.085	1.93
K^{+}	1.70		1.70		1.57		1.66		1.84	
Fe^{2+}/Mg^{2+}	0.056		0.056		0.051		0.053		0.059	
Na^{+}/K^{+}	0.123		0.124		0.172		0.151		0.046	

in the group of analyses averaged was strikingly small. Furthermore, it is apparent that there is in fact little variation in composition within the groups of primary and secondary phlogopites from the different xenoliths.

However, striking differences in composition exist between the group of primary phlogopite grains and the group of secondary phlogopite grains. The secondary phlogopites have appreciably higher TiO_2 and Cr_2O_3 contents, significantly higher Al_2O_3 contents and Fe^{2+}/Mg^{2+} and Na^{+}/K^{+} ratios, and somewhat lower SiO_2 contents.

All the phlogopite microprobe analyses in Tables 1 and 2 have low totals. However, several elements were not determined—notably H_2O^{+}, F, BaO and NiO. Also as the oxidation state of iron was not determined, total iron has been expressed as FeO.

As a check on the microprobe analyses in view of the low totals and also to find out the contents of the other elements thought likely to be present, a bulk mineral separate of phlogopite from garnet lherzolite xenolith BD 1150 (CARSWELL and DAWSON, 1970) was prepared and analysed by Mr. V. A. Somogyi at Sheffield University using a combination of atomic absorption, spectrophotometric, flame photometric and gravimetric techniques. This xenolith contains the highest proportion of apparent primary phlogopite plates in any xenolith so far examined by the author, together with secondary phlogopite rims (up to 0.2 mm in width) around the garnets.

TABLE 2. SECONDARY PHLOGOPITES

Wt.%	CK1	CK3	CK4	CB4	CB6
SiO_2	39.7	39.0	39.2	39.1	39.3
TiO_2	1.45	0.45	0.86	1.36	1.41
Al_2O_3	13.9	16.1	14.5	15.1	14.8
Cr_2O_3	1.60	1.51	1.36	1.57	1.50
*FeO	3.12	3.15	3.17	2.95	2.90
MnO	0.10	0.02	0.14	0.05	0.02
MgO	24.8	25.3	24.5	25.1	24.7
CaO	0.03	0.02	0.03	0.02	0.03
Na_2O	0.92	1.41	1.82	1.05	0.92
K_2O	9.06	7.87	7.38	8.41	9.14
Total	94.7	94.8	93.0	94.7	94.7

*FeO total iron as FeO
CK samples from Kimberley Mines
CB samples from Bultfontein Dumps

STRUCTURAL FORMULAE CALCULATED ANHYDROUS WITH RESPECT TO TWENTY-TWO OXYGENS

Si^{4+}	5.65	7.99		5.52	8.00		5.65	8.00	5.54	8.00		5.59	8.01	
$Al^{3+(IV)}$	2.34			2.48			2.35		2.46			2.41		
$Al^{3+(VI)}$	—			0.194			0.114		0.071			0.076		
Ti^{4+}	0.155			0.048			0.093		0.145			0.151		
Cr^{3+}	0.180			0.168			0.154		0.176			0.169		
Fe^{2+}	0.371	5.99		0.372	6.11		0.382	6.01	0.350	6.06		0.345	5.97	
Mn^{2+}	0.012			0.003			0.017		0.006			0.003		
Mg^{2+}	5.27			5.32			5.25		5.31			5.30		
Ca^{2+}	0.004			0.003			0.004		0.003			0.004		
Na^+	0.253	1.91		0.386	1.81		0.509	1.87	0.288	1.81		0.253	1.92	
K^+	1.65			1.42			1.36		1.52			1.66		
Fe^{2+}/Mg^{2+}	0.070			0.070			0.073		0.066			0.066		
Na^+/K^+	0.154			0.272			0.376		0.189			0.153		

Unfortunately, in order to obtain sufficient material for a complete analysis, a bulk mineral separate of both primary and secondary phlogopite had to be prepared and even then it was found impossible to produce a separate in sufficient quantity which was absolutely free of clinopyroxene grains. However, in view of the very low CaO figures (0.03 wt.% maximum) for all the phlogopites analysed with the microprobe, it was possible to correct the phlogopite analysis to account for the presence of the small amount of clinopyroxene. Accordingly in Table 3, the phlogopite analysis in the first column has been corrected in the second column by reducing the CaO figures from 0.42 to 0.02 wt.% and making appropriate corrections to the other oxide values. This was equivalent to subtracting 2.027 wt.% of clinopyroxene from the analysis, an analysis of the clinopyroxene in BD 1150 having been performed separately.

In both the uncorrected and corrected phlogopite analyses in Table 3, SiO_2 has been determined by difference from 100.00 as insufficient material was available for a gravimetric SiO_2 determination.

The wet analysis for the bulk phlogopite separate shows as suspected the presence of significant amounts of F, BaO and NiO and well over 3 wt.% H_2O^+. The analysis total for the ten elements determined in the microprobe analyses, including total iron expressed as

TABLE 3

Wt.%	Phlogopite BD1150	Corrected phlogopite BD1150	Structural formula on basis of 24 (O, OH, F, Cl)		
*SiO_2	40.4	40.1	Si^{4+}	5.705	7.994
TiO_2	0.51	0.52			
P_2O_5	0.02	0.02	P^{5+}	0.002	
Al_2O_3	13.4	13.6	Al^{3+}	2.287	
Cr_2O_3	0.76	0.73	Ti^{4+}	0.056	6.386
Fe_2O_3	1.06	1.05	Cr^{3+}	0.082	
FeO	2.33	2.35	Fe^{3+}	0.113	
MnO	0.03	0.03	Fe^{2+}	0.280	
NiO	0.22	0.22	Mn^{2+}	0.003	
MgO	27.2	27.5	Ni^{2+}	0.025	
CaO	0.42	0.02	Mg^{2+}	5.827	
BaO	0.41	0.42	Ca^{2+}	0.003	1.958
Na_2O	0.76	0.73	Ba^{2+}	0.063	
K_2O	9.12	9.31	Na^{+}	0.202	
F	0.28	0.28	K^{+}	1.690	
Cl	0.03	0.03			
H_2O^{+}	3.17	3.24	F'	0.126	3.209
Total	100.1	100.1	Cl'	0.007	
Less O ≡ F	0.12	0.12	OH'	3.076	
Less O ≡ Cl	0.01	0.01	*Fe^{2+}/Mg^{2+}		0.067
Adjusted total	100.00	100.00	Na^{+}/K^{+}		0.120

*Fe^{2+}/Mg^{2+} Ratio is based on total iron expressed as FeO as with the other analysed phlogopites.
*SiO_2 SiO_2 by difference from 100.00.

FeO, is 95.81 wt.% showing that the totals for the microprobe analyses (average total 94.42 wt.%) are reasonably respectable although somewhat on the low side. The analysis of the bulk phlogopite separate is as to be expected somewhat intermediate in character between the microprobe primary and secondary phlogopite analyses, but approaches most closely the analyses of the primary phlogopites.

CLINOPYROXENES

Microprobe analyses are presented for both the clear primary clinopyroxene cores (Table 4) and the cloudy porous clinopyroxene rims (Table 5).

As the oxidation state of iron was not determined analytically, the Fe^{2+}/Fe^{3+} ratio must be fixed before the percentage of jadeite molecule in these clinopyroxenes can be estimated. Two independent methods of fixing the Fe^{2+}/Fe^{3+} ratio were attempted. Firstly, from the structural formulae by a calculation procedure which assumed stoichiometry. However, this procedure, which is particularly sensitive to analytical errors in SiO_2, results in all, or virtually all, the iron being calculated as Fe_2O_3 in the majority of these clinopyroxenes.

As such low Fe^{2+}/Fe^{3+} ratios seemed unrealistic, the FeO and Fe_2O_3 figures in Tables 4 and 5 are based on the alternative method of arbitrarily fixing a third of the total iron determined as FeO as Fe_2O_3 in order to give Fe^{2+}/Fe^{3+} ratios which correspond roughly

TABLE 4. PRIMARY CLINOPYROXENE CORES

Wt.%	CK1	CK2	CK3	CK4	CB4	CB6
SiO_2	54.9	55.3	54.8	54.2	54.8	54.6
TiO_2	0.09	0.09	0.08	0.08	0.05	0.15
Al_2O_3	3.37	3.48	3.39	2.30	4.63	2.54
Cr_2O_3	1.89	1.64	1.85	1.61	2.69	1.62
*Fe_2O_3	0.86	0.93	0.93	0.78	0.90	0.81
FeO	1.54	1.67	1.76	1.39	1.62	1.47
MnO	0.09	0.22	0.10	0.20	0.12	0.12
MgO	15.6	15.2	15.4	16.2	14.7	17.0
CaO	19.3	18.2	19.1	20.6	16.5	20.0
Na_2O	2.74	3.12	3.09	2.08	4.02	2.33
K_2O	0.04	0.01	0.05	0.01	0.04	0.07
Total	100.4	99.9	100.6	99.5	100.1	100.7
STRUCTURAL FORMULAE ON BASIS OF SIX OXYGENS						
Si^{4+}	1.97	1.99	1.97	1.97	1.97	1.96
Ti^{4+}	0.002	0.002	0.002	0.002	0.001	0.004
Al^{3+}	0.143	0.148	0.144	0.099	0.196	0.107
Cr^{3+}	0.054	0.047	0.053	0.046	0.076	0.046
Fe^{3+}	0.023	0.025	0.025	0.021	0.024	0.022
Fe^{2+}	0.046	0.050	0.053	0.042	0.049	0.044
Mn^{2+}	0.003	0.007	0.003	0.006	0.004	0.004
Mg^{2+}	0.836	0.816	0.825	0.880	0.787	0.910
Ca^{2+}	0.744	0.702	0.736	0.801	0.635	0.769
Na^{+}	0.191	0.218	0.215	0.147	0.280	0.162
K^{+}	0.002	0.000	0.002	0.000	0.002	0.003
Total	4.01	4.01	4.03	4.02	4.02	4.03
% Jd.	10.2	14.1	11.4	6.3	15.9	6.6
Ca/Ca + Mg	0.471	0.462	0.472	0.477	0.447	0.458

*Fe_2O_3—third total iron as FeO arbitrarily fixed as Fe_2O_3,
Jd—jadeite,
CK—samples from Kimberley Mines,
CB—samples from Bultfontein Dumps.

to the ratios found in general in other ultramafic xenolith clinopyroxenes for which the values were determined analytically. The percentage of jadeite molecule indicated is the average value obtained by two calculation methods—firstly, from the remaining Na^+ after calculation of $NaFe^{3+}Si_2O_6$ and $NaCrSi_2O_6$, and secondly, from the remaining Al^{3+} after the calculation of $CaTiAl_2O_6$ and $CaAl_2SiO_6$ when $Si^{4+} + Al^{3+[IV]} = 2.000$.

It is apparent from a comparison of the analyses in Tables 4 and 5 that by far the most striking difference in composition between the clear clinopyroxene cores and the cloudy porous margins is the decrease in the Al_2O_3 and Na_2O contents in the latter, reflected in the much lower per cent jadeite figures. On the other hand, differences in Cr_2O_3 content are negligible and in Ca/Ca + Mg ratio only minimal—corresponding to equilibrium temperatures only some 20–80°C lower for the rims than the cores on the basis of the solid solution limits in the synthetic diopside-enstatite system at 30 kbar pressure (DAVIES and BOYD, 1966).

TABLE 5. CLOUDY CLINOPYROXENE RIMS

Wt.%	CK1	CK2	CK3	CK4	CB4
SiO_2	54.2	54.7	54.4	53.8	54.1
TiO_2	0.09	0.08	0.08	0.09	0.04
Al_2O_3	2.31	1.43	2.30	1.26	3.44
Cr_2O_3	1.76	1.82	1.82	1.60	2.65
$*Fe_2O_3$	0.80	0.88	0.79	0.82	0.87
FeO	1.43	1.58	1.41	1.49	1.56
MnO	0.09	0.22	0.11	0.20	0.12
MgO	16.2	16.6	16.3	16.2	15.5
CaO	21.0	20.5	20.7	22.7	19.2
Na_2O	2.24	1.76	2.19	0.96	2.29
K_2O	0.07	0.01	0.05	0.00	0.04
Total	100.2	99.6	100.2	99.1	99.8

STRUCTURAL FORMULAE ON BASIS OF SIX OXYGENS

Si^{4+}	1.96	1.99	1.97	1.97	1.96
Ti^{4+}	0.002	0.002	0.002	0.002	0.001
Al^{3+}	0.098	0.061	0.098	0.054	0.147
Cr^{3+}	0.050	0.052	0.052	0.046	0.076
Fe^{3+}	0.022	0.024	0.022	0.023	0.024
Fe^{2+}	0.043	0.048	0.043	0.046	0.047
Mn^{2+}	0.003	0.007	0.003	0.006	0.064
Mg^{2+}	0.875	0.897	0.880	0.888	0.837
Ca^{2+}	0.816	0.800	0.802	0.892	0.743
Na^{+}	0.157	0.124	0.154	0.068	0.161
K^{+}	0.003	0.000	0.002	0.000	0.002
Total	4.03	4.01	4.03	4.00	4.00
% Jd.	5.6	4.4	5.8	0.2	6.3
Ca/Ca + Mg	0.482	0.471	0.477	0.501	0.470

$*Fe_2O_3$—third total iron as FeO arbitrarily fixed as Fe_2O_3,
Jd—Jadeite,
CK—samples from Kimberley Mines,
CB—samples from Bultfontein Dump.

No additional Na_2O and Al_2O_3 rich phase such as plagioclase was detected to be associated with the jadeite depleted clinopyroxene rims, at least in amounts resolvable with the microprobe.

DISCUSSION

The experimental data at present available (KUSHIRO *et al.*, 1967; YODER and KUSHIRO, 1969; MODRESKI and BOETTCHER, 1972) indicates that the stability field of phlogopite is likely to extend down into the upper mantle—perhaps to depths as great as 150–200 km in continental regions with low geothermal gradient. Phlogopite is likely to be stable to appreciably greater depths in the mantle than amphibole (KUSHIRO, 1969; ALLEN *et al.*, 1972).

It is therefore not unreasonable to postulate that in the garnet lherzolite xenoliths studied the large phlogopite plates, showing no apparent disequilibrium towards the other primary mineral phases, as indicated by textural relationships, are themselves part of the primary mineral assemblage. These phlogopites have, however, significantly different chemical compositions from the primary phlogopites described by DAWSON *et al.* (1970) and FLOWER (1969, 1971).

TABLE 6. POSTULATED PRIMARY PHLOGOPITES

Wt.%	A	B	C
SiO_2	41.3	39.98	40.10
TiO_2	0.32	9.13	6.15
Al_2O_3	12.6	13.45	12.12
Cr_2O_3	0.70	0.71	n.d.
Fe_2O_3	—	—	0.63
FeO	2.63	3.57	8.84
MnO	0.02	0.04	0.82
MgO	26.8	18.73	17.40
CaO	0.02	0.00	0.00
Na_2O	0.74	0.06	1.00
K_2O	9.36	9.64	8.36
H_2O	n.d.	n.d.	3.70
Total	94.5	95.31	99.02
Fe^{2+}/Mg^{2+}	0.055	0.107	0.282
Na^+/K^+	0.120	0.009	0.181

A. Mean of five primary phlogopites, this paper.
B. Phlogopite from Lashaine xenolith (BD738)—DAWSON *et al.* (1970).
C. Phlogopite from Jan Mayèn alkali basalt—FLOWER (1969).

In Table 6 the mean of the five postulated primary phlogopites analysed in this paper may be compared with DAWSON *et al.*'s (1970) postulated primary phlogopite from a mica garnet lherzolite (BD 738) from the carbonatite tuff of the Lashaine volcano, and with FLOWER's (1969, 1971) postulated mantle phlogopite which forms xenocrysts in gas vesicles in Jan Mayen alkali basalts.

Both the Lashaine and Jan Mayen phlogopites are characterized by remarkably high TiO_2 contents in contrast with the low TiO_2 contents in the primary phlogopites analysed here.

The undoubted secondary phlogopites in the xenoliths studied here have somewhat higher TiO_2 contents (mean 1.11 wt.%). The highest TiO_2 contents (3.33 wt.%) found in phlogopites by this author occurred in secondary phlogopite around ilmenite in a Monastery Mine ilmenite-clinopyroxene xenolith (MITCHELL *et al.*, 1973).

The postulated primary phlogopites also have a significantly lower Fe^{2+}/Mg^{2+} ratio together with higher Na_2O contents and Na^+/K^+ ratio than the Lashaine phlogopite. They also have a very much lower Fe^{2+}/Mg^{2+} ratio and MnO contents and somewhat lower Na^+/K^+ ratio than the Jan Mayen phlogopite. It is therefore felt on chemical grounds, particularly in view of their much lower TiO_2 contents and Fe^{2+}/Mg^{2+} ratio, that the phlogopite plates described in this paper are more likely to represent a primary phase in equilibrium with the four-phase garnet lherzolite assemblage in the upper mantle than the phlogopites from Lashaine and Jan Mayen.

As the garnet lherzolites studied contained on average 1% by volume of primary phlogopite this suggests that the upper mantle, at depths of the order of 100–150 km, contains on average 0.09 wt.% K_2O and 0.03 wt.% H_2O in phlogopite. Clinopyroxenes, together with the other primary minerals can be expected to contribute at the most about 0.005 wt.% K_2O to the overall value in the upper mantle and, it is assumed, negligibly H_2O—although this assumption has recently been questioned (MARTIN and DONNAY, 1972). Any amphibole present in the garnet lherzolite xenoliths studied by the author occurs adjacent to garnet and appears to be secondary.

One can therefore estimate that the upper mantle at depths of roughly 100–150 km contains on average 0.10 wt.% K_2O and 0.03 wt.% H_2O^+. Clearly, however, the concentration of primary phlogopite in a much larger number of garnet lherzolite xenoliths from different kimberlite localities must be observed before one can place much reliance on these upper mantle K_2O and H_2O estimates. Local variations in the amount of primary phlogopite would lead to very large variations in K_2O and H_2O contents in the upper mantle.

However, the proposed figure of about 0.10 wt.% for K_2O in the upper mantle is within the estimates of 0.02–0.15 wt.% given by KUSHIRO *et al.* (1967) on the basis of a 10% enrichment factor of K_2O in basalts compared with its upper mantle source material, and close to RINGWOOD's (1966) estimate of 0.13 wt.% for his pyrolite model mantle composition. The H_2O figure of 0.03 wt.% is rather lower than the figure of 0.1 wt.% assumed by RINGWOOD (1969) and WYLLIE (1971). However, the possibility of additional water being present in other minerals or in intergranular liquid films cannot at present be ruled out. Indeed recent water determinations by the author on clinopyroxenes and orthopyroxenes from garnet lherzolite xenoliths have indicated the presence of on average 0.2–0.3 wt.% H_2O in both pyroxenes. With about 30% by volume of pyroxenes in such xenoliths this would bring the likely figure for water in the upper mantle up to roughly 0.1 wt.%.

As regards the jadeite depleted marginal zones around the clinopyroxenes in the analysed xenoliths, it seems most likely that the Na_2O and Al_2O_3 released, possibly as a consequence of the pressure decrease during kimberlite emplacement, has been taken up in both the secondary phlogopite and the secondary amphibole which is also present in small amounts. It is noteworthy that the secondary phlogopites have higher Na^+/K^+ ratios than the primary phlogopites and indeed also higher Na^+/K^+ ratios than the phlogopites usually found in the kimberlite pipes (see RIMSAITE, 1971, table 1).

The clinopyroxene of distinctly poikilitic habit in xenolith CB4 has a lower Ca/Ca + Mg ratio than the clinopyroxenes in the other granoblastic textured xenoliths—indicating the highest temperature of crystallization (roughly 1060°C). This xenolith was the only one studied which did not contain apparent primary phlogopite, suggesting that it may have crystallized at temperatures above the melting temperature of phlogopite in the upper mantle. Similarly, BOYD and NIXON (1973) have noted that amongst the garnet lherzolite xenolith suite in the kimberlites of Northern Lesotho, phlogopite is present in the granular textured xenoliths but absent in the higher temperature (roughly >1100°C) assemblages of the sheared xenoliths.

It therefore appears likely that in the garnet lherzolites of the upper mantle equilibrated at relatively shallow depths (<150–200 km) much of the K_2O, and possibly also H_2O, is contained in small amounts of phlogopite, and this phlogopite may be termed primary in the sense that it crystallized in equilibrium with the four-phase garnet lherzolite assemblage before incorporation of the xenolith in the kimberlite pipe. However, at greater depths in

the mantle phlogopite is likely to be unstable (MODRESKI and BOETTCHER 1972) and K_2O (and H_2O) are presumably contained in small amounts of intergranular liquid. The depth at which phlogopite melts in the upper mantle may correspond to the lithosphere/asthenosphere interface.

The texture of xenolith CB4 is important in that it points to the initial crystallization of the four-phase garnet lherzolite assemblage from the solidus. This would be contrary to an interpretation of the granular garnet lherzolites as olivine + orthopyroxene residua in which both garnet and clinopyroxene only appear at sub-solidus temperatures through exsolution from high temperature aluminous orthopyroxene. Nevertheless, NIXON and BOYD (1973) have presented data which indicate that the common granular garnet lherzolite xenoliths are depleted in Na, Ti, Fe, Ca and Al relative to the sheared garnet lherzolites and even more so relative to RINGWOOD's (1966) hypothetical pyrolite mantle composition, and consequently concluded that they represent essentially residual "depleted" mantle after extensive upper mantle partial melting. Such an interpretation of the granular garnet lherzolites casts doubts over any assumption that the levels of K_2O and H_2O contained in the postulated primary phlogopite observed in these xenoliths are representative of the initial levels in the upper mantle source rocks for basaltic and other mantle derived magmas. However, the whole question of whether or not the phlogopite bearing granular garnet xenoliths are suitable source rocks for basaltic magmas, and hence represent "fertile" or "depleted" upper mantle, is still clearly open for debate.

ACKNOWLEDGEMENTS

The kimberlite xenolith specimens studied were kindly supplied by B. Hawthorne of De Beers Consolidated Mines Limited. The microprobe work at the Mineralogisk–Geologisk Museum in Oslo was supported by a grant from The Royal Society and the encouragement of Professor K. S. Heier and valuable assistance of W. L. Griffin and R. Åmli were greatly appreciated. In addition the author wishes to thank V. Somogyi for the wet chemical analysis of phlogopite BD 1150.

REFERENCES

ALLEN, J. C., MODRESKI, P. J., HAYGOOD, C. and BOETTCHER, A. L. (1972) The role of water in the mantle of the Earth. *Report 24th Int. Geol. Cong. Section 2*, 231–40.

BENCE, A. E. and ALBEE, A. L. (1968) Empirical correction factors for the electron microanalysis of silicates and oxides. *J. Geol.* **76**, 382–403.

BOYD, F. R. and NIXON, P. H. (1973) Origin of the lherzolite nodules in the kimberlites of Northern Lesotho. *Int. Conf. Kimberlites–Cape Town, Abstracts of Papers*, pp. 47–50.

CARSWELL, D. A. and DAWSON, J. B. (1970) Garnet peridotite xenoliths in South African kimberlite pipes and their petrogenesis. *Contr. Mineral. Petrol.* **25**, 163–84.

CHEN JU-CHIN (1971) Petrology and chemistry of garnet lherzolite nodules in kimberlite from South Africa. *Amer. Mineral.* **56**, 2098–110.

DAVIES, B. T. C. and BOYD, F. R. (1966) The join $Mg_2Si_2O_6$–$CaMgSi_2O_6$ at 30 kilobars pressure and its application to pyroxenes from kimberlites. *J. Geophys. Res.* **71**, 3567–76.

DAWSON, J. B. and POWELL, D. G. (1969) Mica in the upper mantle. *Contr. Mineral. Petrol.* **22**, 233–7.

DAWSON, J. B., POWELL, D. G. and REID, A. M. (1970) Ultrabasic xenoliths and lava from the Lashaine volcano, northern Tanzania. *J. Petrol.* **11**, 519–48.

ERNST, T. (1936) Der melilith-basalt des Westberges bei Hofgeismar, nördlich von Kassal, also assimilationsprodukt ultrabasischer gesteine. *Chem. Erde* **10**, 631–66.

FLOWER, M. J. F. (1969) Phlogopite from Jan Mayen Island, North Atlantic. *Earth Planet. Sci. Lett.* **6**, 461–6.
FLOWER, M. J. F. (1971) Evidence for the role of phlogopite in the genesis of alkali basalts. *Contr. Mineral. Petrol.* **32**, 126–37.
FYFE, W. S. (1970) Lattice energies, phase transformations, and volatiles in the mantle. *Phys. Earth. Planet. Interiors* **3**, 196–200.
KUSHIRO, I. (1969) Stability of amphibole and phlogopite in the upper mantle. *Carnegie Inst. Washington, Yearb.* **68**, 245–7.
KUSHIRO, I., SYONO, Y. and AKIMOTO, S. (1967) Stability of phlogopite at high pressures and possible presence of phlogopite in the Earth's upper mantle. *Earth Planet. Sci. Lett.* **3**, 197–203.
KUTOLIN, V. A. and FROLOVA, V. M. (1970) Petrology of ultrabasic inclusions from basalts of Minusa and Transbaikalian regions (Siberia, U.S.S.R.). *Contr. Mineral. Petrol.* **29**, 163–79.
LAMBERT, I. B. and WYLLIE, P. J. (1970) Melting in the deep crust and upper mantle and the nature of the low velocity zone. *Phys. Earth Planet. Interiors* **3**, 316–22.
MARTIN, R. F. and DONNAY, G. (1972) Hydroxyl in the mantle. *Amer. Mineral.* **57**, 554–70.
MITCHELL, R. H., CARSWELL, D. A., BRUNFELT, A. O. and NIXON, P. H. (1973) Mineralogy and rare earth geochemistry of an ilmenite–clinopyroxene xenolith from the Monastery Mine kimberlite. In: *Lesotho Kimberlites* (editor P. H. NIXON), pp. 224–9, Cape and Transvaal Printers Ltd.
MITCHELL, R. H. and CROCKET, J. H. (1971) Diamond genesis—a synthesis of opposing views. *Mineral. Deposita* **6**, 392–403.
MATHIAS, M., SIEBERT, J. C. and RICKWOOD, P. C. (1970) Some aspects of the mineralogy and petrology of ultramafic xenoliths in kimberlite. *Contr. Mineral. Petrol.* **26**, 75–123.
MODRESKI, P. J. and BOETTCHER, A. L. (1972) The stability of phlogopite and enstatite at high pressures: a model for micas in the interior of the earth. *Amer. J. Sci.* **272**, 852–69.
NICHOLLS, G. D. (1967) Geochemical studies in the ocean as evidence for the composition of the mantle. In: *Mantles of the Earth and Terrestrial Planets* (editor S. K. RUNCORN), Wiley-Interscience, New York.
NIXON, P. H. and BOYD, F. R. (1973) Petrogenesis of the granular and sheared ultrabasic nodule suite in Kimberlites. In: *Lesotho Kimberlites* (editor P. H. NIXON), pp. 48–56, Cape and Transvaal Printers Ltd.
O'HARA, M. J. (1967) Mineral paragenesis in ultrabasic rocks. In: *Ultramafic and Related Rocks* (editor P. J. WYLLIE), pp. 393–403, J. Wiley & Sons.
O'HARA, M. J. (1970) Upper mantle composition inferred from laboratory experiments and observations of volcanic products. *Phys. Earth Planet. Interiors* **3**, 236–45.
OXBURGH, E. R. (1964) Petrological evidence for the presence of amphibole in the upper mantle and its petrogenetic and geophysical implications. *Geol. Mag.* **101**, 1–19.
RIMSAITE, J. (1971) Distribution of major and minor constituents between mica and host ultrabasic rocks, and between zoned mica and zoned spinel. *Contr. Mineral. Petrol.* **33**, 259–72.
RINGWOOD, A. E. (1966) The chemical composition and origin of the earth. In: *Advances in Earth Sciences* (editor P. M. HURLEY), M.I.T. Press, Cambridge, Mass.
RINGWOOD, A. E. (1969) Composition and evolution of the upper mantle. In: *The Earth's Crust and Upper Mantle* (editor P. J. HART), Geophysics Monograph 13, American Geophysical Union, Washington, D.C.
SCLAR, C. B. (1970) High pressure studies in the system MgO–SiO_2–H_2O. *Phys. Earth Planet. Interiors* **3**, 333.
VARNE, R. (1970) Hornblende lherzolite and the upper mantle. *Contr. Mineral. Petrol.* **27**, 45–51.
WHITE, R. W. (1966) Ultramafic inclusions in basaltic rocks from Hawaii. *Contr. Mineral. Petrol.* **12**, 245–314.
WILSHIRE, H. G. and BINNS, R. A. (1961) Basic and ultrabasic xenoliths from volcanic rocks of New South Wales *J. Petrol.* **2**, 185–208.
WYLLIE, P. J. (1971) The role of water in magma generation and initiation of diapiric uprise in the mantle. *J. Geophys. Res.* **76**, 1328–38.
YODER, H. S. and KUSHIRO, I. (1969) Melting of a hydrous phase: phlogopite, *Amer. J. Sci.* **267**-A, 558–82.

Earth and Planetary Science Letters, 31 (1976) 175–178

[6]

LANTHANIUM, SAMARIUM AND YTTERBIUM ABUNDANCES IN SOME SOUTHERN AFRICAN GARNET LHERZOLITES

ROGER H. MITCHELL

Department of Geology, Lakehead University, Thunder Bay, Ont. (Canada)

and

D.A. CARSWELL

Department of Geology, University of Sheffield, Sheffield (Great Britain)

Received January 5, 1976
Revised version received March 26, 1976

La, Sm and Yb abundances are given for coexisting garnet and clinopyroxene from four granular garnet lherzolites and a garnet pyroxenite. La/Yb ratios of clinopyroxene range from 29 to 398, and are an important factor to be considered in any partial-melting model involving garnet lherzolite. Garnets have REE distributions which conflict with the hypothesis that garnets from granular and sheared lherzolites have different REE distributions. Calculated garnet-liquid distribution coefficients for Sm and Yb average 0.09 and 6.30 respectively. Calculated REE abundances in whole rocks are less than actually found implying that xenoliths are contaminated by light-REE-rich kimberlite. Revised mantle abundances are for La, 0.7 ppm and Yb, 0.2 ppm (La/Yb = 3.5).

1. Introduction

Garnet lherzolite plays a key role in mantle petrology and therefore also in partial-melting models which attempt to account for the rare earth element (REE) distribution patterns of a wide variety of mantle-derived magmas. Shimizu [1] has remarked upon the paucity of information on the REE content of garnet lherzolite and its constituent minerals, in fact the only extant data is that of Shimizu [1], Ridley and Dawson [2], and Philpotts et al. [3]. We present here La, Sm, and Yb data for garnets and coexisting pyroxenes together with whole-rock data for four garnet lherzolites and a garnet pyroxene which have previously been described by Carswell and Dawson [4]. The analyses were made by a radio chemical neutron activation procedure similar to that described by Ragland et al. [5]. Samples were washed in 1*N* HCl prior to analysis. The results are given in Table 1 and presented as chondrite-normalized distribution patterns in Fig. 1.

2. Clinopyroxenes

Fig. 1 shows that clinopyroxenes are enriched in light REE by 8–45 times chondritic abundances, the data being in good agreement with previous studies [1–3]. Of particular interest is the marked depletion in La in some of the samples. Complete analyses for REE would show a maximum at Nd or Ce [1–3]. The REE distribution patterns for clinopyroxenes from these granular garnet lherzolites is similar to Shimizu's [1] granular lherzolite data. La/Yb ratios (Table 1) are very variable, an important factor to be considered in any models of partial melting. For example, consider the partial melting of a lherzolite of composition garnet (5%)–clinopyroxene (5%)–orthopyroxene (20%)––olivine (70%) according to Shaw's [6] partial melting model in which phases melt in the proportions in which they occur in the rock. If the La/Yb ratio of the clinopyroxene were 10, then 2% melting of the rock would result in liquids with a La/Yb ratio of 44, if the La/Yb

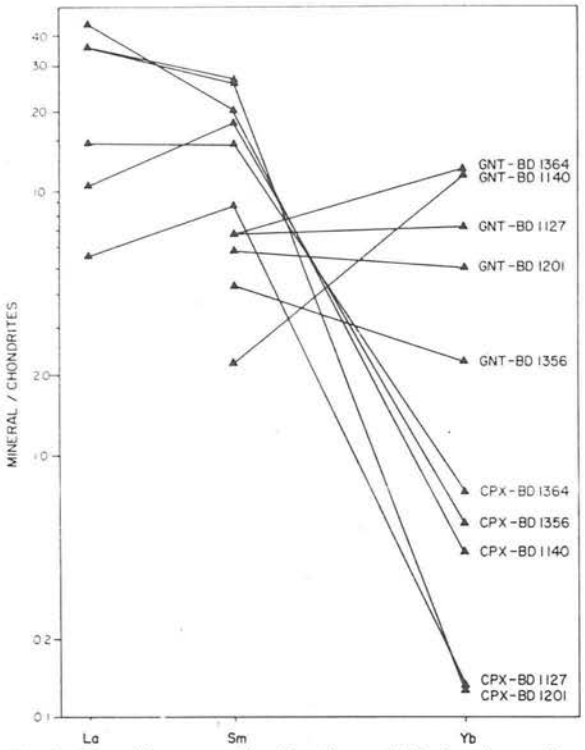

Fig. 1. Chondrite-normalized La, Sm and Yb abundances in coexisting clinopyroxenes and garnet from garnet lherzolites.

ratio of the clinopyroxene were 100, the same degree of melting would result in the melt La/Yb ratio being 87. Crystal-liquid distribution coefficients used in the calculation are for La; (cpx/liq) = 0.1 [7], (gnt/liq) = 0.002 [8], (opx or oliv/liq) = 0.002 (estimated from [7]), and for Yb, (cpx/liq) = 0.23, (gnt/liq) = 4, (opx or oliv/liq) = 0.007 (summarized by [9]).

The only previous data for La/Yb in mantle clinopyroxenes from lherzolites are 64 and 113 for Lashaine lherzolite [2] and 24 for Hawaiian lherzolite [10].

3. Garnets

The garnets have very variable REE abundances, La not being detectable by the analytical procedure employed, and are enriched in the heavy REE. The REE distribution patterns (Fig. 1) have positive or negative slopes. Shimizu [1] has shown that garnets from sheared and granular garnet lherzolites have positive and negative slopes respectively. The present REE data together with that of Ridley and Dawson [2] for granular garnet lherzolites indicates that no generalizations should yet be made concerning REE abundance patterns in the garnets from different textural types of lherzolites, a conclusion which has recently been found to be true for the major element composition of clinopyroxenes and whole rocks [11,12].

4. Clinopyroxene-garnet pairs

Table 1 gives clinopyroxene-garnet partition coefficients for Sm and Yb. These vary by a factor of 10 for rocks which are mineralogically very similar [4] and which have probably equilibrated at similar temperatures and pressures [13,14]. The partition coefficients are in the range reported by Shimizu [1] and Schnetzler and Philpotts [7]. Sm and Yb partition coefficients between the garnet and liquid have been calculated from the garnet/clinopyroxene partition coefficients and the clinopyroxene/liquid partition coefficients of pyroxene GSFC193 [7] as outlined by Shimizu [1]. Results are given in Table 1, the values agree well with published data [1,7]. It is particularly important to note that the Yb garnet-liquid partition coefficient is very much less than the value of 40 recommended by Shaw [8] which is commonly employed in partial-melting calculations. The actual value for Yb is not yet known but must be between 3 and 10 [1,7].

5. Whole rocks

Calculation of whole-rock REE abundances from the mineral data and modal abundances given by Carswell and Dawson [4] assuming that garnet and clinopyroxene contribute overwhelmingly to the whole-rock REE abundances (Table 1) result in calculated REE abundances which are lower than the observed abundances (Table 1). The discrepancy is undoubtedly due to contamination of the xenolith by the kimberlite host which is strongly enriched in light REE [15]. Contamination of xenoliths by kimberlite has previously been noted to occur for potassium by Erlank [16]. We therefore consider that whole-rock REE abundances of garnet lherzolites cannot be used to estimate the REE abundances or La/Yb ratios of the upper mantle. Shaw [8] estimates the upper mantle to contain 2 ppm La and 0.4 ppm Yb (La/Yb = 5). Using our calculated

TABLE 1

	La	Sm	Yb	La/Yb	$K^{Sm}_{cpx/gnt}$	$K^{Yb}_{cpx/gnt}$	$K^{Sm}_{gnt/liq}$	$K^{Yb}_{gnt/liq}$
BD 1364 (Matsoku pyroxenite)								
gnt	–	1.27	2.60	–	2.26	0.058	0.12	3.91
cpx	5.10	2.87	0.15	34.0	–	–	–	–
wr	2.13	1.26	0.54	3.94	–	–	–	–
calc. wr	1.53	1.08	0.51	3.00	–	–	–	–
BD 1201 (Wesselton)								
gnt	–	1.11	1.09	–	4.48	0.027	0.06	8.41
cpx	11.94	4.97	0.03	398.00	–	–	–	–
wr	1.69	0.33	0.11	15.36	–	–	–	–
calc. wr	0.59	0.28	0.03	19.66	–	–	–	–
BD 1356 (Matsoku)								
gnt	–	0.74	0.49	–	4.64	0.245	0.06	0.93
cpx	3.47	3.43	0.12	28.9	–	–	–	–
wr	–	0.22	–	–	–	–	–	–
calc. wr	0.17	0.21	0.03	5.67	–	–	–	–
BD 1140 (Bultfontein)								
gnt	–	0.42	2.44	–	8.92	0.036	0.03	6.30
cpx	14.25	3.75	0.09	158.00	–	–	–	–
wr	2.95	0.51	0.25	11.80	–	–	–	–
calc. wr	0.99	0.31	0.29	3.4	–	–	–	–
BD 1127 (Jagersfontein)								
gnt	–	1.27	1.60	–	1.29	0.019	0.2	11.9
cpx	1.87	1.64	0.03	62.33	–	–	–	–
wr	0.55	0.13	0.05	11.00	–	–	–	–
calc. wr	0.06	0.11	0.08	0.75	–	–	–	–

Abbreviations: gnt = garnet; cpx = clinopyroxene; wr = whole rock; calc. wr = calculated whole rock.

whole-rock REE abundances we would tentatively suggest that these values be revised downwards to 0.7 ppm La and 0.2 ppm Yb (La/Yb = 3.5).

Acknowledgements

J.B. Dawson is thanked for supplying the garnet lherzolites. The analyses were undertaken at the Mineralogisk-Geologisk Museum of the University of Oslo. A.E. Brunfelt is thanked for providing access to the analytical facilities.

References

1 N. Shimizu, Rare earth elements in garnets and clinopyroxenes from garnet lherzolite nodules in kimberlite, Earth Planet. Sci. Lett. 25 (1975) 26–32.

2 W.I. Ridley and J.B. Dawson. Lithophile trace element data bearing on the origin of peridotite xenoliths, ankaramite, and carbonatite from Lashaine volcano, N. Tanzania, Phys. Chem. Earth 9 (1975) 558–569.

3 J.A. Philpotts, C.C. Schnetzler and H.H. Thomas, Petrogenetic implications of some new geochemical data on eclogitic and ultrabasic inclusions, Geochim. Cosmochim. Acta 36 (1972) 1131–1166.

4 D.A. Carswell and J.B. Dawson, Garnet peridotite xenoliths in South African Kimberlite pipes and their petrogenesis, Contrib. Mineral. Petrol. 25 (1970) 163–184.

5 P.C. Ragland, A.O. Brunfelt and P.W. Weigand, Rare earth abundances in Mesozoic dolerite dikes from the eastern United States, in: Activation Analysis in Geochemistry and Cosmochemistry, A.O. Brunfelt and E. Steinnes, eds. (Universitetsforlaget, Oslo, 1970) 227–235.

6 D.M. Shaw, Trace element fractionation during anatexis, Geochim. Cosmochim. Acta 34 (1970) 237–243.

7 C.C. Schnetzler and J.A. Philpotts, Partition coefficients of rare earth elements between igneous matrix material and rock forming mineral phenocrysts, Geochim. Cosmochim. Acta 34 (1970) 331–340.

8 D.M. Shaw, Development of the early continental crust,

1. Use of trace element distribution coefficient models for the protoarchean crust, Can. J. Earth Sci. 9 (1972) 1577–1595.
9 N. Shimizu and R.J. Arculus, Rare earth element concentrations in a suite of basanitoids and alkali olivine basalts from Grenada, Lesser Antilles, Contrib. Mineral. Petrol. 50 (1975) 231–240.
10 J.B. Reid, Jr. and F.A. Frey, Rare earth distributions in lherzolite and garnet pyroxenite xenoliths and the constitution of the upper mantle, J. Geophys. Res. 76 (1971) 1184–1196.
11 J.B. Dawson, J.J. Gurney and P.J. Lawless, Textural and mineralogical studies of peridotite xenoliths from the Bultfontein mine (abstract), Kimberlite Conf., Cambridge (1975).
12 J.J. Gurney, J.B. Dawson, B. Harte and P.J. Lawless, The bulk chemical composition of peridotite facies rocks from the Matsoku and Bultfontein pipes (abstract), Kimberlite Conf., Cambridge (1975).
13 F.R. Boyd and P.H. Nixon, Origins of the ultramafic nodules from some kimberlites of northern Lesotho and the Monastery mine, South Africa, Phys. Earth 9 (1975) 431–454.
14 J.J. Gurney, B. Harte and K.G. Cox, Mantle xenoliths in the Matsoku kimberlite pipe, Phys. Chem. Earth 9 (1975) 507–523.
15 R.H. Mitchell and A.O. Brunfelt, Rare earth geochemistry of kimberlite, Phys. Chem. Earth 9 (1975) 671–686.
16 A.J. Erlank, Distribution of potassium in mafic and ultramafic nodules, Carnegie Inst. Washington Yearbook 68 (1970) 433–438.

Earth and Planetary Science Letters, 34 (1977) 30–38

[4]

GREEN GARNETS FROM THE NEWLANDS KIMBERLITE, CAPE PROVINCE, SOUTH AFRICA

D.B. CLARKE [1]

Department of Geology, Dalhousie University, Halifax, N.S. (Canada)

and

D.A. CARSWELL

Department of Geology, University of Sheffield, Sheffield (Great Britain)

Received September 8, 1976
Revised version received November 24, 1976

Six crystals of green, uvarovite-rich garnet from the Newlands kimberlite have been analysed. The range of Cr_2O_3 is 10.04–14.04% and CaO is 19.18–25.94% (wt.), and thus they are similar to garnets found in only one other kimberlite province, namely Yakutia. By combining data from both the Russian and South African occurrences, four models are considered for the formation of such garnets. The model which best accounts for the available chemical data, and mode of occurrence, involves formation of the uvarovitic garnets during subsolidus recrystallization of spinel wehrlitic cumulates, which themselves had been produced by a fractionating magma at a depth of about 200–250 km.

1. Introduction

Until recently, green garnets had not been recognised in kimberlites; however, they have now been described from the Udachnaya, Dalnaya and Zagadochnaya pipes in Yakutia [1], and dichroic green-violet varieties from the Kao pipe in Lesotho [2]. This paper establishes the Newlands area as another documented locality of Ca,Cr-rich garnets in kimberlite.

The Newlands kimberlite pipes are located 60 km northwest of Kimberley, Cape Province, and consist of five small blows (diameters 15–40 m) joined by a series of kimberlite fissures over a distance of 600 m. These pipes were sampled during a field excursion of the First International Kimberlite Conference and, from four different blocks of kimberlite, six green garnets were recovered. It is the purpose of this paper to describe the chemistry and discuss the possible origin of these garnets.

Recent experimental work on the stabilities of garnet solid solutions, including the uvarovite molecule [3–7] has shown that pyralspite-ugrandite mutual solid solution is extensive at high temperatures and high pressures, and that uvarovite has the highest thermal stability of the common garnet end-members up to ~25 kbars. Since the Newlands green garnets are largely uvarovite-pyrope-grossular solid solutions, these experimental results are particularly relevant to the origin of all such garnets in kimberlite.

2. Petrography

The Newlands kimberlite, from which the green garnets were separated, consists of large, rounded phenocrysts of olivine (~Fo_{90}), up to 2 cm in maximum dimension, which are partly serpentinized and may contain small, red, chrome spinels. The only other

[1] Address until July 1977: Grant Institute of Geology, University of Edinburgh, West Mains Road, Edinburgh EH9 3JW, Great Britain.

large crystals are phlogopite plates up to 5 mm in diameter and red/purple garnets up to 1 cm in diameter. Modally the olivines make up 40–50% of the rock, phlogopite about 5% and total garnets less than 1%. These large crystals are set in a fine-grained groundmass of serpentine, carbonate and opaque oxides. The average analysis of two small octahedra of magnesian chromite from the groundmass was (wt.%): $TiO_2 = 0.4$, $Al_2O_3 = 8.4$, $Fe_2O_3 = 2.3$, $FeO = 15.9$, $Cr_2O_3 = 61.4$, $MnO = 0.4$, $MgO = 11.6$.

In hand specimen and under a stereoscopic microscope the uvarovitic garnets are dark green in colour and are up to 1 cm in diameter. The one green garnet seen in thin section was pale green, isotropic, had rounded to sculptured edges, and was laced with a network of randomly curving cracks. A continuous opaque kelyphitic rim 0.05 mm wide surrounded that particular garnet.

3. Chemistry of the Newlands garnets

The average analyses of six crystals of green garnet are given in Table 1. The following observations and comparisons can be made:

(1) The chemical characteristics of these garnets satisfy all criteria of cluster 7 of Dawson and Stephens [28], except that analyses 1 and 2 have highly anomalous TiO_2 contents. The structural formulae of these two garnets only were calculated considering titanium to be in a trivalent state [33–35] since using conventional Ti^{4+} results in an extremely poor balance between eight- and six-fold co-ordinated cations.

(2) The range of Cr_2O_3 is 10.04–14.04% (wt.) and the substitution of Cr^{3+} for Al^{3+} in the octahedral sites is evident.

(3) The range of CaO is 19.18–25.94% (wt.) and the substitution of Ca for Mg-Fe^{2+}-Mn in the sites with eight-fold co-ordination is also evident. In having more than 50% end-member molecules containing calcium, the Newlands garnets are similar to the most calcic garnets from the Udachnaya and Dalnaya pipes [1]. Comparisons of the Newlands, Yakutian and Kao green garnets are given in Fig. 1A, B and show that: (a) the garnet xenocrysts of Newlands, Dalnaya and Udachnaya are very similar, but different from the xenocrysts of Zagadochnaya and Kao; (b) the green garnet from the Sytikanskaya wehrlite xenolith is similar to the discrete xenocrysts (phenocrysts?), but the other garnets from xenoliths are somewhat lower in Cr and Ca; (c) the knorringitic green garnets from Kao form a compact grouping distinctly different from the uvarovite-rich garnets of Newlands and most of those from Yakutia. Since the Kao garnets plot (Fig. 1A) on a direct continuation of the narrow composition field for garnets from two-pyroxene peridotite assemblages [1, fig. 1] they have probably been derived from such assemblages.

(4) The green garnets from the Zagadochnaya pipe [10] plot as a discrete group in Fig. 1A, B and appear to be related to garnet-pyroxene-kyanite (grospydite) assemblages.

(5) As shown by Fig. 1C, four of the Newlands garnets have compositions which lie beyond the limit of solid solution at 1200°C and 30 kbars [3]. This suggests that they may have formed at pressures greater than 30 kbars.

(6) Analyses 1 and 2 (Table 1) are of two contiguous grains which have a sharp, but irregular, contact with each other. The low-magnesian part (analysis 1) has a very constant composition, whereas the high-magnesian portion (analysis 2) is inhomogeneous showing variable Cr_2O_3 (10.29–11.04%), MgO (9.03–10.72%) and CaO (18.43–20.89%). Because this composite grain is only a fragment, it is inpossible to deduce the nature of the relationship between the two portions. In Fig. 1A, B these two grains have been joined by tie-lines which show that the variations in their CaO, MgO and Fe/Fe+Mg is comparable to the extent of the variation seen in the rest of the individual grains.

4. Origin of the green garnets

We shall now consider some conditions which would favour the formation of uvarovite-rich green garnets of the type found in the Newlands kimberlite. These conditions, and phenomena which must be explained, are as follows:

(1) A high Cr^{3+}/R^{3+} ratio is necessary in the environment of formation, coupled with conditions which permit the formation of garnet with a higher Ca^{2+}/R^{2+} ratio than is normally found in chrome-rich ultrabasic rocks.

(2) Uvarovite-rich green garnets with ΣCa com-

ponents >50% [1] appear to form only a small proportion of the total garnet population in the kimberlites where they occur.

(3) A genetic link between the green garnets and the formation of kimberlitic magmas must be considered, but uvarovite-rich garnets are found in other environments [8,9,28].

(4) Broadly comparable green garnets have been found in three xenoliths from Yakutian kimberlite pipes [1,10]. One of these xenoliths (D-332) is described as a garnet wehrlite, whereas another (S-1) is not specifically described as containing clinopyroxene, although it seems to be implied [1]. On this evidence it would appear that the assemblage olivine + garnet + chrome diopside ± chrome spinel is probably necessary for the formation of such garnets. The green garnet recovered from the grospydite nodule of Zagadochnaya is chemically quite distinct (Fig. 1A, B).

TABLE 1

Newlands green garnets

	1	2	3	4	5	6
SiO_2	38.68	39.04	38.64	38.65	38.40	38.02
TiO_2	1.04 *	1.27 *	0.43	0.52	0.41	0.40
Al_2O_3	12.74	13.26	11.67	12.20	10.80	10.49
Cr_2O_3	10.04	10.51	12.68	12.76	13.57	14.04
Fe_2O_3	3.02	1.80	1.95	1.87	2.74	2.75
FeO	1.51	3.82	2.85	3.51	2.71	3.10
MnO	0.22	0.25	0.31	0.35	0.36	0.37
MgO	6.36	10.13	6.95	8.88	9.15	6.61
CaO	25.94	19.18	24.23	21.07	21.00	23.86
Total	99.55	99.26	99.71	99.81	99.13	99.64
No. in average	23	6	5	3	3	4
Si	5.988 } 6.000	5.988 } 6.000	5.992 } 6.000	5.949 } 6.000	5.969 } 6.000	5.954 } 6.000
Al	0.012	0.012	0.008	0.051	0.031	0.046
Al	2.314	2.383	2.125	2.162	1.948	1.890
Ti	0.121 } 4.015	0.147 } 4.009	0.050 } 3.957	0.060 } 3.991	0.048 } 3.984	0.047 } 3.999
Cr	1.228	1.271	1.555	1.553	1.668	1.738
Fe^{3+}	0.352	0.208	0.227	0.216	0.320	0.324
Fe	0.196	0.492	0.369	0.452	0.352	0.406
Mn	0.029 } 5.985	0.037 } 5.991	0.041 } 6.042	0.046 } 6.010	0.047 } 6.017	0.049 } 6.002
Mg	1.457	2.312	1.606	2.037	2.120	1.543
Ca	4.303	3.150	4.026	3.475	3.498	4.004
Uvar	30.70	31.83	39.71	38.99	42.04	43.47
And	8.80	5.21	5.81	5.02	8.06	7.37
Ti-And	3.03	3.69	–	–	–	–
Pyr	24.28	38.59	27.35	34.10	35.63	25.72
Spess	0.48	0.62	0.69	0.76	0.80	0.82
Gross	29.18	11.85	23.04	13.75	8.68	15.18
Alm	3.27	8.21	3.40	6.97	4.78	6.70
Schor	–	–	0.00	0.42	0.00	0.73
Cations allocated (%)	99.74	99.58	97.88	99.56	99.16	99.69

* Titanium calculated as Ti^{3+} in the structural formulae.

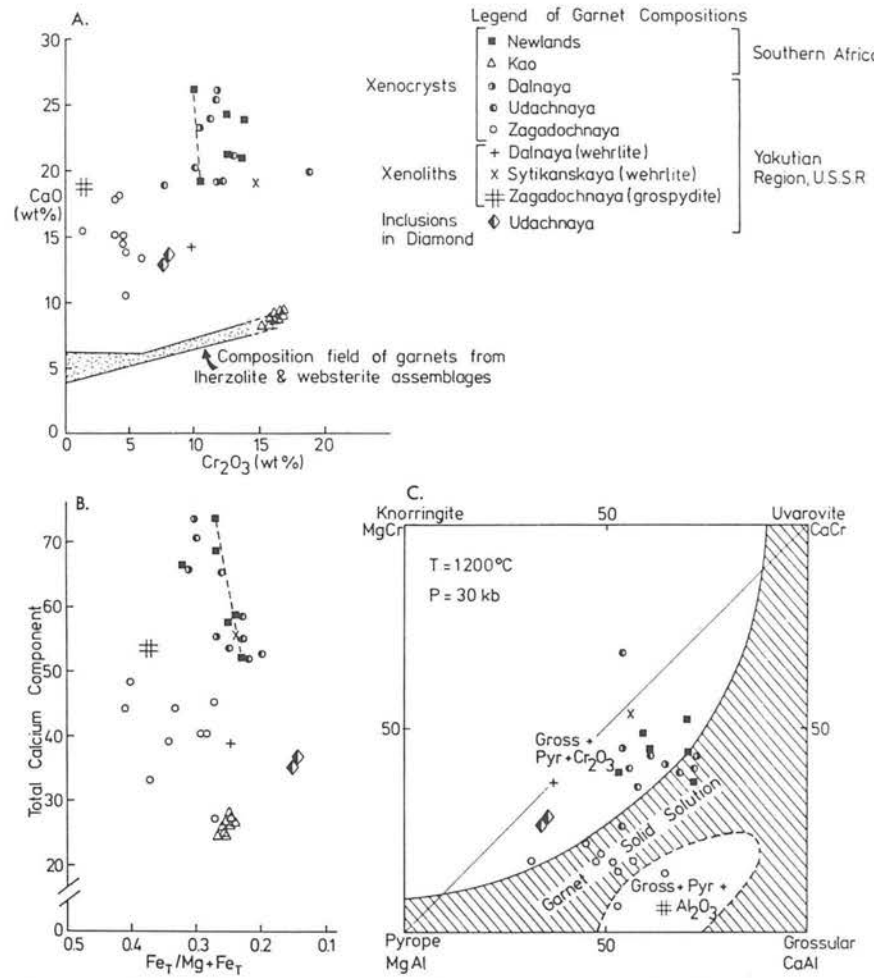

Fig. 1. A. Variation in the CaO and Cr_2O_3 contents of Newlands green garnets compared with those of Yakutia and Kao. The dashed line joins analyses 1 and 2 of Table 1. B. A comparison of the total calcium component (schorlomite + andradite + uvarovite + Ti-andradite + grossular) plotted as a function of the iron ratio for green garnets from Newlands, Yakutia and Kao. C. Chemical composition of uvarovitic garnets compared with the experimentally determined limits of solid solution at 1200°C and 30 kbars [3].

Outlined below are four possible models which might account for the origin of uvarovite-rich green garnets in kimberlites.

Model 1. The green garnets are part of a "normal", i.e. essentially undepleted, mantle peridotite assemblage at great depths (probably >350 km), and have been brought to the surface as accidental xenocrysts in kimberlitic magma.

It has been shown that a "normal" mantle garnet lherzolite may be expected to undergo phase transformations between 350 and 420 km so that the pyroxenes effectively go into solid solution in the garnet [11]. The effect of this transformation on the garnet composition is to change it from essentially a pyrope-almandine to a more grossular-rich composition depending on the amount of clinopyroxene in the original rock. However, this transformation process alone is insufficient to create a garnet of unusually high chrome content in mantle peridotite of both the common granular, and rarer sheared, garnet lherzolite xenolith types [12,13], which have $Cr_2O_3/Cr_2O_3 + Al_2O_3$ ratios generally of 0.10–0.15. Unless there is a large increase with depth in the $Cr_2O_3/Cr_2O_3 + Al_2O_3$ ratio over the values found in mantle peridotites thought to have been derived from depths of roughly 100–220 km [14,15], it is unlikely that the garnet-bearing dunites (possibly with minor chrome diopside persisting at first) expected at depths of greater than 350 km would contain uvarovite-rich garnets.

Model 2. The green garnets have formed as part of the refractory residuum during a deep-level (probably >350 km) partial melting event.

At depths of less than 350 km in the mantle, a small degree of partial melting (10–15%) of garnet lherzolite should result in the formation of harzburgitic residua. It is therefore unlikely that the orthopyroxene-free garnet wehrlite xenoliths in Yakutia [1] could have originated as residua of partial melting in this region of the mantle. However, partial melting of the same bulk composition at greater depths might be expected to leave a residuum of garnet dunite even after 40–50% partial melting. Depending on the distribution coefficient for Cr between the garnet and liquid (K_D^{Cr} gnt/liq > 10?) the chrome content of the garnets may increase as the degree of fractional partial melting increases [36]. Therefore, it may be possible to create a range of garnet compositions with varying Cr contents depending on the degree of partial melting. If the magma is kimberlitic, or can at least differentiate to become a kimberlite, fragments of this refractory mantle may then be erupted with the magma. The individual green garnets found in the Newlands kimberlite may then just be parts of disaggregated, deep-level, refractory mantle xenoliths. A weakness of this model is that one would not expect such deep-level refractory peridotite to contain clinopyroxene as observed in at least one uvarovite-rich garnet-bearing xenolith [1].

Both models 1 and 2 infer depths of origin greater than 350 km for these green garnets. This is considerably in excess of the 100–220 km generally indicated by nodule suites [14,15]. Although greater depths have been suggested [16], no high-pressure polymorphs of other phases [11,17] have been found to corroborate such deep levels of origin.

Model 3. The green garnets are the products of fractional crystallization of magma (not necessarily strictly kimberlitic) produced by the partial melting of mantle peridotite at depths > 250 km.

Fractional crystallization of a magma at, or near, its region of melting in the mantle may produce cumulates of dunite, followed by garnet-bearing dunite and wehrlite. If that magma continued to fractionate in situ to become a kimberlite, possibly as a result of extensive eclogite fractionation [18], then that kimberlitic fluid may occasionally erupt with some of its early cumulates. In this case the green garnets would effectively be cognate xenocrysts or, more likely, parts of disaggregated cognate garnet wehrlite xenoliths created during the formation of the kimberlitic magma. The scarcity of such garnets in kimberlites may be attributed either to their very early crystallization or to the inability of the fractionating magma to remain in situ until it has become kimberlitic and sufficiently gas-charged to result in eruption.

Support for this model and an origin from depths of at least 200 km becomes from the description of uvarovite-rich garnets in a wehrlite association within a Yakutian diamond [19]. On the assumption that the diamonds and the inclusions they contain have crystallized in equilibrium with kimberlitic liquid [20,21], it would appear likely that olivine is the principal liquidus phase at the pressures at which diamond crystallises. Comparison of the graphite ⇌ diamond stability curve [22] with the extrapolated garnet lherzolite solidus [23] renders it unlikely that diamond would be stable at melting temperatures for mantle peridotites at pressures less than about 65 kbars.

Model 4. The green garnets have been derived from disaggregated garnet wehrlite xenoliths formed by subsolidus recrystallization of original spinel wehrlite assemblages (abundant olivine + minor chrome diopside and chrome spinel) precipitated from fractionating kimberlite magma, probably at slightly lower pressures than necessiated in model 3 but still close to, or within, the diamond stability field.

This model differs from model 3 in that the garnets form at subsolidus temperatures through the breakdown of a primary clinopyroxene-spinel assemblage. The simplified subsolidus reaction may be expressed by:

$$\underset{\text{diopsidic cpx}}{2\,Ca(Mg,Fe)Si_2O_6} + \underset{\text{Cr spinel}}{(Mg,Fe)(Cr,Al)_2O_4} \rightleftharpoons \underset{\text{uvarovitic garnet}}{Ca_2(Mg,Fe)(Cr,Al)_2Si_3O_{12}} + \underset{\text{olivine}}{(Mg,Fe)_2SiO_4} \quad (1)$$

(subsolidus recrystallization of spinel wehrlite)

Support for such a subsolidus origin for the uvarovitic garnets is as follows:

(1) The Newlands garnets have relatively high Fe+Mn/Fe+Mn+Mg ratios (0.24–0.34) and are therefore unlikely to represent early crystals phases from a fractionating ultrabasic magma (the uvarovitic garnets found as inclusions in a Yakutian diamond [19], and believed to be liquidus phases, have lower Fe+Mn/Fe+Mn+Mg = 0.15).

(2) Chrome spinels ("chromites") may be fairly common as inclusions in diamonds depending on locality [20,37] suggesting that, in some magmas, chrome spinel rather than chrome garnet is a liquidus phase even at the high pressures (~65 kbars) at which diamond forms. Experimental observations [24,25], and crystal chemical considerations [36], strongly suggest that the distribution coefficient of Cr between liquid and spinel is likely to result in the early spinel phase being extremely rich in chromium.

(3) Both uvarovite-bearing xenoliths described by Sobolev et al. [1] contain chrome spinel.

(4) The observed association of uvarovitic garnets with wehrlitic nodules, and of knorringitic garnets with lherzolitic and harzburgitic nodules, is consistent with equation (1) or equation (2), respectively:

$$\underset{\text{opx}}{4(Mg,Fe)SiO_3} + \underset{\text{Cr spinel}}{(Mg,Fe)(Al,Cr)_2O_4} \rightleftharpoons \underset{\text{knorringitic garnet}}{(Mg,Fe)_3(Al,Cr)_2Si_3O_{12}} + \underset{\text{olivine}}{(Mg,Fe)_2SiO_4} \quad (2)$$

(subsolidus recrystallization of a spinel lherzolite)

thus we believe that the wehrlitic association of the Yakutian green garnet is essential to their formation. Significantly, both the uvarovite-bearing wehrlitic xenoliths from Yakutia [1], and the Newlands kimberlite groundmass, contain chrome spinels with high Cr contents, a chemical characteristic which has been associated with spinel inclusions in diamond [37]. The association of Cr-rich spinels lends support to the idea that the green garnets have formed within the stability field of diamond.

Even with a subsolidus origin for these Ca,Cr-rich garnets, experimental data indicate relatively high-pressure conditions for their formation. Experimental studies in the system $MgO–CaO–Al_2O_3–SiO_2$ [26] have indicated that the CaO contents of pyrope garnets in wehrlitic assemblages increase with pressure. In addition, MacGregor [27] has demonstrated that, with increasing Cr_2O_3/R_2O_3 ratio, the spinel lherzolite ⇌ garnet lherzolite boundary shifts to increasingly higher pressures, and that this reaction is progressive across a five-phase transition zone which expands with increasing Cr_2O_3 content. As a result, the Cr/Al ratio in the garnet may be expected to increase progressively with pressure across this five-phase transition zone, and similarly, in orthopyroxene-free assemblages, across a four-phase (olivine + clinopyroxene + spinel + garnet) transition field.

Fig. 2 illustrates the conditions required for the formation of uvarovite-rich garnets as envisaged in this model. The apparent rarity of such garnets in kimberlites may be explained by the fact that perhaps only in the small (shaded) region of the $P–T$ diagram will the necessary critical conditions occur for precipitation of Cr_2O_3-rich spinel wehrlite, followed by early reaction to garnet wehrlite and subsequent incorporation and disaggregation in an eruptive kimberlite magma.

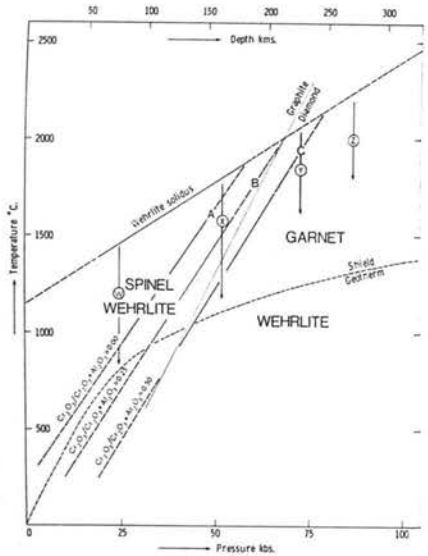

Fig. 2. $P-T$ diagram illustrating various possible cooling histories for mantle wehrlite cumulates in relation to the likely position of the equilibrium boundary between spinel wehrlites and garnet wehrlites for compositions with different $Cr_2O_3/Cr_2O_3 + Al_2O_3$ ratios. This diagram shows how the equilibrium boundary for the reaction pyroxene + spinel ⇌ garnet + olivine in wehrlite compositions (the position and slope of boundary *A* corresponds to boundary S of MacGregor [27, fig. 2]), may be expected to shift to significantly higher pressures with increasing $Cr_2O_3/Cr_2O_3 + Al_2O_3$ ratio (as demonstrated in fig. 5 of MacGregor [27]). Note that spinel may initially persist with garnet into the garnet wehrlite field to the right of boundaries *A*, *B* or *C*. The data of MacGregor [27] and O'Hara et al. [30] suggest that the presence of the small amounts of Fe^{2+} and Fe^{3+} in natural mantle wehrlite assemblages probably have little significant overall effect on the position of the spinel wehrlite ⇌ garnet wehrlite boundary (they may well have minor effects in opposite directions which largely cancel each other out). On the diagram the graphite ⇌ diamond equilibrium curve is from Bundy et al. [22], the "Shield Geotherm" from Clark and Ringwood [31], and the position of the wehrlite solidus is based on the data of Davis and Schairer [32].

In order of increasing depth (and pressure) of precipitation one can recognise the following four different cooling histories (assuming essentially isobaric character) for wehrlite cumulates. *W*: precipitation of spinel wehrlite which is likely to remain as such, even if it ultimately re-equilibrates on the "Shield Geotherm". *X*: precipitation of spinel wehrlite followed by reaction to garnet wehrlite, but only at temperatures close to the "Shield Geotherm". The large temperature interval between precipitation and reaction to garnet wehrlite in this instance, means that the chances of such garnet wehrlites ever again coming into contact with a magma capable of erupting them are probably small. *Y*: precipitation of spinel wehrlite followed by early reaction to garnet wehrlite at temperatures not much below the solidus. In this instance such garnet wehrlites would have a higher probability of being erupted by kimberlite magma than in *X*. Such depths of origin and cooling history corresponds to that envisaged in the favoured model 4, put forward to explain the genesis of the Newlands green garnets. The shaded region indicates the most favourable $P-T$ conditions for forming uvarovitic garnets by this process. *Z*: direct precipitation of garnet wehrlite, as envisaged in petrogenesis model 3.

5. Conclusions

(1) The six green uvarovite-rich garnets from the Newlands kimberlite are chemically very similar to rare green garnets described from two Yakutian kimberlite pipes. The origin of both suites of garnet should be similar and, since similar garnets have also been found in two wehrlitic xenoliths, it is possible that all the individual green garnets are the result of the fragmentation of such xenoliths incorporated in these particular kimberlites.

(2) The description of a fairly similar garnet in a wehrlitic inclusion assemblage within a diamond and the pertinent experimental data on garnet and ultrabasic rock systems suggest formation at high pressures, probably corresponding to depths of at least 200 km.

(3) Of the four models put forward we prefer model 4 as it appears to fit best with the available data. We thus favour an origin of the Newlands green garnets from fragmented garnet wehrlite xenoliths which have formed through the subsolidus recrystallization of spinel wehrlite assemblages, and which are themselves the products of fractional crystallization of a magma that was at least on the way to becoming kimberlitic.

Acknowledgements

The authors wish to thank the organizers of the First International Kimberlite Conference for the opportunity to collect samples at the Newlands Mine. In addition, D.B. Clarke acknowledges generous support by the National Research Council of Canada and Dalhousie University, and D.A. Carswell acknowledges travel grants from The Royal Society and the University of Sheffield.

We also wish to thank Drs. F.G.F. Gibb and J.W. Harris for their critical reading of the manuscript.

References

1 N.V. Sobolev, Yu.G. Lavrent'ev, N.P. Pokhilenko and L.V. Usova, Chrome-rich garnets from the kimberlites of Yakutia and their parageneses, Contrib. Mineral. Petrol. 40 (1973) 39.
2 G. Hornung and P.H. Nixon, Chemical variations in the Knorringite-rich garnets, in: P.H. Nixon, ed., Lesotho Kimberlites (1973) 122.
3 I.G. Malinovsky, A.M. Doroshev and A.A. Godovikov, The stability of garnets of the series pyrope-grossularite-knorringite-uvarovite at 1200°C and 30 kbar, Akad. Nauk S.S.S.R., Sib. Otd., Inst. Geol. Geofiz., Exptl. Invest. Mineral. (1974) 70.
4 I.G. Malinovsky and A.M. Doroshev, Stability of the garnet series uvarovite-knorringite and grossularite-uvarovite at 1200°C and 30 kbar, Akad. Nauk S.S.S.R., Sib. Otd., Inst. Geol. Geofiz., Exptl. Invest. Mineral. (1974) 73.
5 H.G. Huckenholz and D. Knittel, Uvarovite: stability of uvarovite-grossularite solid solution at low pressure, Contrib. Mineral. Petrol. 49 (1975) 211.
6 H.G. Huckenholz, Uvarovite stability in the $CaSiO_3$–Cr_2O_3 join up to 10 kbar, Neues Jahrb. Mineral. Monatsh. (1975) 22.
7 H.G. Huckenholz and D. Knittel, Uvarovite: stability of uvarovite-andradite solid solutions at low pressure, Contrib. Mineral. Petrol. 56 (1976) 61.
8 J.T. Frankel, Uvarovite garnet and South African jade (hydrogrossular) from the Bushveld complex, Transvaal, Am. Mineral. 44 (1959) 565.
9 O. van Knorring, A new occurrence of uvarovite from northern Karelia in Finland, Mineral. Mag. 29 (1951) 594.
10 N.V. Sobolev, I.K. Kuznetsova and N.E. Zyuzin, The petrology of grospydite xenoliths from the Zagadochnaya kimberlite pipes in Yakutia, J. Petrol. 9 (1968) 253.
11 A.E. Ringwood, Phase transformations and the constitution of the mantle, Phys. Earth Planet. Inter. 3 (1970) 109.
12 D.A. Carswell and J.B. Dawson, Garnet peridotite xenoliths in South African kimberlite pipes and their petrogenesis, Contrib. Mineral. Petrol. 15 (1970) 163.
13 P.H. Nixon and F.R. Boyd, Petrogenesis of the granular and sheared ultrabasic nodule suite in kimberlites, in: P.H. Nixon, ed., Lesotho Kimberlites (1973) 48.
14 D.A. Carswell, Comparative equilibration temperatures and pressures of garnet lherzolites in Norwegian gneisses and in kimberlite, Lithos 7 (1974) 113.

15 F.R. Boyd and P.H. Nixon, Origin of the ultramafic nodules from some kimberlites of northern Lesotho and the Monastery Mine, South Africa, Phys. Chem. Earth 9 (1975) 431.
16 P.G. Harris and E.A.K. Middlemost, The evolution of kimberlites, Lithos 3 (1969) 77.
17 A.E. Ringwood and A. Major, The system Mg_2SiO_4–Fe_2SiO_4 at high pressures and temperatures, Phys. Earth Planet Inter. 3 (1970) 84.
18 M.J. O'Hara and H.S. Yoder, Formation and fractionation of basic magmas at high pressures, Scott. J. Geol. 3 (1967) 67.
19 N.V. Sobolev, Z.V. Bartoskinskiy, F.S. Yefimova, Yu.G. Lavrent'yev and L.N. Pospelova, Olivine-garnet-chrome diopside assemblage from Yakutian diamond, Dokl. Akad. Nauk S.S.S.R. 192 (1970) 134.
20 H.O.A. Meyer and F.R. Boyd, Composition and origin of crystalline inclusions in natural diamonds, Geochim. Cosmochim. Acta 36 (1972) 1255.
21 J.J. Gurney and G.S. Switzer, The discovery of garnets closely related to diamonds in the Finsch pipe, South Africa, Contrib. Mineral. Petrol. 39 (1973) 103.
22 F.R. Bundy, H.P. Bovenkerk, H.M. Strong and R.H. Wentorf, Diamond-graphite equilibrium line from growth and graphitization of diamond, J. Chem. Phys. 35 (1961) 383.
23 K. Ito and G.C. Kennedy, The melting and phase relations in a natural peridotite to 40 kilobars, Am. J. Sci. 165 (1967) 519.
24 M.L. Keith, Phase equilibria in the system MgO–Cr_2O_3–SiO_2, J. Am. Ceram. Soc. 37 (1954) 490.
25 J.S. Dickey and H.S. Yoder, Partitioning of chromium and aluminium between clinopyroxene and spinel, Carnegie Inst. Washington Yearb. 71 (1972) 384.
26 I.D. MacGregor, Stability fields of spinel and garnet peridotites in the synthetic system MgO–CaO–Al_2O_3–SiO_2, Carnegie Inst. Washington Yearb. 64 (1965) 126.
27 I.D. MacGregor, The effect of CaO, Cr_2O_3, Fe_2O_3 and Al_2O_3 on the stability of spinel and garnet peridotites, Phys. Earth Planet. Inter. 3 (1970) 372.
28 J.B. Dawson and W.F. Stephens, Statistical classification of garnets from kimberlite and associated xenoliths, J. Geol. 83 (1975) 589.
29 T. Prestvik, Norwegian chromian ugrandite-garnets, Norsk Geol. Tidsskr. 54 (1974) 177.
30 M.J. O'Hara, S.W. Richardson and G. Wilson, Garnet-peridotite stability and occurrence in crust and mantle, Contrib. Mineral. Petrol. 32 (1971) 48.
31 S.P. Clark and A.E. Ringwood, Density distributions and constitution of the mantle, Rev. Geophys. 2 (1964) 35.
32 B.T.C. Davis and J.F. Schairer, Melting relations in the join diopside-forsterite-pyrope at 40 kilobars and at one atmosphere, Carnegie Inst. Washington Yearb. 64 (1965) 123.
33 R.K. Moore and W.B. White, Intervalence electron transfer effects in the spectra of the melanite garnets, Am. Mineral. 56 (1971) 826.

34 P.G. Manning, Optical absorption and electron microprobe studies of some high Ti-andradites, Can. Mineral. 10 (1970) 260.
35 R.K. Moore and W.B. White, Electronic spectra of transition metal ions in silicate garnets, Can. Mineral. 11 (1972) 791.
36 R.G. Burns, Crystal field effects in chromium and its partitioning in the mantle, Geochim. Cosmochim. Acta 39 (1975) 857.
37 J.W. Harris and J.J. Gurney, Inclusions in Diamonds, in: J. Field, ed., The Properties of Diamond (1976) in press.

(Reprinted from Nature, Vol. 276, No. 5689, p. 737 December 14 1978)

Palaeogeotherms: implications of disequilibrium in garnet lherzolite xenoliths

FRASER AND LAWLESS[1] have pointed out that, because of the different diffusion mechanisms involved, the two-pyroxene geothermometer[2,3] and the garnet–orthopyroxene geobarometer[4,5] commonly used[6–8] in the interpretation of the pressure–temperature equilibration conditions and depths of derivation of garnet lherzolite xenoliths in kimberlites may be out of phase and thus generate a spurious apparent geotherm. Whilst this may be the case it should, however, be noted that the lines of constant K for garnet–orthopyroxene equilibria in Fig. 1 of Fraser and Lawless[1] are, in the depth range of interest, effectively sub-parallel to geotherms independently calculated[9] from heat flow–production studies. This essentially makes it impossible to determine whether geotherms calculated from xenolith data are real or spurious in the way suggested.

Their Fig. 1 thus highlights the critical importance of the temperature estimates to the depths of origin inferred for such xenoliths. Their further discussion, therefore, purporting to demonstrate the different diffusion blocking temperatures for element exchange reactions between various mineral pairs in garnet lherzolite xenoliths is crucial but quite unconvincing and rather misleading.

Fraser and Lawless attempted to test the possibility that diffusion between pyroxenes and garnets is less rapid than between coexisting pyroxenes by comparing the distribution coefficients for Mg–Fe^{2+} exchange between garnet–clinopyroxene and garnet–orthopyroxene pairs with temperatures based on the Ca–Mg exchange between coexisting pyroxenes[3]. They interpreted the arrays of data points in their Fig. 2 as indicating that Mg–Fe^{2+} exchange between pyroxenes and garnet is effectively blocked below ~1,100 °C whilst lower temperatures continue to be monitored by Ca–Mg exchange between coexisting pyroxenes. In reaching this conclusion they ignored the fact that the xenoliths concerned have probably been derived from an appreciable depth zone in the mantle and hence may be expected to have equilibrated over a range of pressures as well as temperatures. Furthermore, clearly both Mg–Fe^{2+} exchange between pyroxenes and garnets and Ca–Mg exchange between coexisting pyroxenes depend on pressure as well as temperature, although there are uncertainties as to the magnitudes of the pressure dependence of these exchange reactions[2,10–13]. Certainly it is unreasonable for Fraser and Lawless to expect that the xenoliths would plot along lines defining the temperature dependence of the Mg–Fe^{2+} distribution coefficients at effectively one particular pressure. Indeed the experimental evidence of Råheim and Green[12] that $(Mg/Fe^{2+})_{cpx}/(Mg/Fe^{2+})_{gnt}$ decreases with temperature but increases with pressure suggests that the arrays of points on Fig. 2 of Fraser and Lawless may simply reflect the combined pressure/temperature effects on the distribution coefficients involved.

The variation in $(Mg/Fe^{2+})_{cpx}/(Mg/Fe^{2+})_{gnt}$ between garnet–clinopyroxene pairs in different metamorphic environments[14,15,19] indicates that Mg–Fe^{2+} exchange is normally effective at temperatures well below 1,100 °C. Krogh[16], Råheim and Green[17], for example, have described both prograde and retrograde variations in this distribution coefficient in eclogite assemblages which indicate that above ~700 °C, diffusion rates even in garnets are fast enough to chemically homogenise the minerals. At lower temperatures Mg–Fe^{2+} exchange is not completely blocked but is restricted to the extent that pronounced zoning is produced and retained, especially in the garnets[16].

Thus contrary to the impression given by Fraser and Lawless and to the interpretation which they place on their Fig. 2, petrographic[16–19] and experimental[2,10–12] evidence indicate that Mg–Fe^{2+} exchange reactions between pyroxenes and garnets probably provide far more sensitive geothermometers below 1,100 °C than the Ca–Mg exchange between coexisting pyroxenes. However, the magnitude of the pressure effect on the Mg–Fe^{2+} exchange reactions in garnet lherzolite assemblages and reliable estimates of the Fe^{2+}/Fe^{3+} ratios in these minerals[19] must first be determined before one can hope to obtain geologically meaningful temperatures from even these geothermometers and hence calculate valid geotherms.

I thank Dr W. L. Griffin for his helpful comments.

D. A. CARSWELL

Department of Geology,
University of Sheffield,
Mappin Street,
Sheffield, UK

1. Fraser, D. G. & Lawless, P. J. *Nature* **273,** 220–222 (1978).
2. Davis, B. T. C. & Boyd, R. F. *J. geophys. Res.* **71,** 3567–3576 (1966).
3. Wells, P. R. A. *Contr. Mineral. Petrol.* **62,** 129–139 (1977).
4. MacGregor, I. D. *Am. Mineral.* **59,** 110–110 (1974).
5. Wood, B. J. *Contr. Mineral Petrol.* **46,** 1–15 (1974).
6. Boyd, F. R. *Geochim. cosmochim. Acta* **37,** 2533–2546 (1973).
7. Boyd, F. R. & Nixon, P. H. *Phys. Chem. Earth* **9,** 341–454 (1975).
8. Carswell, D. A., Clarke, D. B. & Mitchell, R. H. *Proc. 2nd Int. Kimberlite Conf.* (in the press).
9. Clark, S. P., Jr. & Ringwood, A. E. *Rev. Geophys.* **2,** 35–88 (1964).
10. Mori, T. & Green, D. H. *Earth planet. Sci. Lett.* **26,** 277–286 (1975).
11. Lindsley, D. H. & Dixon, S. A. *Am. J. Sci.* **276,** 1285–1301 (1976).
12. Råheim, A. & Green, D. A. *Contr. Mineral. Petrol.* **48,** 179–203 (1974).
13. Wood, B. J. *Carnegie Inst. Wash. Ybk* **75,** 571–574 (1977).
14. Banno, S. *Phys. Earth planet. Int.* **3,** 405–421 (1970).
15. Mysen, B. O. & Heier, K. S. *Contr. Mineral. Petrol.* **36,** 73–94 (1972).
16. Krogh, E. J. *Nature* **267,** 17–19 (1977).
17. Råheim, A. & Green, D. H. *Lithos* **8,** 317–328 (1975).
18. Griffin, W. L., Carswell, D. A. & Nixon, P. H. *Proc. 2nd Int. Kimberlite Conf.* (in the press).
19. Carswell, D. A. & Griffin, W. L. (in preparation).

FRASER AND LAWLESS reply—We completely agree[1] with Carswell that the similarity between the temperature dependence of the garnet–orthopyroxene geobarometer[2] and likely geothermal gradients makes it difficult to use this reaction to distinguish between the effects of differences in blocking temperatures and temperature–pressure distributions obtained from samples which have equilibrated at different depths along such geothermal gradients.

In the absence of a suitable alternative geobarometer with a different slope it is difficult to distinguish between these two possibilities or indeed some combination of both. It is, however, unsound to make Carswell's *a priori* assumption that the xenoliths in question are derived from different depths and to use such an assumption to require that the nodules show an appreciable effect of pressure on Fe^{2+}–Mg distribution coefficients. This may indeed be the case as may bulk-compositional effects such as we have mentioned[1]. However, the observed departure of garnet–pyroxene Fe^{2+}–Mg distribution coefficients from the equilibrium values at 30 kbar is equally consistent with increased departure from equilibrium at lower temperature. The extent of low temperature Fe^{2+}–Mg exchange observed in the eclogitic assemblages of Krogh[3] and Råheim and Green[4] results from equilibration over long periods of geological time and cannot be directly compared with the proposed retrograde effects on garnet lherzolite nodules resulting from relatively rapidly changing temperature–pressure conditions during movement towards the Earth's surface before final eruption of the kimberlite.

These important questions can only be resolved by independent tests. The calibration of an alternative geobarometer with different slope is clearly important. Moreover, the bulk chemical homogeneity of the phases in the xenoliths should be critically analysed in terms of likely diffusion models and tests should be made of the homogeneity and equilibration of isotopes and refractory trace elements among different mineral phases. Recently published data[5] show a correlation of pyroxene–garnet Mn/Mg and V/Al ratios with clinopyroxene–orthopyroxene temperatures suggesting equilibration of these trace elements. However, the same authors note grain-by-grain relative inhomogeneities of 25% in Cr and Sc contents of the garnets and similar results have been observed elsewhere[6]. Similarly our work has shown that pyroxene–garnet Cr/Al distribution coefficients are widely scattered for the low temperature group of granular nodules but are more tightly grouped in the case of sheared nodules. Isotopic disequilibrium in garnet and spinel lherzolite nodules has also been reported[7–10] although it seems that in the case of garnet lherzolites this applies only to sheared

nodules, the granular nodules being apparently equilibrated and giving ages close to that of the host kimberlite[7], despite their dominantly lower temperatures.

There are thus several contradictory pieces of evidence concerning equilibrium in garnet lherzolite and xenoliths and hence uncertainty in their use for the calculation of geothermal gradients. When alternative geobarometers and more isotopic, trace element and kinetic data become available these issues should be more easily resolved.

DONALD G. FRASER
Department of Geology & Mineralogy, University of Oxford, Parks Road, Oxford, UK

P. J. LAWLESS
P.P. Box 106,Crown Mines, 2025, South Africa

1. Fraser, D. G. & Lawless, P. J. *Nature* **273,** 220–222 (1978).
2. Wood, B. J. *Contr. Mineral. Petrol.* **46,** 1–15 (1974).
3. Krogh, E. J. *Nature* **267,** 17–19 (1977).
4. Råheim, A. & Green, D. H. *Lithos* **8,** 317–328 (1975).
5. Shimizu, N. & Allègre, C. J. *Contr. Mineral. Petrol.* **67,** 41–50 (1978).
6. Boyd, F. R. & Finger, L. W. *Carnegie Inst. Wash. Ybk* **74,** 519–525 (1975).
7. Allègre, C. J., Manhes, G., Richard, P., Rousseau, D. & Shimizu, N. Abstract, *Int. Conf. Geochronology and Isotope Geol.* (Denver, 1978).
8. Stueber, A. M. & Irkamuddin, M. *Geochim. cosmochim. Acta* **38,** 207–216 (1974).
9. Dasch, E. J. & Green, D. H. *Am. J. Sci.* **275,** 461–469 (1975).
10. Basu, A. R. & Murthy, V. R. *Earth planet Sci. Lett.* **35,** 239–246 (1977).

Printed in Great Britain by Macmillan Production Ltd., Basingstoke, Hampshire

REPRINTED FROM: The Mantle Sample: Inclusions in Kimberlites and other Volcanics.

Proc. 2nd Int. Kimberlite Conference, Vol. 2. 1979

LOWER-CRUSTAL GRANULITES AND ECLOGITES FROM LESOTHO, SOUTHERN AFRICA

W. L. Griffin

Geologisk Museum, Oslo, Norway

D. A. Carswell

Department of Geology, Sheffield University, Sheffield, England

P. H. Nixon

Geology Department, Box 4820 University P.O., Papua, New Guinea

Abstract. Nodules of garnet granulites and "crustal" eclogites occur in many kimberlites around the edge of the Kaapvaal craton, but are apparently absent from pipes within the craton. In most Lesotho pipes this suite is dominated by basic cpx+plag+gnt±opx granulites, with smaller numbers of eclogites, garnet websterites and intermediate/acid granulites. Two-pyroxene granulites are common at Monastery Mine.

The basic granulites are essentially olivine-basaltic, with minor normative Hy or Ne. The absence of plagioclase in eclogites and garnet websterites is controlled mainly by bulk chemistry; only rocks with >45% normative An+Ab contain modal feldspar. Microprobe data for 50 rocks demonstrate the consanguinity of the garnet granulite-eclogite-websterite suite. Clinopyroxenes from all garnetiferous samples are eclogitic (Jd/Ts > ½). Jd/Jd+Ts is proportional to Ab/Ab+An in the coexisting plagioclase (An 5-77%); Jd ranges from <5 to 30%. Garnets in all rock types resemble those from eclogites in gneiss and blueschist. High-sulfur (3.5-6.8% SO_3) scapolite occurs in six samples.

Most samples of the garnet granulite suite yield T-P estimates between 550-700°C and 5-13 Kb, implying an origin in the lower crust. Seismic data on adjacent areas, measured densities, and data on nodule abundances suggest that the lower crust beneath Lesotho contains 50-70% basic granulite+eclogite+websterite, and 50-30% intermediate to acid granulite. Fe-rich garnet websterites give P - T estimates in the range 13-19 Kb, and may represent an important rock type in the uppermost mantle.

Our crustal P-T estimates lie closer to predicted oceanic geotherms than to the "Shield" geotherm, suggesting that the latter is only valid for the deeper parts of the upper mantle. The high T at lower-crustal depths during mid-Cretaceous time presumably was a consequence of the Karroo volcanic activity.

Introduction

Petrological studies of supposed deep-crustal rocks (granulites, eclogites, etc.) usually contain an inherent ambiguity. The exposure of these rocks on the earth's surface implies that they have been brought up from depth by large-scale tectonic movements. Unless this uplift is, geologically speaking, very rapid, the mineralogy and chemistry of the rocks will probably be modified by partial or complete reequilibration at shallower crustal depths. This modification may prevent study, or even recognition, of the original nature of the rocks.

Kimberlite eruption, on the other hand, is an extremely rapid process. McGetchin and Ullrich (1973) estimate that an ascending kimberlite magma would traverse the thickness of the continental crust in less than 15 minutes. Magma temperatures have been estimated to be around 500°C (Sheppard and Dawson, 1975). The circulation of meteoric water, besides causing serpentinization, probably reduces the temperature of emplaced diatreme-facies kimberlite to <100°C in a very short time. Nodules of deep-seated crustal rocks in these diatremes may therefore be regarded as quenched samples, at least by comparison with normal surface outcrops. If they escape hydrothermal alteration during the hydration of the kimberlite, these nodules offer a unique chance to study deep-crustal chemistry and mineral equilibria.

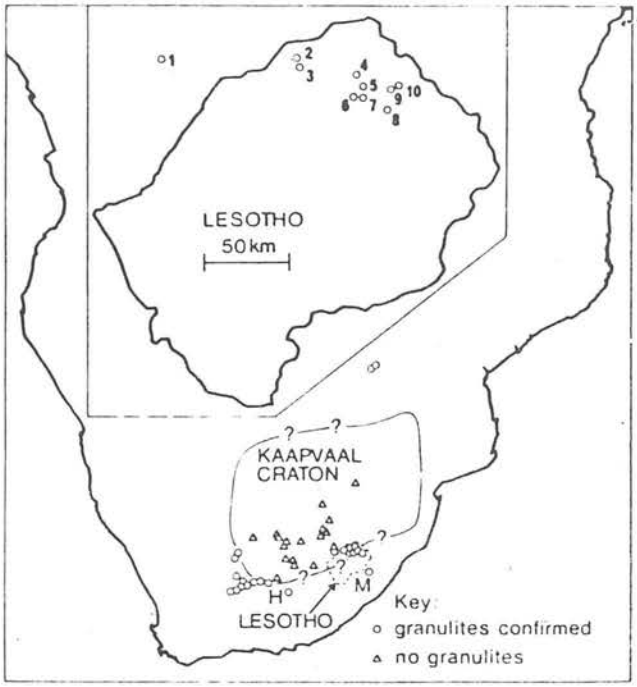

Fig. 1. Distribution of granulite nodules in the kimberlites of Southern Africa, based largely on survey of Rickwood et al. (1969). H, Hanover pipe; M, Melkfontein. Inset: Lesotho, showing sample localities: 1, Monastery Mine; 2, Lipelenang; 3, Khabos; 4, Lemphane; 5, Lighobong; 6, Kao; 7, Pipe 200; 8, Matsoku; 9, Mothae; 10, Letseng-la-Terae.

This paper presents a study of 55 granulite, eclogite and garnet websterite nodules from 11 kimberlites in Lesotho and adjacent South Africa. We have also studied a suite of spinel lherzolites, presumably from the shallow mantle or deep crust, in the Lipelenang and Ngopetseu kimberlites; primary data on these will be presented elsewhere.

Occurrence of granulite-suite nodules

The "garnet granulite suite" described here includes pyroxene-garnet granulites (cpx+gnt+plag±opx), eclogites (cpx+gnt) and garnet websterite (cpx+opx+gnt). The essentially continuous variation in modal composition and mineral chemistry among these three groups (see below) suggests that most, if not all, of these rocks formed through metamorphism of a dominantly mafic suite under a rather restricted range of P and T. Two-pyroxene, garnet-free granulites occur at Monastery Mine.

Our collection includes nodules from nine kimberlites in Lesotho and three (Monastery Mine; Hanover; and Melkfontein, E. Griqualand) in adjoining South Africa. A survey of the literature and available collections shows that garnet granulites ("plagioclase eclogites" of Ringwood et al., 1969) have been found only in kimberlites on, or outside of, the edge of the Kaapvaal craton (Fig. 1). Pipes within the craton apparently lack granulite nodules, and contain eclogite nodules only of the "griquaite" type (Nixon, 1973). Basement xenoliths in the pipes of the craton interior are usually intermediate to acid, amphibolite-facies gneisses that may or may not represent deep-crustal material.

The Kaapvaal craton consists largely of Early Archaean gneisses and greenstone belts. It is bordered by younger mobile belts characterized by high-grade regional metamorphism, commonly in granulite facies. Kröner (1977) argues that these belts were formed primarily by intracratonic reworking of the older rocks, with little addition of new material. The restriction of the granulite nodules to kimberlites lying along the craton-mobile belt boundary may indicate that the granulite suite is a product of the reworking processes. This suggestion is strengthened by the Proterozoic U/Pb ages obtained on zircons from two granulite nodules from Lesotho kimberlites (Davis, 1977). If the granulite suite is present beneath the craton, something must have prevented the kimberlites from sampling it there.

Petrography

Most of our samples are 1-3 cm in size and relatively homogeneous. The larger ones, however, commonly display compositional layering on a scale of mm to cm. Interlayering of eclogite and granulite on these scales is illustrated in "Lesotho Kimberlites" (P. Nixon, ed. 1973) (pl. 43A, our sample KN-195), and by our sample L-12 (Table 1). Many other samples show a foliation defined by thin, discontinuous trains of mafic minerals in plagioclase, or of garnet in clinopyroxene (see "Lesotho Kimberlites", pl. 33A, our PHN-2438).

The dominant texture in all rock types is polygonal granoblastic (see "Lesotho Kimberlites" Pl. 15A, 29B, 34, 40A). The rocks are typically equigranular, with average grain sizes from 0.5-1.5 mm. Despite the compositional layering, dimensional orientation of grains is rare, as is undulatory extinction or other evidence of strain. The textures are interpreted as the result of annealing in a static environment (Nixon, 1973), perhaps reflecting heating during the Karroo volcanic episode (see below).

Clinopyroxene, orthopyroxene, garnet and plagioclase account for >95% of the mode in most samples (Table 1). Within the garnet granulite suite there is essentially continuous modal variation from granulites to eclogites and garnet pyroxenites (as plagioclase ranges from 50% to <1%) and from eclogites to garnet websterites (opx from 0 to 30%) (Fig. 2). Hydrous minerals are rare; where present they

Table 1. Modal Data for Granulites, Eclogites and Pyroxenites

Sample	type	dens.	gr. size	cpx	opx	gnt	plag	%An	scap.	amp.	bio.	ap.	rut.	ilm.	other phases	comments
HANOVER																
PHN-2317	GG	-	F	40	-	38	22	21	-	-	-	-	-	-	Qtz	Foliated
KAO																
K-1	GG*	2.39	M	+		+	+	-	-	-	-	-	-	+	Natrol., seric.	Compl. alt.
K-2	GG	2.94	M/C	26	-	31	40	20	3	-	-	-	+	-	Kspar	Anom. rutile
K-3	GG	3.27	M/C	48	-	34	18	13	-	+	+	-	+	-	Pyrite	Sec. amph.
K-4	GG	-	C	26	-	69	5	77	-	+	-	-	-	-		- " -
K-5	Ec	3.66	C	52	-	42	-	-	-	-	-	-	-	6		
KAO-1	Ec	-	M	46	-	51	-	-	-	-	3	-	+	-		Anom. rutile
KAO-2	Ec	-	M/C	67	-	33	-	-	-	-	+	-	+	-		- " -, sec. bio.
KC-22	Ec	-	M	36	-	64	-	-	-	-	-	-	-	-		
KC-23	Ec	-	M	61	-	39	-	-	-	-	-	-	-	-		
KC-28	GG	-	M	34	-	44	1	50	-	-	-	-	-	21		
KC-29	GG	-	M/C	78	-	20	2	alt.	-	-	-	-	-	-		
KC-30	Ec	-	M/C	49	-	40	-	-	-	2	-	-	-	9		
KC-31	Ec	-	M	44	-	53	-	-	-	-	3	-	+	-		
PHN-2438	GG	2.69	F/M	33	-	21	46	8	-	-	-	-	-	-		"Lesotho Kimb." pl.33A
KHABOS																
PHN-1442j	GG	-	M	8	-	46	44	44	-	-	-	-	-	-	2% Kyan.	Al_2SiO_5/cpx sympl.
LEMPHANE																
PHN-2508	GW	-	M	47	15	15	-	-	-	8	-	+	-	-	15% Mgt.	Gnt. exsol. in pyrox., sec. poik. amph.
LETSENG-LA-TERAE																
LT-2	GG*	2.74	M/C	27	+	23	28	27	+[1]	-	3	+	+	+	18% Qtz.	Opx incl. in cpx.
LT-6	GG	-	M	34	-	22	41	30	-	-	-	-	+	3		
PHN-2003/1	GG	-	M	13	-	20	67	alt.	-	-	+	-	-	-		Heav. alt.
PHN-2567/5	GW	-	M/C	69	9	22	-	-	-	-	-	-	+	+		
LIPELENANG																
L-5	GG*	3.03	M/C	28	4	21	47	52	-	-	-	-	-	-	Sillim., corun., spinel	Coronite. Al_2SiO_5 in plagioclase.
LIQHOBONG																
LQ-1	GW	3.35	M	52	5	40	-	-	-	3	+	-	-	-	Fe, Ni sulf.	Anom. rutile
LQ-2	GG	2.94	M	31	-	43	23	32	3	-	-	-	+	-	Qtz	Altered
LQ-4	GG*	3.24	M	39	-	30	10	5	-	-	-	+	8	3	3% Qtz, 7% Ksp.	- " -
PHN-2494	GG	3.08	F/M	26	-	28	46	12	-	-	-	-	-	-	Ksp. (Ab_{32})	Plag = $Or_{4.5}$
PHN-2495	GG*	3.37	C	52	6	41	tr.	16	-	-	+	+	1	-		Anom. rutile
KN-195	GG	3.16	F/M	26	-	43	31	12	-	-	-	-	+	-	Ksp. (Ab_{35})	"Lesotho Kimb."pl.43A
KN-206	GW	3.50	C	39	30	26	-	-	-	+	-	+	5	+		Anom. rut. (SE Blow)
MATSOKU																
M-1	GG*	3.13	M	32	-	34	34	23	-	-	-	-	-	-	Kyan. (sec.)	Finely layered
M-3	GW	3.37	C	58	23	19	-	-	-	-	-	-	+	+		Anom. rutile
M-5	GW	3.39	M	60	15	25	-	-	-	-	-	-	+	+		- " -
L-9	GW*	3.38	C	75	6	19	-	-	-	-	-	-	+	+		- " -, opx alt.

Table 1, Cont'd.

L-12A	GG*	3.15	M	47	-	23	30	19	-	-	-	-	-	-	Qtz.	
L-12B	Ec*	3.15	M/C	70	-	26	-	-	+	-	-	-	+	+	4% Qtz, pectol.	Layered granul./eclog.
L-13	GG*	3.10	M	37	-	29	34	23	-	-	+	-	+	-	Kyan.(sec.)	
L-16	GW*	3.31	M	60	19	21	-	-	-	-	-	-	+	+		Anom. rut.,opx alt.
L-17	GW*	3.40	M	58	5	37	-	-	-	-	-	-	+	+		
L-20	GG*	3.17	M	26	5	46	20	17	-	-	1	-	+	-	Ksp.	
PHN-1646A	GG	3.21	M	50	-	29	21	19	-	-	+	-	+	-		Anom. rut., (cf.Rogers,
PHN-1670	GG*	3.05	M	20	-	33	47	23	+	-	-	-	+	-		Altered 1977)
PHN-2852	GG*	3.03	M	30	-	32	35	19	3	-	-	-	+	-		Anom. rut.(cf.Rogers,
OVK-F 10303	GG*	3.00	M	19	-	37	44	19	-	-	-	-	+	+	Kyan. (sec.)	Sec. carb. 1977)
																pect.(cf.Rogers,1977)
MONASTERY																
MO-4	PG	3.15	F/M	48	22	-	21	47	-	8	1	-	-	-	Spinel	
MO-6	PG	2.97	M	43	6	-	34	55	-	17	-	-	-	-		
MO-9	SP	-	F	-	40	-	-	-	-	45	-	-	-	-	15% spinel	
PHN-2630/1	GW*	3.52	F/M	33	2	53	-	-	-	-	12	-	-	-		
PHN-2630/2	GG*	3.14	M	38	8	32	18	50	-	-	+	-	-	4		Kelyphite
PHN-2645	PG*	2.94	M	39	10	-	45	35	-	-	4	-	-	-	Ti-mgt	
MOTHAE																
PHN-1919	GG*	-	M	36	-	33	29	18	-	-	2	-	+	+		Heavy alt. "Les.Kimb."
																pl. 15A(cf.Rogers,1977)
PIPE 200																
PHN-2450	Ec	-	C	37	-	61	-	-	-	+	1	-	1	-		Anom. rutile
PHN-2496	Ec	3.34	C	71	-	23	-	-	-	5	1	-	+	-		- " -
PHN-2532	Ec*	3.42	M/C	55	-	36	-	-	-	-	-	+	9	+		Sec. carb.
PHN-2533	GG*	3.13	M	45	-	27	27	12	-	-	1	+	+	+		Kelyphite(cf.Rogers,
																1977)
PHN-2685/1A	Ec*	3.13	C	45	-	50	-	-	-	-	5	-	+	-	Carbonate	Anom.rut.Altered.
MELKFONTEIN																
PHN-3017	GG	-	M/C	45	-	45	5	27	5	-	-	-	-	-		

Rock types: GG, garnet granulite; PG, pyroxene granulite; Ec, eclogite; GP, garnet pyroxenite; SP, spinel pyroxenite.
*Sample analyzed (Table 2).
Grain size: F, fine-grained (<0.5 mm average diameter); M, medium-grained (0.5-1.5 mm); C, coarse-grained (>1.5 mm).
1: One thin section contains no scapolite, another ca. 5%.

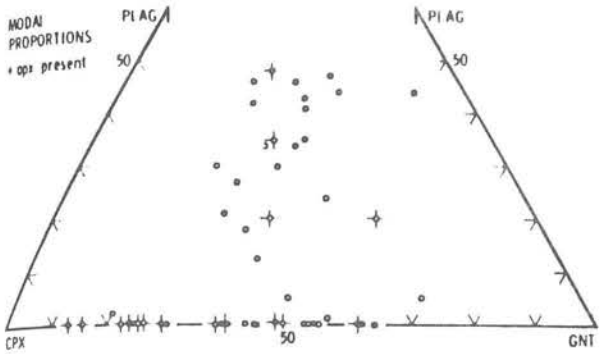

Fig. 2. Modal proportions of pyroxenes, garnet and plagioclase. See also Table 1.

usually appear to be in textural equilibrium with the anhydrous phases. The main exceptions to this rule are the pyroxene granulites from Monastery Mine, in which amphibole surrounds and replaces pyroxenes, and the garnet websterite PHN-2508, which contains abundant poikilitic amphibole. Other cases of disequilibrium features are noted in Table 1.

The most important accessory mineral is rutile, which occurs both as discrete grains and commonly as acicular inclusions in garnet and pyroxene. These needles always show inclined extinction, the result of an unusual habit that appears to be characteristic of rutile inclusions in minerals formed at high P and T (Griffin et al., 1971). Ilmenite, zircon and apatite are also common accessory minerals. Quartz and scapolite are less common, but are abundant ($\bar{<}$15%) in some specimens, as are magnetite, orthoclase, kyanite and sillimanite (Table 1).

Many samples show hydrothermal alteration, presumably by fluids from the kimberlite. Natrolite, pectolite, sericite and carbonate replace feldspars. Orthopyroxene is commonly altered to a brown serpentine-like material, especially in the garnet websterites, and green "kelyphite" rims garnets in a few samples. Scapolite is commonly altered to an unidentified light brown material; nearly complete loss of SO_3 is associated with the early stages of this alteration. Grain boundaries and cracks in the clinopyroxenes of some eclogites and garnet websterites show wide, sharply bounded zones filled with vermicular, apparently empty, channels in a symplectite-like pattern. Similar rims have been observed in garnet lherzolite nodules (Carswell, 1975).

Although equilibrium metamorphic textures are the rule in this nodule suite, some important exceptions should be noted.

(1) Opx in LT-2 occurs only as rounded inclusions in clinopyroxene, suggesting that the reaction opx+plag → cpx+gnt+qtz has taken place.

(2) L-6 is a coronite, showing "primary" Al-rich pyroxenes surrounded by zones of granular garnet with inclusions of spinel and corundum. The following reactions have probably occurred:

(a) $3MgAl_2SiO_6 \rightarrow Mg_3Al_2Si_3O_{12} + 2Al_2O_3$

(b) $MgAl_2O_4 + 3MgSiO_3 + CaAl_2Si_2O_6 \rightarrow$

$CaMgSi_2O_6 + Mg_3Al_2Si_3O_{12} + Al_2O_3$

The plagioclase is full of randomly oriented needles of an Al_2SiO_5 phase (sillimanite?).

(3) In PHN-1442j rinds of coarse-grained garnet surround areas in which poikilitic clinopyroxene encloses tiny garnet euhedra and laths of kyanite. Elsewhere, sheaves of kyanite needles (X-ray identification; B. Harte, pers. comm. 1977) are intergrown with clinopyroxene (cf. Meyer and Brookins, 1976, Fig. 2). A coarser-grained kyanite/cpx intergrowth was seen in a coronite anorthosite from Thaba Putsoa (not analyzed). The reactions involve the breakdown of plagioclase and a primary clinopyroxene rich in Tschermak's molecule, to produce kyanite, a less aluminous secondary clinopyroxene and a Ca, Fe-rich garnet (Table 3). The reactions responsible for the texture may be of the type:

(c) 3Mg-Ts + 3An + Ab → Gros + Py + Jd + 4Kyan

(d) 3Mg-Ts + 3An + 3Ab → 3Di + 3Jd + 6Kyan

The higher Jd content and lower Ts content of the secondary pyroxene and the higher K_D (Fe/Mg) of the secondary gnt + cpx pair indicate that these reactions proceeded with decreasing T.

The intergrowths of kyanite needles with clinopyroxene are also present, though rare, in samples M-1, L-13 and OVK-F10303, all from Matsoku.

(4) In PHN-2508, garnet occurs as small rods, apparently exsolved, in clinopyroxene and orthopyroxene.

(5) The pyroxene granulites from Monastery Mine show extensive exsolution of orthopyroxene lamellae in clinopyroxene, a feature that is rare in the garnet-granulite suite.

Whole-rock Chemistry

Whole-rock analyses and CIPW norms for 25 nodules are presented in Table 2. One strikingly banded nodule (L-12) was split into eclogite and granulite portions for analytical purposes. Analyses were done at the University of Sheffield, mainly by XRF; major elements were analyzed on fusion pellets (1:9 lithium tetraborate), trace elements on pressed powders. Contents of FeO, Na_2O, H_2O and CO_2 were determined separately by standard wet-chemical techniques.

Four of our analyzed samples have also been analyzed by Rogers (1977). The large differences in major-element values between our analyses

Table 2. Whole Rock Analyses and CIPW Norms

Rock Type	Garnet Granulites											Banded Specimen	
Sample Number	PHN 2630/2	LQ 4	PHN 2852	L 20	L 6	PHN 1670	PHN 2533	L 13	M 1	OVKF 10303	LT 2	L 12A	L 12B
SiO_2	42.97	43.97	44.98	46.82	47.23	49.18	49.69	49.89	50.37	50.89	59.93	49.50	49.65
TiO_2	1.86	3.30	1.39	0.06	0.06	0.53	0.67	0.36	0.35	0.26	0.87	0.43	0.69
Al_2O_3	12.25	11.89	16.87	13.81	23.93	18.24	14.69	18.55	18.89	19.12	13.07	16.23	12.80
Fe_2O_3	3.71	5.03	1.35	2.07	0.72	0.61	2.16	0.60	0.71	0.90	0.60	1.07	0.88
FeO	12.40	13.22	8.33	10.24	3.82	6.44	9.09	5.57	5.52	5.73	4.66	6.70	8.22
MnO	0.28	0.27	0.15	0.18	0.07	0.11	0.21	0.13	0.10	0.12	0.10	0.14	0.17
MgO	7.52	5.16	8.27	9.04	8.18	7.75	6.93	8.11	8.05	6.80	2.42	8.70	10.82
CaO	12.46	9.87	10.85	10.91	11.15	10.07	9.30	10.44	10.38	8.59	9.77	11.44	13.33
Na_2O	1.30	2.39	3.16	2.16	2.54	3.09	3.26	3.45	3.46	4.14	4.69	3.41	2.25
K_2O	1.05	1.13	0.39	1.13	0.18	0.96	1.88	0.72	0.88	1.03	0.92	0.47	0.42
P_2O_5	0.44	0.74	0.14	0.25	0.02	0.11	0.03	0.04	0.06	0.05	0.21	0.03	0.03
S	0.08	0.15	0.06	0.05	0.03	0.04	0.04	0.05	0.05	0.04	0.06	0.07	0.16
H_2O	1.65	1.69	3.41	2.05	0.80	1.94	1.19	0.89	1.08	1.20	1.62	0.75	0.43
CO_2	0.92	NIL	NIL	NIL	NIL	NIL	NIL	NIL	NIL	0.36	NIL	0.18	TRACE
Total+	99.39	99.00	99.77	100.55	98.94	99.77	99.58	98.98	100.11	99.65	99.00	99.43	100.25
$\frac{100\ Mg}{Mg+Fe}$	46.0	34.1	60.7	57.1	76.5	66.4	52.8	70.3	70.0	64.9	45.3	66.9	68.1
$\frac{100\ Na}{Na+Ca}$	15.9	30.5	34.5	26.4	29.2	35.7	38.8	37.4	46.6	46.6	46.5	35.0	23.4
PPM													
Ni	156	60	56	114	32	69	39	144	83	59	23	141	221
Co	78	114	80	94	48	60	84	83	90	52	60	88	82
V	425	348	131	225	12	68	309	138	139	96	129	158	268
Cr	223	36	427	261	228	347	174	284	297	254	98	315	890
Zn	121	190	96	107	27	64	235	46	48	50	40	59	65
Cu	200	59	10	51	11	18	18	21	13	21	28	45	127
Rb	52	21	12	21	2	30	24	10	13	15	3	11	5
Sr	396	283	1419	1070	232	3556	652	882	1081	2415	294	812	698
Zr	56	137	29	106	3	29	5	14	19	16	76	18	22
Ba	3611	535	2451	2428	1002	1854	2949	183	237	682	388	1217	358
K/Rb	168	447	268	448	751	266	650	599	561	572	2557	352	689

+ Total includes wt.% Cr_2O_3, NiO, SrO and BaO

Table 2. Cont.

Rock Type	2 Pyroxene Granulite	Garnet Websterites							Eclogite		Highly Altered Xenoliths		
Sample Number	PHN 2645	L 17	PHN 2495	KN 206	L 9	M 5	L 16	M 3	PHN 2630/1	PHN 2532	PHN 2685/1A	PHN 1919	K 1
SiO_2	47.34	45.87	46.98	47.15	47.88	48.07	48.50	48.50	41.06	42.92	32.75	44.57	46.21
TiO_2	0.76	0.71	1.85	1.58	1.24	0.49	0.71	0.51	0.51	2.22	1.36	1.01	0.27
Al_2O_3	13.45	10.54	11.05	7.91	7.75	10.24	8.36	7.79	12.72	12.45	12.23	15.69	19.15
Fe_2O_3	3.20	3.23	2.58	4.23	4.71	4.34	3.01	3.55	1.93	2.76	1.86	3.33	0.45
FeO	7.86	9.55	10.31	16.74	9.47	5.45	6.89	10.50	19.45	12.54	13.88	7.13	1.42
MnO	0.18	0.22	0.21	0.29	0.22	0.20	0.19	0.25	0.58	0.21	0.33	0.19	0.05
MgO	8.59	13.52	13.38	16.48	13.17	16.77	15.70	14.26	9.02	9.52	14.57	9.23	0.20
CaO	8.95	12.46	10.21	4.07	12.39	12.50	13.28	11.21	10.60	12.36	10.12	7.92	8.37
Na_2O	2.60	1.47	1.68	0.79	1.84	0.78	1.56	1.24	0.21	1.74	0.11	5.19	14.07
K_2O	2.42	0.04	0.26	0.03	0.02	0.06	0.06	0.03	0.84	0.02	0.21	0.28	0.15
P_2O_5	0.10	0.11	0.48	0.06	0.04	0.02	0.04	0.03	0.04	0.04	0.20	0.04	0.02
S	0.04	0.00	0.03	NIL	0.09	0.01	0.04	0.08	0.04	0.03	0.40	0.04	0.03
H_2O	1.97	1.36	0.74	1.09	0.98	1.20	1.60	1.53	1.30	1.26	4.76	5.67	7.80
CO_2	0.73	TRACE	NIL	NIL	NIL	NIL	TRACE	NIL	0.42	0.50	4.65	NIL	NIL
Total+	99.74	99.25	100.12	100.42	99.44	100.13	100.57	99.48	98.90	98.66	99.15	100.42	98.22
100 Mg / Mg+Fe	58.8	65.9	65.4	59.2	64.0	76.3	74.5	65.1	43.1	53.0	62.5	61.9	16.3
100 Na / Na+Ca	35.4	17.6	22.9	26.0	21.2	10.1	17.5	16.7	3.5	20.3	1.9	54.3	75.3
PPM													
Ni	87	380	357		264		581		257	114	168	173	8
Co	51	104	111		87		78		77	110	81	84	4
V	268	358	253		418		288		169	410	384	176	19
Cr	157	771	1536		903		3717		679	311	356	149	51
Zn	83	90	113		114		73		81	118	340	97	13
Cu	19	39	41		89		94		31	18	177	99	14
Rb	51	0	1		5		6		77	1	11	22	7
Sr	891	113	163		182		111		67	147	610	252	200
Zr	47	19	146		33		41		399	30	103	16	96
Ba	12611	70	637		64		77		407	123	14172	556	80
K/Rb	395	-	2158		33		83		91	125	162	105	183

+ Total includes wt.% Cr_2O_3, NiO, SrO and BaO

Table 3. Pyroxenes and Garnets from Granulite-suite Nodules

Clinopyroxenes

	PHN 2317	K-2	K-3	K-4	K-5	KAO 2	KC 22	KC 23	KC 28	KC 29	KC 30	KC 31	PHN 2438
Rk type	GG	GG	GG	Ec	Ec	Ec	Ec	Ec	GG	GG	Ec	Ec	GG
SiO_2	51.6	51.9	52.6	51.4	52.3	52.9	53.5	53.4	53.1	51.6	51.8	53.8	53.4
TiO_2	0.4	0.6	0.4	0.6	0.3	0.8	0.5	0.3	0.4	0.3	0.2	0.3	0.8
Al_2O_3	5.3	8.3	6.4	6.6	4.3	8.4	8.6	8.2	7.3	3.8	3.6	6.6	8.3
Fe_2O_3	4.5	1.3	4.7	0.0	5.0	2.2	1.4	3.2	3.9	5.1	3.8	2.6	1.8
FeO	4.1	2.9	4.0	3.6	4.5	1.6	2.2	3.9	1.2	4.2	5.7	0.6	3.0
MnO	-	-	0.1	0.09	0.1	0.15	-	-	0.15	0.15	.0.2	0.15	-
MgO	11.4	12.2	10.6	13.9	11.6	12.0	12.6	9.7	12.0	12.4	12.0	13.6	11.5
CaO	20.0	20.6	17.7	22.7	18.8	17.5	19.5	16.5	17.5	21.3	20.5	19.6	18.4
Na_2O	2.6	2.5	3.8	0.94	2.9	4.0	3.2	4.7	4.0	1.8	1.8	3.1	3.8
Σ	99.9	100.3	100.3	99.83	99.8	99.55	101.5	99.9	99.55	100.65	99.6	100.35	101.0
Si	1.904	1.877	1.921	1.878	1.932	1.909	1.898	1.938	1.921	1.904	1.928	1.926	1.910
Al^{IV}	0.096	0.123	0.079	0.122	0.068	0.091	0.102	0.062	0.079	0.096	0.072	0.074	0.090
Al^{VI}	0.135	0.231	0.197	0.160	0.120	0.267	0.258	0.289	0.233	0.067	0.086	0.206	0.262
Ti	0.012	0.016	0.011	0.015	0.008	0.022	0.014	0.008	0.010	0.008	0.005	0.008	0.020
Fe^{3+}	0.124	0.034	0.129	-	0.139	0.059	0.036	0.088	0.107	0.141	0.106	0.070	0.048
Fe^{2+}	0.126	0.087	0.121	0.111	0.139	0.047	0.064	0.118	0.038	0.129	0.178	0.017	0.089
Mn	-	-	0.003	0.003	0.003	0.005	-	-	0.005	0.005	0.006	0.005	-
Mg	0.627	0.658	0.577	0.758	0.639	0.645	0.666	0.525	0.649	0.679	0.668	0.726	0.614
Ca	0.791	0.798	0.693	0.886	0.744	0.677	0.741	0.642	0.678	0.843	0.819	0.750	0.706
Na	0.186	0.175	0.269	0.067	0.208	0.279	0.220	0.331	0.281	0.128	0.131	0.218	0.261

Table 3 (cont.)

Clinopyroxenes	PHN 1442j prim.	PHN 1442j sec.	PHN 2508	LT 2	LT 6	PHN 2567/5	L 6	LQ 1	LQ 2	LQ 4	PHN 2494	PHN 2495	KN 195
Rk type	GG	GG	GP	GG	GG	GP	GG	GP	GG	GG	GG	GG	GGG
SiO_2	50.5	52.2	52.5	52.0	51.1	54.1	50.3	53.0	52.6	53.6	53.6	53.2	53.7
TiO_2	0.0	-	0.1	0.6	0.7	0.2	0.8	0.4	0.5	0.2	0.5	0.5	0.5
Al_2O_3	9.5	7.0	2.5	4.2	5.7	4.1	7.1	6.9	6.9	7.2	7.7	6.4	7.3
Fe_2O_3	2.7	1.5	3.7	3.2	2.1	1.7	3.5	3.7	0.0	6.5	3.2	3.7	4.0
FeO	0.9	1.5	4.3	5.0	6.1	4.1	1.2	1.6	2.8	5.7	2.4	2.9	1.7
MnO	-	-	0.1	-	0.06	-	-	0.0	0.04	0.1	-	-	-
MgO	12.5	13.4	13.7	12.8	11.7	13.9	14.0	12.3	13.8	7.5	11.4	11.9	11.6
CaO	21.8	22.0	21.2	20.7	20.8	19.8	21.7	19.1	21.5	14.2	17.4	17.8	17.4
Na_2O	2.0	1.5	1.5	1.8	1.8	2.3	1.5	3.4	1.8	5.8	4.2	3.7	4.3
Σ	99.9	99.5	99.6	100.3	100.06	100.2	100.1	100.4	99.94	100.8	100.4	100.1	100.5
Si	1.831	1.896	1.944	1.913	1.890	1.964	1.831	1.911	1.903	1.953	1.927	1.930	1.929
Al^{IV}	0.169	0.104	0.056	0.087	0.110	0.036	0.169	0.089	0.097	0.047	0.073	0.070	0.071
Al^{VI}	0.237	0.196	0.053	0.095	0.139	0.140	0.135	0.205	0.195	0.263	0.254	0.204	0.238
Ti	-	-	0.004	0.015	0.019	0.005	0.022	0.011	0.014	0.008	0.013	0.013	0.013
Fe^{3+}	0.073	0.041	0.103	0.089	0.059	0.047	0.096	0.100	-	0.177	0.086	0.101	0.107
Fe^{2+}	0.027	0.047	0.132	0.154	0.189	0.123	0.035	0.048	0.084	0.174	0.073	0.087	0.052
Mn	-	-	0.003	-	0.002	-	-	-	0.001	0.003	-	-	-
Mg	0.676	0.726	0.756	0.702	0.643	0.752	0.760	0.661	0.747	0.408	0.611	0.643	0.621
Ca	0.847	0.856	0.841	0.816	0.822	0.770	0.846	0.738	0.835	0.556	0.670	0.692	0.670
Na	0.141	0.134	0.108	0.128	0.127	0.162	0.106	0.238	0.123	0.411	0.293	0.260	0.299

Table 3 (cont.)

Clinopyroxenes

	KN 206	M 1	M 3	M 5	L 9	L 12A	L 12B	L 13	L 16	L 17	L 20	PHN 1646A	PHN 1670
Rk type	GP	GG	GP	GP	GP	GG	Ec	GG	GP	GP	GG	GG	GG
SiO_2	53.8	52.2	53.5	53.0	54.0	52.4	53.0	52.7	53.4	53.4	52.8	52.3	52.5
TiO_2	0.26	0.6	0.17	0.2	0.1	0.3	0.3	0.6	0.3	0.2	0.3	0.2	0.7
Al_2O_3	5.9	10.6	4.8	4.2	4.7	9.9	8.7	10.8	5.5	5.1	5.4	4.8	7.4
Fe_2O_3	5.3	1.2	4.0	1.3	3.2	1.3	1.5	1.6	2.6	2.6	2.9	3.7	2.1
FeO	4.2	1.5	3.7	2.9	3.9	2.6	2.9	1.3	2.2	3.2	4.2	2.8	1.8
MnO	-	-	-	-	0.1	0.1	0.1	-	0.1	0.1	0.1	-	-
MgO	10.3	11.5	12.3	14.6	12.2	10.8	11.5	11.3	13.6	12.9	12.1	13.0	12.9
CaO	15.8	19.3	18.5	21.6	18.4	18.2	18.1	19.5	19.9	19.3	19.9	20.0	20.0
Na_2O	4.7	3.5	3.2	1.5	3.3	3.8	3.7	3.7	2.6	2.8	2.6	2.4	2.8
Σ	100.26	100.4	100.17	99.3	99.9	99.4	99.8	101.5	100.2	99.6	100.3	99.2	100.2
Si	1.960	1.866	1.950	1.939	1.969	1.896	1.915	1.865	1.930	1.948	1.928	1.925	1.894
Al^{IV}	0.040	0.134	0.050	0.061	0.031	0.104	0.085	0.135	0.070	0.052	0.072	0.075	0.106
Al^{VI}	0.214	0.312	0.156	0.120	0.171	0.319	0.285	0.315	0.164	0.167	0.160	0.133	0.208
Ti	0.007	0.016	0.005	0.006	0.003	0.008	0.008	0.016	0.008	0.005	0.008	0.006	0.018
Fe^{3+}	0.144	0.033	0.111	0.037	0.087	0.036	0.042	0.042	0.072	0.072	0.080	0.102	0.058
Fe^{2+}	0.127	0.045	0.112	0.089	0.120	0.078	0.088	0.038	0.067	0.099	0.128	0.086	0.053
Mn	-	-	-	-	0.003	0.003	0.003	-	0.003	0.003	0.003	-	-
Mg	0.559	0.613	0.668	0.796	0.663	0.585	0.618	0.596	0.733	0.701	0.658	0.713	0.694
Ca	0.617	0.739	0.722	0.847	0.719	0.705	0.699	0.739	0.771	0.754	0.778	0.789	0.773
Na	0.332	0.243	0.226	0.106	0.233	0.267	0.258	0.254	0.182	0.198	0.184	0.171	0.196

Table 3 (cont.)

Clinopyroxenes

	PHN 2852	OVKF 10303	MO 4	MO 6	PHN 2630/1	PHN 2630/2	PHN 2645	PHN 1919	PHN 2450	PHN 2496	PHN 2532	PHN 2533	PHN 2685/1A	PHN 3017
Rk type	GG	GG	PG	PG	GP	GG	PG	GG	Ec	Ec	Ec	GG	Ec	GG
SiO_2	52.9	53.0	53.0	51.9	52.0	53.4	52.5	52.2	53.5	53.9	53.3	55.0	52.9	49.2
TiO_2	0.6	0.6	0.4	0.3	0.2	0.3	0.2	0.5	0.3	0.3	0.4	0.2	0.5	1.2
Al_2O_3	7.4	9.8	2.6	3.3	2.3	3.8	2.5	7.2	4.7	4.8	7.8	7.9	7.7	8.2
Fe_2O_3	2.4	1.2	1.0	0.6	1.7	0.0	1.4	3.4	1.2	0.0	3.7	0.0	3.3	4.1
FeO	2.9	2.2	4.9	9.8	8.4	8.9	7.8	2.5	3.0	3.9	4.0	6.0	4.6	4.3
MnO	–	–	–	–	–	–	–	–	0.10	0.11	–	–	–	–
MgO	12.4	11.4	15.2	12.7	12.8	11.8	13.5	11.9	14.3	14.1	10.1	10.4	10.3	10.6
CaO	19.4	17.9	22.6	21.2	21.8	20.6	21.4	19.0	21.3	20.8	17.3	16.2	17.0	20 0
Na_2O	3.0	4.0	0.6	0.6	0.7	0.9	0.8	3.2	1.8	1.9	4.3	4.1	4.1	2.4
Σ	101.0	100.1	100.3	100.4	99.9	99.7	100.1	99.9	100.2	99.81	100.9	99.8	100.4	100.0
Si	1.899	1.899	1.942	1.932	1.945	1.996	1.949	1.897	1.938	1.958	1.923	1.995	1.920	1.816
Al^{IV}	0.101	0.101	0.058	0.068	0.055	0.004	0.051	0.103	0.062	0.042	0.077	0.005	0.080	0.184
Al^{VI}	0.212	0.313	0.056	0.076	0.047	0.163	0.059	0.205	0.139	0.164	0.255	0.333	0.251	0.174
Ti	0.016	0.017	0.010	0.009	0.006	0.008	0.006	0.014	0.008	0.008	0.011	0.005	0.013	0.034
Fe^{3+}	0.065	0.031	0.027	0.017	0.048	–	0.038	0.094	0.032	–	0.099	–	0.090	0.114
Fe^{2+}	0.088	0.064	0.150	0.304	0.262	0.278	0.241	0.076	0.092	0.118	0.121	0.182	0.140	0.132
Mn	–	–	–	–	–	–	–	–	0.003	0.003	–	–	–	–
Mg	0.664	0.609	0.830	0.704	0.714	0.657	0.747	0.645	0.772	0.763	0.543	0.562	0.556	0.581
Ca	0.746	0.687	0.885	0.847	0.874	0.825	0.851	0.740	0.827	0.810	0.669	0.630	0.661	0.792
Na	0.209	0.278	0.043	0.043	0.051	0.068	0.058	0.225	0.126	0.134	0.301	0.288	0.288	0.172

Table 3 (cont.)

Orthopyroxenes

	PHN 2508	LT 2	PHN 2567/5	L 6	LQ 1	PHN 2495	KN 206	M 3	M 5	L 9	L 16	L 17	L 20	MO 4	MO 6	PHN 2630/1	PHN 2630/2	PHN 2645
Rk type	GP	GG	GP	GG	GP	GG	GP	GP	GP	GP	GP	GP	GG	PG	PG	GP	GG	PG
SiO_2	53.5	53.1	55.5	54.5	54.8	54.2	53.7	53.8	55.6	54.5	55.0	54.5	54.2	54.1	51.8	52.0	52.6	53.1
TiO_2	0.0	0.5	0.0	0.0	-	0.0	0.0	0.0	0.0	0.0	0.0	-	0.0	0.0	0.0	0.1	0.06	0.0
Al_2O_3	0.75	1.6	1.0	4.0	2.1	1.6	0.83	0.76	2.1	0.85	1.8	1.2	1.7	1.3	1.5	0.94	2.1	1.1
Fe_2O_3	1.1	1.5	0.0	1.9	1.8	0.58	0.0	0.0	0.6	0.0	0.59	1.0	1.1	0.0	0.0	0.78	0.0	0.0
FeO	19.1	19.3	14.3	7.0	10.7	14.7	20.3	18.9	10.5	17.9	11.6	14.2	15.9	17.0	27.1	27.0	26.4	24.0
MnO	0.22	-	-	-	0.1	-	-	-	-	-	0.10	0.1	0.0	-	-	-	-	-
MgO	24.9	24.8	28.8	32.3	30.5	28.0	24.0	25.2	31.1	26.2	30.1	28.3	27.2	26.3	18.6	19.5	17.4	21.3
CaO	0.25	0.36	0.20	0.45	0.28	0.18	0.30	0.35	0.41	0.32	0.35	0.35	0.36	0.43	0.58	0.40	0.40	0.47
Na_2O	0.0	-	-	0.0	0.0	0.0	0.0	0.0	0.0	0.0	0.0	0.0	0.0	0.0	0.0	0.0	0.0	0.0
Σ	99.82	101.16	99.80	100.15	100.28	99.26	99.13	99.01	100.31	99.77	99.54	99.65	100.46	99.13	99.58	100.72	98.96	99.97
Si	1.969	1.930	1.984	1.894	1.933	1.958	1.994	1.985	1.948	1.984	1.954	1.961	1.949	1.976	1.980	1.966	2.032	1.990
Al^{IV}	0.031	0.069	0.016	0.106	0.067	0.042	0.006	0.015	0.052	0.016	0.046	0.039	0.051	0.024	0.020	0.034	-	0.010
Al^{VI}	0.002	-	0.030	0.058	0.020	0.026	0.030	0.018	0.035	0.021	0.030	0.012	0.021	0.033	0.049	0.006	0.096	0.039
Ti	-	0.013	-	-	-	-	-	-	-	-	-	-	-	-	-	0.003	0.002	-
Fe^{3+}	0.029	0.042	-	0.049	0.047	0.016	-	-	0.017	-	0.016	0.028	0.031	-	-	0.022	-	-
Fe^{2+}	0.586	0.587	0.428	0.204	0.316	0.443	0.630	0.583	0.309	0.545	0.344	0.427	0.477	0.519	0.866	0.854	0.853	0.752
Mn	0.007	-	-	-	0.003	-	-	-	-	-	0.003	0.003	-	-	-	-	-	-
Mg	1.366	1.344	1.535	1.673	1.603	1.508	1.328	1.386	1.624	1.422	1.594	1.518	1.458	1.431	1.061	1.099	1.002	1.190
Ca	0.010	0.014	0.008	0.017	0.011	0.007	0.012	0.014	0.015	0.012	0.013	0.013	0.014	0.017	0.024	0.016	0.017	0.019
Na	-	-	-	-	-	-	-	-	-	-	-	-	-	-	-	-	-	-

Table 3 (cont.)

Garnets	KAO 2	KC 22	KC 23	KC 28	KC 29	KC 30	KC 31	PHN 2438	PHN 1442j prim.	PHN 1442j sec.	PHN 2508	LT 2	LT 6
Rk type	Ec	Ec	Ec	GG	GG	Ec	Ec	GG	GG	GG	GP	GG	GG
SiO_2	40.3	41.4	39.5	39.6	38.1	38.4	41.0	40.1	40.3	40.2	38.9	39.5	39.1
TiO_2	0.0	0.0	0.0	0.0	0.0	0.0	0.0	0.0	-	0.0	0.0	0.0	0.0
Al_2O_3	22.4	23.6	22.2	23.7	22.2	21.3	23.5	22.7	23.0	23.2	22.0	21.6	21.6
FeO	15.3	15.0	23.6	18.8	26.9	27.3	13.8	19.1	14.3	15.3	25.1	24.6	23.4
MnO	0.49	-	-	0.71	0.83	1.1	0.57	-	-	-	0.84	-	0.57
MgO	15.3	14.1	7.0	13.7	5.7	6.0	17.3	11.5	11.2	10.4	8.1	8.9	7.4
CaO	5.4	7.1	8.4	4.1	7.5	6.7	4.5	6.0	11.2	11.1	5.6	6.0	8.3
Σ	99.19	101.2	100.7	100.61	101.23	100.8	100.67	99.4	100.0	100.2	100.54	100.6	100.37
Si	2.984	2.998	3.011	2.927	2.948	2.984	2.960	3.009	2.987	2.985	2.984	3.010	3.001
Al^{IV}	0.016	0.002	-	0.073	0.052	0.016	0.040	-	0.013	0.015	0.016	-	-
Al^{VI}	1.942	2.013	1.995	1.995	1.972	1.938	1.960	2.010	1.996	2.015	1.972	1.940	1.955
Ti	-	-	-	-	-	-	-	-	-	-	-	-	-
Fe	0.947	0.909	1.505	1.162	1.737	1.773	0.831	1.198	0.886	0.950	1.610	1.568	1.499
Mn	0.031	-	-	0.044	0.054	0.072	0.035	-	-	-	0.055	-	0.037
Mg	1.686	1.522	0.795	1.514	0.652	0.699	1.864	1.290	1.237	1.151	0.926	1.011	0.851
Ca	0.431	0.551	0.686	0.325	0.624	0.557	0.350	0.481	0.889	0.883	0.460	0.490	0.679

Table 3 (cont.)

Garnets	PHN 2567/5	L 6 inner	LQ 11	LQ 21	LQ 4	PHN 2494	PHN 2495	KN 195	KN 206	M 1	M 3	M 5
:k type	GP	GG	GP	GG	GG	GG	GG	GG	GP	GG	GP	GP
SiO_2	40.4	40.3	40.2	41.1	37.9	40.1	40.0	40.1	39.2	40.7	39.1	40.6
TiO_2	0.0	0.0	0.0	0.0	0.0	0.0	0.0	0.0	0.0	0.0	0.05	0.0
Al_2O_3	22.2	23.5	22.7	23.3	21.6	22.7	22.3	22.8	21.9	23.7	22.0	22.8
FeO	21.1	14.9	18.9	13.6	32.3	20.3	21.0	20.7	25.2	14.2	23.8	16.4
MnO	-	-	0.6	0.41	0.6	-	-	-	-	0.2	-	-
MgO	11.3	15.6	13.6	15.3	4.3	12.1	11.7	12.0	8.7	13.1	9.4	13.9
CaO	5.0	5.5	4.6	6.7	5.2	4.9	4.5	4.8	4.1	7.9	4.7	5.5
Σ	100.0	99.8	100.6	100.41	101.9	100.1	99.5	100.4	99.1	99.8	99.05	99.2
Si	3.032	2.953	2.977	2.992	2.961	2.996	3.014	2.992	3.024	2.991	3.005	3.010
Al^{IV}	-	0.047	0.023	0.008	0.039	0.004	-	0.008	-	0.009	-	-
Al^{VI}	1.964	1.983	1.958	1.988	1.951	1.996	1.981	1.996	1.991	2.041	1.993	1.993
Ti	-	-	-	-	-	-	-	-	-	-	0.003	-
Fe	1.324	0.913	1.170	0.824	2.113	1.269	1.323	1.292	1.626	0.871	1.530	1.017
Mn	-	-	0.038	0.025	0.040	-	-	-	-	0.012	-	-
Mg	1.264	1.704	1.501	1.653	0.501	1.348	1.314	1.334	1.000	1.438	1.077	1.536
Ca	0.402	0.432	0.365	0.519	0.438	0.392	0.363	0.384	0.339	0.621	0.387	0.437

Table 3 (cont.)

Garnets

	PHN 2317	K 2	K 3	K 4	K 5	L 9	L 12A	L 12B	L 13	L 16	L 17	L 20
Rk type	GG	GG	GG	Ec	Ec	GP	GG	Ec	GG	GP	GP	GG
SiO_2	38.6	40.5	39.0	41.1	38.7	40.0	40.4	40.4	40.9	40.7	39.8	40.1
TiO_2	0.0	0.0	0.0	0.0	0.0	0.0	0.0	0.0	0.0	0.0	0.0	0.0
Al_2O_3	21.7	23.1	21.7	22.8	22.2	21.2	23.8	23.6	22.2	22.3	21.6	21.9
FeO	24.1	16.8	24.8	12.9	25.7	23.0	17.2	18.0	15.1	17.7	20.6	22.5
MnO	-	0.3	0.7	0.56	0.6	0.6	0.4	0.4	0.3	0.5	0.5	0.3
MgO	6.7	12.1	8.4	15.4	8.5	11.0	11.8	12.5	13.3	13.8	12.0	10.7
CaO	8.4	8.1	6.0	8.2	5.3	4.6	7.3	5.9	8.4	5.0	4.8	5.3
Σ	99.5	100.9	100.6	100.96	101.0	100.4	100.9	100.8	100.2	100.0	99.3	100.8
Si	2.994	2.984	2.988	2.981	2.958	3.028	2.976	2.974	3.016	3.015	3.014	3.015
Al^{IV}	0.006	0.016	0.012	0.019	0.042	-	0.024	0.026	-	-	-	-
Al^{VI}	1.978	1.990	1.947	1.929	1.958	1.891	2.043	2.025	1.929	1.947	1.928	1.941
Ti	-	-	-	-	-	-	-	-	-	-	-	-
Fe	1.563	1.035	1.589	0.781	1.643	1.456	1.056	1.107	0.931	1.097	1.305	1.415
Mn	-	0.019	0.045	0.034	0.039	0.038	0.025	0.025	0.019	0.031	0.032	0.019
Mg	0.775	1.329	0.959	1.663	0.968	1.241	1.289	1.376	1.462	1.524	1.354	1.199
Ca	0.698	0.639	0.429	0.638	0.434	0.373	0.578	0.468	0.664	0.397	0.389	0.427

Table 3 (cont.)

Garnets

	PHN 1646A	PHN 1670	PHN 2852	OVKF 10303	PHN 2630/1	PHN 2630/2	PHN 1919	PHN 2450	PHN 2496	PHN 2532	PHN 2533	PHN 2685/1A	PHN 3017
Rk type	GG	GG	GG	GG	GP	GG	GG	Ec	Ec	Ec	Ec	Ec	GG
SiO_2	39.1	40.5	40.6	40.2	38.2	39.7	39.5	40.2	39.8	39.4	40.7	39.2	39.4
TiO_2	0.0	0.0	0.0	0.0	0.0	0.0	0.0	0.0	0.0	0.0	0.0	0.0	0.1
Al_2O_3	22.4	23.0	23.1	23.7	21.7	22.5	22.5	23.0	22.7	22.4	23.8	22.1	21.9
FeO	21.6	16.0	19.3	15.9	28.1	26.0	20.5	19.0	19.9	24.2	21.5	23.6	22.3
MnO	-	-	-	-	-	-	-	0.79	0.84	-	-	-	-
MgO	10.7	14.3	11.7	13.2	4.9	4.7	10.9	12.6	11.8	7.2	8.0	8.6	7.9
CaO	5.2	6.3	6.2	7.3	6.7	7.0	6.5	5.2	5.1	7.8	6.1	6.2	8.6
Σ	99.0	100.1	100.9	100.3	99.6	99.9	99.9	100.79	100.14	101.0	100.1	99.7	100.2
Si	2.981	2.980	3.003	2.958	3.001	3.065	2.979	2.979	2.983	2.998	3.054	3.004	3.005
Al^{IV}	0.019	0.020	-	0.042	-	-	0.021	0.021	0.017	0.002	-	-	-
Al^{VI}	1.994	1.974	2.013	2.013	2.009	2.047	1.978	1.987	1.988	2.006	2.105	1.997	1.974
Ti	-	-	-	-	-	-	-	-	-	-	-	-	0.006
Fe	1.377	0.984	1.194	0.978	1.846	1.679	1.293	1.177	1.247	1.540	1.349	1.509	1.421
Mn	-	-	-	-	-	-	-	0.050	0.054	-	-	-	-
Mg	1.216	1.568	1.290	1.448	0.574	0.541	1.225	1.392	1.318	0.816	0.895	0.980	0.894
Ca	0.425	0.497	0.491	0.575	0.564	0.579	0.515	0.413	0.410	0.636	0.490	0.507	0.704

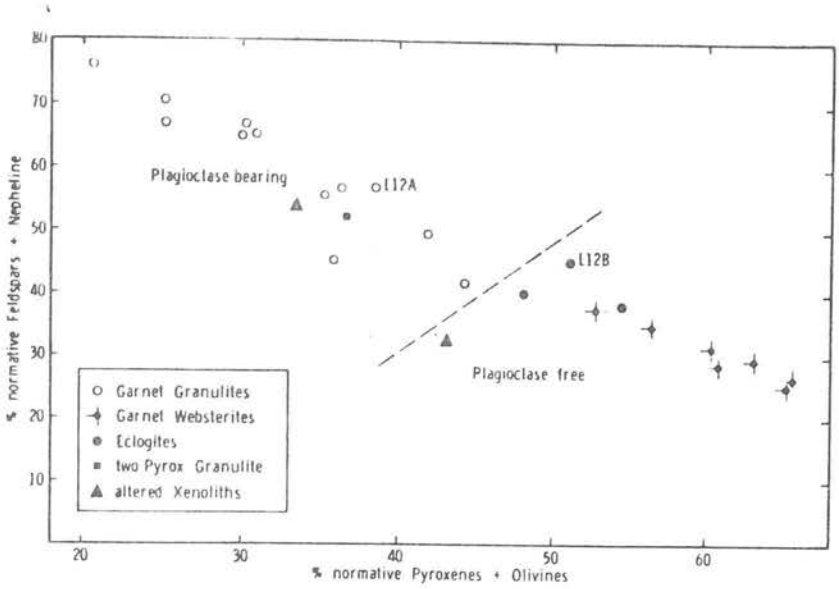

Fig. 3. Chemical controls on the presence of modal plagioclase in the garnet granulite suite.

and his imply that the original samples were quite inhomogeneous (especially OVKF10303).

The basic granulites and eclogite are essentially olivine-basaltic in composition, with minor normative Ne (0-5%) or Hy (0-2%, one with 9%). In contrast, the garnet websterites are more strongly Hy-normative (6-25%, one with 59%). The felsic granulite LT-2 contains significant normative and modal quartz, and is of intermediate composition.

The absence of plagioclase in the eclogites and garnet pyroxenites is largely controlled by rock chemistry. Only rocks with >35% normative plagioclase and <45% normative pyroxenes + olivine contain modal plagioclase (Fig. 3). Plagioclase-bearing nodules also have generally higher Na/Na+Ca than those lacking plagioclase. This compositional control on the presence of plagioclase, and the interlayering of eclogite and granulite on the cm scale (L12A, B) makes it unnecessary to postulate that the eclogites originated at greater depths than the granulites.

The garnet websterites are lower in Al, and higher in Mg/Mg+Fe, than the granulites, as well as being more mafic. This trend is compatible with the websterites being mafic cumulates from a basic magma now represented by the granulites. However, within the granulites there is a well-defined trend toward higher Mg/Mg+Fe in the less mafic samples. This is difficult to explain in terms of crystal fractionation, and argues against a simple genetic relation among the various granulites, or between these rocks and the garnet websterites.

Extensive hydration of primary mafic phases is accompanied in some cases by carbonation (PHN-2685/1A) or natrolitization (PHN-1919, K-1). Many of the fresher samples show similar effects on a smaller scale, especially partial alteration of primary feldspars and scapolite to secondary minerals such as natrolite, pectolite, sericite and carbonate. The fluids responsible for the post-granulite-facies introduction of H_2O, CO_2 and Na_2O presumably come from the enclosing kimberlite, and the alteration may be regarded as analogous to the fenitization that commonly accompanies alkaline-carbonatite complexes.

The contents of LIL elements such as K, Rb, Sr, Ba, Zr, Ti and P are highly variable, and the possibility of contamination from the kimberlite must be considered. In some samples (PHN-2685/1A, PHN-2645) there appears to be a correlation between high Ba and Sr contents and the presence of secondary carbonate, but this does not hold in general. Furthermore, microprobe studies of PHN-2645 show that the Ba mostly resides in tiny (<10μm) K-feldspar inclusions in the plagioclase. The K in most nodules resides in biotite and/or K-feldspar (Table 1), as does, presumably, most of the Rb. Since these phases appear on textural grounds to be in equilibrium with the other members of the granulite-facies or eclogite assemblages, the present levels of K, Rb, Sr and Ba were probably established before or during the granulite-facies metamorphism. The same is probably true of Ti and P, which reside in rutile (or ilmenite) and apatite, respectively; there are no obvious grounds for regarding either of these phases as secondary with respect to the primary metamorphic assemblages.

Analyses of REE in Lesotho granulite nodules (including our samples PHN-1646, -1919, -2852, OVK-F10303) show a wide range in both ΣREE and in the degree of enrichment of the light REE (Rogers, 1977). Samples with low REE have

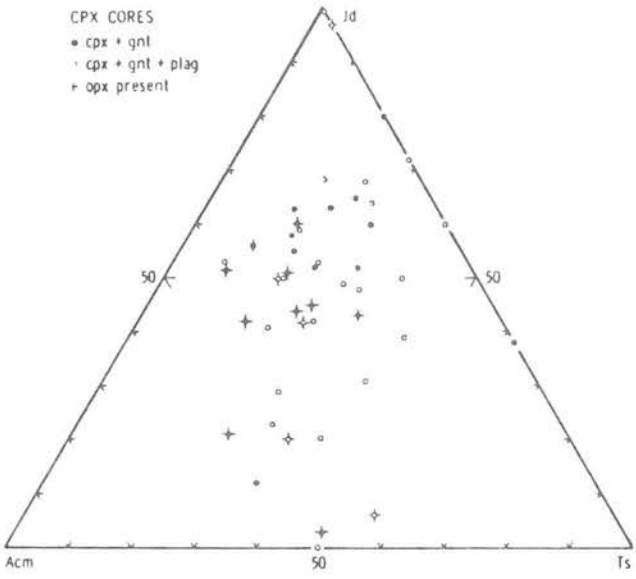

Fig. 4. Proportions of jadeite (Jd), Ca-Tschermak's molecule (Ts) and acmite (Acm) end-members in clinopyroxenes of the garnet granulite suite.

flat, unfractionated or light-REE-depleted patterns relative to chondrites, while increasing REE contents are accompanied by greater enrichment in the light REE. Most samples, however, show pronounced positive Eu anomalies. Both garnet and clinopyroxene also show this positive Eu anomaly (Rogers, 1977; and pers. comm.). This implies that the REE patterns were established, and the Eu^{2+} partly oxidized to Eu^{3+}, prior to the formation of the high-P granulite/eclogite mineral assemblages, which in turn argues against significant contamination from the kimberlite. Rogers (1977) has also shown that other incompatible elements (Nb, Zr, Hf, Ta) vary coherently with the REE, suggesting that the contents of these elements were also relatively little affected by alteration.

Thus, even after discounting kimberlite-contamination effects, the trace-element and minor-element contents of these nodules show wider variations than the major-element concentrations. Many samples show the high K/Rb ratios and low K/Ba ratios characteristic of medium- and high-pressure granulite-facies rocks (Heier, 1973). The very low contents of Ti, K, P and Zr in some nodules are anomalous for basaltic compositions and also suggest depletion. On the Ti-Zr-P discrimination diagram (Floyd and Winchester, 1975) 3 nodules plot as alkali basalts, 10 as tholeiitic basalts, and the rest fall outside any defined fields. Thus the minor and trace-element compositions do not appear to reflect original magmatic distributions. The REE patterns discussed above show very large variations in abundances and degree of fractionation among nodules of similar bulk composition. These variations are difficult to reconcile with an igneous origin, but could be explained by variable removal of incompatible elements during an anatectic event. We conclude that the trace-element and minor-element contents of these nodules reflect modification of some primary distribution(s) by high-grade metamorphic processes, perhaps including anatexis (cf. Rogers, 1977).

Mineral Chemistry

Methods: Minerals were analyzed using a manual ARL-EMX electron microprobe at the Central Institute for Industrial Research, Oslo. Accelerating voltages were 15 kV and sample currents 0.01-0.03 μ amps. Natural and synthetic mineral standards were used, and the data were reduced using the method of Bence and Albee (1968). Fe^{3+} was calculated in the pyroxenes on the assumption of charge balance (program PYROX, by E. R. Neumann). Our experience suggests that this procedure tends to produce maximum values for Fe^{3+}, since analytical errors and non-stoichiometry in the pyroxenes usually produce low values for SiO_2. Analyses with unusually high Fe^{3+}/Fe^{2+} ratios have been run in duplicate to confirm the analyses. Calculated Fe^{3+} values are not given for the garnets, since these values are usually so small (<0.5%) that we interpret them as resulting

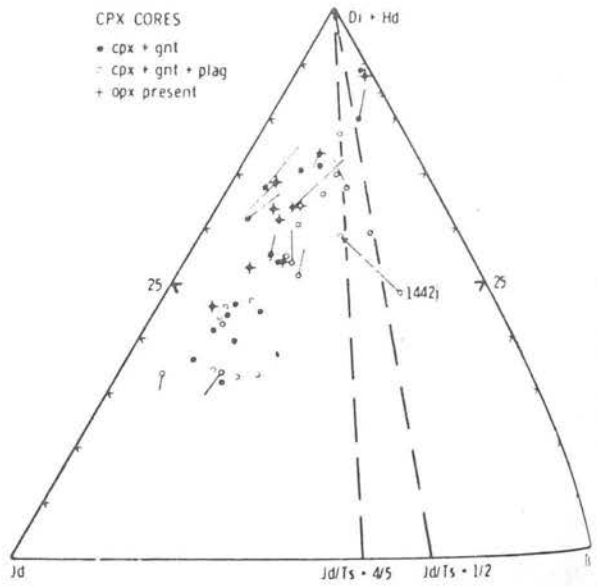

Fig. 5. Proportions of Jd, Ts and diopside + hedenbergite (Di + Hd) end-members in the clinopyroxenes. Short lines connect analyses of the cores of the grains (symbols) with analyses of rims, where zoning was observed. For sample PHN-1442j an arrow runs from the primary to the secondary pyroxene.

from analytical error. This is typical of granulite and eclogite garnets, in our experience.

Clinopyroxenes: Most of the analyzed clinopyroxenes, regardless of rock type, have high contents of Jd+Acm+Ts (Table 3). The relative proportions of these components vary widely, but Jd is usually dominant (Fig. 4). These pyroxenes thus resemble those from metamorphic eclogites. Preliminary single-crystal X-ray studies of pyroxenes from M-1, LQ-1 and LQ-4 show that they have disordered structures (C2/c space group), suggesting crystallization at T >600°C (A. Mottana, pers. comm.). Further studies of pyroxenes are in progress.

The ratio Jd/Ts > ½ usually distinguishes granulite-facies from eclogite pyroxenes (omphacites) (White, 1964). According to this criterion, the analyzed clinopyroxenes of both eclogites and garnet granulites in the Lesotho suite are eclogitic (Fig. 5). The four exceptions are all low in both Jd and Ts, and the errors on both components may be large relative to the absolute contents. Clinopyroxenes from the Monastery pyroxene granulites have lower Jd/Ts and higher Acm. There is a reasonably good correlation of the Jd/Ts ratio of the pyroxenes with the Ab content of the coexisting plagioclase (Fig. 6) in the garnet granulites.

Some of the clinopyroxenes show zoning, usually in the form of lower Jd content within about 100 μm of the rims. The marked zones with tabular channels, described above, also have much lower Jd and Ts contents than their host pyroxenes (Fig. 5). The Jd-depleted rims

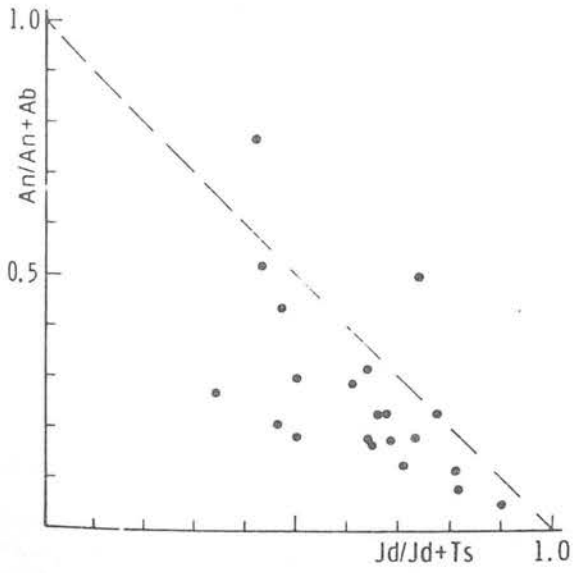

Fig. 6. Relation between plagioclase composition and the Jd/Jd+Ts ratio of coexisting clinopyroxene.

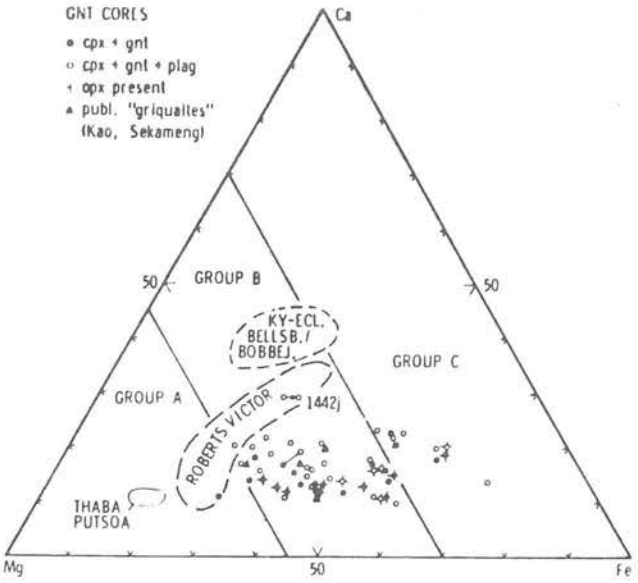

Fig. 7. Atomic proportions of Fe, Mg and Ca in garnets. Group A (eclogites in kimberlites), B (eclogites in gneiss) and C (eclogites in blueschist) are adapted from Coleman et al. (1965). Data on kyanite-eclogites from Bellsbank Fissure and Bobbejaan are by Carswell (unpublished).

are interpreted as the combined result of metasomatism and decompression during the transport of the nodules in the kimberlite, and give an idea of the amount of reequilibration of the mineral assemblages that may have occurred since the nodules were picked up by the kimberlite.

Orthopyroxenes: The orthopyroxenes of the garnet granulite suite show uniformly low CaO contents consist with their relatively low-temperature metamorphic equilibration (see below). The Al_2O_3 contents vary considerably. In the garnet websterites, lower Al_2O_3 contents are systematically related to higher FeO contents, as is characteristic of granulite-facies pyroxenes (Griffin and Heier, 1969). The exception to this trend is PHN-2630/1 from Monastery Mine. The orthopyroxenes from the garnet granulites and pyroxene granulites do not show this Al_2O_3-FeO correlation. No other clear differences in mineral chemistry are observed between the different rock types in the garnet granulite suite.

Garnets: The garnets show a wide range in Fe/Mg, reflecting variations in bulk-rock composition and in the P/T-controlled partitioning between garnet and pyroxenes. The grossular content ranges only between 10 and 23% except for PHN-1442j. The observed ranges in Fe/Mg/Ca are approximately the same for granulites, eclogites and garnet pyroxenites

Table 4. Analyses of Mica, Amphibole and Scapolite

Micas					Amphiboles			
	K-3	LQ-1	LT-2	PHN 2630/1	PHN 2508	206	MO-6	MO-9
SiO_2	40.5	38.1	37.3	36.9	44.0	46.4	42.4	44.3
TiO_2	4.0	3.8	6.0	5.7	0.7	1.1	2.3	0.3
Al_2O_3	11.8	13.7	11.8	13.7	10.7	9.0	12.9	14.6
FeO	8.7	6.9	10.9	17.5	10.1	10.9	14.8	5.2
MnO	-	0.0	-	-	0.1	-	-	-
MgO	19.5	18.7	16.7	12.5	16.1	15.5	10.1	17.0
CaO	0.14	0.06	0.17	-	10.8	8.3	11.4	11.5
Na_2O	0.34	0.38	0.16	0.1	3.4	4.6	1.8	3.0
K_2O	9.7	9.6	9.5	9.4	0.9	0.5	1.6	0.5
BaO	-			-				
Σ	94.7	91.2	92.5	95.8	96.8	98.3	97.3	96.4

Scapolites							
	K-2	PHN 2852	L-12	LQ-2	PHN 1670	PHN 3017	LT-2
SiO_2	47.3	49.2	51.7	48.2	50.1	48.2	48.6
Al_2O_3	27.5	26.9	23.4	25.4	24.4	22.2	24.9
CaO	15.7	14.3	13.7	16.3	15.0	14.7	14.9
Na_2O	4.3	4.9	5.2	4.2	4.8	4.4	4.8
K_2O	0.0	0.1	0.1	0.0	0.1	0.1	0.1
SO_3	3.5	5.0	5.7	3.9	5.0	6.8	4.7
Cl	0.0	0.0	0.0	0.0	0.0	0.0	0.05
Σ	98.3	100.5	99.8	98.0	99.4	97.0	98.05

PHN-3017 also contains MgO 0.3, FeO 0.3.

(Fig. 7). All of the garnets plot in the fields for Group B (eclogites in gneiss) and Group C (eclogites and blueschists) of Coleman et al. (1965), except for K-31 from Kao. Published analyses of "griquaite" garnets from Kao and Sekameng plot in the Group B field together with our analyses, whereas the garnets of type "Griquaites" are generally distinct in composition from ours (Fig. 7). About 30% of our analyzed garnets classify in Group 5 (magnesian almandine) of Dawson and Stevens (1975); the rest fall in Group 3 (calcic pyrope-almandine). This separation does not correspond to differences in rock type.

Micas and amphiboles: The analyzed micas, all of which appear to be in textural equilibrium with pyroxenes and garnet, include both phlogopites and biotites. Some biotites are unusually rich in TiO_2 (Table 4). The amphiboles are Na-rich hornblendes.

Feldspars: Plagioclase compositions range from An_5-An_{77} (Table 1), but cluster in the range An_{10}-An_{35}. K_2O contents are low (Or <5%) and antiperthite is very rare. Zoning (both "normal" and "reversed") of up to 5% An from core to rim of single grains has been observed in a few samples. Homogeneous grains of orthoclase (Ab_{30-35}) occur rarely (Table 1).

Scapolites: High-sulfer scapolites have been recognized in several samples (Table 4). Similar scapolites have been reported from high-P, high-T nodules in the Delegate pipes (Lovering and White, 1964) and in anorthosite interlayered with eclogite in the Bergen Arcs, Norway (Griffin, 1972). The distribution of Na and Ca between these scapolites and the coexisting plagioclase, if compared with experimental work (Goldsmith and Newton, 1977), would imply temperatures >1300°C. Other mineral equilibria (see below) suggest much lower temperatures; the experimental data probably are not applicable to these rocks.

P/T Estimates

The analyzed rocks contain mineral assemblages that allow estimates of the pressure and temperature of equilibration through the use of published geothermometers and geobarometers. Wood (1976) has shown that the P dependence of Fe/Mg partitioning between coexisting garnet and clinopyroxene in the Ca-free system is less than that found by Råheim and Green (1974)

Table 5. P-T Estimates

Sample	Type	K_D (gnt/cpx)	T°, C	P, Kb	Method	Comments
PHN-2317	GG	10.0	560	5.5	1+5	Qtz present
K-2	GG	5.9	690	10	1+5	
K-3	GG	7.9	630	10	1+5	
K-4	GG	3.2	860	10	1+5	Plag An_{77}, no Fe^{3+}
KAO-2	Ec	7.7	590	5	1+4	No plag, minimum P
			630	10.5	1+5	- " -
KC-23	Ec	8.4	580	5	1+4	- " -
			625	11.5	1+5	- " -
KC-28	GG	13.1	550	12	1+5	
PHN-2438	GG	6.4	670	9.5	1+5	
PHN-1442j	GG	12.7	<500	<0	1+5	Disequil. textures (sec. cpx/gnt)
PHN-2508	GW	10.0	590	10.8	1+2	gnt exsolved from pyroxenes
			795	-	7	
LT-2	GG	7.1	630	6.6	1+2	opx incl. in cpx, maximum P
			680	14	1+3	
			<600	~ 0	1+5	
			810	-	7	
LT-6	GG	6.0	660	5	1+5	
L-6	GG	11.6	<650	<0	1+5	Coronite, plag An_{52}
PHN-2567/5	GW	6.4	715	15.8	1+2	
			843	-	7	
LQ-1	GW	10.7	515	1.1	1+2	575°, 10 Kb w/ form. fr / analysis
			550	1	1+5	No plag, minimum P
			700	-	7	
LQ-2	GG	4.4	750	7.5	1+5	Qtz present
LQ-4	GG	9.9	560	5.5	1+4	- " -
			610	10.5	1+5	
PHN-2494	GG	7.9	600	5.5	1+4	
			625	10	1+5	
			650	at 5	6	
			700	at 10	6	
PHN-2495	GG	7.4	650	9	1+2	
			635	9	1+5	
			770	-	7	
KN-195	GG	11.5	550	9.5	1+5	
			700	at 10	6	
KN-206	GW	7.2	690	16.5	1+2	
			750	-	7	
M-1	GG	8.2	575	8	1+4	
			625	10.5	1+5	
M-3	GW	8.5	640	13.6	1+2	
			780	-	7	
M-5	GW	5.9	680	7.9	1+2	
			790	-	7	
L-9	GW	6.5	740	20.5	1+2	
			765	-	7	
L-12A	GG	6.1	680	7.5	1+4	
			710	13.5	1+5	
L-13	GG	10.0	560	4.5	1+4	
			580	11	1+5	
L-16	GW	7.9	605	6.0	1+2	
			790	-	7	
L-17	GW	6.8	695	14.5	1+2	
			775	-	7	
L-20	GG	6.1	680	9.6	1+2	
			660	6.5	1+5	
			720	15.5	1+3	No qtz, maximum P
			730	-	7	

Table 5, (cont.)

Sample	Type	K_D (gnt/cpx)	T°, C	P, Kb	Method	Comments
PHN-1646A	GG	9.4	<550	<0	1+5	
PHN-1670	GG	8.2	600	7	1+5	
PHN-2852	GG	7.0	650	9	1+5	
OVK-F 10303	GG	6.4	645	6.5	1+4	
			695	13	1+5	
PHN-2630/1	GW	8.8	580	5.8	1+2	
			850	-	7	
PHN-2630/2	GG	7.3	615	5.5	1+2	
			660	12	1+3	
			<600	< 0	1+5	Plag An_{50}. Unreliable
			875	-	7	
PHN-1919	GG	9.0	580	8.5	1+5	
PHN-2532	Ec	8.5	570	4.5	1+4	No plag, minimum P
			615	10.5	1+5	
PHN-2533	GG	4.7	760	11	1+4	
			770	11.5	1+5	
PHN-3017	GG	7.0	625	6.5	1+5	

Methods: 1: gnt/cpx; Råheim and Green (1974). 2: opx/gnt; Wood (1974).
3: opx+plag+gnt+qtz; Wood (1975). 4: Di/Ab; Kushiro (1969).
5: cpx/plag; Currie and Curtis (1976). 6: Ab/Or; Stormer (1975).
7: cpx/opx (Fe/Mg); Wells (1977).

in tholeiitic compositions. However, the rocks studied here are basaltic in composition, and the garnets thus contain significant amounts of Ca. We will therefore use the P-T calibration of Råheim and Green (1974). As mentioned above, our procedure for estimating the Fe^{3+} content of the pyroxenes probably biases our estimates toward higher K_D (lower T) and lower Jd (lower P). On the basis of other studies (Mysen and Griffin, 1973) we estimate the probable error resulting from analytical uncertainty to be $\pm$ 75°C and 2 Kb.

The Jd content of diopside coexisting with albite can be used to define the P at given T, using the data of Kushiro (1969); in the absence of quartz this will be a minimum P. Currie and Curtis (1976) have recalibrated this barometer, taking into account the presence of other components in the clinopyroxene and plagioclase. By assuming that the last plagioclase to disappear was albite, a minimum P can also be calculated for eclogites having >20% Jd in the pyroxene.

The Al content of orthopyroxene coexisting with garnet can be used to calculate a P/T relation using the method of Wood (1974), which allows for the presence of Fe in both phases and of Ca in garnet. Wood (1975) has also proposed a geobarometer for opx+gnt+plag+qtz assemblages, but the calibration of this must be regarded as preliminary.

The only available geothermometer for the two-pyroxene granulites from Monastery is that of Wood and Banno (1973) recently recalibrated by Wells (1977). Unfortunately this method appears in our experience to be of dubious reliability at T <800°C (see below). The clinopyroxenes in these rocks contain too little Jd, and the plagioclases too much An, to allow reliable use of the Currie and Curtis (1976) method.

The P-T estimates presented in Table 5 are calculated using the analyses in Table 3, all of which represent the cores of the grains. We regard the marginal zoning observed in some pyroxenes and plagioclase as a result of modification during transport in the kimberlite. The core analyses should therefore give the closest approach to equilibrium conditions.

Five samples give P $\lesssim$0 Kb; two of these have calcic plagioclase and three show disequilibrium textures. In general the Currie and Curtis method gives much higher P than would be estimated from Kushiro's data. As might be expected, the discrepancy is greatest for samples with Fe-rich pyroxenes and calcic plagioclases. There is reasonably good agreement between the Currie and Curtis values and those calculated from opx/gnt partitioning (Wood, 1974) for two samples (PHN-2495, L-20) with sodic plagioclase, but not for PHN-2630/2, in which the plagioclase is An_{50}. We conclude that the Currie and Curtis values are reasonably good for samples with plagioclase less calcic than An_{35}.

Several garnet websterites yield pressures $\gtrsim$15 Kb, and appear anomalous relative to the other samples (Fig. 8). These are all cases in which the orthopyroxene is Fe-rich and Al-poor. These samples otherwise appear, as noted above, to form part of a continuous variation series with the websterites that give much

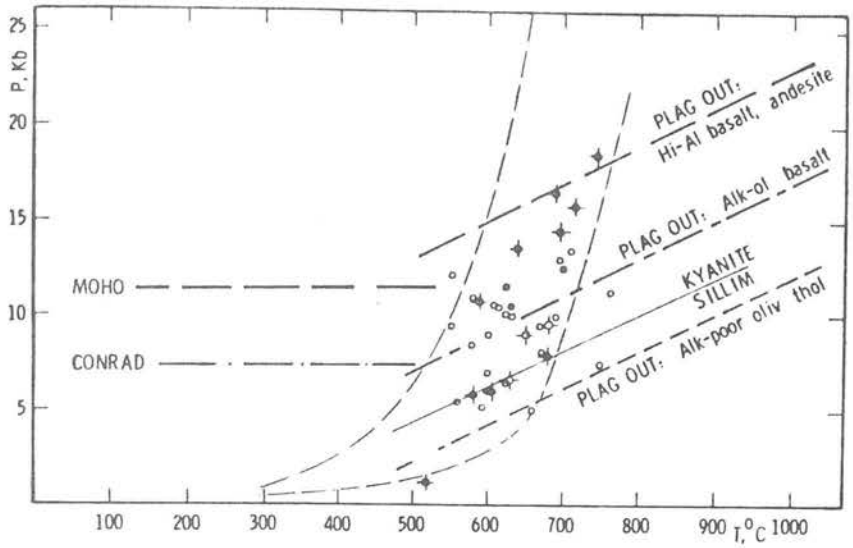

Fig. 8. P-T determinations on nodules of the garnet granulite suite (Table 5). Symbols as in Fig. 3-7. Positions of Moho and Conrad discontinuities are from the Transvaal (Hales and Sacks, 1959). Plag-out curves based on data for relevant compositions at 1100°C, extrapolated at 20 bars/°C (Ringwood, 1975).

lower P, and there is also a correlation of calculated P with whole-rock Fe/Mg.

We therefore prefer to regard these high pressures with caution. The geobarometer of Wood (1974) is calibrated essentially on Mg-rich compositions, and the extrapolation to higher Fe/Mg values may involve a systematic error. The P estimates for these low-Al samples are also very sensitive to K_D (gnt/cpx) and thus to errors in the calculated Fe^{3+} contents of the clinopyroxenes. The effect of overestimating Fe^{3+} is, however, to lower both P and T. For example, calculation of sample L-17 without Fe^{3+} raises P from 14.5 Kb to 28.5 Kb, and T from 695° to 945°C.

The calculated P-T values for the garnet granulites spread mostly between 5-13 Kb and 550-770°C (Fig. 8). There is no obvious correlation of high T with low values of Fe^{3+} in the pyroxenes; both the upper and lower envelopes enclosing the data points on Figure 8 are closely limited by samples with Acm-free clinopyroxenes. Thus the indicated lower-T envelope cannot be moved to significantly higher T. The upper envelope may in fact lie at too high temperatures, but our experience with the calculation of Fe^{3+} in pyroxenes suggests that this is probably not so. Higher T estimates would lead to higher P estimates, and would imply that most of the plagioclase-bearing granulites come from below the Moho; we regard this as unlikely.

The P/T boundaries for the disappearance of plagioclase from garnet-granulites of basaltic composition depend heavily on the details of bulk composition. The boundaries suggested by Green and Ringwood (1972) at 1100°C are plotted in Figure 8, extrapolated to lower T along a gradient of 20 bars/°C as suggested by Ringwood (1975). Most garnet websterites lie above the plag-out line for alkali-poor olivine tholeiite, the closest relevant, experimentally studied composition. All eclogites with >20% Jd in the clinopyroxene plot above the plag-out line for alkali-olivine basalt (cf. analysis of PHN-2532, Table 2). Most of the garnet granulites are equivalent to high-Al olivine basalts, and the experimental boundaries in Figure 8 imply that they should retain plagioclase up to P = 15-17 Kb at their calculated temperatures. The few analyzed granulites with lower Al contents, which should lose their plagioclase at P > 10 Kb, all plot below the plag-out line for alkali-olivine basalts.

The internal consistency between the calculated P-T conditions and the extrapolated experimental boundaries suggests that the P-T estimates are reasonable, though it does not place narrow limits on the possible errors. We conclude that the bulk of the garnet granulite suite probably equilibrated as metamorphic rocks at temperatures between 550-700°C and pressures of 5-13 Kb, and that these nodules come from various levels in the lower crust.

The pyroxene granulites from Monastery Mine must have equilibrated below the garnet-in line for alkali-olivine basalt, which essentially overlaps the lowest plag-out curve in Figure 8. The three analyzed samples (as well as a garnet granulite and a garnet pyroxenite from Monastery) give cpx/opx temperatures ranging from 800 to

900°C by the method of Wood and Banno (1973). This method gives temperatures for the rest of the garnet granulite suite from 780-900° (100-200°C higher than the T given by the other methods). We consider these temperatures to be unrealistically high, but the complete overlap may indicate that the pyroxene granulites from Monastery Mine crystallized at similar T, but lower P than the Lesotho garnet granulite suite.

Three spinel lherzolites from Lipelenang (Carswell and Griffin, unpublished) give temperatures of 820-860°C by both the cpx/opx thermometer of Wood and Banno (1973) and the opx/spinel geothermometer of Obata (1976), and 715-790°C by the thermometer of Wells (1977). We assume that these rocks come from below the base of the crust, but that they crystallized at pressures below the spinel lherzolite/garnet lherzolite boundary. The lower T estimates are similar to those obtained on the garnet granulite suite by the same method. This is consistent with equilibration at P = 12-15 Kb according to the boundary of O'Hara et al. (1971), roughly along the same geotherm as the granulites.

Discussion

Composition of the lower crust: No seismic data are available from Lesotho, so inferences about the crustal structure there must be drawn from geophysical studies of the neighboring regions. Hales and Sacks (1959) used earth tremors in the Witwatersrand to study crustal structure along a traverse from Johannesburg eastward to the coast, across the edge of the Kaapvaal craton. They found the depth to Moho along the traverse to be about 37 km, in agreement with earlier studies. The sub-Moho V_p (7.96 km/sec) is lower than in other parts of the Transvaal. The seismic data define a two-layer crust. The upper layer has V_p = 6.0 km/sec, indicating a low density and probably a "granitic" composition. Well within the craton, the lower layer gives V_p = 6.7 km/sec, and the depth to the Conrad Discontinuity is about 22 km. The V_p increases both with depth within the layer, and along the traverse toward the coast, reaching V_p = 7.2 km/sec near the edge of the craton, as the depth to Conrad increases to about 28 km. Data for both P and S waves at stations outside the edge of the craton suggest a depth to Conrad of ca. 25 km. The seismic data thus indicate the presence of an intermediate-velocity lower-crustal layer beneath both the craton and the bordering mobile belt; this layer appears to be both thicker and denser near the edge of the craton.

If these data can be applied to Lesotho, then our P-T estimates (Table 5, Fig. 8) indicate that the nodules of the garnet-granulite suite come largely, if not entirely, from the sub-Conrad layer. This is not unreasonable, since many lines of evidence suggest that the deep continental crust must consist mainly of granulite-facies rocks (Heier, 1973).

The overall composition of the lower-crustal layer will depend on the proportions of basic granulites, eclogites/garnet websterites and intermediate/acidic granulites. Our sampling was not designed to be representative, and is clearly biased toward the mafic rock types. This is mainly because the more felsic granulites collected by us are typically heavily altered, especially in the smaller nodules. About 12% of the "eclogites" examined by Mathias et al. (1970) contained plagioclase; this is clearly not a representative proportion either.

The most reliable estimate is probably that of Bloomer and Nixon (1973), who counted the proportions of different rock types in a large sample from the Letseng-la-Terae concentrates. Garnet-bearing rocks of presumed lower-crustal origin made up 62% of all nodules and 85% of the crustal ones. Of these, 36% were garnet granulite, 6% eclogites and the rest (58%) acid garnet gneisses, garnet amphibolites, etc. The separation of lower-crustal from upper-crustal lithologies in the last group is difficult, but many of these probably correspond to our sample LT-2, an intermediate granulite. The relative proportions of rock types clearly vary from pipe to pipe: for example, eclogites are quite abundant at Kao. However, a 1:1 ratio of basic granulites + eclogites + garnet websterites to acid + intermediate granulites may be roughly correct for the nodule suite. Is it also correct for the lower crust?

We have measured the density of our samples where they were large enough and fresh enough to give reliable results (Table 1). The average density of the basic garnet granulites is 3.1 g/cm^3; the eclogites and garnet websterites average 3.4 g/cm^3. If these values are combined in the 6:1 proportion found by Bloomer and Nixon (1973), the average density of the garnet-granulite suite is about 3.15 g/cm^3. The only fresh intermediate granulite (LT-2) has a much lower density (2.74 g/cm^3).

The lower-crustal seismic velocities measured by Hales and Sacks (1959) beneath the craton (6.7 km/sec) and beneath the mobile belt (7.2 km/sec) may be converted to average densities using the empirical relation found for granulite-facies rocks by Christensen and Fountain (1975). According to this relation (V_p = 0.33 + 2.27ρ) the cratonic lower crust has an average density of 2.81 g/cm^3, while that beneath the mobile belt has ρ = 3.03 g/cm^3. If the crust is a mixture of the basic granulite suite and intermediate rocks like LT-2, then the proportion of basic rocks must increase from 15-20% beneath the craton to 70-75% beneath the mobile belt. If more acidic rocks are present, or if the very dense eclogites are regarded as mantle rocks, the proportion of mafic rocks must be

somewhat larger in both cases. The lower proportion of basic rocks beneath the craton is consistent with the apparent absence (or great rarity?) of such nodules in the extensively studied cratonic kimberlites.

The estimates based on seismic velocities are only approximate, and assume that seismic data from the Transvaal are relevant to Lesotho. Nevertheless, these data and those of Bloomer and Nixon (1973) imply that the lower crust beneath Lesotho is a roughly equal mixture of basic granulites and intermediate/acid granulites, with smaller proportions of eclogites and garnet websterites. The layered nature of our samples suggests that this part of the crust is compositionally layered on scales ranging from cm to meters. The overall composition may be roughly dioritic, and was proposed for the deep continental crust in general by den Tex (1965). This inference is also consistent with the conclusion of Windom and Boettcher (1976), based on experimental studies of plagioclase-garnet reactions, that a Conrad discontinuity should be observable only in areas where the lower crust contains large amounts of basic rocks. This lower-crustal layer is essentially anhydrous, though small amounts of SO_3 and CO_2 may be stored in scapolites, which are present in at least 15% of our samples.

Origin of the Granulite Complex

The lower crust in continental shield areas is generally believed to be intermediate in average composition, as shown by numerous studies of medium-and high-pressure granulite-facies terranes (Heier, 1973). Our interpretation of the seismic data suggests a larger proportion of basic rocks and a more basic average composition. How has this complex formed?

The basic rocks of the garnet-granulite suite are unlikely to represent recrystallized Karroo-period igneous rocks. The Karroo volcanics are tholeiitic, and lower in Al_2O_3 than the basic granulites. Furthermore, the zircon ages from two nodules indicate that the granulites are Precambrian rocks. Whole-rock chemical data discussed above indicate that the basic rocks are not genetically related to one another as members of a single igneous suite. The trace-element data further suggest that the garnet granulite suite has been depleted in LIL elements, probably during high-grade metamorphism and anatexis.

We therefore envisage the lower-crustal suite as a polygenetic complex with a prolonged history of intrusion, metamorphism and anatexis. These processes have produced a residuum enriched in refractory basic lithologies, and depleted in acidic rocks, relative to the normal continental lower crust. It may be comparable to, for example, the Fraser Range block of the Australian shield, estimated to contain ca. 60% basic granulite-facies rocks (Lambert and Heier, 1968).

The mobile belt bordering the Kaapvaal craton is believed to have formed through multistage reworking of the cratonic rocks (Kröner, 1977). The reworking processes were apparently responsible for both the formation of granulite-facies rocks and for the accumulation of basic rocks in deep crust. We envisage three possible mechanisms: (1) anatexis and subsequent removal of the more acidic components, (2) intrusion of basic rocks into the lower crust during and after orogenic episodes, (3) lateral emplacement of basic material (? oceanic crust) beneath the craton margin by subduction (cf. the apparent existence of subducted oceanic rocks beneath the Colorado Plateau; Helmstaedt and Doig, 1975). The absence of the granulite suite within the craton suggests that these mechanisms were specific to the mobile belt.

Comparison with other suites

(1) Surface outcrops of granulite and eclogite: The Lesotho nodules differ markedly in one respect from most granulite suites; the clinopyroxenes have the high Jd/Ts ratios characteristic of eclogites (Fig. 5). White's (1964) distinction between granulite and eclogite pyroxenes was drawn on the basis of samples from surface outcrops, and has proven to hold true for many granulites and eclogites analyzed since 1964. We interpret the chemistry of the clinopyroxenes in the Lesotho rocks as reflecting a quenched high-pressure pyroxene/plagioclase equilibrium consistent with that predicted from experimental studies (Green and Ringwood, 1967). To our knowledge this relation has not been demonstrated previously.

Under uniform P-T conditions, one would expect a positive correlation of Jd/Jd+Ts in the clinopyroxenes with Ab/Ab+An in the plagioclase over a wide range of bulk compositions. The scatter observed in Figure 6 may be attributed partly to the equilibration of these samples under a range of P-T conditions. Analytical errors, especially in the estimation of Fe^{3+} in clinopyroxene, will also contribute to scatter in the calculated Jd/Jd+Ts. The low Jd/Ts ratios of the pyroxenes in granulites from surface outcrops are probably an effect of reequilibration of the pyroxene-plagioclase pairs during uplift and cooling (Griffin and Carswell, in prep.).

The polygonal granoblastic textures so characteristic of these nodules are apparently not typical of eclogites in gneisses nor of most granulite terranes. These annealed textures may be typical of rocks in the lower crust, where recrystallization has occurred under static conditions over long periods of time (Nixon, 1973; cf. Padovani and Carter, 1977). However, the high heat flow during

the Karroo volcanic period may also have been important in promoting textural equilibrium.

(2) Griquaites: Nixon (1973) has suggested reserving the name "eclogite" for crustal rocks and calling mantle-derived garnet-clinopyroxene rocks "griquaites". Crustal types were to be recognized on the basis of their finer grain size and granoblastic textures. The problem of making this distinction in practice is shown by the fact that four "griquaites" from Kao and Sekameng (Nixon and Boyd, 1973a, b) are indistinguishable in garnet and clinopyroxene chemistry from the granulites and fine-to-medium-grained eclogites analyzed by us (Fig. 7). On the other hand, the type griquaites of Roberts Victor Mine and the similar rocks from Newlands (both diamondiferous), as well as the Thaba Putsoa type with subcalcic diopside, can all be separated from our garnet-granulite suite on the basis of garnet chemistry (Fig. 7). Some of these griquaite garnets have moderate TiO_2 and Cr_2O_3 contents, while our samples are essentially Ti- and Cr-free. The classic griquaites also appear to have lower values of K_D^{Fe-Mg} (gnt-cpx) than the eclogites of the garnet-granulite suite. The use of the term "griquaite" for these mantle-derived eclogites may therefore be useful if the distinction is made on the basis of mineral chemistry.

(3) Other crustal nodule suites: Few comparable nodule suites have been described in detail previously. Irving (1974) has described garnet clinopyroxenites (±plag), garnet websterites and two-pyroxene granulites from the basaltic pipes at Delegate, New S. Wales, Australia. The granulites were inferred to have come from the lower crust, but equilibration temperatures could only be fixed to <1150°C. The garnet pyroxenites and garnet websterites were interpreted as upper mantle (13-17 Kb) cumulates.

Padovani and Carter (1977) describe nodules of two-pyroxene basic granulites and aluminous garnet granulites from the Kilbourne Hole maar, which lies in a region of high heat flow.

McCallum and Eggler (1976) have inferred pressures of equilibration of 12-25 Kb (T = 700-850°C) for garnet websterites from the Sloan diatreme, Wyoming; they also suggested that the lower crust here consists of granulites and pyroxenites, but presented no analyses of these rocks. McGetchin and Silver (1972) presented size/abundance data on the nodule suite from Moses Rock dike, Utah, and concluded that basic garnet granulite ("garnetiferous metagabbro") was the dominant rock type in the lower crust, grading downward to eclogitic rocks and pyroxenites. The Lesotho data suggest that these rocks may in fact "coexist" with granulites, but data on the mineral chemistry of the Moses Rock nodules would be necessary to confirm this.

Meyer and Brookins (1976) described aluminous basic granulites from the Stockdale pipes, Kansas. Their estimated P-T conditions (850°C, 12 Kb) are based on treating all Fe as FeO. Recalculation of the analyses for sample 1128d (the one that satisfies charge-balance requirements) on the basis used here yields P = 5-10 Kb, T = 625-690°, compatible with the estimates for Lesotho. Eclogites from this pipe (Meyer and Brookins, 1971) are similar in mineral chemistry to those described here, and probably come from the lower crust rather than from the mantle.

The available data thus suggest that the lower crust in most areas sampled by kimberlites or basaltic diatremes is dominantly basic in composition. Where heat flow is unusually high, as in areas undergoing basaltic volcanism, these rocks are represented mainly by two pyroxene granulites. In areas of moderate heat flow, garnet granulites, pyroxenites and eclogites dominate the lower-crustal nodule suite.

The Mohorovic Discontinuity beneath Lesotho

The ultramafic nodules from the Lesotho kimberlites have been intensively studied in several laboratories, and their equilibrium P and T have been estimated by reference to experimental work on the Di-En and En-Py systems (Boyd, 1973; Boyd and Nixon, 1975). These estimates define a "pyroxene geotherm" in the depth range 85-150 km, which closely approximates the generalized "Shield geotherm" of Clark and Ringwood (1964). However, these studies have not identified any nodules that originate from the upper mantle at depths between ca. 35 and 85 km. Spinel lherzolites do occur in the kimberlites at Lipelenang and Ngopetseu in Lesotho. However, the rarity of such materials in the Lesotho and South African kimberlites suggests that they do not represent the normal upper mantle beneath this area.

It is possible that the kimberlites simply do not sample the uppermost mantle, for mechanical reasons. Alternatively, the uppermost mantle may be represented by dunites, harzburgites or other lithologies for which P-T estimates are not yet available, but these nodules are also rare in the Lesotho pipes. Carswell et al. (this volume), have argued that the apparent gap in the sampling may be an artifact produced by the calculation procedure. The smaller T dependence of the Ca-rich arm of the Di-En solvus at low temperatures may result in an overestimation of temperatures in the 700-950°C range, and displace all determinations to higher T (and thus higher P) (cf. Mori and Green, 1976; Lindsley and Dixon, 1976). In this case the uppermost mantle may in fact be represented by numerous garnet-lherzolite nodules.

Another possibility is that the upper mantle from 35-85 km depth consists largely of eclogite and garnet websterites, with smaller amounts

of garnet granulites of gabbroic-anorthosite or andesitic composition (Fig. 8). We interpret the eclogites studied here as crustal rocks, because of their similarities to the granulites, but it is important to note that the pressure estimates on these rocks are only minimum values. Several garnet websterites from our suite yield P-T estimates that would place them at depths of 45-60 km (Fig. 8). These high pressures may be spurious, but pending better calibration of the opx/g barometer, we must consider the possibility that these rocks are in fact fragments of the uppermost mantle. The eclogites and websterites have densities corresponding to the measured sub-Moho seismic velocities in the Transvsaal (Vp = 7.9-8.0, Hales and Sacks (1959)).

The arguments against an eclogitic upper mantle (summarized by Ringwood, 1975) are based heavily on large-scale geophysical and geochemical models. They may not be relevant to the existence of a relatively thin (40-50 km) eclogitic layer immediately underlying the continental crust in shield areas. Until some ultrabasic rocks are definitely identified as coming from the uppermost mantle, the possibility of an eclogite- or pyroxenite-rich zone must remain open. This model would imply that the Moho beneath Lesotho represents a narrow zone beneath which eclogite and garnet websterite become the dominant rock types. We envisage such a zone as being produced by an underplating process. Ascending magmas would tend to pond up, at least temporarily, at the base of the crust due to the density contrast, which would reduce their buoyancy. Cumulates from these magmas would be relatively mafic, and on cooling would be converted to eclogites and garnet websterites. Eclogites formed from large cumulate masses in the lower crust would also, with time, tend to sink through the crust and accumulate near the Moho. Eventually, these processes could build up a thick layer of basic rocks with eclogite-facies mineral assemblages. The shallower parts of the garnet-granulite suite, representing most of our samples, may also be the result of these processes, as suggested above.

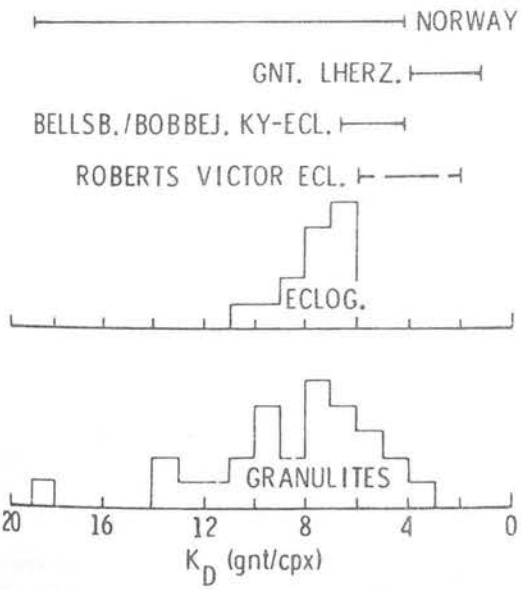

Fig. 9. Ranges of K_D (Fe(Mg)gnt/Fe(Mg)cpx) in the garnet granulite suite and in some comparable suites of eclogites. The Norwegian eclogites are "crustal" (Krogh, 1977), the others are mantle-derived (in part diamondiferous).

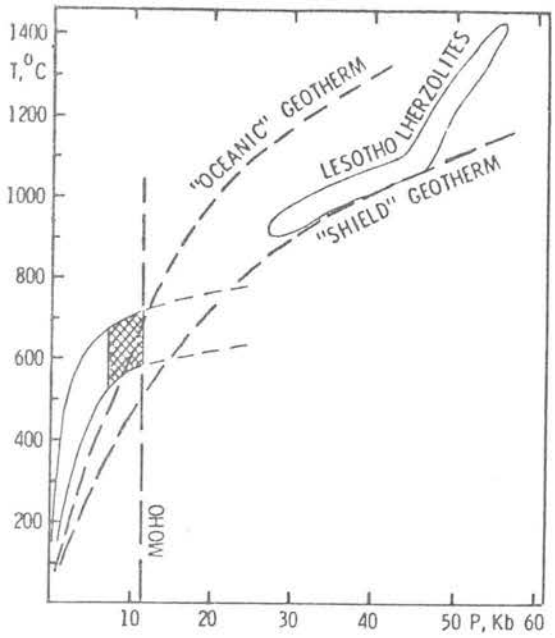

Fig. 10. Relation between the P-T field of the garnet granulite suite (crosshatched) and various proposed geotherms. Crossed dots are the high-Fe, low-Al garnet pyroxenites; these P-T estimates may be spurious.

The Mid-Cretaceous geotherm beneath Lesotho

The P-T estimates in Figure 8 are mostly contained between two curves, which are sharply concave due to the low pressures estimated for a few samples. Moving these samples to higher pressures (and thus higher T) would allow the high-T curve to be smoothed out somewhat, but the positions of these curves in the 6-10 Kb range seem reasonably well-established and imply average temperatures of 600-650°C in this depth interval.

These temperatures are higher by 200-250°C than those predicted by the "Shield geotherm" of Clark and Ringwood (1964) and the low-P extension of the "pyroxene geotherm" of Boyd and Nixon (1975) (Fig. 10). It might be argued that these temperatures are relics after a

granulite-facies regional metamorphic event, and that the mineral assemblages have failed to completely equilibrate during post-metamorphic cooling to a "Shield geotherm". However, the present-day heat flow in the Karroo basin is very high (1.41 h.f.u., Clark and Ringwood, 1964), and presumably was still higher immediately after the Karroo volcanism had ceased ca. 90 m.y. ago. The crustal geotherm defined by the nodule suite is consistent with this high heat flow; this suggests that he equilibration temperatures of the nodules do record the actual crustal temperatures at the time of kimberlite eruption. Such a conclusion is also consistent with the annealed textures of most nodules, which may be ascribed to Karroo-period heating in a static environment.

Gabbroic intrusions of varying size, intruded during the Karroo volcanic activity, would perturb the local geotherm to varying degrees. This effect may explain the wide range in the T estimates, at each P, shown by the garnet granulite suite. The two-pyroxene granulites from Monastery Mine appear to imply somewhat elevated T at shallow P. Since gabbro is one of the most common nodule types at Monastery Mine, the pyroxene granulite nodules may be samples of a widespread contact-metamorphic aureole.

Our data suggest that the "pyroxene geotherm" of Boyd and Nixon (1975) is only valid for the deeper parts of the upper mantle, while temperatures in the uppermost mantle and lower crust lay well above those predicted by the "Shield geotherm". This in turn implies a complicated thermal structure, with several inflections, in the 0-250 km depth region during Cretaceous time.

Acknowledgements. The authors are grateful to the Norwegian Scientific Research Council Nansenfondet, the Natural Evnironmental Research Council and The Royal Society for financial support. P. Kretsen kindly provided important extra samples and useful discussions. The considerable assistance of Dr. R. Kanaris-Sotiriou and V. A. Somogyi with the whole-rock analyses is gratefully acknowledged. We would also like to thank the organizers and guides of the 1973 Lesotho excursions for making this work possible.

References

Bence, A. E., and A. L. Albee, Empirical correction factors for the electron microanalysis of silicates and oxides, J. Geol., 78, 382-403, 1968

Bloomer, A. G., and P. H. Nixon, The geology of the Letseng-la-terae kimberlite pipes, in Lesotho Kimberlites, edited by P. H. Nixon, Lesotho National Development Cooporation, Masern, Lesotho, pp. 20-32, 1973.

Boyd, F. R., A pyroxene geotherm, Geochim. Cosmochim. Acta, 37, 2533-2546, 1973.

Boyd, F. R., and P. H. Nixon, Origins of the ultramafic nodules from some kimberlites of northern Lesotho and the Monastery Mine, South Africa, Phys. Chem. Earth, 9, 431-454, 1975.

Carswell, D. A., Primary and secondary phlogopites and clinopyroxenes in garnet lherzolite xenoliths, Phys. Chem. Earth, 9, 417-429, 1975.

Carswell, D. A., D. B. Clarke, and R. H. Mitchell, The geochemistry of ultramafic nodules from Pipe 200 and their bearing on the nature of the upper mantle beneath Lesotho, Extended Abstracts, Second International Kimberlite Conference, Santa Fe, New Mexico, 1977.

Christensen, N. I., and D. M. Fountain, Constitution of the lower continental crust based on experimental studies of seismic velocities in granulite, Bull. Geol. Soc. Amer., 86, 227-236, 1975.

Clark, S. P., Jr., and A. E. Ringwood, Density distribution and constitution of the mantle, Rev. Geophys., 2, 35-88, 1964.

Coleman, R. G., D. E. Lee, L. B. Beatty, and W. W. Brannock, Eclogites and eclogites: their differences and similarities, Bull. Geol. Soc. Amer., 76, 483-508, 1965.

Currie, K. L., and L. W. Curtis, An application of multicomponent solution theory to jadeitic pyroxenes, J. Geol., 84, 179-194, 1976.

Davis, G. L., The ages and uranium contents of zircons from kimberlites and associated rocks, Extended Abstracts, Second International Kimberlite Conference, Santa Fe, New Mexico, 1977.

Dawson, J. B., and W. E. Stevens, Statistical classification of garnets from kimberlite and associated xenoliths, J. Geol., 83, 589-607, 1975.

den Tex, E., Metamorphic lineages of orogenic plutonism, Geol. Mijnbouw, 44, 103-132, 1965.

Floyd, P. A., and J. A. Winchester, Magma type and tectonic setting discrimination using immobile elements, Earth Planet. Sci. Letters, 27, 211-218, 1975.

Goldsmith, J. R. and R. C. Newton, Scapolite-plagioclase stability relations at high pressures and temperatures in the system $NaAlSi_3O_8$-$CaAl_2Si_2O_8$-$CaCO_3$-$CaSO_4$, Amer. Mineral., 62, 1063-1081, 1977.

Green, D. H., and A. E. Ringwood, An experimental investigation of the gabbro to eclogite transformation and its petrological applications, Geochim. Cosmochim. Acta, 31, 767-833, 1967.

Green, D. H., and A. E. Ringwood, A comparison of recent experimental data on the gabbro-garnet granulite-eclogite transition, J. Geol., 80, 272-288, 1972.

Griffin, W. L., Formation of eclogites and the coronas in anorthosite, Bergen area, Norway, Geol. Soc. Amer. Memoir, 35, 37-63, 1972.

Griffin, W. L., and K. S. Heier, Paragenesis of garnet in granulite-facies rocks,

Lofoten-Vesterålen, Norway, Contr. Mineral. Petrol., 23, 89-116, 1969.
Griffin, W. L., and K. S., Heier, Petrological implications of some corona structures, Lithos, 6, 315-335, 1973.
Griffin, W. L., B. B. Jensen, and S. N. Misra, Anomalously elongated rutile in eclogite-facies pyroxene and garnet, Norsk Geol. Tidsskr., 51, 177-185, 1971
Hales, A. L. and I. S. Sacks, Evidence for an intermediate layer from crustal seismic studies in the Eastern Transvaal, Geophys. J. Roy. Astr. Soc., 2, 15-33, 1959.
Heier, K. S., Geochemistry of granulite facies and problems of their origin, Phil. Trans. R. Soc. Lond., A 273, 429-442, 1973.
Helmstaedt, H., and R. Doig, Eclogite nodules from kimberlite pipes of the Colorado Plateau-samples of subducted Franciscan-type oceanic lithosphere, Phys. Chem. Earth, 9, 95-111, 1975.
Irving, A. J. Geochemical and high pressure experimental studies of garnet pyroxenite and pyroxene granulite xenoliths from the Delegate basaltic pipes, Australia, J. Petrol., 15, 1-40, 1974.
Krogh, E., Evidence of Precambrian continent-continent collision in western Norway, Nature, 267, 17-19, 1977.
Kröner, A., The Precambrian geotectonic evolution of Africa: plate accretion versus plate destruction, Precambrian Res., 4, 163-213, 1977.
Kushiro, I., Clinopyroxene solid solutions formed by reactions between diopside and plagioclase at high pressures, Mineral. Soc. Amer., Spec. Paper, 2, 179-191, 1969.
Lambert, I. S., and K. S. Heier, Geochemical investigations of deep seated rocks in the Australian Shield, Lithos, 1, 30-53, 1968.
Lindsley, D. H., and S. Dixon, Diopside-enstatite equilibria at 850°C to 1400°C, 5 to 35 Kb, Amer. J. Sci., 276, 1285-1301, 1976.
Lovering, J. F., and A. J. R. White, The significance of primary scapolite in granulitic inclusions from deep seated pipes, J. Petrol., 5, 195-218, 1964.
Mathias, M., J. C. Siebert, and P. C. Rickwood, Some aspects of the mineralogy and petrology of ultramafic xenoliths in kimberlites, Contr. Mineral. Petrol., 26, 75-123, 1970.
McCallum, M. E., and D. H. Eggler, Diamonds in an upper mantle peridotite nodule from kimberlite in southern Wyoming, Science, 192, 253-256, 1976.
McGetchin, T. R., and L. T. Silver, A crustal-upper mantle model for the Colorado Plateau based on observations of crystalline rock fragments in the Moses Rock dike, J. Geophys. Res., 77, 7022-7037, 1972.
McGetchin, T. R., and G. W. Ullrich, Xenoliths in maars and diatremes with inferences for the moon, Mars and Venus, J. Geophys. Res., 78, 1832-1853, 1973.
Meyer, H. O. A., and D. G. Brookins, Eclogite xenoliths from the Stockdale kimberlite, Kansas, Contr. Mineral. Petrol., 34, 60-72, 1971
Meyer, H. O. A. and D. G. Brookins, Sapphirine, sillimanite and garnet in granulite xenoliths from Stockdale kimberlite, Kansas, Amer. Mineral., 61, 1194-1202, 1976.
Mori, T., and D. H. Green, Subsolidus equilibria between pyroxenes in the CaO-MgO-SiO_2 system at high pressure and temperature, Amer. Mineral., 61, 616-625, 1976.
Mysen, B. O., and W. L. Griffin, Pyroxene stoichiometry and the breakdown of omphacite, Amer. Mineral., 56, 60-63, 1973.
Nixon, P. H. (ed.), Lesotho Kimberlites, Lesotho Nat. Devel. Corp. 350 pp. 1973.
Nixon, P. H., Perspective, in Lesotho Kimberlites, edited by P. H. Nixon, Lesotho Nat. Devel. Corp. 1973, 350 pp. 1973.
Nixon, P. H. and F. R. Boyd, Deep-seated nodules in Lesotho Kimberlites, edited by P. H. Nixon, Lesotho Nat. Devel. Corp. 1973, 350 pp. 1973a.
Nixon, P. H. and F. R. Boyd, Carbonated ultrabasic nodules from Sekameng, in Lesotho Kimberlites, edited by P. H. Nixon, Lesotho Nat. Devel. Corp. 1973, 350 pp. 1973b.
Obata, M., The solubility of Al_2O_3 in orthopyroxenes in spinel and plagioclase peridotites and spinel pyroxenite, Amer. Mineral., 61, 804-816, 1976.
O'Hara, M. J., S. W. Richardson, and G. Wilson, Garnet-peridotite stability, Contr. Mineral. Petrol., 32, 48-68, 1971.
Padovani, E. R. and J. L. Carter, Granulite facies xenoliths from Kilbourne Hole maar, New Mexico, and their bearing on deep crustal evolution, Extended Abstracts, Second International Kimberlite Conference, Santa Fe, New Mexico, 1977.
Råheim, A., and D. H. Green, Experimental determination of the temperature and pressure dependence of the Fe-Mg partition coefficient for coexisting garnet and clinopyroxene, Contr. Mineral. Petrol., 48, 179-203, 1974.
Rickwood, P. C., J. J. Gurney, and D. R. White-Cooper, The nature and occurrence of eclogite xenoliths in the kimberlites of southern Africa. Upper Mantle Project, Geol. Soc. S. Africa Spec. Publ., 2, 371-393, 1969.
Ringwood, A. E., Composition and Petrology of the Earth's Mantle, McGraw Hill, New York, 618 pp. 1975.
Rogers, N. W., Granulite xenoliths from Lesotho kimberlites and the composition of the lower continental crust, Nature, 270, 681-684, 1977.
Sheppard, S. M. F. and J. B. Dawson, Hydrogen, carbon and oxygen isotope studies of megacryst and matrix minerals from Lesothan and South African kimberlites, Phys. Chem. of the Earth, 9, 747, 764, 1975.
Stormer, J. C., Jr., A practical two-feldspar geothermometer, Amer. Mineral., 60, 667-674, 1975.

Wells, P. R. A., Pyroxene thermometry in simple and complex systems, Contr. Mineral. Petrol., 62, 129-139, 1977.

White, A. J. R., Clinopyroxenes from eclogites and basic granulites, Amer. Mineral., 49, 883-886, 1964.

Windom, K. E., and A. L. Boettcher, The effect of reduced activity of anorthite on the reaction grossular + quartz = anorthite + wollastonite: a model for plagioclase in the lower crust and upper mantle, Amer. Mineral., 61, 889-896, 1976.

Wood, B. J., Solubility of alumina in orthopyroxene coexisting with garnet, Contr. Mineral. Petrol., 46, 1-5, 1974.

Wood, B. J., The influence of pressure, temperature and bulk composition on the appearance of garnet in orthogneisses - an example from South Harris, Scotland, Earth Planet. Sci. Let., 26, 299-311, 1975.

Wood, B. J., The partitioning of iron and magnesium between garnet and clinopyroxene, Geophys. Lab. Wash. Yearbook, 75, 571-574, 1976.

Wood, B. J., and S. Banno, Garnet-orthopyroxene and orthopyroxene-clinopyroxene relationships in simple and complex systems, Contr. Mineral. Petrol., 42, 109-124, 1973.

Reprinted from: "The Mantle Sample: Inclusions in Kimberlites and Other Volcanics", Proc. Second Int. Kimb. Conf., Vol. 2, 1979.

THE PETROLOGY AND GEOCHEMISTRY OF ULTRAMAFIC NODULES FROM PIPE 200, NORTHERN LESOTHO

D. A. Carswell

Department of Geology, University of Sheffield, Sheffield, U.K.

D. B. Clarke

Department of Geology, Dalhousie University, Halifax, Canada

R. H. Mitchell

Department of Geology, Lakehead University, Thunder Bay, Canada

Abstract. The Pipe 200 ultramafic nodule suite is dominated by relatively depleted garnet- and/or chromite-bearing lherzolites (whole rock 100 Mg/(Mg+Fe) 91.0-93.5). These contain olivines (Fa 7.0-8.6), orthopyroxenes (Fs 6.3-7.7) with 0.54-1.04 wt.% Al_2O_3, clinopyroxenes with consistent 100 Ca/(Ca+Mg) (46.0-48.4) but variable Al_2O_3, (1.64-3.99 wt.%), Cr_2O_3 (1.59-4.25 wt.%) and Na_2O (0.81-3.14 wt.%), chrome pyrope garnets and/or primary magnesiochromites. By contrast four ultradepleted chromite harzburgites/lherzolite (100 Mg/(Mg+Fe) 95.0-95.4) contain more magnesian olivines (Fa 4.9-5.0) and orthopyroxenes (Fs 4.1-4.3).

Provisionally preferred P/T estimates for the garnet-bearing lherzolites are 906-949°C and 24.5-30.8 kb, the temperature range being somewhat wider (873-962°C) if one also includes lherzolites in which garnet is absent but is considered likely to have been originally present. An ultradepleted chromite lherzolite nodule, which is unlikely to have ever contained garnet, yields an equivalent equilibration temperature of 950°C. It is concluded that these various ultramafic nodules may all have been derived from much the same depth zone in the mantle (roughly 70-100 km below surface on preferred estimates), the presence or absence of primary chromite relative to garnet being related to shifts in the position of the spinel lherzolite/garnet lherzolite transition boundary for compositions with various $Cr_2O_3/(Cr_2O_3+Al_2O_3)$ ratios. The observed nodule suite does, however, contain one harzburgite nodule with more aluminous primary spinel and orthopyroxene which seems likely to have equilibrated under significantly lower P/T conditions and hence have been derived from depths < 50 km.

Mineralogical and chemical comparison between the Pipe 200 ultramafic nodules and those from other pipes in northern Lesotho and in the Kimberley area, as well as in the Lashaine volcano, indicates that the mantle beneath Pipe 200 and much of northern Lesotho may be extensively depleted down to greater depths, perhaps reflecting the intensive Karroo volcanism in that area.

Introduction

Pipe 200 in northern Lesotho is situated close to the Letele Pass road about 8 km west of the better known kimberlites of the Kao area. The main intrusion of the pipe outcrops on the western bank of the Malibamatso River (see Kresten and Dempster, 1973; including Plate 41B). In addition to numerous nodules of obvious crustal origin (basalts, sandstones, gneisses, etc.) this kimberlite pipe also contains common ultramafic nodules of likely mantle derivation. These are mainly lherzolites with or without small amounts of purple garnet.

We decided to study the whole rock and mineral chemistry of these particular nodules, in order to compare them with the contrasting granular and sheared ultramafic nodule types described by Nixon and Boyd (1973) from other kimberlite pipes in northern Lesotho, notably Thaba Putsoa and Mothae. We also wished to determine whether the presence or absence of garnet in these nodules is related to varying whole rock chemistry or to different depths of derivation in the mantle.

Petrography

All thirty-four ultramafic nodules which we have examined from Pipe 200 are of the common 'coarse grained' or 'granular' textured types as defined by Boullier and Nicholas (1973) and Boyd and Nixon (1972), respectively. Olivines and

TABLE 1. Whole Rock Analyses of

Sample Number	PTH 107	PHT 108	PTH 201	PTH 202	PTH 203	PTH 205	PTH 207	PTH 208	PTH 210	PTH 400	PT 4
Rock Type	CH	(G)CL	SH	(G)CL	CL	(G)CL	GCL	GL	GP	GL	GC
SiO_2	40.49	43.69	44.10	46.07	43.42	43.68	45.69	46.29	52.52	45.55	44.
TiO_2	0.01	0.04	0.17	0.17	0.35	<0.01	0.02	0.16	0.13	0.04	0.
Al_2O_3	0.24	0.51	0.47	0.54	0.14	0.24	0.66	1.18	5.10	0.41	0.
Cr_2O_3	0.09	0.18	0.20	0.23	0.20	0.19	0.34	0.28	0.33	0.16	0.
Fe_2O_3	2.45	2.58	1.73	1.74	1.49	2.91	1.88	1.97	1.53	2.75	1.
FeO	2.27	4.54	4.09	4.57	2.80	3.45	4.20	3.95	2.52	4.93	1.
MnO	0.06	0.12	0.10	0.11	0.07	0.11	0.11	0.11	0.14	0.10	0.
NiO	0.28	0.29	0.29	0.31	0.34	0.33	0.28	0.29	0.07	0.29	0.
MgO	47.48	44.25	45.66	43.50	48.17	44.46	42.83	42.17	22.84	42.10	45.
CaO	0.07	0.92	0.59	0.58	0.18	0.29	0.71	0.73	13.11	1.32	0.
Na_2O	0.02	0.14	0.03	0.12	0.06	0.06	0.09	0.07	0.43	0.26	0.
K_2O	0.02	0.20	0.07	0.12	0.04	0.05	0.05	0.03	0.09	0.13	0.
P_2O_5	0.01	0.03	0.02	0.04	0.04	0.03	0.03	0.04	0.03	0.02	0.
H_2O^-	5.94	2.52	2.26	2.41	2.11	4.04	3.05	2.47	1.11	1.93	2.
CO_2	NIL	NIL	0.48	NIL	NIL	NIL	NIL	NIL	0.27	NIL	0.
TOTAL	99.43	100.01	100.26	100.51	99.41	100.04	99.94	99.74	100.22	99.99	100.
100 Mg/(Mg+Fe)	95.0	92.0	93.5	92.7	95.4	92.7	92.8	92.9	91.3	91.0	91.
100 Cr/(Cr+Al)	20.1	19.1	22.2	22.2	48.9	34.7	25.7	13.7	4.2	20.7	22.

Rock Types: CL - Chromite Lherzolite CH - Chromite Harzburgite SH - Spinel Harzburgite
GCL - Garnet Chromite Lherzolite GL - Garnet Lherzolite GP - Garnet Pyroxenite
(G) - In parentheses indicates that garnet thought likely to be a member of the original primary assemblage, although now absent

enstatites do, however, show evidence of slight deformation with blurred kink band development and more rarely grain flattening giving a crude tabular texture.

Mineralogically most of the Pipe 200 ultramafic nodules are lherzolites with forsteritic olivine (65-75 vol.%) and enstatite (20-30 vol.%) the two dominant minerals. In the analytical tables peridotite nodules are classified as lherzolites if there was any chrome diopside visible in thin section or hand specimen. Amounts of the bright green chrome diopside phase are always small (< 5 vol.%) more typically only 1-2 vol.%. Likewise the amounts of the other characterising phases garnet and/or chromite, are also small (1-2 vol.% on average).

The chrome pyrope garnets invariably have extensive semi-opaque kelyphite alteration rims often coarsening and clearing somewhat towards their outer margin so that one can discern numerous small yellowish or reddish brown spinel grains associated with pale coloured amphibole and/or phlogopite. PTH 202 and 205 now lack garnet but are designated as '(garnet) chromite lherzolites', since characteristic kelyphite alteration patches indicate its previous presence.

Where present, the large discrete deep red brown primary chrome spinels (chromites) are petrographically distinct from the smaller sec dary spinels associated with the breakdown of garnets. PTH 201 is designated a spinel harz ite on analytical evidence that the primary spinels are more aluminous than in the other ules. Of the thirty-four ultramafic nodules studied, sixteen contained only garnet (incl analysed samples PTH 102, 210, 400, 403, 404, 405, 406 and 407), eight contained both prima chromite and garnet (including analysed sampl PTH 207, 401, 409 and 410), two have primary chromite and scarce kelyphite patches indicat the previous presence of garnets (PTH 202 and 205), and eight apparently contained only chr mite (analysed samples PTH 107, 108, 201, 20 301, 302, 303 and 304), although of those PT 108 and 304 may arguably have also originall tained garnet.

The garnet pyroxene nodule, PTH 210, is ex ceptional in that it lacks olivine and has hi

200 Ultramafic Nodules.

PTH 403	PTH 404	PTH 405	PTH 406	PTH 407	PTH 409
GL	GL	GL	GL	GL	GCL
45.73	45.11	46.22	45.82	45.06	44.82
0.04	0.04	0.02	0.03	0.10	0.17
1.16	0.73	1.06	1.64	1.09	0.58
0.40	0.32	0.32	0.32	0.35	0.28
2.98	2.09	2.62	2.27	2.13	2.64
4.30	3.93	4.16	4.59	4.29	3.41
0.12	0.11	0.11	0.12	0.11	0.11
0.26	0.29	0.28	0.29	0.29	0.30
41.13	43.45	42.81	41.54	43.32	43.01
0.98	0.95	0.57	1.22	0.85	0.43
0.13	0.12	0.10	0.12	0.11	0.10
0.12	0.04	0.07	0.09	0.12	0.09
0.04	0.06	0.03	0.03	0.05	0.03
2.63	2.36	1.65	1.66	2.32	4.05
NIL	NIL	NIL	NIL	0.23	NIL
100.02	99.60	100.02	99.74	100.42	100.02
91.3	93.0	92.1	91.8	92.6	93.0
18.8	22.7	16.8	11.6	17.7	24.4

contents of both garnet and clinopyroxene, approximately 15 and 50 vol.% respectively. A garnet granulite nodule and four eclogite nodules from Pipe 200 are described elsewhere by Griffin et al. (1978).

All ultramafic nodules are relatively fresh but do show some serpentinisation and additional infiltration metasomatism effects reflected in the growth of small amounts of secondary phlogopite, carbonate, apatite, ilmenite and/or rutile.

Rock Chemistry

Whole rock analyses for seventeen nodule samples are presented in Table 1. Samples were analysed by a combination of 'wet' chemical techniques (spectrophotometric, gravimetric, titration and atomic absorption) at the University of Sheffield.

Excluding for the moment the garnet pyroxenite nodule PTH 210, it is apparent that the suite of Pipe 200 ultramafic nodules taken as a whole is characterised by high Mg/(Mg+Fe) and Cr/(Cr+Al) ratios, and low CaO and Na_2O contents. This reflects their refractory and highly depleted chemical nature in terms of their basalt-yielding potential. The garnet-bearing lherzolites from Pipe 200 are of broadly similar chemistry (see Table 2) to the granular textured garnet lherzolites in the nearby Thaba Putsoa, Mothae and Liqhobong pipes, but contrast strikingly with the relatively fertile, sheared garnet lherzolite nodules in those pipes (Nixon and Boyd, 1973). They are also somewhat more depleted than in the common granular textured garnet lherzolites found in the Kimberley area pipes and the unbanded coarse grained granular or flaser textured garnet lherzolites from the Matsoku pipe (Carswell and Dawson, 1970; Cox et al, 1973). It should be noted that some Na_2O values for Matsoku ultramafic nodules, as given in Table 26 of Cox et al. (1973), are almost certainly in serious error. Calculation of whole rock compositions using the mineral analyses and modes indicates that the Na_2O values quoted are often unrealistically low. Hence the average Na_2O value quoted for the Matsoku 'common peridotites' in Table 2 involves a correction to the Na_2O figures for the analyses taken from Cox et al., (1973).

Consideration of the internal chemical variation within the suite of analysed Pipe 200 ultramafic nodules (Table 1) shows that there are fairly constant differences in whole rock chemistry between the garnet-only lherzolites, garnet + chromite lherzolites, and chromite-only harzburgites/lherzolites. Mg/(Mg+TFe) and Cr/(Cr+Al) increase and Al_2O_3, CaO and Na_2O contents decrease for the nodule types in that order, with decreasing amounts of chrome diopside as well as garnet. In fact, of the ultra-depleted chromite harzburgites/lherzolites which lack petrographic evidence suggesting that they originally contained garnet, only PTH 203 contains any visible chrome diopside and even then as confirmed by the low CaO and Na_2O contents, only trace amounts. There is also a general increase in MgO/SiO_2 ratio from the garnet lherzolites to the chromite harzburgites/lherzolites reflecting increased modal contents of olivine relative to enstatite. Thus, as illustrated on Figure 1, the chromite harzburgites/lherzolites have more depleted compositions than the garnet lherzolites, indicating that modal mineralogy may be mainly controlled by whole rock chemistry.

The fact that on Figure 1 the composition points for PTH 202 and 108 plot close to the boundary between the garnet-only and garnet + chromite fields supports our petrographic interpretation that these nodules originally contained garnet. PTH 202 (and likewise 205) contains kelyphite patches which indicate the original presence of garnet, whilst PTH 108 contains clusters of small chromite grains associated with coarser phlogopite and chrome diopside which arguably may have formed at the expense of original garnet. On the other hand, the spinel harzburgite PTH 201, which likewise plots in the garnet + chromite field, lacks any petrographic evidence to suggest that it may originally have contained garnet.

As expected, the garnet pyroxenite nodule PTH 210 contrasts strikingly in its chemical composi-

TABLE 2. Comparison of Garnet Lherzolites from Pipe 200 with Those from Other Localities.

Rock Type	A	B	C	D	E	F
SiO_2	46.83	45.80	43.89	47.44	46.56	44.61
TiO_2	0.08	0.03	0.16	0.07	0.08	0.08
Al_2O_3	0.91	0.51	1.85	1.62	1.90	1.85
Cr_2O_3	0.30	0.21	0.22	0.41	0.31	0.44
*FeO	6.43	6.23	8.58	6.48	6.60	6.95
MnO	0.11	0.10	0.12	0.11	0.11	0.12
NiO	0.30	0.18	0.23	0.33	0.29	0.37
MgO	43.97	46.06	42.94	42.39	42.67	44.20
CaO	0.84	0.82	1.86	1.12	1.14	1.22
Na_2O	0.12	0.06	0.21	0.14	0.18	0.17
K_2O	0.08	0.03	0.03	0.11	0.14	0.08
P_2O_5	0.04	0.00	0.00	0.03	0.04	0.08
* Total Fe expressed as FeO and analyses recalculated anhydrous to 100% in all cases.						
100 Mg/(Mg+Fe)	92.4	92.9	89.9	92.1	92.0	92.0
100 Cr/(Cr+Al)	19.4	23.3	7.9	14.8	10.1	14.2

A - Garnet lherzolites from Pipe 200 (mean of 10).

B - Granular garnet lherzolites from Thaba Putsoa, Mothae and Liqhobong (mean of 4) - Nixon and Boyd (1973).

C - Sheared garnet lherzolites from Thaba Putsoa and Mothae (mean of 6) - Nixon and Boyd (1973).

D - Unbanded garnet lherzolites (common peridotites) from Matsoku (mean of 5) - Cox et al. (1973); Carswell and Dawson (1970).

E - Common type garnet lherzolites from Kimberley Mines (mean of 23) - Analyses from Holmes (1936), Ito and Kennedy (1967), Whitfield (1971), Berg and O'Hara (1973), Carswell and Dawson (1970), and unpublished data. The data presented by Chen (1971) are deliberately excluded on the grounds of incompatibility with data from other sources, in particular Mg/(Mg+Fe) values are consistently lower at equivalent CaO, Al_2O_3 and Cr/(Cr+Al) values suggesting that the analytical MgO values are too low.

F - Garnet lherzolites from Lashaine volcano, Tanzania (mean of 5) - Rhodes and Dawson (1975), Ridley and Dawson (1975).

tion with the peridotite nodule suite, especially in its much higher Al_2O_3, CaO and Na_2O contents and lower Cr/(Cr+Al) ratio. In terms of rock chemistry, as well as in modal mineralogy, this nodule resembles certain of the Matsoku pyroxenite/peridotite nodules (Cox et al., 1973) interpreted as mantle cumulates of moderately evolved magmatic liquids (Gurney et al., 1975). However, whilst the Matsoku nodules show a striking trend of decreasing Mg/(Mg+Fe) with increased Al_2O_3, CaO and Na_2O contents, this is not apparent in the Pip 200 garnet pyroxenite. Its 100 Mg/(Mg+Fe) ra (91.3) is in fact within the range of values (91.0-93.5) observed in the common garnet lher lites from Pipe 200. It also has a significan lower Na_2O/CaO ratio (0.033) when compared wi the proposed Matsoku cumulate nodules (mean 0. and does not show the banded texture seen in t of the latter.

The low, but nevertheless variable, content

of 'incompatible' elements such as Ti, K and P in the Pipe 200 nodules merit some comment. The variability in the contents of these elements (especially of Ti) in the various peridotite nodules and comparison with contents in the various primary mineral phases indicate that the base levels for these elements in these mantle-derived samples prior to incorporation in the kimberlite are likely to have been extremely low, probably in the order of 0.01-0.02 wt.% for the oxides of each of these elements. Concentrations above these low base levels seem likely to have resulted from infiltration metasomatism (Harte et al., 1975) due to contamination by the enclosing kimberlite magma.

Mineral Chemistry

The minerals in these nodules were analysed by electron microprobe mostly at Dalhousie University but some at the University of Edinburgh. Most quoted analyses are averages of several point analyses of different grains. The data were acquired on both conventional crystal spectrometry and energy dispersive systems and as a result of background uncertainty and detector sensitivity, considerable uncertainty is associated with concentrations of less than 0.10 wt.%.

Olivine

Olivines in all nodules are highly forsteritic (Table 3). Those in the ultra-depleted chromite harzburgite/lherzolite nodules have lower fayalite contents (4.9-5.0% Fa) than those in the garnet ± chromite lherzolites (7.0-8.6% Fa). The fayalite contents of olivines in the (garnet) chromite lherzolite xenoliths (7.4-8.6% Fa) which now lack garnet (namely PTH 108, 202, 205 and 304) are in line with the latter rather than the former. As with other aspects of its mineral chemistry, the spinel harzburgite PTH 201 is exceptional as it contains olivine with 7.0% Fa composition yet lacks evidence that it ever contained garnet.

Orthopyroxene

Orthopyroxenes in all nodules are enstatites (Table 4) although again 100 Fe/(Fe+Mg) values vary somewhat between the different nodule types. The group of ultradepleted chromite harzburgites/lherzolite (PTH 107, 203, 301, 302 and 303) contain orthopyroxenes with 4.1-4.3% Fs in contrast with the garnet ± chromite lherzolites in which orthopyroxene compositions are 6.3-7.7% Fs. Orthopyroxene compositions (6.5-7.5% Fs) in those chromite lherzolites which arguably contained garnet originally are in line with the latter rather than the former. All orthopyroxene analyses, except PTH 207(S) in Table 4 are of the common large primary grains. Such orthopyroxenes in garnet ± chromite lherzolites are characterised by low Al_2O_3 (0.70-1.04 wt.%), moderate CaO (0.33-0.53 wt.%) and high Cr_2O_3 (0.25-0.50 wt.%) contents. Small amounts of discernible secondary orthopyroxene occur associated with secondary chrome spinel at the outer margins of the kelyphite rims around some garnets. Such secondary orthopyroxene, as represented by analysis PTH 207(S) is quite distinct in

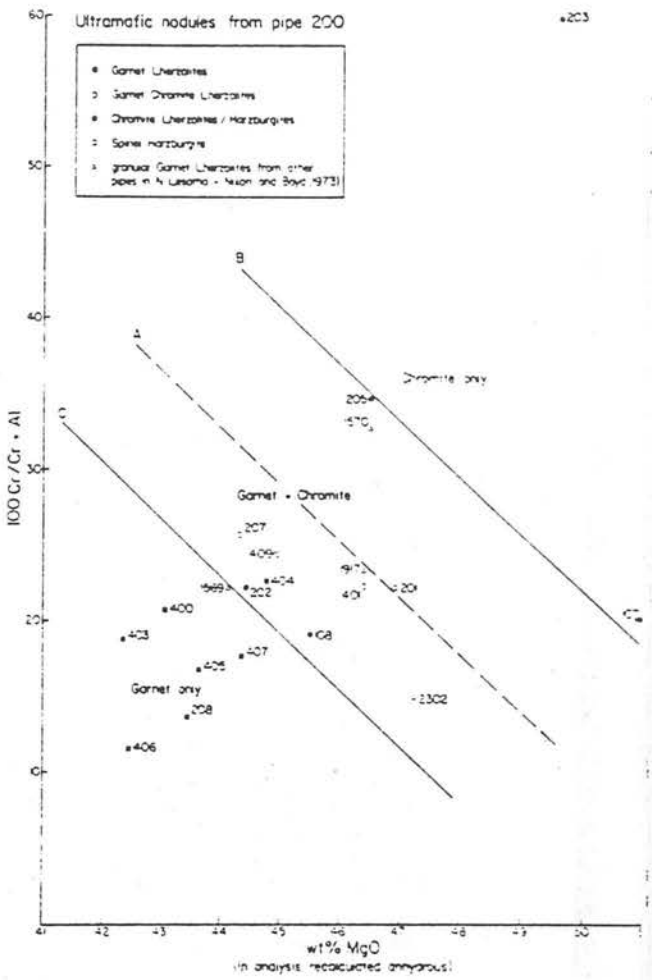

Fig. 1. Whole rock composition plot of wt.% MgO against 100 Cr/(Cr+Al) (in analyses recalculated anhydrous to 100% and with total iron as FeO) for Pipe 200 ultramafic nodules. Compositions for comparable granular textured garnet lherzolites from Thaba Putsoa, Mothae and Liqhobong (Nixon and Boyd, 1973) are also shown. These authors give an analysis for primary chromite in nodule 1570 but do not make it clear whether chromite is absent in the other nodules. Boundaries A and C correspond to those defining the chromite-only, garnet + chromite and garnet-only composition fields for peridotite nodules from the Lashaine volcano (Reid et al., 1973) whilst B represents the approximate position of the chromite + garnet/chromite-only boundary for the Pipe 200 nodules.

TABLE 3. Analyses of Olivines in

Sample Number	PTH 102	PTH 107	PTH 108	PTH 201	PTH 202	PTH 203	PTH 205	PTH 207	PTH 301	PTH 302	PTH 303	PTH 304	PT
Rock Type	GL	CH	(G)CL	SH	(G)CL	CL	(G)CL	GCL	CH	CH	CH	(G)CL	G
SiO_2	41.9	41.9	41.1	41.9	41.1	41.8	41.7	42.1	40.7	41.6	41.5	41.0	40
TiO_2	0.07	n.d.	0.00	0.00	0.00	0.01	0.08	0.05	n.d.	n.d.	n.d.	n.d.	0.
Al_2O_3	n.d.	n.d.	0.03	0.04	n.d.	0.04	n.d.	n.d.	n.d.	n.d.	n.d.	n.d.	0.
Cr_2O_3	0.07	n.d.	0.01	0.10	0.04	0.05	n.d.	0.11	n.d.	n.d.	n.d.	n.d.	0.
*FeO	7.77	4.97	8.26	6.95	7.45	4.78	7.35	7.75	4.86	5.02	4.97	7.34	8.
MnO	0.13	n.d.	0.12	0.01	0.02	0.06	n.d.	0.13	n.d.	n.d.	n.d.	n.d.	0.
NiO	n.d.	0.29	0.44	0.43	n.d.	0.40	n.d.	n.d.	n.d.	n.d.	n.d.	n.d.	0.
MgO	48.5	52.9	49.6	51.8	50.5	51.9	50.4	50.1	52.8	53.7	53.5	51.5	51
CaO	0.06	n.d.	0.01	0.02	n.d.	0.02	0.07	0.05	n.d.	n.d.	n.d.	n.d.	0.
Total	98.5	100.1	99.6	101.2	99.1	99.0	99.6	100.3	98.4	100.3	100.0	99.8	9
100 Fe/(Fe+Mg)	8.3	5.0	8.5	7.0	7.6	4.9	7.6	8.0	4.9	5.0	5.0	7.4	

* All Fe taken as FeO
n.d. Not determined
Sample nomenclature as in Table 1

composition from the primary enstatites with a higher 100 Fe/(Fe+Mg) content (11.4% Fs), an appreciably higher Al_2O_3 content (2.81 wt.%) and much lower CaO (0.16 wt.%) and Cr_2O_3 (0.09 wt.%) contents. Primary orthopyroxenes in PTH 201 and 210 are exceptional in their appreciably higher Al_2O_3 contents, 1.45 and 2.28 wt.% respectively.

Clinopyroxene

Clinopyroxene analyses (Table 5) show variable contents of Al_2O_3 (1.64-3.99 wt.%), Cr_2O_3 (1.59-4.25 wt.%) and Na_2O (0.81-3.14 wt.%). It is clear from Figure 2 that the Al_2O_3 contents vary sympathetically with Na_2O in individual clinopyroxene point analyses, reflecting variable jadeite contents. In most lherzolite nodules individual analyses both of different grains and different points within individual grains show little variation and in these cases the single clinopyroxene analysis given in Table 5 represents the mean value. However, in both PTH 202 and 204 although grain cores are usually of fairly uniform composition, striking jadeite depletion was observed in certain point analyses, notably those from grain rims. For both nodules, the rim analysis given in Table 5 corresponds to the individual point analysis indicating the most extreme jadeite depletion noted in clinopyroxene grains in that rock. The clinopyroxene grains in these nodules have clear cores, but distinctly cloudy margins. The marginal clouding often extends along curved fractures into or even right across individual grains and appears to be due to large numbers of small tubular shaped fluid inclusions. Similar petrographic features and a sociated jadeite depletion have previously bee observed in garnet lherzolite nodules from the Kimberley mines (Carswell, 1975).

The observed jadeite depletion is not accompanied by kosmochlor ($NaCrSi_2O_6$) depletion. T chromite lherzolite PTH 203 contains clinopyro with the highest Cr_2O_3 content and this correla with highest whole rock Cr/(Cr+Al) and Na_2O/Ca ratios. However, plots of Cr/(Cr+Al) Cpx agai Cr/(Cr+Al) rock and of wt.% Al_2O_3 and wt.% Cr_2O in clinopyroxene against Na_2O/CaO in the rock other nodules do not show consistent correlati between rock and clinopyroxene compositions. conclude that the overall variation in Al_2O_3, Cr_2O_3 and Na_2O contents observed in the clinop xenes in these Pipe 200 ultramafic nodules larg reflects the effects of secondary alteration (notably jadeite loss) superimposed on primary chemical and physical controls.

There is only limited variation in 100 Ca/(Mg) (46.0-48.4 excluding rim analyses) amongst the analysed primary clinopyroxenes in the lher lite nodules. Rim analyses do not have consis tently lower or higher Ca/(Ca+Mg) ratios than responding cores. This, together with the fac that there is no significant correlation betwe Ca/(Ca+Mg) and Na_2O content in the clinopyroxe in the various lherzolite nodules, points to broadly similar initial equilibration temperatu for the nodule suite and the non-equilibration the jadeite depleted clinopyroxenes.

In the lherzolite nodules much of what litt clinopyroxene is present tends to be closely a sociated spatially with garnets and its kelyph

200 Ultramafic Nodules.

PTH 401	PTH 403	PTH 404	PTH 405	PTH 406	PTH 407	PTH 409	PTH 410
GCL	GL	GL	GL	GL	GL	GCL	GCL
41.6	41.6	41.5	41.2	41.5	40.8	41.2	41.2
0.01	0.04	0.07	0.01	0.03	n.d.	0.03	0.03
0.04	0.03	0.04	0.03	0.03	0.03	0.03	0.03
n.d.	0.04	0.09	0.04	n.d.	n.d.	n.d.	n.d.
6.83	7.73	7.36	7.37	7.14	7.44	7.16	7.32
0.06	n.d.	0.12	0.11	0.08	0.09	0.11	0.08
n.d.	n.d.	n.d.	0.45	n.d.	n.d.	n.d.	n.d.
51.6	49.5	50.2	50.8	50.1	50.9	49.8	51.3
0.01	0.05	0.05	0.02	0.04	0.04	0.04	0.03
100.2	99.0	99.4	100.0	98.9	99.2	98.4	99.8
7.0	8.1	7.6	7.5	7.4	7.6	7.5	7.4

alteration products or with clusters of phlogopite and spinel grains which arguably may be secondary after garnet. Such clinopyroxene may actually occur within kelyphite or more typically may form a narrow collar around it. This suggested that at least some of the clinopyroxene might be secondary and related to garnet breakdown. However, only in the case of nodules PTH 207 and 403 were we able to detect clinopyroxenes of secondary aluminous types--analyses 207 (S1 and S2) and 403 (S1 and S2) in Table 5. Such clinopyroxenes occur as very small grains on the outermost margins of the semi-opaque kelyphite alteration zones around garnets and have variable compositions reflecting their unequilibrated nature. However, most clinopyroxene grains immediately adjacent to kelyphite zones and also those in clusters with spinels and phlogopites (as in PTH 108) are chrome diopsides essentially indistinguishable in composition from discrete primary grains. Either such clinopyroxene has re-equilibrated with the lherzolite assemblage following garnet breakdown, or poikiloblastic habit of clinopyroxene towards garnet is a feature which pre-dates kelyphite formation in many nodules. It is possible that the marginal clouding and jadeite depletion of clinopyroxene grains as observed in nodules with extensive kelyphite development, such as PTH 202 and 204, are adjustments in composition of the primary clinopyroxene grains which are related to garnet breakdown, and that both features are a consequence of the combined effects of metasomatism and decompression resulting from incorporation in kimberlite and subsequent diatreme emplacement.

The clinopyroxene in the garnet pyroxenite nodule PTH 210 is distinctly different in composition from clinopyroxenes in lherzolite nodules. It has low Al_2O_3, Cr_2O_3 and Na_2O contents coupled with high 100 Ca/(Ca+Mg) = 50.9. These compositional differences, as with those observed in coexisting orthopyroxene and garnet, may simply reflect the different paragenesis and whole rock composition, rather than different equilibration conditions.

Garnet

Garnet analyses (Table 6) for the lherzolite nodules fall within the range of the common chrome pyropes (Group 9 - Dawson and Stevens, 1975) found elsewhere in garnet lherzolite nodules and as common xenocrysts within kimberlites. However, with the exception of PTH 400 they have somewhat higher Cr_2O_3 and CaO contents (see Figure 3) than the most frequent garnets found within the common garnet lherzolite nodules in the Kimberley area and Matsoku pipes (Carswell and Dawson,1970; Cox et al., 1973; Gurney and Switzer, 1973) and in Yakutian pipes (Sobolev et al., 1973). On the other hand the garnets from the granular garnet lherzolite nodules of the Thaba Putsoa and Mothae pipes (Nixon and Boyd, 1973) have broadly comparable Cr_2O_3 and CaO contents.

It is apparent that the more depleted garnet lherzolites with higher Cr/(Cr+Al) and Mg/(Mg+Fe) ratios have garnets which also have higher Cr/(Cr+Al) ratios and in addition show a sympathetic increase in CaO. This garnet composition trend is perhaps also reflected, although in a more extreme fashion, by the analysed chrome pyrope garnet xenocrysts from the nearby Kao kimberlite (Hornung and Nixon, 1973). We suggest that all the Kao garnets plotted on Figure 3 are from disaggregated lherzolite nodules, those with lowest Cr_2O_3 and CaO contents being from nodules of comparable composition to the common type in the Kimberley and Matsoku pipes, intermediate ones from comparatively depleted nodules of the common Pipe 200 type, whilst the extreme chrome-rich green garnets are likely to be from nodules with extremely high Cr/(Cr+Al) ratios. Garnets showing a comparable range in chemistry and thought to be related to similar lherzolite parageneses have been reported as xenocrysts in Yakutian pipes, notably Udachnaya (Sobolev et al., 1973). In addition garnets, intermediate in composition between those in the Pipe 200 nodules and the extreme Kao green garnet types, have been recorded by Gurney and Switzer (1973) as xenocrysts in the Finsch kimberlite pipe, South Africa. These observations indicate that the garnets of Groups 9 and 12 (Dawson and Stevens, 1975) should best be considered as one group, related to lherzolite parageneses with varying Cr/(Cr+Al) ratios.

The garnet in the garnet pyroxene nodule PTH 210 has an appreciably lower Cr_2O_3 content as well as somewhat higher FeO and MnO contents.

TABLE 4. Analyses of Orthopyroxenes

Sample Number	PTH 102	PTH 107	PTH 108	PTH 201	PTH 202	PTH 203	PTH 205	PTH 207(P)	PTH 207(S)	PTH 210	PTH 30
Rock Type	GL	CH	(G)CL	SH	(G)CL	CL	(G)CL	GCL	GCL	GP	G
SiO_2	58.0	58.4	58.0	57.9	57.2	58.4	58.2	57.8	57.6	56.8	58.
TiO_2	0.10	n.d.	0.05	0.00	0.01	0.02	0.08	0.08	0.05	n.d.	n.d.
Al_2O_3	0.86	0.95	0.59	1.45	1.04	0.79	0.74	0.70	2.81	2.28	0.7
Cr_2O_3	0.50	0.48	0.40	0.43	0.33	0.55	0.44	0.46	0.09	0.35	0.3
*FeO	4.83	2.86	5.06	4.52	4.59	2.90	4.77	4.76	7.05	5.94	2.8
MnO	0.14	n.d.	0.14	0.01	0.01	0.07	0.00	0.15	0.13	0.22	n.d
NiO	n.d.	n.d.	n.d.	0.10	n.d.	0.13	n.d.	n.d.	n.d.	n.d.	n.d
MgO	34.0	36.6	34.9	35.9	37.1	35.8	35.3	35.4	30.9	34.4	36.
CaO	0.50	0.34	0.34	0.18	0.29	0.41	0.48	0.47	0.16	0.22	0.1
Na_2O	n.d.	n.d.	0.10	0.02	n.d.	0.16	n.d.	n.d.	n.d.	n.d.	n.d
Total	98.9	99.6	99.6	100.5	100.6	99.2	100.0	99.8	98.8	100.2	98.
100 Fe/(Fe+Mg)	7.4	4.2	7.5	6.6	6.5	4.3	7.0	7.0	11.4	8.8	4.
100 Ca/(Ca+Mg)	1.0	0.6	0.7	0.4	0.6	0.8	1.0	0.9	0.4	0.5	0.
Structural Formulae on the Basis of 6.000 Oxyge											
Si_{IV}	2.005	1.987	1.995	1.969	1.948	1.997	1.989	1.984	2.003	1.950	1.9
Al^{IV}	0.000	0.013	0.005	0.031	0.042	0.003	0.011	0.016	0.000	0.050	0.0
Al^{VI}	0.035	0.025	0.019	0.027	0.000	0.029	0.019	0.012	0.115	0.042	0.0
Ti	0.003	--	0.001	0.000	0.000	0.001	0.002	0.002	0.001	--	--
Cr	0.014	0.013	0.011	0.012	0.010	0.015	0.012	0.012	0.002	0.009	0.0
Fe	0.140	0.081	0.145	0.129	0.131	0.083	0.136	0.137	0.205	0.171	0.0
Mn	0.004	--	0.004	0.000	0.000	0.002	0.000	0.004	0.004	0.006	--
Ni	--	--	--	0.003	--	0.004	--	--	--	--	--
Mg	1.750	1.857	1.789	1.818	1.884	1.827	1.799	1.809	1.598	1.762	1.8
Ca	0.019	0.012	0.013	0.007	0.011	0.015	0.018	0.017	0.006	0.008	0.0
Na	--	--	0.007	0.001	--	0.011	--	--	--	--	--
Total	3.968	3.988	3.989	3.996	4.026	3.985	3.986	3.994	3.935	3.999	3.9

* All Fe as FeO
n.d. Not determined

Spinel

Spinel analyses for various nodules are given in Table 7, and are plotted in a wt.% Cr_2O_3 vs. wt.% MgO variation diagram (Figure 4). Discrete primary spinels are low Al magnesiochromites, i.e. 64.9-81.4% $M^{2+}Cr_2O_4$, except in the spinel harzburgite PTH 201 where they are aluminous chrome spinels with a much lower 100 Cr/(Cr+Al) ratio. The primary chromites in the ultra-depleted harzburgite/lherzolite nodules plot in a slightly different composition field to those in garnet lherzolites (Figure 4) because of their higher absolute Cr_2O_3 and MgO contents. However primary chromites in Pipe 200 garnet lherzolites are similar in composition to those described from comparable granular textured garnet lherzolites in the nearby Thaba Putsoa and Mothae pipes (Nixon and Boyd, 1973) and to those in garnet and/or spinel lherzolite nodules from the Lashaine volcano in northern Tanzania (Reid et al., 1975). Spinels associated with kelyphitic alteration zones around garnets show a wide range of compositions. Those from the innermost parts of kelyphites (PTH 207A, 404, 405A, 407 and 410 in Table 7) are high Al chrome spinels (72.9-77.6% $M^{2+}Al_2O_4$), fairly analogous in composition to the primary spinels in the common lherzolite inclusions in basalts (Ross et al., 1954). These undoubtedly secondary spinels thus appear to be related to partial breakdown of the high pressure garnet lherzolite assemblage to a lower pressure spinel lherzolite assemblage. However, spinels from the outermost parts of kelyphite zones or immediately adjacent to them (PTH 207B, 403B and 405B in Table 7) often have intermediate 100 Cr/

in Pipe 200 Ultramafic Nodules.

PTH 302	PTH 303	PTH 304	PTH 400	PTH 401	PTH 403	PTH 404	PTH 405	PTH 406	PTH 407	PTH 409	PTH 410
CH	CH	(G)CL	GL	GCL	GL	GL	GL	GL	GL	GCL	GCL
58.9	59.3	58.7	57.8	58.1	58.0	58.9	57.8	57.8	57.3	57.7	58.0
n.d.	n.d.	n.d.	0.06	0.03	0.06	0.04	0.03	0.03	0.02	0.05	0.04
0.36	0.41	0.54	0.75	1.04	0.92	0.82	0.88	0.88	0.87	0.82	0.96
0.23	0.76	0.18	0.25	0.37	0.46	0.42	0.48	0.43	0.45	0.40	0.50
2.79	2.92	4.39	5.13	4.28	4.76	4.39	4.46	4.38	4.56	4.57	4.53
n.d.	n.d.	n.d.	0.11	0.11	0.00	0.11	0.09	0.11	0.10	0.12	0.10
n.d.	n.d.	n.d.	0.12	n.d.	n.d.	n.d.	0.11	n.d.	n.d.	n.d.	n.d.
36.7	36.8	35.7	34.7	35.8	34.6	35.0	35.2	35.0	35.6	34.8	35.7
0.22	0.18	0.34	0.48	0.33	0.47	0.53	0.44	0.43	0.45	0.42	0.46
n.d.	n.d.	n.d.	0.13	0.07	n.d.	0.10	0.16	0.08	0.14	0.15	0.17
99.2	99.9	99.8	99.5	100.2	99.2	100.3	99.6	99.1	99.5	99.0	100.4
4.1	4.3	6.5	7.7	6.3	7.2	6.6	6.6	6.6	6.7	6.9	6.6
0.4	0.4	0.7	1.0	0.7	1.0	1.0	0.9	0.9	0.9	0.9	0.9
2.008	2.009	2.003	1.991	1.980	1.997	2.004	1.984	1.991	1.973	1.992	1.976
0.000	0.000	0.000	0.009	0.020	0.003	0.000	0.016	0.009	0.027	0.008	0.024
0.014	0.016	0.022	0.021	0.022	0.034	0.033	0.020	0.027	0.008	0.025	0.015
--	--	--	0.002	0.001	0.002	0.001	0.001	0.001	0.001	0.001	0.001
0.006	0.007	0.005	0.007	0.010	0.013	0.011	0.013	0.012	0.012	0.011	0.013
0.080	0.083	0.125	0.148	0.122	0.137	0.125	0.128	0.126	0.131	0.132	0.129
--	--	--	0.003	0.003	0.000	0.003	0.003	0.003	0.003	0.004	0.003
--	--	--	0.003	--	--	--	0.003	--	--	--	--
1.865	1.858	1.816	1.782	1.821	1.775	1.774	1.802	1.798	1.826	1.791	1.813
0.008	0.007	0.012	0.018	0.012	0.017	0.019	0.016	0.016	0.017	0.016	0.017
--	--	--	0.009	0.005	--	0.007	0.011	0.005	0.009	0.010	0.011
3.981	3.979	3.983	3.993	3.995	3.977	3.977	3.996	3.988	4.007	3.990	4.002

(Cr+Al) ratios. Furthermore, it was somewhat surprising to discover that the three petrographically distinct types of spinel grains in PTH 204 (large discrete primary (?) grains, small idioblastic grains associated with clusters of clinopyroxene and phlogopite grains, and small grains associated with kelyphitic alteration zones around garnet) all have similar compositions of the low Al magnesiochromite type. Small spinels associated with 'pools' of phlogopite and clinopyroxene grains in PTH 108 are of similar low Al type. Thus, if as seems likely, at least some of these spinels (PTH 108, 204, 207B, 403B and 405B) are a secondary generation derived from the breakdown of primary garnet, then it would appear that they have re-equilibrated with the lherzolite assemblage unlike those in the innermost part of kelyphites.

Phlogopite

Phlogopites typically form narrow coronas around the partly kelyphitised garnets but also, as in PTH 108, occur in clusters with spinel and chrome diopside grains. Their general secondary metasomatic character is borne out by partial analyses (not presented here) which indicate that they usually have high, although somewhat variable, TiO_2 (0.21-4.24 wt.%) and Cr_2O_3 (0.84-2.48 wt.%) contents together with 100 Fe/(Fe+Mg) ratios of 5.6-10.6.

Discussion

No garnet-bearing lherzolites with P/T equilibration estimates which indicate derivation from

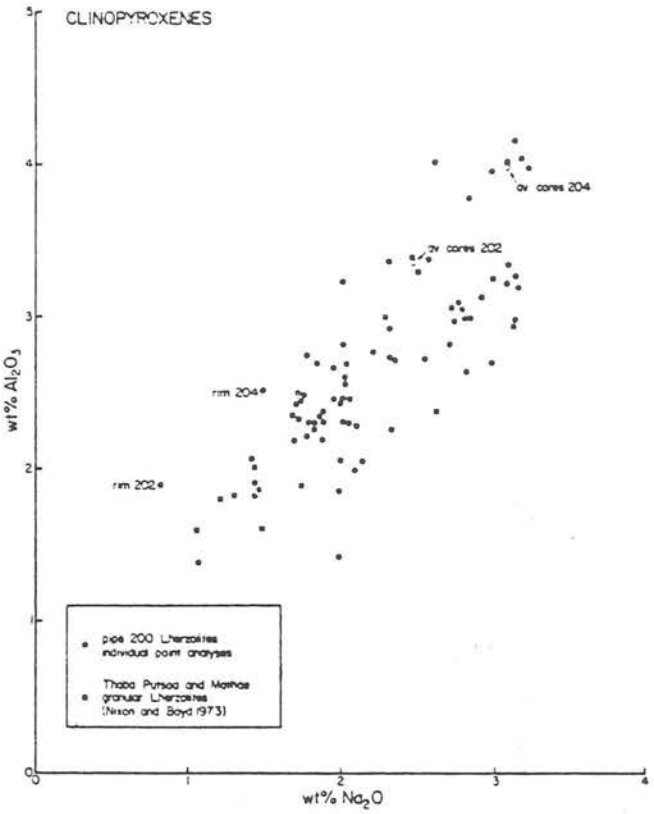

Fig. 2. Wt.% Al_2O_3 against wt.% Na_2O plot for analysed clinopyroxenes from Pipe 200 lherzolite nodules.

the top sixty or so kilometres of the mantle have been recognised in previous studies of nodule suites in Lesotho pipes (Boyd, 1973; Boyd and Nixon, 1975; Gurney et al., 1975; Dawson et al., 1975). This may be due to overestimation of P/T values and implied depths of derivation for certain garnet lherzolites by the P/T calculation procedures adopted by these authors. Alternatively the uppermost mantle may be of highly depleted chemical character, and hence largely comprise garnet-free ultramafic rocks, for which it is currently not possible to fix P/T values and depths of origin. Assuming that both our sampling, and that of the kimberlite, were adequate, consideration of the Pipe 200 ultramafic nodule suite may enable us to resolve this problem and provide a more satisfactory characterisation of the nature of the uppermost mantle beneath northern Lesotho at the time of kimberlite emplacement. We intend to present a more detailed discussion elsewhere as for the present we are obliged to restrict ourselves to just a few pertinent remarks on these matters.

We think it reasonable to conclude that the one primary aluminous spinel harzburgite nodule (PTH 201) was derived from shallower mantle depths than any of the other analysed Pipe 200 nodules. Such primary aluminous spinel nodules are apparently

TABLE 5: Analyses of Clinopyroxenes

Sample Number	PTH 102	PTH 108	PTH 202 (Cores)	PTH 202 (Rim)	PTH 203	PTH 204 (Cores)
Rock Type	GL	(G)CL	(G)CL	(G)CL	CL	GCL
SiO_2	54.6	54.4	54.4	53.0	54.5	54.2
TiO_2	0.13	0.05	0.06	0.08	0.10	0.06
Al_2O_3	1.90	1.64	3.36	1.90	2.64	3.99
Cr_2O_3	2.22	2.74	2.28	2.44	4.25	2.89
*FeO	2.22	2.31	2.38	2.36	1.47	2.14
MnO	0.04	0.08	0.02	0.02	0.09	0.07
NiO	n.d.	n.d.	0.05	n.d.	0.05	n.d.
MgO	15.8	15.6	15.2	18.2	15.0	14.1
CaO	20.6	20.3	19.4	20.5	17.0	18.1
Na_2O	1.44	1.96	2.47	0.81	2.82	3.08
Total	99.0	99.1	99.6	99.3	98.8	99.3
100 Ca/(Ca+Mg)	48.4	48.3	47.8	44.7	46.2	47.7
Si	1.993	1.991	1.974	1.935	1.987	1.977
Al^{IV}	0.007	0.009	0.026	0.065	0.013	0.023
Al^{VI}	0.075	0.062	0.118	0.017	0.101	0.145
Ti	0.004	0.001	0.002	0.002	0.003	0.002
Cr	0.064	0.079	0.065	0.070	0.123	0.083
Fe	0.068	0.071	0.072	0.072	0.045	0.065
Mn	0.001	0.002	0.001	0.001	0.003	0.002
Ni	--	--	0.001	--	0.001	--
Mg	0.860	0.851	0.821	0.992	0.817	0.777
Ca	0.806	0.796	0.753	0.803	0.701	0.707
Na	0.102	0.139	0.174	0.057	0.199	0.218
Total	3.980	4.002	4.007	4.015	3.992	4.002
$\%NaCrSi_2O_6$	6.6	7.9	6.6	6.0	12.4	8.3
$\%NaAlSi_2O_6$	4.2	5.6	9.5	0.0	7.8	12.3

* All Fe taken as FeO. Stiochiometrically calculated Fe^{3+} values not presented as at these very low total iron values slight analytical errors, especially in SiO_2, result in a widely differing Fe^{3+}/Fe^{2+} ratio.

rare amongst the nodule suite from pipes in northern Lesotho, although Boyd and Nixon (1975) described one from Liqhobong, and we have observed others from Lipelenang and Ngopetseu. This rarity is in line with the narrow stability zone (probably < 20 km) at the top of the mantle predicted for such assemblages by relevant experimental studies (MacGregor, 1970; O'Hara et al., 1971).

The primary spinels in other garnet free per-

in Pipe 200 Ultramafic Nodules.

PTH 204 (Rim)	PTH 205	PTH 207(P)	PTH 207(S_1)	PTH 207 S_2	PTH 210	PTH 304	PTH 400	PTH 401	PTH 403(P)	PTH 403(S_1)	PTH 403(S_2)	PTH 404	PTH 405	PTH 407	PTH 409	PTH 410
GCL	(G)CL	GCL	GCL	GCL	GP	(G)CL	GL	GCL	GL	GL	GL	GL	GL	GL	GCL	GCL
52.9	54.4	54.7	49.1	52.6	54.4	54.4	54.2	54.3	54.2	48.6	51.7	55.0	54.2	53.8	54.1	54.5
0.10	0.16	0.10	n.d.	0.17	n.d.	n.d.	0.13	0.01	0.18	0.92	0.40	0.10	0.08	0.01	0.11	0.09
2.52	2.46	2.19	8.12	4.02	1.99	2.95	2.66	2.54	2.84	8.73	4.43	2.34	2.95	2.30	3.26	3.07
3.01	2.88	2.63	3.26	2.19	0.65	3.64	1.59	2.02	3.12	2.25	1.40	2.64	3.20	2.52	3.41	3.33
2.11	2.29	2.34	2.88	3.94	1.59	1.94	2.64	1.79	2.48	4.10	4.45	2.24	2.22	2.17	2.27	2.22
0.08	n.d.	0.06	n.d.	0.48	n.d.	n.d.	0.10	0.07	n.d.	n.d.	0.24	0.05	0.10	0.10	0.08	0.07
n.d.	n.d.	n.d.	n.d.	n.d.	n.d.	n.d.	0.06	n.d.	n.d.	n.d.	n.d.	n.d.	0.04	n.d.	n.d.	n.d.
15.6	15.6	16.1	15.9	21.4	16.5	15.2	16.2	16.1	15.3	15.7	18.6	15.9	15.2	16.1	14.5	15.3
21.1	19.3	19.8	18.8	14.3	23.7	18.2	19.6	20.9	18.6	18.3	16.8	20.0	18.1	19.5	18.0	18.1
1.48	2.01	1.93	0.93	n.d.	0.48	3.14	2.03	1.71	2.49	1.19	1.03	1.88	2.79	2.05	2.94	2.76
98.9	99.1	99.9	99.0	99.6	99.3	99.5	99.2	99.5	99.2	99.7	99.1	100.2	98.9	98.7	98.7	99.5
49.3	47.1	46.9	45.9	32.5	50.9	46.3	46.6	48.2	46.6	45.6	39.4	47.5	46.2	46.5	47.1	46.0
Structural Formulae on the Basis of 6.000 Oxygens																
1.946	1.984	1.980	1.802	1.900	1.981	1.976	1.975	1.973	1.975	1.775	1.890	1.985	1.982	1.974	1.981	1.978
0.054	0.016	0.020	0.198	0.100	0.019	0.024	0.025	0.027	0.025	0.225	0.110	0.015	0.018	0.026	0.019	0.022
0.055	0.090	0.074	0.153	0.071	0.066	0.102	0.089	0.082	0.097	0.151	0.081	0.084	0.109	0.073	0.122	0.109
0.003	0.004	0.003	--	0.005	--	--	0.004	0.000	0.005	0.025	0.011	0.003	0.002	0.000	0.003	0.002
0.088	0.083	0.075	0.095	0.063	0.019	0.105	0.046	0.058	0.090	0.065	0.040	0.075	0.092	0.073	0.099	0.096
0.065	0.070	0.071	0.088	0.119	0.048	0.059	0.080	0.054	0.076	0.125	0.136	0.068	0.068	0.067	0.070	0.067
0.002	--	0.002	--	0.015	--	--	0.003	0.002	--	--	0.007	0.002	0.003	0.003	0.002	0.002
--	--	--	--	--	--	--	0.002	--	--	--	--	--	0.001	--	--	--
0.855	0.846	0.871	0.868	1.152	0.893	0.823	0.879	0.873	0.833	0.855	1.012	0.855	0.825	0.883	0.792	0.828
0.831	0.754	0.769	0.739	0.555	0.925	0.708	0.767	0.814	0.726	0.716	0.658	0.773	0.707	0.767	0.706	0.705
0.106	0.142	0.136	0.066	--	0.034	0.221	0.143	0.120	0.176	0.084	0.073	0.131	0.198	0.146	0.209	0.194
4.006	3.989	4.000	4.008	3.979	3.984	4.019	4.013	4.004	4.002	4.021	4.020	3.990	4.005	4.012	4.001	4.004
8.8	8.4	7.5	6.8	--	1.9	10.6	4.6	5.8	9.0	6.6	4.1	7.6	9.3	7.4	9.9	9.6
0.7	6.1	6.0	0.0	--	1.6	8.0	7.3	5.5	8.2	0.0	0.0	5.8	9.5	4.9	10.8	9.2

% Kosmochlor and % Jadeite calculated in that order, after first calculating $CaTiAl_2O_6$ and $CaAl_2SiO_6$ on the assumption that $Al^{IV} = 2.000 - Si$

n.d. - not determined

dotite nodules from Pipe 200 have 100 Cr/(Cr+Al) ratios which are as high or even higher (Table 7 and Figure 4) than those in the associated garnet lherzolites. This, together with the earlier demonstration of significant differences in whole rock chemistry between these nodule types (Table 1 and Figure 1) negates the necessity to interpret these nodules as having equilibrated at significantly different pressures (and depths). The stability of garnet relative to spinel in lherzolite assemblages is strongly dependent on the 100 Cr/(Cr+Al) ratio in the rock (MacGregor, 1970). In the absence of any way in which we can at present estimate P/T equilibration conditions for the garnet-free peridotites, it is not possible to demonstrate convincingly that they have indeed been derived from depths comparable to those deduced for the associated garnet lherzolites. How-

TABLE 6: Analyses of Garnets in Pipe 200 Ultramafic Nodules.

Sample Number	PTH 102	PTH 204	PTH 207	PTH 210	PTH 400	PTH 403	PTH 404	PTH 405	PTH 406	PTH 407	PTH 409	PTH 410
Rock Type	GL	GCL	GCL	GP	GL	GL	GL	GL	GL	GL	GCL	GCL
SiO_2	41.5	41.8	41.5	41.9	41.7	41.4	41.3	41.4	41.7	40.9	41.4	41.6
TiO_2	0.11	0.02	0.15	n.d.	0.17	0.10	0.10	0.04	0.05	0.04	0.07	0.09
Al_2O_3	18.0	18.1	17.2	23.2	20.3	18.9	17.7	18.9	18.8	18.1	17.9	19.1
Cr_2O_3	7.63	8.00	8.36	1.48	4.29	6.82	7.86	6.29	7.15	7.59	7.68	6.96
$*Fe_2O_3$	0.00	0.00	0.11	0.78	1.91	0.45	0.60	0.46	0.00	1.31	0.03	1.70
FeO	7.04	6.78	6.94	9.06	6.04	6.93	6.43	6.51	6.60	5.62	6.50	5.30
MnO	0.40	0.42	0.40	0.59	0.38	0.25	0.41	0.37	0.39	0.37	0.41	0.35
MgO	18.1	19.0	18.8	18.6	20.6	19.4	19.0	20.1	19.2	19.4	19.2	20.8
CaO	6.72	6.62	6.92	5.72	5.39	6.04	6.82	5.32	6.60	6.50	6.55	5.55
Total	99.5	100.7	100.5	101.3	100.8	100.3	100.2	99.4	100.5	99.8	99.7	101.4
Structural Formulae on the Basis of 24.000 Oxygens												
Si	6.058	6.024	6.024	5.939	5.938	5.970	5.992	5.999	6.001	5.940	6.018	5.911
Al	3.092	3.074	2.947	3.873	3.400	3.211	3.027	3.222	3.192	3.096	3.064	3.197
Ti	0.012	0.002	0.016	--	0.018	0.011	0.011	0.004	0.005	0.004	0.008	0.010
Cr	0.880	0.912	0.959	0.166	0.483	0.778	0.902	0.720	0.814	0.872	0.882	0.781
$*Fe^{3+}$	0.000	0.000	0.013	0.083	0.205	0.049	0.066	0.051	0.000	0.143	0.003	0.181
Fe^{2+}	0.859	0.818	0.842	1.074	0.719	0.837	0.780	0.789	0.795	0.683	0.789	0.630
Mn	0.049	0.051	0.049	0.071	0.046	0.031	0.050	0.045	0.048	0.046	0.050	0.042
Mg	3.942	4.076	4.074	3.926	4.369	4.178	4.113	4.344	4.119	4.204	4.166	4.404
Ca	1.051	1.023	1.076	0.869	0.822	0.934	1.060	0.825	1.018	1.012	1.020	0.844
Total	15.944	15.981	16.000	16.000	16.000	16.000	16.000	16.000	15.991	16.000	16.000	16.000
Percentage of Garnet End Members												
Pyrope	62.2	62.5	63.1	66.1	73.6	66.1	63.8	68.3	65.5	65.8	65.2	69.0
Almandine	14.6	13.7	11.2	18.1	11.5	13.8	11.2	11.7	13.3	11.4	11.5	10.5
Spessartine	0.8	0.9	0.8	1.2	0.8	0.5	0.8	0.8	0.8	0.8	0.9	0.7
Uvarovite	17.8	17.1	18.3	4.2	12.2	15.7	17.7	13.8	17.0	17.0	17.2	14.3
Knorringite	4.6	5.8	6.2	--	--	3.9	4.9	4.3	3.4	5.0	5.1	5.5
Andradite	--	--	--	2.1	1.7	--	--	--	--	--	--	--
Skiagite	--	--	0.3	--	0.3	--	1.7	1.3	--	--	0.1	--
Grossular	--	--	--	8.3	--	--	--	--	--	--	--	--

$*Fe^{3+}$ calculated from anion deficiency in structural formulae based on 16.000 cations

ever, the similarity in clinopyroxene 100 Ca/(Ca+Mg) ratio, and consequently derived temperature estimates for the chromite lherzolite (PTH 203), to the values obtained for the garnet lherzolites suggest that this may well be the case.

It is clear that the Pipe 200 garnet-bearing lherzolite nodules are closely similar in terms of their whole rock and mineral chemistries to the petrographically similar nodules previously described by Nixon and Boyd (1973) in nearby pipes. P/T estimates for all such nodules based on direct application of experimental data for the two-pyroxene solvus (Davis and Boyd, 1966) and garnet-orthopyroxene equilibria (MacGregor, 1974), lie on the non-inflected part of the 'pyroxene' geotherm of Boyd (1973), Boyd and Nixon (1975). It is widely accepted that there is a large measure of uncertainty in the absolute accuracy of such P/T values but it has been assumed (Boyd, 1973; Boyd and Nixon, 1975) that the relative P/T values obtained for different garnet lherzolites should be significant. However, even this may not be the case if there are variations in whole rock chemistry amongst the garnet lherzolite nodules which significantly affect the mineral equilibria.

With this in mind we prefer to use the semi-empirical approaches adopted by Wood and Banno (1973), Wood (1974) and Wells (1977) which attempt to take account of the effect of Fe on the two-pyroxene solvus, and of the complex chemistries of natural garnets and orthopyroxenes. Certainly the low Al_2O_3 contents of the primary orthopyroxenes (0.70-1.04 wt.%) and in their high 100 Cr/(Cr+Al) ratios mean that we cannot justifiably obtain P estimates for the Pipe 200 garnet lherzolites by direct application of MacGregor's (1974) data in the manner followed by Boyd (1973).

The Pipe 200 garnet lherzolites yield T/P estimates of 1034-1071°C/31.4-37.7 kb using the combination of equation (27) of Wood and Banno (1973), and equation (12) of Wood (1974), and 906-949°C/24.5-30.8 kbs. using equation (5) of Wells (1977) and equation (12) of Wood (1974). For both sets of P estimates Cr contents in garnet and orthopyroxene were taken into account in the manner proposed by Wood (1974). Garnet-free lherzolites yield T estimates of 999-1093°C (Wood and Banno, 1973) and 873-962°C (Wells, 1977), but P estimates are unobtainable. These various P/T estimates imply derivation of these nodules from a surprisingly narrow depth zone in the mantle. Whilst it is possible that kimberlite eruptions may be habitually selective in their depth sampling, we consider that the failure of the adopted calculation procedures to adequately take account of the opposing effects of T and P on the clinopyroxene-orthopyroxene and garnet-orthopyroxene equilibria may be responsible for telescoping the derived P/T estimates into an artifically narrow range.

In view of the relative insensitivity of the two-pyroxene thermometer at temperatures below about 1100°C and doubts over the corrections necessary for the effect of P and the presence of

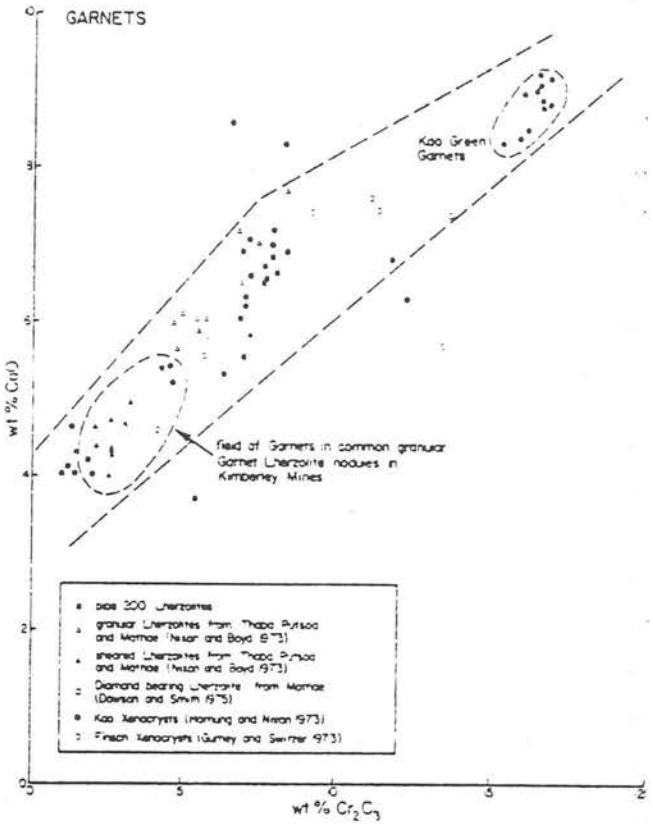

Fig. 3. Wt.% CaO against wt.% Cr_2O_3 plot for analysed garnets from Pipe 200 lherzolite nodules as well as for xenolithic and xenocrystal garnets of likely lherzolite paragenesis from other kimberlites in Lesotho and South Africa.

Al on the two-pyroxene solvus (Mori and Green, 1975, 1976; Lindsley and Dixon, 1976; Dixon and Presnall, 1977) as well as major uncertainties introduced in the extrapolation of experimental data on simple systems to the interpretation of mineral equilibria in more chemically complex natural minerals, we feel that we cannot unquestionably accept any of the so-derived P/T estimates. Derivation of unequivocal P/T values for the Pipe 200 nodules will probably have to await further experimental data on the effect of Cr_2O_3 on the garnet-orthopyroxene equilibria and experimental calibration of the effects of P and T on the Fe-Mg or Mn-Mg distribution coefficients in these ultramafic assemblages. In the meantime our inclination is towards accepting the relatively lower P/T estimates provided by the combined use of equation (5) of Wells (1977) and equation (12) of Wood (1974) as the most realistic. Such values as shown in Figure 5, are the most compatible with preferred P/T estimates for the lower crustal nodules (Griffin et al., 1978) but necessitate substantial revision to the palaeogeothem of Boyd (1973), Boyd and Nixon (1975) in the region of the lower crust and uppermost mantle.

TABLE 7: Analyses of Spinel

Sample Number	PTH 108	PTH 201	PTH 202	PTH 203	PTH 204A	PTH 204B	PTH 204C	PTH 207A	PTH 207
Rock Type	(G)CL	SH	(G)CL	CL	GCL	GCL	GCL	GCL	
SiO_2	0.05	0.13	0.04	0.05	n.d.	n.d.	n.d.	n.d.	n.d.
TiO_2	0.73	0.01	0.27	0.34	n.d.	n.d.	n.d.	0.21	0.4
Al_2O_3	5.35	29.4	14.2	8.75	13.9 ±0.7	14.8 ±0.3	15.0 ±0.2	44.9	12.
Cr_2O_3	59.9	41.5	51.7	63.1	55.0 ±0.7	53.7 ±0.4	53.1 ±0.6	23.0	55.
$*Fe_2O_3$	6.04	0.53	7.04	1.91	3.99 ±0.4	4.09 ±0.2	4.30 ±0.4	2.01	4.0
FeO	15.9	12.2	12.0	10.8	13.7	13.4	13.7	10.09	12.
MnO	0.55	0.07	0.06	0.38	n.d.	n.d.	n.d.	0.57	n.d
NiO	n.d.	0.10	n.d.	0.10	n.d.	n.d.	n.d.	n.d.	n.d
MgO	11.1	16.0	14.7	14.7	13.4 ±0.3	13.6 ±0.3	13.4 ±0.4	18.6	14.
Total	99.1	99.9	19.4	100.0	99.6	99.2	99.1	99.2	99.
100 Cr/(Cr+Al)	88.2	48.6	70.9	82.9	72.6	70.9	70.4	25.6	75.
					Structural Formulae on the Basis of 4.000 Oxyge				
Si	0.002	0.004	0.001	0.002	--	--	--	--	--
Ti	0.018	0.000	0.06	0.008	--	--	--	0.005	0.01
Al	0.212	1.017	0.529	0.331	0.521	0.554	0.562	1.450	0.45
Cr	1.594	0.963	1.288	1.603	1.383	1.348	1.335	0.498	1.47
$*Fe^{3+}$	0.153	0.012	0.167	0.046	0.096	0.098	0.101	0.041	0.09
Fe^{2+}	0.449	0.300	0.317	0.291	0.365	0.356	0.365	0.231	0.33
Mn	0.016	0.002	0.002	0.010	--	--	--	0.013	--
Ni	--	0.002	--	0.003	--	--	--	--	--
Mg	0.556	0.700	0.689	0.706	0.635	0.644	0.635	0.760	0.69
$\%M^{2+}Cr_2O_4$	81.4	48.4	64.9	81.0	69.2	67.4	66.8	25.0	71.
$\%M^{2+}\ Al_2O_4$	10.8	51.0	26.7	16.7	26.0	27.7	28.1	72.9	23.
$\%M^{2+}\ Fe_2{}^{3+}O_4$	7.8	0.6	8.4	2.3	4.8	4.9	5.1	2.1	4.9

$*Fe^{3+}$ Calculated by Charge Balance in the Structural Formulae

n.d. Not determined

In most rocks different spinel grains show little chemical variation and are represented by a single mean analysis. However, spinels in PTH 207, 403 and 405 show a range in chemistry as represented by the two sets of analyses presented. 207A, 403A and 405A, represent spinels in the innermost parts of kelyphites around garnets, whilst 207B, 403B, and 405B represent spinels

The stability of primary spinel relative to garnet in all Pipe 200 nodules other than PTH 201 appears to have been largely controlled by the level of depletion of Al_2O_3, CaO and FeO relative to Cr_2O_3 and MgO in these rocks (Table 1 and Figure 1). It is of interest to consider whether ultramafic nodules from pipes in other areas have similar assemblages at equivalent levels of Cr/(Cr+Al) and Mg/(Mg+Fe) in the rock. Stability of garnet in rocks with higher Cr/(Cr+Al) ratios would imply higher pressures (MacGregor, 1970) and hence deeper levels of origin, thus indicating that the mantle in that area was highly depleted to greater depths if the depth range of sampling was comparable.

For comparison the garnet-only, garnet and chromite and chromite-only composition fields defined by the ultramafic nodules in the Lashaine volcano, Tanzania (Reid et al., 1975) are shown in Figure 1. Unfortunately, the garnet and chromite chromite-only boundary (A) is not closely defined but the apparent lack of overlap in the composition

in Pipe 200 Ultramafic Nodules.

PTH 301	PTH 302	PTH 303	PTH 304	PTH 401	PTH 403A	PTH 403B	PTH 404	PTH 405A	PTH 405B	PTH 407	PTH 409	PTH 410
CH	CH	CH	(G)CL	GCL	GL		GL	GL		GL	GL	GL
n.d.	n.d.	n.d.	n.d.	0.10	n.d.	n.d.	0.12	0.14	0.16	0.19	0.12	0.22
n.d.	n.d.	n.d.	n.d.	0.11	1.39	2.03	0.83	0.29	1.96	0.07	0.49	0.59
11.2	8.03	8.20	9.0	13.8	28.8	15.5	46.3	45.1	33.3	46.7	10.1	48.6
60.1	62.3	61.7	58.6	55.4	38.4	47.8	18.7	22.0	31.4	21.9	57.5	18.7
3.56	4.39	4.91	5.87	3.37	4.11	6.14	2.88	3.07	3.36	1.49	3.80	2.38
9.39	8.79	9.17	13.5	13.5	12.7	15.3	11.0	8.13	12.1	8.64	15.0	9.57
n.d.	n.d.	n.d.	n.d.	0.38	0.24	n.d.	0.31	0.27	0.33	0.23	0.35	0.24
n.d.	n.d.	n.d.	n.d.	n.d.	0.28	0.26	n.d.	0.05	0.21	n.d.	n.d.	n.d.
16.0	16.0	15.7	13.0	13.4	16.6	13.7	18.7	20.2	17.4	20.0	12.2	20.2
99.9	99.5	99.2	99.4	99.7	100.5	100.1	98.6	99.0	99.9	99.0	99.2	100.2
78.3	83.9	83.5	81.4	72.9	46.1	67.4	21.3	24.6	38.7	23.9	79.2	20.5
--	--	--	--	0.003	--	--	0.003	0.004	0.005	0.005	0.004	0.006
--	--	--	--	0.003	0.030	0.048	0.017	0.006	0.042	0.001	0.012	0.012
0.416	0.303	0.311	0.346	0.515	0.977	0.573	1.495	1.444	1.122	1.488	0.389	1.523
1.499	1.579	1.570	1.510	1.392	0.874	1.186	0.405	0.474	0.712	0.468	1.485	0.394
0.085	0.118	0.119	0.144	0.081	0.089	0.145	0.059	0.063	0.072	0.030	0.093	0.048
0.248	0.236	0.247	0.348	0.359	0.306	0.401	0.252	0.185	0.289	0.196	0.410	0.213
--	--	--	--	0.010	0.006	--	0.007	0.006	0.008	0.005	0.010	0.005
--	--	--	--	--	0.006	0.007	--	0.001	0.005	--	--	--
0.752	0.764	0.753	0.632	0.637	0.712	0.641	0.762	0.817	0.745	0.806	0.596	0.799
75.0	78.9	78.5	75.5	70.0	45.0	62.3	20.7	23.9	37.3	23.6	75.5	20.0
20.8	15.2	15.6	17.3	25.9	50.4	30.1	76.3	72.9	58.9	74.9	19.8	77.6
4.2	5.9	5.9	7.2	4.1	4.6	7.6	3.0	3.2	3.8	1.5	4.7	2.4

typically outside, although still adjacent to, turbid kelyphite alteration zones. PTH 204 contains three petrographically distinct types of spinels: (A) large discrete apparently primary grains (B) small idioblastic grains associated with clusters of clinopyroxene and phlogopite grains (C) small grains associated with kelyphitic breakdown of garnet.

Mean and standard deviation are presented for each of these types of spinel grains. In other garnet chromite lherzolites, analyses for PTH 401 and 409 represent primary chromites whilst that for PTH 410 is for secondary spinels associated with garnet breakdown.

fields suggests either derivation from a fairly restricted depth zone or a systematic decrease in the level of depletion with depth. It is apparent that in the ultramafic nodules from Pipe 200 and certain other pipes in northern Lesotho, garnet is stable to significantly higher whole rock Cr/(Cr+Al) values than in the Lashaine nodules (compare also Table 2, columns A, B and F). It therefore seems likely that the mantle is in general more highly depleted to greater depths beneath these northern Lesotho pipes, although in both areas there may well be an overall general decrease in the level of depletion in basalt-yielding constituents with depth. Moreover, as the garnet stable in lherzolites with increased Cr/(Cr+Al) values itself becomes increasing chromiferous, the presence of the exceptionally chrome-rich green garnet xenocrysts in the nearby Kao kimberlite (Figure 3) implies that the mantle beneath northern Lesotho may in places be exceptionally depleted to considerable depths with extremely high Cr/(Cr+Al) ratios This may well reflect the extensive Karroo volcan-

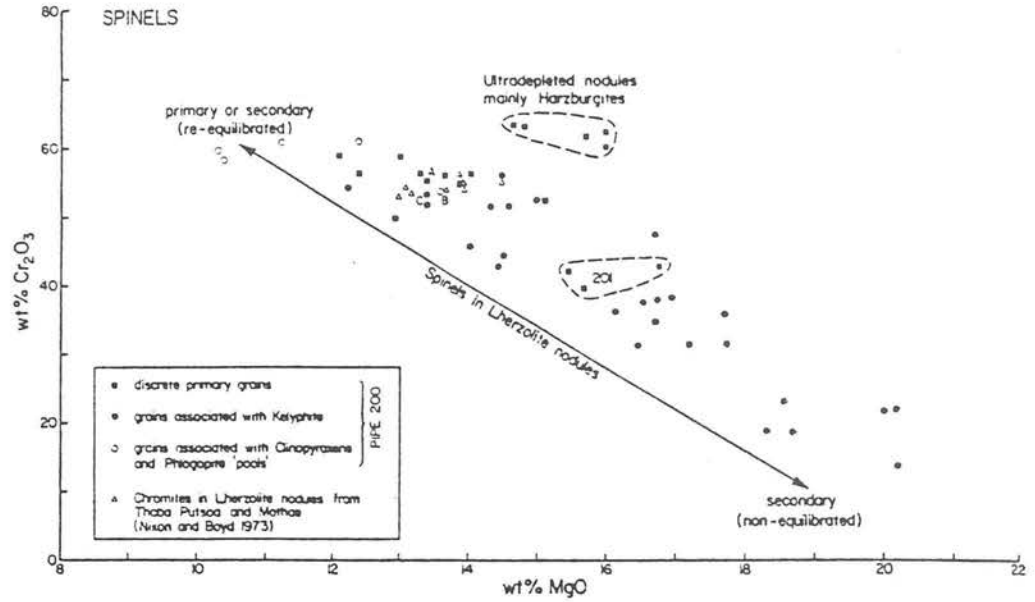

Fig. 4. Wt.% Cr_2O_3 against wt.% MgO plot for analysed spinels from Pipe 200 ultramafic nodules.

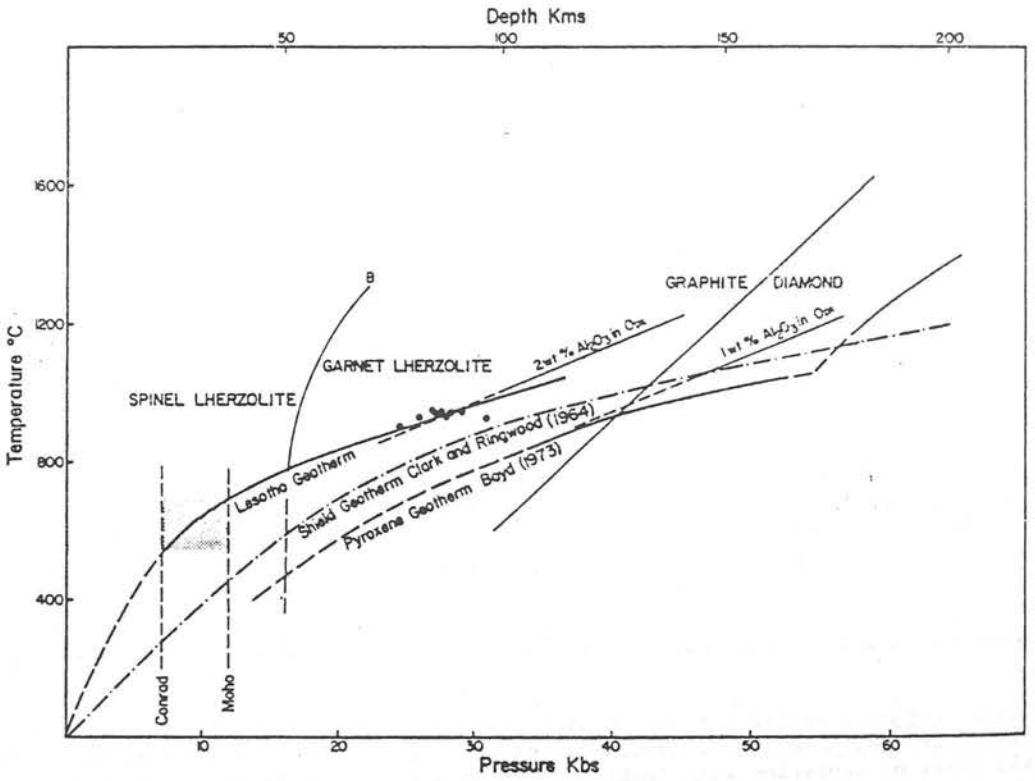

Fig. 5. P/T diagram showing revised Lesotho Geotherm compatible with provisionally preferred P/T estimates for Pipe 200 garnet lherzolite nodules (dots, see text) and P/T estimates for lower crustal granulite/eclogite nodules from Lesotho pipes (stippled field, Griffin et al., 1978). Curve B is the experimentally determined spinel lherzolite/garnet lherzolite boundary for natural materials from O'Hara et al. (1971). The diamond/graphite inversion curve is from Bundy et al. (1961) and the wt.% Al_2O_3 isopleths for orthopyroxene in equilibrium with garnet are from MacGregor (1974). Positions of the Conrad and Moho discontinuities are based on the seismic data for the Transvaal (Hales and Sacks, 1959).

ism which preceded kimberlite emplacement in this area.

Acknowledgements: D. A. Carswell wishes to acknowledge the financial support of The Royal Society, University of Sheffield and Natural Environmental Research Council, D. B. Clarke funding from Dalhousie University and the National Research Council of Canada, and R. H. Mitchell funding from the National Research Council of Canada. J. R. Andrews, M. J. O'Hara and P. Kresten kindly provided additional samples. The considerable assistance of V. A. Somogyi with the whole rock analyses and of P. G. Hill and R. M. MacKay with the probe analyses is gratefully acknowledged. We also wish to thank the organisers and guides of the 1973 Lesotho kimberlite excursions.

References

Berg, W. and M. J. O'Hara, Source mantle, residuum and partial melt compositions deduced from the kimberlite record, Extended Abstracts, First International Kimberlite Conference, Cape Town, 31-33, 1973.

Boullier, A. M., and A. Nicholas, Texture and fabric of peridotite nodules from kimberlite at Mothae, Thaba Putsoa and Kimberley, in Lesotho Kimberlites, edited by P. H. Nixon, pp. 57-66, Lesotho National Development Corp., Maseru, Lesotho, 1973.

Boyd, F. R., A pyroxene geotherm, Geochim. Cosmochim. Acta, 37, 2533-2546, 1973.

Boyd, F. R., and P. H. Nixon, Ultramafic nodules from the Thaba Putsoa kimberlite pipe, Carnegie Inst. Wash. Yearb., 71, 362-373, 1972.

Boyd, F. R., and P. H. Nixon, Origins of the ultramafic nodules from some kimberlites of northern Lesotho and the Monastery Mine, South Africa, Phys. Chem. Earth, 9, 431-454, 1975.

Bundy, F. R., H. P. Bovenkerk, H. M. Strong, and R. H. Wentorf, Jr., Diamond graphite equilibrium line from growth and graphitisation of diamond, J. Chem. Phys., 35, 383-391, 1961.

Carswell, D. A., Primary and secondary phlogopites and clinopyroxenes in garnet lherzolite xenoliths. Phys. Chem. Earth., 9, 417-429, 1975.

Carswell, D. A., and J. B. Dawson, Garnet peridotite xenoliths in South African kimberlite pipes and their petrogenesis, Contr. Mineral. Petrol., 25, 163-184, 1970.

Chen, J. C., Petrology and chemistry of garnet lherzolite nodules in kimberlite from South Africa, Am. Mineral., 56, 2098-2110, 1971.

Clark, S. P., Jr., and A. E. Ringwood, Density distribution and constitution of the mantle. Rev. Geophys., 2, 35-88, 1964.

Cox, K. G., J. J. Gurney, and B. Harte, Xenoliths from the Matsoku Pipe, in Lesotho Kimberlites, edited by P. H. Nixon, pp. 76-92, Lesotho National Development Corp., Maseru, Lesotho, 1973.

Davis, B. T. C., and F. R. Boyd, The join $Mg_2Si_2O_6$-$CaMgSi_2O_6$ at 30 kilobars pressure and its application to pyroxenes from kimberlites. J. Geophys. Res., 71, 3507-3576, 1966.

Dawson, J. B., J. J. Gurney, and P. J. Lawless, Palaeogeothermal gradients derived from xenoliths in kimberlite, Nature, 257, 299-300, 1975.

Dawson, J. B., and J. V. Smith, Occurrence of diamond in a mica-garnet lherzolite xenolith from kimberlite, Nature, 254, 580-581, 1975.

Dawson, J. B., and W. E. Stevens, Statistical classification of garnets from kimberlite and associated xenoliths, J. Geol., 83, 589-607, 1975.

Dixon, J. R., and D. C. Presnall, Geothermometry and geobarometry of synthetic spinel lherzolite in the system CaO-MgO-Al_2O_3-SiO_2, Extended Abstracts, Second International Kimberlite Conference, Santa Fe, New Mexico, 1977.

Griffin, W. L., D. A. Carswell, and P. H. Nixon, Lower crustal granulites and eclogites from Lesotho and South Africa, Proceedings of the Second International Kimberlite Conference, in press.

Gurney, J. J., B. Harte, and K. G. Cox, Mantle xenoliths in the Matsoku kimberlite pipe. Phys. Chem. Earth, 9, 507-523, 1975.

Gurney, J. J., and G. S. Seitzer, The discovery of garnets closely related to diamonds in the Finsch Pipe, South Africa, Contr. Mineral. Petrol., 39, 103-116, 1973.

Hales, A. L., and I. S. Sacks, Evidence for an intermediate layer from crustal seismic studies in the East Transvaal, Geophys. J. Roy. Astr. Soc., 2, 15-23, 1957.

Harte, B., K. G. Cox, and J. J. Gurney, Petrography and geological history of upper mantle xenoliths from the Matsoku kimberlite pipe, Phys. Chem. Earth, 9, 477-506, 1975.

Holmes, A., A contribution to the petrology of kimberlite and its inclusions, Trans. Geol. Soc. S. Africa, 39, 379-428, 1936.

Hornung, G., and P. H. Nixon, Chemical variations in the knorringite-rich garnets, in Lesotho Kimberlites, edited by P. H. Nixon, pp. 122-127, Lesotho National Development Corp., Maseru, Lesotho, 1973.

Ito, K., and G. C. Kennedy, The melting and phase relations in a natural peridotite to 40 kilobars, Am. J. Sci., 265, 519-538, 1967.

Kresten, P., and A. N. Dempster, The geology of Pipe 200 and the Malibamatso dyke swarm, in Lesotho Kimberlites, edited by P. H. Nixon, pp. 172-179, Lesotho National Development Corp., Maseru, Lesotho, 1973.

Lindsley, D. H., and S. A. Dixon, Diopside-enstatite equilibria at 850° to 1400°C, 5 to 35 kb., Am. J. Sci., 276, 1285-1301, 1976.

MacGregor, I. D., The effect of CaO, Cr_2O_3, Fe_2O_3 and Al_2O_3 on the stability of spinel and garnet peridotites, Phys. Earth Planet Inter., 3, 372-377, 1970.

MacGregor, I. D., The system MgO-Al_2O_3-SiO_2: solubility of Al_2O_3 in enstatite for spinel and garnet peridotite compositions, Am. Mineral., 59, 110-119, 1974.

Mori, T., and D. H. Green, Pyroxenes in the system $Mg_2Si_2O_6$-$CaMgSi_2O_6$ at high pressure, Earth Planet. Sci. Letters, 26, 277-286, 1975.

Mori, T., and D. H. Green, Subsolidus equilibria between pyroxenes in the CaO-MgO-SiO_2 systems at high pressures and temperatures, Am. Mineral. 61, 616-625, 1976.

Nixon, P. H., and F. R. Boyd, Petrogenesis of the granular and sheared ultrabasic nodule suite in kimberlites, in Lesotho Kimberlites, edited by P. H. Nixon, pp. 48-56, Lesotho National Development Corp., Maseru, Lesotho, 1973.

O'Hara, M. J., S. W. Richardson, and G. Wilson, Garnet peridotite stability and occurrence in crust and mantle, Contr. Mineral. Petrol., 32, 48-68, 1971.

Reid, A. M., C. H. Donaldson, R. W. Brown, W. I. Ridley, and J. B. Dawson, Mineral chemistry of peridotite xenoliths from the Lashaine volcano, Tanzania, Phys. Chem. Earth, 9, 525-543, 1975.

Rhodes, J. M., and J. B. Dawson, Major and trace element chemistry of peridotite inclusions from the Lashaine volcano, Tanzania, Phys. Chem. Earth, 9, 545-557, 1975.

Ridley, W. I., and J. B. Dawson, Lithophile trace element data bearing on the origin of peridotite xenoliths, ankaramite and carbonatite from Lashaine volcano, North Tanzania, Phys. Chem. Earth, 9, 559-596, 1975.

Ross, C. S., M. D. Foster, and A. T. Myers, Origin of dunites and of olivine-rich inclusions in basaltic rocks, Am. Mineral., 39, 693-737, 1954.

Sobolev, N. V., Yu G. Lavrentev, N. P. Pokhilenko and L. V. Usova, Chrome-rich garnets from the kimberlites of Yakutia and their paragenesis, Contr. Mineral. Petrol., 40, 39-52, 1973.

Wells, P. R. A., Pyroxene thermometry in simple and complex systems, Contr. Mineral. Petrol., 62, 129-139, 1977.

Whitfield, G. G., A petrological and mineralogical study of peridotite and eclogite xenoliths from certain kimberlite pipes, Unpublished M.Sc. Thesis, Rhodes University, South Africa, 1971.

Wood, B. J., The solubility of alumina in orthopyroxene coexisting with garnet, Contr. Mineral. Petrol., 46, 1-15, 1974.

Wood, B. J., and S. Banno, Garnet-orthopyroxene and orthopyroxene-clinopyroxene relationships in simple and complex systems, Contr. Mineral. Petrol., 42, 109-124, 1973.

Mantle derived lherzolite nodules associated with kimberlite, carbonatite and basalt magmatism: A review

D. A. CARSWELL

LITHOS

Carswell, D. A. 1980: Mantle derived lherzolite nodules associated with kimberlite, carbonatite and basalt magmatism: A review. *Lithos 13*, 121–138. Oslo. ISSN 0024-4937.

Occurrences, petrography and major element chemistry of lherzolite nodules are reviewed. Spinel-garnet stability relationships in these nodules are discussed and are shown to be controlled by chemical as well as physical (P/T) considerations. On the basis of a survey of spinel compositions it is proposed that three classes of spinel bearing lherzolite nodules should be recognised: namely Al-spinel lherzolites [spinel 100 Cr/(Cr + Al) < 25], Cr-spinel lherzolites [spinel 100 Cr (Cr + Al) 25–65] and chromite lherzolites [spinel 100 Cr/(Cr + Al) > 65].

All lherzolite nodules yield sub-solidus P/T equilibration estimates and are interpreted as fragments of upper mantle wall rocks incorporated during the volatile charged eruptions. Depths of derivation increase from < 60 kms for most nodules in alkali basaltic magmas to > 150 kms for some nodules in kimberlites. The fact that Al-spinel lherzolites are the most common nodule type in magmas of the alkali basalt suite whilst garnet lherzolites are dominant in kimberlites is attributed to the combined effects of a typically steeper geotherm in the mantle beneath areas of alkali basaltic volcanism and a shallower depth of origin for this type of magmatism. Al-spinel lherzolites do, however, occur in the kimberlites of the western U.S.A. and south-west Greenland in contrast to their apparent absence in the kimberlites of southern Africa and Yakutia, U.S.S.R. This suggests that the uppermost mantle beneath these latter regions (as represented by nodules of chromite lherzolites and chromite or Cr-spinel harzburgites) has a more refractory residual type composition with a higher Cr/(Cr + Al) ratio–although the evidence indicates an overall decrease in the level of depletion in 'basaltic' magma yielding constituents with depth. Lherzolite nodules generally have chemical compositions which are depleted in such constituents relative to the pyrolite model compositions for primitive or pristine mantle; nevertheless their composition range is thought to encompass both highly 'depleted' and essentially 'undepleted' upper mantle compositions.

The fact that consistent temperature estimates can be obtained from the various calibrated element exchange reaction geothermometers for some lherzolite nodules but not for others (notably those with strikingly porphyroclastic textures) may indicate that some lherzolite nodules comprise mantle derived rocks which failed to totally re-equilibrate following the diapiric movements which immediately preceded their incorporation and rapid transportation to the surface.

D. A. Carswell, Department of Geology, University of Sheffield, Sheffield S1 3JD, United Kingdom.

Occurrence and petrography

Ultramafic nodules of likely mantle derivation are extremely abundant in most kimberlite occurrences (Wagner 1914; Williams 1932; Carswell & Dawson 1970; Nixon & Boyd 1973; Sobolev 1977; etc.). They are less common although still of frequent occurrence in basaltic rocks–notably, although not exclusively, in magmas of the alkali basalt-basanite-nephelinite suite (Ross et al. 1954; White 1966; Kuno & Aoki 1970; Frey & Green 1974; Varne 1977; Donaldson 1978; Frey & Prinz 1978; etc.). The most common types are essentially 4-phase lherzolites with a mineral assemblage of olivine-orthopyroxene-clinopyroxene-garnet or spinel. Phlogopite mica and amphibole may be additional minor primary phases in some instances (Erlank 1973; Varne 1970; Carswell 1975; Dawson & Smith 1975a) but are more commonly of secondary replacement origin. The relative uniformity of the mineralogy and chemistry of these lherzolite nodules (for example in the Fe/Mg ratios of constituent minerals) contrasts with the more varied mineralogical and chemical make-up of a second group of ultramafic nodules observed to sometimes occur in both basaltic and kimberlitic magmas (White 1966; Cox et al. 1973; Frey & Prinz 1978). This latter group of ultramafic nodules, which contain more Fe and Ti-rich mineral assemblages and are typified by more clinopyroxene rich types such as websterites and wehrlites, are generally interpreted as magmatic cumulates (Ringwood 1975; Gurney et al. 1975; Frey & Prinz 1978), sometimes possibly of cognate origin, and will not be considered further in this paper.

As far as the lherzolite nodules are concerned,

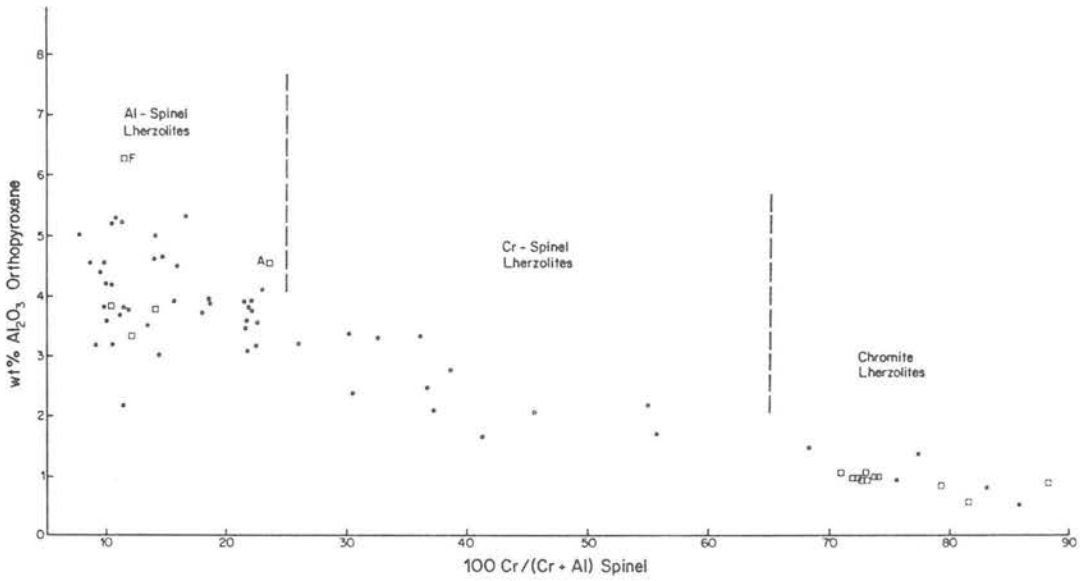

Fig. 1. Plot of 100 Cr/(Cr + Al) ratio in primary spinels against wt.% Al_2O_3 in coexisting orthopyroxenes for garnet free (closed circles) and garnet bearing (open squares) lherzolite nodules. Data from Ross et al. 1954; Kutolin & Frolova 1970; Kuno & Aoki 1970; Nixon & Boyd 1973; Frey & Green 1974; Aoki & Prinz 1974; Emeleus & Andrews 1975; Suwa et al. 1975; Reid et al. 1975; Wallace 1975; Smith & Levy 1976; Berger & Brousse 1976; Ferguson et al. 1977; Varne 1977; Donaldson 1978; Frey & Prinz 1978; Carswell et al. 1979.

kimberlites typically contain spinel free garnet lherzolites whilst garnet free spinel lherzolites are the predominant type in magmas of the alkali basalt suite. However, lherzolite nodules which contain, or have been interpreted to have originally contained, garnet have occasionally been reported from alkali basalt suite magmas (Kuno & Aoki 1970; Berger & Brousse 1976; Berger 1977; Volyanyuk et al. 1976) and garnet free spinel lherzolites have also been reported from kimberlites (Smith & Dawson 1975; Emelus & Andrews 1975; Smith & Levy 1976; Mitchell 1977; Carswell et al. 1979). Occurrences of both garnet lherzolite and spinel lherzolite nodules have also been noted in lamprophyric or ankaramitic rocks associated with extrusive and intrusive carbonatite magmatic activity (Griffin 1973; Reid et al. 1975; Wallace 1975).

On the basis of a compilation of 384 whole rock analyses, Maaløe & Aoki (1977) calculated an average mode for spinel lherzolite nodules of 66.70% olivine, 23.74% orthopyroxene, 7.83% clinopyroxene and 1.73% spinel. It would appear that all except five of these analyses were of nodules contained in magmas of the alkali basalt suite and that the large majority, but not all, of these nodules contained aluminous spinels. Confusion has arisen from descriptions of spinel lherzolite nodules because of dual usage of the name spinel. Spinel is often used as a general name to describe any mineral phase belonging to a chemically complex group, or series of oxides, in addition to its more specific use to describe a mineral which closely approximates in its chemical composition to $MgAl_2O_4$. As lherzolite nodules contain spinels which show significant compositional variation, mostly within the quaternary system $MgAl_2O_4$-$MgCr_2O_4$-$FeAl_2O_4$-$FeCr_2O_4$, it is important that descriptions of such nodules clearly indicate whether the name spinel is being used in a general or specific sense.

Fig. 1 demonstrates that primary spinel grains in lherzolite nodules cover a considerable composition range and that increasing Cr/(Cr + Al) ratio in spinel correlates with decreasing wt. % Al_2O_3 content in coexisting orthopyroxene. It is therefore clearly unsatisfactory to describe all garnet free primary spinel bearing lherzolites simply as spinel lherzolites. Instead it is proposed that three classes of such nodules should be recognised on the basis of spinel compositions, namely: *Al-spinel lherzolites* [spinel 100 Cr/(Cr + Al) < 25], *Cr-spinel lherzolites* [spinel 100 Cr/(Cr + Al) 25–65] and *chromite lherzolites* [spinel 100 Cr/(Cr + Al) > 65].

Petrographic observations (e.g. Carswell et al. 1979) indicate that whilst many garnet lherzolite nodules contain minor secondary aluminous spinel developed as a result of an olivine-garnet break-

down reaction (Reid & Dawson 1972) some nodules contain coexisting primary spinels and garnets. Such spinels are typically low Al magnesio-chromites with 100 Cr/(Cr+Al) > 65 (Reid et al. 1975; Nixon & Boyd 1973; Carswell et al. 1979). However, primary aluminous spinels with 100 Cr/(Cr+Al) <25 which coexist with garnets have been described in a lherzolite nodule from a kimberlite diatreme in S. E. Australia–labelled A in Fig. 1–(Ferguson et al. 1977) and in a comparable nodule from an alkali basalt diatreme in Lozère, France–labelled F in Fig. 1–(Berger & Brousse 1976). Aoki & Prinz (1974) have also described primary aluminous spinels thought to have originally coexisted with garnets in lherzolite nodules in alkali basalts at Itinome-gata, N.E. Japan. However, they entertain the possibility that the compositions of these discrete, petrographically primary, spinels may have been somewhat modified during breakdown of original garnet and higher pressure pyroxenes. It is also doubtful whether Cr-spinel garnet lherzolite nodules from the kimberlites at Green Knobs, New Mexico, U.S.A. (Smith & Levy 1976) and Somerset Island, Canada (Mitchell 1978) represent fully equilibrated assemblages as in these nodules garnets occur as coronas around the Cr-spinels.

Table 1 summarises the occurrences of the various lherzolite nodule types associated with kimberlite, alkali basalt and carbonatite magmatism, taking due account of spinel compositions.

Maaløe & Aoki (1977) have given an average mode for garnet lherzolite nodules of 62.6% olivine, 30% orthopyroxene, 5% garnet, 2% clinopyroxene and 0.4% phlogopite. Using the average whole rock composition of some 61 garnet lherzolite nodules given in Table 7 col. D, and appropriate mineral compositions an average mode of roughly 62% olivine, 27% orthopyroxene, 6% garnet, 4% clinopyroxene and 1% phlogopite can be calculated. This higher figure for phlogopite includes both primary and secondary grains (Carswell 1975) as the common contamination of nodules enclosed in kimberlites by K_2O is not allowed for in the calculation of this mode. Comparison of these average modes for garnet lherzolites with that quoted earlier from Maaløe & Aoki (1977) for spinel lherzolites, indicates that in the Al-spinel lherzolites the lower content of the most aluminous phase (spinel instead of garnet) is typically complemented by an at least doubled clinopyroxene content and a somewhat higher olivine/orthopyroxene ratio.

Olivine and orthopyroxene compositions in the different lherzolite nodule types have similar Fe/(Fe+Mg) ratios–most lying within the ranges 89–93% fayalite and 90–94% enstatite, respectively. Garnets when present are chrome pyropes (Dawson & Stevens 1975). Clinopyroxenes in all cases are essentially chrome diopside but like coexisting orthopyroxenes contain appreciably more Al_2O_3 as the Cr/(Cr+Al) content of any coexisting spinel decreases.

Lherzolite nodules have metamorphic rather than igneous textures (Basu 1975; Mercier & Nicolas 1975; Harte 1977) which reflect varying degrees of deformation and recrystallisation. Harte (1977) has defined four principal textural types–namely coarse, porphyroclastic, mosaic-porphyroclastic and granuloblastic. Coarse textured nodules appear to be the dominant type in kimberlites but porphyroclastic textured nodules may be in alkali basalts (Mercier & Nicholas 1975). However, nodules with various deformation fabrics appear to be associated with all three types of magmatism under consideration (e.g. Nixon & Boyd 1973; Griffin 1973; Wallace 1975; Basu 1977; Coisy & Nicholas 1978).

Some studies have indicated correlations between textures and nodule chemistry (Nixon & Boyd 1973; Francis 1978) but more commonly between textures and equilibration temperatures as deduced from mineral compositions (Boyd & Nixon 1975; MacGregor 1975; Boyd et al. 1976; Danchin & Boyd 1976; Basu 1977). However, other studies (Harte et al. 1975; Dawson et al. 1975) have demonstrated that such correlations do not exist in lherzolite nodule suites from other localities. Thus although lherzolite nodules in kimberlites with highest apparent equilibration temperatures and pressures (Boyd 1973; Boyd et al. 1976; Danchin & Boyd 1976) have striking porphyroclastic or mosaic-porphyroclastic textures it is now clear that increased deformation does not always correlate with increased equilibration P/T conditions and hence greater implied depths of derivation. Indeed some lherzolite nodules show significant variations in the level of deformation over distances of only centimetres indicating that deformation may be very variable and localised in extent (Dawson et al. 1975).

Garnet lherzolite/spinel lherzolite stability relationships

Experimental studies (Green & Ringwood 1967; O'Hara et al. 1971) have shown that spinel lher-

Table 1. Summary of the distribution of the various lherzolite nodule types.

	Al-spinel lherzolites	Cr-spinel lherzolites	Chromite lherzolites	Al-spinel garnet lherzolites	Cr-spinel garnet lherzolites	Garnet lherzolites ±chromite
Kimberlites	New Mexico, U.S.A. (*Smith & Leavy 1976*) S.W. Greenland (*Emeleus & Andrews 1975*) Colorado-Wyoming U.S.A. (*McCallum et al. 1975*)	New Mexico, U.S.A. (*Smith & Leavy 1976*) Arctic Canada (*Mitchell 1977*) Colorado-Wyoming U.S.A. (*McCallum et al. 1975*)	South Africa (*Smith & Dawson 1975*) Lesotho (*Carswell et al. 1979*)	S.E. Australia (*Ferguson et al. 1977*)	New Mexico U.S.A.* (*Smith & Leavy 1976*) Arctic Canada* (*Mitchell 1978*)	S. Africa-Lesotho (*Carswell & Dawson 1970, Nixon & Boyd 1973, etc.*) Yakutia, U.S.S.R. (*Sobolev 1977*) S.W. Greenland (*Emeleus & Andrews 1975*) Arctic Canada (*Mitchell 1978*) Colorado-Wyoming, U.S.A. (*McCallum et al. 1975*)
Alkali basalt – Basanite – Nephelinite suite	Numerous world wide occurrences e.g. Tasmania, Australia, Japan, Hawaii, U.K. (*Varne 1977, White 1966, Kuno & Aoki 1970, Frey & Green 1974, Donaldson 1978, Ross et al. 1954, etc.*)	Ndonyuo Olnchoro Kenya (*Suwa et al. 1975*) S.E. Australia (*Frey & Green 1974*) Itinome-Gata, Japan (*Aoki & Prinz 1974*) Arizona, U.S.A. (*Frey & Prinz 1978*)		Massif Central France (*Berger & Brousse 1976, Berger 1977*) ?Itinome-Gata, Japan (*Aoki & Prinz 1974*)		Vitim Plateau, U.S.S.R. (*Volyanyuk et al. 1976*)
Lamprophyric or ankaramitic rocks associated with carbonatites	Fen, S. Norway (*Griffin 1973*)		S. Westland, New Zealand (*Wallace 1975*) Lashaine, Tanzania (*Reid et al. 1975*)			Lashaine, Tanzania (*Reid et al. 1975*)

* Questionable whether these nodules fully equilibrated as garnets occur as coronas around spinels.

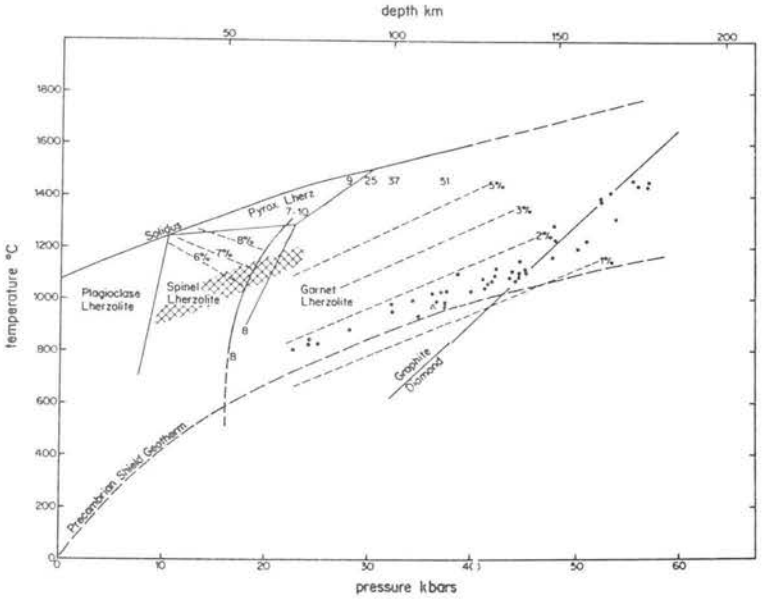

Fig. 2. P/T diagram showing a generalised field (hatched) for the likely equilibration conditions of lherzolite nodules in magmas of the alkali basalt-basanite-nephelinite suite and calculated equilibration conditions for individual garnet lherzolite nodules from kimberlite pipes in Lesotho, southern Africa (the diamond bearing garnet lherzolite nodule described by Dawson & Smith 1975b being shown by separate triangular ornament). The latter estimates were obtained from the Mori & Green (1978) calibration for $K_D^{Gnt\text{-}Cpx}{}_{Fe\text{-}Mg}$ (with all Fe taken as Fe^{2+}) and equation (1.2) of Wood (1974) for garnet-orthopyroxene equilibria (without consideration of substitution of Cr for Al in these minerals). The solid lines defining the P/T stability fields for various lherzolite assemblage types and the solidus curve correspond to those experimentally determined by Green & Ringwood (1967) for a pyrolite model composition (in fact that of Ringwood 1966 given in Table 8), whilst curve B is the experimentally determined spinel lherzolite⇌garnet lherzolite reaction boundary for natural materials from O'Hara et al (1971). Dotted lines correspond to different positions for the spinel lherzolite⇌garnet lherzolite reaction boundary for various Cr/(Cr + Al) ratios (MacGregor 1970). Approximate values for 100 Cr (Cr + Al) are indicated by the numbers alongside these and the other spinel lherzolite⇌garnet lherzolite reaction boundaries. Dashed lines represent experimentally determined isopleths for wt.% Al_2O_3 in orthopyroxenes–those in the garnet lherzolite field after MacGregor (1974), those in the spinel lherzolite field after Dixon & Presnall (1977). The Precambrian shield geotherm is from Clark & Ringwood (1964) and the graphite⇌diamond inversion curve from Bundy et al. (1961).

zolites are stable at lower pressures than garnet lherzolites. However, it is also clear that the transition pressure will increase for rock compositions with higher Cr/(Cr + Al) ratios (MacGregor 1970). Fig. 2 illustrates how the spinel lherzolite ⇌ garnet lherzolite reaction curves determined by Green & Ringwood (1967) and O'Hara et al. (1971) for whole rock compositions with 100 Cr/(Cr + Al) values of 7–10 may be expected to shift to progressively higher pressures for rocks with higher 100 Cr/(Cr + Al) values. At the same time the composition of the spinel phase stable to such increased pressures must itself become more chromiferous. It follows from this that certain Cr-spinel lherzolites and chromite lherzolites may be stable under the same pressure conditions as some garnet lherzolites.

As many lherzolite nodules have 100 Cr/(Cr + Al) values in the range 7–14 (see Tables 5 and 6) the P/T boundary between the Al-spinel lherzolite and garnet lherzolite stability fields for such nodule compositions is probably fairly close to the experimentally determined reaction curves. However, it should be noted that the pronounced curvature of the reaction curve indicated by O'Hara et al. (1971) necessitates much higher minimum pressures for garnet lherzolite stability at low temperatures than indicated by a linear extrapolation of the reaction boundary given by Green & Ringwood (1967).

Petrographic observations of rare instances of lherzolite nodules with co existing primary Al-spinels and garnets (Aoki & Prinz 1974; Berger & Brousse 1976; Ferguson et al. 1977) and of more common occurrences of lherzolite nodules with coexisting primary chromites and garnets (Nixon & Boyd 1973; Reid et al. 1975; Carswell et al. 1979) indicate that garnet lherzolite/spinel lherzolite sta-

Table 2. Temperature estimates (°C) for equilibration of garnet lherzolite nodules in N. Lesotho kimberlites–data from Nixon & Boyd (1973).

Sample No.		Two pyroxene solvus		Al^{VI}-Cr partition between pyroxenes Mysen (1976)	$K_{DFe\cdot Mg}^{Gnt\text{-}Cpx}$	$K_{DFe\cdot Mg}^{Opx\text{-}Cpx}$	$K_{DFe\cdot Mg}^{ol\text{-}Cpx}$	Mean estimate from K_D values	Average of 5 temperature estimates*		Wt.% Al_2O_3 orthopyroxene
		CMS system with Fe corr. Wells (1977)	Natural garnet lherz. comps. Mori & Green (1978)		Experimental calibration of natural garnet lherzolite assemblages Mori & Green (1978)				$\bar{x}$	σn	
Coarse (granular) garnet lherzolites	1595	*888	900	*912	*804	*815	*828	816	849	43	0.93
	1567	920	935	874	884	877	913	891	894	19	0.93
	1592	923	938	887	953	1001	1030	995	959	52	0.96
	1570	938	956	886	830	791	819	813	853	53	0.91
	1573	942	960	924	843	933	941	906	917	37	0.90
	1569	963	982	878	828	828	832	829	866	52	0.92
	1568	933	948	975	983	1158	1129	1090	1036	90	1.01
	1572	939	958	1024	1024	1202	1110	1112	1060	89	0.96
	1917	983	1003	881	973	1003	967	981	961	42	0.71
	1559B	937	960	872	994	1043	1025	1021	974	63	0.79
Porphyroclastic (sheared) garnet lherzolites	1597	1375	1477	1153	1444	1318	1251	1338	1308	100	1.35
	1596	1368	1465	1098	1455	1387	1247	1363	1311	126	1.46
	1566	1353	1467	981	1392	1360	1262	1338	1270	151	1.37
	1610	1330	1447	1074	1412	1417	1271	1367	1300	126	1.38
	1611	1314	1427	1083	1382	1375	1285	1314	1288	109	1.34
	1925	1273	1354	1063	1457	1490	1359	1435	1328	153	1.39
	1924	1258	1332	1009	1436	1475	1340	1417	1304	166	1.27
	E3	1264	1332	1012	1279	1321	1179	1260	1211	110	1.21
	1591	1244	1308	998	1232	1251	1149	1210	1175	96	0.97
	2001	1194	1260	1042	1311	1236	1191	1246	1195	88	0.97
	1582	1055	1130	885	1086	1247	1052	1128	1065	115	0.88

bility relationships are further complicated by the existence of a narrow transitional 5-phase garnet-spinel lherzolite stability field, the width of which probably increases for rock compositions with increased 100 Cr/(Cr+Al) values. Such an interpretation is supported by the preliminary experimental studies of MacGregor (1970) on the effect of Cr_2O_3 on the stability of spinel lherzolites relative to garnet lherzolites.

P/T equilibration conditions and petrogenetic implications

In recent years element partition relationships between the mineral phases in lherzolite nodules have been extensively employed to obtain estimates of their P/T conditions of equilibration (e.g. O'Hara 1967a; Boyd 1973). Most early estimates were obtained by some variant of the two pyroxene solvus geothermometer (usually heavily dependent on the Davis & Boyd (1966) experimental data for the $Mg_2Si_2O_6$-$CaMgSi_2O_6$ join at 30 Kbars) used in conjunction with consideration of the Al_2O_3 contents of the pyroxenes shown to be markedly P/T dependent (MacGregor & Ringwood 1964; O'Hara 1967b; Boyd 1970; MacGregor 1974; Akella 1976). More recently refinements have been made to the experimental calibration of the two pyroxene solvus (Nehru & Wyllie 1974; Mori & Green 1975; Lindsley & Dixon 1976) and semi-empirical extrapolations of the experimental data on simple chemical systems have been developed (Wood & Banno 1973; Wells 1977) in order at least partly to take account of the more complex chemistry of natural pyroxene pairs. In addition Mori & Green (1978) have in fact experimentally calibrated the miscibility gap for coexisting pyroxenes in natural garnet lherzolite assemblages over the range 950–1500 °C and 30–40 Kbars. Further experimentally calibrated geothermometers which can be applied to lherzolite nodule assemblages are provided by consideration of Al^{VI}–Cr partitioning between coexisting pyroxenes (Mysen 1976) and Fe^{2+}–Mg^{2+} partitioning between various mineral pairs (Mori & Green 1978).

Garnet lherzolite nodules in kimberlites

Despite the variety of calibrated geothermometers which can now be applied to garnet lherzolite assemblages there are a number of problems and uncertainties attached to the derived temperature estimates, especially for the nodules which appear to have equilibrated at the highest temperatures.

Several of these problems are illustrated by the various temperature estimates listed in Table 2 for the two contrasting textural types of garnet lherzolite nodules described by Nixon & Boyd (1973) from certain kimberlite pipes in northern Lesotho. Firstly, it may be seen that the various geothermometers yield encouragingly similar temperature estimates for most of the coarse (granular) textured nodules. From this it seems reasonable to conclude that the mineral assemblages of these particular nodules were fully equilibrated before they were incorporated and rapidly transported to the surface and also that these estimates are fairly accurate. However, there is considerable variation between the different temperature estimates obtained for the porphyroclastic (sheared) textured nodules.

The disparity between the Wells (1977) and Mori & Green (1978) two-pyroxene solvus temperatures for these latter nodules may be readily explained by the fact that the lherzolite compositions calibrated by Mori & Green (1978) were somewhat less ferriferous than these particular nodules and hence that the effect of Fe in shrinking the two pyroxene solvus (Lindsley & Munoz 1969) has not been adequately taken into account in deriving temperatures from the Mori & Green (1978) calibration. However, the consistently very much lower temperatures obtained from the Mysen (1976) calibration for Al^{VI}–Cr partitioning between the pyroxenes are clearly much more disturbing. Perhaps the fact that this method appears to give results which are broadly consistent with those obtained from other methods for nodules which appear to have equilibrated at relatively low temperatures but not for the higher temperature nodules indicates that the assumption made in calculating $K_{Al^{VI}\text{-}Cr}^{Opx\text{-}Cpx}$ values that $Al^{VI}=\Sigma Al/2$ (Mysen & Boettcher 1975) only holds for the lower temperature nodules.

If, as has been previously indicated (e.g. Boyd 1973), the higher temperature nodules have also equilibrated under higher pressures, then it is also important to explore the possibility that at least part of the disparity between the various temperature estimates may be due to failure of some of the geothermometers employed to take account of significant pressure effects on the element partition coefficients concerned. Certainly it is likely that both pyroxene miscibility relationships (Mori & Green 1975; Lindsley & Dixon 1976; Howells & O'Hara 1978) and Fe^{2+}-Mg^{2+} partitioning be-

tween mineral pairs (cf. Råheim & Green 1974; Wood 1976) are pressure as well as temperature dependent and that, at least as far as the pyroxene solvus is concerned, the pressure effect becomes more important at higher temperatures. Expectations are that increased pressure will if anything raise the $K_D^{Gnt\text{-}Cpx}_{Fe\text{-}Mg}$ values and widen the two pyroxene solvus. Thus application of a pressure correction factor would in fact raise the temperature estimates obtained from the two pyroxene solvus and from $K_D^{Gnt\text{-}Cpx}_{Fe\text{-}Mg}$ and hence enlarge the discrepancies from the Mysen (1976) values.

The K_D values used to calculate the temperatures listed in Table 2 assume, in the absence of analytically determined Fe^{2+}/Fe^{3+} values, that all Fe is divalent in these minerals. The fact that this assumption leads to temperature estimates based on K_D values which for most nodules are closely similar to values obtained from the two pyroxene solvus geothermometer (Tables 2–4) probably indicates that the Fe^{3+} contents of the silicate minerals in lherzolite nodules are usually very low. However, as analytically determined Fe^{2+}/Fe^{3+} ratios in clinopyroxenes are typically lower than in coexisting ferromagnesian silicates, these K_D values should strictly be viewed as minimum values and the corresponding temperatures as maximum values for these methods. Unfortunately calculation of Fe^{2+}/Fe^{3+} ratios for clinopyroxenes in lherzolite nodules on a charge balance basis (see for example Carswell & Griffin 1980) usually yields unrealistically low Fe^{2+}/Fe^{3+} values.

As none of the above considerations appears to provide a really convincing explanation, perhaps the variable temperature estimates for the porphyroclastic textured nodules reflect internal chemical disequilibrium within these particular nodules due to their failure to fully recrystallise and equilibrate under a particular set of P/T conditions. Comparison of the different textural types of garnet lherzolite nodules in the Matsoku pipe, northern Lesotho (Carswell & Dawson 1970; Cox et al. 1973), the Premier pipe, South Africa (Danchin & Boyd 1976) and the Udachnaya pipe, U.S.S.R. (Boyd et al. 1976; Sobolev 1977) also indicates that the highly deformed nodules typically yield more variable temperature estimates by the various methods. Since kinetic considerations (cf. Fraser & Lawless 1978; Carswell 1978) render it unlikely that Al^{VI}-Cr partitioning between pyroxenes would be adjusted more rapidly than Fe^{2+}-Mg^{2+} partitioning between the mineral phases, such an explanation might be construed to indicate that deformation and recrystallisation of these particular nodules took place in a rising rather than falling temperature environment. Such an interpretation could be compatible with the stress heating theory propounded by Boyd (1973) although recently it has been more in vogue to interpret the deformation and thermal state of these nodules as due to mantle diapirism (Green & Gueguen 1974; Dawson et al. 1975; Harte 1978).

Some petrographic observations (Kuno & Aoki 1970; Suwa et al. 1975; Carswell et al. 1979) have indicated that certain mantle derived lherzolite nodules appear to have moved out of the garnet lherzolite stability field prior to their incorporation and rapid upwards transport in magmatic rocks. Evidence for this comes from the fact that in some lherzolite nodules, pyroxenes and spinels occurring as coarse symplektite intergrowths (considered to have resulted from breakdown of original garnet) have similar compositions to, and thus appear to have equilibrated with, the discrete primary pyroxenes and spinels in the same nodules. Furthermore, although the fine grained intergrowths of secondary aluminous pyroxenes and spinels forming distinct kelyphite rims around garnets in many garnet lherzolite nodules have variable compositions and have clearly not re-equilibrated, observations that the secondary phases of symplektites formed from garnet breakdown are sometimes deformed (Lock & Dawson, personal communication) again points to garnet breakdown having occurred before rather than during incorporation and transport within the magmatic rocks. Whilst mantle lherzolites could move from the garnet lherzolite into the spinel lherzolite stability field simply as a result of a rise in the ambient temperature, the chemistries of the secondary phases resulting from garnet breakdown give no clear indication of increased temperatures (Carswell et al. 1979) and hence it seems most satisfactory to relate garnet breakdown to decompression under essentially isothermal conditions resulting from mantle convection or diapiric movements which preceded the magmatic event.

From the foregoing discussions it is clear that for many of the highly deformed garnet lherzolite nodules there remains considerable uncertainty attached to petrogenetic interpretations dependent on estimates of their equilibration temperatures. Placing particular emphasis on the temperature estimates from the Wells (1977) 'best fit' calibration of the two pyroxene solvus geothermometer and the Mori & Green (1978) calibration of $K_D^{Gnt\text{-}Cpx}_{Fe\text{-}Mg}$ as the most likely to be reliable for the majority of these nodules but taking mean estimates when

the variation between the various estimates for a particular nodule is small, it is tentatively concluded that garnet lherzolite nodules from the kimberlites of southern Africa, for which most data are currently available, have probably equilibrated over the approximate temperature range 850–1400 °C. On the basis of such temperature estimates equilibration pressures in the range 25–54 Kbars can be calculated using equation (12) of Wood (1974) for garnet-orthopyroxene equilibria. Taking only the temperature estimates from $K_D^{Gnt\text{-}Cpx}{}_{Fe\text{-}Mg}$ (Mori & Green 1978) a slightly wider P/T range of 800–1460 °C and 22.5–57.5 Kbars is indicated as illustrated on Fig. 2 for garnet lherzolite nodules in kimberlite pipes in northern Lesotho.

Unfortunately, pressure estimates for garnet lherzolites are, if anything, subject to even more uncertainty than the temperature estimates. In the first place any errors in the latter may well be compounded in the pressure estimates. In addition X_{Al}^{M1} contents of orthopyroxenes coexisting with garnets have to date been experimentally calibrated only for Cr free systems yet orthopyroxenes in lherzolite nodules have significant Cr contents and it is clear, as previously discussed, that whole rock Cr/(Cr + Al) ratios profoundly affect orthopyroxene-garnet-spinel equilibria. Taking into account substitution of Cr for Al in garnets and orthopyroxenes in the manner proposed by Wood (1974) lowers the P estimates quoted above for garnet lherzolite nodules in kimberlites by on average 4 Kbars, but the validity of such a correction may be questioned. Whilst it is encouraging to note that the P/T estimates contained in Fig. 2 extend into the diamond stability field, the only fully documented diamond bearing garnet lherzolite nodule (Dawson & Smith 1975b) in fact plots some 5 Kbars outside the diamond stability field on this calculation basis. Application of the Cr correction procedure of Wood (1974) takes this particular nodule a further 3.4 Kbars away from the diamond/graphite inversion curve of Bundy et al. (1961) and hence only enhances the problem.

There is no a priori reason to consider that the P/T estimates shown in Fig. 2 for the garnet lherzolite nodules in the kimberlites of northern Lesotho define an inflected palaeogeotherm. The inflected or kinked palaeogeotherms indicated by Boyd (1973), Boyd & Nixon (1975) and MacGregor (1975) may well just be artefacts resulting from somewhat subjective interpretation of even less accurate P/T estimates obtained by other methods (cf. Harte 1978; Howells & O'Hara 1978). The P/T equilibration conditions indicated for the garnet lherzolite nodules in the kimberlites of southern Africa are in temperature terms all somewhat elevated above the conditions predicted at upper mantle depths by the Precambrian shield geotherm of Clark & Ringwood (1964) but the nodules derived from the deepest levels appear to be particularly so. With this in mind it is of interest to consider the inferences which may be drawn from the equivalent P/T estimates from garnet lherzolite nodule suites from the kimberlites in other continents. These in fact indicate broadly similar upper mantle geotherms at the time of kimberlite emplacement beneath Yakutia, U.S.S.R. (Boyd et al. 1976; Sobolev 1977) and the Colorado-Wyoming state line region of the U.S.A. (McCallum et al. 1975), a slightly higher geotherm beneath the Arctic Canada (Mitchell 1978) and S. W. Greenland (Emeleus & Andrews 1975) regions, and a substantially higher geotherm beneath New South Wales, Australia (Ferguson et al. 1977). As greater depths are required for diamond stability with higher geotherms (Fig. 2) such variations will certainly have an important influence on the likely economic potential of the kimberlites in these different regions.

Lherzolite nodules in basaltic magmas

Estimates of equilibration temperatures for a suite of Al-spinel lherzolite nodules from Tasmanian basalts (Varne 1977) are given in Table 3. It is clear that the higher Al_2O_3 contents of the pyroxenes in these nodules, as in other lherzolite nodules of this type, restrict the extent of solid solution between the coexisting pyroxenes (Mori 1977; Herzberg 1978). Hence the Wells (1977) and Mori & Green (1978) calibrations of the two pyroxene solvus yield underestimated temperatures for these nodules. The values obtained from the Mori (1977) calibration (equation 16) for the CaO-MgO-Al_2O_3-SiO_2 system are clearly to be preferred, especially as they are closely in line with the temperature estimates based on Al^{VI}-Cr partitioning between the pyroxenes (Mysen 1976) and K_D values (Mori & Green 1978).

Equivalent equilibration temperature estimates for other suites of Al-spinel lherzolite nodules in basaltic magmas (Ross et al. 1954; Kuno & Aoki 1970; Kutolin & Frolova 1970; Frey & Green 1974, etc.) as well as those for Cr-spinel lherzolite nodules occasionally observed in such magmas (Ross et al. 1954; Frey & Green 1974; Aoki & Prinz 1974; Donaldson 1978; Frey & Prinz 1978) mostly lie within the 900–1150 °C range. As in Table 3 most

Table 3. Temperature estimates (°C) for equilibration of Al-spinel lherzolite nodules in basalts from Tasmania (Varne 1977).

Sample No.	Two pyroxene solvus			Al^{VI}-Cr partitioning between pyroxenes Mysen (1976)	$K^{Opx\text{-}Cpx}_{Fe\text{-}Mg}$	$K^{ol\text{-}Cpx}_{Fe\text{-}Mg}$	Mean estimate from K_D values	Average of preferred values (in italics)	Wt% Al_2O_3 orthopyroxene
	CMAS system Mori (1977)	CMS system with Fe corr. Wells (1977)	Natural garnet lherz. comps. Mori & Green		Experimental calibration of natural garnet lherzolite compositions Mori & Green (1978)				
1	*971*	859	887	*997*	1087	1135	*1111*	1026	3.8
2	*996*	876	903	*942*	918	963	*941*	960	3.2
3	*1067*	919	951	*1100*	1119	1135	*1127*	1098	5.2
4	*1128*	949	995	*1050*	939	992	*966*	1048	5.4
5	*1024*	888	922	*991*	801	811	*806*	940	3.2
7	*944*	848	870	–	894	966	*930*	937	3.0
8	*872*	807	826	*1064*	951	956	*954*	963	3.8
9	*1146*	968	1009	*1076*	983	960	*972*	1065	5.3
Mean values $\bar{x}$ for all 8 samples	1018	889	920	1031	959	990	976	1005	
	σn 87	50	58	52	98	98	96	58	

other lherzolite nodules in basaltic magmas yield similar temperature estimates from the various element partition coefficients but a few yield highly variable estimates suggesting that, like certain garnet lherzolites in kimberlites, they may consist of mineral assemblages which have not fully equilibrated.

Uncertainities over the slope of the Al_2O_3 isopleths for othopyroxenes stable in the Al-spinel lherzolite stability field (cf. MacGregor 1974; Herzberg & Chapman 1976; Obata 1976; Presnall 1976; Dixon & Presnall 1977) prevent calculation of unequivocal pressure values for Al-spinel lherzolite nodules. The P/T field for equilibration of lherzolite nodules associated with basaltic magmas is therefore only indicated in a generalised fashion in Fig. 2. The implied upper mantle geotherm beneath regions affected by magmatism of the alkali basalt suite type suggests (with reference to the Al-spinel lherzolite/garnet lherzolite reaction curves of Green & Ringwood 1967 and O'Hara et al. 1971) that the rare garnet bearing lherzolite nodules found in such magmas (Berger & Brousse 1976; Volyanyuk et al. 1976; Berger 1977) have come from depths of roughly 60–75 kilometres – in line with P/T estimates for such nodules of around 1200° and 20 Kbars. However, judging from the lherzolite nodules found in most magmas of the alkali basalt suite, eruptions of such magmas seem likely to have in general originated from depths less than about 60 kilometres.

The equilibration temperature estimates indicated for lherzolite nodules in such magmas clearly reflect sub-solidus recrystallisation and along with textural evidence and various geochemical considerations (e.g. Leggo & Hutchison 1968; Ringwood 1975) indicate that these lherzolite nodules, like those enclosed in kimberlites, represent mantle derived wall rock fragments incorporated during the volatile charged eruptions. They do not represent cognate cumulates derived directly from the host magmas as has sometimes been suggested (O'Hara & Mercy 1963; O'Hara 1967a).

Lherzolite nodules associated with carbonatite magmas

Al-spinel lherzolite nodules in damkjernite of the Fen carbonatite complex, south Norway (Griffin 1973) are similar in their mineralogy and chemistry to the common lherzolite nodules found in alkali basalt suite magmas. Calculated equilibration temperature estimates (Table 4) are therefore not surprisingly also similar and indicate that the upper

mantle geotherm beneath that region at the time of carbonatite emplacement was closely comparable to that normally encountered beneath regions affected by alkali basalt magmatism. On the other hand, the Lashaine carbonatite/ankaramite volcano in Tanzania (Dawson et al. 1970; Reid et al. 1975) contains chromite lherzolite and garnet lherzolite nodules with calculated mean equilibration temperatures of 920°C and 1015°C, respectively. These values combined with a calculated mean pressure estimate of 34 kbars. for the garnet lherzolites, point to a present day upper mantle geotherm beneath the Lashaine volcano closely similar to that beneath southern Africa at the time of kimberlite emplacement some 90 m.y. ago.

Lamprophyric rocks associated with carbonatite at South Westland, New Zealand were described by Wallace (1975) as containing chromite lherzolite nodules. However, the data are ambiguous as two nodules with low Al_2O_3 orthopyroxenes yield a mean equilibration temperature estimate of 960°C by the preferred methods, whilst two nodules with very much more aluminous orthopyroxenes give a mean temperature estimate of 1235°C. It would be surprising if the latter two nodules did not in fact contain Al-spinels rather than the chromites inferred by Wallace (1975).

Garnet free spinel bearing lherzolites in kimberlites

Many kimberlites contain garnet free primary spinel bearing lherzolite nodules in addition to the more common garnet lherzolite nodules. The kimberlites of southern Africa have to date only been noted to contain chromite lherzolite types (Smith & Dawson 1975; Carswell et al. 1979) but Cr-spinel lherzolites have been noted in the kimberlites of Somerset Island, Canada (Mitchell 1977) and the Colorado-Wyoming state line district, U.S.A. (McCallum et al. 1975) and Al-spinel lherzolites in kimberlites of both the latter region and S.W. Greenland (Emeleus & Andrews 1975). Equilibration temperature estimates for these various spinel lherzolite nodule types are on average some 100°C lower than those for the coarse textured garnet lherzolites in the same kimberlite pipes and hence indicate that they have usually been derived from somewhat shallower mantle depths than the associated garnet lherzolite nodules. This is in line with the previously noted similar relationship between associated chromite lherzolites and garnet lherzolites in the Lashaine carbonatite/ankaramite volcano.

Table 4. Temperature estimates (°C) for equilibration of Al-spinel lherzolite nodules in Damkjernite of Fen Carbonatite Complex, South Norway (Griffin 1973).

Sample No.	Two pyroxene solvus			Al^{VI}-Cr partitioning between pyroxenes Mysen (1976)	$K_{DFe\text{-}Mg}^{Opx\text{-}Cpx}$	$K_{DFe\text{-}Mg}^{ol\text{-}Cpx}$	Mean estimate from K_D values	Average of preferred values (in italics)	Wt.% Al_2O_3 orthopyroxene
	CMAS system Mori (1977)	CMS system with Fe corr. Wells (1977)	Natural garnet lherz. comps. Mori & Green		Experimental calibration of natural garnet lherzolite compositions Mori & Green (1978)				
1	*968*	862	885	*982*	1035	1056	*1046*	999	4.20
2	*1260*	1053	1107	*1294*	1166	1186	*1176*	1243	4.56
4	*1065*	915	950	*1019*	1019	1032	*1026*	1037	4.55
7	*1210*	1014	1062	*1005*	1112	1064	*1088*	1101	5.00
8	*978*	866	892	*956*	1136	1045	*1091*	1008	4.66
9	*894*	818	840	*875*	1246	1166	*1206*	992	4.40
10	*1002*	878	907	*1003*	1115	1091	*1103*	1036	4.47
Mean of $\bar{x}$ all 7	1054	915	949	1019	1120	1098	1105	1059	
samples σn	124	80	92	121	69	47	60	82	

Table 5. Average compositions of garnet lherzolite nodules (individual analyses recalculated to 100% on a H_2O and CO_2 free basis with all Fe expressed as FeO).

	A	B	C	D	E	F	G	H
SiO_2	46.56	45.29	46.39	43.89	47.44	44.61	43.77	44.83
TiO_2	0.08	<0.1	0.07	0.16	0.07	0.08	0.17	0.18
Al_2O_3	1.90	1.24	0.82	1.85	1.62	1.85	1.74	3.69
Cr_2O_3	0.31	0.36	0.28	0.22	0.41	0.44	0.43	0.37
FeO	6.60	7.98	6.44	8.58	6.48	6.95	7.98	8.66
MnO	0.11	0.11	0.11	0.12	0.11	0.12	0.11	0.14
NiO	0.29	0.38	0.29	0.23	0.33	0.37	nd.	nd.
MgO	42.67	43.54	44.53	42.94	42.39	44.20	44.39	39.40
CaO	1.14	0.82	0.86	1.86	1.12	1.22	1.33	3.06
Na_2O	0.18	0.16	0.10	0.21	0.14	0.17	0.24	0.23
K_2O	0.14	0.12	0.14	0.03	0.11	0.08	0.15	0.03
P_2O_5	0.04	nd.	0.06	0.00	0.03	0.08	nd.	<0.01
100 Mg/Mg+Fe	92.0	90.7	92.5	89.9	92.1	92.0	90.8	89.0
100 Cr/Cr+Al	10.1	16.3	18.6	7.9	14.8	14.2	14.2	7.4

A. 23 nodules in kimberlites of Kimberley area, South Africa (Holmes 1936; Ito & Kennedy 1967; Whitfield 1971; Berg & O'Hara 1973; Carswell & Dawson 1970; Carswell–unpublished data). B. 41 nodules in kimberlites at Bultfontein, Wesselton and Jagersfontein, South Africa (Chen 1971). C. 16 coarse (granular) nodules in kimberlites of pipe 200, Mothae, Thaba Putsoa, Liqhobong and Ngopetsoeu, Lesotho (Nixon & Boyd 1973; Carswell et al. 1979; and unpublished data). D. 6 porphyroclastic (sheared) nodules in kimberlites of Mothae and Thaba Putsoa, Lesotho (Nixon & Boyd 1973). E. 5 unbanded nodules (common peridotites) from Matsoku kimberlite, Lesotho (Cox et al. 1973; Carswell & Dawson 1970). F. 5 nodules in ankaramite/carbonatite at Lashaine Volcano, Tanzania (Rhodes & Dawson 1975; Ridley & Dawson 1975). G. 6 nodules in kimberlite of Udachnaya Pipe, Yakutia, U.S.S.R. (Sobolev 1977). H. 8 nodules in alkali basalt at Itinome-Gata, Japan. Garnets invariably replaced in these nodules (Kuno & Aoki 1970; Aoki & Shiba 1973).

Major element chemistry of lherzolite nodules and nature of the uppermost mantle

Implicit in the recognition of lherzolites as an abundant and distinctive group of nodules in various types of magmatic rocks is their relative mineralogical and chemical uniformity. This has often been stressed to substantiate the now widely accepted view (Harris et al. 1967, 1972; Carswell & Dawson 1970; Ringwood 1975, etc.) that such nodules have been derived directly from the upper mantle and hence are representative of the predominant rocks in that part of the earth. However, on the basis of the vastly increased number of whole rock analyses of lherzolite nodules which have become available in recent years it is now clear that such nodules show significant variations in their contents of the more fusible chemical components and hence have variable magma yielding potentials (Harris et al. 1972; Nixon & Boyd 1973; Hutchison et al. 1975; Shimizu & Allègre 1978; Carswell et al. 1979). In terms of major element chemistry increasing degrees of depletion in the more fusible (i.e. 'basaltic' magma yielding) constituents are reflected in decreased Al, Ca, Ti, Na and K contents and increased Mg/(Mg+Fe) and Cr/(Cr+Al) ratios.

An extensive study of the whole rock chemical variation in between 18–43 lherzolite nodules from each of five widely spaced localities in the Massif Central, France and of forty such nodules from Dreiser Weiher, Eifel, West Germany, has been reported by Hutchison et al. (1970, 1975) and Harris et al. (1972). They demonstrated significant differences in the compositions of the lherzolite nodule suites from these different localities as well as considerable variation in the level of depletion amongst nodules from individual localities. In their compilation of 384 spinel lherzolite nodule analyses (most but not all being of Al-spinel lherzolite type and from alkali basalt suite magmas) Maaløe & Aoki (1977) pointed to similarities in the mean compositions for such nodules from both continental and oceanic environments but likewise recognised an overall chemical variation thought to encompass both undepleted and depleted upper mantle compositions.

Hutchinson et al. (1975) reported that garnet lherzolite nodules from the Bultfontein kimberlite in South Africa are no less depleted than spinel lherzolite nodules in several alkali basalt localities in the Massif Central. On the other hand, comparison by Maaløe & Aoki (1977) of 202 garnet lherzolite nodule analyses (mostly from the kimberlites of southern Africa) with the 384 spinel lherzolite

analyses indicated significant overall differences in chemical composition, although there is undoubtedly some overlap in the composition ranges of the two groups of lherzolite nodules. They did not consider these differences as evidence of a systematic variation in the chemical composition of the mantle with depth but rather as a reflection of an anomalous upper mantle composition beneath Africa.

The fact is, however, that even in southern Africa there are significant differences in the chemical composition of lherzolite nodules brought up at different localities. The composition data for garnet lherzolite nodules in Table 5 shows, for example, how on average such nodules in the Kimberley area kimberlites have significantly less depleted chemical compositions than the coarse equigranular textured nodules in many of the kimberlites of northern Lesotho (col. C). Moreover even in northern Lesotho, garnet lherzolite nodules in the Matsoku kimberlite pipe appear to be less depleted than say those in Pipe 200 (Carswell et al. 1979) only some 25 kilometres away. Such observations suggest significant lateral variations in the chemical composition of the upper mantle over quite small distances.

In addition it should be noted that the average compositions for lherzolite nodules given in Tables 5 and 6 themselves conceal a fair amount of variation in the level of depletion amongst nodules from individual localities, which can only reflect variable levels of depletion at different depths in the mantle. Nixon & Boyd (1973) have observed that porphyroclastic (sheared) textured garnet lherzolite nodules in two of the kimberlite pipes in northern Lesotho have notably less depleted chemical compositions than the coarse (granular) textured garnet lherzolites in the same pipes (compare cols. C and D in Table 5). As P/T estimates (see Table 2 and related discussion) point to a deeper level origin in the mantle for the former group of nodules, indications are that, at least beneath these particular pipes, the mantle becomes less depleted with depth. On the other hand, Smith & Levy (1976) have deduced that the upper mantle beneath the Green Knobs diatreme on the Colorado Plateau, U.S.A. becomes more depleted with depth–a zone of Al-spinel lherzolite overlying more depleted garnet lherzolite. However, this deduction was based on comparison of the mineral chemistry of xenocrysts (thought to represent disaggregated garnet lherzolites) with that of the Al-spinel lherzolite nodules, not on direct comparison of whole rock nodule compositions.

Further evidence that, at least beneath southern Africa, the upper mantle becomes less depleted with depth is provided by consideration of the relationships between garnet lherzolite and spinel lherzolite nodules. Fig. 2 illustrates that Al-spinel lherzolites can be expected to be stable to higher pressures at increased temperatures and hence that the depth in the mantle at which garnet lherzolites are likely to be encountered will increase for regions with higher upper mantle geotherms. The fact that Al-spinel lherzolites are the common nodule type in magmas of the alkali basalt suite whilst garnet lherzolites are dominant in most kimberlites can therefore be attributed to the combined effects of a typically steeper geotherm in the mantle beneath areas of alkali basaltic volcanism and a shallower depth of origin for this type of magmatism.

Rare occurrences of garnet lherzolite nodules associated with basanitic volcanism (Berger & Brousse 1976; Berger 1977; Volyanyuk et al. 1976) are taken to indicate that occasionally such magmas are erupted from depths ($\simeq$60–75 kms–Fig. 2) which lie within the garnet lherzolite stability field. On the other hand, occurrences of Al-spinel lherzolites in the kimberlites of S.W.Greenland and the Colorado Plateau, U.S.A. when contrasted with their apparent absence in the kimberlites of southern Africa and Yakutia, U.S.S.R., probably at least in part reflect higher upper mantle geotherms beneath these former regions. However, the fact that Al-spinel lherzolites have also been reported from the kimberlites of the Colorado-Wyoming state line district U.S.A. for which a similar upper mantle geotherm to that beneath southern Africa and Yakutia at the time of kimberlite emplacement has been deduced (McCallum et al. 1975) is compatible with the curved Al-spinel lherzolite garnet lherzolite reaction boundary determined by O'Hara et al. 1971 which may be taken to indicate that even under continental shield areas characterised by low heat flows, the uppermost mantle (approximately a 10–15 kilometres thick zone) may be expected to lie in the Al-spinel lherzolite stability field. With this in mind it is considered that the apparent absence of Al-spinel lherzolites in the much studied kimberlites of southern Africa and Yakutia, U.S.S.R., must reflect the fact that the uppermost mantle beneath these areas has a more highly depleted refractory, residual type chemical composition with a higher $Cr/(Cr+Al)$ ratio.

In the kimberlites of southern Africa the uppermost mantle is therefore considered to be represented by the nodules of chromite lherzolites and

Table 6. Average compositions of spinel lherzolite nodules (individual analyses recalculated to 100% on a H_2O and CO_2 free basis with all Fe expressed as FeO).

	A	B	C	D	E	F	G	H	I
SiO_2	44.20	44.64	44.24	44.48	44.79	44.85	42.30	45.31	42.91
TiO_2	0.13	0.05	0.16	0.18	0.12	0.08	tr.	0.11	0.08
Al_2O_3	2.05	2.24	2.18	1.80	3.23	2.11	1.21	0.43	0.52
Cr_2O_3	0.44	0.45	0.23	0.42	0.36	0.42	0.35	0.25	0.36
FeO	8.29	8.09	8.36	8.90	8.61	8.00	6.89	6.52	7.34
MnO	0.13	0.12	0.13	0.14	0.12	0.10	0.17	0.09	0.12
NiO	0.28	0.27	0.30	nd.	nd	0.28	0.18	0.34	0.42
MgO	42.21	41.69	42.70	41.77	39.46	41.53	48.26	46.03	47.54
CaO	1.92	2.25	1.57	2.34	2.70	2.34	0.44	0.56	0.54
Na_2O	0.27	0.16	0.12	0.13	0.35	0.25	0.10	0.13	0.08
K_2O	0.06	0.03	0.03	0.04	0.12	0.01	0.04	0.17	0.04
P_2O_5	0.03	nd.	0.02	<0.01	0.05	nd.	0.06	0.04	0.02
100 Mg/Mg + Fe	90.1	90.2	90.1	89.3	89.1	90.2	92.6	92.6	92.0
100 Cr/Cr + Al	12.6	11.9	6.6	13.5	7.0	11.8	16.2	28.1	31.7

A. 384 nodules mostly in alkali basalt suite and mostly, but not exclusively, Al-spinel lherzolite types (Maaloe & Aoki 1977). B. 150 nodules in alkalic basalts from Massif Central, France (Hutchison et al. 1970). C. 7 Al-spinel lherzolite nodules in ankaramite from Calton Hill, Derbyshire (Hamad 1963; Carswell–unpublished data). D. 13 Al-spinel lherzolite nodules in alkali basalt in Itinome-Gata, Japan (Kuno & Aoki 1970; Aoki & Shiba 1973). E. 4 Al-spinel lherzolite nodules in Damkjernite of Fen Carbonatite Complex, south Norway (Griffin 1973). F. 3 Al-spinel lherzolite nodules in kimberlite at Green Knobs, New Mexico, U.S.A. (Smith & Leavy 1976). G. 3 Cr-spinel lherzolite nodules in nephelinite at Ndonyuo Olnchoro, Kenya (Suwa et al. 1975). H. 5 chromite lherzolite nodules in kimberlites of pipe 200 and Ngopetsoeu, Lesotho (Carswell et al. 1979 and unpublished data). I. 2 chromite lherzolite nodules in ankaramite carbonatite of Lashaine Volcano, Tanzania (Rhodes & Dawson 1975).

chromite or Cr-spinel bearing harzburgites (Smith & Dawson 1975; Carswell et al. 1979). Comparison of whole rock analyses shows that chromite lherzolite nodules have more depleted compositions than both Al-spinel lherzolites from elsewhere (Table 6) and associated garnet lherzolites (Table 5). Thus the present evidence from the nodules occurring in the kimberlites of southern Africa points to an upper mantle stratigraphy beneath that region which comprises an uppermost highly depleted zone predominantly of chromite lherzolite and chromite or Cr-spinel harzburgite (probably of the order of 40 kilometres thick) overlying a zone in which garnet lherzolites predominate but become less depleted at increased depths. Further support for such an interpretation comes from the typically somewhat lower equilibration temperatures indicated for the chromite lherzolite nodules when compared with associated garnet lherzolites.

The presence of chromite lherzolites and harzburgites together with garnet lherzolites as nodules in the Lashaine carbonatite/ankaramite volcano, Tanzania (Reid et al. 1975) and of Cr-spinel lherzolites and harzburgites in nephelinite at Ndonyno Olnchoro volcano, Kenya (Suwa et al. 1975) and the absence of Al-spinel lherzolite nodules in both of these recent volcanoes, strongly suggests that the highly depleted chemical character of the uppermost mantle beneath southern Africa recorded by the Late Cretaceous kimberlites currently extends to beneath East Africa. The occurrence of xenocrysts of particularly chromiferous pyrope garnets of likely lherzolite paragenesis in certain kimberlites in Yakutia, U.S.S.R. (Sobolev et al. 1973) as also in certain pipes in northern Lesotho (see Carswell et al. 1979), is taken to indicate high levels of depletion of the upper mantle to unusually deep levels beneath parts of both these regions.

Observations that in Africa lherzolite nodules of highly depleted chemical character are variously contained in kimberlite, nephelinite and carbonatite/ankaramite magmas and that Al-spinel lherzolite nodules in the kimberlite at Green Knobs, New Mexico, U.S.A. and in the damkjernite of the Fen carbonatite complex, south Norway have closely similar compositions to the common lherzolite nodules found elsewhere in magmas of the alkali basalt suite (Table 6) invalidate any assumption that the uppermost mantle beneath areas of alkali basalt-basanite-nephelinite magmatism normally has a somewhat less depleted chemical composition to that beneath areas of kimberlite or carbonatite magmatism. Instead currently available lherzolite nodule data support the contention that the uppermost mantle beneath a large part of Africa has a more highly depleted chemical com-

Table 7. Lherzolite nodule compositions compared to pyrolite mantle compositions (individual analyses recalculated to 100% on a H_2O and CO_2 free basis with all Fe expressed as FeO).

	A	B	C	D
SiO_2	45.20	45.1	44.2	45.89
TiO_2	0.71	0.2	0.13	0.09
Al_2O_3	3.54	4.6	2.05	1.57
Cr_2O_3	0.43	0.3	0.44	0.32
FeO	8.47	7.9	8.29	6.91
MnO	0.14	0.1	0.13	0.11
NiO	0.20	0.2	0.28	0.29
MgO	37.48	38.1	42.21	43.46
CaO	3.08	3.1	1.92	1.16
Na_2O	0.57	0.4	0.27	0.16
K_2O	0.13	0.02	0.06	0.12
P_2O_5	0.06	0.02	0.03	0.04
100 Mg/Mg + Fe	88.7	89.6	90.1	91.8
100 Cr/Cr + Al	7.5	4.2	12.6	12.0

A. Pyrolite model composition (Ringwood 1966); B. Average mantle pyrolite composition (Ringwood 1975); C. Average of 384 spinel lherzolite nodules (Maaløe & Aoki 1977); D. Average of 61 garnet lherzolite nodules, mostly in kimberlites but also in Lashaine ankaramite/carbonatite volcano. Note that the data of Chen (1971) are deliberately excluded from this average on the grounds of incompatibility, especially in Al_2O_3 contents and Mg/(Mg + Fe) ratios, with data from other sources on equivalent nodules from the same localities.

position than beneath other regions affected by kimberlite, carbonatite or alkali basaltic magmatism, with the possible exception of Yakutia, U.S.S.R.

The data in Table 7 demonstrate that the upper mantle compositions indicated by averaged lherzolite nodule compositions are significantly depleted in potential basaltic magma yielding constituents relative to the pyrolite model compositions for primitive or pristine mantle of Ringwood (1966, 1975). Indeed Ringwood (1975) has proposed that the uppermost mantle, as represented by ultramafic nodules and alpine type peridotites, has a dominantly refractory residual composition which reflects the fact that any basaltic component has already been extracted. Certainly the amounts of garnets, spinels and clinopyroxenes in some lherzolite nodules are sufficiently low that at solidus temperatures these minerals may well have been entirely occluded within refractory magnesian olivines and orthopyroxenes. However, the evidence from the various lherzolite nodule suites strongly indicates the existence of significant lateral and vertical variations in the level of depletion of the uppermost mantle and is taken to support previous suggestions (Hutchison et al. 1975; Maaløe & Aoki 1977) that the chemical composition range exhibited by lherzolite nodules effectively encompasses that of both residual 'depleted' and primitive 'undepleted' mantle. Nevertheless there may well normally be an overall chemical zonation to the upper mantle above the asthenophere with the level of depletion in basaltic magma yielding constituents decreasing with depth.

Concluding remarks

It is apparent that lherzolite nodules represent an abundant and coherent group of comparatively uniform mineralogy and chemistry but that there are nevertheless important variations in the nature and composition of the stable alumina-rich mineral phases (spinel and or garnet) complemented by changes in the modal content and chemical composition of associated pyroxenes. The minerals spinel and garnet show an overall antipathetic relationship but some nodules contain coexisting primary spinels and garnets and it is clear that spinel-garnet stability relationships are complex and are determined by chemical (notable Cr (Cr + Al) ratio) as well as physical (P T) controls. Spinel lherzolites are stable at lower pressures than garnet lherzolites, but the transition pressure increases for more refractory rock compositions. Hence whole rock chemical data, notably Cr (Cr + Al) ratios, are required and must be closely matched to experimentally studied compositions before precise pressure estimates can be obtained for the various lherzolite nodule types. The construction of accurate upper mantle stratigraphic profiles on the basis of observed nodule suites must therefore await a more detailed experimental calibration of garnet-spinel-pyroxenes equilibria in Cr-bearing ultrabasic rock compositions.

The range of spinel compositions in lherzolites is such that it is unsatisfactory to refer to all such nodules simply as spinel lherzolites. Instead it is proposed that the names Al-spinel lherzolite, Cr-spinel lherzolite and chromite lherzolite should be employed depending on spinel compositions. It is also desirable to note whether or not garnet lherzolites contain primary spinel and if so, of which composition type.

Correlations between textures and nodule chemistry or between textures and equilibration temperatures and hence depths derivation have been recorded in certain lherzolite nodule suites in both kimberlites and magmas of the alkali basalt suite but clearly do not hold in all cases. Previous

suggestions of significant inflections in upper mantle palaeogeotherms beneath some regions are considered to be unsubstantiated, especially when due allowance is made for current uncertainties in the pressure/temperature estimates for garnet lherzolite nodules.

Lherzolite nodules both from individual and widely separated localities have somewhat variable contents of the more fusible chemical components indicating that significant vertical and lateral variations exist in the chemical composition and hence 'basaltic' magma yielding potential of the upper mantle. Nodule evidence suggests that the uppermost mantle beneath much of southern, as well as possibly eastern, Africa and Yakutia, U.S.S.R. is particularly depleted in such constituents but that the level of depletion decreases markedly with depth.

Some recent studies of lherzolite nodule suites have provided only compositions of coexisting minerals. However, it is desirable that such data be combined with whole rock composition data. Only then can one reliably assess to what extent the presence of spinel instead of, or in addition to, garnet in particular nodules is due to chemical rather than pressure/temperature controls. In addition such integrated studies, especially if they include REE data, might hopefully lead to a more satisfactory characterization of 'pristine' as opposed to 'depleted' upper mantle compositions than currently exists.

Acknowledgements. – The author's research in this field has been supported by grants from The Royal Society and the Natural Environment Research Council. J. B. Dawson and S. Maaløe are thanked for their constructive reviews of the manuscript and F.G.F. Gibb for his assistance with writing a computer programme to handle the pressure/temperature calculations.

References

Akella, J. 1976: Garnet pyroxene equilibria in the system $CaSiO_3$-$MgSiO_3$-Al_2O_3 and in a natural mineral mixture. *Am. Mineral. 61*, 589–598.

Aoki, K. & Prinz, M. 1974: Chromium spinels in lherzolite inclusions from Itinome-gata, Japan. *Contrib. Mineral. Petrol. 46*, 249–256.

Aoki, K. & Shiba, I. 1973: Pyroxenes from lherzolite inclusions of Itinome-gata, Japan. *Lithos 6*, 41–51.

Basu, A. R. 1975: Hot spots, mantle plumes and a model for the origin of ultramafic xenoliths in alkali basalts. *Earth Planet. Sci. Lett. 28*, 261–274.

Basu, A. R. 1977: Olivine-spinel equilibria in lherzolite xenoliths fom San Quintin, Baja, California. *Earth Planet. Sci. Lett. 33*, 443–450.

Berg, W. & O'Hara, M. J. 1973: Source mantle, residuum and partial melt compositions deduced from the kimberlite record. *Ext. Abst. 1st Intern. Kimberlite Conf., Cape Town, S. Africa*, 31–33.

Berger, E. 1977: Sur la presence d'une lherzolite à granats en enclave dans le basalte alcalin de la Vestide du Pal (Ardeche): Conditions d'equilibre, implications pétrogénétiques et geotectoniques. *C. R. Acad. Sci. Paris, Ser. D. 284*, 709–712.

Berger, E. & Brousse, R. 1976: Une lherzolite à granats du pipe d'Eglazines (Lozère, France) stabilisée a 1400 C et 30 Kbar. *C. R. Acad. Sci. Paris, Ser. D. 282*, 1477–1480.

Boyd, F. R. 1970: Garnet peridotites and the system $CaSiO_3$-$MgSiO_3$-Al_2O_3. *Mineral. Soc. Am. Spec. Pap. 3*, 63–67.

Boyd, F. R. 1973: A pyroxene geotherm. *Geochim. Cosmochim. Acta 37*, 2533–2546.

Boyd, F. R., Fujii, T. & Danchin, R. V. 1976: A noninflected geotherm for the Udachnaya kimberlite pipe, U.S.S.R. *Carnegie Inst. Wash. Year Book, 75*, 523–531.

Boyd, F. R. & Nixon, P. H. 1975: Origins of the ultramafic nodules from some kimberlites of northern Lesotho and the Monastery Mine, South Africa. *Phys. Chem. Earth 9*, 431–454.

Bundy, F. R., Bovenkerk, H. P. & Strong, H. M. 1961: Diamond graphite equilibrium line from growth and graphitisation of diamond. *J. Chem. Phys. 35*, 383–391.

Carswell, D. A. 1975: Primary and secondary phologopites and clinopyroxenes in garnet lherzolite xenoliths. *Phys. Chem. Earth 9*, 417–429.

Carswell, D. A. 1978: Palaeogeotherms: implications of disequilibrium in garnet lherzolite xenoliths. *Nature 276*, 737.

Carswell, D. A. & Dawson, J. B. 1970: Garnet peridotite xenoliths in South African kimberlite pipes and their petrogenesis. *Contrib. Mineral. Petrol. 25*, 163–184.

Carswell, D. A., Clarke, D. B. & Mitchell, R. H. 1979: The petrology and geochemistry of ultramafic nodules from Pipe 200, northern Lesotho. *Proc. Second Intern. Kimberlite Conf. Vol. 2*, 127–144. Am. Geophys. Union.

Carswell, D. A. & Griffin, W. L. 1980: Calculation of equilibration conditions for garnet granulite and garnet websterite nodules in African kimberlite pipes. Submitted to *Contrib. Mineral. Petrol.*

Chen, J. C. 1971: Petrology and chemistry of garnet lherzolite nodules in kimberlite from South Africa. *Am. Mineral. 56*, 2098–2110.

Clark, S. P., Jr. & Ringwood, A. E. 1964: Density distribution and constitution of the mantle. *Rev. Geophys. 2*, 35–88.

Coisy, P. & Nicolas, A. 1978: Regional structure and geodynamics of the upper mantle beneath the Massif Central. *Nature 274*, 429–432.

Cox, K. G., Gurney, J. J. & Harte, D. 1973: Xenoliths from the Matsoku Pipe. In Nixon, P. H. (ed.), *Lesotho Kimberlites*, Lesotho National Devel. Corp. Maseru, Lesotho. pp. 76–92.

Danchin, R. V. & Boyd, F. R. 1976: Ultramafic nodules from the Premier Kimberlite pipe, South Africa. *Carnegie Inst. Wash. Year Book 75*, 531–538.

Davis, B. T. C. & Boyd, F. R. 1966: The join $Mg_2Si_2O_6$-$CaMgSi_2O_6$ at 30 kilobars pressure and its application to pyroxenes from kimberlites. *J. Geophys. Res. 71*, 3507–3576.

Dawson, J. B., Gurney, J. J. & Lawless, P. J. 1975: Palaeogeothermal gradients derived from xenoliths in kimberlite. *Nature 257*, 299–300.

Dawson, J. B., Powell, D. G. & Reid, A. M. 1970: Ultrabasic xenoliths and lava from the Lashaine volcano, Northern Tanzania. *J. Petrol. 11*, 519–548.

Dawson, J. B. & Smith, J. V. 1975a: Chromite-silicate intergrowths in upper mantle peridotites. *Phys. Chem. Earth 9*, 339–350.

Dawson, J. B. & Smith, J. V. 1975b: Occurrence of diamond in a mica-garnet lherzolite xenolith from kimberlite. *Nature 254*, 580–581.

Dawson, J. B. & Stevens, W. E. 1975: Statistical classification of garnets from kimberlite and associated xenoliths. *J. Geol. 83*, 589–607.

Dixon, J. R. & Presnall, D. C. 1977: Geothermometry and geobarometry of synthetic spinel lherzolite in the system CaO-MgO-Al_2O_3-SiO_2. *Ext. Abst. 2nd Intern. Kimberlite Conf.* New Mexico, U.S.A.

Donaldson, C. H. 1978: Petrology of the uppermost upper mantle deduced from spinel-lherzolite and harzburgite nodules at Calton Hill, Derbyshire. *Contrib. Mineral. Petrol. 65*, 363–377.

Emeleus, C. H. & Andrews, J. R. 1975: Mineralogy and petrology of kimberlite dyke and sheet intrusions and included peridotite xenoliths from south-west Greenland. *Phys. Chem. Earth 9*, 179–197.

Erlank, A. J. 1973: Kimberlite potassic richterite and the distribution of potassium in the upper mantle. *Ext. Abst. 1st Intern. Kimberlite Conf. Cape Town, South Africa*, 103–106.

Ferguson, J., Ellis, D. J. & England, R. N. 1977: Unique spinel-garnet lherzolite inclusion in kimberlite from Australia. *Geology 5*, 278–280.

Francis, D. M. 1978: The implications of the compositional dependence of texture in spinel lherzolite xenoliths, *J. Geol. 86*, 473–485.

Fraser, D. G. & Lawless, P. J. 1978: Palaeogeotherms: Implications of disequilibrium in garnet lherzolite xenoliths. *Nature 273*, 220–221.

Frey, F. A. & Green, D. H. 1974: The mineralogy, geochemistry and origin of lherzolite inclusions in Victorian basanites. *Geochim. Cosmochim. Acta 38*, 1023–1059.

Frey, F. A. & Prinz, M. 1978: Ultramafic inclusions from San Carlos, Arizona: petrologic and geochemical data bearing on their petrogenesis. *Earth Planet. Sci. Lett. 38*, 129–176.

Green, D. H. & Ringwood, A. E. 1967: The stability fields of aluminous pyroxene peridotite and garnet peridotite and their relevance in upper mantle structure. *Earth Planet. Sci. Lett. 3*, 151–160.

Green, H. W. & Gueguen, Y. 1974: Origin of kimberlite pipes by diapiric upwelling in the upper mantle. *Nature 249*, 617–620.

Griffin, W. L. 1973: Lherzolite nodules from the Fen alkaline complex, Norway. *Contrib. Mineral. Petrol. 38*, 135–146.

Gurney, J. J., Harte, B. & Cox, K. G. 1975: Mantle xenoliths in the Matsoku kimberlite pipe. *Phys. Chem. Earth 9*, 507–523.

Hamad, S. el D. 1963: The chemistry and mineralogy of the olivine nodules of Calton Hill, Derbyshire. *Mineral. Mag. 33*, 483–497.

Harris, P. G., Hutchinson, R. & Paul, D. K. 1972: Plutonic xenoliths and their relation to the upper mantle. *Phil. Trans. R. Soc. Lond. A, 271*, 313–323.

Harris, P. G., Reay, A. & White, I. G. 1967: Chemical compositions of the upper mantle. *J. Geophys. Res. 72*, 6359–6369.

Harte, B. 1977: Rock nomenclature with particular relation to deformation and recrystallisation textures in olivine-bearing xenoliths. *J. Geol. 85*, 279–288.

Harte, B. 1978: Kimberlite nodules, upper mantle petrology, and geotherms. *Phil. Trans. R. Soc. Lond. A. 288*, 487–500.

Harte, B., Cox, K. G. & Gurney, J. J. 1975: Petrography and geological history of upper mantle xenoliths from the Matsoku kimberlite pipe. *Phys. Chem. Earth 9*, 477–506.

Herzberg, C. T. 1978: Pyroxene geothermometry and geobarometry: experimental and thermodynamic evaluation of some subsolidus phase relations involving pyroxenes in the system CaO-MgO-Al_2O_3-SiO_2. *Geochim. Cosmochim. Acta 42*, 945–957.

Herzberg, C. T. & Chapman, N. A. 1976: Clinopyroxene geothermometry of spinel lherzolites. *Am. Mineral. 61*, 626–637.

Holmes, A. 1936: A contribution to the petrology of kimberlite and its inclusions. *Trans. Geol. Soc. S. Africa 39*, 379–428.

Howells, S. & O'Hara, M. J. 1978: Low solubility of alumina in enstatite and uncertainties in estimated palaeogeotherms. *Phil. Trans. R. Soc. Lond. A. 288*, 471–486.

Hutchison, R., Chambers, A. L., Paul, D. K. & Harris, P. G. 1975: Chemical variation among French ultramafic xenoliths–evidence for a heterogeneous upper mantle. *Mineral. Mag. 40*, 153–170.

Hutchison, R., Paul, D. K. & Harris, P. G. 1970: Chemical composition of the upper mantle. *Mineral. Mag. 37*, 726–729.

Ito, K. & Kennedy, G. C. 1967: The melting and phase relations in a natural peridotite to 40 kilobars. *Am. J. Sci. 265*, 519–538.

Kuno, H. & Aoki, K. 1970: Chemistry of ultramafic nodules and their bearing on the origin of basaltic magmas. *Phys. Earth Planet. Interiors 3*, 273–301.

Kutolin, V. A. & Frolova, V. M. 1970: Petrology of ultrabasic inclusions from basalts of Minusa and Transbaikailian regions (Siberia, U.S.S.R.). *Contrib. Mineral. Petrol. 29*, 163–179.

Leggo, P. J. & Hutchison, R. 1968: A Rb-Sr isotope study of ultrabasic xenoliths and their basaltic host rocks from the Massif Central, France. *Earth Planet. Sci. Lett. 5*, 71–75.

Lindsley, D. H. & Dixon, S. A. 1976: Diopside-enstatite equilibria at 850° to 1400 °C, 5 to 35 kb. *Am. J. Sci. 276*, 1285–1301.

Lindsley, D. H. & Munoz, J. L. 1969: Subsolidus relations along the join hedenbergite-ferrosilite. *Am. J. Sci. 267A*, 295–324.

Maaløe, S. & Aoki, K. 1977: The major element composition of the upper mantle estimated from the composition of lherzolites. *Contrib. Mineral. Petrol. 63*, 161–173.

MacGregor, I. D. 1970: The effect of CaO, Cr_2O_3, Fe_2O_3 and Al_2O_3 on the stability of spinel and garnet peridotites. *Phys. Earth Planet. Interiors 3*, 372–377.

MacGregor, I. D. 1974: The system MgO-Al_2O_3-SiO_2: solubility of Al_2O_3 in enstatite for spinel and garnet peridotite compositions. *Am. Mineral. 59*, 110–119.

MacGregor, I. D. 1975: Petrologic and thermal structure of the upper mantle beneath South Africa in the Cretaceous. *Phys. Chem. Earth 9*, 455–466.

MacGregor, I. D. & Ringwood, A. E. 1964. The natural system enstatite-pyrope. *Carnegie Inst. Wash. Year Book 63*, 161–163.

McCallum, M. E., Eggler, D. H. & Burns, L. K. 1975: Kimberlitic diatremes in northern Colorado and southern

Wyoming. *Phys. Chem. Earth 9*, 149–161.

Mercier, J.-C. C. & Nicolas, A. 1975: Textures and fabrics of upper mantle peridotites as illustrated by xenoliths from basalts. *J. Petrol. 16*, 454–487.

Mitchell, R. H. 1977: Ultramafic xenoliths from the Elwin Bay kimberlite, the first Canadian paleogeotherm. *Can. J. Earth Sci. 14*, 1202–1210.

Mitchell, R. H. 1978: Garnet lherzolite from Somerset Island, Canada and aspects of the nature of perturbed geotherms. *Contrib. Mineral. Petrol. 67*, 341–347.

Mori, T. 1977: Geothermometry of spinel lherzolites. *Contrib. Mineral. Petrol. 59*, 261–279.

Mori, T. & Green, D. H. 1975: Pyroxenes in the system $Mg_2Si_2O_6$-$CaMgSi_2O_6$. *Earth Planet Sci. Lett. 26*, 277–286.

Mori, T. & Green, D. H. 1978: Laboratory duplication of phase equilibria observed in natural garnet lherzolites. *J. Geol. 86*, 83–97.

Mysen, B. O. 1976: Experimental determination of some geochemical parameters relating to conditions of equilibration of peridotite in the upper mantle. *Am. Mineral. 61*, 677–683.

Mysen, B. O. & Boettcher, A. L. 1975: Melting of a hydrous mantle: II. Geochemistry of crystals and liquids formed by anatexis of mantle peridotite at high pressures and high temperatures as a function of controlled activities of water, hydrogen and carbon dioxide. *J. Petrol. 16*, 546–593.

Nehru, C. E. & Wyllie, P. J. 1974: Electron-microprobe measurements of pyroxenes coexisting with H_2O undersaturated liquid in the join $CaMgSi_2O_6$-$Mg_2Si_2O_6$-H_2O, at 30 kilobars with application to geothermometry. *Contrib. Mineral. Petrol. 48*, 221–228.

Nixon, P. H. & Boyd, F. R. 1973: Petrogenesis of the granular and sheared ultrabasic nodule suite in kimberlites. In Nixon, P. H. (ed.), *Lesotho Kimberlites*, Lesotho National Devel. Corp. Maseru, Lesotho, pp. 48–56.

Obata, M. 1976: The solubility of Al_2O_3 in orthopyroxenes in spinel and plagioclase peridotites and spinel pyroxenite. *Am. Mineral. 61*, 804–816.

O'Hara, M. J. 1967a: Crystal-liquid equilibria and the origins of ultramafic nodules in basic igneous rocks. In Wyllie, P. J. (ed.), *Ultramafic and Related Rocks*, Wiley, New York, pp. 346–349.

O'Hara, M. J. 1967b: Mineral paragenesis in ultrabasic rocks. In Wyllie, P. J. (ed.), *Ultramafic and Related Rocks*, Wiley, New York, pp. 393–403.

O'Hara, M. J. & Mercy, E. L. P. 1963: Petrology and petrogenesis of some garnetiferous peridotites. *Trans. Roy. Soc. Edinb. 65*, 251–314.

O'Hara, M. J., Richardson, S. W. & Wilson, G. 1971: Garnet peridotite stability and occurrence in crust and mantle. *Contrib. Mineral. Petrol. 832*, 48–68.

Presnall, D. C. 1976: Alumina content of enstatite as a geobarometer for plagioclase and spinel lherzolites. *Am. Mineral. 61*, 582–588.

Råheim, A. & Green, D. H. 1974: Experimental determination of the temperature and pressure dependence of the Fe-Mg partition coefficient for coexisting garnet and clinopyroxene. *Contrib. Mineral. Petrol. 48*, 179–203.

Reid, A. M. & Dawson, J. B. 1972: Olivine-garnet reaction in peridotites from Tanzania. *Lithos 5*, 115–124.

Reid, A. M., Donaldson, C. H., Brown, R. W., Ridley, W. I. & Dawson, J. B. 1975: Mineral chemistry of peridotite xenoliths from the Lashaine volcano, Tanzania. *Phys. Chem. Earth 9*, 525–543.

Rhodes, J. M. & Dawson, J. B. 1975: Major and trace element chemistry of peridotite inclusions from the Lashaine volcano, Tanzania. *Phys. Chem. Earth 9*, 545–557.

Ridley, I. W. & Dawson, J. B. 1975: Lithophile trace element data bearing on the origin of peridotite xenoliths, ankaramite and carbonatite from Lashaine volcano, N. Tanzania. *Phys. Chem. Earth 9*, 559–569.

Ringwood, A. E. 1966: The chemical composition and origin of the earth. In Hurley, P. (ed.), *Advances in Earth Sciences*, M.I.T. Press, Cambridge, Mass., pp. 287–356.

Ringwood, A. E. 1975: *Composition and Petrology of the Earth's Mantle*, McGraw Hill, New York. 618 pp.

Ross, C. S., Foster, M. D. & Myers, A. T. 1954: Origin of dunites and of olivine rich inclusions in basaltic rocks. *Am. Mineral. 39*, 693–737.

Shimizu, N. & Allègre, C. J. 1978: Geochemistry of transition elements in garnet lherzolite nodules in kimberlites. *Contrib. Mineral. Petrol. 67*, 41–50.

Smith, D. & Levy, S. 1976: Petrology of the Green Knobs diatreme and implications for the upper mantle below the Colorado Plateau. *Earth Planet Sci. Lett. 29*, 107–125.

Smith, J. V. & Dawson, J. B. 1975: Chemistry of Ti-poor spinels, ilmenites and rutiles from peridotite and eclogite xenoliths. *Phys. Chem. Earth 9*, 309–322.

Sobolev, N. V. 1977: *Deep-Seated Inclusions in Kimberlites and the Problem of the Composition of the Upper Mantle*. Am. Geophys. Union, Washington. 279 pp.

Sobolev, N. V., Laurentev, Yu. G., Pokhilenko, N. P. & Usova, L. V. 1973: Chrome-rich garnets from the kimberlites of Yakutia and their paragenesis. *Contrib. Mineral. Petrol. 40*, 39–52.

Suwa, K., Yusa, Y. & Kishida, N. 1975: Petrology of peridotite nodules from Ndonyno Olnchoro, Samburu district, central Kenya. *Phys. Chem. Earth 9*, 273–286.

Varne, P. 1970: Hornblende lherzolite and the upper mantle. *Contrib. Mineral. Petrol. 27*, 45–51.

Varne, R. 1977: On the origin of spinel lherzolite inclusions in basaltic rocks from Tasmania and elsewhere. *J. Petrol. 18*, 1–23.

Yolyanyuk, N. Ya., Semenova, V. G., Yelizar'yeva, T. I. & Bondareva, G. V. 1976: Inclusions of pyrope and pyrope-spinel lherzolite in basanite of the Vitim Plateau. *Doklady Akad. Nauk. SSSR, 228*, 159–162.

Wagner, P. A. 1914: *The Diamond Fields of S. Africa*, Transvaal Leader, Johannesburg. 347 pp.

Wallace, R. C. 1975: Mineralogy and petrology of xenoliths in a diatreme from South Westland, New Zealand. *Contrib. Mineral. Petrol. 49*, 191–199.

Wells, P. R. A. 1977: Pyroxene thermometry in simple and complex systems. *Contrib. Mineral. Petrol. 62*, 129–139.

White, R. W. 1966: Ultramafic inclusions in basaltic rocks from Hawaii. *Contrib. Mineral. Petrol. 12*, 245–314.

Whitfield, G. G. 1971: A petrological and mineralogical study of kimberlite and eclogite xenoliths from certain kimberlite pipes. Unpublished M.Sc. thesis, Rhodes University, South Africa.

Williams, A. F. 1932: *The Genesis of the Diamond*, 2 vols. Benn, London.

Wood, B. J. 1974: The solubility of alumina in orthopyroxene coexisting with garnet. *Contrib. Mineral. Petrol. 46*, 1–15.

Wood, B. J. 1976: The partitioning of iron and magnesium between garnet and clinopyroxene. *Carnegie Inst. Wash. Year Book 75*, 571–574.

Wood, B. J. & Banno, S. 1973: Garnet-orthopyroxene and orthopyroxene-clinopyroxene relationships in simple and complex systems. *Contrib. Mineral. Petrol. 42*, 109–142.

Accepted for publication October 1979
Printed April 1980

MINERALOGICAL MAGAZINE

VOLUME 43 NUMBER 330 JUNE 1980

The uranium content of garnet lherzolite xenoliths from kimberlites

D. A. CARSWELL

Department of Geology, University of Sheffield, Mappin Street, Sheffield, S1 3JD

AND

C. M. RICE

Department of Geology and Mineralogy, University of Aberdeen, Marischal College, Aberdeen, AB9 1AS

SUMMARY. Uranium contents ranging from 0.03–1.18 ppm have been determined by delayed neutron activation analysis in a suite of 19 ultrabasic xenoliths (mostly of the common garnet lherzolite type) from the kimberlites of southern Africa. Consideration of these and previous data lead us to conclude that the U content of *uncontaminated* garnet lherzolite in the uppermost mantle is on average roughly 0.04–0.05 ppm, levels which are sufficient to account for the observed U contents of fresh basalts. Higher U contents in mantle-derived ultrabasic xenoliths are the result of secondary alteration processes, most probably related to infiltration metasomatism stemming from contact with kimberlitic or carbonatitic magma fractions. This introduced U is concentrated along the boundaries of the primary mineral grains and is mostly readily removed by acid leaching. A partial analysis is given for a secondary uraniferous calcium phosphate phase observed in kelyphitic rims around garnets.

IT is generally accepted that the garnet lherzolite xenoliths brought up by kimberlites are representative of the dominant rocks in the uppermost 100–200 km of the mantle (Rickwood, 1969; Carswell and Dawson, 1970; Nixon and Boyd, 1973; Sobolev, 1977, etc.). As such mantle depths probably also correspond to the source region for basaltic magmas (Ringwood, 1975) it is important to decide whether garnet lherzolite xenoliths represent pristine mantle capable of yielding basaltic magmas through feasible partial melting and fractionation processes (O'Hara and Yoder, 1967) or residual mantle depleted in basalt yielding constituents (Ringwood, 1975).

Major element contents of lherzolite xenoliths suggest (Carswell, 1980) that there are significant lateral and vertical variations in the basalt yielding potential of the uppermost mantle rocks. With this in mind it is of interest to determine the U contents of such rocks, especially as they will profoundly influence the heat generating capacity of the uppermost mantle.

Previous studies. Analyses of U contents in rock samples of garnet lherzolites from kimberlites are sparse, surprisingly being fewer in number than analyses of U in griquaite (mantle-derived eclogite) xenoliths which clearly represent a more specialized and subordinate component of the upper mantle. U contents determined in some 17 ultrabasic xenoliths (peridotites) from kimberlites, mostly from localities in southern Africa, range from 0.052–1.2 ppm (Holmes and Paneth, 1936; Heier, 1963; Wakita *et al.*, 1967; Akimov *et al.*, 1968; Fisher, 1970; Morgan and Lovering, 1971; Manton and Tatsumoto, 1971; Kresten, 1974). Discounting the high early values of Holmes and Paneth (1936) and other high values attributable to later alteration processes, the best previous values for the primary U content of garnet peridotite (lherzolite) xenoliths appear to be in the range 0.052–0.276 ppm. On this basis Kresten (1974) suggested that unaltered garnet peridotite xenoliths from kimberlites contain roughly 0.20 ppm U.

By contrast many more analyses are available of the U contents in spinel lherzolite xenoliths brought up in magmas of the alkali basalt–basanite–nephelinite suite. The mean U content

determined in 57 such xenoliths is 0.0425 (σn = 0.0450)—data from Wakita *et al.* (1967); Green *et al.* (1968); Kleeman *et al.* (1969); Fisher (1970); Nishimura (1972); Haines and Zartman (1973); Dostal and Capedri (1976). The mean value for the 22 determinations by neutron activation analysis (0.0385) is reasonably close to, but nevertheless slightly lower than, that for the 35 determinations by fission track analysis (0.0450). Despite some overlap in their U contents, previous analyses thus appear to indicate that spinel lherzolite xenoliths in alkali basalt suite magmas typically have lower U contents than garnet lherzolite xenoliths in kimberlites.

Analytical methods. The U contents of powdered rock and mineral samples were determined by delayed neutron activation analysis using a system directly developed from that of Amiel (1962). Five replicate determinations on sample BD 1133 indicate a precision at 1 σ of 5%. The analyses were carried out by Mr T. Herrington, Analytical Chemistry Group, MOD (PE), at the Atomic Weapons Research Establishment, Aldermaston, Berks., England.

For fission track radiography the samples received a total neutron irradiation of 1×10^{16} n cm^{-2}. Lexan plastic was used as a detector and the prints were etched in 6*N* NaOH at 90 °C for ten minutes.

Uranium contents in rocks. The U contents determined in a suite of 19 ultrabasic xenolith samples from kimberlites are given in Table II, along with notes on the petrography of these samples. The majority of samples are of the common garnet lherzolite type (Carswell and Dawson, 1970; Carswell, 1980) taken to represent the dominant rock type in the uppermost 150–200 km of the mantle. We have classified such xenoliths as garnet lherzolites as long as they contain the 4-phase primary assemblage of olivine + orthopyroxene + clinopyroxene + garnet, despite the fact that the contents of garnet and clinopyroxene are typically < 10%. Some of the xenoliths contain minor amounts of phlogopite interpreted as primary on the basis of its apparent textural and chemical equilibration with the 4-phase garnet lherzolite assemblage (Carswell, 1975). The group of xenoliths studied from the Matsoku pipe in northern Lesotho contains two xenoliths (BD 1354 and 1360) with much higher modal contents of garnet and clinopyroxene. These xenoliths also have lower 100 Mg/(Mg + Fe) ratios and belong to the distinctive banded peridotite–pyroxenite series of xenoliths interpreted to be of cumulate origin (Cox *et al.* 1973; Gurney *et al.* 1975). The group of xenoliths from the Kimberley area mines contains one residual type harzburgite xenolith (BD 1200) totally devoid of garnet and clinopyroxene. Major element analyses of all the BD xenolith samples are given by Carswell and Dawson (1970), whilst analyses for the remaining xenolith samples are given in Table I.

The U contents in these 19 xenolith samples are decidedly variable ranging from 0.03–1.18 ppm, with a mean value of 0.178 ppm (σn 0.254 ppm). In these xenoliths no apparent correlation exists between U content and major element chemical parameters such as 100 Mg/(Mg + Fe) and 100 Cr/(Cr + Al) ratios, which are useful indices of the 'fertile' or 'depleted' chemical character of the mantle in terms of its basalt yielding potential. Instead the variation in U content appears to reflect variation in the type and degree of secondary alteration which has affected these xenolith samples. The dramatically reduced U contents in three xenolith samples after overnight leaching at room temperature in 2*N* HCl indicate that in those samples with highest U contents much of it is in labile sites.

Uranium contents of mineral phases. The U contents determined in mineral separates from certain of our xenolith samples are listed in Table III, along with previous determinations (mainly by fission track analysis) of the U contents of the primary mineral phases in other ultrabasic xenoliths from kimberlites. The U levels determined in our study are more in line with the results obtained by Akimov *et al.* (1968) and Mitchell and Aumento (1974) than with those of Kleeman and Lovering (1973). Whilst Mitchell and Aumento (1974) determined orthopyroxenes as having the highest U contents of the 4-phase garnet lherzolite assemblage, our results for the only xenolith sample for which we have determined U levels in all four mineral phases are in agreement with those of both Akimov *et al.* (1968) and Kleeman and Lovering (1973) to the extent that U appears to be regularly distributed between the phases and decreases in the order garnet > clinopyroxene > orthopyroxene ≥ olivine.

Discussion. Mass balance calculations for those xenoliths for which we have determined the U contents of the mineral phases (making reasonable assumptions for U levels in orthopyroxene and olivine in three out of four cases) yield calculated U contents in rocks reasonably in line with the observed values. However, this is not so if the average U contents for the minerals are used to calculate rock U contents in certain other xenoliths. Fission track mapping on lexan prints shows that in such xenoliths much of the element is concentrated along the boundaries of the primary mineral phases and it is probably this U that is being removed by acid leaching. The precise nature of these secondary U-enriched phases is not entirely clear although the

TABLE I: Additional Analyses of Garnet Lherzolite Xenoliths from Kimberlites

	CB1	CB2	CB4	CK2	CK3	CK4	CK33
SiO_2	45.50	45.55	49.77	44.79	45.09	45.07	45.41
TiO_2	0.07	0.04	0.09	0.00	0.06	0.04	0.02
Al_2O_3	1.85	1.36	2.56	1.90	2.18	2.06	1.68
Cr_2O_3	0.31	0.23	0.42	0.27	0.31	0.32	0.28
Fe_2O_3	2.08	1.82	0.27	1.80	0.97	2.07	2.09
FeO	4.37	4.07	5.04	4.83	5.63	4.56	3.53
MnO	0.10	0.09	0.11	0.11	0.11	0.10	0.09
NiO	0.27	0.28	0.23	0.26	0.26	0.25	0.30
MgO	41.05	42.68	37.73	41.33	40.66	40.92	41.56
CaO	1.19	0.89	0.89	1.14	1.21	1.20	0.51
Na_2O	0.16	0.10	0.12	0.22	0.36	0.17	0.10
K_2O	0.10	0.10	0.06	0.14	0.26	0.16	0.05
P_2O_5	0.06	0.04	0.04	0.08	0.11	0.06	0.03
H_2O^+	3.14	2.62	1.81	2.90	2.95	2.89	4.25
CO_2	0.29	0.25	0.14	0.21	0.24	0.23	0.30
Total	100.54	100.12	99.28	99.98	100.40	100.10	100.20
100 Cr/(Cr + Al)	10.1	10.2	9.9	8.7	8.7	9.4	10.1
100 Mg/(Mg + Fe_T)	92.1	93.0	92.7	91.9	91.8	91.9	93.2

Analyst: V.A. Somogyi, Department of Geology, University of Sheffield, using a combination of atomic absorption, spectrophotometric and gravimetric techniques.

TABLE II: Uranium Contents in Ultrabasic Xenoliths from Kimberlites

Locality	Sample Number	U ppm	Features
Matsoku North Lesotho	BD 1355	0.06	Coarse equigranular textured garnet lherzolite ('Common Peridotite' xenolith type, Cox et al., 1973)
	BD 1356	0.041	Similar to BD 1355, but with more phlogopite - mostly in rims around garnets
	BD 1354	0.03	Coarse textured garnet and clinopyroxene rich garnet lherzolite from banded peridotite-pyroxenite series xenoliths (Cox et al. 1973) interpreted as cumulates
	BD 1360	0.18 (0.079)*	Similar to BD 1355 but with 4 vol.% phlogopite - both as rims around garnets and in metasomatic veins with rutile
	BD 1364	0.06	Similar to BD 1354 but with even more clinopyroxene and less olivine
Kimberley Area Mines South Africa	BD 1140	0.1	Porphyroclastic textured garnet lherzolite. Th 0.26 ppm
	BD 1141	1.18 (0.034)*	Coarse textured garnet lherzolite fairly heavily veined with serpentine
	BD 1150	0.10	Coarse textured garnet lherzolite with abundant phlogopite mostly along grain boundaries but also some discrete primary textured plates
	BD 1200	0.041	Coarse textured harzburgite with 'fingerprint' spinels intergrown with orthopyroxene
	BD 1201	0.041	Coarse equigranular textured garnet lherzolite
	CK 2	0.27	Coarse textured garnet lherzolite with scarce primary textured phlogopite and secondary amphibole rims around garnets
	CK 3	0.41 (0.23)*	Coarse textured garnet lherzolite with scarce primary textured phlogopite and secondary amphibole and phlogopite rims around garnets
	CK 4	0.20	Coarse textured garnet lherzolite with primary and secondary textured phlogopite (Carswell 1975)
	CK 33	0.034	Porphyroclastic textured garnet lherzolite with very scarce clinopyroxene
	CB 1	0.19	Coarse textured garnet lherzolite with minor primary and secondary textured phlogopite
	CB 2	0.13	Porphyroclastic textured garnet lherzolite with minor secondary phlogopite rims around garnets
	CB 4	0.11	Coarse textured garnet lherzolite with minor secondary phlogopite as rims around garnets and clinopyroxene with unusual distinctly poikilitic habit (Carswell 1975)
Jagersfontein Mine South Africa	BD 1127	0.053	Mosaic - porphyroclastic textured garnet lherzolite
	BD 1133	0.154	Coarse textured garnet lherzolite with considerable secondary phlogopite. Range in five uranium determinations 0.143-0.161 ppm

*Values in parenthesis obtained after samples leached in 2N HCl at room temperature overnight

Analyst: J. Herrington

TABLE III: Uranium Contents (in ppm) in the Mineral Phases of Ultrabasic Xenoliths from Kimberlites

Sample Reference \ Mineral		Garnet	Clinopyroxene	Orthopyroxene	Olivine	Analytical Method
This Study	BD 1354	0.07	0.04	-	-	Delayed Neutron Activation Analyses of Mineral Separates
	BD 1364	0.28	0.04	-	-	
	BD 1140	0.5 ± 0.05	0.1 ± 0.05	0.1	<0.05	
	BD 1150	0.21	0.07	-	-	
Akimov et al. (1968)		0.129 (Aver.3)	0.069 (Aver.3)	0.029 (Aver.2)	0.030 (Aver.3)	Fission Track Analysis
Kleeman and Lovering (1973)		0.002-0.14 (Range)	0.007-0.030 (Range)	<0.001-0.0072 (Range)	<0.0003	Fission Track Analysis
Mitchell and Aumento (1974)		0.12 (Aver.8)	0.072 (Aver.10)	0.88 (Aver.20)	0.06 (Aver.17)	Fission Track Analysis
Kramers (1979)		-	≤0.006-0.045 (Range)	-	-	Isotope Dilution Mass Spectrometry on Separates

fact that the sample with the highest U content (BD 1143) also has the highest CO_2 content suggests that at least some of it might be carbonate.

Kimberlites themselves have appreciably higher U contents than the included xenoliths. Thus the average U in 159 determinations in kimberlites from southern Africa is 3.13 ppm—data from Morgan and Lovering (1971); Gurney and Hobbs (1973); Kresten (1974); Fesq *et al.* (1975); and Kramers (1977). This suggests that infiltration metasomatism emanating from the enclosing kimberlite, such as is apparently responsible for the development of secondary micas around garnets (Carswell, 1975), may well be responsible for the elevated U contents in certain xenoliths. However, there is only a poor positive correlation between the U contents of the xenoliths and their K_2O contents which might be taken as a possible index of the degree of contamination from the kimberlite. As carbonatites appear to have typically even higher U contents than kimberlites (Dawson and Gale, 1970; Masaits and Symslov, 1977) and carbonated kimberlites higher U contents than basaltic kimberlites (Kresten, 1974) it is possible that it is the degree of contamination due to a carbonatitic, rather than a strictly kimberlitic, component which is responsible for the elevated U contents in certain xenoliths (*cf.* Brookins *et al.*, 1979).

Some of the xenoliths, notably the CK and CB samples, appear to show a positive correlation between their U and P contents. In view of the suggestion by Fesq *et al.* (1975) and Kable *et al.* (1975) that primary upper mantle apatite might be the principal source for the concentrations of both of these elements in kimberlites, it is important to establish whether apatite exists as a primary phase, albeit in minor amounts, in garnet lherzolite xenoliths. Kleeman *et al.* (1969) observed that primary apatite in small amounts was an important U-bearing phase (with about 35 ppm U) in certain spinel lherzolite xenoliths from Victorian basalts. However, we have not been able to detect primary apatite grains in these xenoliths, either optically or with the microprobe. Microprobe analyses of wt.% P_2O_5 in the mineral phases of xenolith CK4 gave the following values: garnet (0.034), clinopyroxene (0.020), orthopyroxene (0.0043), olivine (0.018), and phlogopite (0.0034). The fact that in the primary mineral assemblage garnet has the highest contents of both U and P may therefore help to explain the positive correlation between these elements in many of these xenoliths. However, the primary mineral phases in CK_4 contain collectively less P_2O_5 than the rock content of 0.06 wt.%, indicating the presence of an additional P-enriched phase. Microprobe examination showed that the kelyphite rims around the garnets in this xenolith contain small grains (maximum dimension about 10 μm) of a uraniferous calcium phosphate phase. A partial analysis (average of five areas) of this phosphate gave P_2O_5 33.7, CaO 48.7, TiO_2 0.04, Y_2O_3 0.08, La_2O_3 0.35, Ce_2O_3 0.59, UO_2 0.032, all in wt.%. We think it unlikely that sufficient, if any, primary apatite occurs in most garnet lherzolite xenoliths to significantly affect the U budget.

Five of our garnet lherzolite samples plus four samples previously studied by Akimov *et al.* (1978), Fisher (1970), and Morgan and Lovering (1971) have U contents in the range 0.034–0.075 ppm, the mean value for these 9 samples being 0.053 ppm. We consider such levels to represent the true background levels of U in garnet lherzolite xenoliths unaffected by contamination associated with secondary alteration processes. Such levels are closely in line with the U levels determined in mantle-derived spinel lherzolite xenoliths from alkali basalt suite magmas, for which a mean value of 0.0425 ppm U for 57 such xenoliths was quoted earlier in this paper.

It is then pertinent to consider whether a U content of the order of 0.04–0.05 ppm in the uppermost mantle is sufficient to account for the levels observed in basaltic magmas if these are taken to be partial melts of such garnet lherzolite source rocks. It is clear that U can be expected to be strongly partitioned into partial melts relative to residual silicate phases. Certainly in the light of U_{Cpx}/U_{melt} partition coefficients most likely to be within the range 0.001–0.024 (Onuma *et al.*, 1968; Kleeman *et al.*, 1969; Kleeman and Lovering, 1973; Seitz, 1973; Seitz *et al.*, 1974; Dostal and Capedri, 1976), there seems to be little problem in generating partial melts with the U levels observed in fresh ridge or intraplate basalts (0.078 ± 0.048 ppm U in 68 samples) (Fisher, 1979) from upper mantle source rocks with 0.04–0.05 ppm U.

On the basis of xenolith studies (Heier, 1963; Wakita *et al.*, 1967; Green *et al.*, 1968; Morgan and Lovering, 1971; and BD 1140 Table II) Th/U rations in the uppermost mantle are likely to be within the range 2–5. Undoubted contamination affects from the enclosing kimberlite make it extremely hazardous to fix upper-mantle K levels on the basis of the K concentrations observed in garnet lherzolite xenoliths. However, best estimates of K/U ratios in the uppermost mantle appear to be within the range 3×10^3–1×10^4 (Wakita *et al.*, 1967; Green *et al.*, 1968; Fisher, 1970, 1979). With these considerations in mind a subcontinental uppermost mantle with on average ~ 0.05 ppm U, ~ 0.19 ppm Th, and ~ 500 ppm K as estimated by Birch (1965) on the basis of heat flow data requirements seems fairly realistic. On the other hand, as emphasized recently by Fisher (1979), if such concentrations are also valid for the sub-oceanic mantle then they are clearly inadequate to explain observed heat flows in those regions on the basis of radiogenic heat generation alone.

Acknowledgements. D. A. Carswell acknowledges support from the Royal Society and the Natural Environmental Research Council.

REFERENCES

Akimov (A. P.), Berzina (I. G.), Gurvich (M. Y.), and Lutts (B. G.), 1968. *Akad. Nauk. SSSR, Dokl.* **181**, 1245–8.

Amiel (S.), 1962. *Anal. Chem.* **34**, 1683–92.

Birch (F. R.), 1965. *Geol. Soc. Am. Bull.* **76**, 133–53.

Brookins (D. G.), Della Valle (R. S.), and Bolivar (S. L.), 1979. In Boyd (F. R.) and Meyer (H. O. A.) (eds.), *Kimberlites, Diatremes, and Diamonds: Their Geology, Petrology and Geochemistry*. Amer. Geophys. Union, 280–8.

Carswell (D. A.), 1975. *Phys. Chem. Earth*, **9**, 417–29.

—— 1980. *Lithos* **13**, 121–38.

—— and Dawson (J. B.), 1970. *Contrib. Mineral. Petrol.* **25**, 163–84.

Cox (K. G.), Gurney (J. J.), and Harte (B.), 1973. In Nixon (P. H.) (ed.), *Lesotho Kimberlites*. Lesotho Nat. Devel. Corp. Maseru, Lesotho, 76–92.

Dawson (J. B.) and Gale (N. H.), 1970. *Chem. Geol.* **6**, 221–31.

Dostal (J.) and Capedri (S.), 1976. *Contrib. Mineral. Petrol.* **54**, 245–54.

Fesq (H. W.), Kable (E. J. D.), and Gurney (J. J.), 1975. *Phys. Chem. Earth*, **9**, 687–707.

Fisher (D. E.), 1970. *Geochim. Cosmochim. Acta*, **34**, 630–4.

—— 1979. Ibid. **43**, 709–16.

Green (D. H.), Morgan (J. W.), and Heier (K. S.), 1960. *Earth Planet. Sci. Lett.* **4**, 155–66.

Gurney (J. J.), Harte (B.), and Cox (K. G.), 1975. *Phys. Chem. Earth*, **9**, 507–23.

—— and Hobbs (J. B. M.), 1973. *Int. Conf. on Kimberlites, Ext. Abstracts*, 143–5.

Haines (E. L.) and Zartman (R. E.), 1973. *Earth Planet Sci. Lett.* **20**, 45–53.

Heier (K. S.), 1963. *Geochim. Cosmochim. Acta*, **27**, 849–60.

Holmes (A.) and Paneth (F. A.), 1936. *Proc. R. Soc. Lond, A*, **154**, 385–413.

Kable (E. J. D.), Fesq (H. W.), and Gurney (J. J.), 1975. *Phys. Chem. Earth*, **9**, 709–34.

Kleeman (J. D.), Green (D. H.), and Lovering (J. F.), 1969. *Earth Planet. Sci. Lett.* **5**, 449–58.

—— and Lovering (J. F.), 1973. *Int. Conf. on Kimberlites, Ext. Abstracts*, 189–90.

Kramers (J. D.), 1977. *Earth Planet. Sci. Lett.* **34**, 419–31.

—— 1979. Ibid. **42**, 58–70.

Kresten (P.), 1974. *Lithos*, **7**, 171–80.

Manton (W. L.) and Tatsumoto (M.), 1971. *Earth Planet. Sci. Lett.* **10**, 217–26.

Masaits (V. L.) and Symslov (A. A.), 1977. *Geochem. Intern.* **14**, 129–40.

Mitchell (W. S.) and Aumento (F.), 1974. *J. Geophys. Res.* **79**, 5529–32.

Morgan (J. W.) and Lovering (J. F.), 1971. In Brunfelt (A. O.) and Steinnes (E.) (eds.), *Activation Analysis in Geochemistry and Cosmochemistry, Universitetsforlaget, Oslo*, 445–54.

Nishimura (S.), 1972. *Chem. Geol.* **10**, 211–21.

Nixon (P. H.) and Boyd (F. R.), 1973. In Nixon (P. H.) (ed.), *Lesotho Kimberlites*, Lesotho Nat. Devel. Corp. Maseru, Lesotho, 48–56.

O'Hara (M. J.) and Yoder (S. J.), 1967. *Scott. J. Geol.* **3**, 67–117.

Onuma (N.), Higuchi (H.), Wakita (H.), and Nagasawa (H.), 1968. *Earth Planet. Sci. Lett.* **5**, 47–51.

Rickwood (P. C.), 1969. *Geol. Soc. S. Africa, Special Publ.* **2**, 395–416.

Ringwood (A. E.), 1975. *Composition and Petrology of the Earth's Mantle*. McGraw Hill, New York, 618 pp.

Seitz (M. G.), 1973. *Carnegie Inst. Wash. Year Book*, **72**, 581–6.

—— Burnett (D. S.), and Bell (P. M.), 1974. Ibid. **73**, 451–4.

Sobolev (N. V.), 1977. *Deep seated inclusions in kimberlites and the problem of the composition of the upper mantle*. Amer. Geophys. Union, Wash. 279 pp.

Wakita (H.), Nagasawa (H.), Vyeda (S.), and Kuno (H.), 1967. *Geochem. J.* **1**, 183–98.

[*Manuscript received 25 October 1979*]

Geochimica et Cosmochimica Acta Vol. 44, pp. 857 to 875
© Pergamon Press Ltd. 1980. Printed in Great Britain

0016-7037/80/0401-0857$02.00/0

Chemistry of micas from kimberlites and xenoliths—II. Primary- and secondary-textured micas from peridotite xenoliths

J. S. DELANEY,* J.V. SMITH
Department of the Geophysical Sciences, University of Chicago, Chicago, IL 60637, U.S.A.

D. A. CARSWELL and J. B. DAWSON
Department of Geology, University of Sheffield, Sheffield S1 3JD, England

(*Received* 1 *August* 1979; *accepted in revised form* 6 *February* 1980)

Abstract—Micas from coarse granular lherzolites in S. African kimberlites may be separated into two groups, those showing primary textural relationships with coexisting silicates and those with secondary, alteration relationships with other silicates. Primary-textured micas form a tight cluster with a mean composition from 10 coarse garnet lherzolites of: SiO_2 41.0, TiO_2 0.18, Al_2O_3 13.5, Cr_2O_3 0.82, total Fe as FeO 2.04, MnO 0.02, MgO 26.0, NiO 0.22, CaO 0.01, BaO 0.29, Na_2O 0.31, K_2O 10.0, Rb_2O 0.028, Cl 0.05, F 3.43 at.%. Primary-textured micas in aggregates with clinopyroxene have higher TiO_2 and four specimens which look similar to the primary group but have textural ambiguities have still higher TiO_2.

Micas with secondary textures have wide ranges of composition which may be correlated with details of the textural parageneses. Micas from kelyphitic rims around garnets tend to be Cr-rich while those from veinlets are Cr-poor. Both groups tend to have higher FeO and TiO_2 than the primary group. Micas produced by alteration of, or filling veinlets through, orthopyroxene have a wide compositional range which overlaps that of the primary-textured micas, especially for harzburgite specimens.

The primary-textured micas show a positive correlation with coexisting pyroxenes for MgO (MgO + FeO) and TiO_2, but not for Cr_2O_3. Secondary-textured micas do not show correlations with coexisting pyroxenes for any elements.

The 'primary-metasomatic' micas described by HARTE and GURNEY (1975) and metasomatic and other micas described by BOETTCHER *et al.* (1979) and BOETTCHER and O'NEIL (1979) are richer in FeO and TiO_2 than the present primary-textured micas, and are attributed to crystallization from fractionated fluids.

INTRODUCTION

AS DESCRIBED in Part I (SMITH *et al.*, 1978), we are studying micas in order to obtain information on the distribution of potassium and other large ions in the upper mantle. Analyses of K, Rb and Ba were summarized in SMITH *et al.* (1979), and the resulting K Rb and K Ba ratios provided constraints on the origin of basaltic rocks. Since publication of Part I the following papers have provided additional chemical analyses of groundmass and phenocryst micas in kimberlites: Elwin Bay and Tunraq kimberlites, Somerset Island, Canada (MITCHELL, 1978, 1979); kimberlitic dyke, Keith township, Ontario, Canada (WATSON *et al.*, 1978); Central West Greenland kimberlites (SCOTT, 1979); Premier Mine, South Africa (ELTHON and RIDLEY, 1979). The first seven analyses in Table 1 of BOETTCHER *et al.* (1979) are apparently of rimmed crystals surrounded by kimberlite matrix. We extend the pioneering study of CARSWELL (1975) in which a distinction was made between the chemistry of primary and secondary micas in peridotite xenoliths. BOYD and NIXON (1978) made a similar distinction between 'mantle-derived' and 'late-stage' micas in ultramafic nodules from the Kimberley pipes, S. Africa.

Igneous, metamorphic and metasomatic processes have modified the rocks and minerals of the upper mantle. Partial melting has generated basaltic liquids and depleted residues. Most liquid has escaped upwards, but some has been trapped, and crystallized. Mineral cumulates have been produced in magma chambers. The resulting heterogeneous suites of rocks have undergone metamorphic recrystallization, which has either partly or completely converted igneous or metasomatic textures into metamorphic ones. Mica is particularly prone to deformation and recrystallization because of its basal cleavage, and is consumed early during partial melting of mica-garnet-lherzolite. Local increase of temperature, and infiltration of fluids into adjacent rocks, can be expected during intrusion of kimberlite magma into peridotitic rocks.

Petrographic textures provide undoubted evidence of the frequent occurrence of metasomatism in peridotite xenoliths transported by kimberlites, but it is unclear how the observed textures relate to the concept of 'precursory metasomatism' prior to eruption of alkali basalts (BOETTCHER and O'NEIL, 1979).

* Present address: American Museum of Natural History, New York, NY 10024, U.S.A.

Table 1. Specimen description

Label	Locality	Rock Type	Mica Type(s)	Reference
BD 1079	Wesselton, S. Africa	Cr-spinel harzburgite[a]	S_o	0
1126	Jagersfontein, S. Africa	Cr-spinel harzburgite	S_o	0
1141A	Bultfontein, S. Africa	lherzolite	P_u	0
1143B	"	garnet lherzolite	P	1
1154B	"	Cr-spinel harzburgite[a]	S_o	0
1155	"	Cr-spinel harzburgite[b]	S_o	0
1197	De Beers, S. Africa	Cr-spinel lherzolite	P_c,P_u	0
1359	Matsoku, Lesotho	rt-gt lherzolite	P_u	1
1368	Monastery, S. Africa	amp-Crsp harzburgite[c]	P,S_m	0
1544	Lashaine, Tanzania	rt-Crsp lherzolite	S_v	0
2125	Mothae, Lesotho	dia-gt lherzolite	P	1
JVS 73-59B	Bultfontein Floors	lherzolite[d]	P	0
73-61	"	harzburgite	S_v	0
73-63	"	garnet lherzolite	P,S_c,S_k	2
73-64	"	garnet lherzolite	P,S_k	2
73-66	"	lherzolite	S_c	0
73-72	"	lherzolite	P	0
73-75A	"	lherzolite	P_c	0
73-76	"	garnet-spinel-lherzolite[d]	P	2
73-81	"	amp - harzburgite	S_v	0
CK1	Kimberley Mines	lherzolite	P,S_o	0
CK2	"	garnet-lherzolite	P_c	0
CK3	"	garnet-lherzolite	S_c	0
CK4	"	garnet-lherzolite	P,S_k	0
CK31	Bultfontein Floors	amp-sp-harzburgite	S_o	0
CK32	"	lherzolite	S_v	0
K1A	Kimberley Mines	lherzolite	S_o,S_c	0
K3	"	Cr-spinel lherzolite[e]	S, S_m	0
K6	"	Cr-spinel lherzolite	S_v	0
K8	"	lherzolite	S_v	0
CB4	Bultfontein Floors	lherzolite	S_k	0
CB6	"	garnet-lherzolite	P,S_k	0
8015	?	garnet-lherzolite	P_c,S_k	0
CHE MON-4	Monastery	lherzolite	P_c	0
CHE BT7	Bultfontein Floors	garnet lherzolite	P_k	1
HOAM 73-1800	Kimberley Mines	garnet wehrlite	P_u	0

Reference: 0 this paper; 1 BISHOP *et al.* (1978); 2 DELANEY *et al.* (1979).

Notes: a rare cpx occurs in separate grains and in symplectite or veins with Cr-spinel and mica. b rare cpx in euhedral grains surrounded by serpentine. c amphibole occurs as single grains partly replaced by mica, and in symplectite with Cr-spinel. e most mica secondary but a few large crystals show primary like texture. d recrystallized mica in deformed areas of primary mica.

Abbreviations: P primary texture, P_c primary texture in which mica tends to associate with clinopyroxene, P_u primary texture but with some unusual features, S_o secondary texture with mica in rims around orthopyroxene, S_c secondary texture with mica in rims around clinopyroxene, S_k secondary texture with mica in kelyphitic rims around garnet, S_m secondary texture with rimming of primary-textured mica, S_v secondary mica in irregular veinlets, usually associated with serpentine.

Here, we describe textures and chemistry of micas occurring in the peridotite xenoliths from kimberlites. In particular, we describe a suite of primary-textured micas with a distinctive chemical composition for geochemical modeling of the upper mantle.

Textural terms and rock nomenclature follow the scheme in HARTE (1977), We emphasize that the present texture of a peridotite xenolith may reflect only the most recent metamorphic event, and that an earlier texture may have been erased completely. A kinematic description of solid-state processes in metamorphic rocks is given by NICHOLAS and POIRIER

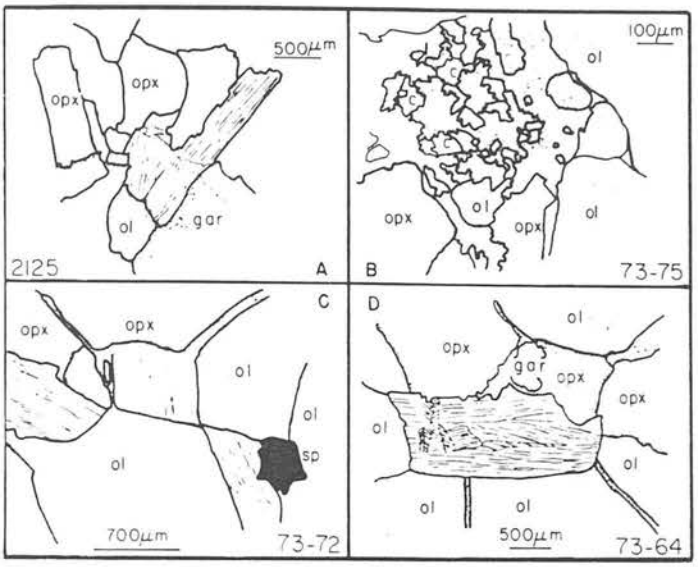

Fig. 1. Drawings of textures involving primary micas. A 2125 Two kink-banded mica grains adjacent to kelyphitic rim of a garnet crystal. All mica grains in five thin sections are next to garnet crystals. Minor alteration in grain boundaries of olivine and orthopyroxene. 3.5 mm across. B 73–75 Aggregate of clinopyroxene (c) and mica crystals surrounded by serpentine (dotted). The clinopyroxene crystals are not optically parallel, and have irregular boundaries. This is an extreme example of intimate association of mica and clinopyroxene, and most agggregates contain only a few crystals with fairly regular boundaries. 1 mm across. C 73-72 Simple texture with slight fracturing of olivine and grain-boundary alteration. 2.8 mm. D 73-64 Simple texture except for deformation and partial recrystallization of mica. Some grain-boundary alteration and fracturing of olivine and orthopyroxene. 4.5 mm.

(1976), and representative textures in peridotite xenoliths are described by BOULLIER and NICHOLAS (1975).

DESCRIPTION OF SPECIMENS

We selected specimens (Table 1) principally from the collections of J. B. Dawson (prefixed JBD), J. V. Smith (JVS), and D. A. Carswell (CK, CB). Additional specimens (K) were obtained from the Fearnsides Collection at the University of Sheffield. Two specimens (CHE) were kindly donated by C. H. Emeleus of the University of Durham and one (HOAM) by H. O. A. Meyer of Purdue University. The original suite was deliberately selected by petrographic examination of polished thin sections to locate large mica grains in apparent textural equilibrium with other silicates. No special effort was made initially to locate specimens with secondary micas because the original suite yielded enough such micas in lherzolites. However, a paucity of secondary micas in harzburgites lead to selection of specimens from the Fearnsides Collection. Eclogites were excluded from the present suite, and will be considered separately.

Micas from xenoliths of mantle peridotites may be crudely subdivided (CARSWELL, 1975) into two *textural* groups: (a) primary-textured micas, denoted P, which occur as large single crystals having 'equilibrium' grain boundaries with adjacent silicate and oxide minerals, and (b) secondary-textured micas, denoted S, which may (i) form alteration rims around other minerals, particularly garnet and orthopyroxene, often penetrating along cleavage traces in the latter, (ii) fill cracks, often in association with serpentine, thereby forming veinlets throughout the rock, and (iii) form rims and veinlets around primary-textured micas. Sub-groups of secondary micas are listed in Table 1.

Grains of primary micas are usually 1–2 mm across, and the exposed cross-sections represent random cuts across thick plates with a thickness-to-width ratio probably varying from near 1:1 to at most 1:5. Grains of secondary micas range widely from a few to several hundreds of micrometers across. Mica grains in alteration products of other minerals tend to be small. The larger grains of secondary mica tend to be more euhedral. Although they may overlap in size with the smaller primary grains, they can be identified as being secondary because of their occurrence in veinlets.

The first complication is the distinct tendency (cf. BOYD and NIXON, 1975; CARSWELL *et al.*, 1979) for coarse mica grains to associate with clinopyroxene, garnet and oxide grains in preference to orthopyroxene and olivine grains (Fig. 1). Particularly striking are pool-like aggregates of mica and clinopyroxene grains, whose texture ranges from a mosaic to an intimate intergrowth (Fig. 1B). Two possible explanations of these aggregates are crystallization from a melt interstitial to olivine and orthopyroxene crystals, and pseudomorphic replacement of an earlier crystal. The first explanation is not tenable because of chemical relationships described later on. The second explanation appears plausible when other specimens are considered (CARSWELL *et al.*, 1979). Kelyphitic rims around garnet consist of fine-grained mixtures of several inhomogeneous minerals including mica, Cr-bearing spinel and Al-rich pyroxenes. Carswell and co-workers found specimens in which the kelyphitic rim has recrystallized into coarse grains of mica, Cr-bearing spinel and Ca-rich pyroxene. Complete transformation of garnet to these three minerals, with prolonged annealing to a coarse texture of chemically-uniform grains may therefore be the origin of the aggregates. Whereas garnets usually occur as equant euhedral crystals, the aggregates tend to be irregular. This can be explained by invoking both deformation and incorporation of some of the adjacent orthopyroxene during the transformation of the garnet. Although the minerals of the aggregates have a primary texture, the likelihood of an earlier history of replacement resulted in the special designation P_c in Table 1 for mica aggregated with clinopyroxene.

What is the explanation of the tendency for a single mica grain to associate with a garnet, or clinopyroxene or oxide

grain in those specimens for which there is no distinctive aggregate texture? Did the mica grain merely nucleate close to one of these other grains, perhaps because olivine and orthopyroxene crystallized earlier leaving a liquid rich in the components of mica, garnet, clinopyroxene and oxide minerals? Or was there a prior episode of metasomatism followed by complete obliteration of any kelyphitic or aggregate texture? From the petrographic viewpoint, the present primary texture merely records that metamorphic equilibration was achieved, thereby removing evidence to decide the above questions.

An important difference between primary- and secondary-textured micas is their relationship to the deformation whose effects are present in most xenoliths of mantle peridotites. Zones of brittle deformation, represented by cracks and kink-bands, cross grain boundaries and are more easily seen in primary micas than in other silicates because of the strong basal cleavage (Fig. 1A, D). The deformation must have occurred late in the history of the rocks because the micas show little healing around fracture planes. Although primary-textured micas must have originally crystallized before deformation, many examples of partial recrystallization occur in the deformed parts of the crystals represented by small euhedral neoblasts of mica in textural equilibrium with one another and sometimes with adjacent portions of the larger crystal fragments. Such late recrystallization, if continued sufficiently long, might under favourable conditions produce an aggregate of crystals obscuring the evidence of strain in the original 'equilibrium' crystal. Continuing strain during recrystallization of an equilibrium primary mica might produce a band or veinlet of smaller mica crystals. The smaller grain size and unstrained character of the secondary micas leaves their relationship to any deformation unclear but is consistent with post-deformational growth (BOYD and NIXON, 1978). The secondary micas have grown in an environment conducive to recrystallization so that evidence of deformation is destroyed.

Four specimens labeled P_u in Table 1 contain special textural features which cast some doubt on assignment to the primary group. Mica grains in 1141A are closely associated with clinopyroxene grains in clusters, but strong deformation has broken up most mica grains. Many olivine grains have recrystallized to a fine-grained aggregate. Although mica grains in 1359 occur randomly and have similar size to their neighbors, the grain size of most specimens tends to be smaller than for peridotites assigned to the P group. Probably 1359 recrystallized to small grains after deformation of a coarser texture. In 1197, all mica grains but one appear to have a primary relationship to the other silicates, with a strong tendency to cluster with spinel grains. However, one mica grain about 2 mm long and 0.2 mm wide cuts completely through an olivine grain about 1 mm across. In 1800, mica grains are very large (~4 mm), but the entire rock is so deformed and net-veined that the extent of preservation of the original texture is unclear.

In none of our specimens has the deformation of the anhydrous silicates proceeded to the degree reported by BOYD (1973) for high-temperature porphyroclastic garnet lherzolites. BOYD and NIXON (1978, p. 1373) noted strong shearing in mantle-derived phlogopite from intensely-deformed Bultfontein rocks, and JBD found mica in most of the sheared garnet lherzolites in his collection from the Bultfontein Mine. A special study is underway to determine the relation between the chemical composition and extent of deformation of micas from these low-temperature porphyroclastic rocks from Bultfontein.

Metasomatic transport of elements including K, Na and Ti is essential for growth of micas rimming garnet and orthopyroxene (types S_k, S_0), though the distance is indeterminate. For primary textured micas, it is possible to invoke an earlier episode of metasomatism prior to metamorphic equilibration, but certainly the primary-textured micas are not the result of post-metamorphic metasomatism, except for the altered rims. Whatever their ultimate origin, the primary-textured micas certainly provide information on the pre-deformation metamorphic era, though not necessarily of an even earlier era.

ANALYTICAL CONDITIONS AND DATA

Although the electron microprobe analyses were obtained by several operators over five years using various conditions, the essential features and correction procedures were as in BISHOP *et al.* (1978). Major elements were referred primarily to Di_{85} Jd_{15} glass, and earlier natural standards for minor elements were replaced by Corning glass standards using the following reference values (glass V: TiO_2 0.80 wt%, Cr_2O_3 0.76; glass W: MnO 0.65; glass X: NiO 0.71).

Analyses of Cl were made at 15 kV and 0.5 μA beam current with 5–20 μm spot dia. Analyses with 1 μA beam current were indistinguishable. The standard (natural scapolite XXXIV; SHAW, 1960) was cross-checked against other natural scapolites and some chlorapatites. No wavelength interferences were found, and an ADP analyzer was used.

Analyses of F required special precautions. False analyses were obtained on F-free specimens when an incorrect aperture was present in the electron-beam column, thereby resulting in electron scattering outside the analyzed area. Contamination was found to occur from diffusion pump oil and a F-free oil (Convolex 10) was used. A TAP analyzing crystal gave a wide peak and wavelength interferences (especially from phosphorus) were reduced to trivial level by careful choice of background positions. Synthetic fluorphlogopite was checked against fluorite and several natural fluorapatites, and a straight line was obtained after correction with the MAGIC on-line computer program.

Special techniques for analysis of Rb and Ba were described by SMITH *et al.* (1979).

Analyses of K_2O and Na_2O tended to be lower than values required for two alkali atoms per formula unit even for optically clean areas. Systematic study of many areas of primary-textured micas usually revealed small regions with the full complement of alkalies. Other elements such as Cr and Ti were not reduced in regions of lowered alkalies.

Table 2 gives representative analyses for micas with primary textures, based on the mean of 4–8 spectrometer analyses taken on spots selected from numerous energy-dispersive analyses. Alkali analyses tend to be lower than those in SMITH *et al.* (1979) because the latter were based on fewer analyses deliberately selected for alkali-rich regions. The BaO and Rb_2O analyses were made only on alkali-rich spots. For these primary-textured micas, minor elements were spatially uniform within $\pm 10\%$.

Table 3 gives representative analyses for micas with secondary textures, usually based on the mean of about 5 spectrometer analyses following a survey with energy-dispersive analyses. A considerable range of compositions was present in most specimens, and for six specimens with particularly large range two representatives analyses are listed. The large and erratic composition range of the secondary micas indicates disequilibrium.

Tables 4 and 5 list analyses of coexisting minerals for specimens not already described in BISHOP *et al.* (1978) and DELANEY *et al.* (1979).

Analyses of the Carswell specimens differ from those given by CARSWELL (1975) because they are the mean values of a larger number of analyses taken at different spots from those used by Carswell.

CHEMISTRY OF MICAS

The chemistry of micas and coexisting minerals can be used to test for equilibrium. Furthermore the poss-

Table 2. Electron microprobe analyses of micas with primary textures

(a) coarse-grained textures with no special features

	CK1	CK4	CB6	1368	2125	73-59B	73-63	73-64	73-76	BT7
SiO_2	40.47	42.50	39.89	42.30	41.7	40.22	41.31	41.07	39.25	41.42
TiO_2	0.25	0.12	0.61	0.01	0.14	0.20	0.03	0.24	0.18	0.06
Al_2O_3	13.64	13.59	12.45	14.24	12.9	13.43	14.05	14.53	13.63	12.42
Cr_2O_3	0.81	0.83	0.67	0.86	0.86	1.01	0.74	0.85	0.87	0.68
FeO	3.23	2.52	2.95	2.36	2.45	2.09	2.57	2.90	2.20	2.70
MnO	0.03	0.00	0.02	0.01	0.01	0.01	0.03	0.02	0.01	0.01
MgO	25.70	25.48	25.22	26.57	26.8	26.03	26.28	24.97	25.82	27.46
NiO	0.20	0.26	0.21	0.22	0.25	0.21	0.20	0.24	0.19	0.23
CaO	0.01	0.00	0.00	0.03	0.00	0.02	0.01	0.02	0.02	0.02
Na_2O	0.42	0.70	0.35	0.27	0.06	0.29	0.19	0.15	0.50	0.21
K_2O	9.30	10.69	10.53	9.02	10.3	10.18	10.58	10.71	9.24	9.48
Cl	0.05	0.09	0.09	0.08	0.11	0.10	0.07	0.10	0.04	0.10
F	0.35	0.26	0.42	0.30	0.73	0.15	0.60	0.47	0.48	0.55
BaO	0.353	0.301	0.167	0.400	0.062	0.697	0.138	0.096	0.565	0.172
Rb_2O	0.027	0.029	0.040	0.023	0.044	0.028	0.024	0.016	0.020	0.026
Total	94.840	97.370	93.617	94.335	95.206	94.665	96.822	96.342	92.465	95.538

(b) associated with clinopyroxene (first six) or with some doubtful textural feature (last four)

	CK2	8015	MON4	1197	73-72	73-75A	1141A	1143B	1359	73-1800
SiO_2	40.87	40.71	41.81	42.84	41.38	41.35	42.16	41.16	41.03	42.49
TiO_2	0.13	0.33	0.12	0.13	0.85	1.20	0.83	0.55	1.37	0.52
Al_2O_3	13.19	13.41	12.93	11.96	12.39	13.47	11.87	12.96	13.48	13.23
Cr_2O_3	0.78	0.75	0.65	0.69	0.58	0.62	0.54	0.67	0.63	1.22
FeO	2.85	3.45	2.31	1.82	2.85	3.30	2.88	2.63	3.23	2.57
MnO	0.02	0.02	0.01	0.00	0.01	0.03	0.02	0.01	0.03	0.03
MgO	25.64	25.12	26.38	26.94	25.21	24.73	25.67	25.18	25.09	24.86
NiO	0.17	0.21	0.17	0.17	0.24	0.17	0.19	0.19	0.20	0.20
CaO	0.02	0.12	0.02	0.01	0.02	0.04	0.02	0.01	0.04	0.02
Na_2O	0.75	0.81	0.76	0.26	0.10	0.17	0.16	0.82	0.10	0.20
K_2O	9.45	9.27	9.85	10.60	10.60	10.60	10.60	9.62	10.20	10.42
Cl	0.08	0.08	0.05	0.05	0.05	0.04	0.04	0.05	0.05	0.08
F	0.15	0.316	0.73	2.16	0.75	0.46	0.81	0.47	1.12	0.88
BaO	0.220	0.435	0.353	0.088	0.035	0.036	0.034	0.202	0.070	0.032
Rb_2O	0.019	0.000	0.016	0.032	0.032	0.036	0.039	0.033	0.037	0.032
Total	94.339	95.031	96.155	97.750	95.107	96.252	95.869	94.555	96.677	96.784

ible role of crystal-liquid partitioning can be tested by using the well-known tendency for Mg and Cr to concentrate into crystalline phases and Fe and Ti to concentrate into liquid during partial melting or fractional crystallization, e.g. MYSEN and BOETTCHER (1975).

In Fig. 2, primary-textured micas have a smaller composition range than secondary ones. Those with unequivocal primary texture (P) fall in a cluster with TiO_2 <0.6 wt% and Cr_2O_3 ranging from 0.6 to 1.0 wt%. Ignoring 73–1800 which was strongly deformed, the remaining primary (?) micas, either aggregated with clinopyroxene (P_c) or with doubtful textural feature (P_u) lie in a narrow band with Cr_2O_3 0.5–0.8 wt% and TiO_2 0–1.4 wt%. Although there is a trend to higher TiO_2 contents for the P_c and P_u micas than for the P micas, as might be expected for micas produced from evolved fluids (i.e. result of partial melting), there is considerable overlap and no clear conclusion appears.

For secondary micas, all those from kelyphitic rims around garnet (c.f. BOYD and NIXON, 1978, Fig. 10; DANCHIN, 1979, Table 2) have high Cr_2O_3 (1–4 wt%) and variable TiO_2 (0–1.5 wt%). Typically the rims are peppered with tiny octahedra of Cr-rich spinel but care was taken to avoid these during analysis (Tables 4 and 5). Because the garnet is richer in Cr_2O_3 than other silicates, the kelyphite can be interpreted as the product of metasomatism by fluids rich in mobile elements including H_2O and K.

The remaining secondary micas scatter widely, but those in veinlets tend to have low Cr_2O_3. The average of the secondary micas is higher in TiO_2 than for the primary micas.

Primary-textured micas fall into one cluster on the FeO vs Cr_2O_3 plot (Fig. 3), and secondary micas tend

Table 3. Electron microprobe analyses of micas with secondary textures

	(a) from harzburgites								(b) from lherzolites					
	CK31	1079	1079	1126	1126	1154B	1155	73-81	CK1	CK3	CK4	CK32	K1A	K3
SiO_2	41.61	41.42	40.63	38.70	39.40	42.52	42.95	42.39	39.62	40.41	40.75	41.0	42.36	40.76
TiO_2	0.51	0.01	0.50	0.43	3.07	0.30	0.02	0.47	1.98	0.13	1.18	0.68	0.06	2.93
Al_2O_3	9.22	12.14	13.52	15.20	13.08	13.71	10.33	11.02	13.56	13.42	14.16	9.70	13.2	12.33
Cr_2O_3	0.35	0.56	1.24	1.30	1.67	0.81	0.51	0.29	1.42	1.00	1.36	0.44	0.54	1.35
FeO	4.54	2.37	2.88	4.36	3.63	2.57	1.77	4.15	3.19	2.81	4.09	4.38	2.71	4.44
MnO	0.02	0.02	0.01	0.07	0.01	0.01	0.02	0.02	0.02	0.02	0.09	0.02	0.01	0.02
MgO	26.73	27.37	25.24	22.87	23.17	26.69	28.80	26.37	25.39	26.00	24.70	26.38	26.5	23.66
NiO	0.21	0.24	0.28	0.00	0.27	0.26	0.27	0.18	0.19	0.18	0.10	0.21	0.23	0.21
CaO	0.00	0.02	0.03	0.05	0.00	0.01	0.01	0.08	0.01	0.01	0.03	0.03	0.01	0.02
Na_2O	0.12	0.25	0.31	0.33	0.40	0.60	0.56	0.21	0.30	1.05	0.32	0.10	0.61	0.21
K_2O	10.76	9.52	9.73	8.56	9.30	9.9	8.5	9.48	9.50	8.43	9.00	10.90	10.1	9.97
Cl	0.02	0.01	0.01	0.03	0.03	0.03	0.03	0.02	0.04	0.08	0.04	0.03	0.03	0.05
F	0.26	0.30	0.43	0.53	0.95	0.12	0.69	0.74	0.50	0.36	0.45	0.24	0.03	0.35
BaO	na	0.297	0.297	0.145	0.145	0.189	0.238	0.200	0.154	0.50	0.108	na	na	na
Rb_2O	na	0.005	<0.005	0.042	0.042	0.036	0.014	0.059	0.025	0.017	0.043	na	na	na
Total	94.35	94.532	95.112	92.617	95.167	97.755	94.712	95.679	95.899	94.417	96.921	94.11	96.39	96.30

	(b) from lherzolites (cont.)													
	K3	K6	K8	K8	CB4	CB6	1368	1544	73-61	73-63	73-63	73-64	73-66	73-66	8015
SiO_2	42.67	41.63	40.08	40.0	39.43	38.61	40.36	40.72	40.03	37.67	39.10	38.95	39.94	41.51	39.71
TiO_2	0.79	0.09	1.93	4.6	1.19	1.23	3.75	7.68	2.61	0.00	0.07	1.54	3.50	1.20	0.52
Al_2O_3	9.96	10.5	10.24	12.0	14.54	14.73	12.95	12.46	13.12	19.95	16.24	17.70	14.85	13.10	14.66
Cr_2O_3	0.56	0.28	0.38	0.2	1.61	1.51	1.41	0.54	1.11	3.77	1.93	1.40	2.05	0.58	1.10
FeO	3.65	2.96	5.30	5.4	2.85	3.09	4.34	5.58	4.46	4.58	3.27	2.99	3.77	3.11	3.58
MnO	0.02	0.02	0.03		0.04	0.02	0.03	0.04	0.03	0.12	0.06	0.01	0.04	0.03	0.02
MgO	26.76	28.58	25.24	22.2	24.17	23.69	22.29	18.92	22.88	21.09	23.38	22.93	22.36	25.30	24.76
NiO	0.21	0.23	0.22		0.14	0.20	0.16	0.10	0.20	0.00	0.11	0.16	0.16	0.21	0.11
CaO	0.02	0.01	0.03		0.06	0.01	0.02	0.18	0.02	0.01	0.01	0.03	0.02	0.10	0.01
Na_2O	0.16	0.29	0.23		0.54	0.94	0.34	0.26	0.23	0.59	0.63	1.34	0.48	0.76	0.29
K_2O	10.0	10.44	10.69	10.6	9.70	9.12	10.2	9.87	10.05	9.88	9.22	8.73	9.64	9.28	9.23
Cl	0.04	0.02	0.03		0.02	0.03	0.03	0.01	0.02	0.05	0.06	0.02	0.02	0.03	0.03
F	1.15	0.01	0.46		0.99	0.50	0.67	0.68	0.86	0.30	0.60	0.61	1.59	2.94	0.35
BaO	na	na	na		0.115	0.228	0.049	0.091	0.035	0.089	0.150	0.143	0.060	0.057	0.132
Rb_2O	na	na	na		0.037	0.018	0.050	0.046	0.055	0.007	0.010	0.025	0.026	0.024	0.015
Total	95.99	95.06	94.86	95.0	95.432	93.926	97.099	97.153	95.640	98.106	94.840	95.578	97.906	98.231	94.517

to have higher FeO. Just as in Fig. 2, secondary micas associated with orthopyroxene (mainly in harzburgites) overlap considerably with primary micas.

Almost all the micas, irrespective of texture, have NiO between 0.16 and 0.26 wt% (Fig. 4). Although micas from kelyphite tend to have lower NiO than primary micas, there is overlap. The lower NiO is not surprising because garnet tends to have low NiO (<0.04 wt%), and an external source of NiO may be necessary for those kelyphitic micas with high NiO.

Because the Fe^{2+}/Fe^{3+} partition ratio cannot be determined from an electron microprobe analysis of a mica, there is uncertainty in atomic assignments. Assuming all iron to be ferrous, the sum of Si^{4+} and Al^{3+} ions is close to 8 for all primary-textured micas (Fig. 5), but tending to a slight excess. Secondary micas lie in a broad band which runs from less than 8 atoms for high-Si micas to greater than 8 atoms for low-Si micas. For those micas with (Si + Al)<8, it is probably necessary to invoke Fe^{3+} ions to fill tetrahedral sites. Ferric iron cannot be ruled out for the low-Si micas, but is not mathematically necessary for filling of tetrahedral sites. Indeed qualitative measurements of the pleochroism (cf. BOETTCHER and O'NEIL, 1979) are consistent with little or no Fe^{3+} in low-Fe primary-textured micas and substantial Fe^{3+} in high-Fe secondary-textured micas.

Figure 6 demonstrates a moderate positive correlation between Al and Cr for all micas. Veinlet micas tend to have lower Al and Cr and kelyphitic micas tend to have higher Al and Cr than primary-textured micas. Secondary micas associated with orthopyroxene overlap with primary-textured micas.

There are large intra-group variations for the mobile elements Na, Cl, F, Ba and Rb, but averages tend to be similar, especially for Na and Rb.

Chlorine is three times higher on average in primary-textured micas than in secondary ones. This

rules out a simple process of generation of primary-textured micas by recrystallization of secondary-textured micas. Of course, an external source of chlorine can be invoked. STEUBER *et al.* (1968) found 0.014–0.028 wt% Cl and 0.019–0.039 wt% F in four garnet peridotites from S. Africa. About one-third of the peridotite would need to be mica if primary-textured mica were the sole source of Cl and up to 10% mica would be needed to account for the F. Such large amounts are quite implausible and the analyses of STEUBER *et al.* apparently indicate the occurrence of one or more phases rich in F and Cl or both. The identity of such a phase or phases is currently unknown. Secondary mica is an even less plausible source for the chlorine. Analyses of F and Cl in ultrabasic inclusions from kimberlites by PAUL *et al.* (1976) show a wide range [0.004–0.025 wt% F; (0.001)–0.021 wt% Cl], for which only lower values could be plausibly accounted for by phlogopite. An important possibility is introduction of Cl into the kimberlites and enclosed xenoliths by percolation of ground water, as postulated for Sr (BARRETT and BERG, 1975). Low values of Cl in various types of mica from kimberlites were found by BOETTCHER and O'NEIL (1979).

Although mean values of K/Rb tend to be close to the 'cosmic' ratio (SMITH *et al.*, 1979), individual ratios vary widely, thereby suggesting local separation of the two elements. Ratios of K/Ba and K/Rb are negatively correlated for micas in peridotite nodules.

CHEMICAL RELATIONS WITH COEXISTING PYROXENES

A test of equilibrium is whether there are systematic trends of element distribution between mica and coexisting silicates (cf. EHRENBERG, 1979). Unfortunately a distribution coefficient for a particular element between two silicates may depend on temperature and pressure as well as bulk composition. A simple linear relationship is not theoretically necessary, but if found for a suite of samples, it is plausible to presume that the samples reached equilibrium.

Systematic trends have been found experimentally for the distribution coefficients of the *mg* ratio [= wt% MgO/(MgO + FeO)] among various silicates, though a substantial temperature variation occurs for some silicates, e.g. garnet and clinopyroxene. Plots of *mg* (mica) vs *mg* (pyroxenes) show systematic positive trends for primary-textured micas (Fig. 7) and considerable scatter for secondary micas. Similar trends (not shown) occur between mica and both olivine and garnet. Kelyphitic micas tend to be slightly richer in Fe than coexisting primary-textured micas. Veinlet micas show the greatest scatter, thereby indicating precipitation from fluids not in equilibrium with primary silicate minerals.

The positive correlation between Ti and Fe in megacrysts from the Malaita alnöite was interpreted in terms of fractionation of these elements into magma as crystallization proceeded (DELANEY *et al.*, 1979). There are no synthesis data, under mantle conditions, to indicate whether the partition of Ti depends significantly on pressure, temperature and composition. Furthermore it is not known how Ti is partitioned between octahedral and tetrahedral sites, with consequent difficulties in choosing appropriate exchange reactions. A good correlation was found for the partition of Ti between primary-textured mica and coexisting clinopyroxene (Fig. 8), with the implication that the exchange reactions are rather straightforward. Kelyphitic micas are richer in Ti than primary-textured micas when referenced to the trend for primary-textured micas. The data points are scattered, and kelyphitic micas are presumably not in equilibrium with the pyroxenes. Furthermore there is not a simple correlation between Ti in kelyphitic mica and garnet.

Primary-textured micas associated with clinopyroxene in aggregates have similar ranges of titanium and *mg* to other primary-textured micas. This does not rule out an earlier kelyphitic replacement texture because subsequent metamorphic annealing could have occurred at similar pressure and temperature to the annealing of the other primary-textured micas.

Chromium is partitioned strongly into crystalline phases from coexisting liquids, as demonstrated clearly by the chemical trends in megacrysts from the Malaita alnöite (DELANEY *et al.*, 1979). Primary-textured micas from clinopyroxene-containing aggregates are not richer in Cr than other primary-textured micas. Whereas primary-textured micas show a simple partitioning of Ti with coexisting pyroxenes, the partitioning of Cr is erratic. Data for primary-textured mica and orthopyroxene fall in a near-elliptical cluster (Fig. 9) without any linear correlation. The spread is even greater between mica and clinopyroxene, and no correlation with bulk composition was detected. Furthermore, no correlation was found with temperature and pressure inferred from pyroxene chemistry. Although no simple partition was found for Cr between primary-textured micas and coexisting pyroxenes, it is not necessary to conclude that they are not in equilibrium. Complex exchange reactions may be responsible for the data. BOYD and FINGER (1975, p. 519) found a greater zoning of Cr and Ti than other elements in pyroxenes and garnets from Lesotho mantle rocks, but minerals from our primary-textured specimens are essentially homogeneous in these elements; the scatter in Fig. 9 is much greater than the intra-specimen composition variation.

Kelyphitic micas tend to fall in a cluster enriched in Cr_2O_3 relative to the primary micas and this is compatible with replacement of Cr-rich garnet rather than Cr-poor olivine and pyroxenes.

ORIGIN OF THE MICAS

Crystal-liquid differentiation, metamorphism and metasomatism have caused major changes in the

chemical distribution of elements in upper-mantle minerals, and evidence accumulates of reaction between peridotite xenoliths and kimberlitic magmas (literature review in Boettcher and O'Neil, 1979). Nevertheless we reaffirm that a suite of micas in peridotite xenoliths have a distinctive primary textural relationship to neighbouring grains of silicate and oxide minerals, and that this textural relationship car-

Table 4. Electron microprobe analyses of other minerals

	BD1079							BD1126					BD1141A		
	ol	opx	cpx	sp[1]	sp[2]	se	ilm[3]	ol	opx	sp[4]	sp[5]	se	ol	opx	cpx
P_2O_5	-	-	-	-	-	-	-	0.004	0.002	-	-	-	-	-	-
SiO_2	42.1	56.1	55.0	0.32	0.2	44.7	0.2	42.3	58.7	0.1	0.3	39.1	40.8	57.8	54.3
TiO_2	-	-	-	0.12	-	-	55.0	0.00	0.00	1.9	2.6	0.3	0.00	0.06	0.23
Al_2O_3	-	2.5	0.5	5.7	12.0	-	0.2	0.00	0.76	13.5	9.6	1.2	0.00	0.41	1.86
Cr_2O_3	-	0.9	1.1	59.9	55.8	-	3.5	0.00	0.21	53.6	55.7	0.4	0.02	0.33	3.61
FeO	7.2	4.9	1.6	22.7	18.9	10.2	25.7	6.72	4.26	17.1	19.2	6.5	8.62	5.36	2.65
MnO	-	-	-	-	-	-	0.3	0.07	0.10	-	-	-	0.14	0.16	0.09
MgO	50.6	34.5	16.3	11.1	13.0	29.2	14.9	51.7	36.5	14.2	13.4	36.9	50.1	35.2	15.8
NiO	-	-	-	-	-	0.2	-	0.44	0.08	-	-	0.2	0.46	0.10	0.09
CaO	-	0.6	23.9	0.2	-	0.7	0.6	0.01	0.14	-	-	0.6	0.01	0.44	19.1
Na_2O	-	-	1.2	-	-	-	-	0.00	0.01	-	-	-	0.01	0.14	2.92
K_2O	-	-	-	-	-	-	-	-	-	-	-	0.2	0.00	0.01	0.03
Sum	100.1	99.5	100.0	100.0	99.8	(85.0)	100.4	101.244	100.762	100.3	100.8	(85.4)	100.16	100.01	99.68

	BD1154B							BD1155					BD1197			
	ol	opx[6]	cpx[7]	sp[8]	sp[9]	sp[10]	sp[11]	ol[12]	opx	cpx[13]	sp[14]	se	ol	opx	cpx	sp
P_2O_5	-	-	-	-	-	-	-	0.002	0.002	-	-	-	-	-	-	-
SiO_2	41.5	57.6	54.8	0.3	0.8	0.3	0.3	41.8	58.1	55.3	0.3	42.7	41.6	59.0	54.7	0.01
TiO_2	-	0.2	-	0.6	1.0	1.5	9.9	0.001	0.002	0.3	1.0	-	0.004	0.016	0.044	0.26
Al_2O_3	-	0.1	1.0	10.0	2.3	7.8	15.7	0.000	0.34	0.3	2.8	1.0	0.01	0.13	1.08	2.90
Cr_2O_3	-	0.8	1.8	53.4	61.1	53.6	22.7	0.006	0.55	1.2	61.9	-	0.03	0.20	4.09	66.3
FeO	7.5	5.2	1.8	25.7	24.8	23.2	31.6	6.64	4.44	2.3	23.3	4.7	5.42	3.26	1.58	16.0
MnO	-	-	-	-	-	-	-	0.09	0.11	-	-	-	0.07	0.07	0.05	0.25
MgO	50.5	35.5	17.0	10.0	9.6	11.6	17.8	51.4	36.4	17.9	10.1	38.3	52.8	37.6	15.7	12.5
NiO	0.5	-	-	-	-	-	-	0.39	0.07	-	-	-	0.40	0.08	0.05	0.08
CaO	-	0.3	23.1	-	-	-	-	0.03	0.12	21.6	-	-	0.02	0.24	19.4	0.00
Na_2O	-	-	1.3	-	-	-	-	0.000	0.02	1.0	-	-	0.03	0.08	2.69	0.00
K_2O	-	0.2	-	-	-	-	-	-	-	-	-	0.2	0.00	0.01	0.00	0.00
Sum	100.0	99.9	100.8	100.0	99.6	98.0	99.0	100.359	100.154	99.9	99.4	86.8	100.354	100.686	99.384	98.280

	BD1368						BD1544							JVS 73-59B		
	ol	opx[15]	opx[16]	amp[17]	amp[18]	sp	ol	opx[19]	opx[20]	cpx	sp	rt[21]	rt[22]	ol	opx	cpx
P_2O_5	0.002	0.002	-	-	-	-	0.006	0.009	0.009	-	-	-	-	0.010	0.005	0.11
SiO_2	41.0	57.7	57.7	46.1	45.2	0.05	40.3	55.8	56.5	54.2	0.04	0.01	0.02	40.96	58.0	55.0
TiO_2	0.002	0.002	0.004	0.03	0.02	0.06	0.021	0.21	0.60	0.30	3.40	87.2	87.2	0.01	0.02	0.03
Al_2O_3	0.001	0.94	1.05	11.5	11.4	17.4	0.020	1.03	0.78	1.40	6.78	0.10	0.04	0.00	0.67	2.10
Cr_2O_3	0.005	0.27	0.94	1.92	2.22	49.1	0.024	0.46	0.83	1.68	50.8	3.62	4.99	0.02	0.32	2.33
FeO	6.51	4.26	4.39	2.39	2.68	18.0	10.27	6.51	4.86	2.58	24.0	2.33	0.78	16.70	4.13	1.45
MnO	0.079	0.098	0.08	0.04	0.02	0.24	0.134	0.15	0.11	0.10	0.28	0.03	0.01	0.08	0.09	0.05
MgO	51.2	36.5	36.3	20.1	20.4	13.2	48.7	34.8	34.0	16.9	11.2	0.23	0.12	52.0	35.6	15.5
NiO	0.42	0.08	0.07	0.12	0.10	0.10	0.35	0.09	0.11	0.05	0.15	0.00	0.03	0.38	0.10	0.06
CaO	0.008	0.19	0.28	11.3	11.1	0.00	0.026	0.56	2.18	21.0	0.00	0.01	0.02	0.017	0.32	20.0
Na_2O	0.000	0.020	0.06	3.25	3.32	0.00	0.000	0.11	0.08	1.64	0.00	0.00	0.00	0.004	0.07	1.95
K_2O	-	-	0.01	1.27	1.29	0.00	-	0.01	0.01	0.01	-	0.00	0.00	-	-	-
Sum	99.227	100.062	100.884	98.02	97.75	98.15	99.851	99.739	100.069	99.86	96.65	93.53	93.21	100.186	99.325	98.58

	JVS 73-61			JVS 73-63				JVS 73-64				JVS 73-66			JVS 73-72		
	ol	opx[23]	opx[24]	gt	ol	opx	cpx	gt	ol	opx	cpx	ol	opx	cpx	ol	opx	cpx
P_2O_5	0.014	0.000	0.003	0.095	0.018	0.004	0.112	0.063	0.012	0.005	0.103	0.011	0.002	-	0.019	0.004	-
SiO_2	40.0	58.0	57.6	42.5	42.0	59.1	54.0	42.0	42.0	58.6	55.6	41.8	58.5	53.9	42.3	58.5	54.6
TiO_2	0.01	0.05	0.07	0.014	0.00	0.003	0.005	0.06	0.005	0.02	0.030	0.008	0.024	0.066	0.02	0.08	0.19
Al_2O_3	0.00	0.01	0.08	21.4	0.01	0.78	2.72	20.9	0.008	0.72	1.76	0.002	0.842	2.1	0.004	0.097	0.82
Cr_2O_3	0.01	0.07	0.26	4.46	0.02	0.30	2.08	4.29	0.02	0.28	1.50	0.010	0.258	2.0	0.017	0.178	3.62
FeO	9.99	5.80	5.73	6.27	6.66	4.12	1.98	7.01	7.56	4.52	2.07	7.51	4.66	1.9	7.01	4.26	2.12
MnO	0.14	0.17	0.16	0.30	0.08	0.09	0.07	0.31	0.08	0.09	0.06	0.08	0.101	0.06	0.08	0.094	0.05
MgO	50.0	35.5	35.1	21.6	52.3	36.7	16.7	21.0	52.2	36.6	16.6	51.9	36.5	15.4	52.0	36.5	15.6
NiO	0.34	0.07	0.08	0.00	0.44	0.12	0.05	0.00	0.39	0.11	0.05	0.41	0.095	0.037	0.38	0.095	0.04
CaO	0.01	0.04	0.17	4.98	0.02	0.41	19.2	5.04	0.021	0.41	20.6	0.01	0.26	20.9	0.014	0.276	20.1
Na_2O	0.00	0.03	0.13	0.02	0.01	0.11	2.34	0.02	0.005	0.096	1.57	0.004	0.06	2.2	0.004	0.070	2.41
K_2O	-	-	-	-	-	-	-	-	-	-	-	-	-	-	-	-	-
Sum	100.514	99.74	99.383	101.639	101.558	101.737	99.257	100.693	102.301	101.451	99.943	101.817	101.302	98.563	101.85	100.15	99.55

Table 4 (continued)

	JVS 73-75A			JVS 73-76				JVS 73-81				HOAM 73-1800			MON-4			
	ol	opx	cpx	gt	ol	opx	cpx	ol	opx	amph[25]	sp	gt	ol	cpx	ol	opx	cpx[26]	cpx[27]
P_2O_5	0.018	0.005	-	0.072	0.023	0.003	0.103	0.007	0.010	-	-	-	-	-	-	-	-	-
SiO_2	42.0	58.4	55.0	42.7	42.4	58.2	55.3	41.5	58.7	56.0	-	42.2	42.2	54.2	40.9	58.8	55.3	55.4
TiO_2	0.020	0.030	0.253	0.027	0.00	0.019	0.06	0.013	0.05	0.32	2.4	0.20	-	-	0.004	0.000	0.03	0.06
Al_2O_3	0.004	0.65	2.34	21.9	0.00	0.81	3.60	0.00	0.03	1.02	0.5	17.4	-	1.4	0.01	0.78	2.67	4.78
Cr_2O_3	0.029	0.34	2.10	3.48	0.013	0.32	2.42	0.007	0.05	0.28	60.0	9.22	-	3.1	0.013	0.31	2.29	3.25
FeO	8.26	4.67	2.82	6.84	6.53	4.08	2.08	9.3	6.1	2.13	30.0	6.12	6.7	1.8	7.41	4.42	1.70	2.40
MnO	0.118	0.12	0.095	0.42	0.07	0.10	0.06	0.12	0.15	0.03	-	0.31	-	-	0.11	0.09	0.05	0.08
MgO	51.6	35.8	16.0	21.6	52.7	36.8	14.8	51.0	36.0	23.0	7.4	20.5	52.7	16.6	50.9	36.3	15.9	15.0
NiO	0.373	0.10	0.045	0.00	0.41	0.09	0.03	0.33	0.07	0.13	-	-	-	-	0.41	0.12	0.03	0.04
CaO	0.027	0.41	18.6	4.38	0.01	0.25	19.6	0.01	0.20	7.1	-	6.2	-	19.0	0.01	0.23	20.27	18.1
Na_2O	0.004	0.16	2.60	0.03	0.03	0.09	3.00	0.00	0.04	3.8	-	-	-	2.1	0.01	0.07	2.43	3.43
K_2O	-	-	-	-	-	-	-	-	-	1.9	-	-	-	-	0.00	0.00	0.00	0.00
Sum	102.453	100.806	99.853	101.443	102.171	100.762	101.053	102.237	101.40	98.71	100.3	102.2	101.6	99.2	99.777	101.11	100.6	100.6

1 in symplectite, 2 rim of separate grain; core similar in composition to symplectite, 3 0.2mm crystals surrounded by serpentine at margin of nodule and kimberlite matrix, 4 mean of isolated grains, 5 symplectite with serpentine, 6 full of inclusions of spinel(?) and mica; TiO_2 0-0.3, Al_2O_3 0-0.5, Cr_2O_3 0-1.8, 7 small crystals between opx and spinel-mica symplectite; Cr_2O_3 0.9-3.8, MgO 15.8-17.1, 8 in mica-spinel symplectite, 9 grains enclosed by mica in vein, 10, 11 core and rim of zoned grains in serpentine, 12 [illegible] grains surrounded by serpentine, 13 [illegible] 14 tiny grains associated with mica in symplectite or veins; variable composition e.g. Al_2O_3 1.3-4.3 TiO_2 1.7-0.2, 15 clean area, 16 inclusion-rich region, 17 remnants of grains partly altered to mica, 18 center of amphibole-spinel symplectite, 19 blade of opx(?) at margin of cumplex region which may result from recrystallization of megacryst of low-Ca pyroxene, 20 clean, recrystallized region, 21 interior of 0.3mm grain; Nb present but not analyzed, 2 interior of 0.3mm grain with Mg,Fe,Cr-rich lamellae; Nb present: Fe,Ni sulfide present, 23,24 center and edge, 25 Cl 0.01 wt.%, F 0.61, 26 inclusion in olivine, 27 normal grain.

Table 5. Electron microprobe analyses of other minerals in Carswell and Fearnsides collections

	CK1 gt	ol	opx	cpx	sp	CK2 gt	ol	opx	cpx[1]	cpx[1]	sp	CK3 gt	ol	opx	cpx	CK4 gt	ol	opx	cpx	sp[2]	sp[3]
P_2O_5	0.02	0.02	0.01	-	-	0.02	0.01	0.01	0.01	0.01	-	0.01	0.01	-	-	0.03	0.02	0.01	-	-	-
SiO_2	42.0	42.0	59.0	54.2	0.09	42.0	42.0	59.0	56.1	55.8	0.03	42.6	40.9	59.0	55.0	42.0	42.69	59.5	55.4	-	2.0
TiO_2	0.06	0.01	0.04	0.07	0.51	0.05	0.02	0.03	0.05	0.09	0.48	0.05	-	0.02	0.06	0.05	0.01	0.04	0.06	0.51	0.90
Al_2O_3	21.59	0.02	0.86	0.28	13	21.13	0.02	0.82	1.90	2.52	12	21.0	0.01	0.74	2.26	22.0	-	0.75	2.11	12	22
Cr_2O_3	3.28	0.02	0.29	2.22	51	3.26	0.03	0.28	2.01	2.05	53	3.16	0.03	0.29	2.27	3.35	-	0.29	2.12	53	40
FeO	8.20	7.85	5.00	2.18	22	8.13	7.96	5.06	2.09	2.54	22	8.10	7.84	5.09	2.31	8.10	7.61	4.90	2.11	22	18
MnO	0.44	0.09	0.11	0.09	-	0.48	0.13	0.12	0.06	0.08	-	0.48	0.11	0.13	0.06	0.48	0.16	0.13	0.05	-	-
MgO	20.0	50.5	35.0	15.2	13	20.3	50.0	35.0	15.5	15.9	13	21.76	50.6	35.0	15.0	20.0	50.0	36.0	16.0	13	17
NiO	-	0.44	0.11	0.06	-	-	0.42	0.11	0.03	0.05	-	0.03	0.44	0.09	0.06		0.44	0.10	0.08	-	-
CaO	4.83	0.01	0.26	20.04	-	4.77	0.01	0.26	20.39	17.81	-	4.88	0.02	0.26	20.97	5.03	0.02	0.32	20.0	-	0.10
Na_2O	0.02	-	0.05	2.01	-	0.020	0.01	0.05	2.15	3.12	-	0.03	-	0.06	2.11	0.03	-	0.12	2.00	-	-
K_2O	-	-	-	0.01?	-	-	-	-	0.02?	0.01?	-	-	-	-	0.01?	-	-	-	0.01?	-	-
Sum	100.44	100.96	100.73	98.36	99.67	100.31	100.61	100.74	100.31	99.98	100.51	102.07	99.96	100.68	100.71	101.04	101.09	102.16	99.94	100.51	100.00

	CK31 ol	opx	amp	sp	rt?	CK39[5] ol	opx	cpx	sp	rt?[4]	CB4 gt	ol	opx	cpx	CSE gt	ol	opx	cpx	sp
P_2O_5	-	-	-	-	-	0.01	-	0.02	-	-	0.04	-	0.01	-	0.03	0.01	-	-	-
SiO_2	41.0	59.0	55.7	1.16	0.06	41.0	59.3	55.0	0.06	-	42.6	42.0	59.0	55.0	42.0	42.0	58.2	54.0	0.42
TiO_2	0.01	0.06	0.31	1.55	66	0.01	0.08	0.11	2.55	60	0.03	-	-	0.07	0.19	0.08	0.08	0.15	1.06
Al_2O_3	0.02	0.04	0.34	0.46	0.03	-	0.04	0.16	0.60	-	21.0	0.01	0.71	3.77	21.0	0.01	0.85	2.19	57
Cr_2O_3	0.03	0.16	0.60	59	19	0.01	0.26	2.08	58	17	4.71	0.04	0.30	3.42	4.4	0.05	0.32	1.95	10
FeO	8.66	5.32	2.35	28	8	8.90	5.27	2.49	29	11	6.65	7.22	4.46	2.50	6.88	7.44	4.67	2.23	9
MnO	0.15	0.16	0.06	-	-	0.13	0.13	0.08	-	-	0.37	0.08	0.10	0.08	0.40	0.09	0.12	0.07	0.14
MgO	49.0	36.0	21.8	9.0	4.1	51.0	36.0	16.4	9.3	3.5	21.0	50.0	35.1	14.0	21.0	50.0	35.0	17.0	24
NiO	0.38	0.09	0.06	-	-	0.35	0.09	0.05	-	-	-	0.42	0.14	0.05	0.02	0.44	0.13	0.07	0.07
CaO	0.01	0.09	4.99	0.03	0.78	0.02	0.27	21.72	-	-	4.05	0.02	0.40	15.49	4.85	0.03	0.44	19.51	-
Na_2O	-	0.03	4.26	-	0.05	-	0.04	1.24	-	-	-	0.02?	0.12	4.00	0.05	0.01?	0.12	2.15	-
K_2O	-	-	4.25	-	0.3?	-	0.01?	0.03?	-	-	-	-	-	0.01?	-	-	0.02?	0.02?	-
Sum	99.26	100.95	94.72	99.20	92.94	101.43	101.81	99.38	99.51	91.5	100.45	99.81	100.34	98.39	100.82	100.37	99.95	99.34	101.69

	K1A ol	opx[6]	cpx	K3 ol	opx	cpx[7]	cpx[7]	sp	K6 ol	opx	cpx	K8 ol	opx	cpx[8]	cpx[8]	rt	sp[9]	8015 gt	ol	opx	cpx
P_2O_5	0.00	0.00	-	0.01	-	-	0.01	-	-	-	-	0.01	0.01	-	0.01	-	-	0.02	0.01	-	0.01
SiO_2	42.0	57.0	54.0	42.0	60.0	55.0	55.0	-	42.0	59.0	54.0	40.0	60.34	54.0	54.0	0.03	-	42.0	42.0	58.0	55.0
TiO_2	0.00	0.01	0.00	0.03	0.09	1.20	0.51	2.13	-	0.01	-	0.03	0.16	1.33	0.39	97.0	13	0.07	0.03	0.05	0.10
Al_2O_3	0.01	0.5	0.70	0.01	0.05	0.64	0.20	1.38	0.01	0.17	0.65	0.02	0.11	0.37	0.70	-	2.2	21.0	0.02	0.83	2.51
Cr_2O_2	0.00	0.35	1.67	0.03	0.17	0.80	2.94	63	0.01	0.13	1.19	0.01	0.58	0.57	0.58	3.3	36	2.90	-	0.25	1.82
FeO	7.93	5.2	2.59	9.0	4.69	3.51	2.62	23	8.09	5.10	2.35	11.0	5.47	2.88	3.91	0.49	31	9.18	9.31	5.56	2.67
MnO	0.11	0.13	0.07	0.11	0.12	0.15	0.11	-	0.12	0.15	0.06	0.18	0.12	0.08	0.10	-	-	0.54	0.13	0.14	0.09
MgO	50.0	36.5	16.75	49.0	36.0	19.53	19.65	12	50.5	37.0	17.27	47.0	33.0	17.5	20.0	0.14	17	20.0	49.0	34.0	15.2
NiO	0.39	0.08	0.05	0.39	0.10	0.03	0.03	-	0.41	0.08	0.05	0.02	0.11	0.07	0.09	-	-	0.04	0.41	0.08	0.05
CaO	0.01	0.85	21.67	0.03	0.31	20.28	19.22	-	-	0.12	22.7	0.15	0.87	22.08	18.27	0.06	0.08	4.67	0.02	0.25	20.47
Na_2O	0.00	0.10?	1.53	0.01?	0.06	0.93	1.45	-	-	0.01	1.25	0.01?	0.17	0.43	1.01	-	0.03	0.01	-	0.06	2.19
K_2O	-	0.2?	0.01?	-	-	0.02?	0.01?	-	-	-	0.01?	-	-	0.01?	0.03?	0.03	0.03	-	-	0.01?	-
Sum	100.45	100.92	99.04	100.62	101.59	102.09	101.75	101.51	101.14	101.87	99.53	98.43	101.36	99.32	99.09	100.91	99.34	100.43	100.93	99.23	100.11

1 two separate grains, 2 separate grain, 3 inclusion in mica, 4 unusual compositions of separate grains, but not checked in detail, 5 large grain of heazlewoodite present, 6 contamination by secondary mica, 7 inclusions in mica, 8 small grains associated with mica, 9 inclusion in rutile.

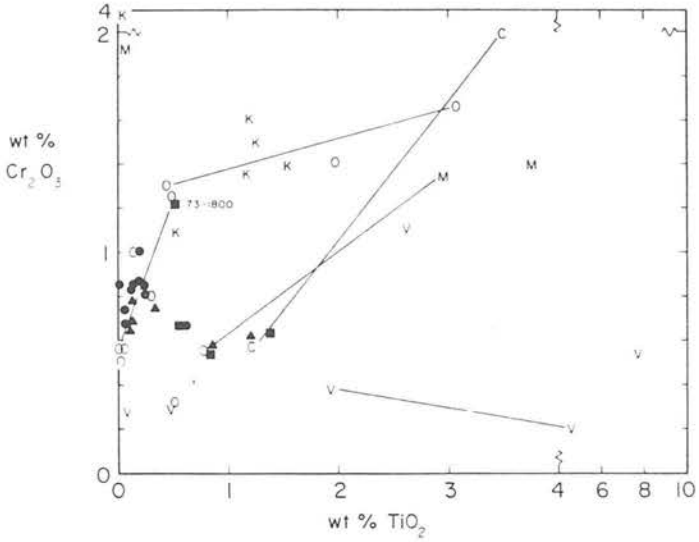

Fig. 2. Cr_2O_3 vs TiO_2 of micas. Filled circle, coarse-grained texture with no special features; filled triangle, primary texture associated with clinopyroxene; filled square, probably primary but with some doubtful feature; K, secondary texture associated with kelyphite rim of garnet; C, secondary texture associated with clinopyroxene; O, secondary texture associated with orthopyroxene; V, secondary texture associated with vein; M, secondary mica fringing mica.

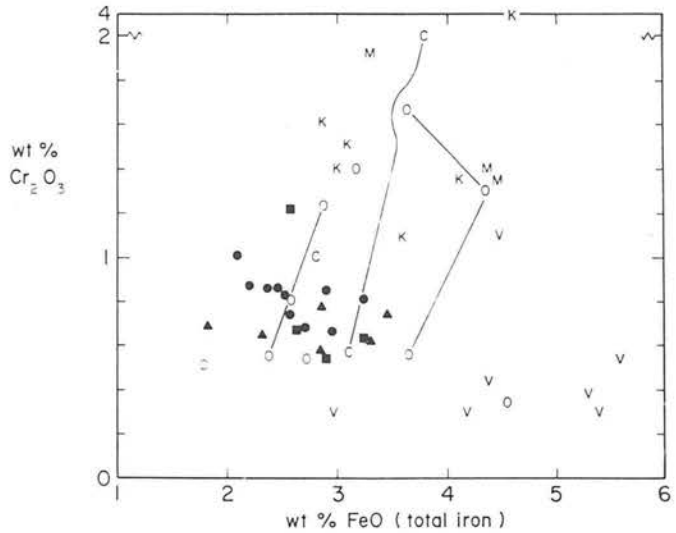

Fig. 3. Cr_2O_3 vs FeO (total) of micas. See Fig. 2 for symbols.

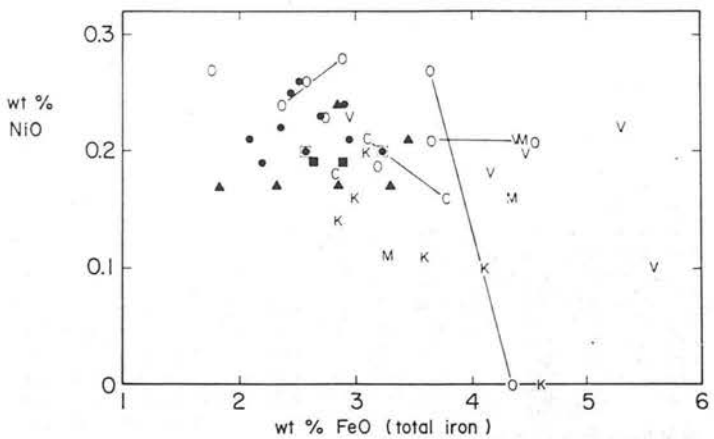

Fig. 4. NiO vs FeO (total) of micas. See Fig. 2 for symbols.

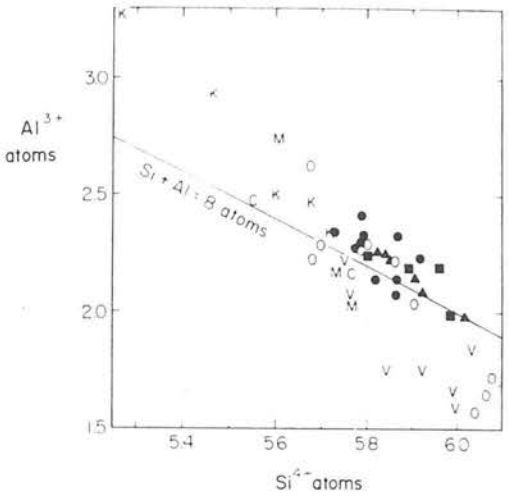

Fig. 5. Al^{3+} vs Si^{4+} atoms for 22 cation charges of micas. See Fig. 2 for symbols.

ries over into a chemical relationship. The suite of primary-textured micas is characterized by coarse grains (>1 mm) of uniform chemical composition except for alteration in the rim and in cracks. The grains are commonly deformed in contrast to secondary micas which occur as small undeformed grains. The deformation may become so severe that mica grains are strongly disrupted, as in specimen 73-1800, and there is then some worry that chemical changes may have taken place. We are concerned that mica grains tend to occur next to clinopyroxene, garnet and spinel grains, but tentatively attribute this to the conditions of crystal nucleation and not to metasomatism, except for the aggregates already discussed. In contrast with the primary-textured micas are the secondary-textured micas, which have been classified into various sub-groups. Those in kelyphitic rims tend to be relatively rich in Cr, whereas those in veinlets tend to be low in Cr, but with a rather wide range of compositions.

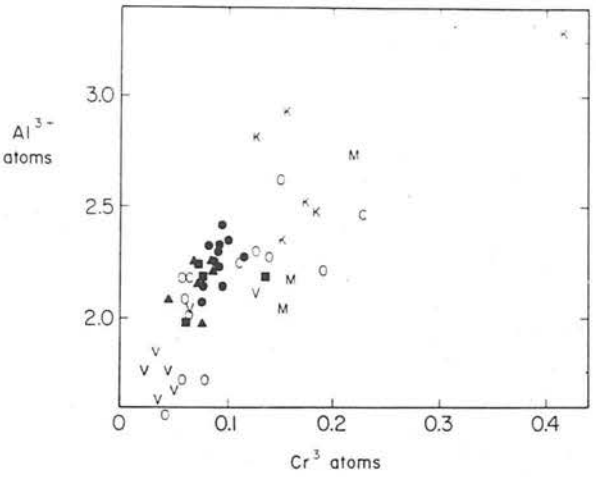

Fig. 6. Al^{3+} vs Cr^{3+} atoms for 22 cation charges of micas. See Fig. 2 for symbols.

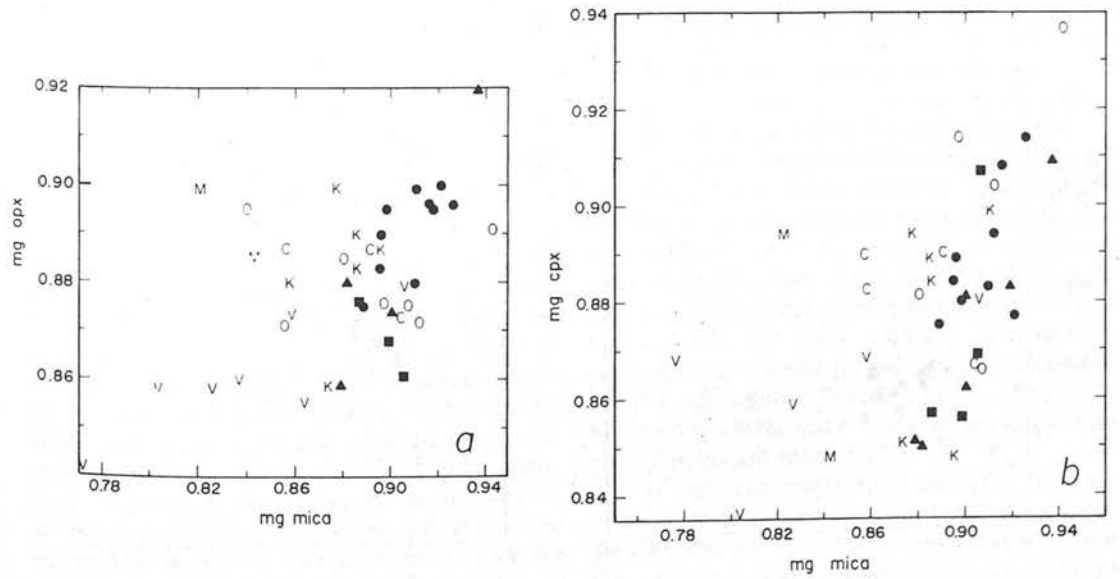

Fig. 7. mg (mica) vs mg (orthopyroxene) and mg (clinopyroxene). See Fig. 2 for symbols.

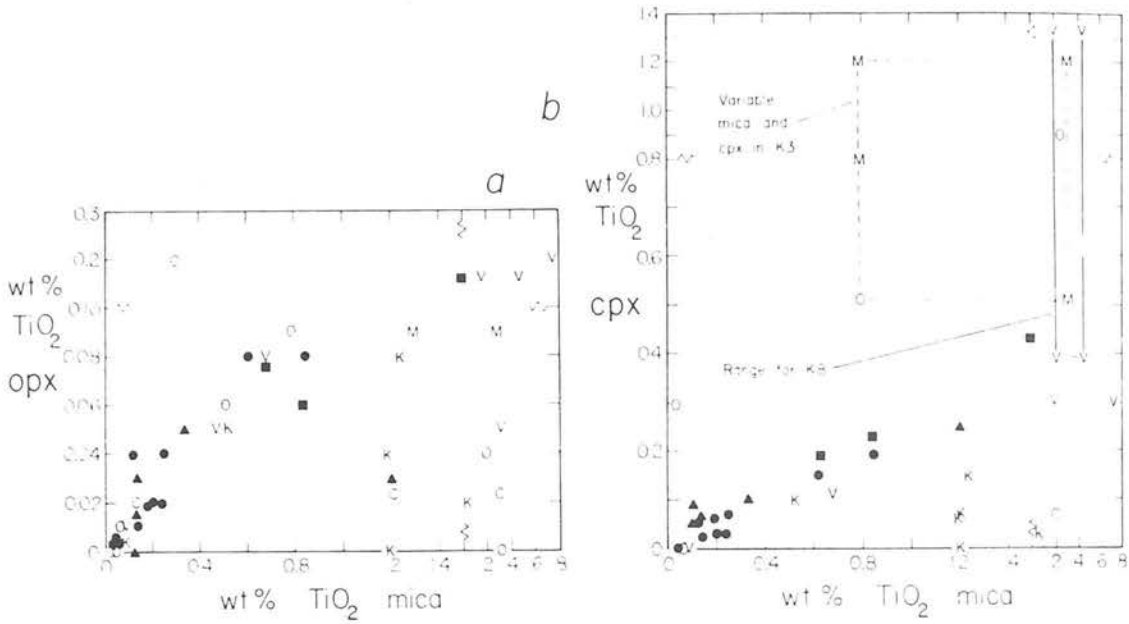

Fig. 8. Wt% TiO_2 (mica) vs TiO_2(orthopyroxene and TiO_2 (clinopyroxene). See Fig. 2 for symbols. Some connecting lines omitted for clarity.

Although primary-textured micas have a restricted range of chemical composition, we emphasize that this range tends to be enclosed by the overall range for all the secondary micas taken together. Furthermore the mean compositions of the secondary micas in harzburgites and lherzolites (Table 6, columns 4 and 5) are quite similar to the mean compositions of primary micas, which are separated into three groups P, P_c and P_u (columns 1–3).

Danchin (1979) suggested that the K content of undepleted lherzolite xenoliths from the Premier mine "is 'primary' in the sense that it has always been present but is not now located in the same site as when these rocks first formed". Thus he favored redistribution of K (and Ti) in the undepleted garnet lherzolites rather than metasomatic introduction from outside. Boyd and Nixon (1978) asserted that 'mantle-derived' phlogopite from Bultfontein was present in peridotites prior to deformation and inclusion in the erupting kimberlite, and that phlogopite selvages on garnet developed after inclusion of peridotite nodules in the kimberlite.

We suggest that the tendency for lower TiO_2 and FeO in the primary-textured and secondary-textured micas may result from the secondary micas inheriting a larger fraction, *on average*, than the primary micas of fractionated liquids. At one extreme, the liquid may be kimberlite magma which invaded the peridotite xenolith causing precipitation of mica and other minerals, especially at grain boundaries. At the other

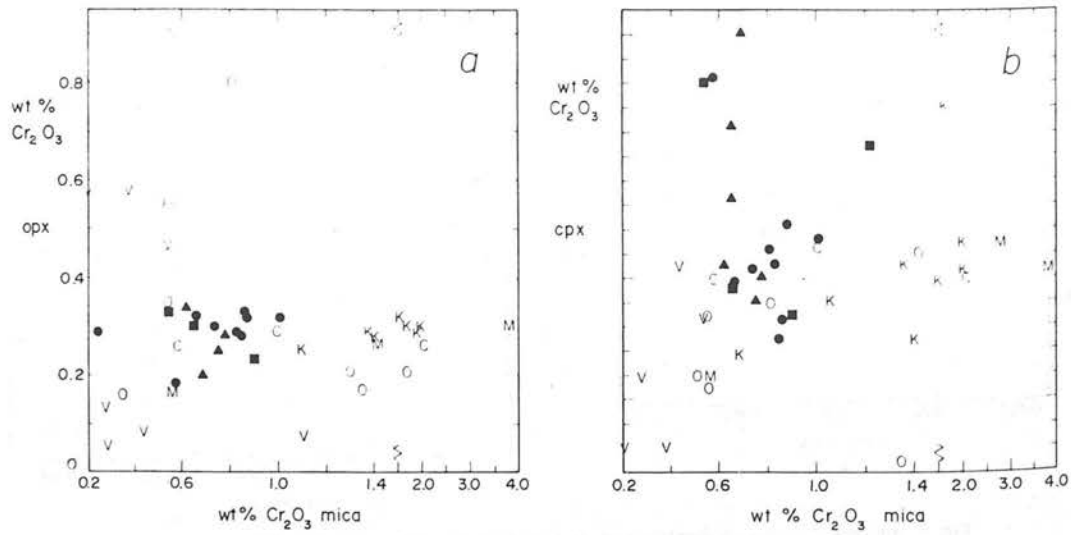

Fig. 9. Wt% Cr_2O_3 (mica) vs Cr_2O_3 (orthopyroxene) and Cr_2O_3 (clinopyroxene). See Fig. 2. for symbols.

Table 6. Mean composition of sub-groups of micas, and selected data from the literature

	1	2	3	4	5	6	7	8	9
SiO_2	41.01	41.49	41.71	42.21	40.25	40.99	41.0-42.7	41.1-42.9	38.7-42.1
TiO_2	0.18	0.46	0.82	0.66	1.79	0.57	1.07-1.59	0.35-0.75	1.04-3.94
Al_2O_3	13.49	12.89	12.89	12.88	13.49	13.26	11.7-13.2	8.2-10.6	9.6-14.6
Cr_2O_3	0.82	0.68	0.77	0.84	1.17	0.78	0.19-0.81	0.03-0.39	0.11-1.41
FeO	2.60	2.76	2.83	3.28	3.84	3.04	2.72-4.57	4.4-8.7	4.3-9.9
MnO	0.02	0.02	0.02	0.02	0.03	0.04	<0.05-0.05	0.01-0.09	0.01-0.05
MgO	26.03	25.67	25.20	25.91	24.15	26.19	23.9-25.5	24.2-26.3	17.7-23.6
NiO	0.22	0.19	0.20	0.21	0.16	0.27	0.16-0.24	-	-
CaO	0.01	0.04	0.02	0.02	0.03	<0.03	<0.05	0.00-0.33	0.00-0.16
Na_2O	0.31	0.48	0.32	0.35	0.51	0.19	0.17-0.43	0.07-0.35	0.05-0.44
K_2O	10.00	10.06	10.21	9.47	9.74	9.99	9.27-9.97	9.1-12.0	9.4-10.7
Cl	0.08	0.06	0.06	0.02	0.03				
F	0.43	0.76	0.82	0.50	0.68				
BaO	0.29	0.19	0.085	0.216	0.137				
Rb_2O	0.028	0.023	0.035	0.029	0.028				
Atoms for 44 cation charges.									
Si	5.817	5.888	5.907	5.881	5.728				
Al	2.255	2.156	2.151	2.065	2.263				
Ti	0.019	0.049	0.087	0.071	0.192				
Cr	0.092	0.076	0.086	0.095	0.132				
Fe	0.308	0.328	0.335	0.391	0.457				
Mn	0.002	0.002	0.002	0.002	0.004				
Mg	5.504	5.430	5.319	5.511	5.123				
Ni	0.025	0.022	0.022	0.024	0.018				
Ca	0.002	0.006	0.003	0.003	0.005				
Ba	0.016	0.011	0.005	0.012	0.008				
Na	0.085	0.132	0.088	0.097	0.141				
K	1.810	1.821	1.845	1.724	1.768				
Rb	0.003	0.002	0.003	0.003	0.003				
Cl	0.020	0.014	0.014	0.005	0.007				
F	0.193	0.341	0.367	0.226	0.306				
mg	0.947	0.943	0.940	0.933	0.917				

1. mean 10 analyses, coarse-grained textures with no special feature (Table 2).
2. mean 6 analyses, associated with clinopyroxene (Table 2).
3. mean 4 analyses, some doubtful textural feature (Table 2).
4. mean 8 analyses, secondary texture in harzburgite (Table 3).
5. mean 21 analyses, secondary texture in lherzolite (Table 3).
6. pale "primary" phlogopite, coarse garnet lherzolite, DANCHIN (1979).
7. "primary-metasomatic" phlogopite, range for 8 xenoliths, Matsoku, HARTE AND GURNEY (1975).
8. range of 10 analyses of phlogopites, with TiO_2<lwt.%, in xenoliths, BOETTCHER et al. (1979).
9. range of 10 analyses of phlogopites, with TiO_2>lwt.%, in xenoliths, BOETTCHER et al. (1979).

extreme, a peridotite could have undergone partial melting with production of local pockets rich in magmatophile elements, including K, Fe and Ti. Deformation is likely during the partial melting, and the melt should move, and in some instances escape completely, and in other instances merely move a short distance. Subsequent cooling would lead to crystallization of melt pockets and ultimately to retrograde metamorphism and establishment of an equilibrium texture. Although there is a tendency for TiO_2 and FeO contents to be lower in primary than in secondary micas, it is necessary to remember the wide range of minor elements for secondary micas and the tendency for some secondary micas to have compositions related to adjacent minerals. Thus kelyphitic micas have higher Cr_2O_3 than veinlet micas, presumably because of contribution of Cr_2O_3 from breakdown of adjacent Cr-rich garnet. In harzburgites, secondary mica adjacent to olivine and orthopyroxene crystals tends to be low in minor elements. We conclude that the chemical composition of micas in peridotite nodules transported by kimberlites can result from both wide-scale factors (e.g. metamorphic equilibrium over large regions: meter to kilometer?) and local factors (e.g. local partial melting; infiltration of kimberlite magma; micrometer to centimeter?). It is necessary to consider textural features as well as chemical ones in discussing the origin of the micas.

Because of the magmatophile nature of TiO_2 and FeO, Fig. 10 is useful in comparing micas from the mantle. Our primary-textured micas are confined to FeO <3.5 wt% and TiO_2 <1.4 wt%, in contrast to many micas with much higher contents of these elements. Actually most primary-textured micas have FeO <3 wt% and TiO_2 <0.8 wt%. Our primary group matches well with the pale 'primary' phlogopite found in coarse garnet lherzolites (Table 6, column 6) by DANCHIN (1979), and the 'mantle-derived' phlogopites of BOYD and NIXON (1978).

It is now convenient to discuss the 'primary-metasomatic' phlogopite in eight xenoliths of garnet lherzolite from Matsoku, Lesotho (HARTE and GURNEY, 1975; HARTE *et al.*, 1975). Three types of phlogopite occur: (a) 'primary-metasomatic' type, occurring

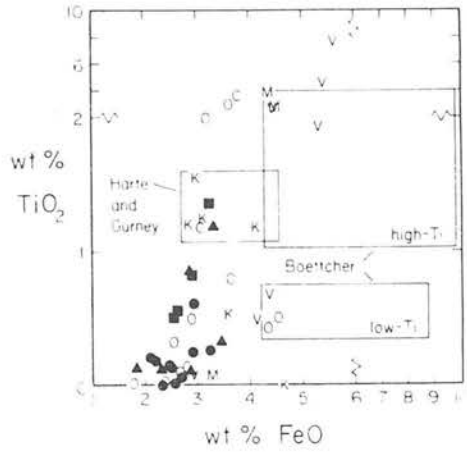

Fig. 10. Wt% FeO vs wt% TiO_2 of micas. Composition ranges are given for 'primary metasomatic micas of HARTE and GURNEY (1975) and for phlogopites in xenoliths (BOETTCHER *et al.*, 1979). See Table 6.

with ilmenite, rutile and sulfide(s) in veins, diffuse patches, small crystals and porphyroblasts (2–3 mm across, (b) 'late-secondary' type, occurring in kelyphitic and phlogopite rims around garnet and in serpentinous material and (c) a third type, whose textural features suggest another kind of 'late-secondary origin'. Because the 'primary-metasomatic' type occurs in veins, a secondary origin is implied with respect to the main body of the peridotite. However, the phlogopite crystals do have 'equilibrium' grain boundaries with respect to adjacent silicate and oxide minerals, as confirmed by B. HARTE (personal communication). Although the original discovery of 'primary-metasomatic' phlogopite was in finer-grained (recrystallized or partly-recrystallized) rocks, it was subsequently found in coarse rocks. A possible explanation of its *primary texture* is that prolonged annealing followed incursion of metasomatizing fluid. Such annealing must have preceded formation of the 'late-secondary' type. The 'primary-metasomatic' type of phlogopite is texturally distinct from our primary-textured type. Furthermore, some of the veins in the Lesotho rocks are much broader (e.g. 1 cm wide in LBM-101) and more regular than the veinlets of our secondary phlogopites; additionally, the veins consistently contain sulfides in contrast to rare and sporadic occurrence in veinlets. In Fig. 10, the composition range of the 'primary-metasomatic' micas lies near the upper limit of the range of Fe and Ti for our primary-textured micas and overlaps with only two specimens one each in the P_c and P_u groups.

BOETTCHER *et al.* (1979) and BOETTCHER and O'NEIL (1979) advocated the occurrence of precursory enrichment by metasomatism of peridotite before transport as xenoliths during magma eruption. Unfortunately they do not give detailed textural descriptions of most of their micas. Their micas from kimberlites tend to be Fe-rich, and we have arbitrarily subdivided them into Ti-rich and Ti-poor groups (Table 6; Fig. 10). The subgroups do not overlap with our primary-textured micas, but do overlap with our veinlet micas. Their specimen Kb-5-1-A is an isolated megacryst in kimberlite matrix. The mica crystals in a garnet lherzolite xenolith Kb-9-1 do not appear to be in textural equilibrium with the other silicate grains. Moreover the crystals average only 0.1 mm diameter in contrast to the >1 mm diameter of our primary-textured micas. We conclude that the specimens described by Boettcher *et al.* are not related to our group of primary-textured specimens.

In a preliminary abstract, SMITH and DAWSON (1975) made a tentative distinction between the chemical composition of micas from the MARID suite (DAWSON and SMITH, 1977) and the megacryst suite, both of which are richer in Fe than the primary-textured micas. The MARID and megacryst suites were attributed to crystallization of phenocrysts from kimberlitic magmas at various stages of ascent, and a third paper will provide detailed documentation. Because the micas described by BOETTCHER *et al.* (1979) are rich in Fe and Ti we attribute them to processes involving crystallization from Fe–Ti-rich liquids, some of which have penetrated into kimberlite: indeed the glimmerite micas described by BOETTCHER and O'NEIL (1979) almost certainly belong to the MARID suite. Although the primary-metasomatic' micas of HARTE and GURNEY (1975) are richer in Ti than all of our micas with undoubted primary texture, they have an overlapping range of Fe. The source of the metasomatizing fluid is unclear, but the close similarity of the Mg/Fe ratios of the 'primary-metasomatic' micas of HARTE and GURNEY and our primary-textured micas rules out derivation of the former from a magma produced by a *small* degree of equilibrium partial melting of the host rocks of the latter. Perhaps the magma responsible for cementing the polymict peridotites described by LAWLESS *et al.* (1979) had a composition similar to the metasomatizing fluids involved in the specimens described by HARTE and GURNEY (1975), being rich not only in K and H_2O but also in S. The phlogopite inclusion in a diamond from the Finsch kimberlite pipe is rich in TiO_2 (1.7 wt%) and FeO (5.4 wt%), which values (GURNEY *et al.*, 1979) are consistent with crystallization of the diamond and included phlogopite from an evolved liquid.

To conclude, there are obviously many uncertainties in the interpretation of the chemistry of micas in peridotite xenoliths, and metamorphism may have totally destroyed earlier textural evidence of metasomatism. Nevertheless there is a fairly well-defined group of coarse primary-textured micas in depleted lherzolite xenoliths, and their mean composition is of value in modeling the composition of *depleted* upper mantle. Fortuitously, the composition in Table 6, column 1, is quite similar to the one listed by WEDEPOHL and MURAMATSU (1979) for the average of a diverse group of phlogopites from "ultramafic rocks of potential mantle origin".

Our primary-textured group has the highest values of Mg/Fe of all micas in mantle peridotites and kimberlites, and it is tempting to ascribe the lower Mg/Fe of other micas to some combination of processes, *one* of which involves concentration of magmatophile elements into a liquid during partial melting of peridotites. At the onset of this investigation we hoped to find clean chemical and textural distinctions between micas from mantle, but ongoing studies by many investigators are indicating that there is some overlap between chemical properties of different textural groups, and that some textural features have ambiguous implications.

Acknowledgements— We thank C. H. EMELEUS and H. O. A. MEYER for supplying specimens, and R. L. HERVIG for making many electron microprobe analyses. Detailed advice from B. HARTE and helpful reviews from A. L. BOETTCHER, F. R. BOYD, F. FREY and D. WONES are much appreciated. Technical assistance from I. M. STEELE, R. DRAUS, I. BALTUSKA and O. DRAUGHN is gratefully acknowledged. Financial support came from NSF grants EAR 76-03604 and 77-27100.

REFERENCES

BARRETT D. R. and BERG G. W. (1975) Complementary petrographic and strontium-isotope ratio studies of South African kimberlite. *Phys. Chem. Earth* **9**, 619–635.

BISHOP F. C., SMITH J. V. and DAWSON J. B. (1978) Na, K, P and Ti in garnet, pyroxene and olivine from peridotite and eclogite xenoliths from African kimberlites. *Lithos* **11**, 155–173.

BOETTCHER A. L. and O'NEIL J. R. (1979) Stable isotope, chemical, and petrographic studies of high-pressure amphiboles and micas: evidence for metasomatism in the mantle source regions basalts and kimberlites. *Am. J. Sci.* in press.

BOETTCHER A. L., O'NEIL J. R., WINDOM K. E., STEWART D. C. and WILSHIRE H. G. (1979) Metasomatism of the upper mantle and the genesis of kimberlites and alkali basalts. In *The Mantle Sample: Inclusions in Kimberlites and other Volcanics* (eds F. R. Boyd and H. O. Meyer), pp. 173–182. American Geophysical Union.

BOULLIER A. M. and NICOLAS A. (1975) Classification of textures and fabrics of peridotite xenoliths from South African kimberlites. *Phys. Chem. Earth* **9**, 467–475.

BOYD F. R. (1973) A pyroxene geotherm. *Geochim. Cosmochim. Acta* **37**, 2533–2546.

BOYD F. R. and FINGER L. W. (1975) Homogeneity of minerals in mantle rocks from Lesotho. *Carnegie Inst. Washington, Yearb.* **74**, 519–525.

BOYD F. R. and NIXON P. H. (1975) Origins of ultramafic nodules from some kimberlites of northern Lesotho and the Monastery mine, South Africa. *Phys. Chem. Earth* **9**, 431–454.

BOYD F. R. and NIXON P. H. (1978) Ultramafic nodules from the Kimberley pipes, South Africa. *Geochim. Cosmochim. Acta* **42**, 1367–1382.

CARSWELL D. A. (1975) Primary and secondary phlogopites and clinopyroxenes in garnet lherzolite xenoliths. *Phys. Chem. Earth* **9**, 417–430.

CARSWELL D. A., CLARKE D. B. and MITCHELL R. H. (1979) The petrology and geochemistry of ultramafic nodules from Pipe 200, northern Lesotho. In *The Mantle Sample: Inclusions in Kimberlites and other Volcanics* (eds F. R. Boyd and H. O. A. Meyer), pp. 127–144. American Geophysical Union.

DANCHIN R. V. (1979) Mineral and bulk chemistry of garnet lherzolite and garnet harzburgite xenoliths from the Premier Mine, South Africa. In *The Mantle Sample: Inclusions in Kimberlites and other Volcanics* (eds F. R. Boyd and H. A. O. Meyer), pp. 104–126. American Geophysical Union.

DAWSON J. B. and SMITH J. V. (1977) The MARID (mica-amphibole-rutile-ilmenite-diopside) suite of xenoliths in kimberlite. *Geochim. Cosmochim. Acta* **41**, 309–323.

DELANEY J. S., SMITH J. V., DAWSON J. B. and NIXON P. H. (1979) Manganesee thermometer for mantle peridotites. *Contrib. Mineral. Petrol.* **71**, 157–169.

EHRENBERG S. N. (1979) Garnetiferous ultramafic inclusions in minette from the Navajo volcanic field. In *The Mantle Sample: Inclusions in Kimberlites and other Volcanics* (eds F. R. Boyd and H. O. A. Meyer), pp. 330–344. American Geophysical Union.

ELTHON D. and RIDLEY W. I. (1979) The oxide and silicate mineral chemistry of a kimberlite from the Premier mine: Implications for the evolution of kimberlitic magmas. In *Kimberlites, Diatremes and Diamonds: Their Geology, Petrology and Geochemistry* (eds F. R. Boyd and H. O. A. Meyer), pp. 206–216. American Geophysical Union.

GURNEY J. J., HARRIS J. W. and RICKARD R. S. (1979) Silicate and oxide inclusions in diamonds from the Finsch kimberlite pipe. In *Kimberlite, Diatremes and Diamonds: Their Geology, Petrology and Geochemistry* (eds F. R. Boyd and H. O. A. Meyer), pp. 1–15. American Geophysical Union.

HARTE B. (1977) Rock nomenclature with particular relation to deformation and recrystallisation textures in olivine-bearing xenoliths. *J. Geol.* **85**, 279–288.

HARTE B. and GURNEY J. J. (1975) Ore mineral and phlogopite mineralisation within ultramafic nodules from the Matsoku kimberlite pipe, Lesotho. *Carnegie Inst. Washington, Yearb.* **74**, 528–536.

HARTE B., COX K. G. and GURNEY J. J. (1975) Petrography and geological history of upper mantle xenoliths from the Matsoku kimberlite pipe. *Phys. Chem. Earth* **9**, 477–506.

LAWLESS P. J., GURNEY J. J. and DAWSON J. B. (1979) Polymict peridotites from the Bultfontein and De Beers Mines, Kimberley, South Africa. In *The Mantle Sample: Inclusions in Kimberlites and other Volcanics* (eds F. R. Boyd and H. O. A. Meyer), pp. 145–155. American Geophysical Union.

MITCHELL R. H. (1978) Mineralogy of the Elwin Bay kimberlite, Somerset Island, N.W.T., Canada. *Am. Mineral.* **63**, 47–57.

MITCHELL R. H. (1979) Mineralogy of the Tunraq kimberlite Somerset Island, N.W.T., Canada. In *Kimberlites, Diatremes and Diamonds: Their Geology, Petrology and Geochemistry* (eds F. R. Boyd and H. O. A. Meyer), pp. 161–171. American Geophysical Union.

MYSEN B. O. and BOETTCHER A. L. (1975) Melting of the hydrous mantle: II Geochemistry of crystals and liquids formed by anatexis of mantle peridotite at high pressures and high temperatures as a function of controlled activities of water, hydrogen and carbon dioxide. *J. Petrol.* **16**, 547–595.

NICHOLAS A. and POIRIER J. P. (1976) *Crystalline Plasticity and Solid State Flow in Metamorphic Rocks*. Wiley.

PAUL D. K., BUCKLEY F. and NIXON P. H. (1976) Fluorine and chlorine geochemistry of kimberlites. *Chem. Geol.* **17**, 125–133.

SCOTT B. H. Petrogenesis of kimberlites and associated potassic lamprophyres from Central West Greenland. In *Kimberlites, Diatremes and Diamonds: Their Geology, Petrology and Geochemistry* (eds F. R. Boyd and H. O. A. Meyer), pp. 190–205. American Geophysical Union.

SHAW D. M. (1960) The geochemistry of scapolite Part II Trace elements, petrology and general geochemistry. *J. Petrol.* **1**, 261–285.

SMITH J. V. and DAWSON J. B. (1975) Chemistry of Mg-rich micas from kimberlites and xenoliths, with implications

for volatiles in upper mantle. *Geol. Soc. Am. Abs. Progrs.* **7**, 1275–1276.

SMITH J. V., BRENNESHOLTZ R. and DAWSON J. B. (1978) Chemistry of micas from kimberlites and xenoliths—I. Micaceous kimberlites. *Geochim. Cosmochim. Acta* **42**, 959–971.

SMITH J. V., HERVIG R. L., ACKERMAND D. and DAWSON J. B. (1979) K, Rb and Ba in micas from kimberlite and peridotitic xenoliths, and implications for origin of basaltic rocks. In *Kimberlites, Diatremes and Diamonds: Their Geology, Petrology and Geochemistry* (eds F. R. Boyd and H. A. O. Meyer), 241–251. American Geophysical Union.

STUEBER A. M., HUANG W. and JOHNS W. D. (1968) Cl and F abundances in ultramafic rocks. *Geochim. Cosmochim. Acta* **32**, 353–357.

WATSON K. D., BRUCE G. S. W. and HALLADAY L. B. (1978) Kimberlitic dyke in Keith township, Ontario. *Can. Mineral.* **16**, 97–102.

WEDEPOHL K. H. and MURAMATSU Y. (1979) The chemical composition of kimberlites compared with the average compositions of three basaltic magma types. In *Kimberlites, Diatremes and Diamonds: Their Geology, Petrology and Geochemistry*, pp. 300–312. American Geophysical Union.

Contrib. Mineral. Petrol. 72, 205–217 (1980)

Contributions to Mineralogy and Petrology

Geological Implications and Validity of Calculated Equilibration Conditions for Ultramafic Xenoliths From the Pipe 200 Kimberlite, Northern Lesotho

R.H. Mitchell[1], D.A. Carswell[2], and D.B. Clarke[3]

[1] Department of Geology, Lakehead University, Thunder Bay, Ontario, Canada P7B 5E1, Canada
[2] Department of Geology, Sheffield University, Sheffield S1 3JD, United Kingdom
[3] Department of Geology, Dalhousie University, Halifax, Nova Scotia, B3H 3J5, Canada

Abstract. Current methods of geothermometry and geobarometry applicable to garnet lherzolite are reviewed with reference to recent experimental studies of the equilibration of natural garnet lherzolite and it is concluded that the Wells and Mori-Green formulations of the two pyroxene solvus provide the most reasonable temperature estimates. Pressures are best estimated by using these temperatures with Wood's formulation of the orthopyroxene-garnet geobarometer without chromium corrections. Pipe 200 garnet lherzolites are considered to have equilibrated at 907°–950° C at 30.0–34.5 kb.

It is shown that the transport times of xenoliths from the mantle are sufficiently long (0.5–24 h) to allow thermal equilibration with kimberlite but are too short to allow chemical re-equilibration to occur. Xenolith suites therefore retain information regarding the pressure/temperature history of the upper mantle despite being heated to the temperature of the kimberlite magma during transport.

The Pipe 200 xenolith suite indicates that the upper mantle beneath Lesotho has been perturbed to temperatures slightly above those defined by steady state geotherms. The Pipe 200 suite is derived from a narrow depth range (90–110 km) and derivation of chromite and garnet lherzolites from similar depths implies that the mantle is heterogeneous over short vertical distances. No simple stratigraphy, in which chromite lherzolites overlie garnet lherzolites is evident. Comparison with other suites of Lesotho garnet lherzolites shows that it is not possible to construct an upper mantle stratigraphy except in the most general terms because of the prevailing lateral and vertical heterogeneity and apparent limited depth range represented by the xenolith suites.

Introduction

The Pipe 200 kimberlite in northern Lesotho is situated close to the Letele pass road about 8 km west of the better known kimberlites of the Kao area. The pipe outcrops on the western bank of the Malibamatso River and it and the associated Malibamatso Blow and kimberlite dike swarm have been briefly described by Kresten and Dempster (1973). In addition to numerous xenoliths of crustal origin the kimberlite contains a suite of mantle-derived ultramafic xenoliths which have been described in detail by Carswell et al. (1979). In that work it was shown that the ultramafic suite was dominated by garnet and/or chromite lherzolites and harzburgites of varying degrees of depletion in 'basaltic components'. Compositional data for the bulk rocks and their constituent minerals were presented but the interpretation of the data in terms of the nature of the upper mantle beneath Northern Lesotho was only briefly touched upon. In this work we explore some of the possibilities of kimberlite-xenolith interaction and the relevance of the xenolith equilibration temperatures and pressures (P/T values) to the thermal and stratigraphic nature of the mantle. The geothermometers available for estimating lherzolite equilibration temperatures are discussed in some detail as the equilibration temperature chosen is critical in evaluating the equilibration pressure and ultimately therefore in arriving at any upper mantle model.

Geothermometry

Temperatures based upon the pyroxene solvus have been extensively utilized for estimating the equilibration parameters of xenoliths. Many of these studies are based upon the Davis and Boyd (1966) 30 kb solvus, which was determined by a combination of optical and XRD methods. The Davis and Boyd (1966) solvus

0010-7999/80/0072/0205/$02.60

Table 1. Pressure and temperature estimates for Pipe 200 ultramafic xenoliths

	PTH 102	PTH 108	PTH 202	PTH 203	PTH 205	PTH 207	PTH 304	PTH 400	PTH 401	PTH 403	PTH 404	PTH 405	PTH 407	PTH 409	PTH 410	PTH 210
Rock type	GL	(G)CL	(G)CL	CL	(G)CL	GCL	(G)CL	GL	GCL	GL	GL	GL	GL	GCL	GL	GP
Pyroxene solvus																
T° C Wells (1977)	947	873	883	952	963	946	880	932	883	946	950	934	929	907	946	823
P kb Wood (1974) No Cr correction	31.5	–	–			34.3		34.5	–	30.0	32.8	32.6	31.1	30.3	32.2	14.4
P kb Wood (1974) Cr correction	31.6	–	–	–		34.8		31.1	–	29.8	28.2	28.4	26.0	24.4	27.5	14.7
T° C Mori-Green (1978)	971	890	896	960	989	969	893	957	896	969	971	953	948	925	967	841
P kb Wood (1974) No Cr correction	32.9	–	–	–	–	35.6	–	36.0		31.2	34.0	33.7	32.1	31.3	33.4	15.3
P kb Wood (1974) Cr correction	33.0	–	–	–	–	36.1	–	32.5	–	31.1	29.3	29.5	27.0	25.4	28.6	15.6
T° C Boyd (1973)	910	915	935	1,005	970	975	1,000	990	920	985	950	1,005	990	965	1,010	800
T° C Wood-Banno (1973)	1,060	999	1,015	1,095	1,081	1,065	1,015	1,047	1,018	1,065	1,073	1,058	1,054	1,034	1,071	945
Garnet-clinopyroxene Fe-Mg exchange																
T° C Akella-Boyd (1974)	1,085	–	–	–	–	1,115	–	1,160	–	1,160	1,110	1,150	1,110	1,185	1,170	875
T° C Mori-Green (1978)	996	–	–	–	–	1,037	–	1,109	–	1,100	1,032	1,097	1,031	1,153	1,122	698

Rock types CL = chromite lherzolite; GCL = garnet chromite lherzolite; GL = garnet lherzolite; GP = garnet pyroxenite. (G) in parentheses indicates that garnet originally thought likely to have been a member of the original primary assemblage, although now absent

position is not consistent with recent experiments employing microprobe techniques. Both Nehru and Wyllie (1974) and Mori and Green (1975, 1976) clearly show that the Davis and Boyd (1966) solvus temperatures are in error, being low relative to the newer values at high temperatures (> 1,100° C) and high at lower temperatures. Boyd (1973) proposed that the pyroxene solvus is essentially insensitive to pressure. Later studies (Mori and Green 1975; Nehru and Wyllie 1974; Lindsley and Dixon 1976) have however demonstrated a pressure effect, the degree of pressure dependence increasing with temperature increase and being most pronounced above 1,200° C. Between 1,200° and 900° C the pressure effects appear to be relatively small, but their extent is poorly known because of insufficient experimental data. Below 900° C the solvus is essentially pressure independent. Wells (1977) has concluded that over much of the temperature range of interest that pressure effects are masked by experimental errors of similar or greater magnitude, a conclusion also reached by Mori and Green (1978) in their study of the solvus in natural garnet lherzolite compositions. We conclude that the present solvus data do not invalidate the assumption that the two pyroxene geothermometer is independent of pressure over the P/T range of interest in the interpretation of these xenoliths.

More serious problems arise in attempting to extrapolate from simple systems to natural assemblages. Boyd (1973) has attempted to make allowance for Fe by use of the Ca/Ca+Mg ratio rather than the Ca/Ca+Mg+Fe ratio of clinopyroxene. Boyd (1973) method temperatures for the Pipe 200 xenoliths are given in Table 1 and are directly comparable with the data employed by Boyd (1973) to define the original version of the Lesotho geotherm. Wood and Banno (1973) derived a semi-empirical expression for correcting for the presence of Fe. Application of the Wood-Banno method to Pipe 200 lherzolites gives temperatures which are 15°–150° C higher than those calculated by the Boyd (1973) method (Table 1). However, as both the above Fe corrections are based on the Davis and Boyd (1966) solvus data, one must question the validity of the temperature estimates.

Wells (1977) incorporating the recent experimental data of Nehru and Wyllie (1974), Mori and Green (1975, 1976), and Lindsley and Dixon (1976) has argued that the Wood-Banno correction gives serious overestimates of temperature for Mg-rich compositions at relatively low temperatures (< 1,100° C), and has devised a new semi-empirical Fe correction. Pressure effects upon the solvus are considered to be minimal and within the experimental errors in the original solvus determinations. Table 1 shows that Wells (1977) temperatures are 118°–143° C lower than those obtained by the Wood-Banno (1973) method.

Mori and Green (1978) have investigated the solvus in a multicomponent system by equilibration of natural mineral mixtures in the range 950°–1,500° C at 30–40 kb pressure. Direct comparison between experimental mixtures and natural garnet lherzolites of similar composition has indicated that previously determined P/T conditions of equilibration, mostly Wood-Banno method, are too high, and that the Lesotho geotherm should be located at much lower temperatures than those proposed by Boyd (1973). The data support Wells (1977) analysis of pyroxene geothermometry. Table 2 gives temperatures of the Mori and Green (1978) and Mori (1976) experimental runs calculated by the Wells (1977) method. Agreement between the Wells temperature and the experimental temperature is surprisingly good, the Wells values being on average about 30° C below that temperature. Similarly calculation of Pipe 200 lherzolite temperatures (Table 1) using the Mori and Green (1978) solvus are about 30° C higher than those obtained by the Wells method. Mori and Green (1978) solvus temperatures are in general higher than the known experimental temperatures when these are calculated for their experimental runs (Table 2).

Table 2. Comparison of experimental and calculated temperatures and pressures of equilibration of natural garnet lherzolites. Experimental data are from Mori (1976)

Experimental runs	C2	T9	T8	T6	FF6	FF7	A7	XII	X8	X6	DD1	DD2	DD3	DD4
T°	1,200	950	1,000	1,050	1,000	1,050	1,450	1,000	1,100	1,200	1,100	1,200	1,250	1,300
P kb	30	30	30	30	30	30	30	30	30	30	40	40	40	40
Pyroxene solvus														
T° C Wells (1977)	1,177	952	1,029	1,051	1,024	1,059	1,391	973	1,070	1,125	1,010	1,115	1,201	1,228
P kb Wood (1974)														
No Cr correction	28.4	20.8	23.2	25.0	29.7	34.1	34.1	23.5	22.5	20.8	31.8	31.6	41.9	34.0
P kb Wood (1974)														
Cr correction	26.5	21.6	24.2	24.6	30.6	35.0	34.0	23.6	21.9	18.7	30.0	30.0	42.9	32.0
T° C Mori-Green (1978)	1,247	1,000	1,091	1,114	1,087	1,128	1,473	1,027	1,146	1,211	1,065	1,194	1,273	1,294
P kb. Wood (1974)														
No Cr correction	31.6	23.2	26.1	28.0	33.0	37.8	37.5	26.2	25.9	24.3	34.8	35.6	45.8	37.1
P kb Wood (1974)														
Cr correction	29.6	23.9	27.2	27.6	34.0	38.8	37.4	26.3	25.2	22.1	33.0	33.8	46.9	35.1

It should be noted at this point that the Wood-Banno, Wells and Mori-Green temperatures in Tables 1 and 2 are calculated by assuming that all Fe is present as Fe^{2+}. These estimates are minimum values, as consideration of stoichiometrically calculated values of Fe^{3+} in the pyroxenes raises the temperature slightly (typically 10°–20° C). In addition the activity of the $Mg_2Si_2O_6$ component in both pyroxenes is calculated assuming ideal mixing of Fe and Mg at the M1 and M2 sites. This is unlikely to be true as demonstrated by Virgo and Hafner (1969) but the errors introduced by this assumption are small compared to the errors inherent in the original solvus data.

Råheim and Green (1974) demonstrated that the distribution coefficient $K_D=(Fe^{2+}/Mg)_{garnet}/(Fe^{2+}/Mg)_{clinopyroxene}$ has potential as a geothermometer for mantle derived rocks. Råheim and Green's (1974) calibrations were for basaltic compositions and are not strictly applicable to garnet lherzolites. In addition a significant pressure effect on K_D was observed. Akella and Boyd (1974) and Mori and Green (1978) have calibrated this distribution coefficient for garnet lherzolite compositions and noted that the pressure effect is much less pronounced than for basaltic compositions. Calculated K_D temperatures for Pipe 200 lherzolites are 1,085°–1,185° C and 996°–1,153° C (Table 1) by the Akella-Boyd (1974) and Mori-Green (1978) methods respectively. Both of these ranges are significantly higher than the Wells (1977) and Mori-Green (1978) solvus temperatures. They are however maximum values for this method, as all Fe is calculated as Fe^{2+}. Assuming that a small amount of Fe^{3+} is present in the natural assemblages and that the Fe^{3+}/Fe^{2+} ratio is higher in clinopyroxene than garnet, the calculated K_D values are too low and the temperature is too high. Reduction of temperatures by as much as 100° C can be achieved by calculating Fe^{3+} on a stoichiometric basis, but this procedure has not been employed here as many of the analysed pyroxenes give unreasonably high Fe^{3+}/Fe^{2+} ratios. Carswell (1978) has noted that the Mg-Fe exchange reaction between pyroxene and garnet is probably more sensitive as a geothermometer below 1,100° C than the pyroxene Ca-Mg exchange. However we caution that until the magnitude of the pressure effects on K_D for lherzolite compositions is known and reliable estimates of Fe^{3+}/Fe^{2+} ratios can be made, that temperatures obtained from the garnet-clinopyroxene thermometer are of doubtful reliability and certainly for the Pipe 200 garnet lherzolites appear to be somewhat too high.

In summary we conclude that the best estimates of equilibration temperatures are probably those given by the Wells (1977) method and to a lesser degree those given by the Mori-Green (1978) solvus method. The close agreement between calculated temperatures for these two thermometers based upon different experiments is encouraging and indicates that earlier temperature estimates for lherzolites are too high.

Geobarometry

MacGregor (1974) showed that the solubility of potential garnet molecule in pyroxenes coexisting with garnet decreases with increasing P for a given temperature. Thus if a temperature estimate is available P may be calculated from the Al_2O_3 content of the pyroxenes.

Boyd (1973) has used 'raw Al_2O_3' contents of orthopyroxenes together with MacGregor's (1974) data to establish equilibrium pressures for Lesotho xenoliths. However, experiments in more complex systems have indicated that the presence of other elements, especially Na, Cr, Fe and Ca profoundly effect the garnet-enstatite equilibria. These 'contaminating' elements in effect reduce the Al_2O_3 content of the orthopyroxene and direct application of MacGregor's (1974) data leads to overestimation of pressures.

Wood (1974) has derived a semi-empirical expression to correct for the more complex character of natural assemblages. Some idea of the effectiveness of the correction can be obtained by applying it to Mori and Green's (1978) laboratory equilibrated assemblages. Pressures calculated using Wells (1977) solvus temperatures are low relative to the known experimental pressure by up to 5 kb, with or without Cr corrections (Table 2). The overall effect of the Cr correction is generally, but not invariably, to reduce calculated pressures relative to those calculated without the correction, as desired by Wood (1974). Pressures calculated using Mori and Green's (1978) solvus temperatures generally give much better agreement with the experimental values, those obtained *without* the Cr correction usually being closer to the actual values. Accordingly we feel that pressures calculated without the Wood (1974) Cr correction seem to be marginally superior to those calculated using it, at least for assemblages with these Cr/Cr+Al ratios. Extension of this conclusion to other assemblages is problematical. The Pipe 200 garnets are much richer in Cr (Cr/Cr+Al=12.4–24.6) than the garnet in the Mori-Green (1978) experimental assemblages (Cr/Cr+Al=3.5–10.3), and we have as yet no way of assessing the validity of the Cr correction for such higher Cr rocks.

In summary we consider that no P estimate can be accepted unequivocally and cannot be until the garnet-orthopyroxene barometer is calibrated for Cr-rich assemblages.

We will however provisionally accept that Wood (1974) pressure estimates with no Cr correction deterined in conjunction with the best temprature estimates, that is the Wells (1977) and Mori-Green (1978) solvus temperatures, give reasonable estimates of equilibration pressures with the provision that the pressures may be too low by several kilobars and also that a Cr correction in Cr-rich systems might reduce calculated pressures further. Hence we are unable to positively state whether the pressure estimates are either too high or too low.

Our recommended P/T estimates for Pipe 200 lherzolites using the Wells (1977)-Wood (1974) methods are:

Garnet lherzolite T° C = 907° 950° C (mean 937° ± 13° C), P kb = 30.0 34.5 kb (mean 32.1 ± 1.5 kb); chromite lherzolite T° C = 873° 963° C.

The single garnet pyroxenite (PTH 210) equilibrated at 823° C and 14.4 kb (Wells/Wood) or 698° C and 8.9 kb (Mori-Green K_D/Wood). The latter values are probably more realistic than the former for this bulk composition.

Interpretive Models of Equilibration Data

The calculated equilibration parameters for the Pipe 200 xenoliths might be interpreted in terms of any of the following models.

Model 1

The P/T data reflect conditions in the upper mantle but are artificially telescoped into a limited P/T range as a consequence of the nature of the geothermobarometers involved. As noted above equilibration temperatures can be reasonably well estimated to within ± 50° C of the 'true' value. Pressure determinations are much less certain, in addition to experimental errors the estimates may be high or low by an unknown magnitude as corrections for the presence of other elements are not sufficiently well understood. Further the Al_2O_3 isopleths are sub-parallel to the theoretical shield geotherms over the critical range of interest. Mori and Green (1975) have noted that the clinopyroxene limb of the Fe-free solvus is less markedly temperature dependent than previously thought, although this may not be true for more complex systems. These problems inherent in the methods can lead to 'telescoping' of the derived P/T values into artificially narrow limits. Moreover experimental studies have shown that the pyroxene solvus is relatively insensitive below 900° C. Fraser and Lawless (1978) have thus noted that because of the different blocking temperatures for diffusion that the two pyroxene geothermometer and the orthopyroxene-garnet geobarometer may be out of phase with one another and generate spurious apparent geotherms. Only further experimental studies will resolve these problems.

Model 2

The P/T data recorded are the result of kimberlite-xenolith thermal interactions and have no relevance to the thermal history of the upper mantle. An assessment of the extent of kimberlite-xenolith interaction has not been previously attempted as it is assumed that such effects do not occur or at the most of minor importance. It is important to demonstrate that this assumption is correct because if it is not, then the whole concept of paleogeotherm determination using xenolith P/T data would be thrown into doubt. The problem can be considered to be one in which there is an interplay of three factors, (a) heat transfer, (b) mass transfer and (c) xenolith transport rates from the mantle in kimberlite. These factors are considered below.

Model 3

The P/T data record information relevant to the thermal history and stratigraphy of the upper mantle. Kimberlite-xenolith interactions are absent. This model is further considered after discussion of Model 2.

Model 2: Kimberlite-Xenolith Interactions

Heat Transfer

Mantle xenoliths incorporated into kimberlite will be subjected to heating by the magma. If the fraction of xenoliths is not too great the magma will possess enough heat to raise their temperature to that of the magma. Heat may also be supplied by the latent heat of crystallization of phases with which the magma is saturated e.g. the discrete nodule association of Boyd and Nixon (1975). Thermal effects can be determined using equations derived for heat conduction in a sphere (Ingersoll et al. 1955) assuming that the xenoliths are approximately spherical and that the magma is not undergoing rapid cooling, this latter assumption being valid only for the magma whilst it remains at depth in the mantle.

The temperature Tx(°C) at r cm from the center of a xenolith radius R cm after t seconds immersion in a magma at temperature Ts, is given by:

$$\frac{\mathrm{Tx}-\mathrm{Ts}}{\mathrm{To}-\mathrm{Ts}}=\frac{2R}{\pi r}\left(\sin y\cdot e^{-x}-\tfrac{1}{2}\sin 2y\cdot e^{-4x}+\tfrac{1}{3}\sin 3y\cdot e^{-9x}\ldots\right)$$

where $y=\pi r/R$ and $x=\pi^2\alpha t/R^2$. To is the original temperature of the xenolith at time $t=0$ and α is

the thermal diffusivity, which here is taken to be 0.010 (Goguel 1976).

The effects for a xenolith of 100 cm radius are shown in Fig. 1. This is a best case possibility with maximum difference between To and Ts. Xenoliths with greater To will heat up faster than those illustrated in Fig. 1, which corresponds to the rise of a kimberitic magma at 1,300° C up into the mantle where it incorporates xenoliths initially at a lower temperature. 1,300° C is taken as a reasonable approximation of initial magma tempratures as Wyllie and Huang (1976) have shown that partial melting of carbonated mantle to give kimberlitic liquids can occur at 1,250°–1,300° C at 50 kb. Figure 1 shows that xenoliths will be essentially uneffected at their cores for times of up to 6 h and that a gradational 'onion skin' temperature profile is developed around the core. This is particularly important as later shattering of large xenoliths would produce a series of small fragments recording this temperature profile, if chemical equilibration also occurs. Such a profile would be meaningless in terms of mantle P/T values. Figure 2 summarizes the times (t) taken for xenolith cores to reach 99% of the magma temperature (Ts). Core temperatures (Tc) are given by the relation (Ingersoll et al. 1955):

$$\frac{Tc-Ts}{To-Ts}=2(e^{-x}-e^{-4x}-e^{-9x}) \quad \text{where } x=\pi^2\alpha t/R^2.$$

Times to reach Ts are not given as the exponential terms in the equation for Tc result in extremely long times for 100% equilibration.

Figure 2 indicates that all xenoliths 10 cm or less in radius. i.e. the typical size of xenoliths found in kimberlite will thermally equilibrate with the magma in 78 min or less. This conclusion being valid for all values of To from 800° C up to Ts.

Clearly the above analysis indicates that thermal interactions between kimberlite and xenoliths can be profound, whether or not thermal equilibration also results in chemical equilibration is however problematical and depends upon diffusion rates between the xenolith minerals and the transport rates of xenoliths to regions where low temperatures block diffusion.

Mass Transfer

Given that xenoliths can thermally equilibrate, will they chemically re-equilibrate? The simplest approach to the problem is to consider it to be one of lattice diffusion and to estimate the amount of diffusion using Fick's Laws. This requires that each phase in the

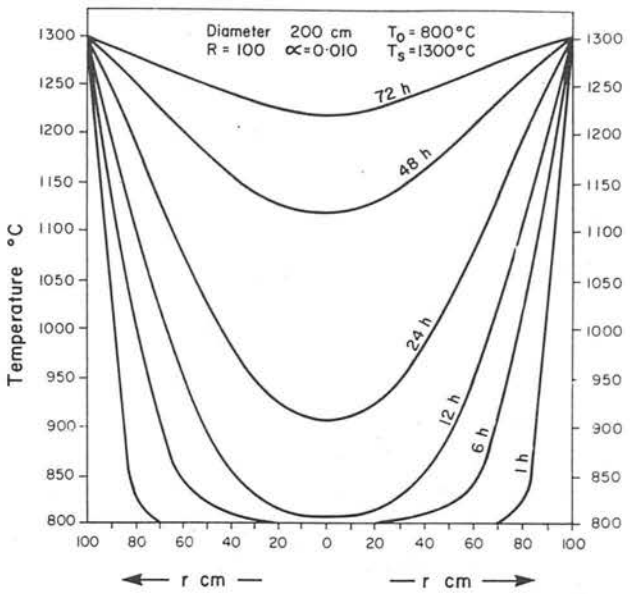

Fig. 1. Temperature profiles developed within a spherical xenolith (radius R = 100 cm) as a function of time (hours) and distance (*r cm*) from the xenolith center. Initial temperatures of the xenolith and host magma assumed to be 800° C and 1,300° C respectively. α = thermal diffusivity

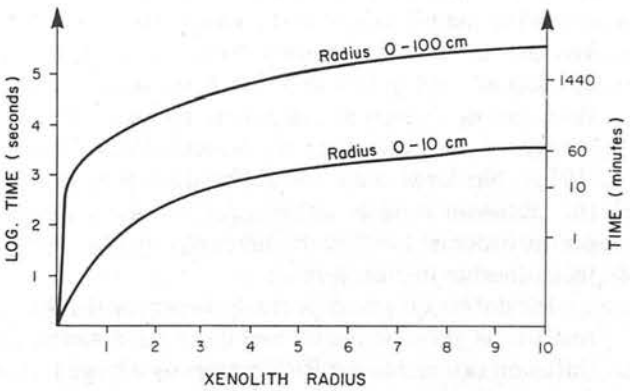

Fig. 2. Times required for spherical xenoliths (initially at 800° C) of up to 100 cm radius to thermally equilibrate to within 99% of the host magma temperature (1,300° C)

xenolith is considered to be a sphere and that diffusion is induced by the temperature rise. Diffusion induced concentration profiles for a given grain can be determined using the relation (Crank 1957).

$$\frac{C-Ci}{Cs-Ci}=1+\frac{2a}{\Pi R}\cdot\sum_{n=1}^{x}\frac{(-1)^n}{n}\sin\frac{n\pi R}{a}\cdot e^{-x}.$$

Where $X=Dn^2\pi^2t/A^2$, Cs = surface concentration, Ci = initial concentration, R = distance from center of a grain radius a cm C = concentration at R after t seconds. D = diffusion coefficient. Results for a grain 0.1 cm in radius are shown in Fig. 3 and indicate

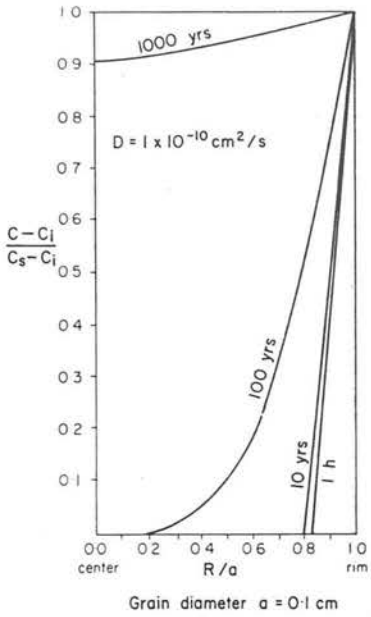

Fig. 3. Diffusion induced concentration profiles for spherical mineral grains, radius a cm, as a function of time and radial distance, R cm, from the grain center. D = diffusion coefficient

that little diffusion occurs in times of up to 10 years for all reasonable values of volume diffusion coefficients for mantle minerals (Hofmann and Hart 1978) and that a zone of diffusion about 20 μm thick will develop around grains in about 1 h. Similar conclusions can be arrived at using more complex diffusion models of the type given by Anderson and Buckley (1973). No large scale re-equilibration is implied in the diffusion models unless equilibration times are on the order of 1,000 years, times clearly not relevent to kimberlite intrusion times.

Ideal diffusion models are, however, probably unrealistic as grain boundary and dislocation controlled diffusion can increase diffusion rates by a large factor. Experimental studies have demonstrated that the equilibration of mechanical mixtures of mantle minerals (Mori and Green 1978: O'Hara et al. 1971) in the presence of small amounts of water proceeds very rapidly. Only 1–24 h is required for the attainment of equilibrium. Similar rapid equilibration might be expected in nature as most xenoliths show evidence of alteration involving water e.g. kelyphitization, serpentinization, secondary phlogopite formation.

Evidence from the xenolith populations have not been studied in detail from this viewpoint. Narrow zones of markely different composition to the bulk of the grain do not appear to be common, but such zones might easily be obscured by later serpentinization and kelyphitization. Such rims are found around clinopyroxenes but the origin of these might be more related to decompression than to kimberlite-xenolith interaction (Carswell et al. 1979). No zoned xenoliths of the type described by Wilshire and Jackson (1975) in basalts have been found in kimberlites. Heterogeneity in such xenoliths can be ascribed to magma-xenolith re-equilibration of the type described by the thermal profiles given in Fig. 1. Boyd and Finger (1975) have shown that intergrain compositional variation in Lesotho xenoliths is very slight, however this result is to be expected if the xenoliths have undergone rapid and complete re-equilibration, and the observation is not diagnostic of the origin of the homogeneity. Harte and Gurney (1975) have described from Matsoku, lherzolites containing primary metasomatic minerals formed at depth in the mantle and have noted that 'extensive chemical equilibration with the host rock silicates was attained' (Harte and Gurney 1975, p. 534) during this metasomatism. As Harte and Gurney (1975) consider that the source of the metasomatic fluids was perhaps the kimberlite itself, this would clearly imply that interaction with kimberlite has occurred therefore that the P/T values given by the xenoliths are not necessarily those of the ambient mantle. The small spread in the P/T data seen some xenolith suites may represent a 'mixing line' between mantle values and those of the magma.

Transport Rates

For thermal and chemical equilibration *not* to occur transport must be rapid if small xenoliths are not to be equilibrated. Pooling of the magma at any stage is not permissible. In terms of rise velocity profiles, kimberlite intrusion may be divided into three stages, (1) upper mantle-lower crust transit, (2) transit within the upper crust as dikes and (3) fluidized intrusion as diatremes. The mechanics of stages 2 and 3 are reasonably well understood but nothing is actually known about stage 1, the portion which is critical to understanding kimberlite-xenolith interactions. McGetchin (1968) has studied the problem by a fluid dynamics approach based upon the Bernoulli equation. The method provides adequate treatment for stages 2 and 3 but is less acceptable for stage 1 for reasons outlined below. Table 3 gives approximate transport times averaged from McGetchin's (1968) velocity profiles. Case M is considered by McGetchin to provide a reasonable analogy to the Kimberley diatreme. An important result of the model is that ca. 97% of the total transport time is spent in the lower crust and mantle. Adiabatic cooling effects and rapid transport rates, if valid, indicate that thermal effects on xenoliths associated with stages 2 and 3 will be minimal, in agreement with the well known lack of thermal effects associated with diatreme for-

Table 3. Average velocities and rise times for stages in kimberlite intrusion as calculated from McGetchins' (1968) model

	Model F			Model M			Model T		
	Velocity range	V	Time	Velocity range	V	Time	Velocity range	V	Time
Stage 3 (0–1 km) diatreme	59–222	134	7 s	318–750	555	2 s	1,005–1,506	1,291	1 s
Stage 2 (1–10 km) dike	16– 59	34	5 min	76–318	186	48 s	392–1,005	673	13 s
Stage 1 (10–100 km)?	16– 0	12	125 min	76– 0	61	25 min	392– 0	259	6 min

All velocities in meters per second. V = average velocity for each stage

mation. However, fluidized emplacement times of less than 2 s would appear to us to be geologically improbable. Flow in kimberlite dikes might be similar to that of CO_2-rich ultrabasic lamprophyres. Currie and Ferguson (1970) estimated flow rates of 20 m/s for such magmas, in agreement with McGetchin's (1968) estimated of 20–60 m/s for the Moses Rock dike. McGetchin's model neglects lateral dike flow of any extent. Such flow might be significant in view of the tendency for kimberlites to be aligned along linear features over distances of tens of kilometers. Such travel would increase transport time and the opportunity for re-equilibration.

During stage 1 of the ascent, McGetchin (1968) indicates that velocities are essentially uniform over a distance of 90 km. This conclusion is the result of considering the ascent to be analogous to flow of a Newtonian fluid in a pipe. As outlined below we feel that this approach may be incorrect, and will overestimate velocities, as a significant non-Newtonian aspect may be involved in the early stages of the ascent.

Kimberlites are considered to form at depths on the order of 150 km by small (1–3%) degrees of partial melting of 'garnet lherzolite' (Mitchell and Brunfell 1975; Wyllie and Huang 1976). The protokimberlite melt will be of small volume relative to the residual mantle (restite) which will be in thermal and chemical equilibrium with the liquid. Mitchell (1978) has postulated that the restite contains material derived from depths greater than 150 km, transported upwards by the diapiric flow which initiates magmatism, these xenoliths however do not record higher P/T values because of continual equilibration during slow diapir transport. Maximum teperatures recorded by xenoliths might give an estimate of P/T at the time of melt segregation. Whether the restite will be transported or not depends upon xenolith settling velocities relative to magma ascent velocities and during the initial stages as the liquid segregates into a larger volume, from the restite, one might expect a considerable loss of xenoliths. This may be one reason for the rarity of high temperature xenoliths of the kind found at Thaba Putsoa (Boyd 1973). At first the mixture of liquid plus restite will be a slurry showing transport characteristics which change from settling to non-settling as the magma accelerates away from the parent diapir. The high proportion of solid to liquid will give the flow non-Newtonian rheological properties (Holland 1973). In such a flow regime McGetchin's (1968) analysis is not valid. Transport rates for non-Newtonian flow are lower than predicted for Newtonian fluids, and at the same time a higher proportion of solid can be carried as the non-Newtonian characteristics alter the transport properties of the matrix fluid. Hence for example, the presence of large numbers of xenoliths in a magma does not necessarily imply a high flow rate. Sparks et al. (1977) have previously demonstrated how these concepts apply to xenoliths in basalts, and that calculated velocities can differ by up to factors of forty.

As the kimberlite ascends, elutriation may occur and new material (true xenoliths) may be added, plucked from the conduit walls. Eventually as the fluid phase expands in the upper portion of the mantle the flow regime will change to one of compressible Newtonian flow and enter stage 2 of the intrusion sequence.

Numerical analysis of the above model is beyond the scope of this paper and in any case is fraught with difficulties, as for example we have no idea of the geometry or method of propogation of the conduit, whether the magma flow is in discrete pulses or is continuous and what is the ratio of non-Newtonian slurry transport to Newtonian turbulent flow. The former may persist to high levels as evidenced by intrusions which contain a very high proportion of xenoliths to liquid e.g. West Greenland, Matosku, Roberts Victor. The xenolith population in any intrusion maybe affected by conduit wall-induced eddies and Magnus effects which might trap the xenoliths at depth or concentrate them in the center of the conduit respectively. Significant amounts of xenolith sorting may occur in the mantle depending upon the ascent velocities and the rheological chracteristics of the kimberlite magma.

In summary, transport rates of xenoliths are likely to be very rapid in the upper crust but we can only place very broad limits on mantle transit times. These may be as short as 25 min, McGetchin's (1968) 'best estimate' to as long as several hours as indicated by the preservation of diamond and coesite (Smyth and Hatton 1977) in kimberlite. McCallister et al.'s (1979) study of pyroxene exsolution microstructures indicates transit times below a maximum of 15 h.

The above discussion indicates that the bulk of the xenolith load is likely to thermally equilibrate with the kimberlite host magma. However, the predicted rates of diffusion are too low for any significant mass transfer and chemical re-equilibration to occur during the short transport times. Laboratory studies indicate that where a fluid phase is present diffusion rates are greatly increased and that chemical re-equilibration might occur within times commensurate with the transport times. However whether these experiments involving finely ground materials can be extrapolated to coarse grained xenoliths is questionable. Xenolith suites which exhibit extensive metasomatic effects and give a limited range of equilibration P/T might be suspected of having undergone re-equilibration with kimberlite, but we cannot conclusively assess whether or not this has occurred until further experiments utilizing coarse grained materials have been undertaken.

In summary it appears that the assumption that xenolith suites retain information regarding the thermal history of the mantle is correct, despite the xenoliths being heated to the temperature of the kimberlite magma during transport through the mantle. The P/T data for the Pipe 200 xenolith suite is therefore interpreted according to model 3 below.

Model 3: Thermal and Stratigraphic Inferences From Pipe 200 Xenoliths

Thermal Inferences

Pressures and temperatures of equilibration of Pipe 200 xenoliths based upon the Wells-Wood method with no Cr correction are plotted in Fig. 4. No high temperature-high pressure xenoliths of the Thaba-Putsoa type are present and there is no indication of a perturbed geotherm, i.e. an array of data points defining a P/T trend at a high angle to a reasonable steady state shield geotherm. The Pipe 200 lherzolites have P/T values similar to those of other Lesotho granular lherzolites (Fig. 4 and see below) and plot above the steady state shield geotherms of Clark and Ringwood (1964) and Pollack and Chapman (1977)

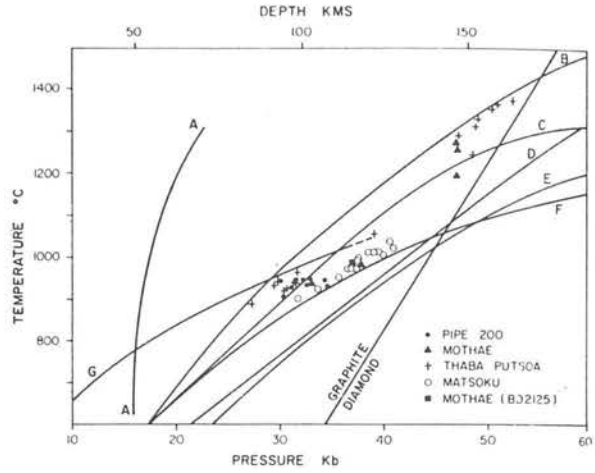

Fig. 4. Temperatures (Wells, 1977) and pressures (Wood 1974, no Cr correction) of equilibration of Lesotho garnet lherzolites relative to some theoretical continental geotherms. Data sources are as follows: Pipe 200 (Carswell et al. 1979), Mothae, Thaba Putsoa (Nixon and Boyd 1973), Matsoku, (Cox et al. 1973), Mothae diamond-bearing lherzolite BD2125 (Dawson and Smith 1975). Curve *AA* is O'Hara et al's (1971) spinel to garnet lherzolite phase transition for Cr-poor assemblages. Conduction-related geotherms-curve *F* (42 mWm^{-2}), Clarke and Ringwood (1964), curves *B* (50 mWm^{-2}) and *E* (40 mWm^{-2}), Pollack and Chapman (1977). Convection-related geotherms – curves *C* (44 mWm^{-2}) and *D* (40 mWm^{-2}), Gurney and Harte (in press). Curve-*G* is an extrapolation of the Lesotho lower crustal geotherm of Griffin et al. (1979). Diamond-graphite univariant (Kennedy and Kennedy 1976)

for heat flows of 42 mWm^{-2} and 40 mWm^{-2} respectively. The P/T values falling at these positions relative to these geotherms supports our use of Wells geothermometry as use of the Wood-Banno method results in many of the Lesotho xenoliths plotting at P/T values below these shield geotherms. As these steady state geotherms can be considered to define the locus of points of minimum P and T for the upper mantle, any magmatism associated with either convection or diapirism should raise local mantle P/T values above these minimum values. Figure 4 also includes geotherms constructed by Gurney and Harte (in press) for convecting mantle as described by Harte (1978). The Pipe 200 data are compatible with a point on the 44 mWm^{-2} convection-related geotherm. The Pipe 200 data also plot below an extension of a lower crustal geotherm defined by Griffin et al. (1979) using P/T data derived from lower crustal eclogites and granulites found in N. Lesotho (including Pipe 200). Use of Wood's (1974) Cr correction shifts some of the data points onto this geotherm but the majority remain below it. The lherzolites are evidently not recording the same thermal events as the lower crustal xenoliths. In fact there is no a priori reason why the two should be compatible as the lower crustal xenoliths may be recording pre-kimberlite events, par-

ticularly as they are unlikely to have re-equilibriated with the kimberlite during transport. Both xenolith suites do however demonstrate that the mantle beneath N. Lesotho had been disturbed to temperatures above those defined by steady state geotherms during the Cretaceous, in keeping with diapiric models of magmatism.

Stratigraphic Inferences

The P/T conditions of equilibration of the garnet lherzolites indicate derivation from depths of 90–110 km, a surprisingly narrow depth range, but in agreement with data obtained for other Lesotho kimberlites (see below). Use of Wood's (1974) Cr correction does not substantially widen this depth range e.g. 75–110 km.

MacGregor (1970) showed that the stability of garnet in the mantle is dependent upon the whole rock Cr/Cr+Al ratio. Rocks with high Cr/Cr+Al require higher pressures to stabilize garnet than those with lower Cr/Cr+Al. Thus at a given pressure and temperature in the mantle the whole rock Cr/Cr+Al determines whether the garnet lherzolite or chromite lherzolite assemblage is stable. At Pipe 200 lherzolites with similar bulk composition (Cr/Cr+Al= 0.15–0.25) fall into two groups with chromite lherzolites having in general lower equilibration temperatures than the garnet lherzolites (Table 1). This is also a point in favour of there being no major kimberlite-xenolith interactions in the Pipe 200 suite as heating of the xenoliths in the kimberlite might bring them into the chromite lherzolite stability field and give higher temperatures of equilibration. Whether or not this would occur would however depend upon the pressure drop during transport and the slope of the reaction boundary for the garnet to chromite lherzolite transition, both of which are unknown. This effect might be the origin of the secondary spinels and pyroxenes associated with the kelyphitic coronas around garnets, although other origins such as decompression can also be advocated for these assemblages (Carswell et al. 1979).

Pressures cannot be determined for the chromite lherzolites but lower temperatures might imply lower pressures of equilibration and thus derivation from slightly higher levels in the mantle than the garnet lherzolites of similar Cr/Cr+Al (e.g., ca. 70–90 km). In this suite of xenoliths we may in fact be recording P/T conditions close to those of the chromite to garnet lherzolite reaction boundary for these compositions.

The chromite lherzolites (and harzburgites) which form a highly depleted assemblage with higher Cr/Cr+Al and Mg/Mg+Fe ratios than the garnet lherzolites give similar temperatures of equilibration to these latter rocks. If the similar temperatures imply similar depths of origin then the absence of garnet in these more depleted assemblages is a bulk compositional effect of the type described by MacGregor (1970), the pressure not being high enough to stabilize garnet. Derivation of these contrasting lherzolites from similar levels, implies that the mantle is heterogeneous over short vertical distances.

Xenoliths derived from higher levels in the mantle are rare in the Pipe 200 suite and we have recognized only 2 in a suite of over 30 ultramafic xenoliths, a garnet websterite (PTH 210) and a spinel harzburgite (PTH 201).

The garnet websterite has similar Mg/Mg+Fe ratios to other Pipe 200 ultramafic xenoliths but is richer in Al_2O_3, CaO and Na_2O and has a lower Cr/Cr+Al ratio (Carswell et al. 1979). This difference in bulk composition makes determination of P/T values problematical. The Wells-Wood method gives 823° C at 14.4 kb, the Mori-Green (K_D)-Wood method 698° C at 8.9 kb with no Cr corrections. Both sets of P/T data indicate derivation from significantly higher levels than the bulk of the xenolith suite. Although the P estimates can at best be regarded as being only approximate, we consider that the K_D temperature estimate for this bulk composition may be reasonable and implies, as this estimate is a maximum value, a crustal derivation for this websterite. This further emphasizes the differences between PTH 210 and garnet websterites of upper mantle origin found in the Matosku kimberlite (Gurney et al. 1975; Carswell et al. 1979).

Sample PTH 201 is a primary aluminous spinel harzburgite. No P/T estimate can be determined easily for this xenolith but we believe that it was derived from relatively shallow depths in the mantle as O'Hara et al. (1971) have determined that a narrow zone of spinel lherzolite is to be expected at the top of the mantle for relatively undepleted lherzolites with low Cr/Cr+Al ratios (0.09–0.13). Such aluminous spinel-bearing peridotites are scarce amongst the Lesotho xenolith suites but have been noted also at Lipelang and Ngopoetsu. With reference to curve A on Fig. 4 and a crude equilibration temperature of 650°–800° C for PTH 201 based upon the Al_2O_3 content of orthopyroxene and the equilibrium constant for the reaction, opx+spinel=olivine+opx (Obata 1976) it seems probably that this xenolith is likely to have been derived from depths of less than 50 km.

In summary, the Pipe 200 kimberlite has sampled a very limited suite of possible mantle material, the bulk being derived from a narrow depth range of 90–110 km. The data are sufficient to construct only

a sketchy upper mantle stratigraphy in which significant compositional heterogeneity over a limited depth range is evident. The mantle sampled is a complex mixture of chromite and garnet lherzolites of varying degrees of depletion.

Comparison With Other Lesotho Xenolith Suites

The Thaba-Putsoa and Mothae pipes are similar in containing a bimodal suite of xenoliths, a high temperature (1,055°–1,375° C) relatively Fe-rich group of porphyroclastic lherzolites and a low temperature group (888°–983° C) of relatively Fe-poor granular lherzolites. The high temperature group appear to have been derived from greater depths than the granular group and plot on Fig. 4 well above the 42 mWm^{-2} and 40 mWm^{-2} steady state geotherms.

This group of data defines the inflected portion of Boyd and Nixon's (1975) perturbed geotherm. The Thaba Putsoa bimodal suite can however be interpreted to be samples derived from two points on the geotherms reflecting higher heat flows i.e. 45–50 mWm^{-2} (Pollack and Chapmann 1977) or greater than 44 mWm^{-2} (Gurney and Harte, in press). In this interpretation no inflection in the geotherm is required. The Mothae granular samples have however equilibrated at somewhat higher T and P than the Thaba Putsoa granular samples and at P/T values close those of the 42 mWm^{-2} shield geotherm of Clark and Ringwood (1964). The Mothae suite includes a diamond-bearing garnet lherzolite (Dawson and Smith 1975) which gives Wells-Wood P/T values well outside of the diamond stability field (Fig. 4). This might be construed to indicate that our P/T estimates are low and unrealistic. However if the lherzolite were originally derived from depths at which diamond was thermodynamically stable but has subsequently been carried to higher levels in the mantle by diapiric action at a rate such that silicate re-equilibration was not inhibited, then we would not expect the P/T estimates to reflect those at which the diamond gew. Here diamond may persist metastably, not having a co-existing C-bearing phase to re-equilibrate rapidly with and so invert to graphite.

The Thaba Putsoa suite of granular textured lherzolites has equilibrated at similar P/T to the Pipe 200 suite, implying similar depths of origin (Fig. 4) and again limited sampling of the mantle. The Pipe 200 assemblage is however more depleted than the Thaba Putsoa (and Mothae) assemblages as evidenced by the garnets and clinopyroxenes at Pipe 200 being richer in Cr and also in the occurrence of the extremely depleted chromite harzburgites. Thaba Putsoa granular lherzolites also contain primary chromites similar in composition to those found in the Pipe 200 lherzolites (Carswell et al. 1979).

Xenoliths in the Matsoku kimberlite comprise a suite of garnet lherzolites similar to those found at Pipe 200 together with a group of relatively Fe-rich garnet websterites which appear to represent cumulates which have equilibrated within the mantle (Gurner et al. 1975). The garnet lherzolites have equilibrated at 903°–1,050° C at 31.7–41.2 kb and plot on Fig. 4 close to the Clark and Ringwood geotherm at P/T values similar to those of the Mothae samples. Matsoku lherzolites include both granular and porphyroclastic types but no distinction between types can be made on the basis of the P/T of equilibration (Gurney et al. 1975). The lherzolites have equilibrated at slightly greater P/T than the Pipe 200 suite and are not as depleted (Gurney et al. 1975; Carswell et al. 1979). Many of the Matosku xenoliths in addition show evidence of infiltration metasomatism which involved extensive re-equilibration of all phases within the mantle (Gurney and Harte, in press).

Nature of the Upper Mantle Beneath Northern Lesotho

Individual kimberlite pipes, as shown above, each present us with a unique suite of xenoliths both in terms of their degrees of depletion and P/T of equilibration. In some cases a bi-modal population of xenoliths is evident. Samples representative of the upper portions of the mantle appear to be scarce and the bulk of the xenolith suites are comprised of chromite and garnet lherzolites together with lesser amounts of garnet websterite, eclogite and chromite harzburgite and rare spinel harzburgite and dunite (Boyd and Nixon 1975; Gurney et al. 1975; Carswell et al. 1979). The different suites found in each pipe indicate that the upper mantle is heterogeneous both laterally and vertically on a scale of tens of kilometers. A simple stratigraphy in which 'spinel lherzolite' overlies garnet lherzolite is certainly not present. Because of the heterogeneity plus the apparent limited depth range represented in the xenolith suites it would not seem possible to construct an upper mantle stratigraphy except in the most general terms.

The above conclusions highlight two problems in determining the upper mantle stratigraphy, why are samples confined to an apparently limited depth range and why are xenoliths from the uppermost mantle so poorly represented in the xenolith suites? Both of these problems may be artifacts of our methods of determining the P/T values as noted above. The choice of geothermometer is critical in this record, as the pressures calculated and hence depths of deriva-

tion are very strongly dependent upon the equilibration temperature chosen. This effect is well illustrated by the upper mantle models based upon the Davis-Boyd (1966) and Wood-Banno (1973) versions of the pyroxene solvus e.g., Boyd and Nixon (1975) and Dawson (1977). In these models a very large apparent gap in the upper mantle succession from the Moho to 125–150 km depth occurs. If one accepts the P/T estimates one then has to account for the failure to recognize garnet-bearing lherzolites of any shallower origin both in Pipe 200 and other kimberlite pipes on a world wide basis. A conventional explanation is to argue that the uppermost 80–90 km of the mantle has a highly depleted composition and consists of dunites and harzburgites for which it is impossible to assign P/T values by existing methods. Such xenoliths do indeed occur in kimberlites, but they are rare. This should not be the case if such materials form the major part of mantle on the ascent path of the kimberlite as implied by such mantle models. Some of the dunites sampled (Boyd and Nixon 1975) do not fit a depleted model of this type being relatively iron rich and in fact appearing to be cumulates. Moreover in cases such as are found at Pipe 200 where scarce clinopyroxene can be found in the depleted xenoliths, the temperatures determined indicate a deep origin for these rocks and the very similar clinopyroxene-free xenoliths.

Use of Wells-Wood geothermobarometry does not eliminate these problems, only the magnitude of the apparent gap is much reduced, i.e. to about 30 km from 80–100 km. As noted above the solvus geothermometer and the garnet-orthopyroxene geobarometer may not be in phase at these temperatures and correction for these effects and the presence of Cr might reduce the gap even further.

However failing the above explanations of the apparent stratigrahic gap one must consider that either the mechanical behaviour of xenoliths varies with depth and/or paragenesis or that kimberlites habitually sample the mantle selectively. We can think of no valid grounds for proposing that spinel harzburgites and lherzolites should behave mechanically differently to garnet lherzolites during transport. Though if the former materials were comminuted during transport it would be very difficult to recognize them in the final consolidated kimberlite. Selective sampling is perhaps the better alternative but it is difficult to envisage why a kimberlitic magma should extensively sample deeper mantle material, fail to sample the uppermost mantle and then sample the lower crust. Such selective sampling might imply drastic changes in the flow regime and/or nature of the conduit. Kimberlites in the uppermost mantle might for example traverse 'swept conduits' utilized by many batches of magma, and fail to pick up any xenoliths in these regions.

With regard to the thermal nature of the mantle beneath N. Lesotho we consider that the P/T values recorded in the xenoliths reflect thermal events in the mantle. The data do not however neccessarily define geotherms as advocated by Boyd and Nixon (1975). Mitchell (1978) has proposed that the high temperature xenolith suite, which defines the inflected portion of the Boyd and Nixon (1975) perturbed geotherm, records a transient pseudogeotherm generated in response to the thermal effects of a rising diapir. Similar interpretations have also been recently advanced by Gurney and Harte (in press). The diapir is considered to be parental to the kimberlite and the high temperature xenolith suite to be made up of material derived from two sources, the thermal aureole around the diapir above the point of kimberlite segretation, ca. 150 km, (i.e., true xenoliths) and diapir material which has partially melted to form kimberlite plus a residual lherzolite (i.e., restite). This latter population of xenoliths is considered to have been derived from depths greater than 150 km and to have been carried up to higher levels by diapiric action. We have proposed above that the Mothae diamond-bearing lherzolite has also been transported upwards by diapiric action and has re-equilibrated in terms of its silicate mineralogy to a P/T characteristic of depths much less than those of its actual depth of origin. A similar process might be advocated for all the low temperature suites of xenoliths and they may represent assemblages which are the integrated result of many episodes of diapirism and magmatism, hence the lateral and vertical heterogeneity and variety of textural types. This juxtaposition of a variety of lherzolites may have occurred as a part of the general evolution of the mantle throughout geological time prior to the onset of the kimberlite magmatism which removed them from the mantle. The temperatures recorded however are probably associated with the last major thermal episode which affected this portion of the matle i.e. the Jurassic Karroo volcanism, and we are seeing in the xenolith P/T values points along the thermal decay curve towards the steady state heat flow values sampled by Cretaceous kimberlite magmatism. The similar temperatures found in S. Africa and Lesotho for these low temperature xenoliths are to be expected as the time scale for re-equilibration processes are sufficient to allow continual equilibration as the heat flow declines. The thermal aureole associated with the diapir which initiated kimberlite magmatism in this model is not considered to extend to levels in the mantle from which the low temperature xenoliths were derived (Mitchell 1978).

Our interpretation of the sub-continental mantle as a dynamic and heterogeneous system throws doubt upon the details of models of the sub-continental mantle as presented by Jordan (1978) in which the 'paleogeotherms' recorded in the xenolith suites are considered to be representative of the present day geotherms and especially in view of our predilection towards lower equilibration temperatures than used by Jordan (1978).

Conclusions

1. Previous estimates of the temperatures of equilibration of mantle-derived xenoliths are too high, especially in the light of the equilibration experiments of Mori and Green (1978). This conclusion requires that the geotherms of Boyd and Nixon (1975) be substantially revised.

2. All pressure estimates are subject to considerable uncertainties in view of the possible lack of equilibrium between the solvus geothermometer and the garnet-orthopyroxene geobarometer and the uncertain nature of the corrections to be made for the presence of minor elements in the natural assemblages.

3. The P/T data can be interpreted to be (a) an artifact of the methods of derivation and of little geological significance, (b) the result of kimberlite-xenolith thermal interactions or (c) to present thermal and stratigraphic information with regard to the nature of the upper mantle. No one of these three alternatives can be accepted unequivocally. Components of all three may play a role in determining the range of P/T values found for a given xenolith suite.

4. The upper mantle beneath N. Lesotho is probably laterally and vertically heterogeneous and consists essentially of chromite and garnet lherzolites of varying degrees of depletion in basaltic components with lesser amounts of eclogite, garnet websterite and harzburgite. Carswell et al. (1979) have also demonstrated that the upper mantle beneath N. Lesotho is considerably more depleted than the mantle beneath the Kimberley area, S. Africa and the Lashaine area, Tanzania. This higher degree of depletion accounts for the scarcity of aluminous spinel lherzolites in the Lesothon xenolith suites. Their place is taken instead by chromite harzbugites.

Acknowledgements. This research is supported by the National Research Council of Canada (RHM and DBC), the Royal Society and the Natural Environment Research Council of the U.K. (DAC). We wish to thank the organisers and guides of the 1973 excursions to the Lesotho kimberlites for the opportunity to visit Pipe 200.

References

Akella, J., Boyd, F.R.: Petrogenetic grid for garnet peridotites. Carnegie Inst. Washington Yearb. **73**, 269–273 (1974)

Anderson, D.E., Buckley, G.R.: Zoning in garnets – diffusion models. Contrib. Mineral. Petrol. **40**, 87–104 (1973)

Boyd, F.R.: A pyroxene geotherm. Geochim. Cosmochim. Acta **37**, 2533–2546 (1973)

Boyd, F.R., Finger, L.W.: Homogeneity of minerals in mantle rocks from Lesotho. Carnegie Inst. Washington Yearb. **74**, 519–525 (1975)

Boyd, F.R., Nixon, P.H.: Origins of ultramafic nodules from some kimbelites of northern Lesotho and the Monastery mine, South Africa. Phys. Chem. Earth **9**, 431–545 (1975)

Carswell, D.A.: Palaeogeotherms: implications of disequilibrium in garnet lherzolite xenoliths. Nature **276**, 737 (1978)

Carswell, D.A., Clarke, D.B., Mitchell, R.H.: The petrology and geochemistry of ultramafic nodules from Pipe 200, northern Lesotho. In: Proc. 2nd. Int. Kimberlite Conf. **2**, 127–144 (1979)

Clark, S.P., Ringwood, A.E.: Density distribution and constitution of the mantle. Rev. Geophys. **2**, 35–88 (1964)

Cox, K.G., Gurney, J.J., Harte, B.: Xenoliths from the Matsoku pipe. In: Lesotho kimberlites (P.H. Nixon, ed.). Lesotho National Development Corp. Maseru, 76–92 (1973)

Crank, J.: The mathematics of diffusion. Oxford Univ. Press, 1956

Currie, K.L., Ferguson, J.: The mechanism of intrusion of lamprophyre dikes indicated by 'offsetting' of dikes. Tectonophysics **9**, 525–535 (1970)

Davis, B.T.C., Boyd, F.R.: The join $Mg_2Si_2O_6 - CaMgSi_2O_6$ at 30 kilobars pressure and its application to pyroxenes from kimberlites. J. Geophys. Res. **71**, 3567–3576 (1966)

Dawson, J.B.: Sub-cratonic crust and upper mantle models based on xenolith suites in kimberlite and nephelinitic diatremes. J. Geol. Soc. London **134**, 173–184 (1977)

Dawson, J.B., Smith, J.V.: Occurrence of diamond in a mica-garnet lherzolite xenolith from kimberlite. Nature **254**, 580–581 (1975)

Fraser, D.G., Lawless, P.J.: Paleogeotherms: implications of disequilibrium in garnet lherzolite xenoliths. Nature **273**, 220–221 (1978)

Goguel, J. Geothermics. 200 p. New York: McGraw-Hill 1976

Griffin, W.L., Carswell, D.A., Nixon, P.H.: Lower crustal granulites and eclogites from Lesotho and South Africa. In: Proc. 2nd Int. Kimberlite Conf. **2**, 59–86 (1979)

Gurney, J.J., Harte, B.: Chemical variations in upper mantle nodules from Southern African Kimberlites (in press)

Gurney, J.J., Harte, B., Cox, K.G.: Mantle xenoliths in the Matsoku kimberlite pipe. Phys. Chem. Earth **9**, 507–523 (1975)

Harte, B.: Kimberlite nodules, upper mantle petrology and geotherms. Phil. Trans. Roy. Soc. London Ser. A**288**, 487–500 (1978)

Harte, B., Gurney, J.J.: Ore mineral and phlogopite mineralization within ultramafic nodules from the Matsoku kimberlite pipe, Lesotho. Carnegie Inst. Washington Yearb. **74**, 528–536 (1975)

Hensen, B.J.: Pyroxenes and garnets as geothermometers and geobarometers. Carnegie Inst. Washington Yearb. **78**, 527–534 (1973)

Hofmann, A.W., Hart, S.R.: An assessment of local and regional isotopic equilibrium in the mantle. Earth Planet. Sci. Lett. **38**, 44–62 (1978)

Holland, F.A.: Fluid flow for chemical engineers, 269 p. London: Edward Arnold Ltd. 1973

Ingersoll, L.R., Zobel, O.J., Ingersoll, A.C.: Heat conduction with geological and other applications. 240 p. London: Thames Hudson 1955

Jordan, T.H.: Composition and development of the continental tectosphere. Nature **274**, 544–548 (1978)

Kennedy, C.S., Kennedy, G.C.: The equilibrium boundary between graphite and diamond. J. Geophys. Res. **81**, 2467–2470 (1976)

Kresten, P., Dempster, A.N.: The geology of Pipe 200 and the Malibamatso dyke swarm. In: Lesotho Kimberlites (P.H. Nixon, ed.). Lesotho National Development Corp. Maseru, 172–179 (1973)

Lindsley, D.H., Dixon, S.A.: Diopside-enstatite equilibria at 850° C to 1,400° C, 5 to 35 kb. Am. J. Sci. **276**, 1285–1301 (1976)

MacGregor, I.D.: The effect of CaO, Cr_2O_3, Fe_2O_3 and Al_2O_3 on the stability of spinel and garnet peridotites. Phys. Earth Planet. Interiors **3**, 372–377 (1970)

MacGregor, I.D.: The system $MgO-Al_2O_3-SiO_2$: solubility of Al_2O_3 in enstatite for spinel and garnet peridotite compositions. Am. Mineral. **59**, 110–119 (1974)

McCallister, R.H., Meyer, H.O.A., Aragon, R.: Partial thermal history of two exsolved clinopyroxenes from the Thaba Putsoa kimberlite pipe Lesotho. In: Proc. 2nd. Int. Kimberlite Conf. **2**, 244–247 (1979)

McGetchin, T.R.: The Moses Rock dike: Geology, petrology and mode of emplacement of a kimberlite-bearing breccia dike, San Juan County, Utah. Ph.D. Thesis. California Inst. of Technology, Pasadena, 405 p. (1968)

Mitchell, R.H.: Garnet lherzolites from Somerset Island, Canada and aspects of the nature of perturbed geotherms. Contrib. Mineral. Petrol. **67**, 341–347 (1978)

Mitchell, R.H., Brunfelt, A.O.: Rare earth geochemistry of kimberlite. Phys. Chem. Earth **9**, 671–686 (1975)

Mori, T.: Pyroxene equilibria in ultramafic rocks. Ph.D. Thesis Australian National University, Canberra, 239 p. (1976)

Mori, T., Green, D.H.: Pyroxenes in the system $Mg_2Si_2O_6-CaMgSi_2O_6$ at high pressure. Earth Planet. Sci. Lett. **26**, 277–286 (1975)

Mori, T., Green, D.H.: Subsolidus equilibria between pyroxenes in the $CaO-MgO-SiO_2$ system at high pressures and temperatures. Am. Mineral. **61**, 616–625 (1976)

Mori, T., Green, D.H.: Laboratory duplication of phase equilibria observed in natural garnet lherzolites. J. Geol. **86**, 83–97 (1978)

Nixon, P.H., Boyd, F.R.: Petrogenesis of the granular and sheared ultrabasic nodule suite in kimberlites. In: Lesotho Kimberlites (P.H. Nixon, ed.). Lesotho National Development Corp. Maseru, 48–56 (1973)

Nehru, C.E., Wyllie, P.J.: Electron microprobe measurement of pyroxenes coexisting with H_2O-undersaturated liquid in the join $CaMgSi_2O_6-Mg_2Si_2O_6-H_2O$ at 30 kb with application to geothermometry. Contrib. Mineral. Petrol. **48**, 221–228 (1974)

O'Hara, M.J., Richardson, S.E., Wilson, G.: Garnet peridotite stability and occurrence in crust and mantle. Contrib. Mineral. Petrol. **32**, 48–68 (1971)

Pollack, H.N., Chapman, D.S.: On the regional variation of heat flow, geotherms and lithospheric thickness. Tectonophysics **38**, 279–296 (1977)

Raheim, A., Green, D.H.: Experimental determination of the temperature and pressure dependence of the Fe – Mg partition coefficient for coexisting garnet and clinopyroxene. Contrib. Mineral. Petrol. **48**, 179–203 (1974)

Smyth, J.R., Hatton, C.J.: A coesite sanidine-grospydite from the Roberts Victor kimberlite. Earth Planet. Sci. Lett. **34**, 284–290 (1977)

Sparks, R.S.J., Pinkerton, H., MacDonald, R.: The transport of xenoliths in magmas. Earth Planet. Sci. Lett. **35**, 234–238 (1977)

Virgo, D., Hafner, S.S.: Fe^{2+}, Mg order-disorder in heated orthopyroxenes. Mineral. Soc. Am. Spec. Paper **2**, 67–81 (1969)

Wells, P.R.A.: Pyroxene geothermometry in simple and complex systems. Contrib. Mineral. Petrol. **62**, 129–139 (1977)

Wilshire, H.G., Jackson, E.D.: Problems in determining mantle geotherms from pyroxene compositions of ultramafic rocks. J. Geol. **83**, 313–329 (1975)

Wood, B.J.: The solubility of alumina in orthopyroxene coexisting with garnet. Contrib. Mineral. Petrol. **46**, 1–5 (1974)

Wood, B.J., Barno, S.: Garnet-orthopyroxene and orthopyroxene-clinopyroxene relationships in simple and complex systems. Contrib. Mineral. Petrol. **42**, 109–124 (1973)

Wyllie, P.J., Huang, W.L.: Carbonation and melting relations in the system $CaO-MgO-SiO_2-CO_2$ at mantle pressures with geophysical and petrological applications. Contrib. Mineral. Petrol. **54**, 79–107 (1976)

Received September 7, 1979; Accepted January 17, 1980

Contrib. Mineral. Petrol. 74, 403–416 (1980)

Contributions to Mineralogy and Petrology

Geothermometry of Garnet Lherzolite Nodules with Special Reference to Those from the Kimberlites of Northern Lesotho

D.A. Carswell and F.G.F. Gibb

Department of Geology, University of Sheffield, Mappin Street, Sheffield, S1 3JD, United Kingdom

Abstract. Different published geothermometric methods have been tested on a large suite of garnet lherzolite nodules from the kimberlites of Northern Lesotho. Comparison of the various calculated equilibration temperature estimates indicates that several of these methods yield unreliable results and should therefore be rejected. However, there is little to choose between the values obtained from five other methods based on three different element exchange reactions. Accordingly we conclude that the petrogenesis of garnet lherzolite nodules is best discussed with reference to the mean temperature estimates derived from these five preferred methods. The late Cretaceous palaeogeotherm for Northern Lesotho is revised on this basis and found to be of a similar form to previous estimates but is significantly displaced to higher temperatures.

Introduction

Estimation of equilibration temperatures for garnet lherzolite nodules is crucial to the evaluation of their equilibration pressures and hence to deducing the depths of derivation of such nodules and ultimately to the construction of models for the stratigraphy of the upper mantle (see for example Boyd 1973; Nixon et al. 1973; Dawson et al. 1975; Mitchell et al. 1980).

Most early equilibration temperature estimates for such nodules (e.g., O'Hara 1967; Boyd 1973; Carswell 1974) were obtained by some variant of the two pyroxene solvus geothermometer based on the experimental data of Boyd and Schairer (1964) and/or Davis and Boyd (1966) for the simple system $Mg_2Si_2O_6$–$CaMgSi_2O_6$. More recently the experimental calibration of the two pyroxene solvus has been refined (Nehru and Wyllie 1974; Mori and Green 1975; Lindsley and Dixon 1976) and semi-empirical extrapolations of the experimental data for the simple enstatite-diopside system have been developed (Wood and Banno 1973; Wells 1977) in an attempt to take account of the more complex chemistry of natural coexisting pyroxenes. Furthermore the size of the miscibility gap for coexisting pyroxenes in simulated natural garnet lherzolite assemblages has been experimentally evaluated by Mori and Green (1978) over the temperature range 950°–1.500° C between 30 and 40 kbars pressure.

Additional mineralogical thermometers applicable to garnet lherzolite assemblages are provided by the experimentally based calibrations (in some cases involving thermodynamic extrapolation of data for appropriate simple chemical systems) which have been published in the last few years for partitioning of Fe^{2+} and Mg^{2+} between various mineral pairs (Raheim and Green 1974; Mori and Green 1978; Ellis and Green 1979; Ganguly 1979; Saxena 1979; O'Neill and Wood 1979), for partitioning of Al^{VI} and Cr between coexisting pyroxenes (Mysen 1976), and for Ca–Mg exchange reactions in garnet-clinopyroxene-orthopyroxene assemblages (Powell 1978).

There are, therefore, several mineralogical geothermometers (including a number of different calibrations for some of these) applicable to the garnet-two pyroxenes-olivine assemblages of garnet lherzolite nodules. Unfortunately some of these have only been tested by their originators on a limited number of selected samples or over restricted ranges of bulk composition, temperature and pressure. Because of this and the not infrequent large inconsistencies in the results obtained from the different geothermometers and calibrations it has become necessary to evaluate the various methods to try to assess which

Reprint requests to: D.A. Carswell

0010-7999/80/0074/0403/$02.80

Table 1. Calculated temperature (and paired pressure) values for the garnet lherzolite nodules

Method / Sample number		Two pyroxene solvus			K_D: $Fe^{2+}-Mg^{2+}$ partitioning between Garnets and Clinopyroxenes				
		Wood and Banno	Wells[a]	Mori and Green[a]	Raheim and Green	Mori and Green[a]	Ellis and Green[a]	Ganguly	Saxena
Nodules from Thaba Putsoa and Mothae Pipes									
PHN 1595	*T*	1,023	889	901	943	804	906	987	807
	P	34.8	27.3	28.0	30.4	22.6	28.3	32.8	22.7
PHN 1567	*T*	1,050	920	936	1,074	884	956	1,040	866
	P	37.8	30.4	31.3	39.2	28.3	32.4	37.3	27.3
PHN 1592	*T*	1,054	923	938	1,176	953	1,017	1,097	925
	P	38.0	30.5	31.4	45.0	32.2	35.9	40.5	30.7
PHN 1570	*T*	1,065	938	956	998	830	903	999	798
	P	38.8	31.5	32.6	35.0	25.3	29.5	35.0	23.5
PHN 1573	*T*	1,071	942	960	988	843	968	1,025	909
	P	36.9	29.8	30.7	32.3	24.2	31.2	34.4	27.9
PHN 1569	*T*	1,112	964	969	1,020	828	942	1,016	845
	P	43.3	34.6	35.0	38.0	26.7	33.4	37.7	27.7
PHN 1568	*T*	1,065	933	948	1,188	983	1,070	1,030	1,025
	P	36.8	29.4	30.3	43.7	32.2	37.1	40.4	34.5
PHN 1572	*T*	1,066	940	958	1,281	1,024	1,096	1,163	1,072
	P	38.5	31.3	32.4	50.7	36.1	40.2	44.0	38.8
PHN 1917	*T*	1,108	983	1,004	1,284	973	1,066	1,136	1,025
	P	45.4	37.8	39.0	56.0	37.2	42.8	47.0	40.4
PHN 1559B	*T*	1,057	937	960	1,278	994	1,084	1,149	1,065
	P	40.2	33.1	34.5	53.2	36.5	41.8	45.6	40.7
PHN 1597[b]	*T*	1,396	1,375	1,476	1,872	1,444	1,413	1,452	918
	P	53.6	52.4	58.0	79.6	56.2	54.5	56.7	27.4
PHN 1596[b]	*T*	1,394	1,370	1,467	1,855	1,455	1,415	1,455	941
	P	52.3	51.0	56.2	77.2	55.6	53.4	55.6	27.9
PHN 1566[b]	*T*	1,360	1,353	1,467	1,763	1,392	1,373	1,415	1,040
	P	50.7	50.4	56.7	72.6	52.5	51.5	53.7	33.4
PHN 1610[b]	*T*	1,335	1,330	1,447	1,791	1,412	1,383	1,426	1,155
	P	49.2	49.0	55.3	74.0	53.4	51.8	54.2	39.5
PHN 1611[b]	*T*	1,325	1,315	1,428	1,762	1,382	1,356	1,406	1,143
	P	49.4	48.8	55.0	73.2	52.5	51.0	53.8	39.4
PHN 1925[b]	*T*	1,320	1,273	1,354	1,898	1,457	1,410	1,457	1,188
	P	49.5	47.0	51.4	81.2	57.0	54.4	57.0	42.3
PHN 1924[b]	*T*	1,313	1,258	1,332	1,893	1,436	1,411	1,452	1,235
	P	50.1	47.1	51.2	82.3	56.9	55.6	57.8	45.8
E 3[b]	*T*	1,327	1,264	1,332	1,624	1,279	1,293	1,344	1,109
	P	50.9	47.2	50.9	67.0	48.0	48.7	51.5	38.6
PHN 1591[b]	*T*	1,312	1,245	1,309	1,614	1,232	1,301	1,335	1,201
	P	52.5	48.6	52.3	69.7	47.9	51.8	53.8	46.2
PHN 2001[b]	*T*	1,258	1,194	1,260	1,791	1,311	1,338	1,385	1,328
	P	50.8	47.0	50.9	81.7	53.9	55.4	58.1	54.8
PHN 1582[b]	*T*	1,109	1,055	1,130	1,410	1,086	1,128	1,207	1,246
	P	42.3	39.1	43.5	59.9	41.0	43.4	48.1	50.3
BD 2125[c]	*T*	1,111	988	1,010	1,262	975	1,053	1,128	995
	P	44.3	37.0	38.3	53.3	36.2	40.9	45.3	37.4

[a] Preferred methods
[b] Sheared texture
[c] Diamond bearing

$K_{Ca-Mg}^{Gnt-Cpx}$ Opx	$K_{Fe^{2+}-Mg^{2+}}^{Gnt-Ol}$	$K_{Al^{VI}}^{Opx}$ Cpx $_{Cr}$	Mean of 10 methods	Mean of 5 preferred methods[a]
Powell	O'Neill and Wood[a]	Mysen	All except Powell	
718	854	912	903	871
12.9	25.4	28.6	28.1	26.3
701	883	874	948	916
7.8	28.3	27.7	32.0	30.1
666	864	887	983	939
−1.2	27.2	38.5	35.0	31.4
735	910	886	928	907
11.6	29.9	28.5	31.0	29.8
709	798	924	943	902
16.2	21.7	28.7	29.8	27.5
710	937	878	951	928
14.0	33.1	29.6	33.9	32.6
646	829	975	1.005	953
−0.2	23.6	31.8	34.0	30.5
671	921	1.024	1.054	988
−17.6	30.2	36.1	37.8	34.0
757	1.056	881	1.052	1.016
3.4	42.2	31.7	42.0	39.8
735	992	872	1.039	993
0.9	36.4	29.3	39.1	36.5
1.489	1.502	1.153	1.400	1.442
40.2	59.4	40.3	53.8	56.1
1.487	1.526	1.098	1.398	1.447
40.6	59.4	36.3	52.5	55.1
1.429	1.370	981	1.351	1.391
38.7	51.3	30.2	50.3	52.5
1.439	1.375	1.074	1.373	1.389
40.5	51.4	35.0	51.2	52.2
1.461	1.299	1.083	1.350	1.356
41.7	47.9	36.1	50.7	51.0
1.500	1.344	1.063	1.376	1.368
51.7	50.8	35.5	52.6	52.2
1.460	1.355	1.009	1.369	1.358
50.4	52.4	33.3	53.2	52.6
1.387	1.321	1.012	1.291	1.298
44.5	50.3	33.2	48.7	49.0
1.240	1.323	998	1.287	1.282
33.5	53.8	34.6	51.1	50.9
1.427	1.372	1.042	1.328	1.295
63.6	57.4	38.3	54.8	52.9
−14.801	1.046	885	1.130	1.089
−2.120.4	38.6	29.2	43.5	41.1
749	1.128	886	1.054	1.031
−1.0	45.3	30.9	40.9	39.5

are most likely to yield reliable, and hence geologically meaningful, results. In this paper we seek to do this by testing all the methods together using a large set of published analytical data.

Geothermometers and Barometers Employed

We have chosen to use the published compositions of the minerals in the garnet lherzolite nodules from the Thaba Putsoa, Mothae, Letseng, Pipe 200 and Matsoku kimberlite diatremes in northern Lesotho as test data, in part because of the particularly wide range of equilibration temperatures indicated for these nodules by earlier studies (Boyd 1973; Boyd and Nixon 1975) but also to see whether consideration of alternative temperature estimates confirms or refutes the suggestion by these authors that the Late Cretaceous palaeogeotherm in the upper mantle beneath northern Lesotho was significantly inflected. The mineral compositions used to calculate the equilibration temperature/pressure estimates for these nodules as listed in Table 1 were taken from Carswell and Dawson 1970; Nixon and Boyd 1973; Cox et al. 1973; Dawson and Smith 1975; Bishop et al. 1978; and Carswell et al. 1979. The actual temperature/pressure values were calculated by a FORTRAN program NODMINS 2 which we have developed for the purpose.

With the exception of the paired pressure (P) temperature (T) values derived by simultaneous solution of the two P-T dependent exchange reaction equations proposed by Powell (1978), all the other tabulated T values are coupled with P values determined by employing equation (12) of Wood (1974) for garnet-orthopyroxene equilibria. Since in our view the Wood (1974) geobarometer does not adequately take account of the influence of varying Cr/(Cr+Al) ratios on garnet-orthopyroxene equilibria we have serious doubts about the accuracy of these P estimates (Carswell et al. 1979; Carswell and Gibb 1980; Carswell 1980). In those cases where the element partition relationships concerned are recognised to be both temperature and pressure dependent (namely the Ellis and Green 1979; Raheim and Green 1974; Ganguly 1979; Saxena 1979; and O'Neill and Wood 1979, methods) and the appropriate equation is solved simultaneously with that of Wood (1974), any errors in the P estimates are carried through into the T estimates and vice-versa. In the other cases where the geothermometer employed was taken to be independent of pressure (namely the Wells 1977; Wood and Banno 1973; Mori and Green 1978; and Mysen 1976, methods) the P values were calculated after the T values hence errors in T may affect P but not vice-versa. These possible sources of error must be borne in mind when attempting to assess the validity of the various T (and P) estimates in both absolute and relative terms.

We have applied the thermodynamically formulated equations of Powell (1978) for Ca – Mg exchange reactions in garnet-orthopyroxene-clinopyroxene assemblages to these nodules in the hope that they might provide an independent check on the P/T estimates obtained from the various geothermometers in combination with the Wood (1974) geobarometer. Simultaneous solution of Powell's (1978) equations yields reasonably consistent and realistic P/T values for most of the higher temperature nodules (the sheared textured nodules of Nixon and Boyd 1973) – the ludicrous values for nodule PHN 1582 (Table 1) being due, we suspect, to an analytical error in the clinopyroxene. However, for the coarse granular textured garnet lherzolite nodules this method yields T values which, in comparison with those obtained by all the other methods (Table 1) clearly seem too low and are coupled with unrealistically low (in several cases negative) P values. Indeed even nodule PHN 1592, one of the two samples which Powell used to test his method, yields a negative P estimate when one actually calculates the P/T

Table 1. (continued)

	Sample number		Two pyroxene solvus			K_D: $Fe^{2+}-Mg^{2+}$ partitioning between Garnets and Clinopyroxenes				
			Wood and Banno	Wells[a]	Mori and Green[a]	Raheim and Green	Mori and Green	Ellis and Green[a]	Ganguly	Saxena
Pipe 200	PTH 102	*T*	1,065	947	971	1,233	996	1,104	1,153	1,042
		P	38.2	31.5	32.9	47.8	34.3	40.4	43.2	36.9
	PTH 207	*T*	1,067	946	967	1,362	1,037	1,163	1,203	1,155
		P	41.5	34.3	35.6	58.9	39.7	47.2	49.5	46.7
	PTH 400	*T*	1,050	932	957	1,421	1,109	1,159	1,226	1,181
		P	37.9	31.1	32.5	59.2	41.2	44.1	48.0	45.4
	PTH 403	*T*	1,066	946	969	1,358	1,100	1,230	1,246	1,222
		P	36.6	30.0	31.2	52.9	38.5	45.7	46.6	45.3
	PTH 404	*T*	1,074	950	971	1,312	1,032	1,143	1,188	1,096
		P	39.9	32.8	34.0	53.6	37.5	43.9	46.5	41.2
	PTH 405	*T*	1,059	934	953	1,435	1,097	1,159	1,225	1,160
		P	39.9	32.6	33.7	61.8	42.1	45.7	49.6	45.7
	PTH 407	*T*	1,055	929	948	1,299	1,031	1,128	1,179	1,099
		P	38.2	31.0	32.1	52.2	36.9	42.4	45.4	40.8
	PTH 409	*T*	1,034	907	925	1,511	1,153	1,261	1,290	1,285
		P	37.6	30.3	31.3	65.2	44.5	50.8	52.4	52.2
	PTH 410	*T*	1,070	946	967	1,448	1,122	1,181	1,242	1,158
		P	39.3	32.2	33.4	61.0	42.3	45.7	49.2	44.4
Matsoku Pipe	LBM 9	*T*	1,093	974	999	1,488	1,090	1,153	1,226	1,205
		P	44.6	37.4	38.9	68.5	44.4	48.2	52.6	51.3
	LBM 11	*T*	1,095	976	1,001	1,362	1,086	1,130	1,202	1,136
		P	39.4	32.7	34.1	54.5	38.9	41.4	45.5	41.7
	LBM 16[b]	*T*	1,116	999	1,026	1,592	1,229	1,246	1,310	1,309
		P	40.7	34.1	35.6	67.6	47.1	48.1	51.7	51.6
	BD 1355	*T*	1,135	1,015	1,040	1,217	938	1,001	1,090	930
		P	46.5	39.4	40.9	51.5	34.7	38.5	43.9	34.2
	BD 1359	*T*	1,062	943	967	1,483	1,143	1,165	1,244	1,207
		P	36.8	32.0	33.4	63.1	43.5	44.8	49.3	47.2
	BD 1355[c]	*T*	1,063	933	950	1,052	836	908	1,008	810
		P	41.8	34.1	35.1	41.2	21.8	32.6	38.5	26.7
	BD 1356[c]	*T*	1,158	1,050	1,083	1,217	940	1,011	1,096	904
		P	47.6	41.2	43.1	51.1	34.6	38.9	43.9	32.4
Letseng	BD1870/2	*T*	922	836	881	1,142	891	943	1,045	902
		P	33.6	28.4	31.1	47.0	31.8	34.9	41.0	32.4

[a] Preferred methods
[b] Flaser texture
[c] Wet chemical analyses of mineral separates with analytically determined Fe^{2+} and Fe^{3+} values

intersection of the two Powell reaction equations (cf. Fig. 4 of Powell 1978). Problems with Powell's proposed method probably arise because in many cases it is not possible to ascertain the necessary site occupancies (in particular the ratio of Ca/Mg in the M2 sites in the orthopyroxenes) with adequate precision. Thus as this method does not yield realistic P/T values for the majority of the nodules considered in this paper, it cannot be regarded as generally applicable and will not be considered further here.

In another attempt to obtain alternative P estimates we have tried using Equation (3) of Herzberg (1978) for garnet-clinopyroxene equilibria. With the Wells (1977) T estimates this equation gives geologically reasonable P values in the range 30–55 kbars for the majority of lower temperature nodules but unrealistic pressures up to 222 kbars for the higher temperature nodules. Simultaneous solution of this Herzberg (1978) equation with that of Ellis and Green (1979) yields realistic P/T values for only a handful of lower temperature nodules and improbably high values for the rest. We therefore conclude that the geobarometer of Herzberg

$K_{Ca-Mg}^{Gnt-Cpx-Opx}$	$K_{Fe^{2+}-Mg^{2+}}^{Gnt-Ol}$	$K_{Al^{VI}-Cr}^{Opx-Cpx}$	Mean of 10 methods	Mean of 5 preferred methods[a]
Powell	O'Neill and Wood[a]	Mysen	All except Powell	
780	943	901	1.036	992
12.0	31.3	28.9	36.5	34.1
721	970	937	1.081	1.017
4.2	35.7	33.7	42.3	38.5
659	984	944	1.096	1.028
− 14.5	34.1	31.8	40.5	36.6
653	964	870	1.097	1.042
− 4.5	31.0	25.7	38.3	35.3
746	910	869	1.055	1.001
4.4	30.4	28.1	38.8	35.7
443	923	905	1.085	1.013
− 48.1	32.0	30.9	41.4	37.2
689	949	883	1.050	997
− 2.1	32.2	28.4	38.0	34.9
519	982	879	1.123	1.046
− 27.9	34.6	28.7	42.8	38.3
426	964	889	1.099	1.036
− 51.8	33.2	28.9	41.0	37.4
626	920	892	1.104	1.027
− 26.2	34.1	32.4	45.2	40.6
470	893	891	1.077	1.017
− 46.5	28.0	27.9	38.4	35.0
−780	866	913	1.161	1.073
−259.2	26.6	29.2	43.2	38.3
746	1.105	874	1.034	1.020
− 1.7	44.8	30.9	40.5	39.7
363	987	952	1.115	1.041
− 68.6	34.5	32.5	41.7	37.6
860	–	850	934	907
− 8.5		29.1	34.1	32.5
−443	–	917	1.042	1.021
−201.0		33.2	40.7	39.4
681	805	935	930	871
− 17.2	26.5	34.4	34.1	30.5

is only of limited use in the present context and, despite the reservations expressed above, we have no option at present but to rely upon the garnet-orthopyroxene geobarometer, in particular as formulated by Wood (1974).

To aid evaluation of the various geothermometers we have computed statistical correlations between the sets of T values obtained by each of the methods for the nodule suite. Correlation coefficients, intercepts and slopes for the results from each of the methods versus each of the other methods plus the average of ten of the methods (all except that of Powell) and the average of five 'superior' (see below) methods are presented in Table 2. The best correlations between results of individual methods are those between the two pyroxene geothermometer of Mori and Green and that of O'Neill and Wood and between the methods of Ganguly and Ellis and Green. It would seem at first glance to be a simple matter to select from Table 2 as the most probably reliable methods, those which consistently give correlation coefficients and slopes close to 1.0 and low intercepts but the statistical data can be misleading. For example, the method of Ganguly looks particularly good against the average of ten methods, but, as can be seen from Fig. 1g, the actual temperatures tend to be consistently high by some 100° C; conversely the Mori and Green K_D method does not appear to be particularly good when compared with the average of ten (Table 2) but this is because the relatively high slope of the line produces big discrepancies at temperatures above 1,400° C and below 900° C whereas within the range applicable to the garnet lherzolite nodules the correlation is very good (see below and Fig. 1e). Also, it is self evident that methods based on the same or similar chemical/mineralogical parameters will tend to yield better correlation coefficients than those utilising different approaches. In view of this latter factor the good correlation between the results obtained by the method of O'Neill and Wood and those from the two pyroxene geothermometer of Mori and Green seems noteworthy.

In order to further evaluate the relative merits of the various geothermometers we have plotted the temperatures obtained by each of the methods, other than that of Powell (1978), against the mean value given by all ten methods in Fig. 1. In the light of this (and the discussion below) we have then plotted in Fig. 2 the T values yielded by each of the five methods we consider 'superior' against the mean values from these methods.

The rationale behind our evaluation, namely that the mean of a set of independently arrived at results is more 'correct' than any individual result, may be unjustified. It is conceivable that one of the methods is correct and the rest in error but there is no evidence (Fig. 1) that this is the case over the temperature range in question. Consequently, we have elected to seek a 'concensus' result using a number of different methods and refining it by eliminating any method which consistently yields values departing significantly from the mean.

Evaluation of the Temperature Estimates

(a) Geothermometers Based on the Two-Pyroxene Solvus

Experimental studies of the simple system $Mg_2Si_2O_6-CaMgSi_2O_6$ (Boyd and Schairer 1964; Davis and Boyd 1966; Nehru and Wyllie 1974; Mori and Green 1975; Lindsley and Dixon 1976) have shown that the two pyroxene solvus should provide a sensitive geothermometer above about 900° C. Pressure effects upon the solvus are minimal at low temperatures, but may become significant above 1,200° C. More serious errors are likely to arise in extrapolating the solvus data for the simple system to the chemically more complex natural pyroxenes. The presence of Fe has a particularly important effect on the extent of solid solution between coexisting pyroxenes (Lindsley and Munoz 1969; Ross et al.

Table 2. Correlations between the individual geothermometers and averages (The three values under each entry are the correlation coefficient, the intercept and the slope)

	Wood and Banno	Wells	Mori and Green 2PX.	Raheim and Green	Mori and Green K_D	Ellis and Green	Ganguly	Saxena	Powell	O'Neill and Wood	Mysen
Wells	0.986 367 0.7										
Mori and Green 2PX.	0.977 473 0.6	0.998 136 0.8									
Raheim and Green	0.817 639 0.4	0.836 361 0.5	0.839 267 0.6								
Mori and Green K_D	0.843 572 0.5	0.861 271 0.7	0.866 159 0.8	0.990 −130 1.4							
Ellis and Green	0.795 440 0.6	0.814 90 0.8	0.816 −55 1.0	0.977 −566 1.7	0.984 −314 1.2						
Ganguly	0.807 329 0.7	0.827 −64 0.9	0.830 −242 1.1	0.988 −876 1.9	0.988 −525 1.3	0.989 −152 1.1					
Saxena	0.164 995 0.1	0.198 813 0.2	0.205 800 0.3	0.622 172 1.2	0.578 283 0.8	0.650 416 0.7	0.635 552 0.6				
Powell	0.595 1.041 0.1	0.590 913 0.2	0.582 932 0.2	0.443 1.039 0.2	0.475 973 0.2	0.464 1.055 0.1	0.449 1.125 0.1	0.096 1.086 0.0			
O'Neill and Wood	0.942 561 0.5	0.951 266 0.7	0.947 162 0.9	0.844 255 1.1	0.851 279 0.8	0.820 527 0.6	0.836 620 0.6	0.204 932 0.1	0.679 −1.056 1.7		
Mysen	0.806 −44 1.3	0.826 −574 1.7	0.830 −854 2.1	0.755 −1.144 2.7	0.786 −792 2.0	0.736 −270 1.5	0.730 −83 1.4	0.171 756 0.3	0.606 −3.405 4.4	0.785 −968 2.1	
Average of 10	0.907 336 0.7	0.927 −50 1.0	0.928 −221 1.2	0.977 −580 1.8	0.982 −323 1.3	0.965 31 1.0	0.972 174 0.9	0.514 505 0.5	0.523 −1.411 1.9	0.921 −381 1.3	0.814 480 0.4
Average of 5	0.953 426 0.7	0.970 75 0.9	0.970 −70 1.1	0.938 −207 1.5	0.952 −67 1.1	0.924 255 0.8	0.933 370 0.8	0.383 713 0.3	0.579 −1.270 1.9	0.958 −198 1.2	0.831 543 0.4

1973). Significant amounts of Na and Al probably also affect the solvus relationships (Akella 1976; Mori 1977) but these effects have not yet been fully quantified.

We can compare three sets of T values calculated from the three alternative equations which have been derived for the two pyroxene solvus geothermometer. That of Wood and Banno (1973) involves a semi-empirical extrapolation of the Davis and Boyd (1966) solvus data to take account of the effect of Fe on the solvus, whilst that of Wells (1977) has been derived in a similar fashion but provides a best fit calibration of both the Davis and Boyd (1966) data and the later solvus data of Nehru and Wyllie (1974), Mori and Green (1975), and Lindsley and Dixon (1976). On the other hand the Mori and Green (1978) calibration is based on their own experimental determination of the two pyroxene solvus in simulated garnet lherzolite compositions, including some natural mineral mixes, over the ranges 950°–1,500° C and 30–40 kbars. It does not, however, incorporate any correction factor for Fe and is thus strictly only applicable to assemblages containing orthopyroxenes with Fe/(Fe+Mg) ratios between 0.04 and 0.13.

From these considerations and comparison of Fig. 1a–c, it is clear that the Wells (1977) and Mori and Green (1978) equations are superior to the earlier one of Wood and Banno (1973) which overestimates

and erroneously bunches together the T values for the apparent lower temperature group of nodules. This is because it is now known that the diopside arm of the solvus is much steeper below about 1,200° C than allowed for by Wood and Banno (1973). There is little to choose between the other two equations although on balance we judge that of Mori and Green (1978) to be marginally superior for these garnet lherzolites. The main differences are in the higher temperature group of nodules for which the Mori and Green (1978) equation appears to overestimate the temperatures slightly, probably because it does not allow for the effect of Fe on the miscibility relationships in these relatively more iron-rich nodules. By contrast the Wells (1977) equation appears to somewhat underestimate the temperatures for this group of nodules probably because it fails to allow for the predicted P effect (see for example Fig. 3 of Lindsley and Dixon 1976) on the solvus at such high pressures and temperatures.

(b) Geothermometers Based on Fe^{2+}–Mg^{2+} Partitioning Between Coexisting Garnets and Clinopyroxenes

The partition coefficient $K_D=(Fe^{2+}/Mg^{2+})_{Gnt}/(Fe^{2+}/Mg^{2+})_{Cpx}$ is strongly temperature dependent and hence provides an extremely useful and sensitive geothermometer for eclogite facies assemblages (Banno 1970; Mysen and Heier 1972). Råheim and Green (1974) suggested that K_D was, however, more markedly pressure dependent than predicted by Banno (1970) from thermodynamic considerations for equilibria in simple systems. On the other hand, Mori and Green (1978), in their experimental study of phase equilibria in both synthetic ultramafic compositions and natural mineral mixes, were unable to detect any significant pressure effect on K_D between 30 and 40 kbars. This conflict has, however, recently been resolved by the experimental data of Ellis and Green (1979) which demonstrate that the Råheim and Green (1974) P-T calibration of K_D overestimates the pressure effect on K_D due to comparison of data at differing pressures for garnets with widely different Ca contents, which reflect non-ideal Ca – Mg substitutions in both garnet and clinopyroxene. The revised Ellis and Green (1979) calibration thus expresses K_D as a function of T, P and the Ca content of the garnet and appears to provide a satisfactory geothermometer for garnet-clinopyroxene pairs in a wide range of rock compositions.

In a different approach to deriving a practical K_D geothermometer, Ganguly (1979) has integrated the appropriate available thermodynamic mixing data with thermochemical and selected earlier experimental data to produce an equation which expresses K_D as a function of T, P and the Ca and Mn contents of the garnet. Saxena (1979) has extended this approach to also take into account the effect of Na in the clinopyroxene on K_D.

Temperature estimates calculated from the five different available K_D equations are listed in Table 1. The K_D values used assume total Fe as Fe^{2+} in both garnets and clinopyroxenes in all cases except nodules BD 1355 and BD 1356 for which FeO values have been determined in analysed mineral separates. Comparison of the various temperature values and of Fig. 1d–h demonstrate that the Ellis and Green (1979) and Mori and Green (1978) K_D equations yield more satisfactory T values for these garnet lherzolites than the other three equations. The Råheim and Green (1974) equation, as might be expected from the preceding comments, progressively overestimates the temperatures for the nodules which equilibrated at the higher P/T conditions – the garnets in these particular nodules having only a limited range of Ca contents. The Ganguly (1979) equation also appears to consistently overestimate the equilibration temperatures for these nodules although not so dramatically, whilst the Saxena (1979) equation yields erratic results which are perhaps not too unreasonable for many of the lower temperature group of nodules, but are clearly anomalously low for the group of porphyroclastic textured nodules, which according to all the preferred estimates have equilibrated at the highest temperatures. We therefore conclude that neither of the last two K_D methods yields reliable T estimates for these garnet lherzolite nodules.

There appears to be little to choose between the T values obtained from the Ellis and Green (1979) and Mori and Green (1978) K_D equations although Fig. 2f does indicate that the former tends to yield T values which for the majority of these nodules are somewhat higher than the mean of the five preferred T values. The T values obtained from the Mori and Green (1978) equation (Fig. 2e) span a rather wider temperature range and might superficially appear to be better. However, it should be remembered that this particular equation does not include a term to allow for the influence of pressure on K_D, hence is only really valid over the 30–40 kbars range. It just so happens that many of these garnet lherzolite nodules have probably equilibrated within or at least close to this pressure range.

The wide range of equilibration temperatures indicated for these garnet lherzolites by both of the preferred K_D equations appears to refute the suggestion by Fraser and Lawless (1978) that in such nodules $Fe^{2+}-Mg^{2+}$ exchange between pyroxenes and garnet

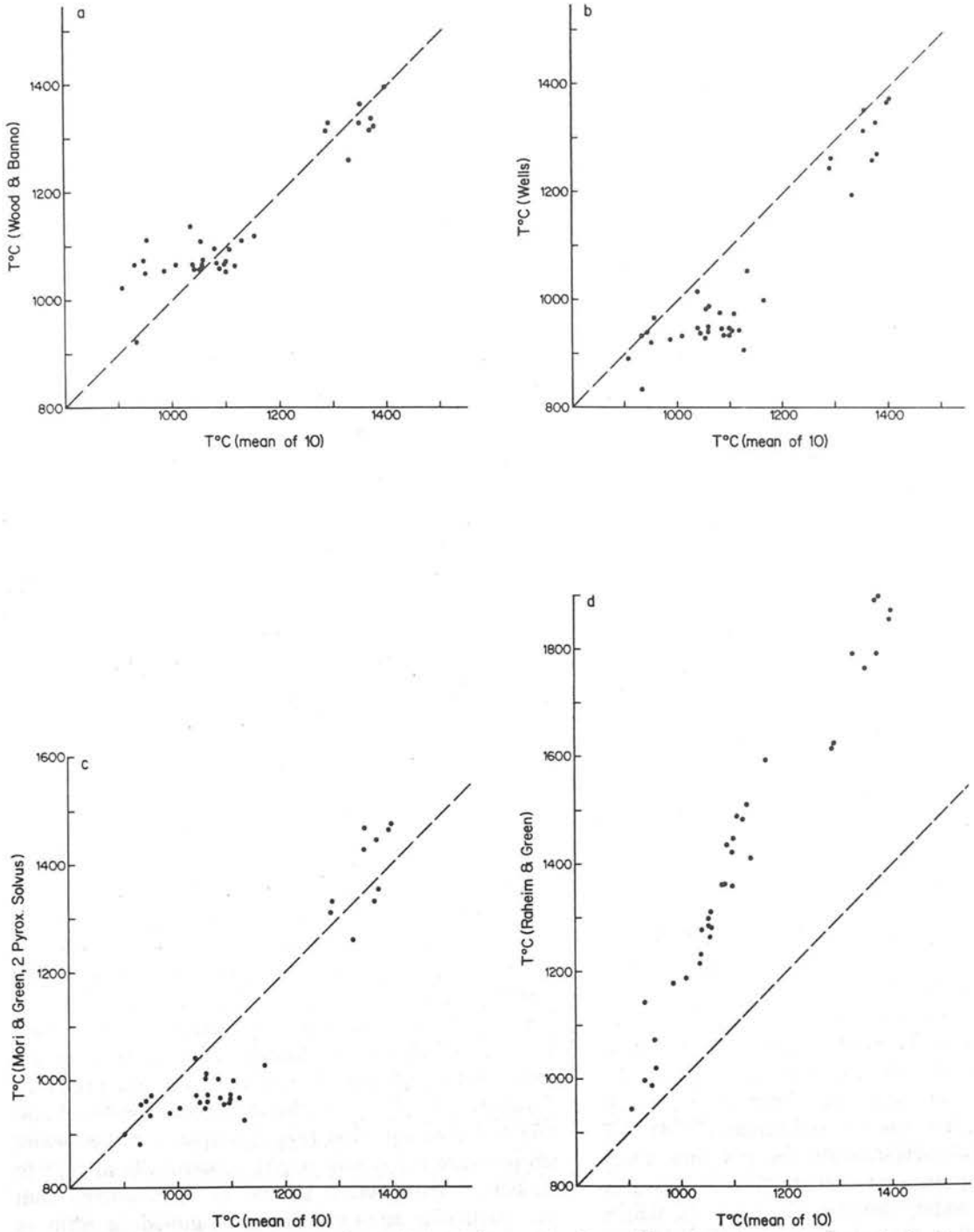

Fig. 1a–j. Equilibration temperature values calculated from each of ten different geothermometric methods plotted against the mean temperature values from all ten methods

is effectively blocked below ~1,100° C whilst lower temperatures continue to be monitored by Ca–Mg exchange between co-existing pyroxenes. Indeed petrographic and experimental evidence indicates that on the contrary K_D values provide a more sensitive geothermometer in the lower part of the temperature range of interest than does the two pyroxene solvus (Carswell 1978).

It should be appreciated that all T estimates derived from the K_D geothermometer may be in serious error if K_D values are calculated from electron microprobe data or any other mineral analyses which do not quantify the amounts of Fe^{2+} and Fe^{3+} (see, for example, Carswell and Gibb 1980; Carswell and Griffin, in press). Determination of $Fe^{2+}/(Fe^{2+}+Fe^{3+})$ ratios in mineral separates of garnets and

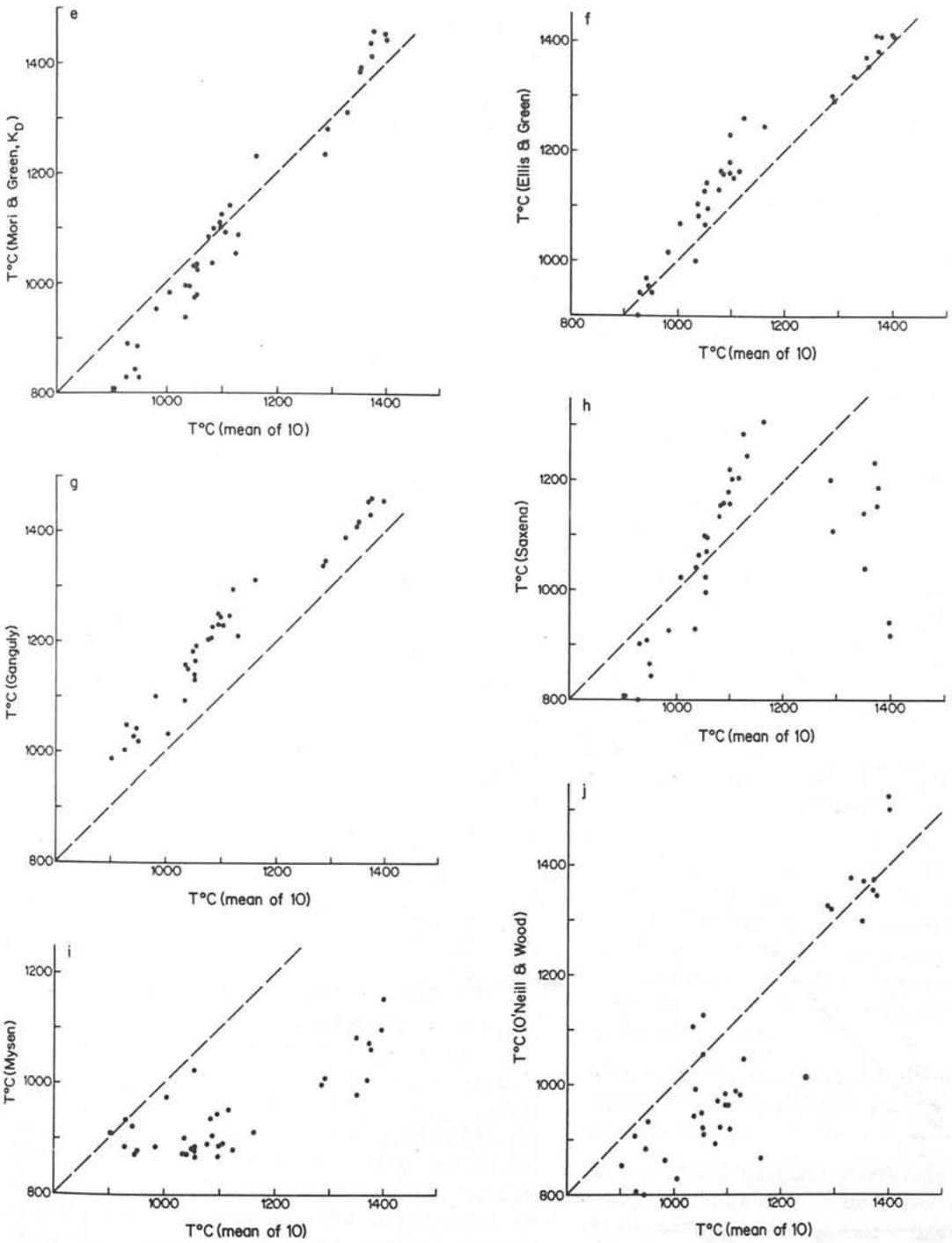

clinopyroxenes in garnet lherzolites (Carswell and Dawson 1970 and unpublished data) indicates that although Fe^{3+} contents in these minerals are fairly low, they are generally higher in clinopyroxenes than in coexisting garnets. Hence K_D values which assume all Fe as Fe^{2+} are in effect minimum values and hence yield T estimates which can be expected to be on the high side.

The minerals in almost all of the garnet lherzolite nodules considered here were analysed by electron microprobe and hence $Fe^{2+}/(Fe^{2+}+Fe^{3+})$ ratios have not been determined. Thus all the T values derived from the K_D geothermometer which are plotted in Figs. 1 and 2 assume total Fe and Fe^{2+}. However, for comparison T values are also tabulated for two garnet lherzolite nodules for which wet chemical anal-

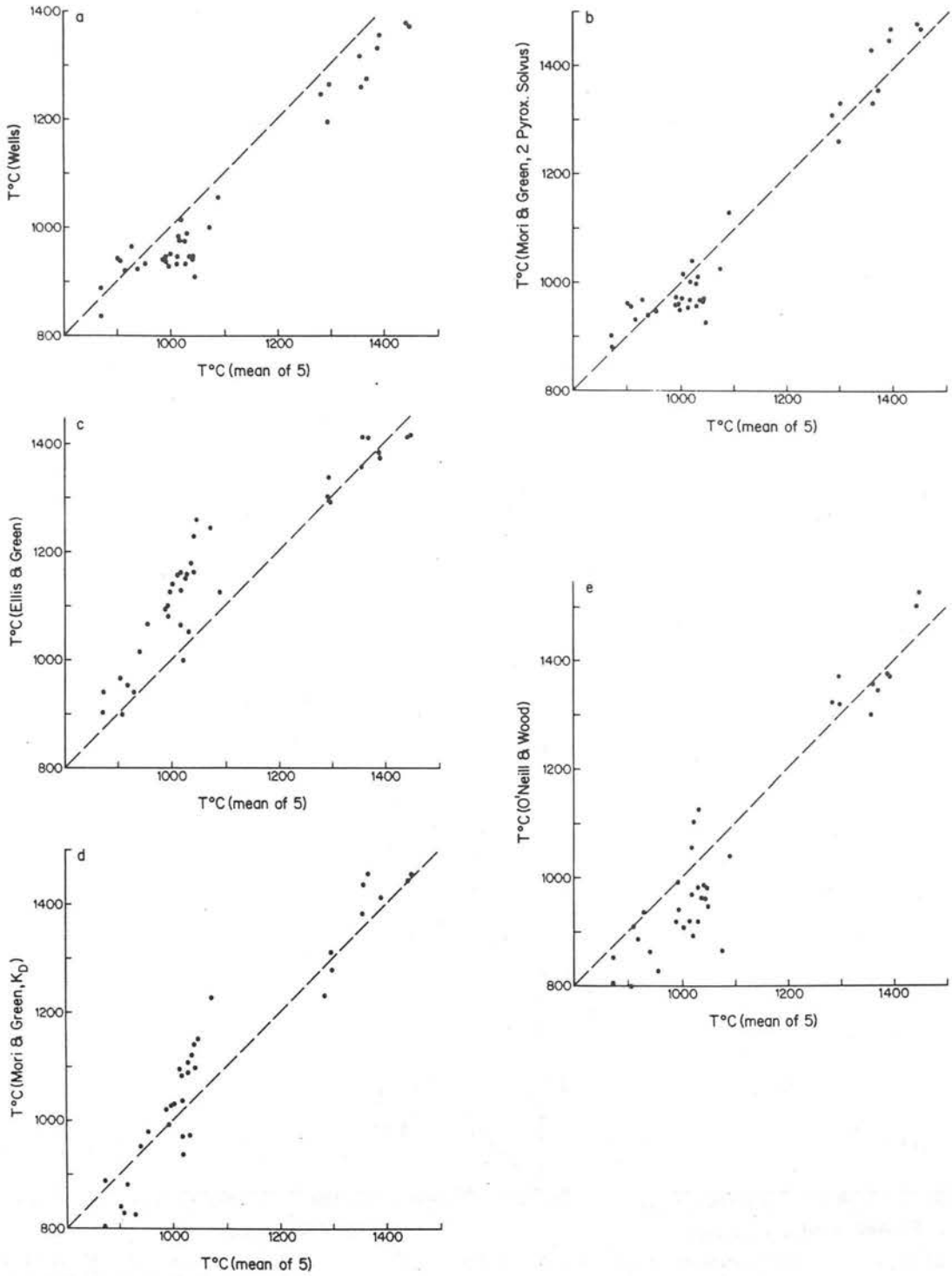

Fig. 2. Equilibration temperature values from each of the five geothermometric methods judged to give 'superior' results for these garnet lherzolite nodules, plotted against the mean temperature values obtained from these five preferred methods

yses including separate FeO and Fe_2O_3 values for mineral separates are available. It is apparent that the higher K_D values obtained from these analyses result in T values from the preferred Ellis and Green (1979) and Mori and Green (1978) equations which are roughly 100° C lower than those based on the assumption of all Fe as Fe^{2+} in both garnets and clinopyroxenes. This could well account for the fact that the Ellis and Green (1979) K_D equation, on the assumption of all Fe as Fe^{2+}, yields T values for

the majority of the nodules which are on the high side of the mean preferred T values.

Unfortunately, it does not appear to be possible to overcome the problem of the lack of analytical data on the $Fe^{2+}/(Fe^{2+}+Fe^{3+})$ ratios in the garnets and clinopyroxenes by calculating the Fe^{2+} and Fe^{3+} values on the basis of charge balance in the structural formulae. Attempts to do so result in unreasonably low $Fe^{2+}/(Fe^{2+}+Fe^{3+})$ ratios for the clinopyroxenes in many garnet lherzolite nodules, when compared with the ratios in rocks for which Fe^{2+} and Fe^{3+} data are available from mineral analyses.

(c) Geothermometer Based on $Fe^{2+}-Mg^{2+}$ Partitioning Between Coexisting Garnets and Olivines

$Fe^{2+}-Mg^{2+}$ partitioning between garnets and olivines, as expressed by the partition coefficient $K_{Fe-Mg}^{Gnt-Ol}=(Fe^{2+}/Mg^{2+})_{Gnt}/(Fe^{2+}/Mg^{2+})_{Ol}$, is not as temperature sensitive as that between garnets and clinopyroxenes (Mori and Green 1978). However, with this partition coefficient the effects of variable Fe oxidation state and of Al substitution on the activities of components in the clinopyroxenes which complicate the use of the K_D geothermometer are essentially avoided. O'Neill and Wood (1979) have provided an experimental calibration of K_{Fe-Mg}^{Gnt-Ol} as a function of T, P, the Ca content of the garnet, and the Fe/(Fe+Mg) ratio of the phases.

We have calculated T estimates for the suite of garnet lherzolites using the appropriately corrected versions (O'Neill and Wood 1980) of Eqs. (26) and (27) of O'Neill and Wood (1979) in a reiterative simultaneous solution with the geobarometric equation of Wood (1974). The tabulated results are reasonably in line with those obtained from the preferred equations for the two pyroxene solvus and the K_D geothermometers (see Figs. 1 and 2). They span a slightly wider temperature range than that indicated by the other preferred geothermometric methods but are neither consistently higher nor lower than the mean of all five preferred T estimates. The scatter about the mean may well simply reflect the relatively low temperature sensitivity of the K_{Fe-Mg}^{Gnt-Ol} partition coefficient especially at the higher temperatures.

(d) Geothermometer Based on $Al^{VI}-Cr$ Partitioning Between Coexisting Pyroxenes

Mysen (1976) has presented an experimental calibration of $Al^{VI}-Cr$ partitioning between coexisting pyroxenes which provides a potential geothermometer for garnet lherzolite assemblages. However, this yields T values which for the majority of nodules are clearly too low (Fig. 1j) especially for those nodules which equilibrated at the highest temperatures. The T values which we have calculated from this geothermometer assume that $Al^{VI}=$ Total Al/2. The clinopyroxenes in particular almost certainly have $Al^{VI}>Al^{IV}$, but unfortunately $Al^{VI}/(Al^{VI}+Al^{IV})$ ratios calculated from the structural formulae are extremely sensitive to even small errors in the SiO_2 analyses and thus yield highly variable $K_{Al^{VI}-Cr}^{Opx-Cpx}$ partition coefficients. We therefore conclude that uncertainty over the $Al^{VI}/(Al^{VI}+Al^{IV})$ ratios in the pyroxenes in these nodules prohibits satisfactory evaluation of this particular geothermometer and is also likely to restrict its usefulness in practice.

(e) Conclusions

In the light of the preceding analysis of the T estimates obtained by the various geothermometric methods for the suite of garnet lherzolites from the kimberlites of northern Lesotho, we consider that the most reliable T estimates are those obtained from the Wells (1977) and Mori and Green (1978) equations for the two pyroxene solvus geothermometer, the Ellis and Green (1979) and Mori and Green (1978) equations for the K_D geothermometer, and the O'Neill and Wood (1979) equation for the K_{Fe-Mg}^{Gnt-Ol} geothermometer. We do not feel that there are grounds for selecting any one of these five preferred geothermometric methods as being superior to the others when applied to garnet lherzolite assemblages. Rather we conclude that it is preferable to evaluate the equilibration conditions of such nodules on the basis of the mean result from the five 'superior' methods for the following reasons:

(a) the relative sensitivities of the individual geothermometers vary in different parts of the temperature range of interest;

(b) the various partition coefficients used are dependent to differing degrees on pressure and hence any errors in the pressure estimate will differentially affect the temperatures yielded by the individual methods;

(c) $Fe^{2+}/(Fe^{2+}+Fe^{3+})$ ratios in the minerals are generally unknown and the inaccuracies in considering all Fe as Fe^{2+} will result in errors of different magnitudes in the temperatures yielded by the various methods.

The fact that five different methods based as they are on three different element partition relationships, yield reasonably close temperature values for the majority of the nodules encourages us to the view that

our approach is justified and to think that the 5-method mean temperature valves should be sufficiently accurate to be geologically meaningful.

The Late Cretaceous Geotherm for Northern Lesotho

The preferred mean T estimate for each garnet lherzolite nodule (taken together with its paired mean P estimate) is plotted in Fig. 3, where the relationship of these P/T estimates to various postulated geotherms and key experimentally determined reaction curves can be assessed. All the estimates lie well within the garnet lherzolite stability field (Green and Ringwood 1967; O'Hara et al. 1971) but in a P/T band which although it extends into the diamond stability field for the highest temperature nodules is nevertheless significantly different from that of the earlier P/T estimates used by Boyd (1973) to define the late Cretaceous 'pyroxene geotherm' for the upper mantle beneath Lesotho. Nevertheless, as with these earlier P/T estimates, our new ones for this suite of nodules likewise fall into two groups – those in the higher temperature group all being for nodules with strikingly deformed fabrics from the Thaba Putsoa and Mothae pipes. However, the apparent correlation between deformation and equilibration temperature amongst the garnet lherzolite nodules from these particular pipes (Boyd and Nixon 1975) does not hold elsewhere (Harte et al. 1975; Dawson et al. 1975) – not even in the nearby Matsoku pipe.

On Fig. 3 our P/T estimates for the lower temperature group of nodules plot close to, but slightly above, the predicted Precambrian shield geotherm of Clark and Ringwood (1964) whilst the higher temperature group of nodules plots considerably above this geo-

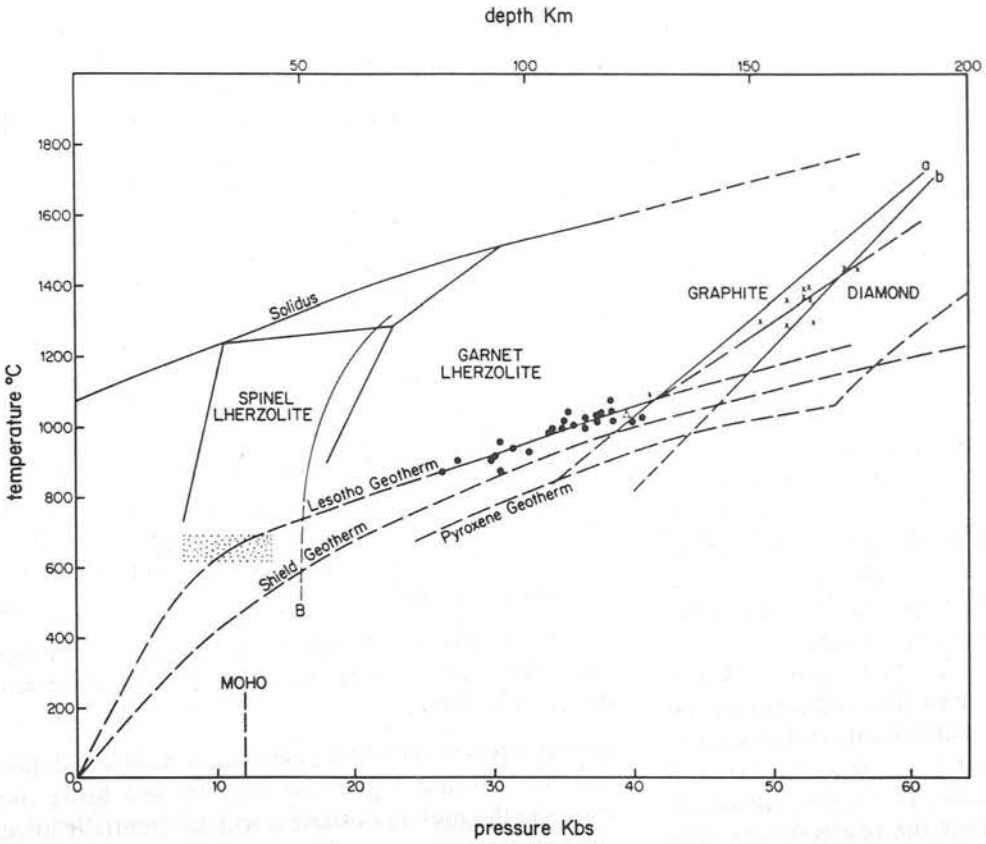

Fig. 3. P/T diagram showing the positions of our 'best' P/T estimates (as discussed in the text) for these garnet lherzolite nodules relative to various key mineral reaction curves and proposed geotherms. *Crosses* are for the sheared nodules from the Thaba Putsoa and Mothae pipes and the *triangular symbol* for the diamond bearing nodule BD 2125. The *solid lines* defining the P/T stability fields for various lherzolite assemblage types and the *solidus curve* are from Green and Ringwood (1967), whilst *curve B* is the experimentally determined spinel lherzolite⇌garnet lherzolite reaction boundary of O'Hara et al. (1971). The alternative *graphite ⇌diamond inversion curves* (*a*, *b*) are from Bundy et al. (1961) and Kennedy and Kennedy (1976), respectively. The Precambrian shield geotherm is from Clark and Ringwood (1964), the pyroxene geotherm from Boyd (1973), whilst the Lesotho geotherm is drawn to be broadly compatible with our P/T estimates for the garnet lherzolite nodules and 'best' estimates (stippled field covers one standard deviation about the mean) of the equilibration conditions for garnet granulite and garnet websterite nodules of suggested lower crustal origin (Carswell and Griffin, in press)

therm. Superficially this could be taken as confirmation of the earlier suggestions of Boyd (1973) and Boyd and Nixon (1975) that the upper mantle geotherm beneath northern Lesotho was significantly inflected at the time of kimberlite emplacement. However, as discussed by Mitchell et al. (1980) uncertainty exists as to whether the P/T estimates for mantle derived nodules in kimberlite do in fact define a palaeogeotherm which reflects the ambient conditions in the upper mantle at the time of kimberlite emplacement. Inaccuracies in the equilibration pressure estimates derived from the garnet-orthopyroxene geobarometer (as discussed earlier), possible lack of equilibrium between the geothermometers and geobarometers employed (Fraser and Lawless 1978), or kimberlite-nodule thermal interactions (Mitchell et al. 1980) could all result in the P/T estimates producing a spurious geotherm. Alternatively the P/T values recorded in such nodules, especially for the high temperature group, may simply reflect a transient geotherm generated in response to the localised thermal effects of a rising mantle diapir immediately prior to kimberlite eruption (Green and Gueguen 1974). With these considerations in mind we feel that our new P/T estimates for these garnet lherzolite nodules do not unequivocally confirm or refute the existence of a significant inflection in the late Cretaceous palaeogeotherm and have therefore drawn (Fig. 3) alternative projections of the Lesotho geotherm for depths >130 km.

We do, however, have sufficient confidence in our preferred equilibration temperature estimates for these nodules to conclude that, especially when taken together with the P/T estimates for nodules of lower crustal derivation from the same kimberlites (Griffin et al. 1979; Carswell and Griffin, in press), they indicate that the late Cretaceous palaegeotherm beneath northern Lesotho was appreciably steeper than implied by the 'pyroxene geotherm' of Boyd (1973) and somewhat steeper than the shield geotherm of Clark and Ringwood (1964) (see also discussion in Carswell et al. 1979; Griffin et al. 1979). The only independent check which we have on the accuracy of the pressure estimates for these nodules is provided by the existence of diamond in nodule BD 2125 (Dawson and Smith 1975). Our equilibration pressure estimate (Table 1) for this nodule falls 5.5 kbars below the diamond stability field as defined by Kennedy and Kennedy (1976) but lies within the error brackets on the diamond–graphite equilibrium boundary as determined by Bundy et al. (1961). It is noteworthy that the latter boundary is more consistent with independently calculated equilibration conditions for diamond bearing eclogite nodules from the Roberts Victor kimberlite (Carswell et al., in press).

Acknowledgements. D.A. Carswell wishes to acknowledge financial support from the Royal Society and the Natural Environment Research Council.

References

Akella J (1976) Garnet pyroxene equilibria in the system $CaSiO_3-MgSiO_3-Al_2O_3$ and in a natural mineral mixture. Am Mineral 61:589–598

Banno S (1970) Classification of eclogites in terms of physical conditions of their origin. Phys Earth Planet Inter 3:405–421

Bishop FC, Smith JV, Dawson JB (1978) Na, K, P and Ti in garnet, pyroxene and olivine from peridotite and eclogite xenoliths from African kimberlites. Lithos 11:155–173

Boyd FR (1973) A pyroxene geotherm. Geochim Cosmochim Acta 37:2533–2546

Boyd FR, Nixon PH (1975) Origins of the ultramafic nodules from some kimberlites of northern Lesotho and the Monastery Mine, South Africa. Phys Chem Earth 9:431–454

Boyd FR, Schairer JF (1964) The system $MgSiO_3-CaMgSi_2O_6$. J Petrol 5:275–309

Bundy FP, Bovenkerk HP, Strong HM, Wentorf RH Jr (1961) Diamond-graphite equilibrium line from growth and graphitization of diamond. J Chem Phys 35:383–391

Carswell DA (1974) Comparative equilibrium temperatures and pressures of garnet lherzolites in Norwegian gneisses and in kimberlite. Lithos 7:113–121

Carswell DA (1978) Palaeogeotherms: Implications of disequilibrium in garnet lherzolite xenoliths. Nature 276:737

Carswell DA (1980) Mantle derived lherzolite nodules associated with kimberlite, carbonatite and basalt magmatism: A review. Lithos 13:121–138

Carswell DA, Clarke DB, Mitchell RH (1979) The petrology and geochemistry of ultramafic nodules from Pipe 200, northern Lesotho. Proc 2nd Int Kimberlite Conf. Vol 2, pp 127–144. Am Geophys Union

Carswell DA, Dawson JB (1970) Garnet peridotite xenoliths in South African kimberlite pipes and their petrogenesis. Contrib Mineral Petrol 25:163–184

Carswell DA, Dawson JB, Gibb FGF (1980) Equilibration conditions of upper mantle eclogites: implications for kyanite-bearing and diamondiferous eclogites. Mineral Mag (in press)

Carswell DA, Gibb FGF (1980) The equilibration conditions and petrogenesis of European crustal garnet lherzolites. Lithos 13:19–29

Carswell DA, Griffin WL Calculation of equilibration conditions for garnet granulite and garnet websterite nodules in African kimberlite pipes. Tshermaks Mineral Petrog Mitt (in press)

Clark SP Jr, Ringwood AE (1964) Density distribution and constitution of the mantle. Rev Geophys 2:35–88

Cox KG, Gurney JJ, Harte B (1973) Xenoliths from the Matsoku pipe. In: Nixon PH (ed) Lesotho Kimberlites, Lesotho National Devel. Corp Maseru, Lesotho, pp 76–92

Davis BTC, Boyd FR (1966) The join $Mg_2Si_2O_6-CaMgSi_2O_6$ at 30 kilobars pressure and its application to pyroxenes from kimberlites. J Geophys Res 71:3567–3576

Dawson JB, Gurney JJ, Lawless PJ (1975) Palaeogeothermal gradients derived from xenoliths in kimberlite. Nature 257:299–300

Dawson JB, Smith JV (1975) Occurrence of diamond in a mica-garnet lherzolite xenolith from kimberlite. Nature 254:580–581

Ellis DJ, Green DH (1979) An experimental study of the effect of Ca upon garnet-clinopyroxene Fe–Mg exchange equilibria. Contrib Mineral Petrol 71:13–22

Fraser DG, Lawless PJ (1978) Palaeogeotherms. Implications of disequilibrium in garnet lherzolite xenoliths. Nature 273:220–222

Ganguly J (1979) Garnet and clinopyroxene solid solutions, and geothermometry based on Fe–Mg distribution coefficients. Geochim Cosmochim Acta 43:1021–1029

Green DH, Ringwood AE (1967) The stability fields of aluminous pyroxene peridotite and garnet peridotite and their relevance in upper mantle structure. Earth Planet Sci Lett 3:151–160

Green HW, Gueguen Y (1974) Origin of kimberlite pipes by diapiric upwelling in the upper mantle. Nature 249:617–620

Griffin WL, Carswell DA, Nixon PH (1979) Lower crustal granulites and eclogites from Lesotho, southern Africa. Proc 2nd Int Kimberlite Conf, Vol 2, pp 59–86

Harte B (1978) Kimberlite nodules, upper mantle petrology and geotherms. Philos Trans R Soc London, Ser A 288:487–500

Harte B, Cox KG, Gurney JJ (1975) Petrography and geological history of upper mantle xenoliths from the Matsoku kimberlite pipe. Phys Chem Earth 9:477–506

Herzberg CT (1978) The bearing of phase equilibria in simple and complex systems on the origin and evolution of some well-documented garnet websterites. Contrib Mineral Petrol 66:375–382

Kennedy SC, Kennedy GC (1976) The equilibrium boundary between graphite and diamond. J Geophys Res 81:2467–2470

Lindsley DH, Dixon SA (1976) Diopside-enstatite equilibria at 850° to 1,400° C, 5 to 35 Kb. Am J Sci 276:1285–1301

Lindsley DH, Munoz JL (1969) Subsolidus relations along the join hedenbergite-ferrosilite. Am J Sci 267A: 295–324

MacGregor ID (1974) The system $MgO-Al_2O_3-SiO_2$: Solubility of Al_2O_3 in enstatite for spinel and garnet peridotite compositions. Am Mineral 59:110–119

Mitchell RH, Carswell DA, Clarke DB (1980) Geological implications and validity of calculated equilibration conditions for ultramafic xenoliths from the Pipe 200 kimberlite, northern Lesotho. Contrib Mineral Petrol 72:205–217

Mori T (1977) Geothermometry of spinel lherzolites. Contrib Mineral Petrol 59:261–279

Mori T, Green DH (1975) Pyroxenes in the system $Mg_2Si_2O_6-CaMgSi_2O_6$ at high pressure. Earth Planet Sci Lett 26:277–286

Mori T, Green DE (1978) Laboratory duplication of phase equilibria observed in natural garnet lherzolites. J Geol 86:83–97

Mysen BO (1976) Experimental determination of some geochemical parameters relating to conditions of equilibriation of peridotite in the upper mantle. Am Mineral 61:677–683

Mysen BO, Heier KS (1972) Petrogenesis of eclogites in high grade metamorphic gneisses, exemplified by the Hareidland eclogite, western Norway. Contrib Mineral Petrol 36:73–94

Nehru CE, Wyllie PJ (1974) Electron-microprobe measurements of pyroxenes coexisting with H_2O undersaturated liquid in the join $CaMgSi_2O_6-Mg_2Si_2O_6-H_2O$ at 30 kilobars with application to geothermometry. Contrib Mineral Petrol 48:221–228

Nixon PH, Boyd FR (1973) Petrogenesis of the granular and sheared ultrabasic nodule suite in kimberlites. In: Nixon PH (ed) Lesotho Kimberlites, Lesotho National Devel Corp Maseru, Lesotho, pp 48–56

Nixon PH, Boyd FR, Boullier A-M (1973) The evidence of kimberlite and its inclusions on the constitution of the outer part of the earth. In: Nixon PH (ed) Lesotho Kimberlites, Lesotho National Devel Corp Maseru, Lesotho, pp 312–318

O'Hara MJ (1967) Mineral paragenesis in ultrabasic rocks. In: Wyllie PJ (ed) Ultramafic and Related Rocks, Wiley, New York, pp 393–403

O'Hara MJ, Richardson SW, Wilson G (1971) Garnet peridotite stability and occurrence in crust and mantle. Contrib Mineral Petrol 32:48–68

O'Neill HStC, Wood BJ (1979) An experimental study of Fe–Mg partitioning between garnet and olivine and its calibration as a geothermometer. Contrib Mineral Petrol 70:59–70

O'Neill HStC, Wood BJ (1980) An experimental study of Fe–Mg partitioning between garnet and olivine and its calibration as a geothermometer: corrections. Contrib Mineral Petrol 72:337

Powell R (1978) The thermodynamics of pyroxene geotherms. Philos Trans R Soc London, Ser A 288:457–469

Raheim A, Green DH (1974) Experimental determination of the temperature and pressure dependence of the Fe–Mg partition coefficient for coexisting garnet and clinopyroxene. Contrib Mineral Petrol 48:179–203

Ross M, Huebner JS, Dowty E (1973) Delineation of the one atmosphere augite-pigeonite miscibility gap for pyroxenes from Lunar basalt 12021. Am Mineral 58:619–635

Saxena SK (1979) Garnet-clinopyroxene geothermometer. Contrib Mineral Petrol 70:229–235

Wells PRA (1977) Pyroxene thermometry in simple and complex systems. Contrib Mineral Petrol 62:129–139

Wood BJ (1974) Solubility of alumina in orthopyroxene coexisting with garnet. Contrib Mineral Petrol 46:1–15

Wood BJ, Banno S (1973) Garnet-orthopyroxene and orthopyroxene-clinopyroxene relationships in simple and complex systems. Contrib Mineral Petrol 42:109–124

Received April 21, 1980; Accepted August 11, 1980

TMPM Tschermaks Min. Petr. Mitt. 28, 229–244 (1981)

TMPM Tschermaks Mineralogische und Petrographische Mitteilungen

From the Department of Geology, University of Sheffield, Sheffield, United Kingdom, and the Mineralogisk-Geologisk Museum, Oslo, Norway

Calculation of Equilibration Conditions for Garnet Granulite and Garnet Websterite Nodules in African Kimberlite Pipes

D. A. Carswell and W. L. Griffin

Received August 12, 1980;
accepted November 10, 1980

Summary

Pressure/temperature estimates based on different combinations of calibrated mineralogical thermometers and barometers and alternative assumptions concerning the $Fe^{2+}/(Fe^{2+} + Fe^{3+})$ ratios in the mineral phases are compared for a suite of fourteen nodules. Preferred *P/T* values have been obtained by simultaneous solution of eq. (12) of *Wood* (1974) for garnet-orthopyroxene equilibria and the *Ellis* and *Green* (1979) equation defining the *P,T,X* dependence of the Fe^{2+}–Mg^{2+} partition coefficient for coexisting garnet and clinopyroxene. However, to obtain realistic results it is first necessary to calculate the Fe^{3+} contents in the minerals – conveniently done on a charge balance basis. The favoured mean *P/T* estimates of 654 ± 36°C and 10.8±3.1 kbs are compatible with a lower crustal origin for this nodule suite.

Zusammenfassung

Berechnung von Gleichgewichts-Bedingungen von Granat-Granulit und Granat-Websterit-Xenolithen in afrikanischen Kimberliten

Druck-Temperatur-Berechnungen auf Grund verschiedener Kombinationen von kalibrierten mineralogischen Thermometern und Barometern sowie alternativer Modelle der $Fe^{2+}/(Fe^{2+} + Fe^{3+})$-Verhältnisse in den Mineralen einer Gruppe von 14 Einschlüssen werden verglichen. Bevorzugte *P/T*-Werte ergaben sich durch simultane Lösung der Gl. (12) für Granat-Orthopyroxen-Gleichgewichte von *Wood* (1974) und der Gleichung von *Ellis* und *Green* (1979), die die *P-T-X*-Abhängigkeit des Fe^{2+}—Mg^{2+}-Verteilungskoeffizienten für koexistierende Granat und Clinopyroxen definiert. Um realistische Ergebnisse zu erhalten, ist es jedoch zuerst notwendig, die Fe^{3+}-Gehalte der Minerale zu berechnen, vorzugsweise auf der Grundlage des Ladungsausgleichs. Die bevorzugten Durchschnittswerte von 654° ± 36°C und 10.8–3.1 kb sind in guter Übereinstimmung mit einer Herkunft aus der unteren Kruste.

0041-3763/81/0028/0229/$ 03.20

Numerous recent papers, e.g. *Råheim* and *Green* (1975), *Jackson* and *Harte* (1977), *Krogh* (1977), *Rogers* (1977), *Ernst* and *Dal Piaz* (1978), *Lappin* and *Smith* (1978), *O'Hara* and *Yarwood* (1978), *Griffin* et al. (1979), *Medaris* (1980), *Savage* and *Sills* (1980), use *P* (pressure)/*T* (temperature) estimates for granulites and eclogites to reconstruct geothermal gradients, thickness of ancient crust, etc. Such estimates are commonly based on two-pyroxene or pyroxene-garnet geothermometers/barometers that are experimentally calibrated on simple systems and/or far outside the crustal *P*/*T* range. The application of these methods to complex crustal rocks involves important assumptions, but the effect of alternative assumptions is not seriously considered in many such studies. This article empirically compares several of these methods, and attempts to evaluate their ability to give geologically realistic values of *P* and *T* for crustal rocks.

Many kimberlite pipes in southern Africa contain nodules of unexposed crustal rock types in addition to the extensively studied suite of mantle-derived nodules. Nodules of high grade metamorphic rocks (granulites, garnet websterites, eclogites) are particularly in evidence in the kimberlites around the edge of the Kaapvaal craton – notably in Lesotho and at Monastery Mine and other kimberlites in adjacent Cape Province, South Africa. The petrography, mineral and whole rock chemistry of a large suite of such nodules has been described elsewhere (*Griffin* et al., 1979). It was concluded that most (possibly all) of these nodules had been derived from the lower crust.

This paper provides a more detailed consideration of the problems and pitfalls involved in the estimation of *P*(pressure)/*T*(temperature) equilibrium conditions for these nodules, in the light of several new thermometric/barometric calibrations which have appeared since the former paper was presented. For present purposes we have restricted our discussion to nodules with the dominant primary mineral assemblages garnet + clinopyroxene + + orthopyroxene + plagioclase or garnet + clinopyroxene + orthopyroxene (garnet granulites and garnet websterites, respectively) (Table 1).

The mineral compositions (Table 2) on which the *P*/*T* estimates have been made were obtained by electron microprobe analysis, as with most other recent studies of kimberlite nodule suites. Certain key composition parameters and partition coefficients used to calculate the *P*/*T* estimates for these nodules are listed in Table 3. Despite the general superiority of electron microprobe analyses compared to "wet" analysis of mineral separates when considering element partition between coexsiting mineral phases, the lack of any analytical data on the $Fe^{2+}/(Fe^{2+} + Fe^{3+})$ ratios in the various minerals is a serious draw-back. Many recent papers involving *P*/*T* estimates for kimberlite nodule suites based on element partition coefficients (e.g.

Table 1. *Petrographic Data for Analysed Samples*

Sample No.	Locality	Rock Type	Mineral Assemblage
PHN2508	Lemphane	Garnet Websterite	Orthopyroxene–Clinopyroxene–Garnet–Magnetite: Considerable Secondary Amphibole
LQ1	Liqhobong	Garnet Websterite	Orthopyroxene–Clinopyroxene–Garnet: Minor Amphibole, Mica and Sulphide
KN206	Liqhobong	Garnet Websterite	Orthopyroxene–Clinopyroxene–Garnet–Rutile: Minor Amphibole and Ilmenite
PHN2495	Liqhobong	Garnet Granulite	Orthopyroxene–Clinopyroxene–Garnet–Plagioclase (Minor): Accessory Rutile
PHN2567/5	Letseng	Garnet Websterite	Orthopyroxene–Clinopyroxene–Garnet: Minor Rutile and Ilmenite
LT2	Letseng	Garnet Granulite	Orthopyroxene (Minor)–Clinopyroxene–Garnet–Plagioclase–Quartz: Minor Scapolite, Biotite, Rutile and Ilmenite
M3	Matsoku	Garnet Websterite	Orthopyroxene–Clinopyroxene–Garnet: Accessory Rutile and Ilmenite
M5	Matsoku	Garnet Websterite	Orthopyroxene–Clinopyroxene–Garnet: Accessory Rutile and Ilmenite
L9	Matsoku	Garnet Websterite	Orthopyroxene–Clinopyroxene–Garnet: Accessory Rutile and Ilmenite
L16	Matsoku	Garnet Websterite	Orthopyroxene–Clinopyroxene–Garnet: Accessory Rutile and Ilmenite
L17	Matsoku	Garnet Websterite	Orthopyroxene–Clinopyroxene–Garnet: Accessory Rutile and Ilmenite
L20	Matsoku	Garnet Granulite	Orthopyroxene–Clinopyroxene–Garnet–Plagioclase: Minor Biotite, K-Feldspar and Rutile
PHN2630/1	Monastery	Garnet Websterite	Orthopyroxene–Clinopyroxene–Garnet: Considerable Secondary Biotite
PHN2630/2	Monastery	Garnet Granulite	Orthopyroxene–Clinopyroxene–Garnet–Plagioclase: Minor Biotite and Ilmenite

Table 2. *Representative Microprobe Analyses of Coexisting Minerals*

Sample No.	PHN2508			LQ1			LT2			L20			PHN2630/1		
Mineral	*Opx*	*Cpx*	*Gt*	*Opx*	*Cpx*	*Gt*	*Opx*	*Cpx*	*Gt*	*Opx*	*Cpx*	*Gt*	*Opx*	*Gpx*	*Gt*
SiO_2	53.5	52.5	38.9	54.8	53.0	40.2	53.1	52.0	39.5	54.2	52.8	40.1	52.0	52.0	38.2
TiO_2	0.0	0.1	0.0	–	0.4	0.0	0.5	0.6	0.0	0.0	0.3	0.0	0.1	0.2	0.0
Al_2O_3	0.75	2.5	22.0	2.1	6.9	22.7	1.6	4.2	21.6	1.7	5.4	21.9	0.94	2.3	21.7
Fe_2O_3*	–	3.8	1.2	–	3.7	1.7	–	3.2	1.0	–	2.9	0.8	–	1.7	0.0
FeO	20.1	4.2	24.0	12.3	1.6	17.3	20.6	5.0	23.7	16.9	4.2	21.8	27.7	8.4	28.1
MnO	0.22	0.1	0.84	0.1	0.0	0.6	–	–	–	0.0	0.1	0.3	–	–	–
MgO	24.9	13.7	8.1	30.5	12.3	13.6	24.8	12.8	8.9	27.2	12.1	10.7	19.5	12.8	4.9
CaO	0.25	21.2	5.6	0.28	19.1	4.6	0.35	20.7	6.0	0.36	19.9	5.3	0.40	21.8	6.7
Na_2O	0.0	1.5	–	0.0	3.4	–	–	1.8	–	0.0	2.6	–	0.0	0.7	–
Total	99.7	99.6	100.6	100.1	100.4	100.8	101.0	100.3	100.7	100.4	100.3	100.9	100.6	99.9	99.6
No. of Oxygens	6	6	12	6	6	12	6	6	12	6	6	12	6	6	12
Si	1.973	1.944	2.975	1.940	1.910	2.965	1.938	1.913	3.003	1.954	1.928	3.009	1.969	1.945	3.003
Al	0.033	0.109	1.983	0.088	0.293	1.974	0.069	0.182	1.936	0.072	0.232	1.937	0.042	0.101	2.011
Ti	0.000	0.003	0.000	0.000	0.011	0.000	0.014	0.017	0.000	0.000	0.008	0.000	0.003	0.006	0.000
Fe^{3+}	–	0.105	0.067	–	0.101	0.097	–	0.087	0.058	–	0.080	0.045	–	0.049	0.000
Fe^{2+}	0.620	0.131	1.538	0.365	0.048	1.070	0.630	0.155	1.506	0.509	0.128	1.367	0.877	0.262	1.847
Mn	0.007	0.003	0.054	0.003	0.000	0.038	–	–	–	0.000	0.003	0.019	–	–	–
Mg	1.369	0.756	0.023	1.609	0.661	1.495	1.349	0.702	1.008	1.461	0.658	1.197	1.100	0.713	0.574
Ca	0.010	0.841	0.459	0.011	0.738	0.364	0.014	0.816	0.489	0.014	0.778	0.426	0.016	0.874	0.564
Na	0.000	0.108	–	0.000	0.238	–	–	0.128	–	0.000	0.184	–	0.000	0.051	0.000
Total	4.011	4.000	8.000	4.015	4.000	8.000	4.014	4.000	8.000	4.010	4.000	8.000	4.007	4.000	8.000

* Calculated by charge balance in structural formulae.

Table 3. *Important Mineral Composition Parameters and Partition Coefficients*

Sample No.	X_{Fe}^{Opx}	$a_{Mg_2Si_2O_6}^{Opx}$	$a_{Mg_2Si_2O_6}^{Cpx}$	$K_{Ca-Mg}^{Cpx-Opx}$	X_{Al}^{MI}	K_D^1	K_D^2	X_{Ca}^{gt}
PHN2508	0.312	0.463	0.021	0.046	0.016	5.56	9.61	0.151
LQ1	0.185	0.637	0.008	0.013	0.044	3.47	9.94	0.119
KN206	0.322	0.443	0.014	0.031	0.018	3.33	7.15	0.114
PHN2495	0.236	0.564	0.018	0.033	0.034	3.43	7.38	0.121
PHN2567/5	0.218	0.591	0.036	0.061	0.021	4.61	6.38	0.134
LT2	0.318	0.448	0.024	0.052	0.034	4.49	6.76	0.160
M3	0.296	0.480	0.020	0.041	0.016	4.27	8.50	0.129
M5	0.166	0.658	0.028	0.043	0.044	4.23	5.93	0.146
L9	0.277	0.506	0.018	0.035	0.018	3.76	6.11	0.120
L16	0.184	0.633	0.022	0.035	0.038	3.84	7.58	0.130
L17	0.230	0.573	0.020	0.035	0.026	4.00	6.50	0.126
L20	0.258	0.528	0.013	0.025	0.036	3.74	5.88	0.140
PHN2630/1	0.444	0.300	0.033	0.109	0.021	7.39	8.76	0.189
PHN2630/2	0.460	0.259	0.048	0.185	0.047	7.33	7.33	0.207

X_{Fe}^{Opx} = Fe/(Fe+Mg) in orthopyroxene X_{Ca}^{gt} = Ca/(Ca+Mg+Mn) in garnet

$a_{Mg_2Si_2O}^{Opx}$ and $a_{Mg_2Si_2O_6}^{Cpx}$ = mol. fractions of enstatite in orthopyroxene and clinopyroxene respectively

$K_{Ca-Mg}^{Cpx-Opx} = a_{Mg_2Si_2O_6}^{Cpx}/a_{Mg_2Si_2O_6}^{Opx}$

X_{Al}^{MI} = the fraction of Al in the MI sites in orthopyroxene

$K_D^1 = (Fe^{2+}/Mg^{2+})gnt/(Fe^{2+}/Mg^{2+})\,Cpx$ with all Fe taken as Fe^{2+}

$K_D^2 = (Fe^{2+}/Mg^{2+})gnt/(Fe^{2+}/Mg^{2+})\,Cpx$ with calculated Fe^{3+} contents in both minerals excluded

Boyd and *Nixon*, 1975; *Rogers* and *Nixon*, 1975; *Jackson* and *Harte*, 1977; *Fraser* and *Lawless*, 1978) assume that all iron is present in the divalent state and that the *P/T* values for different nodules obtained on such an assumption are at least valid on a comparative basis. The first assumption is almost certainly not true for crustal rocks, and the second will only be the case if the oxidation state of the analysed nodules is similar.

An alternative approach to this problem is to calculate $Fe^{2+}/(Fe^{2+} + Fe^{3+})$ ratios for the various mineral analyses; this is conveniently done on the basis of charge balance (*Neumann*, 1976). However, this method is sensitive to analytical errors, notably in SiO_2. In this paper we present *P/T* estimates based both on the assumption of all iron as Fe^{2+} and on calculated $Fe^{2+}/(Fe^{2+} + Fe^{3+})$ ratios, and consider the likely geological validity of both sets of estimates for these nodules.

Boyd and *Schairer* (1964), *Davis* and *Boyd* (1966) showed that the diopside limb of the two-pyroxene solvus in the $Mg_2Si_2O_6-CaMgSi_2O_6$ system is strongly temperature dependent between 900–1400°C. Since then this mineralogical thermometer has been widely applied to rocks containing coexisting Ca-rich and Ca-poor pyroxenes, including kimberlite nodules (e.g. *Boyd*, 1973; *Carswell*, 1974). The two pyroxene solvus is probably relatively insensitive to pressure, at least below about 1000°C (*Mori* and *Green*, 1975; *Lindsley* and *Dixon*, 1976). Enrichment in FeO will cause the two pyroxene field to shrink progressively (*Lindsley* and *Munoz*, 1969; *Ross* et al., 1973), but since ultramafic nodules in kimberlites typically contain highly magnesian pyroxenes (orthopyroxenes commonly 4–13% $Fe_2Si_2O_6$) their equilibration temperatures have often been deduced directly from the *Davis* and *Boyd* (1966) data for the Fe-free system. However, a crude allowance for the effect of Fe on the two pyroxene solvus has usually been made (*Boyd*, 1973; *Carswell*, 1974; *Boyd* and *Nixon*, 1975) by estimating the temperature from the Ca/(Ca + Mg) ratio rather than the Ca/(Ca + Mg + Fe) ratio of the clinopyroxene phase.

The clinopyroxenes in the garnet granulite and garnet websterite nodules considered here have 100 Ca/(Ca + Mg) ratios ranging from 50.6–55.7; the *Davis* and *Boyd* (1966) data would imply equilibration temperatures of at most 800°C and often considerably less. However, precise temperature values probably cannot be obtained for these nodules in this manner, as *Davis* and *Boyd* (1966) did not present any experimental data below 950°C. Even if they had done so, the appreciable Na_2O and Al_2O_3 contents in these clinopyroxenes (Table 2) and their relatively iron-rich nature (coexisting orthopyroxenes 16.6–46.0% $Fe_2Si_2O_6$) render it extremely unlikely that the *T* values derived in this manner would be sufficiently accurate to be geologically meaningful.

Wood and *Banno* (1973) derived a semi-empirical expression designed to correct the *Davis* and *Boyd* (1966) data for the effect of Fe on the pyroxene miscibility relations. They adopted an ideal two-site solution model where the contents of Al^{3+}, Cr^{3+}, Ti^{4+} and Fe^{3+} in M1 and Ca^{2+}, Na^{+} and Mn^{2+} in M2 are first substracted before obtaining the fraction of these sites filled by Mg^{2+} and Fe^{2+}. Mg^{2+} and Fe^{2+} were assumed to be distributed between the two sites in proportion to the $Mg^{2+}/(Mg^{2+} + Fe^{2+})$ ratio.

More recent experimental studies of the two pyroxene solvus (*Nehru* and *Wyllie*, 1974; *Mori* and *Green*, 1975, 1976; *Lindsley* and *Dixon*, 1976) have cast serious doubts over certain aspects of the earlier *Davis* and *Boyd* (1966) data. Together these new data indicate that the clinopyroxene limb of the solvus is probably somewhat steeper below 1200°C than was indicated by *Davis* and *Boyd* (1966) and hence is less sensitively dependent on temperature. By incorporating these data with further additional data by *Ross* et al. (1973) and others on the iron bearing pyroxene system and using ideal mixing models and a semi-empirical approach similar to that of *Wood* and *Banno* (1973), *Wells* (1977) obtained a new best fit calibration of the two pyroxene geothermometer.

Temperature values (Table 4) obtained from the *Wells* (1977) equation are for most nodules lower than those calculated from the *Wood* and *Banno* (1973) equation. We judge these *Wells* (1977) temperature estimates to be superior both from the previously outlined considerations and because they more closely approach the values which may be obtained from consideration of $Fe^{2+}-Mg^{2+}$ partition coefficients (see below). However,

Table 4. *Calculated Pressure-Temperature Estimates*

Sample Number	T Estimates from Two Pyroxene Solvus				Ca-Mg Exchange Between Gnt-Cpx-Opx		T Estimates Based on Fe^{2+}-Mg^{2+} Partitioning Between Garnets and Clinopyroxene							
	T°C Wells	P.Kbs Wood	T°C Wood & Banno	P.Kbs Wood	T°C Powell	P.Kbs Powell	K_D	T°C Råheim & Green	P.Kbs Wood	T°C Ellis & Green	P.Kbs Wood	T°C Ganguly	P.Kbs Wood	T°C Saxena	P.Kbs Wood
PHN 2508	747	19.2	780	21.1	594	5.0	1	790	21.7	752	19.5	881	27.0	955	31.4
							2	592	10.2	596	10.4	744	19.0	-	-
LQ1	628	5.6	725	10.4	390	-37.0	1	914	19.6	867	17.3	988	23.2	858	16.8
							2	529	0.9	543	1.6	706	9.5	-	-
KN206	690	16.6	733	19.2	211	-54.8	1	1098	40.8	924	30.5	1032	36.9	1113	41.7
							2	697	17.0	640	13.6	796	22.9	-	-
PHN 2495	725	12.8	788	16.1	354	-33.3	1	961	25.0	887	21.2	998	27.0	1031	28.7
							2	631	8.0	621	7.4	775	15.5	-	-
PHN 2567/5	825	23.1	876	26.0	535	-6.3	1	872	25.8	800	21.7	923	28.7	944	29.9
							2	727	17.5	689	15.4	829	23.4	-	-
LT2	764	12.4	791	13.8	626	3.6	1	791	13.8	809	14.7	918	20.2	887	18.6
							2	637	6.1	677	8.1	805	14.6	-	-
M3	736	20.0	776	22.4	484	-19.5	1	947	32.6	834	25.9	953	33.0	1042	38.3
							2	644	14.5	609	12.5	762	21.6	-	-
M5	791	13.3	873	17.2	674	-0.5	1	811	14.2	815	14.4	928	19.9	751	11.4
							2	679	7.9	699	8.9	832	15.3	-	-
L9	721	18.2	770	21.1	454	-24.9	1	1006	34.9	872	27.0	993	34.1	1050	37.5
							2	754	20.0	694	16.5	843	25.2	-	-
L16	751	12.9	831	16.9	555	-15.3	1	878	19.2	842	17.4	962	23.4	844	17.5
							2	612	5.9	620	6.3	772	13.9	-	-
L17	739	16.0	801	19.4	529	-17.1	1	914	25.6	838	21.4	961	28.2	954	27.8
							2	697	13.7	671	12.3	819	20.4	-	-
L20	683	9.0	746	12.2	532	-13.6	1	887	19.2	863	18.0	973	23.6	915	20.7
							2	691	9.4	700	9.9	837	16.8	-	-
PHN 2630/1	831	19.0	807	17.7	740	24.1	1	631	8.0	684	10.9	800	17.3	800	17.3
							2	579	5.2	637	8.4	760	15.2	-	-
PHN 2630/2	918	12.9	862	10.4	782	30.2	1	558	-3.4	675	1.9	784	6.8	678	2.1
							2	558	-3.4	675	1.9	784	6.8	-	-
$\bar{x}$	753	15.1	797	17.4	533	-11.4	1	861	21.2	819	18.7	935	25.0	916	24.3
σn	69	4.5	47	4.4	147	22.3	1	136	10.7	70	6.9	69	7.4	118	10.8
$\bar{x}$	-	-	-	-	-	-	2	645	9.5	648	9.5	790	17.1	-	-
σn	-	-	-	-	-	-	2	64	6.3	45	4.3	39	5.1	-	-

K_D^1 - Assumes all Fe as Fe^{2+}

K_D^2 - Excludes Calculated Fe^{3+} in both Minerals

because of the strictly limited temperature dependence of the two pyroxene solvus below about 1000°C and uncertainties over the correction factors necessary to extend experimental data from simple pyroxene systems to the more chemically complex natural pyroxenes, we consider that it is probably unrealistic to expect that the two pyroxene solvus geothermometer can yield equilibration temperatures for these nodules which are sufficiently accurate to be geologically interesting. The comparative T data presented in Table 4 show that the temperature estimates obtained from this geothermometer may differ from other, probably more reliable, estimates by as much as 200+°C. We have calculated both the *Wells* (1977) and *Wood* and *Banno* (1973) temperature estimates on the assumption that all Fe is divalent in both pyroxenes. Calculations taking into account calculated $Fe^{2+}/(Fe^{2+} + Fe^{3+})$ ratios yield slightly higher T values but the differences are small compared to the overall uncertainty which we feel should be attached to all T estimates for these nodules based on Ca–Mg exchange between the coexisting pyroxenes.

Neither the *Wells* (1977) nor the *Wood* and *Banno* (1973) equations take account of any pressure effect on the two pyroxene solvus as experimentally demonstrated by *Mori* and *Green* (1975) and *Lindsley* and *Dixon* (1976). However, it would appear that below 1000°C the magnitude of the pressure dependence is small and hence that any errors introduced by ignoring it are relatively minor.

Geobarometry Based on Garnet-Orthopyroxene Equilibria

The solubility of Al_2O_3 in orthopyroxenes coexisting with garnets is strongly P/T dependent (*Boyd* and *England*, 1964; *MacGregor* and *Ringwood*, 1964; *MacGregor*, 1974; *Akella*, 1976). X_{Al}^{Ml} in orthopyroxene in equilibrium with garnet decreases with pressure but increases with temperature. Direct application of experimental data for the simple $MgO-Al_2O_3-SiO_2$ system (*MacGregor*, 1974) cannot be expected to yield meaningful P estimates for these nodules as the presence of other elements, notably Fe, is certain to affect the orthopyroxene-garnet equilibria. However, *Wood* and *Banno* (1973) and *Wood* (1974) have formulated semi-empirical expressions for this potentially useful geobarometer which are designed to take account of the more complex chemistry of natural garnet-orthopyroxene pairs.

The pressure values paired with the *Wells* (1977) and *Wood* and *Banno* (1973) temperatures in Table 4 were obtained from eq. (12) of *Wood* (1974). As the calculated pressures are strongly temperature dependent, any errors in the initial T estimates will of course be carried through into the P estimates. Hence these particular P values are considered to be of dubious validity.

Geothermometry/Barometry Based on Ca–Mg Exchange Reactions Involving Co-Existing Pyroxenes and Orthopyroxene-Garnet

Powell (1978) has presented two thermodynamically formulated equations for Ca–Mg exchange reactions between orthopyroxene-clinopyroxene and orthopyroxene-garnet pairs which should be applicable to the assemblages in these nodules. As these exchange reactions are both pressure and temperature dependent, it is necessary to solve these equations simultaneously to obtain P/T estimates as given in Table 4. It may be seen that the T values are generally rather low as well as inconsistent whilst the P values are mostly negative. Indeed even one of the garnet lherzolite nodules used by *Powell* (1978) as a test of this methods yields a negative equilibration pressure when the P/T intersection of the two reaction equations is calculated, as do several other garnet lherzolite nodules from the Lesothan kimberlites (*Carswell* and *Gibb*, 1980). We conclude that *Powell*'s (1978) method does not yield reliable estimates for the P/T equilibration conditions of the garnet granulite and garnet websterite nodules being considered here, probably because it is impossible to ascertain the required cation site occupancies in the pyroxenes with sufficient precision.

Geothermometry/Barometry Based on Fe^{2+}—Mg^{2+} Partitioning Between Garnets and Clinopyroxenes and Garnet-Orthopyroxene Equilibria

Fe^{2+}—Mg^{2+} partition coefficients between coexisting garnets and clinopyroxenes, commonly expressed as $K_D = (Fe^{2+}/Mg^{2+})Gnt/(Fe^{2+}/Mg^{2+})Cpx$, are strongly temperature dependent (*Banno*, 1970; *Mysen* and *Heier*, 1972). *Råheim* and *Green* (1974) experimentally calibrated K_D as a function of both P and T for a series of natural basaltic rock compositions, and indicated that K_D is more markedly P dependent than estimated by *Banno* (1970) on thermodynamic grounds for simple system equilibria. However, the subsequent experimental results of *Wood* (1976) and *Mori* and *Green* (1978) showed that, at least in the case of ultramafic rock compositions, the P dependence of K_D is considerably less than indicated by *Råheim* and *Green* (1974). Thankfully the situation has recently been clarified by the experimental study of *Ellis* and *Green* (1979) who demonstrate that a combination of non-ideal Ca–Mg substitutions in both garnet and clinopyroxene can result in other changes in the compositions of these minerals which profoundly affect K_D, and that the net effect of these changes is most conveniently measured by the Ca content of the garnet (X_{Ca}^{gt}). In addition *Ganguly* (1979) has attempted to integrate the available thermodynamic mixing data with thermochemical and selected earlier experimental data to derive equations which express K_D as a function of P, T and the Ca and Mn

contents of the garnet, whilst *Saxena* (1979) has extended this approach in an attempt to also take account of the influence on K_D of substantial Na_2O contents in the clinopyroxene.

In Table 4 are listed in turn the T values for these garnet granulite and garnet websterite nodules calculated from each of these four K_D calibrations, paired with P values obtained by simultaneous solution of the appropriate equations with equation (12) of *Wood* (1974) for garnet-orthopyroxene equilibria.

The *Ganguly* (1979) calibration gives fairly consistent, but on average the highest, T estimates for these nodules and, as commented by *Ellis* and *Green* (1979), it seems likely that this particular calibration does not adequately describe the effect of varying mineral compositions on K_D. Indeed *Ganguly* (1979) clearly indicated that his geothermometric expressions should only be applied to Na poor compositions whilst most of the nodules being considered here have quite jadeitic clinopyroxenes (see Table 2 and *Griffin* et al., 1979). On the other hand the mineral assemblages of these nodules fall within the composition range encompassed by *Saxena*'s (1979) geothermometer but this calibration again yields rather high and in addition rather more variable T estimates for the various nodules. We therefore tend to the view that this calibration likewise falls to adequately account for the influence of the mineral compositions on K_D.

The Ca contents of the garnets of these nodules are fairly low and span only a limited range (X_{Ca}^{gt} = 0.114–0.207, Table 3). The mean values obtained for this suite of nodules from both the *Råheim* and *Green* (1974) and *Ellis* and *Green* (1979) equations are not greatly different (Table 4) but it is noteworthy that the *Ellis* and *Green* (1979) T estimates which take account of the effect of X_{Ca}^{gt} on K_D are significantly less variable and are certainly to be preferred.

A serious potential source of error in all T estimates derived from the K_D partition coefficients arises from uncertainty over the $Fe^{2+}/(Fe^{2+} + Fe^{3+})$ ratios in the garnets and clinopyroxenes of these nodules, analysed as they were by electron microprobe. Hence in Table 3 we list two sets of K_D values, the first based on the assumption that all Fe is Fe^{2+} in both minerals – the second excluding Fe^{3+} in the minerals calculated on a charge balance basis (*Neumann*, 1976). As calculated $Fe^{2+}/(Fe^{2+} + Fe^{3+})$ ratios in the clinopyroxenes are very much lower (mean value 0.65) than in the garnets (mean value 0.98) the second set of K_D values are generally much higher and hence yield substantially lower T estimates (Table 4). Since analytical errors and non-stoichiometry in the clinopyroxenes typically produce low values for SiO_2, our experience is that calculation of Fe^{3+} on a charge balance basis tends to produce maximum K_D values. Thus whilst the assumption of all Fe as Fe^{2+} yields K_D values which may be expected to be too low and hence give maximum T estimates, exclusion of calculated

Fe^{3+} contents in most cases gives maximum K_D values and hence minimum T estimates. The key question is which of these two sets of T estimates is closest to reality.

It can be seen from Table 4 that the two sets of T estimates derived from the preferred *Ellis* and *Green* (1979) calibration of K_D vary by up to 324°C for individual nodules, whilst the difference between the means of the two sets of estimates is 171°C. It is just such differences in the T (and corresponding P) estimates which have given rise to quite contrasting interpretations for the depths of origin of such nodules (cf. *Griffin* et al., 1979; *Rogers*, 1977; *Jackson* and *Harte*, 1977). The P/T estimates based on K_D with all Fe as Fe^{2+} necessitate an upper mantle origin for most of these nodules, whilst the second set of P/T estimates (K_D excluding calculated Fe^{3+} contents) is broadly compatible with derivation of this nodule suite from the lower crust.

For the majority of individual nodules the T estimate given by the *Wells* (1977) calibration of the two pyroxene solvus geothermometer lies within the alternative T estimates calculated from K_D by the *Ellis* and *Green* (1979) equation. The mean *Wells* T estimate for the whole nodule suite is in fact somewhat closer to that calculated from K_D assuming all Fe as Fe^{2+} than to that based on K_D excluding calculated Fe^{3+} contents. However, we have previously expressed our reservations over the ability of the two pyroxene solvus geothermometer to produce accurate T estimates for the equilibration of these nodules and certainly it is disconcerting to observe that taken overall there is a clear inverse relationship between the *Wells* T estimates and those based on the first set of K_D values for this suite of nodules. This reflects the fact that both the *Wells* T estimates and the K_D values (when all Fe is taken as Fe^{2+}) tend to increase in the more ferriferous nodule assemblages.

Whilst the data in Table 3 show the expected increase in $K_{Ca-Mg}^{Cpx-Opx}$ with X_{Fe}^{Opx}, the fact that the *Wells* T estimates also tend to increase with X_{Fe}^{Opx} might be taken to indicate that the empirical correction applied by *Wells* (1977) to take account of the effect of iron on the two pyroxene solvus is inadequate. However, we suspect that the problem may be more complex than this since it is apparent that the nodules with more ferriferous assemblages (notably those from Monastery Mine) tend to have the least jadeitic clinopyroxenes. The addition of Fe clearly results in an increase in the extent of solid solution between the coexisting pyroxenes, relative to the $Mg_2Si_2O_6 - CaMgSi_2O_6$ system, whilst the presence of Na_2O and Al_2O_3 may well have the opposite effect (e. g. *Akella*, 1976). Certainly the two ferriferous Monastery Mine nodules with low Na_2O clinopyroxenes give anomalously high *Wells* T estimates when compared to those based on both sets of K_D values.

Neither *Råheim* and *Green* (1974) nor *Ellis* and *Green* (1979) observed any detectable influence of varying rock Mg/(Mg + Fe) ratios on K_D, such as might explain the tendency for the K_D values based on all Fe as Fe^{2+} to be higher in the nodules with lower Mg/(Mg + Fe) ratios. Moreover, such a correlation disappears when K_D is calculated after exclusion of calculated Fe^{3+} contents as does the disturbing inverse relationship between the *Wells* and the *Ellis* and *Green* *T* estimates. We take this as confirmation of the fact that the clinopyroxenes in most of these nodules do indeed contain significant Fe^{3+} contents and hence that the second set of *Ellis* and *Green* *T* estimates is the more realistic.

These preferred *T* estimates range from 543–700°C for this suite of nodules, the mean value being 648 ± 45°C. The corresponding *P* estimates obtained by simultaneous solution of the *Ellis* and *Green* (1979) equation with the geobarometric equation of *Wood* (1974) are 1.6–15.4 kbs, with a mean value of 9.5 ± 4.3 kbs. Clearly the *P/T* estimates for a few individual nodules are anomalously low. In the case of LQ1 this doubtless reflects a K_D value which is too high due to the calculation of an excessive amount of Fe^{3+} in the clinopyroxene. However the low *P* estimate for Monastery Mine nodule PHN 2630/2 which reflects the unusually high X_{Al}^{MI} in the orthopyroxene in this rock considering the high X_{Fe}^{Opx} value (in the other nodules X_{Al}^{MI} shows the expected decrease with increasing X_{Fe}^{Opx}) cannot be readily explained.

Discussion

We have shown that a wide range of *P/T* estimates may be obtained for a single suite of similar nodules depending on whose calibration of various mineralogical thermometers is employed and on the assumptions made regarding the $Fe^{2+}/(Fe^{2+} + Fe^{3+})$ ratios in the minerals. We consider that at the likely temperatures of equilibration of these nodules the two pyroxene solvus geothermometer is not sufficiently sensitive to give reliable results. $Fe^{2+}-Mg^{2+}$ partitioning between the garnets and clinopyroxenes is much more sensitive at such temperatures and the best calibration appears to be that of *Ellis* and *Green* (1979). However, to obtain meaningful *T* estimates from this geothermometer it is necessary when calculating K_D values to take account of the likely Fe^{3+} contents in the minerals, especially the clinopyroxenes. With microprobe minerals analyses this is best done by charge balance in the structural formulae, although in some cases this overestimates the Fe^{3+} contents and leads to somewhat underestimated temperatures. However, taking all Fe as Fe^{2+} in these minerals yields *T* values are in all likelihood serious overestimates.

Simultaneous solution of the *Ellis* and *Green* (1979) equation for the K_D geothermometer with the geobarometric equation of *Wood* (1974) for garnet-orthopyroxene equilibria gives preferred mean *P/T* estimates for this nodule suite of 654 ± 36°C and 10.8 ± 3.1 kbs when the obviously suspect estimates for nodules LQ1 and PHN 2630/2 are excluded. Although we are reasonably confident in the ability of the combination of the *Ellis* and *Green* (1978)/*Wood* (1974) geothermometer-barometer to give geologically meaningful *P/T* values for crustal rocks with appropriate mineral assemblages, it would obviously be comforting to have an alternative geobarometer to that of *Wood* (1974) to confirm the equilibration pressures and hence depths of origin of such rocks. Unfortunately the alternative method provided by *Powell* (1978) based on Ca–Mg exchange in garnet-clinopyroxene-orthopyroxene assemblages yields negative pressures for the majority of the nodules considered here, as does combining eq. (3) of *Herzberg* (1978) for garnet-clinopyroxene equilibria with the *Ellis* and *Green* (1979) K_D equation.

Our preferred *P/T* estimates for the garnet granulite and garnet websterite nodules viewed in conjunction with the general petrological, geochemical and geophysical considerations outlined by *Griffin* et al. (1979) lead us to conclude that these nodules were probably derived from the seismically distinct lower crustal layer which currently underlies this region at a depth of some 22–37 kilometres (*Hales* and *Sacks*, 1959). Furthermore these preferred *P/T* estimates are broadly consistent with the likely Cretaceous lower crustal temperatures implied by measurements of the present day heat flow in the Karroo Basin (*Clark* and *Ringwood*, 1964). We therefore view the suggestion by *Jackson* and *Harte* (1977) that the petrologically equivalent nodules which they have studied from the Matsoku pipe in Lesotho have been derived from sub-Moho depths and that granulite facies rocks therefore extend down some 33 kilometres below the Moho beneath northern Lesotho as unlikely.

The *P/T* estimates for individual nodules do not define a realistic geotherm, such as might suggest derivation from a significant depth range. Indeed consideration both of the partition coefficients considered above and of others such as $K_{Fe-Mg}^{Cpx-Opx}$ and $K_{Fe-Mg}^{Gnt-Opx}$ does not indicate consistent relative equilibrium *P/T* values for the individual nodules. Neither is there any indication that the garnet granulite nodules have equilibrated at consistently different *P/T* conditions to the garnet websterites. We therefore conclude that most likely both nodule types were derived from a limited depth range in the lower crust and that bulk chemical considerations control the presence or absence of plagioclase in the assemblages (see *Griffin* et al., 1978).

Contrary to our foregoing conclusions concerning the applicability of the different mineral thermometers, *Fraser* and *Lawless* (1978) have recently suggested that in ultramafic nodules from certain South African kimberlites

the $Fe^{3+}-Mg^{2+}$ exchange between coexisting garnet and pyroxenes is effectively "blocked" at temperatures below 1100°C, whereas lower temperature equilibration continues to be monitored by Ca–Mg exchange between the coexisting pyroxenes. However, we find the arguments which they put forward in support of this point unconvincing, especially as they have discounted any effect of pressure on the $Fe^{2+}-Mg^{2+}$ exchange reactions (*Carswell*, 1978). Certainly their condition does not appear to hold for the garnet granulite and garnet websterite nodules which we have considered in this paper.

Acknowledgements

The authors wish to acknowledge financial support from the Natural Environmental Research Council and the Royal Society (D.A.C.); and the Norwegian Scientific Research Council and Nansenfondet (W.L.G.). Dr. *F. G. F. Gibb* kindly assisted with writing a computer program to undertake *P/T* calculations.

References

Akella, J., 1976: Garnet pyroxene equilibria in the system $CaSiO_3-MgSiO_3-Al_2O_3$ and in a natural mineral mixture. Am. Min. *61*, 589–598.

Banno, S., 1970: Classification of eclogites in terms of physical conditions of their origin. Phys. Earth Planet. Inter. *3*, 405–421.

Boyd, F. R., 1973: A pyroxene geotherm. Geochim. Cosmochim. Acta *37*, 2533–2546.

– *England, J. L.*, 1964: The system enstatite-pyrope. Carnegie Inst. Washington Year Book *63*, 157–161.

– *Nixon, P. H.*, 1975: Origins of the ultramafic nodules from some kimberlites of northern Lesotho and the Monastery Mine, South Africa. Phys. Chem. Earth *9*, 431–454 (1975).

– *Schairer, J. T.*, 1964: The system $MgSiO_3-CaMgSi_2O_6$. J. Petrol. *5*, 275–309.

Carswell, D. A., 1974: Comparative equilibration temperatures and pressures of garnet lherzolites in Norwegian gneisses and in kimberlite. Lithos *7*, 113–121.

– 1978: Palaeogeotherms: Implications of disequilibrium in garnet lherzolite xenoliths. Nature *276*, 737.

– *Gibb, F. G. F.*, 1980: Geothermometry of garnet lherzolite nodules with special references to those from the kimberlites of northern Lesotho. Contr. Min. Petr. *74*, 403–416.

Clark, S. P., Jr., *Ringwood, A. E.*, 1964: Density distribution and constitution of the mantle. Rev. Geophys. *2*, 35–88.

Davis, B. T. C., Boyd, F. R., 1966: The join $Mg_2Si_2O_6-CaMgSi_2O_6$ at 30 kilobars pressure and its application to pyroxenes from kimberlites. J. Geophys. Res. *71*, 3567–3576.

Ellis, D. J., Green, D. H., 1979: An experimental study of the effect of Ca upon garnet-clinopyroxene Fe–Mg exchange equilibria. Contr. Min. Petr. *71*, 13–22.

Ernst, W. G., Dal Piaz, G. V., 1978: Mineral paragenesis of eclogitic rocks and related mafic schists of the Piemonte ophiolite nappe, Brueil-St-Jacques area, Italian Western Alps. Am. Min. *63*, 621–640.

Fraser, D. G., Lawless, P. J., 1978: Palaeogeotherms: Implications of disequilibrium in garnet lherzolite xenoliths. Nature *273*, 220–222.

Ganguly, J., 1979: Garnet and clinopyroxene solid solutions, and geothermometry based on Fe–Mg distribution coefficient. Geochim. Cosmochim. Acta *43*, 1021–1029.

Griffin, W. L., Carswell, D. A., Nixon, P. H., 1979: Lower crustal granulites and eclogites from Lesotho, southern Africa. Proc. 2nd Internat. Kimberlite Conference *2*, 59–86, Amer. Geophys. Union.

Hales, A. L., Sacks, I. S., 1959: Evidence for an intermediate layer from crustal seismic studies in the East Transvaal. Geophys. J. Roy. Astr. Soc. *2*, 15–23.

Herzberg, C. T., 1979: The bearing of phase equilibria in simple and complex systems on the origin and evolution of some well documented garnet-websterites. Contr. Min. Petr. *66*, 375–382.

Jackson, P. M., Harte, B., 1977: The nature and conditions of formation of granulite facies xenoliths from the Matsoku kimberlite pipe, Lesotho. Extended Abstracts, 2nd Internat. Kimberlite Conference, Santa Fe, New Mexico.

Krogh, E. J., 1977: Evidence of Precambrian continent-continent collision in Western Norway. Nature *267*, 17–19.

Lappin, M. A., Smith, D. C., 1978: Mantle-equilibrated orthopyroxene eclogite pods from the Basal Gneisses in the Selje District, Western Norway. J. Petrol. *19*, 530–584.

Lindsley, D. H., Dixon, S. A., 1976: Diopside-enstatite equilibria at 850° to 1400°C, 5 to 35 kb. Am. J. Sci. *276*, 1285–1301.

– *Munoz, J. L.*, 1969: Subsolidus relations along the join hedenbergite-ferrosilite. Am. J. Sci. *267A*, 295–324.

MacGregor, I. D., 1974: The system $MgO-Al_2O_3-SiO_2$: Solubility of Al_2O_3 in enstatite for spinel and garnet peridotite compositions. Am. Min. *59*, 110–119.

– *Ringwood, A. E.*, 1964: The natural system enstatite-pyrope. Carnegie Inst. Washington Year Book *63*, 161–163 (1964).

Medaris, L. G., 1980: Convergent metamorphism of eclogite and garnet-bearing ultramafic rocks of Lien, Almklovdalen, West Norway. Nature *283*, 470–472.

Mori, T., Green, D. H., 1975: Pyroxenes in the system $Mg_2Si_2O_6$-$CaMgSi_2O_6$ at high pressure. Earth Planet. Sci. Lett. *26*, 277–286.

– – 1976: Subsolidus equilibria between pyroxenes in the $CaO-MgO-SiO_2$ system at high pressures and temperatures. Am. Min. *61*, 616–625.

– – 1978: Laboratory duplication of phase equilibria observed in natural garnet lherzolites. J. Geol. *86*, 83–97.

Mysen, B., Heier, K. S., 1972: Petrogenesis of eclogites in high grade metamorphic gneisses, exemplified by the Hareidland eclogite, Western Norway. Contr. Min. Petr. *36*, 73–94.

Nehru, C. E., Wyllie, P. J., 1974: Electron-microprobe measurement of pyroxenes coexisting with H_2O undersaturated liquid in the join $CaMgSi_2O_6-Mg_2Si_2O_6-H_2O$ at 30 kilobars with application to geothermometry. Contr. Min. Petr. *49*, 221–228.

Neumann, E. R., 1976: Two refinements for the calculation of structural formulae for pyroxenes and amphiboles. Norsk Geol. Tidsskr. *56*, 1–6.

O'Hara, M. J., Yarwood, G., 1978: High pressure-temperature point on an Archaean geotherm, implied magma genesis by crustal anatexis and consequences for garnet-pyroxene thermometry and barometry. Phil. Trans. R. Soc. Lond. A *288*, 441–456.

Powell, R., 1978: The thermodynamics of pyroxene geotherms. Phil. Trans. R. Soc. Lond. A *288*, 457–469.

Råheim, A., Green, D. H., 1974: Experimental determination of the temperature and pressure dependence of the Fe–Mg partition coefficient for co-existing garnet and clinopyroxene. Contr. Min. Petr. *48*, 179–203.

– – 1975: *P, T* paths for natural eclogites during metamorphism – a record of subduction. Lithos *8*, 317–328.

Rogers, N. W., 1977: Granulite xenoliths from Lesotho kimberlites and the composition of the lower continental crust. Nature *270*, 681–684.

– *Nixon, P. H.*, 1975: Geochemistry of lower crustal granulite xenoliths from Lesotho kimberlites. Ann. Report Res. Inst. of African Geol., Univ. of Leeds *19*, 38–41.

Ross, M., Huebner, J. S., Dowty, E., 1973: Delineation of the one atmosphere augite-pigeonite miscibility gap for pyroxenes from Lunar basalt. Am. Min. *58*, 619–635.

Savage, D., Sills, J. D., 1980: High pressure metamorphism in the Scourian of NW Scotland: Evidence from garnet granulites. Contr. Min. Petr. *74*, 153–163.

Saxena, S. K., 1979: Garnet-clinopyroxene geothermometer. Contr. Min. Petr. *70*, 229–235.

Wells, P. R. A., 1977: Pyroxene thermometry in simple and complex systems. Contr. Min. Petr. *62*, 129–139.

Wood, B. J., 1974: Solubility of alumina in orthopyroxene coexisting with garnet. Contr. Min. Petr. *46*, 1–5.

– 1976: The partitioning of iron and magnesium between garnet and clinopyroxene. Carnegie Inst. Washington Year Book *75*, 571–574.

– *Banno, S.*, 1973: Garnet-orthopyroxene and orthopyroxene-clinopyroxene relationships in simple and complex systems. Contr. Min. Petr. *42*, 109–124.

Authors' addresses: Dr. *D. A. Carswell*, Department of Geology, University of Sheffield, Mappin Street, Sheffield S1 3JD, U.K.; Dr. *W. L. Griffin*, Mineralogisk-Geologisk Museum, Sarsgate 1, N-Oslo 5, Norway.

Herausgeber, Eigentümer und Verleger: Springer-Verlag, Mölkerbastei 5, A-1011 Wien. — Für den Textteil verantwortlich: Prof. Dr. E. F. Stumpfl, Institut für Mineralogie und Petrologie, Montan-Universität, A-8700 Leoben. — Für den Anzeigenteil verantwortlich: Mag. Bruno Schweder, Mölkerbastei 5, A-1011 Wien. — IBM-Composersatz: Springer-Verlag Wien. — Reproduktion und Offsetdruck: Adolf Holzhausens Nfg., Kandlgasse 19-21, A-1070 Wien. — Printed in Austria.

MINERALOGICAL MAGAZINE, MARCH 1981, VOL. 44, PP. 79-89

Equilibration conditions of upper-mantle eclogites: implications for kyanite-bearing and diamondiferous varieties

D. A. CARSWELL, J. B. DAWSON, AND F. G. F. GIBB

Department of Geology, University of Sheffield, Mappin Street, Sheffield S1 3JD, UK

ABSTRACT. New mineral data for kyanite-bearing eclogites supplement existing data for eclogite nodule suites from the Roberts Victor and Bellsbank kimberlite intrusions, South Africa. Calculation of equilibration temperatures using the refined K_D calibration of Ellis and Green (1979) indicates that the majority of these eclogites equilibrated over a considerably narrower range (940-1185 °C) than implied by earlier estimates which did not take account of the influence of the Ca-component of garnet on K_D. Most of the Roberts Victor diamondiferous eclogites appear to have equilibrated in the lower part of this range, whilst the equilibration temperatures for the Roberts Victor diamond-free eclogites extend to higher values than those from Bellsbank. The petrogenetic implications of the (calculated) temperature and pressure equilibration conditions for these eclogite suites are discussed with particular reference to possible upper-mantle geotherms and available data on the graphite-diamond transition boundary.

IN most of the kimberlites of southern Africa, eclogite nodules are greatly subordinate in numbers to peridotite nodules, of which garnet lherzolites are a characteristic and widely prevalent type (Mathias *et al.*, 1970; Carswell, 1980; etc.). However, the kimberlites of the Roberts Victor Mine some 40 km east of Bishof in the Orange Free State and of the Bellsbank Main and Bobbejaan fissures at Bellsbank some 50 km north of Barkly West in the Cape Province are unusual in that nodules of eclogite are much more abundant than peridotite suite nodules (Rickwood, 1969; Rickwood *et al.*, 1969). The nodule suites in the Rietfontein kimberlite further west in Cape Province (Gurney *et al.*, 1971) and in the Orapa kimberlite in Botswana (Shee and Gurney, 1979) are apparently also exceptional in this respect.

Reddish-orange garnet and green omphacitic clinopyroxene are the dominant mineral phases in the Roberts Victor and Bellsbank eclogites, but additional primary phases include kyanite, corundum, rutile, graphite and, or, diamond. Mineralogical considerations suggest that the majority of such eclogite nodules are of upper-mantle origin, as distinct from the eclogite nodules of lower crustal origin (Griffin *et al.*, 1979) observed in the Monastery Mine and North Lesothan kimberlites emplaced around the edge of the Kaapvaal craton. Certainly the earlier suggestion by Nixon *et al.* (1963) that kyanite-bearing eclogites are necessarily of crustal origin can be discounted because of the discovery of diamond in certain of these nodules (Dawson, 1968; Rickwood and Mathias, 1970; Switzer and Melson, 1969).

In this paper we present new mineral analyses for a number of kyanite-bearing eclogites from the Roberts Victor, Bellsbank Main and Bobbejaan kimberlites to supplement existing data for these localities which are mostly on the essentially bimineralic and diamond-bearing eclogite varieties. Since the outcrops of the Main and Bobbejaan fissures in the Bellsbank area are only about a kilometre apart and they apparently contain similar nodule suites, they may perhaps be linked at depth, and so for the purposes of comparison with the eclogite nodule suite in the Roberts Victor Mine kimberlite some 125 km away, we have pooled the data on the eclogites from these two dykes and refer to them simply as 'Bellsbank'.

Petrography

MacGregor and Carter (1970) recognized two groups of eclogite nodules from the Roberts Victor Mine kimberlite, primarily on the basis of textural distinctions. Their Group I eclogites were considered to show cumulate textures sometimes with a well-defined mineralogical layering, whereas Group II eclogites were said to have a tightly interlocking texture sometimes with a crude planar fabric reflecting metamorphic recrystallization of what were interpreted as high-pressure liquid precipitates. However, the textural and chemical basis for this subdivision does not appear to have found

favour with later workers (e.g. Lappin and Dawson, 1975; Harte and Gurney, 1975; Lappin, 1978). In general it seems likely that such eclogite nodules represent disrupted fragments of high-pressure magmatic precipitates whose present mineralogy and textures reflect varying responses at subsolidus temperatures to subsequent tectono-metamorphic processes.

Bellsbank Main Fissure. The two analysed kyanite eclogites from this locality (CK/3 and CK 22/7) were similar sized (2 by 2 cm) fragments from the mine concentrate piles. They contain elongate pale-blue kyanite crystals (typically 300–400 microns across) which occur both marginal to and enclosed within the pale honey-coloured garnets and fairly unaltered pale-green clinopyroxenes. However, CK 22/7 also shows striking exsolution of sub-parallel plates of garnet (150–200 microns across) and kyanite (averaging about 50 microns across) within clinopyroxene grains. Lappin (1978) has previously described a 'necklace texture' of alternate millimetre-sized garnet and kyanite crystals along clinopyroxene grain boundaries in a Roberts Victor Mine grospydite nodule which he interpreted as reflecting incoherent grain-boundary exsolution of these minerals from the high-Al clinopyroxenes. The recognition of structurally coherent lamellae of both garnet and kyanite in clinopyroxene grains in nodule CK 22/7 strongly suggests an exsolution origin for at least some of the garnet and kyanite from what must originally have been extremely aluminous clinopyroxenes in certain of these kyanite-bearing eclogite nodules. It is worth noting that O'Hara and Yoder (1967) reported an orientated intergrowth of kyanite in clinopyroxene in a kyanite eclogite from the Dodoma mine, Tanzania. Their view that this kyanite had exsolved from an originally more aluminous higher-temperature clinopyroxene was strengthened by their demonstration that on heating a sample of this eclogite to 1525 °C at 30 kb pressure, nearly all the kyanite disappeared leaving clinopyroxene and garnet as the major crystalline phases at the beginning of melting.

Bellsbank Bobbejaan Fissure. The three analysed kyanite eclogites from this nearby locality (CK 27/3, CK 27/4, and CK 27/7) were again just small fragments (maximum size 3 by 4 cm) from the mine concentrates. All three contain laths of pale-blue kyanite (up to 3 mm long in CK 27/4, but < 1 mm long in the other two samples) enclosed within and adjacent to both the pale honey-coloured garnets and pale-green clinopyroxenes. In CK 27/7 there are also large (up to 2 mm across) primary corundum grains.

Roberts Victor Mine. By contrast, the analysed sample (RV 9) from this locality was a large, 8 by 10 cm, mineralogically banded eclogite nodule in which the following contrasting layers can be recognized:

LAYER A (> 5 cm thick) contains large (up to 3 mm long) deep-blue kyanites both enclosed within, and marginal to, the pale-red garnets and greyish altered clinopyroxene.

LAYER B (about 0.5 cm thick) contains rarer small (< 0.5 mm long) kyanites enclosed in garnets and less altered yellowish-green clinopyroxenes.

LAYER C (about 1.5 cm thick) is garnet-rich and lacks kyanite but does contain a little clinopyroxene.

LAYER D (> 2 cm thick) contains more nearby equal amounts of garnet and clinopyroxene together with a high content of mid-brown mica, but no kyanite.

Brown phlogopitic mica, which is taken to be of replacement origin, is a conspicuous mineral in most eclogite nodules in kimberlites, being concentrated along the boundaries of the primary mineral grains and in fractures through the garnets.

Alteration features. Although clinopyroxene is sufficiently well preserved in sample CK 22/7 to show exsolution textures, in all analysed samples it shows at least some marginal alteration of the type seemingly characteristic of most kyanite eclogite nodules in kimberlites (Switzer and Melson, 1969; Mathias *et al.*, 1970). In the most extreme samples (CK 27/4, 27/7, and RV9 layer A), the highly altered clinopyroxenes are grey in hand specimen and dark brown, nearly opaque, in transmitted light. Only isolated relic cores of fresh clinopyroxene are retained in these instances and the semi-opaque altered portions are optically irresolvable. However, locally the altered areas are more transparent and may be seen to consist of intergrowths of secondary pyroxene, plagioclase, spinel, hornblende, mica, calcite, and patches of pale-brown, largely devitrified, glass. The alteration characteristics of the clinopyroxene are thus similar to those previously described by Switzer and Melson (1969) and Lappin (1978), and attributed by them to partial melting in response to incorporation within, and eruption of, the host kimberlite. Veins of secondary clinopyroxene and plagioclase, with amphibole, mica, and calcite as common additional phases, cut across garnet grains in some cases and testify to the mobilization of a partial melt phase commonly modified through the addition of H_2O, CO_2, and K_2O.

In three of the samples, namely CK22/3, 27/3, and 27/4, kyanite grains show clear evidence of replacement by intergrowths of acicular corundum crystals with interstitial plagioclase ranging in composition from An_{29-42} similar to that illustrated by Dawson (1980, fig. 66). This secondary replacement would appear to relate to breakdown in the stability of kyanite with the jadeite and Ca-tschermak's molecules in the clinopyroxenes—according to the following reactions:

$$NaAlSi_2O_6 + Al_2SiO_5 \rightleftharpoons Al_2O_3 + NaAlSi_3O_8$$
$$CaAl_2SiO_6 + Al_2SiO_5 \rightleftharpoons Al_2O_3 + CaAl_2Si_2O_8$$

Switzer and Melson (1969) noted the common occurrence of corundum at kyanite margins but considered that neither the garnet nor the kyanite was involved in a major way in the generation of the partial melt. However, in the nodules which we have examined it does appear that kyanite has also been commonly, though not invariably, so involved and that breakdown of the aluminous clinopyroxene–kyanite assemblage has led, by way of an intermediate partial melt, to its replacement by an assemblage of plagioclase + corundum + a much less aluminous clinopyroxene (the place of which has often been taken by hornblende and, or, mica where appreciable H_2O and, or, K_2O has been introduced).

Mineral chemistry

The constituent minerals in these kyanite eclogites were analysed by electron microprobe. In all samples, other than RV9, the analysis given is the mean of several point analyses.

Garnet analyses are given in Table I. With the obvious exception of the layered sample RV9, little variation was found in the compositions of different grains; nor is any consistent and significant zoning present. Other than for a slightly higher Na_2O content, the lamellar garnets exsolved from the clinopyroxenes in sample CK 22/7 have essentially the same composition as the larger discrete garnets. However, the garnets in kyanite-bearing eclogites have appreciably higher CaO (grossular) contents than those in associated kyanite-free eclogites (see also fig. 1), a feature which is even more apparent in the compositionally even more extreme grospydite nodules (O'Hara and Mercy, 1966; Smyth and Hatton, 1977; Lappin, 1978; Dawson, 1980).

All iron in the garnets has been assumed to be divalent in the microprobe analyses as presented. The contents of trivalent cations in the structural formulae indicate that Fe^{3+} contents are almost certainly low. This was confirmed by a 'wet' chemical determination of FeO and Fe_2O_3 in a mineral separate of garnet from RV9 which gave values of 12.90 and 1.64 wt‰ respectively. In the absence of data on the Fe_2O_3 contents of most of the garnets, the Xg, values (Ca/(Ca + Mg + Fe + Mn)) in Table I may be taken to provide a reasonable approximation of the proportion grossular end-member in these garnets. On this basis, the garnets in all the analysed kyanite-bearing samples contain less than 50 mol% grossular and these samples are hence classified as kyanite eclogites rather than grospydite (Sobolev *et al.*, 1968; Lappin, 1978).

Clinopyroxene analyses (Table II) again show major differences in composition between kyanite-bearing and kyanite-free eclogites with the former having appreciably higher Na_2O contents (see also fig. 1). Jadeite contents in the clinopyroxenes, calculated assuming zero acmite content (since $Fe^{2+}/(Fe^{2+} + Fe^{3+})$ ratios have not been determined) are extremely high in all the kyanite eclogites, ranging from 54–71 mol%, but drop to 25–32 mol% in the kyanite-free layers in sample RV9. In all cases the jadeite/Ca tschermak's molecule ratio is very high as is to be expected in high-pressure eclogite-facies clinopyroxenes (White, 1966; Kushiro, 1969).

Kyanite and *corundum* analyses (Table III) involved long counting times in order to improve the analytical accuracy for the various minor elements. These kyanites and corundums all contain low, but nevertheless significant, amounts of Fe and Cr. The most intensely blue-coloured kyanite, that in RV9, has the highest total Fe as Fe_2O_3 content. However, the Fe_2O_3 and Cr_2O_3 contents in all these analysed kyanite are small compared with the values of 0.79 and 4.80 wt%, respectively, determined by Sobolev *et al.* (1968) in an intensely blue kyanite from a chrome-rich band in a grospydite nodule from the Zagadochnaya kimberlite pipe in Yakutia. Even higher Cr_2O_3 contents (up to 12.86 wt%, equivalent to up to 18 mol% admixture of Cr_2SiO_5) have been reported by Sobolev *et al.* (1968) for kyanites intergrown with green-violet garnets from the same kimberlite. From the analyses in Table III it is apparent that the secondary corundums developed in the reaction coronas around kyanites have higher Fe_2O_3 and Cr_2O_3 contents than the primary corundums.

Equilibration conditions

The eclogite nodule suites from the Roberts Victor and Bellsbank kimberlites both show an over-all tendency (figs. 1A–B) for higher grossular contents in garnets and higher jadeite contents in coexisting clinopyroxenes in the kyanite-bearing samples. Such a trend is well illustrated by the analyses of the mineral phases in the layered eclogite, sample RV9, but curiously is not shown in the clinopyroxenes in an eclogite nodule analysed by Lappin and Dawson (1975) which contained both kyanite-free and kyanite-bearing bands (as in RV9).

TABLE I: Analyses of Garnets from Kyanite Eclogite Nodules

	RV9 LAYER A	RV9 LAYER B	RV9 LAYER C*	RV9 LAYER D*	CK22/3	CK22/7	CK27/3	CK27/4	CK27/7
SiO_2	39.23	40.6	40.8	40.8	40.1	39.6	40.0	39.8	40.1
TiO_2	0.43	0.33	0.35	0.32	0.11	0.16	0.13	0.12	0.13
Al_2O_3	22.2	22.5	22.1	22.1	23.0	22.9	23.1	23.0	23.2
Cr_2O_3	0.04	0.03	0.11	0.11	0.06	0.06	0.02	0.05	0.01
*FeO	14.9	15.5	16.9	17.9	9.59	10.2	11.0	10.6	10.2
MnO	0.39	0.44	0.64	0.68	0.15	0.15	0.14	0.13	0.12
MgO	7.30	10.8	13.6	13.9	11.9	9.84	12.0	11.8	12.5
CaO	15.6	10.6	5.80	5.07	15.7	17.3	14.2	14.4	13.9
Na_2O	0.14	0.12	0.13	0.08	0.03	0.09	0.02	0.02	0.02
TOTAL	100.2	100.9	100.4	100.9	100.6	100.3	100.6	99.9	100.2
Structural Formulae on the Basis of 12 Oxygens									
Si	2.963	3.000	3.009	3.002	2.938	2.935	2.932	2.939	2.940
Ti	0.024	0.018	0.019	0.018	0.006	0.009	0.007	0.007	0.007
Al	1.973	1.958	1.921	1.915	1.985	2.001	1.998	2.002	2.004
Cr	0.002	0.002	0.006	0.006	0.004	0.004	0.001	0.003	0.004
Fe	0.942	0.956	1.044	1.103	0.587	0.631	0.676	0.655	0.625
Mn	0.025	0.028	0.040	0.042	0.009	0.009	0.009	0.008	0.008
Mg	0.822	1.195	1.499	1.527	1.297	1.086	1.317	1.297	1.371
Ca	1.261	0.836	0.458	0.400	1.234	1.372	1.120	1.140	1.095
Na	0.020	0.017	0.019	0.011	0.004	0.013	0.003	0.003	0.003
TOTAL	8.033	8.010	8.015	8.024	8.064	8.060	8.063	8.054	8.059
x_{Ca}^{gt}	0.413	0.277	0.151	0.130	0.395	0.443	0.359	0.368	0.353

* Total Fe as FeO $x_{Ca}^{gt} = Ca/(Ca + Mg + Fe + Mn)$

* Layers C and D in Nodule RV9 are Kyanite Free

TABLE II: Analyses of Clinopyroxenes from Kyanite Eclogite Nodules

	RV9 LAYER A	RV9 LAYER B	RV9 LAYER C*	RV9 LAYER D*	CK22/3	CK22/7	CK27/3	CK27/4	CK27/7
SiO_2	56.8	57.2	56.3	55.4	56.0	55.7	56.8	55.7	55.4
TiO_2	0.33	0.28	0.35	0.30	0.12	0.15	0.18	0.16	0.18
Al_2O_3	18.8	19.4	7.55	5.65	15.6	17.4	16.7	15.9	17.0
Cr_2O_3	0.02	0.04	0.14	0.16	0.09	0.06	0.07	0.05	0.04
*FeO	2.10	1.96	5.45	6.11	1.19	1.04	1.10	1.40	0.99
MnO	0.03	0.01	0.09	0.14	0.01	0.01	0.02	0.01	0.01
MgO	4.68	4.26	11.2	12.4	7.54	6.54	6.72	7.20	6.72
CaO	8.45	7.10	14.4	15.6	11.7	10.8	10.4	11.2	10.7
Na_2O	9.26	10.2	5.10	4.09	8.39	8.88	9.01	8.60	8.71
TOTAL	100.5	100.5	100.6	99.8	100.6	100.6	101.0	100.2	99.7
Structural Formulae on the Basis of 6 Oxygens									
Si	1.955	1.966	2.005	2.005	1.944	1.930	1.955	1.943	1.933
$Al^{[4]}$	0.045	0.034	0.000	0.000	0.056	0.070	0.045	0.057	0.067
$Al^{[6]}$	0.721	0.750	0.317	0.241	0.584	0.640	0.633	0.596	0.632
Ti	0.009	0.007	0.009	0.008	0.003	0.004	0.005	0.004	0.005
Cr	0.001	0.001	0.004	0.005	0.002	0.002	0.002	0.002	0.001
Fe	0.060	0.056	0.162	0.185	0.035	0.030	0.032	0.041	0.029
Mn	0.001	0.000	0.003	0.004	0.000	0.000	0.001	0.000	0.000
Mg	0.240	0.218	0.596	0.667	0.390	0.338	0.345	0.374	0.350
Ca	0.311	0.261	0.552	0.604	0.434	0.400	0.384	0.418	0.401
Na	0.619	0.683	0.352	0.287	0.565	0.597	0.601	0.582	0.590
TOTAL	3.962	3.976	4.000	4.006	4.013	4.011	4.003	4.017	4.008

* Total Fe as FeO * Layers C and D in RV9 are Kyanite Free

TABLE III: Analyses of Kyanites and Corundums from Kyanite Eclogite Nodules

	KYANITES						CORUNDUMS — PRIMARY	CORUNDUMS — SECONDARY
	RV9	CK22/3	CK22/7	CK27/3	CK27/4	CK27/7	CK27/7	CK27/4
SiO_2	36.8	36.7	36.6	37.0	36.6	36.7	0.01	0.00
TiO_2	0.11	0.02	0.02	0.03	0.03	0.02	0.01	0.03
Al_2O_3	63.1	62.8	62.3	63.7	62.3	62.3	99.8	99.7
Cr_2O_3	0.04	0.13	0.07	0.05	0.08	0.07	0.06	0.13
$*Fe_2O_3$	0.26	0.18	0.13	0.13	0.22	0.13	0.16	0.46
MnO	0.01	0.00	0.00	0.00	0.00	0.00	0.01	0.00
MgO	0.07	0.02	0.01	0.01	0.02	0.01	0.03	0.00
CaO	0.00	0.01	0.00	0.01	0.00	0.00	0.00	0.00
TOTAL	100.4	99.9	99.1	100.9	99.3	99.2	100.1	100.3

* All Fe expressed as Fe_2O_3

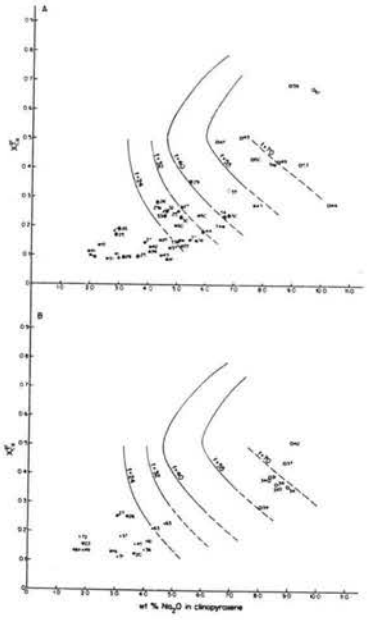

FIG. 1. Plot showing the relationship between the Ca (grossular) content of garnet and Na_2O content of coexisting clinopyroxene in the various eclogite nodule types from A. Roberts Victor Mine, B. Bellsbank Main and Bobbejaan fissures.

Closed ornaments—kyanite free; open ornaments—kyanite-bearing. Diamond ornament signifies diamond bearing. Arrows indicate zoning trends. For comparative purposes the compositions of the coexisting phases in lower crustal eclogites from the Monastery Mine and Northern Lesotho kimberlites (Griffin *et al.*, 1979) are shown by crosses on diagram B.

The numerals adjacent to all points are the 'f' numbers (100 Fe/(Fe+Mg) in garnet) which should be compared with the 'f' lines which are from Sobolev *et al.* (1968, fig. 12).

Sobolev *et al.* (1968) noted, for the kyanite eclogite–grospydite nodule suite from the Zagadochnaya pipe, that in different nodules clinopyroxenes with different Na_2O contents coexist with garnets with essentially the same grossular content. They attributed this to the effect of increased Fe/(Fe+Mg) ratios in the case of those samples with the most sodic clinopyroxenes. Whilst fig. 1A and B show that there is a definite tendency for more grossular-rich garnets to coexist with more sodic clinopyroxenes in the more ferriferous assemblages, as monitored by the Fe/(Fe+Mg) ratio in the garnet, the mineral composition relationships in the Roberts Victor and Bellsbank eclogites neither correspond to, nor are as simple as, those illustrated by Sobolev *et al.* (1968, fig. 12). The lack of correspondence may well largely reflect higher equilibration pressures for these eclogite suites since they contain associated diamond-bearing samples, suggesting pressures of the order of 40–50 kb compared with 20–30 kb estimated by Sobolev *et al.* (1968) for the Zagodochnaya nodules. It seems likely that the compositions of the coexisting garnets and clinopyroxenes in eclogites are controlled by the interplay of several factors, the most important of which are probably the Fe/(Fe+Mg), Na/(Na+Ca) and Al/(Al+Si) ratios in the rock and the pressure (and to a lesser extent the temperature) of equilibration. For example, the eclogite nodules in the Monastery Mine and Northern Lesotho kimberlites, interpreted as being of lower crustal derivation (Griffin *et al.*, 1979), contain low-grossular garnets, and clinopyroxenes with comparatively low-jadeite contents (fig. 1B) despite the highly ferriferous nature of many of these nodules—doubtless reflecting their much lower pressure–temperature equilibration conditions.

It is well known that Fe^{2+}–Mg^{2+} partitioning between coexisting garnets and clinopyroxenes is strongly temperature dependent and hence provides a potentially valuable mineralogical thermometer applicable to eclogites (Banno, 1970; Råheim and Green, 1975). However, Råheim and Green (1974) in their experimental calibration of $K_D = \frac{(FeO/MgO)_{gnt}}{(FeO/MgO)_{cpx}}$ indicated that K_D is significantly dependent on pressure as well as temperature.

K_D values, calculated assuming all Fe as Fe^{2+} in both minerals, are listed in Table IV both for the newly analysed kyanite eclogites and previously analysed associated eclogites from the Roberts Victor, Bellsbank Main and Bobbejaan localities (data from references listed in Table IV). The observed variations in K_D values (2.13–5.74 for Roberts Victor Mine eclogites and 3.35–6.84 for Bellsbank area eclogites in Table IV) have led some authors (MacGregor and Carter, 1970; Reid *et al.*, 1976) to previously suggest that such eclogites have equilibrated over a wide range of temperatures and hence were probably derived from a considerable depth range in the upper mantle.

As diamondiferous eclogites have been reported from each of these localities at least some of the eclogite nodules in these particular kimberlites must have equilibrated within the diamond

TABLE IV A: Eclogite Nodules from Roberts Victor Mine

Sample Number	X^{gt}_{Ca}	K_D^*	T°C at 47 Kb Råheim & Green (1974)	T°C at 47 Kb Ellis & Green (1979)	Reference	Special Features
RV9/A	0.413	4.55	1032	1138	1	Kyanite
RV9/B	0.277	3.10	1177	1177	1	Kyanite
RV9/C	0.151	2.56	1262	1137	1	Garnet Rich
RV9/D	0.130	2.61	1253	1105	1	-
1175	0.203	3.74	1102	1021	2	-
1178	0.154	2.56	1261	1135	2	-
1185	0.136	2.90	1205	1061	2	-
1187	0.087	2.19	1339	1145	2	-
1188	0.264	4.92	1006	974	2	Primary ? Amphibole
1190	0.267	3.42	1137	1122	2	-
1191	0.236	2.91	1204	1164	2	-
1692	0.154	2.68	1241	1118	2	-
1698	0.100	3.06	1182	1002	2	-
SRV1	0.502	5.42	976	1146	3	Kyanite + Coesite Grospydite
111060	0.324	4.58	1030	1054	4	Kyanite + Diamond
110752	0.489	5.74	958	1113	4	Kyanite
RV15	0.422	4.66	1024	1136	5	Kyanite
8534/1	0.685	4.55	1032	1385	6	Kyanite Grospydite
8534/2	0.671	4.41	1043	1388	6	Kyanite Grospydite
6913/1	0.274	3.76	1100	1087	7	-
6913/2	0.431	4.80	1014	1132	7	Kyanite
6914	0.414	3.46	1133	1262	7	Graphite
R1	0.231	3.97	1080	1024	8	Diamond
R2	0.098	2.65	1246	1063	8	Diamond
R3	0.282	4.55	1032	1019	8	Diamond
R4	0.183	3.30	1152	1054	8	Diamond
R5	0.094	2.70	1238	1051	8	Diamond
R6	0.355	3.97	1080	1141	8	Diamond
R7	0.231	3.53	1124	1072	8	Diamond
R8	0.237	3.54	1124	1077	8	Diamond
R9	0.267	3.72	1104	1085	8	Diamond
KA1	0.202	2.87	1210	1136	9	-
KA2	0.147	2.42	1290	1162	9	-
KA3	0.128	2.50	1273	1124	9	-
KA4	0.102	2.29	1315	1138	9	-
KA5	0.094	2.14	1350	1165	9	-
KA6	0.087	2.13	1353	1159	9	-
11063	0.153	2.41	1291	1170	10	-
11062	0.146	2.50	1273	1143	10	-
11060	0.135	2.53	1267	1125	10	-
11061	0.114	2.44	1285	1120	10	-
11064	0.115	2.30	1314	1152	10	-
HRV247-BAC	0.191	3.67	1109	1017	11	Diamond + Graphite
HRV247-BAE	0.175	3.61	1115	1007	11	Diamond + Graphite
HRV247-FC	0.254	4.10	1069	1034	11	Diamond + Graphite
HRV247-FE	0.239	4.13	1066	1016	11	Diamond + Graphite

TABLE IV B : Eclogite Nodules from the Bellsbank Main and Bobbejaan Fissures

Sample Number	X^{gt}_{Ca}	K_D^*	T°C at 47 Kb Råheim & Green (1974)	T°C at 47 Kb Ellis & Green (1979)	Reference	Special Features
CK27/3	0.359	5.59	966	1011	1	Kyanite
CK27/4	0.368	4.63	1026	1090	1	Kyanite
CK27/7	0.353	5.51	970	1011	1	Kyanite + Corundum
1829/1	0.156	3.68	1108	982	2	-
1829/2	0.126	5.54	968	814	2	-
2029/1	0.511	6.84	907	1067	2	Kyanite + Corundum
2029/3	0.381	5.70	960	1024	2	Kyanite + Corundum
2031/1	0.290	4.31	1051	1047	2	-
2031/2	0.253	4.42	1042	1003	2	-
2031/3	0.253	6.12	939	891	2	-
2032/2	0.132	3.35	1145	997	2	-
CK22/3	0.394	5.11	994	1075	1	Kyanite
CK22/7	0.443	6.51	921	1028	1	Kyanite

* All Fe as Fe^{2+} in K_D Calculation

References:
1. This paper
2. Bishop et al. 1978
3. Smyth & Hatton 1977
4. Switzer & Nelson 1969/Sobolev 1977
5. Sobolev 1974
6. Lappin 1978
7. Lappin & Dawson 1975
8. Reid et al. 1976
9. Kushiro & Aoki 1968
10. O'Hara et al. 1975
11. Hatton & Gurney 1979

stability field. Graphite, rather than diamond, has been observed in a few of the eclogites (e.g. 6914 of Lappin and Dawson, 1975), whilst Hatton and Gurney (1979) have described an eclogite nodule (HRV 247) from Roberts Victor Mine which contains numerous grains of diamond and graphite, both considered to be primary constituents. Possible upper-mantle geotherms defined by preferred pressure and temperature estimates for garnet lherzolite nodules in kimberlites from southern Africa (Carswell and Gibb, 1980; and fig. IV) intersect the various theoretically and experimentally determined diamond $\rightleftharpoons$ graphite equilibrium curves in the 39–51 kb range. In the absence of any method by which we could obtain a precise fix on the equilibration pressure for particular eclogite nodules from mineralogical considerations alone we assumed a pressure 47 kb in order to calculate an equilibration temperature for each eclogite nodule from the K_D value. Using the equation given by Råheim and Green (1974) temperatures ranging from 958 to 1353 °C for the Roberts Victor mine and from 907 to 1145 °C for the Bellsbank eclogite suites were obtained (Table IV). Assuming any other constant pressure would likewise yield large temperature ranges for these suites, thus precluding the possibility that all nodules were derived from a relatively narrow range of depths in the upper mantle.

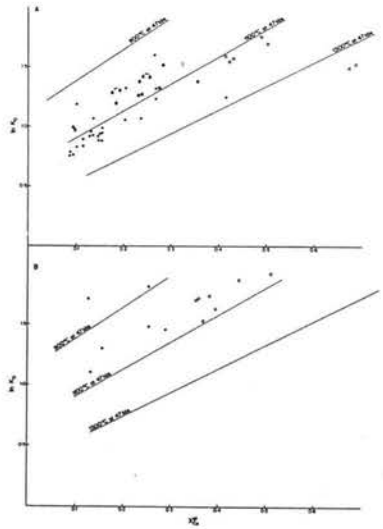

FIG. 2. Plot showing the relationship between $ln\ K_D$ and the mole fraction of Ca in the garnet for the various eclogite nodule types from A. Roberts Victor Mine, B. Bellsbank Main and Bobbejaan fissures.

Sample ornaments as in fig. 1.

The solid lines on these diagrams show the predicted variation in $ln\ K_D$ with X^{gt}_{Ca} at particular PT values as calculated from equation (9) of Ellis and Green (1979).

However, it is apparent from Table IV that the K_D values in kyanite eclogite and grospydite nodules are generally higher than in the kyanite-free essentially bimineralic eclogites, suggesting that there may be a significant compositional influence on K_D. This is born out by plots (fig. 2A and B) of $ln\ K_D$ *v.* X^{gt}_{Ca} for these eclogite nodule suites which demonstrate that K_D values are considerably higher in those eclogites with the more calcic garnets. Moreover, Ellis and Green (1979) have recently demonstrated experimentally that a combination of non-ideal Ca–Mg substitutions in coexisting garnets and clinopyroxenes results in composition changes which profoundly influence the Fe^{2+}–Mg^{2+} partition coefficient values; and that the net effect of these compositional changes on K_D is conveniently monitored by X^{gt}_{Ca}. Equilibration temperature estimates for the individual eclogite nodules calculated by this same equation, again at an assumed pressure of 47 kb, are listed in Table IV. These values indicate that when allowance is made for the observed compositional influence on K_D then the temperature estimates for the majority of eclogite nodules from both the Roberts Victor Mine and Bellsbank area localities are much more tightly grouped, pointing to derivation from a more restricted source region in the upper mantle than indicated by the values calculated from the Råheim and Green (1974) equation. For example, the Ellis and Green (1979) equation yields equilibration temperatures which cluster around 1100 °C at an assumed 47 kb pressure for most of the eclogite nodules from Roberts Victor Mine (fig. 2A). Although there is an overlap in the ranges of equilibration temperatures for the diamond-bearing and diamond-free eclogites from this locality, there are nevertheless differences in the mean equilibration temperature estimates for these two groups (1051 and 1126 °C, respectively) which may be significant. Nevertheless, there is the possibility that the difference may be solely due to the presence or absence of free carbon.

We consider that the particularly high calculated temperatures for the two layers in the grospydite nodule 8534 of Lappin (1978) may be erroneous and hence have not included them in the calculated mean temperature value for the diamond-free nodules from Roberts Victor Mine. We suspect

that these anomalously high temperature values are attributable to either non-equilibration between the garnets and clinopyroxenes in this sample which shows textural evidence of exsolution of kyanites and garnets from pyroxene, or the fact that the minerals in this particularly ferriferous nodule contain appreciable Fe^{3+} not taken into account in the calculation of the K_D values.

Although the assumption which we have made in all cases of all Fe as Fe^{2+} in both garnets and clinopyroxenes is unlikely to be strictly correct, $Fe^{3+}/(Fe^{2+}+Fe^{3+})$ ratios in upper-mantle minerals are likely to be very low (c.f. Burns *et al.*, 1972), particularly in diamond- or graphite-bearing assemblages. Also, since the oxidation state of the upper mantle is unlikely to vary greatly, at least the temperature estimates based on K_D values with all Fe as Fe^{2+} should be valid on a relative basis for the eclogite nodule suites. We have tried calculating $Fe^{3+}/(Fe^{2+}+Fe^{3+})$ ratios for the minerals on the basis of charge balance in the structural formulae (Neumann, 1976) but it is clear that the errors inherent in this procedure are too large, especially for the clinopyroxenes with low total Fe. In the absence of analytically determined $Fe^{3+}/(Fe^{2+}+Fe^{3+})$ ratios in the minerals for the majority of these eclogite nodules, it is therefore necessary to base any discussion of the relative equilibration temperatures of these nodules on K_D values which assume all Fe as Fe^{2+}, but it should be borne in mind that in absolute terms such temperature estimates are likely to be maxima. Certainly K_D values which include only analytically determined Fe^{2+} contents are much higher in the six Roberts Victor Mine eclogite samples for which Kushiro and Aoki (1968) analysed bulk mineral separates and consequently yield Ellis and Green (1979) temperature estimates which are on average some 178 °C lower. On the other hand, the analytically determined $Fe^{3+}/(Fe^{2+}+Fe^{3+})$ ratios in certain other eclogites (Switzer and Melson, 1969; Sobolev, 1977; O'Hara *et al.*, 1975) do not indicate such consistent substantial overestimation of equilibration temperatures when all Fe is taken as Fe^{2+} in the calculation of K_D values.

The variation in the equilibration temperature estimates obtained for different portions of layered eclogite nodules (e.g. 72 °C in the case of RV9) suggests that additional composition influences and, or, analytical errors may account for at least some of the over-all variation in the values obtained for the various eclogite nodules. Exsolution textures (c.f. Lappin, 1978; Harte and Gurney, 1975) clearly demonstrate that at least some, and possibly all, of the eclogites originally crystallized at substantially higher temperatures, most likely as crystal cumulates from trapped upper-mantle partial melts. It would appear that at solidus temperatures at least some of the present garnet and kyanite in the kyanite eclogites was occluded in even more aluminous pyroxenes.

As suggested previously, with reference to eclogite nodule 8534 of Lappin (1978), some of the variation in the temperature estimates for the different eclogite nodules may reflect failure of the mineral assemblages in certain nodules to fully re-equilibrate subsequent to their initial igneous crystallization.

We are tempted to conclude that the unusually high proportion of eclogite nodules in the Roberts Victor and Bellsbank kimberlites reflects the fact that each kimberlite during its ascent happened to intersect substantial layered complexes of such cumulates (varying from essentially bimineralic eclogites to grospydites) close to the site of initiation of their rapid eruption through an otherwise peridotitic upper mantle. However, there is no *a priori* justification for our initial assumption that all these eclogite nodules have come from essentially the same depth and hence have all equilibrated at much the same pressure, and indeed the fact that certain nodules contain diamond and others graphite strongly suggests that this is unlikely.

Implications for geothermal gradients

From their K_D values, we can represent the equilibration conditions for individual nodules by a line in *P* (pressure)-*T* (temperature) space. On the assumption that each nodule equilibrated at the ambient conditions of its site of derivation, it is possible to uniquely fix the *PT* equilibration conditions for each nodule on the basis of the intersection of the *PT* line with the likely upper-mantle geotherm. The latter may be predicted either from geophysical considerations (e.g. Clark and Ringwood, 1964) or from consideration of other nodule types (especially garnet lherzolites) found in kimberlites which enable determination of unique *PT* estimates (e.g. Boyd, 1973). Unfortunately such nodule types are rare in the particular kimberlites under consideration and currently no analyses are available. We have therefore deduced the likely geotherm in the upper mantle beneath these kimberlites from analyses of peridotite nodules in adjacent kimberlite diatremes.

In fig. 3A and B we present two possible alternative upper-mantle geotherms based on 'preferred' (Carswell and Gibb, 1980) *PT* estimates for garnet lherzolite and pyroxenite nodules from the Frank Smith Mine (data from Boyd, 1974) and for garnet lherzolite nodules from the Kimberley Mines (data from Boyd and Nixon, 1978, and Bishop *et al.*, 1978). The inflected geotherm in fig. 3B has the form of the 'Pyroxene Geotherm' favoured by Boyd (1973, 1974) although it is somewhat displaced in absolute terms with the lower-temperature limb essentially coincident with the 'Shield Geotherm' of Clark and Ringwood (1964).

In fig. 4A and B we show the deduced *PT* estimates for individual eclogite nodules based on the intersection of the K_D-determined *PT* lines with the two possible geotherms. [Note that the different bar symbols across the geotherms do not signify a *PT* range but are used simply as a means of distinguishing between different groups of eclogite nodules. The only points of relevance in *PT* terms

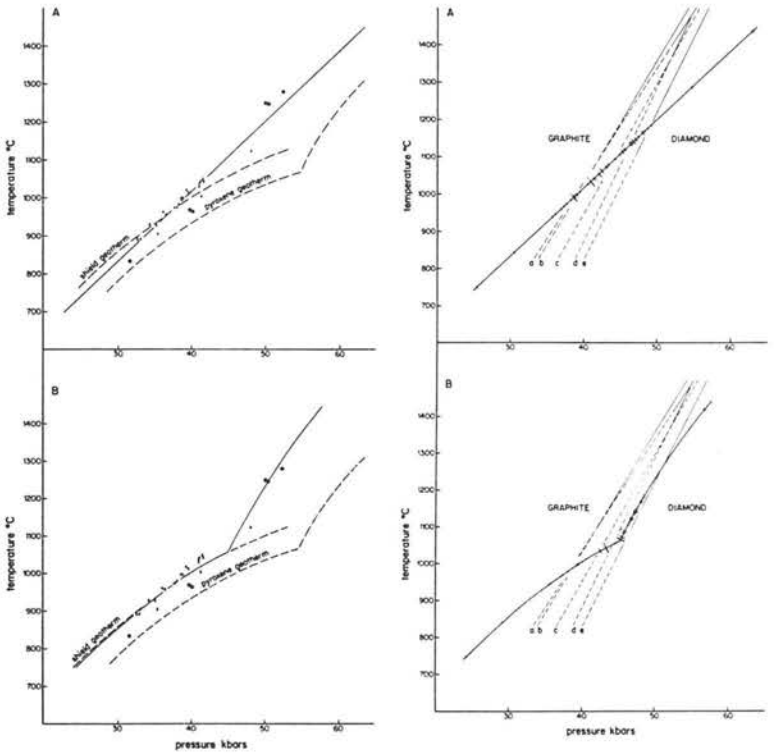

FIGS. 3 and 4. FIG. 3 (*left*). Diagrams showing alternative linear (A) and inflected (B) Late Cretaceous palaeogeotherms for the upper mantle beneath this part of South Africa based on *PT* estimates for garnet lherzolite nodules from the Kimberley Mines kimberlites (crosses) and garnet lherzolite-pyroxenite nodules from the Frank Smith Mine (closed circles). Also shown are the 'Pyroxene' geotherm for Northern Lesotho from Boyd (1973) and the 'Shield' geotherm of Clark and Ringwood (1964). FIG. 4 (*right*). Diagrams showing the *PT* estimates for the eclogite nodules as deduced from the intersection of *PT* lines based on K_D values with the alternative linear (A) and inflected (B) Late Cretaceous palaeogeotherms indicated in fig. 3. The bar symbols in order of decreasing lengths signify Roberts Victor diamond-bearing eclogites; Roberts Victor diamond-free eclogites; and Bellsbank area eclogites; respectively. The various diamond-graphite equilibrium boundaries are from (a) Strong and Chrenko (1971); (b) Bundy *et al.* (1961); (c) Berman (1979); (d) Strong and Hanneman (1967); and (e) Kennedy and Kennedy (1976).

are the intersections of the bars with the geotherms.] Projecting the *PT* line for individual nodules on to the geotherms extends the implied ranges of equilibration temperatures for the suites of nodules compared to those obtained assuming a single pressure value.

As discussed above, the two highest *PT* points (for the two layers in nodule 8534) are most likely erroneous, as probably also is the next highest point which is for the graphite-bearing eclogite 6914 of Lappin and Dawson (1975). On the other hand, the two lowest *PT* estimates which are for the bimineralic eclogites 2031/3 and 1829/2 from Bellsbank–Bobbejaan fissure, may well genuinely reflect substantially higher levels of derivation for these two nodules. Although these particular nodules are not especially ferriferous, it is tempting to equate them with the suite of eclogite nodules of postulated lower crustal origin (Griffin *et al.*, 1979) observed in certain other kimberlites in southern Africa. Preferred *PT* estimates for garnet granulite and garnet websterite nodules associated with the latter group of eclogites, and likewise taken to have been derived from the lower crust, are 654 ± 34 °C and 10.8 ± 3.1 kb (Carswell and Griffin, in prep.). Assuming a comparable equilibration pressure of 10 kb, lowers the equilibration temperature estimates for these two Bobbejaan eclogites even further (to 753 and 703 °C, respectively). Making due allowance for possible further lowering of these temperature estimates if K_D values had been based on analytically determined Fe^{2+} values rather than taking all Fe as Fe^{2+}, it certainly seems conceivable that these two particular eclogites have been derived from the lower crust.

The equilibration temperature estimates for the rest of the eclogite nodules on the geotherms in fig. 4A and B all lie between 940 and 1185 °C and, if correct, point to derivation of these eclogites from depths between 110 and 150 km, although only down to about 135 km in the case of the analysed Bellsbank area eclogite nodule suite. Unfortunately no analyses are available for diamond-bearing eclogites from the Bellsbank localities, but there does appear to be an unexpected, but none the less significant, tendency for the diamond-bearing eclogites from Roberts Victor Mine to have equilibrated at somewhat lower *PT* values, and hence to have come from somewhat shallower depths, than the majority (though not all) of the associated diamond-free eclogites.

Diamondiferous eclogites

It is important to assess the validity of above *PT* estimates in the light of both theoretical predictions and direct experimental evidence on the pressure-temperature conditions for the diamond ⇌ graphite equilibrium boundary, for which five alternative positions are indicated in fig. 4. Boundary (e) represents the most recent experimental determination of Kennedy and Kennedy (1976) which they state to be almost coincident with the earlier and previously much quoted boundary of Bundy *et al.* (1961). However, we have replotted, as boundary (b), the experimentally determined boundary of Bundy *et al.* (1961) and find that it lies at substantially lower pressures than that of Kennedy and Kennedy (1976). Bundy *et al.* (1961) in fact indicated a *PT* band between the diamond and graphite stability fields on the basis of several different experiments. The boundary (b) which we have drawn represents a mean position drawn along this band, such that the error brackets on this boundary in pressure terms are roughly ±1.2 kb. Also shown in fig. 4 are boundaries (a) and (d) based on gross linear extrapolations of two different pairs of high-temperature equilibration points, experimentally determined by Strong and Chrenko (1971) and Strong and Hanneman (1967), respectively; and boundary (c) which is the thermodynamically calculated boundary of Berman (1979). These various boundaries thus indicate that the degree of uncertainty over the precise location of the diamond ⇌ graphite equilibrium boundary amounts to some 5 kb in pressure terms at the likely equilibration temperatures of these eclogite nodules.

From fig. 4 it is immediately apparent that on the basis of the diamond ⇌ graphite boundary of Kennedy and Kennedy (1976), the *PT* estimates for all the diamond-bearing eclogites fall outside the diamond stability field, regardless of which geotherm is assumed. This could be interpreted as indicating inaccuracies in the methods used either in determining these *PT* estimates or in delimiting the geotherms. However, if the alternative diamond ⇌ graphite boundaries of Bundy *et al.* (1961) and Strong and Chrenko (1971) are taken to be correct, then the *PT* estimates for all the diamond-bearing eclogites lie essentially within the diamond stability field. It may be fortuitous but it is none the less encouraging to note that the diamond-bearing eclogite which plots with lowest *PT* equilibration values on the geotherms (essentially at the intersection of the geotherms with the Bundy *et al.* (1961) and Strong and Chrenko (1971) diamond ⇌ graphite equilibrium boundaries) is nodule HRV 247 of Hatton and Gurney (1979) reported to contain coexisting primary diamond and graphite.

Acknowledgements. D. A. Carswell and J. B. Dawson thank the organizers and guides of the 1973 excursions to the South African kimberlites, and wish to acknowledge financial support from the Royal Society and the Natural Environmental Research Council.

REFERENCES

Banno, S. (1970). *Phys. Earth Planet. Inter.* **3**, 405–21.
Berman, R. (1979). In Field (J. E.) (ed.). *The properties of diamond*, Academic Press, London, 1–22.
Bishop, F. C., Smith, J. V., and Dawson, J. B. (1978). *Lithos*, **11**, 155–73.
Boyd, F. R. (1973). *Geochim. Cosmochim. Acta*, **37**, 2533–46.
——(1974). *Carnegie Inst. Wash. Yearb.* **73**, 285–94.
—— and Nixon, P. H. (1978). *Geochim. Cosmochim. Acta*, **42**, 1367–82.
Bundy, F. P., Bovenkerk, H. P., Strong, H. M., and Wentorf, R. H., Jr. (1961). *J. Chem. Phys.* **35**, 383–91.
Burns, R. G., Huggins, F., and Drickamer, H. G. (1972). *Proc. 24th Int. Geol. Cong. Scot.* **14**, 113–23.
Carswell, D. A. (1980). *Lithos*, **13**, 121–38.
—— and Gibb, F. G. F. (1980). *Contrib. Mineral. Petrol.* **74**, 403–16.
Clark, S. P., Jr., and Ringwood, A. E. (1964). *Rev. Geophys.* **2**, 35–88.
Dawson, J. B. (1968). *Econ. Geol.* **63**, 504–11.
——(1980). In *Kimberlites and their xenoliths*, Springer Verlag, Heidelberg.
Ellis, D. J., and Green, D. H. (1979). *Contrib. Mineral. Petrol.* **71**, 13–22.
Griffin, W. L., Carswell, D. A., and Nixon, P. H. (1979). *Proc. Second Intern. Kimberlite Conf.* **2**, 59–86.
Gurney, J. J., Mathias, M., Siebert, C., and Moseley, G. (1971). *Contrib. Mineral. Petrol.* **30**, 46–52.
Harte, B., and Gurney, J. J. (1975). *Phys. Chem. Earth*, **9**, 367–87.
Hatton, C. J., and Gurney, J. J. (1979). *Proc. Second Intern. Kimberlite Conf.* **2**, 29–36.
Kennedy, S. C., and Kennedy, G. C. (1976). *J. Geophys. Res.* **81**, 2467–70.
Kushiro, I. (1969). *Mineral. Soc. Am. Spec. Pap.* **2**, 179–91.
—— and Aoki, K.-I. (1968). *Am. Mineral.* **53**, 1347–67.
Lappin, M. A. (1978). *Contrib. Mineral. Petrol.* **66**, 229–41.
—— and Dawson, J. B. (1975). *Phys. Chem. Earth*, **9**, 351–65.
MacGregor, I. A., and Carter, J. L. (1970). *Phys. Earth Planet. Inter.* **3**, 391–7.
Mathias, M., Siebert, J. C., and Rickwood, P. C. (1970). *Contrib. Mineral. Petrol.* **26**, 75–123.
Neumann, E. R. (1976). *Norsk Geol. Tidsskr.* **56**, 1–6.
Nixon, P. H., von Knorring, O., and Rooke, J. M. (1963). *Am. Mineral.* **48**, 1090–132.
O'Hara, M. J., and Mercy, E. L. P. (1966). *Nature*, **212**, 68–9.
—— and Yoder, H. S., Jr. (1967). *Scott. J. Geol.* **3**, 67–117.
—— Saunders, M. J., and Mercy, E. L. P. (1975). *Phys. Chem. Earth*, **9**, 571–604.
Råheim, A., and Green, D. H. (1974). *Contrib. Mineral. Petrol.* **48**, 179–203.
—— ——(1975). *Lithos*, **8**, 317–28.
Reid, A. M., Brown, R. W., Dawson, J. B., Whitfield, G. G., and Siebert, J. C. (1976). *Contrib. Mineral. Petrol.* **58**, 203–20.
Rickwood, P. C. (1969). *Geol. Soc. S. Africa Spec. Pap.* **2**, 397–416.
—— and Mathias, M. (1970). *Lithos*, **3**, 223–35.
—— Gurney, J. J., and White-Cooper, D. R. (1969). *Geol. Soc. S. Africa Spec. Pap.* **2**, 371–93.
Shee, S. R., and Gurney, J. J. (1979). *Proc. Second Intern. Kimberlite Conf.* **2**, 37–49.
Sobolev, N. V. (1977). In *Deep-seated inclusions in kimberlites and the problem of the composition of the upper mantle*, Am. Geophys. Union, Washington.
—— Kuznetsova, I. K., and Zyuzin, N. I. (1968). *J. Petrol.* **9**, 253–80.
Smyth, J. R., and Hatton, C. J. (1977). *Earth Planet. Sci. Lett.* **34**, 284–90.
Strong, H. M., and Chrenko, R. M. (1971). *J. Phys. Chem.* **75**, 1838–43.
—— and Hanneman, R. E. (1967). *J. Chem. Phys.* **46**, 3668–76.
Switzer, G., and Melson, W. G. (1969). *Smithsonian Contrib. Earth Sci.* **1**, 1–9.
White, A. J. R. (1966). *Am. Mineral.* **49**, 883–8.

[*Manuscript received 11 August 1980*]

[Note: Enlarged copies of the four figures are available on request from the authors.]

Kimberlites. II: The Mantle and Crust—Mantle Relationships, by J. Kornprobst (Editor), pp. 229—243

PERIDOTITE NODULES FROM THE NGOPETSOEU AND LIPELANENG KIMBERLITES, LESOTHO: A CRUSTAL OR MANTLE ORIGIN

by D.A. CARSWELL, W.L. GRIFFIN and P. KRESTEN

Abstract - Variations in whole rock and mineral chemistries allow the recognition of four distinct groups of peridotite nodules within these kimberlite occurrences. Equilibration temperature estimates together with general geochemical considerations strongly suggest that the relatively ferriferous Group 1 (Cr-spinel wehrlites and lherzolites) and Group 2 (Al-spinel lherzolites) nodules represent basaltic cumulates of likely lower crustal origin. By contrast the more magnesian peridotites are considered to have been derived from the upper mantle with the Group 3 nodules (Cr-spinel lherzolites and harzburgites) originating from shallower levels than those of Group 4 (garnet harzburgites). These data imply the existence of a Cr-spinel peridotite zone up to 30 kms thick at the top of the mantle beneath this region, at the time of kimberlite emplacement. Nodule samples of such rocks commonly show subsolidus deformation and recrystallisation effects leading to the development of mosaic and symplectite textures. Element partition considerations indicate that such textures have developed during cooling from an earlier temperature maximum; this cooling may have accompanied slow diapiric upwelling in the uppermost mantle.

1 INTRODUCTION

In contrast to previously described nodule suites from the kimberlites of northern Lesotho, the occurrences in Lipelaneng near Butha-Buthe in north-western Lesotho (No. 99 on Fig. 54 of Nixon & Kresten, 1973) and at Ngopetsoeu near Roma in west-central Lesotho contain an unusually high proportion of spinel bearing, garnet free peridotite nodules. Studies of such nodule samples are clearly important in view of current uncertainties concerning the nature of the uppermost mantle beneath this region (see for example Nixon et al. 1973; Jackson & Harte 1977; Carswell et al. 1979) and the possible existence of a spinel peridotite ⇄ garnet peridotite transition within the upper mantle beneath such cratonic regions. Other than the brief general description provided by Nixon & Kresten (1973) published data on the Lipelaneng nodule suite are limited to that for a coronitic garnet granulite (Griffin et al. 1979) and to the abstract of data on granulite and peridotite suite nodules provided by Jackson (1979). The nodule suite from Ngopetsoeu has not previously been studied.

2 PETROGRAPHY

Petrographic details for individual analysed peridotite nodule samples are given, together with whole rock and mineral chemistry data, in a separate appendix (Volume III "Documents") but are summarised below:

2.1 Lipelaneng samples

The 7 analysed samples from here fall into two groups, readily distinguished in thin section. Samples Lip 1-4 (Group 1) are olivine rich, pyroxene poor, spinel lherzolites or wehrlites with on average around 5 vol.% of dark brown (near opaque) spinel. Rock textures in these samples are dominantly granuloblastic with largely strain-free grains. Samples 5-7 (Group 2) are more pyroxene-rich spinel lherzolites with similar modal contents of spinel. In thin sections spinel is tan coloured in Lip 5 and 7, but olive green in Lip 6. Rock textures are again dominantly granuloblastic but in Lip 6 there is conspicuous development of narrow orthopyroxene coronas around clusters of clinopyroxene sub-grains and spinels. Larger orthopyroxene grains contain abundant fine-grained rutile and less common clinopyroxene exsolution lamellae and often have turbid marginal reaction zones.

2.2 Ngopetsoeu samples

No Group 1 type nodules have been recorded in this xenolith suite. Sample PHN 2873/1 bears a close resemblance to the Group 2 nodules from Lipelaneng with its conspicuous dark olive green spinel and abundant orthopyroxene, again with fine scale rutile and clinopyroxene exsolution lamellae. However, in this sample orthopyroxene ($\sim$ 60 vol.%) is much more abundant than olivine ($\sim$ 10 vol.%) and there are approximately equal amounts ($\sim$ 12 vol.%) of clinopyroxene and a pale green amphibole which appears to be in textural equilibrium with the other mineral phases. Overall the texture is granuloblastic with an absence of any obvious reaction features.

By contrast the majority of peridotite nodule samples from Ngopetsoeu comprise a large group (Group 3) of spinel lherzolites and harzburgites with <2 vol.% each of clinopyroxene and dark orange spinel. Spinel commonly occurs as fine grained symplectitic intergrowths with orthopyroxene, and rarer clinopyroxene, in a similar fashion to the so-called 'finger print' spinels described by Dawson & Smith (1975) in peridotite nodules from kimberlites elsewhere in both Lesotho and South Africa. Overall rock textures are sometimes near equant or tabular granuloblastic but more commonly mosaic-porphyroclastic (Harte 1977).

In addition there is a much smaller group (Group 4) of garnet harzburgite nodules, comprising samples PHN 1905, 2873/3 and 2873/7, which lack clinopyroxene but contain small amounts of garnet (2-5 vol.%) which in two out of three samples coexists with trace amounts of dark red spinel.

3 WHOLE ROCK CHEMISTRY

Whole rock analyses of selected nodule samples, for both major and certain trace elements, demonstrate significant differences between the four petro-

graphically distinct groups of peridotite nodules recognised.

Compared with the common upper mantle derived garnet or spinel bearing lherzolite nodules found globally associated with kimberlite and alkali basalt magmatism, respectively (Carswell 1980) the Groups 1 and 2 peridotite nodules from these two kimberlite localities are significantly less magnesian. The two analysed Group 1 nodules from Lipelaneng have low 100 Mg/(Mg+Fe) values (81.7-84.2) coupled with low Al_2O_3, CaO and Na_2O contents and unusually high 100 Cr/(Cr+Al) values (37.4-39.3). However, in the Group 2 nodules from both Lipelaneng and Ngopetseu low 100 Mg/(Mg+Fe) values (78.0-87.4) are combined with enhanced Al_2O_3, CaO and Na_2O contents and low Cr/(Cr+Al) values (5.1-8.7). As the whole rock compositions of the Groups 1 and 2 peridotites appear dissimilar to any observed or projected upper mantle peridotite compositions (e.g. Ringwood 1966, 1975)[a] we conclude that an upper mantle derivation of such nodules is unlikely.

By contrast, the Group 3 spinel peridotite nodules have significantly higher whole rock 100 Mg/(Mg+Fe) values (89.7-93.5) coupled with low Al_2O_3, CaO and Na_2O contents and high Cr/(Cr+Al) values (20.9-31.1). These nodules are comparable in their composition to a solitary, previously analysed, spinel harzburgite nodule from the Pipe 200 kimberlite (sample PTH 201, Carswell et al. 1979) and may represent relatively 'depleted' uppermost mantle samples. The garnetiferous peridotite nodules (Group 4) have broadly similar 'depleted' chemical compositions with 100 Mg/(Mg+Fe) = 91.0-92.9 and 100 Cr/(Cr+Al) = 15.8-31.1 to the Group 3 spinel peridotites. However, the presence of Cr pyrope garnet rather than Cr spinel points to a somewhat deeper level origin in the mantle at higher pressures.

4 MINERAL CHEMISTRY

The coexisting mineral phases in 24 nodule samples have been analysed by electron microprobe at the University of Oslo using either wavelength dispersive or energy dispersive techniques. Most quoted analyses (Volume III "Documents") are averages of several point analyses of chemically similar grains.

4.1 Olivines

There are clear differences in olivine compositions between the various analysed nodule samples with the olivines in Groups 1 and 2 nodules being significantly less magnesian than those in Groups 3-4 nodules. Ranges of forsterite contents in olivines from the four nodule groups are as follows: Group 1 - Fo_{81-85}; Group 2 - $Fo_{80-88.5}$; Group 3 - $Fo_{91.5-93}$; Group 4 - $Fo_{92.5-93.5}$.

4.2 Orthopyroxene

There are similarly significant differences in the enstatite contents of the orthopyroxenes between the various nodules with the composition ranges as follows: Group 1 - $En_{82.3-85.6}$; Group 2 - $En_{81.7-86.7}$; Group 3 - $En_{92.8-93.6}$; Group 4 - $En_{93.4-94.2}$. Ranges of Al_2O_3 contents of orthopyroxenes in the various nodule groups are: Group 1 - 1.56-1.89 wt.%; Group 2 - 2.82-3.25 wt.%; Group 3 - 0.96-3.01 wt.%; Group 4 - 0.98-1.21 wt.%. It is clear that the orthopyroxenes in the Group 1 spinel lherzolites/wehrlites are appreciably less aluminous than those in the Group 2 spinel lherzolites. The Group 4 garnet harzburgites contain orthopyroxenes with consistently low Al_2O_3 contents, whilst those in the Group 3 spinel lherzolites/harzburgites have variable Al_2O_3 contents depending largely on the textural type present. In nodules of the latter group with good partially recrystallised mosaic-porphyroclastic textures the orthopyroxene porphyroblasts have higher Al_2O_3 contents than the smaller recrystallised neoblasts. Orthopyroxenes occurring as symplectite intergrowths with spinel have lower Al_2O_3 contents than discrete grains in the same nodule. In these Group 3 nodules the overall trend is of decreased Al_2O_3 contents in orthopyroxenes resulting from deformation induced subsolidus recrystallisation.

4.3 Clinopyroxene

Significant compositional differences exist between clinopyroxenes in the different nodule groups and in the Group 3 nodules between different textural types of grains. The clinopyroxenes in the Groups 1 and 2 nodules have highest Fe/Mg ratios, and are typically more titaniferous and aluminous. Stoichiometric end member calculations involving Fe^{3+} calculation (Essene & Fyfe, 1967; Mysen & Griffin, 1973) suggest that the clinopyroxenes in these particular nodules all have significant acmite contents. Jadeite contents are generally negligible except in those of the Group 2 nodules. The Ngopetsoeu Group 2 spinel lherzolite nodule PHN 2873/1 is, however, an exception to this. The composition of the clinopyroxene in this particular nodule reflects equilibration with abundant coexisting hornblende into which Al, Ti, Cr and Na have clearly been preferentially partitioned. The clinopyroxenes in the Group 3 nodules are highly diopsidic, particularly in the recrystallised neoblasts and where intergrown with spinel as symplectite (Di_{80-89}), and are characterised by low contents of both jadeite and Ca-tschermaks molecules.

4.4 Garnets

The garnets in the Group 4 garnet harzburgite nodules are all Cr pyropes ($Pyrope_{71-75}$, $Uvarovite_{9-14}$, $Almandine_{9-13}$), similar to the type 9 garnets of Dawson & Stephens (1975) which comprise the typical garnets in the dominant

garnet lherzolite/harzburgite nodules encountered in most kimberlites.

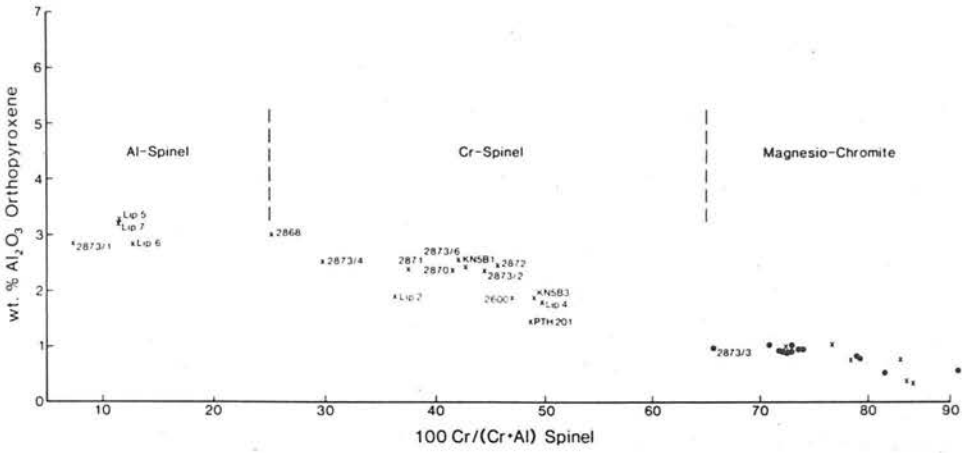

Fig. 1. Plot of 100 Cr/(Cr+Al) ratios in discrete spinels against wt.% Al_2O_3 in coexisting 'primary' orthopyroxenes from garnet free spinel peridotite nodules (crosses) and garnet bearing spinel peridotite nodules (closed circles). Additional data from Nixon & Boyd (1973)[a], Boyd and Nixon (1975) and Carswell et al. (1979). Unlabelled points in the magnesio-chromite field are for various Groups 4 and 5 nodules from the Thaba Putsoa, Mothae and Pipe 200 kimberlites.

4.5 Spinels

As with the other mineral phases, there are notable differences in the chemical compositions of the spinels in the various nodule groups. Group 1 nodules contain Cr spinels that are much more ferriferous and notably more titaniferous than those in the Group 3 nodules. On the other hand Group 2 nodules contain Al spinels with low Cr contents. The Cr spinels in the Group 3 nodules have somewhat variable Cr contents (25.2-48.4% $M^{2+}Cr_2O_4$). Unlike in the coexisting orthopyroxenes no consistent differences were detected between discrete spinel grains and those in symplectite intergrowths with pyroxenes in particular nodules. The spinel associated with the late stage phlogopite in PHN 1899 is a magnesio-chromite (75.8% $M^{2+}Cr_2O_4$) as is the spinel coexisting with garnet in the Group 4 nodule PHN 2873/3 (64.3% $M^{2+}Cr_2O_3$).

The differences in composition of the spinels in the various nodules and their correlation with the Al_2O_3 content of the coexisting orthopyroxenes are highlighted in Fig. 1, which also includes mineral analyses from other spinel-only or spinel + garnet peridotite nodules recorded in the Pipe 200, Thaba

Putsoa, Mothae and Liqhobong kimberlites of northern Lesotho (Nixon & Boyd, 1973[a]; Boyd & Nixon, 1975; Carswell et al., 1979). The Group 2 spinel lherzolite nodules all plot as a well defined group with Al spinels and orthopyroxenes with around 3 wt.% Al_2O_3. Such spinel-orthopyroxene pairs are somewhat akin to those of the common mantle derived spinel lherzolite nodules frequently encountered in alkali basalt suite magmas (e.g. Ross et al. 1954; Kuno & Aoki, 1979; Varne, 1977; Donaldson, 1978; Frey & Prinz, 1978). However, the assemblages in the latter nodules are less ferriferous and frequently contain orthopyroxenes with even higher Al_2O_3 contents (see Fig. 1, Carswell, 1980). The Cr spinel-orthopyroxene pairs of Groups 1 and 3 nodules plot together in Fig. 1, but as noted earlier the former assemblage is much more ferriferous.

The spinels in the Group 1 nodules have quite high stoichiometrically calculated Fe^{3+} contents, corresponding to some 13-31% $M^{2+}Fe^{3+}_2O_4$ in contrast to the negligible calculated $M^{2+}Fe^{3+}_2O_4$ contents in the spinels of the Group 3 nodules. Previously analysed spinel harzburgite nodules PTH 201 from Pipe 200 (Carswell et al., 1979) and PHN 2600 from Liqhobong (Boyd & Nixon, 1975) have mineral assemblages with spinel-orthopyroxene compositions similar to the Group 3 nodules at Ngopetsoeu. Although primary spinel has been analysed in only one Ngopetsoeu Group 4 nodule, comparison with similar nodules with coexisting spinel and garnet from other kimberlites in northern Lesotho confirms that such nodules characteristically contain magnesio-chromite and low Al orthopyroxene. Fig. 1 further indicates that these other kimberlites also contain an additional group (Group 5) of garnet-free spinel lherzolite/harzburgite nodules again with coexisting magnesio-chromite and low Al orthopyroxene. However, overall such nodules are even more refractory and magnesian with whole rock 100 Mg/(Mg+Fe) values of 95.0-95.4 in comparison to values of 91.3-93.5 in the nodules with coexisting garnet and magnesio-chromite.

5. EQUILIBRATION CONDITIONS

On the assumption that the mineral assemblages in these nodules equilibrated under the ambient P/T conditions of their sites of derivation, mineralogical geothermometers/barometers based on various mineral equilibria should indicate the likely depths of derivation of the various groups of peridotite nodules. Unfortunately calibrated barometers only exist for the garnetiferous Group 4 nodules and only assumed pressures can be indicated for the other nodules. However, a number of appropriate calibrated thermometers exist based on several different mineral equilibria. The various calculated equilibrium temperatures and corresponding pressure estimates are listed in Table 1.

TABLE 1 Summary of pressure-temperature estimates for documented peridotite nodule samples.

Sample Number	Y^{Sp}_{Cr}	Mg^{2+}-Fe^{2+} Spinel-Olivine T^oC(1)	Mg^{2+}-Fe^{2+} Spinel-Olivine T^oC(2)	Oliv-Opx Spinel T^oC(3)	Two Pyrox Solvus T^oC(4)	Mg^{2+}-Fe^{2+} Gnt-oliv T^oC(5)	Gnt-Opx Pkbs(6)	5 Phase Assembl. Pkbs(7)
Group 1								
LIP 1[a]	0.35	658	(499)[i]	-	-	-	-	-
LIP 2[a]	-	-	-	-	768	-	-	-
LIP 3[a]	0.38	824	718[i]	-	-	-	-	-
LIP 4[a]	0.38	(944)	732[i]	1339	730	-	-	-
Group 2								
LIP 5[a]	0.11	692	656[i]	905	499	-	-	-
LIP 6[a]	0.12	739	662[i]	936	666	-	-	-
LIP 7[a]	0.11	743	694[i]	966	739	-	-	-
PHN 2873/1[a]	0.07	732	631[i]	862	598	-	-	-
Group 3								
PHN 2867[a]	-	-	-	-	780	-	-	-
PHN 2870[a]	0.41	840	876[ii]	924	710	-	-	-
PHN 2871[a]	0.37	770	808[ii]	882	763	-	-	-
KN 581[a]	0.42	794	835[ii]	956	-	-	-	-
PHN 2873/2[a]	0.44	887	863[ii]	943	692	-	-	-
PHN 2873/4[a]	0.30	753	779[ii]	850	-	-	-	-
PTH 201[b]	0.48	916	869[ii]	791	-	-	-	-
PHN 2600[c]	0.48	879	942[ii]	842	-	-	-	-
PHN 2868[a]	0.25	742	757[ii]	807	755	-	-	-
PHN 2872[a]	0.46	823	873[ii]	805	681	-	-	-
PHN 1899[a]	0.46	813	863[ii]	606	-	-	-	-
PHN 2873/4[a]	0.30	-	-	697	736	-	-	-
PHN 2873/6[a]	0.41	-	-	658	661	-	-	-
Group 4								
PHN 2873/3[a]	0.64	906	1054[iii]	-	-	760 ——→ 21.2 913 ——————→ 27.1		
PHN 2873/7[a]	-	-	-	-	-	781 ——→ 19.8		
PHN 1905[a]	-	-	-	-	-	1018 ——→ 36.0		
PTH 207[b]	0.71	-	1452[iii]	-	-	946 ——————→		29.8
PTH 409[b]	0.76	-	1104[iii]	-	-	967		31.6
PHN 1595[c]	0.69	-	1278[iii]	-	-	882		29.0
PHN 1567[c]	0.68	-	1182[iii]	-	-	899		29.9
PHN 1592[c]	0.69	-	1197[iii]	-	-	889		29.7
PHN 1570[c]	0.70	-	1200[iii]	-	-	912		28.9
PHN 1573[c]	0.68	-	1152[iii]	-	-	840		29.2
PHN 1572[c]	0.69	-	1150[iii]	-	-	924		29.0

Additional Notes:
PHN 2867 to PHN 2600 - 'Primary' assemblages with high Al orthopyroxene and discrete spinels.
PHN 2868 to PHN 1899 - Recrystallised mosaic textured assemblages.
PHN 2873/4 to PHN 2873/6 - Pyrox-spinel symplectite with low Al opx.

P/T Calibrations:
1. Henry & Medaris 1980
2. Engi (in press)
3. Sachtleben & Seck 1981
4. Wells 1977
5. O'Neill and Wood 1979, 1980
6. Wood 1974
7. O'Neill 1981

Data Sources:
a. This paper
b. Carswell et al. 1979
c. Nixon & Boyd 1973

Assumed Pressures: i. 10 Kbars
ii. 15 Kbars
iii. 30 Kbars

5.1 Clinopyroxene-orthopyroxene equilibria

The inconsistent temperatures calculated by the Wells (1977) calibration of this thermometer for the various nodule groups probably reflect errors resulting both from the imprecision of this method at these temperatures and its failure to satisfactorily take account of the influence of pressure and various compositional factors on the two pyroxene solvus (Lindsley & Dixon, 1976; Herzberg 1978[a]; Mori 1978). Accordingly it would seem injudicious to attempt to discriminate between possible lower crustal and uppermost mantle nodules on the basis of these particular temperature estimates.

5.2 Olivine-spinel equilibria

Fe^{2+}-Mg^{2+} partitioning between olivine and spinel is a potentially valuable geothermometer for spinel peridotites (Irvine, 1965; Evans & Frost, 1975; Fujii, 1977)[b]. Here we have utilised the most recent calibrations of this geothermometer as provided by Henry & Medaris (1980) and Engi (in press). The Henry & Medaris calibration follows the earlier treatment of Evans & Frost (1972) and involves normalisation of the partition coefficient to $Y^{Sp}_{Fe^{3+}} = 0.05$. The Engi calibration has a more thorough experimental and theoretical basis with corrections introduced both for the Fe^{3+} content of the spinel and the pressure dependence of the partition coefficient.

For the Groups 1 and 2 nodules, if the two wayward values are excluded, the Henry & Medaris calibration gives mean and standard deviation temperature values of 731 ± 51°C (with no P correction) and the Engi calibration 682 ± 36°C (with an assumed P = 10 Kbars). These values look reasonable for ambient temperatures to be expected near the base of the crust beneath a relatively stable cratonic region. They are also in line with independent equilibration temperature estimates for postulated lower crustal granulite suite nodules (Griffin et al.,1979; Carswell & Griffin, 1981) from the kimberlites of southern Africa. By contrast olivine-spinels equilibration temperatures for the Group 3 nodules are significantly higher, the mean and standard deviation values in 8 nodules with discrete spinels being 803 ± 43°C with the Henry & Medaris calibration or 832 ± 43°C with the Engi calibration (assuming P = 15 K bars). There is in fact no overlap in calculated temperatures for individual nodules in nodules of Groups 1 and 2 compared with Group 3, if the more consistent and preferred values given by the Engi calibration are accepted. The temperature difference between these nodules cannot be solely attributed to differences in the assumed P, since increasing the assumed pressure to 15 Kbars for the Groups 1 and 2 nodules only increases the mean calculated temperature given by the Engi calibration to 695°C. The existence of equilibration temperature differences between the Groups 1 and 2 and Group 3 nodules is further substantiated by the higher calculated temperatures for comparable Group 3 type nodules from Pipe 200 (PTH

201) and Liqhobong (PHN 2600) also included in Table 1. Hence the differences in the calculated olivine-spinel temperatures are considered to be real and to reflect equilibration at uppermost mantle depths (Group 3) and lower crustal depths (Groups 1 and 2).

The one Group 4 nodule from Ngopetsoeu with analysed coexisting primary spinel and garnet (PHN 2873/3) yields even higher olivine-spinel equilibration temperatures of 906°C with the Henry & Medaris calibration and 1054°C with the Engi calibration (assuming P = 30 Kbars). Comparable Group 4 type garnet-spinel lherzolite/harzburgite nodules from Pipe 200 and Thaba Putsoa (data from Nixon & Boyd, 1973[a] and Carswell et al., 1979) all yield consistently high temperatures (>1100°C) with the Engi calibration (assuming P = 30 Kbars). In addition the separate group of 'ultradepleted' garnet free magnesio-chromite bearing lherzolite/harzburgite nodules also recorded in the Pipe 200 and Thaba Putsoa kimberlites (Boyd & Nixon 1975; Carswell et al., 1979) again all yield olivine-spinel equilibration temperatures >1100°C with the Engi calibration (P = 30 Kbars). Some of the calculated temperatures for individual nodules are excessively high but it seems reasonable to conclude that both these nodules and the Group 4 type garnetiferous nodules have been derived from deeper mantle levels than the Group 3 Cr spinel bearing lherzolite/harzburgite nodules.

5.3 Olivine-orthopyroxene-spinel equilibria

Recent experimental and theoretical studies (Fujii, 1976; Obata, 1976; Danckwerth & Newton, 1978) have shown that the Al-isopleths for orthopyroxenes in equilibrium with forsterite and spinel are nearly independent of pressure and therefore provide a useful geothermometer. Sachtleben & Seck (1981) have derived a calibration for this geothermometer which empirically corrects for the control on the Al solubility in the orthopyroxene exerted by $Cr/(Cr+Al+Fe^{3+})$ ratio (Y_{Cr}^{Sp}) of the coexisting spinel.

The inconsistent and generally high temperatures calculated from this thermometer for the Groups 1 and 2 nodules probably reflect a general lack of equilibrium in the Al distribution in the mineral assemblages of these nodules, certain of which contain coronitic reaction textures. Amongst the Group 3 nodules, the most important point to emerge is of the lower calculated temperatures for the recrystallised mosaic textured low Al orthopyroxene bearing assemblages and for the orthopyroxene-spinel symplectite intergrowths. Apparent 'primary' assemblages based on assumed equilibration of higher Al orthopyroxene porphyroclasts and discrete spinels yield temperatures which seem appropriate for uppermost mantle depths although the values obtained for individual samples are mostly somewhat higher than those indicated by the Engi calibration of the olivine-spinel geothermometer at P = 15 Kbars.

5.4 Olivine-orthopyroxene-garnet equilibria

It is possible to derive unique P/T estimates for Group 4 nodules with this assemblage using a combination of the experimentally based P/T dependent calibrations for Al solubility in orthopyroxene (Wood, 1974) and Fe^{2+} - Mg^{2+} partitioning between the garnet and olivine (O'Neill & Wood, 1979, 1980). However, this procedure yields unsatisfactorily inconsistent results which may at least in part reflect the fact that the Wood (1974) calibration does not adequately take account of the influence of Cr on garnet-orthopyroxene equilibria.

5.5 Olivine-orthopyroxene-clinopyroxene-garnet-spinel equilibria

The Cr_2O_3 contents of naturally occurring peridotites result in the stability of this 5 phase divariant assemblage over a fairly wide pressure interval (MacGregor, 1970; O'Neill, 1981) between the recognised 4 phase spinel lherzolite and garnet lherzolite stability fields (O'Hara et al., 1971; Jenkins & Newton, 1979). In the 5 phase assemblage Cr is heavily partitioned into the spinel phase. Hence in peridotites with the levels of whole rock 100 Cr/(Cr+Al) ratios (16-31) encountered in these Group 4 Ngopetsoeu nodules the coexisting spinels are typically magnesio-chromites with 100 Cr/(Cr+Al) > 65 (Carswell et al., 1979; Carswell, 1980; this study). O'Neill (1981) has utilised experimentally determined data on the equilibrium between spinel lherzolite and garnet lherzolite and added corrections to take account of the influence of Cr and Fe on the mineral equilibrium to derive a geobarometer applicable to the garnet + spinel five phase assemblages in natural peridotites. Unfortunately only Ngopetsoeu nodule PHN 2873/3 has the appropriate analysed 5 phase assemblage but data also exist on comparable nodules from Pipe 200 (Carswell et al., 1979) and Thaba Putsoa (Nixon & Boyd, 1973)[a]. The procedures for the calculation of these particular P/T estimates largely follows that proposed by O'Neill (1981) with temperatures calculated first from the O'Neill & Wood (1979, 1980) calibration for Fe^{2+} - Mg^{2+} partitioning between the garnet and olivine at an assumed P = 30 Kbars. However, to take account of more recent experimental data (O'Neill, pers.comm.) a correction of -10% has been applied to the nominal pressure obtained for the reaction in CMAS, corrected for the Cr content of the spinel, before calculation and implementation of the appropriate Fe^{2+} correction. The P/T values thus obtained for the 9 nodules concerned are reasonably consistent and look geologically realistic - the mean and standard deviation values for the 9 samples being 897 ± 46°C and 29.1 ± 1.1 Kbars. For the 8 nodules from Pipe 200 and Thaba Putsoa these values can be compared with mean values of 944°C/32.0 Kbars obtained by the preferred methods applicable to 4 phase garnet lherzolite assemblages (Carswell & Gibb, 1980)[b]. In conclusion, the P/T estimates for the Group

4 type garnetiferous nodules are considered to correspond to sub-Moho conditions expected on the Lesotho 'geotherm' at depths below surface of approaching 100 kilometres (see Fig. 1, Carswell & Gibb, 1980)[b].

6. DISCUSSION

The symplectite intergrowths of spinel with pyroxenes which are a notable feature of the Group 3 spinel lherzolite/harzburgite nodules, present several problems in interpretation. Dawson & Smith (1975) have observed that similar intergrowths are of widespread occurrence in garnet-free spinel peridotite nodules from various kimberlites in southern Africa. Evidence that the mineral phases involved have the same composition in individual nodules whether they occur as discrete grains or are intergrown as symplektites led them to hesitatingly reject interpretations involving metasomatic replacement, exsolution, or the breakdown or reaction of earlier phases in favour of an interpretation of the intergrowths as a primary crystallisation phenomenon.

In the Ngopetsoeu Group 3 nodules most symplectite intergrowths are of orthopyroxene + Cr spinel but some are of orthopyroxene + Cr spinel + minor clinopyroxene. In the latter instances there is in fact no clinopyroxene elsewhere in the nodule. On the other hand, orthopyroxene is common in all the nodules and the symplectite often takes the form of a kind of overgrowth on larger orthopyroxene grains. Whilst our microprobe data confirm the absence of significant composition differences between spinels intergrown in symplectites and those occurring as isolated grains in the same nodule, we have observed consistent differences between the compositions of the pyroxenes of the symplectites and primary porphyroclast pyroxene grains. On the other hand both orthopyroxenes and clinopyroxenes intergrown with spinel in symplectites have compositions similar to those of corresponding recrystallised pyroxene neoblasts in those nodules with distinct mosaic-porphyroclastic textures.

As noted earlier, the lower Al contents of the orthopyroxenes in both neoblasts and symplectites provides strong evidence that both formed in response to deformation-induced recrystallisation at significantly reduced temperatures. The consistent compositions of the discrete and symplectite spinels can be explained if both have re-equilibrated under the changed P/T conditions. Certainly rapid re-equilibration of spinels appears to have occurred in certain Pipe 200 peridotite nodules (Carswell et al., 1979) where spinels associated with the outer parts of kelyphites resulting from garnet breakdown, spinels intergrown with clusters of Cr diopside and phlogopite grains, and discrete spinels may all have the same composition in individual nodules.

One feasible explanation is that the symplectites are the result of reaction between olivine and pre-existing Cr-rich garnet. Scan analyses of clinopyroxene bearing symplectites, if recalculated to 16 oxygens have approximately $M^{3+} = 2$

and M^{4+} = 4, as would be expected from a mixture of olivine + garnet (Bell et al., 1975; Smith, 1977). The high CaO contents (13.2-17.8 wt.%) would imply an original pyrope-uvarovite garnet unlike those usually encountered in upper mantle peridotites. However, a considerable amount of orthopyroxene component resulting from the olivine + garnet reaction may have crystallised as overgrowths on the adjacent large orthopyroxenes and thus been 'lost' from the actual symplectite areas. If this has occurred then the pyrope (and knorringite) content of the original garnet would have been correspondingly higher. This calculation also ignores the presence of clinopyroxene free symplectites in the same rock. If these are included in an average, the hypothetical garnet becomes still lower in Ca. However, the symplectite texture is usually accepted as evidence of rapid growth rates and slow diffusion rates, so that such an 'averaging' would seem to be of dubious validity. The postulated original garnets in these nodules may have had compositions approaching those of the Cr rich green garnet xenocrysts (with around 25 mol.% each of uvarovite and knorringite) found in the Kao kimberlite (Hornung & Nixon, 1973). These green garnets conceivably were derived from disaggregated highly depleted garnet lherzolite nodules (see Fig. 3, Carswell et al., 1979). However, the olivine + garnet reaction interpretation does not explain the source of the Na in the symplectite unless original jadeite- or kosmochlor-rich clinopyroxene is assumed to have been involved in the breakdown reaction.

An alternative interpretation of the symplectites involves the breakdown of a complex pyroxene by a sliding reaction of the type $pyrox._{ss} + spin_1 \longrightarrow opx + spin_2 \pm cpx$. This would require that the primary pyroxene was extremely rich in Al + Cr. The amount of secondary pyroxene 'lost' as overgrowths on larger grains is difficult to estimate, as noted above, so that this problem may be only apparent.

Breakdown of an original high pressure olivine + Cr-rich garnet assemblage to a lower pressure pyroxene + spinel assemblage in these nodules implies diapiric movements in the mantle preceeding kimberlite generation (Smith, 1977). Certainly such an interpretation would be in keeping with the abundant evidence of deformation induced recrystallisation textures in these particular nodules. The alternative origin by breakdown of complex pyroxenes implies cooling from a previous temperature maximum. This does not require vertical movements, but cooling might well have been related to upward transport of material.

An analysed olivine megacryst from Ngopetsoeu has a composition ($Fo_{83.6}$) within the range recorded (Fo_{83-87}) in olivine megacrysts from the Letseng-laterae kimberlite of northern Lesotho (Boyd & Nixon, 1975; Dawson et al., 1981) which in turn have similar compositions to the olivines in rare nodules of porphyroclastic textured Fe rich dunites observed in the Thaba Putsoa (Boyd & Nixon 1975) and Bultfontein (Dawson et al., 1981) kimberlites. The Fe rich nature of

these megacrysts and dunites suggests that they represent cumulates rather than residua of partial melting of upper mantle peridotites, but it seems unlikely that such olivines were precipitated directly from kimberlite liquids (Dawson et al., 1981). Olivine-liquid partition considerations (Roeder & Emslie, 1970) instead suggest that such olivines were precipitated from basaltic magmas. This raises the interesting possibility that such olivine megacrysts, dunites and the Groups 1 and 2 spinel peridotite nodules described in this paper may all represent fragments of ultramafic cumulates of earlier basalt magmas (perhaps of Karroo age) trapped near the base of the crust as envisaged by Cox (1980). Certainly such an origin would seem appropriate for the relatively ferriferous Grouns 1 and 2 peridotite nodules and is in keeping with the relatively low calculated olivine-spinel equilibration temperature for these nodules as discussed earlier.

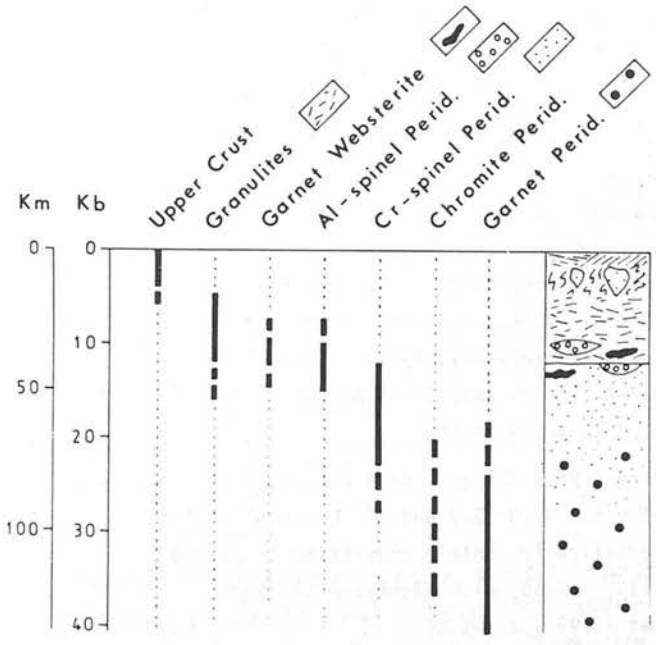

Fig. 2. Depth ranges of various xenolith types beneath NW Lesotho, based on geothermometry/geobarometry calculations (Carswell et al., 1979; Carswell and Griffin, 1981; Griffin et al., 1979; and this paper). Assemblages for which only temperature could be calculated (spinel lherzolites) have been assigned a depth by comparison with a generalised Lesotho geotherm constructed from the above references. Group 1 Cr spinel peridotite nodules have probably been derived from similar depths to the Group 2 Al spinel peridotites, in contrast to the indicated uppermost mantle zone of Group 3 type Cr spinel peridotite.

7. SUMMARY

Our observations and analytical data on the nodule suites at Lipelaneng and Ngopetsoeu, taken together with previously published data on the nodule suites from other kimberlites in Lesotho, lead us to recognise the existence of five distinct groups of primary spinel bearing peridotite nodules. These have been derived, as illustrated schematically in Fig. 2, from various stratigraphic levels in the lower crust-uppermost mantle section traversed by these kimberlites during their volatile charged emplacement. The five spinel bearing peridotite nodule groups are as follows:

Group 1 nodules - recognised so far only at Lipelaneng, contain Cr spinel (Y_{Cr}^{Sp} = 0.35-0.38) with quite high $M^{2+}Fe_2^{3+}O_4$ contents. Indeed the whole mineral assemblage is more ferriferous than that normally encountered in mantle derived peridotite nodules. Olivines are Fo_{81-85} and orthopyroxenes $En_{82.86}$ with fairly low Al_2O_3 contents (1.56-1.86 wt.%).

Group 2 nodules - encountered at both Lipelaneng & Ngopetsoeu, are similarly ferriferous (olivines Fo_{80-88}) but contain Al spinels (Y_{Cr}^{Sp} = 0.07-0.12) which coexist with aluminous orthopyroxenes (2.83-3.25 wt.% Al_2O_3).

Group 3 nodules - particularly conspicuous at Ngopetsoeu but also previously noted at Pipe 200 and Liqhobong, have quite 'depleted' whole rock chemical compositions (100 Mg/Mg+Fe = 89.7-93.0 and 100 Cr/Cr+Al = 20.9-29.9) and contain Cr spinels (Y_{Cr}^{Sp} = 0.25-0.48) with magnesian olivines (Fo_{91-93}) and orthopyroxenes (En_{93-94}). Many of these nodules show subsolidus deformation and recrystallisation effects leading to the development of mosaic-porphyroclastic and symplectite intergrowth textures. Coarse grained orthopyroxene porphyroclasts have higher Al_2O_3 contents (2.32-3.01 wt.%) than associated mosaic (0.96-2.43 wt.%) and symplectite (1.20-1.75 wt.%) textured grains.

Group 4 nodules - recorded at Ngopetsoeu, Pipe 200 and Thaba Putsoa, have similar whole rock compositions (100 Mg/Mg+Fe = 91.0-92.9 and 100 Cr/Cr+Al = 15.8-31.1) to Group 3 nodules but characteristically contain coexisting Cr pyrope garnet and magnesio-chromite spinel (Y_{Cr}^{Sp} > 0.60) with magnesian olivines (Fo_{92-94}) and low Al_2O_3 orthopyroxenes (0.99-1.21 wt.%).

Group 5 nodules - not observed at Lipelaneng or Ngopetsoeu but recorded at Pipe 200, Thaba Putsoa and Mothae, have extremely depleted whole rock chemical compositions (100 Mg/Mg+Fe = 95.0-95.4 and 100 Cr/Cr+Al = 20.1-48.9) and contain highly magnesian olivines (Fo_{93-95}), low Al_2O_3 orthopyroxenes (0.36-1.05 wt.%) and magnesio-chromite spinels (X_{Cr}^{Sp} = 0.69-0.80) without garnet.

Geochemical considerations and calculated P/T equilibration conditions for the mineral assemblages in the various nodule groups, lead us to conclude that the peridotite nodules of Groups 1 and 2 have been derived from near the base of

the crust and may well represent ultramafic cumulates derived from trapped bodies of earlier basaltic magmas. Nodules of Groups 3-5 are by contrast of undoubted mantle derivation, with those of Group 3 having been derived from the uppermost few tens of kilometres of the mantle and those of Groups 4 and 5 from somewhat deeper levels. There is thus strong evidence for the existence of a garnet free Cr-spinel peridotite zone at the top of the mantle sections sampled by the Ngopetsoeu, Pipe 200 and Liqhobong kimberlites. It seems likely that a similar uppermost mantle zone, dominated by Cr-spinel peridotite was also sampled by the well documented kimberlites of the Kimberley area (e.g. Williams, 1932; Holmes, 1936; Dawson & Smith, 1975). Furthermore, the absence of garnetiferous peridotite nodules which have demonstrably equilibrated in approximately the top 45 kilometres of the mantle (see for example Fig.3, Carswell & Gibb, 1980)[b] makes us strongly suspect that such an uppermost mantle Cr-spinel peridotite zone may occur extensively beneath southern Africa. This hypothesis can be tested by a program of geothermometry on the common spinel harzburgite nodules.

It should be emphasised that no magnesian Al-spinel peridotite nodules, analogous to those habitually encountered in alkali basalt suite magmas, have been recorded in these, or indeed any other, kimberlites in southern Africa. The occurrence instead of Group 3 type Cr-spinel peridotite nodules indicates that the uppermost 45 or so kilometres of the mantle section transected by these kimberlites has a more highly 'depleted' peridotite composition than is usually encountered at similar mantle depths beneath regions undergoing alkali basalt suite magmatism. Additional nodule evidence, such as the occurrence of Group 4 type peridotite nodules with coexisting Cr pyrope garnet and magnesiochromite spinel, indicates that this highly depleted chemical character often extends down some 70 or more kilometres in the sub-Moho mantle section beneath Lesotho, perhaps as a consequence of the voluminous earlier Karroo basalt magmatism.

8. ACKNOWLEDGEMENTS

We wish to acknowledge financial support from the Natural Environmental Research Council and The Royal Society (DAC), and the Norwegian Scientific Research Council and Nansenfondet (WLG). Thanks are also due to the organisers and guides of the 1973 Lesotho excursions, to Peter Nixon who collected the majority of Ngopetsoeu nodules, and to Martin Engi who kindly provided a preprint of his paper on the olivine-spinel geothermometer.

Ann.Sci.Univ.Clermont-Fd. II
(1984) 74: 167-178.

PERIDOTITE NODULES FROM THE NGOPETSOEU AND LIPELANENG KIMBERLITES, LESOTHO: A CRUSTAL OR MANTLE ORIGIN - APPENDIX

by D.A. CARSWELL, W.L. GRIFFIN and P. KRESTEN

TABLE 1

Petrographic Details of Analysed Peridotite Nodule Samples

Sample Number	Locality	Rock Type	Nodule Group	Modal Mineralogy					Other Features
				Olivine	Ortho-Pyroxene	Clino-Pyroxene	Spinel	Garnet	
LIP 1	LIPELANENG	Spinel Wehrlite	1	X	-	Z	Z	-	
LIP 2		Spinel Lherzolite	1	X	Z	Z	Z	-	
LIP 3		Spinel Werhlite	1	X	-	Z	Z	-	Minor carbonate
LIP 4		Spinel Lherzolite	1	X	Z	Z	Z	-	Minor carbonate
LIP 5		Spinel Lherzolite	2	X	Y	Y	Z	-	
LIP 6		Spinel Lherzolite	2	X	Y	Y	Z	-	Conspicuous coronitic reaction textures
LIP 7		Spinel Lherzolite	2	X	Y	Y	Z	-	Minor reaction coronites
PHN1899		Spinel Lherzolite	3	X	Y	Z	Z	-	Phlogopite and chromite associated with late infiltration metasomatism
PHN1905		Garnet Harzburgite	4	X	Y	-	-	Z	Secondary phlogopite as rims around garnets
PHN1906		Spinel Lherzolite	3	X	Y	Z	Z	-	
PHN2867		Spinel Lherzolite	3	X	Y	Z	Z	-	Minor spinel limited to symplektitic intergrowths with pyroxenes
PHN2868		Spinel Lherzolite	3	X	Y	Z	Z	-	Good mosaic - porphyroclastic texture
PHN2870		Spinel Lherzolite	3	X	Y	Z	Z	-	Spinel-pyroxene symplektites
PHN2871		Spinel Lherzolite	3	X	Y	Z	Z	-	Spinel as both discrete grains and symplektitic intergrowths with pyroxene
PHN2872		Spinel Lherzolite	3	X	Y	Z	Z	-	Mosaic - porphyroclastic texture

PHN 2873/1	NGOPETSOEU	Spinel Lherzolite	2	Y	X	Y	Z	-	∿12 vol.% amphibole
PHN 2873/2		Spinel Lherzolite	3	X	Y	Z	Z	-	Good mosaic-porphyroclastic texture
PHN 2873/3		Garnet Harzburgite	4	X	Y	-	Z	Z	Extensive kelyphite reaction rims around garnets. Primary chromite.
PHN 2873/4		Spinel Lherzolite	3	X	Y	Z	Z	-	Both discrete spinels and coarse symplektitic intergrowths with Opx and Cpx
PHN 2873/5		Mica Lherzolite	3	X	Y	Z	Z	-	Considerable late stage hydration with phlogopite development
PHN 2873/6		Spinel Lherzolite	3	X	Y	Z	Z	-	Cpx limited to symplektitic intergrowths with spinel.
PHN 2873/7		Garnet Harzburgite	4	X	Y	-	Z	Z	Secondary phlogopite rims around garnets. Trace primary chromite
PHN 2873/8		Spinel Lherzolite	3	X	Y	Z	Z	-	
PHN2874		Olivine Megacryst	-	X	-	-	-	-	Single coarse megacryst
KN 4		Spinel Lherzolite	3	X	Y	Z	Z	-	Mosaic-porphyroclastic texture - both discrete and symplektitic spinels
KN 5B1		Spinel Lherzolite	3	X	Y	Z	Z	-	
KN 5B3		Spinel Lherzolite	3	X	Y	-	Z	-	Coarse grained with large discrete spinels
KN 5B7		Spinel Lherzolite	3	X	Y	Z	Z	-	Spinel-pyroxene symplektites
WLG 1		Ortho-Pyroxene Megacryst	-	-	X	Z	-	Y	Exsolved single orthopyroxene megacryst

Modal Percentages by Volume X > 30; Y 10-30; Z < 10

TABLE 2 - Whole rock analyses of selected nodule samples

SAMPLE NO.	LIP 3	LIP 4	LIP 5	LIP 6	LIP 7	PHN 1899	PHN 1905	+PHN 1906	PHN 2871	PHN 2872	PHN 2873/1	PHN 2873/2	PHN 2873/3	PHN 2873/7	PHN 2873/8	PHN 2874	+KN 4	+KN 5B7
SiO_2	36.60	37.49	43.91	41.38	43.74	42.98	43.11	45.0	43.26	44.20	50.02	43.68	43.99	42.07	43.12	38.80	43.5	47.3
TiO_2	0.13	0.04	0.08	0.20	0.08	0.09	0.05	0.05	0.01	0.01	0.11	0.02	0.06	0.15	0.03	0.03	0.07	0.06
Al_2O_3	1.75	1.21	4.55	7.21	4.36	0.71	0.84	0.8	0.81	0.66	5.96	0.69	0.49	1.07	0.78	0.00	0.5	0.9
Cr_2O_3	1.69	1.08	0.63	0.82	0.62	0.28	0.28	0.35	0.38	0.42	0.46	0.38	0.33	0.30	0.38	0.01	0.27	0.41
Fe_2O_3	5.14	4.42	1.80	4.37	2.27	2.01	1.42	1.1	1.44	1.53	1.68	1.51	2.61	3.03	1.86	3.36	1.0	1.3
FeO	11.57	10.27	7.55	10.78	7.46	5.22	4.50	4.3	5.04	5.03	6.29	4.83	4.66	4.48	4.38	12.05	5.0	4.4
MnO	0.14	0.15	0.14	0.22	0.12	0.09	0.11	0.11	0.06	0.04	0.13	0.09	0.06	0.09	0.08	0.13	-	0.11
NiO	0.44	0.39	0.27	0.23	0.28	0.32	0.28	-	0.31	0.34	0.16	0.32	0.36	0.27	0.31	0.11	-	-
MgO	40.70	42.55	35.80	29.24	35.65	43.27	42.29	42.7	44.96	44.28	27.92	44.91	41.15	41.06	45.13	43.08	44.7	40.8
CaO	0.37	0.55	2.64	3.70	2.50	0.52	0.69	0.5	0.18	0.37	4.96	0.36	0.77	1.22	0.55	0.07	0.4	0.5
Na_2O	0.05	0.03	0.34	0.85	0.33	0.18	0.10	<0.1	0.02	0.12	0.24	0.05	0.17	0.11	0.24	0.02	0.1	0.1
K_2O	0.02	0.04	0.07	0.12	0.13	0.39	0.14	<0.1	0.01	0.11	0.15	0.08	0.15	0.37	0.22	0.03	0.1	0.1
P_2O_5	0.02	0.04	0.03	0.03	0.05	0.04	0.04	0.01	0.00	0.03	0.01	0.01	0.05	0.05	0.08	0.02	0.05	0.01
S	0.01	0.00	0.03	0.04	0.08	0.04	0.09	0.12	0.02	0.02	0.06	0.03	0.02	0.07	0.02	0.02	0.02	0.02
H_2O^+	0.93	0.97	2.29	1.64	1.99	4.16	4.98	4.3	2.98	2.66	1.30	3.51	4.27	5.97	3.78	2.35	3.5	3.5
CO_2	0.73	0.65	0.34	0.00	0.24	0.25	0.35	0.22	0.00	0.00	0.16	0.00	0.37	0.59	0.00	0.00	0.14	0.11
TOTAL	100.29	99.88	100.47	100.83	99.90	100.55	99.27	99.55	99.48	99.82	99.63	100.47	99.51	100.90	100.96	100.08	99.44	99.56
Rb ppm	4	3	3	11	1	16	3	-	2	7	5	7	8	20	7	3	-	-
Sr	17	44	41	111	36	43	37	-	0	39	16	13	68	108	65	6	-	-
Ba	12	49	74	269	80	322	50	-	16	66	57	43	300	102	75	18	-	-
V	113	42	59	80	59	26	24	-	19	33	121	18	27	29	31	3	-	-
Zn	77	67	50	108	52	43	38	-	36	37	38	35	44	44	37	109	-	-
Cu	30	23	29	49	31	24	13	-	10	18	113	7	15	12	11	15	-	-
100Mg/Mg+Fe	81.7	84.2	87.4	78.0	87.0	89.7	92.9	93.5	92.7	92.5	86.4	92.8	91.3	91.0	93.0	83.6	93.1	92.9
100Cr/Cr+Al	39.3	37.4	8.5	7.1	8.7	20.9	18.3	22.7	23.9	29.9	5.1	27.0	31.1	15.8	24.6	-	26.6	23.4

+ Analyses by P. Kresten at University of Stockholm. All other analyses performed in Department of Geology, University of Sheffield mainly by X-ray fluorescence

TABLE 3
Analyses of Olivines in Nodule Samples

Sample Number	LIP 1	LIP 2	LIP 3	LIP 4	LIP 5	LIP 6	LIP 7	PHN 1899	PHN 1905	PHN 2867	PHN 2868	PHN 2870	PHN 2871	PHN 2872
SiO_2	39.8	38.8	39.6	39.1	39.5	38.3	39.6	41.0	41.2	41.4	41.2	41.2	41.3	41.5
FeO	15.2	15.5	14.7	17.9	11.5	18.9	11.4	7.38	6.57	6.39	7.13	7.08	6.94	7.33
MnO	0.13	-	0.11	0.18	0.27	0.35	0.25	0.0	0.17	0.07	0.16	0.0	-	0.17
MgO	45.4	45.4	45.7	42.9	48.2	42.1	48.3	51.4	52.1	51.6	51.9	51.8	51.9	51.6
Total	100.4	99.6	100.0	100.0	99.4	99.7	99.5	99.8	100.0	99.9	100.4	100.1	100.2	100.6
%Fo	84	84	85	81	88	80	88.5	92.5	93.5	93	93	93	93	92.5

Sample Number	PHN 2873/1	PHN 2873/2	PHN 2873/3	PHN 2873/4	PHN 2873/5	PHN 2873/6	PHN 2873/7	KN 5B1	KN 5B3
SiO_2	40.0	40.9	41.2	41.2	41.4	41.5	41.2	42.0	41.8
FeO	12.4	6.96	6.69	7.03	8.47	7.23	7.39	6.7	6.7
MnO	0.10	0.0	0.12	0.0	0.24	0.0	0.0	-	-
MgO	47.5	51.8	51.7	50.9	51.0	51.6	50.9	50.6	50.4
Total	100.0	99.6	99.7	99.3	99.2	100.2	99.5	99.3	98.9
%Fo	87	93	93	93	91.5	93	92.5	93	93

TABLE 7
Analyses of garnets, phlogopites and amphiboles in nodule samples

Sample No.	PHN 1905	PHN 1905	PHN 2873/1	PHN 2873/3	PHN 2873/5	PHN 2873/7	WLG 1
Mineral Phase	Gnt.	Phl.	Amph.	Gnt.	Phl.	Gnt.	Gnt.
SiO_2	42.0	41.3	45.1	41.7	40.0	41.6	41.8
TiO_2	0.0	0.10	0.50	0.0	3.21	-	-
Al_2O_3	20.6	13.5	12.1	21.9	14.1	21.5	22.2
Cr_2O_3	5.33	0.85	0.48	3.17	2.17	3.86	2.66
FeO^T	5.99	2.43	4.55	7.14	4.06	7.52	10.3
MnO	0.28	0.0	0.10	0.40	0.0	0.39	0.39
MgO	21.4	25.6	17.7	20.5	22.7	19.8	19.0
CaO	5.56	0.14	12.5	5.55	0.0	5.76	5.03
Na_2O	-	0.18	1.52	-	0.27	-	-
K_2O	-	10.3	0.40	-	9.84	-	-
TOTAL	101.1	94.4	95.0	100.4	96.4	100.4	101.4

FeO^T - Total Fe as FeO

GNT = Garnet; PHL = Phlogopite; AMPH = Amphibole

TABLE 4

Analyses of Orthopyroxenes in Nodule Samples

Sample Number	LIP 2	LIP 4	LIP 5	LIP 6	LIP 7	PHN 1899	PHN 1905	PHN 2867	PHN 2867	PHN 2868	PHN 2868	PHN 2870	PHN 2871	PHN 2872	PHN 2872
Form	D^1	D^1	D^1	D^1	D^1	D^1	D^1	D^1	D^2	D^1	D^2	D^1	D^1	D^1	D^2
SiO_2	55.0	55.0	54.9	53.9	54.7	57.5	57.4	57.4	56.9	56.0	56.4	56.4	56.4	56.6	56.8
TiO_2	0.13	0.0	0.10	-	0.21	-	0.0	0.0	0.0	0.0	0.0	0.0	0.0	0.0	0.0
Al_2O_3	1.89	1.56	3.27	2.84	3.22	0.96	0.99	2.23	1.62	3.01	2.43	2.37	2.37	2.48	1.62
Cr_2O_3	0.20	0.18	0.22	0.14	0.22	0.24	0.42	0.36	0.26	0.61	0.37	0.66	0.44	0.48	0.36
FeO^T	9.69	11.89	7.73	12.0	7.56	4.66	4.01	4.30	4.78	4.44	4.88	4.64	4.49	4.78	4.66
MnO	-	0.26	0.27	0.37	0.26	0.23	0.0	0.13	0.09	0.30	0.15	0.10	0.10	0.17	0.0
MgO	32.4	31.0	32.8	30.0	32.9	36.2	36.2	35.3	35.4	35.4	35.4	35.2	35.6	35.9	35.5
CaO	0.15	0.37	0.39	0.39	0.47	0.20	0.45	0.47	0.17	0.28	0.25	0.39	0.25	0.32	0.21
Total	99.5	100.3	99.7	99.6	99.5	100.0	99.5	100.2	99.2	100.0	99.9	99.8	99.6	100.7	99.2
Structural Formulae on the Basis of 6.000 Oxygens															
Si	1.938	1.944	1.915	1.919	1.912	9.967	1.970	1.957	1.963	1.920	1.936	1.938	1.938	1.928	1.959
Ti	0.003	0.000	0.003	-	0.005	-	0.000	0.000	0.000	0.000	0.000	0.000	0.000	0.000	0.000
Al	0.078	0.065	0.134	0.119	0.133	0.038	0.040	0.090	0.066	0.122	0.098	0.096	0.096	0.100	0.066
Cr	0.006	0.005	0.006	0.004	0.006	0.006	0.011	0.010	0.008	0.016	0.010	0.018	0.012	0.013	0.010
Fe	0.286	0.352	0.226	0.358	0.221	0.133	0.115	0.123	0.138	0.127	0.140	0.133	0.129	0.136	0.134
Mn	-	0.008	0.008	0.011	0.008	0.007	0.000	0.004	0.003	0.009	0.004	0.003	0.003	0.005	0.000
Mg	1.699	1.634	1.708	1.594	1.712	1.850	1.851	1.795	1.817	1.806	1.811	1.804	1.821	1.822	1.826
Ca	0.006	0.014	0.015	0.015	0.018	0.007	0.016	0.017	0.006	0.010	0.009	0.014	0.009	0.012	0.008
%En	85.6	82.3	88.3	81.7	88.6	93.3	94.2	93.6	92.9	93.4	92.8	93.1	93.4	93.0	93.1

TABLE 4

Analyses of Orthopyroxenes in Nodule Samples (continued)

Sample Number	PHN 2873/1	PHN 2873/2	PHN 2873/3	PHN 2873/4	PHN 2873/4	PHN 2973/5	PHN 2873/6	PHN 2873/6	PHN 2873/7	KN 5B1	KN 5B3	WLG 1
Form	D^1	D^1	D^1	D^1	S	D^1	D^1	S	D^1	D^1	D^1	Host
SiO_2	55.1	56.4	57.4	56.7	57.6	57.7	56.6	57.6	57.6	56.8	57.9	57.3
TiO_2	0.0	0.0	0.0	0.0	0.0	0.0	0.0	0.0	0.0	-	-	-
Al_2O_3	2.82	2.38	0.98	2.52	1.75	0.96	2.56	1.20	1.21	2.42	1.38	1.07
Cr_2O_3	0.10	0.59	0.29	0.40	0.34	0.27	0.59	0.50	0.27	0.70	0.52	0.26
FeO^T	8.94	4.64	4.45	4.63	4.75	4.93	4.77	4.71	4.56	4.36	4.50	6.84
MnO	0.20	0.10	0.12	0.09	0.08	0.22	0.10	0.12	0.10	-	-	0.10
MgO	32.6	35.3	36.4	35.0	36.0	35.9	34.9	35.6	36.0	34.5	35.1	34.8
CaO	0.35	0.49	0.18	0.43	0.04	0.43	0.47	0.36	0.30	0.47	0.29	0.36
Total	100.1	99.9	99.8	99.8	100.6	100.4	100.0	100.1	100.0	99.3	100.2	100.7
Structural Formulae on the Basis of 6.000 Oxygens												
Si	1.923	1.935	1.967	1.946	1.959	1.970	1.940	1.970	1.969	1.956	1.973	1.966
Ti	0.000	0.000	0.000	0.000	0.000	0.000	0.000	0.000	0.000	-	-	-
Al	0.116	0.096	0.040	0.102	0.070	0.039	0.104	0.048	0.049	0.098	0.076	0.043
Cr	0.003	0.016	0.008	0.011	0.009	0.007	0.016	0.014	0.007	0.019	0.014	0.007
Fe	0.261	0.133	0.128	0.133	0.135	0.141	0.137	0.135	0.130	0.126	0.128	0.196
Mn	0.006	0.003	0.004	0.003	0.002	0.006	0.003	0.004	0.003	-	-	0.003
Mg	1.697	1.808	1.857	1.788	1.825	1.829	1.783	1.816	1.835	1.770	1.782	1.781
Ca	0.013	0.018	0.007	0.016	0.002	0.016	0.017	0.013	0.011	0.017	0.011	0.013
%En	86.7	93.1	93.6	93.1	93.1	92.8	92.9	93.1	93.4	93.4	93.3	90.1

FeO^T Total Fe taken as FeO

D^1 Discrete grains, apparently primary

D^2 Recrystallised smaller neoblasts

S Intergrown with spinel in symplectites

TABLE 5

Analyses of Clinopyroxenes in Nodule Samples

Sample Number	LIP 1	LIP 2	LIP 3	LIP 4	LIP 5	LIP 6	LIP 7	PHN 1899	PHN 2867	PHN 2868	PHN 2870	PHN 2871	PHN 2872
Form	D[1]	D[1]	D[1]	D[1]	D[1]	D[1]	D[1]	D[1]	D[1]	D[2]	D[1]	D[1]	D[2]
SiO_2	52.2	52.2	51.4	53.1	53.1	52.2	53.0	53.6	52.8	53.7	53.5	53.9	54.0
TiO_2	0.71	0.50	0.99	0.21	-	1.30	-	0.38	0.14	0.0	0.0	0.0	0.0
Al_2O_3	4.06	4.48	4.82	3.37	6.06	6.42	6.19	0.93	2.19	3.76	2.31	2.56	1.87
Cr_2O_3	0.78	0.95	1.25	0.73	0.54	0.51	0.60	0.68	1.21	1.21	0.91	1.00	1.03
FeO^T	3.04	3.41	3.38	4.28	2.46	4.33	2.39	3.90	1.23	1.20	1.29	0.93	1.15
MnO	0.0	-	0.0	0.12	0.13	0.14	0.14	0.28	0.0	0.11	0.0	0.20	0.16
MgO	14.8	15.0	14.4	15.0	14.3	12.8	14.2	19.1	17.3	16.1	17.2	16.6	17.2
CaO	22.3	21.3	21.6	20.9	20.5	18.7	19.8	19.7	23.4	22.4	23.6	22.9	23.5
Na_2O	1.68	1.79	1.94	2.07	2.81	3.42	2.73	1.01	0.71	1.44	0.90	1.01	0.92
Total	99.6	99.6	99.8	99.8	99.9	99.8	99.1	99.6	99.0	99.9	99.7	99.1	99.8
Structural Formulae on the Basis of 6.000 Oxygens													
Si	1.913	1.910	1.886	1.944	1.922	1.904	1.930	1.958	1.936	1.940	1.946	1.963	1.959
Ti	0.020	0.014	0.027	0.006	-	0.036	-	0.010	0.004	0.000	0.000	0.000	0.000
Al	0.176	0.193	0.209	0.146	0.259	0.276	0.266	0.040	0.095	0.160	0.099	0.110	0.080
Cr	0.023	0.028	0.036	0.021	0.016	0.015	0.017	0.020	0.035	0.035	0.026	0.029	0.030
Fe	0.093	0.104	0.104	0.131	0.074	0.132	0.073	0.119	0.038	0.036	0.039	0.028	0.035
Mn	0.000	-	0.000	0.004	0.004	0.004	0.004	0.009	0.000	0.003	0.000	0.006	0.005
Mg	0.809	0.818	0.789	0.821	0.772	0.694	0.769	1.039	0.944	0.869	0.932	0.900	0.930
Ca	0.877	0.836	0.848	0.820	0.796	0.733	0.774	0.770	0.920	0.868	0.918	0.895	0.916
Na	0.119	0.127	0.138	0.147	0.197	0.242	0.193	0.072	0.050	0.101	0.063	0.071	0.065
%CaTiTs	1.9	1.4	2.7	0.6	-	3.5	-	1.1	0.4	0.0	0.0	0.0	0.0
% CaTs	6.2	7.7	7.5	6.3	9.1	4.2	8.2	0.0	2.8	6.6	3.9	3.8	3.3
% Jad	1.2	1.0	0.2	0.6	7.8	11.9	10.1	0.0	0.0	2.8	0.0	3.3	0.0
% Kosm.	2.2	2.7	3.6	2.1	1.5	1.5	1.7	2.0	3.6	3.4	2.6	2.9	3.0
% Acm.	8.4	8.9	9.9	11.8	7.5	11.9	7.2	5.2	1.6	3.6	3.8	0.9	3.5
% Di	78.1	72.5	73.5	73.0	70.3	62.3	68.4	71.5	88.1	79.7	88.5	83.2	88.1

TABLE 5

Analyses of Clinopyroxenes in Nodule Samples (continued)

Sample Number	PHN 2873/1	PHN 2873/2	PHN 2873/4	PHN 2873/5	PHN 2873/6	KN 5B1	WLG 1
Form	D^1	D^2	S	D^1	S	S	EX
SiO_2	52.4	53.4	53.9	53.8	53.6	54.0	54.2
TiO_2	0.10	0.00	0.00	0.24	0.00	-	-
Al_2O_3	1.89	1.90	2.30	2.85	1.99	1.94	2.45
Cr_2O_3	0.17	0.87	0.97	1.78	1.02	1.16	1.54
FeO^T	2.38	1.11	1.29	2.38	1.52	1.30	3.05
MnO	0.10	0.14	0.05	0.00	0.00	-	0.0
MgO	17.1	17.2	17.6	16.6	16.9	16.8	16.0
CaO	24.6	23.5	23.9	19.3	23.6	23.0	20.7
Na_2O	0.22	0.82	0.78	2.25	0.90	0.84	2.07
Total	99.0	98.9	100.8	99.2	99.5	99.0	100.0
Structural Formulae on the Basis of 6.000 Oxygens							
Si	1.933	1.955	1.939	1.962	1.954	1.971	1.969
Ti	0.003	0.000	0.000	0.007	0.000	-	-
Al	0.082	0.082	0.098	0.122	0.086	0.084	0.105
Cr	0.005	0.025	0.028	0.051	0.029	0.036	0.044
Fe	0.073	0.034	0.039	0.072	0.046	0.040	0.093
Mn	0.003	0.004	0.002	0.000	0.000	-	0.000
Mg	0.940	0.940	0.945	0.899	0.918	0.914	0.867
Ca	0.974	0.922	0.921	0.752	0.924	0.900	0.806
Na	0.016	0.058	0.054	0.159	0.064	0.059	0.146
% CaTiTs	0.3	0.0	0.0	0.7	0.00	-	-
% CaTs	1.3	3.2	3.3	3.7	3.4	2.9	4.6
% Jad.	0.0	0.0	0.0	3.4	0.0	2.5	1.3
% Kosm.	0.5	2.5	2.8	5.1	3.0	3.3	4.6
% Acm.	1.1	3.3	2.7	7.2	3.4	0.1	8.8
% Di	90.5	89.2	88.9	70.4	88.4	83.5	75.1

FeO^T Total Fe taken as FeO

D^1 Discrete grains apparently primary

D^2 Recrystallised smaller neoblasts

S Intergrown with spinel in symplektites

EX Exsolved from orthopyroxene

TABLE 6

Analyses of Spinels in Nodule Samples

Sample Number	LIP 1	LIP 3	LIP 4	LIP 5	LIP 6	LIP 7	PHN 1899	PHN 1899	PHN 2868	PHN 2870	PHN 2871	PHN 2872
Form	D	D	D	D	D	D	D^1	D^2	D	D	D	D
SiO_2	-	-	-	-	-	-	-	-	0.0	-	0.0	-
TiO_2	1.67	0.87	0.93	0.0	0.0	-	-	-	0.0	-	0.0	-
Al_2O_3	26.9	27.4	20.3	56.5	52.1	56.6	31.4	10.3	47.0	34.2	37.9	31.5
Cr_2O_3	28.2	30.9	30.0	10.8	11.3	11.0	40.3	59.4	23.6	36.1	33.8	39.3
$*Fe_2O_3$	10.8	9.51	16.5	1.09	3.44	1.05	0.70	3.81	0.18	0.70	0.0	0.05
FeO	25.3	21.8	24.8	12.9	19.5	13.0	12.5	16.2	10.0	11.0	11.2	12.0
MnO	0.28	0.23	0.39	0.16	0.10	0.0	0.56	0.0	0.0	0.21	0.10	0.41
MgO	8.17	9.93	6.99	18.2	13.5	18.2	15.9	11.7	19.3	17.0	17.6	15.9
Total	101.3	100.6	100.0	99.6	99.9	99.8	101.4	101.4	100.1	99.2	100.6	99.2
100 Cr/Cr+Al	41.3	42.7	49.7	11.5	12.7	11.5	46.3	79.5	25.2	41.5	37.4	45.6
100 $Fe^{2+}/Fe^{2+}+Mg$	63.8	55.5	66.9	28.7	44.9	28.6	31.6	43.6	22.6	27.0	26.5	30.3
Structural Formulae on the Basis of 4.000 Oxygens												
Si	-	-	-	-	-	-	-	-	-	-	-	-
Ti	0.039	0.020	0.023	-	-	-	-	-	-	-	-	-
Al	0.981	0.991	0.778	1.754	1.684	1.751	1.066	0.391	1.492	1.161	1.251	1.087
Cr	0.690	0.749	0.770	0.224	0.245	0.228	0.919	1.516	0.504	0.823	0.749	0.911
$*Fe^{3+}$	0.251	0.220	0.406	0.022	0.071	0.021	0.015	0.093	0.004	0.015	0.000	0.001
Fe^{2+}	0.655	0.560	0.673	0.283	0.446	0.286	0.302	0.436	0.226	0.265	0.263	0.293
Mn	0.007	0.006	0.011	0.004	0.002	-	0.014	-	-	0.005	0.002	0.010
Mg	0.376	0.454	0.339	0.713	0.551	0.714	0.684	0.564	0.774	0.730	0.735	0.696
% $M^{2+}Cr_2O_4$	35.9	38.2	39.4	11.2	12.2	11.4	45.9	75.8	25.2	41.2	37.5	45.4
% $M^{2+}Al_2O_4$	51.0	50.6	39.8	87.7	84.2	87.6	53.3	19.6	74.6	58.0	62.5	54.4
% $M^{2+}Fe_2^{3+}O_4$	13.1	11.2	20.8	1.1	3.6	1.0	0.8	4.6	0.2	0.8	0.0	0.1

TABLE 6

Analyses of Spinels in Nodule Samples (continued)

Sample Number	PHN 2873/1	PHN 2873/2	PHN 2873/3	PHN 2873/4	PHN 2973/4	PHN 2873/6	KN 5B1	KN 5B1	KN 5B3
Form	D	D	D	D	S	S	D	S	D
SiO_2	0.0	-	0.0	0.0	0.0	0.47	-	0.71	0.26
TiO_2	0.0	-	0.0	0.0	0.0	0.0	-	-	-
Al_2O_3	58.2	32.6	18.6	43.5	42.6	33.3	32.7	33.4	29.0
Cr_2O_3	6.89	38.8	52.9	27.4	28.1	35.9	36.3	35.4	41.6
$*Fe_2O_3$	3.93	0.65	1.92	0.07	0.52	0.96	0.67	0.55	1.22
FeO	13.7	10.8	13.1	10.5	9.81	11.4	11.2	11.2	10.8
MnO	0.18	0.10	0.18	0.12	0.33	0.46	0.61	0.35	0.52
MgO	18.1	17.2	14.4	18.5	18.7	16.9	16.1	17.2	16.8
Total	101.0	100.0	101.1	100.1	100.1	99.4	97.6	98.8	100.2
100 Cr/Cr+Al	7.4	44.4	65.7	29.7	30.6	42.0	42.7	41.5	49.0
100 $Fe^{2+}/Fe^{2+}+Mg$	30.0	26.1	34.0	24.4	23.3	28.1	29.2	27.4	27.4
Structural Formulae on the Basis of 4.000 Oxygens									
Si	-	-	-	-	-	0.014	-	0.021	0.008
Ti	-	-	-	-	-	-	-	-	-
Al	1.781	1.104	0.671	1.404	1.379	1.133	1.137	1.138	0.998
Cr	0.141	0.881	1.285	0.594	0.610	0.819	0.847	0.809	0.960
Fe^{3+}	0.077	0.014	0.044	0.001	0.011	0.021	0.015	0.012	0.027
Fe^{2+}	0.296	0.259	0.335	0.241	0.225	0.274	0.276	0.271	0.264
Mn	0.004	0.002	0.005	0.003	0.008	0.011	0.015	0.009	0.013
Mg	0.699	0.739	0.660	0.756	0.767	0.728	0.708	0.741	0.731
% $M^{2+}Cr_2O_4$	7.1	44.1	64.3	29.7	30.5	41.5	42.4	41.3	48.4
% $M^{2+}Al_2O_4$	89.1	55.2	33.5	70.2	69.0	57.4	56.9	58.1	50.3
% $M^{2+}Fe_2^{3+}O_4$	3.8	0.7	2.2	0.1	0.5	1.1	0.7	0.6	1.3

$*Fe^{3+}$ Calculated by charge balance in the structural formulae

TABLE 8

Scan analyses of pyroxene-spinel symplectites in nodule PHN 2870

	4	6	10	Average of 6
SiO_2	39.04	37.98	42.07	36.34
Al_2O_3	10.16	9.59	8.78	9.73
Cr_2O_3	9.99	9.97	8.93	9.71
FeO	4.09	4.27	3.84	4.97
MnO	(0.16)	(0.05)	(0.10)	(0.10)
MgO	17.72	17.33	17.23	18.41
CaO	16.25	15.78	17.79	13.18
Na_2O	1.05	1.02	0.82	0.79
Σ	98.46	95.99	99.53	93.11

O = 16

Si	3.996	3.995	4.236	3.891
Al	1.226	1.189	1.041	1.254
Cr	0.808	0.829	0.710	0.839
Fe	0.350	0.370	0.321	0.460
Mg	2.704	2.717	2.584	3.013
Ca	1.782	1.778	1.918	1.495
Na	0.209	0.208	0.157	0.166

O = 12, after subtraction of olivine = $\frac{1}{2}$ ($\Sigma M^{2+} - \frac{3}{2} \Sigma M^{3+}$) (ignoring Na)

Si	3.026	3.025	3.253	2.920
Al	1.195	1.169	1.079	1.230
Cr	0.788	0.815	0.768	0.823
Fe	0.167	0.183	0.105	0.271
Mg	1.070	1.045	0.630	1.341
Ca	1.738	1.746	1.988	1.467

Contrib Mineral Petrol (1987) 95:499–511

Contributions to Mineralogy and Petrology

Evaluation of mineral thermometers and barometers applicable to garnet lherzolite assemblages

D.A. Carswell and F.G.F. Gibb
Department of Geology, University of Sheffield, Mappin Street, Sheffield S1 3JD, UK

Abstract. We have tested the ability of some 12 different barometer and 20 different thermometer formulations to reproduce the experimental $P-T$ equilibration conditions of 'natural' multi-component garnet lherzolite assemblages. For natural rock compositions it is essential to take account of the influence of both Cr and Fe on the garnet-orthopyroxene Al exchange reaction customarily used as a barometer for such assemblages and accordingly our results demonstrate that the formulation of Nickel and Green (1985) is the most satisfactory. No single thermometer formulation was judged to be reliable throughout the $P-T$ range of interest. In our view equilibration temperatures are best assessed by consideration of a combination of the most satisfactory thermometer formulations, based on the two-pyroxene solvus and the $Fe^{2+}-Mg^{2+}$ exchange reactions between mineral pairs. Our results further indicate that use of the barometer (MacGregor 1974) and thermometer formulations recommended by Finnerty and Boyd (1984 and 1986) will lead to inaccurate assessment of the temperatures and pressures of equilibration for most garnet lherzolite xenolith assemblages and hence to incorrect interpretation of their depth of derivation within the mantle.

Background

Garnet lherzolite assemblages (olivine + orthopyroxene + clinopyroxene + garnet) in ultramafic rocks with upper mantle geochemical affinities are occasionally preserved in alpine-type peridotite bodies which probably mark the sites of palaeo-continental plate collision sutures within exhumed deep level, high pressure, crustal metamorphic complexes (e.g., Carswell and Gibb 1980a; Carswell 1986; Carswell and Cuthbert 1986). They are more extensively recorded as xenoliths (nodules) brought up by volatile charged alkaline eruptives, notably kimberlites (e.g., Nixon and Boyd 1973; Ringwood 1975; Sobolev 1977; Dawson 1980; Carswell 1980).

In recent years there has been considerable interest in the application of various mineral thermometers and barometers to these assemblages with a view to deducing their depths of derivation. Moreover there has been a steady increase in the number of available calibrations proposed for the various element exchange equilibria which form the basis of these thermometers and barometers. However, there is currently little or no consensus as to which particular calibrations provide the most accurate and hence geologically meaningful values for the equilibration temperatures (T) and pressures (P) of such garnet lherzolite assemblages.

Previously we presented (Carswell and Gibb 1980b) a comparison of the thermometers then available, using garnet lherzolite xenoliths from the kimberlites of northern Lesotho (southern Africa) as a test sample suite. There is good evidence that the different textural types of these garnet lherzolite xenoliths (Nixon and Boyd 1973; Boyd 1973; Carswell et al. 1979) have equilibrated over a wide temperature range-probably of the order of 500 °C. From calculated results we selected five thermometers judged to be the best then available, since they consistently gave results closest to the mean temperature value for all ten of the methods tested for each particular xenolith sample. This approach led us to reject those thermometers judged to be inaccurate and/or imprecise. We concluded that without being excessively subjective we could do no better than recommend that, at the then current 'state of the art', the best available temperature estimate for each xenolith was an average of the temperatures given by the five selected thermometers. This recommendation was subsequently criticised by Finnerty and Boyd (1984) on the grounds that there was no reason to accept the mean temperature derived from the five thermometers as any more accurate than an estimate made with just one thermometer.

Following a rather different approach, Finnerty and Boyd (1984, 1986) attempted a test of the accuracy of selected pairings of thermometers and barometers through reference to the $P-T$ constraints provided by experimental data on the diamond-graphite univariant transition (Kennedy and Kennedy 1976) and on phlogopite stability (Eggler and Wendlandt 1979). Finnerty and Boyd (1984) concluded that the most accurate $P-T$ values for the northern Lesotho garnet lherzolite xenolith suite were those obtained by a combination of a two-pyroxene solvus thermometer based on the experimental data of Lindsley and Dixon (1976) for the diopside limb of the diopside-enstatite miscibility gap in the simple $CaO-MgO-SiO_2$ (CMS) system, with a barometer based on the experimental data of MacGregor (1974) for the Al_2O_3 content of orthopyroxene coexisting with garnet in the $MgO-Al_2O_3-SiO_2$ (MAS) system. This choice seemed surprising to us on several grounds.

Firstly, the selected calibration of the two-pyroxene solvus thermometer assumes a fixed pressure value of 20 kbar

Offprint requests to: D.A. Carswell

and thus takes no account of the influence of pressure on the solvus as stressed by Lindsley and Dixon (1976) themselves. Neither does it incorporate any corrections to take account of the expected effect on the solvus relationships (cf. Wells 1977; Nickel et al. 1985) of additional chemical components (notably Fe, Al, Cr and Na) in the pyroxenes present in natural garnet lherzolite assemblages. In acknowledgement of this latter problem, Finnerty and Boyd (1984) did attempt to minimise the influence of Fe and the other components through calculation of the enstatite component in these natural clinopyroxenes as 1-[2Ca/(Ca + Mg)]. The use of a barometer based simply on the uncorrected wt.% Al_2O_3 isopleths of MacGregor (1974) for enstatite coexisting with pyrope in the MAS system may be questioned on similar grounds. Several other experimental studies (e.g., MacGregor 1970; O'Neill 1981; Harley 1984a; Nickel and Green 1985; Webb and Wood 1986) have demonstrated the profound influence exerted on garnet-orthopyroxene equilibria by additional components (such as Fe, Cr and Ca) in natural mineral assemblages.

Finnerty and Boyd (1986) have provided a revised evaluation which considers thermometer and barometer calibrations which have become available since their earlier paper. The barometer based on the MacGregor (1974) data is still judged to be the best available in terms of meeting their imposed petrologic constraints. However, they have presented a revised formulation for the two-pyroxene solvus thermometer which comprises a geometrically constrained empirical fit of the diopside limb which takes account of the more recent reversed experimental determinations of the two-pyroxene miscibility gap at pressures up to 60 kbar (Nickel and Brey (1984); Brey and Huth (1984)). This formulation (Finnerty and Boyd (1986) thus incorporates a pressure correction, though the magnitude of the pressure effect on the miscibility gap is considerably less than that indicated by the earlier experimental data of Lindsley and Dixon (1976). Finnerty and Boyd (1986) consider that their formulation currently yields the most accurate equilibration T values for garnet lherzolite xenolith assemblages and is preferable to the thermodynamically modelled formulations for enstatite and diopside component exchange, based on essentially the same data, given by Nickel and Brey (1984).

The assessments by Finnerty and Boyd (1984, 1986) of the 'best' available thermometer and barometer have been largely governed by the locations in $P-T$ space of calculated values for one diamond bearing xenolith (BD2125; Dawson and Smith 1975) and one primary graphite bearing xenolith (PHN1569; Nixon and Boyd 1973) relative to the diamond⇌graphite inversion curve of Kennedy and Kennedy (1976). Not only is the number of constrained xenolith samples involved uncomfortably small but other experimental (Bundy et al. 1961; Bundy 1980) and thermodynamic (Berman 1979) data on the diamond-graphite transition suggest that the location in $P-T$ space of the Kennedy and Kennedy (1976) curve may be in error by some 100° C or 2.5 kbar, in the range of $P-T$ values concerned. As admitted by Finnerty and Boyd (1984), the additional phlogopite constraint is poor because of uncertainty in the $P-T$ location of the stability curve for natural phlogopites.

Approach

The accuracy of thermometer and barometer formulations based on experimentally determined phase equilibria is crucially dependent on a number of factors, mostly associated with the experiments themselves, which can be very difficult to assess. For example, unless the reaction in question has been reversed experimentally considerable doubt must exist as to whether true equilibrium has been obtained and even when reactions have been reversed they may not have been bracketed tightly enough for accurate thermometer/barometer formulations. Also, errors are often present in recorded experimental temperature and pressure values (particularly in the piston/cylinder apparatus experiments generally used for the type of thermometers and barometers in question). Still further uncertainty arises from the necessarily large extrapolations involved (a) in applying experimental data derived from relatively simple systems to the much more chemically complex natural rocks, and (b) in extending the $P-T$ ranges of the thermometers and/or barometers beyond the generally limited ranges of experimental values. Attempts have been made to apply thermodynamically derived corrections to allow such extrapolations but the data on which these are themselves based are often meagre and/or subject to equally large uncertainties.

With so many sources of possible error, most of which are extremely difficult to quantify (not least because of the frequent paucity of published detail concerning experimental conditions), there is little prospect of being able to evaluate the cumulative effects of such errors and the most useful exercise is to attempt an evaluation of the overall accuracy of the thermometers and barometers.

Previous attempts to do this for mineral thermometers and barometers applicable to general lherzolite assemblages (Carswell and Gibb 1980b; Finnerty and Boyd 1984, 1986) have all involved calculation of $P-T$ values from mineral analyses for naturally occurring xenolith assemblages using specific pairings of thermometers and barometers (termed thermobarometers by Finnerty and Boyd). Since the majority of available thermometers include a pressure term and all barometers a temperature term, the $P-T$ values have to be obtained either through simultaneous solution of two equations or by a reiterative calculation procedure. Either way propagation of any errors will occur, whether arising from the use of inaccurate and/or imprecise thermometers or barometers or from poor quality mineral analyses. Consequently it is difficult to judge where the sources of error lie in the $P-T$ values calculated from a paired thermometer/barometer for any particular xenolith sample.

Accordingly we report here results obtained from a radically different approach to the evaluation of the accuracy of the various available thermometers and barometers. This has involved testing each thermometer and barometer independently against experimentally calibrated mineral composition data for 'natural' multi-component garnet lherzolite assemblages. Such experimental data unfortunately are rather limited and may be subject to some of the errors and uncertainties mentioned above, but at least they provide a more rigorous test of individual thermometers and barometers than those previously attempted.

Calculation of equilibration temperatures and pressures for garnet lherzolite assemblages from mineral composition data has been facilitated by a highly flexible, interactive computer program (NODMINS 3) giving the operator complete freedom to choose which of 22 thermometers and 13 barometers are to be paired together to form the thermobarometer for calculation of $P-T$ values. Where the selected thermometer contains a pressure term and the ba-

rometer a temperature term, the calculation is performed on a reiterative basis until the change in the calculated values is less than 0.1 °C and 1 bar. Most importantly, there is also an option to enter a preset temperature or pressure value, a facility essential to the evaluation exercise reported here. A further important option is that the $P-T$ calculations may be done either on the mineral composition data as entered (usually electron microprobe analyses with all Fe expressed as FeO) or on recalculated mineral analyses where the respective values of Fe^{2+} and Fe^{3+} in garnet, clinopyroxene and orthopyroxene have been calculated by stoichiometric charge balance (e.g., Neumann 1976). Additional flexibility allows the use of different variants of certain mineral composition parameters (such as X^{gt}_{Ca}) in particular calculations.

Test data

Ideally the test data should satisfy the following requirements:

(i) Natural multi-component rock compositions and mineral phases should have been used in the experiments. These rock and mineral compositions and the experimental $P-T$ conditions should have been close to those observed with the naturally occurring garnet lherzolite assemblages.

(ii) Experimental procedures and run times should have been such as to ensure satisfactory equilibration of the mineral assemblages.

(iii) Good quality electron microprobe analyses of the coexisting mineral phases should be available.

The data which appear to meet these requirements best are those provided by Nickel (1983) and by Akella (1976).

The Nickel (1983) data are for two ultramafic rock compositions; TP-40 corresponding to Tinaquillo peridotite minus 40% olivine (Jaques and Green 1980) and TP-40C the same peridotite mix with 1.6% Cr_2O_3 added. These rock compositions were equilibrated at $T=1000$–$1400°$ C and $P=35$ kbar, with run times between 8 and 168 h. Mineral equilibration was judged by Nickel (1983) to have been generally good, especially at the higher temperatures. However, some Cr/(Cr+Al) zonation was recorded in garnets, especially in the lower T runs with the more chrome-rich composition TP-40C. In addition some Fe loss to Ag–Pd capsules was reported in the 1100° C and 1200° C runs which might be expected to affect thermometers based on Fe–Mg exchange between minerals due to possible differences in Fe loss rate from the different minerals.

Akella (1976) reported experimentally calibrated mineral composition data for a natural mineral mixture of forsteritic olivine + enstatitic orthopyroxene + diopsidic clinopyroxene + pyropic garnet designed to simulate naturally occurring garnet lherzolite assemblages. Experimental runs were done at 1100° C and 1300° C with pressures of 31, 38 and 44 kbar. It is claimed that considerable care was taken to ensure satisfactory equilibration and production of homogeneous mineral phases. Where necessary total run times were extended beyond 16 h by recycling sample runs two or three times. Loss of Fe was avoided by use of graphite capsules with tight-fitting lids.

Mori and Green (1978) have provided considerable mineral composition data on garnet lherzolite assemblages derived from experimental runs on a synthetic ultramafic composition and a natural mineral mix. Their experiments were conducted over a wider range of $P-T$ conditions, viz 950–1500° C and 30–40 kbar, but run times were mostly short and hence satisfactory equilibration was often in doubt. There was also uncertainty over possible Fe loss to capsules. The most pertinent set of experimental run data presented by Mori and Green (1978) is that for a mechanical mixture (C2) comprising an equal weight proportion of olivine, orthopyroxene, clinopyroxene and garnet separated from Norwegian garnet lherzolites. All their mineral composition data for runs on the sintered synthetic pyrolite minus 40% olivine composition (consisting of <1 micron size olivine, orthopyroxene, clinopyroxene, plagioclase, ilmenite and chromite) have been used as test data although some are of doubtful quality. The Mori and Green (1978) runs on synthetic glass rich in pyroxene components or its sintered equivalent have, however, been excluded.

Mineral composition data from Kushiro et al. (1972) for a garnet lherzolite assemblage formed at 1450° C and 30 kbar from a starting material comprising a mix of natural olivine, orthopyroxene, clinopyroxene and garnet separated from a garnet lherzolite xenolith in kimberlite, to which 2 wt% synthetic fluor-phlogopite was added, have also been considered. However, the run time involved was only 50 min and our results clearly indicate extremely poor equilibration in this assemblage.

Finally, the early experimental data provided by Green (1973) for a garnet lherzolite assemblage formed at 30 kbar, 1250° C from a pyrolite minus 40% olivine composition and on mineral phases found near the liquidus of an olivine-rich basanite at 27–29 kbar, 1220–1260° C have been scrutinised but rejected as unsatisfactory. Our tests using these data indicated very poor chemical equilibration within these experimental charges (especially with respect to $Fe^{2+}-Mg^{2+}$ exchange reactions). Moreover the quality of the mineral analyses provided is poor as demonstrated, for example, by the poor cation totals in the calculated structural formulae.

Doubts over whether satisfactory equilibration was achieved in some of the experimental data employed means that our thermometer and barometer tests were not as rigorous as we would wish, but are the best that can be done with the experimental data available.

Barometers tested

Experience has indicated that the content of Al^{3+} cations in the octahedral sites (M1) in orthopyroxene coexisting with garnet is particularly pressure dependent and thus provides the best means of assessing the equilibration pressures of garnet lherzolite assemblages. Hence 11 out of 12 of the barometer variants tested here (barometer P10 is the exception) are based on this orthopyroxene composition parameter. Most of the experimental data on which the various barometer calibrations are based are for the simple MAS and CMAS systems (e.g., MacGregor 1974; Perkins and Newton 1980), but in some cases semi-empirical thermodynamically derived corrections (e.g., Wood 1974) have been introduced to take account of the more complex chemistries of the naturally occurring mineral assemblages. Most recently Nickel (1983), Nickel and Green (1985) have presented empirical barometer calibrations based on experimental data for the CMAS and $SiO_2-MgO-Al_2O_3-CaO-Cr_2O_3$ (SMACCR) systems. With the addition of thermodynamic/empirical corrections for the influence of FeO, their barometric formulations most closely model the compositions of naturally occurring garnet lherzolites.

Applications of all variants of this garnet-orthopyroxene barometer are subject to possible errors arising from uncertainty over the value of the X^{M1}_{Al} composition parameter in orthopyroxenes. The actual mineral reaction which forms the basis of this barometer may be expressed as:

$$(Mg\ Fe\ Ca)_2\ Si_2\ O_6 + (Mg\ Fe\ Ca)\ Al_2SiO_6$$
ORTHOPYROXENE
$$= (Mg\ Fe\ Ca)_3\ Al_2\ Si_3\ O_{12}$$
GARNET

In more chemically complex orthopyroxenes, any Cr^{3+}, Ti^{4+} and Fe^{3+} cations are usually taken to be restricted to the $M1^{[6]}$ sites whereas Al^{3+} cations are partitioned be-

tween the $M1^{[6]}$ and $Z^{[4]}$ sites depending on the $P-T$ conditions of formation.

Three different approaches are possible for the evaluation of X_{Al}^{M1} in orthopyroxenes from mineral analyses, using cation contents recalculated to the standard 6 oxygens.

(1) $Al^{[4]}$ may be calculated as $2.000-Si^{4+}$ and hence X_{Al}^{M1} as total Al^{3+} cations (Al^T) minus $Al^{[4]}$. A major problem with this is that the Al contents of orthopyroxenes in garnet lherzolite assemblages are rather low and hence the deduced partitioning of Al^{3+} cations between the $M1^{[6]}$ and $Z^{[4]}$ sites is seriously prone to even small errors in the SiO_2 analysis.

(2) X_{Al}^{M1} may be taken simply as half of the total Al^{3+} cations (Al^T). This assumes that all Al^{3+} cations are present as (Mg Fe Ca) Al_2SiO_6, i.e. Tschermak's molecule type substitutions.

(3) Allowing for the presence of Cr^{3+}, Ti^{4+} and Fe^{3+} in M1 and Na^+ in M2 sites, X_{Al}^{M1} may be taken as $[Al^T-(Cr^{3+}+Fe^{3+}+2Ti^{4+}-Na^+)]/2$. The term $(Cr^{3+}+Fe^{3+}+2Ti^{4+}-Na)$ corrects for the presence of Al^{3+} in $Z^{[4]}$ as in $MgCrAlSiO_6$, $MgFe^{3+}AlSiO_6$ and $MgTiAl_2O_6$ type molecules after first accounting for Cr^{3+} and Fe^{3+} combined with Na^+ in $NaCrSi_2O_6$ and $NaFe^{3+}Si_2O_6$. In the event of there being more Na^+ than $(Cr+Fe^{3+}+2Ti)$ then the Al^{3+} combined with Na^+ in $NaAlSi_2O_6$ has to be subtracted before calculation of X_{Al}^{M1}.

In several of the barometer variants tested X_{Al}^{M1} in orthopyroxene is taken as $Al^T/2$ as indicated by the original authors. However, since orthopyroxenes in garnet lherzolite assemblages contain significant contents of Cr^{3+} in particular there are strong arguments in favour of using the X_{Al}^{M1} values determined by the third approach (here termed X_{Al-Cr}^{M1}), as proposed by Nickel and Green (1985) for barometer P9. It should be noted that for three of the barometers tested (namely P4, P11 and P12), Finnerty and Boyd (1984, 1986) have fitted the experimental data concerned to equations of the form

$$\ln \frac{\text{wt\% } Al_2O_3^{opx}}{100} = \frac{a+bP}{T} + C.$$

Hence in these particular barometers, aluminium partitioning between orthopyroxene and garnet has been only rather crudely assessed as the weight fraction of Al_2O_3 in the orthopyroxene.

Summary details of the various barometer calibrations tested are as follows:

P1: equation (12) of Wood (1974) based on a combination of the experimental data of MacGregor (1974) for the MAS system and Wood (op. cit.) for the $FeO-MgO-Al_2O_3-SiO_2$ (FMAS) and $CaO-FeO-MgO-Al_2O_3-SiO_2$ (CFMAS) systems, with X_{Al}^{M1} taken as $Al^T/2$.

P2: equation (12) of Wood (1974) but with allowance made for Cr^{3+} contents by use of the modified X_{Al-Cr}^{M1} orthopyroxene parameter and with modification to the (l–y)gt composition parameter to take account of Cr substitution for Al in garnet.

P3: as P1 but with the addition of an extra term relating to Ca–Cr interaction in garnet as proposed by Finnerty and Boyd (1984).

P4: the Finnerty and Boyd (1984) formulation (A3) based on the MAS data of MacGregor (1974).

P5: equation (5) of Harley and Green (1982), a semi-empirical calibration based on experiments in the FMAS and CFMAS systems with X_{Al}^{M1} in orthopyroxene taken as $Al^T/2$.

P6: as P5 but with allowance for Cr, Ti and Na contents in orthopyroxene through use of the X_{Al-Cr}^{M1} composition parameter.

P7: equation (15) of Harley (1984a) based on FMAS and CFMAS experimental data as in Harley and Green (1982) but incorporating what was considered to be a more rigorous and thermodynamically reasonable regular solution model; X_{Al}^{M1} taken as $Al^T/2$.

P8: as P7 but with allowance for Cr, Ti and Na contents in orthopyroxene through use of the X_{Al-Cr}^{M1} composition parameter.

P9: equation (9) of Nickel and Green (1985) based on experiments in the CMAS and chrome bearing SMACCR systems with thermodynamic modelling and addition of Fe correction terms. As recommended, the modified X_{Al-Cr}^{M1} composition parameter has been used in the calculation.

P10: equation (105) of Nickel (1983), an empirical barometer which considers the Cr^{3+} content of orthopyroxene coexisting with garnet, again based on experiments in the CMAS and SMACCR systems with thermodynamic modelling and Fe correction. X_{Cr}^{M1} in orthopyroxene is taken as the total Cr^{3+} cation content in the standard 6 oxygens formula unit.

P11: the Finnerty and Boyd (1986) formulation from experimental data by Perkins et al. (1981) for the MAS system, modified by the assumption of linear rather than gently curved alumina isopleths.

P12: the Finnerty and Boyd (1986) formulation from experimental data by Perkins and Newton (1980) for the CMAS system.

Results of barometer tests

To facilitate comparison and assessment of the accuracy of the various barometers tested, our calculated pressures for the test data set are presented in Table 1 as differences between the calculated and experimentally recorded values.

In the light of earlier discussion over the procedures and compositions used to acquire the experimentally calibrated test data, it is considered that most weight should be placed on the Nickel (1983) and Akella (1976) data. Results for certain of the Mori and Green (1978) experiments (notably T9, FF7 and DD3) and for the Kushiro et al. (1972) run data are especially suspect probably due to poor equilibration.

All three variants (P1, P2 and P3) based on the Wood (1974) data tend to underestimate relative to P_{EXP}, though P3 least so. Indeed eliminating the anomalously high and low values from suspect experimental runs, the majority of P3 values are within $\pm 10\%$ relative of P_{EXP}. With the most Cr rich samples (TP40C and C2) P3 tends, in fact, to slightly overestimate unlike the case with most of the other test samples.

P4, the barometer favoured by Finnerty and Boyd (1984, 1986) based on the MacGregor (1974), data, can be seen almost invariably to overestimate seriously the pressures involved – especially for the most chromiferous samples. Consequently, we have little confidence in its ability to accurately measure the equilibration pressures of natural garnet lherzolite assemblages.

P11 and P12 based on the data of Perkins et al. (1981)

Table 1. Differences between calculated (P_{CALC}) and experimental (P_{EXP}) pressures for the tested barometers

Sample run	Ref	T_{EXP}	P_{EXP}	P1–P_{EXP}	P2–P_{EXP}	P3–P_{EXP}	P4–P_{EXP}	P5–P_{EXP}	P6–P_{EXP}	P7–P_{EXP}	P8–P_{EXP}	P9–P_{EXP}	P10–P_{EXP}	P11–P_{EXP}	P12–P_{EXP}
TP40	1	1000	35	−5.3	−4.6	−3.3	+1.4	−4.3	−1.8	−6.5	−4.3	−0.9	−3.2	−0.3	−1.8
TP40	1	1100	35	−4.1	−3.6	−1.5	+4.0	−3.3	−0.8	−6.0	−3.8	+0.3	−1.4	+1.1	+0.3
TP40	1	1200	35	−4.6	−5.9	−2.8	+3.5	−4.4	−4.1	−7.4	−7.2	−2.2	−3.0	+0.1	−0.8
TP40	1	1300	35	−2.6	−2.8	−0.5	+6.3	−3.3	−1.5	−4.8	−3.2	+0.3	same	+1.7	+1.6
TP40	1	1400	35	−3.5	−4.9	−1.5	+5.9	−4.8	−4.2	−5.7	−5.1	−1.1	−0.5	+0.9	+0.6
TP40C	1	1000	35	−5.5	−3.1	−0.7	+1.8	−4.2	+1.7	−6.4	−1.2	+2.4	−4.6	same	−1.4
TP40C	1	1100	35	−4.4	−3.4	+2.0	+4.8	−3.3	+2.2	−5.8	−1.0	+3.0	−1.4	+1.7	+1.1
TP40C	1	1200	35	−4.7	−5.9	same	+4.2	−4.5	−1.8	−6.8	−4.5	−0.4	−5.1	+0.6	−0.1
TP40C	1	1300	35	−2.9	−3.4	+1.9	+7.1	−3.3	+0.3	−5.7	−2.6	+1.2	−4.0	+2.3	+2.4
TP40C	1	1400	35	−2.5	−3.5	+1.9	+8.1	−3.6	−0.4	−5.1	−2.3	+1.8	−3.8	+2.5	+2.8
N8	2	1100	31	−3.3	−1.8	−2.8	+3.5	−3.0	−1.0	−5.8	−4.1	+0.8	−7.9	+1.6	−0.4
N7	2	1300	31	−0.3	−0.4	+0.5	+8.3	−1.0	−0.3	−4.4	−3.8	+2.8	+0.2	+4.2	+3.5
N10	2	1300	44	−6.5	−5.4	−6.1	+1.4	−7.3	−5.7	−11.9	−10.5	−2.7	−15.2	−4.1	−3.2
N13	2	1100	38	−5.0	−4.7	−4.5	+1.9	−5.0	−3.7	−7.8	−6.9	−1.8	−8.6	−1.2	−1.8
C2	3	1200	30	−0.4	−2.4	+3.7	+8.5	−0.3	−3.9	−2.0	−0.8	+2.4	+1.7	+5.2	+4.3
DD1	3	1100	40	−3.3	−1.3	−1.5	+3.3	−3.2	+0.8	−6.4	−2.9	+2.0	–	−0.6	−0.3
DD2	3	1200	40	−3.9	−5.2	−2.1	+4.5	−4.0	−3.6	−8.4	−8.0	−0.8	−1.9	−0.3	+0.4
DD3	3	1250	40	+4.6	+10.4	+6.2	+12.0	+4.3	+12.2	−1.0	+5.8	+13.8	−1.2	+5.2	+7.8
DD4	3	1300	40	−2.7	−4.1	−0.8	+5.4	−3.2	−2.6	−7.0	−6.5	−0.5	+0.8	−0.1	+0.8
DD7	3	1250	30	−0.8	+1.0	+1.4	+8.6	−1.0	+2.6	−3.6	−0.4	+4.4	+3.8	+4.9	+4.1
X6	3	1200	30	−6.1	−8.2	−3.5	+2.8	−6.2	−6.2	−8.4	−8.3	−3.5	+7.2	+0.8	−1.6
X7	3	1150	30	−3.0	−2.7	−1.2	+5.2	−2.9	−1.2	−5.5	−4.0	+1.3	+8.2	+2.9	+1.1
X8	3	1100	30	−6.0	−5.0	−4.1	+2.1	−5.7	−3.1	−7.1	−4.8	−1.6	+6.0	+0.8	−0.7
X9	3	1050	30	−6.2	same	−4.3	+2.4	−5.5	+2.2	−6.9	same	+4.1	+0.8	+1.3	−1.2
X11	3	1000	30	−5.0	−4.9	−3.4	+2.7	−4.0	−2.8	−5.8	−4.7	−1.5	+2.6	+1.8	−0.6
FF6	3	1000	30	−1.3	−0.5	+1.1	+6.3	−0.3	+2.4	−2.5	−0.1	+3.5	+1.5	+4.6	+3.0
FF7	3	1050	30	+3.8	+4.6	+6.4	+11.8	+4.6	+7.5	+1.4	+3.9	+8.5	+5.4	+8.5	+8.5
FF8	3	1250	30	−3.5	−5.5	−0.4	+6.4	−3.6	−3.2	−5.4	−5.1	−0.6	+7.5	+3.3	+1.8
T6	3	1050	30	−4.8	−5.3	−3.4	+4.3	−3.6	−3.1	−5.5	−5.0	−1.0	−10.2	+2.8	+0.8
T7	3	1020	30	−9.1	−6.0	−6.2	−0.1	−7.9	−2.9	−9.2	−4.7	−1.3	−6.2	−0.5	−3.6
T8	3	1000	30	−8.0	−7.0	−5.4	+1.0	−6.5	−4.0	−8.0	−5.7	−2.6	−3.2	+0.5	−2.4
T9	3	950	30	−9.0	−8.4	−6.9	−0.5	−7.2	−5.3	−8.7	−7.0	−3.8	−1.8	−0.3	−3.6
T10	3	1200	30	−5.2	−5.3	−2.5	+3.4	−5.3	−3.2	−6.7	−4.9	−1.2	−0.5	+1.2	−0.9
T11	3	1150	30	−6.4	−6.4	−2.7	+3.3	−6.0	−3.2	−7.4	−4.9	−1.2	+6.7	+1.4	−0.8
T12	3	1100	30	−7.5	−8.8	−4.2	+2.1	−6.6	−5.6	−8.8	−7.9	−3.6	+5.2	+0.8	−1.7
KUSH	4	1450	30	+1.4	−0.1	+9.0	+14.0	−0.8	+5.4	−1.2	+2.7	+5.4	+2.2	+8.0	+8.5

Values of $P_{CALC} - P_{EXP}$ given in kilobars, temperatures in degrees centigrade
References to Exp run data: *1* Nickel (1983); *2* Akella (1976); *3* Mori and Green (1978); *4* Kushiro et al. (1972)
P1 Wood (1974) A; P2 Wood (1974) B; P3 Wood (1974) C; P4 MacGregor (1974); P5 Harley and Green (1972) A; P6 Harley and Green (1972) B; P7 Harley (1984a) A; P8 Harley (1984a) B; P9 Nickel and Green (1985); P10 Nickel (1983) Cr; P11 Perkins et al. (1981); P12 Perkins and Newton 1980)

and Perkins and Newton (1980), respectively, yield much more accurate pressures than P4 (the majority being within ±5% of P_{EXP}), despite the similarly rather inadequate formulations involved. There seems to be little to choose between the P11 and P12 values but P12 is marginally preferred on the basis of a more even distribution of over- and underestimates relative to P_{EXP}.

P9, the more complex barometer of Nickel and Green (1985) formulated for a multi-component system which most closely approaches that of the natural garnet lherzolite assemblages, yields values closely comparable to P12. There is again an even distribution of over- and underestimates relative to P_{EXP}, the majority being within ±5% and all, bar the three most suspect sample runs, within ±15%. P9 is preferred as a barometer to P12 because of its more comprehensive formulation, its use of the X^{M1}_{Al-Cr} parameter and the fact that it yields superior pressure estimates for the better equilibrated (higher T) runs on the most Cr rich samples.

P5 (Harley and Green 1982) although formulated for a multi-component (though Cr-free) system seriously and consistently underestimates the pressures (again excluding

Table 2. Differences between calculated and experimental temperatures for the tested thermometers

Sample run	Ref	P_{EXP}	T_{EXP}	$T1_D$	$T2_D$	$T3_D$	$T4_D$	$T5_D$	$T6_D$	$T7_D$	$T8_D$	$T9_D$	$T10_D$	$T11_D$
TP40	1	35	1000	+ 35	+ 84	+ 20	+110	+ 25	+ 18	+ 74	+ 92	+ 18	+107	+ 41
TP40	1	35	1100	− 22	+ 29	− 32	+ 59	− 20	− 13	+ 34	+ 19	− 20	+ 98	− 6
TP40	1	35	1200	+ 38	+ 94	+ 49	+ 72	− 3	same	+ 56	+ 33	+ 92	+136	+ 74
TP40	1	35	1300	+ 96	+158	+130	+ 42	+ 33	− 44	+146	+ 63	+143	+131	+132
TP40	1	35	1400	+124	+190	+177	+ 45	+ 80	− 50	+230	+ 79	+128	+157	+156
TP40C	1	35	1000	+ 60	+109	+ 47	+119	+ 31	− 28	+ 79	+104	+ 46	+ 39	+ 67
TP40C	1	35	1100	+ 34	+ 86	+ 31	+ 88	+ 13	− 38	+ 71	+ 56	+ 50	+ 72	+ 56
TP40C	1	35	1200	+ 60	+116	+ 73	+ 68	+ 9	+ 11	+ 80	+ 51	+118	+158	+ 97
TP40C	1	35	1300	+ 37	+ 96	+ 61	+ 3	− 26	− 85	+ 69	+ 13	+ 93	+ 80	+ 73
TP40C	1	35	1400	+ 92	+158	+141	+ 21	+ 45	− 37	+185	+ 51	+122	+168	+130
N8	2	31	1100	+ 89	+129	+ 91	+118	+ 57	+ 5	+126	+ 94	+117	+110	+106
N7	2	31	1300	+ 23	+ 66	+ 43	− 22	− 42	− 58	+ 63	− 1	+ 75	+ 79	+ 50
N10	2	44	1300	+ 64	+161	+ 97	− 18	− 48	−267	+ 47	+ 33	+124	+ 34	+120
N13	2	38	1100	− 50	+ 9	− 62	same	− 81	− 20	− 28	+ 1	− 55	+ 99	− 30
C2	3	30	1200	− 9	+ 28	− 7	+ 37	− 23	− 33	+ 47	− 3	+ 26	+ 77	+ 9
DD1	3	40	1100	+ 37	+106	+ 36	− 14	− 91	− 22	− 35	+ 66	+ 62	+124	+ 74
DD2	3	40	1200	+ 43	+117	+ 56	− 34	− 85	+ 11	− 7	+ 38	+111	+194	+ 95
DD3	3	40	1250	+ 63	+142	+ 87	+ 8	− 49	−112	+ 23	+ 44	+121	+ 60	+110
DD4	3	40	1300	+ 13	+ 91	+ 36	− 6	− 72	−101	− 6	− 5	+ 82	+ 91	+63
DD7	3	30	1250	+ 49	+ 82	+ 66	− 22	− 65	− 59	+ 20	+ 31	+ 97	+ 72	+ 71
X6	3	30	1200	− 13	+ 24	− 11	− 32	− 75	+ 9	+ 11	− 2	+ 28	+130	+ 8
X7	3	30	1150	+ 53	+ 90	+ 57	+ 16	− 33	+ 15	+ 47	+ 59	+ 90	+137	+ 72
X8	3	30	1100	+ 6	+ 40	− 3	+ 24	− 30	− 7	+ 46	+ 47	+ 12	+ 99	+ 12
X9	3	30	1050	+ 39	+ 72	+ 27	+ 44	− 14	+ 28	+ 58	+ 85	+ 38	+126	+ 41
X11	3	30	1000	− 35	− 5	− 60	+ 51	− 28	+ 30	+ 27	+ 67	− 79	+ 96	− 59
FF6	3	30	1000	+ 26	+ 58	+ 7	+ 93	+ 24	− 1	+ 86	+ 89	− 2	+ 61	+ 13
FF7	3	30	1050	+ 37	+ 71	+ 26	+ 72	+ 9	− 40	+ 78	+ 80	+ 29	+ 31	+ 36
FF8	3	30	1250	− 45	− 8	− 41	− 41	− 83	− 64	+ 2	− 40	− 4	+ 60	− 25
T6	3	30	1050	− 31	+ 1	− 50	+ 71	+ 1	+ 8	+ 64	+ 33	− 56	+ 91	− 41
T7	3	30	1020	− 32	− 1	− 55	+ 97	+ 31	+ 17	+ 99	+ 53	− 68	+ 96	− 50
T8	3	30	1000	− 9	+ 23	− 31	+ 99	+ 29	− 15	+ 91	+ 72	− 47	+ 43	− 28
T9	3	30	950	− 68	− 39	−102	+ 87	+ 1	+ 47	+ 50	+ 12	−137	+102	−117
T10	3	30	1200	− 4	+ 32	− 2	− 1	− 53	+ 6	+ 25	+ 3	+ 36	+124	+ 16
T11	3	30	1150	+ 25	+ 61	+ 25	+ 14	− 35	− 44	+ 44	+ 40	+ 50	+ 65	+ 38
T12	3	30	1100	+ 37	+ 72	+ 32	+ 58	+ 8	+ 13	+ 87	+ 64	+ 54	+119	+ 48
KUSH	4	30	1450	−138	− 99	−120	−190	−272	−163	−219	−154	− 81	− 42	−111

spurious results from the experimental sample runs T9, FF7, DD3 and KUSH). However, use of orthopyroxene composition parameter X^{M1}_{Al-Cr} rather than X^{M1}_{Al}, significantly improves the accuracy to the extent that the majority of the estimates (P6) are then within $\pm 10\%$ of P_{EXP}, most notably and significantly for the Nickel (1985) and Akella (1976) experimental data. Indeed for the most Cr-rich samples, P6 yields results encouraging close to P_{EXP}.

P7, presented by Harley (1984a) as an improved calibration based on the same experimental data base as P5 (Harley and Green 1982), in fact yields poorer pressure values, in almost all cases underestimating P_{EXP} by at least 10% and often by much more. The suggestion of Harley (1984a) that X^{gt}_{Ca} should be taken as $Ca+Mn/(Ca+Mn+Mg+Fe^{2+})$ in natural manganese bearing garnets rather than as $Ca/(Ca+Mg+Fe^{2+})$ has been tested but only serves to increase the disparity between P_{CALC} and P_{EXP}. The basis for this proposal was that the behaviour of Ca and Mn in pyrope-almandine garnets is likely to be essentially identical. Use of the alternative orthopyroxene parameter X^{M1}_{Al-Cr} rather than X^{M1}_{Al} in the Harley (1984a) barometer has been tested as P8 and does help to reduce the disparities between P_{CALC} and P_{EXP}. However, as most P8 values are still serious underestimates of P_{EXP}, this barometer seems best rejected. Indeed it can be noted that Harley (1984b) himself noted that the Harley (1984a) barometer consistently underestimated P relative to the Harley and Green (1982) calibration, especially when measured values of $K^{gnt-opx}_{Fe-Mg}$ are high. However, the latter values can scarcely be regarded as high in the data tested here.

Finally, it is apparent from Table 1 that P10, the Cr barometer of Nickel (1983), yields mostly less accurate P estimates than the preferred Al barometer (P9). Whilst some of the inconsistent results may be attributable to analytical errors with the relatively low levels of X^{M1}_{Cr} in some orthopyroxenes, the serious underestimates for most of the Cr-rich TP40C runs and 3 out of 4 of the Akella (1976) runs are particularly disconcerting and probably signal poor Cr equilibration between the mineral phases in these experiments. Indeed Nickel (1983) has indicated that disequilibrium $Cr/(Cr+Al)$ zoning was apparent in garnets in experiments with the TP40C composition, especially at the lower temperatures. Hence we conclude that the Cr barometer (P10) should be used with caution and generally limited to samples where $X^{M1}_{Cr} > 0.1$ in orthopyroxene and adequate chemical equilibration is likely.

$T12_D$	$T12R_D$	$T13_D$	$T13R_D$	$T14_D$	$T15_D$	$T16_D$	$T17_D$	$T17R_D$	$T18_D$	$T19_D$	$T19R_D$	$T20_D$	$T20R_D$	T^*_D
+ 75	+ 37	+ 61	+ 21	+133	+ 41	+ 32	− 10	− 10	same					+25
+ 54	+ 46	+ 44	+ 36	+ 97	− 1	+ 17	− 57	− 41	− 12					−13
+ 11	+122	+ 5	+124	+ 51	−115	+ 9	−190	− 95	−165					+ 4
+ 66	+116	+ 71	+ [illegible]	+ 84	−132	+138	+ 5	+ 80	+344					+34
+ 48	+ 48	+ 60	+ [illegible]	+ 53	−346	+167	− 7	− 7	+630					+64
+ 80	+ 50	+ 66	+ 33	+133	+ 41	+ 22	− 4	+120	+ 1					+31
+ 91	+100	+ 84	+ 94	+118	+ 18	+ 31	− 28	− 16	+ 31					+20
− 19	+ 46	− 27	+ 43	+ 19	−164	− 50	− 81	+ 16	+ 49					− 9
+ 4	− 6	+ 5	− 6	+ 22	−259	+ 11	−108	−108	+114					−11
+ 9	+117	+ 17	+136	+ 12	−318	+ 70	− 61	+126	+422					+27
−161	−405	−180	−431	− 75	−263	−125	−154	−169	−155					+57
− 85	−325	− 90	−343	− 39	−217	− 45	−238	−326	− 99					−64
− 45	−286	− 52	−306	+ 1	−170	− 44	−208	−348	−200					−10
− 41	−668	− 57	−696	+ 26	−118	− 86	− 66	−101	− 44					−67
same	+226	− 5	+239	+ 35	−135	+ 2	− 48	+322	+205	+ 12	+786	− 30	+570	−17
+147	−142	+141	−164	+193	+197	+170	− 22	+ 1	+ 23	+ 60	+103	+ 59	+ 92	−25
− 1	−230	− 1	−251	+ 42	− 2	− 30	+142	− 75	− 7	−113	same	− 84	+ 8	− 8
− 70	+ 29	− 80	+ 26	− 19	−400	− 84	−209	− 63	−203	−179	+ 76	−178	+ 31	+19
− 93	−164	−101	−177	− 47	−312	−102	−230	−216	−199	−163	−137	−185	−164	−18
+ 3	−210	+ 2	−224	+ 31	−157	+ 33	−158	−147	+ 15	− 22	+ 1	− 56	− 38	−38
− 8	− 74	− 14	− 84	+ 32	−101	+ 9	−126	−304	+ 33	−132	− 22	−126	− 43	−83
− 2	−154	− 40	−171	+ 47	− 80	+ 6	−131	+ 96	− 33	− 96	− 35	− 89	− 43	−43
+ 90	+ 90	+ 84	+ 84	+132	+ 22	+107	− 41	−105	+ 99	+ 17	+ 17	+ 14	+ 14	−21
+ 76	+ 56	+ 66	+ 45	+122	+ 51	+ 54	− 19	+ 39	+ 81	+ 25	+129	+ 43	+122	− 6
+ 76	+ 3	+ 63	−113	+131	+ 37	+ 49	− 39	− 63	− 3	+ 21	+104	+ 46	+184	−18
+ 1	+ 34	− 15	+ 19	+ 64	− 22	− 48	− 41	+ 7	+ 7	− 7	+ 77	+ 24	+ 87	+ 2
+ 17	− 15	+ 4	− 30	+ 72	− 16	− 16	− 78	− 40	− 33	− 97	− 37	− 60	− 15	+ 6
− 22	− 40	− 25	− 44	+ 6	−153	− 15	− 95	−173	+159	+ 52	+ 52	+ 8	+ 8	−70
+ 23	− 51	+ 11	− 66	+ 64	− 37	− 47	− 35	+ 54	+ 29	− 55	+ 87	− 18	+ 95	−12
+ 72	+ 91	+ 61	+ 81	+113	+ 19	+ 15	− 20	+ 7	+ 35	+ 7	+ 52	+ 43	+ 78	+24
+ 81	+ 76	+ 64	+ 69	+121	+ 49	+ 14	− 19	+ 10	+ 14	+ 12	+ 62	+ 53	+ 92	+24
+ 97	− 15	+ 84	− 42	+141	+ 72	+ 21	− 24	− 24	− 38	− 9	− 9	+ 50	+ 50	− 8
+ 79	−223	+ 79	−240	+106	− 5	+129	− 74	−107	+150	+148	+233	+ 81	+146	−64
+ 93	−148	+ 94	−163	+114	+ 14	+ 89	− 35	− 1	+152	+ 75	+547	+ 60	+426	−35
+ 60	− 99	+ 53	−114	+ 90	− 32	+ 16	− 87	− 68	− 22	+ 13	+155	+ 34	+145	+20
−220	−1432	−223	−1447	−206	−400	−264	−296	−457	− 76	−142	+384	−186	+240	–

Values of $T_D = T_{CALC} - T_{EXP}$ given in degrees centigrade; pressures in kilobars

Two pyroxene solvus thermometers: *T1* Lindsley and Dixon (1976) 20 kbar; *T2* Lindsley and Dixon (1976); *T3* Finnerty and Boyd (1986); *T4* Wood and Banno (1973); *T5* Wells (1977); *T6* Sachtleben and Seck (1981); *T7* Mori and Green (1978); *T8* Kretz (1982); *T9* Nickel and Brey (1984) En; *T10* Nickel and Brey (1984) Di; *T11* Nickel et al. (1985)

$K_{Gnt-Cpx}^{Fe^{2+}-Mg}$ thermometers: *T12* Ellis and Green (1979); *T13* Powell (1985); *T14* Ganguly (1979); *T15* Saxena (1979); *T16* Mori and Green (1978)

$K_{Gnt-Opx}^{Fe^{2+}-Mg}$ thermometers: *T17* Harley (1984b); *T18* Mori and Green (1978)

$K_{Gnt-Oliv}^{Fe^{2+}-Mg}$ thermometers: *T19* O'Neill and Wood (1979); *T20* Kawasaki

T^* – 'Best' estimate (see text)

Thermometers tested

We report here on the ability of a total of 20 different thermometer formulations to reproduce the experimental temperatures of the same test data. These thermometers fall into two principal groups depending upon the nature of the element exchange reactions involved.

A. Thermometers based on the two-pyroxene solvus

The extent of mutual solubility between coexisting Ca-rich and Ca-poor pyroxenes has long been recognised to provide a valuable and sensitive thermometer, especially at temperatures above about 900° C (e.g., Boyd and Schairer 1964; Davis and Boyd 1966; Boyd 1973). However, more recent experimental data have also demonstrated a significant pressure influence on this miscibility gap (e.g., Lindsley and Dixon 1976; Mori and Green 1975; Brey and Huth 1984). Thus two-pyroxene solvus thermometer calibrations which do not include a pressure correction term are suspect outside of the experimental pressure range used to establish the calibration. Numerical formulations of these thermometers (e.g., Finnerty and Boyd 1984, 1986; Nickel and Brey 1984; Nickel et al. 1985) have been favoured over graphical methods (e.g., Lindsley and Dixon 1976; Lindsley 1983; Davidson and Lindsley 1985) because of ease of application.

Most experimental data on which the various formulations of the two-pyroxene solvus thermometer are based are for the simple diopside-enstatite (CMS) system. How-

ever, Wood and Banno, followed by Wells (1977), pioneered the development of thermodynamic formulations based on a simple ideal solution model for the coexisting pyroxenes designed to take account of the influence exerted on the $Ca^{2+}-Mg^{2+}$ exchange reaction by the presence of other elements (notably Fe) occupying M1 and M2 sites. Nevertheless, as cautioned by Nickel et al. (1985), there remains considerable uncertainty over the correct thermodynamic model to be applied to the pyroxene miscibility relationships and hence thermometer formulations based primarily on data for the simple CMS or CMAS systems are of doubtful validity when applied to the more chemically complex natural pyroxenes.

Here we have tested the following formulations of the two-pyroxene solvus thermometer:

T1: the formulation (A1) derived and recommended by Finnerty and Boyd (1984), based on the Lindsley and Dixon (1976) CMS data at 20 kbar without any pressure correction term.

T2: as T1 but also incorporating a pressure correction term based on the Lindsley and Dixon (1976) data.

T3: the empirical fit of the diopside limb of the solvus as derived and recommended by Finnerty and Boyd (1986). It incorporates a P correction based on the experimental data of Brey and Huth (1984), Nickel and Brey (1984).

T4: the semi-empirical formulation [Eq. (27)] of Wood and Banno (1973). No pressure term involved.

T5: the semi-empirical formulation [Eq. (5)] of Wells (1977), effectively a revised version of T4 – again without a pressure correction term.

T6: the formulation of Sachtleben and Seck (1981) derived for the enstatite limb of the solvus from the Lindsley and Dixon (1976) CMS data at 15 kbar. No pressure term incorporated.

T7: the formulation of Mori and Green (1978) based on their experimentally determined phase equilibria for natural compositions – again without a pressure correction term.

T8: the formulation [Eq. (19a) or (19b), depending on temperature] of Kretz (1982) based on a combination of CMS data (Lindsley and Dixon 1976) and natural pyroxene data. No pressure term involved.

T9: the formulation [Eq. (4)] of Nickel and Brey (1984) for enstatite component exchange between pyroxenes derived from a thermodynamic regular solution model applied to their CMS experimental data, with pressure term incorporated. Enstatite component calculated as [1–2Ca/(Ca+Mg)], as recommended by Finnerty and Boyd (1986), in order to minimise the influence of additional elements present in the M1 and M2 sites of natural pyroxenes.

T10: the formulation [Eq. (5)] of Nickel and Brey (1984) for diopside component exchange between pyroxenes. Similar derivation to T9, again with a pressure correction term. Diopside component calculated as 2Ca/(Ca+Mg), as recommended by Finnerty and Boyd (1986).

T11: the empirical formulation [Eq. (1)] of Nickel et al. (1985) for enstatite component exchange between pyroxenes based on their CMS and CMAS data, with pressure correction term. Enstatite component calculated as in T9.

B. Thermometers based on $Fe^{2+}-Mg^{2+}$ exchange between minerals

Several experimental studies (e.g., Ellis and Green 1979; Mori and Green 1978; O'Neill and Wood 1979; Harley 1984b) have demonstrated that $Fe^{2+}-Mg^{2+}$ exchange reactions between coexisting mineral phases encountered in garnet lherzolite assemblages are strongly temperature dependent and thus provide the bases for sensitive thermometers applicable to such assemblages. As pressure exerts a significant, though lesser, influence such thermometers should also include a pressure correction term.

A serious problem with the application of such thermometers arises from uncertainty over the oxidation state of iron in minerals analysed by electron microprobe. An assumption that all iron is present as Fe^{2+} in the mineral phases of upper mantle derived garnet lherzolite xenoliths in kimberlites might perhaps be justified by the strongly reduced nature of the mineral assemblages as witnessed by the occasional presence of diamond or graphite (cf., Haggerty 1986). Also with good quality microprobe analyses, stoichiometric charge balance calculations generally provide little evidence of significant Fe^{3+} contents in the constituent garnets and pyroxenes. There is, however, uncertainty over the oxidation state of iron under the experimental procedures used to generate the experimentally calibrated test data. Also in some experiments Fe loss to capsules appears to have been a problem. Hence possible different rates of loss of Fe from different minerals may affect the application of thermometers based on $Fe^{2+}-Mg^{2+}$ exchange reactions between coexisting minerals.

Nickel (1983) has reported that some Fe^{3+} was present in the initial compositions but was probably mostly reduced to Fe^{2+} under experimental conditions. Stoichiometric charge balance calculations suggest the presence of at most only minor amounts of Fe^{3+} in the resulting garnets and pyroxenes. The Nickel (1983) data for the highest temperature experiments (1300 and 1400° C) may be expected to be the most reliable for application of $Fe^{2+}-Mg^{2+}$ exchange reaction thermometers because of the use of graphite lined capsules and elimination of Fe loss.

Graphite capsules with tight fitting lids were also used by Akella (1976) to avoid Fe loss. However, stoichiometric charge balance calculations for these mineral data indicate significant Fe^{3+} contents, especially in the clinopyroxenes. However, it is uncertain as to whether these are real or reflect poor mineral analyses, though we suspect the latter. The same is true for the Kushiro et al. (1972) data, but as the results of all applications of thermometers and barometers to this data set are poor (suggesting unsatisfactory equilibration) they seem best rejected.

Oxygen fugacities were apparently not controlled in the experimental runs of Mori and Green (1978). Also Fe loss was suspected in many runs. Hence caution is necessary over application of $Fe^{2+}-Mg^{2+}$ exchange thermometers to this data set. Accordingly, it seemed appropriate to consider temperatures calculated both on initial mineral analyses which assume all Fe as Fe^{2+} and on recalculated analyses with respective Fe^{3+} and Fe^{2+} contents calculated by stoichiometric charge balance.

The full list of the various $Fe^{2+}-Mg^{2+}$ exchange reaction thermometers which we have tested is as follows, with grouping into sub-groups:

B1. Thermometers based on $Fe^{2+}-Mg^{2+}$ exchange between garnet and clinopyroxene

T12: equation (9) of Ellis and Green (1979) based on their experiments in the CFMAS system.

T13: equation (17) of Powell (1985), being a slightly modified version of T12 derived through a more rigorous mathematical assessment of the experimental data of Ellis and Green (1979) together with that of Raheim and Green (1974).

T14: the formulation [Eq. (10a or 10b), depending upon temperature] of Ganguly (1979) which involved thermodynamic extrapolation of selected experimental data to compositions in the CFMAS+MnO system.

T15: the formulation [Eq. (10)] of Saxena (1979) which involved thermodynamic extrapolation of experimental data to compositions in the CFMAS+MnO+Na_2O system.

T16: the formulation of Mori and Green (1978) based on their experimental phase equilibria for natural compositions. Note that it does not involve a pressure correction term.

Thermometers based on $Fe^{2+}-Mg^{2+}$ exchange between garnet and orthopyroxene

T17: equation (11) of Harley (1984b) based on experimental data in the FMAS and CFMAS systems.

T18: the formulation of Mori and Green (1978) based on their experimental phase equilibria for natural compositions – without pressure correction term.

Thermometers based on $Fe^{2+}-Mg^{2+}$ exchange between garnet and olivine

T19: the formulation [Eq. (26, 27)] of O'Neill and Wood (1979), as corrected by O'Neill and Wood (1980), based on thermodynamic extrapolation of their experimental data for the FMAS and CFMAS systems.

T20: the formulation [Eq. (9)] of Kawasaki (1979) based on a thermodynamic analysis of experimental data for the FMAS system.

Results of thermometer tests

Temperatures calculated for the test data set using the 20 different thermometer formulations tested here are presented in Table 2 as the differences between the calculated and experimentally recorded values. As might be expected from earlier comments, the results for the Kushiro et al. (1972) experimental data are consistently poor and seem best ignored. For several other samples, most notably DD3, DD4, T10 and T11 of Mori and Green (1978), chemical equilibration of Fe^{2+} and Mg^{2+} between the mineral phases appears to have been poor. It is noteworthy that these suspect data are for samples with only relatively short (i.e. 1 h) experimental run times. More surprising are the poor results for $Fe^{2+}-Mg^{2+}$ exchange thermometers applied to garnet, clinopyroxene and orthopyroxene in the Akella (1976) experiments. Stoichiometric charge balance calculations point to the possibility to significant Fe^{3+} contents in all three minerals in these experimental products. However, calculated temperatures which take these Fe^{3+} contents into consideration (T12R, T13R, T17R, T19R and T20R) are even worse (Table 2) than those based on the assumption of all Fe as Fe^{2+}. Moreover, graphite capsules with tight fitting lids were reportedly used in order to avoid Fe loss and oxidation. We can only conclude that either the mineral analyses concerned are of unsatisfactory quality or that Fe and Mg compositional inhomogeneities have persisted in these particular run products.

Thermometers based on the two-pyroxene solvus

T5 (Wells 1977) is judged to be the currently best available calibration of the two-pyroxene solvus for assemblages equilibrated at less than about 37 kbar. It yields temperatures encouragingly close to T_{EXP} (within $\pm 50°$ C) for all but one of the Nickel (1983) experimental run data. It does not, however, include a term to correct for the influence of pressure on the pyroxene miscibility relationship and hence there are indications, from the test data for 38–44 kbar experiments, that as a result it underestimates T at such higher pressures. Indeed at $P>37$ kbar, amongst the various calibrations of the two-pyroxene solvus T4 (Wood and Banno 1973) and T8 (Kretz 1982) yield temperatures closest to T_{EXP}. These results seem fortuitous, however, since again neither calibration actually includes a pressure correction term. Moreover, there is clear evidence that both T8 and, especially, T4 seriously overestimate T_{EXP} at the lower temperatures ($T<1100°$ C).

Our calculations indicate that, for the majority of experimental data, T3 (the formulation favoured by Finnerty and Boyd 1986) yields temperatures more disparate from T_{EXP} than T5 (Wells 1977). In particular, T3 consistently yields substantial (50–150° C) overestimates for the higher temperature ($T>1200°$ C) run data.

T9 (Nickel and Brey (1984), enstatite component exchange – with X_{En}^{Cpx} calculated as [1–2Ca/(Ca−Mg)] as suggested by Finnerty and Boyd (1986), yields temperatures reasonably close to T_{EXP} for the lower T run data of Nickel (1983). However, for the higher T run data ($T>1200°$ C) it habitually overestimates (like T3) relative to T_{EXP}, typically by some 100° C. The complimentary thermometer T10 (Nickel and Brey 1984, diopside component exchange) is judged to be even less satisfactory than T9 since it also yields unreliable temperatures for the lower T run data, probably because of insensitivity due to the low concentrations of diopside component in the orthopyroxenes at these lower temperatures. In cautioning against use of the T9 and T10 thermometers in natural garnet lherzolite assemblage, we note that Nickel and Brey (1984) themselves considered the equations which they presented for enstatite and diopside exchange reactions in coexisting pyroxenes based on CMS data to provide only "a good starting point for a development or more reliable thermometers based on the miscibility gap".

T11 (Nickel et al. 1985) yields gross overestimates (mostly $>200°$ C) relative to T_{EXP} if, as indicated by these authors, the enstatite component in the pyroxenes is calculated as $[(1-(Al/2))\times(1-Ca)]$. However, as emphasised by Nickel et al. (1985), this formulation is only for pyroxene compositions within the CMS and CMAS systems and is invalid for natural pyroxenes, especially those with significant Na contents. A modified calculation of T11 (with the enstatite component taken as [1–2Ca/(Ca+Mg)], in an at-

tempt to minimise the influence of other elements present (Finnerty and Boyd 1984, 1986), yields temperatures (as tabulated in Table 2) which are certainly closer to T_{EXP} but are still mostly inaccurate. Indications are that with this modified formulation T11 still tends to yield overestimates relative to T_{EXP} for the higher T (>1200° C) experimental data but by contrast tends to underestimate at the lowest temperatures (<1100° C).

T1 (based on Lindsley and Dixon 1976 with P fixed at 20 kbar – as recommended by Finnerty and Boyd 1984 but now superseded in their opinion by T3) yields values reasonably close to T_{EXP} for the lower temperature data but, as with T3 and T9–11, again consistently overestimates at temperatures over 1200° C. T2 (based on Lindsley and Dixon (1976), with pressure correction) is even more inaccurate, almost invariably overestimating relative to T_{EXP} – especially for the highest $P-T$ data. Errors are at least in part attributable to the fact that the pressure influence on the miscibility gap is likely to be appreciably less (Brey and Huth 1984; Nickel and Brey 1984) than indicated by Lindsley and Dixon (1976).

T6 (the simple formulation derived by Sachtleben and Seck (1981) for the enstatite limb of the solvus from the Lindsley and Dixon (1976) CMS data at 15 kbar) somewhat surprisingly yields temperatures within ±50° C of T_{EXP} for most of the test samples. However, indications are that, in the absence of a P correction term, T6 tends to increasingly underestimate relative to T_{EXP} as pressures increase.

Thermometers based on $Fe^{2+}-Mg^{2+}$ exchange between garnet and clinopyroxene

The best calibrations of this thermometer are undoubtedly T12 (Ellis and Green 1979) and T13 (Powell 1985). Differences between T12 and T13 values are small (mostly <15° C). However, there are indications that T12 more closely reproduces T_{EXP} at temperatures over 1200° C whereas T13 seems preferable below 1200° C where it yields values which are slightly lower than T12 and closer to T_{EXP}. Despite some uncertainty over the possible presence of some Fe^{3+} in the constituent mineral phases of some experimental studies (especially those of Mori and Green 1978), temperatures calculated assuming all Fe as Fe^{2+} are, in the great majority of cases, closer to T_{EXP} than those where Fe^{3+} contents calculated by stoichiometric charge balance have been taken into consideration (T12R and T13R). Only in samples DD3, X11 and T9 of Mori and Green (1978) are the latter values significantly closer to T_{EXP}, whilst in other samples gross disparities from T_{EXP} are apparent. Since calculated Fe^{3+}/Fe^{2+} ratios in minerals are highly susceptible to any analytical errors (notably in SiO_2), it is recommended that greater weight should be placed on temperatures calculated assuming all Fe is present as Fe^{2+}. However, where small amounts of Fe^{3+} do exist in garnets and clinopyroxenes (especially the latter) such temperatures may be expected to be slight overestimates. This may explain why, when calculated on this basis, the T12 and T13 values tend to overestimate relative to T_{EXP}.

T14 (Ganguly 1979) and T16 (Mori and Green 1978) both tend to yield overestimates relative to T_{EXP}, although indications are that T14 most seriously overestimates below 1200° C whereas T16 overestimates worst at the higher temperatures. T15 (Saxena 1979) is the least satisfactory of the thermometer calibrations based on $Fe^{2+}-Mg^{2+}$ exchange between garnets and clinopyroxene, typically underestimating relative to T_{EXP} by at least 100° C at around 1200° C and by 300° C at around 1400° C.

Thermometers based on $Fe^{2+}-Mg^{2+}$ exchange between garnet and orthopyroxene

T17 (Harley 1984b) is judged to be a more reliable calibration than T18 (Mori and Green 1978) but even so mostly yields temperature underestimates relative to T_{EXP}. Some of the worst results are for samples (such as DD3 and DD4) for which we have serious doubts over whether satisfactory $Fe^{2+}-Mg^{2+}$ equilibration between the mineral phases was achieved during the experiments. Consideration of just small amounts of Fe^{3+} in either garnet or orthopyroxene, calculated by stoichiometric charge balance (T17R), leads to rather erratic variations from the temperatures calculated assuming all Fe is present as Fe^{2+} and from T_{EXP}.

T18 generally yields highly inaccurate results, especially at the higher temperatures where it frequently overestimates by >100° C relative to T_{EXP}.

Thermometers based on $Fe^{2+}-Mg^{2+}$ exchange between garnet and olivine

The absence of analytical data for olivines in the Nickel (1983) and Akella (1976) experiments means that tests on these thermometers are restricted to the data of Mori and Green (1978) and Kushiro et al. (1972). Unfortunately, the latter yield unacceptable temperatures for the same reasons as before.

Results for the two different formulations tested, namely T19 (O'Neill and Wood 1979, 1980) and T20 (Kawasaki 1979) are rather inconsistent in their ability to reproduce T_{EXP}. This may well reflect the uneven quality of the Mori and Green (1978) data. Certainly the results for samples DD3, DD4, T10 and T11 are especially poor, but as they also yielded inaccurate temperatures on consideration of $Fe^{2+}-Mg^{2+}$ exchange between garnet-clinopyroxene and garnet-orthopyroxene pairs overall, unsatisfactory equilibration with respect to $Fe^{2+}-Mg^{2+}$ partitioning seems likely in these particular samples. As far as the other test samples are concerned, T19 yields values mostly rather closer to T_{EXP} than T20 and is therefore preferred. Whilst in some of these samples (C2, X8, X9, X11, T7, T8 and T9) the assumption that all Fe is present as Fe^{2+} in both minerals yields satisfactory temperatures, in certain others (DD2, DD7, FF7 and X8) calculations which take account of Fe^{3+} contents in garnets calculated by charge balance yield temperatures (T19R and T20R) closer to T_{EXP}. However, the Fe^{3+} contents calculated in these garnets may be spurious rather than real (a consequence of poor quality microprobe analyses) as for certain are those calculated for the garnets in samples C2 and X11.

Conclusions and strategy for determination of P–T equilibration conditions for garnet lherzolite assemblages

Our results indicate that the barometer-thermometer combinations favoured by Finnerty and Boyd (1984 and 1986) represent unfortunate choices and can both be expected to yield incorrect values for the pressures and temperatures of equilibration of most mantle derived garnet lherzolite xenolith assemblages. Such $P-T$ values will in turn lead

to incorrect assessment of the depths of origin of many such xenoliths. We consider the erroneous $P-T$ values to be a consequence of the fact that both their favoured barometer (P4: MacGregor 1974) and thermometers (T1: Lindsley and Dixon 1976 at 20 kbar; T3: Finnerty and Boyd 1986) have been formulated from experimental data for simple MAS, CMS and CMAS systems and do not adequately take account of the influence exerted on the element exchange reactions by the presence of other elements in the structural sites of the minerals concerned.

From the results of our tests we conclude that the most accurate pressures for garnet lherzolite assemblages equilibrated under uppermost mantle $P-T$ conditions are those provided by P9, the barometer of Nickel and Green (1985). In our view this is the only barometer formulation currently available which adequately takes account of the profound influence of X_{Al}^{M1} in orthopyroxene coexisting with garnet that results from the presence of significant Cr and Fe contents. Even with P9 (Nickel and Green 1985) there are some indications that pressures may be somewhat overestimated in the case of particularly chromiferous assemblages (i.e. $X_{Cr}^{M1}>0.02$ in orthopyroxene), especially when spinel is present as an additional phase incorporating Cr and Al.

We feel unable to select with the same conviction a single 'best' thermometer for garnet lherzolite xenolith assemblages. In our view none of the 11 different formulations of the two-pyroxene solvus thermometer tested is satisfactory throughout the whole $P-T$ range of interest but T5 (Wells 1977) is judged to be the least unsatisfactory. It considers M1 and M2 site occupancies by elements additional to Ca and Mg but lacks a pressure correction term and as a result increasingly underestimates the equilibration temperature for pressures above about 37 kbar. By contrast T3 (Finnerty and Boyd 1986) does not adequately take account of the influence of elements other than Ca and Mg on the pyroxene solvus but probably contains a satisfactory pressure correction term. Our assessment is that T3 is somewhat less accurate than T5 over the $P-T$ range covered by our tests (950–1450° C; 30–44 kbar) and in particular seriously overestimates T above 1200° C. Since equilibration temperatures and pressures may be expected in general to increase together for garnet lherzolite assemblages in mantle derived xenolith suites, and the deduced errors in T3 and T5 are in opposite directions in the highest $P-T$ samples tested, we rather tentatively conclude that at present the two-pyroxene solvus temperature for assemblages equilibrated at $P>37$ kbar is most accurately reproduced by the average of the values obtained from the thermometer formulations T3 (Finnerty and Boyd 1986) and T5 (Wells 1977).

As none of the two-pyroxene solvus thermometer formulations is entirely satisfactory, we consider it prudent to also take account of the equilibrium temperatures indicated by thermometers based on the $Fe^{2+}-Mg^{2+}$ exchange reactions between mineral pairs in garnet lherzolite assemblages, despite uncertainty over whether all Fe is present as Fe^{2+} in these minerals.

$Fe^{2+}-Mg^{2+}$ exchange between garnet and clinopyroxene is especially temperature sensitive. From our tests we judge T12 (Ellis and Green 1979) to be the most accurate calibration of this thermometer when $T>1200°$ C but T13 (Powell 1985) to be somewhat superior when $T<1200°$ C. However, there are indications that, when all Fe is assumed to be present as Fe^{2+}, both T12 and T13 tend to slightly overestimate actual equilibration temperatures. This suggests that small amounts of Fe^{3+} may often be present, especially in the clinopyroxenes. T17 (Harley 1984) is judged to be the most accurate calibration available for $Fe^{2+}-Mg^{2+}$ exchange between garnet and orthopyroxene but nevertheless appears to fairly consistently underestimate actual equilibrium temperatures. Finally T19 (O'Neill and Wood 1979, 1980) is considered to be the best available calibration for $Fe^{2+}-Mg^{2+}$ exchange between garnet and olivine. It does not appear to consistently over- or underestimate and the fact that it is rather erratic in its ability to reproduce the actual run temperatures in our test samples is considered more likely to reflect inconsistent $Fe^{2+}-Mg^{2+}$ equilibration between garnet and olivine in the Mori and Green (1978) experiments than any inherent error in this thermometer calibration.

From these observations, and taking note of the fact that expected errors from T12/T13 for garnet-clinopyroxene pairs and T17 for garnet-orthopyroxene pairs are likely to be in opposite directions, we conclude that as far as the $Fe^{2+}-Mg^{2+}$ exchange reaction thermometers are concerned it is best to calculate a mean value from T12 or T13 (depending on temperature), T17 and T19 for each assemblage. However, we consider it advisable to reject any individual value derived from these thermometers which differs by $>75°$ C from the calculated two-pyroxene solvus temperature for that assemblage. Unsatisfactory and spurious results may arise in specific instances from analytical errors, compositional inhomogeneities (inadequate equilibration) or the presence of Fe^{3+}.

Our final 'best' equilibration temperature value (T^*; Table 2) for each garnet lherzolite assemblage is then an average of the assessed two-pyroxene solvus and $Fe^{2+}-Mg^{2+}$ exchange reaction temperatures derived as outlined above. Inspection of Table 2 shows that the T* values are within 35° C of T_{EXP} for 26 out of 34 of the test samples, a significantly better result than that obtained by application of any single thermometer. Moreover, the less accurate results for at least some of the aberrant test samples (notably N8, N7 and N13 of Akella 1976) are probably attributable to unsatisfactory mineral analyses or compositional inhomogeneities.

$P-T$ results calculated by our preferred calibrations and procedures for actual garnet lherzolite xenolith suites and discussion of their implications will be presented elsewhere.

Acknowledgements. We wish to thank Klaus Nickel for helpful suggestions and permission to use his unpublished formulation for the Cr-barometer and results for experimentally equilibrated garnet lherzolite assemblages from his thesis. Tony Finnerty and Joe Boyd kindly provided us with a preprint of their latest paper evaluating thermobarometers. Research on assessment of equilibration conditions for garnet lherzolite assemblages has been supported by grants from the Natural Environment Research Council to D.A.C.

References

Akella J (1976) Garnet pyroxene equilibria in the system $CaSiO_3-MgSiO_3-Al_2O_3$ and in a natural mineral mixture. Am Mineral 61:589–598

Berman R (1979) Thermal properties. In: Field JE (ed) The properties of diamond. Academic Press, London

Boyd FR (1973) A pyroxene geotherm. Geochim Cosmochim Acta 37:2533–2546

Boyd FR, Schairer JF (1964) The system $MgSiO_3-CaMgSi_2O_6$. J Petrol 5:275–309

Brey G, Huth J (1984) The enstatite-diopside solvus to 60 kbar. In: Kornprobst J (ed) Kimberlites II: The mantle and crust-mantle relationships. Proc Third Int Kimb Conf. Developments in Petrology 11B:257–264. Elsevier, Amsterdam

Bundy FP (1980) The P, T phase and reaction diagram for elemental carbon, 1979. J Geophys Res 85:6930–6936

Bundy FP, Bovenkerk HP, Strong HM, Wentorf RH Jr (1961) Diamond-graphite equilibrium line from growth and graphitisation of diamond. J Chem Phys 35:383–391

Carswell DA (1980) Mantle derived lherzolite nodules associated with kimberlite, carbonatite and basalt magmatism: a review. Lithos 13:121–138

Carswell DA (1986) The metamorphic evolution of Mg–Cr type Norwegian garnet peridotites. Lithos 19:279–297

Carswell DA, Cuthbert SJ (1986) Eclogite facies metamorphism in the lower continental crust. In: Dawson JB, Carswell DA, Hall J, Wedepohl KH (eds) Nature of the Lower Continental Crust. Geol Soc Lond Special Publ 24:193–209

Carswell DA, Gibb FGF (1980a) The equilibration conditions and petrogenesis of European crustal garnet lherzolites. Lithos 13:19–29

Carswell DA, Gibb FGF (1980b) Geothermometry of garnet lherzolite nodules with special reference to those from the kimberlites of Northern Lesotho. Contrib Mineral Petrol 74:403–416

Carswell DA, Clarke DB, Mitchell RH (1979) The petrology and geochemistry of ultramafic nodules from Pipe 200, northern Lesotho. In: Boyd FR, Meyer HOA (eds) The mantle sample: Inclusions in Kimberlites and other volcanics. Proc Second Int Kimb Conf 2:127–144. Am Geophys Union, Washington

Davidson PM, Lindsley DH (1985) Thermodynamic analysis of quadrilateral pyroxenes Part II: Model calibration from experiments and applications to geothermometry. Contrib Mineral Petrol 91:390–404

Davis BTC, Boyd FR (1966) $Mg_2Si_2O_6-CaMgSi_2O_6$ at 30 kilobars pressure and its application to pyroxenes from kimberlites. J Geophys Res 71:3567–3576

Dawson JB (1980) Kimberlites and their xenoliths. Springer Berlin

Dawson JB, Smith JV (1975) Occurrence of diamond in a mica-garnet lherzolite xenolith from kimberlite. Nature 254:580–581

Eggler DH, Wendlandt RF (1979) Experimental studies on the relationship between kimberlite magmas and partial melting of peridotite. In: Boyd FR, Meyer HOA (eds) Kimberlites, diatremes, and diamonds: their geology, petrology and geochemistry. Proc Second Int Kimb Conf 1:330–338. Am Geophys Union, Washington

Ellis DJ, Green DH (1979) An experimental study of the effect of Ca upon garnet-clinopyroxene Fe–Mg exchange equilibria. Contrib Mineral Petrol 71:13–22

Finnerty AA, Boyd FR (1984) Evaluation of thermobarometers for garnet peridotites. Geochim Cosmochim Acta 48:15–27

Finnerty AA, Boyd FR (1986) Thermobarometry for garnet peridotite xenoliths: a basis for upper mantle stratigraphy. In: Nixon PH (ed) Mantle xenoliths. J Wiley and Sons, New York

Ganguly J (1979) Garnet and clinopyroxene solid solutions, and geothermometry based on Fe–Mg distribution coefficients. Geochim Cosmochim Acta 43:1021–1029

Green DH (1973) Conditions of melting of basanite magma from garnet peridotite. Earth Planet Sci Lett 17:456–465

Haggerty SE (1986) Diamond genesis in a multiply-constrained model. Nature 320:34–38

Harley SL (1984a) The solubility of alumina in orthopyroxene coexisting with garnet in $FeO-MgO-Al_2O_3-SiO_2$ and $CaO-FeO-MgO-Al_2O_3-SiO_2$. J Petrol 25:665–696

Harley SL (1984b) An experimental study of the partitioning of Fe and Mg between garnet and orthopyroxene. Contrib Mineral Petrol 86:359–373

Harley SL, Green DH (1982) Garnet-orthopyroxene barometry for granulites and peridotites. Nature 300:697–701

Jaques AL, Green DH (1980) Anhydrous melting of peridotite at 0–15 kbar pressure and the genesis of tholeiitic basalt. Contrib Mineral Petrol 73:287–310

Kawasaki T (1979) Thermodynamic analyses on the Mg–Fe exchange equilibrium between olivine and garnet: an application to the estimation of $P-T$ relations of ultramafic rocks. J Jpn Ass Mineral Petrol Econ Geol 74:395–405

Kennedy CS, Kennedy GC (1976) The equilibrium boundary between graphite and diamond. J Geophys Res 81:2467–2470

Kretz R (1982) Transfer and exchange equilibria in a portion of the pyroxene quadrilateral as deduced from natural and experimental data. Geochim Cosmochim Acta 46:411–421

Kushiro I, Shimizu N, Nakamura Y (1972) Compositions of coexisting liquid and solid phases formed upon melting of natural garnet and spinel lherzolites at high pressures: a preliminary report. Earth Planet Sci Lett 14:19–25

Lindsley DH (1983) Pyroxene thermometry. Am Mineral 68:477–493

Lindsley DH, Dixon SA (1976) Coexisting diopside and enstatite at 20 kbar and 900°–1200° C. Am J Sci 276:1285–1301

MacGregor ID (1970) The effect of CaO, Cr_2O_3 and Al_2O_3 on the stability of spinel and garnet peridotite. Phys Earth Planet Int 3:372–377

MacGregor ID (1974) The system $MgO-Al_2O_3-SiO_3$: solubility of Al_2O_3 in enstatite for spinel and garnet peridotite compositions. Am Mineral 59:110–119

Mori T, Green DH (1978) Laboratory duplication of phase equilibria observed in natural garnet lherzolites. J Geol 86:83–97

Neumann E-R (1976) Two refinements for the calculation of structural formulae for pyroxenes and amphiboles. Norsk Geol Tidsskr 56:1–6

Nickel KG (1983) Petrogenesis of garnet and spinel peridotites. Unpubl PhD Thesis, University of Tasmania

Nickel KG, Brey G (1984) Subsolidus orthopyroxene-clinopyroxene systematics in the system $CaO-MgO-SiO_2$ to 60 kb: a re-evaluation of the regular solution model. Contrib Mineral Petrol 87:35–42

Nickel KG, Green DH (1985) Empirical geothermobarometry for garnet peridotites and implications for the nature of the lithosphere, kimberlites and diamonds. Earth Planet Sci Lett 73:158–170

Nickel KG, Brey GP, Kogarko L (1985) Orthopyroxene-clinopyroxene equilibria in the system $CaO-MgO-Al_2O_3-SiO_2$ (CMAS): New experimental results and implications for two-pyroxene thermometry. Contrib Mineral Petrol 91:44–53

Nixon PH, Boyd FR (1973) Petrogenesis of the granular and sheared ultrabasic nodule suite in kimberlites. In: Nixon PH (ed) Lesotho Kimberlites. Lesotho Nat Devel Corp Maseru, Lesotho

O'Neill HStC (1981) The transition between spinel lherzolite and garnet lherzolite, and its use as a geobarometer. Contrib Mineral Petrol 77:185–194

O'Neill HStC, Wood BJ (1979) An experimental study of Fe–Mg partitioning between garnet and olivine and its calibration as a geothermometer. Contrib Mineral Petrol 70:59–70

O'Neill HStC, Wood BJ (1980) An experimental study of Fe–Mg partitioning between garnet and olivine and its calibration as a geothermometer: corrections. Contrib Mineral Petrol 72:337

Perkins III D, Newton RC (1980) The compositions of coexisting pyroxenes and garnets in the system $CaO-MgO-Al_2O_3-SiO_2$ at 900–1100° C and high pressures. Contrib Mineral Petrol 75:291–300

Perkins III D, Holland TJB, Newton RC (1981) The Al_2O_3 contents of enstatite in equilibrium with garnet in the system $MgO-Al_2O_3-SiO_2$ at 15–40 kbar and 900°–1600° C. Contrib Mineral Petrol 78:99–109

Powell R (1985) Regression diagnostics and robust regression in geothermometer/geobarometer calibration: the garnet-clinopyroxene geothermometer revisited. J Metam Geol 3:231–243

Raheim A, Green DH (1974) Experimental determination of the temperature and pressure dependence of the Fe–Mg partition

coefficient for coexisting garnet and clinopyroxene. Contrib Mineral Petrol 48:179–203
Ringwood AE (1975) Composition and petrology of the earth's mantle. McGraw Hill, New York
Sachtleben Th, Seck HA (1981) Chemical control on the Al-solubility in orthopyroxene and its implications on pyroxene geothermometry. Contrib Mineral Petrol 78:157–165
Saxena SK (1979) Garnet-clinopyroxene geothermometer. Contrib Mineral Petrol 70:229–235
Sobolev NV (1977) Deep-seated inclusions in kimberlites and the problems of the composition of the upper mantle. Am Geophys Union, Washington
Webb SAC, Wood BJ (1986) Spinel-pyroxene-garnet relationships and their dependence on Cr/Al ratio. Contrib Mineral Petrol 92:471–480
Wells PRA (1977) Pyroxene thermometry in simple and complex systems. Contrib Mineral Petrol 62:129–139
Wood BJ (1974) Solubility of alumina in orthopyroxene coexisting with garnet. Contrib Mineral Petrol 46:1–15
Wood BJ, Banno S (1973) Garnet-orthopyroxene and orthopyroxene-clinopyroxene relationships in simple and complex systems. Contrib Mineral Petrol 42:109–124

Received August 21, 1986 / Accepted January 21, 1987

Contrib Mineral Petrol (1987) 97:473–487

Contributions to Mineralogy and Petrology

Garnet lherzolite xenoliths in the kimberlites of northern Lesotho: revised *P–T* equilibration conditions and upper mantle Palaeogeotherm

D.A. Carswell and F.G.F. Gibb
Department of Geology, University of Sheffield, Mappin Street, Sheffield S1 3JD, UK

Abstract. Evidence is presented that the inflected palaeogeotherm for northern Lesotho, previously highlighted by Boyd (1973), Boyd and Nixon (1973, 1975), Finnerty and Boyd (1984, 1987), is essentially an artifact of the unsatisfactory, over-simplified barometer formulation (based on MacGregor 1974) employed. The absence of an inflection in the palaeogeotherm for Udachnaya, Siberia based on *P–T* estimates for garnet lherzolite xenoliths calculated with the same barometer, does not prove the reality of an inflected palaeogeotherm for northern Lesotho. Rather, it reflects, at least in part, chemical differences between the equivalent deformed, high-*T* xenoliths in these two areas – most importantly expressed in the respective contents of jadeite relative to ureyite in the constituent orthopyroxenes. Accurate estimation of *P–T* equilibration conditions for garnet lherzolite xenoliths requires both complete and precise mineral analyses and adequate consideration of the influence of minor elements, such as Cr and Na, on the element exchange reaction thermometers and barometers employed. The barometer formulation of Nickel and Green (1985) is judged to be the best currently available. As no single thermometer is entirely satisfactory and dependable throughout the *P–T* range of interest, equilibration temperatures are currently best assessed as a mean value obtained from application of the most accurate formulations for both the two-pyroxene solvus thermometer (Bertrand and Mercier 1985) and $Fe^{2+}-Mg^{2+}$ exchange reactions between garnet-clinopyroxene (Powell 1985), garnet-orthopyroxene (Harley 1984a) and garnet-olivine (O'Neill and Wood 1979) mineral pairs. Such 'best' $P-T$ estimates for xenoliths in the kimberlites of northern Lesotho indicate a somewhat elevated, non-inflected, upper mantle palaeogeotherm, compatible with a 120–145 km thick thermally conductive lithosphere above a convecting asthenosphere. The common coarse textured, chemically depleted, garnet lherzolite xenoliths appear mostly to have originated from close to the base of the lithosphere whilst the contrasting deformed, higher *T*, more chemically fertile xenoliths have come from the underlying asthenosphere. There is evidence for slight variations in the heat flux within the mantle beneath northern Lesotho at the time of emplacement of the Thaba Putsoa and Mothae kimberlites, only some 16 km apart, and also possibly for a regional variation in the thickness of the lithosphere.

Background

Boyd (1973), Nixon and Boyd (1973a), Boyd and Nixon (1973, 1975) pioneered the application of element exchange reaction thermobarometers to mantle-derived garnet lherzolite xenolith suites encountered in kimberlites. Calculated equilibrium pressures (*P*) and temperatures (*T*) for individual xenoliths have been taken to indicate prevailing $P-T$ conditions in the upper mantle immediately prior to entrainment in the enclosing kimberlite, and the array of $P-T$ points defined by an analysed suite of xenoliths at a particular kimberlite locality taken to represent the upper mantle geotherm beneath the area at that time.

Garnet lherzolite xenoliths with contrasting coarse (granular) or deformed (sheared) textures (Boullier and Nicolas 1973; Harte 1977) have been documented by Nixon and Boyd (in Nixon 1973) from various kimberlite localities in northern Lesotho, southern Africa. The majority of their analysed xenoliths were from the Thaba Putsoa and Mothae pipes but individual samples from the Matsoku, Kao, Lemphane and Liqhobong pipes, two from Letseng-la-Terae and one from Monastery Mine close to the NW border of Lesotho in Orange Free State, South Africa, were also considered. Boyd (1973), Boyd and Nixon (1973, 1975) further demonstrated that the deformed xenoliths have equilibrated at considerably higher temperatures than the coarse, undeformed xenoliths. Whilst the lower temperature, coarse grained group of xenoliths was shown to have equilibrated at $P-T$ conditions close to the shield geotherm of Clark and Ringwood (1964), the higher temperature, deformed xenoliths were believed to define a marked deviation away from the predicted steady-state conductive mantle geotherm at depths exceeding 150–180 km (depending on the actual barometer used). Furthermore it was suggested that the point of inflection in the deduced 'pyroxene' geotherm corresponded to the lithosphere/asthenosphere boundary during the Late Cretaceous (the time of emplacement of these kimberlites) and that the perturbation of the geotherm was a consequence of stress heating of the deformed garnet lherzolites in response to horizontal shearing connected with the break-up and dispersal of Gondwanaland.

This stimulating interpretation has prompted considerable further analysis and interpretation of the peridotite xenolith suites in the kimberlites of northern Lesotho and

elsewhere. Deformed garnet lherzolite xenoliths in kimberlites at certain other localities [such as Premier Mine near Pretoria, South Africa (Danchin 1979), and Frank Smith Mine to the NW of Kimberley, South Africa (Boyd 1974)] have likewise equilibrated at appreciably higher temperatures than associated coarse grained xenoliths and have also been taken to define inflected palaeogeotherms. However, elsewhere [as in the Kimberley area kimberlites (Dawson et al. 1975; Boyd and Nixon 1978), and in the Matsoku pipe in northern Lesotho (Cox et al. 1973; Harte et al. 1975)] deformed garnet lherzolites have mineral chemistries which indicate that they have equilibrated under essentially the same $P-T$ conditions, as associated undeformed xenoliths. By contrast, deformed garnet lherzolite xenoliths in the Udachnaya kimberlite, USSR, have been shown (Boyd 1984) to have equilibrated at appreciably higher temperatures than associated coarse, undeformed xenoliths but at $P-T$ conditions which lie on the continuation of a cratonic area geotherm calculated for a 40 mW m^{-2} surface heat flow above a conductive mantle (Pollack and Chapman 1977).

It is thus apparent that there is no general correlation between degree of deformation, equilibration temperature and depth of origin. However, in kimberlites with a bimodal temperature distribution within the observed garnet lherzolite xenolith suite, the higher temperature xenoliths invariably have deformed (porphyroclastic or mosaic-porphyroclastic) textures. Why they define inflected geotherms in some instances (northern Lesotho, Premier Mine) but not in others (Udachnaya) has never been adequately explained, but the reality of inflected geotherms seems to have been widely accepted.

Suggestions that inflected geotherms may be spurious and result from the use of inaccurately calibrated mineral thermometers and barometers (Howells and O'Hara 1978) or from unsatisfactory application of mineral thermometers and barometers based on equilibria in simple chemical systems to xenoliths with more complex and differing chemistries (Mercier and Carter 1975) have received little attention. In addition, Harte (1978) has pointed out that as far as the xenoliths from the northern Lesotho kimberlites are concerned, those from *individual* pipes may be interpreted as defining linear or gently curved dT/dP gradients without obvious inflections. This interpretation was endorsed by Harley (1984b) and by Harley and Thompson (1984) who also emphasised that $P-T$ estimates are critically dependent upon the choice of thermometer-barometer pairing and hence that the uncertainties are such that unequivocal interpretations of the $P-T$ arrays are impossible.

Despite these reservations, Finnerty and Boyd (1984, 1987) have recently published results of an extensive evaluation of thermobarometers applicable to garnet lherzolite xenoliths and emphasised the existence of an inflection in the northern Lesotho palaeogeotherm for almost every combination of thermometer and barometer tested. With the large number of independent thermometers tested it was stated that the inflection cannot be an artifact of the method of temperature estimation but they conceded that it could be due to a problem with the barometer employed.

Since the first description by Boyd (1973) of the inflected northern Lesotho palaeogeotherm, there has probably been more debate over its interpretation than its reality. The original interpretation that it reflected stress (shear) heating of deformed asthenospheric garnet lherzolite during plate movements associated with the break-up of Gondwanaland now has to be rejected on several grounds. Firstly, a comparable inflected palaeogeotherm has been described from the xenolith suite in the Precambrian Premier Mine kimberlite (Danchin and Boyd 1976; Danchin 1979). Secondly, Mercier and Carter (1975) have argued from mechanical considerations that shear heating is likely to be negligible for the viscosities and strain rates expected at the $P-T$ conditions of the inflected geotherms. Furthermore, comparative thermometry on analysed porphyroclast and recrystallised neoblast assemblages in deformed high-temperature garnet lherzolite xenoliths from northern Lesotho gives no indication of shear heating. Recorded chemical differences between porphyroclasts and neoblasts are small (Mercier and Carter 1975; Lock 1980) or insignificant (Boyd 1975) and, if anything, point to cooling rather than heating during deformation.

Dislocation studies and the limited recovery, recrystallisation and grain growth shown by some deformed xenoliths indicate that they have been subjected to high stress and high strain rate deformation only shortly before eruption of the enclosing kimberlite (Goetze 1975; Harte 1978). Consequently, explanations of the thermal anomalies associated with inflected palaeogeotherms have shifted to alternative models involving convective heat transfer either in rising mantle diapirs (Green and Gueguen 1974) or plumes (Parmentier and Turcotte 1974) connected with kimberlite generation, or to thermal aureole effects resulting from close proximity to bodies of 'protokimberlite' magma (Harte 1983; Mitchell 1984) – possibly the magma responsible for the crystallisation of the Cr-poor megacryst (discrete nodule) suites (Gurney and Harte 1980; Harte and Gurney 1981) also observed in the kimberlites in northern Lesotho (Nixon and Boyd 1973b) and elsewhere. Mercier (1979) has argued that the high stress, sheared textures characteristic of the deformed high-temperature xenoliths formed within a few hours (at most) of sampling by the kimberlite and seem more appropriately ascribed to the rapid, high stress, process of kimberlite conduit formation than to slower major geotectonic processes such as the ascent of large mantle diapirs or convection-related flow.

Nixon and Boyd (1973a), Boyd and Nixon (1975), Nixon et al. (1981) have drawn attention to the bulk rock chemical differences between the deformed (sheared) high-T and coarse (granular) low-T garnet lherzolite xenoliths in the northern Lesotho kimberlites. The deformed high-T xenoliths have been shown to have relatively fertile (undepleted in basaltic components) compositions with higher Fe, Ti, Ca, Al and Na contents and Fe/(Fe+Mg) ratios than the coarse low-T xenoliths. They attributed these differences to the derivation of the former xenoliths from more pristine mantle in the asthenosphere and the latter from the depleted (residual) overlying lithosphere. By contrast, Gurney and Harte (1980) and Harte (1983) have emphasised the importance of metasomatism associated with earlier magmatic intrusions at depth in the mantle as a process leading to the Fe–Ti enrichment and general 'fertilisation' of the deformed high-T garnet lherzolites. The apparent influence of diffusive metasomatism on the chemistry of deformed high-T xenoliths from northern Lesotho is demonstrated by observed enrichment in Ti, Fe and Na and depletion in Cr of garnet porphyroclast rims (Smith and Boyd 1986). However, it is debatable as to what extent there is a direct inter-relationship between this metasoma-

tism, the deformation, the deduced high equilibration temperatures for certain xenoliths and inflected palaeogeotherms.

Metasomatic effects (including Fe–Ti enrichment) associated with pyroxenite sheet emplacement have been well documented in the banded peridotite/pyroxenite xenolith suite from the Matsoku pipe in northern Lesotho (Harte et al. 1975; Gurney and Harte 1980; Harte and Hunter 1986). However, in the Matsoku xenolith suite there is no apparent correlation between this metasomatism and observed deformation. Furthermore, our $P-T$ calculations confirm earlier indications (Harte et al. 1975; Harte 1978) of comparable $P-T$ equilibration conditions for the Matsoku peridotite/pyroxenite xenolith suite regardless of the extent of metasomatism or deformation.

Similar diffusive Fe–Ti enrichment and Cr depletion in garnet porphyroclast rims to those observed in deformed high-T xenoliths from the northern Lesotho kimberlites, have also been documented in rather lower temperature deformed garnet lherzolite xenoliths from the Kimberley area mines (Smith and Boyd 1986) and Udachnaya, Siberia (Sobolev et al. 1986) which do not define inflected palaeogeotherms. Moreover, Smith and Boyd (1986) have argued that, since olivine compositions in the deformed high-T xenoliths from northern Lesotho are distinctly more fayalitic than those in the associated coarse lower-T xenoliths and olivine compositions are likely to be relatively insensitive to any infiltration metasomatism, significant bulk rock composition differences (notably in Fe/Mg) between the high-T and low-T xenoliths probably existed prior to any late-stage metasomatism and tectonic mixing. This view appears to be substantiated by their respective trace element and isotopic signatures. Data for deformed high-T xenoliths from northern Lesotho indicate internal Nd and Sm isotopic equilibrium at the time of sampling by the kimberlite with REE and isotopic signatures resembling those of somewhat depleted (high Sm/Nd, low Rb/Sr) MORB-type mantle from the convective asthenosphere. Thus Richardson et al. (1985) comment that the trace element and isotopic systematics of these relatively more fertile peridotites do not require a more complex origin involving diffusive introduction of a basaltic or protokimberlitic component from megacryst forming magmas as proposed by Gurney and Harte (1980); and Harte (1983). By contrast, lower temperature coarse and deformed garnet lherzolite xenoliths (with depleted major element compositions) from the Kimberley area kimberlites display either internal isotopic equilibrium or inverse isotopic equilibrium attributable to addition of a mantle metasomatic component without re-equilibration and have overall isotopic signatures indicative of variably enriched (low Sm/Nd, high Rb/Sr) old subcontinental lithospheric mantle.

Available evidence thus indicates fundamentally different bulk rock chemistries and origins for the deformed high-T and coarse low-T garnet lherzolite xenolith suites in the kimberlites of northern Lesotho. We proceed here to assess the respective $P-T$ equilibration conditions for these two groups of xenoliths taking full account of their contrasted bulk rock chemistries in order to ascertain whether the inflected palaeogeotherm, which is a key feature of many interpretative models, is real or spurious. We also aim to resolve the enigma as to why deformed high-T garnet lherzolite xenolith suites apparently define inflected palaeogeotherms for some areas (e.g., northern Lesotho) but not for others (e.g., Udachnaya, Siberia). Boyd (1975) has taken the fact that inflections based on $P-T$ estimates derived from pyroxene compositions are sometimes present and sometimes not to indicate that they are real and not an artifact of the thermobarometric methods employed. Here we explore the possibility that the presence or absence of inflections in derived palaeogeotherms may be due to chemical differences between the respective xenolith suites.

Thermometer and barometer selection

$P-T$ equilibration conditions for garnet lherzolite assemblages may be determined through application of paired thermometers and barometers (thermobarometers) based on calibrated element exchange reaction equilibria. The most sensitive thermometers in the $P-T$ range of interest are those which consider $Ca^{2+} \rightleftharpoons Mg^{2+}(Fe^{2+})$ exchange between the coexisting pyroxenes (two pyroxene solvus thermometer) and $Fe^{2+} \rightleftharpoons Mg^{2+}$ exchange between garnet and coexisting pyroxene or olivine ($K_{Gnt-Cpx}^{Fe-Mg}$, $K_{Gnt-Opx}^{Fe-Mg}$, $K_{Gnt-Oliv}^{Fe-Mg}$ exchange thermometers). The most appropriate barometer is that which considers the extent of Tschermak's molecule type substitution $(MgFeCa)_{M2}Al_{M1}^{VI}\,Al_{Z}^{IV}\,SiO_6$ – in orthopyroxene coexisting with garnet. As several different formulations and experimental or semi-empirical calibrations have been proposed for these thermometers and barometers, it is first necessary to assess which provide the most accurate and geologically meaningful $P-T$ estimates for natural garnet lherzolite assemblages. A serious problem is that most calibrations are based on experimental data for simple chemical systems which do not precisely simulate natural rock systems, although some formulations incorporate semi-empirical, thermodynamically-derived corrections aimed at taking account of the more complex chemistries of the naturally occurring mineral assemblages.

Finnerty and Boyd (1984, 1987) have attempted to evaluate the accuracy of $P-T$ estimates obtained for the garnet lherzolite xenolith suite in the kimberlites of northern Lesotho from selected pairings of thermometers and barometers by reference to he $P-T$ constraints provided by experimental data on the diamond-graphite transition curve (Kennedy and Kennedy 1976) and on phlogopite stability (Eggler and Wendlandt 1979). In practice the phlogopite constraint is poor with different generations of phlogopite growth frequently present (e.g., Carswell 1975) and uncertainty over the location in $P_{TOTAL}-T$ space of the stability curve for natural phlogopites. Hence the assessments by Finnerty and Boyd (1984, 1987) of the most accurate combination of thermometer and barometer (thermobarometer) have been influenced largely by consideration of the calculated $P-T$ estimates for just one diamond bearing xenolith, BD 2125 from Mothae (Dawson and Smith 1975), and one primary graphite bearing xenolith, PHN 2569 from Thaba Putsoa (Nixon and Boyd 1973a), relative to the diamond-graphite transition curve of Kennedy and Kennedy (1976). Finnerty and Boyd (1987) have concluded that the most accurate $P-T$ equilibration estimates for the garnet lherzolite xenolith suite from northern Lesotho are those provided by their revised formulation (FB87) for the two-pyroxene solvus thermometer in combination with a barometer formulation (MC74) based on the experimental data of MacGregor (1974) for the weight percent Al_2O_3 content of orthopyroxene coexisting with garnet in the $MgO-Al_2O_3-$

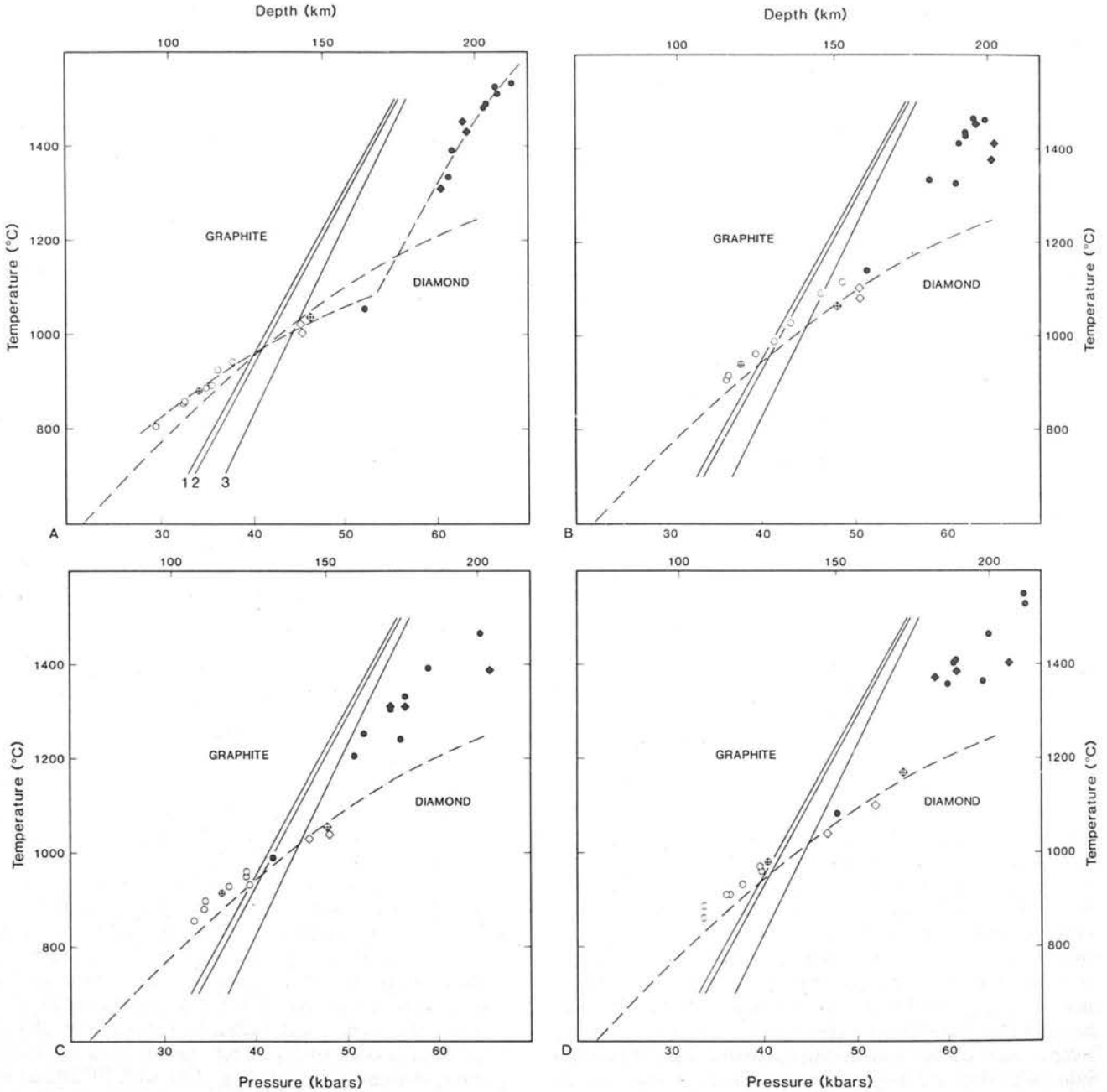

Fig. 1 A–D. $P-T$ equilibration estimates for xenolith suites from Thaba Putsoa: ● deformed, ○ coarse, ⊕ coarse (graphite), and Mothae: ◆ deformed, ◇ coarse, ⌖ coarse (diamond), calculated using the barometer formulated from MacGregor (1974) in combination with: **A** The two-pyroxene solvus thermometer of Finnerty and Boyd (1987); **B** The thermometer for $Fe^{2+} \rightleftharpoons Mg^{2+}$ exchange between garnet-clinopyroxene pairs (Powell 1985); **C** The thermometer for $Fe^{2+} \rightleftharpoons Mg^{2+}$ exchange between garnet-orthopyroxene pairs (Harley 1984a); **D** The thermometer for $Fe^{2+} \rightleftharpoons Mg^{2+}$ exchange between garnet-olivine pairs (O'Neill and Wood 1979). Also indicated are the continental shield geotherm (—·—·—) of Pollack and Chapman (1977) calculated for a 40 mW m^{-2} surface heat flow above a conductive mantle and an inflected palaeogeotherm (— — —) of the form proposed by Finnerty and Boyd (1984, 1987) based on the calculated $P-T$ values for xenoliths from Thaba Putsoa and Mothae. The different $P-T$ locations indicated for the diamond-graphite transition curve are: 1 Based on thermodynamic data of Berman (1979); 2 Based on experimental data of Bundy et al. (1961), Bundy (1980); 3 Based on experimental data of Kennedy and Kennedy (1976). Sources of analytical data for xenolith suites are indicated in the general text

SiO_2 (MAS) system. This thermobarometer (FB87 v MC74) yields $P-T$ estimates for the northern Lesotho xenolith suite which indicate a markedly inflected palaeogeotherm (reproduced in Figs. 1 A and 5B) with the deformed high-T xenolith group plotting at temperatures elevated well above the predicted conductive shield geotherm. An inflected palaeogeotherm is especially evident when $P-T$ data for xenoliths from different northern Lesotho kimberlite localities are aggregated together (Fig. 5B) and the low-temperature part of the palaeogeotherm is constrained to be sub-parallel to the conductive shield geotherm.

We have recently published (Carswell and Gibb 1987) the results of a different approach to the evaluation of thermometers and barometers applicable to garnet lherzolite

assemblages, in which we tested the ability of individual thermomemeters and barometers to reproduce the $P-T$ conditions of experimentally equilibrated multi-component garnet lherzolite assemblages (Akella 1976; Nickel 1983; Mori and Green 1978) which closely approach the compositions of the natural assemblages encountered as xenoliths in kimberlites. We concluded that the best barometer formulation is that provided by Nickel and Green (1985) based on experimental data for the $CaO-MgO-Al_2O_3-SiO_2$ (CMAS) and chrome bearing $SiO_2-MgO-Al_2O_3-CaO-Cr_2O_3$ (SMACCR) systems with the content of Al^{3+} in the octahedral sites (M1) of orthopyroxenes present as a result of Tschermak's molecule type substitution, evaluated as:

$$X_{Al}^{M1}=[Al^{Total}-(Cr^{3+}+Fe^{3+}+2Ti^{4+}-Na^{+})]/2.$$

The term $(Cr^{3+}+Fe^{3+}+2Ti^{4+}-Na^{+})$ takes account of the presence of Al^{3+} in tetrahedral sites as expressed in $MgCrAlSiO_6$, $MgFe^{3+}AlSiO_6$ and $MgTiAl_2O_6$ type molecules after first correcting for the Cr^{3+} and Fe^{3+} combined with Na in $NaCrSi_2O_6$ and $NaFe^{3+}Si_2O_6$. However, when $Na^{+}>(Cr^{3+}+Fe^{3+}+2Ti^{4+})$ then the Al^{3+} combined with Na^{+} in jadeite ($NaAlSi_2O_6$) has to be subtracted in order to obtain the correct amount of Al^{3+} present in M1 sites as a result of Tschermak's molecule type substitution.

We have since tested in the same manner an additional barometer formulation proposed by Bertrand et al. (1986), which is unusual in that it considers the content of Al^{3+} in tetrahedral (Z) rather than octahedral (M1) sites as a measure of the degree of Tschermak's molecule type substitution in orthopyroxenes. Our tests indicate that this formulation is not as good as that of Nickel and Green (1985) and in many instances seriously underestimates equilibration pressures. Problems arise with this barometer formulation when orthopyroxenes have $Cr^{3+}>0.82\ Na^{+}$ (as is frequently the case) since $MgCrAlSiO_6$ type substitutions are not considered and hence the excess Cr^{3+} leads to overestimated X_{Al}^{Z} values and hence underestimated pressures.

From our thermometer tests (Carswell and Gibb 1987) we concluded that no single thermometer formulation is satisfactory throughout the entire $P-T$ range of interest, and proposed that equilibration temperatures for garnet lherzolite xenolith assemblages should be assessed from a combination of the most reliable formulations of the two-pyroxene solvus thermometer (Wells 1977; Finnerty and Boyd 1987) and $Fe^{2+}\rightleftharpoons Mg^{2+}$ exchange reaction thermometers between the different mineral pairs (Ellis and Green 1979; Powell 1985; Harley 1984a; O'Neill and Wood 1979). Our tests also indicated that the two-pyroxene solvus thermometer formulation (FB87) favoured by Finnerty and Boyd (1987) tends to yield underestimates at temperatures $<1000°$ C and more serious overestimates at $T>1200°$ C. These problems probably arise because the simple formulation used, with reference to CMS system experimental data, as a measure of the enstatite component in clinopyroxenes, namely 1-[2Ca/(Ca+Mg)], is inadequate for more chemically complex natural pyroxenes. We further demonstrated that the alternative formulation (WE77) of Wells (1977), which attempts to correct for the effect on the $Ca^{2+}\rightleftharpoons Mg^{2+}$ exchange reaction between coexisting pyroxenes produced by the presence of other elements (especially Fe) in the M1 and M2 sites, yields more satisfactory temperature estimates for assemblages equilibrated in the lower part of the $P-T$ range considered but seriously underestimates at pressures greater than about 37 kbar since it does not incorporate a correction factor to take account of the influence of pressure on the pyroxene miscibility relationships.

As no single formulation of the two-pyroxene solvus thermometer tested was judged satisfactory throughout the $P-T$ range of interest, we concluded (Carswell and Gibb 1987) that two-pyroxene solvus temperatures for garnet lherzolite xenolith assemblages were probably best assessed by WE77 in the lower part of the $P-T$ range but by an average of the WE77 and FB86 values for assemblages equilibrated at $P>37$ kbar, when errors from the two methods are likely to be in opposite directions. We have since tested a further formulation (BM85) of the two-pyroxene solvus thermometer, proposed by Bertrand and Mercier (1985), which incorporates corrections for the influence of Fe, Na and pressure on $Ca^{2+}\rightleftharpoons Mg^{2+}$ exchange as observed in the CMS system. We now consider BM85 to be the best single formulation currently available for the two-pyroxene solvus thermometer for the $P-T$ range encountered in the garnet lherzolite xenolith assemblages. However, it is rather critically dependent upon the availability of accurate analyses for Na in orthopyroxenes (it should *not* be used when Na contents in orthopyroxenes have not been determined) and there are some indications that it may tend to slightly overestimate at the highest temperatures.

Our barometer tests (Carswell and Gibb 1987) have shown that the formulation (MC74) favoured by Finnerty and Boyd (1984, 1987) seriously overestimates the experimentally recorded equilibration pressures for test data (Akella 1976; Nickel 1983; Mori and Green 1978) which either correspond to or closely simulate natural garnet lherzolite compositions. This overestimation is worst at the highest temperatures and for the most chrome-rich compositions. In the MC74 barometer as formulated by Finnerty and Boyd (1984) the extent of Tschermak's molecule type substitution in orthopyroxene is simplistically taken as the total weight fraction of Al_2O_3 present. This is reasonably satisfactory for orthopyroxene compositions within the MAS system on which the barometer is based but is inappropriate for more chemically complex orthopyroxenes such as those in garnet lherzolite xenoliths with significant contents of Fe, Ca, Na, Ti and Cr. More recent experimental data (O'Neill 1981; Nickel and Green 1985; Webb and Wood 1986) have demonstrated that the content of Cr can be expected to have a particularly profound influence on the garnet-orthopyroxene equilibrium. It is therefore clear that a barometer based on this equilibrium must take adequate account of the influence of these other chemical components and be formulated along the lines proposed by Nickel and Green (1985).

From the foregoing we certainly would not expect the thermobarometer favoured by Finnerty and Boyd (1987) based on a combination of the FB87 two-pyroxene solvus thermometer and the MC74 barometer to yield the most accurate and geologically meaningful values for the $P-T$ equilibration conditions of the garnet lherzolite assemblages encountered as xenoliths in kimberlites.

Reality of the inflected palaeogeotherm

Our conclusion that the FB87 two-pyroxene solvus thermometer tends to underestimate equilibration temperatures for the lower-T xenoliths and overestimate temperatures for the higher-T xenoliths can not alone explain away the

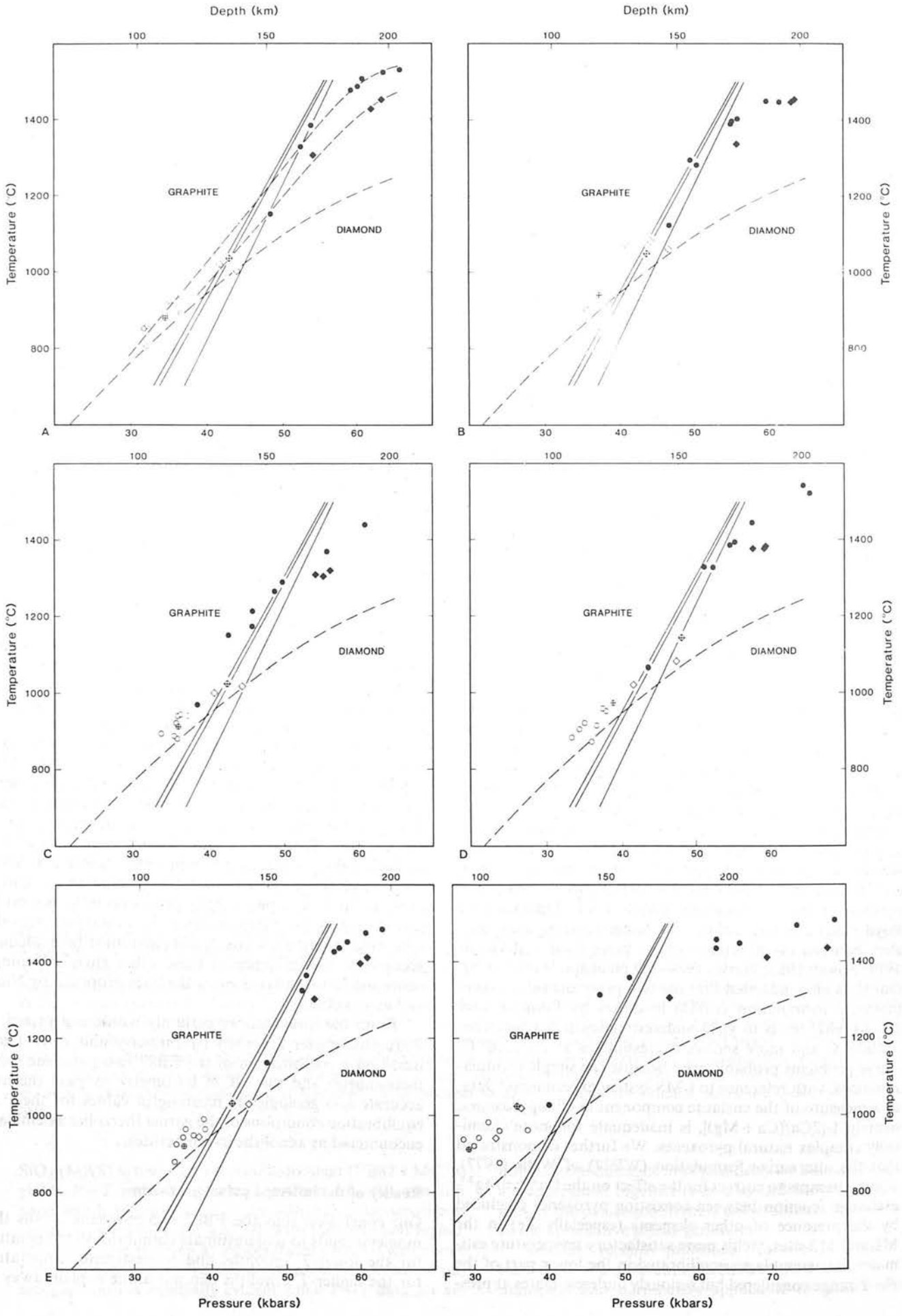
Depth (km)
100
150
200
1400
1200
1000
800
Temperature (°C)
GRAPHITE
DIAMOND
A
B
C
D
E
F
30
40
50
60
70
Pressure (kbars)

inflected palaeogeotherm for the northern Lesotho garnet lherzolite suite. Comparison of Fig. 1A with Fig. 1B D demonstrates that combination of the MC74 barometer formulation with alternative thermometers for $Fe^{2+} \rightleftharpoons Mg^{2+}$ exchange reactions between different mineral pairs produces significant changes in the $P-T$ estimates for individual xenoliths from the Thaba Putsoa and Mothae kimberlites but in each case it is still possible to infer an inflected palaeogeotherm. We therefore agree with Finnerty and Boyd (1984) that the apparent inflection in the geotherm cannot just be an artifact of the particular thermometer used.

Figure 2A–D show comparative $P-T$ estimates for the same xenolith populations obtained by the use of the same four thermometers in combination with the barometer formulation of Nickel and Green (1985), which we would expect to yield the most accurate pressure values (Carswell and Gibb 1987). In addition, equivalent $P-T$ estimates obtained using the two-pyroxene solvus thermometer formulation of Bertrand and Mercier (1985) rather than that of Finnerty and Boyd (1986) are shown in Fig. 2E. We conclude from Fig. 2A–E that if the doubtful constraint that the lower $P-T$ points should lie on a geotherm subparallel to the expected conductive shield geotherm is discarded, then the $P-T$ arrays can be more appropriately interpreted as defining palaeogeotherms somewhat elevated overall above the 40 mW/m^2 shield geotherm shown, rather than markedly inflected palaeogeotherms of the form described by Boyd (1973) and Finnerty and Boyd (1984, 1987). An interesting additional feature, arising from the use of the improved and more sophisticated barometer formulation of Nickel and Green (1985), is that the $P-T$ arrays for the Thaba Putsoa and Mothae xenolith suites are largely distinct and thus, as illustrated in Fig. 2A, appear to define separate, non-inflected palaeogeotherms. This suggests a marginally higher heat flux in the mantle beneath Thaba Putsoa than at Mothae at the time of sampling by kimberlites only some 16 km apart.

Comparison between the $P-T$ arrays in Figs. 1 and 2 thus confirms our view that inflections in the upper mantle palaeogeotherm(s) for northern Lesotho are artifacts which result largely from the use of over-simplified and inadequate barometer formulations. The MC74 barometer is particularly unsatisfactory in this respect leading to a marked, but nonetheless spurious, inflection when combined with the FB87 thermometer (Figs. 1A and 5B). With the MC74 barometer the progressive pressure overestimation expected from our tests (Carswell and Gibb 1987) is only in evidence along the lower temperature part of the geotherm, subparallel to the conductive shield geotherm. On the other hand, the deformed high-T group of xenoliths plots at elevated temperatures and dramatically reduced pressures relative to the shield geotherm. The reason for this unexpected pressure reduction is that the orthopyroxenes in the xenoliths concerned have significant jadeite contents.

The presence of jadeite substitution is demonstrated in Fig. 3A where it can be seen that orthopyroxenes in these deformed high-T xenoliths almost invariably have $Na^+ > Cr^{3+}$ and that the excess Na^+ correlates with Al^{3+}. The jadeite contents of these orthopyroxenes reflect the more fertile Na-enriched bulk rock compositions of these high-T xenoliths compared to the coarse low-T xenoliths (Nixon and Boyd 1973a; Carswell 1980, Table 5). By contrast what little Na is present in orthopyroxenes of the coarser lower-T xenoliths appears to be effectively combined in ureyite ($NaCrSi_2O_6$) and jadeite contents are negligible.

Failure of the MC74 barometer to allow for Al^{3+} combined with Na^+ as jadeite in the deformed high-T xenoliths, means that the amount of Al taken to be involved in Tschermak's molecule substitution is overestimated. Hence calculated equilibration pressures in these xenoliths are reduced relative to the overestimated values normally expected from MC74 based on tests on Na-free or Na-poor rock compositions (Carswell and Gibb 1987). With the combined FB87 v MC74 thermobarometer recommended by Finnerty and Boyd (1987) the apparent inflection of the palaeogeotherm for northern Lesotho is further enhanced by erroneously high temperatures for the deformed high-T group of xenoliths.

Revised pressure-temperature estimates and interpretation

As no single thermometer formulation applicable to garnet lherzolite assemblages is entirely satisfactory throughout the entire $P-T$ range observed in kimberlite xenoliths (Carswell and Gibb 1987), significant differences arise between the $P-T$ equilibration conditions deduced for individual xenoliths depending on the particular thermometer employed (Fig. 2A–E). Also with only a single temperature estimate for a xenolith based on one particular element exchange reaction it is not possible to identify erroneous values resulting from analytical errors or unsatisfactory equilibration between the selected mineral pair. As stated previously we therefore calculate equilibration temperatures for such xenoliths as an average value obtained from consideration of the best available calibrations for several different element exchange reactions between different mineral pairs. We have calculated these temperatures in combination with pressures obtained from the Nickel and Green (1985) barometer formulation.

Our revised 'best' values for the pressure (P^*) and temperature (T^*) equilibration conditions of garnet lherzolite assemblages in the analysed xenolith suites from Thaba Putsoa and Mothae (data from Nixon and Boyd 1973a; Boyd and Finger 1975; Dawson and Smith 1975) are listed in

Fig. 2A–F. $P-T$ equilibration estimates for garnet lherzolite xenoliths from Thaba Putsoa: ● deformed, ○ coarse, ⊕ coarse (graphite), and Mothae: ◆ deformed, ◇ coarse, ◈ coarse (diamond) calculated using the following thermometer-barometer combinations: **A** Two-pyroxene solvus thermometer (Finnerty and Boyd 1987) – barometer (Nickel and Green 1985); **B** Thermometer for $Fe^{2+} \rightleftharpoons Mg^{2+}$ exchange between garnet-clinopyroxene pairs (Powell 1985) – barometer (Nickel and Green 1985); **C** Thermometer for $Fe^{2+} \rightleftharpoons Mg^{2+}$ exchange between garnet-orthopyroxene pairs (Harley 1984a) – barometer (Nickel and Green 1985); **D** Thermometer for $Fe^{2+} \rightleftharpoons Mg^{2+}$ exchange between garnet-olivine pairs (O'Neill and Wood 1979) – barometer (Nickel and Green 1985); **E** Two-pyroxene solvus thermometer (Bertrand and Mercier 1985) – barometer (Nickel and Green 1985); **F** Two-pyroxene solvus thermometer (Bertrand and Mercier 1985) – barometer (Bertrand et al. 1986). Note the change of pressure scale relative to the other diagrams. Diamond-graphite inversion curves and shield geotherm as in Fig. 1. Separate palaeogeotherms based on the $P-T$ arrays for the Thaba Putsoa and Mothae xenolith suites are only shown in **A** but can also be deduced for the other $P-T$ plots

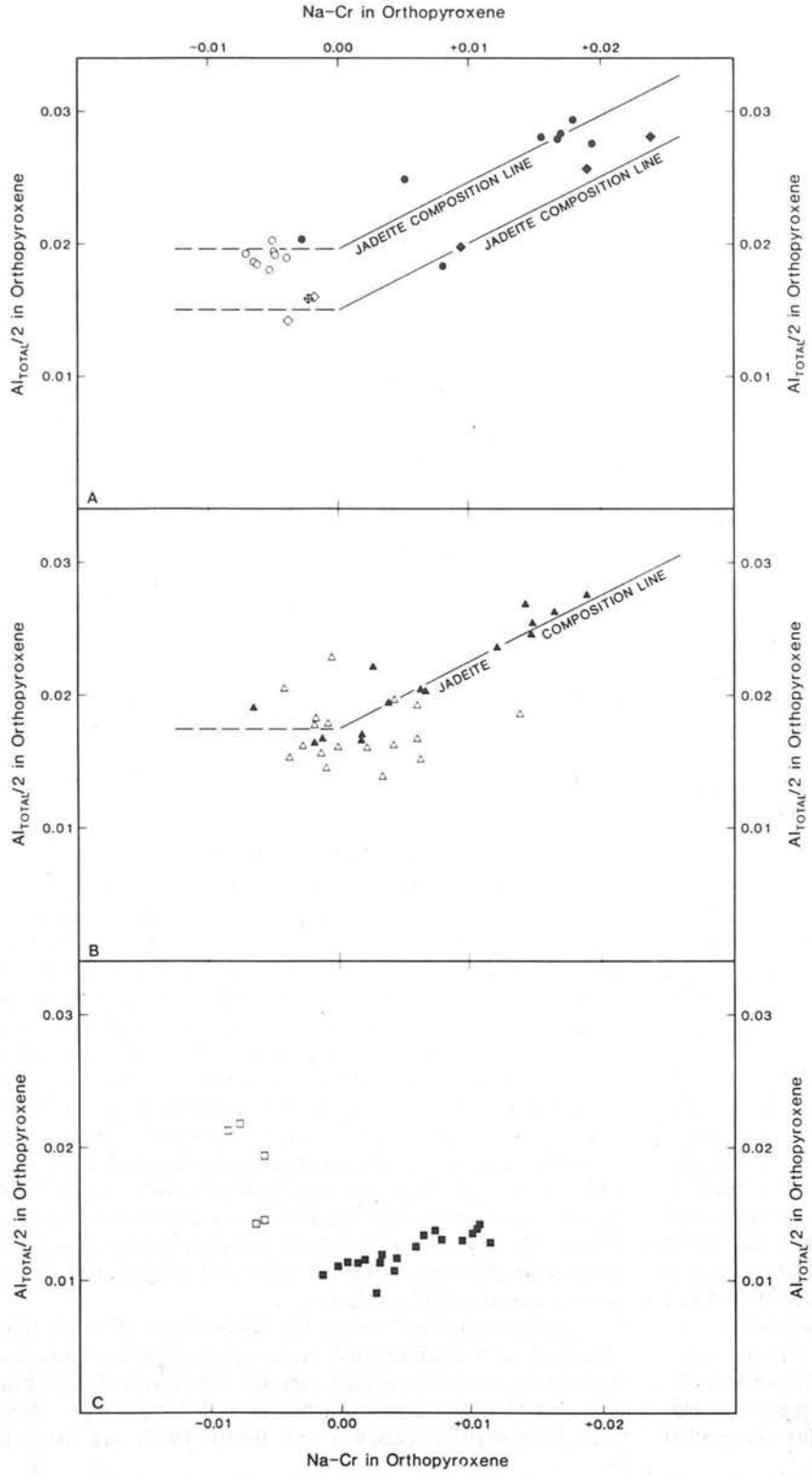

Fig. 3A–C. Comparison of orthopyroxene compositions in terms of total Al 2 vs (Na − Cr) in 6-oxygen formulae for deformed and coarse textured garnet lherzolite xenoliths from: **A** Thaba Putsoa; ● deformed, ○ coarse and Mothae: ◆ deformed, ◇ coarse, ⌖ coarse (diamond): **B** Letseng Main and Satellite Pipes; ▲ deformed, △ coarse: **C** Udachnaya, Siberia: ■ deformed, □ coarse – data from Boyd (1984) and Carswell (unpublished)

Table 1 and plotted in Fig. 4A. P^* and T^* values were calculated as follows:

i. A two-pyroxene solvus temperature was calculated using the formulation of Bertrand and Mercier (1975), these values usually being close to those from the Wells (1977) formulation for lower-T xenoliths and between those from the Wells (1977) and Finnerty and Boyd (1987) formulation for higher-T xenoliths.

ii. An $Fe^{2+} \rightleftharpoons Mg^{2+}$ exchange reaction temperature was calculated by averaging results for $Fe^{2+} \rightleftharpoons Mg^{2+}$ exchange between garnet-clinopyroxene, garnet-orthopyroxene and garnet-olivine pairs obtained from the thermometer formulations of Powell (1985), Harley (1984a) and O'Neill and Wood (1979), respectively. For garnet-clinopyroxene pairs the formulation of Powell (1985) was preferred to that of Ellis and Green (1979) since our tests indicated that it yields better values at $T < 1200°$ C and closely similar values to that of Ellis and Green (1979) at higher temperatures.

Table 1. Calculated pressure (kbar)-temperature (°C) estimates for garnet lherzolite xenoliths from Thaba Putsoa and Mothae

Locality	Texture	Sample numbers	Thermometer									
			2-Pyroxene solvus			$Fe^{2+}\rightleftharpoons Mg^{2+}$ exchange			Best 2-Px solvus	Best $Fe\rightleftharpoons Mg$ exchange	T^*	P^*
			WE77	FB87	BM85	Gnt–Cpx POW.85	Gnt–Opx HAR.84	Gnt–Oliv OW.79	T	T	Mean	NG 85
Thaba Putsoa	Coarse	PHN 1595	889	807	878	912	888	909	878	903	891	35.7
		PHN 1569[a]	911	881	918	938	918	962	918	939	929	36.8
		PHN 1567	920	852	925	949	937	922	925	936	930	35.6
		PHN 1592	923	860	942	1003	945	914	942	954	948	36.5
		PHN 1570	938	886	946	909	939	949	946	932	939	37.2
		PHN 1573	943	893	963	980	(890)	(889)	963	980	972	39.4
		PHN 1568	933	925	962	1055	909	897	962	954	958	36.4
		PHN 1572	939	941	989	1079	941	966	989	995	992	39.0
	Deformed	PHN 1582	1054	1151	1132	1122	(1020)	1079	1132	1122	1127	47.2
		PHN 1591	1240	1327	1321	1285	(1213)	1323	1321	1304	1312	52.0
		E 3	1264	1383	1359	1300	(1209)	1327	1359	1314	1336	51.8
		PHN 1610	1330	1485	1433	1405	(1319)	1394	1433	1400	1416	56.7
		PHN 1566	1353	1503	1447	1395	(1331)	1389	1447	1392	1420	56.7
		PHN 1611	1315	1476	1425	1401	(1284)	1439	1425	1420	1422	56.7
		PHN 1596	1369	1522	1473	1450	(1403)	1529	1473	1461	1467	60.9
		PHN 1597	1375	1528	1481	1453	1452	1512	1481	1472	1477	63.0
Mothae	Coarse	PHN 1559B	937	1020	(948)	1071	1007	1021	(948)	1033	1033	42.3
		BD 2125[b]	988	1037	1031	1045	1028	(1119)	1031	1036	1034	43.0
		PHN 1917	983	1002	1029	1061	1024	1072	1029	1052	1041	45.6
	Deformed	PHN 2001	1193	1306	1303	1331	1311	1364	1303	1335	1319	55.0
		PHN 1924	1258	1427	1393	1432	1334	1381	1393	1382	1388	60.0
		PHN 1925	1273	1449	1408	1439	1348	1379	1408	1389	1398	60.7

[a] Primary graphite bearing
[b] Primary diamond bearing – Dawson and Smith (1975)
All other data from Nixon and Boyd (1973a) or Boyd and Finger (1975)

iii. T^* was then calculated as the mean of the two-pyroxene solvus and $Fe^{2+}\rightleftharpoons Mg^{2+}$ exchange temperatures, and a corresponding 'best' pressure estimate (P^*) calculated at T^* from the Nickel and Green (1985) barometer.

For some xenoliths certain temperature estimates have been excluded from the calculation of T^* because they are clearly out of line (usually by $>75°$ C) with the other values. As discussed later such anomalous values may arise for a number of reasons including innate errors in the thermometer concerned, analytical errors and chemical disequilibrium between the selected analysed points in mineral grains, most likely related to compositional inhomogeneities in the minerals concerned. The most obvious anomalous values are those calculated from $Fe^{2+}\rightleftharpoons Mg^{2+}$ exchange between garnet-orthopyroxene pairs (Harley 1984a) for the majority of the deformed xenoliths from Thaba Putsoa (see Table 1). Also, the two-pyroxene solvus temperature for PHN 1559B from Mothae was rejected since it is appreciably lower than those calculated from the $Fe^{2+}\rightleftharpoons Mg^{2+}$ exchange thermometers, which may be expected to be somewhat more sensitive and reliable at the low temperature concerned.

iv. Finally the complete sequence of calculations was reiterated with the provisional P^* value used during calculation of revised temperature estimates and ultimately final T^* and P^* values obtained. In practice these usually differ little from the initial T^* and P^* values calculated.

There is uncertainty over the oxidation state of iron in mantle derived garnet lherzolite assemblages analysed by electron microprobe but we have found that with good quality analyses stoichiometric charge balance calculations indicate that little or no Fe^{3+} is present in the silicate mineral phases. This is especially the case in orthopyroxenes where $NaFe^{3+}Si_2O_6$ substitution need not be considered. Hence in our $P-T$ calculations based on electron microprobe analyses, we have made the reasonable assumption that all iron is present as Fe^{2+} in the garnet lherzolite assemblages. This assumption can be further justified by the fact that $Fe^{2+}\rightleftharpoons Mg^{2+}$ exchange reaction temperatures calculated on this basis are mostly closer to two-pyroxene solvus temperatures than when any stoichiometrically calculated Fe^{3+} contents are taken into consideration. The latter can arise spuriously through analytical inaccuracies or even just imprecision, especially in the determined SiO_2 contents. The presence of diamond or graphite in certain garnet lherzolite xenoliths is also indicative of the strongly reduced nature of these mineral assemblages (Haggerty 1986).

In Fig. 4A, our P^*–T^* estimates for the Thaba Putsoa and Mothae xenolith suites again appear, as in Fig. 2A, to define separate, elevated but non-inflected, palaeogeotherms for these two localities. However, compared with Fig. 2A the overall range of indicated equilibration temperatures (and hence of implied derivation depths) is somewhat reduced. As in Fig. 2A one particular Thaba Putsoa xenolith (PHN 1582) appears to be anomalous in that it plots on the Mothae palaeogeotherm. The explanation of this is not clear, but could be attributable to incorrect temperature assessment resulting from analytical error(s) in the cli-

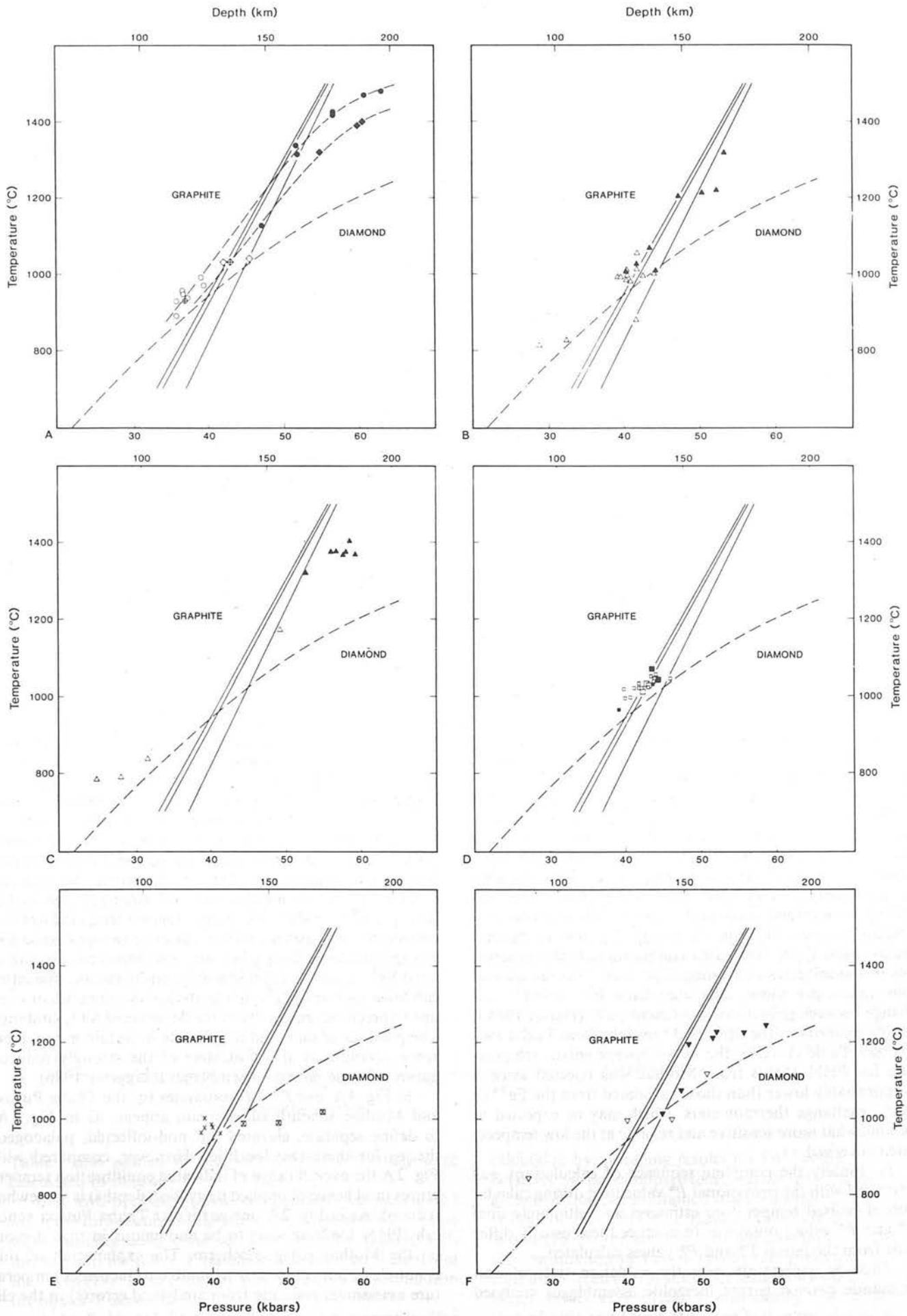
Depth (km)
100
150
200
1400
1200
1000
800
Temperature (°C)
GRAPHITE
DIAMOND
A
B
C
D
E
F
30
40
50
60
Pressure (kbars)

nopyroxene (the published analytical total is only 98.21 wt%). The fact that the calculated $P-T$ equilibration conditions for this particular xenolith are separated in $P-T$ space from those for all other Thaba Putsoa and Mothae deformed xenoliths perhaps supports such an interpretation. However, this xenolith is also unusual in other respects. In particular it is relatively Fe and Ti rich compared with other xenoliths and contains only minor pyroxenes and garnet relative to an unusually fayalitic olivine (Fo_{84}) and also primary ilmenite intergrown with the silicate phases. Hence, the seemingly anomalous $P-T$ equilibration values for this xenolith may be due to failure of the thermometers and barometers employed to adequately take account of such chemical differences from other Thaba Putsoa xenoliths.

It will be noted in Fig. 4A (as also in Fig. 2A, B, C and E) that $P-T$ equilibration values for the diamond bearing xenolith PHN 2125 from Mothae lie about 2.5 kbar below the pressures required for diamond stability as indicated by the diamond-graphite transition curve of Kennedy and Kennedy (1976) – the critical constraint exercised by Finnerty and Boyd (1984, 1987) in their barometer selection. However, we emphasise that other experimental (Bundy et al. 1961; Bundy 1980) and thermodynamic (Berman 1979) data on the diamond-graphite transition indicate that the Kennedy and Kennedy (1976) curve may well be some 2.5 kbar too high (or 100° C too low) in the $P-T$ range concerned. We therefore consider the $P-T$ values shown for PHN 2125 in Fig. 4A to be compatible with diamond stability, given the uncertainties which should be attached to the location in $P-T$ space of the diamond-graphite stability curve and to the $P-T$ estimates.

Our equivalent P^*-T^* estimates of equilibration conditions for garnet lherzolite xenoliths from other kimberlites in northern Lesotho are plotted in Fig. 4B–F. Xenolith data from the Main (Fig. 4B) and Satellite (Fig. 4C) Pipes at Letseng-la-Terae are from Boyd in Nixon (1973), Bishop et al. (1978), Lock and Dawson (1980), and Lock (1980). (In accordance with his analytical tests and recommendations, the Al_2O_3 contents in orthopyroxenes from xenoliths in the Satellite Pipe reported by Lock (1980) have been reduced by 15% relative.) The $P-T$ points for three xenoliths from the Letseng Main Pipe which plot below the 40 mW m^{-2} shield geotherm can probably be accounted for by inaccurate analyses or internal chemical disequilibrium (Lock 1980). As can be discerned from Fig. 5A the majority of the xenoliths from the Letseng Pipes appear to lie closer to the non-inflected, palaeogeotherm for the geographically nearer Mothae locality than to that for Thaba Putsoa. An interesting feature at Letseng is that although both kimberlite pipes have incorporated mantle xenoliths from different depths, the depths of derivation for most xenoliths differ in the two pipes (cf., Fig. 4B and C). Thus individual kimberlite eruptions appear to be selective regarding the depths from which they incorporate wall-rock xenoliths, at least in an uncomminuted state. Certainly the Letseng Satellite Pipe is unusual in that, unlike the other studied kimberlites in northern Lesotho, it does not appear to have incorporated garnet lherzolite xenoliths of the common, coarse textured, depleted type from depths of around 120–145 km. Also a single xenolith (BD 1910) has been recorded with an unusually high equilibration temperature (1170° C) for a coarse textured xenolith. However, as in the Thaba Putsoa and Mothae xenolith suites, an overall pattern of higher $P-T$ equilibration conditions (and greater depths of origin) for deformed xenoliths is also apparent at Letseng although there are some exceptions, namely three analysed lower-T deformed xenoliths from the Main Pipe. An interesting observation by Lock (1980) is that whilst comparative thermometry for porphyroclasts and neoblasts in the higher-T deformed xenoliths from Letseng points to cooling during deformation, in the lower-T deformed xenoliths slight heating is indicated.

Xenolith data from the Matsoku Pipe plotted in Fig. 4D are from Cox et al. (1973), Boyd and Nixon in Nixon (1973), and Bishop et al. (1978). All garnet lherzolite xenoliths from Matsoku, whether belonging to the common peridotite or banded peridotite/pyroxenite groups (Cox et al. 1973; Harte et al. 1975) and whether or not they have deformed textures, appear to have equilibrated under a very restricted range of $P-T$ conditions. It is possible that the range of $P-T$ conditions indicated for these Matsoku xenoliths in Fig. 4D is a reflection of the degree of uncertainty which could be attached to such $P-T$ estimates because of inaccuracy in the mineral analyses and/or the thermometer and barometer formulations employed (see below). Accordingly we hesitate to suggest other than that in the Matsoku Pipe all the xenoliths are derived from approximately the same depth in the mantle. This depth (130–140 km) may correspond to the base of the lithosphere and mark the depth at which there was a significant change in the character and velocity of the kimberlite eruption.

Likewise in Pipe 200 (Fig. 4E) indications are again that all the analysed garnet lherzolite xenoliths (Carswell et al. 1979) probably have been derived from essentially the same mantle depth, although this depth appears to have been rather shallower (around 125 km) than for the Matsoku Pipe. $P-T$ equilibration conditions for the three xenoliths from Pipe 200 which plot below the 40 mW m^{-2} geotherm are undoubtedly in error because Na contents have not been determined for the orthopyroxenes. Orthopyroxenes in the highly depleted garnet lherzolite xenoliths from Pipe 200 are notably chromiferous and failure to take account of the Cr combined with Na as ureyite has resulted in anomalously high equilibration pressure estimates for these three xenoliths. This emphasises the fact that accurate estimation of $P-T$ equilibration conditions for garnet lherzolite xenoliths requires complete and accurate mineral analyses plus careful consideration of the effects of minor element contents on the element exchange reaction thermometers and barometers employed especially when X_{Al} values in orthopyroxenes are low.

The interpretation problems which can arise from the calculation of $P-T$ equilibration conditions from unsat-

Fig. 4A–F. P^*-T^* (see text) equilibration estimates for garnet lherzolite xenoliths from various individual kimberlite pipes in northern Lesotho. Note how slightly separate palaeogeotherms (– – – – –) are indicated for **A** Thaba Putsoa: ● deformed, ○ coarse, ⊕ coarse (graphite) and Mothae: ◆ deformed, ◇ coarse, ◈ coarse (diamond) xenolith suites. Diamond-graphite inversion curves and shield geotherm as in Fig. 1. **B** Letseng Main Pipe: ▲ deformed, △ coarse. **C** Letseng Satellite Pipe: ▲ deformed, △ coarse. **D** Matsoku Common Peridotites: ■ deformed, □ coarse, Banded Xenoliths ▪ deformed, ▫ coarse. **E** Pipe 200 × coarse, ⊞ (Na not determined in orthopyroxenes. **F** Kao: ▼ deformed, ▽ coarse

isfactory analytical data are well illustrated in Fig. 4F for garnet lherzolite xenoliths from the Kao kimberlite. Analytical data for a single deformed high-T xenolith (2273) from Kao provided by Boyd and Nixon in Nixon (1973) yield $P-T$ estimates which lie close to the palaeogeotherm defined by the Mothae xenolith suite (Fig. 5A). However, $P-T$ estimates calculated for both deformed and coarse granular xenoliths from the data provided by MacGregor (1979) are widely scattered on Fig. 4F and must be treated with caution. Although the Na contents of orthopyroxenes were reported by MacGregor (1979) for all the xenoliths plotted, totals for many of the mineral analyses are poor and there are some apparent printing errors in the published table of analyses.

Comprehensive quantification of the 'error brackets' which should be attached to individual $P-T$ results is difficult due to the multivariate nature of the problem (Carswell and Gibb 1987). The errors arise basically from three sources. Firstly, from incorrect 'calibration' of the thermometer and/or barometer (whether as a result of experimental error or inappropriate formulation or application). Secondly, there are limitations on the precision and accuracy of electron probe microanalyses and, thirdly, there may be inhomogeneities in the analysed minerals, which may be undetectable within the precision of the analysis but are nevertheless real in at least some xenolith samples (Boyd and Finger 1975). Errors of the first type are potentially the most serious and have already been discussed at length (see also Carswell and Gibb 1987). Errors due to the last two sources are difficult to separate and we have used the multi-analysis data of Boyd and Finger (1975) to compute the maximum combined errors to be expected from these two sources over the range of P and T derived for this contribution by our recommended method. Details of these errors and the underlying rationale will be presented elsewhere (D.A. Carswell and F.G.F. Gibb, in preparation) but the calculations show that, because the calculated pressure is strongly influenced by the derived temperature, serious error propagation can occur. Moreover, the 'error boxes' are not orthogonal, as might be inferred from the attempt to estimate such errors by Boyd and Finger (1975), but are strongly elongated sub-parallel to the geotherm. Consequently, the potential presence of such errors, unlike those of the first type, can not be used to argue for or against the reality or otherwise of an inflected palaeogeotherm. These errors (or compositional uncertainties) will, however, when present, lead to a spreading of the calculated $P-T$ values for the members of a xenolith suite along the palaeogeotherm thus implying a greater variation in their depth of derivation than is, in fact, the case.

A composite plot of P^*-T^* values for all garnet lherzolite xenoliths from northern Lesotho for which reliable analytical data are available is presented in Fig. 5A. The banded peridotite/pyroxenite group of xenoliths from Matsoku have been omitted to avoid overcrowding of points at around 1025° C and 42.5 kbar. Only single xenoliths have been included from Kao (2273) and Liqhobong (data from Nixon and Boyd in Nixon 1973) and from Monastery Mine (data from Boyd and Finger 1975) just over the NW border of Lesotho. The individual xenoliths from each of these three localities plot close to the elevated but non-inflected, palaeogeotherms indicated for the Mothae and Thaba Putsoa localities during the late Cretaceous, the time of emplacement of these kimberlites. A composite palaeogeotherm for northern Lesotho is of questionable validity but would lie between the separate palaeogeotherms indicated for Mothae and Thaba Putsoa.

Overall sampling and analysis of xenoliths from the kimberlites of northern Lesotho may well have been biased towards the deformed garnet lherzolites. Nevertheless, it is clear that the most common garnet lherzolite xenoliths are those with relatively depleted major and trace element chemistries and isotopic signatures probably indicative of old sub-continental lithospheric mantle (Richardson et al. 1985). Such xenoliths mostly have coarse (granular) textures but some have porphyroclastic or mosaic-porphyroclastic textures indicative of deformation and sometimes slight heating (Lock 1980) only shortly before or possibly even during entrainment in the erupting kimberlites. As $P-T$ equilibration conditions for these xenoliths mostly lie in the range 930°–1050° C and 36–45 kbar, with implied depths of origin of 120–145 km, it would seem that they have been derived from, or close to, the base of the sub-continental lithosphere. The slight, but systematic, differences in the depths of origin for such xenoliths apparent in Fig. 5A for different kimberlite localities may perhaps signal regional variations in the thickness of the lithosphere beneath northern Lesotho. Alternatively, it may reflect variations in the 'take-off' depth for rapid kimberlite eruption through the lithosphere. If the former interpretation is correct, then it would appear that, under the prevailing $P-T$ conditions in the mantle beneath northern Lesotho at the time of kimberlite emplacement, the lithosphere may only have been thick enough to permit diamond stability close to its base at certainly localities, notably at Mothae. Xenoliths derived from higher levels in the mantle lithosphere and from the lower crust (Griffin et al. 1979) also occur in the kimberlites of northern Lesotho but appear to be less common overall.

The deformed, high-T xenoliths with more fertile major and trace element compositions have REE and isotopic signatures compatible with MORB-type mantle from the convective asthenosphere (Richardson et al. 1985). Indications are of considerable variations in the depths of derivation of such xenoliths from within the asthenosphere in the different kimberlites of northern Lesotho, although some clustering of $P-T$ points for individual kimberlites is apparent in Fig. 5A.

The form of our revised palaeogeotherm(s) for northern Lesotho bears some similarity, but does not correspond precisely, to the convection related geotherm calculated by Harte (1978) – see Fig. 5A – which assumes a 44 mW m^{-2} surface heat flow, a 200 km thick lithosphere, and an enhanced temperature at the base of the lithopshere caused by a hot diapir or plume in the asthenosphere. From this we conclude that the palaeogeotherm(s) for northern Lesotho indicated by our revised $P-T$ estimates for garnet lherzolite xenoliths may be adequately explained as corresponding to a conductive geotherm in the lithosphere related to a somewhat elevated, cratonic margin, surface heat flow of 41–42 mW m^{-2} modified by an enhanced heat flux from the top of the asthenosphere. The latter may have been due to convective upwelling in the asthenosphere possibly directly associated with the generation and uprise of protokimberlite magma. The slight indication of a decrease in the geothermal gradient at depths greater than about 175 km (Figs. 4A and 5A) is more in line with what would be expected in a thermally convecting asthenosphere be-

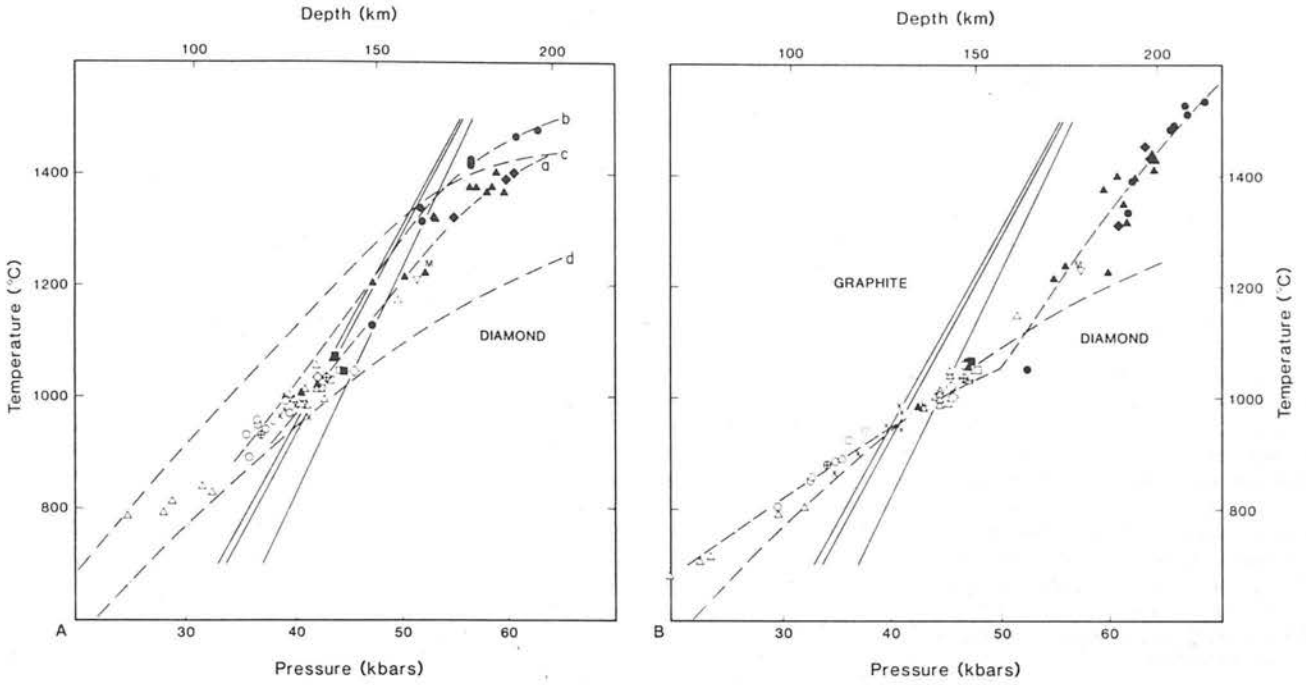

Fig. 5 A, B. **A** Composite $P-T$ diagram showing P^*-T^* equilibration estimates for garnet lherzolite xenoliths from kimberlites throughout northern Lesotho relative to deduced palaeogeotherms for the xenolith suites at Mothae (◆ deformed, ◇ coarse, ⊹ coarse with diamond), Thaba Putsoa (● deformed, ○ coarse, ⊕ coarse with graphite), Pipe 200 (×), Matsoku CP (■ deformed, □ coarse), Letseng (▲ deformed, △ coarse), Kao (▽), Liqhobong (*L*) and Monastery (*M*). Also shown are the deduced palaeogeotherms for Mothae (*a*) and Thaba Putsoa (*b*), the convection-related shield geotherm (*c*) calculated by Harte (1978) and the conductive shield geotherm (*d*) of Pollack and Chapman (1977) calculated for a 40 mW/m^2 surface heat flow. **B** Composite $P-T$ diagram based on $P-T$ estimates for garnet lherzolite xenoliths from kimberlites throughout northern Lesotho calculated from the Finnerty and Boyd (1987) formulation of the two-pyroxene solvus thermometer in combination with their barometer formulation based on MacGregor (1974). Data and locality symbols as in **A**. Note the inflected palaeogeotherm (– – – –) inferred from these particular $P-T$ estimates, in contrast to those indicated in **A** for the Mothae and Thaba Putsoa xenolith suites. Diamond-graphite inversion curves and shield geotherm as in Fig. 1

neath a more rigid, thermally conducting, lithosphere (Mercier and Carter 1975; Harte 1978) than a palaeogeotherm inflected dramatically away from the adiabat as indicated by Finnerty and Boyd (1984, 1987) with the point of inflection taken to mark the lithosphere-asthenosphere boundary.

A similar, convex upwards, non-inflected, convection-related palaeogeotherm has recently been suggested by Bertrand et al. (1986) for the Thaba Putsoa xenolith suite on the basis of $P-T$ estimates derived by combining the two-pyroxene solvus thermometer of Bertrand and Mercier (1985) with their own proposed barometer formulation. However, because of pressure underestimation by the Bertrand et al. (1986) barometer, $P-T$ estimates for the Thaba Putsoa and Mothae xenolith suites (Fig. 3F) calculated by this combination of thermometer and barometer are significantly displaced to lower pressures, to the extent that the values for the diamond bearing xenolith BD 2125 from Mothae plot some 8 kbar below the minimum pressure required for diamond stability.

$P-T$ estimates for garnet lherzolite xenoliths obtained by Boyd (1984) and Finnerty and Boyd (1987), using the MC74 barometer in combination with various two-pyroxene solvus thermometer formulations, do not indicate an inflected palaeogeotherm for Udachnaya, Siberia in contrast to that for northern Lesotho. Contrary to the statement by Boyd (1975), this does not prove the reality of the inflected palaeogeotherm for northern Lesotho but, merely reflects contrasting bulk rock and mineral chemistries in the deformed, high-T garnet lherzolite xenolith suites from these two areas.

There is a scarcity of satisfactorily complete, bulk-rock chemical analyses of adequately documented xenoliths from Udachnaya. However, a single analysis of a deformed, high-T xenolith (Ud.5 – Sobolev 1977; Borley 1975) indicates that, in contrast to the equivalent xenoliths from the northern Lesotho kimberlites, any enhanced Na content may be coupled with Cr. This appears to be further borne out by analyses of constituent orthopyroxenes in Udachnaya xenoliths (Boyd 1984; Carswell, unpublished data) which reveal lower jadeite contents (and correspondingly higher ureyite contents) compared with orthopyroxenes in deformed, high-T xenoliths from Thaba Putsoa, Mothae and Letseng in northern Lesotho (cf., Fig. 3A–C). Hence pressure estimates for the deformed, high-T xenoliths from Udachnaya obtained by the MC74 barometer will not be subject to the same large reduction due to its failure to take account of appreciable jadeite contents in orthopyroxenes as observed in equivalent xenoliths from the northern Lesotho kimberlites. Our P^*-T^* estimates for both the coarse, low-T and deformed, high-T garnet lherzolite xenoliths from Udachnaya certainly lie close to a conductive geotherm associated with a 40 mW m^{-2} surface heat flow such as might be expected for a stable cratonic region (D.A. Carswell, in preparation).

Acknowledgements. D.A.C. wishes to acknowledge grants from the Natural Environment Research Council supporting research into equilibration conditions for garnet lherzolite assemblages.

References

Akella J (1976) Garnet pyroxene equilibria in the system $CaSiO_3 - MgSiO_3 - Al_2O_3$ and in a natural mineral mixture. Am Mineral 61:589–598

Berman R (1979) Thermal properties. In: Field JE (ed) The properties of diamond. Academic Press, London

Bertrand P, Mercier J-CC (1985) The mutual solubility of coexisting ortho- and clinopyroxene: towards an absolute geothermometer for the natural system? Earth Planet Sci Lett 76:109–122

Bertrand P, Sotin C, Mercier J-CC, Takahashi E (1986) From the simplest chemical system to the natural one: Garnet peridotite barometry. Contrib Mineral Petrol 93:168–178

Bishop FC, Smith JV, Dawson JB (1978) Na, K, P and Ti in garnet, pyroxene and olivine from peridotite and eclogite xenoliths from African kimberlites. Lithos 11:155–173

Borley GD (1975) Mantle deformation beneath the South African and Siberian platforms. Nature 254:489–491

Boullier AM, Nicholas A (1973) Texture and fabric of peridotite nodules from kimberlite at Mothae, Thaba Putsoa and Kimberley. In: Nixon PH (ed) Lesotho kimberlites: 57–66. Lesotho Nat Dev Corp Maseru, Lesotho

Boyd FR (1973) A pyroxene geotherm. Geochim Cosmochim Acta 37:2533–2546

Boyd FR (1974) Ultramafic nodules from the Frank Smith kimberlite pipe, South Africa. Carnegie Inst Washington Yearb 73:285–294

Boyd FR (1975) Stress-heating and compositional variations in enstatites from sheared lherzolites. Carnegie Inst Washington Yearb 74:525–528

Boyd FR (1976) Inflected and noninflected geotherms. Carnegie Inst Washington Yearb 75:521–531

Boyd FR (1984) Siberian geotherm based on lherzolite xenoliths from the Udachnaya kimberlite, USSR. Geology 12:528–530

Boyd FR, Finger LW (1975) Homogeneity of minerals in mantle rocks from Lesotho. Carnegie Inst Washington Yearb 74:519–525

Boyd FR, Nixon PH (1973) Structure of the upper mantle beneath Lesotho. Carnegie Inst Washington Yearb 72:431–445

Boyd FR, Nixon PH (1975) Origins of the ultramafic nodules from some kimberlites of Northern Lesotho and the Monastery Mine, South Africa. Phys Chem Earth 9:431–454

Boyd FR, Nixon PH (1978) Ultramafic nodules from the Kimberley Pipes, South Africa. Geochim Cosmochim Acta 42:1367–1382

Bundy FR (1980) The P, T phase and reaction diagram for elemental carbon, 1979. J Geophys Res 85:6930–6936

Bundy FR, Bovenkerk HP, Strong HM, Wentorf RH Jr (1961) Diamond-graphite equilibrium line from growth and graphitization of diamond. J Chem Phys 35:383–391

Carswell DA (1975) Primary and secondary phlogopites and clinopyroxenes in garnet lherzolite xenoliths. Phys Chem Earth 9:417–429

Carswell DA (1980) Mantle derived lherzolite nodules associated with kimberlite, carbonatite and basalt magmatism: a review. Lithos 13:121–138

Carswell DA, Gibb FGF (1980) Geothermometry of garnet lherzolite nodules with special reference to those from the kimberlites of Northern Lesotho. Contrib Mineral Petrol 74:403–416

Carswell DA, Gibb FGF (1987) Evaluation of mineral thermometers and barometers applicable to garnet lherzolite assemblages. Contrib Mineral Petrol 95:499–511

Carswell DA, Clarke DB, Mitchell RH (1979) The petrology and geochemistry of ultramafic nodules from Pipe 200, Northern Lesotho. In: Boyd FR, Meyer HOA (eds) The mantle sample: inclusions in kimberlites and other volcanics. Am Geophys Union Washington, Proc 2nd Int Kimb Conf 2:127–144

Clark SP Jr, Ringwood AE (1964) Density distribution and constitution of the mantle. Rev Geophys 2:35–88

Cox KG, Gurney JJ, Harte B (1973) Xenoliths from the Matsoku Pipe. In: Nixon PH (ed) Lesotho Kimberlites. Lesotho Nat Dev Corp Maseru, Lesotho, pp 76–100

Danchin RV (1979) Mineral and bulk chemistry of garnet lherzolite and garnet harzburgite xenoliths from the Premier Mine, South Africa. In: Boyd FR, Meyer HOA (eds) The mantle sample: inclusions in kimberlites and other volcanics. Am Geophys Union, Washington, Proc 2nd Int Kimb Conf 2:104–126

Danchin RV, Boyd FR (1976) Ultramafic nodules from the Premier kimberlite pipe, South Africa. Carnegie Inst Washington Yearb 75:531–538

Dawson JB, Smith JV (1975) Occurrence of diamond in a mica-garnet lherzolite xenolith from kimberlite. Nature 254:580–581

Dawson JB, Gurney JJ, Lawless PJ (1975) Palaeogeothermal gradients derived from xenoliths in kimberlite. Nature 257:299–300

Eggler DH, Wendlandt RF (1979) Experimental studies on the relationship between kimberlite magmas and partial melting of peridotite. In: Boyd FR, Meyer HOA (eds) Kimberlites, diatremes and diamonds: their geology, petrology and geochemistry. Am Geophys Union Washington, Proc 2nd Int Kimb Conf 1:330–338

Ellis DJ, Green DH (1979) An experimental study of the effect of Ca upon garnet-clinopyroxene Fe – Mg exchange equilibria. Contrib Mineral Petrol 71:13–22

Finnerty AA, Boyd FR (1984) Evaluation of thermobarometers for garnet peridotites. Geochim Cosmochim Acta 48:15–27

Finnerty AA, Boyd FR (1987) Thermobarometry for garnet peridotite xenoliths: a basis for upper mantle stratigraphy. In: Nixon PH (ed) Mantle Xenoliths. J Wiley and Sons, New York

Goetze C (1975) Sheared lherzolites: from the point of view of rock mechanics. Geology 3:172–173

Green HW, Gueguen Y (1974) Origin of kimberlite pipes by diapiric upwelling in the upper mantle. Nature 249:617–620

Griffin WL, Carswell DA, Nixon PH (1979) Lower-crustal granulites and eclogites from Lesotho, southern Africa. In: Boyd FR, Meyer HOA (eds) The mantle sample: inclusions in kimberlites and other volcanics. Am Geophys Union Washington, Proc 2nd Int Kimb Conf 2:59–86

Gurney JJ, Harte B (1980) Chemical variations in upper mantle nodules from southern African kimberlites. Philos Trans R Soc London A 297:273–293

Haggerty SE (1986) Diamond genesis in a multiple-constrained model. Nature 320:34–38

Harley SL (1984a) An experimental study of the partitioning of Fe and Mg between garnet and orthopyroxene. Contrib Mineral Petrol 86:359–373

Harley SL (1984b) Comparison of the garnet-orthopyroxene geobarometer with recent experimental studies and applications to natural assemblages. J Petrol 25:697–712

Harley SL, Green DH (1982) Garnet-orthopyroxene barometery from granulites and peridotites. Nature 300:697–701

Harley SL, Thompson AB (1984) Xenolithic mineral assemblages in kimberlites, palaeogeotherms, and the thermal structure of the mantle. In: Kornprobst J (ed) Kimberlites. II. The mantle and crust-mantle relationships. Proc 3rd Int Kimb Conf Development in Petrology, Elsevier, Amsterdam, 11B:277–287

Harte B (1977) Rock nomenclature with particular relation to deformation and recrystallisation textures in olivine-bearing xenoliths. J Geol 85:279–288

Harte B (1978) Kimberlite nodules, upper mantle petrology and geotherms. Philos Trans R Soc London A288:487–500

Harte B (1983) Mantle peridotites and processes – the kimberlite sample. In: Hawkesworth CJ, Norry MJ (eds) Continental basalts and mantle xenoliths. Shiva Geology Series, pp 46–91

Harte B, Gurney JJ (1981) The mode of formation of chromium poor megacryst suites from kimberlites. J Geol 89:749–753

Harte B, Hunter RH (1986) Speculations concerning the importance of metasomatic melt migration in the formation of pyroxenite sheets in garnet-peridotite xenoliths from Matsoku, Lesotho. 4th Int Kimb Conf Perth. Geol Soc Australia Abst 16:184–186

Harte B, Cox KG, Gurney JJ (1975) Petrography and geological history of upper mantle xenoliths from the Matsoku kimberlite pipe. Phys Chem Earth 9:477–506

Howells S, O'Hara MJ (1978) Low solubility of alumina in enstatite and uncertainties in estimated palaeogeotherms. Philos Trans R Soc London A288:471–486

Kennedy CS, Kennedy GC (1976) The equilibrium boundary between graphite and diamond. J Geophys Res 81:2467–2470

Lock NP (1980) The geology of the Letseng kimberlites, Lesotho. Unpublished Ph D thesis, University of Sheffield

Lock NP, Dawson JB (1980) Garnet-olivine reaction in the upper mantle: evidence from peridotite xenoliths in the Letseng-la-Terae kimberlites, Lesotho. Trans R Soc Edinburgh: Earth Sci 71:47–53

MacGregor ID (1974) The system $MgO-Al_2O_3-SiO_2$: solubility of Al_2O_3 in enstatite for spinel and garnet peridotite compositions. Am Mineral 59:110–119

MacGregor ID (1979) Mafic and ultramafic xenoliths from the Kao kimberlite pipe. In: Boyd FR, Meyer HOA (eds) The mantle sample: inclusions in kimberlites and other volcanics. Am Geophys Union, Washington, Proc 2nd Int Kimb Conf 2:156–172

Mercier J-CC (1979) Peridotite xenoliths and the dynamics of kimberlite intrusions. In: Boyd FR, Meyer HOA (eds) The mantle sample: inclusions in kimberlites and other volcanics. Am Geophys Union, Washington, Proc 2nd Int Kimb Conf 2:197–212

Mercier JCC, Carter NL (1975) Pyroxene geotherms. J Geophys Res 80:3349–3362

Mitchell RH (1984) Garnet lherzolites from the Hanaus-I and Louwrensia kimberlites of Namibia. Contrib Mineral Petrol 86:178–188

Mori T, Green DH (1978) Laboratory duplication of phase equilibria observed in natural garnet lherzolites. J Geol 86:83–97

Nickel KG (1983) Petrogenesis of garnet and spinel peridotites. Unpublished Ph D thesis, University of Tasmania

Nickel KG, Green DH (1985) Empirical geothermobarometry for garnet peridotites and implications for the nature of the lithosphere, kimberlites and diamonds. Earth Planet Sci Lett 73:158–170

Nixon PH (1973) (ed) Lesotho Kimberlites. Lesotho Nat Dev Corp Maseru, Lesotho, p 350

Nixon PH, Boyd FR (1973a) Petrogenesis of the granular and sheared ultrabasic nodule suite in kimberlites. In: Nixon PH (ed) Lesotho kimberlites. Lesotho Nat Dev Corp Maseru, Lesotho, pp 48–56

Nixon PH, Boyd FR (1973b) The discrete nodule association in kimberlites from northern Lesotho. In: Nixon PH (ed) Lesotho kimberlites. Lesotho Nat Dev Corp Maseru, Lesotho, pp 67 75

Nixon PH, Rogers NW, Gibson IL, Grey A (1981) Depleted and fertile mantle xenoliths from southern African kimberlites. Ann Rev Earth Planet Sci 9:285–309

O'Neill HStC (1981) The transition between spinel lherzolite and garnet lherzolite, and its use as a geobarometer. Contrib Mineral Petrol 77:185–194

O'Neill HStC, Wood BJ (1979) An experimental study of Fe–Mg partitioning between garnet and olivine and its calibration as a geothermometer. Contrib Mineral Petrol 70:59–70

Parmentier EM, Turcotte DL (1974) An explanation fo the pyroxene geotherm based on plume convection in the upper mantle. Earth Planet Sci Lett 24:209–212

Pollack HN, Chapman DS (1977) On the regional variation of heat flow, geotherms and lithospheric thickness. Tectonophysics 38:279–296

Powell R (1985) Regression diagnostics and robust regression in geothermometer/geobarometer calibration: the garnet-clinopyroxene geothermometer revisited. J Metamorph Geol 3:231–243

Richardson SH, Erlank AJ, Hart SR (1985) Kimberlite-borne garnet peridotite xenoliths from old enriched subcontinental lithosphere. Earth Planet Sci Lett 75:116–128

Smith D, Boyd FR (1986) Compositional heterogeneities in minerals from peridotite nodules. 4th Int Kimb Conf Perth. Geol Soc Australia Abst 16:335–337

Sobolev NV (1977) Deep-seated inclusions in kimberlites and the problems of the composition of the upper mantle. Am Geophys Union, Washington

Sobolev NV, Pokhilenko NP, Carswell DA, Rodinov AS (1986) Sheared lherzolites from kimberlites of Yakutia. 4th Int Kimb Conf Perth. Geol Soc Australia Abst 16:338–339

Webb SAC, Wood BT (1986) Spinel-pyroxene-garnet relationships and their dependence on Cr/Al ratio. Contrib Mineral Petrol 92:471–480

Wells PRA (1977) Pyroxene thermometry in simple and complex systems. Contrib Mineral Petrol 62:129–139

Received December 22, 1986 / Accepted August 4, 1987

C. **General papers or papers based on high pressure metamorphic rocks from other geological settings**

MINERALOGICAL MAGAZINE

VOLUME 40 NUMBER 314 JUNE 1976

The geochemistry of 'charnockites' and their constituent ferromagnesian minerals from the Precambrian of south-east Sri Lanka (Ceylon)

D. E. DE S. JAYAWARDENA[1] AND D. A. CARSWELL

Department of Geology, University of Sheffield, Sheffield, S1 3JD

SUMMARY. A chemical and petrographic study of charnockites and pyroxene/hornblende-bearing granulites has been undertaken, and the data used in an interpretation of the petrogenesis of these rocks. Major- and trace-element analyses of fourteen rocks are presented, together with major-element analyses of seven orthopyroxenes, seven clinopyroxenes, two garnets, and three hornblendes. The compositions of the coexisting ferromagnesian minerals are used to obtain estimates of the likely pressure temperature conditions of equilibration (5–7 kbar and 700±50 °C) of the various mineral assemblages.

Geological setting. The Precambrian rocks of Ceylon are divided into the *Highland Series* (metasediments and charnockites) and the *Vijayan Series* (granites, granitic gneisses, and migmatites)—Cooray (1962). The area studied in the south-east of Sri Lanka straddles the boundary between the Highland Series and the Vijayan Series, the most significant features being the absence of a transitional zone and the presence of acid charnockites in the form of circular domes in the Vijayan Series. This is in contrast to the findings of Cooray (1961), who mapped an area north of the present area of study.

The prominent rock types encountered are: Highland Series: charnockites (acid, intermediate, and basic); undifferentiated metasediments (garnetiferous granulites, garnetiferous biotite gneisses, garnet–sillimanite–biotite gneisses); khondalites (quartz–feldspar–garnet–sillimanite–graphite schists); quartzites; crystalline limestones; calc-gneisses and calc-granulites; amphibole granulites; and amphibolites. These rocks are found closely associated with each other and this association is invariably of an interbanded nature.

The area immediately east of the Highland Series is underlain by rocks grouped under the Vijayan Series (Balendran, 1968): hornblende–biotite gneisses; granites; granitic gneisses and migmatites; acid to intermediate charnockites; calc-granulites

[1] Present address: Geological Survey Department, 48 Sri Jinaratana Road, Colombo—2, Sri Lanka.

and calc-gneisses; and amphibolites. The hornblende–biotite gneisses are the main lithological unit in this area and the granites and pink granite gneisses have been demarcated purely on their field relations to the hornblende–biotite gneisses. Acid to intermediate charnockites occur as circular domes and are in a different environment as compared to those of the Highland Series, where the charnockites are mostly associated with metasediments. Charnockites are rare in the Vijayan Series and were regarded by Cooray (1962) as relicts of an earlier metamorphic event.

In a recent examination of a Gondwanaland re-assembly of Peninsular India and part of east Antarctica, Sri Lanka is accommodated, without displacement relative to India, in the Antarctic Ocean re-entrant immediately off Lützow-Holm Bay, which is composed of a charnockitic group and a granitic group (Tatsumi and Kizaki, 1969). The recent geological mapping of the south-eastern coastal belt has revealed a similar lithological association in the Vijayan Series (Balendran, 1968).

Geochronology and metamorphism. The interpretation of existing structural, metamorphic, and isotopic-age data relevant to the question of the geological relationship between the Highland Series and Vijayan Series rocks remains controversial (see, for example, Cooray, 1961, 1962; Katz, 1971; Berger, 1973).

Vijayan Series rocks dated by Crawford and Oliver (1969) define a whole-rock isochron at 1150±60 Myr—the suggested date for the regional scale almandine–amphibolite facies metamorphism and migmatization, which have affected these rocks. Unfortunately the charnockites found as scattered occurrences within the eastern Vijayan have not so far been dated.

Charnockites from the Highland Series have yielded Rb/Sr ages (Crawford and Oliver, 1969) ranging from roughly 1250 to 3000 Myr. They regarded the older ages as relicts of earlier events, suggesting that there have been several episodes of metamorphism affecting these rocks and leading to charnockite development. Alternatively the range of dates could perhaps be interpreted as the result of varying degrees of isotopic re-equilibration of old (at least 3000 Myr) metamorphic rocks during the most recent major metamorphic event (about 1250 Myr). In either case it seems probable that the Highland Series rocks underwent fairly extensive recrystallization and isotopic homogenization under still essentially granulite facies conditions at roughly the same time as the Vijayan Series rocks suffered regional scale almandine–amphibolite facies metamorphism.

Petrography. The rock types studied in detail were charnockites (acid, intermediate, and basic types as defined by Cooray, 1962), pyroxene granulites, and an amphibole granulite.

The charnockites from the Highland Series vary from acid to basic types. Both intermediate and basic charnockites contain coexisting ortho- and clino-pyroxenes, as do the pyroxene granulites although in greater quantities. Biotite is sometimes present and hornblende almost invariably. The hornblende, both in green and brown varieties, usually occurs closely associated with pyroxene. Whilst in many cases it appears to be of late development, in other instances it may well be of earlier origin, as, for example, where rimmed by orthopyroxene in one rock. Garnet is a frequent constituent in the basic charnockites. Plagioclase shows a wide range in composition

(An_{16-60}) and the potash feldspar is commonly a microperthitic orthoclase. The amphibole granulite sample studied has a very high modal content of hornblende and clinopyroxene with an absence of orthopyroxene and garnet.

The acid charnockites from the Vijayan Series are characterized by an abundance of quartz and feldspar with small amounts of highly altered subidiomorphic orthopyroxene, and a total absence of both clinopyroxene and garnet. These charnockites differ from those of the Highland Series in their much higher modal contents of perthitic orthoclase. The perthites are mainly of the replacement type and generally show a myrmekitic intergrowth at plagioclase margins.

TABLE I. *Modal mineralogy of charnockites and pyroxene/amphibole granulites from SE. Sri Lanka*

	Highland Series									Vijayan Series				
	1	2	3	4	5	6	7	8	9	10	11	12	13	14
Quartz	—	—	—	—	14	7	10	28	Maj	Maj	7	20	26	—
K Feldspar	4	1	2	2	2	8	4	13	Maj	Maj	34	59	50	2
Plagioclase	28	9	31	47	38	55	39	26	Maj	Maj	27	15	13	32
Biotite	—	—	—	2	4	10	12	2	Acc	Maj	10	—	1	2
Garnet	10	Tr	15	—	17	—	—	Tr	Min	—	—	—	—	—
Hornblende	15	5	5	16	9	1	14	—	Min	Min	8	3	5	45
Orthopyroxene	18	30	18	14	5	8	6	28	Acc	Acc	2	2	3	—
Clinopyroxene	20	55	27	16	9	9	11	—	—	—	—	—	—	17
Opaques	5	1	2	2	2	2	4	2	Acc	Acc	2	1	2	2
% An in Plag.	46	48	56	40	60	36	36	42	30	12	14	12	12	36

Maj = Major minerals >10 % Min = Minor minerals 2–10 %
Acc = Accessory minerals <2 % Tr = Trace <0·5 %

1. Basic charnockite, 48/116.
2. Pyroxene granulite, 49/87/1.
3. Pyroxene granulite, J/50/2.
4. Basic charnockite, 49/16/1.
5. Basic charnockite, 48/28/3.
6. Intermediate charnockite, 42/7.
7. Intermediate charnockite, 48/104/1.
8. Acid charnockite, 42 81 1.
9. Acid charnockite, J 49 2.
10. Acid charnockite, J 51 7.
11. Acid charnockite, J 51 2 2.
12. Acid charnockite, J 51 10.
13. Acid charnockite, J 51 5.
14. Amphibole granulite, 48 64.

From Table I it is apparent that the samples analysed in this study fall into the following mineral assemblages: orthopyroxene–clinopyroxene–garnet–hornblende±biotite–plagioclase; clinopyroxene–hornblende–biotite–plagioclase; and orthopyroxene±hornblende±biotite–plagioclase. K feldspar is invariably present and quartz commonly so.

Rock chemistry. The major- and trace-element analyses of the charnockites and their associated rocks are presented in Table II. When plotted on an ACF diagram all the rocks fall within the diopside–anorthite–hypersthene field corresponding to the granulite facies assemblages observed. The low Fe_2O_3/FeO ratio for all samples suggests low partial pressures of oxygen (Goldschmidt, 1954). A general tendency for MgO, CaO, and FeO contents to increase with basicity was noted.

When the chemical changes in the rocks are plotted on variation diagrams based on

Larsen's method, modified by Nockolds and Allen (1953), there is a marked change in the trends of K, Na, and Al curves for the Vijayan Series and Highland Series charnockites and granulites. This trend is also evident from fig. 1 where the basic charnockites plot close to basaltic rocks and the compositional trend from basic to acid members is towards increasing K. The AFM diagram (fig. 2) also illustrates the compositional trend from basic to acid charnockites with the increasing alkali content.

TABLE II. *Chemical analyses of charnockites and pyroxene/amphibole granulites from SE. Sri Lanka*

	Highland Series									Vijayan Series				
	1	2	3	4	5	6	7	8	9	10	11	12	13	14
SiO_2	45·50	48·81	47·77	48·21	50·87	53·90	56·12	66·47	70·62	64·02	64·90	68·59	72·09	48·89
TiO_2	1·96	0·42	2·46	1·77	2·84	1·38	0·89	1·24	0·84	0·69	0·49	0·40	0·41	1·29
Al_2O_3	13·55	13·41	13·06	13·20	12·95	16·19	17·55	12·21	11·66	16·57	14·90	14·49	13·75	13·95
Fe_2O_3	4·08	2·34	0·00	3·95	6·30	3·45	2·70	1·74	1·62	1·06	1·18	1·88	1·03	3·10
FeO	13·07	7·22	16·91	9·79	10·90	6·13	4·97	6·30	4·68	3·81	3·56	2·51	1·91	8·90
MnO	0·20	0·18	0·21	0·22	0·28	0·17	0·14	0·12	0·13	0·10	0·09	0·12	0·03	0·19
MgO	7·30	12·16	5·95	7·58	2·98	3·95	3·77	2·83	1·00	1·29	2·02	0·12	0·27	7·45
CaO	10·92	12·80	10·50	10·58	8·89	7·87	6·79	3·19	3·64	3·53	3·71	1·59	1·37	12·10
Na_2O	2·50	1·42	2·53	2·85	0·89	3·70	4·27	3·17	2·51	4·42	4·74	4·53	3·79	2·32
K_2O	0·40	0·13	0·26	0·50	0·57	1·77	1·14	1·75	2·20	3·30	2·72	5·13	5·38	1·00
P_2O_5	0·30	0·04	0·40	0·19	1·53	0·72	0·28	0·28	0·17	0·24	0·11	0·06	0·08	0·13
SO_3	0·46	0·00	0·40	0·72	0·36	0·07	0·05	0·09	0·10	0·07	0·09	0·03	0·02	0·36
H_2O^+	0·34	0·39	0·11	0·28	0·27	0·33	0·32	0·14	0·13	0·12	0·28	0·18	0·20	0·38
H_2O^-	0·10	0·22	0·11	0·16	0·05	0·17	0·07	0·10	0·09	0·12	0·13	0·09	0·04	0·07
Total	100·68	99·54	100·67	100·00	99·68	99·80	99·06	99·63	99·39	99·34	98·92	99·72	99·67	100·13
Trace elements (in ppm):														
Ba	128	58	91	58	662	1218	625	538	—	—	347	497	407	—
Co	80	64	71	54	49	34	28	32	—	—	11	6	3	—
Cr	175	283	160	166	120	52	95	129	—	—	121	22	28	—
Cu	78	32	117	98	206	142	31	28	—	—	13	9	5	—
Mn	1779	1387	1642	1680	1753	1188	1199	871	—	—	693	717	378	—
Ni	116	64	90	44	19	115	72	63	—	—	24	3	10	—
Rb	5	2	3	7	23	42	18	51	—	—	92	96	176	—
Sr	246	137	130	127	142	651	660	211	—	—	275	111	69	—
V	426	227	378	336	69	232	166	119	—	—	55	—	11	—
Y	40	14	59	38	102	38	28	32	—	—	49	94	99	—
Zn	124	101	131	135	179	95	79	68	—	—	91	73	69	—
Zr	138	19	157	73	526	131	107	223	—	—	214	609	297	—

Both major and trace elements determined by X-ray fluorescence analysis, except for Na_2O, H_2O, and FeO, which were determined by atomic absorption, gravimetric, and Wilson's vanadium-reagent–titration methods, respectively. Analyst: D. E. de S. Jayawardena.

The column numbers equate with those in Table I, for which a sample key is provided.

Fig. 3 shows the variation in content of various trace elements plotted against the major element differentiation index (⅓Si+K)−(Ca+Mg) for the analysed rock suite. It is clear that there is a relative enrichment in Cr, Ni, V, and to a lesser extent Co in the basic charnockites and pyroxene granulites. Zr is low in the basic charnockites but increases in the intermediate group; however, values drop somewhat in the more acid rocks from the Highland Series, although they rise to a peak again in the acid charnockites of the Vijayan Series. Sr increases rapidly with increasing plagioclase content in the basic to intermediate charnockites and then decreases towards the acid end. Highest Ba contents are likewise found in the intermediate charnockites, whilst

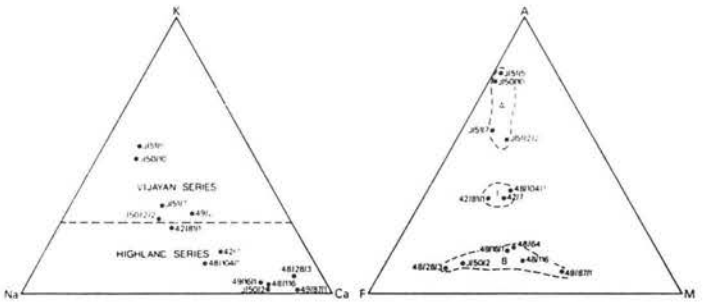

FIGS. 1 and 2: FIG. 1 (left). K:Na:Ca variation diagram for the analysed charnockites/granulites from SE. Sri Lanka. FIG. 2 (right). AFM variation diagram illustrating chemical distinctions between the analysed acid charnockites (A), intermediate charnockites (I), basic charnockites and granulites (B).

Rb is at its highest in the acid types. The content of Zn and Cu was found to be generally uniform with a slight increase in the intermediate types.

The variation of major and trace elements for acid to basic charnockites and pyroxene granulites is generally similar to that shown by the Madras charnockite series (Howie, 1955). In general the acid charnockites from the Vijayan Series show a depletion in Ni, Cr, Co, V, and Sr, and are enriched in Zr and Rb as compared to the basic to intermediate charnockites of the Highland Series. There is no significant variation in the trace elements in acid charnockites from the Highland and Vijayan Series.

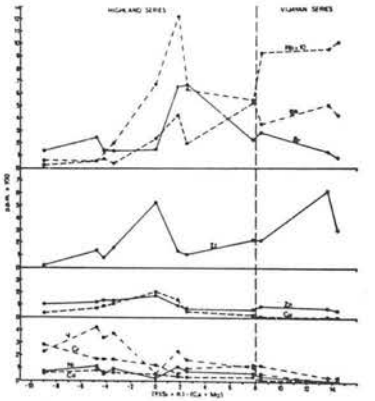

FIG. 3. A plot showing the variation in trace-element content against differentiation index for the analysed Highland Series and Vijayan Series charnockites/granulites.

The determined major and trace elements give a broad indication that the basic charnockites closely resemble basaltic rocks and the variation from the basic to acid members is similar to that shown by a normal igneous differentiation series probably of a calc-alkaline nature. However, the marked increase in Na, K, Rb, and to a lesser extent Al in the Vijayan Series charnockites may reflect some form of alkali metasomatism or granitization, as these rocks are closely associated with granites and migmatites in the field.

Mineral chemistry

Orthopyroxenes. The analytical results for major oxides in seven orthopyroxenes are presented in Table III, together with their structural formulae. The samples were all from the acid to basic charnockites and pyroxene granulites of the Highland Series. The 100 Mg/(Mg+Fe+Mn) ratios calculated vary from 46·0 to 67·9, compared with 35·3–49·0 for orthopyroxenes from the Madras charnockite series (Howie, 1955).

Alumina is generally lower than in the Madras charnockite series and varies from 0·98 wt. % Al_2O_3 for J/50/2 (pyroxene granulite—with garnet) to 1·86 wt. % Al_2O_3 (acid charnockite). However, the orthopyroxene in pyroxene granulite 49/87/1 has an appreciably higher Al_2O_3 content of 4·34 wt. %.

The experimental work of Green and Ringwood (1967) has indicated that the Al_2O_3 content of coexisting pyroxenes may be expected to increase from low- to high-pressure granulite assemblages for rocks of comparable chemistry. However, this is only true for garnet-free assemblages. Once garnet becomes stable in a particular rock, the Al_2O_3 content of the pyroxenes will in fact begin to drop with increasing pressure as further garnet forms (Boyd and England, 1964). Clearly the Al_2O_3 contents of granulite pyroxenes are controlled not only by the *PT* conditions of crystallization, but by chemical control on mineralogy (Howie, 1965).

As regards the pyroxene granulite 49/87/1 the effect of the higher Mg/Fe and Ca/Na ratios in this rock, compared with the other analysed rocks, appears to have been to restrict the content of highly aluminous phases, namely garnet and plagioclase, under the prevailing *PT* conditions of formation, thus resulting in the presence of more aluminous pyroxenes in this rock. Such an explanation is in line with the experimental evidence of Green and Ringwood (1967), which indicated that under granulite facies *PT* conditions garnet appears at lower pressures in rocks with lower Mg/Fe ratios, and plagioclase is stable to higher pressures in rocks with lower Ca/Na ratios.

Clinopyroxenes. The results of chemical analyses for major oxides in seven clinopyroxenes are presented in Table III, together with their structural formulae. In these clinopyroxenes the amount of tetrahedral aluminium is generally greater than octahedral aluminium, the replacement of Si by Al not exceeding 7 %. In the majority of clinopyroxenes Al_2O_3 does not exceed 3 wt. %, but in 49/87/1 the clinopyroxene has an appreciably higher Al_2O_3 content (4·55 wt. %) as did its associated orthopyroxene as discussed above.

The CaO content of the clinopyroxene is fairly constant varying from 20·73 wt. % to 21·06 wt. %, except for 49/87/1, which has a significantly higher CaO content of 22·19 wt. %. Although temperature has a major effect on the extent of solid solution between coexisting pyroxenes (Boyd and Schairer, 1964; Davis and Boyd, 1966), increasing Fe/Mg ratio in the pyroxenes may also be expected to lead to progressive shrinkage of the two-pyroxene field (Lindsley and Munoz, 1969). Thus the higher CaO content of the clinopyroxene in 49/87/1 does not necessarily indicate a lower crystallization temperature than in the other analysed rocks, but may just reflect the significantly lower Fe/Mg ratio in this rock and its constituent minerals.

Two samples of *garnets* were analysed from a pyroxene granulite (J/50/2) and a

TABLE III. *Chemical analyses of pyroxenes*

	Orthopyroxenes							Clinopyroxenes						
	1	2	3	4	5	6	7	1′	2′	3′	4′	5′	6′	7′
SiO_2	49·14	49·15	49·51	49·60	50·50	50·60	50·92	51·59	51·17	50·50	50·54	50·87	50·53	50·49
TiO_2	0·30	0·12	0·12	0·14	0·11	0·13	0·10	0·20	0·23	0·28	0·24	0·21	0·28	0·47
Al_2O_3	0·98	1·86	1·59	1·50	1·27	1·55	4·34	2·14	2·41	2·61	2·09	2·10	2·79	4·55
Fe_2O_3	—	—	—	—	—	—	—	1·54	1·87	3·57	4·02	2·63	3·06	2·28
FeO	33·40*	31·93*	31·34*	30·43*	25·30*	27·63*	19·69*	12·06	10·40	10·46	8·61	8·18	8·21	5·00
MnO	0·33	0·53	0·46	0·91	1·03	0·59	0·34	0·17	0·42	0·26	0·30	0·50	0·24	0·17
MgO	13·93	16·14	15·21	16·30	18·38	18·28	23·79	10·94	12·03	11·13	11·87	12·84	12·36	14·16
CaO	0·92	0·42	0·96	0·98	1·05	0·71	1·07	20·74	20·86	20·73	20·89	20·73	21·06	22·19
Na_2O	0·02	0·01	0·03	0·01	0·04	0·01	0·02	0·42	0·41	0·46	0·46	0·54	0·47	0·54
K_2O	0·01	0·01	0·01	0·03	0·04	0·01	0·01	0·04	0·05	0·02	0·03	0·07	0·03	0·01
P_2O_5	0·01	0·00	0·00	0·00	0·01	0·01	0·00	0·04	0·02	0·04	0·03	0·03	0·04	0·02
SO_3	0·00	0·00	0·01	0·06	0·01	0·00	0·02	0·03	0·09	0·08	0·07	0·09	0·03	0·04
Total	99·04	100·17	99·24	99·96	97·74	99·52	100·30	99·82	99·99	100·14	99·24	98·79	99·10	99·92
Cation proportions on the basis of 6 oxygens:														
Si	1·960	1·922	1·950	1·937	1·967	1·949	1·874	1·956	1·933	1·914	1·922	1·933	1·914	1·870
Al^{iv}	0·040	0·078	0·050	0·063	0·033	0·051	0·126	0·044	0·067	0·086	0·078	0·067	0·086	0·130
Al^{vi}	0·006	0·008	0·074	0·006	0·025	0·010	0·062	0·052	0·040	0·031	0·016	0·027	0·039	0·069
Ti	0·009	0·004	0·004	0·004	0·003	0·004	0·003	0·006	0·007	0·008	0·007	0·006	0·008	0·013
Fe^{3+}	—	—	—	—	—	—	—	0·044	0·053	0·102	0·115	0·075	0·087	0·064
Mg	0·828	0·941	0·893	0·949	1·067	1·049	1·305	0·619	0·677	0·629	0·673	0·727	0·698	0·781
Fe^{2+}	1·114	1·004	1·032	0·994	0·894	0·890	0·666	0·383	0·329	0·332	0·274	0·260	0·260	0·155
Mn	0·011	0·018	0·015	0·030	0·034	0·019	0·011	0·005	0·013	0·008	0·013	0·016	0·008	0·005
Ca	0·039	0·018	0·041	0·041	0·044	0·029	0·042	0·844	0·845	0·842	0·851	0·844	0·855	0·880
Na	0·002	0·001	0·002	0·001	0·003	0·001	0·001	0·031	0·030	0·034	0·034	0·040	0·035	0·039
K	0·001	0·000	0·001	0·001	0·002	0·000	0·000	0·002	0·002	0·001	0·001	0·003	0·001	0·000
Σ (Al^{iv} to Mn)	1·968	2·015	2·018	1·983	1·953	1·981	1·987	1·109	1·119	1·110	1·098	1·111	1·100	1·087
Σ (Ca, Na, K)	0·042	0·019	0·044	0·043	0·049	0·030	0·043	0·877	0·877	0·877	0·886	0·887	0·891	0·919
Mg	41·80	46·98	45·42	47·83	55·14	53·30	66·82	32·82	35·65	33·18	35·37	38·09	36·42	41·92
Fe	56·23	52·12	52·49	50·10	42·58	45·22	31·03	22·43	19·85	22·42	19·92	17·71	17·92	11·32
Ca	1·97	0·90	2·09	2·07	2·27	1·47	2·15	44·75	44·50	44·40	44·70	44·21	45·19	46·76

* Total Fe value (XRF) quoted as FeO in orthopyroxenes. FeO determined by Wilson's procedure in clinopyroxenes. Na_2O by atomic absorption: all other elements by X-ray fluorescence. Analyst: D. E. de S. Jayawardena.

All pyroxene separates from Highland Series rocks:

1 and 1′ from pyroxene granulite J/50/2.
2 from acid charnockite 42/81/1.
2′ from amphibolic granulite 48/64.
3 and 3′ from basic charnockite 48/116.
4 and 4′ from intermediate charnockite 42/7.
5 and 5′ from intermediate charnockite 48/104/1.
6 and 6′ from basic charnockite 49/16/1.
7 and 7′ from pyroxene granulite 49/87/1.

basic charnockite (48/28/3) and the analyses are presented in Table IV. These garnets were found to be richer in andradite, grossular, and spessartine, and poorer in almandine when compared to garnets from the gneisses (Jayawardena, 1973). The low MnO content, (FeO+MnO)/MgO ratio, and the almandine content of the garnets are in agreement with those from similar metamorphic terraines (Miyashiro, 1953; Sturt, 1962; Engel and Engel, 1960). It is, however, apparent that the host-rock composition plays an important role in controlling the chemical composition of garnets and it is difficult to separate the variation due to host rock from that due to grade of metamorphism.

TABLE IV. *Chemical analyses of garnets and partial analyses of hornblendes*

	Garnets		Hornblendes				Structural formulae				
	1	2	3	4	5		1′	2′	3′	4′	5′
SiO_2	37·94	37·99	41·91	41·86	40·38	Si	3·005	3·036	6·264	6·247	6·088
TiO_2	0·10	0·14	2·24	2·18	2·60	Al^{iv}	—	—	1·736	1·753	1·912
Al_2O_3	20·28	20·30	11·63	11·13	12·38	Al^{vi}	1·893	1·912	0·312	0·204	0·288
Fe_2O_3	2·84	0·39	4·72	4·67	4·26	Ti	0·006	0·008	0·252	0·245	0·295
FeO	24·87	28·20	11·81	13·09	14·79	Fe^{3+}	0·169	0·023	0·531	0·524	0·483
MnO	0·95	0·82	0·17	0·23	0·91	Fe^{2+}	1·648	1·885	1·476	1·634	1·865
MgO	4·51	4·01	10·75	11·24	9·05	Mn	0·064	0·478	0·022	0·029	0·116
CaO	7·51	6·85	11·57	11·40	11·11	Mg	0·533	0·056	2·395	2·500	2·034
Na_2O	0·01	0·04	1·45	1·12	2·06	Ca	0·637	0·586	1·853	1·823	1·795
K_2O	0·01	0·02	1·52	1·53	1·01	Na	0·002	0·006	0·420	0·324	0·602
						K	0·001	0·002	0·290	0·291	0·194
Total	99·02	98·76	97·77	98·45	98·55	O	12·000	12·000	23·000	23·000	23·000
						% Almandine	57·2	61·4	*X* 2·563	2·438	2·591
						% Andradite	8·8	1·2	*Y* 4·986	5·136	5·081
						% Grossular	13·3	19·0	*Z* 8·000	8·000	8·000
						% Pyrope	18·5	16·4			
						% Spessartine	2·2	1·9			

All elements determined by X-ray fluorescence analysis except Na_2O (atomic absorption) and FeO (Wilson's vanadium-reagent method). Analyst: D. E. de S. Jayawardena.

All mineral separates from Highland Series rocks:

1 and 1′ garnet from basic charnockite 48/28/3.
2 and 2′ garnet from pyroxene granulite J/50/2.
3 and 3′ hornblende from basic charnockite 49/16/1.
4 and 4′ hornblende from amphibole granulite 48/64.
5 and 5′ hornblende from basic charnockite 48/116.

Three samples of *hornblendes* from 48/64 (amphibole granulite) and 48/116 and 49/16/1 (basic charnockites) were analysed (Table IV). Their compositions lie between the fields of common hornblende and pargasite. When their compositions are calculated as pargasite–ferropargasite and magnesiohastingsite–hastingsite end-members (Gilbert, 1966), they plot diagonally across the end-members pargasite and hastingsite and exhibit less scatter than those from Madras (Howie, 1955). The compositions of the hornblendes studied are similar to those from Kondapalli, India (Fig. 1, Leelanandam, 1970).

In the hornblendes of the present study the number of Ca atoms per formula unit varies from 1·87 to 1·93 and falls within the hornblende field (Deer *et al.*, 1961). The replacement of Mg by Fe^{2+} shows a wide variation when expressed as 100 $Mg/(Mg+Fe^{2+}-Fe^{3+}-Mn)$ and Fe^{3+}/Fe^{2+} is less than 1. The relatively high TiO_2 contents and Al^{vi} values in hornblendes from basic charnockites and amphibole granulites as compared to hornblendes from gneisses and amphibolites suggest somewhat higher temperatures and pressures of crystallization for the Highland Series (Jayawardena, 1973). However, it is difficult to distinguish between the compositional control imposed by the whole rock chemistry and that due to the prevailing temperatures and pressures of crystallisation.

Petrogenesis: Temperature estimates

Coexisting pyroxenes. Six pairs of coexisting pyroxenes have been analysed from Highland Series charnockites/granulites. In all cases, the Ca-rich pyroxenes have lower Fe^{2+}/Mg^{2+} ratios than the associated Ca-poor pyroxenes. Hence pyroxene tie-lines on the En–Wo–Fs diagram cut the En–Wo side-line when extended, as to be expected for assumed equilibrium assemblages (Howie, 1965).

The Mg^{2+}–Fe^{2+} distribution coefficient K_D (Kretz, 1961) or K_μ (Bartholomé, 1962) between the coexisting pyroxenes can be used to estimate the likely temperature of equilibration of these mineral assemblages. The range of K_D values (Table V) is rather large, particularly with the analytically determined Fe^{2+} values—no doubt at least in part reflecting the difficulty in obtaining accurate Fe^{2+}/Fe^{3+} ratios with standard geochemical techniques as employed here. A comparison with temperature estimates and corresponding K_D values for coexisting pyroxenes in rocks for Madras (Howie, 1955, 1965), Colton area (New York; Engel *et al.*, 1964), Saltora (India; Sen and Rege, 1966), and Amaravathi (Andhra Predesh; Ramaswamy and Murty, 1973), suggest equilibration temperatures in the range 700±100 °C for the mineral assemblages from south-east Sri Lanka.

Manna and Sen (1974) have indicated that garnetiferous basic granulites have lower K_D values and thus lower equilibration temperatures as compared to associated garnet-free basic granulites in the Saltora district of West Bengal. However, the values in Table V do not show any systematic differences in K_D between the garnetiferous and garnet-free granulites studied here. It is, however, apparent that higher whole-rock Fe/Mg ratios seem to have favoured the formation of garnet in certain of these basic charnockites under the prevailing *PT* conditions. This is in line with the experimental evidence of Green and Ringwood (1967). However, it has to be pointed out that the samples in this study were collected over a wide area, unlike the rock suite studied by Manna and Sen (1974), hence regional variation in the *PT* conditions of metamorphism are more likely in this instance.

The $Ca/(Mg+Fe^{2+})$ ratio in the clinopyroxenes can also be used to give an estimate of the temperature of crystallization by comparison with solid-solution limits for the coexisting pyroxene pairs in the synthetic $MgSiO_3$–$CaMgSi_2O_6$ system (O'Hara and Mercy, 1963; Boyd and Schairer, 1964). It has been shown experimentally (Davis and Boyd, 1966) that pressure has little effect on the position of the diopside solvus. The

solvus limits extrapolated on to the $MgSiO_3$–$CaMgSi_2O_6$ join for the curves representing the two-pyroxene field of the present study are approximately Ca_1Mg_{99} and $Ca_{48}Mg_{52}$ (Jayawardena, 1973) and give an approximate temperature of equilibration of 850±150 °C (Boyd and Schairer, 1964). Unfortunately this geothermometer is rather insensitive at such temperatures, as the solvus boundaries become almost parallel to the temperature axis at low temperatures. The semi-empirical method of Wood and Banno (1973) for calculating the equilibrium temperatures from the coexisting pyroxene data gives closely similar values (858±11 °C as the mean temperature and standard deviation for the six pyroxene pairs).

TABLE V. Ca/(Ca+Mg) *ratios and* K_D *values for coexisting pyroxenes*

Sample Number	CPX			OPX			K_D	
	Ca	Mg	$\frac{Ca}{Ca-Mg}$	Ca	Mg	$\frac{Ca}{Ca-Mg}$	*Calc. Fe^{2+}	†Det. Fe^{2+}
J/50/2	44·75	32·82	0·577	1·97	41·80	0·045	0·514	0·519
48/116	44·40	33·18	0·572	2·09	45·42	0·044	0·551	0·521
42/7	44·70	35·37	0·558	2·07	47·83	0·041	0·505	0·450
48/104/1	44·21	38·09	0·537	2·27	55·14	0·040	0·550	0·505
46/16/1	45·91	36·42	0·558	1·47	53·30	0·027	0·528	0·476
49/87/1	46·76	41·92	0·527	2·15	66·82	0·031	0·500	0·524

* These K_D values are based on Fe^{2+} values obtained following calculation of the Fe^{2+}/Fe^{3+} ratios in these pyroxenes from the structural formulae assuming stoichiometry, by a similar procedure to that used by Mysen and Heier (1972).

† These K_D values are based on the determined Fe^{2+} values.

Coexisting garnet and clinopyroxene. Only one coexisting garnet–clinopyroxene pair has been analysed in this study, but the partitioning of Fe^{2+} and Mg between these mineral phases can also be used to give an indication of the equilibration temperature. Banno (1970) used the derived distribution coefficient K' to obtain a rough estimate of temperature for the purpose of a genetic classification of eclogites and according to him the pressure effect on K' is negligible.

The distribution coefficient K' calculated for sample J/50/2 is 6·37 and using the compiled analyses and temperature estimates for calibration of the $K' = f(T)$ geothermometer of Mysen and Heier (1972) a value of 670 °C can be deduced. Råheim and Green (1974) have demonstrated through experimental work that K' is more highly dependent on pressure than originally thought by Banno (1970), and their derived expression for relating K' to equilibration temperature gives a value of 656 °C if a pressure of 7 kb is assumed as a first approximation.

As errors in K', and likewise K_D, can be introduced by inaccurate Fe^{2+}/Fe^{3+} ratio determinations, it is also worth considering the distribution coefficient K'' for Mn and Mg between the garnet and clinopyroxene. The calculated K'' for J/50/2 is 15·33 and from fig. 4 (Carswell, 1974) an approximate temperature of 675 °C can be estimated. The temperature estimates derived from the Fe^{2+}/Mg and Mn/Mg partition coefficients

are thus in close agreement, although it is realistic to put error limits of at least ±50 °C on these values.

It is apparent that there is a discrepancy of close to 200 °C between the values derived from consideration of the Ca distribution between the coexisting pyroxenes and from the Fe^{2+}–Mg–Mn distribution between coexisting garnet and clinopyroxene. It is considered that the higher estimates based on the former method are more likely to be in serious error and hence that a value of 700±50 °C is probably most appropriate for the final equilibration of these assemblages. As the various estimates are based on analyses of bulk mineral separates, it may be that the range of temperature values reflect the temperature range from that of initial formation down to final equilibration of the charnockite/granulite terrain during subsequent cooling/unloading.

Pressure estimates

Green and Ringwood (1967) carried out an experimental investigation of the gabbro to eclogite transformation, resulting in a subdivision of basic granulite assemblages into low-, intermediate-, and high-pressure types.

The SiO_2 undersaturated pyroxene granulites and charnockites studied are characterized by orthopyroxene+clinopyroxene−garnet−plagioclase and orthopyroxene−clinopyroxene−plagioclase assemblages. The Lewisian metamorphic rocks of Scourie, Sutherland, described by O'Hara (1961) similarly contain the assemblage orthopyroxene+clinopyroxene+garnet+plagioclase in undersaturated basic rocks. De Waard (1964) described an area in the Adirondacks where he drew attention to the intermingling of orthopyroxene+clinopyroxene+plagioclase+quartz−hornblende and clinopyroxene+garnet+plagioclase−quartz+hornblende assemblages. This intermingling was explained by De Waard (op. cit.) as due to the presence of mineral assemblages from both sides of the reaction orthopyroxene+plagioclase = clinopyroxene+garnet+quartz. This reaction is now recognized as taking place at the boundary between the high-pressure and intermediate-pressure granulite fields. The granulites and charnockites of Madras (Howie, 1955) have a stable mineral assemblage of orthopyroxene+clinopyroxene+plagioclase+quartz+hornblende and this is true for granulite facies terrains in Uganda (Groves, 1935), Varberg (Sweden; Quensel, 1954), and Broken Hill (New South Wales; Binns, 1964).

The assemblage orthopyroxene±clinopyroxene±garnet+plagioclase+quartz± hornblende−biotite in oversaturated rocks of the Highland Series of south-east Sri Lanka therefore appears to have been formed under the *PT* conditions of the intermediate-pressure granulite field (Green and Ringwood, 1967). This is further borne out by the presence of coexisting sillimanite+K-feldspar and absence of muscovite and kyanite in the metasedimentary gneisses that are closely intermixed with the charnockites of the Highland Series.

The charnockites of the Vijayan Series are characterized by the assemblage orthopyroxene+plagioclase+quartz±hornblende±biotite and can therefore also be grouped under the intermediate-pressure granulite field.

The most likely *PT* field of equilibration of the charnockites and pyroxene granulites from both the Vijayan Series and Highland Series is shown on fig. 4. With the favoured

temperature estimates of 700±50 °C, best load-pressure estimates would be in the range 5 to 7·5 kbar. With metamorphic temperatures of that order, the general lack of evidence of crustal partial melting in the Highland Series rocks, the absence of muscovite, and the scarcity of hornblende compared with pyroxenes, together indicate that in general the water pressure must have been significantly less than the total pressure during the granulite facies metamorphism.

Conclusion

From the rock chemistry it is difficult to decide whether the marked increase in Na, K, Rb, and to a lesser extent Al in the Vijayan Series charnockites reflects the typical compositions of the more acid members of a calc-alkaline type differentiation series or whether it is due to alkali metasomatism or granitization during metamorphism. However, the field association of these rocks with granites and migmatites would appear to favour the latter interpretation.

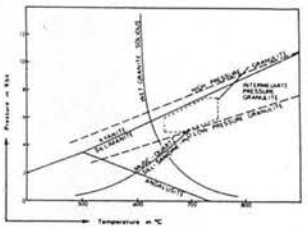

FIG. 4. The stippled field indicates the estimated P–T conditions of equilibration of the SE. Sri Lanka charnockites/granulites in relation to the extrapolated P–T boundaries for the intermediate-pressure granulite field (Green and Ringwood, 1967), the likely stability field of the Al_2SiO_5 polymorphs (Newton, 1966; Fyfe and Turner, 1966; Holdaway, 1971), the experimentally determined reaction curve muscovite + quartz = sillimanite + sanidine + water (Evans, 1965), and the minimum melting curve for water-saturated 'granite' (Bowen and Tuttle, 1958).

Consideration of the partitioning of various elements between coexisting pyroxenes and coexisting clinopyroxene and garnet indicates equilibration temperatures in the range 700±50 °C. Amongst the suite of samples studied there was no evidence that garnetiferous granulites have consistently lower equilibrium temperatures than garnet-free granulites as indicated by Manna and Sen (1974).

The charnockites and pyroxene granulites studied from both the Highland Series and Vijayan Series have mineral assemblages that fall into the intermediate-pressure granulite field of Green and Ringwood (1967), suggesting formation at load pressures in the range 5 to 7·5 kbar, corresponding to crustal depths of roughly 17 to 25 kilometres. Water pressure is thought likely to have been in general significantly less than the load pressure during the granulite facies metamorphism.

On the basis of the mineral data presented and the available age dates, we tentatively suggest that the charnockites of both the Highland Series and Vijayan Series may have equilibrated at broadly similar P_{LOAD}/T conditions at roughly the same time (1150–1250 Myr) as the development of the associated Vijayan Series gneisses, migmatites, and granites. The development of the latter rock types on a regional scale we attribute to the prevalence of much higher P_{H_2O} conditions during this metamorphic event in the Vijayan Series rocks than in the Highland Series rocks. There is, however, a need for further studies, including age dates, on the associated charnockites, gneisses, and granites in the Eastern Vijayan Series to help resolve the question of the genetic relationship between these rocks, and between the Highland and Vijayan Series as a whole.

Acknowledgements. D. E. de S. Jayawardena wishes to acknowledge the advice and assistance of Dr. R. Kanaris-Sotiriou and Mr. V. A. Somogyi with analytical procedures and to thank Professor L. R. Moore for the use of Department facilities during the tenure of a technical Assistance Study Fellowship from the British Council. He also wishes to thank the Director, Geological Survey of Sri Lanka, for permission to publish this paper.

REFERENCES

BALENDRAN (V. S.), 1968. Unpublished 1″ geological sheets of Tirrukkovil and Westminster Abbey. Geological Survey of Ceylon.
BANNO (S.), 1970. *Phys. Earth Planet. Interiors*, **3**, 405–21.
BARTHOLOMÉ (P.), 1962. Iron-magnesium ratio in associated pyroxenes and olivines. *Petrologic studies—A volume in honour of A. F. Buddington*, 1–20, *Geol. Soc. Amer.*
BERGER (A. R.), 1973. *Geol. Rundsch.* **62**, 342–7.
BINNS (R. A.), 1946. *Journ. Geol. Soc. Austr.* **11**, 283–330.
BOWEN (N. L.) and TUTTLE (O. F.), 1958. *Geol. Soc. Amer. Mem.* **74**.
BOYD (F. R.) and ENGLAND (J. F.), 1964. *Carnegie Inst. Wash. Yearbk.* **63**, 157–61.
—— and SCHAIRER (J. F.), 1964. *Journ. Petr.* **5**, 275–309.
CARSWELL (D. A.), 1974. *Lithos*, **7**, 113–21.
COORAY (P. G.), 1961. The Geology of the Country around Rangala—*Memoir* **2**, *Geological Survey of Ceylon.*
—— 1962. *Quart. Journ. Geol. Soc.* **118**, 239–73.
CRAWFORD (A. R.), 1974. *Tectonophysics*, **22**, 141–57.
—— and OLIVER (R. L.), 1969. *Spec. Publ. Geol. Soc. Australia*, **2**, 283–306.
DAVIS (B. T. C.) and BOYD (F. R.), 1966. *Journ. Geophys. Res.* **71**, 3567–76.
DEER (W. A.), HOWIE (R. A.), and ZUSSMAN (J.), 1961. *Rock-forming minerals*, **2**, London (Longmans).
DE WAARD (D.), 1964. *Koninkl. Ned. Akad. Wetenschap Proc. Ser. B*, **67**, 344–62.
ENGEL (A. E. J.) and ENGEL (C. G.), 1960. *Bull. Geol. Soc. Amer.* **71**, 1–58.
—— ENGEL (C. G.), and HAVENS (R. G.), 1964. *Journ. Geol.* **72**, 131–56.
EVANS (B. W.), 1965. *Amer. Journ. Sci.* **263**, 647–67.
FERNANDO (L. J. D.), 1948. *Bull. Imp. Inst.* **46**, 303–25.
FYFE (W. S.) and TURNER (F. J.), 1966. *Contr. Min. Petr.* **12**, 354–64.
GILBERT (M. C.), 1966. *Amer. Jour. Sci.* **264**, 698–742.
GOLDSCHMIDT (J. R.), 1954. *Geochemistry*, Oxford University Press.
GREEN (D. H.) and RINGWOOD (A. E.), 1967. *Geochimica Acta*, **31**, 767–833.
GROVES (A. W.), 1935. *Quart. Jour. Geol. Soc.* **91**, 150–207.
HAPUARACHCHI (D. J. A. C.), 1957. In *Admin. Report. Govt. Mineralogist for 1956*, Colombo, Ceylon.
HOLDAWAY (M. J.), 1971. *Amer. Journ. Sci.* **271**, 97–131.
HOWIE (R. A.), 1955. *Trans. Roy. Soc. Edin.* **62**, 725–68.
—— 1965. *Controls of Metamorphism* (ed. Pitcher and Flinn), 319–26. London (Oliver & Boyd).
JAYAWARDENA (D. E. DE S.), 1973. *A geochemical study of rocks and ferro-magnesian minerals from a selected area in the south-eastern sector of the Pre-Cambrian of Ceylon.* Unpublished M.Sc. thesis, Geology Department, University of Sheffield.
KATZ (M. B.), 1971. *Geol. Rundsch.* **60**, 1523–49.
KRETZ (R.), 1961. *Journ. Geol.* **69**, 361–87.
LEELANANDAM (C.), 1970. *Journ. Petr.* **11**, 475–505.
LINDSLEY (D. A.) and MUNOZ (J. L.), 1969. *Amer. Jour. Sci.* (*Schairer Vol.*), **267A**, 297–324.
MANNA (S. S.) and SEN (S. K.), 1974. *Contr. Min. Petr.* **44**, 195–218.
MIYASHIRO (A.), 1953. *Geochimica Acta*, **4**, 179–208.
MYSEN (B. O.) and HEIER (K. S.), 1972. *Contr. Min. Petr.* **36**, 73–94.
NEWTON (R. C.), 1966. *Science*, **151**, 1222–5.
NOCKOLDS (S. R.) and ALLEN (R. S.), 1953. *Geochimica Acta*, **4**, 105–42.

O'HARA (M. J.), 1961. *Journ. Petr.* **2**, 248–76.
—— and MERCY (E. L. P.), 1963. *Trans. Roy. Soc. Edin.* **65**, 251–314.
QUENSEL (P.), 1954. The charnockite series of the Varberg district in the south-west coast of Sweden. *Arkiv. Min. Geol.* **1**, No. 10.
RÅHEIM (A.) and GREEN (D. H.), 1974. *Contr. Min. Petr.* **48**, 179–203.
RAMASWAMY (A.) and MURTY (M. S.), 1973. *Min. Mag.* **39**, 74–7.
SEN (S. K.) and REGE (S. M.), 1966. Ibid. **35**, 759–62.
STURT (B. A.), 1962. *Journ. Petr.* **3**, 181–91.
TATSUMI (T.) and KIZAKI (K.), 1969. *Geology of the Lützow-Holm Bay region and the 'Yamato Mountains' (Queen Fabiola Mountains)*. In CRADDOCK, C. (co-editor), 1969–70. *Geologic Maps of Antarctica, Antarctic Map Folio*, 12—Amer. Geogr. Soc., New York.
WICKRAMASINGHE (O. C.), 1969. *The geochemistry and geochronology of the charnockites and associated rocks of Ceylon.* Unpublished Ph.D. thesis, Department of Earth Sciences, University of Leeds.
WOOD (B. J.) and BANNO (S.), 1973. *Contr. Min. Petr.* **42**, 109–24.

[*Manuscript received 24 January 1975; revised 23 June 1975*]

Bull. Minéral.
(1983), 106, 761-774

Petrology of garnet-clinopyroxene rocks in a granulite facies environment, Bohemian massif of Lower Austria

by HEINZ G. SCHARBERT* and DENNIS A. CARSWELL**

* Institut für Petrologie, Universität Wien, Dr. Karl Lueger Ring 1, 1010 Wien, Austria.

** Department of Geology, University of Sheffield, Mappin Street, Sheffield S1 3JD, U.K.

Abstract. — Whole rock and mineral analyses are presented for garnet-clinopyroxene rocks found intimately associated with possible mantle derived garnetiferous peridotite bodies in a high pressure granulite facies terrain. Although garnets are pyropic (48-76 % pyrope) these rocks are not true eclogites since their constituent clinopyroxenes are not omphacites but rather Al-augites or Cr-diopsides with Al^{IV}/Al^{VI} ratios, mostly > 1.0. Element partitioning considerations between garnet-clinopyroxene and clinopyroxene-orthopyroxene pairs are taken to indicate arrested equilibration under pressure-temperature conditions compatible with those previously deduced for the surrounding granulite facies rocks. However, mineral zoning profiles and exsolution textures clearly indicate that the current metamorphic mineral assemblages have formed in response to cooling from an earlier temperature (and pressure ?) maximum. It is considered that these garnet-clinopyroxene rocks may represent the partially recrystallised crystalline products of trapped upper mantle partial melts of olivine tholeiite to picrite composition in which highly aluminous pyroxenes were the dominant original phases formed on the liquidus. The present metamorphic character and lithological associations of such rocks may accordingly bear witness to deep-seated tectonic interactions between the upper mantle and lower continental crust during a profound compressional orogenic event.

Key words : granulite facies, eclogite, garnet group, clinopyroxene, geothermometry.

Pétrologie des roches à grenat-clinopyroxène dans un environnement du domaine des granulites. Massif de Bohème de la Basse Autriche.

Résumé. — Des analyses de roches totales et de minéraux sont données pour des roches à grenat et clinopyroxène découvertes intimement associées à des massifs de péridotite à grenat probablement issues du manteau et incorporées dans un domaine granulitique de haute pression.

Bien que leurs grenats soient riches en pyrope (48-76 % pyrope) ces roches ne sont pas de vraies eclogites etant donné que leurs clinopyroxenes ne sont pas des omphacites, mais plutôt des augites alumineuses ou des diopsides chromifères avec des rapports Al^{IV}/Al^{VI} bien supérieurs à 1. Les informations fournies par les coefficients de partage entre les couples grenat-clinopyroxène et clinopyroxène-orthopyroxène permettent d'établir des conditions de pression et température de formation compatibles avec celles déjà trouvées pour les roches granulitiques encaissantes. Cependant, les structures zonées des minéraux et les figures d'exsolution indiquent clairement que les parageneses métamorphiques courantes ont été formées lors d'un épisode de refroidissement intervenant après un premier maximum de température (et de pression ?).

On considère que ces roches à grenat-clinopyroxène peuvent représenter le matériel cristallin piégé partiellement recristallisé issu des produits de fusion partielle du manteau supérieur, de composition tholéiitique à olivine, à picritique, dans lesquels les pyroxènes riches en alumine furent les phases initiales principales formées sur le liquidus. Le caractère métamorphique actuel et les associations lithologiques de telles roches peuvent éclairer d'un jour nouveau les interactions tectoniques profondes entre le manteau supérieur et la partie inférieure de la croûte continentale lors d'un évenement orogénique intense, de type compressif.

Mots-clés : facies granulite, éclogite, grenat, clinopyroxène, géothermométrie.

INTRODUCTION

Granulite facies rocks, leucocratic potash feldspar rich gneisses (Gföhl gneiss), pyrope-bearing peridotites and garnet-clinopyroxene rocks ("eclogites") (Becke *et al.*, 1914 ; Köhler, 1941) have been recognized as a typical lithological association of the Gföhl unit (Fuchs, 1971) within the Moldanubian Zone of the Bohemian massif in Lower Austria. Comparable features on the Czechoslovakian side have been presented by Fiala (1966) and Kopecký and Sattran (1966).

The granulite facies rocks have been investigated in some detail, lately by Scharbert and Kurat (1974), by Scharbert *et al.* (1976) and by

Fuchs und Scharbert (1979). Physical conditions with pressures exceeding 10 kbar (low P_{H_2O}) and a minimum temperature of 760 °C seem to have prevailed during the deep-seated granulite facies metamorphism of Caledonian age (Arnold und Scharbert, 1973) in this area.

It has been previously suggested that the garnet peridotites and associated garnet-clinopyroxene rocks are of Upper Mantle origin and have been emplaced into low crustal granulite facies environments in the solid state by deep-reaching tectonic movements (Kappel, 1967 ; Rost und Grigel, 1969 ; Scharbert, 1973). Matura (1974) noticed the distribution of the ultramafic rocks in narrow zones which are concordant with the internal structure of the granulite facies bodies. An Upper Mantle origin of garnet peridotites and associated eclogites and their tectonic emplacement into high grade metamorphic terrains have also been suggested elsewhere by several authors (Carswell, 1968*a*,*b* ; Carswell and Gibb, 1980 ; Ernst, 1978 ; Kornprobst, 1969 ; Medaris, 1980 ; O'Hara and Mercy, 1963 ; and others).

Two occurrences of Moldanubian garnet-clinopyroxene rocks (''eclogites'') have been investigated previously by Kappel (1967). He proposed the following scheme to explain the development of these rocks and their association with garnetiferous peridotites.

1. Crystallisation of the garnet peridotites from a ''pyrolitic magma'' at pressures of around 23 kbar.

2. Formation of the ''eclogites'' from locally concentrated basaltic ''residual magma'' with crystallisation temperatures of 1 530-1 630 °C at a minimum pressure of 23 kbar.

3. Equilibration of the present garnet-clinopyroxene assemblage at around 1 000 °C on cooling still at mantle depths.

4. Tectonic emplacement of these mantle rocks into lower continental crust subject to granulite facies conditions, with attendant retrogression of the mantle derived rocks.

There is some confusion over what Kappel meant by crystallisation from a 'pyrolitic magma' and by the 'residual magma' as well as uncertainty concerning the respective equilibration conditions of the garnet clinopyroxenites and the encompassing granulite facies rocks.

Dempsey and Scharbert (1981) have demonstrated that the high pressure (20-30 kbar) melts of a typical Moldanubian garnet clinopyroxenite specimen (1096) quench to highly aluminous pyroxenoid phases which may have been the primary crystallisation products from such melts in the mantle.

Recent observations have revealed a somewhat more variable modal mineralogy in the garnet clinopyroxene rocks than previously recognised. Garnet and clinopyroxene may be joined by orthopyroxene and spinel in various proportions, the appearance of minor olivine leads towards a lherzolitic character in some instances, and the appearance of minor plagioclases provides a possible link with pyriclasites (Scharbert, 1963) — considered to represent basaltic rocks metamorphosed under high pressure granulite facies conditions. The pyriclasites consist of garnet, clinopyroxene, plagioclase, orthopyroxene, pargasitic amphibole, manganese ilmenite and scarce spinel. Formerly they have been called ''plagioclase eclogites'' (Tertsch, 1921), a most unsatisfactory name.

The principal aim of the present contribution is to demonstrate with new data on several occurrences the results of a closer investigation of the mineralogical adjustment of the garnet-clinopyroxene rocks to lower crustal granulite facies conditions.

PETROGRAPHY AND ROCK CHEMISTRY

The garnet-clinopyroxene rocks appear in the form of layers of variable thickness (up to 40 cm) within the sometimes strongly serpentinised garnet peridotite bodies. They may also appear as tectonically disrupted lenses of fragments of irregular shape (cf. Kappel, 1967, p. 269). The localities of investigated garnet-pyroxene rocks can be deduced from figure 1.

The geological mode of occurrence of all these rocks closely resembles that described for similar rocks by Kornprobst (1969) from Beni Bouchera (Morocco), by Dickey (1970) and Obata (1980) from the Sierra de la Ronda (Spain), by Dickey (1970) and Conquéré (1971) from l'Etang de Lerz (France), and by Carswell (1968*a*, 1973) and Medaris (1980) from Norwegian localities.

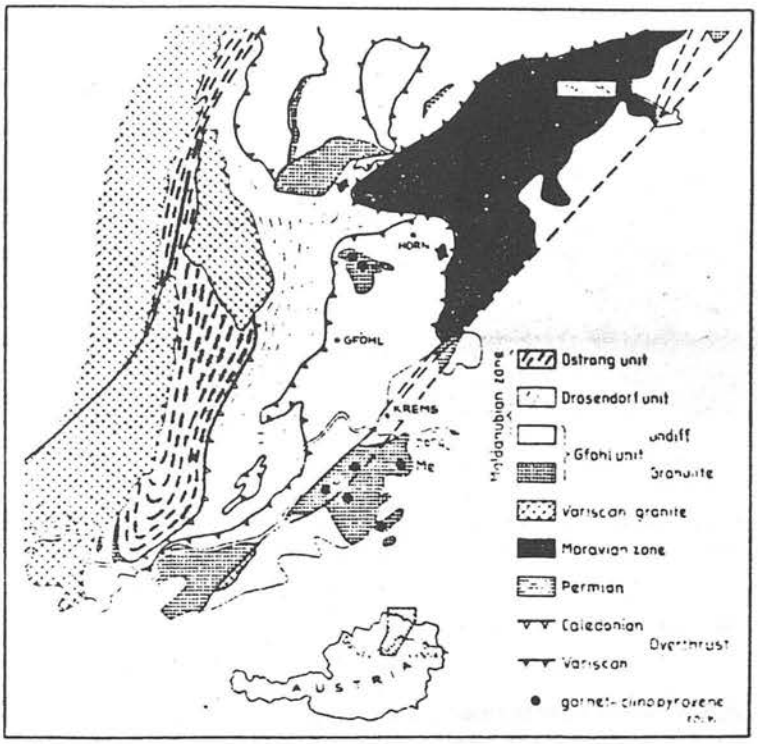

FIG. 1. — *Simplified map of the tectonic units of the Lower Austrian Moldanubian Zone* (Fuchs, 1971). Dots indicate garnet-clinopyroxene localities considered in this paper.

Carte simplifiée des unités tectoniques de la Zone Moldanubienne de la Basse Autriche (Fuchs, 1971). Les points indiquent les localisations des clinopyroxénites à grenat considerees dans cet article.

As previously indicated by Kappel (1967), the Lower Austrian garnet-clinopyroxene rocks usually have metamorphic textures though frequently with evidence of textural disequilibrium. No "primary" crystallisation products have been observed, with the possible exception of specimen 857 which is a clinopyroxenite with a relatively sub-calcic clinopyroxene as the sole mineral phase.

Mineralogical and textural features are considered to justify recognition of the following petrographic variants :

1. Garnet websterite I (garnet + clinopyroxene + orthopyroxene),
2. Garnet websterite II (garnet + clinopyroxene + orthopyroxene, with sometimes olivine, spinel, minor MgO-rich ilmenite and brown amphibole),
3. Garnet clinopyroxenite (garnet + clinopyroxene, minor plagioclase),
4. Spinel-bearing garnet clinopyroxenite (garnet + clinopyroxene + spinel, minor plagioclase),
5. Spinel-bearing garnet websterite (garnet + clinopyroxene + orthopyroxene + spinel).

Only rock types 1-3 are considered in detail in this paper.

Garnet websterites I contain dark-red garnets of variable size and amount. In some of the specimens garnet becomes the predominant constituent, reaching up to 5 mm in diameter. Some of the samples have kelyphite rims around garnets, especially those with high MgO-contents. Exsolution of orthopyroxene from clinopyroxene is a typical feature of this group of garnet websterites. The exsolved orthopyroxene occurs in the form of small spindles, lamellae or grainlets within the clinopyroxene host (Figure 2) or between adjacent clinopyroxene grains. Exsolution of garnet from clinopyroxene, as described by Beeson and Jackson (1970), Green (1966) or Kornprobst et Conquéré (1972), has locally been

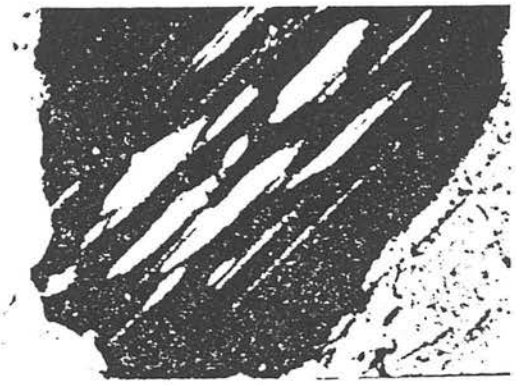

FIG. 2. — *Orthopyroxene exsolution in clinopyroxene. Garnet websterite I.* Crossed nicols, 60×.

Exsolution d'orthopyroxène dans un clinopyroxène. Websterite à grenat I. Polariseurs croisés, × 60.

observed and will be described more fully in a future paper.

Garnet websterites II contain a medium to fine-grained matrix of two pyroxenes. Occasionnally, large clinopyroxene porphyroclasts with or without exsolved orthopyroxene, are situated in the recrystallised matrix. Coarse-grained garnets are irregularily distributed. They are often kelyphitised (Figure 3) or surrounded by brown amphibole. Cr-bearing spinel occurs as a minor constituent in the matrix. In one specimen (850), MgO-rich ilmenite has been found

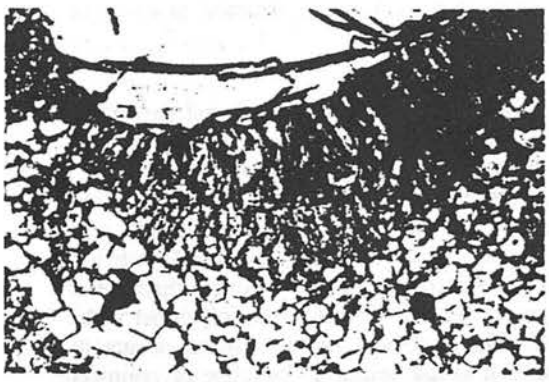

FIG. 3. — *Kelyphitized garnet and two pyroxene mosaic with inserted spinels. Garnet websterite II.* Plane light, 60×.

Mosaïque de grenat kélyphitisé et de deux pyroxènes avec inclusions de spinels. Websterites à grenat II. Lumière naturelle, × 60.

(Scharbert, 1979). MgO-rich samples may also carry forsteritic olivine, with up to 0.5 weight-% NiO.

Garnet clinopyroxenites (Kappel's "eclogites") mainly consists of medium- to coarse-grained garnets and clinopyroxenes. Zones of crushing and undulous extinction in the clinopyroxenes demonstrate some deformational influence. Clinopyroxenes of slightly different composition constitute the recrystallised fine grained mosaic fabric. The garnets are sometimes surrounded by rims of minute plagioclase grains with compositions between An_{33} and An_{71} (Kappel, 1967, p. 272). Anomalous birefringent garnets have also been described by this author. This is the rock type which lead Kappel to reach his final conclusion concerning its Upper Mantle origin and later adjustment to the granulite facies tectonisation.

Whole rock analyses for major and trace elements in selected rock samples are given in tables I and II. Specimens 844, 846 and 1096 are

	Gt-WbI		Gt-WbII	Gt-Cpxite		
	1096	846	844	Me	851	852
SiO_2	46.24	48.45	48.60	46.89	47.47	47.83
TiO_2	0.16	0.13	0.30	0.07	0.12	0.12
Al_2O_3	11.57	11.21	9.22	16.48	12.68	12.87
Cr_2O_3	0.13	0.29	1.31	0.09	0.09	0.11
Fe_2O_3	0.88	0.97	0.43	0.28	1.25	0.62
FeO	7.12	5.12	7.80	4.01	6.34	6.89
MnO	0.20	0.18	0.21	0.18	0.18	
MgO	18.90	20.10	15.94	15.14	14.95	
CaO	13.67	12.21	15.16	14.68	14.55	
Na_2O	0.73	0.84	1.20	1.70	1.62	
K_2O	0.02	0.07	0.10	0.14	0.10	
H_2O	0.16	0.16	0.20	0.21	0.12	
P_2O_5	0.09	0.07	-	0.07	0.05	
total	99.87	99.82	100.63	100.07	100.01	
CIPW-norm :						
q	-	-	-	-	-	-
or	0.1	0.4	-	0.65	0.6	0.8
ab	5.8	7.2	2.0	1.1	14.9	9.2
ne	0.3	-	-	5.6	-	3.0
an	27.4	25.7	22.9	38.2	26.0	26.7
di	34.4	26.0	15.7	28.0	29.2	34.5
hy	-	14.7	33.0	-	6.1	-
ol	34.6	24.5	24.1	26.1	21.6	24.8
mt	0.9	1.0	0.4	0.3	1.3	0.6
il	0.2	0.2	0.4	0.1	0.2	0.2
ap	0.2	0.1	0.1	-	0.1	0.2
cr	0.1	0.3	1.4	-	-	-
100 Mg / Mg + Fe	81.0	85.6	91.6	87.0	77.1	78.2

TABLE I. — *Bulk chemical composition of selected garnet websterites and garnet clinopyroxenites.*

Composition chimique de quelques websterites à grenat et de clinopyroxénites à grenat.

	Gt-Wb I		Gt-Wb II	Gt-Cpxite		
	1096	846	844	Me	851	852
	311	708	1483	270	371	333
	804	1998	8398	600	823	711
	114	84	138	350	143	164
	115	5	139	26	72	132
	50	38	49	60	43	47
	36	42	24	-	34	30
	118	16	22	10	27	18
	60	1	23	-	194	221
	166	23	53	-	102	31
	1	2	1	-	2	5
	-	-	-	-	-	-
	30	4	11	10	27	18
	4.2	-	-	-	-	-
	0.8	-	0.76	-	0.9	-
	0.3	-	0.9	-	1.1	-
	2.65	-	1.09	-	1.95	-
	5.22	-	0.26	-	0.55	-
	1.15	-	0.14	-	0.20	-
	1.57	-	-	-	-	-
	2.51	-	0.80	-	0.75	-
	0.40	-	0.14	-	0.14	-

ABLE II. — *Trace elements contents in selected garnet websterites and garnet clinopyroxenites* (in ppm).

Teneurs en éléments traces de quelques webstérites à grenat et de clinopyroxénites (en ppm).

arnet websterites, with 844 olivine-bearing. pecimens 851, 852 and Me (Meidling im Tal, appel, 1967) are garnet clinopyroxenites. Obious distinctions exist between the two groups : e former have higher MgO contents (espeally the olivine bearing sample) and lower $_2O_3$, CaO and alkali contents. All the rocks ve relatively high Cr and Ni contents (again otably the olivine bearing garnet websterite) d are low in incompatible elements, such as a, Rb and REE. The consistently high normae olivine contents reflect the fact that these cks have an olivine tholeiite to picritic basalt emistry in line with experimental and petrolocal deductions of the likely character of primive upper mantle partial melts (Carswell, 968*a* ; Conquéré, 1971 ; Dickey *et al.*, 1977 ; oubet and Allègre, 1982 ; O'Hara, 1965 ; ray, 1982 ; Stolper, 1980).

MINERAL CHEMISTRY

arnets

In table III, a selection of microprobe analys is summarised. The three groups of rocks are designated as A-C. The analyses are listed according to their increasing FeO content in grain cores, if zoned. The garnets of the websterites I (A) are homogeneous in many specimens. However they are occasionally surrounded by narrow rims of slightly different composition. The pyrope-contents of grain cores always exceed 63 mol.-% ; those of the rims are somewhat lower. Almandine contents are higher in the rims. There is usually no great difference in CaO content, with respect to cores and rims. MnO is higher in the rims. Cr_2O_3 contents of garnets range up just less than 1 wt.%. The garnets of the websterites II (B) are similar in composition. 850 has an almandine-rich rim, whose MnO content is also high. TiO_2 of this garnet reflects the overall enrichment in TiO_2 of this sample, which contains ilmenite and TiO_2-rich pyroxenes. All these phases in sample 850 are also higher in iron.

The wet chemical analyses of the garnets in specimens "Mi" (Mitterbachgraben) and "Me" (Meidling im Tal) by Kappel (1967, p. 282) are shown in table III for comparison with the new microprobe analyses for the garnets of the garnet clinopyroxenites (C). Zoning appears in varying intensities : 851 has a homogeneous central part, 853 has a weak zonation, whereas 852 is homogeneous throughout. The element distribution patterns for CaO, MnO and FeO appear similar with those given by Kurat and Scharbert (1972), Scharbert and Kurat (1974) and Fuchs und Scharbert (1979) for garnets in associated granulite facies rocks. Generally, this latter group of garnets is lower in MgO and Cr_2O_3 and higher in FeO and MnO, than the websterite garnets.

Figure 4 shows the direction of the compositional zonation marked by arrows. The websterite garnets are characterised by differences in FeO and MgO between the homogeneous cores and the narrow rims, whereas the garnets of the clinopyroxenites show major differences in CaO and FeO between cores and rims.

Clinopyroxenes

Clinopyroxenes of different compositional types occur in these rocks. They can roughly be subdivided into two main categories, viz. Cr-diopsides and Al-augites (Wilshire and Shervais, 1975 ; Wass, 1979). The chemical analyses are

A

	1088	820		819		1096	827a
		c	r	c	r		
SiO_2	41.7	41.3	40.5	41.4	40.8	41.8	41.7
TiO_2	0.17	0.19	0.09	0.16	0.09	0.19	0.12
Al_2O_3	23.1	22.1	22.0	22.0	22.1	23.5	23.7
Cr_2O_3	0.35	0.72	0.93	0.34	0.34	0.13	0.07
FeO	6.96	7.3	8.5	8.0	13.1	9.5	9.6
MnO	0.33	0.34	0.35	0.35	0.48	0.33	0.26
MgO	22.0	23.6	21.8	19.5	18.3	21.0	19.1
CaO	4.22	5.3	5.3	8.8	6.8	5.6	5.6
total	98.83	101.85	100.47	100.55	102.01	102.05	99.15
Pyr	75.5	74.8	70.0	63.9	59.4	69.7	66.4
Alm	13.4	13.4	17.1	16.6	23.9	17.6	19.5	
Gros	11.4	11.7	12.4	20.8	16.8	12.1	14.0
Sp	0.7	0.6	0.7	0.7	0.9	0.6	0.6
X_{Mg}	0.857	0.841	0.744	0.777	0.708	0.724	0.713

B

	846		844		850	
	c	r	c	r	c	r
SiO_2	40.9	41.7	41.7	41.6	40.3	39.1
TiO_2	0.11	0.05	0.1	0.1	0.42	0.34
Al_2O_3	23.3	22.5	22.1	22.0	22.4	21.8
Cr_2O_3	0.24	0.24	1.0	0.9	0.39	0.45
FeO	10.0	12.9	6.4	9.6	14.1	19.2
MnO	0.26	0.52	0.2	0.2	0.42	0.87
MgO	21.8	18.7	23.6	20.8	18.1	13.9
CaO	4.51	4.72	5.4	5.4	5.4	5.7
total	100.73	101.12	100.5	100.6	101.53	101.36
Pyr	70.6	62.4	75.7	69.9	59.9	47.5
Alm	16.2	24.9	11.5	17.9	26.2	36.8
Gros	10.5	11.7	12.4	12.8	13.2	14.0
Sp	0.5	1.0	0.4	0.4	0.7	1.7
X_{Mg}	0.743	0.606	0.849	0.741	0.563	0.435

C

	1847		Me	853		346	
	c	r		c	r	c	r
SiO_2	42.1	41.8	41.29	39.9	40.3	40.2	40.2
TiO_2	0.09	0.04	0.06	0.3	0.3	0.3	0.1
Al_2O_3	23.4	23.4	23.72	22.3	22.6	23.5	23.2
Cr_2O_3	0.13	0.13	-	-	-	-	-
FeO	9.47	10.5	9.65	10.3	11.6	10.7	13.4
MnO	0.25	0.26	0.52	0.3	0.3	0.3	0.3
MgO	17.5	17.8	16.3	16.2	15.2	15.9	17.4
CaO	7.36	6.02	8.25	11.4	9.4	9.5	5.7
total	100.30	99.97	99.25	100.7	100.0	100.2	100.3
Pyr	61.9	67.2	57.9	53.4	52.6	55.0	59.6
Alm	19.8	20.9	19.6	19.0	22.5	20.8	25.8
Gros	16.7	15.3	21.4	27.0	24.2	23.6	14.1
Sp	0.5	0.5	1.1	0.6	0.6	0.6	0.6
X_{Mg}	0.697	0.669	0.661	0.645	0.579	0.622	0.568

	Mi	852	851	
			c	r
SiO_2	41.31	40.1	40.6	39.9
TiO_2	0.08	0.07	-	-
Al_2O_3	23.81	23.4	22.4	22.0
Cr_2O_3	-	0.23	0.1	0.1
FeO	10.83	11.6	12.2	14.7
MnO	0.41	0.35	0.4	0.4
MgO	14.71	17.0	16.7	16.3
CaO	8.89	9.43	8.5	6.6
total	100.04	100.18	100.09	100.0
Pyr	53.2	57.3	55.9	55.1
Alm	22.4	22.0	22.8	28.0
Gros	23.6	25.9	22.5	16.1
Sp	0.9	0.7	0.8	0.8
X_{Mg}	0.579	0.617	0.592	0.492

TABLE III. — *Chemical composition of garnets.* A : *garnet websterites I* ; B: *garnet websterites II* ; C : *garnet clinopyroxenites.* Me and Mi are taken from Kappel (1967, p. 282). Analyses are arranged according to increasing FeO contents in the cores. All iron as FeO. c = core, r = rim.

Composition chimique des grenats. A : *websterites à grenat I* ; B : *websterites à grenat II* ; C : *clinopyroxénites à grenat.* Me et Mi d'après Kappel (1967, p. 282). Les analyses sont disposées selon l'augmentation de la teneur en FeO au centre des grenats. Fer total en FeO, c = centre, r = bordure.

summarised in table IV (A-C), in the same order as in table III.

The clinopyroxenes of the garnet websterites I (A) are distinguished by Al_2O_3 contents from 3.4 to 6 wt.% ; Cr_2O_3 is mostly over 0.15 wt.%, reaching up to 0.5 wt.%. TiO_2 is usually low. $100 \times Mg/(Mg + \Sigma Fe)$ ranges from 88.3 to 94.3 ; $100 \times Ca/(Ca + Mg)$ lies between 45.0 and 49.9. Al^{IV} has an average of 0.133 on the basis of 6 oxygens. These clinopyroxenes mostly fall below the 1:1 dividing line in the diagram of Aoki and Shiba (1973), indicating Al^{IV}/Al^{VI} ratios mostly over 1. These Cr-diopsides can therefore be taken as granulite facies type clinopyroxenes.

The composition of the clinopyroxenes of the garnet websterites II (B) is very similar to the former ones. Two generations of clinopyroxenes have been identified in the specimens 844 and 850. 844a represents a clinopyroxene porphyroclast of a presumably older generation, in comparison to 844b, which is the analysis of neoblasts in the matrix. The main differences lie in the higher CaO of the latter and the higher Al_2O_3, Cr_2O_3 and Na_2O of the former. As already mentioned, specimen 850 is rich in FeO and TiO_2, a feature which is also expressed in the clinopyroxenes a and b. In contrast to specimen 844, there are no major differences in this specimen between the different clinopyroxene texture types and it is thought that the matrix pyroxenes (b) may just be mechanically disintegrated, unrecrystallised, large grains (a). Al^{IV}/Al^{VI} reaches 5.41 in 844 and even 7.14 in

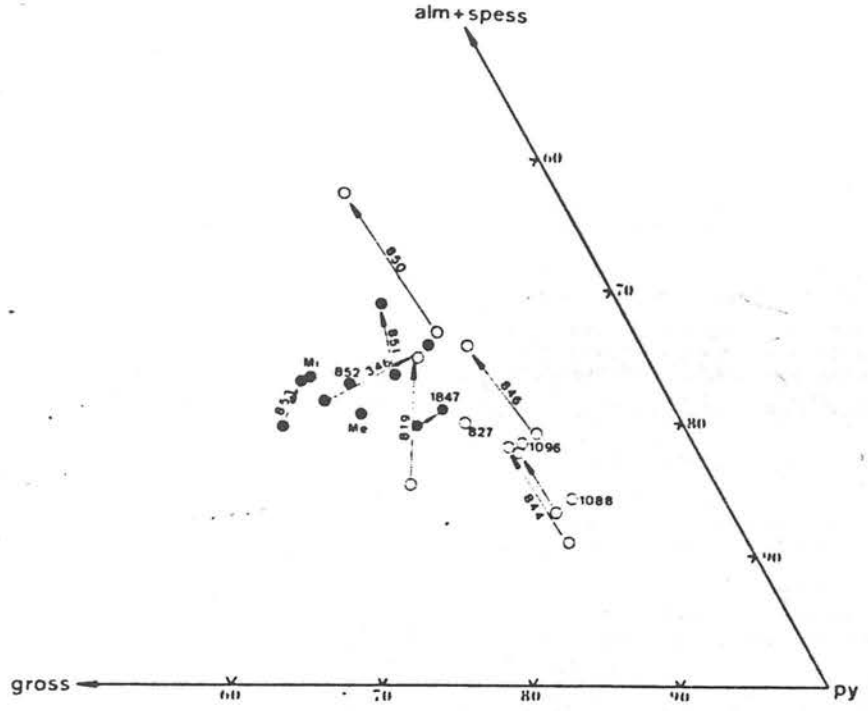

FIG. 4. — *Garnet zoning*. Arrows point to rim compositions. Single signs stand for homogeneous grains. See text for explanation. Open circles : garnet websterites, closed circles : garnet clinopyroxenites.

Zonation du grenat. Les flèches indiquent les compositions des bordures. Les signes simples indiquent les grains homogenes. Voir le texte pour les explications. Cercles ouverts : websterites à grenat ; cercles pleins : clinopyroxenites a grenat.

850b. There is no Al^{VI} in 850a, though this may reflect inaccuracy in the SiO_2 determination for this particular sample.

As already pointed out by Kappel (1967, p. 284), the Meidling im Tal (''Me'') and Mitterbachgraben (''Mi'') clinopyroxenes of the garnet clinopyroxenites (C) are highly aluminous. During the course of the present study, similar clinopyroxenes have been detected in further samples from the Mitterbachgraben area (Figure 1). Al_2O_3 ranges from roughly 7 to 10 wt.%. These clinopyroxenes have lower MgO contents and are higher in Na_2O, compared with the websterite clinopyroxenes. They seem best called Al-augites. Cr_2O_3 and TiO_2 contents are low. Al^{IV}/Al^{VI} is always less than 1. $100 \times Mg/(Mg + \Sigma Fe)$ ranges from 84.0 to 92.9, $100 \times Ca/(Ca + Mg)$ from 46.7 to 53.8.

Column D in table IV represents the analysis of a monomineralic clinopyroxenite. Al_2O_3 is high, Al^{IV}/Al^{VI} is comparable with the group C-clinopyroxenes. $100 \times Ca/(Ca + Mg)$ is low. The mineral is a moderately sub-calcic Al-augite.

The consideration of total Fe as FeO in the calculation of the end members of the garnet websterite clinopyroxenes ignores the possible acmite contents in favour of jadeite. If one reverses the calculation order, then jadeite is lowered and considerable acmite is indicated. Reiteration then enables derivation of stoichiometrically calculated Fe_2O_3 contents (Mysen and Griffin, 1973). However, we have not included these values in table 4 as in most cases too much acmite and insufficient jadeite has been calculated, since end member calculation necessitates converting all the Fe to Fe^{3+} in many of the websterite clinopyroxenes. This may reflect analytical errors (notably in SiO_2) or perhaps these crystals are genuinely non-stoichiometric. We cannot therefore obtain the jadeite/Ca-tschermaks ratios in these clinopyroxenes in a reliable

	A						E
	1088	820	819	1096	827a	846	R44a
SiO_2	51.3	50.2	52.8	52.2	51.7	51.0	50.8
TiO_2	0.12	0.19	0.11	0.27	0.24	0.12	0.06
Al_2O_3	4.52	5.77	4.91	3.45	6.05	5.22	5.31
Cr_2O_3	0.29	0.47	0.28	0.15	0.06	0.16	0.53
Fe_2O_3	*	-	-	-	-	-	-
FeO	2.35	1.97	3.12	2.64	3.92	2.88	2.26
MnO	0.11	0.07	0.11	-	0.04	0.07	0.1
MgO	18.0	18.2	17.2	18.6	16.6	17.0	17.6
CaO	21.6	22.6	19.6	22.6	20.8	23.5	21.6
Na_2O	1.76	0.99	1.17	0.9	1.21	1.18	1.41
K_2O	-	<0.02	0.03	-	-	-	-
total	100.05	100.46	95.33	100.81	100.62	101.13	99.67
Ca	44.5	45.7	42.6	44.7	44.4	47.7	44.8
Mg	51.7	51.2	52.0	51.2	49.1	47.8	51.5
Fe	3.8	3.1	5.4	4.1	6.5	4.5	3.7
$\frac{100 \times Mg}{Mg + \Sigma Fe}$	93.1	94.3	90.6	92.6	88.3	91.4	93.2
$\frac{100 \times Ca}{Ca + Mg}$	46.3	47.1	45.0	46.6	47.5	49.9	46.5
Fe/Mg	0.073	0.06	0.103	0.080	0.132	0.094	0.072
Al^{IV}/Al^{VI}	2.13	2.33	0.65	2.78	1.04	2.17	1.65

	B					D
	853	W1	852	851	857	
SiO_2	50.7	50.49	51.7	52.2	51.2	
TiO_2	0.13	0.14	0.31	0.1	1.04	
Al_2O_3	9.4	9.33	9.4	9.4	7.76	
Cr_2O_3	0.12	-	0.07	0.13	-	
Fe_2O_3	2.04	1.48	-	-	-	
FeO	1.67	3.23	3.6	3.1	5.25	
MnO	0.06	0.1	0.09	0.16	0.13	
MgO	13.6	13.43	12.8	12.6	16.42	
CaO	21.1	19.51	19.1	20.4	15.52	
Na_2O	1.67	1.98	2.12	2.0	1.36	
K_2O	-	0.11	-	-	0.02	
total	100.49	99.80	99.19	100.09	98.70	
Ca	49.4	46.7	48.1	50.6	36.5	
Mg	44.3	44.8	44.9	43.5	53.8	
ΣFe	6.3	8.5	7.0	5.9	9.7	
$\frac{100 \times Mg}{Mg + \Sigma Fe}$	87.5	84.0	86.5	88.1	84.9	
$\frac{100 \times Ca}{Ca + Mg}$	52.7	51.0	51.4	53.8	40.4	
$\Sigma Fe/Mg$	0.142	0.190	0.156	0.136	0.180	
Al^{IV}/Al^{VI}	0.77	0.75	0.44	0.43	0.67	

	C					
	844b	850a	850b	1847	346	Me
SiO_2	51.4	48.9	50.8	52.85	52.6	50.76
TiO_2	0.06	0.62	0.69	0.17	0.04	0.09
Al_2O_3	3.3	4.1	4.0	6.89	9.20	10.01
Cr_2O_3	0.4	0.15	0.17	0.15	0.27	-
Fe_2O_3	-	-	-	-	-	0.89
FeO	2.03	4.2	5.1	2.94	3.1	1.83
MnO	0.08	0.13	0.11	0.10	0.14	0.10
MgO	17.2	16.4	17.5	14.2	14.4	15.97
CaO	24.6	24.6	22.1	20.0	20.1	19.31
Na_2O	1.01	0.75	0.78	2.02	1.58	1.54
K_2O	*	-	0.02	-	-	0.09
total	100.09	99.85	101.25	99.32	101.43	100.27
Ca	49.6	49.2	43.9	47.4	47.4	44.7
Mg	48.1	50.5	48.2	47.1	46.9	51.0
Fe	3.1	7.0	7.9	5.5	5.7	4.3
$\frac{100 \times Mg}{Mg + Fe}$	93.9	87.8	85.9	89.5	89.1	92.2
$\frac{100 \times Ca}{Ca + Mg}$	50.4	49.5	47.6	50.1	50.2	46.7
Fe/Mg	0.064	0.139	0.164	0.117	0.122	0.094
Al^{IV}/Al^{VI}	5.41	-	7.14	0.37	0.53	0.87

TABLE IV. — *Chemical compositions of clinopyroxenes.* A : *garnet websterites I* ; B : *garnet websterites II* ; C : *garnet clinopyroxenites*. Me and Mi are taken from Kappel (1967, p. 284). All iron as FeO in the columns A, B and D. Fe_2O_3 has been stoichiometrically calculated in the C-clinopyroxenes.

Compositions chimiques des clinopyroxènes. A : *websterites à grenat I* ; B : *websterites à grenat II* ; C : *clinopyroxénites à grenat*. Me et Mi d'après Kappel (1967, p. 284). Fer total en FeO dans les colonnes A, B et D. Fe_2O_3 a été calculé stoechiometriquement dans la colonne C - clinopyroxènes.

manner. It can only be said that the generally high Al^{IV}/Al^{VI} values (Table 4A and B) suggest low jadeite/Ca-Ts ratios.

On the other hand, the clinopyroxenes of the garnet clinopyroxenites are rather less of a problem. They yield better stoichiometric end member calculations with little Fe^{3+} indicated. These minerals have consistently low Al^{IV}/Al^{VI} ratios. For comparative purposes Ca:Mg:Fe values are again given with total Fe as FeO.

Orthopyroxenes

This phase only appears in the garnet websterites, viz. as an exsolution feature in type I and as individual grains in type II. The modal content of orthopyroxene in garnet websterites II is always much less than that of clinopyroxene. In table V, orthopyroxene compositions are summarised. In both groups the orthopyroxenes have quite similar compositions. $100 \times Mg/(Mg + \Sigma Fe)$ varies from 81 to 91, lower than in all the coexisting clinopyroxenes. Al_2O_3 is higher or lower than in the clinopyroxenes of the garnet websterites I, but consistently lower in the garnet websterites II. Al^{IV}/Al^{VI} varies unsystematically. The 850 orthopyroxene is again characterised by the highest FeO and TiO_2 in this study.

						B		
	1088	820	819	1096	827a	846	844b	850b
	53,2	53,1	54,0	53,1	55,0	53,7	53,5	53,7
	0,07	-	0,02	0,08	0,04	0,03	0,08	0,17
	5,76	5,4	5,2	5,2	4,8	4,6	4,3	2,87
	0,07	0,27	0,23	0,19	0,06	0,12	0,25	0,11
	6,3	6,8	12,3	7,1	10,1	8,7	7,3	13,0
	0,15	0,13	0,28	0,12	0,09	0,13	0,14	0,11
	35,7	34,9	28,3	34,2	30,3	33,0	33,8	30,8
	0,91	0,47	0,76	0,88	0,38	0,61	0,37	0,54
	<0,02	<0,02	<0,02	<0,02	0,02	-	-	0,03
	100,16	101,07	101,91	100,87	100,79	100,89	99,74	100,92
	1,6	0,9	1,5	1,6	0,9	1,1	0,7	1,1
	89,5	89,4	79,1	88,2	83,4	86,1	88,6	80,0
	8,8	9,7	19,2	10,2	15,7	12,7	10,7	18,9
	91,0	90,2	80,3	89,6	84,2	87,1	89,2	80,9
	0,248	0,108	0,240	0,115	0,188	0,147	0,120	0,236

TABLE V. — *Chemical compositions of orthopyroxenes.* A : *garnet websterites I* ; B : *garnet websterites II*. FeO is total Fe.

Compositions chimiques des orthopyroxènes. A : *websterites à grenat I* ; B : *websterites à grenat II*. FeO : fer total.

	A	B	C
SiO_2	40.14	0.44	-
TiO_2	2,42	-	55.1
Al_2O_3	16.24	61.8	-
Cr_2O_3	0.35	6.14	0.06
FeO	6.60	11.4	39.6
MnO	0.05	-	0.38
MgO	18.00	19.9	5.21
CaO	10.81	-	-
Na_2O	3.42	-	-
K_2O	0.14	-	-
total	98.17	99.68	100.35
Si	5.76	$MgAl_2$	76.1	MgTi	16.7
Mg	0.93	$FeCr_2$	6.3	FeTi	80.4
$(Na+K)_A$	1.03	$FeAl_2$	17.1	MnTi	0.4
Ti	0.26	$FeFe_2$	0.3	Ti	0.1

TABLE VI. — A : *Chemical composition of amphibole* (850) ; B : *spinel* (844) ; C : *ilmenite* (850) *in garnet websterites II.*

A : *composition chimique de l'amphibole* (850) ; B : *spinelle* (844) ; C : *ilménite* (850) *dans les websterites à grenat II.*

Amphibole

Pale to medium brown amphibole with rather weak pleochroism is a constituent of the garnet websterite II 850. It appears only as rims around some of the garnets. It is characterised by high MgO and substantial amounts of TiO_2 and Cr_2O_3 (Table IVA). Following Leake (1978), this amphibole can be classified as *pargasite*.

Spinel

In the rocks of this study, spinel only appears as a scarce secondary phase. The composition of the chromian spinel in the garnet websterite II 844 is given in table 6B. It is situated within the fine-grained clinopyroxene-orthopyroxene fabric joining the radially aggregated kelyphitic rims around pyrope-rich garnets.

Opaque phases occur only in 850 and are MgO-rich ilmenites (cf. Scharbert, 1979).

Plagioclase

This mineral occurs in very restricted amounts as a secondary phase in some of the garnet clinopyroxenites. Individual grains occur preferentially in the neighbourhood of garnet. Their An-content varies from 33 to 71 mol.-% (Kappel, 1967, p. 272), a feature confirmed by the present study.

CONDITIONS OF RECRYSTALLISATION

First of all we should stress that no *primary mineral phases* originating from any high pressure crystallisation of possible basaltic melts can be observed. Therefore, we are for the most part limited to an attempt to deduce the conditions of the recrystallisation of the present assemblages in these rocks, which clearly demonstrate metamorphic textures.

Recently, Carswell and Gibb (1980) emphasised that the mantle-derived garnet lherzolites in Norwegian and Alpine high grade metamorphic gneiss terrains equilibrated *after*, rather than *before*, their tectonic emplacement. By applying new geothermometric methods, they deduced lower recrystallisation temperatures (734-893 °C) than previously thought. The necessary high pressures (> 20 kbar) required to stabilise such assemblages in the lower continental crust were considered to be a consequence of transient subduction (Krogh, 1977 ; Cuthbert *et al.*, 1981).

The idea of a "subfluence" was recently put forward by Behr (1978) in connection with the development of high pressure granulites in Central Europe. In the Bohemian Massif, Behr (1978) recognised eight granulite belts with garnet-bearing ultramafic rocks. These belts delimit major shear zones which extend down to the deeper crust, along which subfluence processes have taken place. These subfluence zones are characterised by nappes, thrust structures, blastomylonitic horizons, etc. By means of access of water, the granulites have been permitted to ascend into the higher crust along these zones.

Rocks of close association in the present context are found in the Moldanubian complex of the Bohemian Massif of NW-Bohemia and have been described by Fiala (1966) and Kopecky and Sattran (1966). Carswell (1974) previously calculated 1 000-1 100 °C and 33-34 kbar for the equilibration conditions of these garnet lherzolites, values which are now considered to be doubtful, if compared with those for the Alpine and Norwegian occurrences (Carswell and Gibb, 1980, p. 21). In the Austrian part of the Moldanubian Zone of the Bohemian Massif, detailed studies of garnet lherzolites have not yet been undertaken. Therefore, we are limited in the calculation of pressure-temperature estimates to only those rocks considered in this paper.

Pyroxene solubility relationships, $K_{Fe-Mg}^{gt\text{-}cpx}$ (i.e. K_D) partitioning, and the generally high Al contents of the pyroxenes seem to point to relatively high temperature/moderate pressure equilibration conditions. Actual P-T values calculated for the Lower Austrian garnet-clinopyroxene samples (Table VII), are, however, very variable, probably in part reflecting disequilibrium between individual mineral analyses used for the calculations.

In particular, P estimates obtained from the Wood (1974) garnet orthopyroxene geobarometer are very variable (some samples even yielded negative values) and use of Herzberg's (1978) equation (3) which considers the Ca-tschermaks contents of clinopyroxenes gives even more inconsistent results. Clearly, certain of the individual P estimates are unrealistically low, but most point to comparatively low pressures, < 15 kbar.

garnet websterites I		$T^{gt\text{-}cpx}$ °C Fe-Mg	ESG	WOOD P kbar	$K_D^{cpx\text{-}opx}$ Fe-Mg	WELLS(1977) T°C	WOOD P kbar
1068		2.42	1001	18.4	0.744	766	8.2
827	core	2.80	916	10.0	0.555	867	8.1
	rim	4.03	776	4.5			8.0
819	core	2.26	1151	13.3	0.426	1077	11.1
	rim	3.95	815	5.9			13.1
1096		3.19	980	8.4	0.696	897	5.1
827a		2.25	1074	15.8	0.702	977	12.0
445	core	3.71	842	10.7	0.639	920(?)	(-4.1?)
	rim	4.21	756	5.0			
garnet websterites II							
444	core	3.1*	907	14.8	0.61(**)	855	9.8
	rim	3.69	816	6.7			9.6
446	core	3.47	863	12.8	0.670	920	15.7
	rim	3.74	797	7.9		907	14.2
mean values	cores	3.45	866	14.0	0.705	907	10.8
	rims	4.10	787	6.9			

*) cpx porphyroclasts involved in calculation

**) pyroxene pairs in garnet contained

***) All garnet websterite samples; unspecified analyses also taken to correspond to grain cores.

garnet clinopyroxenites (10 kbs assumed)		$K_D^{gt\text{-}cpx}$ Fe-Mg	ELLIS & GREEN T°C	WELLS (1979) T°C
1047	core	2.57	1034	1048
	rim	2.87	942	995
346	core	3.13	999	964
	rim	3.58	952	925
Re		4.06	878	891
857	core	2.47	1145	1063
	rim	2.87	1027	989
[illegible]		2.17	1169	1121
852		2.42	1086	1071
851	core	2.87	989	995
	rim	3.67	863	914
mean values	*) cores	2.82	1042	1019
	rims	3.28	921	956

*) unspecified analyses also taken to correspond to grain cores.

TABLE VII. — *Temperature-pressure estimates on garnet websterites I and II and on garnet clinopyroxenites*. For the latter, a pressure of 10 kbar was assumed for the calculation.

Estimations de la température et de la pression pour les webstérites à grenat I et II et pour les clinopyroxénites à grenat. Pour ces dernières, une pression de 10 kbar a été adoptée pour le calcul.

Best temperature estimations are considered to be those based on the calibrations given by Ellis and Green (1979) and Wells (1977, 1979). In table VII, the results of these calculations are summarised, together with P results according to

Wood (1974), for the garnet websterites I and II. For the garnet clinopyroxenites, lacking orthopyroxene, pressures of 10 kbar have been assumed for calculation of the Ellis and Green (1979) and Wells (1979) temperatures.

The majority of the Wells (1977) two pyroxene solvus temperatures are in the 850-950 °C range and are probably meaningful. The mean value of the Wells/Wood pairings are 907 °C and 10.8 kbar.

Fe-Mg partitioning between garnet and clinopyroxene is strongly temperature dependent (Raheim and Green, 1974 ; Ellis and Green, 1979) and it is clear from table VII that the K_D values increase from cores to rims reflecting consistently higher Fe/Mg ratios in garnet rims compared to cores. This zoning sense is clearly retrograde, i.e. reflects decreasing temperatures. For the garnet clinopyroxenites, with an assumed pressure of 10 kbar, the mean temperature for grain core pairs is 1 042 °C according to Ellis and Green (1979) and 1 016 °C according to Wells (1979). The lower temperature values for the calculations involving garnet rims are 921 °C and 956 °C respectively For garnet websterites I and II, taken together, the combination of the Ellis and Green (1979) K_D thermometer and the Wood (1974) barometer yields mean values for grain cores of 988 °C and 14.0 kbar and for grain rims of 787 °C and 5.9 kbar.

The zoning pattern, if any, is the same in all three lithological groups, and this is combined with the broadly similar calculated equilibration temperatures. This strongly suggests, that all three groups of rocks considered in this paper have had a similar metamorphic evolutionary history.

The K_D values listed in table VII have been calculated on the assumption that all Fe in both garnets and clinopyroxenes is present as Fe^{2+} (cf. tables 3 and 4). Stoichiometric considerations indicate that this is unlikely, especially in the clinopyroxenes, which in all probability have higher $Fe^{3+}/(Fe^{3+} + Fe^{2+})$ ratios than the co-existing garnets. Hence it is likely that these K_D values are in fact *minimum* values and that accordingly, the derived temperatures are *maximum* estimates.

With this in mind, it seems reasonable to conclude that the garnet-clinopyroxene grain rim assemblages in the rocks considered in this paper may well have equilibrated under the same P-T conditions as those indicated by the minimum values of P = 11 kbar and T = 760 °C, previously deduced by Scharbert and Kurat (1974) and recently endorsed by Newton (written communication, 1982 ; T > 770 °C, P > 9.4 kbar) for the dominant granulite facies rocks of the Moldanubian Zone of the Bohemian massif.

The K_D zoning profiles and the pyroxene exsolution textures clearly indicate that these garnet-clinopyroxene rocks have cooled from an earlier temperature maximum. This begs further questions such as whether these earlier high temperatures reflect original igneous crystallisation temperatures of these rocks on intrusion into a lower crustal granulite complex or into upper mantle peridotitic rocks, or simply reflect previously higher ambient P-T conditions affecting these rocks either in the lower crust or in the upper mantle prior to tectonic emplacement. Full answers to such questions must await further studies of the structural, geochemical and geochronological relationships between the garnet-clinopyroxene rocks, the garnetiferous peridotites and the encompassing granulite facies rocks (including the garnet pyriclasites) and a comparison of the P-T evolutionary paths followed by these various rocks.

In the meantime, if one considers the process of unmixing of the pyroxenes and the crystallisation of the garnet rims as one common stage in the metamorphic history of the garnet-clinopyroxene rocks then it is worth considering whether it might be permissible to combine the garnet cores and theoretical 'reconstituted' clinopyroxenes to characterise an earlier stage in that history. Table VIII gives the theoretical values of such clinopyroxenes calculated from the clinopyroxene and orthopyroxene analyses in samples of garnet websterites I. They have been recalculated on the basis of a ratio of clinopyroxene:orthopyroxene of 5:1 and the pyroxene relationships are presented graphically in the pyroxene quadrilateral (Figure 5).

The mean K_D value of 2.21 for the garnet core-'reconstituted' clinopyroxene assemblages yields a temperature value of 1 129 °C (at an assumed pressure of 20 kbar) using the Ellis and Green (1979) calibration. This is 140 °C higher than the mean temperature estimate for the present garnet and clinopyroxene grain core assem-

	1088	820	819	1096	827a	846
SiO_2	51,6	52,3	53,0	52,2	52,4	51,5
TiO_2	0,11	0,16	0,1	0,24	0,21	0,2
Al_2O_3	4,4	4,0	5,0	3,7	5,8	5,1
Cr_2O_3	0,09	0,44	0,28	0,16	0,06	0,15
FeO	3,2	3,51	4,7	3,38	5,0	3,9
MnO	0,12	0,08	0,11	0,04	0,05	0,08
MgO	20,4	20,6	17,4	21,2	18,9	19,7
CaO	18,6	19,4	17,4	19,0	17,4	19,7
Na_2O	0,65	0,66	1,0	0,75	1,0	0,63
Ca	37,6	38,3	37,2	37,2	36,5	39,3
Mg	57,3	56,3	54,4	57,7	55,3	54,6
Fe	5,1	5,4	8,2	5,1	8,2	6,1
$\frac{100 \times Ca}{Ca + Mg}$	39,6	40,4	41,6	39,2	39,8	41,8

TABLE VIII. — *Theoretical composition of "reconstituted" clinopyroxenes.*

Composition théorique de clinopyroxènes "reconstitués".

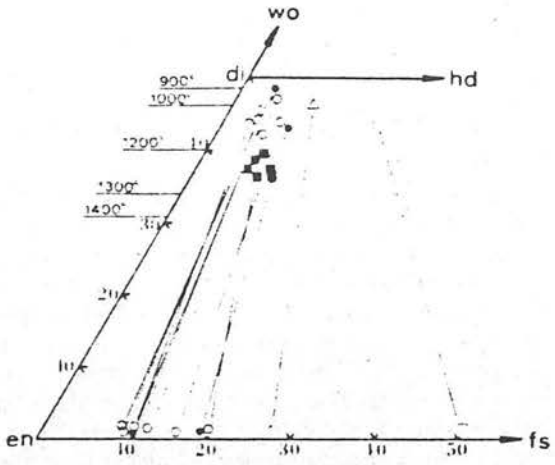

FIG. 5. — *Pyroxene quadrilateral.* Open circles : Garnet websterites I ; closed circles : garnet websterites II ; triangles : pyriclasite (unpubl.) ; open square : acid pyroxene granulite ; closed squares : "reconstituted" clinopyroxenes ; large open circle (partly overlapped) : clinopyroxene (whole rock) plot of 857.

Quadrilatère des pyroxènes. Cercles ouverts : websterites à grenat I ; cercles pleins : websterites à grenat II ; triangles : pyriclasites (non publiées) ; carré ouvert : granulite acide à pyroxène ; carrés fermés : clinopyroxènes "reconstitués" ; grand cercle ouvert (partiellement recouvert) : clinopyroxène (roche totale) position de 857.

blages in these garnet websterites. However, there is no certainty that the 'reconstituted' clinopyroxene compositions are valid and hence that the deduced temperature estimates are meaningful, especially as there is no proof that such higher temperature clinopyroxenes in fact coexisted with garnet. Moreover, the occasional petrographic evidence of garnet exsolution from clinopyroxene in these rocks and the experimental evidence (Dempsey and Scharbert, 1981) that at pressures of 20-30 kbar and temperatures of 1 300-1 500 °C melts of these garnet-clinopyroxene rocks may have crystallised entirely to highly aluminous pyroxenes, suggest that the higher temperature clinopyroxenes would have been significantly more aluminous than indicated in table VIII. A further indication that the early higher temperature clinopyroxenes may not have coexisted with garnet is provided by the clinopyroxenite sample 857 (Table IV.D) which lacks garnet and contains an apparently relict higher temperature sub-calcic clinopyroxene whose composition overlaps that of the 'reconstituted' clinopyroxenes in figure 5.

On current mineralogical evidence, we clearly cannot determine with any degree of certainty just at what temperatures and pressures (and hence depths) the 'primary' assemblages of the garnet-clinopyroxene rocks originally crystallised. However, in view of their chemical character and their distinctive field association with magnesian peridotite bodies, we favour the view that these rocks may well represent the trapped products of primitive basaltic partial melts which initially crystallised at high pressures and temperatures within the uppermost mantle but were subsequently extensively recrystallised during their tectonic intercalation into the lower continental crust.

ACKNOWLEDGMENTS

The authors are indebted to the Cultural Division of the Lower Austrian provincial government, Vienna, for financial support during the fieldwork (Proj. III/2-WF-64/4). Furthermore H.G.S. thanks the 'Fonds zur Förderung der wissenschaftlichen Forschung' for the provision of an electron microprobe ARI-SEMQ (Proj. 1939). W. Richter and F. Koller undertook critical reading of the earlier drafts. The rock analy-

ses were done during a stay in the Geological Department of Manchester University by the first author. REE, U, Th, Hf were analysed by W. Kiesl (University of Vienna).

REFERENCES

AOKI, K.-I. and SHIBA, T. (1973). — Pyroxenes from lherzolite inclusions of Itinomegata, Japan. *Lithos, 6*, 41-51.

ARNOLD, A. und SCHARBERT, H.G. (1973). — Rb-Sr-Altersbestimmungen an Granulites der südlichen Böhmischen Masse in Österreich. - Schweizer. *Mineral. Petr. Mitt., 53*, 61-78.

BECKE, F., HIMMELBAUER, A., REINHOLD, F. und GÖRGEY, R. (1914). — Das niederösterreichische Waldviertel. *Tschermaks Mineral. Petr. Mitt., 32*, 185-217.

BEESON, M.H. and JACKSON, E.D. (1970). — Origin of the garnet pyroxenite xenoliths at Salt Lake Crater, Oahu. *Spec. Pap. Mineral. Soc. Amer., 3*, 95-112.

BEHR, H.-J. (1978). — Subfluenzprozesse im Grundgebirgsstockwerk Mitteleuropas. *Z. dt. Geol. Ges., 129*, 283-318.

CARSWELL, D.A. (1968*a*). — Picritic magma-residual dunite relationships in garnet peridotite at Kalskaret, Tafjord, South Norway. *Contr. Mineral. Petr., 19*, 97-124.

CARSWELL, D.A. (1968*b*). — Possible primary upper mantle peridotite in Norwegian basal gneisses. *Lithos, 1*, 322-355.

CARSWELL, D.A. (1973). — Garnet pyroxenite lens within Ugelvik layered garnet peridotite. *Earth Planet Sci. Lett., 20*, 347-352.

CARSWELL, D.A. (1974). — Comparative equilibration temperatures and pressures of garnet lherzolites in Norwegian gneisses and in kimberlites. *Lithos, 7*, 113-121.

CARSWELL, D.A. and GIBB, F.G.F. (1980). — The equilibration conditions and petrogenesis of European crustal garnet lherzolites. *Lithos, 13*, 19-29.

CONQUERÉ, F. (1971). — Les pyroxénolites à amphibole et les amphibolites associées aux lherzolites du gisement de Lherz (Ariege, France) : un exemple du rôle de l'eau au cours de la cristallisation fractionnée des liquides issus de la fusion partielle de lherzolites. *Contrib. Mineral. Petr., 33*, 32-61.

CUTHBERT, S.J., CARSWELL, D.A. and HARVEY, M.A. (1981). — A plate tectonic model for the metamorphic evolution of the basal gneiss complex of Western South Norway - a working hypothesis. *Terra cognita, 1*, 41-42.

DEMPSEY, M.J. and SCHARBERT, H.G. (1981). — Phase relations in Moldanubian garnet pyroxenites (Bohemian Massif of Lower Austria) : an experimental study. Progr. in Exp. Petr., 5th rep., NERC, D/18, 70-73.

DICKEY, J.S. (1970). — Partial fusion products in alpine-type peridotites : Serrania de la Ronda and other examples. *Spec. Pap. Min. Soc. Amer., 3*, 33-49.

DICKEY, J.S., OBATA, M. and SUN, C.J. (1977). — Partial fusion versus fractional crystallization : hypotheses for the differentiation of the Ronda ultramafic massif of southern Spain. Oregon Dept. *Geol. Min. Indust. Bull., 96*, 79-89.

ELLIS, D.J. and GREEN, D.H. (1979). — An experimental study of the effect of Ca upon garnet-clinopyroxene Fe-Mg exchange equilibria. *Contr. Mineral. Petr., 71*, 13-22.

ERNST, G.W. (1978). — Petrochemical study of lherzolite rocks from the Western Alps. *J. Petrol., 19*, 341-392.

FIALA, J. (1966). — The distribution of elements in mineral phases of some garnet lherzolites from the Bohemian Massif. *Krystallinikum, 4*, 31-53.

FUCHS, G. (1971). — Zur Tektonik des östlichen Waldviertels. *Verh. geol. B.A.*, Vienna, 424-440.

FUCHS, G. und SCHARBERT, H.G. (1979). — Kleinere Granulitvorkommen im niederösterreichischen Moldanubikum und ihre Bedeutung für die Granulitgenese. *Verh. geol. B.A.*, Vienna, 29-49.

GREEN, D.H. (1966). — The origin of the "eclogites" from Salt Lake Crater, Hawaii. *Earth Planet. Sci. Lett., 1*, 414-420.

HERZBERG, C.T. (1978). — Pyroxene geothermometry and geobarometry : experimental and thermodynamic evolution of some subsolidus phase relations involving pyroxenes in the system CaO-MgO-Al_2O_3-SiO_2. *Geochim. Cosmo. Acta, 42*, 945-957.

KAPPEL, F. (1967). — Die Eklogite Meidling im Tal und Mitterbachgraben im niederösterreichischen Moldanubikum südlich der Donau. *N. Jb. Min. Abh., 107*, 266-298.

KOHLER, A. (1941). — Die moldanubischen Gesteine des Waldviertels und seiner Randgebiete. *Fschr. Mineral., 25*, 253-316.

KOPECKY, L. and SATTRAN, V. (1966). — Buried occurrences of pyrope-peridotites and the structures of the crystalline basement in the extreme southwest of the 'Ceské stredohori' mountains. *Krystallinikum, 4*, 65-86.

KORNPROBST, J. (1969). — Le massif ultrabasique des Beni Bouchera (Rif Interne, Maroc) : Etude des péridotites de haute température et de haute pression, et des pyroxénolites à grenat qui leur sont associées. *Contr. Mineral. Petr., 23*, 283-322.

KORNPROBST, J. et CONQUÉRÉ, F. (1972). — Les pyroxénolites à grenat du massif de lherzolites de Moncaup (Haute-Garonne, France) : caractères communs avec certaines enclaves des basaltes alcalins. *Earth Planet Sci. Lett., 16*, 1-14.

KROGH, E.J. (1977). — Evidence of precambrian continent-continent collision in Western Norway. *Nature, 267*, 17-19.

KURAT, G. and SCHARBERT, H.G. (1972). — Compositional zoning in garnets from granulite facies rocks of the Moldanubian Zone, Bohemian Massif of Lower Austria, Austria. *Earth Planet. Sci. Lett., 16*, 379-387.

LEAKE, B.E. (1978). — Nomenclature of amphiboles. *Mineral. Mag., 42*, 533-563.

LOUBET, M. and ALLÈGRE, C.J. (1982). — Trace elements in orogenic lherzolites reveal the complex history of the upper mantle. *Nature, 298*, 809-814.

MATURA, A. (1974). — Bericht 1973 über Aufnahmen auf den Blättern Mautern (37) und Krems (38). *Verh. geol. B.A.*, Vienna, A79.

MEDARIS, L.G. Jr. (1980). — Petrogenesis of the Lien peridotite and associated eclogites, Almklovdalen, western Norway. *Lithos, 13*, 339-353.

MYSEN, B.O. and GRIFFIN, W.L. (1973). — Pyroxene stoichiometry and the breakdown of omphacite. *Amer. Mineral., 58*, 60-63.

OBATA, M. (1980). — The Ronda peridotite : garnet-, spinel- and plagioclase lherzolite facies and the P-T-trajectories of a high-temperature mantle intrusion. *J. Petrol., 21*, 533-572.

O'HARA, M.J. (1965). — Primary magmas and the origin of basalts. *Scott. J. Geol., 1*, 19-40.

O'HARA, M.J. and MERCY, E.L.F. (1963). — Petrology and petrogenesis of some garnetiferous peridotites. *Trans Roy. Soc. Edinburgh, 65*, 251-314.

RAHEIM, A. and GREEN, D.H. (1974). — Experimental determination of the temperature and pressure dependence of the Fe-Mg partition coefficient for coexisting clinopyroxene and garnet. *Contr. Mineral. Petr., 48*, 179-203.

ROST, F. und GRIGEL, W. (1969). — Zur Geochemie und Genese granatführender Ultramafitite des mitteleuropäischen Grundgebirges. *Chemie der Erde, 28*, 91-177.

SCHARBERT, H.G. (1963). — Zur Nomenklatur der Gesteine in Granulitfazies. *Tschermaks Mineral. Petr. Mitt., 8*, 591-598.

SCHARBERT, H.G. (1973). — Pyrope-rich garnet from Moldanubian garnet pyroxenites, Bohemian Massif of Lower Austria, Austria. *N. Jb. Min. Mh.*, 89-93.

SCHARBERT, H.G. (1979). — Mg-reicher Ilmenit in einem Granat-Websterit im Granulitkorpet von St. Leohard, Mittleres Kamptal, Niederösterreich. Anz. Akad. Wiss., Vienna, *Math.-Natw. Kl.*, 161-165.

SCHARBERT, H.G. and KURAT, G. (1974). — Distribution of some elements between coexisting ferromagnesian minerals in Moldanubian granulite facies rocks, Lower Austria, Austria. *Tschermaks Mineral. Petr. Mitt., 21*, 110-134.

SCHARBERT, H.G., KORKISCH, J. and STEFFAN, I. (1976). — U, Th and K in granulite facies rocks, Bohemian Massif of Lower Austria, Austria. *Tschermaks Mineral. Petr. Mitt., 23*, 223-232.

SPRAY, J.G. (1982). — Mafic segregations in ophiolite mantle sequences. *Nature, 287*, 366-368.

STOLPER, E. (1980). — A phase diagram for mid-ocean ridge basalts : preliminary results and implications for petrogenesis. *Contr. Mineral. Petr., 74*, 13-27.

TERTSCH, H. (1921). — Studien am Westende des Dunkelsteiner Granulitmassives. *Tschermaks Mineral. Petr. Mitt., 35*, 177-214.

WASS, S.Y. (1979). — Multiple origin of clinopyroxenes in alkali basaltic rocks. *Lithos, 12*, 115-132.

WELLS, P.R.A. (1977). — Pyroxene thermometry in simple and complex systems. *Contr. Mineral. Petr., 62*, 129-139.

WELLS, P.R.A. (1979). — Chemical and thermal evolution of sialic crust, southern West Greenland. *J. Petrol., 20*, 187-226.

WILSHIRE, H.G. and SHERVAIS, J.W. (1975). — Al-augite and Cr-diopside ultramafic xenoliths in basaltic rocks from the western United States. *Phys. Chem. Earth, 9*, 257-272.

WOOD, B.J. (1974). — The solubility of alumina in orthopyroxene coexisting with garnet. *Contr. Mineral. Petr., 46*, 1-15.

Eclogite facies metamorphism in the lower continental crust

D.A. Carswell & S.J. Cuthbert

SUMMARY: Occurrences of medium-temperature eclogite-facies assemblages in the Norwegian Caledonides, Western Alps and Central European Variscides are reviewed with reference to a generalized tectono-thermal model for their stabilization in continental plate collision zones involving A-type subduction. It is demonstrated that the respective pressure-temperature-time paths for lower continental crust and uppermost mantle during such orogenesis contrast with that for upper crust, and that mineralogical features, such as chemical zoning in garnets, may monitor the tectonic location and thermal evolution of different crustal levels in the resultant thrust-nappe stack. Phanerozoic orogenic belts of this type typically show evidence of the generation of early eclogite-facies assemblages subjected to partial greenschist- or amphibolite-facies overprint some 40–60 Ma later. The survival and ultimate surface exposure of the high-pressure assemblages requires that their exhumation is rapid (mean uplift rate around 1 mm year) relative to the rate of thermal relaxation in the tectonically thickened continental crust.

Introduction

The minimum lithostatic pressures required for the stability of eclogite-facies rocks (Fig. 1) are best experimentally defined for quartz-normative metabasaltic rocks, with the plagioclase free essentially bimineralic assemblages of pyralspite garnet + omphacitic clinopyroxene diagnostic of eclogites (*sensu stricto*), and for garnetiferous meta-peridotites. Whilst a detailed discussion of the definition of this metamorphic facies is perhaps not appropriate here, it is pertinent to note that in some felsic rocks albitic plagioclase may still be stable relative to jadeite + quartz (Fig. 1) under eclogite-facies P_{LOAD}-T conditions where omphacitic pyroxene and grossular bearing garnet are stable relative to plagioclase in metabasaltic rocks. Accordingly mineral assemblages of quartz + K feldspar + plagioclase + garnet + orthopyroxene ± clinopyroxene ± kyanite in quartzo-feldspathic gneisses customarily designated as high-P granulites may in fact be cofacial with eclogites, as also may be garnet + phengite + quartz ± kyanite ± zoisite in metapelites and jadeite + garnet + zoisite + K feldspar + quartz in metagranitoids (Compagnoni 1977; Heinrich 1982).

Eclogites are known to have formed in a variety of geological environments, which are reflected in their varying modes of occurrence and mineral chemistry (Eskola 1921; Coleman *et al.* 1965; Smulikowski 1960, 1964, 1968; and Banno 1970). In this contribution we are primarily concerned with those found as layers or lenses in terrains of dominant amphibolite- or granulite-facies continental crust (broadly forming 'Group B' of Coleman *et al.* 1965, and the 'Common Eclogites' of Smulikowski 1968). Mineral thermometers such as that based on $K^{Gnt\text{-}Cpx}_{Fe^{2+}-Mg^{2+}}$ partition coefficients, indicate that these eclogites have generally equilibrated at temperatures between 500–900 °C (e.g. Carswell *et al.* 1985; Griffin *et al.* 1985) higher than those deduced for eclogites in blueschist-facies terrains (e.g. Brown & Bradshaw 1979) and lower than those for mantle derived xenoliths in alkalic eruptive rocks (e.g. Carswell *et al.* 1981). We consider it appropriate to refer to such rocks as 'medium-T eclogites'.

If Ringwood's (1975) linear (dP/dT = 20 bar/°C) extrapolation of the high-T experimental reaction boundary for plagioclase elimination in a quartz tholeiite composition (Fig. 1) is valid, then eclogite should be stable towards the base of continental crust of average 35 km thickness at temperatures less than about 600 °C. Such lower crustal thermal conditions are to be expected in stable continental regions with observed surface heat flows $< 65\ mW\ m^{-2}$ (Chapman, this volume). On the other hand, petrological studies of exposed lower crust gneiss terrains and of lower crustal derived xenolith suites, as well as deep seismic investigations, are generally taken to indicate (as exemplified by several other papers in this volume) that granulite-facies assemblages are dominant in the lower continental crust. In tectonically inactive regions, such lower crustal granulites, most likely to have formed in response to an enhanced thermal flux during some previous tectono-thermal event, may customarily be preserved metastably under P_{LOAD}-T conditions corresponding to the eclogite facies. During establishment of the expected ambient thermal conditions, transformation of lower continental crust rocks to eclogite-facies assemblages along a cooling path under stress-free conditions may well be effectively blocked for kinetic reasons.

From: Dawson, J.B., Carswell, D.A., Hall, J. & Wedepohl, K.H. (eds) 1986, *The Nature of the Lower Continental Crust*, Geological Society Special Publication No. 24, pp. 193–209.

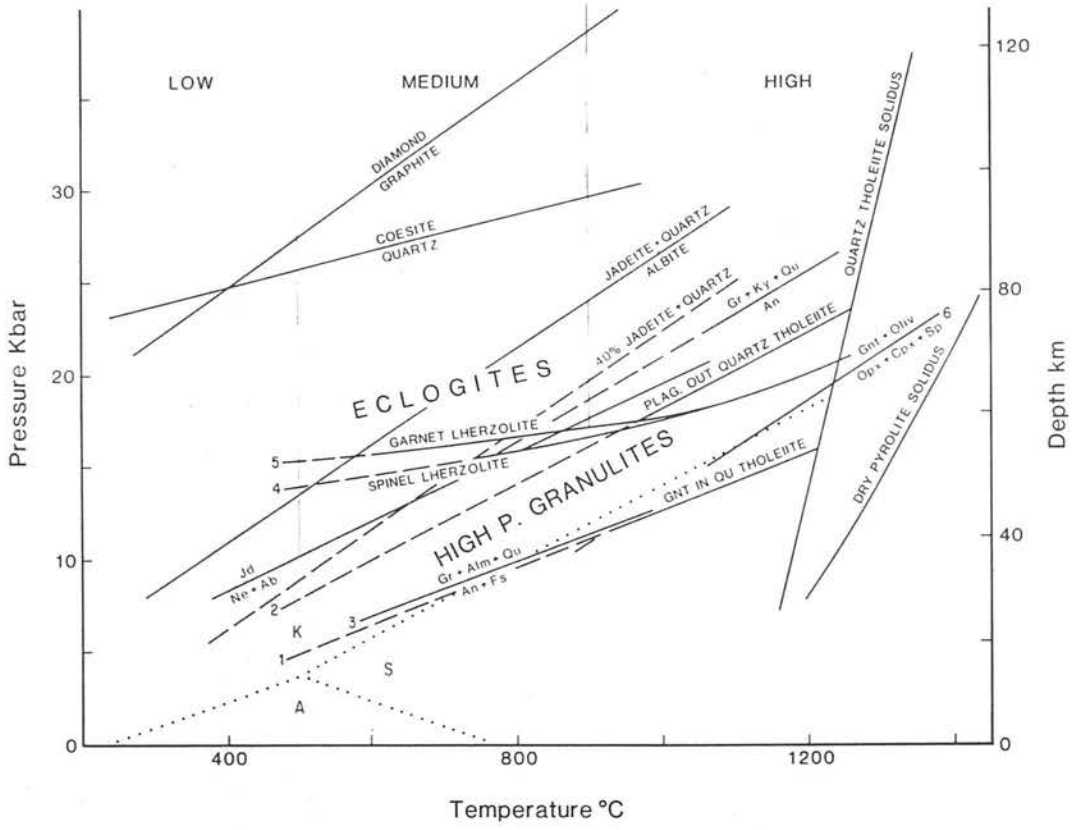

FIG 1. Pressure (depth)-temperature diagram showing the stability fields for low, medium and high temperature eclogite-facies assemblages relative to the following experimentally determined reaction equilibria: Garnet-in (1) and plagioclase-out (2) reaction curves and extrapolations in quartz tholeiite compositions (Green & Ringwood 1967a; Ringwood 1975). Calculated reaction curve (3) for 3 anorthite + 3 ferrosilite = grossular + 2 almandine + 3 quartz from Bohlen *et al.* (1983); 3 anorthite = grossular + 2 kyanite + quartz: Goldsmith (1980); albite = jadeite + quartz: Holland (1980). Estimated stability curve for 40% jadeite + quartz: Kushiro (1969); nepheline + albite = 2 jadeite: Robertson *et al.* (1957). Univariant reaction curve (4) for spinel lherzolite ⇌ garnet lherzolite reaction in natural garnet peridotite composition: O'Hara (1975). Curve (5) for the same reaction in more magnesian compositions: O'Hara *et al.* (1971). Reaction curve (6) for pyroxenes + spinel = garnet + olivine in the CMAS system: MacGregor (1970). Quartz ⇌ coesite: Mirwald & Massonne (1980); graphite ⇌ diamond: Berman (1979). Stability fields for alumino-silicates (K-Kyanite; S-sillimanite; A-andalusite: Holdaway (1971). Solidus for quartz tholeiite composition (Green & Ringwood 1967a). Dry pyrolite (periodotite) solidus (Green & Ringwood, 1967b). The low pressure boundary conditions for the eclogite-facies are best defined by the reaction curves for spinel lherzolite ⇌ garnet lherzolite and for plagioclase disappearance in quartz tholeiite basalt compositions.

Current exposure of medium-T eclogites within continental crust bears witness to special tectonic processes responsible both for their stabilization and their survival during transport to the surface. In this review we highlight certain features common to occurrences of medium-T eclogites and cofacial rocks in the Norwegian Caledonides, the western Alps and the Central European Variscides. We attempt to deduce their formation within the framework of a generalized model for the tectono-thermal behaviour of continental collision zones.

A tectono-thermal model for eclogite formation in continental crust

Here we examine the general thermal and metamorphic consequences of crustal thickening in a collision zone involving two continental lithospheric plates. A simplistic model showing underthrusting (A-type subduction; Hodges *et al.* 1982) of one continental plate beneath the other and detachment around the Moho in the overthrust plate is illustrated in Fig. 2. In reality an intensely imbricated thrust-nappe stack is likely to evolve in response to prolonged crustal shortening (compression) but the contrasted thermal effects and resultant metamorphic responses in the lower and upper plates can be expected to persist. In the upper plate overthrusting (nappe translation) will bring deep level warmer rocks over cooler rocks, whereas in the lower plate progressive underthrusting (with thrusts stepping down with time) will place original high level colder rocks beneath warmer rocks. The main thermal contrast is still, however, likely to be across the principal plate suture.

Tectonic processes can be expected to operate rapidly compared with the rate at which thermal surfaces re-equilibrate by thermal conduction after disturbance, as emphasized by thermal model calculations (Oxburgh & Turcotte 1974; England & Thompson 1984). Thus the perturbed P–T (depth) profile (Fig. 2 c–d) resulting from the tectonic thickening of continental crust will only gradually decay over a time scale of at least some tens of millions of years. The actual P-T-t (time) paths followed by the rocks will in fact depend on the balance between the rates of resultant thermal relaxation and of surface erosion (exhumation). Whilst the metamorphic temperatures (T_{max}) attained are likely to be largely governed by thermal relaxation towards a steady state geotherm for thickened crust, the maximum pressures recorded by the rocks will be critically dependent upon the erosion rate (England & Thompson 1984).

The predicted forms of the P-T-t paths for original cool upper crustal rocks in the upper part of the underthrust plate and for warmer lower crustal rocks sited in the lower part of the overthrust plate are illustrated in Figs 2e and 2f, respectively. In the former case, the rocks may be expected to enter the eclogite-facies stability field along a prograde (heating) path, whilst in the second case eclogite-facies assemblages may be stabilized along a cooling path. Similarly, any cool oceanic crustal rocks (ophiolites) caught up in the suture zone may be expected to follow a prograde metamorphic path subsequent to collision, whereas any tectonically intercalated subcontinental upper mantle rocks would follow cooling paths. This may help to discriminate between the suggested alternative origins of metaperidotite bodies in such orogenic belts. Contrasted P-T-t paths for the metamorphic evolution of three possible eclogite-facies samples generated in a continental plate collision zone are illustrated in Fig. 3, with reference to a time sequence (a–e) of lithospheric cross-sections.

We now proceed to review the tectonic setting and interpretation of various European occurrences of medium-T eclogites in the light of this generalized model. In particular we examine evidence which might indicate that different rocks have indeed generated their eclogite-facies assemblages along contrasted P-T-t paths, depending on their pre- and post-collision locations in an evolving plate collision zone. In this connection, a consideration of chemical zoning profiles in minerals, notably garnets, is especially important (Spear *et al.* 1984).

High-P metamorphism in the Western Gneiss region, Norwegian Caledonides

Medium-T eclogites occur sporadically over a substantial tract of the Scandinavian Caledonides (see Fig. 1 in Bryhni *et al.* 1977) but are particularly in evidence in the Western (also called Basal) Gneiss Region of southern Norway. Here metabasic eclogite lenses are widely preserved within dominantly amphibolite-facies quartzo-feldspathic gneisses whilst cofacial garnet lherzolite and garnet websterite assemblages and more rarely also eclogites (*sensu stricto*) occur within 'alpine type' peridotite bodies. This region represents a deeply eroded core zone of the Scandinavian Caledonides which structurally underlies a thick pile of Caledonian nappes which now outcrop mostly to the east and south (see, for example, Roberts *et al.* 1981, and Figs. 1 & 2 in Cuthbert *et al.* 1983).

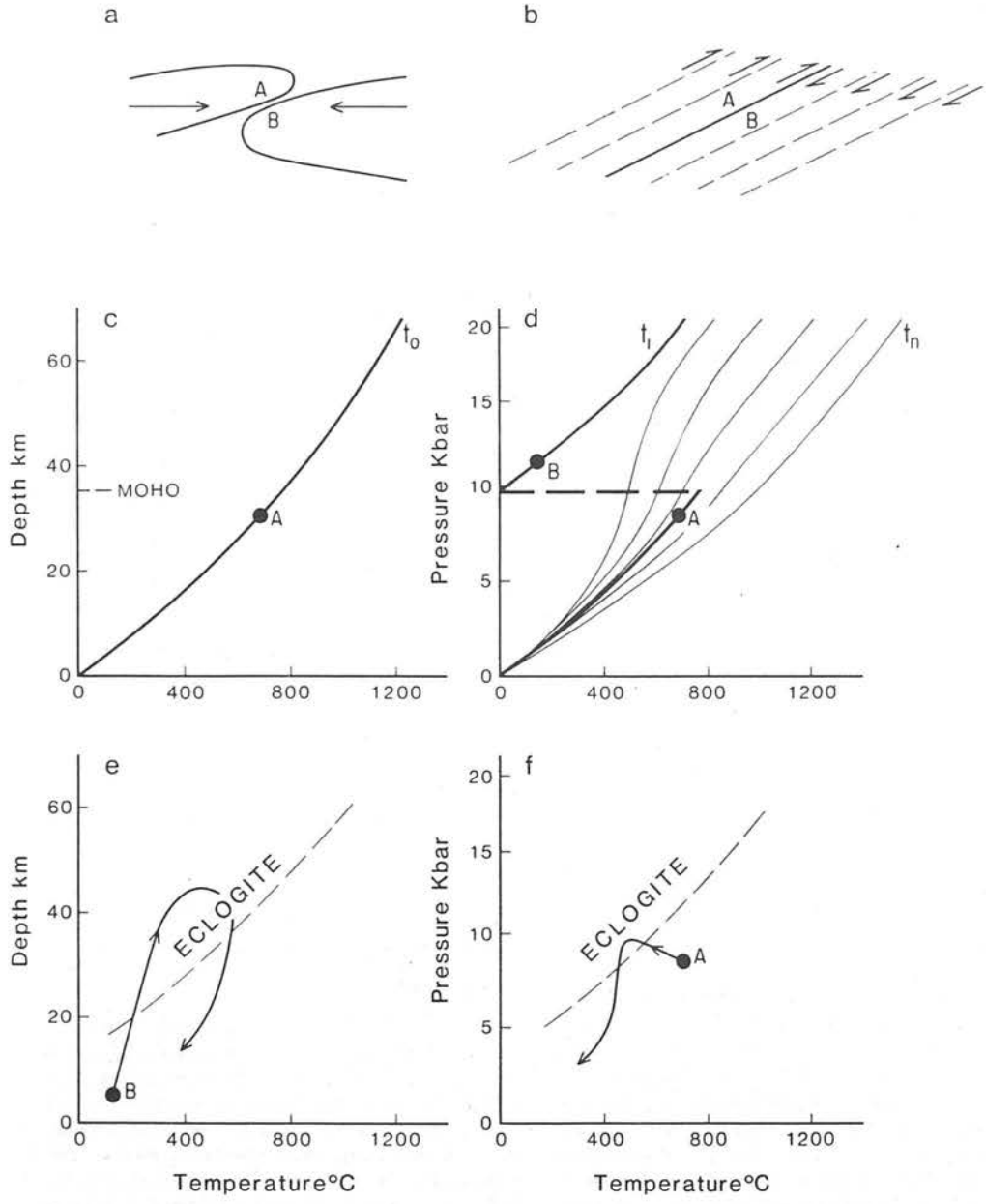

FIG. 2. Tectono-thermal model for the generation of eclogite-facies assemblages in continental crust. (a) A-type subduction as a result of collision between two continental plates. (b) Evolution of thrust-nappe stack in tectonically thickened continental crust. (c) Assumed pre-collisional (time = t_0) 'steady state' continental geotherm of 80 m W/m^2 (Chapman, this volume), appropriate for a partially cooled previous extensional regime with granulite-facies assemblages dominant in the lower continental crust. (d) Perturbed geotherm at t_1 immediately following collision and overthrusting of continental crust slab with assumed detachment at the Moho. Thermal relaxation over some tens of millions of years would eventually lead to a new 'steady state' geotherm at t_n appropriate for the thickened continental crust. (e) Prograde metamorphic path in P-T space leading to the stabilization of eclogite-facies assemblages in original upper crustal rocks (B) of the underthrusting plate. Note that P_{max} is reached before T_{max} and the initial, near isothermal, decompression during exhumation. (f) P-T-t path leading to possible generation on cooling of eclogite-facies assemblages from original granulite-facies lower crustal rocks (A) near the sole of the overthrust slab. An initial (perhaps exaggerated) pressure increase due to thrust-nappe stacking in the overthrust slab is assumed but is not critical to the model. Any tectonically intercalated slices of sub-continental mantle peridotite may be expected to follow a similar path.

K-Ar, Rb-Sr, U-Pb and Sm-Nd mineral ages for various lithologies (including eclogites) mostly fall between 380–450 Ma (e.g. Krogh *et al.* 1973; Gebauer *et al.* 1982; Griffin & Brueckner 1980, 1982; Mearns & Lappin 1982) and confirm the profound influence of the Caledonian orogeny on the rocks of this region. Field differentiation between reworked Precambrian basement and metamorphosed Late Precambrian ('Eocambrian')-Lower Palaeozoic cover rocks has proved extremely difficult (Bryhni 1966; Bryhni & Grimstad 1970; Carswell 1973; Strand 1960) but it seems that the Western Gneiss Region comprises an interfolded and intensely imbricated sequence of both autochthonous and allochthonous cover rocks and pre-Caledonian basement. This is corroborated by recent work in the east of the region (Krill 1985).

Rb-Sr whole rock isochrons and U-Pb zircon 'upper' concordia intersection ages as well as geochemical features (Harvey 1983; Krill 1983; Lappin *et al.* 1979) indicate that substantial volumes of acid-intermediate gneisses within this region represent recrystallized mid-Proterozoic igneous rocks. These and possible genetically related, spatially associated rocks such as anorthosites, titaniferous gabbros-norites and peridotites (Carswell *et al.* 1983; Harvey 1983) appear to have been intruded into the lower continental crust at around 1500 Ma.

High-P/medium-T eclogite facies assemblages are best preserved in the western coastal parts of the region and are generally more thoroughly retrogressed further east. Such high-P relicts are most conspicuously preserved in rocks of basic or ultrabasic composition (eclogites and garnetiferous peridotites, respectively) which are typically mantled by shells of later amphibolite. For the most part the dominant acid-intermediate gneisses have biotite and hornblende-bearing amphibolite-facies assemblages but locally almandine rich garnet and clinopyroxenes are preserved in less deformed rocks (Bryhni 1966; Carswell & Harvey 1985; Krill 1983; Lappin *et al.* 1979) indicating the earlier stability of the high-pressure assemblage: perthitic orthoclase + plagioclase + quartz + garnet + clinopyroxene. Scarce pelitic rocks frequently contain relict garnet and kyanite as well as symplektitic intergrowths of biotite and feldspars indicating that the high-P mica phengite may have been initially stable (cf. Heinrich 1982).

Whilst most eclogite lenses have sheared and amphibolitized margins against the encompassing gneisses, a few preserve intrusive contact relationships (Cuthbert & Carswell 1982; Griffin & Carswell 1985) which indicate that they originally formed dykes or larger bodies within the plutonic igneous precursors of the quartzo-feldspathic gneisses. Moreover, some of the large bodies have retained zones of original igneous textured doleritic-gabbroic rocks (Cuthbert & Carswell 1982; Gjelsvik 1952; Griffin & Råheim 1973; Mørk 1982). Indeed it is possible to observe all stages of conversion from the original igneous protoliths through rocks with coronitic development of the high-P garnet and omphacitic clinopyroxene replacing the original low P mineral phases, to thoroughly recrystallized granoblastic textured eclogites.

There is, therefore a growing volume of evidence which suggests that at least a substantial proportion of the exposed Western Gneiss Region witnessed the high-P metamorphism responsible for eclogite formation. It appears that evidence for this 'early' eclogite-facies metamorphic event is generally only retained in the more massive and structurally competent rock masses which have escaped the extensive late deformation and concurrent recrystallization to amphibolite-facies assemblages. Recent evidence provided by Sm-Nd and U-Pb data (Gebauer *et al*; Griffin & Brueckner 1980, 1982; Mearns & Lappin 1982) indicates a Caledonian (400–450 Ma) age for eclogite formation in western Norway. Such observations and the recognition of the development of the high-P eclogite-facies assemblages from a variety of crustal protoliths contradicts certain previous interpretations (O'Hara 1975; Lappin & Smith 1978; Smith 1980, 1981, 1982) that the Norwegian medium-T eclogites invariably represent foreign 'bodies' of deep seated, mostly mantle, origin tectonically emplaced into lower grade continental crust gneisses late in the Caledonian orogenic cycle. An ultimate upper mantle origin does, however, seem likely from general petrological and geochemical considerations for the forsteritic olivine-bearing 'alpine-type' periodite bodies which occasionally retain high-P garnet lherzolite, garnet websterite and eclogite assemblages (O'Hara & Mercy 1963; Carswell & Gibb 1980; Carswell *et al.* 1983; Medaris 1980, 1984).

Application of mineral thermometers and barometers to the high-P (eclogite-facies) metamorphic relicts in the Western Gneiss Region indicate (Krogh 1977; Griffin *et al.* 1985) a regional variation in the maximum T–P conditions attained, which varies from around 775 °C and 22 kbar in the coastal regions of Møre and Romsdal to around 550 °C and 12.5 kbar further south in Sunnfjord (Carswell 1981; Carswell & Gibb 1980; Carswell *et al.* 1984; Giffin *et al.* 1985; Krogh 1977, 1980a and b).

We have previously presented a tectonic model relating the features described above to northwes-

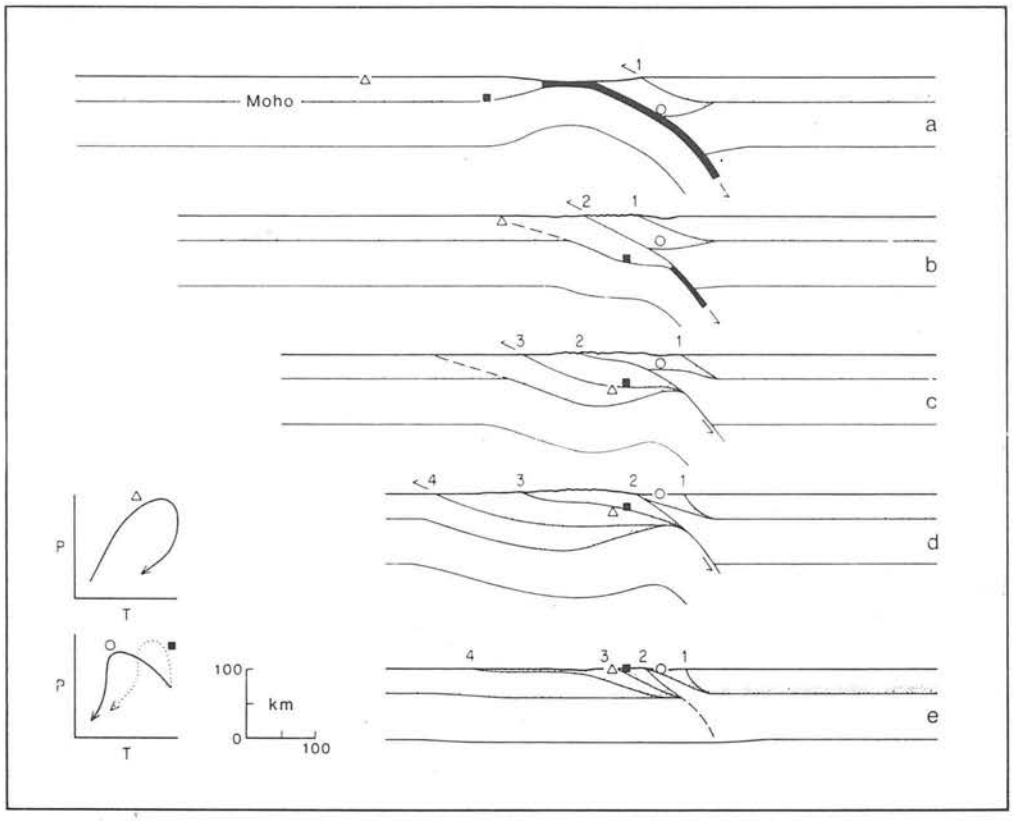

FIG. 3. Schematic lithospheric cross-sections showing the evolution of three eclogite-facies samples (open circle, closed square, triangle) in a continental collision-type orogen. Inset graphs show path of each sample in P-T space (compare with examples in text and Figs. 2 and 4). Lower crust is stippled, oceanic crust black. Numbers indicate successive major thrusts stepping back into the underthrusting plate. Accretion/obduction of oceanic crust (ophiolites) is omitted for clarity.

terly subduction of the margin of the Baltic continental plate beneath the leading edge of the Greenland continental plate on closure of Iapetus Ocean during the Caledonian orogeny (Cuthbert *et al.* 1983). The expected initial thermal perturbation of the regional conductive thermal gradient (Bird *et al.* 1975; England & Thompson 1984) associated with envisaged crustal thickening to about 80 km would have promoted the formation of eclogite-facies assemblages in the lower parts of the thickened prism. However, the survival of such assemblages and their apparent exposure at the surface by the early mid-Devonian, only some 65 Ma later, necessitates their rapid exhumation. Estimates of uplift rates based on considerations of isostacy and fluvial/glacial erosion alone (England & Richardson 1977; Anhert 1971) suggest that the rapid erosional exhumation may have been aided by tectonic stripping near the surface associated with eastwards translation of the allochthonous Caledonian nappes on to the Baltic foreland. More importantly, crustal imbrication in the Baltic foreland, leading to further northwestwards underthrusting beneath the currently exposed Western Gneiss Region is thought to have resulted in the exposure of the high pressure lithologies above a normal thickness of continental crust.

Whereas in the northwesternmost part of the Western Gneiss Region the eclogite-facies mineral phases are largely chemically homogeneous (due to the high temperatures of formation) further south garnets often display marked compositional prograde growth zonation (as exemplified in Fig. 5A for an eclogite sample from the Dalsfjord area) and may enclose mineral inclusions interpreted as relicts of earlier amphibolite- or blueschist-facies assemblages (e.g. Bryhni & Griffin 1971; Krogh 1982). This evi-

dence indicates that such rocks have initially followed a prograde P–T path (as illustrated in Fig. 4) through the blueschist facies into the eclogite facies. This was followed by rapid decompression (reflected in symplektitic development of granulite-facies assemblages) and ultimately, if deformation permitted access to aqueous fluids, the development of lower-T amphibolite-facies assemblages. Such a P-T-t path, characterized by heating during compression on the prograde segment, is compatible with these rocks having originally resided in the lower underthrusting continental plate (cf. Fig., 2e and Fig. 4). By contrast, as outlined by Carswell *et al.* (1983) and Medaris (1980, 1984), the medium-T eclogite-facies assemblages in the alpine-type peridotite bodies show evidence, from diffusion controlled 'retrograde' garnet zoning profiles (e.g. Fig. 5B) and rarely preserved exsolution textures, of equilibration (albeit sometimes arrested) in response to cooling. Such observations are compatible with their emplacement from the upper mantle into thickened continental crust on tectonic imbrication across the crust-mantle interface during the major continental collision event.

High-P metamorphism in the Sesia-Lanzo zone, Western Alps

Important information on the tectonic and metamorphic processes affecting lower continental crust rocks during the collision between the NW European (Penninic) and Austro-alpine (Insubric) continental plates is recorded in the Sesia-Lanzo Zone, the most southeasterly (internal) unit of the Western Alps. The Sesia-Lanzo Zone is now taken to represent a tectonic slice of the Austro-alpine continental crust (Compagnoni *et al.* 1977) which structurally overlies the meta-ophiolites and schistes lustrés of the Piemonte Zone (presumed relicts of the Jurassic Piemonte oceanic crust). The Piemonte Zone (Nappe) has in turn been thrust on to the margin of the Penninic continental plate, portions of which are exposed in the tectonic windows represented by the Monte Rosa, Gran Paradiso and Dora Maira Massifs as well as the Grand Saint Bernard-Briançonnais Nappe further west.

It would appear that the Austro-alpine, Piemonte and Penninic units of the Western Alps have all had a similar metamorphic history during the Alpine orogeny, characterized by an early Eo-Alpine high-P eclogite-/blueschist-facies event and a later (Lepontine) greenschist-facies overprint of variable intensity (Compagnoni *et al.* 1977; Compagnoni 1977; Caby *et al.* 1978; Lardeaux *et al.* 1982; Chopin & Maluski 1980). The latter has been reliably dated at 38–40 Ma but there is considerably more doubt over the date of the early high-P metamorphism. Compagnoni *et al.* (1977) indicated a 70–90 Ma date but, on the basis of the age data provided by Hunziker (1974) and Oberhaensli *et al.* (1982), Rubie (1984) has concluded that the eclogite-/blueschist-facies conditions in the Sesia-Lanzo Zone were initiated 100–130 Ma ago but may have persisted until 60 Ma. Caron (1984) has taken the available data to indicate that the high-P metamorphic conditions were attained at different times in the different structural units—namely at 110–130 Ma in the Sesia-Lanzo Zone, 40–70 Ma in the Piemonte schistes lustrés and at 40–50 Ma in some Briançonnais units. Chopin & Malaski (1980) have dated the early high P event at 60–75 Ma in phengites and paragonites from the Gran Paradiso nappe of the Pennine Zone.

According to Compagnoni *et al.* (1977) the Sesia-Lanzo Zone comprises heterogeneous pre-Alpine continental basement rocks which are subdivided into two main, lithologically contrasted, tectonic units—the lower *Eclogitic Micaschist Complex* (EMS) and the upper *Seconda Zona Dioritico-Kinzigitica* (II DK). The latter comprises mostly amphibolite- and locally granulite-facies gneisses (kinzigites) of probable mainly Hercynian age, and recrystallization to early Alpine high-P assemblages or late greenschist-facies assemblages is restricted to local high strain zones. The II DK has close lithological similarity to the Ivrea Zone, to the east of the Insubric Line (Fault Zone), which appears to have been largely unaffected by the Alpine metamorphism and deformation and exposes similar gneisses structurally underlain by peridotites. The Ivrea Zone is widely taken to represent a tectonic slice through the pre-Alpine lower continental crust into the upper mantle (Mehnert 1975; Rivalenti *et al.* 1980).

The lower EMS unit consists of dominant micaschists and metabasites which only rarely retain high temperature pre-Alpine mineral assemblages as they have suffered near pervasive recrystallization to Early Alpine eclogite-/blueschist-facies assemblages. However, in the western part of the Sesia-Lanzo Zone these rocks have been extensively retrograded to Late Alpine greenschist-facies assemblages (Gneiss Minuti Complex). A further important feature of the EMS unit is the occurrence of Permian granitoid bodies (such as at Mt. Mucrone) in which the original sodic plagioclase has been replaced by intergrowths of jadeite and zoisite and the biotite by phengite and garnet in response to the Early Alpine high-P metamorphism (Compagnoni 1977; Oberhaensli *et al.* 1982).

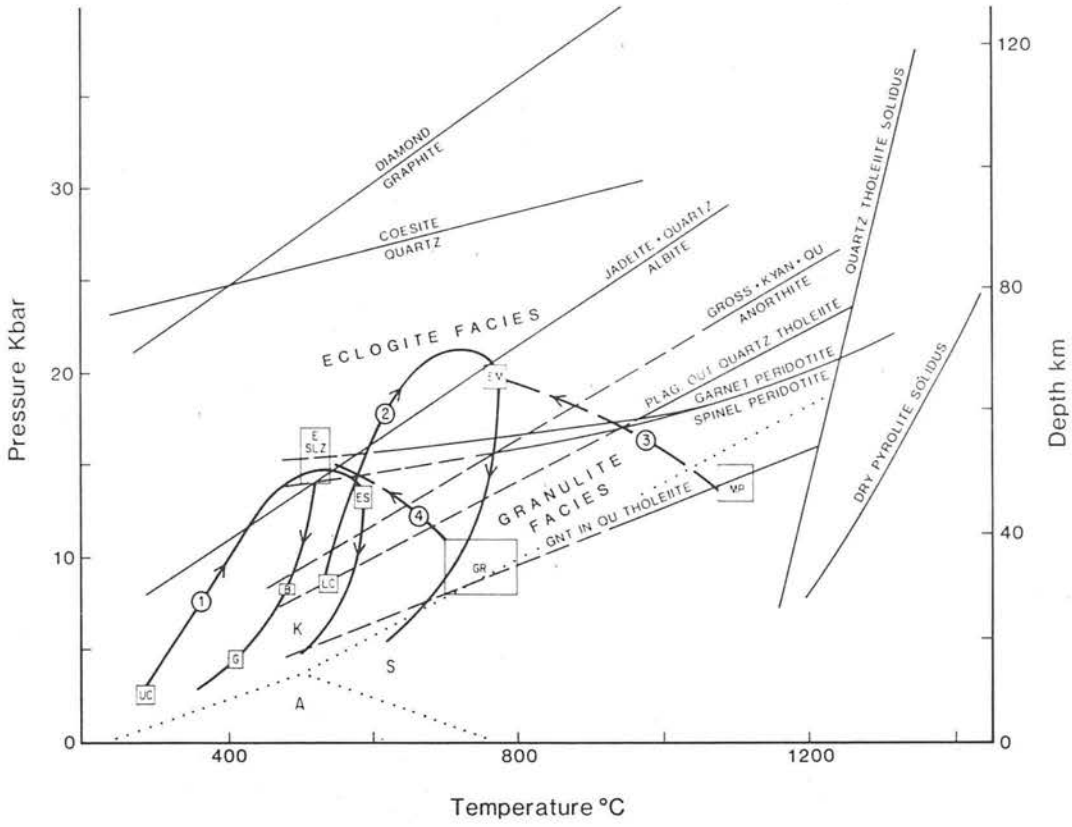

FIG. 4. Pressure (depth)-temperature diagram illustrating contrasted P-T-t paths for the generation and exhumation of eclogite-facies assemblages in protoliths from different structural levels in continental collision zones as follows: (1) along a prograde (heating) P-T-t path for Sunnfjord Dalsfjord, west Norway [ES] from original upper–middle crustal rocks [UC] in underthrusting lower plate. (2) along a prograde path for the Møre district, west Norway [EM] from a deep crustal level [LC] in underthrusting lower plate. (3) along a cooling path for tectonically intercalated sub-continental mantle peridotite slices [MP] in the Møre district, west Norway. (4) formation by re-equilibration at lower temperature of original lower crustal granulites-amphibolites [GR] in overthrusting slab for the Sesia-Lanzo Zone [ESLZ]. western Alps.

The P-T-t path for the Sesia-Lanzo Zone rocks is based on data provided by Lardeaux *et al.* (1982) with [B] and [G] representing indicated conditions for formation of retrograde blueschist- and greenschist-facies assemblages, respectively. However, note that as discussed in the text and also indicated in Carswell *et al.* (1982), the cooling paths (heavy dashed lines) leading to stabilization of medium-T eclogite-facies assemblages from lower crustal [GR] and upper mantle [MP] protoliths may well not be as direct as indicated in this diagram.

In all instances the initial uplift path for the high-P assemblages is characterized by rapid, near isothermal, decompression. Data sources for the various reaction curves as in Fig. 1.

Best estimates of temperatures during the high-P metamorphism in the Sesia-Lanzo rocks are 500–540 C (Lardeaux *et al.* 1982) with probable pressures of 14–17 kbar—the minimum value being constrained by the observed stability of effectively pure jadeite+quartz (see Fig. 1). By contrast, Lardeaux *et al.* (1982) have indicated the P–T conditions for formation of the pre-Alpine granulite-facies assemblages to have been 700–800 C and 8–11 kbar.

A P-T-t path for the Sesia-Lanzo Zone rocks (Fig. 4) based on these observations might, on first consideration, be taken to be compatible (cf. Fig. 2f) with eclogite formation during Alpine upthrusting and cooling of granulite-facies lower continental crust. However, although the tectonic location within the Alpine belt appears correct, various geological, mineralogical and geochronological observations (Compagnoni *et al.* 1977; Lardeaux *et al.* 1982; Zingg 1983; Kruhl 1984) indicate that the Sesia-Lanzo Zone rocks (like those of the Ivrea and Strona-Ceneri Zones to the east) were already at a fairly high crustal level prior to the Alpine orogeny. Controversy persists over the age of the granulite-facies metamorphism, although Zingg (1983) favours the interpretation that it was Caledonian. However, these continental crust segments are considered to have remained at depth until the Variscan orogeny, which caused limited amphibolite- to greenschist-facies retrogression (Lardeaux *et al.* 1982; Kruhl 1984), but to have been uplifted and cooled to *c.* 300 C by *c.* 180 Ma on the basis of K-Ar mica ages (Zingg 1983). Chemical zoning profiles in garnets from Sesia-Lanzo Zone rocks are unfortunately rather variable and complex (Desmons & Ghent 1977) but suggestive of different episodes of garnet growth and diffusive re-equilibration.

High-P metamorphism in the European Variscan fold belt

Sparse relicts of high-P metamorphic assemblages (mostly medium-T eclogites or high-P granulites) are widely distributed in several basement massifs (Bohemian, Polish Sudetan, Vosges-Schwarzwald, Massif Central, S. Armorican, N.W. Iberian) of the Variscan fold belt of western and central Europe (e.g. Dudek & Fediukova 1974; Kappel 1967; Matthes 1978; Pin & Vielzeuf 1983; Smulikowski & Bakum-Czubarow 1973). Interpretation of the tectonometamorphic evolution of these particular high-P rocks is clouded by general uncertainty over the geochronology of the seemingly complex sequence of Caledonian to Hercynian orogenic events which appears to have been involved in the Palaeozoic consolidation of median Europe (Ziegler 1984)—compounded by the limited, and spatially separated, nature of the exposure.

Early ideas (e.g. Zoubek 1969) of a Precambrian age for these high-P assemblages have been disproved by more recent Rb-Sr and U-Pb dating (Gebauer & Grünenfelder 1979; van Breemen *et al.* 1982; Vidal *et al.* 1980) which indicate that they have formed from protoliths of both Proterozoic and Early Palaeozoic age. However, major divergences of opinion remain over the actual age of the high-P assemblages. Pin & Vielzeuf (1983), in their review, support a Caledonian age (400–450 Ma) for their formation throughout Variscan median Europe, a view supported by the radiometric age determination of Arnold & Scharbert (1973) in Lower Austria and Jäger & Watznauer (1969) in Saxony. However, much younger Hercynian ages of 345 ± 5 Ma and 320^{+29}_{-36} Ma, respectively, have been indicated by van Breeman *et al.* (1982) in the Moldanubian Zone of the Czech part of the Bohemian Massif and by Gebauer *et al.* (1981) in the Massif Central. On the other hand, an intermediate 380^{+14}_{-22} Ma (Acadian-Ligerian) age has been demonstrated by Gebauer & Grünenfelder (1979) for eclogites in the Munchberg Massif of the northern Saxo-Thuringian Zone of the Bohemian Massif. Acadian ages have also been deduced for eclogites in the W. Iberian Massif of Western Galicia (Van Calsteren *et al.* 1979) and for blueschists on the Ile de Groix, S. Armorican Massif (Peucat & Cogné 1977). This situation is not fully resolved and the possibility must be considered that the development of the medium-T eclogite/high-P granulite association was not synchronous across the central European Variscides. We tentatively favour the interpretation put forward by Autran & Cogné (1980), Santallier *et al.* (1978), Matte & Burg (1981) and Zeigler (1984) for a dominant Acadian-Ligerian (i.e. Eo-Hercynian) age of around 380 Ma for the high-P metamorphism, in response to collision of the Gondwana-derived Intra-Alp, Iberian and Avalon allochthonous terrains with the southern margin of the Laurasian craton previously consolidated during the Caledonian orogenic cycle (Ziegler 1984). As in the Norwegian Caledonides and the Western Alps, there is abundant evidence in the Central European Variscides for a later (*c.* 320 Ma) retrograde (lower-P) metamorphic overprint on the early high-P assemblages during the now most apparent tectono-metamorphic phase of the Hercynian orogeny.

As emphasized by Pin & Vielzeuf (1983) a particular feature of the Variscan fold belt is the close spatial association of medium-T eclogites,

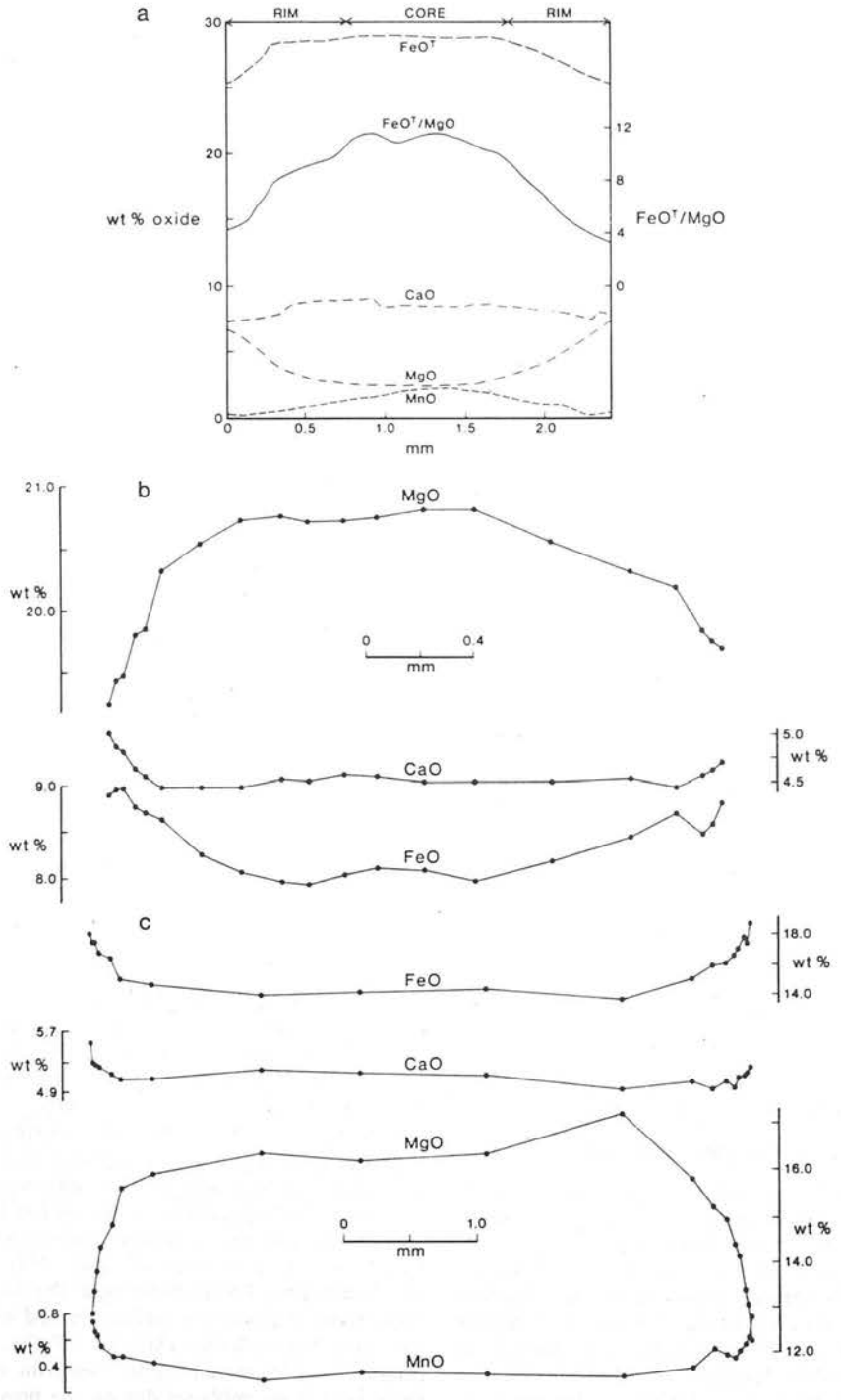

FIG. 5. Chemical zoning profiles across garnet grains in eclogite-facies rocks. Analyses all performed on the Microscan IX electron microprobe at the University of Sheffield. A. Garnet showing prograde growth zoning in eclogite from Dalsfjord, west Norway. Mineral inclusion suites are tschermakitic amphibole + zoisite + ilmenite/rutile in the core zone, and omphacitic clinopyroxene + rutile ± barroisitic amphibole in the rim zones. B. Garnet clast showing extensive diffusion controlled 'retrograde' zoning indicative of a prolonged cooling history—in porphyroclastic textured garnet peridotite from Ugelvik, Otrøy, west Norway. C. Garnet clast again showing extensive 'retrograde' zoning in porphyroclastic garnet pyroxenite associated with peridotite within the St. Leonhard granulite complex at Reitmuhle, Kamptal, lower Austria.

garnet peridotites and garnet websterites with quartzo-feldspathic gneisses. The gneisses have a dominant high-P granulite facies assemblage of quartz-perthite-plagioclase-garnet-kyanite with minor orthopyroxene and/or clinopyroxene in scarcer more mafic variants. This association is particularly in evidence in the Moldanubian Zone of the Bohemian Massif in Southern Czechoslovakia (Dudek & Fediukova 1974; Misar *et al.* 1983), in Lower Austria (Kappel 1967; Scharbert & Carswell 1983) and in the Oberfalzwald of N.E. Bavaria (Busch 1970; Matthes 1978).

Scharbert & Kurat (1974) have estimated minimum P–T conditions for formation of quartz-feldspathic granulites in Lower Austria to have been 11 kbar and 760°C, consistent with formation in the lower continental crust. Czech geologists (e.g. Vesela 1967) have often favoured interpreting the dominant felsic granulites as metamorphosed rhyolites and tuffs stratigraphically associated with more mafic granulites of presumed meta-sedimentary origin. However, recently Vrana & Jakes (1982) have described the deformation induced transformation of relatively pristine unfoliated garnet bearing hypersolvus leucogranites into highly flattened and recrystallized felsic garnet granulites. They view such plutonic igneous rocks to have been the products of relatively dry ($P_{H_2O} < 2$ kbar) anatectic melting in the lower continental crust with crystallization under granulite-facies conditions at $P_{Total} > 7$ kbar and $T > 800$°C. However, van Breeman *et al.* (1982) have interpreted the initial crystallization of the lower crustal rocks of the Moldanubian Zone to have been largely accomplished during the Cadomian orogenic cycle (*c.* 550 Ma) but the actual granulite-facies metamorphism to have occurred much later during the Hercynian orogeny at 345 ± 5 Ma.

Spatially associated medium-T eclogites, garnet websterites and garnet peridotites occur within the quartzo-feldspathic granulites at numerous localities within the Moldanubian Zone of the Bohemian massif. These garnetiferous peridotite bodies and enclosed metabasic rocks, taken to represent the partially recrystallized products of trapped partial melts of olivine tholeiite to picrite compositions (Scharbert & Carswell 1983), have been widely interpreted as tectonic intercalculations of upper mantle rocks (Kappel 1967; Fiala 1966; Scharbert 1973; Matthes 1978; Dudek & Fediukova 1974). Such rocks invariably show evidence of static recrystallization to lower pressure granulite-facies assemblages as well as later deformation induced retrogression to amphibolite-facies assemblages, as also widely observed in the felsic granulites.

Garnets in the eclogite-facies rocks from Lower Austria have conspicuous retrograde chemical zoning profiles (see Fig. 5c) and pyroxenes show extensive exsolution. Comparable mineralogical features are observed in the associated granulites. Unfortunately it is currently only possible to indicate minimum P–T conditions for formation of the quartzo-feldspathic granulites (Scharbert & Kurat 1974) and the extensive metamorphic retrogression suffered by the basic and ultrabasic rocks makes thermobarometry of their relict high P assemblages rather hazardous. However, we suggest that the lower continental crust and upper mantle lithologies were in effective tectonic juxtaposition early in the metamorphic evolution and that their respective high-P/medium-T mineralogies were in effect both coeval and cofacial. We further suggest that the stabilization of these high-P assemblages in the Moldanubian Zone rocks may have been caused by them having been underthrust from the north-west by cooler continental lithosphere in the manner illustrated in Fig. 3. In addition we speculate that the implied earlier high-T assemblages both in the lower crust and uppermost mantle have been generated in response to an enhanced mantle heat flux during a precursive phase of continental lithospheric extension.

Confirmation that the lower continental crust rocks of the Moldanubian Zone were subjected to P–T conditions appropriate for the stability of medium-T eclogites early in the Variscan orogenic cycle requires further isotopic age data and proof that undoubted eclogite-facies assemblages were also developed in crustal protoliths. In the latter connection it is worth noting the reported significant range of eclogite rock compositions (Dudek & Fediukova 1974; Matthes 1978) and the fact that not all eclogite occurrences are directly associated with mantle-derived peridotite bodies. However, clearly more field and analytical data are required to consolidate the interpretation of the high-P rocks in the Moldanubian Zone of the Bohemian Massif and indeed elsewhere in the Variscides.

Discussion

The controversial medium-T eclogite-facies assemblages sporadically preserved in certain amphibolite or granulite-facies terrains are considered to have been generated largely from continental crust protoliths. Mineral-chemical evidence indicates that their formation requires substantial crustal thickening (up to or even in excess of 70 km). A likely tectonic scenario for this is considered to be the collision of two continental lithospheric plates during which the

leading edge of one plate undergoes transient subduction beneath the other (Fig. 3). Subsequent further thickening may occur as thrusts progressively step 'down' and back into the underthrust plate, as outlined by Hodges *et al.* (1982).

Continental plate collision would be expected to perturb the steady state temperature-depth profile and result in the stabilization of eclogite-facies assemblages along prograde P-T-t paths in the underthrust plate. In addition the lower crust of the upper plate may be cooled by being brought into contact with underthrust upper crust. However, in this instance kinetic barriers may limit re-equilibration to eclogite-facies assemblages to high strain zones. Eclogite stabilization would be enhanced by any tectonic thickening of the upper plate and may be repeated during continued crustal shortening each time a major new thrust becomes operational in the underthrusting foreland.

Mineral features may monitor the origin and location of rocks during the tectonic events responsible for eclogite stabilization. Garnet zoning and mineral inclusion suites can show an evolution involving increasing T as well as P_{Load} (Fig. 5a) indicating that the rocks probably represent previous upper–middle crust (e.g. Sunnfjord, western Norway). Alternatively zoning may indicate cooling (Figs. 5B & C), with or without an initial pressure increase, indicative of previous lower continental crust (Moldanubian Zone; Sesia-Lanzo Zone?) or, in the case of garnetiferous alpine-type peridotites, tectonically intercalated upper mantle (Moldanubian Zone; western Norway).

The survival and ultimate exposure of medium-T eclogites requires that the rate of exhumation is fast relative to the rate of thermal relaxation following continental underthrusting (England & Richardson 1977; Draper & Bone 1980). Thermobarometry on widely developed retrogressive symplektites and kelyphites with granulite-facies assemblages corroborates this rapid uplift hypothesis, showing that initial uplift and decompression was usually accomplished with little change in temperature. Geochronological evidence for the Caledonides, Alps and Variscides whilst still controversial, indicates that eclogite-facies assemblages formed early in the evolution of each belt and were superimposed upon appreciably older (Proterozoic or Palaeozoic) crustal material. The time interval between the early high-P metamorphism and later extensive lower-P greenschist- or amphibolite-facies assemblages may have been only some 40–60 Ma, indeed our best estimate for complete unroofing of the eclogite-bearing terrain in Western Norway is some 65 Ma. The necessary average erosion rate of around 1 mm/year is encouragingly in line with estimates of current and recent uplift rates along the Indus–Tsangpo suture zone in the Himalaya (Zeitler *et al.* 1982; Melita 1980).

Buoyant uplift of terrains bearing eclogite-facies assemblages may be aided by continued underthrusting of crustal wedges below them (Fig. 3), allowing eclogites in lower crustal rocks to be exposed above a normal thickness of crust. Thrusts such as the Main Boundary Thrust of the Himalaya may be responsible for such a process. Sequential foreland propagation of such thrusts (Fig. 3) may produce eclogites of different ages at different tectonostratigraphic levels in an orogen (as suggested by Caron (1984) for the western Alps) and may be responsible for the presence of high-P metamorphic rocks at several levels in the Caledonian allochthon of Scandinavia (Bryhni *et al.* 1977). Tilting of the crust as a consequence of underthrusting (Windley 1983) may also aid eventual exposure of high-P rocks from deep levels in the thrust-nappe stack.

Competition between thermal and mechanical effects can have a significant effect on the resulting mineral assemblages. Factors such as the previous thermal structure of the crust, the rate of plate convergence and the rate of uplift will all control the nature of the rocks reaching the surface. It is perhaps significant that in the three areas reviewed the peak metamorphic and retrogressive mineral assemblages are significantly different, probably reflecting different thermal regimes. Rubie (1984) has developed a model for the Sesia-Lanzo zone in which prolonged subduction of oceanic lithosphere beneath the thickened crust retarded relaxation of the isotherms and produced the unusually low equilibration temperatures recorded there. Whilst this model may significantly overestimate the period of oceanic subduction (Tricart, 1984 indicates that ocean closure commenced at *c.* 80 Ma, significantly later than Rubie's (1984) estimate of 130–100 Ma) it serves to illustrate the blanketing effect of thrusting cold material below an evolving eclogite-facies terrain. Retardation of uplift may result from density increases brought about by up-pressure phase transformations (Richardson & England 1979); a reduced rate of plate convergence or even climatic factors affecting erosion rates. Such retardation may allow thermal relaxation in the thickened crust to obliterate the medium-T eclogite-facies assemblages. Thus some exposed apparent 'lower crustal' granulite facies terrains may have originally been at eclogite-facies, particularly those regions containing high P granulites.

Medium-T eclogites appear to be a particular

feature of Phanerozoic continental collision belts, although a recent geochronological study of comparable eclogites in the Eastern Glenelg Lewisian inlier of NW Scotland (Sanders *et al.* 1984) has indicated a Late Proterozoic (Grenville) age. We know of no proven examples of Archaean crustal eclogites. This might be indicative of the fact that only more recently in the earth's history has the continental crust been sufficiently thick, cool and rigid (cf. Tarling 1980) to permit the degree of Type A subduction necessary for the stabilization and survival of medium-T eclogites. On the other hand, England & Bickle (1984) have recently argued that the Archaean continental crust was not greatly different in thickness and thermal structure from that of the Phanerozoic era.

The Himalayan collision zone currently lacks medium-T eclogites at outcrop, although high-P granulites have been found (Windley 1983). Eclogites might be expected to exist at deeper levels in the thrust-nappe stack and their eventual exposure may be aided by erosion and underthrusting along faults such as the Main Boundary Fault.

ACKNOWLEDGEMENTS: We wish to acknowledge research grants (DAC) and a research studentship (SJC) from the Natural Environment Research Council which have supported our studies of eclogite-facies rocks.

References

AHNERT, F. 1970. Functional relationship between denudation, relief and uplift in mid-latitude drainage basins. *Am. J. Sci.* **268,** 243–263.

ARNOLD, A. & SCHARBERT, H.G. 1973. Rb-Sr alterbestimmungen an granuliten der Südlichen Böhmischen masse in Österreich. *Schweiz. Mineral. Petrogr. Mitt.*, **53,** 61–78.

AUTRAN, A. & COGNÉ J. 1980. La zone interne de l'orogène varisque dans l'ouest de la France et sa place dans le developpement de la chaîne hercynienne. *In*: COGNÉ, J. & SLANSKY, M. (eds) *Geologie de l'Europe du Precambrian aux bassins sedimentaries posthercyniens*. Mem. B.R.G.M. **107,** 87–92.

BANNO, S. 1970. Classification of eclogites in terms of physical conditions of their origin. *Phys. Earth Planet. Interiors*. **3,** 405–421.

BERMAN, R. 1979. Thermal properties. *In*: FIELD J.E. (ed.). *The Properties of Diamond*. Academic Press, London.

BEST, M.G. 1982. *Igneous and Metamorphic Petrology*. Freeman, San Francisco.

BIRD, P., TOKSOZ, M.N. & SLEEP, N.H. 1975. Thermal and mechanical models of continent-continent convergence zones. *J. Geophys. Res.*, **80,** 4405–4416.

BOHLEN, S.R., WALL, V.J. & BOETTCHER, A.L. 1983. Geobarometry in granulites. *In*: SAXENA, S.K. (ed.), *Kinetics and Equilibrium in Mineral Reactions*. Advances in Physical Geochemistry, Vol. 3, Springer-Verlag, New York.

BROWN, E.H. & BRADSHAW, J.Y. 1979. Phase relations of pyroxene and amphibole in greenstone, blueschist and eclogite from the Francisan Complex, California. *Contrib. Mineral. Petrol.* **71,** 67–83.

BRYHNI, I. 1966. Reconnaissance studies of gneisses, ultrabasites, eclogites and anorthosites in Outer Nordfjord, Western Norway. *Nor. Geol. Unders.*, **241,** 1–68.

—— & GRIFFIN, W.L. 1981. Zoning in eclogite garnets from Nordfjord, West Norway. *Contrib. Mineral. Petrol.* **32,** 112–125.

—— & GRIMSTAD, E. 1970. Supracrustal and infracrustal rocks in the gneiss region of the Caledonides west of Breimsvatn. *Nor. Geol. Unders.* **266,** 105–140.

——, KROGH, E. & GRIFFIN, W.L. 1977. Crustal derivation of Norwegian eclogites: A review. *Neues Jb. Miner. Abh.* **130,** 49–68.

BUSCH, K. 1970. Die Eklogitvorkommen des Kristallinen Grundgebirges in N.E. Bayern. IV. Die Eklogite der Oberfalz und ihr metamorpher Abbau. *Neues Jb. Miner. Abh.* **113,** 138–178.

CABY, R., KIENAST, J.-R. & SALIOT, P. 1978. Structure, métamorphism et modèle d'evolution tectonique des Alps occidentales. *Rev. Geogr. Phys. Geol. Dyn.* **XX,** 307–322.

CARON, J.M. 1984. The diversity of geodynamic regimes leading to high pressure-low temperature metamorphism (Western Alps and Corsica). *Terra Cognita*, **4,** 39–43.

CARSWELL, D.A. 1973. Garnet pyroxenite lens within Ugelvik layered garnet peridotite. *Earth Planet Sci. Lett.* **20,** 347–352.

—— 1980. Mantle derived lherzolite nodules associated with kimberlite, carbonatite and basalt magmatism: A review. *Lithos*, **13,** 121–138.

—— 1981. Clarification of the petrology and occurrence of garnet lherzolites, garnet websterites and eclogite in the vicinity of Rödhaugen, Almklovdalen, West Norway. *Nor. Geol. Tidsskr.* **61,** 249–260.

——, DAWSON, J.B. & GIBB, F.G.F. 1981. Equilibration conditions of upper-mantle eclogites: implications for kyanite-bearing and diamondiferous varieties. *Mineral. Mag.* **44,** 79–89.

—— & GIBB, F.G.F. 1980. The equilibration conditions and petrogenesis of European crustal garnet lherzolites. *Lithos*, **13,** 19–29.

—— & HARVEY, M.A. 1985. The intrusive history and tectono-metamorphic evolution of the Basal Gneiss Complex in the Moldeford area, West Norway. *In*: GEE, D.G. & STURT, B.A. (eds) *The Caledonide Orogen*. John Wiley, London.

——, HARVEY, M.A. & AL-SAMMAN, A. 1983. The petrogenesis of contrasting Fe-Ti and Mg-Cr garnet peridotite types in the high grade gneiss complex of Western Norway. *Bull. Mineral.* **106,** 727–750.

——, KROGH, E. & GRIFFIN, W.L. 1985. Norwegian orthopyroxene eclogites: Calculated equilibration

conditions and petrogenetic implications. *In*: GEE, D.G. & STURT, B.A. (eds) *The Caledonide Orogen*. John Wiley, London.

CHOPIN, C. & MULUSKI, H. 1980. ^{40}Ar-^{39}Ar dating of high pressure metamorphic micas from the Gran Paradiso area (Western Alps): Evidence against the blocking temperature concept. *Contrib. Mineral. Petrol.* **74,** 109–122.

COLEMAN, R.G., LEE, D.E., BEATTY, J.B. & BRANNOCK, W.W. 1965. Eclogites and eclogites: Their differences and similarities. *Bull. Geol. Soc. Am.* **76,** 483–508.

COMPAGNONI, R. 1977. The Sesia-Lanzo zone: High pressure-low temperature metamorphism in the Austroalpine continental margin. *Rend. Soc. Ital. Mineral. Petrol.* **33,** 335–374.

——, DAL PIAZ, G.V., HUNZIKER, J.C., GOSSO, G., LOMBARDO, B. & WILLIAMS, P.F. 1977. The Sesio-Lanzo zone, a slice of continental crust with alpine high pressure–low temperature assemblages in the western Italian Alps. *Rend. Soc. Ital. mineral. Petrol.* **33,** 281–334.

CUTHBERT, S.J. & CARSWELL, D.A. 1982. Petrology and tectonic setting of eclogites and related rocks from the Dalsfjord area, Sunnfjord, western Norway. *Terra Cognita*, **2,** 315.

——, HARVEY, M.A. & CARSWELL, D.A. 1983. A tectonic model for the metamorphic evolution of the basal gneiss complex, western South Norway. *J. Metamorphic Geol.* **1,** 63–90.

DAWSON, J.B. 1980. *Kimberlites and their Xenoliths*. Springer-Verlag, Berlin.

DESMONS, J. & GHENT, E.D. 1977. Chemistry, zonation and distribution coefficients of elements in eclogitic minerals from the Eastern Sesia Unit, Italian Western Alps, *Schweiz. Mineral. Petrogr. Mitt.* **57,** 397–411.

DRAPER, G. & BONE, R. 1981. Denudation rates, thermal evolution and preservation of blueschist terrains. *J. Geol.* **89,** 601–613.

DUDEK, A. & FEDIUKOVA, E. 1974. Eclogites of the Bohemian Moldanubian. *Neues Jb. Miner. Abh.* **121,** 127–159.

ELLIS, D.J. & GREEN, D.H. 1979. An experimental study of the effect of Ca upon garnet-clinopyroxene Fe-Mg exchange equilibra. *Contrib. Mineral. Petrol.* **71,** 13–22.

ENGLAND, P. & BICKLE, M. 1984. Continental thermal and tectonic regimes during the Archaean. *J. Geology*, **92,** 353–367.

—— & RICHARDSON, S.W. 1977. The influence of erosion upon the mineral facies of rocks from different metamorphic environments. *J. geol. Soc. London*, **134,** 201–213.

—— & THOMPSON, A.B. 1984. Pressure-temperature-time paths of regional metamorphism. 1. Heat transfer during the evolution of regions of thickened continental crust. *J. Petrol.* **25,** 894–928.

ERNST, W.G. 1977. Tectonics and prograde versus retrograde P-T trajectories of high pressure metamorphic belts. *Rend Soc. Ital. Mineral. Petrol.* **33,** 221–252.

ESKOLA, P. 1921. On the eclogites of Norway. *Sr. Norske vidensk-Akad. i Oslo Mat. Natur. Kl.* **8,** 1–118.

FIALA, J. 1966. The distribution of elements in mineral phases of some garnet lherzolites from the Bohemian Massif. *Krystalinikum*, **4,** 31–53.

GJELSVIK, T. 1952. Metamorphosed dolerites in the gneiss area of Sunnmøre on the west coast of southern Norway. *Nor. Geol. Tidsskr.* **31,** 31–134.

GOLDSMITH, T.R. 1980. The melting and breakdown reactions of anorthite at high pressures and temperatures. *Am. Mineral.* **65,** 272–284.

GREEN, D.H. & RINGWOOD, A.E. 1967a. An experimental investigation of the gabbro to eclogite transformation and its petrological applications. *Geochim. Cosmochim. Acta*, **31,** 767–833.

—— & —— 1967b. The stability fields of aluminous pyroxene peridotite and garnet peridotite and their relevance in upper mantle structure. *Earth Planet. Sci. Letters*. **3,** 151–160.

GRIFFIN, W.L. & BRUECKNER, H.K. 1980. Caledonian Sm-Nd ages and a crustal origin for Norwegian eclogites. *Nature*, **285,** 319–321.

—— & 1982. Rb-Sr and Sm-Nd studies of Norwegian eclogites. *Terra Cognita*, **2,** 324.

—— & CARSWELL, D.A. 1985. Geochronological setting of in situ eclogite metamorphism in western Norway. *In*: GEE, D.G. & STURT, B.A. (eds) *The Caledonide Orogen*. John Wiley, London.

——, AUSTRHEIM, H. *et al.* 1985. High pressure metamorphism in the Scandinavian Caledonides. *In*: GEE, D.G. & STURT, B.A. (eds) *The Caledonide Orogen*, John Wiley, London.

—— & RÅHEIM, A. 1973. Convergent metamorphism of eclogites and dolerites, Kristiansund area, Norway. *Lithos*, **6,** 21–40.

GEBAUER, D., BERNARD-GRIFFITHS, J. & GRÜNENFELDER, M. 1981. U-Pb zircon and monazite dating of a mafic-ultramafic complex and its country rocks. Example: Sauviat-sur-Vige, French Central Massiff. *Contrib. Mineral. Petrol.* **76,** 292–300.

—— & GRÜNENFELDER M. 1979. U-Pb zircon and Rb-Sr mineral dating of eclogites and their country rocks. Example: Munchberg Gneiss Massif, northeast Bavaria. *Earth Planet Sci. Lett.* **42,** 35–44.

——, LAPPIN, M.A., GRÜNENFELDER, M., KOESTLER, A. & WYTTENBACH, A. 1982. Age and origin of some Norwegian eclogites. A U-Pb zircon and REE study. *Terra Cognita*, **2,** 323.

HARTE, B. 1983. Mantle peridotites and processes—the kimberlite sample. *In*: HAWKESWORTH C.J. & NORRY, M.J. (eds) *Continental Basalts and Mantle Xenoliths*. Shiva geology series.

HARVEY, M.A. 1983. A geochemical and Rb-Sr study of the Proterozoic augen orthogneisses on the Molde Peninsula, west Norway. *Lithos*, **16,** 325–338.

HEINRICH, C.A. 1982. Kyanite-eclogite to amphibolite facies evolution of hydrous mafic and pelitic rocks, Adula Nappe, central Alps. *Contrib. Mineral. Petrol.* **81,** 30–38.

HELMSTAEDT, H. & GURNEY, J.J. 1984. Kimberlites of southern Africa—are they related to subduction processes? *In*: KORNPROBST, J. (ed.) *Kimberlites I:*

Kimberlites and Related Rocks. Elsevier, Amsterdam.

HODGES, K.V., BARTLEY, J.M. & BURCHFIEL, B.C. 1982. Structural evolution of an A-type subduction zone, Lofoten-Rombak area, northern Scandinavian Caledonides. *Tectonics*, **1**, 441–462.

HOLDAWAY, M.J. 1971. Stability of andalusite and the aluminium phase diagram. *Am. J. Sci.* **271**, 97–131.

HOLLAND, T.J.B. 1980. The reaction albite = jadeite + quartz determined experimentally in the range 600–1200 C. *Am. Mineral.* **65**, 1129–134.

HUNZIKER, J.C. 1974. Rb-Sr and K-Ar age determination and the alpine tectonic history of the western Alps. *Mem. Ist Geol. min. Univ. Padova*, **31**, 54 pp.

JÄGER, E. & WATZNAUER, A. 1969. Einige Rb/Sr datierungen an granuliten des Sachsischen granulitgebirges. *Monatber. Dtsch. Akad. Wiss.* **11**, 420–426.

KAPPEL, E. 1967. Die Eklogite Meidling im Tal und Mitterbach graben im Niederösterreichischen Moldanubikum südlich der Donau. *Neues Jb. Miner. Abh.* **107**, 266–298.

KRILL, A.G. 1983. Rb-Sr study of rapakivi granite and augen gneiss from the Risberget Nappe, Oppdal, Norway. *Nor. Geol. Unders.* **380**, 51–65.

—— 1985. Relationships between the western gneiss region and the Trondheim region: stockwerk-tectonics reconsidered. *In*: GEE, D.G. & STURT, B.A. (eds) *The Caledonide Orogen* John Wiley, London.

KROGH, E.J. 1977. Evidence of precambrian continent-continent collision in western Norway. *Nature*, **267**, 17–19.

—— 1980a. Geochemistry and petrology of glaucophane-bearing eclogites and associated rocks from Sunnfjord, western Norway. *Lithos*, **13**, 355–380.

—— 1980b. Compatible P–T conditions for eclogites and surrounding gneisses in the Kristiansund area, western Norway. *Contrib. Mineral. Petrol.* **75**, 387–393.

—— 1982. Metamorphic evolution of Norwegian country-rock eclogites, as deduced from mineral inclusions and compositional zoning of garnets. *Lithos*, **15**, 305–321.

KROGH, T.E., MYSEN, B.O. & DAVIS, G.L. 1973. A palaeozoic age for the primary minerals of a Norwegian eclogite. *Carnegie Inst. Wash. Yearb.* **73**, 575–576.

KRUHL, J.H. 1984. Metamorphism and deformation of the N.W. margin of the Ivrea Zone, Val Loana (Italy). *Schweiz Mineral. Petrog. Mitt.* **64**, 151–167.

KISHIRO, I. 1969. Clinopyroxene solid solutions formed by reactions between diopside and plagioclase at high pressure. *Mineral. Soc. Am. Sp. Pap.* **2**, 179–191.

LAPPIN, M.A. 1966. The field relationships of basic and ultrabasic masses in the basal gneiss complex of Stadlandet and Almklovdalen, Nordfjord, S.W. Norway. *Nor. Geol. Tidsskr.* **46**, 439–495.

—— 1977. Crustal and in situ origin of Norwegian eclogites. *Nature*, **269**, 730.

——, PIDGEON, R.T. & VAN BREEMAN, O. 1979. Geochronology of basal gneisses and mangerite syenites of Stadlandet, west Norway. *Nor. Geol. Tidsskr.* **59**, 161–181.

—— & SMITH, D.C. 1978. Mantle equilibrated orthopyroxene eclogite pods from the basal gneisses in the Selje District, western Norway. *J. Petrol.* **19**, 530–584.

LARDEAUX, J.-M., GOSSO, G., KIENAST, J.-R. & LOMBARDO, B. 1982. Relations entre le métamorphisme et la déformation dans la zone Sésia-Lanzo (Alps occidentales) et le problème de l'eclogitisation de la croûte continentale. *Bull. Soc. Geol. France*, **24**, 793–800.

MACGREGOR, I.D. 1970. The effect of CaO, Cr_2O_3, and Al_2O_3 on the stability of spinel and garnet peridotites. *Phys. Earth Planet. Int.* **3**, 372–377.

MATTE, P.L. & BURG, J.P. 1981. Sutures, thrusts and nappes in the Variscan Arc of western Europe: Plate tectonic implications. *In*: MCCLAY, K.R. & PRICE, N.J. (eds.), *Thrust and Nappe Tectonics*. Spec. Publ. Geol. Soc. Lond. **9**, 353–358.

MATTHES, S. 1978. The eclogites of southern Germany. A summary. *Neues Jahrb. Mineral. Monatsch.* **3**, 93–109.

MEARNS, E.W. & LAPPIN, M.A. 1982. A Sm-Nd isotopic study of 'internal' and 'external' eclogites, garnet lherzolites and grey gneiss from Almklovdalen, western Norway. *Terra Cognita*, **2**, 324.

MEDARIS JR., L.G. 1980. Petrogenesis of the Lien peridotite and associated eclogites, Almklovdalen, western Norway. *Lithos*, **13**, 339–353.

—— 1984. A geothermobarometric investigation of garnet peridotites in the western gneiss region of Norway. *Contrib. Mineral. Petrol.* **87**, 72–86.

MEHTA, P.K. 1980. Tectonic significance of the young mineral dates and dates of cooling and uplift in the Himalayas. *Tectonophys.* **62**, 205–217.

MEHNERT, K.R. 1975. The Ivrea Zone. A model of the deep crust. *Neues Jb. Miner. Abh.* **125**, 156–199.

MIRWARD, P.W. & MASSONNE, H.J. 1980. The low-high quartz and quartz-coesite transition to 40 kbar between 600°C and 1600°C and some reconnaissance data on the effect of $NaAlO_2$ component of the low quartz-coesite transition. *J. Geophys. Res.* **85**, 6983–6990.

MISAR, Z., JELINEK, E. & JAKES, P. 1983. Inclusions of peridotite, pyroxenite and eclogite in granulite rocks of pre-Hercynian upper mantle and lower crust in the East Bohemian Massif (Czechoslovakia). *Ann. Sci. Univ. Clermont-Fd. II*, **74**, 85–95.

MIYASHIRO, A. 1973. *Metamorphism and Metamorphic Belts*. John Wiley, New York.

MØRK, M.B.E. 1982. A gabbro-eclogite transition on Flemsøy, Sunnmøre, western Norway. *Terra Cognita*, **2**, 316.

NIXON, P.H. & BOYD, F.R. 1973. Petrogenesis of the granular and sheared ultrabasic nodule suite in kimberlites. *In*: NIXON, P.H. (ed.) *Lesotho Kimberlites* Lesotho Nat. Devel. Corp. Maseru, Lesotho.

O'HARA, M.J. 1975. Pressure required to stabilise garnet-peridotite and eclogite at low temperatures. *Abst. Int. Conf. Geotherm. Geobarom. Penn State University, U.S.A.*

—— & MERCY, E.L.P. 1963. Petrology and petrogenesis of some garnetiferous peridotites. *Trans. Roy. Soc. Edinb.* **65**, 251–314.

——, RICHARDSON, S.W. & WILSON, G. 1971. Garnet peridotite stability and occurrence in crust and mantle. *Contrib. Mineral. Petrol.* **32**, 48–68.

—— & YODER JR., H.S. 1967. Formation and fractionation of basic magmas at high pressures. *Scott. J. Geol.* **3**, 67–117.

OBERHAENSLI, R., HUNZIKER, J.C., MARTINOTTI, G. & STERN, W.B. 1982. Mucronites: An example of Eo-Alpine eclogitisation of Permian granitoids, Italy. *Terra Cognita*, **2**, 325.

OXBURGH, E.R. & TURCOTTE, D.L. 1974. Thermal gradients and regional metamorphism in overthrust terrains with special reference to the Eastern Alps. *Schweiz. Mineral. Petrogr. Mitt.* **54**, 641–662.

PEUCAT, J.J. & COGNÉ, J. 1977. Geochronology of some blueschists from Ile de Groix, France. *Nature*, **268**, 131–132.

PIN, C. & VIELZEUF, D. 1983. Granulites and related rocks in Variscan Median Europe: A dualistic interpretation. *Tectonophysics*, **93**, 47–74.

RINGWOOD, A.E. 1975. *Composition and petrology of the earth's mantle*. McGraw Hill, New York.

RIVALENTI, G., GARUTI, G., ROSSI, A., SIENA, F. & SINIGOI, S. 1981. Existence of different peridotite types and of a layered igneous complex in the Ivrea Zone of the western Alps. *J. Petrol.* **22**, 127–153.

ROBERTS, D., THON, A., GEE, D.G. & STEPHENS, M.B. 1981. Scandinavian Caledonides—Tectonstratigraphy map, scale 1–1,000,000. Uppsala Caledonide Symp.

ROBERTSON, E.C.F., BIRCH, F. & MACDONALD, G.L.F. 1957. Experimental determination of jadeite stability relations to 25,000 bars. *Amer. J. Sci.* **255**, 115–137.

ROBINSON, D.N., GURNEY, J.J. & SHEE, S.R. 1984. Diamond eclogite and graphite eclogite xenoliths from Orapa, Botswana. *In*: KORNPROBST, J. (ed.) *Kimberlites II: The Mantle and Crust-Mantle Relationships*. Elsevier, Amsterdam.

RUBIE, D.C. 1983. A thermal-tectonic model for high-pressure metamorphism and deformation in the Sesia Zone, western Alps. *J. Geol.* **92**, 21–36.

SANDERS, I.S., VAN CALSTEREN, P.W.C. & HAWKESWORTH, C.J. 1984. A Grenville Sm-Nd age for the Glenelg eclogite in north-west Scotland. *Nature*, **312**, 439–440.

SANTALLIER, D., FLOCH, J.P. & GUILLOT, P.L. 1978. Quelques aspects du métamorphisme dévonien en bas-limousin (Massif Central, France). *Bull. Mineral.* **101**, 77–88.

SCHARBERT, H.G. 1973. Pyrope-rich garnet from Moldanubian garnet pyroxenites, Bohemian Massif, Lower Austria, Austria. *Neues Jb. miner. Abh.* **H-2**, 89–93.

—— & CARSWELL, D.A. 1983. Petrology of garnet-clinopyroxene rocks in a granulite facies environment, Bohemian Massif of Lower Austria. *Bull. Mineral.* **106**, 761–774.

—— & KURAT, G. 1974. Distribution of some elements between coexisting ferromagnesian minerals in Moldanubian granulite facies rocks, Lower Austria, Austria. *Tschermaks Mineral. Petrogr. Mitt.* **21**, 110–134.

SMITH, D.C. 1980. A tectonic mélange of foreign eclogites and ultramafites in west Norway. *Nature*, **287**, 366–368.

—— 1981. A reappraisal of factual and mythical evidence concerning the metamorphic and tectonic evolution of eclogite-bearing terrain in the Caledonides. *Terra Cognita*, **1**, 73.

—— 1982. A review of the controversial eclogites in the Caledonides. *Terra Cognita*, **2**, 304.

SMULIKOWSKI, K. 1960. Comments on eclogite facies in regional metamorphism. *Rep. Int. Geol. Congr. XXI Copenhagen* Pt. **XIII**, 372–382.

—— 1964. Chemical differentiation of garnets and clinopyroxenes in eclogites. *Bull. Acad. Pol. Sc. Ser. Geol. Geogr.* **XII**, 11–18.

—— 1968. Differentiation of eclogites and its possible causes. *Lithos*, **1**, 89–1012.

—— & BARUM-CZUBAROW, N. 1973. New data concerning the granulite-eclogite rock series of Stary Gieraltow, East Sudetes, Poland. *Bull. Acad. Pol. Sc. Ser. Geol. Geogr.* **XXI**, 25–34.

SPEAR, F.S., SELVERSTONE, J., HICKMOTT, D., CROWLEY, P. & HODGES, K.V. 1984. P-T paths from garnet zoning: A new technique for deciphering tectonic processes in crystalline terranes. *Geology*, **12**, 87–90.

STRAND, T. 1960. The region with basal gneiss in the N.W. part of S. Norway. *Nor. Geol. Unders.* **208**, 230–245.

TARLING, D.H. 1980. Lithosphere evolution and changing tectonic regimes. *J. geol. Soc. London*, **137**, 459–467.

TRICART, P. 1984. From passive margin to continental collision: A tectonic scenario for the western Alps. *Amer. J. Sci.* **284**, 97–120.

VAN BREEMAN, O., AFTALION, M. *et al.* 1982. Geochronological studies of the Bohemian Massif, Czechoslovakia and their significance in the evolution of central Europe. *Trans. Roy Soc. Edinb. Earth Sci.* **73**, 89–108.

VAN CALSTEREN, P.W.C., BUELRIJK, N.A.I.M., *et al.* 1979. Isotopic dating of older elements (including the Cabo Ortegal Mafic-Ultramafic Complex) in the Hercynian orogen of N.W. Spain. Manifestations of a presumed early palaeozoic mantle-plume. *Chem. Geol.* **24**, 35–56.

VESELA, M. 1967. On the stratigraphical position of granulites in the Moldanubicum. *Krystalinikum*, **5**, 137–152.

VIDAL, PH., PEUCAT, J.J. & LASNIER, B. 1980. Dating of granulites involved in the Hercynian Fold Belt of Europe: An example taken from the granulite-facies orthogneisses at La Picherais, southern Armorican Massif, France. *Contrib. Mineral. Petrol.* **72**, 283–289.

VRANA, S. & JAKES, P. 1982. Orthopyroxene granulites from a segment of charnockitic crust in southern Bohemia. *Vest. Ustr. Ustav. Geol.* **57**, 129–143.

WINDLEY, B.F. 1983. Metamorphism and tectonics of the Himalaya. *J. geol. Soc. London*, **140**, 849–865.

TAHIKRHELI, R.A.K. 1982. Fission-track evidence for Quaternary uplift of the Nanga Parbat region, Pakistan. *Nature*, **298**, 255–257.

ZIEGLER, P.A. 1984. Caledonian and Hercynian crustal

consolidation of western and central Europe—a working hypothesis. *Geol. Mijnbouw*, **63**, 93–108.

ZEITLER, P.K., JOHNSON, N.M., NAESER, C.W. & TAHIRKHELI, R.A.K. 1982. Fission-track evidence for Quaternary uplift of the Nanga Parbat region, Pakistan. *Nature*, **298**, 255–257.

ZINGG, A. 1983. The Ivrea and Strona-Ceneri Zones (southern Alps, Ticino and N-Italy)—A Review. *Schweiz. Mineral. Petrogr. Mitt.* **63**, 361–392.

ZOUBEK, V. 1969. Age relations in metamorphic terrains of the Bohemian Massif: Some methods and results. *Geol. Ass. Can Spec. Pap.* **5**, 73–81.

D.A. CARSWELL, Department of Geology, University of Sheffield, Mappin Street, Sheffield, S1 3JD, UK.

S.J. CUTHBERT, Exploration Division, BRITOIL plc., 150 St. Vincent Street, Glasgow, G2 5LJ, UK.